Second Series *October 1, 1931* *Vol. 38, No. 7*

THE
PHYSICAL REVIEW

X-RAY ABSORPTION BY A THOMAS-FERMI ATOM

By Louis C. Roess and E. H. Kennard*
Department of Physics, Cornell University

(Received August 24, 1931)

Abstract

Calculations were made on the K shell of tin, the K electron being assumed to move according to the Dirac relativistic equation in a modified Fermi-Thomas field. The ionization potential for a K electron thus found exceeds the observed energy of the K absorption edge by only 0.48 percent. Mass absorption-coefficients for the K shell for wave-lengths 1, 1.5 and 2.5 times the absorption-edge wave-length were found to be 2.42, 12.10, 37.42 respectively, as against Richtmyer's observed values of 2.36, 11.0, 37.0.

The Model and the Results

FORMULAS for the mass absorption coefficient of the K shell have been obtained[1] from both relativistic and nonrelativistic quantum mechanics on the assumption that for the heavy elements a hydrogen-like atom constitutes a sufficiently good approximation; agreement with experiment could be secured by the introduction of a screening constant of arbitrary but plausible size. A much better approximation and one involving no such arbitrary element should be obtained by employing the Thomas-Fermi field;[2] presumably the Hartree-Fock[3] field would be still better, but it would involve much more laborious calculations.

In the present paper are reported a few calculations made for tin with the Thomas-Fermi field. An atom in the middle range of atomic numbers was chosen because there the hydrogen-like model has become rather poor while at the same time the Thomas-Fermi field should give a better approximation than it does for lighter elements. In the first calculations the field for a K electron in an atom of nuclear charge Ze was taken to be that for a neutral atom of charge $(Z-1)e$ plus the Coulomb field of an extra proton

* This investigation was supported by a grant from the Heckscher Research Foundation.

[1] H. Hall and J. R. Oppenheimer, Phys. Rev. **38**, 57 (1931); L. C. Roess, Phys. Rev. **37**, 532 (1931), and references in the latter paper. The work of Hall and Oppenheimer shows that the neglect of retardation is not important for wave-lengths relatively close to the K edge.

[2] L. H. Thomas, Proc. Camb. Phil. Soc. **23**, 542 (1927); E. Fermi, Zeits. f. Physik **48**, 73 (1928).

[3] D. R. Hartree, Proc. Camb. Phil. Soc. **24**, 89, 111 (1928); V. Fock, Zeits. f. Physik **61**, 126 (1930).

in the nucleus, e being the numerical electronic charge. Such a field has been used elsewhere for a valence electron;[4] its use for an interior electron is open to question but it seems also doubtful whether any attempt at further refinement of the essentially rough Thomas-Fermi method is really worth while. However, for the last calculation such an attempt was made;† the field was taken to be: Thomas-Fermi field of atom of charge $(Z+1)e$ minus Coulomb field of proton in nucleus minus field of one valence electron minus half the field due to K electrons of atom of charge Ze. This potential may be justified by the following reasoning. The contraction of the outer electrons when one K electron is removed suggests the use of a Thomas-Fermi field corresponding to atomic number $Z+1$, corrected by subtracting the Coulomb field of one proton. A further correction must be made for the extra valence electron; this may be accomplished roughly by taking its potential to be that of a spherical shell of charge e and radius a, where a is the "atomic radius," determined, say, from x-ray measurements on crystals. To obtain the field in which the K electron moves, half the potential due to the K-shell itself was then subtracted; this potential was taken as that due to the Thomas-Fermi charges, of density $\rho(r)$, located within a sphere of such radius r_0 that $\int_{r=0}^{r=r_0}\rho(r)d\tau=-2e$.

The second field of potential thus obtained is about one percent higher than the first (at points well inside the atom). The ionization potential for a Dirac electron in this field exceeds the observed energy of the K absorption edge for tin by 0.48 percent as against a deficit of 1.6 percent when the first Thomas-Fermi field was used.

Values of the mass absorption coefficient of the K shell were obtained with the first field for $\lambda_k/\lambda=1.5$ and 2.5, and with the second field for $\lambda=\lambda_k$, λ_k being the wave-length of the absorption edge. The results are shown in Table I in comparison with the experimental values.

TABLE I. *Mass absorption coefficient* $(\tau_p/\rho)_k$ *for tin.*

λ in X.U.	λ_k/λ	Calculated		Observed	
		Thomas-Fermi	Screened Coulomb[6]	Richtmyer[5]	Allen[5]
169.58	2.5	2.421	1.9	2.365	3.16 to 3.28
282.63	1.5	12.104	9.03	11.0	13.9 to 14.6
423.94	1.0	37.42	28.5	37.0	45.9 to 47.7

[4] E. Fermi, Zeits. f. Physik **49**, 550 (1928); F. Rasetti, Zeits. f. Physik **49**, 546 (1928).

† *Note added by E. H. Kennard.*—A third possibility would be simply to subtract the assumed potential due to one K electron from the Fermi-Thomas field of the actual atom; this seemed less plausible because no allowance is then made for increased concentration of the remaining electrons. Now, classically, the work done in the reversible removal of a relatively small charge from a system in equilibrium is measured by the mean of the potentials at its location in the system before and after the removal. This consideration suggests that, as a final refinement, we might use the mean of the third field just mentioned and the second field described in the paper.

[5] F. K. Richtmyer, Phys. Rev. **27**, 1 (1927); **30**, 755 (1927). S. J. M. Allen, Phys. Rev. **28**, 907 (1926).

[6] L. C. Roess, Phys. Rev. **37**, 532 (1931).

Inspection of the table shows a much improved agreement with experiment, especially if Richtmyer's values are taken to be more nearly correct.

THEORY

The mass absorption coefficient of the K shell is given by the following formula (ref. 6, Eq. (49)):

$$\left(\frac{\tau_\nu}{\rho}\right)_k = \frac{4\pi e^2 \lambda N}{3A}\left[\frac{8}{3}\left|\int_0^\infty F_0 G_1^* r^2 dr\right|^2 + 3\left|\int_0^\infty F_{-2}^* G_0 r^2 dr + \frac{1}{3}\int_0^\infty F_0 G_{-2}^* r^2 dr\right|^2\right] \tag{1}$$

in which N is the Loschmidt number, A the atomic weight, λ the wave-length of the incident radiation, and F_l and G_l are radial functions satisfying the simultaneous differential equations (ref. 6, Eq. (11)):

$$\begin{aligned} &\frac{2\pi}{h}\left(\frac{W+eV}{c}+mc\right)F_l + \frac{dG_l}{dr} - \frac{l}{r}G_l = 0, \\ &-\frac{2\pi}{h}\left(\frac{W+eV}{c}-mc\right)G_l + \frac{dF_l}{dr} + \frac{l+2}{r}F_l = 0, \end{aligned} \tag{2}$$

where W is the energy and V the potential.

For an atom of atomic number Z, the first field described above is given by

$$V_1 = \frac{e}{r}\left\{1 + (Z-1)\phi\left(\frac{r}{\mu_{z-1}}\right)\right\} \tag{3}$$

where $\phi(x)$ is the Thomas-Fermi function[2] satisfying the relations

$$\phi'' = \frac{\phi^{3/2}}{x^{1/2}}, \quad \phi(0) = 1, \quad \int_0^\infty \phi^{3/2} x^{1/2} dx = 1, \tag{4}$$

and

$$\mu_z = \left(\frac{9\pi^2}{128z}\right)^{1/3} \cdot a_0, \quad a_0 = \frac{h^2}{4\pi^2 m e^2}. \tag{5}$$

In order to obtain the second field, we must determine the potential due to the K shell. We start with a total potential $V=(Ze/r)\phi(r/\mu_Z)$ and a corresponding charge density

$$\rho(r) = -\frac{1}{4\pi r^2}\frac{d}{dr}\left(r^2\frac{dV}{dr}\right) = -\frac{Ze}{4\pi r}\frac{d^2\phi}{dr^2}, \tag{6}$$

from which we obtain for the charge inside any radius $r=\mu_Z y$

$$\int \rho(r) d\tau = -Ze\int_0^y y\phi'' dy = -Ze[y\phi'(y) + 1 - \phi(y)],$$

and as the equation defining $y_0 = r_0/\mu_Z$,

$$y_0\phi'(y_0) + 1 - \phi(y_0) = 2/Z. \tag{7}$$

Half the potential due to the distributed charge inside the radius r_0 will then be

$$
\begin{aligned}
&-\frac{4\pi}{2r}\int_0^r \rho(r)r^2dr - \frac{4\pi}{2}\int_r^{r_0}\rho(r)rdr, \quad (r \leqq r_0),\\
&-\frac{e}{r} \quad (r \geqq r_0),\\
&= \begin{cases} -\dfrac{Ze}{2\mu_z y}[y\phi'(y_0) + 1 - \phi(y)] & (y \leqq y_0),\\ -\dfrac{e}{\mu_z y} & (y \geqq y_0). \end{cases}
\end{aligned} \tag{8}
$$

The remainder of the derivation of the second field is elementary, and we obtain finally, putting $r = \mu_{Z+1}x$,

$$
V_2 = \begin{cases} \dfrac{(Z+1)e}{\mu_{z+1}x}\phi(x) + \dfrac{Ze}{2\mu_{z+1}x}\left\{\dfrac{\mu_{z+1}x}{\mu_z}\phi'(y_0) + 1 - \phi\left(\dfrac{\mu_{z+1}}{\mu_z}x\right)\right\} \\ \qquad + \dfrac{e}{a} - \dfrac{e}{\mu_{z+1}x}, \quad (0 \leqq x \leqq x_0), \\ \dfrac{(Z+1)e}{\mu_{z+1}x}\phi(x) + \dfrac{e}{a} \qquad \left(x_0 \leqq x \leqq \dfrac{a}{\mu_{z+1}}\right), \\ \dfrac{(Z+1)e}{\mu_{z+1}x}\phi(x) + \dfrac{e}{\mu_{z+1}x} \qquad \left(\dfrac{a}{\mu_{z+1}} \leqq x\right). \end{cases} \tag{9}
$$

If we transform Eq. (2) by putting $r = \mu_{1,2}x$, with $\mu_1 = \mu_Z$, $\mu_2 = \mu_{Z+1}$, and writing

$$W = mc^2 + h(\nu - \nu_k) \tag{10}$$

$$A_{1,2} = \frac{4\pi mc}{h}\mu_{1,2} \tag{11}$$

$$\epsilon_{1,2} = 2\pi\mu_{1,2}\left(\frac{1}{\lambda} - \frac{1}{\lambda_k}\right) \tag{12}$$

$$\alpha = \frac{2\pi e^2}{hc} \tag{13}$$

$$V_{1,2} = \frac{e}{\mu_{1,2}x}\phi_{1,2}(x), \tag{14}$$

we obtain

$$
\begin{aligned}
&\left[A_{1,2} + \epsilon_{1,2} + \frac{\alpha\phi_{1,2}}{x}\right]F_l + \frac{dG_l}{dx} - \frac{l}{x}G_l = 0,\\
&-\left[\epsilon_{1,2} + \frac{\alpha\phi_{1,2}}{x}\right]G_l + \frac{dF_l}{dx} + \frac{l+2}{x}F_l = 0.
\end{aligned} \tag{2'}
$$

In Eq. (1) the subscripts 0 refer to the discrete spectrum and the subscripts 1 and -2 to the continuous spectrum. For these values of l and these conditions on ϵ, Eqs. (2′) are to be integrated numerically, the solutions normalized to unity, and then the integrals in Eq. (1) evaluated by numerical quadrature.

Numerical Methods

For the discrete spectrum $l=0$, and F_0 and G_0 have no nodes inside the range of integration. We use this fact to obtain a single nonlinear first-order equation from Eqs. (2′). Put

$$\eta = F/G, \quad \eta'/\eta = F'/F - G'/G; \tag{15}$$

then from (2′)

$$\eta' = \epsilon + (A+\epsilon)\eta^2 - \frac{1}{x}[2\eta - \alpha\phi(1+\eta^2)], \tag{16}$$

$$G'/G = -\left[A + \epsilon + \frac{\alpha\phi}{x}\right]\eta. \tag{17}$$

Having obtained η we can find G from (17) by numerical quadrature.

Since (16) has a singular point at the origin, a series development must be used to determine η for small values of x. Knowing[7] that $\phi(x)$ is an analytic function of $x^{1/2}$ near the origin, we write

$$\phi(x) = \sum_0^\infty a_n x^{1/2n}, \quad \eta(x) = \sum_0^\infty b_n x^{1/2n}, \quad \eta^2(x) = \sum_0^\infty c_n x^{1/2n}, \tag{18}$$

and find

$$b_0 = \frac{\alpha Z}{1+\rho} = \frac{1-\rho}{\alpha Z}, \text{ where } \rho = (1-\alpha^2Z^2)^{1/2}, \quad b_1 = 0,$$

$$(2\rho+1)b_2 = Ab_0^2 + (\epsilon - \alpha a_2)(1+b_0^2), \tag{19}$$

$$(2\rho + \tfrac{1}{2}n)b_n = (A+\epsilon)c_{n-2} + \alpha\left[a_0(1+b_0^2) + Z\sum_1^{n-1} b_\nu b_{n-\nu} + \sum_1^{n-1} a_\nu c_{n-\nu}\right], \quad (n>2).$$

The value of ϵ, which in the discrete case is negative, must be chosen so that η is everywhere finite. This is done by a method of trial and error, and fortunately the dependence of η on ϵ was so strong that comparatively few values of η were necessary to judge the correctness of the trial ϵ. The values of η and η' at the first four points were obtained from the series (18) and the solution was then extended by applying Milne's[8] method of numerical integration.

[7] E. B. Baker, Phys. Rev. **36**, 630 (1930).
[8] W. E. Milne, Am. Math. Monthly **33**, 455 (1926).

In the continuous spectrum l takes on the values 1 and -2, and ϵ is positive. Near the origin the solution proceeds exactly as in the discrete case, with

$$b_0 = \frac{\alpha Z}{l+1+\rho_l} = \frac{l+1-\rho_l}{\alpha Z}, \quad \text{where } \rho_l = ((l+1)^2 - \alpha^2 Z^2)^{1/2},$$

and ρ_l substituted for ρ in Eq. (19). The equation for η can be used except near a root of G, where $\xi = 1/\eta$ may sometimes be used; but to continue this solution to infinity by the usual method is naturally out of the question.

The method employed for values of x greater than the first zero of either F or G follows readily from a suggestion made by Madelung.[9] We first transform Eq. (2′) to the normal form for the second order by putting

$$g = \frac{xG}{\left(A+\epsilon+\frac{\alpha\phi}{x}\right)^{1/2}}, \quad f = \frac{xF}{\left(\epsilon+\frac{\alpha\phi}{x}\right)^{1/2}} \tag{20}$$

and obtain for g

$$\frac{d^2g}{dx^2} + J(x,\epsilon)g = 0 \tag{21}$$

in which

$$\begin{aligned} J(x,\epsilon) = {} & \epsilon(A+\epsilon) + (A+2\epsilon)\frac{\alpha\phi}{x} + \left(\frac{\alpha\phi}{x}\right)^2 - \frac{l(l+1)}{x^2} \\ & + \frac{l+1}{x\left(A+\epsilon+\frac{\alpha\phi}{x}\right)}\left(\frac{\alpha\phi}{x}\right)' + \frac{1}{2\left(A+\epsilon+\frac{\alpha\phi}{x}\right)}\left(\frac{\alpha\phi}{x}\right)'' \\ & - \frac{3}{4\left(A+\epsilon+\frac{\alpha\phi}{x}\right)^2}\left[\left(\frac{\alpha\phi}{x}\right)'\right]^2. \end{aligned} \tag{22}$$

The asymptotic form of J being $J = \epsilon(A+\epsilon) = \text{const.}$, we put

$$g = BW \sin\left\{\int_{x_0}^{x} \frac{dx}{W^2} + \beta\right\} \tag{23}$$

in which B and β are constants, and obtain from Eq. (21)

$$W'' + JW - 1/W^3 = 0. \tag{24}$$

We want to find that solution of Eq. (24) which has a known simple form at infinity and which fluctuates as little as possible over a large range of x, since such a solution will be easily computed and will moreover give at once the asymptotic form of g. As Madelung[9] has indicated, such a solution can be found by means of the following iteration process:

[9] E. Madelung, Zeits. f. Physik **67**, 516 (1931).

$$JW^4{}_{n+1} = 1 - W_n{}^3 \cdot W_n'', \; W_0 = J^{-1/4}. \tag{25}$$

For the particular form of J given by Eq. (22) one can readily show that the iteration process converges for sufficiently large x, and that $\lim_{x\to\infty} W = J(\infty, \epsilon)^{-1/4} = [\epsilon(A+\epsilon)]^{-1/4}$. It is worth mentioning that when $\epsilon \to 0$ a numerical simplification results if one puts $W = (2a)^{1/2}x^{1/4}V$, also $x = (ay)^2$ $(a = 1/2(A\alpha)^{-1/2})$ in Eq. (24), and then obtains V by means of a similar iteration process.

Having thus determined W, we choose B and β to make the solution g join smoothly onto the solution G already found near the origin. If the subscript 0 means the values of the functions at the junction point, x_0, one finds readily that

$$\tan\beta = \frac{1}{W_0[W_0 g_0'/g_0 - W_0']}, \quad B = \frac{g_0}{W_0 \sin\beta}. \tag{26}$$

By use of the first of Eqs. (2′) and Eqs. (23) and (20), we find that F and G have the asymptotic forms

$$\begin{aligned} F &\sim M_x \frac{B}{(A+\epsilon)^{1/2}W(\infty)} \frac{\cos\left[[\epsilon(A+\epsilon)]^{1/2}x + \delta(x)\right]}{x} \\ G &\sim M_x (A+\epsilon)^{1/2} BW(\infty) \frac{\sin\left[[\epsilon(A+\epsilon)]^{1/2}x + \delta(x)\right]}{x} \end{aligned} \tag{27}$$

in which $\delta(x)$ is a slowly-varying function of x, and M_x is the "radial" normalizing factor in terms of x. Comparing Eq. (27) with Eq. (36) of reference 6 shows that F and G have the same asymptotic form here as there, and that

$$C = (A+\epsilon)^{1/2}BW(\infty), \quad D = 1/(A+\epsilon)W(\infty)^2. \tag{28}$$

Therefore, with the proper change of variable, the normalization can be carried out here exactly as it was done there and one obtains

$$M_x{}^2 = \frac{2\mu}{hc}\frac{1}{DC^2} = \frac{2\mu}{hc}\frac{1}{B^2}. \tag{29}$$

We now have the solutions for both the discrete and continuous spectrum properly normalized, so that the evaluation of Eq. (1) is readily accomplished. In all numerical quadratures the interval of integration was taken small enough so that Simpson's rule gave the desired accuracy.

THE PERIODIC SYSTEM OF ATOMIC NUCLEI AND THE PRINCIPLE OF REGULARITY AND CONTINUITY OF SERIES

By William D. Harkins
George Herbert Jones Laboratory
The University of Chicago

(Received August 6, 1931)

Abstract

New relations which concern the existence and stability of atomic nuclei are presented, together with a discussion of evidence for the relations given earlier as exhibited by the newer data on the existence of isotopes. It is shown that the four series, the helium, uranium, lithium and beryllium series, exhibit a considerable amount of regularity and are now almost continuous. The more abundant species of odd atomic number keep in general to a constant isotopic number as the atomic number increases, or else the isotopic number increases by the same amount as the atomic number. There is a general tendency as the atomic number increases for the isotopic number of the most abundant isotope of elements of both even and odd atomic number (a) to remain constant, (b) to increase at the same rate as the atomic number or (c) to decrease along a line of constant electronic number.

The atomic, mass, isotopic, and electronic numbers of all known isotopes are given in figures which exhibit the periodic and other relations of atomic nuclei. Many undiscovered atomic species (isotopes of each element) between atomic numbers 61 and 18, are predicted, and the general relations predict the existence of a considerable number of additional species among elements of lower number.

These relations are presented in the form of fourteen rules, several of which are new, and three are fundamental laws presented earlier. The bearing of the newer data on these rules is discussed.

The paper discusses nuclear stability and abundance as related to the pairing of nuclear electrons and the oddness and evenness of the electronic number, to the evenness and oddness of the nuclear charge (atomic number) as exhibited by the most recent work on the composition of the crust of the earth, the meteorites, and the atmosphere of the sun, and to the ratio of nuclear electrons to protons.

The neutron, or nuclear neutral particle may play a part in atom building. The figures, fundamental laws, rules, and relations presented, especially the principle of continuity and regularity of series, when taken in connection with known facts, seem to indicate that atomic nuclei are built in steps, and, except in the simplest cases, not as single events. That is the general picture revealed by all of these appears to be in discord with the theory of Millikan and Cameron.

1. Introduction

THE atomic species, often, but incorrectly, called isotopes, give a pattern which exhibits a considerable number of regularities when they are plotted in any natural way. The most important of these regularities have been expressed by the writer in the form of a set of relations or rules in a series of papers.[1,2]

[1] Harkins and Wilson, J. Am. Chem. Soc. **37**, 1367–9 (1915), Phil. Mag., (1915).

[2] Harkins, J. Am. Chem. Soc. **39**, 859, Table II (1917); Science **50**, 580–1; Phys. Rev. **15**, 85 (1920); Phil. Mag. **42**, (1921); J. Am. Chem. Soc. **42**, 1976 (1920); J. Am. Chem. Soc. **43**, 1050 (1921); J. Franklin Inst. **195**, 554 (1923); J. Am. Chem. Soc. **45**, 1426 (1923).

While the most important of these rules have thus been known for a considerable time, the present paper gives additional interesting relations whose importance is revealed by more recent work. This has been so extensive, due to the efforts of Aston and others, that every one of the first sixty elements, except only columbium, masurium, rhodium, and palladium, has been tested for isotopes. While the number of isotopes which exist for such elements as strontium and barium is much larger than the number thus far found, the attainment of the present stage of completeness makes it essential to examine the relations which exist between the species now known.

2. Periodic System of the Atomic Species (Elements 1 to 60)

The values for two experimentally determined variables which relate to atomic nuclei, are well known. These variables are the mass number (P), supposed to give the number of protons in the nucleus, and the atomic number (Z). A derived variable, $P-Z$, is supposed to give the number of nuclear electrons (N).

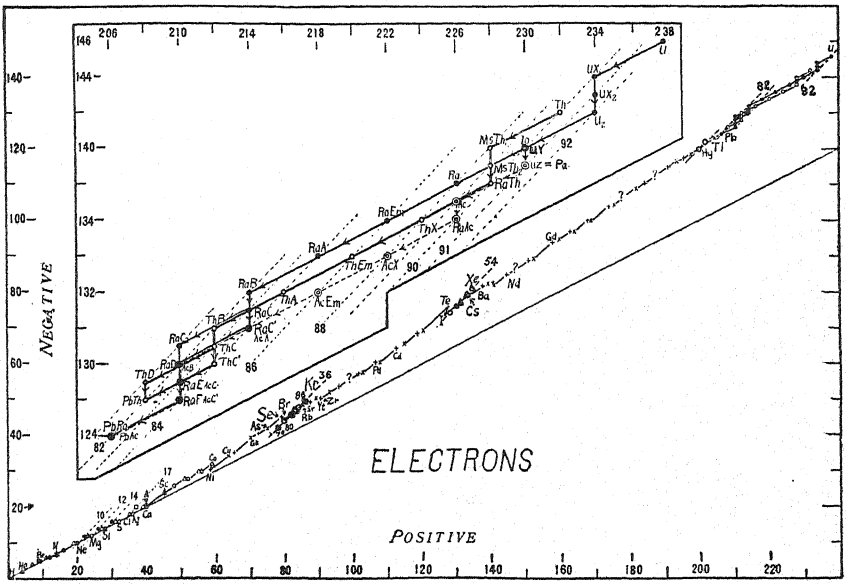


Fig. 1. The negative electron content of atomic nuclei as a function of the number of protons (positive electrons)

Fig. 1 shows the general form of the diagram which is obtained when the number of protons is plotted on the X-axis and the number of electrons on the Y-axis. The most abundant atomic species are found to lie in this plot on a line with a slope of $\frac{1}{2}$ which passes through the origin, and all of the other species are found to lie on 54 other equidistant lines above and parallel to this line. The scale of Fig. 1 is too small to show these lines except in the enlarged section in which the radioactive species are shown. These 55 parallel lines, when numbered, give the isotopic number, (n), a number as natural as, and on a par with, the atomic number.

The isotopic number has been defined by the writer[3] by the equations:

$$n = P - 2Z \quad (1)$$

$$n = 2N - P \quad (2)$$

$$n = N - Z. \quad (3)$$

If the formula of any nucleus is written as $(p_2e)_z(pe)_n$, then n is the isotopic number if p represents a proton and e, an electron.

If Fig. 1 is now rotated clockwise through the angle whose sine is $\frac{1}{2}$, and skewed so that the lines of constant atomic number are vertical, Fig. 2 results. This is the most compact and simple diagram which presents the relations between atomic nuclei. This and other forms of representation have been discussed by Harkins and Madorsky.[4]

In the figure every intersection of a vertical with a horizontal line represents a possible atomic species. The general position of the symbols which represent the atomic species shows that the band of greatest stability has somewhat the form of one limb of an hyperbola.

Species which belong to the thorium series ($P=4M$) are designated by circles, those of the uranium series ($P=4M+2$) by diamond shaped symbols, those of the lithium series ($P=4M+3$) by triangles, and those of the beryllium series ($P=2M+1$) by squares. M is taken to represent any whole number. The thorium and uranium series are named for the radioactive series which they include and the other two series begin with the principal isotope of lithium and of beryllium, respectively.

The principal general pattern of Fig. 2 is that of a double network of squares, produced by the lines which give the atomic and the isotopic number. The heavier lines of this network represent even and the light lines odd numbers. It is evident that the greatest number of species occur where heavy horizontal lines meet heavy vertical lines.

The considerable regularity in the pattern exhibited is in accord with the rules listed in the next section.

It may be noted that the proton or hydrogen nucleus has an atomic number 1 and an isotopic number -1. The electron has an atomic number -1 and an isotopic number 2.

In Fig. 2, the lines of slope -1 give the number of nuclear electrons, and the dashed lines of slope -2 give the number of protons or the mass number. The double arrow-heads designate the mean atomic weight for the element. If these are not shown the mean value coincides somewhat closely with that for the principal isotope of the element.

The ratio N/P of negative electrons to protons is given by the lines which radiate from the origin.

The most abundant isotope of columbium or of rhenium has not been found by the positive ray method but the existence of both these species is indicated by the atomic weight of the element, so they are included in the figure.

[3] W. D. Harkins, Phil. Mag 42, 305 (1921)

[4] W. D. Harkins and S. L. Madorsky, Phys. Rev. 19, 135 (1922).

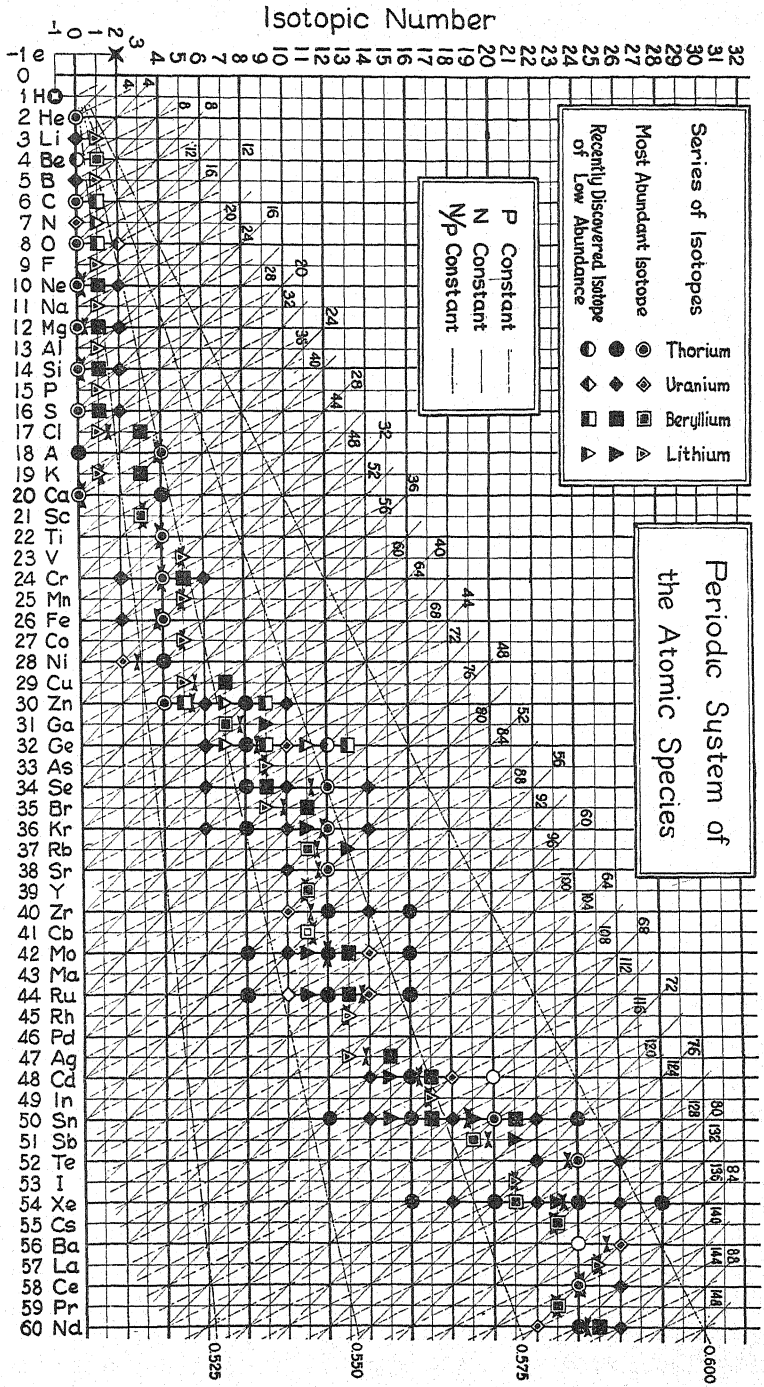


Fig. 2. Periodic system of atomic nuclei of nuclear charges −1 to 60.

The isotopic number has been defined by the writer[3] by the equations:

$$n = P - 2Z \quad (1)$$

$$n = 2N - P \quad (2)$$

$$n = N - Z. \quad (3)$$

If the formula of any nucleus is written as $(p_2e)_z(pe)_n$, then n is the isotopic number if p represents a proton and e, an electron.

If Fig. 1 is now rotated clockwise through the angle whose sine is $\frac{1}{2}$, and skewed so that the lines of constant atomic number are vertical, Fig. 2 results. This is the most compact and simple diagram which presents the relations between atomic nuclei. This and other forms of representation have been discussed by Harkins and Madorsky.[4]

In the figure every intersection of a vertical with a horizontal line represents a possible atomic species. The general position of the symbols which represent the atomic species shows that the band of greatest stability has somewhat the form of one limb of an hyperbola.

Species which belong to the thorium series ($P=4M$) are designated by circles, those of the uranium series ($P=4M+2$) by diamond shaped symbols, those of the lithium series ($P=4M+3$) by triangles, and those of the beryllium series ($P=2M+1$) by squares. M is taken to represent any whole number. The thorium and uranium series are named for the radioactive series which they include and the other two series begin with the principal isotope of lithium and of beryllium, respectively.

The principal general pattern of Fig. 2 is that of a double network of squares, produced by the lines which give the atomic and the isotopic number. The heavier lines of this network represent even and the light lines odd numbers. It is evident that the greatest number of species occur where heavy horizontal lines meet heavy vertical lines.

The considerable regularity in the pattern exhibited is in accord with the rules listed in the next section.

It may be noted that the proton or hydrogen nucleus has an atomic number 1 and an isotopic number -1. The electron has an atomic number -1 and an isotopic number 2.

In Fig. 2, the lines of slope -1 give the number of nuclear electrons, and the dashed lines of slope -2 give the number of protons or the mass number. The double arrow-heads designate the mean atomic weight for the element. If these are not shown the mean value coincides somewhat closely with that for the principal isotope of the element.

The ratio N/P of negative electrons to protons is given by the lines which radiate from the origin.

The most abundant isotope of columbium or of rhenium has not been found by the positive ray method but the existence of both these species is indicated by the atomic weight of the element, so they are included in the figure.

[3] W. D. Harkins, Phil. Mag **42**, 305 (1921)

[4] W. D. Harkins and S. L. Madorsky, Phys. Rev. **19**, 135 (1922).

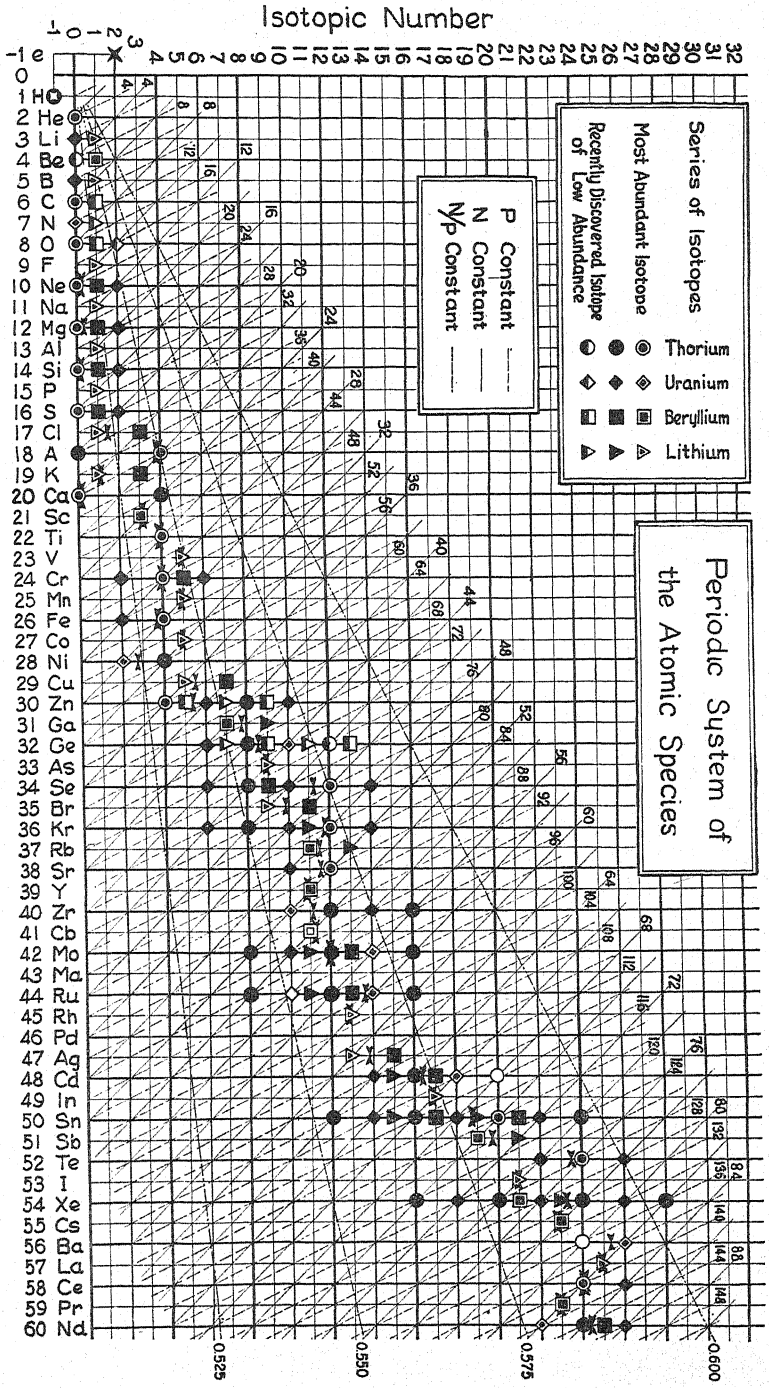


Fig. 2. Periodic system of atomic nuclei of nuclear charges −1 to 60.

3. Rules Concerning the Abundance and Stability of Atomic Nuclei

The most important rules which concern the stability and abundance of atomic nuclei are given below with special reference to Fig. 2, which emphasizes the fact that these rules are of even more general import than the limited earlier knowledge revealed.

In order to exhibit the extent to which the rules themselves apply it is necessary to consider a third dimension, to represent either abundance or stability, in connection with Fig. 2. Certain abundance relations are shown in Fig. 6.

Rule 1. Nearly all atomic nuclei contain an even number of electrons. Thus there seem to be at least 125 atoms of even to one atom of odd electronic number in the earth's crust. The extremely striking evidence for this rule is presented in Section 11, and the more detailed evidence in earlier papers by the writer. Corollary: Most atomic species have an even electronic number. Thus of the 156 known species for elements 1 to 60 inclusive, 125 have an even and 31 an odd electronic number. In Fig. 2 species of even electronic number lie on lines of slope -1, and those of odd number half way between the lines.

Rule 2. The number of electrons in the nucleus of any atom, other than hydrogen, is in no case less than half the number of protons (See Fig. 12).

Rule 3. Nearly all atomic nuclei have an even net nuclear charge, that is the atomic number is almost always even. The remarkable new evidence for this rule is presented in Section 10, and the more detailed earlier evidence in former papers of this series. Corollary: Most atomic species have an even atomic number. For example, of the 156 known species represented in Fig. 2 the atomic number is even for 116, and odd for 40.

Rule 4. Nearly all atomic nuclei contain an even number of protons. Corollary: More atomic species have an even than an odd mass number. Thus Fig. 2 shows 90 species with an even to 66 with an odd protonic number.

Rule 5. The number of protons in atomic nuclei is more often divisible by 4 than is to be expected by chance.

This relation is not so apparent in the number of species as it is in abundance especially of the light atoms. Thus 46 of the 156 species shown in Fig. 2 have mass numbers divisible by 4, and 43 divisible by 2 but not by 4. The number of species with mass numbers divisible by 3 should be 4/3 times the number divisible by 4, or 58, while the number found in Fig. 2 is 50.

However Rule 5 is of considerable significance, since all of the 5 most abundant species known in the meteorites have mass numbers divisible by 4.

Rule 6. If N is even then P is more often even than odd, and if N is odd, P is more often odd than even. Thus there is a certain matching of N and P with respect to evenness or oddness. There are almost no atoms in which the number of nuclear electrons is odd and the number of protons even. The 3 species of this type which exist are lithium 6, boron 10, and nitrogen 14, of isotopic number 0. They are the only species known which belong to Class IV according to Table I.

Rule 7. For light atoms (up to $Z=28$) the isotopic number which represents the chemical atomic weight is in general higher for odd than for even-numbered elements. Above atomic number 28 this value is usually higher for even than for odd-numbered elements; that is, the relation is inverted.

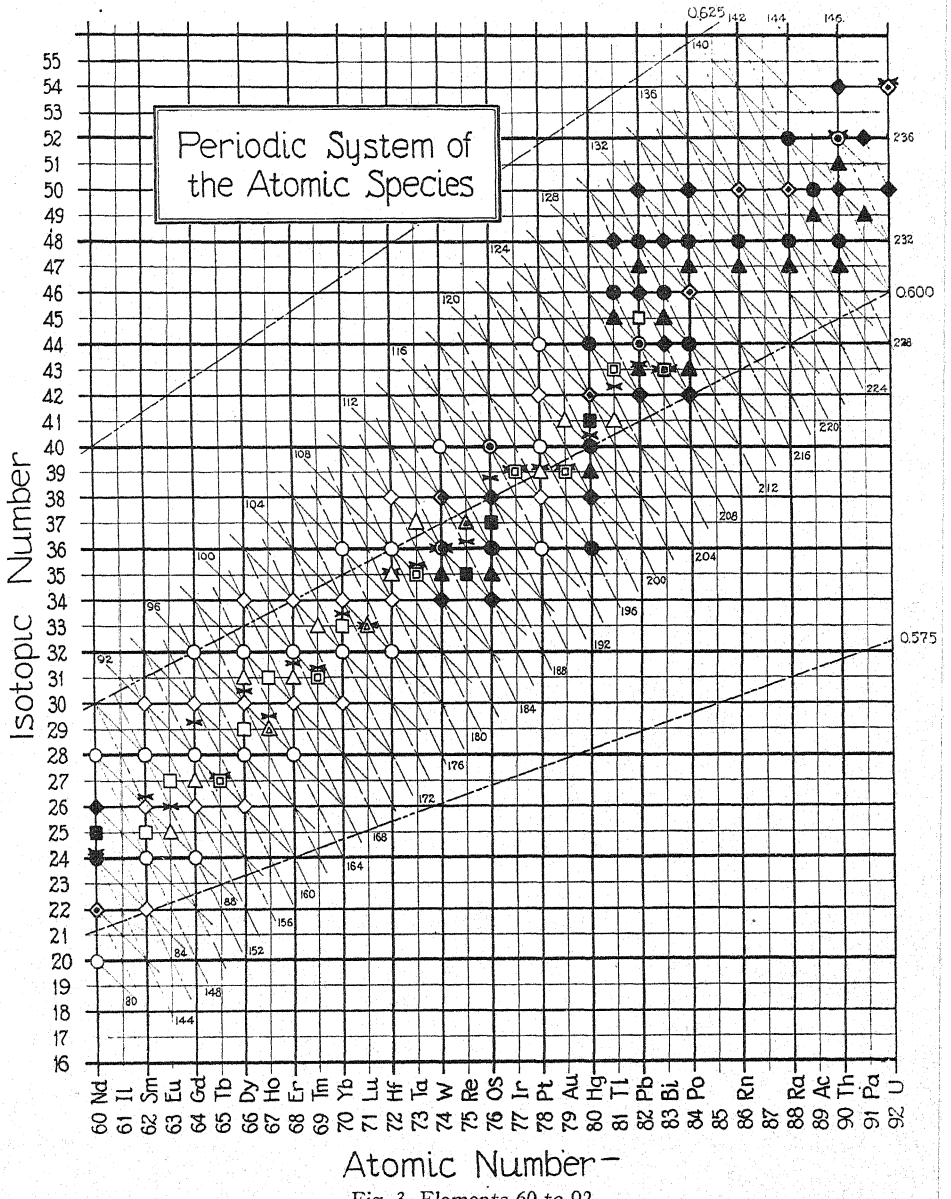


Fig. 3. Elements 60 to 92.

The above seven rules were discovered by the writer. An eighth found by Aston is as follows:

Rule 8. Not more than two isotopes are known for any element of odd atomic number, except among the radioactive elements.

TABLE I. *Classification of atomic nuclei according to even and odd number of electrons, and the corresponding abundance in the meteorites and the crust of the earth.*

Class			Abundance in Atomic Percentage	
			Earth's crust	Meteorites
Class I	N=even	P=even	87.4	95.4
Class II	N=even	P=odd	10.8	2.1
Class III	N=odd	P=odd	1.8	2.5
Class IV	N=odd	P=even	0.0007	0.0

Only 3 species of Class IV are known, and all of these have an isotopic number zero: lithium 6, boron 10, and nitrogen 14.

To the above may be added the following relation:

Rule 9. The difference of isotopic and of mass number between the two isotopes of an element of odd atomic number is always 2, except where species of Class IV of isotopic number 0 occur. (Li^6, B^{10}, N^{14}). The first two of these species have a mass number less by 1 than that of the more abundant isotopes.

4. Periodic System of the Atomic Species (Elements 60 to 92)

The general pattern for elements 60 to 92 is shown in Fig. 3, in which the symbols have the same significance as in Fig. 2.

Undiscovered species which are almost certain to be discovered later are designated by open symbols. A line around the inner part of the symbol indicates the most abundant isotope of the element.

From illinium (61) to tantalum (73) no atomic species have been found since these elements have not been investigated. It may be expected that all of the species listed in this region will be found when these elements are tested by methods with a moderate degree of sensitivity. The general pattern may be expected to be just that given. With more delicate methods the limits may be expected to extend beyond the species listed.

The more abundant isotope for each element of odd number is indicated, and the predictions may be expected to be correct in each case for which the chemical atomic weight is known.

It may be seen that rhenium and thallium are in discord with the otherwise general rule that the lighter of the two isotopes of an element of odd number is the more abundant.

Two other exceptions to this rule are found in lithium and beryllium, but this is due to the abnormal occurrence of isotopes of an entirely different class, those of Class IV according to one of the important schemes of classification introduced by the writer.

5. The Radioactive Series

The radioactive series are shown in Fig. 4. The atomic weight of members of the actinium series are unknown. The values given are those generally thought the most probable. If they are correct, the actinium series is a part

of the lithium series. On this basis, the members of this series have odd isotopic numbers and give odd isotopes to the elements of even number. The atomic weights or number of protons, and the number of electrons are given in the figure. Thus for radium the atomic weight is 226 and the number of electrons 138.

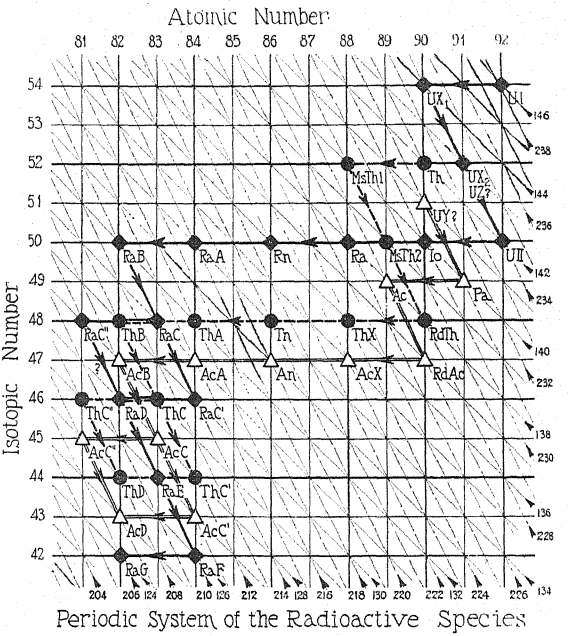


Fig. 4. The radioactive elements.

6. Variation in Abundance of Isotopes

Rule 10. For light elements of even number the most abundant isotopic species in an element of even number has an isotopic number of zero, or one divisible by 4, that is the most abundant isotope belongs to the helium-thorium ($4M$) series.

Up to element 38 there are only three exceptions: beryllium, nickel, and germanium.

Rule 11. For light elements of odd number the most abundant isotope has first an isotopic number 1, which increases (by 4) to 5 for elements 23 to 29.

Thus for either even or odd elements the most abundant isotopes tend to lie on lines of constant isotopic number, which, when varied increase by 4 as the atomic number rises.

Rule 12. (a) For light elements (up to 30) the most abundant isotope of an element of even number has the same electronic number as the next preceding element of odd number. For elements of higher number this relation is commonly reversed.

Rule 12. (b) Thus successive most abundant isotopes often lie on a line of constant electronic number. For example, the electronic number is 82 for the principal isotope of Ba (56), La (57), Ce (58), Pr (59), and Nb (60), and it is 50 for the principal isotope of Sr (38), Yr (39), and Zr (40).

An interesting relation is revealed by Fig. 3. The principal isotope of each element of odd number from Tb (65) to Ir (77) lies on a straight line of slope 1. On this same straight line lie the principal isotopes of the even-numbered elements Nd (60), Hg (80), Ra (88), Th (90), and U (92), and one of the two most abundant isotopes of W (74).

The increment along such a line is p_3e_2 between adjacent elements and p_6e_4 between odd (or even) elements. That this relation is not fortuitous, at least for the elements of odd number, is shown by the fact that the principal isotopes of Rh (45), In (49), Sb (51), I (53), Cs(55), and La (57) also lie on another line of slope 1. The same is true of Cu (29), Ga (31), and As (33), and also of K (19), Sc (21), and V (23).

Rule 13. In general for elements of odd number, with increase of atomic number:

(a) the isotopic number of the principal isotope remains constant, so the mass number increases by 4, and the electronic number by 2—that is the increment has the composition of an alpha-particle, or

(b) the isotopic number increases at the same rate as the atomic number, —that is the increase in mass number is 6, and in number of electrons is 4.

In one case, from lanthanum to praeseodymium, Rule 12 becomes more prominent and the isotopic number decreases along a line of constant electronic number.

The relations expressed by Rule 13 are expressed in Fig. 5.

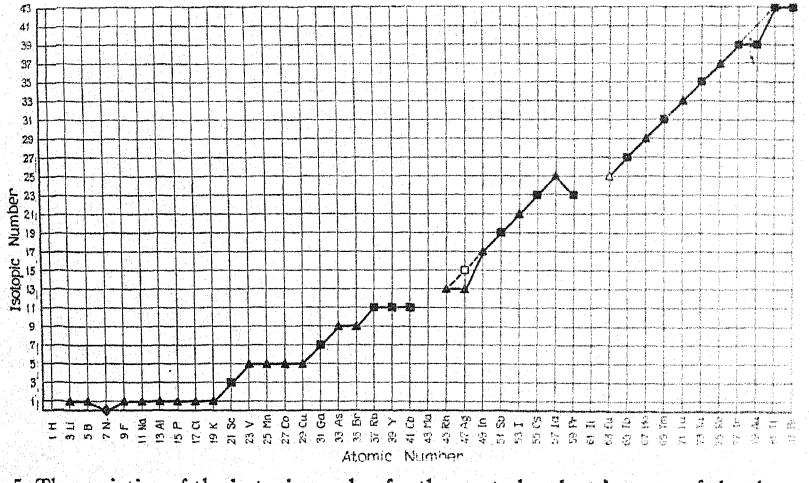


Fig. 5. The variation of the isotopic number for the most abundant isotopes of the elements of odd number. The two isotopes of silver have almost the same abundance.

7. Distribution of Abundance among Isotopes

The distribution of abundance among isotopes is very simple for elements of odd number.

Rule 14. The more abundant of the two isotopes of an element of odd number has in general the lower isotopic and the lower mass number.

This is not true for two elements, lithium and boron, which have isotopes

of the exceptional Class IV, but is true for nitrogen. As with certain other rules, some exceptions are found in elements of high atomic number. Thus in rhenium (75) and thallium (81) the higher isotope is the more abundant. In silver the two isotopes have almost the same abundance as judged from the chemical atomic weight and the packing fraction (See Fig. 5).

The variation in abundance of the isotopes of 9 well distributed elements is shown in Fig. 6. The vertical distance between two adjacent horizontal lines represents 50 percent, except for oxygen, at the top where the distance is twice as great, or 100 percent. The values for small percentages are printed in the figure. Thus oxygen consists of 99.9 percent isotopic number 0, 0.01

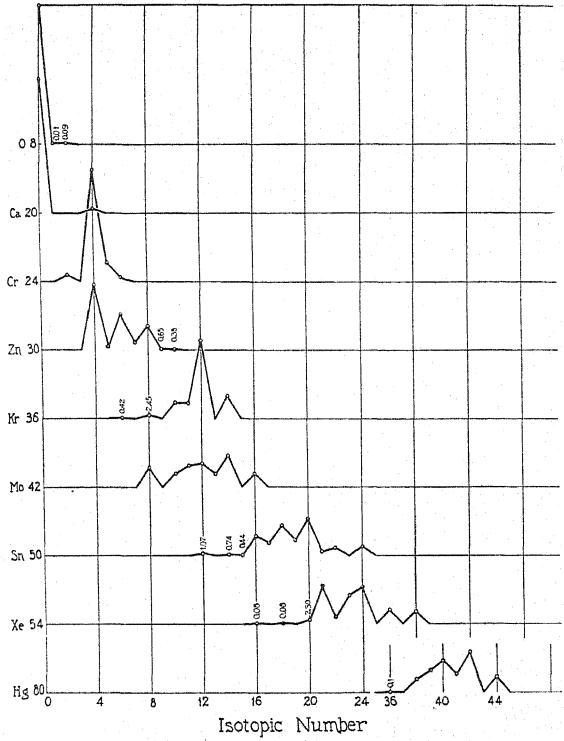


Fig. 6. Abundance of isotopes.

percent number 1, and 0.09 percent number 2. The pattern for neon, magnesium, silicon and sulphur, is in each case the same as for oxygen, except that isotopes 1 and 2 are relatively more abundant, especially for magnesium. The patterns for calcium and argon are the inverse of each other, with isotopes of number 0 and 4, with almost the whole material concentrated in the 0 isotope of calcium, and in isotope 4 of argon. Fig. 2 indicates the probability that both argon and calcium have undiscovered species of number 2, and probably 3, and that argon and possibly calcium probably contain species of isotopic number 1.

As the atomic number increases several peaks of abundance become prom-

inent instead of the single high peak found for oxygen, neon, magnesium, silicon, sulphur, argon, calcium, chromium, and krypton. Also, Rule 15, the abundance is much higher on the whole for even than for odd isotopic numbers. In xenon isotopes 21 and 24 are the most abundant, which represents an exceptional case in so far as 21 is concerned.

The distribution of abundance for two other elements is as follows; as found by Aston:

Ruthenium, atomic number = 44		
Isotopic number	Mass number	Percent
8	96	5
10	98	?
11	99	12
12	100	14
13	101	22
14	102	30
16	104	17

Ruthenium, like molybdenum (42) has the maximum of abundance at isotopic number 14, and the two patterns are much alike.

Osmium, atomic number = 76		
Isotopic number	Mass number	Percent
34	186	1.0
35	187	0.6
36	188	13.5
37	189	17.3
38	190	25.1
40	192	42.6

Here is an exceptional case, in that the highest isotope (thus far found) is the most abundant.

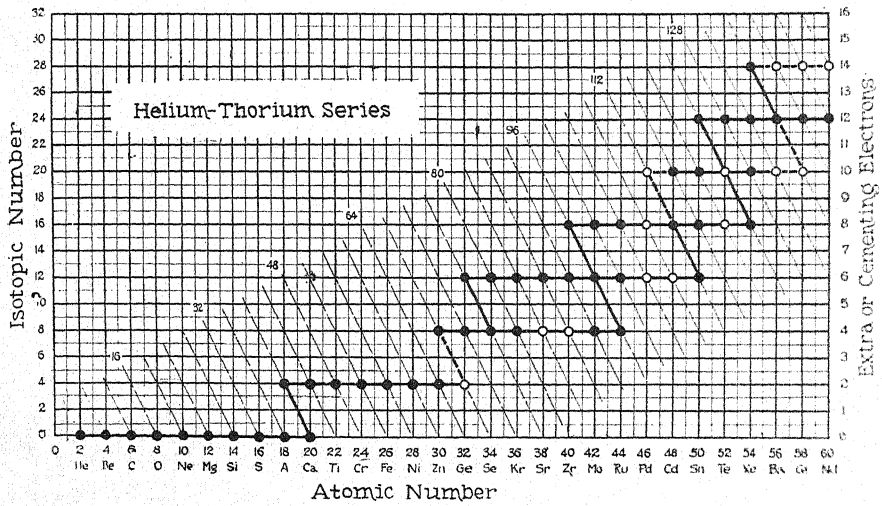


Fig. 7. Continuity in the helium-thorium series.

8. The Principle of Continuity and Regularity of Series of Atomic Nuclei (Atomic Species)

Certain regularities in the system of atomic nuclei are made more apparent by a separation of the atomic species into the four following series:

A. Even Series
   1. Helium-Thorium ($4M$) Series
   2. (Lithium 6) -Uranium ($4M+2$) Series

B. Odd Series
   3. Lithium 7 or lithium ($4M+3$) Series
   4. Beryllium 9 or beryllium ($4M+1$) Series

Thus the helium-thorium series (Fig. 7) exhibits a regular pattern as shown: the isotopic number increases by 4 at each step, and between calcium

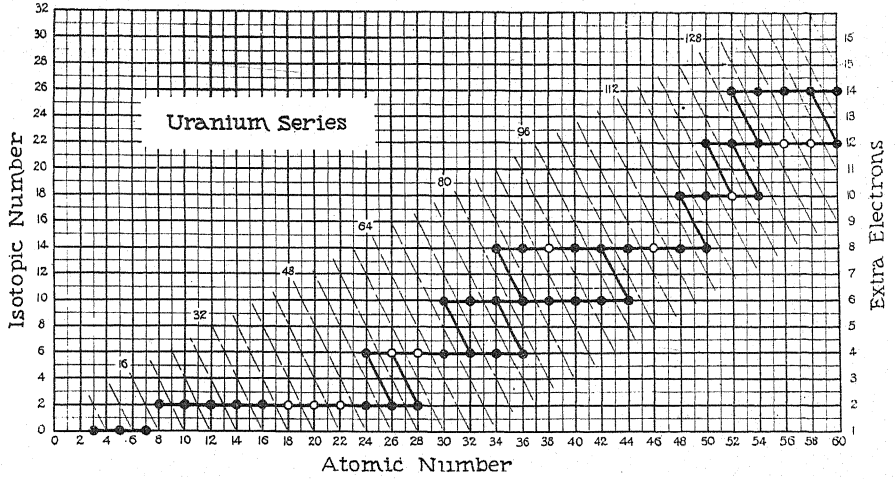


Fig. 8.

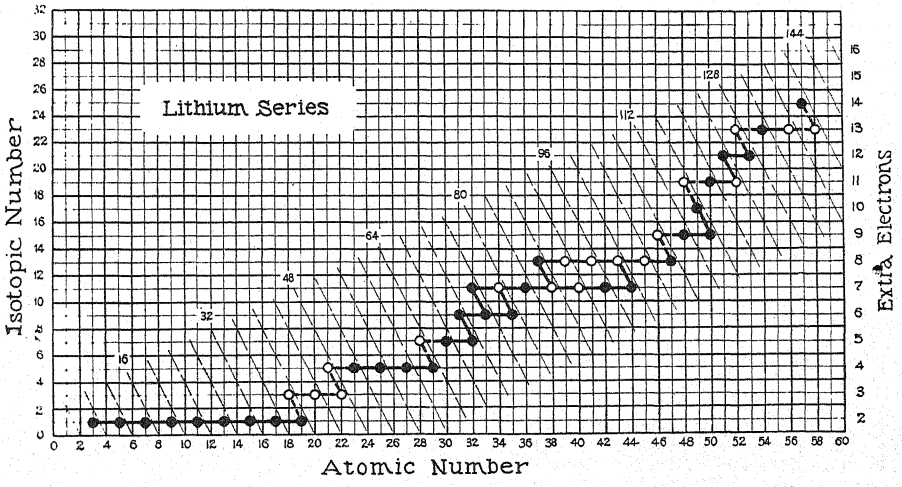


Fig. 9.

($P=40$, $n=0$) and argon ($P=40$, $n=4$) the atomic number decreases by two as the isotopic number makes its first step above zero. According to the principle of continuity all species which belong to the series and which lie on a line of constant isotopic number between the limits of known species are in general supposed to exist.

Thus the principle of continuity definitely predicts the following species: strontium ($n=8$, $P=84$), zirconium ($n=8$, $P=88$), palladium, two unknown species ($n=12$, $P=104$, and $n=16$, $P=108$), cadmium ($n=12$, $P=108$), tellurium, two unknown species ($n=12$, $P=120$ and $n=16$, $P=126$), or seven species in all, while 47 of the 54 species are now known.

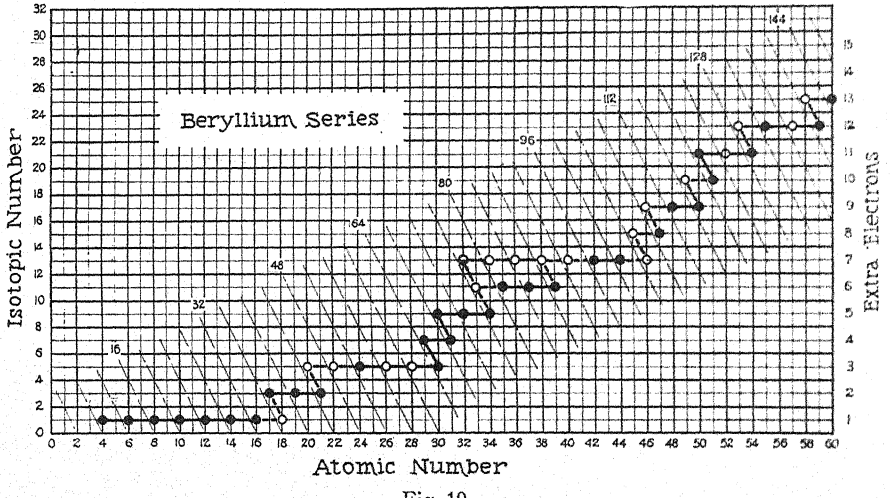


Fig. 10.

Species such as germanium ($n=4$, $P=68$) are not so definitely predicted, for here the existence of nickel ($n=8$, $P=64$) would meet the condition of regularity as well. It is also not so certain that the particular type of regularity which would be preserved by the existence of either of these two species is so persistent as the general form of the pattern otherwise.

There are undoubtedly great differences in the stability of species along any line of constant isotopic number, just as in the radioactive series. It, therefore, need not be surprising if a small number of species predicted by this principle remain undiscovered until much more delicate means of detection are discovered.

What is more apparent, however, is that the isotopic composition now given for such elements as strontium and barium is entirely inadequate, that zirconium contains a lower isotope than is now known, etc. The principle indicates that masurium ($Z=43$) has either an isotope of mass number 97 or of 99, and that probably both are present. The following table gives the length of each level as at present known:

This agrees with Latimer's nuclear model which is based on a part of the above relation expressed by Fig. 7, as given by the writer[5] in 1921.

[5] Harkins, Phil. Mag. **42**, 306, Pl. XII (1921).

Level	Isotopic Number	Number of Species Between Known Limits In Table	
1	0	10	10
2	4	7	8
3	8	8	8
4	12	10	10
5	16	8	8

The helium-thorium series is shown in another form in Fig. 11 in which lines of constant atomic number have a slope of 2, and the atomic number at the X-axis is twice the number of α-particles, and the number of electrons 2 times the number of α-particles plus the number of cementing or extra

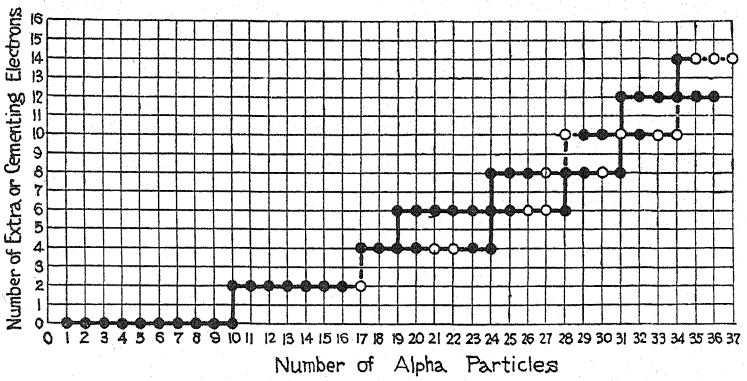


Fig. 11. The helium-thorium series. The atomic number is twice the number of alpha particles minus the number of cementing or extra electrons.

electrons. This form of representation was used early by the writer and has been adopted by Gamow and others.

The uranium series is much like the thorium series, but shifted two isotopic numbers higher.

A marked difference occurs in that the two lowest levels are only two isotopic numbers apart, but this is due to the presence of the three abnormal species of Class IV.

Level	Isotopic Number	Number of Species in Known Series
0	0	(3)
1	2	11
2	6	7
3	10	8
4	14	9

Here as in the thorium series levels 1 and 4 are the longest.

Odd Series. The odd series exhibit extremely interesting relations. Thus the two series would become almost coincident if the atomic number of every species in the beryllium series were increased by one. Unlike the even series, which occupy even isotopic levels but not in common (exception Class IV), each of the two odd series occupies every odd isotopic level. Like the even series the first level is especially long.

The lithium and the beryllium series together constitute what may be considered as a single combined or odd series.

9. The Ratio of Nuclear Electrons to Protons and the Isotopic Number

The isotopic number, defined in Section 1, has not come into general use, because, although it is an entirely natural and necessary number, it does not seem to be related to a sufficiently simple characteristic of atom nuclei to make it easily comprehensible to physicists or chemists in general. If, as in Fig. 12, the ratio of nuclear electrons to protons is plotted on one axis, and the atomic number (or the number of protons) on the other, it is found that every point which represents an atomic species lies on one of 55 lines. These

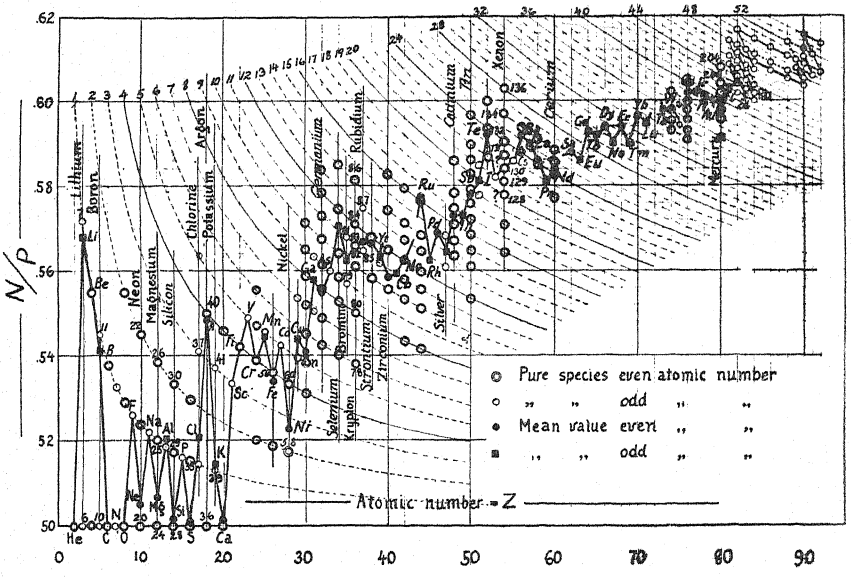


Fig. 12. Variation of the relative negativeness (N/P) of atomic nuclei with their net positive charge (z).

lines give the isotopic number. In Fig. 12 one of these lines is straight, while each of the others has nearly the form of one branch of an equilateral hyperbola. The straight line, which is thus different from all the rest, is given the isotopic number zero, and the curved lines are numbered from 1 to 54.

As has already been shown by the writer the stability of an atomic nucleus is highly dependent upon the values of N/P and Z. Thus as the net positive nuclear charge (Z) grows larger the relative negativeness (N/P) of the nucleus must also increase if the nuclei formed are to be stable. For any value of Z stable nuclei have a certain range of values of N/P.

The present known range for N/P is largest for lithium (0.071), is 0.055 for beryllium and oxygen, 0.045 for selenium, and almost this last value for tin and germanium. The range of N/P decreases in general as the nuclear positive charge (Z) increases. It is appreciably less than 0.02 for mercury or any radioactive element.

The range in the known isotopes of sulphur ($Z=16$) is 0.029, which is abnormally low for a light element. According to the early theory of the writer, adopted in Latimer's recent nuclear model, this is due to the fact that in the sulphur nucleus the first pair of cementing elections, which are present in argon 40 ($Z=18$), have not as yet entered the nucleus. Thus in addition to a matching of N/P and Z in the nucleus, certain specific constituitive influences affect the stability.

No atomic species is known in which the ratio N/P is greater than 0.62.

10. The High Abundance of the Chemical Elements of Even Number (Rule 3)

The theory of nuclear structure and stability developed by the writer[1] in 1915 indicated that the elements of even number should be much more stable and abundant than those which are odd. It is very surprising that such an important and striking fact should have remained so long unrecognized.

The data which supported this rule were considered comprehensively in the 1917 paper.[2] However the great progress made since that time in the investigation of the abundance of the elements in the rare earths by Goldschmidt, in the meteorites and in the earth's crust by Ida and Walter Noddack, in the atmosphere of the sun by Russell, and in the stars by Payne, as carried out by x-ray and ordinary spectroscopic methods,[6] makes it essential to consider the relationship between the rule and the newer data. This is particularly important, since, as was predicted when the rule was discovered, its application in connection with cosmic composition is now found to be of fundamental importance.

Thus the newest data indicate that the atomic nuclei of the elements of even number are 50 times more abundant in the meteorites, 10 times more abundant in the surface of the earth, 10 times more abundant in the atmosphere of the sun, and more abundant, by an unknown factor, in the stars than the elements of odd number.

The meteorites give the best idea of the composition of material in general, since they are more available for analysis than the stars, and come from much more widely distributed regions than the crust of the earth. The six most abundant elements in the meteorites are all even in atomic number, and these six alone contain 97 percent of all of the atoms in the meteorites. Their relative abundance in terms of number of atoms is as follows:

Oxygen	1
Iron	0.59
Silicon	0.30
Magnesium	0.25
Nickel	0.42
Sulphur	0.04

[6] V. Goldschmidt and Thomassen, Videnskaps. Skrift. I. Mat.-naturw. Kl. 1924, No. 5. I. and W. Noddack, Naturwissenschaften **18**, 757 (1930); H. N. Russell, Astrophys. J. **70**, 11 (1929); Miss Payne ,Stellar Atmospheres (Harvard Observatory Monographs, No. 1), Cambridge, Mass., p. 184 (1925).

The recent data of Ida and Walter Noddack are represented in Fig. 13. All of the high peaks are for elements of even number. Of all of the 31 peaks only one, for arsenic, represents an element of odd number. This element

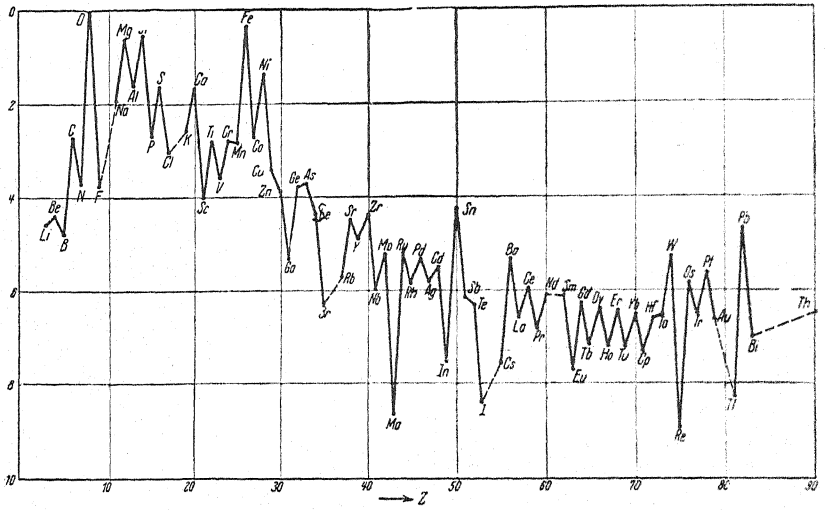


Fig. 13. Logarithm of the atomic abundance of the elements in the meteorites (Noddack). (Abundance of oxygen taken as unity).

seems anomalous in the earth's crust also, with an abnormally high abundance (only 5.5×10^{-6} parts by weight, however) and is found to have an abnormally

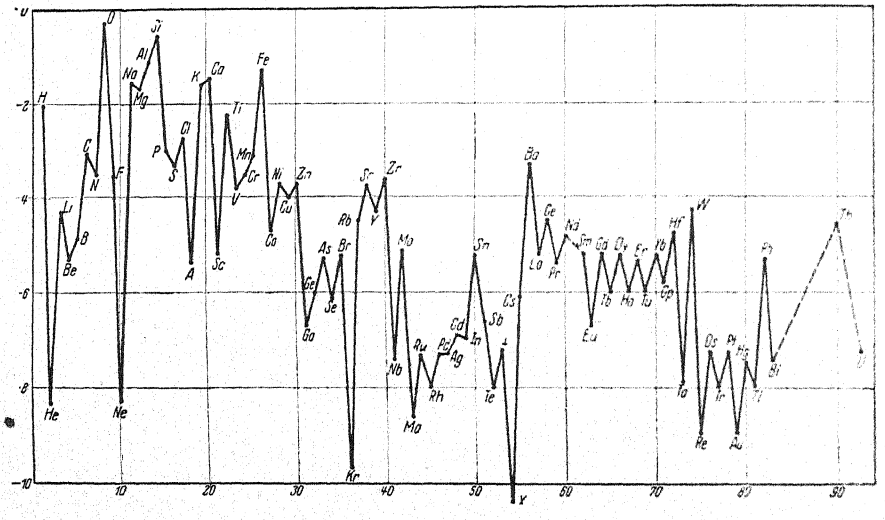


Fig. 14. Logarithm of the atomic abundance of the elements in the earth's crust. (Noddack). (Fraction of the total number of atoms.)

low abundance in the atmosphere of the sun. Fig. 14 represents the crust of the earth, in which 32 of the 34 peaks (hydrogen excluded) represent elements of even number.

The fact that the lowest troughs occur for the rare gases indicates that here the chemical and physical characteristics rule, and not the stability of the nuclei. Otherwise masurium, rhenium, and gold are the rarest in the earth's crust, and masurium and rhenium in the meteorites.

In general in both the meteorites and the earth's crust, each element of even number is much more abundant than either of the two adjacent elements of odd number. In individual cases where this is not true the element of even number is more abundant than the arithmetic mean of the two that of the two adjacent elements of odd number.

Concerning the atmosphere of the sun Russell states "Every element of even number except beryllium, is more abundant than the mean of the adjacent elements, and every odd element less abundant, with the exception of europium, for which the data are uncertain. Among the rare earths only those with even atomic numbers have been conclusively identified in the sun". He adopts the early idea of the writer that the low abundance of lithium and beryllium may be due to the small number of the component parts of which their nuclei are built: too few to give high stability. It should be remembered that there are several types of stability.

11. The Pairing of Nuclear Electrons and the High Abundance of Atomic Nuclei of Even Electronic Number (Rule 1)

The theory that the electrons in the nucleus are almost always associated in pairs was developed on the basis of the "hydrogen-helium" theory[1] according to which the nucleus of the atom is built up of groups of the composition of alpha particles, and other groups, almost all of which contain a pair of electrons. In addition it was noticed that cementing electrons occur in general in pairs. Thus in the 26 light species listed in 1917[7] the formulae give 209 pairs of electrons to 2 unpaired electrons. The pairs seem to be more prominent still in the heavier atoms.[8]

The theory that the electrons are associated in pairs suggested Rule 1, according to which nuclei in which the electronic number is even are extremely more abundant than those in which it is odd.

Only two species of odd electronic number for which the atomic fraction in the earth's crust is greater than 1×10^{-5} are known;—magnesium 24 and silicon 29. Of the 214 atomic species listed in Figs. 2 and 3 as discovered by radioactive means, by positive rays, or by band spectra, 52 or nearly one-fourth have an odd electronic number. However, the species of odd electronic number have an extremely small abundance. Thus there seem to be at least 125 atoms of even to one of odd electronic number in the earth's crust. The most important experiment in this connection would be to determine accurately the quantitative isotopic composition of silicon and magnesium.

Although recent theory attributes nuclear spin entirely to the protons of the nucleus, and although there seems to be some connection between nuclear spin and stability, the above considerations seem to indicate that the

[7] W. D. Harkins, J. Am. Chem. Soc. 39, Table II, 859 (1917).
[8] W. D. Harkins, Phys. Rev. 15, Tables II and III, pages 85 and 86 (1920).

pairing of nuclear electrons is a more fundamental phenomenon in relation to stability than spin. Up to the present time the new quantum mechanics has not been successful in bringing this most fundamental pairing into the theory. This type of pairing seems in some way to be associated with the presence of protons. The pairing of electrons in the nucleus, as discovered by the writer, is more general, and represents a much more intimate association, than their pairing in molecules as found by Stark and G. N. Lewis.

12. Atom Building in Steps

The general relations presented in this paper, especially those concerned with the principle of continuity and regularity of series, and with the relations of the most abundant isotopes, suggest strongly that atom nuclei are built in steps, and not in single events. That is they seem to be in entire disagreement with the idea that atomic nuclei are all formed almost instantaneously (say 10^{-12} seconds) as is assumed in the theory of Millikan and Cameron.[9]

That atoms are actually built in steps under some conditions is demonstrated by the well known synthesis of oxygen 17 from nitrogen 14.

13. Atom Building by Neutrons

There is no evidence whatever that neutrons, or electrically neutral nuclear particles, play any part in atom building, or even that they exist. However the difficulty which a positively charged particle would in general have in penetrating the potential barrier around a nucleus of high charge, suggests that some other process may be utilized in the formation of atomic nuclei. Proceeding from this point of view both Rutherford and Harkins suggested independently in 1920 that such neutral nuclear particles (neutrons) may add themselves to atomic nuclei.[10] The same idea has been revived by Langer and Rosen[11] who seem to consider it to be an entirely new suggestion. Neutrons could not be detected by chemical means, and their percentage in the earth's crust would be very minute, provided they exist.

Rule 2, according to which the ratio of electrons to protons in any nucleus which contains both, is in no case less than $\frac{1}{2}$, is not in discord with this idea, but the fact, shown so plainly in Fig. 12, that there is no known nucleus in which this ratio is more than 0.62, shows that the existence of neutrons would give an entirely different order of magnitude for this ratio. This seems to indicate that neutrons may not exist, but the simple neutron (*pe*) represents a limiting case, which might well be an exception to the rule.

If, as is now supposed, nuclear spin is associated entirely with electrons, the simple neutron would be expected to exhibit a spin of $h/2\pi$. The general properties of neutrons and neutronal material as assumed by Langer and Rosen are the same as those given earlier.

[9] R. A. Millikan and Cameron, Phys. Rev. **31**, 921 (1928).

[10] W. D. Harkins, J. Am. Chem. Soc. **42**, 1965 (1920), Chemical Reviews, **5**, 431 (1928). Ernest Rutherford, Proc. Roy. Soc., London, **42**, 1964 (1920).

[11] R. M. Langer and N. Rosen, Phys. Rev. **37**, 1579 (1931).

MULTIPLET STRUCTURE AND ZEEMAN EFFECT

By J. B. Green* and R. A. Loring
Mendenhall Laboratory of Physics, Ohio State University

(Received August 4, 1931)

Abstract

Houston's method as applied to triplets and singlets cannot account for any inversions in the triplet terms. This is probably due to the fact that spin-spin and mutual spin-orbit interactions are neglected. The results of Houston's and Goudsmit's work are applied to the Zeeman effects of the spectra of Sn III and Sb I, and the agreement is found to be very satisfactory.

THE relation of multiplet structure to Zeeman effect has been discussed in detail by Houston[1] for the case of one *s*-electron and one other electron. The arguments used by Houston and the formulas he derives have been shown by Laporte[2] and by Condon[3] to apply equally well to the case of one *s*-electron and a shell of other electrons lacking one for completion. Houston's results depend on the previous work of Heisenberg[4] on the spectrum of helium, which has since been done more rigorously by Gaunt,[5] using Dirac's method.

Briefly, the method consists in setting up the Hamiltonian function as an operator in three parts, (1) the ordinary kinetic and potential energy, (2) the electrostatic interaction of the two electrons, (3) the other perturbations, such as the interaction of each electron spin with its orbital momentum, the magnetic interaction of the two electrons, and the interactions between each electron spin and the orbit of the other. Of the last named perturbations, only the individual spin-orbit interaction involves the atomic number Z, so that for high effective atomic numbers, the others may be neglected as being of order $1/Z$ compared with it.

This is the case that Houston has considered in his work. As a consequence, his results can apply only to cases for which the effective atomic number is large, and should not be expected to fit the cases where either the real atomic number is small, or where we are dealing with a "nonpenetrating orbit." A comparison of Heisenberg's results with Houston's shows this very clearly. Both Heisenberg and Gaunt get an inversion for the triplet spectra of He I and Li II, as is really the case, while Houston's results do not yield the possibility of accounting for any such inversions. On the other hand, both Heisenberg's and Gaunt's calculations depend on the assumption of a large

* John Simon Guggenheim Memorial Fellow.

[1] Houston, Phys. Rev. **33**, 297 (1929).

[2] Laporte and Inglis, Phys. Rev. **35**, 1337 (1930).

[3] Condon and Shortley, Phys. Rev. **35**, 1342 (1930).

[4] Heisenberg, Zeits. f. Physik. **38**, 411 (1926).

[5] Gaunt, Phil. Trans. Roy. Soc. **A228**, 151 (1929).

spin-orbit interaction, i.e., a large energy difference between the triplet and singlet terms of the same electron configuration, so that they are of no use in considering several of the cases covered by Houston's work.

These partial inversions also occur in the two-electron spectra of high atomic number elements, such as the ^3F terms of Tl II and Pb III.[6] Here, the cause of the inversion is possibly attributable to the nonpenetrating character of the orbits, so that the terms are nearly hydrogenic and the effective Z is small, and the neglect of the higher order terms in the perturbations is not permissible. It seems, therefore, that the theory should be extended to cover these cases too, by the calculation of these spin-spin and mutual spin-orbit interactions. However, the mathematical tedium is probably too great and so it has not yet been done.

In spite of these drawbacks, Houston's results do give us one good clue as a help in spectral classification where the triplet terms are in their normal order. The positions for Russell-Saunders coupling measured from the center of gravity of the triplet are $L-1$, and $-L-1$. If the center triplet level is lower than -1, then we should look for the related singlet level higher than L. If the center triplet level is higher than -1, then we should look for the related singlet level lower than $-L-1$. An application of this method to the spectrum of Pb III indicates that Smith's choice of 7^1D_2 is probably incorrect, and that the term he has called pp^1D_2 is the proper choice for 7^1D_2.

The method also gives us an excellent comparison of interval ratios and Zeeman effects, as Houston has already shown. But there has been no very careful check on the g-values of highly-ionized atoms. With a view toward supplying this deficiency, we have carefully remeasured our plates for Sn III.[7] These had previously been measured for qualitative purposes, principally for use in spectral classification. Even so, certain anomalies in the Zeeman patterns of the lines were noticed. The new measurements appear in Table I.

TABLE I. *Zeeman patterns of Sn III lines.*

Wave-length	Classification	Zeeman pattern			
4585	$^3S_1{}^3P_2$	(0) (0.502)	(1.002)	1.508	1.984
4856	$^3S_1{}^3P_1$	(0.535)	1.442	1.983	
5291	$^3P_1{}^3D_1$	0.479	(0.926)	1.445	
5369	$^3P_0{}^3D_1$	(0) 0.512			
4330	$^1P_1{}^3S_1$	(0.95)	1.06	2.01	

The weighted g-values based on the intensities of the components and the ease of the setting of the microscope, together with the Landé g-values and those calculated with the aid of Houston's formulas are as follows. The agreement between Houston's formulas and experiment is seen to be quite good, probably well within the limits of experimental error. For the last two levels, belonging to the same electron configuration, Pauli's g-sum rule is satisfied.

[6] Smith, Phys. Rev. **34**, 393 (1929).

[7] Green and Loring, Phys. Rev. **30**, 574 (1927).

TABLE II. *Observed and calculated g-values for Sn III.*

Level	Observed	Landé	Houston
$^3S_1$	2.001	2	2
$^3P_2$	1.505	3/2	3/2
$^3D_1$	.503	1/2	1/2
$^3P_1$	1.447	3/2	1.456
$^1P_1$	1.055	1	1.044

Goudsmit's[8] extension of Houston's and Slater's methods also gives us a method of comparing Zeeman effect data with the theory of interval ratios. As examples, the p^2 configuration of Sn I and Pb I serve excellently. The formula for the g-value in this case becomes

$$g = \frac{(5/2)E - 3X - (7/2)A}{2E - 2X - 3A}$$

TABLE III. *Observed and calculated g-values in the spectra of Sn I and Pb I.*

Element	Level	Landé	Observed	Calculated
Sn I	$^3P_2$	3/2	1.45	1.46
	$^1D_2$	1	1.05	1.04
Pb I	$^3P_2$	3/2	1.27	1.29
	$^1D_2$	1	1.23	1.21

whence we find the values of g given in Table III. For the configuration ^3P+s the g-formula is

$$g = \frac{(10/3)E - (8/3)X + 8A}{2E - X + 5A}$$

and we find in the spectrum of Sb I the g-values given in Table IV. It is not

TABLE IV. *Observed and calculated g-values in the spectrum of Sb I.*

Level	Landé	Observed	Calculated
$^4P_{1/2}$	8/3	2.333	2.370
$^2P_{1/2}$	2/3	1.004	0.963

possible to carry out the same sort of calculation for the $^4P_{3/2}$ and $^2P_{3/2}$ levels of the same configuration, for the partial g-sum is not constant as in the above examples, where $j=\frac{1}{2}$, for all types of coupling, but is influenced by the proximity of the $(^1D_2+s)^2D_{3/2}$ term.

[8] Goudsmit, Phys. Rev. **35**, 1327 (1930).

THE ROTATIONAL ANALYSIS OF THE FIRST NEGATIVE GROUP OF OXYGEN (O_2^+) BANDS

By Daniel S. Stevens
Ryerson Physical Laboratory, University of Chicago

(Received August 24, 1931)

Abstract

The uitraviolet O_2^+ bands have been produced by a hollow cathode discharge, or with greater intensity from a mixture of helium with a small amount of oxygen in a large discharge tube. Photographs were taken in the second order of a 21 foot Rowland grating (dispersion = 1.32A/mm). The following bands were used for a rotational analysis: 1–8; 0–8; 1–9; 0–9. As was expected, since NO and O_2^+ have the same number of electrons, these bands correspond to a $^2\Pi \rightarrow {}^2\Pi$ transition like the double headed β bands of NO. The lower $^2\Pi$ is case a as in NO. Unlike the case of NO, however, the upper $^2\Pi$ is case b. The lower $^2\Pi$ is regular, with a doublet separation A'' (corresponding to zero rotation) of 195 cm^{-1}. In the upper $^2\Pi$ the value of the spin-orbital coupling coefficient A' is +8.2. Each band consists of eight branches (four P and four R), the Q branches apparently being too weak to appear on the plates. This is in agreement with theory. Λ-type doubling is negligible in the upper $^2\Pi$ but is present in the lower $^2\Pi$ state. Alternate levels in each successive Λ-type doublet are missing. This is as prediced by the quantum theory of homopolar molecules, since it is known that the nuclear spin of the oxygen atom is zero. The probable electronic configuration of the upper $^2\Pi$ state is given as $\cdots 2p\pi^3\, 3d\pi^2$, and that of the lower $^2\Pi$ state as $\cdots 2p\pi^4\, 3d\pi$. The constants of the molecule in the two electronic states are given by: $B' = 1.048 - 0.014\, v'$; $B'' = 1.610 - 0.009\, v''$; $r_e' = 1.41 \times 10^{-8}$ cm; $r_e'' = 1.14 \times 10^{-8}$ cm; $A' = +8.2$ cm^{-1}; $A'' = +195$ cm^{-1}.

Introduction

A SYSTEM of double headed bands lying in the region λλ4400–2000 can be obtained[1] by passing a discharge through pure oxygen. These bands are called the first negative group of oxygen and are attributed to O_2^+. From the type of transition and the molecular constants determined by the present rotational analysis there can be no doubt that O_2^+ is actually the emitter.

The vibrational analysis of these bands has been recently investigated by Ellsworth and Hopfield.[2] It seems probable that the v'' numbering as given by these investigators should be increased by two units. This was pointed out by Mulliken[3] from the intensity distribution in the band system. Stueckelberg[4] has shown that such a revised v'' numbering is the most probable from the Franck-Condon principle of transition probabilities. Ellsworth and Hopfield also found evidence on their plates of band progressions to lower final vibrational states than the level they called $v'' = 0$. For these reasons the bands which were used in the present rotational analysis have been called 1–8;

[1] J. Stark, Ann. d. Physik 43, 319 (1914); R. C. Johnson, Proc. Roy. Soc. A105, 683 (1924).
[2] V. Ellsworth and J. Hopfield, Phys. Rev. 29, 79 (1927).
[3] R. S. Mulliken, Phys. Rev. 32, 213 (1928).
[4] E. C. G. Stueckelberg, Phys. Rev. 34, 66 (1929).

0–8; 1–9; 0–9; although they were designated by Ellsworth and Hopfield as 1–6; 0–6; 1–7; 0–7.

Since NO and O_2^+ have the same number of electrons it would be expected that their band systems would be similar. The beta bands of NO and the first

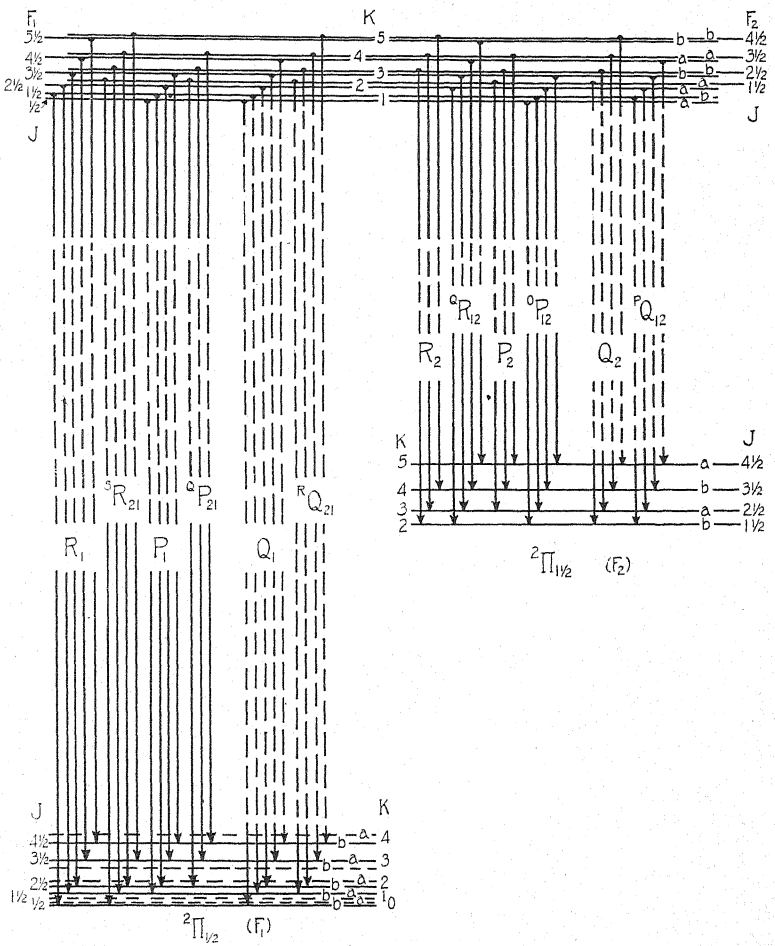


Fig. 1. First few rotational terms for the initial state $v'=0$ and final state $v''=9$ of the first negative group of oxygen (O_2^+) bands. The possible transitions are grouped into branches. The Q branches (shown dashed) were not found in the bands. The other branches were all definitely located and established the case b $^2\Pi \rightarrow$ case a $^2\Pi$ nature of transition. All the rotational levels are drawn to the same scale except that the Λ-type doubling is magnified 50X. Even then, it shows only in the lower $^2\Pi_{\frac{1}{2}}$ state. The levels shown dashed do not exist physically (cf. section on Λ-type doubling). The a and b classification on the levels shown in full is in all cases for the level actually present.

negative group of O_2^+ bands lie in the same spectral region and are similar in appearance, (both are double headed and degrade toward the red). The NO beta bands have been analyzed[5] and found to be $^2\Pi \rightarrow {}^2\Pi$, both states being

[5] F. A. Jenkins, H. A. Barton and R. S. Mulliken, Phys. Rev. **30**, 150–174 (1927); **30**, 175–188 (1927).

case *a*. For each of the two heads there is a strong *R* and a strong *P* branch, also a very weak *Q* branch. It was expected that the first negative group of O_2^+ bands would have a similar structure. But four strong branches were found in each head of each band. This situation can be accounted for[6] if the transition is from a case *b* state to a case *a* state rather than between two case *a* states.

In transitions between two case *a* states, there are the selection rules $\Delta\Sigma=0$ and $\Delta J=0, \pm 1$. In case *b*, Σ is no longer a quantum number,[7] and the selection rule $\Delta\Sigma=0$ no longer holds in case *b*→case *a* transitions but the selection rule $\Delta J=0, \pm 1$ still holds. The various branches[8] which can appear in a $^2\Pi$ case *b*→ $^2\Pi$ case *a* transition are shown by Fig. 1.

The *Q* branches, which are shown with broken lines in the figure, were too weak to be found in the bands. The other branches, however, have all been definitely located and establish the case *b*→case *a* type of transition. The "main" *R* and *P* branches (R_1 and P_1; R_2 and P_2) are of about equal intensity and have their maximum at about $J=20\frac{1}{2}$. The "satellite" branches ($^SR_{21}$ and $^QP_{21}$; $^QR_{12}$ and $^OP_{12}$) are somewhat weaker than the main branches.

Experimental Procedure

The bands were produced in a hollow cathode discharge. The tube was similar to that described by Frerichs.[9] It was, however, found advantageous to construct the cathode with a block of tin instead of the aluminum used by Frerichs. Cooling coils were embedded in the tin so that a large current (1.5 amp.) could be passed through the cathode for many hours (50–100). Some bands due to the cathode material appeared on the high frequency side of the 1–8 and 0–8 O_2^+ bands, but those foreign bands did not interfere with the analysis. The bands were photographed in the second order of a 21 foot Rowland grating giving a dispersion of 1.32 A/mm.

Recently Drs. S. M. Naudé and W. Weizel, while photographing the visible O_2^+ bands in this laboratory, have found a more intense source of O_2^+ spectra by using helium with a small amount of oxygen in a discharge tube similar to that described by Naudé and Christy.[10] They have kindly furnished me with a plate taken in the same region as mine. By means of this plate it was possible to show that there were no errors due to the presence of the tin bands. Only a few faint lines of the tin bands had appeared inside the heads of the 1–8 and 0–8 bands of O_2^+.

Data and Results

Due to the presence of many branches the appearance of the bands was rather complex and many of the lines were blends. This was especially true

[6] Cf. R. S. Mulliken, Reviews of Modern Physics **3**, 128–146 (1931).

[7] For a discussion of cases *a* and *b* cf. R. S. Mulliken, Reviews of Modern Physics **2**, 105–108 (1930).

[8] For the nomenclature of the branches, cf. R. S. Mulliken, Reviews of Modern Physics **3**, 119 (1931).

[9] R. Frerichs, Zeits. f. Physik **35**, 683 (1926).

[10] S. M. Naudé, and A. Christy, Phys. Rev. **37**, 492 (1931).

TABLE I. *Wave number and intensity data for the 0—8; 1—8; 0—9; 1—9 bands of the first negative group of oxygen (O_2^+) bands. The first six numbers represent the wave number of a given line, the next figure in bold-face type gives the number of times the line was used in the scheme of analysis and the last figure is an estimate of the relative intensity of the line. The letter d means that the line appeared diffuse and A means atomic line.*

1—8 Band, First head

$J''+\frac{1}{2}$	$^SR_{21}$	$^QP_{21}$	R_1	P_1
1	28620.644		28613.733*d*	
2	21.344		13.033*d*	28605.921
3	21.244	28607.311	11.311	00.411
4	20.744	02.436	09.122	28594.111
5	19.222	28597.236	05.821	87.212
6	16.712*d*	89.9310	01.136	78.412*d*
7	13.533*d*	82.625	28596.336	69.211
8	09.222	73.824	89.1310	58.512
9	03.736	64.624	82.625	47.513
10	28597.036	53.925	73.624	34.313
11	89.9310	42.827	64.524	21.614
12	81.012	29.826	53.525	06.414
13	72.111	16.728	42.727	28491.215*d*
14	61.314	01.928	29.826	74.215
15	50.114	28486.725*d*	16.828	57.215
16	37.515	69.827	02.128	38.316
17	24.513	52.6210	28487.125*d*	19.324
18	09.613	33.728	70.227	28398.326
19	28494.814	14.744	53.6210	77.315
20	77.614	28393.514	34.428	54.115
21	61.014	72.412	15.444	31.315
22	41.913	49.212	28394.436	06.015
23	23.422*d*	26.112	73.612	28280.915
24	02.048*d*	01.212	50.512	53.926*d*
25	28381.124*d*	28276.124	27.712	27.015
26	58.025	49.011	02.512	28197.725*d*
27	35.711	22.311	28277.724	68.937*d*
28	10.612	28193.311	49.912	37.715
29	28285.311	64.211		06.915
30	57.623	33.711		28073.114*d*
31	30.511			40.825*d*
32	01.412			05.415
33	28173.712			27970.715
34				33.115
35				27896.514

1—8 Band, Second head

$J''+\frac{1}{2}$	R_2	P_2	$^QR_{12}$	$^OP_{12}$
2	28429.421		28420.622	28413.222
3	29.521	28415.344	19.324	08.424
4	28.211	10.921	17.511	02.348*d*
5	26.511	04.911	13.222	28394.436
6	24.122*d*	28398.326	08.424	85.526*d*
7	20.622	90.311	02.348*d*	75.824
8	15.344	81.124	28396.111	64.726*d*
9	09.721	69.726	88.413*d*	53.124
10	02.348*d*	59.313	79.414	39.912
11	28394.436	47.012	69.626	26.122
12	85.526*d*	34.112	58.125	10.622
13	75.824	20.012	46.412	28294.812
14	64.726*d*	04.512	33.112	77.424
15	52.724	28288.613	19.112	59.213
16	38.912	71.214	03.813	39.913
17	25.212	53.126	28287.713	19.614
18	09.613	33.515	70.212	28198.125
19	28293.513	13.415	52.112	76.012*d*
20	76.124	28191.012	32.412	52.514
21	57.613	69.537*d*	12.312	28.214
22	37.914	45.715	28190.712	02.314*d*
23	17.814	21.715	68.137*d*	28076.015
24	28195.914	28095.516	44.613	48.328*d*
25	73.724	69.025*d*	20.312	19.814
26	49.915	41.125*d*	28094.212	27989.815
27	25.615	12.926	67.712	59.714
28	28099.215	27982.227	39.712	27.214
29	74.228*d*	52.326	13.026	
30	45.915		27982.727	
31	18.012		52.326	
32	27987.611		19.812	
33	57.111			
34	24.111			
35	27892.112*d*			

TABLE I. (*Cont.*)

0−8 Band, First head

$J''+\frac{1}{2}$	${}^{S}R_{21}$	${}^{Q}P_{21}$	R_1	P_1
1	27747.311		27740.121	
2	48.725		40.121	27732.712
3	49.825	27735.411	39.224	28.124
4	49.925	31.028*d*	37.411	22.423*d*
5	48.825	25.923	34.225	14.815
6	46.214*d*	19.225*d*	30.828*d*	07.315
7	43.616*d*	12.211	25.823	27698.212
8	39.224	03.511	19.125*d*	87.412
9	34.525	27694.624	13.026*d*	76.914
10	28.124	84.224	04.726	64.612
11	21.723*d*	73.413	27696.013	51.812
12	13.026*d*	61.013*d*	85.413	37.312
13	04.726	48.313	74.914	22.5210
14	27694.624	34.014	62.714	06.228
15	84.224	19.114	50.217	27589.426
16	72.014	03.015	35.917	71.025
17	59.814	27586.713	21.7210	52.637
18	45.814	68.213	05.928	32.1510*d*
19	31.717	50.024	27589.426	11.715
20	15.514	29.713	71.025	27489.635
21	27599.314	09.636	52.937	67.114
22	81.515*d*	27487.111	32.8510*d*	42.813
23	63.514	65.124	12.814	18.613
24	43.511	41.422	27490.713	27392.513
25	23.525	16.911	68.715	66.515
26	01.418	27390.711	44.712	38.112
27	27479.324	64.912	20.714	10.524
28	55.813	37.524	27394.813	27280.113
29	32.012	09.122	68.825	50.422
30	05.724*d*	27278.711	40.911	18.122
31	27380.212	49.022	13.411	27186.635
32	52.011	18.022	27283.424	52.422
33	25.014	27186.635	53.413	
34	27294.711	52.422	21.712	
35	65.011	18.713	27190.212	
36	33.311		56.511	
37	02.011		23.111	

0−8 Band, Second head

$J''+\frac{1}{2}$	R_2	P_2	${}^{Q}R_{12}$	${}^{O}P_{12}$
2	27557.921		27549.434	27542.311
3	58.211	27543.711	47.911	36.911
4	57.421	38.923*d*	45.522	30.313
5	55.811	33.1410*d*	42.321	23.225
6	53.037	26.135	37.711	14.513
7	49.734	18.623	32.8410*d*	05.113
8	45.122	09.836	26.135	27494.213
9	40.323*d*	00.325	18.623	82.714
10	33.1410*d*	27489.635	09.436	69.914
11	26.135	78.117	00.325	56.414
12	17.413	65.124	27489.635	41.422
13	08.312	51.711	78.724	25.915*d*
14	27497.612	37.027	65.712	09.116*d*
15	86.712	21.525	52.512	27391.613
16	73.712	04.514	37.527	72.714
17	60.413	27387.213	22.125	53.213
18	45.713	68.313	05.724*d*	32.315
19	30.415*d*	48.813	27388.216	10.524
20	13.614	27.913	69.325	27287.816
21	27396.412	06.413	50.112	64.116
22	77.713	27283.424	29.311	39.114
23	58.413	60.123	08.012	13.714
24	37.524	35.113	27285.012	27186.635
25	16.313	10.014	61.823	59.313
26	27293.414	27182.714	36.614*d*	30.214
27	70.311	55.514	11.512	01.214
28	45.214	26.314	27184.211	
29	20.015	27097.214	57.412	
30	27193.012		27.912	
31	65.912		27099.013	
32	36.813			
33	07.714			

TABLE I. (*Cont.*)
1−9 Band, First head

$J''+\frac{1}{2}$	${}^{S}R_{21}$	${}^{Q}P_{21}$	R_1	P_1
1	26972.326		26965.721	
2	74.224		65.721	26959.111
3	75.911	26961.611	64.628	53.926
4	74.811	57.316	63.114	49.211
5	73.924	52.128	60.426	41.712
6	72.126	45.928*d*	56.012	33.713
7	69.612*d*	38.9310	51.928	25.31*A*
8	64.728	30.3310	45.928*d*	14.813
9	60.426	21.214	38.9310	04.013
10	53.826	10.714	30.3310	26891.413
11	47.315	00.014	22.014	78.713
12	38.9310	26887.514	11.713	64.413
13	30.3310	74.914	01.313	49.613
14	20.114	60.516	26888.914	33.311
15	09.615	46.114	76.515	16.715
16	26897.715	29.514	62.216	26798.416
17	85.314	12.913	48.015	79.738
18	71.015	26795.014	31.615	59.4410
19	56.815	76.736	15.415	38.938
20	40.315	56.314	26796.915	16.6410
21	24.815	36.312	78.938	26694.926
22	06.513	14.113*d*	49.4410	70.524
23	26788.513*d*	26692.112	39.038	46.415
24	68.024	67.512	16.6410	20.3310
25	48.413	43.812	26694.926	26594.225
26	26.114	17.514	70.524	66.224
27	04.314*d*	26591.812	46.415	38.323
28	26680.318	63.525	20.2310	08.125
29	56.726*d*	35.536*d*	26594.225	78.425
30	30.113	05.711	66.824	
31	04.327*d*		38.323	
32	26576.3310		08.125	
33	49.215*d*		26478.425	
34	19.227			
35	26489.415			

1−9 Band, Second head

$J''+\frac{1}{2}$	R_2	P_2	${}^{Q}R_{12}$	${}^{O}P_{12}$
2	26785.035		26776.736	26769.711
3	85.335	26771.639	75.711	65.025
4	84.435	66.523*d*	72.839	58.211
5	82.612	60.7110	69.424	50.813*d*
6	79.938	53.7310	65.125	42.513
7	76.836	46.411	59.6410	33.01*A*
8	71.639	37.126	52.7310	22.214
9	66.723*d*	27.826	45.613*d*	10.715
10	60.4410	17.0410	37.126	26697.814
11	53.0310	05.727	27.626	84.316
12	44.212	26692.928	17.3410	69.614
13	34.838	79.628	05.827	54.114
14	24.314	64.62*A*	26693.128	37.517
15	13.014	49.126	79.628	20.1310
16	00.113	32.424*d*	64.72*A*	01.115
17	26687.015	15.028	49.626	26581.515
18	72.015	26596.025	32.624*d*	60.616
19	56.726	76.6310	15.128	39.218
20	39.917	55.613	26596.725	16.217
21	22.617	34.236	77.1310	26492.617
22	04.127*d*	11.218	56.912	68.015
23	26584.417	26488.115	35.236	
24	63.515	63.113		
25	42.216			
26	19.227			
27	26495.917			
28	71.117			

TABLE I. (*Cont.*)

0−9 Band, Second head

$J''+\frac{1}{2}$	R_2	P_2	$^QR_{12}$	$^OP_{12}$
2	25913.538		25905.012	25898.523
3	14.238	25899.611	03.912	93.325
4	13.738	95.122	01.712	86.612
5	12.327	89.224	25898.523	79.313
6	09.525*d*	82.824	94.122	71.113
7	06.712	75.83*A*	89.224	61.515*d*
8	02.412	67.037	82.824	51.517
9	25897.3210	57.537	75.83*A*	40.016
10	91.314	46.925	67.637	27.616
11	84.614	36.125	58.614	14.516
12	76.63*A*	23.815	48.528*d*	00.316
13	67.637	11.015	37.714	25785.115
14	57.537	25796.616	25.628	68.716
15	46.925	81.816	12.928	51.72*A*
16	34.716	65.328*d*	25798.616	33.548*d*
17	22.116	48.716*d*	84.037	14.727
18	08.018	30.518*d*	67.814	25694.627
19	25793.517	11.818	51.32*A*	73.712
20	77.517	25691.718	33.548*d*	51.425
21	61.117	71.017	14.727	28.716
22	43.218	48.917	25694.627	04.716
23	24.918	26.6110	74.312	25580.116
24	04.818	02.519	52.311	53.62*A*
25	25684.618	25578.117	30.228	
26	62.718	52.118	06.213	
27	40.718*d*		25582.013	
28	16.718		56.02*A*	
29	25592.718			
30	66.818			
31	40.918			

0−9 Band, First head

$J''+\frac{1}{2}$	$^SR_{21}$	$^QP_{21}$	R_1	P_1
1	26102.426		26095.048	
2	04.326		95.548	26088.411*d*
3	05.228	26091.137	95.148	84.226
4	05.528	86.624	93.411*d*	78.427
5	04.526	81.9210*d*	90.837	71.126
6	02.326	75.113	86.624	63.228*d*
7	26099.814	68.115*d*	81.9210*d*	54.312
8	95.548	59.918	76.014	44.411
9	91.237	51.517*d*	69.515	33.424
10	85.226	41.115	61.416	21.525
11	79.127	30.716	53.427*d*	09.112
12	71.126	18.716	43.326	25995.012
13	63.228*d*	06.728	33.424	80.715
14	53.227*d*	25992.615	21.525	64.716
15	43.626	78.528*d*	09.716	48.715
16	31.914	62.926	25996.016	30.717
17	20.413	47.015	82.317	13.028
18	06.928	29.315	66.718	25893.325
19	25993.515	11.827	51.218	73.713
20	78.128*d*	25892.213	33.918	52.213
21	62.926	73.013	16.518	30.628*d*
22	45.613	51.526	25897.3310	07.226
23	28.613	30.228*d*	78.115	25784.037
24	09.525*d*	07.026	56.937	58.728*d*
25	25890.612	25784.237	35.725	33.548*d*
26	69.612	59.128*d*	12.929	06.314
27	48.828*d*	34.348*d*	25790.316	25679.514
28	25.628	07.011	65.328	50.313
29	03.512	25680.411	40.813	21.913
30	25778.612	51.425	13.613	25590.814
31	54.211	23.111	25687.316	60.314
32	27.413	25592.2210	58.517	
33	01.111	62.011	30.228	
34	25672.512		25599.513	
35	44.415		69.614	
36	13.711		36.913	

near the heads, where the assignment of lines was difficult. In the second head of each band the branches were better separated. The structure of the bands was determined by locating first the branches in the second head and from them calculating the positions of the rotational levels of the upper electronic state. Knowing these levels and one or two branches in the first head, the remaining branches in the first head could be calculated. The wave numbers of the lines which form the various branches are given in Table I.

Determination of the Δ_2F's

By reference to Fig. 1, it will be seen that various internal combinations can be obtained in each band. For the first heads of the bands, the relations for the lower $^2\Pi$ are:

$$^SR_{21}(J-1) - {}^QP_{21}(J+1) = R_1(J-1) - P_1(J+1)$$
$$= F_1''(J+1) - F_1''(J-1) \equiv \Delta_2F_1''(J) \quad (1)$$

and for the second heads:

$$^QR_{12}(J-1) - {}^OP_{12}(J+1) = R_2(J-1) - P_2(J+1)$$
$$= F_2''(J+1) - F_2''(J-1) \equiv \Delta_2F_2''(J). \quad (2)$$

Similar relations that give the Δ_2F's of the upper electronic state are:

$$^SR_{21}(J) - {}^QP_{21}(J) = R_2(J) - P_2(J) = \Delta_2F_2'(J) \quad (3)$$
$$R_1(J) - P_1(J) = {}^QR_{12}(J) - {}^OP_{12}(J) = \Delta_2F_1'(J). \quad (4)$$

All of these Δ_2F's are listed in Tables II and III. The vibrational quantum numbers of the four bands used in the analysis were such that the rotational levels associated with two adjacent vibrational levels ($v'=0, 1$; $v''=8, 9$) of both the upper and lower electronic states were obtained. Furthermore every Δ_2F in both the upper and lower states is determined independently four times by the differences of four pairs of lines. In the following tables data are given only for the vibrational states $v'=0$ and $v''=9$. Similar data for the vibrational states $v'=1$ and $v''=8$ may readily be obtained from the wave numbers of Table I.

After a series of lines had been located in a band it was not possible to tell immediately what branch it corresponded to. The combination relations just given were used to determine the proper designations of the series. The combinations between the series were first obtained. Then by reference to Fig. 1 it will be seen that for a given J value any member of the $^SR_{21}$ branch would have a larger wave number than the corresponding member of the R_1 branch. Exactly the same relation held between the $^QP_{21}$ branch and the P_1 branch.

Values of the Constants B, D and A

The terms of the upper $^2\Pi$ state can be represented accurately by Hill and Van Vleck's equation (see Eq. (9) following). This state, however, is so close to Hund's case b that the terms, except for the lowest K values, can also be represented by the following equation:[7]

TABLE II. *The first set of data gives the values of $\Delta_2F_1''(J)$ for the 9 vibrational state obtained from Eq. (1). The second set of data gives the values of $\Delta_2F_2''(J)$ for the 9 vibrational state obtained from Eq. (2). The J values have been omitted from the column headings so that R_1-P_1 really stands for $R_1(J-1)-P_1(J-1)$. Other column headings are exactly similar.*

$\Delta_2F_1''(J)$						$\Delta_2F_2''(J)$					
	0−9 Band		1−9 Band				0−9 Band		1−9 Band		
$J+\frac{1}{2}$	${}^sR_{21}-{}^QP_{21}$	R_1-P_1	${}^sR_{21}-{}^QP_{21}$	R_1-P_1	*av.*	$J+\frac{1}{2}$	R_2-P_2	${}^QR_{12}-{}^OP_{12}$	R_2-P_2	${}^QR_{12}-{}^OP_{12}$	*av.*
2	11.3	10.8	10.7	13.4	11.6	3	18.4	18.4	18.5	18.5	18.5
3	17.7	17.1	16.9	16.5	17.1	4	25.0	24.6	24.6	24.9	24.8
4	23.3	24.0	23.8	22.9	23.5	5	30.9	30.6	30.7	30.3	30.8
5	30.4	30.2	28.9	29.4	29.7	6	36.5	37.0	36.2	36.4	36.5
6	36.4	36.5	35.0	35.1	35.8	7	42.5	42.6	42.8	42.9	42.7
7	42.4	42.2	41.8	41.2	41.4	8	49.2	49.2	49.0	48.9	49.0
8	48.3	48.5	48.4	47.9	48.3	9	55.5	55.2	54.6	54.9	55.1
9	54.4	54.5	54.0	54.5	54.4	10	61.2	61.3	61.0	61.3	61.2
10	60.5	60.4	60.4	60.2	60.4	11	67.5	67.3	67.5	67.5	67.5
11	66.5	66.4	66.3	65.9	66.3	12	73.6	73.5	73.4	73.5	73.5
12	72.4	72.7	72.4	72.4	72.5	13	80.0	79.8	79.6	79.8	79.8
13	78.5	78.6	78.4	78.4	78.5	14	85.8	86.0	85.7	85.7	85.8
14	84.7	84.7	84.2	84.6	84.6	15	92.2	92.1	91.9	92.0	92.2
15	90.3	90.8	90.6	90.5	90.6	16	98.2	98.2	98.0	98.1	98.1
16	96.6	96.7	96.7	96.8	96.7	17	104.2	104.6	104.1	104.1	104.3
17	102.6	102.7	102.7	102.8	102.7	18	110.3	110.3	110.4	110.4	110.4
18	108.6	108.6	108.6	109.1	108.7	19	116.3	116.4	116.4	116.4	116.4
19	114.7	114.5	114.7	115.0	114.7	20	122.5	122.6	122.5	122.5	122.5
20	120.5	120.6	120.5	120.5	120.5	21	128.6	128.8	128.7	128.7	128.7
21	126.6	126.7	126.2	126.4	126.6	22	134.5	134.6	134.5		134.5
22	132.7	132.5	132.7	132.5	132.6	23	140.7	141.0	141.0		140.9
23	138.6	138.6	139.0	139.1	138.8	24	146.8				146.8
24	144.4	144.6	144.7	144.8	144.6	25	152.7				152.7
25	150.4	150.6	150.5	150.4	150.6						
26	156.3	156.2	156.6	156.6	156.4						
27	162.7	162.6	162.6	162.4	162.6						
28	168.4	168.4	168.8	168.0	168.4						
29	174.2	174.5	174.6		174.3						
30	180.4	180.5			180.5						
31	186.4				186.4						
32	192.2				192.2						

TABLE III. *The first set of data gives the values of $\Delta_2F_1'(K=J-\frac{1}{2})$ for the 0 vibrational state obtained from Eq. (4). The second set of data gives the values of $\Delta_2F_2'(K=J+\frac{1}{2})$ for the 0 vibrational state obtained from Eq. (3). The J values have been omitted from the column headings so that R_1-P_1 really stands for $R_1(J)-P_1(J)$. Other column headings are exactly similar.*

$\Delta_2F_1'(K=J-\frac{1}{2})$						$\Delta_2F_2'(K=J+\frac{1}{2})$					
	0−8 Band		0−9 Band				0−8 Band		0−9 Band		
$J+\frac{1}{2}$	R_1-P_1	${}^QR_{12}-{}^OP_{12}$	R_1-P_1	${}^QR_{12}-{}^OP_{12}$	*av.*	$J+\frac{1}{2}$	${}^SR_{21}-{}^QP_{21}$	R_2-P_2	${}^SR_{21}-{}^QP_{21}$	R_2-P_2	*av.*
2	7.4	7.1	7.1	6.5	7.0	3	14.4	14.5	14.1	14.6	14.4
3	11.1	11.0	10.9	10.6	10.9	4	18.9	18.5	18.9	18.6	18.7
4	15.0	15.2	15.0	15.1	15.1	5	22.9	22.7	22.6	23.1	22.8
5	19.7	19.1	19.7	19.2	19.4	6	27.0	26.9	27.2	26.7	26.9
6	23.5	23.2	23.4	23.0	23.3	7	31.4	31.1	31.7	30.9	31.1
7	27.7	27.7	27.6	27.7	27.7	8	35.4	35.3	35.6	35.4	35.4
8	31.7	31.9	31.6	31.3	31.8	9	39.1	40.0	39.7	39.8	39.6
9	36.1	35.9	36.1	35.8	36.0	10	43.9	43.5	44.1	44.4	44.0
10	40.1	39.5	39.9	40.0	39.9	11	48.3	48.0	48.4	48.5	48.4
11	44.2	43.9	44.3	44.1	44.1	12	52.0	52.3	52.4	52.8	52.4
12	48.1	48.2	48.3	48.2	48.2	13	56.4	56.6	56.5	56.6	56.5
13	52.4	52.8	52.7	52.6	52.6	14	60.6	60.6	60.6	60.9	60.7
14	56.5	56.6	56.8	56.9	56.7	15	65.1	65.2	65.1	65.1	65.1
15	60.8	60.9	61.0	61.2	61.0	16	69.0	69.2	69.0	69.4	69.2
16	64.9	64.8	65.3	65.1	65.0	17	73.1	73.2	73.4	73.4	73.3
17	69.1	68.9	69.3	69.3	69.2	18	77.6	77.4	77.6	77.5	77.5
18	73.8	73.4	73.4	73.2	73.4	19	81.7	81.6	81.7	81.7	81.7
19	77.7	77.7	77.5	77.6	77.6	20	85.8	85.7	85.9	85.8	85.8
20	81.4	81.5	81.7	82.1	81.9	21	89.7	90.0	89.9	90.1	90.0
21	85.8	86.0	85.9	86.0	85.9	22	94.4	94.3	94.1	94.3	94.3
22	90.0	90.2	90.1	89.9	90.0	23	98.4	98.3	98.4	98.3	98.3
23	94.2	94.3	94.1	94.2	94.2	24	102.1	102.4	102.5	102.3	102.3
24	98.2	98.4	98.2	98.7	98.4	25	106.6	106.3	106.4	106.5	106.4
25	102.2	102.5	102.2		102.3	26	110.7	110.7	110.5	110.6	110.6
26	106.6	106.4	106.6		106.5	27	114.4	114.8	114.5		114.6
27	110.2	110.3	110.8		110.4	28	118.3	118.9	118.6		118.6
28	114.7		115.0		114.8	29	122.9	122.8	123.1		122.9
29	118.4		118.9		118.7	30	127.0		127.2		127.1
30	122.8		122.8		122.8	31	131.2		131.1		131.2
31	126.8		127.0		126.9	32	134.0		135.2		135.2
32	131.0				131.0	33	138.4		139.1		139.1
						34	142.3				142.3
						35	146.3				146.3

$$T = T_0^e + G(v) + B_v[K(K+1) - \Lambda^2 + \overline{G^2}] + f(K, J-K) + \phi_i(K, J) + D_v K^2(K+1)^2 + \cdots \quad (5)$$

The lower $^2\Pi$ state is co close to Hund's case a that the terms can be represented by the following equation:[7]

$$T = T_0^e + G(v) + A\Lambda\Sigma + B_v^*[J(J+1) - \Omega^2 + \overline{G^2} + S_{perp}^2] + \phi_i(\Sigma, J) + D_v J^2(J+1)^2 + \cdots \quad (6)$$

By use of Eq. (5), the $\Delta_2 F$'s of the upper $^2\Pi$ state should be given very closely by the relation:

$$\Delta_2 F'(K) = 2B_v(2K+1) \quad (7)$$

From Eq. (6), the $\Delta_2 F$'s of the lower $^2\Pi$ state should be given by:

$$\Delta_2 F''(J) = 2B_v^*(2J+1). \quad (8)$$

The use of these simplified expressions for the $\Delta_2 F$'s can be justified except for the lowest values of K of the upper $^2\Pi$ state and for the highest values of the rotational quantum number in either electronic state. In both Eqs. (5) and (6), the ϕ function represents the Λ-type doubling. In the upper electronic state the Λ-type doubling is experimentally found to be negligible. There is Λ-type doubling in the lower electronic state, but the rate of change of the ϕ function with J is so small that it does not affect the $\Delta_2 F$'s. The same argument can be applied to the other neglected terms which are either constant or change very slowly with respect to J. The last statement holds for the term

TABLE IV. *B values.*

	upper $^2\Pi$	
	$v'=0$	$v'=1$
$B(F_1)$	1.050	1.030
$B(F_2)$	1.047	1.037
$B(av)$	1.048	1.034
	lower $^2\Pi$	
	$v''=8$	$v''=9$
$B^*(F_1)$	1.525	1.520
$B^*(F_2)$	1.550	1.538
$B(av)$	1.538	1.529

involving D for rotational quantum numbers less than 15. For values above this number, the $\Delta_2 F$'s are increasingly less than those given by Eqs. (7) and (8), since D is inherently negative. [$D = -4B_e^3/\omega_e^2$]. From this relation, for the upper electronic state $D' = 5.6 \times 10^{-6}$ and for the lower electronic state $D'' = 4.6 \times 10^{-6}$. D values calculated from the departure of the $\Delta_2 F$'s from a straight line agree with these fairly well. This would be expected for the upper electronic state which is case b but not necessarily for the lower case a electronic state.

Considering Eqs. (7) and (8), it is seen that they predict a linear relation between the Δ_2F's and the rotational quantum numbers; the slope of the line in each case being $4B$. The plot of the actual Δ_2F's in each case lay on a straight line for moderate values of the rotational quantum number, and the slope of the line was used to obtain the B values listed in Table IV. Since K has integral values and J half-integral values for these states, it would be expected that the intercept of the line on the axis of rotational quantum numbers would be close to a whole number for the upper $^2\Pi$ state and close to a half-number for the lower $^2\Pi$ state. This was found to be the case.

Since the upper $^2\Pi$ in case b, B_v should have practically the same value for the F_1 and F_2 sets of rotational levels. This was observed. For the lower $^2\Pi$ state, which is case a, the observed B_v's are called B_v^* since they are not true B_v values. The values of B_v^* differ for the F_1 and F_2 sets of levels as follows:[11]

$$B_v^* = B_v(1 \pm B_v/A\Lambda)$$

with $\pm B_v/\mathrm{A}$ according as $\Sigma = \pm\frac{1}{2}$

From the above equation the difference between the B_v^* values for the F_2 and F_1 sets of levels of the lower $^2\Pi$ state should be ≈ 0.023. This is close to the observed values. The true B_v is obtained by taking the average of $B_v^*(F_1)$ and $B_v^*(F_2)$.

B_v is related to other molecular constants[12] by the equations:

$$B_v = B_e - \alpha(v + \tfrac{1}{2}) = B_0 - \alpha v,$$
$$B_e = h/8\pi^2\mu c r_e^2 = 27.70 \times 10^{-40}/\mu r_e^2.$$

Values of some of these constants are given in Table VII.

The value of A'', the parameter governing the doublet separation of the lower $^2\Pi$ state, can be calculated from Eq. (6). This is done by taking the difference between a line in the first head and a line in the second head which come from the same upper level and end on lower levels of the same J value. An expression for this term difference involving A'' may be obtained from Eq. (6). The smallest J values, for which the data were considered most reliable, were chosen to calculate A''. The result was $A'' = 195$ cm^{-1}.

The value of A' for the upper $^2\Pi$ state can be determined by the use of Hill and Van Vleck's formula:[13]

$$T = T_0^e + G(v) + B_v\{(J+\tfrac{1}{2})^2 - \Lambda^2 \pm \tfrac{1}{2}[4(J+\tfrac{1}{2})^2 - 4A\Lambda^2/B_v + A^2\Lambda^2/B_v^2]^{1/2} + \overline{G^2}\} + \phi_i(J) + \cdots \quad (9)$$

This equation is quadratic in A and gives two possible values, i.e., for the upper electronic state $A' = +8.2$ or -4.0. One can decide between these

[11] For a discussion of B^* cf. R. S. Mulliken, Reviews of Modern Physics **2**, 113 (1930); **3**, 110 (1931).

[12] Cf. R. S. Mulliken, Reviews of Modern Physics **2**, 65–67 (1930).

[13] E. L. Hill and J. H. Van Vleck, Phys. Rev. **32**, 261–2 (1928).

two values in the following way. Either A' value will give the same term value for all rotational levels except the lowest ($J=\frac{1}{2}$). Also for every J value except the lowest, there are two rotational levels, one of which can be classified as an F_1 level and the other level as belonging to the F_2 set. There is only one level for $J=\frac{1}{2}$.[14] According as A' is positive or negative the position of this level should from the theory be such that it would be naturally classified with the F_1 set or with the F_2 set of levels.

By reference to Fig. 1 it will be seen that one more line near the origin would be added to the P_1 and ${}^OP_{12}$ branches than to the ${}^QP_{21}$ and P_2 branches if the level $J=\frac{1}{2}$ belongs to the F_1 set of levels. The converse will be true if this level belongs to the F_2 group of levels. In most of the bands it was not possible to decide definitely between the two possible positions of the level $J=\frac{1}{2}$. In four instances, however, it appeared that this level belonged to the F_1 set of levels rather than to the F_2 set, thus indicating that $A'=+8.2$. [The first line of each of the following branches appears to come from the level $J=\frac{1}{2}$: P_1 of the 0–9 and 1–9 bands, ${}^OP_{12}$ of the 1–9 band. On the other hand a line from this level appeared to be definitely absent in the case of P_2 branch of the 1–8 band.]

Calculation of the Δ_1F's of the Upper $^2\Pi$ State

Since there were no Q branches present, it was impossible to obtain the Δ_1F's directly by combinations between the lines. In the upper electronic state for each value of K there is an F_2 level with $J=K-\frac{1}{2}$, slightly above an F_1 level with $J=K+\frac{1}{2}$. The relative position of the F_2 and F_1 levels is a function of A/B_v.[15] The separation of these two levels for a given value of K will be called the spin-doubling distance (ϵ_K) since it is due to the two orientations of the spin vector with respect to K.

For moderate and large values of K the spin-doubling distance changes very slowly with K, so it can be obtained with sufficient accuracy from the lines in the following way. By reference to Fig. 1 it is seen that:

$$\begin{aligned} {}^SR_{21}(J-1) - R_1(J-1) &= {}^QP_{21}(J+1) - P_1(J+1) \\ &= R_2(J-1) - {}^QR_{12}(J-1) \\ &= P_2(J+1) - {}^OP_{12}(J+1) \\ &= \Delta_1F_1'(J+\tfrac{1}{2}) + \epsilon_{K=J+1/2}. \end{aligned} \tag{10}$$

[For definition of Δ_1F cf. end of next section on p. 1309] From Eq. (10):

$$\Delta_1F_1'(J+\tfrac{1}{2}) + \epsilon_{K=J+1/2} + \Delta_1F_1'(J-\tfrac{1}{2}) + \epsilon_{K=J-1/2} = \Delta_2F_1'(J) + 2\epsilon_{K=J}. \tag{11}$$

In the right hand member of Eq. (11) the sum of the two ϵ terms corresponding to $K=J-\frac{1}{2}$ and $K=J+\frac{1}{2}$ is practically the same as twice the value which ϵ_K would have for a hypothetical intermediate level with $K=J$.

Values of ϵ are readily calculated from Eq. (11) since the $\Delta_2F'_1(J)$ terms can be obtained directly from the line differences according to Eq. (4), or by

[14] Cf. R. S. Mulliken, Reviews of Modern Physics **2**, 109 (1930).
[15] Cf. R. S. Mulliken, Reviews of Modern Physics **2**, 114 (1930).

reference to Table III. Fig. 2 is a plot of ϵ against K. The solid line shows the values obtained by Hill and Van Vleck's formula and the circles are the values obtained from the lines by the method outlined. For the lowest K values many of the lines were not resolved. The lowest term differences, that were considered most reliable, were used to determine the constants in Hill and Van Vleck's equation, and then the position of the lowest rotational levels was calculated. The first members of the branches could then be located. The first values of ϵ in Fig. 2 are from these blended lines.

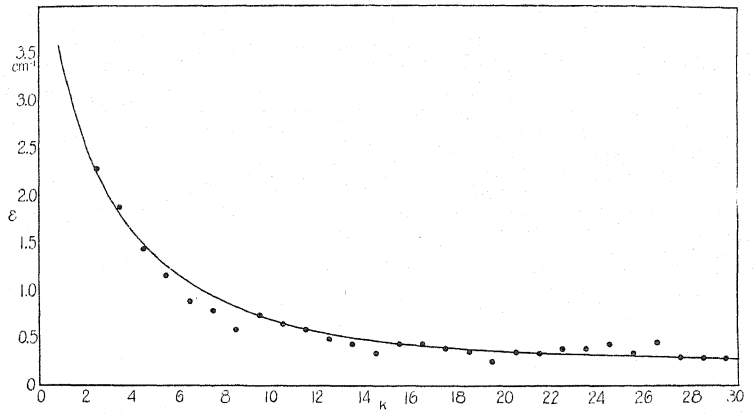


Fig. 2. A graph of ϵ_K (the spin-doubling distance) for the upper $^2\Pi$ state against K. The solid line is drawn from values obtained from Hill and Van Vleck's equation. The circles are values obtained from the lines according to Eq. (11).

The quantities given by Eq. (10) are listed in columns 2 through 10 of Table V. By subtracting the ϵ's from these quantities the $\Delta_1 F$'s of the upper $^2\Pi$ state are obtained. These are listed in columns 11 and 12 of Table V.

Calculation of the $\Delta_1 F^*$'s of the Lower $^2\Pi$ State

The $\Delta_1 F^*$'s of this state were obtained in a similar manner. The $\Delta_1 F^*$'s of the vibrational state $v''=9$ as listed in Table VI will be taken as an example. In columns 2 and 6 is listed the difference:

$$^sR_{21}(J) - R_1(J+1)$$

and in columns 4 and 8

$$^qP_{21}(J) - P_1(J+1)$$

These columns are labelled uncorrected since they must be corrected by subtracting the proper ϵ_K (already obtained, cf. Fig. 2) from each difference to obtain the $\Delta_1 F_1^*$ of the lower state. This will be seen by reference to Fig. 1. It will be noted that the ϵ_K to be subtracted from any one member of columns 2 and 6 is for a K value two units greater than the ϵ_K to be subtracted from the corresponding member of columns 4 and 8. These two values of ϵ are practically the same for moderate and high values of K but not so for low values of K (cf. Fig. 2). The columns labelled uncorrected have the appear-

TABLE V. *Values of* $\Delta_1F_1'(K=J)$ *and* $\Delta_1F_2'(K=J)$ *for the 0 vibrational state obtained from Eqs. (10) and (11). The J values have been omitted from the column headings, so that;* (1) $^SR_{21}-R_1$ *stands for* $^SR_{21}(J-1)-R_1(J-1)$; $R_2-{}^QR_{12}$ *stands for* $R_2(J-1)-{}^QR_{12}(J-1)$; *and* (2) $^QP_{21}-P_1$ *stands for* $^QP_{21}(J+1)-P_1(J+1)$; $P_2-{}^OP_{12}$ *stands for* $P_2(J+1)-{}^OP_{12}(J+1)$.

	0−8 Band				0−9 Band						
$J+\frac{1}{2}$	$^SR_{21}-R_1$	$^QP_{21}-P_1$	$R_2-{}^QR_{12}$	$P_2-{}^OP_{12}$	$^SR_{21}-R_1$	$^QP_{21}-P_1$	$R_2-{}^QR_{12}$	$P_2-{}^OP_{12}$	*av.*	$\Delta_1F_2'(K\equiv J)$ $=av-\epsilon_{K=J-\frac{1}{2}}$	$\Delta_1F_1'(K\equiv J)$ $=av-\epsilon_{K=J+\frac{1}{2}}$
1	7.2	7.3		6.8	7.4	6.9		6.3	7.0	3.6	4.5
2	8.6	8.6	8.5	8.6	8.8	8.2	8.5	8.5	8.5	6.0	6.5
3	10.6	11.1	10.3	9.9	10.1	10.8	10.3	9.9	10.4	8.4	8.7
4	12.5	11.9	11.9	11.6	12.1	11.9	12.0	11.7	11.9	10.2	10.4
5	14.6	14.0	13.5	13.5	13.7	13.8	13.8	14.3	13.9	12.4	12.7
6	15.4	16.1	15.3	15.6	15.7	15.5	15.4	15.5	15.6	14.4	14.6
7	17.8	17.7	16.9	17.6	17.9	18.1	17.5	17.5	17.6	16.6	16.6
8	20.1	19.6	19.0	19.7	19.5	19.6	19.6	19.3	19.6	18.6	18.8
9	21.5	21.6	21.7	21.7	21.7	21.6	21.5	21.6	21.8	21.0	21.1
10	23.4	23.7	23.7	23.7	23.8	23.7	23.7	23.5	23.6	22.9	22.9
11	25.7	25.8	25.8	25.8	25.7	26.0	26.0	25.9	25.8	25.1	25.2
12	27.6	27.8	27.8	27.9	27.8	27.9	28.1	27.9	27.8	27.2	27.2
13	29.8	29.7	29.6	29.9	29.8	29.8	29.9	30.1	29.8	29.2	29.3
14	31.9	32.0	31.9	31.8	31.7	32.2	31.9	31.8	31.9	31.4	31.4
15	34.0	34.1	34.2	34.0	33.9	34.0	34.0	34.0	34.0	33.5	33.6
16	36.1	36.1	36.2	36.0	35.9	36.0	36.1	35.9	36.0	35.6	35.6
17	38.1	38.3	38.3	38.2	38.1	38.1	38.1	38.1	38.2	37.8	37.8
18	39.9	40.1	40.0	40.1	40.2	40.0	40.2	40.3	40.1	39.7	39.7
19	42.3	42.5	42.2	42.3	42.3	42.4	42.2	42.3	42.3	41.9	41.9
20	44.5	44.3	44.3	44.3	44.2	44.3	44.0	44.2	44.3	43.9	43.9
21	46.4	46.5	46.3	46.4	46.4	46.2	46.4	46.5	46.4	46.2	46.0
22	48.7	48.9	48.4	48.5	48.3	48.3	48.6	48.9	48.6	48.2	48.2
23	50.7	50.4	50.4	50.7	50.5	50.7	50.6		50.6	50.2	50.2
24	52.8	52.6	52.5	52.5	52.6	52.8	52.5		52.6	52.2	52.3
25	54.8	54.4	54.5	54.3	54.9	54.8	54.4		54.6	54.3	54.3
26	56.7	57.4	56.8		56.7	56.7	56.5		56.8	56.5	56.5
27	58.6	58.7	58.8		58.5	58.5	58.7		58.6	58.3	58.3
28	61.0	60.6	61.0		60.3	60.6	60.7		60.7	60.4	60.5
29	63.2	62.4	62.6		62.7	62.8			62.7	62.5	62.5
30	64.8	65.6	65.1		65.0				65.1	64.9	64.9
31	66.8		66.9		66.9				66.9	66.7	66.7
32	68.6				68.9				68.8	68.6	68.6
33	71.6				70.9				71.2	71.0	71.0
34	73.0				73.0				73.0	72.8	72.8

TABLE VI. *The values of* $\Delta_1 F_1''^*(J+\frac{1}{2})$ *for the 9 vibrational state.*

$J+\frac{1}{2}$	0−9 Band $R_{21}(J)-R_1(J+1)-\epsilon_{K=J+1\frac{1}{2}}$ uncorr.	corr.	${}^QP_{21}(J)-P_1(J+1)-\epsilon_{K=J-\frac{1}{2}}$ uncorr.	corr.	1−9 Band $R_{21}(J)-R_1(J+1)-\epsilon_{K=J+1\frac{1}{2}}$ uncorr.	corr.	${}^QP_{21}(J)-P_1(J+1)-\epsilon_{K=J-\frac{1}{2}}$ uncorr.	corr.	$\Delta_1 F_1''^*(J+\frac{1}{2})$ av. of corr.
1	6.9	4.4			6.6	4.1			4.3
2	9.2	7.2			9.6	7.6			7.4
3	11.8	10.1	12.7	10.2	12.8	11.1	12.4	9.9	10.3
4	14.7	13.2	15.5	13.5	14.4	12.9	15.6	13.6	13.3
5	17.9	16.7	18.7	17.0	17.9	16.7	18.4	16.7	16.7
6	20.4	19.4	20.8	19.3	20.2	19.2	20.6	19.1	19.3
7	23.8	22.8	23.7	22.5	23.7	22.7	24.1	22.9	22.7
8	26.0	25.2	26.5	25.5	25.8	25.0	26.3	25.3	25.2
9	29.8	29.1	30.0	29.0	30.1	29.4	29.8	28.8	29.1
10	31.8	31.1	32.0	31.2	31.8	31.1	32.0	31.2	31.1
11	35.8	35.2	35.7	35.0	35.6	35.0	35.6	34.9	35.0
12	37.7	37.1	38.0	37.3	37.6	37.0	37.9	37.2	37.1
13	41.7	41.2	42.0	41.4	41.4	40.9	41.6	41.0	41.2
14	43.5	43.0	43.9	43.3	43.6	43.1	43.8	43.2	43.1
15	47.6	47.2	47.8	47.3	47.4	47.0	47.7	47.2	47.2
16	49.6	49.1	49.9	49.4	49.7	49.3	49.8	49.3	49.3
17	53.7	53.3	53.7	53.3	53.7	53.3	53.5	53.1	53.3
18	55.7	55.3	55.6	55.2	55.6	55.1	56.1	55.7	55.3
19	59.6	59.2	59.6	59.2	59.9	59.5	60.1	59.7	59.5
20	61.6	61.4	61.6	61.2	61.4	61.0	61.4	61.0	61.2
21	65.6	65.2	65.8	65.4	65.4	65.0	65.8	65.4	65.3
22	67.5	67.1	67.5	67.1	67.5	67.1	67.7	67.3	67.1
23	71.7	71.3	71.5	71.1	71.9	71.5	71.8	71.4	71.3
24	73.8	73.5	73.5	73.1	73.1	72.8	73.3	72.9	73.1
25	77.7	77.4	77.9	77.5	77.9	77.7	77.6	77.2	77.4
26	79.3	79.0	79.6	79.3	79.7	79.4	79.2	78.9	79.2
27	83.5	83.2	84.0	83.7	84.1	83.8	83.7	83.4	83.4
28	84.8	84.6	85.1	84.8	86.1	85.9	85.1	84.8	84.8
29	89.9	89.7	89.6	89.3	89.9	89.7			89.6
30	91.3	91.1	91.1	90.8	91.8	91.6			91.1
31	95.7	95.5			96.2	96.0			95.7
32	97.2	97.0			97.9	97.7			97.3
33	101.6	101.4							101.4
34	102.9	102.7							102.7
35	107.5	107.3							107.3

TABLE VI (*Continued*). *The values of* $\Delta_1 F_2''^*(J+\frac{1}{2})$ *for the 9 vibrational state*

$J+\frac{1}{2}$	0–9 Band $R_2(J)-{}^QR_{12}(J+1)-\epsilon_{K=J+1\frac{1}{2}}$ uncorr.	corr.	$P_2(J)-P_{12}(J+1)-\epsilon_{K=J-\frac{1}{2}}$ uncorr.	corr.	1–9 Band $R_2(J)-{}^QR_{12}(J+1)-\epsilon_{K=J+1\frac{1}{2}}$ uncorr.	corr.	$P_2(J)-{}^QP_{12}(J+1)-\epsilon_{K=J-\frac{1}{2}}$ uncorr.	corr.	$\Delta_1 F_2''^*(J+\frac{1}{2})$ av. of corr.
2	9.6	7.6			9.3	7.3			7.5
3	12.5	10.8	13.0	10.5	12.5	11.8	13.4	10.9	11.0
4	15.2	13.7	15.8	13.8	15.0	13.5	15.7	13.7	13.7
5	18.2	17.0	18.1	16.4	17.5	16.3	18.2	16.5	16.4
6	20.3	19.3	21.3	19.8	20.3	19.3	20.7	19.2	19.4
7	23.9	22.9	24.3	23.1	24.1	23.1	24.2	23.0	23.0
8	26.6	25.8	27.0	26.0	26.0	25.2	26.4	25.4	25.6
9	29.7	29.0	29.9	28.9	29.6	28.9	30.0	29.0	29.0
10	32.7	32.0	32.4	31.6	32.8	32.1	32.7	31.9	31.9
11	36.1	35.5	35.8	35.1	35.7	35.1	36.1	35.4	35.3
12	38.9	38.3	38.7	38.0	38.4	37.8	38.8	38.1	38.0
13	42.0	41.5	42.3	41.7	41.7	41.2	42.1	41.5	41.5
14	44.6	44.1	44.9	44.3	44.7	44.2	44.5	43.9	44.1
15	48.3	47.9	48.3	47.8	48.3	47.9	48.0	47.5	47.8
16	50.7	50.3	50.6	50.1	50.5	50.1	50.9	50.4	50.3
17	54.3	53.9	54.1	53.7	54.4	54.0	54.4	54.0	53.9
18	56.7	56.3	56.8	56.4	56.9	56.5	56.8	56.4	56.4
19	60.0	59.6	60.4	60.0	60.0	59.6	60.4	60.4	60.0
20	62.8	62.4	63.0	62.6	62.8	62.4	63.0	62.6	62.5
21	66.5	66.1	66.3	65.9	65.7	65.3	66.2	65.8	65.8
22	68.9	68.5	68.8	68.4	68.9	68.5			68.5
23	72.6	72.2	73.0	72.6	74.3	73.9			72.6
24	74.6	74.3							74.3
25	78.4	78.1							78.1
26	80.7	80.4							80.4
27	84.7	84.4							84.4

ance of giving combination agreements except near the origin and this caused considerable confusion before the branches had been classified.

It should be noted that the quantities above called $\Delta_1 F$ or $\Delta_1 F^*$ are not "true" $\Delta_1 F'$s, because of the existence of Λ-type doubling. As explained in the following section on Λ-type doubling, each rotational level has an a and b component. A "true" $\Delta_1 F(J+\frac{1}{2})$ would be the distance from the a or b component of the J level to the a or b component respectively of the $J+1$ levels. In the case of O_2^+, however, alternate levels in the successive Λ-type doublets are missing. Because of this the quantity which has physical existence is the distance from the a level of J to the b level of $J+1$ (cf. Fig. 3), or from the b level of J to the a level of $J+1$. This quantity, for the lower

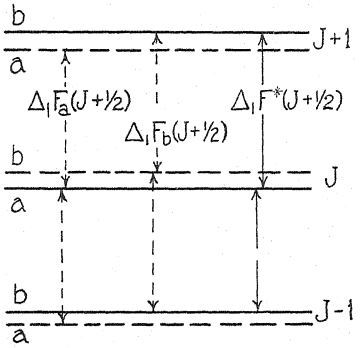


Fig. 3. The relation of the $\Delta_1 F^*$'s to the $\Delta_1 F$'s.

$^2\Pi$ state, will be denoted as $\Delta_1 F''^*$. In the upper $^2\Pi$ state this distinction will not be made since the Λ-type doubling in this state cannot be detected experimentally. This means that a $\Delta_1 F_1'^*$ is identical within experimental error with a "true" $\Delta_1 F'$.

Λ-TYPE DOUBLING

For an electronic state with $\Lambda > 0$, the rotational levels are double, one level of the doublet being classified as an a level and the other as a b level.[16] However O_2^+ is a homonuclear molecule and the angular momentum (I) of the oxygen atom is zero,[17] as is known from the atmospheric oxygen bands. This means that alternate levels in the successive Λ-type doublets should be missing (cf. Fig. 3).

Alternate levels were actually observed to be missing. This is shown by the fact that the number of lines in any one series was the same as though there were no Λ-type doubling. But the lines were staggered since each rotational level was in effect slightly displaced, i.e., every other line was of slightly greater or smaller wave number than if there had been no Λ-type doubling. The staggering was made evident by plotting successive differences

[16] For a discussion of the nomenclature of these levels cf. R. S. Mulliken, Reviews of Modern Physics 3, 93 (1931).

[17] For a discussion of homonuclear molecules cf. R. S. Mulliken, Reviews of Modern Physics 3, 146 (1931).

of the lines of a branch against an arbitrary number. A straight line could be drawn between the points such that alternate points lay on opposite sides of this line. If there had been no Λ-type doubling the points would all have been on this line.

The Λ-type doubling should also appear in a plot of the $\Delta_1 F^*$'s. This causes the $\Delta_1 F^*$'s to stagger similarly to the series discussed above. The amount of this staggering is equal to the width of the Λ-type doublet, i.e., the distance which there would be between an a and b level of the same J value if both levels physically existed in the case of O_2^+.

When the $\Delta_1 F^*$'s were plotted it was found that there was Λ-type doubling in the lower $^2\Pi$ state, but not an appreciable amount in the upper $^2\Pi$

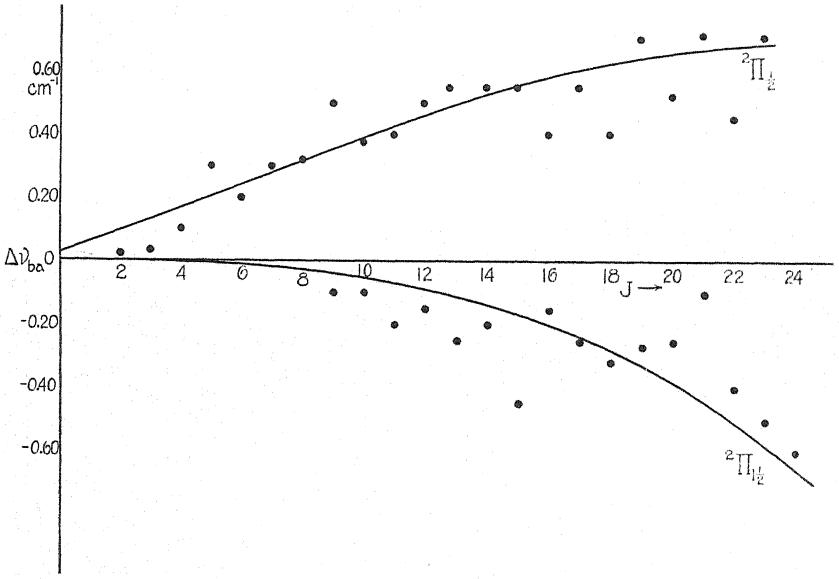


Fig. 4. Comparison of experimentally observed Λ-type doublet widths with the theoretical curves of Eqs. (12) and (13). The value of p was obtained from the slope of the initial portion of the curve through the points of the lower $^2\Pi_{\frac{1}{2}}$ state.

state. The Λ-type doublet widths are shown by Fig. 4. The following theoretical relations are expected:[18]

For a case a $^2\Pi_{\frac{1}{2}}$ state

$$\Delta\nu_{ba} = p(J + \tfrac{1}{2}). \tag{12}$$

For a case a $^2\Pi_{1\frac{1}{2}}$ state

$$\Delta\nu_{ba} = [p/Y^2 + 2q/Y](J - \tfrac{1}{2})(J + \tfrac{1}{2})(J + 3/2). \tag{13}$$

These relations represent the data fairly well and give $p = 0.036$, $q = 0.0027$.

There are reasons for believing that the upper electronic state of O_2^+ is $^2\Pi_u$ and the lower state $^2\Pi_g$. If this is true, then since for oxygen the complete ψ is Sy and for an atom with $I = 0$ ψ_{nu} is s, only—rotational levels can

[18] R. S. Mulliken and A. Christy, Phys. Rev. 38, 94 (1931).

exist in the upper $^2\Pi$ state and + rotational levels in the lower $^2\Pi$ state.[17] If these conditions are correct, then the designations a and b as assigned here correspond respectively to the c and d classes of rotational levels.[16]

From an examination of the staggering of the $\Delta_1F''^*$'s in the lower $^2\Pi_{\frac{1}{2}}$ state, it is found that those $\Delta_1F''^*$ (N)'s, where $N=J+\frac{1}{2}$, for which N is an odd integer have slightly larger values than they would have if there were no Λ-type doubling. Also those $\Delta_1F''^*(N)$'s, for which N is an even integer have slightly smaller values than they would have if there were no Λ-type doubling. This means that for the lower $^2\Pi_{\frac{1}{2}}$ state the a levels are above the b levels in each Λ-type doublet. For the lower $^2\Pi_{1\frac{1}{2}}$ state the reverse is true, i.e., the b levels are above the a levels. This difference is in agreement with theory.[18]

Conclusion

A possible explanation why the upper $^2\Pi$ is case b can be found by considering the probable electron configuration[19] of this state. The electronic configuration of normal O_2^+ has been designated as $1s\sigma^2\ 2p\sigma^2\ 2s\sigma^2\ 3p\sigma^2\ 3d\sigma^2\ 2p\pi^4\ 3d\pi^2$. The removal of a $3d\pi$ electron probably gives the lower $^2\Pi$ state of O_2^+ with the electronic configuration $\cdots\ 3d\sigma^2\ 2p\pi^4\ 3d\pi$. The removal of a $2p\pi$ electron would give the electronic configuration $\cdots\ 3d\sigma^2\ 2p\pi^3\ 3d\pi^2$. Such a configuration would give several electronic states one of which is a $^2\Pi$ state that would be expected to have a small coupling of the spin with the electric axis, corresponding to the upper $^2\Pi$ case b state.

TABLE VII. *Values of the molecular constants.*

upper $^2\Pi$	lower $^2\Pi$
$A'=+8.2$ cm^{-1}	$A''=+195$ cm^{-1}
$B'=1.048-0.014v'$	$B''=1.610-0.009v''$
(observed $v'=0$, 1)	(observed $v''=8$, 9)
D' (cal.) $=5.6\times10^{-6}$	D'' (cal.) $=4.6\times10^{-6}$
D' (obs.) $\approx 5\times10^{-6}$	$r_e''=1.14\times10^{-8}$ cm
$r_e'=1.41\times10^{-8}$ cm	$p=0.036$
	$q=0.0027$

In conclusion I wish to thank Professor R. S. Mulliken for proposing the problem and for his many valuable suggestions; also Dr. A. Christy for his interest and advice during the investigation.

[19] Cf. R. S. Mulliken, Phys. Rev. **37**, 1711 A (1931).

SECONDARY EMISSION FROM NICKEL BY IMPACT OF METASTABLE ATOMS AND POSITIVE IONS OF HELIUM

By Marshall C. Harrington
Palmer Physical Laboratory, Princeton University, Princeton, N. J.

(Received August 24, 1931)

Abstract

Experiments on the secondary electron emission from Ni electrodes due to bombardment by positive ions and metastable atoms in a helium discharge under conditions similar to those obtaining in a glow discharge are reported. The method of measurement is similar to that of Uyterhoeven and Harrington.[1] The proportion of the measured current at the cathode which is carried by electrons is found to be 15 to 50 percent depending on experimental conditions. Similarly the number of electrons per slow positive ion is found to range between about 8 and 20 percent. The secondary electrons originate at the surface of the collector with about 15 volts maximum initial energy.

THE experiments of W. Uyterhoeven and the author[1] on the secondary electron emission from nickel by impact of metastable atoms and positive ions of neon under conditions similar to those in a glow discharge have been extended to helium with a similar apparatus. As was to be expected from the similarity of the two gases, the data indicate that helium behaves in an analogous manner. Here, as in neon, the condition for emission by impact of slow positive ions is fulfilled, namely $V_i \geqq 2\phi$, where V_i is the ionization potential and ϕ is Richardson's work functions.[2] ($V_i = 24$ and ϕ = about 4.5 or 5).

Apparatus

The experimental arrangement was similar to that of the previous experiments in neon.[1] The discharge tube (see Fig. 1) was spherical in shape (20 cm diameter) with four side arms. The anode and cathode occupied two of these; a third at the bottom housed the main experimental electrode; the fourth at the top contained the movable electrode C. The cathode K was of a standard type of the General Electric Company consisting of an oxide coated nickel cylinder heated by a tungsten filament within. The anode A was a nickel cylinder. The main experimental electrode P (see Fig. 2) was a circular nickel disk (diameter 18.2 mm) with a coplanar concentric guard ring G (outer diameter 29.2 mm). The former was supported by the cylinder M and the latter by the outer cylinder L. The joints were made by electric spot welding. The cylinder L was protected by the cylindrical glass cover H in order to avoid drawing larger currents than necessary from the main dis-

[1] Uyterhoeven and Harrington, Science **70**, 586 (1929); Phys. Rev. **35**, 124 (1930); **35**, 438 (1930); **35**, 1421 (1930); **36**, 709 (1930).

[2] Holst and Oosterhuis, Physica **4**, 375 (1924).

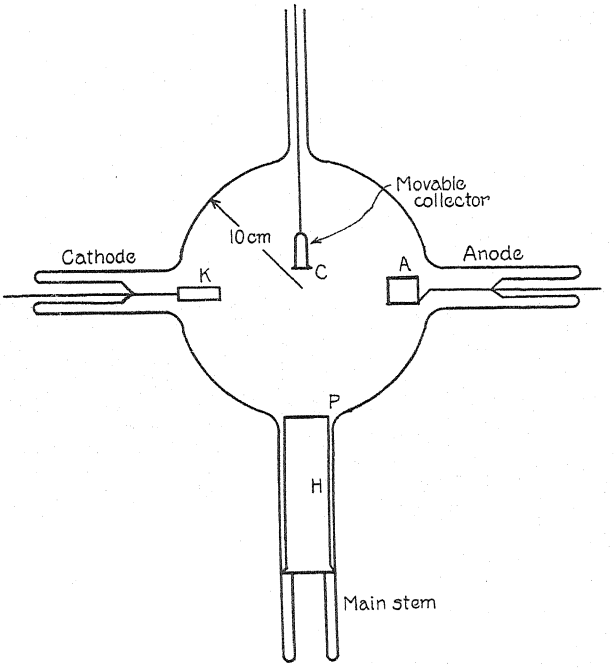


Fig. 1. The experimental tube.

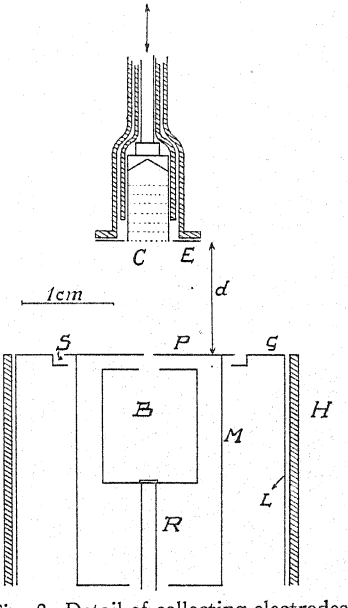


Fig. 2. Detail of collecting electrodes.

charge. The cylinder M protected the Faraday box B, which was at its center, from whatever charged or uncharged particles may have come through the annular slit S between the plate P and its guard ring G. The Faraday box B itself was a nickel cylinder closed at its top and bottom and supported by the rod R. In the center of the upper cover of B there was a circular hole (diameter 2 mm) which was immediately below a small hole (diameter 0.74 mm) in the center of the plate P.

The collector C was a small cylinder of nickel with one open end exposed to the discharge. This open end was covered with nickel gauze in order to allow the electrons which came to it to be trapped without much reflection. The sides and back were protected by glass. This was fitted with a plane annular guard ring E concentric and coplanar with the exposed end of C. The collector C was movable along its axis, that is, in a direction perpendicular to the plane of the plate P, opposite to which it was placed.

The metal used in the construction of the electrodes was outgassed by the induction furnace in the usual manner.

The discharge was run at about 0.5 to 1 ampere, and a more or less uniform luminosity filled the whole sphere. The helium gas used was constantly circulated and purified by a misch-metal arc, and liquid air traps were used to avoid condensible vapors. The tube was baked out before being used for about five hours at approximately 425° C with the pumps running until the pressure was no longer readable on a McLeod gauge.

Experimental Methods and Results

Two of the methods described in the paper[3] reporting the experiments in neon were used here. The first method[4] gave a measurement of the proportion of measured current carried by electrons at the plate P. The cylinder C was placed at a fixed distance d from the plate P and given a definite negative potential $(V_C)_A$ measured with respect to the anode so that it drew a positive current i_C. The potential of the plate $(V_P)_A$ measured with respect to the anode was lowered from about $(V_C)_A+50$ to $(V_C)_A-100$. The currents to the plate i_P and to the cylinder i_C were measured. The latter current was also put through a mirror galvanometer compensated with an opposing current in order to make a sensitive measurement of the variations in i_C from an arbitrary zero point. Some difficulty was encountered in making this steady due to fluctuations in the discharge. A typical curve of i_C *vs.* $(V_P)_A$ is given in Fig. 3.

Secondary electrons emitted from the plate P were accelerated by the drop across the sheath on the plate P, and a certain proportion of them arrived at the outer edge of the sheath on the collector C. The rest were scattered on the way. When the drop across the sheath on the plate P was greater than that on C, the electrons were received at C, giving a decrease (Fig. 3) in the measured current i_C. Actually since secondary electrons had some initial velocity, they started to come in when the negative potential $(V_P)_A$

[3] Uyterhoeven and Harrington, Phys. Rev. **36**, 709 (1930).
[4] See reference 3, pp. 712 ff.

was somewhat less than $(V_C)_A$, say about 15 volts. Table I gives some illustrative material.

TABLE I.

$(V_C)_A$	I	V	Δi_C	$\bar{i}_P$	i_P	γ
−100	0.520	29	18.3	30	250	12
−125	0.525	30	20.5	34.2	255	13
−150	0.520	31	20.9	34.9	260	13.5
−175	0.520	31	22.2	36.9	264	14
−200	0.520	31	24.0	40	269	15

I=total current in tube in amperes. V=drop across the tube in volts. Δi_C=electron current received at C in $\mu A/cm^2$. $\bar{i}_P$=electron current originating at plate calculated from Δi_C using measured distance d=4.3 cm and mean free path. $\gamma=\bar{i}_P/i_P$ in percent. Pressure=1.5 $\times 10^{-2}$ mm of Hg.

The electron current originating from the plate P was calculated from Δi_C by assuming an exponential decrease. The gas kinetic mean free path was taken as 0.1259 cm at 1 mm.[5] The value of the proportion γ of the current i_P carried by electrons is given in the table. This is about the same as that found in neon, and varied with the discharge conditions.

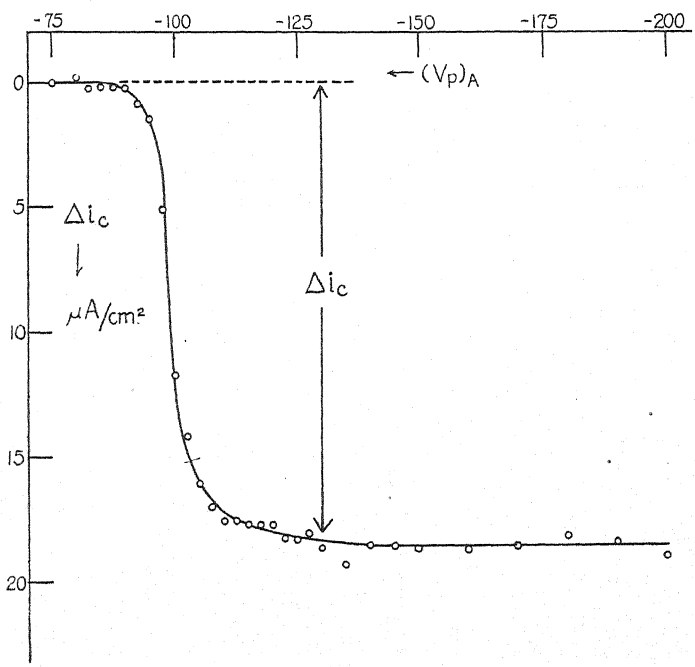


Fig. 3. i_C *vs.* $(V_P)_A$.

It is to be noted that electron reflection or secondary electron emission[6] due to impact of electrons at the collector C would introduce an error in

[5] Compton and Van Voorhis, Phys. Rev. **26**, 450 (1925).

[6] Compton and Langmuir, Revs. Mod. Phys. **2**, 171 (1930). See section 7 and references cited there.

Δi_C, which would make the calculated electron current i_P, and consequently γ, too small. In view of the fact that the electrode C was constructed especially to minimize reflection, and that the percentage reflection is only 3 or 4 in any case, the error thus introduced is not large.

Another method[7] enabled the secondary electron current to be separated into two parts, one part due to the bombardment of positive ions and the other due to the impact of neutral particles. This gave data on the number α of electrons emitted per impinging positive ion. The movable collector C was withdrawn into its side tube, as it was not used. The plate P and its guard ring G were put at some definite negative potential $(V_P)_A$ (say -100 v) measured with respect to the anode. The plate P and guard ring G thus drew

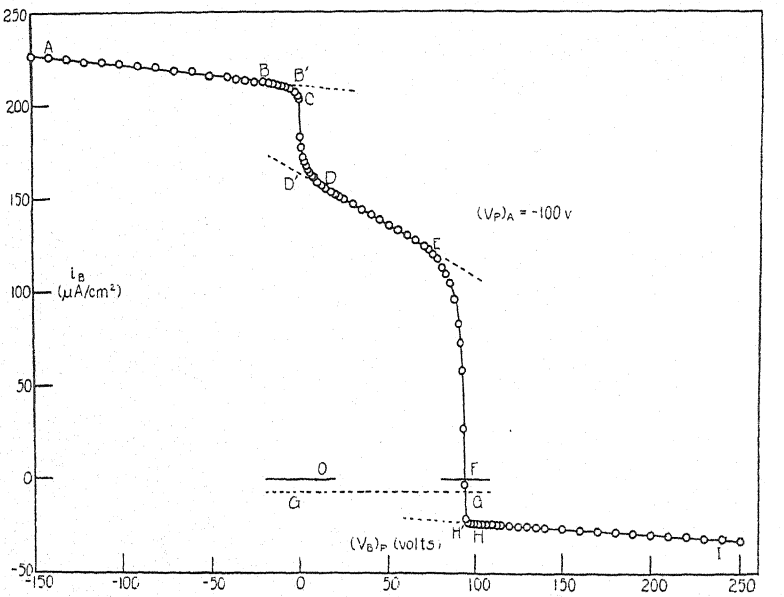


Fig. 4. Box currents i_B *vs.* box potential $(V_B)_P$ for plate potential $(V_P)_A = -100$ v.

a definite positive current i_P which was composed in part of a positive ion current i^+ coming in and in part of an electron current i^- going out. The ions received at P were accelerated by the potential drop across the sheath which existed above P, and hit the latter with the corresponding energy. Some ions went through the hole in the plate P and on into the box B beneath whenever the potential $(V_B)_P$ of the box (measured with respect to the plate P) permitted them. Fig. 4 gives a typical plot of the current i_B received at the box B as a function of the box potential $(V_B)_P$.

The general behavior of the currents in helium was the same as that in neon in the experiment previously described[3] and the interpretation given to the data is the same. The box B was first made negative and its potential $(V_B)_P$ raised from -250 to $+250$. The positive ions which came through the hole in the plate were received at the box until the potential of the box

[7] See reference 3, pp. 720 ff.

became equal to that of the space outside the sheath above the plate P from which the ions came. (Points $ABCDEFII$ of Fig. 4). As can be seen in Fig. 4, the potential $(V_B)_P$ at which this occurred was very nearly equal to $-(V_P)_A$, indicating that the space from which the ions came had a potential almost equal to that of the anode. This gave a very good method of measuring the space potential, and was in all cases more definite than the method used by Langmuir and others.[8] It is to be noted, however, that in this case the information needed was the actual potential drop across the sheath when the plate was receiving considerable current. This was in all likelihood somewhat different from the space potential existing when the plate was floating, for the semilog plots according to Langmuir's method[8] indicated a somewhat lower potential. The positive ions thus received when $(V_B)_P$ equalled $-(V_P)_A$ went into the box B through the hole in its upper cover, and any electrons emitted because of them had a very small chance of escape. This offered opportunity to measure the actual positive ion current.

Uncharged particles, however, came through the hole in the plate P in a more or less random direction. Of these some, such as metastable atoms, had sufficient potential energy for the ejection of electrons from surfaces at which they lost their potential energies. This process does not necessarily occur at the surface first struck, for according to Oliphant[9] metastable atoms can be reflected from metal surfaces. Kenty[10] has pointed out that there should be included with the metastable atoms, the photons of the resonance radiation which have very nearly the same energy. The photoelectric efficiency of visible light is too small to account for the magnitudes of the currents found previously in neon[3] or here in helium. So far as is known to the author, there are aside from Kenty's work[10] no estimates of the photoelectric efficiency of the resonance light of the noble gases. Obviously, however, the experimental method used here does not distinguish between the photoelectric effect and the metastable atom effect. In order, however, to simplify the wording of the explanation of the data here presented, the phrase "metastable atoms" is to be understood as "metastable atoms and photons of resonance radiation."

A portion of the metastable atoms (see Fig. 2) went into the interior of the box B along with the positive ions, and any secondary electrons arising therefrom were trapped within and were not recorded. The rest, however, hit either the box B on its outer surfaces, or the under side of the plate P or cylinder M, and electrons ejected flowed to or from B as the potential $(V_B)_P$ permitted. As in neon,[3] it was found that the electrons had certain initial velocities of which the maximum was about 15 volts, corresponding to the difference between the potential energy of the metastable atoms and the work function of nickel ($V_m = 19$ and $\phi =$ about 5). This checks the value found by the other method described above. The dip $B\ C\ D$ in the curve i_B vs. $(V_B)_P$ (see Fig. 4) is due to these currents, which flowed first one way and then the

[8] Langmuir and Mott-Smith, Gen. Elec. Rev. **27**, 810 (1924) and other papers referred to therein.

[9] Oliphant, Roy. Soc. Proc. **A124**, 228 (1929).

[10] Kenty, Phys. Rev. **38**, 377 (1931) and private communication.

other as the potential $(V_B)_P$ was raised. The negative current i_1 from the box B, for instance, flowed when $(V_B)_P$ was less than $+15$ volts, and was proportional to CD' where D' is the point where ED extended backward cuts the axis of zero potential. The other current i_2, which flowed to the box, was received when $(V_B)_P$ was more than -15 volts, and was proportional to CB' where B' is the intersection of AB extended and the zero axis.

The exact position of the point C where the curve (Fig. 4) crosses the axis of zero voltage was somewhat in doubt, since the curve had a vertical inflection there and varied rapidly with the voltage. However, the total of these two currents i_1 and i_2 was $B'D'$, and this was divided in the same ratio as the areas $BB'C$ and $CD'D$ between the curve and the extrapolated lines which respectively determine B' and D'.

The real positive ion current i^+ received by the box at $(V_B)_P=0$ was thus the apparent positive ion current OD' plus the current i_2, which was received when $(V_B)_P>-15$ volts. As the potential of the box was raised, the ion current received gradually decreased (points D to E of Fig. 4). This may have been due to the presence of slow ions which were repelled from the box in increasing numbers as the potential was raised or to distortion of the fields around the hole in the plate as the potential of the box was changed. At $(V_B)_P=-(V_P)_A$ the ion current was entirely cut off, and the residual current FH' (points H to I, Fig. 4) was negative partly because of the current i_2 mentioned above and partly because of secondary electrons liberated by the impact on the underside of the plate of ions repelled by the box and subsequently received by the box. FH' was then composed of two parts $FG=B'C=i_2$ and $GH'=i_3$ which was ascribable to the effect of the ions. This latter current was divided by i^+ to give the number α of electrons per positive ion. All currents were reduced to amperes per cm² in order that they might be compared directly. The current received by the plate was thus divided by the area of the plate, and the currents received at the box were divided by the area of the hole in the plate. Here, as in the first method described above, an estimate of the proportion γ of measured current which was carried by electrons could be made. Illustrative material is presented in Table II.

TABLE II.

p	I	V	$(V_P)_A$	i_P	i^+	i_3	α	i^-	γ
4 $\times10^{-2}$	0.483	32	−100	358	171	15	9	187	52
	0.481	34	−120	376	167	14	9	209	55
	0.479	37	−140	388	169	14	9	219	56
	0.478	37	−160	413	173	15	9	240	57
	0.480	36	−180	440	181	17	9	259	59
	0.480	35	−200	454	173	19	8	286	62
2 $\times10^{-2}$	0.730	37	−160	413	329	26	8	84	21
2 $\times10^{-2}$	0.493	32	−160	275	230	21	9	45	20
4.5$\times10^{-2}$	0.415	56	−150	315	96	19	20	219	69

p=pressure in mm of Hg. I=total current through tube in amperes. V=drop across tube in volts. $(V_P)_A$=potential of plate. i_P=apparent current at plate in $\mu A/cm^2$. i^+=positive ion current in $\mu A/cm^2$. i_3=secondary electron current due to positive ions in $\mu A/cm^2$. $\alpha=100i_3/i^+$. $i^-=i_P-i^+$. $\gamma=100i^-/i_P$.

Discussion

The measurements offer some inherent difficulties which unfortunately affect adversely the accuracy of the results. In general, the curves for helium were not as smooth or as consistent as those reported for neon.[3] The runs given in Table II are typical of results obtained during several months. The variations must be due to undetected changes in gas purity or in the surface condition of the electrodes caused by sputtering or by surface layers. This gives an indication as to the variations which may be anticipated under conditions which appear to be excellent as regards the present best technique of gas and electrode purification.

The values of α (8 to 20) found in helium (Table II) were about the same as those reported for neon[3] (14 to 20).

The values of γ (Table II) found by the second method were in general considerably higher than those found by the first method (Table I). However, the electrostatic field which existed between the edge of the sheath and the plate P was such that the effective size of the hole in P was less than its measured size, as can be seen from the following argument.[11] Consider the edge of the sheath S above P as a plane at zero potential emitting positive ions of zero velocity at a definite uniform rate. The points of plate P (at, say, -100 volts) are therefore the termini of the lines of force beginning on S. These lines of force will be parallel, running perpendicular both to S and to P except at P in the neighborhood of the hole where the lines will spread as they approach P. The locus of the termini on S of the lines of force which touch the edge of the hole in P is then a circle of area A_1 smaller than that of the hole A_2. Charged particles of zero mass liberated at S would follow these lines, but since the positive ions have considerable mass, they will go along lines of less curvature. The area A_3 on S from which the positive ions will go through the hole A_2 in the plate is thus larger than A_1, but not as large as A_2. The error in i^+ introduced in this manner is obviously not inconsiderable, but unfortunately difficult to calculate exactly. The value of $i^-=i_P-i^+$ is thus larger than it should be and consequently γ also. The errors in the two methods are such that, if allowance be made, the values of γ would be more nearly the same.

The values of γ reported here for helium are of the same order as those found in neon.[3]

Since the work on neon[3],[12] was reported a number of papers on related problems have appeared. Massey[13] presented a theoretical paper on the extraction of electrons from metals by positive ions and metastable atoms. The theory of the effect is presented from the point of view of the Sommerfeld theory of metals and the analytic method of wave mechanics, and the conclusion is drawn that the mechanism assumed is adequate to account for the neutralization of positive ions and the emission of electrons by metastable

[11] Semenoff and Walther, *Die physikalischen Grundlagen der electrischen Festigkeitslehre*, Springer, p. 23, and Mott-Smith and Langmuir, Phys. Rev. **27**, 760 (1926).

[12] For references to older work see Langmuir and Compton, Revs. Mod. Phys. **2**, 175–181 (1930), Sections 8 and 9.

[13] Massey, Camb. Phil. Soc. Proc. **26**, 386–401 (1930).

atoms. Langmuir and Found[14] report some interesting experiments on the production by resonance radiation in neon of metastable atoms which in turn eject electrons. An arc was run in a small portion of the total length of a long tube. Metastable atoms were produced considerably beyond the end of the arc as shown by secondary electron emission from electrodes. Similar emission from the walls left them positively charged. The metastable atoms from the discharge fall off $1/e$th for each 0.4 radius of the tube along the tube, so that metastable atoms from the discharge did not produce the effect. A shutter in the tube also showed that metastable atoms were produced at the end of the tube by something which traveled in straight lines, i.e., light. Kenty,[15] on the other hand, is of the opinion that in neon under conditions similar to those obtaining in Langmuir and Found's experiment,[14] the preponderance of the emission is attributable to the direct photoelectric action of the resonance radiation (about 700A) on the electrodes. His electrodes consisted of a nickel disk which could be turned about an axis perpendicular to the axis of the tube so that its plane could be placed either parallel or perpendicular to the axis of the tube, and a gauze cylinder surrounding it. The main discharge was maintained at another part of the tube some centimeters away. The disk was made negative, and the current collected was several times greater when the disk was perpendicular to the axis of the tube than when it was parallel, indicating direct photoelectric action rather than the effect of metastable atoms produced near the electrodes by the resonance radiation. In each of these experiments, since the electrodes were at a considerable distance from the discharge, the effect of positive ions was small. As has been mentioned above, the method used in the experiments reported here and previously in neon[3] does not permit a distinction between the photoelectric effect and that of metastable atoms.

Penning[16] has continued his experiments on the liberation of electrons from metal surfaces by positive ions. In neon he finds $\alpha=3$ to 5 for ions of zero velocity on degassed tungsten. This is somewhat lower than that (about 7) found last year in this laboratory for neon on nickel.[3] Penning has also used ions of velocity (500 volts) much higher than those used here, and reports $\alpha=20$ for tungsten in neon and $\alpha=32$ for tungsten in the presence of mercury.

Güntherschulze[17] in some work on the liberation of electrons from copper by positive ions at low gas pressure has used a method which involves the measurement of the heat delivered at the electrode. However, there was no possibility of distinction between secondary electron emission due to positive ion bombardment and that due to the impact of metastable atoms or to the photoelectric effect. His results, as far as they go, coincide with those presented here.

In conclusion the author wishes to thank Professor Karl T. Compton of the Massachusetts Institute of Technology, Professor Louis A. Turner of Princeton University and Dr. W. Uyterhoeven of N. V. Phillips Lamp Works, Eindhoven, Holland, for their assistance and advice.

[14] Langmuir and Found, Phys. Rev. **36**, 604 (1930).
[15] Kenty, Phys. Rev. **38**, 377 (1931).
[16] Penning, K. Akad. v. Wet. Amst. Proc. **33**, 841–857 (1930).
[17] Güntherschulze, Zeits. f. Physik **62**, 600–606 (1930).

SCATTERING OF HIGH VELOCITY ELECTRONS BY THIN FOILS

By H. V. Neher
Norman Bridge Laboratory, California Institute of Technology

(Received August 25, 1931)

Abstract

With a narrow, homogeneous beam of electrons, scattering by thin foils of aluminum, silver and gold has been investigated. Voltages up to 145 kv ($\beta=0.63$) were used. Under conditions where single scattering was predominate and secondary electrons were absent, the amount of scattering was studied as a function of the primary energy, atomic number and angle. Absolute values were also obtained. The above investigations have lead to the following results: (1) Secondary electrons are defined and a means of eliminating them is proposed and used. (2) Wentzel's criterion for single scattering is tested over a wide range of energies. The value of $\theta/4\omega_{\min}$ for aluminum is found to increase from 3.3 at 45 kv to 6.1 at 145 kv. (3) A more critical criterion for single scattering by thin foils is obtained which depends on the shape of the curve connecting ρ, the amount of scattering, with angle. (4) Dependence of scattering on energy of primary beam is found to agree well with either Mott's equation or with the relation k/V^2, but is at variance with the classical relativistic theory. (5) Comparison of values of scattering for aluminum, silver and gold shows that ρ increases faster than Z^2. (6) Scattering is obtained as a function of angle from 95° to 173°. For aluminum the dependence found experimentally agrees well with either Mott's or Rutherford's equation. The latter also gives the correct dependence on angle for silver and gold. Mott's equation is not applicable for these heavy elements. (7) Absolute values of scattering for aluminum compared with theory give $\rho=1.32$ of the value given by Mott's equation. This relation is valid within the ranges $\theta=95°$–$173°$, $V=56$–145 kv. (8) Secondary electrons coming from the foil are distributed according to the simple cosine law. (9) No evidence of loss of energy due to radiation is found up to one-half the energy of the primary beam.

Introduction

THE experimental study of scattering of high velocity electrons by atomic nuclei is far more difficult than the corresponding problem using α-particles. At least three fundamental complications are encountered when electrons are used for the bombarding particles. First, the relativity change of mass of the electron becomes increasingly important at energies above 40,000 volts. Second, secondary electrons emitted by the scatterer are indistinguishable from the primary electrons scattered by the nuclei. Third, effects due to loss of energy of the primary electron through radiation may be important for the light elements and large angles.

Investigations on scattering of high velocity electrons have been made with both β-rays and cathode rays. Chadwick and Mercier[1] using radium E as a source of β-rays obtained approximate agreement with the classical,

[1] Chadwick and Mercier, Phil. Mag. 50, 208 (1925).

theoretical prediction that the amount of scattering should increase with the square of the atomic number. Comparison of absolute values with Darwin's classical relativistic equation showed the experimental results to be 25 percent too large. However, a lack of homogeniety of the β-rays together with the difficulties encountered from the γ-rays make scattering experiments with radioactive sources unreliable. Schonland,[2] using cathode rays with energies up to 79 kv obtained agreement with Darwin's theory for absolute magnitude of the scattering as well as a correct dependence upon energy and atomic number.

Because of the lack of sufficient and accurate data and the increased theoretical interest in the problem, the following more extended investigations were undertaken.

Theories of Nuclear Scattering

Rutherford's equation giving the probability of an α-particle of mass m and charge $2e$ being scattered within the solid angle $d\omega$ at an angle θ to the original direction of motion by a nucleus of atomic number Z may be written as follows:

$$d\rho = \frac{ntZ^2e^4}{m^2v^4}\operatorname{cosec}^4\frac{\theta}{2}\,d\omega, \tag{1}$$

where n is the number of nuclei per cm^3, t is the thickness of matter traversed and v is the velocity of the particle. This equation does not include a relativity correction and is not applicable in the case of high velocity electrons where β is large.

Darwin[3] has calculated the orbit of a high velocity electron in the field of a heavy positive nucleus, taking into account change of mass as the electron passes the nucleus. He arrived at the result that if the electron comes within a certain critical distance p_0 it will spiral in and be absorbed by the nucleus. This can have no physical meaning since no transmutation of the elements is observed. Using Darwin's result, Crowther and Schonland[4] deduced the angular distribution of the electrons scattered by nuclei, neglecting those which spiraled into the nucleus. The value for the scattering between 90° and 160° for Al, Cu and Ag found experimentally by Schonland[5] agreed well with that deduced from Darwin's orbits. Later Schonland[6] showed that these spiralling electrons could not be neglected in his case and in order to get a solution to the problem he assumed that they emerged uniformly in all directions. This gave a result at variance with his experimental work.

The equation of Crowther and Schonland, both in the original and in the latter form given by Schonland, gives a dependence on β and θ as well as an absolute magnitude not found in this work. There is also some confusion as

[2] B. F. J. Schonland, Proc. Roy. Soc. **A113**, 87 (1926–27).
[3] C. J. Darwin, Phil. Mag. **25**, 201 (1913).
[4] J. A. Crowther and B. F. J. Schonland, Proc. Roy. Soc. **A100**, 526 (1921–22).
[5] Reference 2.
[6] B. F. J. Schonland, Proc. Roy. Soc. **A119**, 673 (1928).

to the form of the correction to be applied.[7] In addition, from considerations of wave mechanics, it appears quite clear that we can no longer regard the electron as a point when the distances of approach become of the order of h/mv, the wave-length to be associated with the electron. Comparison of Darwin's relativistic scattering equation with experiment is given in Table IV. It will be noticed that the relative as well as the absolute magnitudes do not agree over a wide range of energies. Consequently we shall not consider this theory further.

Perhaps the best treatment of the problem has been given by Mott[8] who uses Dirac's wave equation which includes corrections for both relativity and spin. The result arrived at may be expressed as

$$d\rho = \frac{ntZ^2e^4}{4m_0^2c^4}\left(\frac{1-\beta^2}{\beta^4}\right)\left[\operatorname{cosec}^4\frac{\theta}{2} - \beta^2\operatorname{cosec}^2\frac{\theta}{2} + \beta\pi\frac{2\pi e^2}{hc}Z\frac{\cos^2\theta/2}{\sin^2\theta/2} + \text{terms in}\left(\frac{2\pi e^2}{hc}Z\right)^2\right].$$

For the angles θ_1 and θ_2 this becomes,

$$\rho = \frac{\pi ntZ^2e^4}{m_0^2c^4}\left(\frac{1-\beta^2}{\beta^4}\right)\left[\cot^2\frac{\theta_1}{2} - \cot^2\frac{\theta_2}{2} - 2\beta^2\log\frac{\sin\theta_2/2}{\sin\theta_1/2} + \frac{2\pi\beta Z}{137}\left(\sin\frac{\theta_1}{2} + \operatorname{cosec}\frac{\theta_1}{2} - \sin\frac{\theta_2}{2} - \operatorname{cosec}\frac{\theta_2}{2}\right) + \cdots\right]. \quad (2)$$

The quantity ρ in this equation gives the ratio of the number of electrons scattered between the angles θ_1 and θ_2 to the total number of electrons incident on the scatterer.

Description of Apparatus

The apparatus in general is similar to that used by Schonland[9] for studying the same problem. A general view of the apparatus is shown in Fig. 1.

The electron "gun".

All metal parts were turned from copper. This metal has the advantages of being nonmagnetic as well as having a low vapor pressure. To eliminate the possibility of cold emission all metal parts were given two coats of nickel, then plated with chronium and finally given a very high polish. Metal to glass seals were used throughout. This eliminated entirely waxes and greases and made possible the attaining of a high vacuum in a minimum time. The metal shield extending back over the cathode was designed to protect the glass. No difficulty was experienced when working at 145 kv after the tube had been outgassed by continuous operation at lower voltages.

The filament was of the concentrated type wound with 10 mil tungsten

[7] E. E. Rutherford, Radiation from Radioactive Sources, 225 (1930).
[8] N. F. Mott, Proc. Roy. Soc. **A124**, 425 (1929).
[9] See reference 2 and B. F. J. Schonland, Proc. Roy. Soc. **108**, 187 (1925).

wire in the form of a helix and bent back on itself. This type was found to give a more intense beam finally emerging into the scattering chambers than that given by a number of other designs constructed. The position of the filament in relation to the end of the metal tube in which it was situated had to be adjusted very accurately to secure a maximum of current. It was also found that

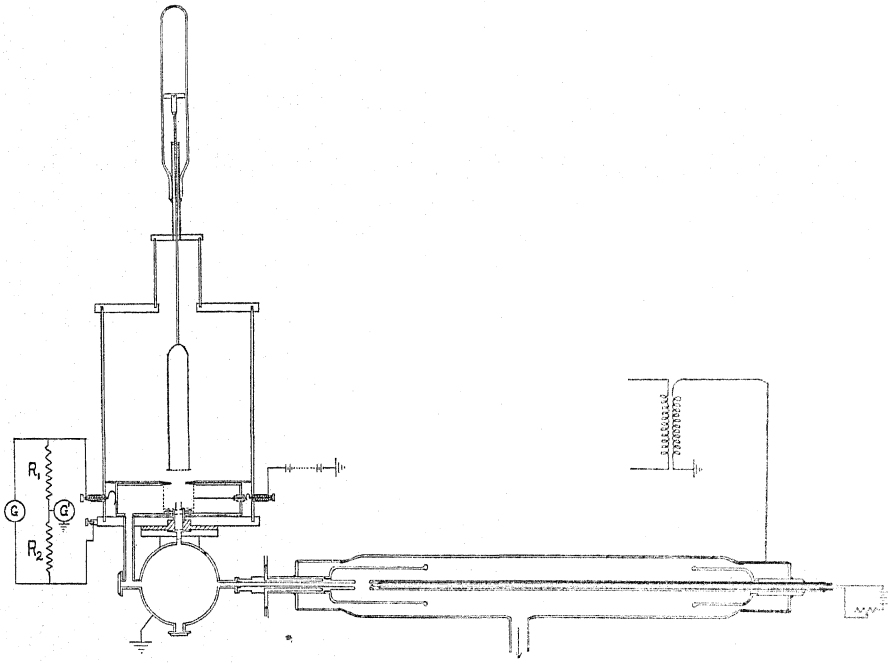


Fig. 1. Cross-section of apparatus showing electron-gun, solenoid, scattering chambers, method of varying angle and electrical connections.

a resistance of several hundred thousand ohms, placed between the filament and the metal tube surrounding it, increased the focusing action of the electric field between the cathode and anode and very materially strengthened the current received into the scattering chambers for a given total emission.

The solenoid.

This consisted of a brass cylinder 13 cm in diameter and 50 cm long wound with two layers of copper wire 1.63 mm in diameter. A section 10 cm long in the middle of the cylinder was partitioned from the remaining and could be evacuated with the rest of the apparatus. Each end of the solenoid was water cooled. Special precautions were taken to eliminate all magnetic substances in the neighborhood of the solenoid, since the maximum field was only 250 gauss.

As the solenoid was used not only as a means of obtaining a homogeneous beam but also for measuring the voltage of the electrons, it was necessary to know its constant. For an electron bent in a magnetic field,

$$(H\rho) = \frac{m_0 v}{e(1-\beta^2)^{1/2}},$$

while the energy of the electron after falling through a potential V is,

$$Ve = m_0c^2\left(\frac{1}{(1-\beta^2)^{1/2}} - 1\right).$$

Eliminating β between these two equations,

$$(H\rho)^2 = \frac{1}{c^2}\cdot\frac{2m_0c^2}{e}\left(V + \frac{e}{2m_0c^2}V^2\right).$$

At low voltages,

$$(H\rho)^2 = kI^2 = k'V.$$

The relation between high and low voltages can then be written in terms of the respective currents in the solenoid as,

$$I^2 = \frac{1}{K}(V + 0.982 \times 10^{-6}V^2) \tag{3}$$

where $K = V/I^2$ for low voltages. V has been expressed in volts, I in amperes and the values of the constants inserted. The quantity K will be defined as the constant of the solenoid. Calibrations were made at high voltages with a standard sphere gap and by an electrical deflection method. The two methods gave results agreeing to within 1/2 percent. The constant obtained was,

$$K = 737 \pm 3 \text{ volt amp.}^{-2}.$$

Scattering chambers.

The arrangement of the scattering chambers can best be described by referring to Fig. 2. The purpose of using chambers of such large diameter

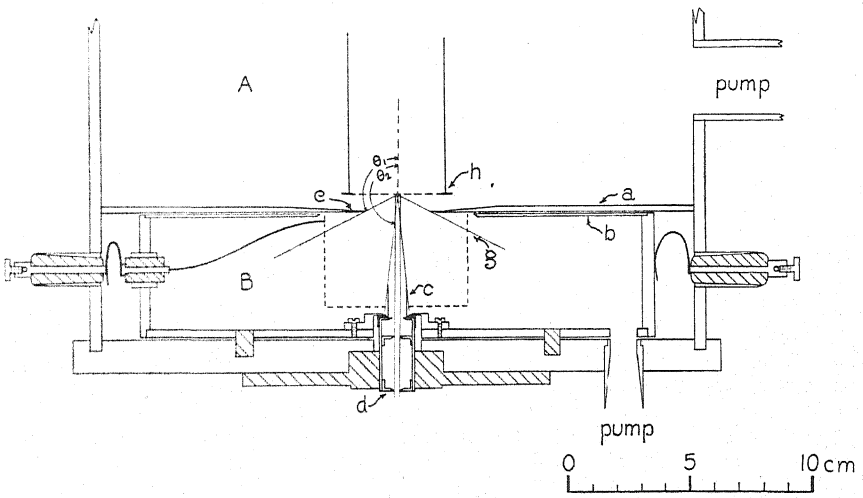


Fig. 2. Enlarged view of lower scattering chamber showing the relations of scatterer, grid and collector. The angles between which the scattered electrons were collected are also shown.

(20 and 25 cm) was to eliminate as far as practical the effect of reflected electrons going from one into the other. When the inside was brass the reflection

from the upper into the lower chamber amounted to 0.0003–0.0009 of the main beam. When the whole inside was lined with aluminum this value was reduced to 0.0001–0.0003.

The electrons were admitted from the solenoid into the scattering chambers through four collimating openings made of aluminum which were all grounded. The first three openings were 2.8 mm in diameter and the last was 4 mm. The purpose of this last opening was to stop scattered electrons from the openings below entering the lower chamber. The small, thin aluminum cylinder c was fastened to d and extended up into B a distance of 1.8 cm. It performed two functions: (1) it further prevented stray electrons from the openings below reaching B, and (2) it definitely fixed the larger angle of scattering.

Chamber B was insulated from A by thin (0.05 mm) mica disks. The metal disks a and b were fastened to A and B respectively. A thin aluminum ring 0.015 cm thick, 0.8 cm wide, with a 2.83 cm opening in its center formed the final separation between A and B. The disk b had an opening in it slightly larger than the grid g. This was found necessary since many electrons collect in the space within the grid and part of them would be collected by B if b extended beyond the edge of g.

Grids to stop secondary electrons.

For investigating secondary electrons up to 2000 volts, a wire grid was constructed. It consisted of a 4 mm mesh cylindrical framework made of 2

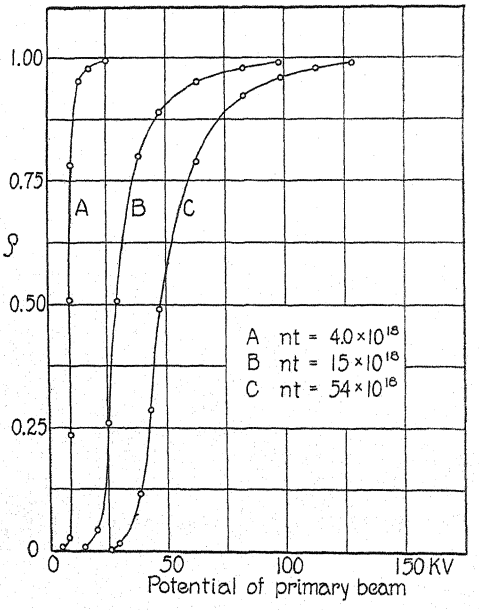


Fig. 3. The stopping power of aluminum foils of different thicknesses. The "range" may be obtained approximately from the lower knee of the curve.

mil nickel wire. The ratio of wire to total space was 0.025. The reflection coefficient of nickel is 0.30, hence a correction of 1.6 percent was applied to the readings when this grid was used.

When secondary electrons with energies greater than 2000 volts were investigated, because of the ionization currents produced and the attendant insulation difficulties, other means were resorted to than that of using actual potentials. Such a means was furnished by thin foils. Referring to Fig. 3 it will be noticed from the curve for aluminum connecting ρ (the ratio of transmitted electrons to the total number incident) with the voltage of the primary beam, that no electrons are transmitted up to a certain voltage after which there is a sudden increase. At voltages ordinarily used, from 90 to 145 kv, even a piece of aluminum 0.01 mm thick is very transparent and at the same time acts as an equivalent stopping potential of 50 to 55 kv. A small correction for voltages below 120 kv can be applied to account for those electrons scattered elastically which are stopped by this foil if it is used as a grid to stop secondary electrons. Although such foils do not form a barrier as perfect as would be furnished by an actual stopping potential, they do afford a means

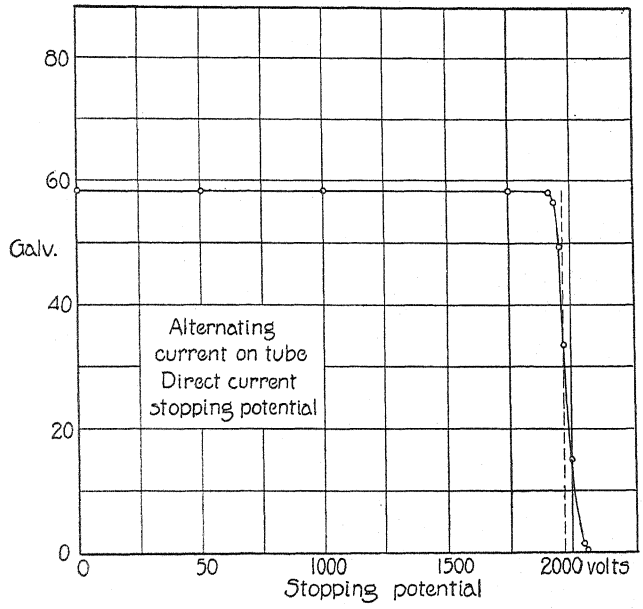


Fig. 4. Homogeniety of electron beam shown by applying D. C. stopping potentials. Dotted line represents computed voltage from known constant of solenoid.

of obtaining equivalent stopping potentials with an accuracy sufficient for the problem under consideration. This will appear more clearly in what follows.

Secondary electrons will also be set free from the foil grid on the collector side by the electrons which go through. To investigate this point a fine wire grid was placed around the foil grid and a stopping potential of 2000 volts applied. A decrease in the current received in B of 1 to 2 percent was found if the primary voltage was of the order of 50 kv, but for 100 kv the effect decreased to 0.3 to 0.4 percent. When necessary this correction was applied to the readings.

A means is thus provided by which secondary electron velocities up to

one-half the energy of the initial beam can be investigated. Reasons will be given later why one-half the energy of the initial beam is the upper limit to the energies of the secondary electrons.

Method of varying angle.

The foil acting as the scatterer was mounted on a thin metal ring, h, 3 cm in diameter, supported by a nickel wire 0.6 mm in diameter. The whole could be raised and lowered by means of a magnetic control as shown in Fig. 1, The height of the foil above the opening e could be measured to within 0.008 cm. The screw on the control mechanism was calibrated with a traveling microscope. The angles between which the electrons were collected were determined by the size of the openings c and e and by the height of the foil.

Homogeniety of beam.

The homogeniety of the beam for the case of alternating current applied to the tube was tested with d.c. stopping potentials. The result is shown in Fig. 4. Such a test was desirable since an alternating current transformer was used as a source of high voltage. The dotted line in the figure represents the voltage of the electrons computed from the constant of the solenoid. It will be noticed that the distribution of energies is almost symmetrical about the computed value. If $\pm\Delta V$ represents the heterogeneity of the beam, then if each side of the true value is considered, (cf. Eq. (1))

$$\rho' = \frac{k}{(V+\Delta V)^2} = \frac{k}{V^2}\left(1 - \frac{2\Delta V}{V} + \cdots\right)$$

$$\rho'' = \frac{k}{(V-\Delta V)^2} = \frac{k}{V^2}\left(1 + \frac{2V}{V} + \cdots\right)$$

$$\frac{\rho' + \rho''}{2} \doteq \frac{k}{V^2} = \rho.$$

If the beam of electrons is symmetrical about a mean voltage given by the constant of the solenoid, this same reasoning will apply to all $\pm\Delta V$'s and if the spread of voltage is not more than 5 percent on either side, the error introduced into the experimental results due to the lack of homogeniety will be negligible.

Determination of nt.

It was soon found that the variations in the thickness of the foils were too great to permit weighing a large sheet of the material and computing the average value of nt. Consequently a quartz torsion balance which had a constant of 0.1214×10^{-6} gm/div. was constructed. The constant was determined by weighing small sections of very fine wire a long piece of which had been previously weighed on an analytical balance. Aluminum foils 5×10^{-5} cm thick and 3 mm square could be weighed to 1 percent.

If m is the mass of a piece of foil of area A, then the product nt is given by: $nt = 6.06\times10^{23}\, m/MA$, where M is the atomic weight of the element compos-

ing the foil. The value of nt which enters directly into the scattering equation, is independent of the density of the material. Since that portion of the foil where the beam passed through was cut out and weighed, local variations in uniformity should not introduce a large error if the beam were uniform. This point was tested with the thinnest foils by rotating the foil one turn and taking readings every 45°. Variations of not more than 2 percent were observed while the average variation was 1 percent.

Experimental Procedure

The current in the solenoid was set and kept at a constant value while the voltage of the electron beam was increased until a maximum current came through into the scattering chambers as indicated by the galvanometer G'. (See Fig. 1). R_2 was kept constant at 10^4 ohms and R_1 adjusted until G read zero deflection. A change of resistance in R_1 of 0.1 ohm would give a deflection of G of approximately 5 mm. Since R_2 was 10^4 ohms, changes in ρ of 1 part in 10^6 of the main beam could be detected. When a balance of G was obtained, the drop in potential across R_2 was the same as that across R_1 and the apparent value of scattering within the given angles was then given by,

$$\rho = \frac{R_1}{R_1 + R_2}.$$

To this value of ρ several corrections must be applied.

1. A correction for the value of ρ when no foil was present. It varied with the height of the ring h, the kind of foil used as a stopping potential and the potential of the primary beam. This "zero correction" was checked at various times. A typical selection of values is given in the table below for a foil with an equivalent stopping potential of $-27{,}000$ volts.

Table I.

V	θ_1	θ_2	ρ (correction)
68.9 kv	95°10′	172°5′	0.00022
96.9	95°10′	172°5′	0.00026
129.0	95°10′	172°5′	0.00028
145.0	95°10′	172°5′	0.00030

This "zero correction" is to be subtracted from the apparent value of ρ.

2. A correction for the wire of which the grid was constructed. It amounted to 0.8 percent for the foil covered grids and 1.6 percent for the fine mesh wire grid. This correction is to be added.

3. A correction for the stopping power of the foil grids for elastically scattered electrons. This was obtained from Fig. 3 and amounted at most to only a few percent. This is to be added.

4. A correction for the reflection out of chamber B and for the absorption by the foil grid of electrons reflected from the walls of B. Two experimental methods could be used to determine the magnitude of these two effects. (1) The dimensions of the scattering chamber could be increased and an extrapolation to an infinitely large one made; or, (2) the chamber could be lined

with different metals of known reflection coefficients and an extrapolation to zero reflection made. The latter method was chosen as the more practical. Consequently, the reflection coefficients of aluminum and brass were determined as well as the angular distribution of these reflected electrons. The ratio of the coefficients for aluminum and brass is $0.13/0.29=0.45$. A typical example showing the effect of lining the chamber B with brass and aluminum is given below:

Metal	V	θ_1	θ_2	V_s	ρ
Al	96.9 kv	108°	173°	−27 kv	0.001260
Brass	96.9 kv	108°	173°	−27 kv	0.001253

The effects increased slightly for lower voltages and decreased for higher voltages. In most cases the correction was negligible.

When the foil grid was used it was connected electrically to chamber A. This was necessary since B was to collect only those electrons scattered elastically while A was to collect all others. Secondaries emitted from the foil or other parts of A subtracted in one place but added in another so that the net result was nil.

Results

Secondary electrons.

It is of great importance to eliminate the effect of secondary electrons if nuclear scattering is to be studied. When stopping potentials are applied to the electrons coming from a thin metal foil which is being bombarded with a homogeneous beam of high velocity electrons, it is found that the electrons so emitted have a wide distribution of energies. A large number have energies below 100 volts, but an appreciable number, compared with the electrons which have been scattered elastically, have much higher energies. It is necessary to determine how high a stopping potential must be applied to stop all secondary electrons and still not stop those scattered elastically.

Secondary electrons have been defined by other investigators in various ways. Becher[10] and Stehberger,[11] working at energies below 12,000 volts defined as secondary electrons all those with energies below 36 volts. Wagner[12] defined all electrons coming from the material bombarded as secondary. In this paper a different definition based upon the process of collision of two electrons will be adopted. It is well known that as a purely mechanical process, when two electrons collide, one of them being initially at rest, they part at an angle of 90° to one another. We shall distinguish them after collision by defining the one with the greater energy as the primary and the one with the lesser energy as the secondary.

It will be apparent from the above considerations that for a sufficiently thin foil, many secondary electrons formed in the center of the foil will have

[10] A. Becher, Ann. d. Physik **78**, 288 (1925).
[11] K. H. Stehberger, Ann. d. Physik **86**, 825 (1928).
[12] P. B. Wagner, Phys. Rev. **35**, 98 (1930).

sufficient energy to emerge. If stopping potentials equal to one-half the energy of the initial beam are applied it is certain that all secondaries are stopped and that the remaining electrons are those which have been scattered by nuclei alone.

The effect of applying successively higher stopping potentials to the electrons emitted by thin foils of aluminum bombarded with 128 kv electrons is shown in Fig. 5. The ordinate gives the ratio of the number of electrons penetrating the stopping potential (given by the corresponding abscissa) to the total number of primary electrons incident on the scatterer. The angles between which the scattered particles were collected in each case were 95° and 172°. The values of ρ given in Fig. 5 refer only to curve (a).

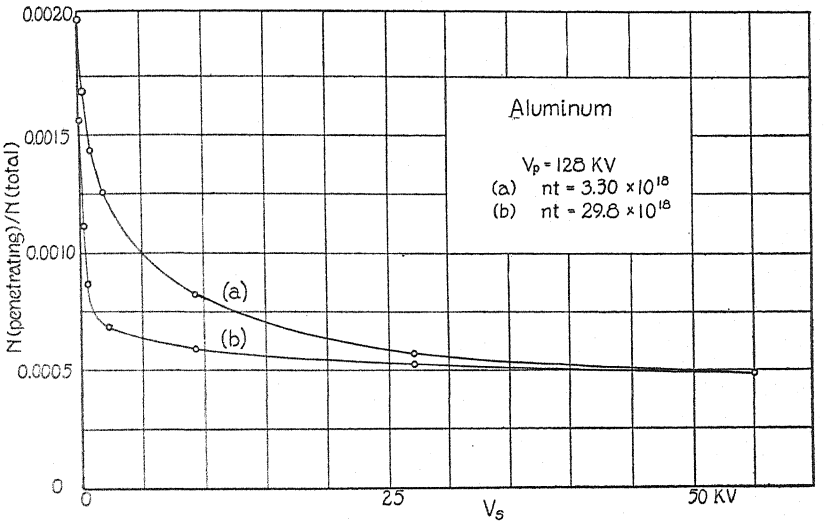


Fig. 5. Shows (1) that an appreciable number of secondary electrons are present from a thin foil at very high energies, (2) that secondary electrons are more important for a thinner foil. Curve (b) fitted to (a) at 55 kv.

The relative importance of secondary electrons for thin foils is greater than for thicker foils. This is shown in curve (b) where the foil was eight times the thickness of that used in obtaining curve (a). (b) is fitted to (a) at 55 kv. This difference of relative importance of secondary electrons may be explained by the greater probability of a secondary electron emerging from the thinner foil. In each case the probability of the nuclearly scattered primary electron emerging is practically 1.

It might be thought that the electrons stopped between 25 and 55 kv were those which had been scattered by the nuclei but which had gradually lost sufficient energy to other electrons in the foil so that they were stopped by a potential less than half their original value. If this were so one would expect the curve for the thicker foil to nearly coincide with the one for the thinner foil. It therefore appears that there are a few secondary electrons at very high energies, although they form an appreciable percentage of the total number collected.

It is interesting to note that Schonland used 150 volts stopping potential and assumed that all secondary electrons were eliminated.

Single scattering.

Experimentally if ρ increases linearly with nt single scattering is the predominating factor. The results of these tests are shown in Fig. 6. Wentzel[13] has

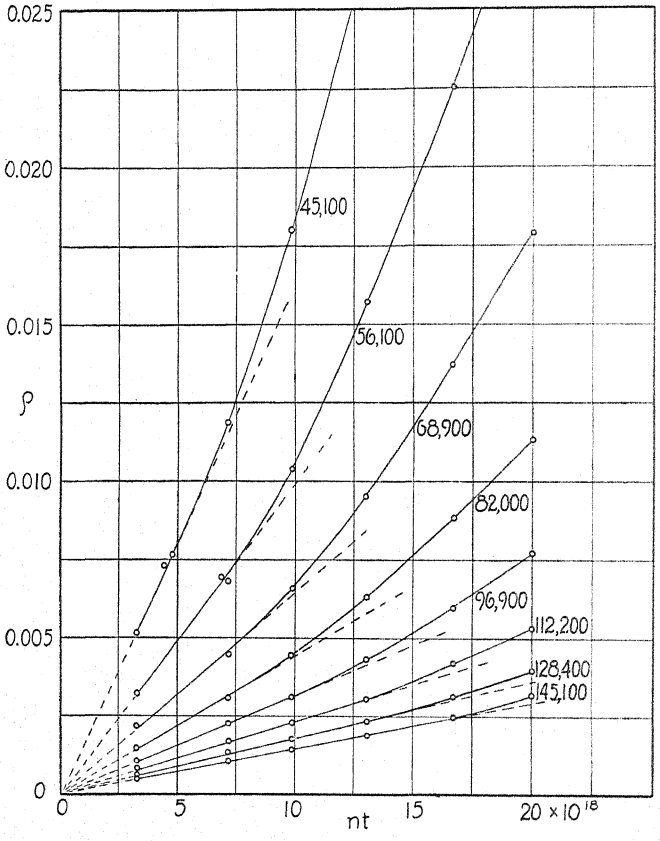


Fig. 6. Tests of single scattering—ρa nt. Angles: $\theta_1 = 95° 10'$, $\theta_2 = 172° 5'$.

obtained a criterion based on classical reasoning which must be satisfied for single scattering to be the predominating factor. It may be stated as follows: If

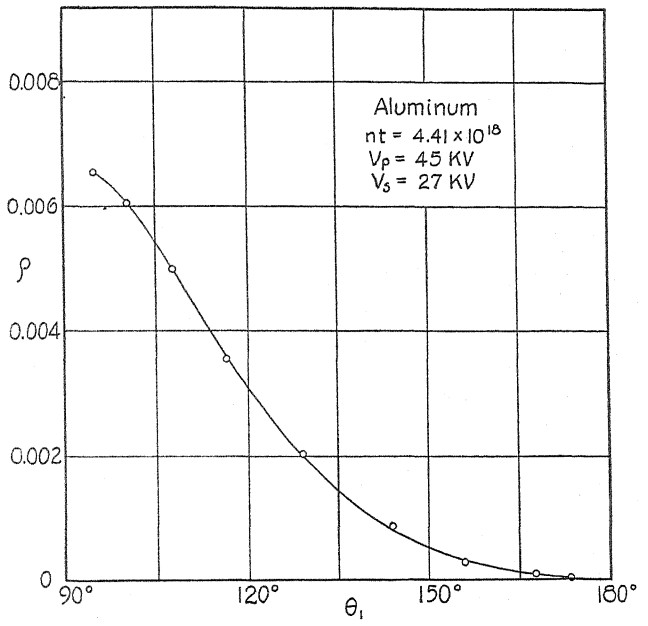
$$4\omega_{\min} = 8 \cot^{-1} \frac{2V}{Ze} \left(\frac{2}{\pi nt} \right)^{1/2},$$

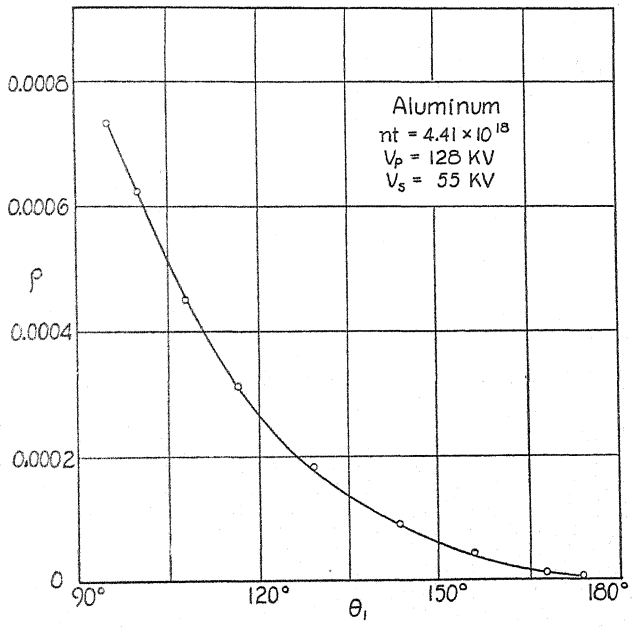
then for single scattering,

$$\frac{\theta}{4\omega_{\min}} = 3 \text{ or } 4.$$

If we apply Wentzel's criterion to the point where the curves depart from linearity in Fig. 10 we obtain the values given in Table II.

[13] G. Wentzel, Ann. d. Physik 69, 333 (1922).





Figs. 7 and 8. More accurate test of single scattering by thin foils. Hump in Fig. 7 disappears for $V_p > 90$ kv for a foil of this thickness as shown in Fig. 8.

TABLE II. *Aluminum.*

	$\theta_1=95°10'$	$\theta_2=172°5'$	
nt	V	$4\omega_{min}$	$\theta_1/4\omega_{min}$
6.0×10^{18}	45.0	28°56′	3.3
7.4	56.0	25°52′	3.7
8.3	68.9	22°40′	4.2
9.4	82.0	20° 0′	4.7
11.3	96.9	18°40′	5.0
13.2	112.5	17°20′	5.5
15.5	129.0	16°24′	5.8
17.6	145.0	15°36′	6.1

The factor $\theta/4\omega_{min}$ is not a constant but increases with the voltage. The value reported by Schonland is $\theta/4\omega_{min}=3.0$, which is for both 60 and 80 kv. Judging from the results given here this value is much too low.

A more accurate criterion for single scattering from a foil can be obtained experimentally from the shape of the curve showing the variation of ρ with angle. Near 90° a scattered electron emerging from the foil must go a greater distance through the metal than one coming out at larger angles, and the probability of a second collision is increased. This will have the effect of decreasing the slope of the curve near 90°. These plurally scattered electrons will be partially thrown into larger angles and will give the hump shown in Fig. 7, which is for 45,000 volts with a stopping potential of 27,000. Fig. 8, for the same foil ($nt=4.41\times10^{18}$) but a primary voltage of 128,000 and a stopping potential of 55,000, shows how the hump has completely disappeared. The shape of the curve for this particular thickness of aluminum foil remains unchanged from 90 to 145 kv. A necessary and sufficient condition for single scattering at angles from 90° to 180° when a foil is bombarded normally is that the curve connecting ρ with θ shall not change its shape when the primary potential is increased.

TABLE III. *Aluminum.*

$V_s=-27{,}000$ kv, $\theta_1=95°10'$, $\theta_2=172°5'$							
kv	56.1	68.9	82.0	96.9	112.2	128.4	145.1
$\frac{\rho}{nt}$	9.47	6.35	4.38	3.05	2.34	1.63	1.35×10^{-22}
	9.65	6.41	4.31	3.14	2.29		
	9.69	6.38	4.43	3.09	2.31	1.71	1.41
	8.70	6.31	4.17	2.97	2.31	1.72	
	8.92	6.12	4.38	3.10	2.28	1.73	1.35
av.	9.29	6.31	4.33	3.07	2.31	1.70	1.37×10^{-22}

An indication of the accuracy obtainable, using foils of such thickness in each case that single scattering was predominate, is shown in the following table for five different foils. The value ρ/nt should be constant for constant voltages, angles and atomic number. The stopping potential, V_s, in each case was 27,000 volts.

Dependence of scattering on energy of primary beam.

The variation of the amount of scattering for aluminum between the angles of 95°10′ and 172°5′ as a function of the energy of the beam is shown in Fig. 9. Plotted in the same figure are the relations k/V^2 and the relative values computed from Mott's equation, each being fitted to the experimental value at 56 kv.

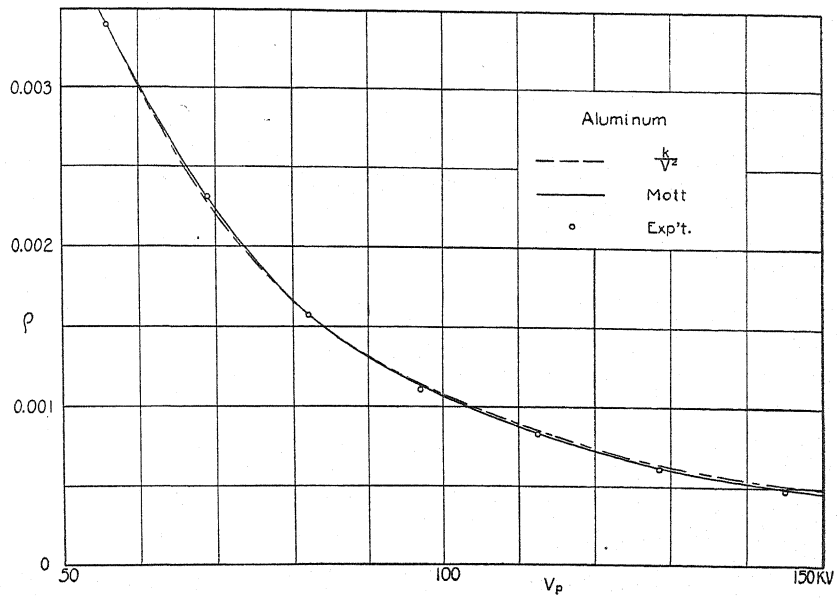


Fig. 9. Dependence of ρ upon energy of primary beam with appropriate stopping potentials in each case.

TABLE IV. *Aluminum.*

$nt=3.68\times10^{18}$		$\theta_1=95°10'$		$\theta_2=172°5'$	
β	V	Relative values of ρ			
		Exp	Mott	Darwin	k/V^2
0.436	56.1 kv	0.00340	0.00340	0.00340	0.00340
0.474	68.9	0.00231	0.00229	0.00241	0.00226
0.511	82.0	0.00157	0.00157	0.00178	0.00160
0.543	96.9	0.00110	0.00114	0.00134	0.00115
0.574	112.2	0.00082	0.00084	0.00104	0.00085
0.603	128.4	0.00061	0.00064	0.00088	0.00065
0.630	145.1	0.000485	0.000495	0.00077	0.000505
β	V	Absolute values of ρ			
		Exp	Mott	Darwin	Rutherford ($\alpha 1/V^2$)
0.436	56.1 kv	0.00340	0.00257	0.00460	0.00264
0.474	68.9	0.00231	0.00174	0.00326	0.00176
0.511	82.0	0.00157	0.00118	0.00242	0.00124
0.543	96.9	0.00110	0.00086	0.00182	0.00089
0.574	112.2	0.00082	0.00063	0.00141	0.00066
0.603	128.4	0.00061	0.00049	0.00119	0.00051
0.630	145.1	0.000485	0.000375	0.00104	0.00039

A comparison of the relative as well as the absolute values of ρ is given in Table IV. The following points should be noted: (1) The dependence on energy of beam given by Mott's equation and by the empirical relation k/V^2 agrees well with experiment, while the equation based on relativity correction of the classical theory does not agree. (2) Absolute values of scattering within the angles given do not agree with any of the theories. Rutherford's equation cannot be written proportional to $1/V^2$ above 30 to 40 kv. Mott's result is the one we shall consider most seriously. Comparing with the experimental values we obtain,

$$\text{Exp} = 1.32 \text{ Mott}$$

which represents the facts quite closely for aluminum. It will be shown later that Mott's equation also gives the correct dependence on θ. The above relation, then, is valid in the case of aluminum within the ranges, $V=56{,}000$ to 145,000 volts and $\theta=95°$ to 173°.

Dependence of scattering on Z.

In Table V the factor $\rho/ntZ^2f(\theta/2)$ is compared for Al, Ag and Au at $\theta_1=95°10'$ and $\theta_2=172°5'$ for $\beta=0.603$ and $\beta=0.630$. All the theories require that this factor should be a constant for all elements but it actually increases. Schonland also reports a value too high for gold and attributes it to an abnormal emission of secondary electrons. This explanation is hardly tenable for the results reported here because of the stopping potentials used. It may be pointed out here that Mott's equation applies best to the lighter elements and neglecting further terms in the expansion (see Eq. (2)) is scarcely justifiable in the cases of silver and gold.

TABLE V.

	$\beta=0.603$			$\beta=0.630$		
	Al	Ag	Au	Al	Ag	Au
Mott	1.52	1.77	2.41×10^{-24}	1.24	1.38	1.95×10^{-24}
Ruth.	1.18	1.65	2.50	0.94	1.19	1.77

In view of the fact that plural scattering contributed something to the value of ρ for the thinnest silver and gold foils (800A and 1200A respectively) it would be expected that the value would be high. Wentzel's criterion for both these elements gives $4\omega_{\min}=5.3$ at 128,000 volts. We should then expect mostly single scattering and the large values obtained for these elements must indicate that ρ increases faster than Z^2.

Dependence of scattering on angle.

C. E. Eddy[14] has studied the angular distribution of β-rays scattered by thin foils from 0° to 50° but under conditions where plural scattering was very prominent. Kemplerer[15] working with voltages between 10 kv and 40 kv

[14] C. E. Eddy, Proc. Camb. Phil. Soc. **25**, 50 (1929).
[15] Klemplerer, Ann. d. Physik **3**, 849 (1929).

found an angular dependence between 10° and 120° not given by any existing theory. The accuracy of this latter work, however, was probably insufficient to warrant conclusions. Certain definite angles have been used by other observers, but a consistent effort to obtain an accurate dependence on angle has not been made.

The dependence of scattering on angle found experimentally is well illustrated in Fig. 10 which is for aluminum. θ_1 is plotted as abscissa so that any ordinate gives the value of the ratio of the number of electrons collected between θ_1 and θ_2 to the total number of electrons incident on the foil. θ_2

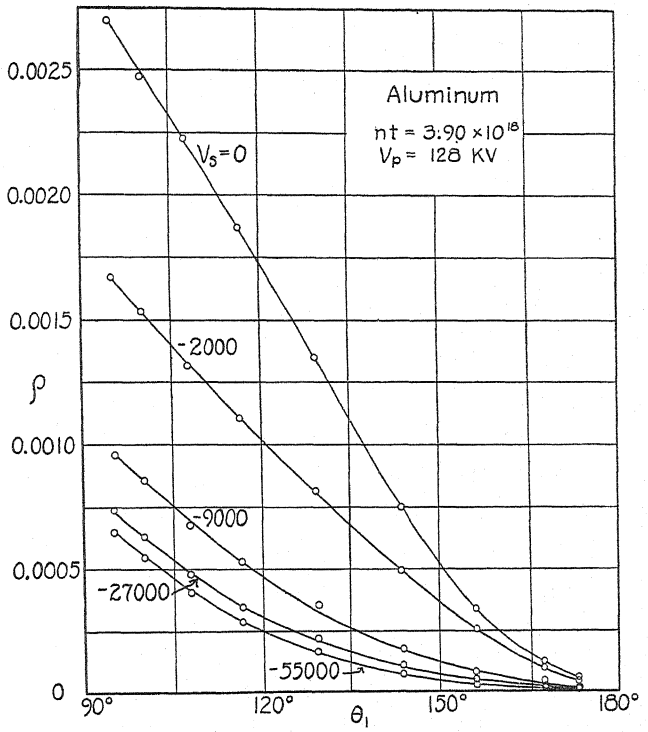


Fig. 10. Dependence of ρ upon angle. Shows effect of applying successively higher stopping potentials both on absolute magnitude and shape of curve.

varies from 172° when $\theta_1 = 95°$, to 178° when $\theta_1 = 173°$. The primary voltage for each curve is 128,000. The four curves plotted are for the stopping potentials given. In Fig. 11 plotted with values for $V_s = -55{,}000$ volts and fitted at 95°10′ is given the variation with θ from both Mott's and Rutherford's equations. All curves which have been obtained from 97 to 145 kv are very similar in shape to the one given in Fig. 11 if the proper stopping potential is applied. At voltages below 97 kv, the hump shown in Fig. 7 begins to appear for the thinnest foil available, and no comparison with theory based on the assumption of single scattering can be made. For sufficiently high voltages either the equation of Mott or Rutherford gives a dependence on θ between 95° and 173° which agrees well with experiment.

Similar curves have been obtained for gold and silver. The angular dependence for these two metals agrees well with Rutherford's $\cot^2 \theta/2$ relation but the agreement is not as good with Mott's equation. This deviation is probably due to the fact that, as mentioned before, neglecting further terms in the expansion is not permissible for the heavy elements.

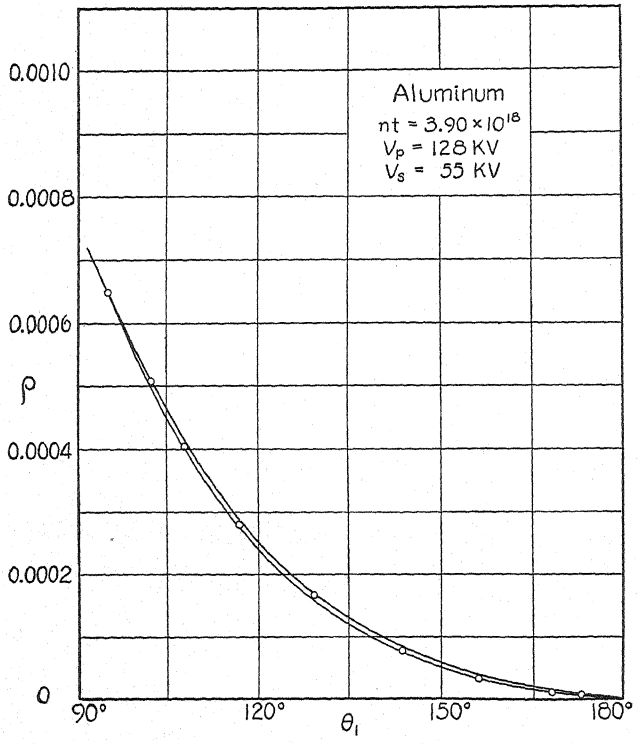


Fig. 11. Lowest curve of Fig. 10 compared with the angular distribution given by Mott and Rutherford. Theoretical curves fitted at 95°.

Angular distribution of secondary electrons.

To find the dependence on angle of the secondary electrons emitted between two energies, we need only to take the difference in ordinates of two curves for two different stopping potentials. Fig. 12 shows the result for aluminum taken from Fig. 10. It was found that the points agree very well with the curve $k'(\sin^2 \theta_1 - \sin^2 \theta_2)$. Since the second term in the parenthesis is small compared with the first this may be written as $k' \sin^2 \theta_1$. If this is differentiated with respect to θ and divided by $\sin \theta$ the result is $2k \cos \theta$, which represents the intensity of the secondary electrons at the angle θ. The following conclusions may then be drawn: The electrons that come from a thin foil when bombarded with high velocity electrons may be divided into two definite and distinct groups:

1. Those that are scattered without an appreciable loss of energy and have an intensity distribution given by either Rurtherford's $\text{cosec}^4 \theta/2$ law, or Mott's equation.

2. Those that come off with low velocities and have an intensity distribution given by cos θ. It is interesting to note that the cosine distribution is also obtained for the emission of electrons from solid surfaces.

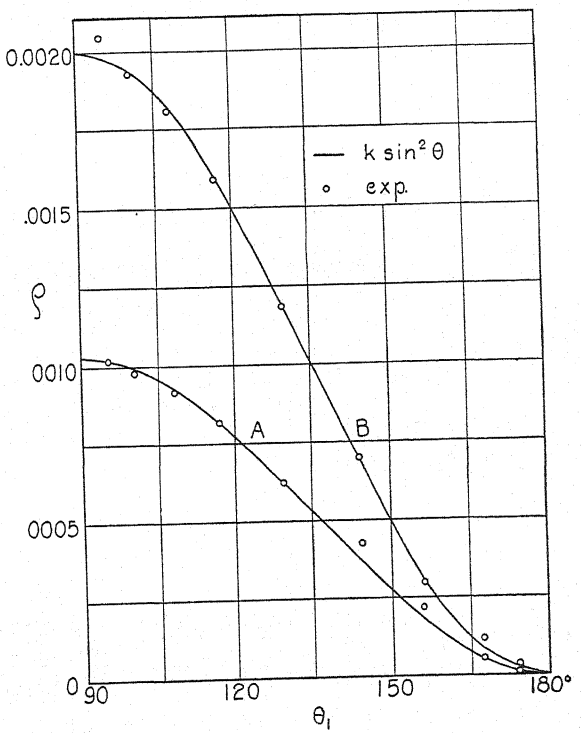


Fig. 12. Angular distribution of secondary electrons from a thin foil taken from Fig. 10. Curve A,0 to 55 kv, curve B,2 to 55 kv.

Effects Due to Radiation

When an electron is accelerated energy is lost due to radiation. The continuous x-ray spectrum is due to the hyperbolic orbits of the electron around the nuclei of the atoms composing the x-ray target. Some electrons will lose all their energy through radiation and these will give the short wave-length limit or the maximum frequency of the radiation emitted according to the relation of Duane and Hunt, $Ve = h\nu_{max}$. Kramers[16] has computed the amount of energy lost by an electron deflected through an angle θ upon the assumption that the orbit is not appreciably disturbed. He finds the expression,

$$R = \frac{4}{3}(\tfrac{1}{2}mv^2)\frac{\beta^3}{Z}\tan^5\frac{\theta}{2}\left[(\pi+\theta)\left(1+\tfrac{1}{2}\operatorname{cosec}^2\frac{\theta}{2}\right)+3\cot\frac{\theta}{2}\right].$$

For a 50,000 volt electron deflected through 90° by an aluminum nucleus, the relative amount of energy lost is ten percent according to the above relation.

Mott[17] has considered the effect of radiation forces on the angular distribu-

[16] H. A. Kramers, Phil. Mag. **46**, 826 (1923).
[17] N. F. Mott, Proc. Camb. Phil. Soc. **27**, II, 255 (1931).

tion of nuclearly scattered electrons. Although an exact solution is not obtained, he concludes that the correction to be applied to the scattering equation is an addition of not more than a few percent. However, until a more accurate calculation is made, especially to determine the dependence on angle, no definite conclusions can be drawn.

Qualitative tests may be made experimentally as follows:

1. For large angles it might be expected that many electrons have lost a large portion of their energy and that an appreciable number would be stopped by $-55{,}000$ volts if the original energy were 110,000. If this were true the curve showing the variation of ρ with θ would come close to the axis $\rho=0$ at large angles. No such effect is noticed.

2. Since light atoms 2, according to Kramer's equation cause a greater loss of energy than heavier atoms, we should expect a differently shaped curve connecting ρ and θ for aluminum and gold. Both elements follow the same law experimentally.

3. The relative loss of energy according to Kramers is proportional to β^3. We should expect, then, that for two widely different potentials with one-half the primary voltage used as a stopping potential in each case, we should get departures from scattering equations that are based on purely elastic scattering. No such departures are found.

What can be said, then, about the electrons that generate the continuous x-ray spectrum? There seem to be at least two possible explanations. Either, (1) The number losing one-half their energy or more is inappreciable compared with a given fraction of the main beam collected between 140° and 180°, or, (2) Momentum relations are such as to distribute over various angles those electrons losing energy.

Discussion of Errors

It is thought that the main error entering into the measurement of ρ experimentally came from an inaccurate knowledge of the "zero correction" when the foil was in place. The foil distributed the electrons going through in a different way than was the case when the "zero correction" was taken with the foil present. It is estimated that this error was not more than 1 or 2 percent; first, because of the small "zero correction" when the foil was absent, (about 0.0002 of the main beam), and second, because with a very thin foil, where the "zero correction" was comparable with the true value of ρ, the main beam was not scattered appreciably.

An analysis showed that the error due to the finite size of the beam and its slight divergence was negligible.

To make certain that no appreciable impurities of large atomic number were present in the aluminum foil used, some very pure aluminum from Siegbahn's laboratory was tested. The values of ρ/nt agreed to within 1 percent of those obtained with the foils regularly used.

The value of nt could be determined to 1 percent and the error in measuring the angle on the factor $\cot^2\theta_1/2$ was of the same magnitude.

It may, therefore, be concluded that the experimental error in the absolute

value of ρ for aluminum cannot be greater than 3 or 4 percent. For gold and silver the error may be slightly larger since only three and not five different foils were used for each in determining the final average values of ρ/nt.

Conclusions

Comparison with theory.

The experimental results when compared with existing theories may be summarized as follows:

1. Dependence on energy of primary beam: Either Mott's equation or the empirical relation k/V^2 gives good agreement within the range 56 to 145 kv.

2. Dependence on atomic number: According to Mott's equation, ρ increases faster than Z^2. This is found experimentally but the increase is not sufficient to give good agreement. All other equations give ρ proportional to Z^2.

3. Dependence on angle: Either Rutherford's or Mott's equation gives good agreement.

4. Absolute values of ρ: Within the ranges $\theta = 95°$ to 173°, and $V = 56$ to 145 kv, absolute values of scattering by aluminum are given by, Exp. $= 1.32$ Mott.

The classical relativistic result of Darwin as applied by Crowther and Schonland does not agree with the experimental values reported here, either in absolute magnitude or in its dependence on θ and β.

The difference in absolute magnitude between theory and experiment is the most outstanding discrepancy. The effect of a nuclear magnetic moment has been computed by Massey[18] and was found to be negligible. Also, it appears both from an experimental point of view and from Mott's theoretical investigation that radiative forces cannot account for the difference. The explanation must be looked for elsewhere. It might be expected that since the discrepancy becomes less for lighter elements, some information might be obtained by using hydrogen, helium and beryllium. It is planned to extend this work to the case of gases in the near future.

Comparison with other observers.

The absolute values of ρ for aluminum obtained in this paper are from one-half to two-thirds those obtained by Schonland. The results on silver and gold given here are from 0.7 to 0.8 of his values. It is quite apparent that the difference is mainly due to secondary electrons. A comparison with the work of Chadwick and Mercier can hardly be made since they used much smaller angles and an extrapolation is not permissable at this stage of experimental knowledge.

The writer wishes to take this opportunity to express his appreciation to Professor E. C. Watson who suggested the problem and who has continuously been interested in the work. His sincere thanks are also due Dr. R. A. Millikan for the personal interest he has shown.

[18] H. S. W. Massey, Proc. Roy. Soc. A127, 666 (1930).

THE CAPTURE AND LOSS OF ELECTRONS BY HELIUM IONS IN HELIUM

By Philip Rudnick
University of Chicago

(Received August 26, 1931)

Abstract

Mean free paths for capture (L_1) and loss (L_0) of electrons by helium ions in helium have been measured by a method whose chief novelty is the use of an ion source which gives quite strictly homogeneous velocities. In the range of velocities 0.6×10^8 cm/sec. to 1.0×10^8 cm/sec. L_0, reduced to 760 mm, is found to decrease from 21.5×10^{-4} cm to 8.6×10^{-4} cm and L_1 is practically constant at 1.2×10^{-4} cm. These results are compared to similar measurements by other observers, particularly with regard to the manner of dependence on velocity. The relation of the results to available information on ionization and energy loss is discussed.

INVESTIGATION of hydrogen canal rays has shown that there is a definite probability, varying with the velocity of the rays and with the nature of the gas through which they pass, that any proton in the beam may capture an electron[1,2,3,4,5,6] without appreciable loss of velocity.[2] The rapidly moving neutral atom thus formed may again lose an electron. If the beam traverses field-free space an equilibrium is established in which the numbers of charged and uncharged particles are in direct proportion to the probabilities of the changes which produce them. When fast alpha-particles penetrate matter similar interchanges occur between doubly and singly charged states.[7,8,9] At lower velocities the equilibrium shifts; the doubly charged ions disappear and neutral helium atoms appear. The present experiments are in this lower velocity range. They report probabilities for the interchanges between neutral and singly charged helium atoms in helium.

A simple quantitative theory of this phenomenon has been given by Wien[1] and more recently discussed by Rüchardt.[10] If a beam is initially composed of a fraction F_0 of neutral atoms and the remaining portion $(1-F_0)$ of ions, the fraction F of all the atoms which will be neutral at any subsequent point x in the path is given by

[1] W. Wien, Sitz. d. K. P. Akad. d. Wiss., July 1911, p. 773.
[2] J. Koenigsberger u. J. Kutschewski, Ann. d. Physik **37**, 161 (1912).
[3] A. Rüttenauer, Zeits. f. Physik **4**, 267 (1921).
[4] E. Rüchardt, Ann. d. Physik **71**, 377 (1923).
[5] H. Bartels, Ann. d. Physik **6**, 957 (1930).
[6] F. Goldmann, Ann. d. Physik **10**, 460 (1931).
[7] E. Rutherford, Phil. Mag. **47**, 277 (1924).
[8] G. H. Henderson, Proc. Roy. Soc. **A109**, 157 (1925).
[9] J. C. Jacobsen, Phil. Mag. **10**, 401 (1930).
[10] R. Rüchardt, Handbuch der Physik XXIV, p. 90.

$$F = F_\infty + (F_0 - F_\infty)e^{-(1/L_0+1/L_1)x} \tag{1}$$

where dx/L_1 and dx/L_0 are the respective probabilities for capture and loss of an electron by a particle in the distance dx and F_∞ is the equilibrium value approached by F, determined by

$$F_\infty = L_0/(L_0 + L_1) \tag{2}$$

L_1 and L_0 have the interpretation of mean free paths and are inversely proportional to the pressure. If the beam, originally neutral, traverses a path distance x along which a transverse electric field continuously removes all positive ions as they form, before there is time for them to return to the neutral state, the intensity decreases according to a simple absorption law depending only on L_0:

$$I = I_0 e^{-x/L_0}. \tag{3}$$

Preliminary Experiments

Some early experiments were performed with the apparatus shown in Fig. 1, of the type used by Rüchardt and earlier workers. Helium canal rays from a discharge tube were deviated through an angle of about five degrees

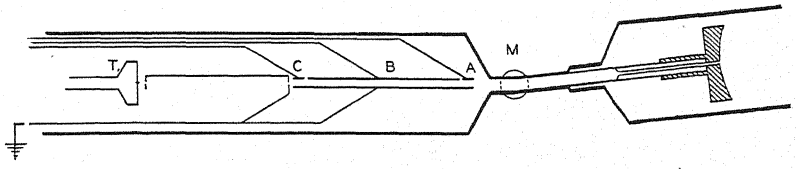


Fig. 1. Preliminary apparatus. M, magnetic field. A, B, C, deflecting condensers. T, thermocouple.

by the magnetic field M, from which ions of relatively homogeneous velocity proceeded to the thermocouple T, passing between the condenser plates A, B, and C. By applying deflecting potentials to these condenser plates one could remove all positive ions existing in the beam at one or both of the points A and C, or continuously over the path ABC. The relative reduction of intensity at the thermocouple was observed when a deflecting field was applied at A only, at C only, at C after A had previously been applied, and finally along B and C after A had previously been applied. Any two of these four measurements could be used to deduce values for the two independent parameters in Eqs. (1) and (3), that is to say F_∞ and $(1/L_0+1/L_1)$, or equivalently L_0 and L_1. This could be accomplished in many different ways varying in precision and convenience; in practice F_∞ and L_0 were most reliably and directly determined. In any event there remained two independent measurements with which to check the validity of the exponential relation (1), without recourse to determination of the variation of L_0 and L_1 with pressure, which is of course another important check.

The results were unsatisfactory in two respects. First, observations were not reproducible from day to day; fluctuations of from ten to fifteen percent in values of F_∞ and L_0 could not be eliminated, though attention was given

to careful electrical control of the discharge and to removal of traces of water and mercury vapors by repeated flaming of the tube. The second difficulty was a consistent indication, in each set of observations, of a departure from the behavior implied in Eq. (1) in the sense that F approached its ultimate value F_∞ more rapidly on the early part of the path, between M and A, Fig. 1, than later, between A and C. In other words, $(1/L_0+1/L_1)$ appeared to decrease along the path.

Since the resolution of velocities employed here was necessarily imperfect because of intensity limitations, it seemed that the remaining inhomogeneity was the most probable cause of the difficulties, and a strictly homogeneous source of ions was accordingly sought. Experiments with such a source are described in the following sections; the results there obtained were satisfactorily reproducible, and not significantly different from averages of the values obtained above. The second question, of deviations from the exponential law (1) is not definitely answered because the new apparatus was not adapted to a direct measurement of $(1/L_0+1/L_1)$.

Final Apparatus

The tube in which final measurements were made employed a source of homogeneous ions similar to that used by Batho and Dempster[11] in a study of the Doeppler effect, with which they obtained very sharp displaced lines, indicating homogeneity in velocity. Fig. 2 shows the arrangement. A low

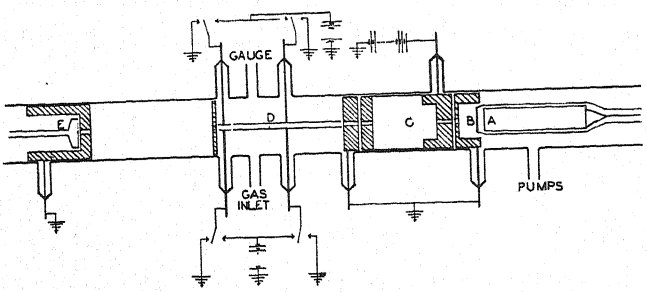


Fig. 2. Diagram of apparatus. A, anode. B, hot cathode. C, accelerating electrode. D, deflecting condensers. E, thermocouple.

voltage arc is operated between the hot cathode B, at ground potential, and the anode A, a hollow cylinder with open ends. Ions thus produced are drawn through the intervening diaphragm into electrode C, which is charged to a high negative potential. Within C many of the ions lose their charge; only these neutral atoms can proceed beyond the retarding field which exists between C and the succeeding grounded diaphragm. Thus a completely neutral beam enters the observation space, in which deflecting condensers D and thermocouple E follow the earlier arrangement except that the condenser A of Fig. 1 is omitted here.

[11] H. F. Batho and A. J. Dempster, to be published shortly in the Astrophysical Journal. Abstract, Phys. Rev. 37, 100 (1931).

The filament and anode at one end, and the thermocouple at the other, were carried on ground joints, permitting of convenient removal for visual alignment of parts within the tube. The entire path length from filament to thermocouple was 28 cm. The two condensers were 7.5 cm and 1 cm long, their plates about 3 mm apart. These plates were made of nickel gauze in such fashion as to minimize the possibility of specular reflection of ions to the thermocouple. All diaphragm openings were circular, of 2 mm diameter, except the one immediately in front of the filament, which was a half-millimeter larger.

The arrangement of the tube was such that the thermocouple was not exposed to direct radiation from any hot surface, the filament being located off the axis of the tube, and the anode hollow. Those parts which are cross-hatched in Fig. 2 were of solid aluminum of substantial thickness, and probably contributed materially to the adequate protection of the thermocouple from filament radiation. This consideration was important, since in operation the filament end of the tube became decidedly hot to the touch, while the thermocouple was sensitive to temperature changes of the order of 0.001°C. With the arrangement shown, any disturbance caused by the filament was less than that arising from variations in room temperature, and so gradual as to be unnoticed. The shield immediately surrounding the thermocouple protected it in large degree from short period fluctuations in room temperature.

The thermocouple itself was a single junction of a fine platinum wire and an extruded bismuth wire of diameter 0.01 inch. These two were spot-welded to a small piece of platinum foil of area about 1 mm^2 which served as a target for the impinging rays. The two outer ends were joined to the supporting wires with other strips of platinum foil. This couple was connected directly to a galvanometer of resistance 16 ohms and sensitivity 168 megohms.

Helium was purified by two passages through charcoal at liquid air temperature, the second time at low pressure immediately before use. Gas was streamed through the apparatus during all experiments, entering and leaving through liquid air traps. Pressures were measured with a McLeod gauge, also separated from the tube by a liquid air trap.

Storage batteries maintained the hot cathode arc and supplied potentials to the deflecting condensers. A steady accelerating potential was supplied to C, Fig. 2, by a high tension transformer with half-wave rectification, and a condenser in parallel. This potential was measured with an electrostatic voltmeter which had been calibrated against a micrometer sphere gap.

Measurements and Results

Determinations of F_∞ and L_0 were made at pressures between 0.007 mm and 0.070 mm of mercury, and with accelerating potentials between 7.5 kv and 21 kv. The lower limit of pressure was set by the decreasing number of ions formed in the arc. L_0 was determined from Eq. (3) by observing the intensity at the thermocouple with all condensers grounded and again with deflecting potentials applied to both the long and short condensers.

$1/L_0$ was proportional to the pressure at all pressures over 0.015 mm within an experimental uncertainty of about ten percent. At the lowest pressures $1/L_0$ appeared to be 30 to 40 percent higher than was to be expected from the linear relation at higher pressures. No definite explanation is offered for this result.The values at the lowest pressures were omitted from the averages, which are given in Table I, column 4, reduced to 760 mm pressure. The long condenser was considered to extend right up to the electrode C, Fig. 2, where the beam contained only neutral particles. Actually it failed to do so by about 15 mm. The error thus introduced is easily computed and was found to be negligible at all except the highest pressures, where the appropriate small corrections were applied to the data.

TABLE I.

1 Accelerating potential in kv	2 Velocity in cm per sec.	3 F_∞	4 L_0	5 L_1	6 $1/L_0$	7 $2/(L_0+L_1)$
21	1.00×10^8	0.87	8.6×10^{-4}	1.3×10^{-4}	1160	2000
15	.84	.90	10.5	1.2	950	1700
11	.72	.93	14.0	1.1	710	1300
7.5	.60	.95	21.5	1.1	460	880
5	.49		40		250	

The mean free paths are expressed in centimeters, reduced to 760 mm pressure, but uncorrected for temperature. The kinetic theory mean free path in helium at 760 mm and 300°A is 1.9×10^{-5} cm.

For the arrangement of potentials shown in Fig. 2 the beam approached equilibrium from an initial neutral state, for which $F_0=1$. It was also possible to allow a beam to come to equilibrium from an initial state consisting entirely of ions, for which $F_0=0$, by grounding electrode C and applying a high positive potential to all parts shown to the right of C in Fig. 2. F was measured, both for $F_0=1$ and for $F_0=0$, by observing the intensity at the thermocouple with the condensers grounded, and again with a deflecting potential applied to the short condenser only. The two values of F so obtained agreed within an experimental uncertainty of from one to two percent for pressures above 0.020 mm and were then considered to give the equilibrium value F_∞. At the highest pressures F showed small decreases attributable to the finite length of the short condenser. The following figures are the averages obtained for F_∞ at pressures between 0.020 mm and 0.030 mm: 0.86, 0.89, 0.90, 0.94 for the respective accelerating potentials 21, 15, 11, and 7.5 kv. When L_1 was computed by Eq. (2), taking F_∞ from above and L_0 from Table I, the results were somewhat irregular and too high to explain the differences observed between F and F_∞ at low pressures. It will be noted that very small changes in F_∞ give large variations in the computed value of L_1. It was found that the low pressure observations could be fitted by using the values of F_∞ given in Table I, which are higher than those given above by differences of a few percent, only slightly more than the experimental uncertainty. The figures for L_1 in the table, which follow

from the adjusted values of F_∞, have a relatively large uncertainty, so that the variation with velocity shown in the table is not at all positively established.

The adjustments made in F_∞ are in the same direction as, and less than, the correction for finite length of the short condenser considered by Rüchardt.[10] This correction is applicable when the condenser removes all ions formed between the plates as well as those which enter as ions. This could not be shown to be the case in these experiments. Curves of thermocouple intensity against deflecting potential showed approximate saturation below 500 volts, as was to be expected, but slight dependence of intensity on voltage persisted up to 2000 volts, as far as the observations were carried. Hence it appears that Rüchardt's full correction should not be applied.

The anode voltages in the arc were always less than 100 volts and the occurrence of doubly charged ions in the arc was considered improbable on the basis of experiments such as those of Bleakney.[12] Extrapolation of Rutherford's data for alpha-particles also indicates that doubly charged ions should be few in number at these velocities.

It was found necessary to use a weak magnetic field to protect the thermocouple from secondary electrons which were accelerated away from electrode C when it was negatively charged. Errors from this cause are present in preliminary data already reported.[13]

Observations with Argon

When these same experiments were tried with argon satisfactory intensity was not obtained at any pressure, and none at all above 0.02 mm. This was in marked contrast to helium, where an abundance of ions reached the thermocouple at all pressures up to the arcing point, about 0.2 mm. This suggests much stronger absorption by scattering in argon than in helium. This factor may enter in the results of Kallman and Rosen,[14] who have also observed greater absorption in argon than in helium. These workers ascribe the absorption to neutralization, but reference to a recent paper by Cox[15] will show that scattering is an equally tenable explanation. The absorption mentioned above, however, could not be attributed to neutralization, as neutral atoms and ions affect the thermocouple equally.

Good measurements were not obtained with argon, but the trials roughly indicated values for F_∞ about the same as in helium, and for L_0 one-half to one-fourth of the values for helium.

Discussion of Results

The results in Table I and similar measurements of other observers are plotted logarithmically as a function of velocity in Fig. 3. The free path for capture of an electron varies approximately as v^5 for the alpha-particles

[12] W. Bleakney, Phys. Rev. **36**, 1303 (1930).
[13] P. Rudnick, Phys. Rev. **37**, 1707 (1931), abstract.
[14] H. Kallmann and B. Rosen, Zeits. f. Physik **61**, 61 (1930).
[15] I. W. Cox, Phys. Rev. **34**, 1426 (1929).

(curve A), but shows no certain variation at all with velocity for the slower helium ions studied here (curve E). The measurements of Rüchardt and Goldmann (curves C and C') were made by very different experimental means and should therefore be compared with some caution, but if one accepts the indication that the free path for capture of an electron by a proton in hydrogen has a minimum in the region of 10^8 cm/sec., it is not surprising that the curve for helium should be nearly horizontal in this same region.

The free path for loss of an electron varies approximately as the inverse square of velocity for both hydrogen (curve D) and helium (curve F) at the lower velocities, but increases with velocity for the singly charged alpha-particle (curve B). This contrast probably corresponds at least roughly to the

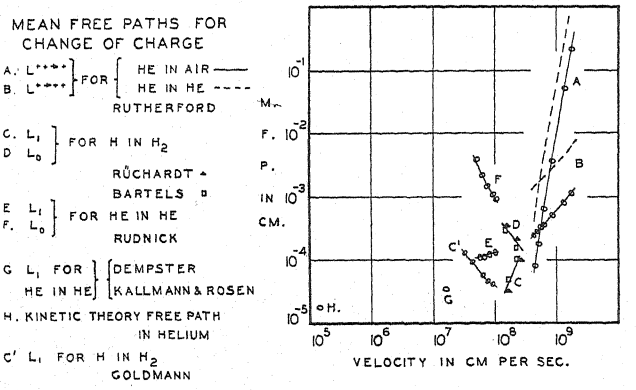


Fig. 3.

occurrence of the maximum of the Bragg ionization curve at intermediate velocities. The broken curve shown for alpha-particles in helium is Rutherford's statement that a few experiments with helium indicated free paths five or six times as great as in air.

Dempster has determined the value 3.5×10^{-5} cm as a mean free path for absorption of 900 volt helium ions in helium.[16] Data for virtually the same experiment given by Kallmann and Rosen[14] permit computation of the free path 3.7×10^{-5} cm for 400 volt ions. An average of these two is plotted in Fig. 3. It will be noted that the point falls below the practically horizontal curve for neutralization of helium ions at higher velocities, as one would expect if the absorption studied at the lower velocities involved scattering as well as neutralization.

If we suppose in these experiments that the fast neutral atoms are in the normal state and hence identical with the molecules of the gas through which they pass, then collisions in which the fast atom ionizes an atom at rest will be just as frequent as collisions in which the fast atom is itself ionized. This means that each particle, in describing its free path as a neutral atom, ionizes only one atom in the gas at rest, although according to kinetic

[16] A. J. Dempster, Phil. Mag. 3, 115 (1927).

theory about 45 collisions occur over the same path. $1/L_0$ is then the number of ion pairs produced by a neutral atom per centimeter of its path as a neutral. This ionization becomes $1/(L_0+L_1)$ when expressed as the number of ions per centimeter of the path described in both charged and neutral states. If the neutral atoms are not in the normal state[17] they will probably ionize less frequently than they are ionized, and their efficiency of ionization will then be less than $1/L_0$. The increase in $1/L_0$ with velocity, shown in column 6 of Table I, accords with the known increase of ionizing power with velocity for alpha-particles in this range.[18]

From the table the ionizing power of the neutral atom is 1160 ions per cm for the velocity 10^8 cm/sec. In contrast to this, an electron of the same velocity has an energy of only 3 volts and hence no ionizing power whatever in helium. Even at its maximum the ionizing efficiency of electrons,[19] achieved at a velocity of 6 or 8 times 10^8 cm/sec., is only about equal to the value mentioned above for the slower atoms.

For each capture of an electron, a positive ion is formed in the gas; each electron lost also remains in the gas. Accordingly, each particle produces a pair of ions in the distance (L_0+L_1), or $1/(L_0+L_1)$ ion pairs per cm by capture and loss of electrons. Combining this with the ionization by neutral atoms considered above gives $2/(L_0+L_1)$ for the ionization per particle per cm in the composite beam attributable to the neutral atoms and to the alternations of charge. Ionization in excess of this would presumably be produced only by the positive ions. Numerical values are given in column 7 of Table I. The value for $v=10^8$ cm/sec., when multiplied by 24.6, the ionization potential of helium, indicates energy dissipation due to ionization of at least 5×10^4 equivalent volts per cm.

Recent range-velocity data[20] for slow alpha-particles, combined with the value 0.179 for the relative stopping power of helium,[21] show that helium particles of velocity 10^8 cm/sec. lose their energy in helium at a rate of about 1.6×10^5 volts per cm. Thus the minimum ionization $2/(L_0+L_1)$ deduced above represents about one-third of the total energy dissipated by the particles.

The remaining two-thirds of the energy could be spent in either or both of two ways: first, in additional ionization by the positive ions along their short paths, which however, still involve about seven collisions according to kinetic theory, compared to about 45 for the neutral free path; second, in elastic or inelastic collisions not involving ionization. The first of these alternatives is suggested by the conclusion reached by Gurney[22] that alpha-particles in helium expend almost all of their energy in ionization. This result seems clearly established for the average behavior at least below $v=10^9$

[17] M. L. E. Oliphant, Proc. Roy. Soc. **A124**, 228 (1929).
[18] G. H. Henderson, Phil. Mag. **42**, 538 (1921).
[19] P. T. Smith, Phys. Rev. **36**, 1293 (1930).
[20] P. M. S. Blackett and F. C. Champion, Proc. Roy. Soc. **A130**, 380 (1931).
[21] R. W. Gurney, Proc. Roy. Soc. **A107**, 340 (1925).
[22] R. W. Gurney, Proc. Roy. Soc. **A107**, 332 (1925).

cm/sec. A direct estimate of ionizing power at $v=10^8$ cm/sec. from Henderson's curve[18] and the relative value 1.3 for ionization in helium[22] also supports the first hypothesis, as it indicates roughly the formation of 9000 ions per cm, requiring an energy of 2.2×10^5 volts per cm, more than the total dissipation 1.6×10^5 volts per cm estimated above. It thus appears probable that the helium particles studied here produce ionization several times the minimum estimate $2/(L_0+L_1)$, and that the ionization in excess of this minimum must be attributed to the positive ions. This conclusion has the somewhat surprising corollary that the positive helium ion has an ionizing power in helium about 28 times that of the neutral helium atom at the velocity 10^8 cm/sec.

It is a pleasure to acknowledge the many essential suggestions and constantly helpful advice and criticism which Professor A. J. Dempster has given in the course of this work.

IONIZATION OF CAESIUM VAPOR BY LIGHT*

By F. W. Cooke
University of Illinois

(Received August 12, 1931)

Abstract

The photo-ionization of caesium vapor as a function of the wave-length of the light has been measured at low pressure. The curve has a maximum at the principal series limit, decreases to a minimum at 2800A, and rises again at shorter wave-lengths. The pressure was too low for the ionization by line absorption to be observed. The absolute value of the atomic ionization coefficient at the series limit was found to be 6×10^{-19}, in fair agreement with Mohler's value, which is 2.3×10^{-19}.

The Problem

When the monatomic vapor of an alkali metal is irradiated by monochromatic light of sufficiently high frequency, the atoms may absorb some of the light and thereby become ionized. If the frequency ν of the light is higher than the convergence frequency ν_0 of the principal series of the element, then the ejected electron leaves the atom with a velocity v given by the equation

$$h(\nu - \nu_0) = \tfrac{1}{2}mv^2,$$

where h is Planck's constant, and m is the mass of the electron.

Consider a beam of monochromatic light incident on a given volume of the vapor. Let J_ν be energy flux density in ergs per cm² per sec.; A the cross-section area of vapor column taken normal to the light path; x the length of absorbing column of vapor; and N the number of atoms per cc of the vapor. Then the number of quanta absorbed per sec. is

$$n = \frac{KNAxJ_\nu}{h\nu}$$

and the "atomic absorption coefficient" is $K = n \cdot 1/NAx \cdot h\nu/J_\nu$ quanta absorbed per atom per quantum per cm² of incident energy. If I is the saturation ionization current and e the electron charge, the number of positive ions produced per sec. is I/e, which is the number of quanta absorbed per sec., assuming that the absorption of one quantum produces one positive ion and one electron. Hence the "atomic ionization coefficient" is

$$k = \frac{I}{e} \cdot \frac{1}{NAx} \cdot \frac{h\nu}{J_\nu}$$

positive ions per atom per quantum per cm² of incident energy. It may be determined by the measurement of the ionization current produced by the

* Preliminary note, Phys. Rev. 37, 1707 (1931).

light. On the basis of the simple assumption above, it is identical with the "atomic absorption coefficient" at the frequency ν. The latter coefficient may be measured by the absorption of the vapor directly.

The "atomic ionization coefficient" as a function of the frequency of the light has been studied in recent years for the metals caesium, rubidium, and potassium. Following the detection of the ionization produced by the absorption of ultraviolet light by caesium vapor by Kunz and Williams,[1] Mohler, Foote and Chenault,[2] Little,[3] Mohler and Boeckner,[4] and Lawrence and Edlefsen[5] have determined the shape of the ionization curve on both sides of the principal series limit of caesium. Little used the "direct" method, while the others used the sensitive method of neutralization of the space-charge surrounding a heated filament. Ionization on the long-wave side of the series limit seems to be a definite fact, with maxima in the curve corresponding to the principal series lines $1s$–$5p$ to $1s$–$9p$. Ionization is a maximum at the series limit. The curves of Little and Mohler have a minimum near 2750A with a rise at shorter wave-lengths to 60 and 40 percent, respectively, of the maximum. The curve of Lawrence is monotone on the short-wave side.

Little[3] made the first absolute measurement of the "atomic ionization coefficient," and found the value 2.2×10^{-21} ions per atom per quantum per cm^2 of incident light at 3130A. Mohler and Boeckner[4] obtained the value 1.85×10^{-19} at 3130A, and 2.3×10^{-19} at the limit 3184A, which is one hundred times larger than the value given by Little. However, Mohler and Boeckner[4] measured directly the percentage change in absorption of the 3130A line of mercury between 100°C and 218°C, from which they deduced that the atomic absorption coefficient is about 3×10^{-19} at 3130A.

Ionization by line absorption has been explained by Mohler and Boeckner,[6] also independently by Freudenberg,[7] on the basis of Franck's suggestion[8] of the formation of a molecule ion by the collision of an excited caesium atom with a normal atom. Other hypotheses that have been proposed are shown to be incapable of explaining the observed ionization.

The work reported here was undertaken with three objects in view: (a) To determine by the "direct" method whether ionization at long wave-lengths is real, as found with the space-charge method; and to study it. (b) To settle the discrepancy between the magnitudes of the atomic ionization coefficient as given by Little and by Mohler and Boeckner. (c) To find whether the ionization curve rises again at short wave-lengths; and if so, the reason.

[1] Kunz and Williams, Phys. Rev. **15**, 550 (1920); **22**, 456 (1923).
[2] Mohler, Foote and Chenault, Phys. Rev. **27**, 37 (1926).
[3] Little, Phys. Rev. **30**, 109 (1927); correction **30**, 963 (1927).
[4] Mohler and Boeckner, Bur. Stand. J. Res. **3**, 303 (1929); **5**, 51 (1930).
[5] Lawrence and Edlefsen, Phys. Rev. **34**, 233 (1929).
[6] Mohler and Boeckner, Bur. Stand. J. Res. **5**, 51 (1930).
[7] Freudenberg, Zeits. f. Physik **67**, 417 (1931).
[8] Gudden, "Lichtelektrische Erscheinungen," p. 226 (1928).

Experimental Procedure

In the direct method there are two serious difficulties not inherent in the space-charge method. In the first place there is a large dark current which may be as great as the ionization current of the vapor, or even greater. This dark current is due to the conductivity of the glass tube, to the conductivity of the alkali metal film on the glass, to the thermal ionization of the vapor, and to thermal emission from caesium surfaces. The ionization tube was constructed in such a way as to keep the two surface conductivities and the thermal emission from caesium surfaces at a minimum. Thermal ionization of the vapor can not be avoided, however, in any case.

In the second place, the photoionization of the vapor can easily be masked by surface photoionization, caused by light striking any surface on which there is an alkali metal film. Direct tests for this were made, and it is believed it did not cause serious error.

The continuous radiation from a water-cooled hydrogen discharge tube, in series with a Hilger E2 spectrograph, was used as a source of light. The beams transmitted were about 20A wide at 3000A. The hydrogen tube was similar to the design of Lawrence and Edlefsen,[9] but with the quartz tube silvered on the inside. The discharge was operated at 4.7 amperes. The intensity was proportional to the current.

The ionization tube was made of Pyrex glass with platinum electrodes and plane quartz windows. In preliminary tests with many Pyrex tubes, the Pyrex glass showed a surprising conductivity at low temperatures, with indications of an electrolytic electromotive force. Ordinary soda glass and fused quartz showed no electromotive force or conductivity up to 200°C, and practically none up to 250°C, while Pyrex showed a large electromotive force and conductivity beginning at about 100°C. A somewhat similar behavior of heated Pyrex glass has been recently reported by Mitchell,[10] who found that treatment with hydroflouric acid was most effective in restoring the low conductivity, and attributed the effect to a surface characteristic of the glass.

On account of this behavior of Pyrex, the collecting electrode connected to the electrometer was insulated from the body of the ionization tube by a section of quartz tubing five cm long. In other respects the arrangement of electrodes and internal and external guard cylinders of platinum was similar to that of Little.

A long side tube extended through the wall of the main furnace and contained the caesium, which was vaporized by a separate furnace, as in the work of Mohler and Boeckner. In order to reduce the surface conductivity due to a caesium film, the experiments were made with a large temperature difference between the ionization tube and the caesium reservoir, at least 100°C at all times. The empty tube became conducting near 220°C, hence the main furnace was kept at a temperature near 180°C. The caesium reservoir

[9] Lawrence and Edlefsen, Rev. Sci. Inst. **1**, 45 (1930).
[10] Mitchell, Phil. Mag. **11**, 748 (1931).

was heated to about 60°C in the experiments. At higher temperatures the dark current became relatively too large.

The ion current was measured by the rate of drift of a quadrant electrometer. A drift of one mm per minute was produced by a current of 2.51×10^{-15} amp. During all the measurements the insulation of the ionization tube was excellent, as indicated by a negligible leak of the electrometer when it was charged sufficiently to produce a large deflection.

The energy of the ionizing light entering the tube was determined by means of a potassium photoelectric cell in quartz, the cell being calibrated throughout the spectrum with a mercury arc and thermopile, the latter being calibrated from a Hefner lamp. The measurements were corrected for absorption and reflection by the quartz windows of the tube.

The cross-section area of the beam of light for each of four wave-lengths was measured at two places near the ends of the collecting electrode and the mean value plotted against wave-length. An area from this curve multiplied by the length of the collecting electrode (9 cm) gave the volume of illuminated vapor for any desired wave-length.

The number of atoms per cubic centimeter of the vapor was calculated from the vapor pressure, which was found from Rowe's equation[11] based on Kroner's data at 250°–350°C:

$$\log_{10} p = 7.1650 - \frac{3966}{T},$$

where p is the pressure in mm of mercury corresponding to the absolute temperature T.

Results

The data for one set of measurements are given in Table I. Another set gave somewhat larger values for the atomic ionization coefficient, with 7.6×10^{-19} at the series limit. The curve in Fig. 1 is drawn for the mean of both sets.

(a) At higher caesium pressures the dark current became excessive, so that the photoionization current, due to the small energy in the beam of light, could not be found with sufficient accuracy. In accord with the work of Mohler and Boeckner only slight ionization was found for wave-lengths greater than the series limit, since the direct method restricts the observations to pressures too low for the effect of line absorption found by others with the more sensitive space-charge method to be detected, even though a continuous source was used.

(b) The mean absolute value at the series limit of the atomic ionization coefficient, 6×10^{-19}, with an uncertainty of the same order of magnitude, agrees fairly well with the determination of Mohler and Boeckner, which is 2.3×10^{-19} at the series limit, and is in complete disagreement with the value of Little, which is 100 times smaller than that of Mohler and Boeckner.

[11] Rowe, Phil. Mag. **3**, 534 (1927).

In Little's experiment, the internal earthed guard ring was very close to the "collecting" electrode, with good opportunity for a caesium film to settle in this region, since no appendix was used as a caesium reservoir. It seems possible in view of the present work, that the surface conductivity in this region resulted in partially earthing the collecting electrode itself. This would be the equivalent of a second shunt resistance on the electrometer,

TABLE I.

Wave-length A	Caesium Temper-ature °C	I/e ions per sec. $\times 10^4$	N atoms per cc $\times 10^{11}$	A area of beam cm²	$J_\nu/h\nu$ quanta per cm² per sec. $\times 10^{11}$	k ions per atom per quantum per cm² $\times 10^{-19}$	mean k $\times 10^{-19}$
3263	55	3.3	3.45	0.96	2.70	0.42	0.22
	58	zero	—	—	—	zero	
3232	57	10.3	4.12	0.95	2.84	1.06	1.34
	54	13.9	3.19		2.84	1.86	
	58	11.1	4.47		2.84	1.06	
3184	55	28.4	3.45		2.87	3.36	4.92
	55	50.0	3.45		2.87	5.92	
	55	46.0	3.45		2.87	5.46	
3174	55	28.0	3.45		2.94	3.26	3.64
	57	39.6	4.12		2.94	3.84	
	54.5	31.6	3.32	0.95	2.94	3.80	
3154	55	19.8	3.45	0.94	2.97	2.28	2.28
3090	53	21.8	2.97	0.94	3.17	2.76	2.76
3006	53	22.8	2.97	0.93	3.44	2.70	2.46
	56	24.2	3.80	0.93	3.44	2.22	
2900	56	27.6	3.80	0.91	3.65	2.44	2.22
	58	26.6	4.47	0.91	3.65	2.00	
2804	55	23.2	3.45	0.90	3.80	2.18	2.18
2707	55	19.0	3.45	0.89	3.88	1.78	1.78
2597	57	29.6	4.12	0.88	3.80	2.38	2.38
2498	57	37.2	4.12	0.86	3.72	3.14	2.64
	56	23.4	3.80	0.86	3.72	2.14	
2396	58	30.6	4.47	0.85	3.40	2.62	2.62
2302	56	28.6	3.80	0.84	2.93	2.90	2.80
	58	26.8	4.47	0.84	2.93	2.70	
2225	55	17.6	3.45	0.83	2.40	2.94	2.94
	54	16.2	3.19	0.83	2.40	2.94	

and if it were 100 times less than the shunt resistance intentionally used (and measured), then only one percent of the ionization current would be measured by the electrometer.

(c) In the region of continuous absorption there is a rise of the ionization curve at short wave-lengths, in agreement with the results of Mohler and Boeckner, but not in agreement with the curve of Lawrence and Edelfsen. The curve has a minimum at 2800A and rises at 2200A to 60 percent of the maximum at the series limit. The shape of the curve remains an unsettled question, especially so, in the light of the conflicting results of Mohler and Lawrence, who both used the more sensitive space-charge method.

To test this point further, absorption photographs of the caesium vapor were made at various temperatures, with an absorbing vapor column of 14

inches. Twelve or more lines of the principal series were very clearly shown at the higher temperatures. Comparison of microphotometer records of photographs at room temperature and at 265°C lead to an absorption curve

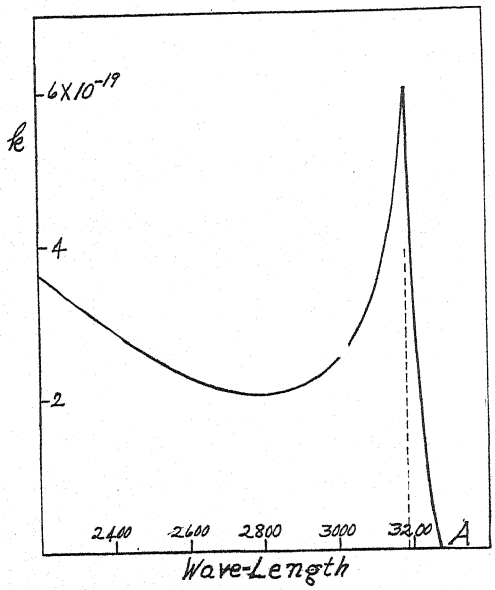


Fig. 1. The atomic ionization coefficient k.

decreasing from the limit and becoming asymptotic to the wave-length axis near 2700A. These experiments should, however, be continued.

ACKNOWLEDGMENTS

This investigation was suggested by Professor J. Kunz and carried out under his direction, and the writer is greatly indebted to him for his continued interest and advice throughout the progress of the investigation. Thanks are due to Professor C. T. Knipp for assistance with the experiments on the conductivity of the Pyrex glass tubes. The writer wishes also to express his thanks to Professor F. W. Loomis, Head of the Department of Physics, for valuable suggestions and for his interest in the work, and to Professor Loomis and Professor A. P. Carman for providing the equipment and for the use of the facilities of the laboratory.

SOME ELECTRICAL PROPERTIES OF SPECTROSCOPICALLY PURE ZINC CRYSTALS

By A. G. Hoyem
Physical Laboratory, State University of Iowa

(Received August 11, 1931

Abstract

With single crystal specimens of *spectroscopically pure* zinc (99.9999 percent zinc), the Thomson coefficient at 49.5°C has been measured as a function of orientation. A very accurate confirmation of the Voigt-Thomson symmetry relation is obtained, the principal values of the Thomson coefficient being: $\sigma_\perp = 0.86 \times 10^{-6}$ cal./coul./deg., and $\sigma_\parallel = 0.34 \times 10^{-6}$ cal./coul./deg. The thermal e.m.f. of these same specimens against copper has been determined as a function of orientation throughout the temperature range −180° to 200°C. From these data, the values of the Peltier coefficient, the Thomson coefficient, and the difference in principal Thomson coefficients have been computed as functions of temperature by means of the relations given by the Kelvin thermodynamical theory of thermoelectricity. The values of the Peltier coefficient of $Zn_\perp$ against $Zn_\parallel$ thus obtained are: $\pi = 658$ microvolts at 49.5°C and $\pi = 1080$ micro-volts at 125°C. For the difference in the principal Thomson coefficients, the values are: $\sigma_\perp - \sigma_\parallel = 0.58 \times 10^{-6}$ cal./coul./deg. at 49.5°C and $\sigma_\perp - \sigma_\parallel = 1.20 \times 10^{-6}$ cal./coul./deg. at 125°C. The predictions of the Kelvin theory regarding $\sigma_\perp - \sigma_\parallel$ are thus found to be in agreement with the direct determinations by Ware and the writer. The Voigt-Thomson law is found to hold also in the case of thermoelectric power and the other thermoelectric properties to which it should apply. The dependence of resistivity on temperature has been investigated for the temperature range −170° to 25°C. The average value of the temperature coefficient of resistivity obtained is: $\alpha = 4.058 \times 10^{-3}$. For comparison purposes, a direct determination of the Thomson coefficients of single cyrstal specimens of *Kahlbaum's best* zinc at 49.5°C has also been made, as well as a study of the dependence of their resistivities on temperature. For this less pure zinc, the principal values of the Thomson coefficient are: $\sigma_\perp = 0.91 \times 10^{-6}$ cal./coul./deg. and $\sigma_\parallel = 0.38 \times 10^{-6}$ cal./coul./deg. For the temperature coefficient of resistivity, the average value is: $\alpha = 4.009 \times 10^{-3}$. A variation in the values of α for specimens of the same grade of zinc is observed which is considerably greater than can be attributed to experimental error.

Introduction

THAT the presence of even slight amounts of impurity may have a very pronounced influence on some of the properties of metals is well known. Consequently, in trying to ascertain the properties truly characteristic of a metallic element, it is obviously of great importance that the specimens studied be as free from foreign substances as possible. If at the same time simplicity and uniformity characterize the spatial arrangement of the atoms throughout the specimen, such as is the case in single crystals, it is evident that the characteristics obtained ought to be even more closely associated with the true properties of the element itself. Several investigations dealing with the electrical properties of zinc single crystals have been reported, none, however, for zinc of exceedingly high purity. Linder,[1] Bridgman,[2] and

[1] E. G. Linder, Phys. Rev. **26**, 486 (1925), **29**, 554 (1927).

[2] P. W. Bridgman, Nat. Acad. Sci. Proc. **11**, 608 (1925); Proc. Amer. Acad. Sci. **61**, 101 (1926).

Grüneisen and Goens[3] have measured the thermal e.m.f. of zinc against copper, and from the thermoelectric power thus obtained have computed by means of the customary thermodynamical relations the Peltier coefficients of the zinc crystals (against copper) and the difference in the Thomson coefficients of the two principal orientations as functions of temperature. Specific resistance and the temperature coefficient of resistivity have been measured by Grüneisen and Goens,[4] Bridgman,[2] and Ware.[5] Direct determinations of the Thomson coefficient have been made by Ware[5] and by Veleger.[6] None of these investigators give the exact analysis of the zinc used except to state that it was Kahlbaum's, Kahlbaum's best, or Merck's brand of zinc. Hence it is reasonable to assume that the specimens varied considerably in purity and that all contained not less than 0.01 percent impurity, the percentage of impurity usually present in chemically pure zinc. The zinc used in the present investigation was obtained through the courtesy of the New Jersey Zinc Company and is known as *spectroscopically pure* zinc. Its analysis is given as 99.9999 percent pure.[7] On single crystal specimens made from this S. P. zinc, a direct determination was made of the Thomson coefficient, together with measurements of thermal e.m.f. against copper, of specific resistance,[8] and of the temperature coefficient of resistivity. From the thermal e.m.f. data, the Peltier coefficient against copper and the difference in the principal Thomson coefficients, $(\sigma_\perp - \sigma_\parallel)$, were computed as functions of temperature. Thus, in view of the fact that the thermal e.m.f. and the Thomson coefficient measurements were obtained for the same crystal specimens, it is possible to make a better comparison between the predictions of thermodynamical theory and the results of direct measurement than would have been possible in using only the results of previous investigators for comparison purposes. In addition, in order that the comparison between the results for the S. P. zinc and less pure grades of zinc might be more trustworthy, the Thomson coefficient, specific resistance,[8] and temperature coefficient of resistivity were also determined for a set of single crystal specimens made from Kahlbaum's best zinc.

Apparatus and Experimental Procedure

1. Production of the single crystals

The Czochralski-Gomperz method, described in considerable detail in a recent paper by the writer and E.P.T. Tyndall,[9] was used with a few slight modifications in growing the single crystal specimens. Due to the fact that the quantity of zinc available was comparatively small, approximately 250

[3] E. Grüneisen and E. Goens, Zeits. f. Physik **37** 278, (1926).
[4] E. Grüneisen and E. Goens, Zeits. f. Physik **26**, 250 (1924).
[5] L. A. Ware, Phys. Rev. **35**, 989 (1930).
[6] H. Veleger, Ann. d. Physik **9**, 366 (1931).
[7] The writer is very grateful to the New Jersey Zinc Company for providing him with a quantity of this exceedingly pure material. For a description of its properties and the method of production, see H. M. Cyr, Tran. Amer. Electrochem. Soc. **52**, 349 (1927).
[8] E. P. T. Tyndall and A. G. Hoyem, Phys. Rev. **37**, 101 (1931).
[9] A. G. Hoyem and E. P. T. Tyndall, Phys. Rev. **33**, 81 (1929).

grams, and the fact that the greater the purity of the metal the more readily it oxidizes when it is in the molten state, it was very necessary to minimize the two chief sources of waste, namely, loss of specimens due to imperfections caused by occasional unsteadiness of the crystal growing apparatus, and loss of material due to oxidation. To overcome the former difficulty, a new drawing mechanism was constructed, the square brass rod and the slides used in the former apparatus being replaced by a hexagonal brass rod which was guided by two sets of three ball-bearings. Oxidation was eliminated by having the entire growth process take place inside of a Pyrex glass tube, 5 cm in diameter and 25 cm tall, which contained a mixture of hydrogen and nitrogen. In order to avoid the possiblities of contamination, the crucible, as well as the tools used for handling the zinc, were also made of Pyrex.

The crystals were all grown in the "region of successful growth" designated in the earlier paper.[9,10] These S. P. crystals are extremely ductile and as a consequence are very difficult to handle without bending. Though the near zero degree orientations are the most brittle, they are not nearly as much so as the corresponding orientations of crystals made from Kahlbaum or other grades of zinc. Twenty-six crystals in all were grown ranging from fifteen to twenty centimeters in length and having a mean diameter of from two to three millimeters. Prior to the growing of these crystals, numerous K zinc crystals were grown under practically the same conditions with the double purpose of establishing the technique of crystal growth in the new apparatus and to provide material for the comparison between the S. P. zinc and a grade of zinc more nearly like that used by previous investigators.

2. The Thomson coefficient

The Thomson coefficient was measured by means of the Nettleton[11] method described by Ware[5] with further slight modifications.[12] In brief, the essential features of the method are as follows: The two ends of a single crystal specimen of zinc are maintained at different, but constant, temperatures. The Thomson effect, which is positive for zinc, will then cause an e.m.f. to be set up within the crystal, directed from the colder to the hotter portion. If an electric current is now set up in the crystal so that it flows down the temperature gradient, there will be a generation of heat in the crystal, a portion of which will be caused by the resistance of the crystal, the remainder being caused by the fact that the current is flowing in opposition to the Thomson

[10] Some recent work by Mr. H. K. Schilling performed in this laboratory seems to indicate that this region is successful growth may be considerably extended provided exceeding care be taken to minimize vibration and temperature fluctuation during the growth process. This raises the question as to whether the apparatus and procedure described here were not sufficiently improved over the first set-up so that crystals might also have been grown outside of the "region of successful growth." The only positive evidence of this is that attempts to grow Kahlbaum crystals of nearly 0° orientation at too high or at too low temperatures were definite failures. Aside from this the growth of crystals was purposely confined to what was believed to be the only suitable conditions.

[11] H. R. Nettleton, Proc. Phys. Soc. Lond. **34**, 77 (1921) ; **29**, 59 (1916).

[12] For diagrams of the apparatus and the electrical circuits involved see the article by Ware, Figs. 1, 2, and 3.

e.m.f. If the same current through the specimen is reversed, the Joulean heat will be of the same magnitude as before, but the Thomson effect will now produce an absorption of heat, hence the temperature of the specimen will be different in the two cases. On reversal, however, the current may be automatically increased to such a value that the temperature of the specimen remains constant. When such a state is reached that the temperature of the specimen does not change when the current is reversed, it has been shown by Nettleton[11] that if certain conditions are met, the Thomson coefficient, σ, will be equal to i_0R/JU calories per coulomb per degree, where i_0 is the above mentioned difference in currents corresponding to no temperature change, R is the resistance of the crystal, J is the mechanical equivalent of heat in joules per calorie, and U is the difference in temperature between the two ends. The two end temperatures used were 99° and 0°, respectively.

The accuracy with which the balancing current, i_0, can be determined hinges essentially on the sensitivity of the device used in detecting temperature changes in the crystal and on the constancy of the end temperatures. In order to increase this accuracy, the following modifications in Ware's procedure were made: The length of the bolometer coils was approximately doubled and better heat insulation provided in the entire bolometer-bridge circuit. The capacity of both the hot and cold reservoirs was increased so as to make it possible to maintain the temperatures at the ends of the crystal very constant throughout longer periods. The constancy of the hot end was further increased by heating the water by means of a different coil than the one which was used in mounting the crystal. This auxiliary coil was wound on the surface of the boiler as far removed from the end of the specimen as possible thus greatly diminishing the variations in temperature caused by occasional fluctuations in the heating current. With these modifications, the uncertainty in the determination of the balancing current, i_0, for most of the crystals was reduced to less than two percent. Two thermocouples, permanently imbedded in the reservoir blocks adjacent to the block-crystal junctions, served in determining the temperatures at the ends of the crystal.

3. Thermal e.m.f.

The thermal e.m.f. of zinc against copper was measured immediately following the determination of the Thomson coefficient of each crystal specimen, that is, while the specimen was still in the Thomson apparatus. A diagram of the circuit is shown in Fig. 1. Determination of the temperature at the ends of the crystal was made by connecting the potentiometer across terminals 1 and 4, and 2 and 3, respectively. These constantan-copper thermocouples are the two couples referred to in the preceding section. Readings across terminals 1 and 3 gave the thermal e.m.f. of the crystal against copper. In obtaning the various temperature differences, the cold end of the Thomson apparatus was maintained at 0°C, while the hot end served as the variable junction. The necessary low temperatures were secured by draining the boiler chamber and then introducing various quantities of liquid air directly into the chamber, the depth of the temperature obtained at the junction naturally depending

on the amount of liquid air introduced and on the extent of the heat insulation. To obtain the high temperatures, use was made of the heating element

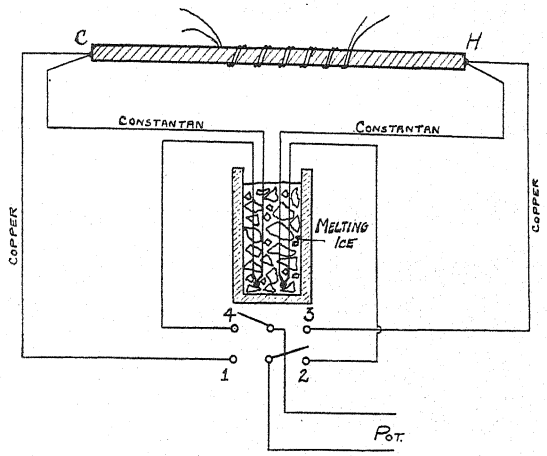


Fig. 1. The thermal e.m.f. circuit.

located in the boiler near the end of the crystal, currents ranging from 0.5 to 1.5 amperes being used. At both the high and the low temperatures, the fluc-

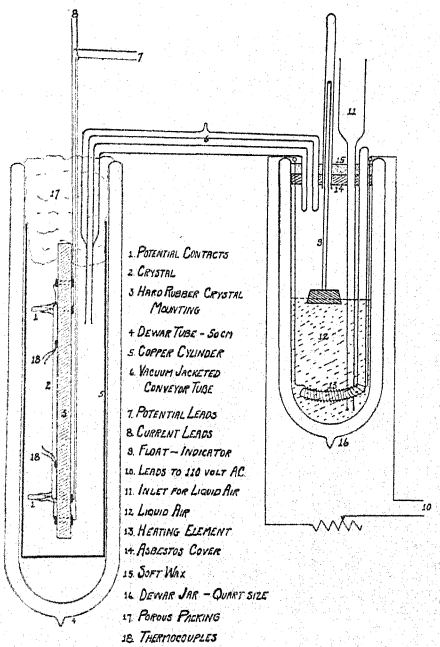


Fig. 2. Cross-sectional view of apparatus used in determining the resistance of the specimens at temperatures ranging from 25° to −170°C.

tuation encountered while the readings of temperature and the thermal e.m.f. were being taken and checked was usually less than half a degree.

4. Temperature coefficient of resistivity

The apparatus used in the determination of the temperature coefficient of resistivity is shown in Fig. 2. It employs the method for the production of low temperatures described by Cioffi and Taylor[13], namely, the evaporation of liquid air by the use of a heating element and the subjection of the specimens under investigation to the stream of cold dry air thus produced, the degree of cold depending on the rate of evaporation and on the insulation used in the transfer of the cold air. In this apparatus cold dry air, obtained by the forced evaporation of the liquid air in the small Dewar container, was transferred by means of the vacuum-jacketed tube into the large Dewar container, the entire apparatus being entirely enclosed in heat insulating material. Two crystal specimens were investigated simultaneously, being placed in parallel grooves on the hard rubber mounting. Chisel-shaped pieces of zinc, held in contact with the specimens by means of springs, served in obtaining the potential drop across any desired portions. These contacts were devised so as to eliminate the possibility of effects which might be due to contamination by soldered connections or due to irregularities in the crystal structure caused by cutting. The current leads were attached to the ends of the specimens. To insure greater constancy and uniformity of temperature throughout the region containing the specimens, the specimens and the mounting were placed inside of a copper cylinder fitting closely in the large Dewar container. Two thermocouples placed about ten centimeters apart between the two specimens furnished the means of determining the exact temperature as well as to show the absence of any appreciable vertical temperature gradient. The temperature coefficient was computed by using the relationship:

$$\alpha = \frac{1 - p}{t_2 p - t_1}$$

where p is the ratio of R_1 to R_2, R_1 and R_2 being the resistances of the specimen at the temperatures t_1 and t_2, respectively. The resistance measurements were made by the usual potentiometer method, the current used in the crystals being 0.5 ampere.

This low temperature apparatus proved very satisfactory particularly in regard to the constancy with which the temperature could be maintained and the fact that a temperature as low as $-170°$C could be obtained without excessive consumption of liquid air. At this temperature the consumption was approximately three liters per hour, but less, of course, at higher temperatures.

Results

1. Thomson coefficient

The experimental results obtained in the direct determination of the Thomson coefficient are represented graphically in Fig. 3. The values obtained for the S.P. crystals are represented by circles, the values for the K crystals being denoted by dots. Both sets of data are for a mean temperature of 49.5°C.

[13] P. P. Cioffi and L. S. Taylor, Opt. Soc. Amer. J. 6, 906 (1922).

In agreement with Ware's findings, both sets of data indicate that the Voigt-Thomson symmetry relationship for the Thomson coefficient holds at this temperature, the linearity being particularly definite in the case of the S.P. zinc. It is only fair to state that the greater regularity in the results for the S.P. zinc is largely due to the greater care taken in this case and that with the possible exception of the two points for the K zinc at $\cos^2\theta=0$ and at $\cos^2\theta=0.74$, the deviations are no larger than the probable experimental error.

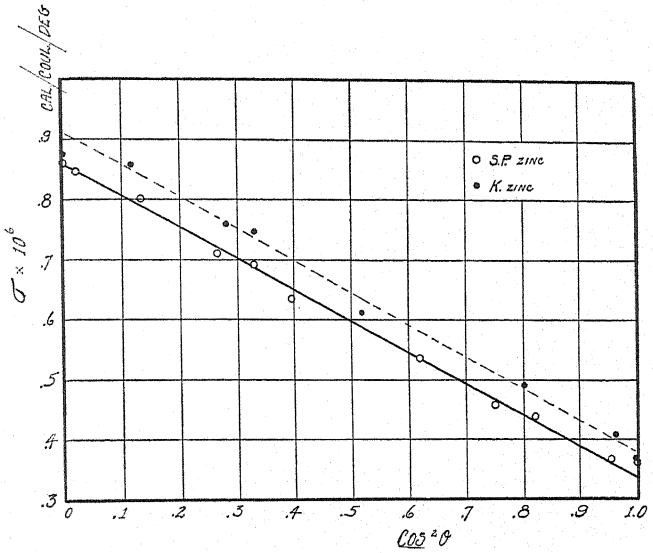


Fig. 3. Directly determined values of the Thomson coefficient plotted against $\cos^2\theta$. The S.P. values are represented by O————O, and the K zinc values by ●- - - - -●.

The values for $\sigma_\perp$ and $\sigma_\parallel$ for the S.P. zinc, expressed in micro-calories per coulomb per degree, are 0.86 and 0.34, respectively, while for the K zinc the values are 0.91 and 0.38, respectively, in fairly good agreement with Ware's values of 0.98 and 0.38 respectively, for the same grade of zinc. Comparing the results for the S.P. crystals with the writer's K crystals it is evident that the effect of impurity is to cause a practically constant increase in the Thomson coefficient for all orientations, the ratio, $\sigma_\perp/\sigma_\parallel$, and the difference, $\sigma_\perp-\sigma_\parallel$, being almost identical for the two sets of crystals. The effect of impurity on specific resistance is apparently of the same type.[8]

2. Thermal e.m.f.

The observed values of the thermal e.m.f. of zinc against copper are represented graphically in Fig. 4, the e.m.f. being considered positive when it is directed from the hot to the cold junction through the zinc. The four different notations used in plotting these values were used merely for the sake of clarity to aid in associating the various points with the curves to which they belong. The numbers alongside the curves indicate the crystal orientations. Representing these curves by empirical equations of the form: $E=at^3+bt^2+ct$,

where a, b, and c are constants which are characteristic of the individual curves, and differentiating these equations with respect to t, equations giving the value of the thermoelectric power, $e(=dE/dt)$, are obtained. Fig. 5 shows the values of the thermoelectric power, obtained in this manner, plotted against the square of the cosine of the angle of orientation. The ordinate

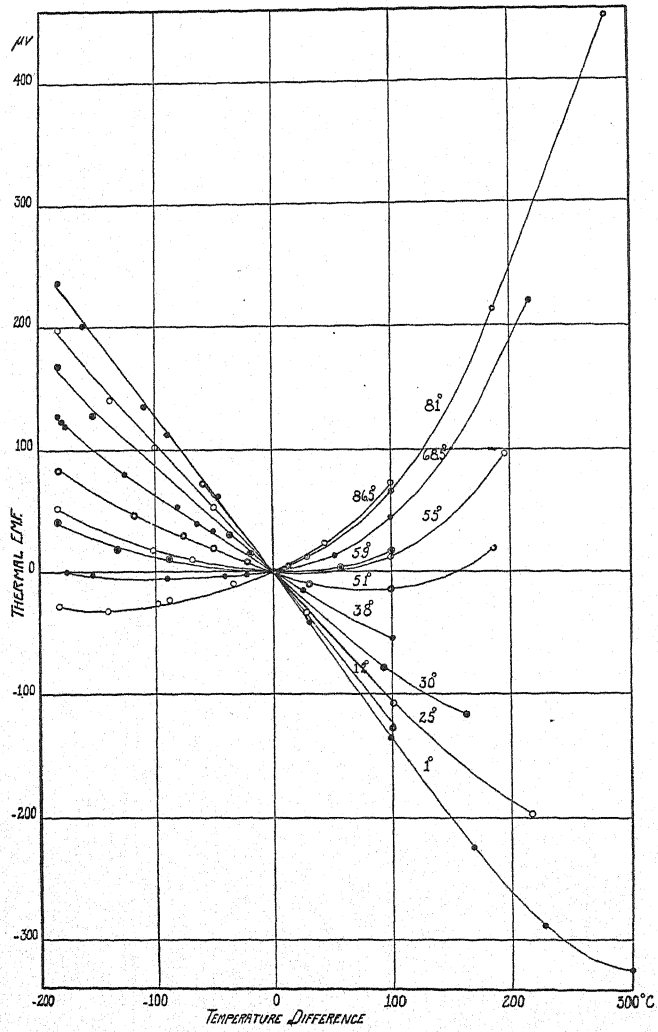


Fig. 4. Thermal e.m.f. of S.P. zinc against copper represented as a function of temperature difference. The crystal orientations are indicated on the curves.

scale indicated applies to the curve for the temperature of $-180°$. To avoid confusion, the origin for the values corresponding to a temperature of $-150°$ is shifted upward one whole unit, the origin for those corresponding to $-100°$ being shifted upward two whole units, etc. That the Voigt-Thomson symmetry relation holds for this zinc throughout the range of temperature investigated seems quite evident. The slight scattering of points for the tempera-

ture of 180° is believed to be due to the fact that the probable error in the determination of e is greatest here, since this region is for some of the crystals very near the upper limit for the thermal e.m.f. measurements and is also a region for which e changes quite rapidly.

The thermoelectric properties of single crystals may be obtained without reference to any other metal by expressing the characteristic values for the one principal orientation ($\theta=90°$), against those for the other principal orientation ($\theta=0°$). These values for thermal e.m.f. were obtained by using

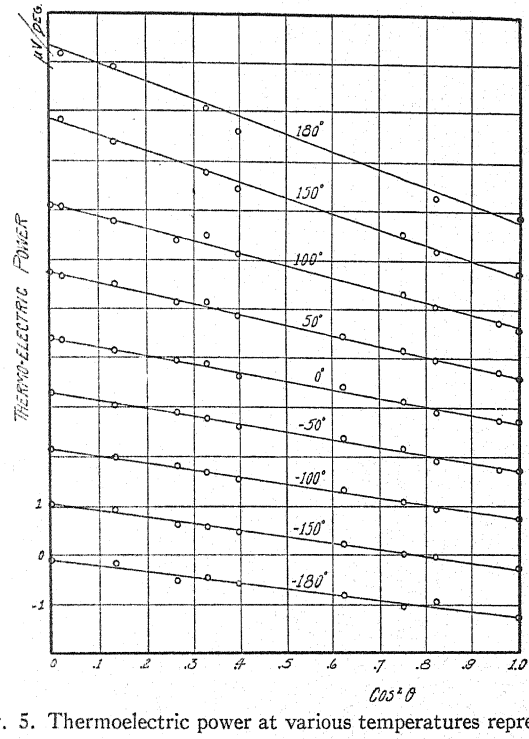


Fig. 5. Thermoelectric power at various temperatures represented as a function of $\cos^2\theta$.

the empirical equations for E and plotting values of E against $\cos^2\theta$ in the same manner as e is represented in Fig. 5. Definite straight line relations were obtained from which the values of $E_\perp$ and $E_\parallel$ were observed and their difference plotted against the corresponding temperature. The results are represented in Fig. 6 by the circles and the solid, heavy curve. The results obtained by Linder[1] and by Grüneisen and Goens[3] are also shown, being represented by the double circles and the dots, respectively. In order to make this comparison, the writer's results had to be reduced by the use of the law of intermediate temperatures, whereby

$$E(t, -253°) = E(0°, -253°) + E(t, 0°).$$

The value of $E(0°, -253°)=483.6\mu v$, taken from the work of Grüneisen and Goens, was used in carrying out the reduction. It is to be noted that the writer's results are in closest agreement with those of Grüneisen and Goens.

By noting the values of $e_\perp$ and $e_\parallel$, in Fig. 5, and plotting their difference against temperature, the variation of thermoelectric power for $Zn_\perp$ against $Zn_\parallel$ is obtained. This is represented in Fig. 7.

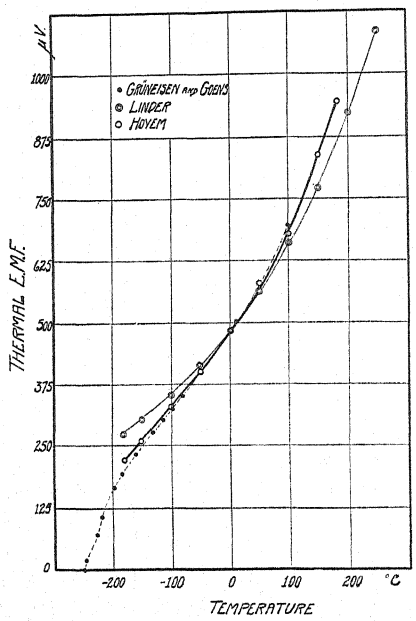


Fig. 6. Thermal e.m.f. of $Zn_\perp$ against $Zn_\parallel$.

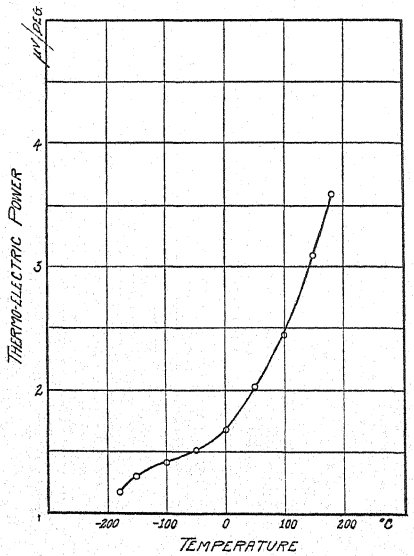


Fig. 7. Thermoelectric power of $Zn_\perp$ against $Zn_\parallel$.

The Peltier coefficient, π, for $Zn_\perp$ against $Zn_\parallel$ and the difference in the principal Thomson coefficients, $\sigma_\perp - \sigma_\parallel$, are, according to the Kelvin thermodynamical theory, given by Te and $T(de/dt)$, respectively, where T is the

absolute temperature and e is the thermoelectric power for $Zn_\perp$ against $Zn_\parallel$. The Peltier coefficient, π, obtained in this manner, is represented in Fig. 8 as a function of temperature. Similar results obtained by Linder[1] and by

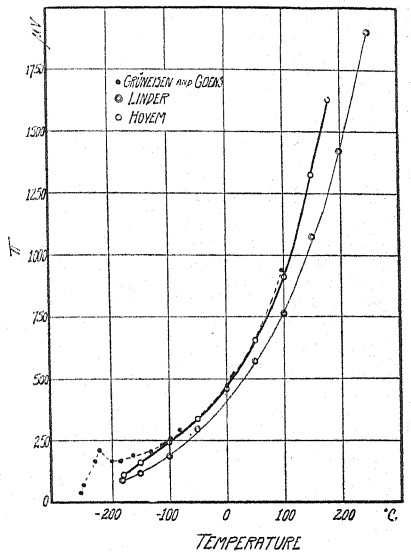


Fig. 8. The Peltier coefficient of $Zn_\perp$ against $Zn_\parallel$.

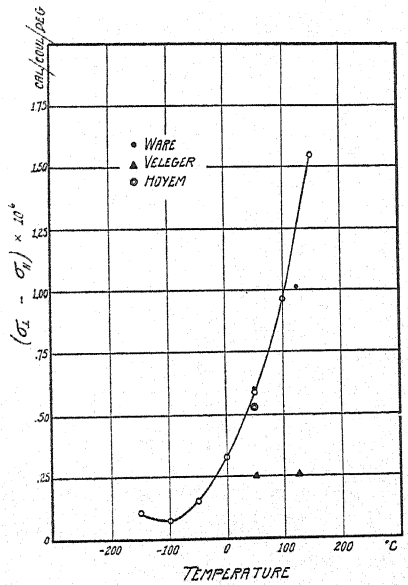


Fig. 9. The difference in the principal Thomson coefficients represented as a function of temperature.

Grüneisen and Goens[3] have been included on the graph for comparison. The values obtained by the writer throughout the greater part of the range are seen to be in very close agreement with those obtained by Grüneisen and

Goens. The writer's measurements did not extend below the temperature of liquid air, consequently all that can be said about the slight maximum in the Peltier coefficient at low temperatures obtained by these earlier investigators is that there is no definite indication of such an increase in the present results.

In Fig. 9 the difference in the principal Thomson coefficients,[14] $\sigma_\perp - \sigma_\parallel = (T/J)(de/dt)$, is represented also as a function of temperature. The value of de/dt used in the above computations was obtained by differentiation of a series of second degree equations which represented overlapping sections of the thermoelectric power versus temperature curve shown in Fig. 7. These equations were of the form: $e = at^2 + bt + c$, where a, b, and c were constants characteristic of the various sections of the curve. This method for determing de/dt was chosen primarily because of its simplicity and because of its superiority to the graphical method of measuring the slopes of tangents drawn to the curve. The graph indicates that for temperatures above $-100°$C there should be a very definite increase in the difference in Thomson coefficients with temperature. On this graph are also indicated the values of $\sigma_\perp - \sigma_\parallel$ taken from the direct determinations of Ware,[5] Veleger,[6] and the writer. The writer's values for the S.P. zinc and for the K zinc are represented by the one double circle at $t = 49°$C, the two values being practically identical. The results of Ware and Veleger are represented by dots and by triangles, respectively. Very good agreement is seen to exist between the predictions of the thermodynamical theory, as exemplified by the curve in the figure, and the directly determined results of Ware and the writer. Veleger's results, on the other hand, show considerable disagreement both as to magnitude and as to variation with temperature. In view of the fact that all other "indirectly determined" values of the difference in the principal Thomson coefficients, such as those by Linder,[1] Bridgman,[2] and Grüneisen and Goens,[3] are in much better agreement with the writer's results than with those of Veleger, it seems very improbable that the discrepancy in the latter's results can denote any failure on the part of the thermodynamical theory.[15] It should be borne in mind here that the writer's "indirectly determined" values, given by the curve in the figure, were obtained from the same set of S.P. specimens as were used in the direct determination for the S.P. zinc.

It is possible also to obtain from the thermal e.m.f. curves (Fig. 4) the Thomson coefficient of any specimen as a function of temperature, the procedure being as follows: Differentiating the empirical equations for E twice with respect to t and multiplying by the absolute temperature, T, one obtains $T(d^2E/dt^2) = \sigma_{ZN} - \sigma_{CU}$. By adding the Thomson coefficient of copper at the given temperature, the coefficient for the zinc specimen results. This has been done for crystals representing the extreme orientations, using a 1° crystal to get $\sigma_\parallel$ and two crystals, 81° and 86.5°, for $\sigma_\perp$. The 81° crystal was used since the thermal e.m.f. curve for the highest orientation (86.5°) did not extend above 100°C. From 0° to 100°C the range common to both, the crystals yield

[14] Expressed in calories per coulomb per degree, the units previously used for the Thomson coefficient.

[15] See for instance Table 6 in Veleger's article.

practically identical values. The results of this computation are shown in Fig. 10. The values of the Thomson coefficient for copper at various temperatures were taken from the work of Berg[16] and Borelius and Gunneson,[17] a mean value being adopted. Since the writer, of course, used a different specimen of copper, the results shown in Fig. 10 cannot be expected to represent absolute values. The variation with temperature, to obtain which the computations were especially made, is considered somewhat more reliable. In this connection it is to be noted that this variation of σ with temperature is very different from that recently obtained by Veleger, but in good agreement with Ware's results, as may be seen in the figure.

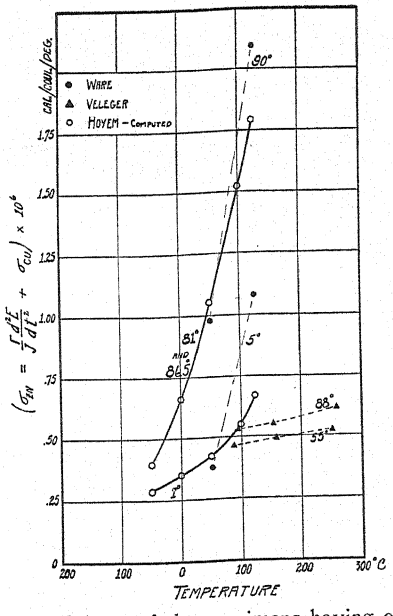


Fig. 10. The Thomson coefficients of the specimens having orientations 86.5°, 81°, and 1°, represented as functions of temperature. Veleger's directly determined values are indicated by ▲------ ▲-, Ware's by ●-------●.

If in Fig. 10 the difference in the ordinates of the two curves corresponding to a given temperature be noted, the difference should obviously be very nearly equal to $\sigma_\perp - \sigma_\parallel$. Values so obtained are found to be in very good agreement with the $\sigma_\perp - \sigma_\parallel$ values given in Fig. 9. It should be mentioned here that while the first method of computing $\sigma_\perp - \sigma_\parallel$ makes use only of first derivatives of empirical equations, the second uses second derivatives. The agreement between the two methods thus serves as a double check on the reduction of the results. It need hardly be said that the values obtained by the first method are more reliable, depending as they do on data for all the crystals, whereas data for only two crystals are used in the second method. The second method can obviously be extended to include all the crystals, but it is not considered worthwhile to do so.

[16] O. Berg, Ann. d. Physik **32**, 477 (1910).
[17] G. Borelius and F. Gunneson, Ann. d. Physik **65**, 520 (1921).

3. Temperature coefficient of resistivity

The observed values of the temperature coefficient of resistivity are listed in Table I. These results were obtained by plotting the resistance of the

TABLE I.

S.P. crystals		K crystals	
θ	α	θ	α
1	4.043×10^{-3}	26.5	3.994×10^{-3}
12	4.086	34	3.960
16	4.039	40	3.986
22.5	4.019	44	4.019
25	4.049	66	3.963
28.5	4.059	90	4.069
30	4.042	90	4.069
33	4.043		
37	4.064		
39	4.046		
42	4.051		
44	4.004		
52	4.072		
53	4.049		
55	4.051		
59	4.067		
61.5	4.080		
65	4.055		
68.5	4.071		
71	4.058		
81	4.086		
81	4.096		
86.5	4.081		
Average value	4.058×10^{-3}		4.009×10^{-3}

various specimens against temperature on millimeter cross-section paper, the dimensions of the graph being approximately one by one and a half meters. On this immense scale nine-tenths of the points fall within one millimeter of the lines as drawn, the remaining points having deviations which would lead to errors in α not to exceed three-tenths of one percent. Hence the relationship between resistance and temperature throughout the entire ranged used, ($-170°$ to 25°C), is considered to be accurately linear. With this degree of accuracy it is evident that the difference in the values of α for the individual crystals must be thought of as real. The distinct difference which exists between the average value of α for the K specimens and the average value for the S.P. specimens, α in general being higher for the S.P. group, is in accord with what would be expected in view of the higher purity of the S.P. zinc. It might be argued that the variation of α within a group (such as the S.P.) should also be used as an indication of difference in purity, with the idea that either contamination occurred during the growth of the crystals or that some purifying process took place, the residue of zinc in the crucible getting more impure with time. In either case there should be a correlation between the order of growing a crystal and its value of α. No such correlation exists. Moreover it may be pointed out that if α is taken as an indicator of relative purity within a group, there should be a corresponding well-marked effect in the specific resistance. This, however, is not true. In spite of the over-lapping of

the α-values in the two groups, S.P. and K crystals, the resistivities of the S.P. crystals are almost without exception lower than those of the K crystals, comparing, of course, corresponding orientations. It may be further remarked that other properties, such as the Thomson effect, the unusual mechanical properties of the very pure zinc crystals, etc., should also give some clue to any possible purity difference of individual crystals in the same group. No such effects are found. Hence the difference in α amongst crystals made from the same grade of zinc must be attributed to some other factor than purity. There is an indication that α may increase with orientation, but the presence of several anomalous cases, high values for low orientations and vice versa, makes it difficult to consider α as purely a function of orientation. This variation of α amongst specimens made from the same grade of zinc is therefore a rather open question.

Ware in his determination obtained an average value of 0.00425 for the temperature coefficient in the temperature range, 20° to 110°C. In this connection, the writer wishes to point out that prior to the measurements of the temperature coefficient of resistivity just mentioned, an oil bath arrangement similar to that described by Ware was employed using a temperature range, 20° to 110°C. The average value of α obtained with that apparatus for K specimens was in very close agreement with Ware's results. It was, however, observed that with the writer's set-up, the resistance-temperature relationship was not linear in all cases, the departure from linearity being greater the longer the specimens had been immersed in the oil bath and always of such a type as to make the curves concave upward. This apparent increase in the resistance of the specimens, when the readings are taken starting with low temperatures, tends to give α a high value. An investigation proved that the zinc was being dissolved in the oil, the increased resistance of the specimens being exactly accounted for by the loss in weight. The effect was first noted with the same grade of oil that was used by Ware and the dissolution was more pronounced the longer the oil had been in use. At this time the oil was heated in a tin container with the heating element and its asbestos board form directly immersed in the oil. Removing the heating element from contact with the oil, using a Pyrex container, and a different grade of oil did not eliminate the effect. Since there is no indication of any departure from linearity in the upper range of the low temperature determinations and in view of the effect of the oil bath, it seems very unlikely that there is any departure of the resistance-temperature curves from linearity in the temperature range 20° to 100°C. Hence only the values obtained from the low temperature determinations have been listed in the table and in all probability these will apply to the higher temperature range as well.

The writer wishes to express his sincere thanks to the members of the staff of the Physics department of the State University of Iowa for their assistance and suggestions throughout the course of this investigation. The writer wishes in particular to express his appreciation to Dr. E. P. T. Tyndall for suggesting and directing this problem and for the encouragement and the many helpful criticisms he has so generously given.

THE INTERNAL MOLECULAR POTENTIAL BETWEEN THE SUBSTITUENT GROUPS IN A BENZENE RING AS DERIVED FROM THE HEATS OF COMBUSTION*

By H. A. Stuart[1]

(Received August 6, 1931)

Abstract

It is shown that differences in the observed heats of combustion of isomeric benzene derivatives can be interpreted as the internal molecular potential existing between their substituent groups. A like interpretation can be given for the differences between the values observed for the heats of combustion of certain nonisomeric benzene derivatives and those calculated by the rule of additivity. This internal potential, to which the attractive and repulsive forces between the groups are due, results from the electrostatic potential of the group moments (dipole effect), the polarization of the substituents and of the ring (induction effect), the dispersion effect, and from steric hindrance. We have, therefore, a new and direct method of measuring the internal potential, which determines both the internal motion of groups within an organic molecule and its most stable configuration. The values thus measured are in good agreement with values theoretically evaluated from the above intermolecular (van der Waals) forces. From the data derived by this method we conclude in the case of o-xylene that valence angles of 120° between the C–CH_3 bond and the aromatic C–C bonds are extremely stable, for the energy required to distort these angles through 10° is greater than 2 K cal/mole. We find, also, very restricted rotation for the butane molecule, from which it follows that saturated aliphatic hydrocarbons in the gaseous state tend to form zigzag chains. Such restricted rotation is found for the ether molecule as well.

Introduction

ONE of the most interesting structure problems at present is the question as to the rotation of groups around a bond and to their most stable orientation within an organic molecule. This rotational motion of course is governed by the forces acting between the different groups, that is, by the internal molecular potential between them. It is necessary, therefore, to study by means of theory the nature and distance of action of these forces, and to develop experimental methods for determining the mutual influence and the potential energy of the neighboring groups.

As to the nature and classification of these forces we will make the following assumptions, which agree nicely with our empirical knowledge. The forces leading to a chemical bond between two atoms are given principally by the interchange binding forces and can be calculated only by the methods of quantum mechanics. The forces between two neighboring atoms, not too close together, are the van der Waals forces. These intermolecular forces can be

* Contribution from the Chemical Laboratory of the University of California.

[1] Universität Königsberg, at present International Research Fellow University of California, Berkeley, California.

treated by classical and wave mechanics methods. If two atoms not connected by a chemical bond approach each other too closely, there are produced strong repulsive forces, which have not yet been treated theoretically, and which we will classify generally as caused by steric hindrance. We shall use this scheme in interpreting the results derived in this paper from the heat of combustion as it is all we have at present. It may be pointed out, however, that most of our conclusions are independent of the nature of the assumed forces. The sphere of action is determined by the surface at which we have equilibrium between repulsive and attractive forces, i.e. a minimum of potential energy.

Of the different methods which permit us to study the rotation within, and the most stable configuration of a molecule, we may mention measurements and discussions of electric moments,[2] investigations of the Kerr effect,[3] x-ray[4] and electron beam[5] interferences. The interference methods yield direct information concerning the distance between the atoms in a molecule. By the use of all these methods we may determine whether repulsive or attractive forces act between these atoms. But none of these methods gives us the internal potential energy between the atoms and atom groups, by which the internal motion of groups and the configuration of the molecule are determined.

It is therefore justifiable and useful to look for other methods, which may allow us to measure directly the internal potential and settle these questions of structure.

Such a method is given by the discussion of the heats of combustion, especially of isomeric compounds. It will be shown here that the differences in the energies of the molecules can be easily interpreted as the differences in the internal potential of the substituent groups, which is due to the attractive and repulsive forces acting between them.

As is well known, simple addition of the different bond energies concerned yields a value, correct to within a few percent, for the heat of formation of an organic molecule. This value is approximate because the value of any bond energy may depend in some measure upon the nature of the other bonds acting on the same atom[6] since such bonds often influence each other. If we take isomeric compounds such as isomeric benzene derivatives, however, where the same bonds act on the corresponding atoms, we expect constant heats of formation and therefore also constant heats of combustion so long as there is no marked difference in the internal potential energy between the sub-

[2] See for instance H. Sack, Erg. d. exakt. Naturw. **8**, 307 (1929) and H. A. Stuart, Phys. Zeits. **31**, 80 (1930); L. Meyer, Zeits. f. physik. Chem. **B, 8**, 27 (1930).

[3] H. A. Stuart, Zeits. f. Physik **63**, 533 (1930) and H. A. Stuart, Erg. d. exakt. Naturw. **10** (1931) in press.

[4] P. Debye, Phys. Zeits. **30**, 84, 524 (1929); **31**, 142 (1930). L. Bevilogna, ibid. **32**, 265 (1931).

[5] H. Mark and R. Wierl, Zeits. f. Physik **60**, 741 (1930); R. Wierl, Phys. Zeits. **31**, 366, 1028 (1930) and Leipziger Vorträge 1930, (1930).

[6] So we generally find differences in the aromatic and aliphatic bond energies, see H. Grimm and H. Wolff, Handbuch d. Physik **24**, 526 (1926).

stituents. We further expect that, on substituting in a benzene ring several groups, one after the other, the energy which is necessary for the successive groups will be independent of the presence of other substituents, so long as the internal potential between the substituents may be neglected. In this case the heat of combustion of the compound ought to be equal to the heat of combustion of benzene plus the amounts of energy characteristic of each substituent. The deviations from this additivity rule ought to increase with the potential energy between the substituents.

We shall first show that these ideas are in agreement with experimental data, and that deviations of the observed heats of combustion from the additivity rule can be interpreted quantitatively as potential energies between the substituent groups.

Experimental Data

In Table I, column 3, are summarized the observed heats of combustion of benzene and some simple derivatives in K cal/mole. As we have to compare the heats of combustion of the free molecules, or the heats of combustion for the gas at room temperature, we have to add to these observed values the heats of vaporization and in the case of solids also the heat of fusion, which are tabulated in columns 4 and 5. For our purpose it is sufficient to use the

Table I. *Thermal data and amounts of energy characteristic of each substituent for various benzene derivatives.*

Substance	Formula	H. Comb[7] obs. K cal/mole	H. Fusion K cal/mole	H. Vap. K cal/mole	H. Comb gas obs. K cal/mole	Q_{subst}
Benzene	C_6H_6	783.4		7.4	790.8	
Toluene	$C_6H_5 \cdot CH_3$	936		8	944	+153.2
Phenol	$C_6H_5 \cdot OH$	732	2.8	9	743.8	−47.0
Benzoic Acid	$C_6H_5 \cdot COOH$	771.2	(5)	(10.5)	786.7	−4.1
Aniline	$C_6H_5 \cdot NH_2$	812		9	821	+30.2
Nitrobenzene	$C_6H_5 \cdot NO_2$	739		10	749	−41.8
Fluorobenzene	$C_6H_5 \cdot F$	747.2		7.6	754.8	−36.0

[7] All data of heats of combustion are taken from the Intern. Crit. Tables, which are based on the critical compilation by M. S. Kharasch, Bureau of Standards, J. of Research, *2*, 359 (1929).

heats of fusion and of vaporization for the melting and the boiling point respectively. Where the heats of vaporization are not known, they are calculated by means of the Trouton rule, heat of vaporization $= 20 \times T_{abs}$ cal/mole. The heats of fusion, when not measured, are interpolated and extrapolated. All values for the heat of fusion and heat of vaporization, which are not known by direct measurements, are put in parantheses in this and the following tables. The values corrected for the gaseous state are tabulated in column 6 and in the last column we find the differences between the heats of combustion of benzene and the different derivatives, that is the energy Q_{subst} characteristic of the substitution for the different groups.

In order to show how far the energy necessary to substitute a certain group is independent of the presence of other substituents, we give, in Table II, the observed heats of combustion of some p-derivatives which are cor-

rected to the gaseous state. In column 4 we find the heats of combustion calculated by adding the Q_{subst} values (Table I, last column) to the heat of combustion of the benzene. The energy differences ΔU between the observed and calculated values are given in column 5. The plus sign shows that the observed value is greater than the calculated one. In the next column, 6, are tabulated the electric moments of the substituents together with their direction. A minus sign means that the group is negative with respect to the carbon atom of the ring. We recognize that the energy differences ΔU or the deviations of the additivity rule are increasing with the electric moment of the

TABLE II. *Comparison of observed and calculated heats of combustion of various p-derivatives.*

Substance	Substituents	H. Comb.[8] (gas obs.) K cal/mole	H. Comb. (calc.) K cal/mole	Energy difference ΔU K cal/mole	Elec. moments $\mu \times 10^{18}$
p-Xylene	CH_3; CH_3	1097.7	1097.2	+0.5	+0.4; +0.4
p-Nitrotoluene	NO_2; CH_3	903	902.2	+0.8	−3.8; +0.4
p-Fluoronitrobenzene	NO_2; F	714	713	+1.0	−3.8; −1.3
p-Nitrophenols	NO_2; OH	701[9]	702	−1.0	−3.8; +1.6
p-Nitrobenzoic Acids	NO_2; COOH	747.8	744.9	+2.9	−3.8; (2.7 and 1.6)[10]
p-Nitranilines	NO_2; NH_2	777[9]	779.2	−2.2	−3.8; (+1.5)
p-Dinitrobenzenes	NO_2; NO_2	712.5	707.2	+5.3	−3.8; −3.8

[8] The observed data for the liquid state and the heats of fusion and vaporization are tabulated in Table III.

[9] Heat of Comb. observed = 686; H. Fusion (5.5); H. Vap. (9.5) gives for H. Comb. for the gas 701; K cal; for p-nitraniline the values are 761; 5; (11), respectively, which gives 777 K cal for the gas.

[10] The moment of the COOH group consists of three bond moments: $\mu_{c=o} = 2.3.10^{-18}$; $\mu_{o-H} = 1.6.10^{-18}$ and $\mu_{c-o} = 0.7.10^{-18}$.

substituents, i.e., with the electrostatic potential of the groups. The differences for the first four compounds are within the limits of experimental error. We further find a negative deviation where the electric moments have different signs and therefore attract each other. This is to be expected since a negative difference must be interpreted as attraction.

In Table III are shown as a further example of the connection between the deviation from the additivity rule and the internal potential of the groups the heats of combustion of some isomeric di- and tri-substituted benzene derivatives. We always find that these energy differences ΔU given in the last column increase in the order para, meta and ortho positions. That is to be expected, since the potential between the groups, which is for these compounds, excepting for p- and m-nitraniline always repulsive, increases in the same direction. Besides the electrostatic potential and the polarization of the benzene ring we have in the case of the o-compounds always steric hindrance, that means strong repulsion.

CALCULATION OF THE INTERNAL MOLECULAR POTENTIAL BETWEEN THE SUBSTITUENT GROUPS

The question arises now, how far can these deviations from the additivity rule be interpreted as the internal potential of the substituents and how far

TABLE III. *Observed and calculated heats of combustion of some di- and tri-substituted benzene derivatives.*

Substance	Heat Comb. observed K cal/mole			H. Fusion K cal/mole			H. Vap. K cal/mole			H. Comb. gas K cal/mole observed			calc.	Energy Differences ΔU K cal/mole		
	p	m	o	p	m	o	p	m	o	p	m	o		p	m	o
Fluoronitrobenzene	703_s	706	707	(21)				9.5		714.5	715.5	716.5	713	+1.5	+2.5	+ 3.5
Nitrotoluene	889_s	893	897	(3)				(10)		902	903	907	902.2	−0.2	+0.8	+ 4.8
Nitrobenzoic Acid	728_s	729_s	735_s	8.8	4.6	6.7		(11)		747.8	744.6	752.7	744.9	+2.9	−0.3	+ 7.8
Dinitrobenzene	695_s	697_s	703.2_s	6.5	4.2	5.3	(11)	(11.5)	(11.5)	712.5	712.7	720	707.2	+5.3	+5.5	+12.8
Xylene	1089.1	1089.6	1092[11]				8.6	8.6	8.7	1097.7	1098.2	1100.7	1097.2	+0.5	+1.0	+ 3.5
	sym. 1, 3, 5	asym. 1, 2, 4		sym.	asym.		sym.	asym.		sym.	asym.			sym.	asym.	
Trinitrobenzene	664	674		(5.5)	3		(13)	(13)		682.5	690		665.4	+17.1	+24.6	

[11] Instead of 1093 K cal as given in the Int. Crit. Tables, we use 1092 K cal, as Richards and Barry, J. Amer. Chem. Soc. **37**, 993 (1915) find for the difference between p- and o- xylene 2.6 K cal.

can they be explained by the well-known forces acting between different molecules, i.e., the van der Waals forces.

There are three effects which contribute to the potential of molecules or in our case to the potential of the substituent groups. First of all the electrostatic potential of the permanent electric moments associated with the substituent groups, the dipole effect, secondly the induction effect (Debye effect) caused by the polarization of the molecule by the electric field of the moments of the substituents.[12] In this connection we must consider not only the mutual polarization of the substituents but also the polarization of the benzene ring, which contributes large amounts to the potential energy. The third effect is the so called dispersion effect, which has been introduced by London[13] into the theory of molecular forces. This effect consists in the mutual perturbation of the rapid internal motion of the electrons and always gives attraction.[14]

The energy of the dispersion effect can be approximately calculated, according to London, by the following relation.

$$E_{\text{disp.}} = -\frac{3}{4}\frac{h\nu_0 \cdot \gamma^2}{r^6}$$

γ is the polarizability, that is the electric moment, induced by the unit of electric intensity, r the distance of the groups; for $h\nu_0$ the ionization potential may be used. This effect is in meta- and para-position always negligible (50 to 100 cal/mole), in ortho-position greater, for instance for two NO_2 groups 1500 cal/mole. But as we usually have steric hinderance in ortho-position, i.e., strong repulsion, the dispersion effect will be overcompensated.

The dipole effect may be neglected for para- and meta-positions, excepting in the case of two NO_2 groups. The electrostatic potential of two dipoles whose vectors lie in a plane can be calculated by means of the following expression

$$E_{\text{dipole}} = -\frac{\mu_1 \cdot \mu_2}{r^3}[2 \cos \alpha_1 \cos \alpha_2 - \sin \alpha_1 \sin \alpha_2].$$

α_1 and α_2 are the angles between the direction of the electric moments 1 and 2 and the line connecting both dipoles.

The energy contribution of the induction effect is given by the formula

$$E_{\text{ind.}} = -\tfrac{1}{2}\gamma F^2.$$

F is the electric intensity of the dipole moments. This energy may be neglected as far as the mutual induction of the substituents is concerned, excepting for a very strong group moment, such as the moment of NO_2 with $\mu = 3.8 \times 10^{-18}$. Considering the polarization of the benzene ring we find that

[12] In this case the groups and molecules behave as systems with static charge distribution, dipoles, quadrupoles and so on, which polarize each other.

[13] F. London, Zeits. f. Physik **63**, 245 (1930); Zeits. f. physik. Chem. **B, 11**, 222 (1930).

[14] The van der Waals forces of the noble gases and of nonpolar molecules can be explained only by this effect.

this effect involves very large energies. If we substitute, for instance, one NO_2 group in the benzene ring the field of the group moment will polarize the rest of the molecule, first of all the six aromatic C–C bonds, 1, 2, 3 . . . 6, see Fig. 1. The energy of this polarization effect for the bonds 1 and 6 amounts to 3650 cal for each bond. For the 2 and 5 bonds we find 250 cal and for the 3 and 4 bonds 50 cal each. The total energy is therefore 7900 cal/mole.[15]

If we substitute two or more groups, we have to calculate the resulting field of all group moments acting on the different C–C bonds. It turns out that the energy contributed from the induction by one group depends on the presence of the other ones and that the total energy of the induction effect is not the sum of the energies characteristic of the single groups, whereas the potentials of the dipole and the dispersion effect are always additive and independent of the benzene ring. As long as the groups have electric moments

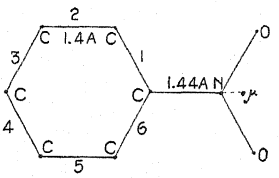


Fig. 1.

with the same direction with respect to the ring, the fields of the single moments weaken each other in most cases so that we get less energy for the induction effect. This corresponds to an increase in the total potential energy or in the heat of combustion.

In Table IV are given some of these calculated energies which arise from the polarization of the ring. In column 1 we find the number and nature of the substituents and in column 2 the energies of the induction effect. Column 3 shows the deviations from the energies we should find if each substituent would polarize the ring independently. These deviations, as mentioned above,

TABLE IV. *Calculated energies which arise from a polarization of the ring.*

Substituent	Induction effect calc. K cal/mole	Deviation from additivity K cal/mole
1 NO_2	−7.9	
2×NO_2 p	−12.7	+3.1
m	−11.3	+4.5
o	−15.9	+0.7
3×NO_2 sym.	−10.9	+12.8
asym.	−15.1	+8.6
1 F	−1.5	
1 F and 1 NO_2 p	−8.2	+1.2
m	−7.5	+1.9
o	−8.5	+0.9
1 NH_2	−1.9	
1 NH_2 and 1 NO_2 p	−10.6	−0.8
1 CH_3	0	
1 CH_3 and 1 NO_2 p	−7.9	0

[15] The fact that all aromatic bond energies are larger than the aliphatic ones may be to some extent due to this induction effect.

in so far as they are positive, increase the total potential and this corresponds to repulsion or higher heat of combustion.

In the calculations the following distances and assumptions are used. The distances of the atoms are known from x-ray diffraction data, which give us for C–C_{ar} 1.4, for C–C_{al} 1.5, and for C–N 1.44A; the distance C–F is about 1.6A. The electric moment of the NO_2 group is localized at a point 0.4A behind the N-atom. The distance between this moment and the C-atom of the ring is therefore 1.84A and the distance between the moment of the C–F bond and the C atom is 1.4A.[16] The refraction R of the six aromatic C–C bonds is equal to the molecular refraction of benzene minus the refraction of the six C–H bonds, i.e., $26.18-6\times1.7=16$. The polarizability, $\gamma=3R/4\pi N$, of one C–C bond amounts therefore to $10.6.10^{-25}$. The C–C bonds are treated as polarizable spheres located in the middle of the bond.

After we have determined in this way the energy amounts caused by the induction of the C–C bonds, we can calculate the total internal potential of the substituent groups for some simple derivatives. In Table V, columns 2

TABLE V.

Substance[17]	Dipole effect cal K—— mole	Disp. effect cal K—— mole	Induct. of subst. cal K—— mole	Induct. of ring cal K—— mole	Total int. potential calc. cal K—— mole	Energy diff. ΔU obs. cal K—— mole	Potential of steric hindrance cal K—— mole
p-dinitrobenzene	+1.6	0	0	+3.1	+4.7	+5.3	0
m- "	+1.8	0	0	+4.5	+6.3	+5.5	0
o- "	+7.7	−1.9	−1.0	+0.7	+5.5	+12.8	+7.3
1, 3, 5, trinitrobenzene	+5.3	0	0	+12.8	+18.1	+17.1	0
1, 2, 4 "	+10.8	−1.9	−1.0	+8.6	+16.5	+24.6 (20.8)	+8.1
p-fluoronitrobenzene	+0.5	0	0	+1.2	+1.7	+1.5	0
m- "	+0.8	0	0	+1.9	+2.7	+2.5	0
o- "	+3.2	−1.7	−0.2	+0.9	+3.2	+3.5	+0.3
p-nitrotoluene	−0.1	0	0	0	−0.1	−0.2	0
m- "	−0.1	0	0	0	−0.1	+0.8	0
o- "	−0.8	−1.6	−0.4	0	−2.8	+4.8	+7.6
p-nitraniline	−0.6	0	0	−0.8	−1.4	−2.2	0
p-xylene	0	0	0	0	0	+0.5	0
m- "	0	0	0	0	0	+1.0	0
o- "	0	−1.0	0	0	−1.0	+3.5	+4.5

[17] The values for m- and o-nitraniline, the nitrobenzoic acids, and the nitrophenols are not given, as we do not know enough about the situation, the orientation, and the amount of the moments associated with these groups, which are not in the plane of the ring.

to 5, are given the energy amounts of the dipole and dispersion effects as well as of both induction effects. In column 6 and 7 we find the sum, i.e., the total potential energy together with the observed energy differences ΔU taken from Table III, last column.

[16] The distances N–O and O–O are 1.13 and 2.09A respectively. Using the fact that for the N=O bond the center of the positive charges is located at 1/4th of the distance N=O near the oxygen atom, we can localize the moment of the NO_2 group (see L. Meyer, Zeits. f. physik. Chem. **B, 8,** 27 (1930)).

[18] For these calculations the following data are used. The polarizabilities are for NO_2 32.2×10^{-25}, for CH_3 24.9×10^{-25} and for F about 7×10^{-25}, the ionization potentials are for Cl 13 volts, for F 16.9, for NO_2 estimated to 13 volts and for CH_3 estimated to 10 volts.

There is an excellent agreement between the observed and calculated values, excepting for the ortho- compounds where we have steric hindrance. The agreement is surprisingly good considering the simplifying assumptions, which are the dipole moments are localized at a point and that the polarizable C–C bonds are substituted by polarizable spheres in the middle of the bonds. In the case of p-nitraniline we find in agreement with the observation an attractive potential and for p- and m-xylene within the limits of experimental error no internal potential at all. We are therefore justified in interpretating an observed energy difference ΔU as the internal potential between the substituent groups.

In the case of the ortho-compounds and of 1, 2, 4 trinitrobenzene the observed energy differences are always much greater than anticipated. The calculation of the electrostatic potential is in these cases somewhat uncertain because the distances of the group moments are comparable with the real dimensions of the dipoles. However we can best explain these deviations as caused principally by steric hindrance, which produces strong repulsive forces. These potentials of steric hindrance or these deviations are tabulated in the last column of Table V. We expect an increase in these deviations with an increase in the diameter of the substituent groups, as is observed. Fluoronitrobenzene has the smallest repulsion potential 0.3 K cal, o-xylene 4.5 K cal, nitrotoluene 7.6 K cal, dinitrobenzene 7.3 K cal and 1, 2, 4 trinitrobenzene 8.1 K cal. The two last compounds have, as is to be expected within the limits of experimental error, the same repulsive potential.

The total internal potential of o-xylene, which is given by the energy difference of the para- or meta- and ortho-compound, as there is no internal potential in p- and m-position, amounts to about 3 K cal.[19] In order to find the internal potential for the higher CH_3 derivatives we have tabulated in Table VI the heat of combustion for each of these compounds together with

TABLE VI.

Substance	H. Comb. obs. K—— cal / mole	H. Fusion K—— cal / mole	H. Vap. K—— cal / mole	H. Comb. gas obs.	K cal/mole calc.	Internal potential K—— cal / mole
1,2,4 Trimethylbenzene (Pseudocumene)	1241.7		9	1250.7	1250.4	+0.3
1,2,4,5 Tetramethylbenzene (Durol)$_s$	1393.6	(5)	9.5	1408.1	1403.6	+4.5
Pentamethylbenzene$_s$	1554	(4)	(10)	1568.0	1556.8	+11.2
Hexamethylbenzene$_s$	1711.9	(6)	10.5	1728.4	1710.0	+18.4

the values calculated according to the additivity rule. The last column gives us the energy difference ΔU or the internal potential. We recognize that these energies are increasing with the number of the substituents as is to be expected. We see furthermore that these potentials are within the limits of

[19] This value depends only on the relative accuracy of the measurements of the heats of combustion of the three xylenes and is therefore more reliable than the difference of 3.5 K cal between the observed and calculated heat of combustion of o-xylene.

error, 6×3, 4×3, and 2×3 K cal, for hexamethylbenzene, pentamethylbenzene and tetramethylbenzene respectively.[20] Because the CH_3 groups have no induction effect where the energy is not additive, and because the p- and m-compounds have no marked internal potential, the total internal potential for hexamethylbenzene is six times as large as the single potentials between two neighboring CH_3 groups. Thus we find that two neighboring groups in hexamethylbenzene have practically the same repulsive potential as in o-xylene. This result is not obvious. Using it we can draw some conclusions regarding the stability of the valence angles between the C–CH_3 and the C–C bonds.

Conclusions

It is known from Lonsdale's x-ray[21] investigations of the crystal structure of $C_6(CH_3)_6$ that the carbon atoms of the CH_3 groups are situated in the plane of the ring, in spite of the repulsive forces (this already shows the stability of the valence angles). We have therefore valence angles of 120° between C–CH_3 bonds and the aromatic C–C bonds. In the case of o-xylene both groups may yield to the repulsive forces but remain in the plane of the ring so that we get a deviation of these valence angles. The angles will not be

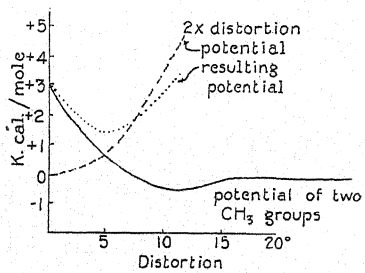


Fig. 2.

distorted more than 10° each, as this change is already sufficient to increase the distance between the carbon atoms of the two CH_3 groups from 2.9 to 3.4A where we certainly have equilibrium or even attraction of the two groups.

As we find for the o-position in xylene the same potential energy of 3 K cal as for the ideal 120° position in hexamethylbenzene, the decrease of the repulsive potential caused by the increasing C–C distance in case of o-xylene must be compensated by the energy, which is necessary to distort both valence angles. Such a compensation is only possible if the energy which is necessary to bend the angles so far that the two CH_3 groups are in the equilibrium position, is greater than the energy difference between the ideal 120° position, and this equilibrium position.[22]

[20] The values for hexa-and pentamethylbenzene are very reliable as here experimental errors do not effect the value for the internal potential energy very much. This is not true for trimethylbenzene where the observed heat of combustion is certainly too small.

[21] K. Lonsdale, Proc. Roy. Soc. (London), **A123**, 494 (1929).

[22] If the distortion potential for this equilibrium angle is equal or smaller than 4.5 K cal, the resulting potential, see Fig. 2, has a minimum and therefore the total potential for o-xylene would be less than 1/6 of the potential of hexamethylbenzene, therefore the distortion energy must be greater than about 2 K cal for each angle.

This energy difference is about 4 K cal since the minimum potential due to the dispersion attraction is about 1 K cal, and the energy required to distort the valence angles between a C–CH_3 and C–C bonds in a benzene ring through 10° is therefore greater than 2 K cal. Thus we see how stable the valence angles are. It may be mentioned that this result is in agreement with values which the author[23] has calculated for the stability of the valence angles of some molecules such as HCN, C_2H_2, CO_2, CS_2, where the fundamental frequencies are known. The distortion energies for these molecules vary between 700 and 4000 cal/mole for a deviation of 10°.

From the heats of combustion for the xylenes we found that two CH_3 groups have a repulsion potential of about 3 K cal/mole. On the other hand the very exact measurements of the heats of combustion of the nine isomeric heptanes established by the Bureau of Standards give nearly constant energies. There are some small deviations which might indicate a slight attraction between two CH_3 groups bound to the same carbon atom, but not a re-

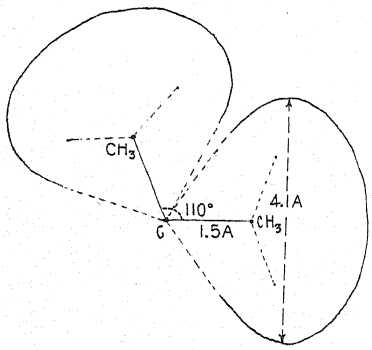


Fig. 3a.

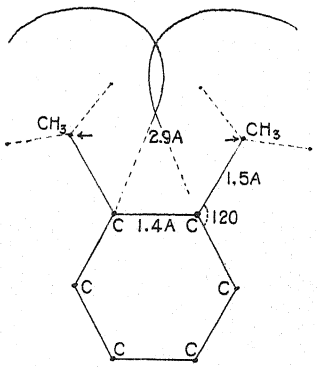


Fig. 3b.

pulsion,[24] although the carbon atoms are only 2.5A distant. From this result we recognize very distinctly that the potential of two CH_3 groups depends, as is to be expected, not only on their distance, but also on their orientation. Therefore the diameter of the sphere of action of a CH_3 group is not the same in all directions. The shape will be very irregular, but will have approximately rotational symmetry around the direction of the C–CH_3 bond. The following form of the sphere of action, see Fig. 3a and b, may explain that we have no marked repulsion for two CH_3 groups bound on the same carbon atom, but a strong one in o-xylene. The greatest diameter perpendicular to the direction of the fourth valence may be taken from Lonsdale's data for the crystal structure of hexamethylbenzene. She finds for the closest distance, to which two CH_3 groups in different molecules can approach each

[23] H. A. Stuart, Phys. Zeits. **32** (1931) in press.

[24] As an alternative to the assumption of zero repulsion, we should have to assume that any possible changes in the internal potentials of adjacent CH_3 groups are just compensated by bond energy changes resulting from the replacement of C-H by C-C bonds. That such compensation exists in all nine isomers with their different configurations is, of course, highly improbable.

other, 4.1A.[25] The greatest radius of the group taken from the C-atom as the center will probably be in the direction of the C–H bonds. We see that for o-xylene the spheres of action overlap each other.

Finally we will discuss the most stable positions of saturated hydrocarbons and of the ether molecule, using the fact that two CH_3 groups in o-xylene have a repulsive potential of about 3 K cal. In the butane molecule where the valence angles are 110° (tetrahedron angle of the quadrivalent carbon atom), we have rotation of the last CH_3 group around the C–C bond. In position II the distance of the two carbon atoms is only 2.6A, so we must have a greater repulsive potential than that in o-xylene, where the dis-

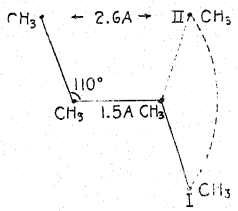


Fig. 4.

tance is 2.9A, or more, and the potential amounts to 3 K cal. As this energy is much greater than the energy of the temperature motion, KT about 600 cal at room temperature, it follows that position II is impossible.[26] In position I (180°) we certainly have no repulsion, perhaps a little attraction, so we probably have at room temperature torsional vibrations with great amplitudes around position I. We may therefore expect for the saturated hydrocarbons also in the gaseous state a tendency towards zigzag chains, as they are observed in liquids and crystals. Nevertheless it is possible that we will find for long chains something like a closed form which, of course, is oriented very far from a planar configuration, especially if the chain has large dipoles on its ends.

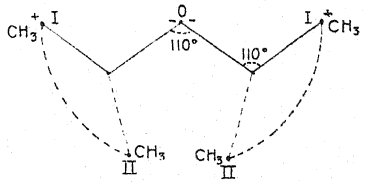


Fig. 5.

Let us consider now the ether molecule, see Fig. 5. We assume as usual 110° for the valence angle of the oxygen atom. We recognize then that position II is absolutely impossible as we have here an enormous steric hindrance, the distance of the carbon atoms of the CH_3 groups being only 1.7A. If at the same time we turn both CH_3 groups through 90°, the distance is still 3.2

[25] This diameter is very reasonable, as with a smaller one, about 3.4A, we could not understand the repulsion in o-xylene

[26] A rotation through 90° to 120° from position II will be sufficient to avoid the repulsive forces as the distance is 3.0A for 60° and 3.5A for 120°.

to 3.3 and becomes, at about 110°, 3.5A, where the repulsion disappears. A configuration with one group in II, the other in I, also seems to be impossible as we have then a repulsive potential similar to that in butane (distance C–C 2.5A). On the other hand, position I is, on account of the dipole attraction, energy approximately equal to $\frac{1}{2}KT$, the most stable one, so that we have in the ether molecule rotation vibrations of about 70° around position I. This is in excellent agreement with results derived by the author from discussions of electric moments in homologous series[27] and from observations of the Kerr constant[28] of the ether molecule, which show directly that position I is the most stable one.

If we had more and, what is of even greater importance, more exact data for the heats of combustion of other isomeric compounds, such as the CH_3 and Cl derivatives of methane, ethane, ethylene, benzene, etc., we should be able to draw very precise conclusions regarding the internal potential of the substituent groups as a function of the distance and the orientation and also as to the mutual influence of the bond energies. This paper may be considered as a first attempt to employ heats of combustion in answering questions as to the free rotation and the stable configuration of groups in an organic molecule.

In conclusion the author wishes to express his thanks to Professor Lewis for his hospitality, and to Professor Pauling, and the other members of the University of California with whom he has had the privilege of discussing this problem.

[27] H. A. Stuart, Phys. Zeits. **31**, 81 (1930).
[28] H. A. Stuart, Zeits. f. Physik **63**, 533 (1930).

FURTHER APPLICATION OF HUANG'S GENERAL EQUATIONS OF ENERGY AND ENTROPY OF GASES: THE GENERAL ADIABATIC EQUATION OF GASES

By Tzu Ching Huang
Department of Chemistry, National Tsing Hua University, Peiping, China

(Received August 14, 1931)

Abstract

From Huang's general equation of entropy there is deduced a general adiabatic equation,

$$\int \psi(v)dv - \int \frac{\partial F}{\partial T} dv + \int c_{v\alpha} \frac{dT}{T} = \text{const},$$

for any gas of the type, $p = T\Psi(v) - \Phi(v) - F(v, T)$. The result is tested satisfactorily with perfect gas as gases obeying van der Waal and Beattie-Bridgeman's equations of state.

THE present short paper aims to deduce a general adiabatic equation of gases belonging to the type,

$$p = T\Psi(v) - \Phi(v) - F(v, T), \tag{1}$$

in which p is the pressure, T the temperature of the gas, $\Psi(v)$ and $\Phi(v)$ are functions of volume, and $F(v, T)$ the function of volume and temperature.

Recently, the author[1] showed that for any gas in the form of Eq. (1), its entropy s is

$$s = \int \Psi(v)dv - \int \frac{\partial F}{\partial T} dv + \int c_{v\alpha} \frac{dT}{T} + k \tag{2}$$

in which $c_{v\alpha}$ = heat capacity of the gas at constant volume and at infinite dilution. Since the necessary condition for any gas to be in adiabatic state is s = const, we have immediately,

$$\int \Psi(v)dv - \int \frac{\partial F}{\partial T} dv + \int c_{v\alpha} \frac{dT}{T} = \text{const}, \tag{3}$$

as the general adiabatic equation of gases. The following applications show the validity and usefulness of this equation.

(1) Perfect gas:

$$p = \frac{RT}{v}.$$

Referring to Eq. (1) and applying Eq. (3), we get

$$Tv^{R/c_v} = \text{const}.$$

[1] Huang, Phys. Rev. **37**, 1171 (1931).

(2) van der Waal's equation of state:

$$p = \frac{RT}{v - b} - \frac{a}{v^2}.$$

Eqs. (1) and (3) give

$$T(v - b)^{R/c_v}.$$

The above results are well known in classical thermodynamics.

(3) Beattie-Bridgeman's equation of state:[2]

$$p = \frac{RT}{v^2}\left[v + B_0\left(1 - \frac{b}{v}\right)\right] - \frac{A_0}{v^2}\left(1 - \frac{a}{v}\right) - \frac{cR}{v^3T^2}\left[v + B_0\left(1 - \frac{b}{v}\right)\right].$$

Eqs. (1) and (3) give

$$R \ln v - \frac{R}{v}\left(B_0 + \frac{2c}{T^3}\right) + \frac{RB_0}{v^2}\left(\frac{b}{2} - \frac{c}{T^3}\right) + \frac{2bcRB_0}{3v^3T^3} + \int c_{v\alpha}\frac{dT}{T} = \text{const.}$$

[2] Beattie and Bridgeman, Proc. Am. Art. Sci. **63**, 231 (1928).

LETTERS TO THE EDITOR

Prompt publication of brief reports of important discoveries in physics may be secured by addressing them to this department. Closing dates for this department are, for the first issue of the month, the twenty-eighth of the preceding month; for the second issue, the thirteenth of the month. The Board of Editors does not hold itself responsible for the opinions expressed by the correspondents.

Intensity of Raman Lines in Estimating the Concentration of the Components Present in Benzene-Toluene Mixtures

Every substance gives its characteristic Raman spectrum in which the frequency shifts of the modified lines can be attributed to the presence of particular groups and linkages in the molecule, and the intensity of the lines under given conditions can be related to the molecular density.[1] Dadieu and Kohlrausch[2] have obtained Raman spectra of binary mixtures in which the characteristic lines of the two components appear without change of frequency, except in a few cases where a slight shift occurs due to the high dipole moment of the molecule. It seemed, therefore, probable that for ordinary liquid mixtures a fair estimate of the concentration of the components present could be made from measurements of the relative intensity of the Raman lines.

Photographs were taken of Raman spectra of benzene-toluene mixtures of varying concentration using a Hg arc as source of excitation as described by R. W. Wood. Experimental conditions were maintained, as nearly as possible, the same for each series of spectra photographed.

The first spectra obtained indicated that a difference of 25 percent in concentration of either component was easily perceptible. Photometric measurements with a Moll densitometer showed a marked change in the contour as well as in the height of the intensity curves of the Raman lines. Some of the results for 25 percent change in concentration are listed in Table I which gives the relative height of the intensity curve for three of the characteristic benzene and toluene lines excited by their respective Hg lines.

TABLE I. *Relative intensity [Ht. in mm].*

Hg Line	4046	4358	4358
	T	*B*	*T*
Raman line	2917	1178	1207
B % *T*			
100– 0	7.1	36.3	2.2
75– 25	18.2	25.6	12.3
50– 50	26.5	22.0	17.8
25– 75	31.0	18.9	23.4
0–100	35.7	12.6	27.2

Five percent variations in concentration could be less readily discerned from the Raman plates; however, intensity curves showed, without doubt, that decided differences existed, as can be seen in part from the measurements given in Table II.

TABLE II. *Relative intensity [Ht. in mm].*

Hg line	4358	4358	4347
	T	*B*	*B*
Raman line	781	884	991
B % *T*			
100– 0	3.2	9.8	19.0
95– 5	7.0	9.0	14.0
90–10	7.3	7.6	11.0
85–15	7.8	6.6	8.5

At present no attempt has been made to determine less than 5 percent change in concentration. Longer exposures as well as change in other conditions may yield more quantitative results, especially when one of the components is present at low concentration.

The experiments indicate, that with proper control of conditions, concentrations of a given mixture, to within at least 5 percent, can be estimated from a study of the relative intensity of the Raman lines.

ELIZABETH A. CRIGLER
Chemistry Laboratory,
Johns Hopkins University,
September 10, 1931.

[1] Daure, P., Comptes Rendus **186**, 1833 (1928); Venkateswaran, S. Ind. J. Phys. **3**, 105 (1928).

[2] Dadieu, A. and Kohlrausch, K. W. F., Phys. Zeits. **31**, 514 (1930).

X-ray Diffraction Patterns of Mixtures[1]

In the March 15 Physical Review, Mr. Roy W. Drier reported that in a number of instances which had come to his attention the x-ray diffraction pattern of mixtures did not correspond to a composite pattern of the components, but on the contrary some lines of the components were absent and new lines appeared. Somewhat earlier,[2] he had reported elsewhere the detection of extremely small amounts of silver (as low as 0.003%) in samples of copper. A comment by Mr. Cyril S. Smith[3] on this earlier paper has already been published to the effect that the silver lines might very well be due to the molybdenum K-beta radiation diffracted by the copper lattice. In private correspondence, we had called Mr. Drier's attention to this interpretation, but it was not entirely convincing to him since his experiments had indicated that spectroscopically silver-free copper did not give the so-called silver lines.

These two papers of Mr. Drier's bring up so clearly the question of the interpretation of the diffraction patterns of mixtures obtained with the General Electric apparatus and his inferences are so surprising that we feel them worthy of comment.

With regard to the presence of silver in copper, we found it quite possible, using sodium chloride as a sample, to demonstrate the presence of molybdenum K-beta radiation under experimental conditions similar to Mr. Drier's. Furthermore, contrary to his experience, we found we could obtain these lines with a sample of copper which was spectroscopically silver-free. On the other hand, we found that palladium, which has an atomic number differing only by one from that of silver but has different lattice dimensions, could not be detected in mechanical mixtures with copper unless present in amounts of the order of 1 to 2 percent. We may add that a copper specimen[4] containing 0.03 percent silver, which gave the apparent silver lines when irradiated with molybdenum, failed to show any silver lines when exposed to copper radiation. We believe, therefore, with Mr. Smith that the effect Mr. Drier observed was due to the inhomogeneity of the radiation employed and that no trustworthy evidence for the presence or absence of silver could be adduced from his experiments.

Our experimental results likewise differ from Mr. Drier's in the study of other mixtures such as those of barium sulfate-titanium dioxide. The barium sulfate pattern itself contains so many lines as to render the titanium dioxide pattern difficult to isolate, and there is the further factor that titanium dioxide may exist in three crystalline forms. In a considerable number of experiments, however, we have found no instance of a diffraction pattern from a mixture of these materials which could not be explained as a composite of the patterns of the components. We repeated Mr. Drier's experiments with copper-zinc mixtures, which he instanced as a particularly good case, and again failed to reproduce his results. The diffraction patterns contained all the strong lines of copper and of zinc and we detected no lines attributable to alpha-brass. If, as Mr. Drier reported, as many as eight lines of alpha-brass could be detected, the strongest of these (111 and 100) must have been of appreciable intensity, but we failed to develop even them.

It is difficult for us to offer an explanation of Mr. Drier's experimental findings, but we think that the question of the homogeneity of the radiation has not been carefully considered and also the possibility of a shift in the position of lines by diffraction from the edges of opaque samples. In any case, it seems to us that the explanation for these surprising effects should first be sought in a very careful examination of the technique rather than in speculations as to the formation of new phases.

A. W. KENNEY
HENRY AUGHEY

Wilmington, Delaware,
September 10, 1931.

[1] Communication No. 80 from the Experimental Station of E. I. duPont de Nemours & Co., Inc., Wilmington, Delaware.

[2] Drier, Ind. Eng. Chem. **23**, 404–5 (1931).

[3] C. S. Smith, Ind. Eng. Chem. **23**, 969–70 (1931).

[4] We wish to acknowledge the assistance of the American Brass Company, who gave us a number of samples of copper containing varying amounts of silver which had been accurately determined.

A New Method of Producing Negative Ions

In some recent experiments on the bombardment of metal surfaces with positive ions, negative ions formed at the surface by the positive ion impacts were observed. The apparatus used was an adaptation of the Dempster type mass spectrograph in which the negative particles formed could be analysed. Platinum targets were used in most cases and the impacting ions were of lithium (chiefly Li_7^+) produced by a spodumene source on a hot filament. The positive ions were accelerated through 500 volts to the target where any negative particles formed would be driven back to the first slit of the mass spectrograph with the same velocity as the impinging positives. Identification of the negative particles was made from the calibration of the spectrograph with known positive ions. All experiments were made in a good vacuum of the order of 10^{-6} mm of mercury.

In this way negative ions of $OH^-=17$ and $Cl^-=35$ were found to result from the bombardment with positive lithium ions. Secondary electrons were also observed together with two ions which were probably H_1^- and H_2^-; the latter two ions were not easily analysed due to the width of the slits and the small values of the magnetic field at which they were observed. For platinum targets which had not been outgassed the negative OH ion was strong and steady over a period of several hours; its intensity was of the same order of magnitude as the electron emission. The H_1 and H_2 ions accompanied the OH ion, H_1 being several times as intense as H_2. The Cl ion was not resolved into its components and was not always observed; its presence was more noticeable when the target was coated with spodumene showing that it probably arose from some chance contamination of the target. Strong outgassing of the platinum target did not affect the electron emission but caused the negative ions to disappear.

This method of forming negative ions while of interest in itself may also be of importance in interpreting related experiments. It is possible that in studies of ionization and secondary electrons produced by positive ions this type of emission may contribute to the effects observed. The general presence of water vapor in most metals and compounds will probably give rise to negative ions as well as electrons while the negative chlorine ion indicates that other substances may form other ions under the influence of positive ion bombardment.

Negative ions have been observed previously by J. J. Thomson[1] and O. H. Smith[2] as the retrograde rays formed in discharge tubes. These ions, presumably of H_2^- and O_2^-, were formed just in front of the cathode by gas molecules acquiring a negative charge. O. W. Richardson[3] and H. A. Barton[4] have reported a few cases of negative ions formed by direct heating of the salt. Very recently Mueller and Smyth[5] have reported negative hydrogen and hydroxyl ions formed by electron impacts in apparatus containing water vapor. Further work on this type of emission is being carried out and will be reported on later.

JAMES S. THOMPSON

Ryerson Physical Laboratory,
University of Chicago,

Armour Institute of Technology,
Chicago, Ill.,
September 12, 1931.

[1] J. J. Thomson, "Rays of Positive Electricity," pp. 137–138.

[2] O. H. Smith, Phys. Rev. 7, 625 (1916).

[3] O. W. Richardson, "Emission of Electricity from Hot Bodies."

[4] H. A. Barton, Phys. Rev. 26, 360 (1925).

[5] D. W. Mueller and H. D. Smyth, Program of Schenectady Meeting, American Physical Society, Abstract 11, Aug. 26, 1931.

Variations in the Grating Constant of Calcite Crystals

With the development of the double crystal spectrometer for measuring x-ray wavelengths and the use of the high precision photographic spectrometers now employed, the question of a possible variation in the grating constant of calcite is of considerable importance. Also the chemical purity and density of the crystals should be examined.

In the present experiments optically clear crystals have been secured from four localities, Iceland, Spain, Montana, and Argentina. The crystals were carefully cleaved and the part of the surface used for diffracting the x-rays was almost free from "steps." Small pieces of each crystal were cut from a region very close to the part of the crystal used and a chemical

TABLE I.

Crystal	Silica	Alumina	Ferrous oxide	Manganous oxide	Magnesium oxide	Calcium carbonate
Iceland	absent	absent	0.006%	0.007%	absent	99.98%
Montana	absent	absent	0.005	0.011	absent	99.97
Argentina	absent	absent	0.006	0.010	absent	99.97
Spain	0.004%	absent	0.007	0.006	absent	99.98

analysis of these pieces has been made. The results of these analyses are shown in Table I. Thus chemically there appears to be very little difference between the various samples.

A preliminary determination of the density of each crystal indicated that the density was the same for all crystals within 1 part in 4000. A more precise determination of the densities will be made before a final report of the experiment is given.

The spectrometer was a high precision double crystal spectrometer built by the Société Génevoise. An attempt was made to calibrate the circle with a telescope but no consistent error of as much as 0.5″ was found. This was just about the error of setting the cross hairs in the telescope. A more precise method of testing the circle was as follows: The diffracting angle of the same crystal in the 4th order was determined in three 120° positions of the circle. These agreed to within 0.4″ with an average variation of 0.2″. This average diffracting angle has been used as the absolute value and all other measurements have been made relative to this.

The first crystal of the spectrometer was an Iceland calcite set to diffract the $K\alpha_1$ line of molybdenum over the main axis of the spectrometer. This crystal was made parallel to the spectrometer axis to within 1′ of arc. The surface of the second crystal was mounted on the axis and parallel to it to within 5″ of arc. The correction which must be made in the measured diffraction angle, due to the height of the slits, was determined experimentally in the 4th order. This agreed, however, very closely with the calculated correction. The correction for the thermal expansion of the crystal has been made using Larsson's value[1] ($\alpha = 1.09 \times 10^{-6}$) of the expansion coefficient. The results are for a crystal temperature of 18°C. In calculating the wave-lengths the theoretical value of the index of refraction ($1-\mu = 1.85 \times 10^{-6}$) has been used and the grating space of the crystal was assumed to be 3.02904A in the first order.

The results given for the 4th order are much more reliable than any others. Eight independent determinations have been made on each crystal in the 4th order and the average variation in each case was about 0.2″. In each of the other orders only two or three determinations have been made and the average

[1] Larsson, Inaugural-Dissertation, Uppsala 1929.

Diffraction angles.

Order	Iceland	Montana	Argentina	Spain
1	6° 42′ 35.4″	6° 42′ 35.6″	6° 42′ 35.5″	6° 42′ 35.3″
2	13° 30′ 44.9″	13° 30′ 45.2″	13° 30′ 45.7″	13° 30′ 45.3″
3	20° 31′ 0.3″	20° 31′ 1.3″	20° 31′ 1.1″	20° 31′ 0.8″
4	27° 51′ 34.0″	27° 51′ 34.6″	27° 51′ 34.7″	27° 51′ 34.4″
5	35° 44′ 28.5″	35° 44′ 30.8″	35° 44′ 29.9″	35° 34′ 29.9″

Wave-lengths.

1	0.707833A	0.707838	0.707837	0.707832
2	0.707827	0.707831	0.707836	0.707832
3	0.707832	0.707841	0.707839	0.707836
4	0.707830	0.707834	0.707835	0.707833
5	0.707827	0.707838	0.707834	0.707834

variation was from 0.2″ to 0.5″. The average wave-length as given by the 4th order is

$$\text{Mo}K\alpha_1 = 0.707833\text{A}$$

Compton[2] has recently reported a precise determination of the diffraction of the $\text{Mo}K\alpha_1$ line in the 4th order using calcite. His value of the diffracting angle is 27° 51′ 32.9″ or a wave-length 0.707824A as calculated above. This is considerably smaller than any of my results, however, Larsson's results[1] agree very closely with the present values obtained with the Iceland crystal.

[2] Compton, Phys. Rev. **37**, 1694 (1931).

The index of refraction of the x-rays in the crystal has been calculated from the 1st and 2nd orders and the 1st and 4th orders. The average values for all crystals are

$$\text{1st and 2nd order } (1-\mu) = 1.90\times10^{-6}$$
$$\text{1st and 4th order } (1-\mu) = 1.86\times10^{-6}.$$

These values are in fair agreement with Larsson's[1] results but differ considerably from the value $(1-\mu) = (2.10\pm0.15)\times10^{-6}$ reported by Compton.[2]

J. A. BEARDEN

Johns Hopkins University,
September 10, 1931.

Thermocouples of Longitudinally and Transversely Magnetized Wires

Recently (Phys. Rev. **38**, 179, (1931)) William H. Ross has performed some experiments designed to give the thermal *emf* between longitudinally and transversely magnetized elements of the same ferromagnetic substance. In these experiments a short length of wire was placed parallel to the magnetic field between the poles of an electromagnet. At each end of this short length the wire was bent at right angles, so that two long segments came out parallel to each other from between the poles of the magnet. These long ends were connected to a galvanometer. The two bends between the magnet poles were kept at different temperatures and when the magnet was excited a thermoelectromotive force was observed.

We may consider that the circuit contains three thermoelectrically distinct metals:—(1) longitudinally magnetized metal, (2) transversely magnetized metal, (3) unmagnetized metal. Assume the junctions of (3) and (2) to be situated at the edges of the magnet poles. These junctions will then be at different temperatures as a result of conduction of heat along the wires, and the resultant *emf* will be partly due to the combination of (2) and (3). The title of the paper by Ross implies the existence of only the elements (1) and (2).

Of course, practically, there is no sharp line of demarcation between the elements (2) and (3), but the results are essentially unchanged in the experiment where a temperature gradient in a nonuniform magnetic field replaces the sharp boundary considered above.

Another point of view would consider the longitudinal thermomagnetic potential differences in the transverse sections of wire. The total *emf* would then involve an integration over a varying magnetic field and a varying temperature gradient.

These considerations are brought forward in order to point out the difficulty of interpreting in a simple way the experiments of Ross. There are conflicting experiments in this field of research and it is highly desirable to keep the various elements clearly segregated in any particular experiment in order to make comparison possible with other results.

C. W. HEAPS

Department of Physics,
Rice Institute,
Houston, Texas,
September 7, 1931.

BOOK REVIEWS

Das Jahrhundert der Strahlen. JOSEF ROSENTHAL. Pp. 29, Figs. 18, Georg Thieme Verlag, Leipzig 1930.

In this little book (the substance of a lecture) the author reviews in a popular and concentrated manner the whole field of radiation. He describes the corpuscluar rays: cathode and canal rays, alpha and beta rays, and covers the entire region of what he calls ether-rays. He refers to them as Herz-, heat-, light-, chemical-, Roentgen-, gamma and Hess-rays. These names indicate that the contribution of German scientists to our knowledge in the field of radiation has been particularly emphasized. The tendency of referring as much as possible to German scientists evidently contributed to make the lecture popular and the article is popular in the best sense of the word. Probably it is for the same reason the author refers to the electromagnetic radiation as ether-rays without hinting at any of the modern theories. Sand and water jets are referred to as corpuscular rays and sound waves are discussed in order to prepare the mind for the ether waves. Special emphasis is laid on the practical importance of roentgen rays, particularly in medicine. The book gives a good lesson in how to make scientific discoveries popular to the newcomers who must answer in the affirmative the last question, "Ist es nicht schön das Wunderland der Strahlen?"

K. W. STENSTROM
University of Minnesota

Statistical Mechanics. R. H. FOWLER. Pp. 570. figs. 28, tables 59. University Press, Cambridge, 1929, and the Macmillan Company, New York.

In this monumental volume, R. H. Fowler has assembled all the work done by him and his fellow-workers since, say, 1922 when the first article of Darwin and Fowler appeared. Although of course, he treats very thoroughly the work done elsewhere, still the book reflects very strongly the methods and the interests of what one might call the Cambridge school. The book, which grew out of an essay to which was awarded the Adams Prize, is devoted mainly to the statistical method and its applications. Consequently the book is devoted practically entirely as the subtitle indicates to the theory of the properties of matter in equilibrium. The kinetic method, or as Jeans calls it the method of collisions, in which one has to consider more in detail the elementary interaction processes, and by which one is only able to treat systems not in equilibrium (as in the theory of heatconduction, viscosity, etc.), is only given in the last chapters (Chapters 17 and 19). Fowler does not here discuss the theory of nonequilibrium states; he only considers what restrictions are imposed on the laws of interaction by the theory of equilibrium states. From this point of view the principle of detailed balancing and its consequences are carefully treated. The H-theorem of Boltzmann is proved for collisions with central forces and considered then as a proof of detailed balancing. Though this is of course correct, still in the opinion of the reviewer it does not give full justice to the famous theorem. Because of the cycle-proof of Boltzmann, which Fowler does not mention, we know that the theorem is more general than the principle of detailed balancing. Also its role in the explanation of the laws of thermodynamics is, I think, not sufficiently stressed.

The statistical method is presented from the point of view which characterises the equilibrium state as the average state. The mathematical method of evaluating the summations which occur is that of the generating functions, or partition functions as Fowler calls them. Together with the method of steepest descent for the approximate evaluation of complex integrals, it forms a very powerful tool, which was for the first time applied to problems in statistical mechanics in the well known articles of Darwin and Fowler in the Phil. Mag. These elegant and in the best sense of the term "witty" methods give the book a great unity in the mathematical treatment; and furthermore they have the advantage that in principle one can judge the degree of approximation at every stage of the calculation. Yet the reviewer regrets that the simple approximation method of Gibbs (as Pauli presents it for instance in the Zeits. f.

Physik **41**, 81, (1927)) is not given, and that the usual derivation of the Maxwell-Boltzmann distribution law, etc., as the most probable state is also omitted. I am not quite convinced by Chapter 6, on the connection with classical thermodynamics, that one is allowed to omit the latter; and the consideration of the most probable state would certainly make the mathematics much simpler.

But these criticisms are perhaps quite irrelevant, because the book is not intended to be a textbook for beginners, and the weight obviously lies not so much on the careful discussion of first principles and methods, as on the applications. And here one can only admire the thoroughness with which the great number of subjects have been treated.

The first four chapters give the general method and the more simple applications. Very interesting is the careful discussion connecting the specific heat and the band spectrum data. Though the agreement is in general good, there remain some very surprising discrepancies. Chapter 5 gives the theory of dissociation and sublimation, which links up with the very fine discussion of the Nernst heat theorem and the chemical constants in Chapter 7. Striking are also the next two chapters on the theory of imperfect gases and the chapters on interatomic forces, which was contributed by Lennard-Jones. With the renewed interest at present in the theory of the equation of state, they will become more and more useful. The next chapters bring the theory of thermionics (Chapter 11), of the dielectric and the dia- and paramagnetic constants of gases (Chapter 12) and of the properties of dilute solutions, including the Debye theory of strong electrolytes (Chapter 13). Then follows (Chapter 14, 15, 16) the study of the properties of matter at high temperatures, which formed the original Adams Prize essay. Fowler's work in this field is so well known that there is no need to give the contents of these chapters in more detail. There is further still a chapter on chemical kinetics, and a short account of the theory of fluctuations. The theory of the Brownian motion is only touched upon. The book closes with a Chapter on the new statistics, with applications to the theory of metals.

All this can give only a small idea of the wealth of material, and the completeness with which most of the subjects have been treated. I am certain that for a long time to come Fowler's work will be an indispensable reference book for all those who are interested in the wide field of the kinetic theory of matter.

GEORGE E. UHLENBECK
University of Michigan

La Topographie sans Topographes. F. OLLIVIER. Pp. 301, figs. 158. Revue d'Optique theorique et instrumentale, Paris, 1929. Price, 42 francs.

Surveying by means of the photographic camera on a practical basis had its beginning about 1860 in the work of Colonel Laussedat in France. Considerable attention was given to these methods in various European countries and the major contributions to the subject were made by European engineers.

About 1885 the photographic method was introduced in America by the Canadian government in connection with surveys in the Rocky Mountains and southeastern Alaska. In the latter the U. S. Coast and Geodetic Survey participated in connection with the preliminary reconnaissance for the boundary between Alaska and British Columbia. Aside from this use by the Canadian and United States government in mountain topographic surveys, the photographic method was used comparatively little in North America until the advent of aerial photography since the World War.

This book by Commandant Ollivier of the French army engineers is a treatise on phototopographic surveying. Its three hundred pages embrace an introduction and nine chapters.

Chapter one is devoted to an excellent historical outline of the method from its early development by Colonel Laussedat together with an explanation of the fundamental principles. The second chapter is devoted to a theoretical consideration of methods and instruments for revealing to the eye the topographic relief as a basis for the surveying and mapping. Monocular, binocular, and stereoscopic methods are treated.

The principles underlying the stereoscopic method of phototopographic surveying are developed in chapter three, and the following chapter is devoted to the instruments and apparatus used in the field and in the office work. Special attention is given to the elaborate modern

instruments for mechanically plotting the control points and contours from the original photographs.

In chapters five and six a very full consideration is given to the subject of precision, errors and corrections. Chapters seven and eight are devoted to the methods of reducing the data and plotting the maps. In conclusion, a number of general topics are considered in the final chapter.

This book should be an important addition to the literature of the subject. With the increased use of photography in aerial surveying, it is inevitable that greater attention will be given in the United States to photographic methods and that more books in the English language will appear, in addition to the current periodical literature in the technical press.

O. M. LELAND
University of Minnesota

A Handbook of Physics Measurements, Vol. II. E. S. FERRY in collaboration with O. W. SILVEY, G. W. SHERMAN, JR., D. C. DUNCAN. Pp. xi+277, figs. 143., Third Edition corrected, John Wiley and Sons Inc., 1929. Price, $2.50.

Each of the four chapters in this self contained manual is divided into two parts. The first part includes definitions, descriptions of apparatus and the derivation of the general theory and equations used in the experiments. In the second part each experimental measurement is described in detail as to manipulation and computation.

One suspects that the manual is written for sophomore engineers who are taking calculus, as mathematics including differential equations is used in developing the theory.

The variation of difficulty in the experiments is marked. In all of the chapters except the first on vibratory motion, experiments are found which might well be used for a liberal arts course with a mathematical prerequisite of only high school algebra. All of the first chapter and part of the others contain plenty of experiments that might well be used in an advanced general laboratory with a calculus prerequisite. This dual characteristic is perhaps best illustrated by chapter four on electricity and magnetism where the twenty-four experiments listed might well be those given in a general physics laboratory plus those given in a special course in electrical measurements for electrical engineers.

It appears to be to the disadvantage of the book that the most difficult theory presented is in the first twenty five pages.

Not the least interesting part of this book is the forty two page supplement listing thirty nine projects so designed that the ambitious student may do extra work in the laboratory. The book contains tables of the most used physical constants.

The preface states that experiments are included "which experience has shown to be most available for college and industrial laboratories." One may not agree with the statement but certainly a list of well written and unusual experiments are offered. Any person in charge of a physics laboratory can hardly afford to miss the wealth of suggestions offered in this volume.

C. J. LAPP
State University of Iowa

Vorlesungen über einige Klassen nichtlinearer Integralgleichungen und Integro-differentialgleichungen. L. LICHTENSTEIN, x+164 pp. Springer, Berlin, 1931. Price, RM 16.80.

Although linear equations have played the conspicuous rôle in mathematical physics to date, some mathematicians have thought that important physical concepts may be gained from a study of nonlinear equations. This monograph represents a beginning in this direction.

For nonlinear integral equations *im kleinen* (where the functions are small in absolute value), the method of successive approximations is shown to be applicable. According as the homogeneous equation has not or has eigenfunctions, the regular or the branching case subsists. This theory is extended to systems of nonlinear integral equations. Certain nonlinear integro-differential equations can be reduced to such systems, but even when a reduction is not possible, there are many cases in which the method of successive approximations is capable of justification.

When there is no restriction on the absolute value of the functions, other methods may be

used to solve the integral equation. The problem may be transformed to an extremal problem, which is solved by using the Ritz method in conjunction with a process of selection from the minimal sequence.

In treating all the special cases, the author goes through the same motions time and again, reminding one of the ancient tale in which "another grasshopper went in and brought forth another grain of corn." (Even then, the grasshoppers had made hardly a dent in the corn pile, when the king protested his weariness and ordered the narrator to cease.) It would seem more to the point to make a thorough study of a typical case, rather than to rely on induction to furnish the final theory.

The book contains many references to the literature, and may be of some interest to specialists, even though of a temporary nature.

JAMES H. BARTLETT, JR.
University of Illinois

Annales de L'Institut Henri Poincaré, Vol. I, sections i, ii, and iii, (Under the direction of MM. CH. MAURAIN, E. BOREL, J. PERRIN, AND P. LANGEVIN. Edited by MM. L. BRILLOUIN L. DE BROGLIE, AND M. FRÉCHET). Pp. 308. Les Presses Universitaires de France, Paris.

The purpose of this new journal is the publication of "conferences" given at l'Institut Henri Poincaré by distinguished men of science, the special fields considered being theoretical physics and the calculus of probabilities. The first volume has appeared in three sections.

In section i, the first article is a discussion by Einstein of his unitary field theory. The idea of parallelism at a distance is developed, and it is shown how certain general field equations may be obtained, which reduce in the first approximation to the well-known gravitational and electromagnetic equations. The tentativeness of the theory is emphasized. Darwin next shows how various phenomena may be regarded from the wave point of view. Finally, Fermi gives a clear account of the Dirac radiation theory, but the degree of approximation does not permit of a detailed discussion of dispersive processes. A short treatment of the Compton and Doppler effects concludes the article.

In section ii, De Donder writes on "La gravifique Einsteinienne," using the original general relativity theory, and claims to give a unitary theory of gravitational, electromagnetic, and quantum-mechanical phenomena. The treatment is based on an article of J. M. Whittaker, who attempted to generalize the Dirac wave equation to the case where an external gravitational field is present. This article is more readable than De Donder's version, although it is open to question as to whether the correct generalization has really been found.

There follow articles dealing more with the calculus of probabilities. Paul Levy derives the Gaussian error law for independent errors, showing what the underlying assumptions are. Polya, from certain postulates, finds the possible error functions for this case, obtaining somewhat greater generality. For observations which are interdependent, such as in contagion and heredity, one finds a Gaussian distribution in many cases, but the criterion for such a distribution is as yet unknown. Kostitzin, in the concluding article, tells about the hereditary physics of Volterra. When the hereditary influence is limited to a short interval of time, the equations describing the situation have infinitely many solutions. The author believes that these may have physical reality, saying that we measure by adopting statistical averages and that we invent statistical theories to explain experiment. In the opinion of the reviewer, this point deserves the attention of phyisicists interested in fundamental problems.

In section iii, after explaining the matrix mechanics and the theory of radioactive disintegration, Born speculates about catalysis by adsorption. The width of spectral lines in then calculated by the method of Weiskopf and Wigner. Brillouin points out the difficulties in solving an hyperbolic equation with spherical boundary conditions, and in determining the rate of propagation of solidification in a sphere. He concludes that the present methods are not suited to the study of these problems.

These "Annales" merit a place in the modern physics library, for many interesting topics are treated with unusual clarity.

JAMES H. BARTLETT, JR.
University of Illinois

Radiations from Radioactive Substances. SIR ERNEST RUTHERFORD, DR. JAMES CHADWICK AND DR. C. D. ELLIS. Pp. 588, figs. 140, Cambridge University Press, and The Macmillan Company, New York. Price, $6.50.

Those interested in radioactivity, I am sure feel greatly indebted to Sir Ernest Rutherford for the assistance he rendered through the publication of his earlier volume entitled "Radioactive Substances and their Radiations." Concerning the then rapidly developing subject that volume still stands as a remarkably accurate presentation. Recently there appeared from the Cambridge University Press, a new volume under the joint authorship of Rutherford, Chadwick and Ellis entitled "Radiations from Radioactive Substances." It is inevitable that again those interested in radioactivity will come to feel indebted to Professor Rutherford as well as his co-authors.

As was to be expected under the circumstances, the volume devotes only the first chapter to the radioactive transformations, the character of which is now quite fully established and has been fully treated by various authors. The new volume therefore being devoted primarily to the radioactive radiations, treats more or less consecutively the alpha, beta and gamma-rays. While the three authors have cooperated in the preparation of the volume as a whole, the treatment of the alpha-rays is, according to the preface, primarily due to Professor Rutherford, the subject of scattering of alpha and beta-rays including artificial disintegration to Dr. Chadwick and the treatment of beta and gamma-rays to Dr. Ellis.

Towards the end is a chapter on atomic nuclei followed by a chapter on miscellaneous topics involving questions of technique and standards. The volume has 588 pages and the illustrations and workmanship are on a par with the earlier volume referred to above. As the authors are among the foremost authorities in the field of Radioactivity, the volume is highly authoritative. The volume is virtually nonmathematical but the fullness of the treatment makes it valuable as a reference book as well as a text in radioactivity.

HENRY A. ERIKSON
University of Minnesota

A Survey of Physics for College Students. FREDERICK A. SAUNDERS. Pp. 635+x. Henry Holt and Company, New York, 1930. Price, $3.75.

Professor Saunders has given us an attractive, and very interesting text; his diction is clear and concise, the figures are excellent and in many cases unique.

In mechanics, the practice of placing the chapters on hydrostatics at the beginning of the treatise seems hardly justified, even by the demands of elementary laboratory work. The chapters on 'motion,' and 'force and motion' are more logically developed. The treatment of rotation, while entirely correct and concise seems to have a lack of concreteness which raises the question whether it shall prove teachable to the average beginner in this subject.

Coming to the topics, elasticity and rigidity, one is impelled to wonder: "How long, Oh Lord"!—until a writer of English texts shall have the courage of convictions to make the proper use of these two terms. One can only marvel why, in spite of the fact that Tait so clearly stated, more than a half-century ago: "A substance is said to be *elastic*, when on being left free it recovers wholly . . . or partially, from a deformation," and farther, "sometimes it is more convenient to speak of the property of *resistance to stress*, as when we speak of a body's *Rigidity*" and adds, significantly, "Young's treatment of the subject of Elasticity is one of the few really imperfect portions of his great work,"—the muddled state of presentation persists through the century in this field,—in which the work of Tait, Thomson, Stokes and de St. Venable leaves no want of precision and clarity whatsoever. In this matter Dr. Saunders is strictly conventional.

In the treatment of electricity, magnetism and optics Dr. Saunders has been successful in introducing the conceptions of modern physics along with the essentials of classic science, for the most part. Geometrical optics is so largely based upon light 'rays' that it would seem questionable whether the studied avoidance of this conception, and method of development of the simpler laws of lenses and reflectors is worth the while an elementary text; the loss in clearness and simplicity seems hardly compensated for in the nearer approach to verity in conceptions.

In his treatment of physical optics, especially in the chapter on dispersion and spectra the author has been particularly happy in his blending of the classic with modern physics.

The text as a whole shows evidence of painstaking work and careful editing, although an occasional error has slipped through, for example, the behavior of a diamagnetic substance in a *uniform* magnetic field is not that which is suggested by the illustration of Fig. 19–12, a field which is *not* uniform being required to produce the action characteristic of diamagnetic media.

On the whole, this text constitutes a distinct and worth while contribution in the field of science teaching, and the teachers of physics in the decade just beginning are to be greatly indebted to Dr. Saunders for such a stimulating and generally well-ordered text.

JOHN E. ALMY
University of Nebraska

Applied Geophysics in the Search for Minerals. A. S. EVE AND D. A. KEYES. Pp. 253, figs. 92. Macmillan Company, New York, 1929. Price $3.00.

This little book gives the elementary principles, a description and operation of instruments and some details of field practice of all the methods of geophysical prospecting which have had practical application. Nearly half of the space in the book is given to electrical and electromagnetic methods, and the rest is about evenly divided between magnetic, gravimetric and seismic methods with a very brief discussion of a few other methods and of salt domes.

The treatment of the electrical and electromagnetic methods reflects the author's experience with them and many details of field apparatus and field procedure are given. In all, there are 18 different methods of electrical and electromagnetic prospecting which are described and for most of these the result and effectiveness based on actual field experience are given. The theoretical treatment is elementary, but sufficient to give the working principles of all the methods described.

The treatment of magnetic, gravitational and seismic methods is apparently based much more on published accounts and less on field experience. The theoretical foundations of these methods are clearly presented, although quite brief. A particular example is the very clear development of the elusive curvature quantity measured by the torsion balance. The discussions of field procedure are brief and in some cases slightly erroneous.

The book is the only one in English to which one can turn as an elementary reference on all the applied methods of geophysical prospecting. Because of its emphasis on electrical and electromagnetic methods, it is probably more useful to the geologist or engineer interested in metal deposits, than to those interested in the larger and deeper oil bearing structures for the location of which the seismograph, torsion balance and magnetometer are much more useful.

L. L. NETTLETON
The Gulf Companies

Uber ungëdanpfte elektrische Ultrakurzwellen. K. KOHL. From Vol. 9. Ergebnisse der exakten Naturwissenschaften. Pp. 276–341. Springer, Berlin, 1930.

The various methods of producing very short electrical waves are reviewed briefly. The greater part of the work is devoted to a discussion of the production of waves of lengths between 3.5 and some 100 cm by means of high vacuum tubes, the emphasis being placed on the experimental results and methods rather than on the somewhat unsatisfactory theoretical explanations. The main points of the several theories are, however, pointed out, as are their weaknesses, also. A chapter on the use of the magnetron for short wave production is included. The final chapter deals with the several suggestions which have been made for the practical use of the special properties of ultrashort waves. This chapter contains some hints on reception methods.

Those interested in any one of the many ramifications of the short-wave problem will find this booklet a helpful reference.

F. B. LLEWELLYN
Bell Telephone Laboratories

Artificial Sunlight. N. LUCKIESH, Pp. 254, figs. 65, plates 8, D. Van Nostrand Company, New York, 1930. Price. $3.75.

"Combining radiation for health with light for vision" is the subtitle of this delightfully written book. Its objective is to call attention to the possible usefulness of some new types of electric light bulbs. At first the author makes the point that light is necessary not only for vision but also for maintenance of health. The majority of the population in this country is working indoors and for them the amount of exposure to unfiltered sunshine is very slight. Radiation of wave-lengths between 2800 and 3100A is assumed to be particularly beneficial physiologically. This radiation is stopped by ordinary window glass and also by the glass used in the ordinary type of incandescent electric bulbs. It is present to a relatively great extent in the carbon arcs and the quartz mercury arcs, which are being used by physicians for light treatments. Sunlight, which has been proven to be of particular value for health also contains a portion of rays in this region. The author proposes that a continuous exposure to small intensities of this radiation in hospitals, homes and offices may be of value and he describes how this can be done. A number of tables and charts are given showing the spectral distribution of the radiation energy: in the solar radiation; from a black body and certain incandescent solids at various temperatures; from carbon arcs and some other electric arcs. A short discussion of the whole electromagnetic spectrum is given. Some biological effects are referred to and the erythemal skin reaction is especially considered. The number of foot-candle-minutes necessary to produce an erythema with different light sources is given in tabulated form. Media suitable for transmission and reflection are discussed with suitable data. The permanency of such media is also considered and the extent to which the transmission of these media changes with age is demonstrated by figures. Infrared radiation and its medical use is considered in some of the chapters but ultraviolet radiation constitutes the main subject of the book. A special chapter is devoted to methods available for quantitative measurements of this radiation.

After all the fundamental problems are thoroughly considered the author describes the new "Sunlight" S-1 lamp. This is a combination of a tungsten filament lamp and a mercury arc housed in a bulb made of Corex D glass, which transmits radiation in the ultraviolet region referred to as specially important. This type of burner requires a transformer as it uses much lower voltage than the ordinary types of bulbs do. Finally the possibility of using tungsten filament burners with bulbs made of Corex D and other glasses transmitting far down in the ultraviolet is considered. Such lamps made for 110 volts can be used instead of the ordinary electric bulbs in the home. Special fixtures and reflectors can be made to enhance the efficiency of the installation. Data on measurements are given which show that erythema producing rays are present though of low intensity. These new types of bulbs are now on the market.

The book contains a collection of data which is of great value. It is easy to read and should prove of interest to physicists and physicians as well as to others of college training. When reading the book it is, however, well to remember that the action of radiation on the human system is quite complicated and that our knowledge in this field is as yet very limited. Such a "new era of lighting" as the author proposes may be of very great importance for the health and should be considered seriously. It will, however, take a long time before definite conclusions can be reached. The possibility that some injurious effects may result from too rapid change is not excluded. Will our eyes stand such continuous exposure for a number of years? How about people who are supersensitive to ultraviolet rays? Let us not be too pessimistic. The author's arguments are quite convincing and the book is a very valuable contribution in the field of light and health.

K. W. STENSTROM
University of Minnesota

Second Series *October 15, 1931* *Vol. 38, No. 8*

THE
PHYSICAL REVIEW

A NEW EXPERIMENT BEARING ON COSMIC-RAY PHENOMENA

By L. M. Mott-Smith and G. L. Locher
The Rice Institute

(Received September 4, 1931)

Abstract

This new experiment consists in combining a Wilson cloud expansion apparatus with Geiger-Müller electron-counters in a manner which allows the simultaneous study of individual cosmic-ray particles by the two methods. Its purpose was to see whether the coincidence effect in electron-counters is actually caused by the passage of an ionizing particle through them as has been generally assumed. This was considered desirable because it was felt that the several conflicting cosmic-ray experiments could perhaps be more satisfactorily explained by assuming the coincidences to be produced by photons. In this work a series of expansion photographs was taken under experimental conditions which allowed a definite correlation of an ion-track appearing in the expansion chamber with a discharge of a Geiger-Müller counter. It was found that the discharges of a counter due to cosmic radiation are accompanied by ion-tracks resembling those due to fast β-rays from radioactive sources. This result means that, in accord with previous beliefs, the coincidence effects are caused by ionizing particles. The best assumption we can make at present appears to be that these are high-energy electrons. The possibility that these effects are due to photons appears to be excluded, so that the reconciliation of the conflicting experimental data in this field will have to follow other lines.

Introduction

SINCE the discovery by Bothe and Kolhörster[1] that the cosmic radiation produces simultaneous discharges when passing through two Geiger-Müller[2] electron-counters placed one above the other, it has been generally assumed that this "coincidence effect" is caused by the passage of an ionizing material particle (presumably a high-energy electron) through the counters. This view appeared entirely reasonable, for the only other simple hypothesis, that the effect is caused by the passage of a photon through the counters, was shown by these investigators to be unable to account for their result unless some new phenomenon was concerned. On the other hand it is interesting to note that the recent failure of attempts by Rossi[3] and by Mott-Smith[4] to produce a magnetic deviation of these corpuscles could perhaps be more satis-

[1] W. Bothe and W. Kolhörster, Zeits. f. Physik **56**, 751 (1929). See also the more recent work of B. Rossi, Cim. (N. S.) **8**, 49, (1931) No. 2.
[2] H. Geiger and W. Müller, Phys. Zeits. **29**, 839 (1928).
[3] B. Rossi, Rend, Acc. dei Lincei **2**, 478 (1930).
[4] L. M. Mott-Smith, Phys. Rev. **37**, 1001 (1931).

factorily explained on the basis of photons. In these experiments, which were made with apparatus involving coincidences in electron-counters, no detectable magnetic deflection of these supposed electrons was observed, though in the work by Mott-Smith, electrons with an energy of as large a value as 2×10^9 e-volts would have given a readily measurable effect. As has been pointed out by the above investigator, there are at present certain serious difficulties in interpreting these experiments to mean that an electronic radiation of such enormous energy exists. If, however, the coincidence effects were produced by the passage of a photon through the apparatus, the lack of deflection is at once explained. In addition, if this were the case it would be clear at once why the Bothe and Kolhörster[1] absorption experiments with counters gave the same cosmic-ray absorption coefficient as that obtained by the electroscope work. It must be added, however, that essential additions to the known properties of photons would have to be postulated to allow this interpretation. In view of our relatively uncertain experimental knowledge with regard to the nature of γ-type radiation having the penetrating power of the cosmic-rays it is believed that such a procedure might be allowable.

A further difficulty with ascribing the coincidence effects to photons comes from the work of Skobelzyn.[5] From his work with the Wilson expansion-chamber it is known that the earth's surface is being bombarded by a radiation composed of high-energy electrons whose energy, intensity, and distribution about the vertical indicate that it is in some way connected with the cosmic radiation. It has been assumed that this radiation is the same as that responsible for the coincidence effects. However, this assumption rests on rather indirect and approximate considerations which might be questioned in view of the result of the deflection experiments as well as the other difficulties in this field.

Consideration of the foregoing type led us to look for a direct experimental method which could decide between these two possibilities.

Experimental

General considerations.

It was decided that a suitable method consisted in combining a Wilson cloud-chamber with Geiger-Müller counters in a manner that permitted the simultaneous study of individual cosmic-ray particles (or photons) by the two methods. For example, if a cloud-chamber is interposed between two counters so that every particle which operates the counters by passing through them must also pass through the chamber, ion-tracks appearing in the chamber can be correlated with the discharges of the counters. This correlation can be made quite definite. A track in the chamber will only be formed during a time-interval of about 0.05 sec. just after the expansion is completed, so that only particles which operate the counters during this interval can be expected to produce a track. Since with the counting-rates attainable the chance of obtaining more than one discharge during the "sensitive" interval is negligibly small, the appearance of tracks at the expansions

[5] D. Skobelzyn, Zeits. f. Physik **54**, 686 (1929).

for which the counters discharged during this interval is a definite indication that the discharge and the track were produced by the same particle.

If a correlation between such tracks and the counter discharges were found, it would be good evidence that the coincidence effects in electron-counters are caused by ionizing particles. A failure to find tracks associated with the discharges would speak in favor of photons if these are assumed to have the properties of ordinary γ-rays, since such photons are known to produce no observable track in traversing a cloud-chamber. The question arises, however, whether it is possible to distinguish in this manner between ionizing particles on one hand, and on the other, photons for which the minimum of new properties are postulated which suffice to account for the coincidence effects. In order that a cosmic-ray photon may cause the observed coincidence phenomena it must be nearly certain to produce at least one ion in each counter through which it passes. On the Compton theory the average energy given to the recoil electrons is in the case of cosmic radiation so great that the "mean free path" of the photon is too large to give even a fair probability of production of an ion in each counter. What is needed here is an additional process, by which such a photon can produce a series of low-energy ions along its path in a manner analagous to the ion-track formation by β-particles or other ionizing particles. To explain the coincidences, these "photon-tracks" would need to have only one or less ion-pairs per cm path in air under normal conditions. Hence such an interpretation might be allowable without contradicting existing experimental facts, particularly since such a process need be postulated only for high-energy photons. However, it appears fairly certain that these hypothetical photon-tracks cannot be assumed to have anything approaching the density of ionization of those due to even the fastest β-particles. This is on account of the unallowably great loss of energy which the photon would undergo in passing through absorbing media. Accordingly, the presence or absence of ion-tracks associated with the counter-discharges can be expected to give the desired information.

Apparatus and preliminary tests.

The apparatus which was actually set up differs from the arrangement described above (for purposes of illustration) on account of certain experimental difficulties. Instead of placing two counters one above and one beneath the expansion-chamber, a single counter was used, located directly above the chamber. This simplification was found necessary because it turns out that with any feasible arrangement involving two counters the passage of cosmic-ray corpuscles through the pair is altogether too infrequent to render the experiment possible. However, our single-counter arrangement is capable of giving just as significant results. In the first place, as will appear below, we can expect that a sufficiently large fraction of the discharges of the single counter are due to cosmic-ray corpuscles which pass through the expansion chamber. Secondly, it is known from the work of Bothe and Kolhörster and others that the ratio of the cosmic-ray counting-rate for the single impulses of one counter to that for paired coincidences in two such counters is about what is expected from the geometry of the arrangement, assuming

that all the particles which give the single impulses would give coincidences if a second counter were in position to receive them. Accordingly, there can be little doubt that in our experiments with the single counter we are studying the corpuscles which are responsible for the coincidence effects.

The relative positions of the expansion chamber E and the Geiger-Müller counter T_1, T_2, as well as of the cameras C for taking the expansion-photographs are indicated by Fig. 1 which represents two side-elevations of the apparatus. (The cameras have been schematically represented in this figure by simply drawing the plates and lenses.) It will be noted that two counters are shown (at T_1 and T_2). These, however, are connected to the amplifier (see Fig. 2) in such a manner that they operate exactly like a single counter of larger cross-sectional area, and can be so considered in what follows.

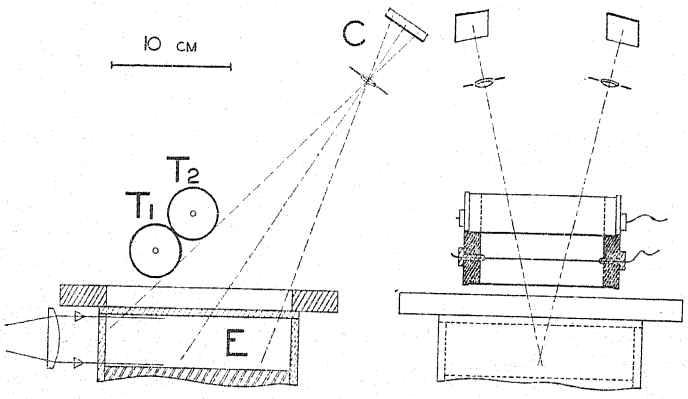


Fig. 1.

The expansion-chamber is the same as that previously described by Locher;[6] its details need not be entered into here. The operation of the chamber was tested by observing the tracks due to recoil β-particles produced by the γ-radiation from a small quantity of radium, filtered through 3 mm of lead. This test was repeated at frequent intervals during the taking of the expansion photographs to insure that the expansion-chamber and associated apparatus remained in proper working condition. The source of illumination was a new type of mercury "flash" arc, developed by the junior author, a full account of which will be published in a separate article.

The Geiger-Müller counters were of a simple construction similar to that used in the first work of Bothe and Kolhörster.[1] A section through one of them is shown in Fig. 1. The tubes were brass of 1.0 mm wall thickness with hard rubber end-pieces carrying little brass holders to which the central wire was attached. The wire was tungsten about 0.076 mm in diameter and had no special treatment of the surface except careful removal of dust just before introduction into the counter. The counter contained air at about 7 cm of mercury pressure.

Tests of the counting-rates of the two counters gave a value of about 55 impulses per minute for each, a rate which is about normal for tubes of these

[6] G. L. Locher, J.O.S.A. & R.S.I. 19, 58 (1929).

dimensions and under our conditions of sea level and about one meter water-equivalent shielding by the parts of the building above the apparatus. Sensitivity tests with γ-radiation from a small quantity of radium were also satisfactory, one milligram of radium at 4.6 meters increasing the count to about 150 discharges per minute.

It is also necessary to know what fraction of the counter-discharges are due to cosmic radiation. To find what fraction of the count is due to radioactive γ-radiation from the surroundings, the counting-rate of one of the counters was determined while it was shielded on all sides by a lead shield approximately 2.5 cm thick. This shield reduced the count from 58.8 to 34.5 per minute. The effect of this shield on the intensity of the local γ-radiation was calculated by taking the absorption coefficient of this radiation to be 0.49 per cm of lead. Its effect on the cosmic radiation could be neglected. It is also necessary to allow for the "zero count" due to the radioactivity of the counter itself and other internal causes. For this the value 6 impulses per minute based on the determination by Bothe and Kolhörster was taken. This approximation was made on account of the difficulty of making tests with the

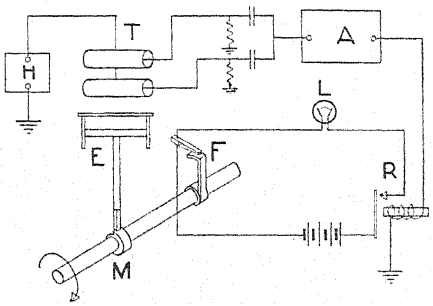


Fig. 2.

counter in a completely radiation-free region. In this manner it was determined that 0.30 ± 0.05 of the discharges of the counters were due to cosmic radiation.

Fig. 2 shows very schematically the auxiliary apparatus of interest. The source of potential for the counters, H, consisted of a thermionic rectifier and condenser furnishing the required potential of about 1500 volts. The amplifier A was of the usual three-stage vacuum-tube variety. It operated the relay R which had a fairly light armature and was adjusted to operate with as short a time lag as possible. Oscillographic tests showed that the relay remains closed for somewhat less than 0.01 sec. at each counter-impulse. This relay closed the circuit as indicated. The purpose of this circuit and associated apparatus was to signal the occurrance of a counter-discharge during the time interval that the expansion-chamber is in the sensitive condition, an event which may be termed a coincidence. The operation of this "coincidence signal" will be clear from an examination of the figure. The expansion is made by setting the cam M into rotation as indicated by the arrow. Carried on the same shaft with the cam is a finger F which closes a pair of contacts just after the expansion is completed and keeps them closed for a predetermined inter-

val. This finger was adjusted so that it held the contacts closed only during the sensitive interval. (The adjustment was made by observing tracks due to photoelectrons from a short flash of x-rays which could be made to occur at varying time intervals after the expansion. Tests with an oscillograph showed that these contacts remained closed for an interval of 0.06 sec.) Thus the signal lamp L will only light when a coincidence occurs. Observation of the signal lamp during the taking of the expansion photographs allowed the coincidence photographs (on which a track might be expected) to be distinguished from those for which there was no discharge of the counter. For convenience the coincidence photographs are designated as C-photographs while the rest are called N-photographs.

Procedure and results.

The principal experiment consisted in setting the counters in operation and taking a series of expansion photographs. These were separated into the C and N groups with the aid of the coincidence signal by marking on the films (just after taking the photograph) those exposures for which a coincidence occurred.

In agreement with the work of Skobelzyn, an examination of these photographs revealed a considerable number of very thin straight tracks resembling those due to the fastest of ordinary β-rays, but somewhat thinner. An inspection of magnified sections of several of these tracks indicated that the number of ions per cm path was about half of the value observed for an average recoil β-particle from radium C γ-rays filtered through 3 mm of lead. We were not equipped to show, in the manner done by Skobelzyn,[5] that a majority of these tracks were not appreciably deflected in a magnetic field of such strength that it could strongly deflect β-rays from radioactive sources. However, on account of the positive result of the present experiment it cannot be doubted that a considerable fraction of these tracks were due to cosmic corpuscles. Further evidence in this direction came from a study of the distribution about the vertical for the 134 thin straight tracks which were found on our photographs. It was found that this distribution was in approximate agreement with the distribution of cosmic-ray particles observed by Tuwim.[7]

It was necessary to know the position and direction of each of these tracks not only for obtaining the distribution just mentioned but also on account of the following circumstance. In attempting to establish a correlation between a certain track appearing on a C-photograph and the discharge of the counter, we must make use of only the tracks whose prolongation passes through the counter. Tracks which do not fulfill this condition are due to cosmic corpuscles which entered the chamber without passing through the counter, to radioactive β-particles originating within the chamber, or other spurious causes. These tracks, of course, must be excluded from consideration. For these reasons a stereoscopic analysis was made of the 134 tracks. This was done by a visual reconstruction method similar to that used by Curtiss[8]

[7] Leo Tuwim, Berliner Ber. No. 4/5, p. 91, (1931).
[8] F. L. Curtiss, Bureau of Stds. Jour. of Res. 4, 663 (1930).

which allowed fair accuracy with considerably less labor than an analytical method.

With the present single-counter arrangement, it is evident that not all the C-photographs can be expected to show a track of the significant kind. Besides, a certain number of such tracks must be expected on the N-photographs due to spurious causes. Hence what must be looked for is whether there is a significantly larger probability of finding a track (of the required type) on a C-photograph than on an N-photograph. Accordingly, the probability of finding such a track on a photograph was computed for each of the two classes of photographs from the experimental data.

TABLE I. *Numerical results.*

Series	Number of		Number of significant tracks observed on		Probability of occurrence of a track on	
	C-Phot.	N-Phot.	C-Phot.	N-Phot.	C-Phot.	N-Phot.
1	—	659	—	15	—	0.023 ± 0.004
2	68	—	6	—	0.088 ± 0.024	—
3	69	448	6	11	0.087 ± 0.024	0.025 ± 0.005
Averages and totals	137	1107	12	26	0.088 ± 0.017	0.024 ± 0.003

The numercial results are presented in Table I. It will be noted that the data for the C-photographs are missing for the first series while those for the N-photographs are for the second. This apparent inconsistency is due to the fact that during the taking of the first series only the upper of the two counters (T_2) was employed. After examination of both the N and the C-photographs in this series, it was found that the chance of a cosmic-ray particle passing through this counter and the chamber was too small to render the experiment feasible. In order to increase this quantity to a reasonable value, the second counter (T_1) was added before taking the remainder of the photographs. Since the examination and stereo-analysis of the numerous N-photographs involved considerable labor, this class of exposures for the second series was not examined but those from the first series are to be used for comparison with the C-photographs of the second. This procedure is legitimate since no changes were made in the manner of taking the photographs or in the expansion chamber, and the taking of the N-photographs is quite independent of the presence of the counters.

Comparing the probability of finding a significant track on an N-photograph to that on a C-photograph, it is seen that a considerably higher value is found for the latter. The probable error has been computed by taking the statistical error of the number of observed tracks to be $0.67\ N^{1/2}$, where N is this number. The difference between the two averages (0.088 and 0.024) is 0.064, while the probable error of the difference is 0.017. Accordingly it is very unlikely that this differences is accidental. The fact that the values for the last series check with the previous ones even better than could be hoped is also evidence in this direction.

This result indicates a definite correlation between the discharges of the counter and the appearance of a track in the chamber. Or, in other words, at least one of the agents which cause the discharges of the counter produces tracks in the expansion-chamber. It must now be shown that this agent is the cosmic-radiation. One possibility is that our result is due to β-particles from radioactive sources. One simple way to account for it is to assume that a β-particle which originates inside the counter reaches the interior of the chamber, or vice versa. This particle must do so without undergoing much deviation and while still endowed with considerable energy. In order to pass from counter to chamber the β-particle has to penetrate through an amount of material corresponding to about 4 meters of air. It is evident that ordinary β-particles or recoil electrons due to γ-radiation from radioactive sources do not have sufficient penetrating power to make such an event possible. Another way by which the present result might be explained is to assume that a primary γ-ray or cosmic-ray photon produces a recoil electron in the counter and that the scattered photon in turn produces a second recoil electron in the chamber, whose track is observed. This process has been considered by Bothe and Kolhörster[1] as a possible explanation of coincidences between two counters. Their analysis also applies to our case. They found that the chance of occurrence of this compound process is so small that it can only account for a negligibly small part of the observed coincidences. Accordingly we can conclude that our result cannot be explained in this way. It seems that the only possibility remaining is the one previously indicated, namely that the track is produced by a cosmic-ray particle which travels through both the counter and the chamber. Further evidence for the correctness of this view comes from the following calculation of the probability of finding a track on a *C*-photograph which may be expected on this assumption.

Calculation of C-probability.

In making this calculation two numerical factors are needed, the first due to the fact that not all the counter-discharges are due to cosmic radiation, the second on account of the circumstance that only a part of the cosmic-ray corpuscles striking the counters will pass through the expansion-chamber. The first factor, the fraction of the counter impulses due to cosmic radiation, was found in the manner already described to be 0.30 ± 0.05. The second quantity is the quotient of the number of particles passing through both the counter and the chamber by the total number striking the counter. It was approximately calculated by a simple geometrical consideration and under the assumption (justified by the work of Tuwim[7] and others) that the cosmic-radiation can be considered as all arriving within an angle of 70° from the vertical. The absorption of the radiation in passing from the counter to the interior of the chamber could, of course, be neglected. In this manner the value 0.066 ± 0.015 was found for the calculated probability of occurrence of a track on a *C*-photograph. In comparing this value with the experimental value 0.088 it must be noted that a portion of the tracks on the *C*-photographs are due to spurious causes. A rough assumption which may be made to allow for this fact is to take the probability of finding a spurious track on a *C*-

photograph to be the probability of occurrence of a track on an N-exposure. Accordingly the experimental value becomes 0.088–0.024 or 0.064 which is in good agreement with the calculated quantity. The closeness of this agreement is, of course, accidental on account of the uncertainties in both values but the comparison shows that our experimental value is about what can be expected.

Discussion

It seems reasonable to conclude from the foregoing that the cosmic-ray corpuscles which cause the coincidence effects in Geiger-Müller counters produce ion-tracks resembling β-ray tracks. It does not appear possible that such tracks could be produced by photons, so that, in agreement with previous beliefs, it appears that the coincidence effects are due to material particles. Accordingly the present result indicates that attempts to explain the coincidences by the direct action of photons must be abandoned.

Another interpretation of this experiment which requires consideration is to suppose that the observed tracks were due to a particle of secondary origin produced by a primary corpuscle which causes the coincidences but whose passage through the cloud chamber was not detected.* As had been indicated above, these tracks could not be due to a secondary recoil electron produced by a photon as the primary corpuscle. However, the possibility remains that they were produced by a primary material particle, such as a high-energy electron, whose passage through the chamber was not detected, perhaps because the track of ions which it leaves is too thin to be observable. Although further work on this subject may show this to be the correct interpretation of the present experiment, it appears to us that the following circumstances speak against this view. The foregoing calculation of the chance of finding a track on a C-photograph shows that practically all the cosmic particles which pass through both the counter and the chamber produce an ion-track. This means that to render this hypothesis tenable, every primary particle passing through the chamber must produce a secondary one therein. Moreover, on account of the requirement that the observed tracks must be directed to pass through the counters, these secondary particles must be set off roughly in the direction of the primary one. If the primary particle were to produce relatively high velocity secondary ones as frequently as is necessary to account for the present result, its penetrating power would be less than is observed unless it is assumed to have an excessively high initial energy. Furthermore, it is felt that the second requirement cannot be readily met, though in absence of any exact knowledge of such a process in this region of energy little more can be said. Accordingly, it seems that the best assumption we can at present make is that both the discharge of the counter and the associated track are directly caused by a single cosmic-ray particle as originally supposed.

With regard to the character of these material particles very little can be said with assurance. At first sight it would seem that the thin tracks we have

* While this article was in preparation, a paper by Jeans appeared in which he states that the result of the magnetic deflection experiments must be taken to mean that the coincidence effects are due to photons. We believe that our present result renders this view untenable. J. H. Jeans, Nature **128**, 103 (1931).

observed could be produced by nothing other than high-energy electrons. Furthermore, if, as seems fairly certain, these tracks are of the same character as those observed by Skobelzyn, from this work comes additional strong evidence in this direction. However, if such were the case, it would have to be assumed, on account of the electron-counter absorption experiments,[1] that these electrons constitute the major part of the primary cosmic radiation. Then the magnetic deviation experiments as well as the observed lack of dependence of the intensity of the cosmic radiation on the magnetic latitude[9] would require that the energy of these electrons be the enormous value of the order of 10^{11} e-volts. This at present seems improbable not only on the grounds of explaining how the electron acquires this enormous energy but also because on present theoretical ideas the penetrating power of such an electronic radiation would be considerably greater than is observed for the cosmic-radiation. The same sort of difficulties would apply if the coincidences were due to protons and perhaps if they were due to heavier particles, through the observed small density of ionization seems to speak against the possibility that they are even of the mass of a proton.[10]

Another possibility which should be mentioned is that we may be dealing with a totally new type of particle. Recently the existence of such a particle, the "neutron," has been tentatively postulated by Langer and Rosen[11] and also by Pauli.[12] As Pauli has pointed out, if the coincidences were produced by such a particle, the absence of magnetic effects is at once clear, since, as its name indicates, it carries no charge. It is evident, however, that this particle would be required to have properties similar to those of an electron as far as ionizing ability is concerned. Though, according to Pauli, this may turn out to be the case, the whole matter is as yet too uncertain to allow even a tentative explanation on this basis at the present time. If it turns out that the neutron possibility must be excluded, it seems on the whole that the best assumption we can make is that these particles are electrons.

It has been the object of this paper to present what we believe to be strong experimental evidence that the coincidence effects are directly due to ionizing material particles, to the definite exclusion of photons. The authors feel that the question of the nature of these particles and the related problem of the general significance of this result for cosmic-ray theory must be left open since they believe that no definite conclusion can be reached at present.[13,14]

[9] R. A. Millikan, Phys. Rev. **36**, 1595 (1930); R. A. Millikan and G. H. Cameron, Phys. Rev. **37**, 235 (1931).

[10] Geiger has recently obtained experimental evidence in favor of protons. See, Discussion on Ultra-Penetrating Rays, Proc. Roy. Soc. **A128**, 331 (1931).

[11] R. M. Langer and N. Rosen, Phys. Rev. **37**, 1579 (1931).

[12] W. Pauli. Presented in a speech at "Symposium on Nuclear Structure" at the summer meeting of the A.A.A.S., June 16, 1931. As yet unpublished.

[13] The present position of the investigation in this field is well presented by "L. H. G." in a summary in Nature **127**, 859 (1931).

[14] A part of the expenses of this experimental work were met by a grant to the junior author from the National Research Council.

THE EFFECT OF GENERAL RADIATION IN THE DIFFRACTION OF X-RAYS BY LIQUIDS

By W. C. Pierce
Department of Chemistry, University of Chicago

(Received May 20, 1931)

Abstract

Previous work has shown that the amount of general radiation transmitted by a single filter may cause peaks in the diffraction pattern of liquids. Balanced strontium and zirconium filters are used to study the magnitude of this effect in x-rays from a molybdenum tube operating at 35 kv. Zirconium alone does not give sufficient filtration under these conditions, but by use of the two filters the effects of the general and characteristic radiation may be completely separated.

IT IS well known that the elimination of hard general radiation is more important in scattering experiments with liquids than with crystalline substances. Thibaud and Trillat,[1] Clark and Stillwell[2] and Stewart and Morrow[3] have independently shown that the presence of hard general radiation in the x-ray beam causes an "inner ring" in the diffraction pattern. Meyer[4] compared the scattering of a monochromatic beam, obtained by crystal reflection, with that of a filtered direct beam. The latter gave a diffraction pattern having much broader peaks and in some cases additional peaks not found for the monochromatic beam.

His method of obtaining a monochromatic beam is not generally applicable for use with an ionization spectrometer because of the low intensity, but the effect of a fairly monochromatic part of the beam may be obtained by the use of balanced filters as suggested by Ross.[5] The present work was undertaken with the objects (1) of testing the balanced filter method and (2) of quantitatively determining the effect due to the hard general radiation.

Apparatus

An ionization spectrometer was used in conjunction with a molybdenum target Coolidge x-ray tube operating at a peak voltage of 35 kv. The entire high tension equipment and the x-ray tube were oil-immersed as described elsewhere.[6] The ionization chamber was 20 cm in length. It was constructed from pure copper, in order to avoid the presence of alpha particles, and was fitted with thin aluminum windows at front and rear. Bakelite insulation was used between the chamber and guard ring, and amber between the guard ring and the collecting rod. A Compton electrometer was used for measuring the

[1] Thibaud and Trillat, C. R. **189**, 751, 907 (1929).
[2] Clark and Stillwell, Radiology **15**, 86 (1930).
[3] Stewart and Morrow, Phys. Rev. **30**, 232 (1927).
[4] Meyer, Ann. d. Physik. (5) **5**, 701 (1930).
[5] Ross, Phys. Rev. **28**, 425 (1926).
[6] Bennett, Gingrich and Pierce, Rev. Sci. Inst. **2**, 226 (1931).

ionization current. It had a scale sensitivity of 25,000 mm per volt with the scale at a distance of 3 m. The capacity of the chamber-electrometer system was estimated at about 50 e.s.u.

Argon was used in the chamber in most of the experiments. Although absorption is not complete in 20 cm of this gas it has the advantage of freedom from clean-up by reaction with the material of the chamber, and gave sufficient sensitivity of detection.

Soller[7] slits were used as recommended by Stewart.[3] Various lengths were employed but all of the results are for slits 15 cm in length and spaced 0.08

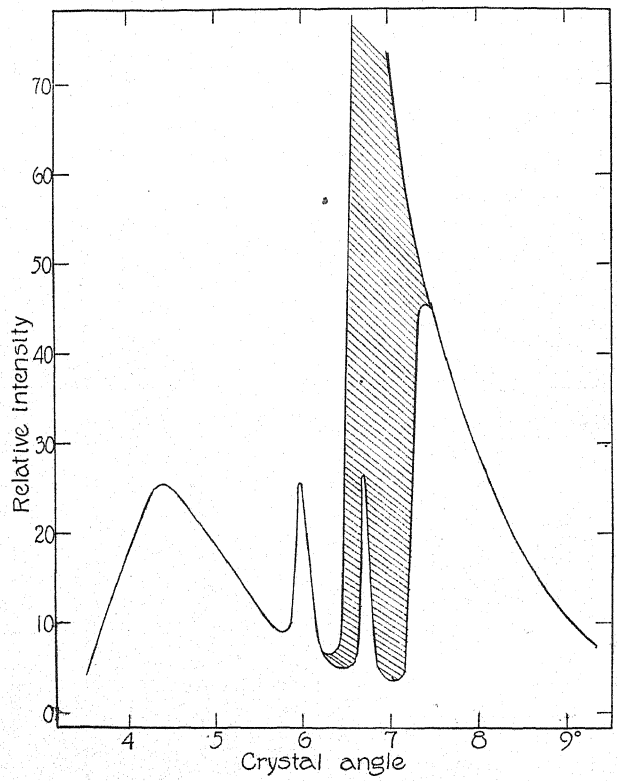


Fig. 1. Transmission of zirconium and strontium filters. Shaded portion represents radiation absorbed by strontium but transmitted by zirconium. Calcite crystals, $d=3.03$A.

cm apart. Intensity may be gained without the sacrifice of too much resolution by using shorter slits; but in the present work the intensity was sufficiently large.

The liquid sample was held in a container mounted on the center of the spectrometer table. In selecting a container for the experiments two objects were held in mind: (1) the container should be so constructed that its scattering of the x-rays would be small in comparison to the scattering of the volume of liquid used, and (2) the thickness of the sample should be less than the

[7] Soller, Phys. Rev. **24**, 139 (1924).

optimum value of $1/\mu$.[8] Flat metal containers with plane cellophane windows gave very little scattering, but no satisfactory glue was found for attaching the windows when used with good solvents.[9] A glass container was finally selected for use with such liquids. It was a very thin walled Pyrex tube, 6 mm in diameter. The beam was narrowed so that only the central portion of the tube was exposed. The scattering of the empty container (and of the air in the axis of the spectrometer) was first determined and this value, corrected for the absorption of the sample, subtracted from the observed scattering of the liquids investigated.

Filters. Since the critical absorption limits of strontium and zirconium lie at 0.7693A and 0.6872A respectively they show a great difference in transmission for rays of wave-length between these values. The zirconium filter was one supplied by the General Electric Company and the strontium filter was constructed by suspending strontium oxide in paraffin at a concentration of about 0.03 gm per cm^2. The latter filter was experimentally balanced against the zirconium by carefully shaving down until the two gave the same transmission for rays in the region 0.4–0.6A. After balancing, the transmission of the two filters was determined over the entire wave-length range by analysis of the transmitted beam with a calcite crystal spectrometer. Results of the analysis are shown in Fig. 1, in which the shaded area represents the radiation transmitted by the zirconium and not by the strontium. Argon was used in the chamber for this determination. A similar one with methyl bromide in the ionization chamber gave higher intensity throughout and showed a greater amount of general radiation, but the balance of the two filters agreed as well as when argon was used.

In making a determination of the intensity of scattered radiation successive readings of the intensity were taken with each of the filters. The difference in the ionization current for the two represents the contribution due to the $K\alpha$ lines.

Effect of the General Radiation

N-hexyl alcohol was chosen as the scattering liquid because it gives two well-defined peaks in the intensity curve and because the results obtained could be readily checked by comparison with those of Stewart and Morrow.[3] Separate scattering curves for each filter and for the balanced filter are shown in Fig. 2a and 2b, taken respectively with methyl bromide and argon in the ionization chamber. The strontium filter curves give the results of general radiation, while the zirconium filter curve gives the results of general plus characteristic radiation. A fairly true curve is obtained with the zirconium filter alone when argon is used for the detector, the effect of the general radiation being shown only by a general elevation of the intensity. With methyl bromide, on the other hand, the more complete absorption of the white radiation causes a peak at 6.5°. When higher voltages are employed this peak shifts to smaller angles as found by Thibaud and Trillat.[1] When a

[8] This was done because of the effective filtration of the beam by the sample (see Thibaud and Trillat, Ref. 1).

[9] Ambroid Liquid Cement was the most resistant one tried. For liquids that did not attack celluloid, windows were constructed of this and attached by Duco Household Cement.

photographic method of detection is used the effect of the general radiation is more pronounced because of the greater absorption in a photographic emulsion than in a gas-filled ionization chamber.

The corrected diffraction pattern of n-hexyl alcohol is given by curve 4 of Fig. 2b. This is in very close agreement with the result of Stewart and Morrow[3] for this liquid, and confirms their conclusion that the minor peak at 3° is due to the same radiation as the main peak.[10]

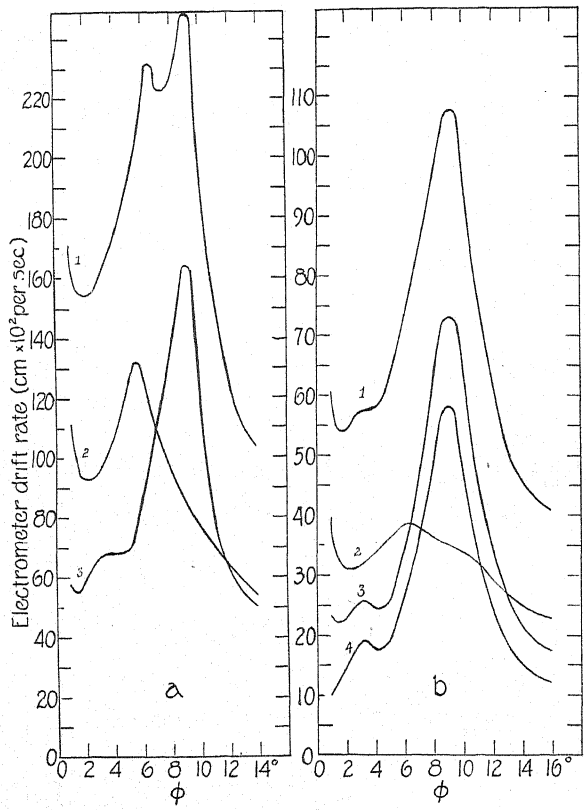


Fig. 2. Intensity-angle curves for n-hexyl alcohol. 2a. Methyl bromide in ionization chamber. (1) Zirconium filter. (2) Strontium filter. (3) Balanced filter- difference between (1) and (2). 2b. Argon in ionization chamber. (1) Zirconium filter (2) Strontium filter (3) Balanced filter-uncorrected (4) Balanced filter-corrected for scattering of container.

Conclusions

(1). The balanced filter is a satisfactory agent for isolating the effects of the general and characteristic radiation. (2). Under the conditions of the experiment the rays transmitted by the zirconium filter contain more general than characteristic radiation. (3). The diffraction pattern of a liquid for general radiation shows a sharp peak at an angle determined by the effective wave-length of x-rays. (4). Argon is a satisfactory detector for molybdenum x-rays when the relative intensity alone is desired. (5). The small angle peak found by Stewart and Morrow for n-primary alcohols is confirmed.

[10] Debye and Menke [Ergebnisse der technischen Röntgenkunde, **2**, 1 (1931)] suggest that perhaps this maximum is due to the general radiation.

HIGHER ORDER EFFECTS IN THE DIFFRACTION OF X-RAYS BY LIQUIDS

By W. C. Pierce
Department of Chemistry, University of Chicago

(Received July 13, 1931)

Abstract

The x-ray diffractions of liquid carbon tetrachloride, chloroform, benzene, solutions of carbon tetrachloride in benzene, o-dichlorbenzene and m-dichlorbenzene have been determined for Mo$K\alpha$ rays by the ionization spectrometer. All give a main peak characteristic of liquids and in addition the halogen compounds give other maxima in the intensity-angle curve at large angles. This effect is the same for carbon tetrachloride, pure or in solution, and is consequently thought to be due to internal interference caused by scattering from the chlorine atoms. Debye's relation for the scattering of single atoms cannot be applied because the positions of the peaks obtained from solutions are masked by the molecular scattering of the solvent.

DEBYE,[1] in a theoretical study of x-ray scattering by liquids, showed that the interference of radiation scattered by neighboring molecules would lead to an intensity peak at small angles and that interference between rays scattered by the separate atoms in the molecule would cause other peaks at larger angles. The two effects were called respectively the outer and inner. He also made the prediction that the inner effect could best be investigated through scattering experiments with gases since the effect of molecular arrangement could be neglected. This prediction has been verified in the later work of Debye[2] and his students, for they have developed the experimental technique and the theory of gaseous scattering, obtaining thereby very precise measurements of interatomic distances within the molecule.

The success of the work with gases emphasizes the importance of interatomic interference in liquid scattering, for on account of the experimental difficulty of obtaining diffraction measurements with organic compounds in the vapor state it would be desirable to obtain such data directly from the liquids. Of the large number of liquids whose x-ray scattering has been investigated only carbon tetrachloride, chloroform, water, and mercury have been reported as giving large angle maxima in the diffraction pattern. The data for these liquids are summarized in Table I, in which the locations of the peaks are expressed as Bragg distances ($n\lambda = 2d \sin \phi/2$) in order to facilitate comparison.

Prins, Meyer, and Debye have attributed some of these peaks to the inner scattering but Debye has shown, by a comparison of the liquid and gas diffraction patterns for carbon tetrachloride, that the positions of the liquid peaks do not coincide with those for the gas. His results for the two cases, re-

[1] Debye, Jour. of Math. and Phys. Mass. Inst. Tech. **4**, 153 (1925).
[2] See Bewilogua, Phys. Zeits **32**, 265 (1931) for a complete review of this work.

TABLE I. *Large angle scattering of certain liquids.*

Substance	Observer	Position of intensity peaks (Bragg distances)			
CCl_4	Prins[3]	5.34	2.86	2.01	1.41A
	Debye[4]	4.9*	2.8*	2.0*	1.4*
$CHCl_3$	Prins[3]	5.3	2.9		
H_2O	Meyer[5]	3.135	2.13	1.35	0.89
	Stewart[6]	3.24	2.11	1.13	
Hg	Prins[3]	2.76	1.41	1.01	
	Debye[4]	2.5*	1.3*	0.9*	

* Values calculated from published curves.

duced to the same intensity for comparison, are plotted in Fig. 1. He has in addition shown[4] that the entire diffraction pattern of mercury may be accounted for by the molecular interference and has deduced distribution curves for the molecules from the observed scattering. From the foregoing he infers that the higher order interference found for carbon tetrachloride is the combined effect of the atomic and molecular interferences.

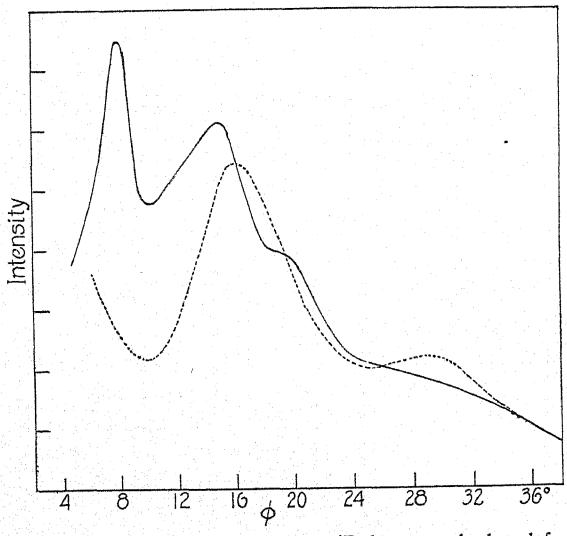


Fig. 1. Diffraction pattern of carbon tetrachloride (Debye, recalculated for $\lambda=0.71$A) Solid line—liquid. Dotted line—gas.

The present work was undertaken with the object of testing this point by a study of solutions of carbon tetrachloride. By using as solvent a liquid giving no higher order maxima it was thought that any effect obtained could be attributed only to interatomic interference as in the case of gases.

[3] Prins, Zeits. f. Physik **56**, 617 (1929).
[4] Debye and Menke, Ergebnisse der Tech. Röntgenkunde **2**, 1 (1931). Debye, Phys. Zeits. **31**, 348 (1930).
[5] Meyer, Ann. d. Physik **5**, 701 (1930).
[6] Stewart, Phys. Rev. **35**, 1426 (1930).

EXPERIMENTAL

Monochromatic x-rays of wave-length 0.71A were obtained from a molybdenum tube by the use of balanced strontium and zirconium filters as previously described.[7] The ionization spectrometer method was used for determining the intensity of scattered radiation. The liquid sample was held in a flat container 1 mm in thickness between thin celluloid windows. Soller slits, each 5 cm in length, were used for collimating and analyzing the beam. No correction was applied for the change in absorption with scattering angle or for the polarization factor, but a correction was made for the scattering of the empty container and of the air. Experimental values of this scattering were corrected for absorption in the sample and these values subtracted from the observed intensity at each spectrometer setting.

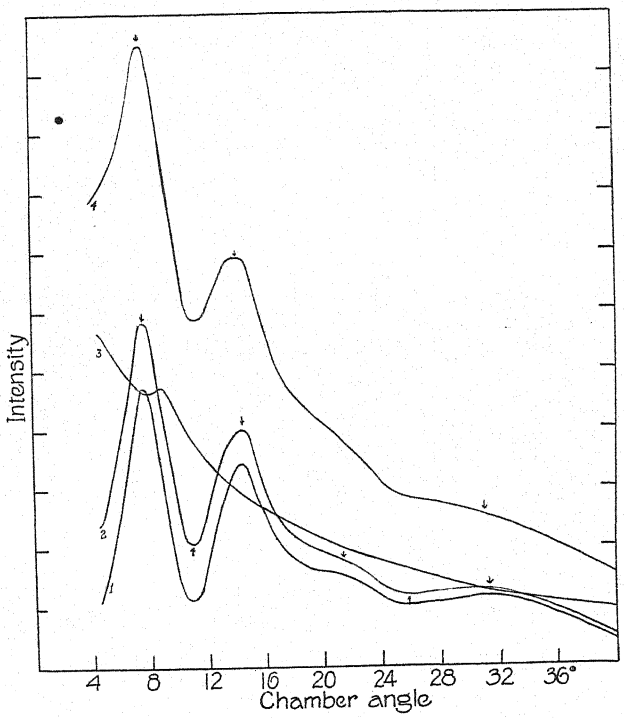


Fig. 2. Diffraction pattern of carbon tetrachloride. $\lambda=0.71$A 1. Balanced filter-corrected for scattering of container. 2. Balanced filter-uncorrected. 3. Strontium filter. 4. Zirconium filter.

RESULTS

1. Carbon tetrachloride. The results as shown in Fig. 2 are in fair agreement with those of Debye, the chief difference being in the position of the second peak and in the prominence of the third. In the present experiment this peak is too broad to be definitely located although repeated experiments have shown it to be a true effect. The difference may possibly be due to the

[7] Pierce, Phys. Rev. preceding paper.

experimental procedure for both Debye and Prins reflected the radiation from a free liquid surface, a method that may cause the effect of the surface molecules to be emphasized more than in transmission scattering as used here. Comparison of the results with the balanced filter and the zirconium filter show that the effect of general radiation is small in the region of large angle scattering.

2. Solutions of carbon tetrachloride in benzene. Solutions of concentrations ranging from 0–100 mol percent were investigated. Pure benzene gives a diffraction pattern showing only the main peak characteristic of molecular interference. Solutions give a pattern having the second and fourth peaks of

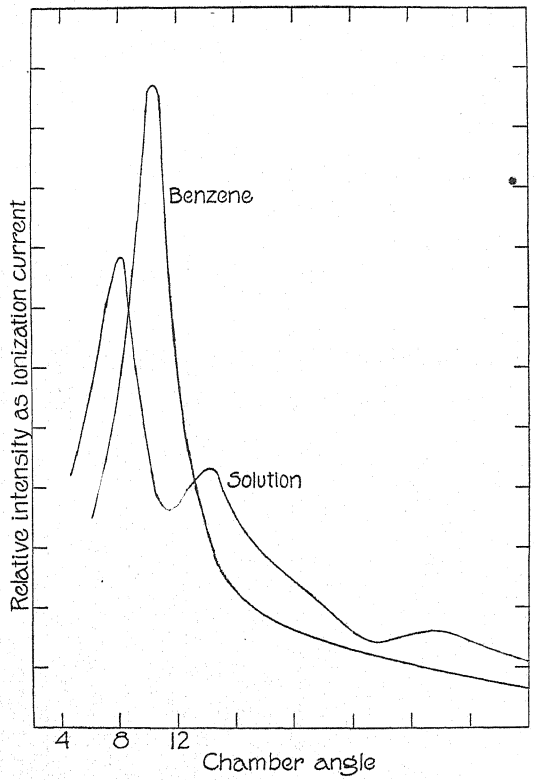


Fig. 3. Diffraction pattern of benzene (upper) and 50 percent solution of carbon tetrachloride in benzene. Taken with balanced filter for $\lambda = 0.71$A.

carbon tetrachloride at the same angular positions as the pure liquid, but the faint third peak could not be identified. The intensity of the higher order peaks decreased with dilution but they could be identified with concentrations as low as 20 mol percent. The results for pure benzene and for a 50 mol percent solution are shown in Fig. 3.

3. Chloroform. The scattering curve is shown in Fig. 4. The first maximum is broader and is at a larger angle than the corresponding one for carbon tetrachloride, indicating that the molecular diameter is smaller. The intensity

at the second peak is much less than for carbon tetrachloride, a result in harmony with that found for the gas scattering.[2] The position of this peak is at a slightly smaller angle than for the former compound.

4. Dihalogenated benzene derivatives. Ortho- and meta-dichlorbenzene were investigated as they are liquid at ordinary temperature. Both give higher order peaks, the ones for the meta-compound being at smaller angles, corresponding to the greater interatomic distances. Both first and second orders of the internal scattering may be identified but neither can be accurately placed, for the first order peak is close to the main liquid peak and the second order is too broad.

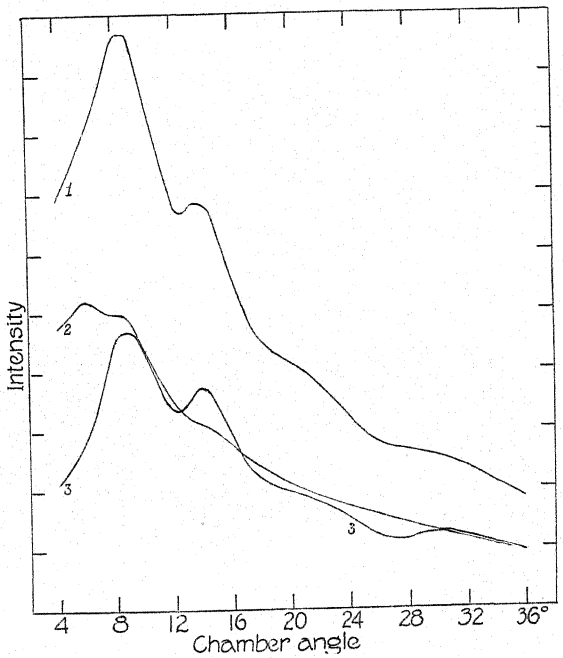


Fig. 4. Diffraction pattern of chloroform. 1. Zirconium filter, 2. Strontium filter, 3. Balanced filter.

Conclusions

The results indicate that the higher order peaks found for the compounds investigated are mainly due to the inner scattering. Evidence is found in the following:

1. Of the compounds investigated all having two or more atoms of high scattering power to the molecule give the effect.
2. The positions of the peaks are the same for pure carbon tetrachloride or for solutions in benzene.
3. Organic molecules in general, even highly symmetrical ones, do not give a higher order scattering detectable with the apparatus used. (See results for benzene.)

4. The relative prominence of the second peak for liquids is about the same as for the first peak with gases.

Although the explanation given is qualitatively satisfactory, quantitative evidence is lacking, for when the atomic distances are calculated for these compounds according to Debye's procedure for gases the results are not in good agreement.[8] This is shown in Table II in which the Cl−Cl distances calculated from the various maxima and minima of the liquid curve are listed together with corresponding distances obtained from the gas scattering curves.

TABLE II. *Cl–Cl distances* from liquid and gas scattering curves.*

Subst.	Peak position	Distance liquid	Distance gas[2]
CCl_4	1 min	3.0	3.00
	1 max	3.4	2.97
	2 min	2.9	2.98
	2 max	3.0	3.01
	3 min		3.00
	3 max		2.96
$CHCl_3$	1 min	2.64	3.13
	1 max	3.4	3.15
	2 min	2.8	3.13
	2 max	2.9	3.14

* Debye has derived a general relation for scattering from N points at fixed distances, but of random orientation with respect to the direction of the x-ray beam

$$I_\phi \propto \frac{1+\cos^2\phi}{2} \sum_1^N{}_i \sum_1^N{}_j \frac{\sin \chi_{ij}}{\chi_{ij}}$$

in which I_ϕ is the intensity at angle ϕ, $x=(4\pi d_{ji}/\lambda)\sin(\phi/2)$, $(1+\cos^2\phi)/2$ is the correction for polarization, d is the distance from the ith to the jth atom, λ is the wave-length, and the double summation indicates that the operation is to be carried out individually for each point over all the other points. When this is applied to the scattering of atoms occupying fixed points within a molecule the equation must be modified to take into account the distribution of electrons in each atom. When this is done for carbon tetrachloride, and the interference in the rays scattered by the central carbon atom is taken into account, the summation gives the relation (neglecting polorization)

$$I_\phi \propto 4\psi_{Cl}^2\left[1+3\frac{\sin \chi_{Cl-Cl}}{\chi_{Cl-Cl}}\right]+8\psi_{Cl}\psi_C\frac{\sin \chi_{Cl-C}}{\chi_{C-Cl}}+\psi_C^2$$

in which ψ_{Cl} is the atomic amplitude factor for the Cl atom (structure factor), ψ_C is the factor for the carbon atom, and

$$\chi_{C-Cl}=\frac{4\pi d_{C-Cl}}{\lambda}\sin\phi/2.$$

By substitution of the proper distances this equation gives values which may be plotted to give a curve whose maxima and minima exactly coincide with those of the experimental curve obtained from gaseous carbon tetrachloride. For a full description of the method see reference 2.

This lack of agreement may be due to masking of the peak positions by either diffuse large angle scattering by the liquid or by large angle maxima and minima, due to the outer effect, in the liquid diffraction. Since solutions give the same diffraction pattern it seems that the shifting is due to the diffuse scattering, for effects based on molecular distances should be changed as the molecular distances are changed by dilution.

The large angle maxima and minima found for water may be similarly explained, i.e., as due to interference in the rays scattered by oxygen atoms of a single complex molecule. Meyer[5] holds this view, but on the basis of calculations of particle size from the width of peak he regards the complex molecule as composed of many molecules. Stewart[6] considers all the peaks due to planar spacings in the cybotactic group and emphasizes the similarity of the diffraction pattern of the liquid and solid.

Mercury alone, of the substances investigated, gives large angle interference maxima due wholly to the molecular arrangement.[9] This is probably because the high concentration of electrons in the atom and the symmetry of the monatomic molecules give a condition favorable to close packing and regular arrangement of the molecules. On the other hand the lack of symmetry of polyatomic organic molecules and the much looser packing of the scattering atoms in these molecules make a very unfavorable condition for the observation of any but first order effects.

The results show that solutions do not offer a satisfactory source for obtaining accurate interferometric measurements but indicate that they may be used for approximate results. Unless the molecule under investigation is a very symmetrical one the diffraction pattern of the pure liquid is more suitable for such measurements because of the greater intensity in the higher order effects.

[9] Even here the possibility may be considered that complex molecules are formed in the liquid state, although the satisfactory analysis made by Debye and Menke furnishes strong evidence to the contrary.

THE REGULAR REFLECTION OF X-RAYS FROM QUARTZ CRYSTALS OSCILLATING PIEZOELECTRICALLY

By Gerald W. Fox and James M. Cork
Iowa State College and University of Michigan

(Received August 27, 1931)

Abstract

Laue patterns from quartz crystals oscillating piezoelectrically have been observed to be more intense than similar patterns from nonoscillating crystals. In this investigation, regular Bragg reflections from the face of crystals oscillating and nonoscillating have been observed in order to notice any variation in intensity or line width. No effect of this kind has been observed. These results are interpreted as negating the existence of Zwicky blocks, rocking slightly by the piezoelectric oscillations, as proposed by Langer. An explanation of the observed effect with Laue spots based upon the extinction effect in perfect crystals is proposed.

Introduction

IT HAS been observed[1] that the intensity of Laue patterns obtained with quartz crystals, oscillating piezoelectrically, is greater than for corresponding patterns with the crystals not oscillating. This result at first glance appears contrary to expectations when one considers the usual effect of temperature elevation and static deformation of the crystal upon Laue patterns. Explanations to account for the phenomenon have been proposed by B. E. Warren[2] and R. M. Langer.[3]

In order to throw more light upon the nature of this phenomenon it was considered desirable to examine the effect obtained with the crystal oscillating and nonoscillating mounted as the reflecting crystal in a Bragg spectrometer.

Apparatus and Manipulation

The general arrangement of apparatus is shown in Fig. 1. The front metal electrode for producing oscillations was cut away at the center so as to expose a portion of the crystal face, 4 mm wide, to the x-ray beam. In this spectrometer the distances between first slit and crystal axis and photographic plate and crystal axis were each made equal to 55 cm. This large distance gave a dispersion of better than 5 x.u. per mm which, together with the use of a fine slit, made it easy to observe any variation in line-width.

The crystals used in this experiment were cut parallel to the hexagonal crystal face and were 0.553 mm in thickness. They oscillated with a wavelength of 84 meters as measured by a standard wave meter agreeing with the

[1] G. W. Fox and P. H. Carr, Phys. Rev. **37**, 1622 (1931).
[2] B. E. Warren, Phys. Rev. **38**, 572 (1931).
[3] R. M. Langer, Phys. Rev. **38**, 574 (1931).

approximate expression $n = 2700/t(\text{mm})$ kilocycles, showing that the actual motion was normal to the face. No frequency corresponding to a lateral vibration could be found. The polished surfaces were etched lightly with hydroflouric acid to improve x-ray reflection.

In some of these exposures only the top part of the plate was exposed with the crystal oscillating and then a shield inverted and the bottom part subjected to an identical exposure with the nonoscillating crystal. Another procedure employed was to expose the full height of the photographic plate to a

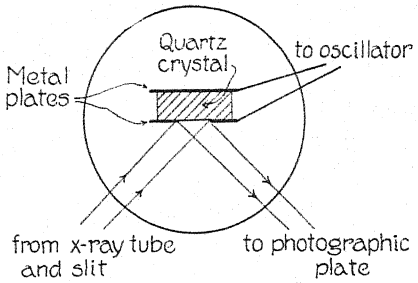


Fig. 1. General arrangement of spectrometer and oscillator.

reflection from the oscillating crystal and then the plate holder was shifted laterally and an identical exposure taken with the nonoscillating crystal. This could be repeated successively several times giving parallel lines whose relative intensity and width could be readily observed. Some such exposures were taken with the crystal in fixed position and others with the crystal rotating with uniform angular velocity through a small angle.

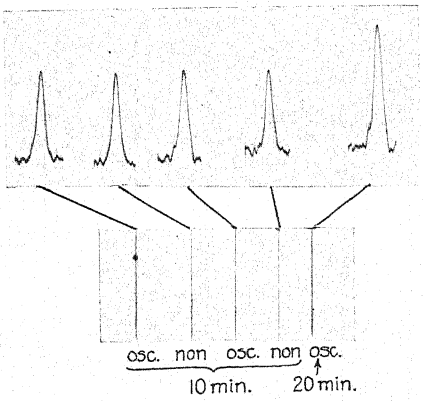


Fig. 2. $L\beta_1$ line in second order from face of oscillating and nonoscillating quartz crystal.

Fig. 2 shows a reproduction of a typical plate taken as described with the crystal in a fixed position. The x-ray emission line employed is in each case the β_1 line in the 2nd order L series of tungsten. In order to test the ability to compare intensities on this plate, the four exposures at the left are each ten minute exposures alternately oscillating and nonoscillating while the line

at the right was obtained with a twenty minute exposure with the oscillating crystal. A microphotogram of the plate is shown accompanying the figure.

Results and Discussion

In no case was it possible to observe any change in intensity or variation in line-width produced by making the quartz crystal oscillate piezoelectrically.

The actual line width as shown in Fig. 2 was about 0.15 mm, with a slight accompanying diffuseness on each side. Now from the geometry of the spectrometer it is seen that a distance of 0.1 mm on the photographic plate corresponds to a rotation of the crystal of approximately 19 seconds of arc.

The proposal of Warren that the spots in the Laue patterns were due to tungsten characteristic K-series lines, rather than the usual continuous spectrum, has been effectively negated by Fox and Carr who repeated their earlier results with voltages much less than the critical voltage for the tungsten K-series.

Now Langer would explain the effect by considering the crystal as a mosaic conglomerate in which the little crystal blocks (following Zwicky)[4] normally having an ideal parallel orientation, take on a rocking motion of a few minutes of arc due to the piezo-oscillations. Due to the Bragg focussing principle a rocking of such small crystal blocks through a few minutes of arc would produce no observable diffuseness of the reflected spectral line in the case of regular Bragg reflection, since for such a small angular displacement, their front faces extended would not be sensibly displaced from the spectrometer axis. This rocking would, however, be accompanied with increased intensity in the reflected line, since a much greater volume of the crystal would be effective in producing reflection when extinction effects are considered. From x-ray reflections one must conclude that quartz is a very perfect crystalline substance. The integrated reflection from a polished face may be many times that from a freshly cleaved surface. Since in this experiment the surface was freshly etched, it would approximate a cleaved surface and a rocking of crystal blocks might be expected to be comparable with the effect of lightly polishing the surface. The absence of this intensity variation can only be interpreted as negating the block idea of the crystalline structure.

This same consideration of extinction effect leads to a satisfactory explanation of the observed results with the Laue method. If the oscillating crystal be considered as a standing wave oscillator with node at center, then the interplanar distance d for atomic planes at the surface will not vary, while that at the center will take small positive and negative increments periodically. This is shown in Fig. 3 in which (a) shows the actual displacement of planes, while (b) shows the variation in the lattice distance Δd which is proportional to the slope of the displacement curve and is always zero at the ends and varies from positive values through zero to a negative value with the acoustic wave.

[4] F. Zwicky, Proc. Nat. Acad. 15, 819 (1929).

A heterogeneous x-ray beam which strikes the crystal face normally and makes a Laue spot at some angle θ, will, when the crystal oscillates, find at internal layers most of the time an altered lattice, and thus the Laue spot will be due to a band of wave-lengths from the continuous spectrum rather than a single wave-length as would have been the case in the ideally perfect crystal at rest. Now it might be thought that if a different wave-length is reflected at successive depths, then the deficiency in the ideal wave-length would be equal to the added energy of the other wave-lengths contributing to the Laue spot and no change in energy would be expected. Because of the extinction effect, this would not be the case, for in the nonoscillating crystal

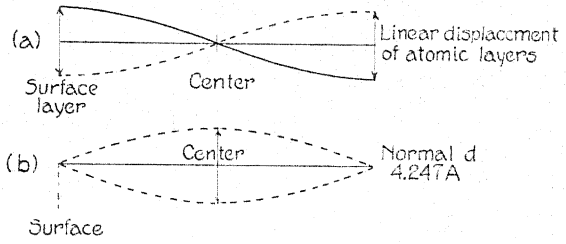


Fig. 3. Variation in lattice constant with distance from center due to acoustic wave.

the diffracted beam must traverse the crystal at an angle just right for reflection and the absorption coefficient may be many times the ordinary absorption coefficient. However, in the oscillating crystal, except for the instant when a normal configuration exists, at no time must the beam reflected from any depth element travel through an appreciable crystal thickness at exactly the correct angle for reflection, and the absorption coefficient it will encounter will be the normal one unmodified by extinction. Any diffuseness in the Laue spot caused by this slight angular variation would hardly be observed, since the spot is already large in the nonoscillating crystal, due to the appreciable thickness of the crystal.

THE SCATTERING OF X-RAYS FROM PARAFFIN, ALUMINUM, COPPER, AND LEAD

By Allen W. Coven
Physics Department, The College of Wooster

(Received August 28, 1931)

Abstract

The radiation from a tungsten-target x-ray tube operated at 80 kv was filtered through 0.244 cm of aluminum and the intensities of the scattered radiations from paraffin, aluminum, copper, and lead were observed by the ionization method. The scattered intensities at angles in the range of 30° to 120° with the forward direction of the primary beam were compared with the scattered intensities at 90°. Values of the intensity at 90° for paraffin were compared with the intensity at 90° for the other materials. The scattering from paraffin and aluminum was at an effective wave-length of 0.32A; from copper 0.26A, and from lead 0.27A. The Dirac value of the scattering from paraffin at 90° was used as the basis for calculating the absolute values of the scattering per gram and the scattering per electron.

Introduction

THE newer conceptions of the relations between waves and quanta have led to considerable development of the theory of the intensity of scattered x-rays. The scattering from monatomic gases has been successfully predicted and some progress has been made in developing a theory of the intensities scattered from solid materials. Further progress may be made possible by the accumulation of data on the scattering from solids at different wave-lengths. The experiment described in this paper was started with the hope of obtaining more accurate relative values of the angular distribution of scattered x-rays from some of the heavier elements. After collecting part of the data it became apparent that the scattering values could be put upon an absolute basis by comparison with the value of the scattering from paraffin at 90°. Hence great care was taken to compare the intensities from each of the metals used as scatterers in the experiment with the intensity from paraffin under the same experimental conditions. It is hoped that the values of the scattering per electron obtained for these metals may be useful in future theoretical developments.

Apparatus and Procedure

Fig. 1 shows the general arrangement of the apparatus used to measure the intensity of the radiation scattered from blocks of paraffin, aluminum, copper, and lead. A 30 m.a., radiator type, tungsten target, Coolidge x-ray tube was the source of the primary radiation. A General Electric x-ray transformer supplied current to the tube at a potential of 80 kv. The primary rays were limited to a beam of small cross section by the circular apertures at S_1 and S_2. A cylindrical ionization chamber having inside dimensions of 8 by 42 cm, with brass walls approximately 0.6 cm thick was mounted on an arm

arranged to rotate about an axis at R. The chamber was filled with ethyl bromide vapor and an excess of the liquid was kept in the bottom of the chamber at all times to insure saturation. The potential across the ionization chamber electrodes was 135 V. Currents in the chamber were measured by a Compton electrometer. Lead shielding around the x-ray tube and around the primary and scattered beams prevented all radiation except that scattered from the scattering block at R from reaching the chamber. Stray radiation was also kept from reaching the electrometer system by lead shields. The longer wave-lengths of the continuous spectrum emitted by the tungsten target were filtered out by 2.44 mm of aluminum placed in the primary beam at F_p. The wave-lengths having intensities greater than 0.1 of the maximum in the filtered beam occupied a band about an octave and a half broad. An

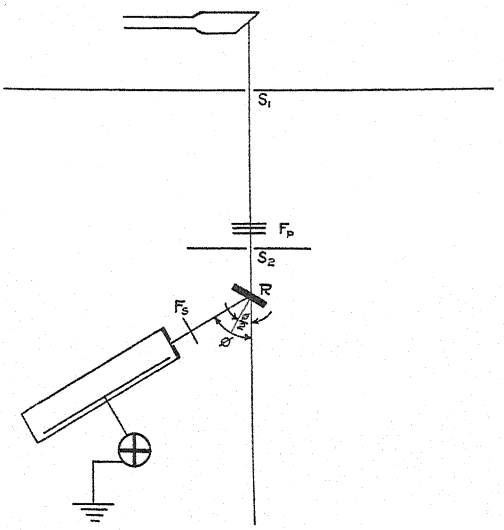


Fig. 1. Arrangement of apparatus.

aluminum sheet 0.812 mm thick was used as a filter in the scattered beam at F_s. This was found to be sufficient to remove the characteristic radiation excited in the scattering materials. The window of the ionization chamber was of 0.255 mm aluminum.

Ratios for each material, of the scattered intensities at angles between 30° and 120° inclusive, compared with the intensities at 90° were first determined. For paraffin and aluminum the scatterers were thin plates of the material, so oriented that the normal to the face of the plate from which the primary beam emerged after passing through the plate made an angle of $\phi/2$ with the forward direction of the primary beam. Thus the scattered rays penetrated the same thickness of the plate as did the primary rays. The copper and lead plates used as scatterers were so thick that none of the primary radiation penetrated them. They were so oriented that rays scattered from the incident face entered the ionization chamber and the glancing angle of the primary rays on the plates was always $\phi/2$.

After the determination of the angular distribution of the scattered radiation for each of the four materials, comparisons of the scattered intensities at 90° between the different materials were made. The ratio of the intensity scattered by paraffin at 90° to that by aluminum at 90° was found to be 6.56. The mass per unit area of the paraffin plate was 0.483 and that of the aluminum plate was 0.0659g/cm². Scattering from the incident face of a 0.812 mm thick aluminum plate was compared with the scattering from the copper and lead plates, each at 90°. The ratio of the intensity from the aluminum plate to that from the copper was found to be 2.64. The intensity from aluminum compared with lead was 2.84. The intensities between copper and lead were also compared directly and found to be in the ratio 1.075, in exact agreement with the ratio 2.84/2.64 from the comparisons with aluminum.

The linear absorption coefficient of the primary rays in aluminum by measurement was 2.51, and in paraffin 0.192. The absorption in paraffin was measured in the block from which the scattering plate had been cut. At the 90° position the rays scattered from paraffin and aluminum had absorption coefficients differing from the coefficient for the primary rays by a negligibly small amount. The hardening of the rays by absorption in the scattering plates was approximately annuled by the increase of wave-length of the rays on scattering. The absorption coefficients for the scattered rays in copper and lead were calculated respectively as 67.8 and 258. Measurement of the absorption in aluminum for the rays scattered from copper and lead gave the same value of absorption coefficient at 30°, 60°, and 90°. The absorption coefficients of the rays scattered from paraffin and aluminum varied slightly with direction of scattering, but were sufficiently constant to produce only a very small change in the corrections made for absorption of the scattered rays in the scattering plates. Consequently these corrections were calculated on the basis of the value of the absorption coefficient at 90°.

Calculations and Results

The scattering per gram of rays penetrating a thin plate of material oriented so that the normal to the plate makes an angle $\phi/2$ with the primary beam is given by

$$s/\rho = (I_\phi/i_\phi)(\cos\phi/2)(1/\omega m), \tag{1}$$

where I_ϕ is the intensity scattered in a direction ϕ, i_ϕ is the intensity of the primary rays penetrating the plate, ω is the solid angle subtended by the ionization chamber window, and m is the mass per unit area of the plate. i_ϕ is given by

$$Ie^{-m\mu/\rho\cos(\phi/2)}$$

where I is the primary ray intensity at the incident face of the scattering plate, and μ/ρ is the mass absorption coefficient of the primary rays in the plate. The ratio of the scattering per gram in any direction compared with that in a direction at right angles to the primary beam may be set up from Eq. (1), and then I does not appear in the ratio, since it is the same at all angles of scattering. This ratio applies to the cases of paraffin and aluminum

scattering in the experiment. A similar ratio derived from Eq. (1) will give the scattering per gram at 90° from aluminum compared with paraffin.

For a plate in which the primary rays are completely absorbed and which is oriented with the incident face at an angle $\phi/2$ with the primary beam, the scattering per gram is

$$s/\rho = (\mu/\rho)I_\phi/I \tag{2}$$

Eq. (2) will thus give the ratio for copper and lead of the scattering per gram at any angle compared with that at 90°. The intensity scattered from the incident face of the 0.812 mm aluminum plate is, however, less than the intensity that would be scattered from a plate of aluminum thick enough to absorb all of the primary radiation. If the maximum path of the x-rays in the aluminum plate is s, the scattered intensity is proportional to $1-e^{-\mu s}=0.437$ for the rays scattered at 90°. The measured intensities of the Al/Cu and Al/Pb scattering at 90° must thus be divided by 0.437 to get the true ratio of the relative intensities to use in calculating the scattering per gram from copper and lead compared with that from aluminum.

When nonhomogeneous radiation is scattered, the wave-lengths entering the ionization chamber will differ for different materials because of the difference in absorption of the different wave-lengths present in the primary beam. The effective wave-length scattered from each material was determined from the spectrum of the scattered beam in each case, according to the equation

$$\lambda_{\text{eff.}} = \int_0^\infty \lambda I_\lambda d\lambda \Big/ \int_0^\infty I_\lambda d\lambda. \tag{3}$$

This meant plotting of the spectral curve for each case of scattering and the curve whose abscissas were the same as the abscissas of the spectral curve, but whose ordinates were equal to the fraction $\lambda I_\lambda/I_\lambda$ of the ordinates of the spectral curve, then measuring the areas under each curve with a planimeter and using their ratio for the effective wave-length. In this way the wave-lengths were found to be

0.32A scattered from paraffin
0.32A scattered from aluminum
0.26A scattered from copper
0.27A scattered from lead.

In the comparison of the scattering from aluminum with that from copper and lead a correction must be made to the measured intensities because of the difference in the wave-lengths scattered. The effective wave-length scattered from the 0.812 mm aluminum plate was estimated to be 0.29A. Thus the measurement of intensities gave the following scattering ratios.

(Al at 0.29A)/(Cu at 0.26A)
(Al at 0.29A)/(Pb at 0.27A)

The ratios desired are, since the angular distributions of the scattered intensities were determined at an effective wave-length for aluminum of 0.32A,

(Al at 0.32A)/(Cu at 0.26A)

(Al at 0.32A)/(Pb at 0.27A).

Hence we need to multiply each of the measured ratios by the ratio

(Al at 0.32A)/(Al at 0.29A).

Coade[1] has measured the mass scattering coefficient for a number of metals at several different wave-lengths. He gives values for aluminum from which the variation of the coefficient with wave-length may be determined. By use of his data it is found that the scattering from aluminum at 0.32A is about 1.14 times the scattering at 0.29A. Hence the intensity ratios comparing the scattering from copper and from lead with that from aluminum were increased 14 percent in calculating values of the scattering per gram ratios, to correct for the actual difference in scattering.

Because of the difference in the wave-lengths entering the ionization chamber in getting the Al/Cu and Al/Pb ratios there will be a different fraction of the rays absorbed in the chamber and an additional correction must be made for this fact. Compton[2] has shown the means of comparing the intensities of two x-ray beams of different wave-lengths in terms of the ionization which they produce. His expression for the intensity ratio has the form

$$I_1/I_2 = (i_1/i_2)(f_1/f_2)(R_2/R_1)(e^{-x_2}/e^{-x_1}) \tag{4}$$

where i_1 and i_2 are the ionization currents, f_1 and f_2 are the fractions of the beams absorbed in the ethyl bromide, R_1 and R_2 are the ratios of the energy spent in producing ionization to the total absorbed energy, e^{-x_1} and e^{-x_2} are the fractions of the beams penetrating all the material in the path of the rays. The ionization current ratio is known from measurement, the fractions of the two beams absorbed in the chamber may be calculated. Compton[2] shows how to calculate the ratio of the energy spent in producing ionization to the total absorbed energy. The absorption in filters and scatterers is known, so the last term may be calculated, neglecting the absorption in air which is very small. The ratio of the intensities was thus found to be about 18 percent greater than it should be for the measured values of aluminum compared with copper, hence the experimental ratio was divided by the factor 1.18. The ratio of the scattering per gram of wave-length 0.32A by aluminum to wave-length 0.26A by copper is thus

$$\frac{2.64}{0.437} \times \frac{1.14}{1.18} \times \frac{(\mu/\rho)_{\mathrm{Al}}}{(\mu/\rho)_{\mathrm{Cu}}}.$$

The ratios of the scattering per gram at 90° calculated from the experimental intensity ratios after making these corrections for difference of scattered wave-length and for difference of ionization are, relating each metal to paraffin as unity,

[1] E. N. Coade, Phys. Rev. **36**, 1109 (1930).
[2] A. H. Compton, Phil. Mag. **8**, 961 (1929).

Paraffin	[1.0]	at 0.32A
Aluminum	1.05	at 0.32A
Copper	1.47	at 0.26A
Lead	4.11	at 0.27A

Fig. 2 shows the curve for scattering from paraffin on the basis of the Dirac theory which gives the angular distribution of intensity proportional to $(1+\cos^2\phi)(1+\alpha \text{ vers}\,\phi)^{-3}$. The experimental points are shown along with the theoretical curve. It is seen that there is good agreement between the experimental and theoretical values in the range 60° to 120°. This is in accord with the results of Jauncey and Harvey[3] who found very good agreement between the scattering from paraffin and the Dirac theory near 90° and for

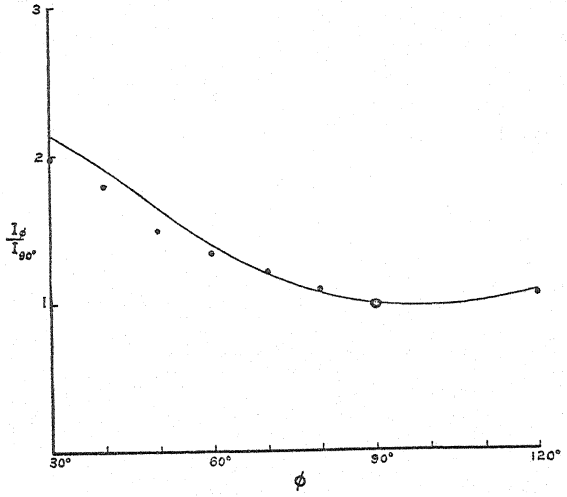


Fig. 2. Scattering from paraffin. Curve from Dirac theory, dots are values from experiment.

wave-lengths of about 0.3A. For the scattering per gram on the Dirac theory we have

$$s/\rho = 0.0238(Z/W)(1+\cos^2\phi)(1+\alpha \text{ vers}\,\phi)^{-3}. \tag{5}$$

for unpolarized x-rays. Here Z is atomic number, W atomic weight, $\alpha = 0.0242/\lambda$. The average formula for paraffin is $C_{24}H_{50}$ and hence Z/W has a value of 0.5, whereupon the scattering per gram from paraffin at 90° is 0.0095, for the wave-length 0.32A. Using this combined with the experimental distributions in angle and ratios at 90°, the values of the scattering for each of the four materials have been calculated and are shown in Table I.

The scattering per electron relative to the classical scattering from a free electron is perhaps of most theoretical interest. For modified radiation this is given by

$$S = (1+\alpha \text{ vers}\,\phi)^{-3}. \tag{6}$$

[3] G. E. M. Jauncey and G. G. Harvey, Phys. Rev. **37**, 698 (1931).

TABLE I. *Scattering per gram.*

Angle	Paraffin 0.32A	Aluminum 0.32A	Copper 0.26A	Lead 0.27A
30°	0.0189	0.0332	0.0542	0.234
40	.0170	.0235	.0391	.169
50	.0142	.0173	.0293	.104
60	.0127	.0134	.0236	.0752
70	.0115	.0116	.0173	.0534
80	.0105	.0109	.0151	.0417
90	.0095	.0100	.0140	.0390
120	.0106	.0114	.0142	.0362

At the wave-length used in the experiment the scattered rays from paraffin are almost all modified, and at 90° the value of S given by Eq. (6) would be a true value for paraffin. If we compare the value of S at 90° for one material with the value for another material at the same angle we shall have

$$S_1/S_2 = (s/\rho)_1(Z/W)_2/(s/\rho)_2(Z/W)_1. \tag{7}$$

Hence the S values at 90° are related as follows

Paraffin	[1.0]
Aluminum	1.09
Copper	1.60
Lead	5.13

In Table II are shown the values of the scattering per electron based on the value 0.803 for paraffin at 90° by the Dirac formula.

TABLE II. *Scattering per electron, S, relative to the classical scattering from a free electron.*

Angle	Paraffin 0.32A	Aluminum 0.32A	Copper 0.26A	Lead 0.27A
30°	0.91	1.66	2.85	14.10
40	.90	1.30	2.27	11.22
50	.84	1.07	1.91	7.75
60	.85	.94	1.73	6.34
70	.86	.91	1.43	5.06
80	.86	.93	1.35	4.28
90	.80	.88	1.28	4.12
120	.68	.80	1.05	3.05

DISCUSSION

Fig. 3 shows the scattering per electron plotted against values of $(\sin \phi/2)/\lambda$. Curve I is for paraffin and shows that the scattering for the wave-length and range of angles investigated is approximately in accord with a theory of the scattering from free electrons. Curve II is for aluminum, Curve III for copper, and Curve IV for lead. These indicate that the electrons in the atoms of the elements cooperate to an increasing amount as the atomic number of the scatterer is increased. They also show that the cooperation of the electrons becomes more effective as the direction of scattering approaches the forward direction of the incident primary radiation, and how particularly effective is their cooperation in heavy elements such as lead, where the elec-

trons are concentrated near the center of the atom. Were there no interference effects between neighboring atoms the cooperation at zero angle should be such that each electron would scatter Z times as much as a free electron scattering independently, where Z is the atomic number of the atom. It is possible that where the atoms are close together constructive interference between rays from neighboring atoms will increase the value of S beyond that of the atomic number of the scattering atom.

The probable experimental error in the intensity measurements is estimated to be about 3 percent. The absolute values of the scattering from cop-

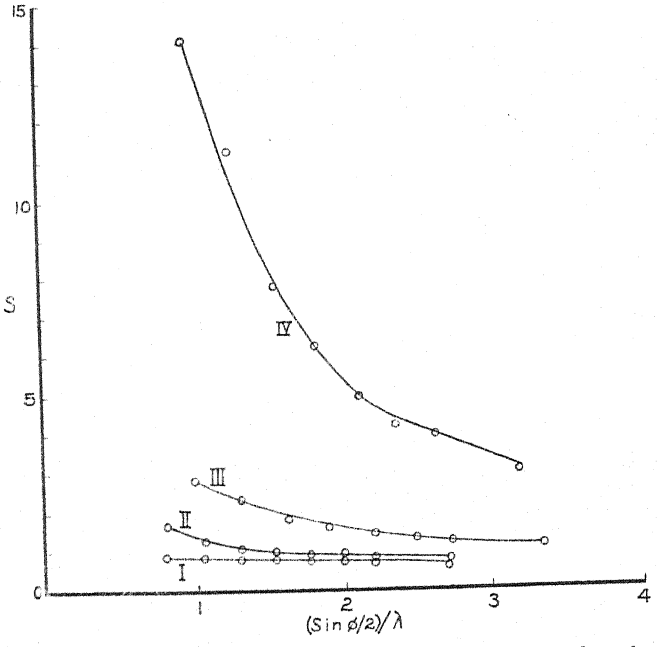


Fig. 3. Scattering per electron relative to the classical scattering from a free electron. Curve I paraffin, curve II aluminum, curve III copper, curve IV lead.

per and lead, depending as they do upon the determination of the Al/Cu ratio which was corrected by a slightly uncertain calculation allowing for the difference in the scattered wave-lengths, may be slightly more in error than the paraffin and aluminum values.

The author is grateful to Professor W. R. Westhafer of the College of Wooster, in whose department the experimental work was done, for supplying the Compton electrometer and other apparatus and material without which the experiment would not have been possible. It is a pleasure also to acknowledge the helpful suggestions regarding the methods of estimating the wave-lengths and of calculating the corrections which were so kindly given by Professor A. H. Compton of the University of Chicago.

INFRARED BANDS OF SLIGHTLY ASYMMETRIC MOLECULES

By Harald H. Nielsen
Mendenhall Laboratory, Ohio State University

(Received August 26, 1931)

Abstract

As an aid in the interpretation of the infrared spectra of nearly linear, slightly asymmetric molecules, calculations have been made upon molecular models of varying degrees of asymmetry in order to determine the general characteristics of their infrared bands. A_x, A_y, and A_z have been chosen as the principal moments of inertia and the atoms comprising the molecule have been taken to be coplanar such that $A_x = A_y + A_z$. For convenience of calculation, a parameter ρ has been chosen where $\rho = A_z/A_y$ and calculations have been made for ten values of ρ, varying in steps of $\Delta\rho = 0.02$ from $\rho = 0.20$ to $\rho = 0.00$. In the computation of the intensities of lines, Boltzmann factors were used corresponding to a largest moment of inertia $A_x = 2.0 \times 10^{-39}$ gm · cm². As in the work of Dennison on completely asymmetric molecules, of which this is essentially an extension, charts have been prepared depicting the general characteristics of the three types of bands which may occur.

Type A bands. Type A bands arise from vibrations of the electric moment along the z-axis or least axis of inertia and may be seen to consist of P, Q, and R branches. The members of the P and R branches are not single lines as in the symmetric rotator, but are groups of closely spaced lines spreading out as ρ increases. The Q branch also is complex and decreases in intensity as ρ decreases finally vanishing in the limiting linear case where $\rho = 0$.

Type B bands. Type B bands arise from vibration of the electric moment along the y-axis or intermediate axis of inertia. They too may be seen to consist, not of single lines, but of groups of closely spaced lines. As ρ decreases the spacing between these groups becomes coarser and coarser until finally where $\rho = 0$, this type of band vanishes completely. Type B consists essentially only of one branch.

Type C bands. Type C bands arise from vibrations of the electric moment along the x-axis or the largest axis of inertia and for the class of molecules here considered are very similar to type B bands. As in the former case the spacing between line groups becomes coarser and coarser, the band finally vanishing completely where $\rho = 0$.

THE infrared rotational-vibrational bands of molecules belonging to the symmetrical rotator class have been fairly well understood for several years, a fact which may be ascribed to their relative simplicity and because solutions to the problem of the symmetric rotator in the quantum mechanics[1] have been available for some time. In bands of this kind, each line may be described as due to certain definite quantum transitions and the spacings between the lines have certain definite meanings in terms of the moments of inertia of the molecules.

Only recently, however, have quantum mechanics solutions to the asymmetric rotator been made available[2] and in bands arising from such mole-

[1] D. M. Dennison, Phys. Rev. **28**, 318–333 (1926); F. Reiche and H. Rademacher, Zeits. f. Physik **39**, 444 (1926); R. de L. Kronig and J. J. Rabi, Phys. Rev. **29**, 262 (1927).

[2] H. A. Kramers and G. P. Ittmann, Zeits. f. Physik **53**, 553–565, (1929); S. C. Wang, Phys. Rev. **58**, 730–734 (1929); O. Klein, Zeits. f. Physik **58**, 730–734 (1929).

cules, the relations of the spacings between lines to the molecular constants are far less apparent. In infrared bands such as those of water vapor[3] and hydrogen sulphide[4] the fine structure lines cannot be arranged in a linearly spaced series and the chief difficulty in their interpretation lies in the inability to ascribe to the observed lines definite quantum transitions. Another complication is, that what frequently is observed as a relatively intense line may indeed be a group of lines lying very close together, incompletely resolved, arising from many different quantum transitions.

In view of these difficulties, it has seemed important to make calculations on molecular models of various degrees of asymmetry, more clearly to understand what would be the general appearances of their bands. In a recent number of Reviews of Modern Physics, Dennison[5] has given two charts illustrating the characteristics of two of the kinds of bands that may occur in completely asymmetric molecules. The purpose of this paper is to extend the work of Dennison and give similar charts demonstrating what will be the behavior of the bands of slightly asymmetric molecules, namely those which approach the linear rotator as their limit. In a later paper it is hoped to discuss characteristic examples of the spectra of such molecules.

A_x, A_y and A_z have been chosen as the three principal moments of inertia where $A_x > A_y > A_z$, and in addition the atoms comprising the molecule have been restricted to lie in one plane, hence $A_x = A_y + A_z$. As in Dennison's work, for convenience of calculation a parameter $\rho = A_z/A_y$ has been chosen and the types of bands occurring have been determined for values of $\rho = 0.20$ to $\rho = 0$ where ρ was made to vary in steps of $\Delta\rho = 0.02$.

The energy value of a given rotational state is according to Wang:

$$E = (h^2/8\pi^2)\left[J(J+1)/2(1/A_x + 1/A_y) + W\left\{1/A_z - (1/A_x + 1/A_y)/2\right\}\right] \quad (1)$$

where W is one of the $2J+1$ roots of the secular determinant which occurs in the Wang-Klein solution of the asymmetric top.

In order to solve this determinant for the values of W, it is first factored into four algebraic equations. These may then in turn be solved for the W's which in general are functions of a parameter b defined by Wang:

$$b = \frac{(1/A_x - 1/A_y)}{2[1/A_z - (1/A_x + 1/A_y)/2]}. \quad (2)$$

The algebraic equations from which the W's may be calculated have been obtained for the values of J from $J=0$ to $J=10$ by factoring the corresponding secular determinants and are given below. These may be shown to be identical to those obtained by Dennison[5] who determined them for J values, $J=0$ to $J=8$ from the Lamé functions used by Kramers and Ittmann in their solution to the asymmetric rotator.

[3] W. W. Sleator, Astrophys. J. **48**, 125 (1918); W. W. Sleator and E. R. Phelps, Astrophys. J. **62**, 28 (1925).

[4] H. H. Nielsen and E. F. Barker, Phys. Rev. **37**, 727–732 (1931).

[5] D. M. Dennison, Reviews of Modern Physics **3**, 280 (1931).

$J = 0 \quad W = 0$

$J = 1 \quad W = 0$

$W^2 - 2W + (1 - b^2) = 0$

$J = 2 \quad W - 1 + 3b = 0$

$W - 1 - 3b = 0$

$W - 4 = 0$

$W^2 - 4W - 12b^2 = 0$

$J = 3 \quad W - 4 = 0$

$W^2 - 4W - 60b^2 = 0$

$W^2 - (10 - 6b)W + (9 - 54b - 15b^2) = 0$

$W^2 - (10 + 6b)W + (9 + 54b - 15b^2) = 0$

$J = 4 \quad W^2 - 10(1 - b)W + (9 - 90b - 63b^2) = 0$

$W^2 - 10(1 + b)W + (9 + 90b - 63b^2) = 0$

$W^2 - 20W + (64 - 28b^2) = 0$

$W^3 - 20W^2 + (64 - 208b^2)W + 2880b^2 = 0$

$J = 5 \quad W^2 - 20W + 64 - 108b^2 = 0$

$W^3 - 20W^2 + (64 - 528b^2)W + 6720b^2 = 0$

$W^3 - W^2(35 - 15b) + W(259 - 510b - 213b^2) - (225 - 3375b - 4245b^2 + 675b^3) = 0$

$W^3 - W^2(35 + 15b) + W(259 + 510b - 213b^2) - (225 + 3375b - 4245b^2 - 675b^3) = 0$

$J = 6 \quad W^3 - W^2(35 - 21b) + W(259 - 714b - 525b^2) - 225 + 4725b + 9165b^2 - 3465b^3 = 0$

$W^3 - W^2(35 + 21b) + W(259 + 714b - 525b^2) - 225 + 4725b + 9165b^2 + 3465b^3 = 0$

$W^3 - 56W^2 + W(784 - 336b^2) - 2304 + 9984b^2 = 0$

$W^4 - 56W^3 + W^2(784 - 636b^2) - W(2304 - 34144b^2) - 483840b^2 + 55440b^4 = 0$

$J = 7 \quad W^3 - 56W^2 + W(784 - 784b^2) - 2304 + 20736b^2 = 0$

$W^4 - 56W^3 + W^2(784 - 2296b^2) - W(2304 - 99360b^2) - 870912b^2 + 353808b^4 = 0$

$W^4 - W^3(84 - 28b) + W^2(1974 - 2324b - 1162b^2) - W(12916 - 52948b - 70660b^2 + 13636b^3) + 11025 - 308700b - 847098b^2 + 566244b^3 + 61425b^4 = 0$

$W^4 - W^3(84 + 28b) + W^2(1974 + 2324b - 1162b^2) - W(12916$

$$+ 52948b - 70660b^2 - 13636b^3) + 11025 + 308700b - 847098b^2$$
$$- 5662446b^3 + 61425b^4 = 0$$

$J = 8$ $W^4 - W^3(84 - 36b) + W^2(1974 - 2988b - 2250b^2) - W(12916$
$- 68076b - 127620b^2 + 39420b^3) + 11025 - 396900b - 1455930b^2$
$+ 1477980b^3 + 363825b^4 = 0$

$W^4 - W^3(84 + 36b) + W^2(1974 + 2988b - 2250b^2) - W(12916$
$+ 68076b - 127620b^2 - 39420b^3) + 11025 + 396900b - 1455930b^2$
$- 1477980b^3 + 363825b^4 = 0$

$W^4 - 120W^3 + W^2(4368 - 1656b^2) - W(52480 - 138528b^2) + 147456$
$- 2428416b^2 + 118800b^4 = 0$

$W^5 - 120W^4 + W^3(4368 - 4176b^2) - W^2(52480 - 430848b^2)$
$+ W(147456 - 12266496b^2 + 1797120b^4) + 92897280b^2$
$- 92897280b^4 = 0$

$J = 9$ $W^4 - 120W^3 + W^2(4368 - 3096b^2) - W(52480 - 243360b^2) - 147456$
$- 4068864b^2 + 668304b^4 = 0$

$W^5 - 120W^4 + W^3(4368 + 7056b^2) - W^2(52480 - 702720b^2)$
$+ W(147456 - 19528704b^2 + 6441984b^4) + 1459814406^2$
$- 291962880b^4 = 0$

$W^5 - W^4(165 - 45b) + W^3(8778 - 7380b - 4086b^2) - W^2(172810$
$- 387630b - 536130b^2 + 100710b^3) + W(1057221 - 7388820b$
$- 19565154b^2 + 11135340b^3 + 822149b^4) - 893025 + 40186125b$
$+ 1893447906^2 - 2689645506^3 - 450528056^4 + 93980256^5 = 0$

$W^5 - W^4(165 + 45b) + W^3(8778 + 7380b - 4086b^2) - W^2(172810$
$+ 387630b - 536130b^2 - 100710b^3) + W(1057221 + 7388820b$
$- 19565154b^2 - 11135340b^3 + 822149b^4) - 893025 - 40186125b$
$- 1893447806^2 + 2689645506^3 - 450528056^4 - 93980256^5 = 0$

$J = 10$ $W^5 - W^4(165 - 55b) + W^3(8778 - 9020b - 6886b^2) - W^2(172810$
$- 473770b - 865810b^2 + 224290b^3) + W(1057221 - 9030780b$
$- 30555954b^2 + 23531860b^3 + 6390549b^4) - 893025 + 49116375b$
$+ 2884823106^2 - 5422180506^3 - 3464730456^4 + 622140756^5 = 0$

$W^5 - W^4(165 + 55b) + W^3(8778 + 9020b - 6886b^2) - W^2(172810$
$+ 473770b - 865810b^2 - 224290b^3) + W(1057221 + 9030780b$
$- 30555954b^2 - 23531860b^3 + 6390549b^4) - 8903025 - 49116375b$
$+ 2884823106^2 + 5422180506^3 - 3464730456^4 - 622140756^5 = 0$

$W^5 - 220W^4 + W^3(16368 - 5456b^2) - W^2(489280 - 932800b^2)$

$$+ W(5395456 - 46095104b^2 + 3165184b^4) - 14745600$$
$$+ 639452160b^2 - 252702720b^4 = 0$$
$$W^6 - 220W^5 + W^4(16368 - 11396b^2) - W^3(489280 - 2215840b^2)$$
$$+ W^2(5395456 - 138188864b^2 + 20438704b^4) - W(14745600$$
$$+ 3177400320b^2 - 26974166640b^4) - 218972160000b^2$$
$$+ 77803545600b^4 - 20314800000b^4 = 0$$

The selection rules for the asymmetric rotator have been correctly stated by Kramers and Ittmann[6] in their third paper and again in a more simple manner by Dennison.[5] In both papers, it is shown that there are three sets of rules depending upon whether the electric moment vibrates along the x-axis, the y-axis or the z-axis. In accord with these, asymmetric molecules may in general have, as we shall see, three different kinds of infrared bands.

The intensity with which a line will occur in the spectrum corresponding to a given quantum transition is expressed by the relation:[7]

$$I^{J\tau}_{J'\tau'} = K(A^{J'\tau'}_{J\tau})^2 N(J) g_{J'}/g_J e^{-E(J,\tau)/kT} \qquad (4)$$

where $N(J)$ is the number of molecules in the state J, g_J and $g_{J'}$, the *a priori* probabilities of the initial states and final states respectively. $A(J'\tau'/J\tau)$ are the amplitudes which in the case of the symmetric rotator are well known.[1] For the asymmetric rotator, the amplitudes for a $(J, \tau, M-J', \tau', M')$transition can be calculated from the already known amplitudes of the symmetric rotator and from the characteristic functions. Once the values of W have been obtained, a set of matrix equations may be obtained from which these characteristic functions may be determined. The actual $J\tau - J'\tau'$ intensity can then be found by summing over all the Zeemann components. Kramers and Ittmann[6] have, however, devised a method which, while it is entirely equivalent to the above procedure, seems more adaptable for numerical work. This method was here used for the most asymmetrical case (i.e. $\rho = 0.2$) and the results compared with those given by the symmetric amplitudes for corresponding transitions. The divergence between the two was found to be so slight that in the remaining cases, the latter were used. Certain transitions may of course occur here for which there are no corresponding ones in the symmetrical case, but for the range of molecules under consideration, these take place with an intensity only slightly different from zero, and may well be neglected.

A complete picture of each of these types of bands should of course include the most intense lines of the spectrum, i.e., those which will be intense enough to be distinguishable from neighboring lines. Just how many values of J will be needed to do this must depend to a large extent upon the moments of inertia of the molecule, since for larger values of the energy the Boltz-

[6] H. A. Kramers and G. P. Ittmann, Zeits. f. Physik **60**, 663–681 (1930).

[7] R. C. Tolman, Statistical Mechanics with Applications to Physics and Chemistry, New York, 1927.

mann factor of Equation (4) becomes an important item in determining the intensity of a line. For example; in the case of lighter molecules, only a few values of J might be required, while for heavier molecules, several might be necessary.

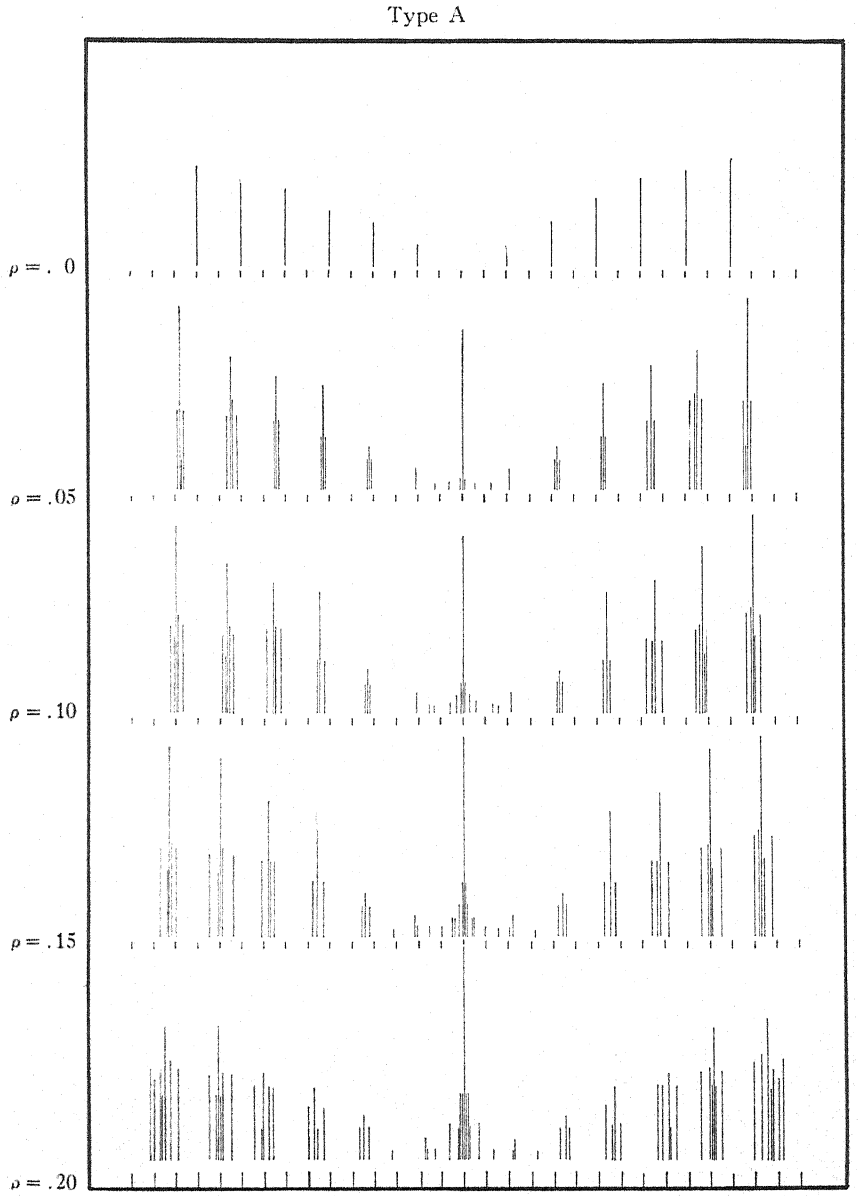


Fig. 1.

Thus for such molecules as formaldehyde ($\begin{matrix}H\\H\end{matrix}\!\!>\!\!-C=O$) where two of the moments of inertia are quite large (of the order of 2.0×10^{-39} gm·cm²) and the third small, a fairly good idea as to the appearance of the bands, especially

near the center, may be had with values of J up to say $J=6$. Since it is thought that these calculations will prove most useful to molecules of just this kind, Boltzmann factors have been used throughout corresponding to a largest moment of inertia. $A_x=2.0\times10^{-39}$ gm·cm². The forty-nine levels of $J=0, 1, 2, 3, 4, 5, 6$ were used to determine the positions of the lines in these bands. The results of these computations are plotted in Figures 1, 2 and 3.

In Figure 1 is shown the type of band arising when the electric moment changes along the least axis (Z-axis) of inertia. This type of band we designate as type A. It consists of P, Q and R branches of which the Q branch diminishes as ρ approaches zero. This becomes apparent by inspection of Equation (1), for keeping A_x constant, then as ρ decreases, the energy values where $W\neq0$* become greater and greater while at the same time the corresponding Boltzmann factors become smaller and smaller until in the limiting case, the linear rotator where $\rho=0$, they become zero. In the latter case the Q branch vanishes completely, as is well known from the HCl-like spectra. From Figure 1 it is clear that to give a complete picture of this type of band showing all the line groups that would be observable in the case of the molecule which we have chosen, many more values of J would be required than have here been used. From the six values used, however, a fairly good idea may be had how the band appears near the center and how each line in the linear case becomes a group of closely spaced lines as ρ becomes different from zero. The scale to which these values have been plotted is indicated on the diagram where the unit it taken as $h/8\pi^2A_x$. Hence two lines on the diagram which are separated by say n units differ in frequency by an amount $nh/8\pi^2A_x$. It should also be pointed out that in such cases where two lines were found to lie extremely close together they have been plotted as one line of their combined intensities.

In Figure 2 is shown the kind of band arising when the electric moment vibrates along the intermediate (y-axis) of inertia and it is denoted as type B. It should be emphasized that the scale to which these values have been plotted is much smaller than before. The unit used and indicated in Figure 2 is taken as $5h/8\pi^2A_x$. As is indicated in the diagram, as ρ decreases, the spacing between lines or groups of lines becomes coarser and coarser until in the limiting case where $\rho=0$, this type of band completely vanishes. In other words the ratio between the spacings of groups of lines in type B and in type A becomes larger and larger as ρ decreases. The reason for this becomes clear upon inspection of the selection rules and of the energy equation (1). It was pointed out in the preceeding section that as ρ is decreased, the energy values where $W\neq0$ become larger and larger. The increase of spacing in type B as ρ is decreased is inherent with this same effect since the permitted transitions are just between such levels which as they increase in energy, also spread farther and farther apart. One observers, moreover, that as the spacing between lines increases, corresponding lines on opposite sides of the center of

* For the molecules which we are here dealing with, one of the W values for each value of J is found to be practically zero. In fact its value decreases with ρ and where $\rho=0$ this value of W becomes identically zero.

the band begin to vary widely in their intensities. It is evident that this should be so for the line on one side of the center corresponding to one on the other side of the center arising from a $J'\tau' - J''\tau''$ transition is a line arising from a $J''\tau'' - J'\tau'$ transition; the ratio of their intensities being given by:

$$\lambda = e^{-(E''-E')/kT} . \tag{5}$$

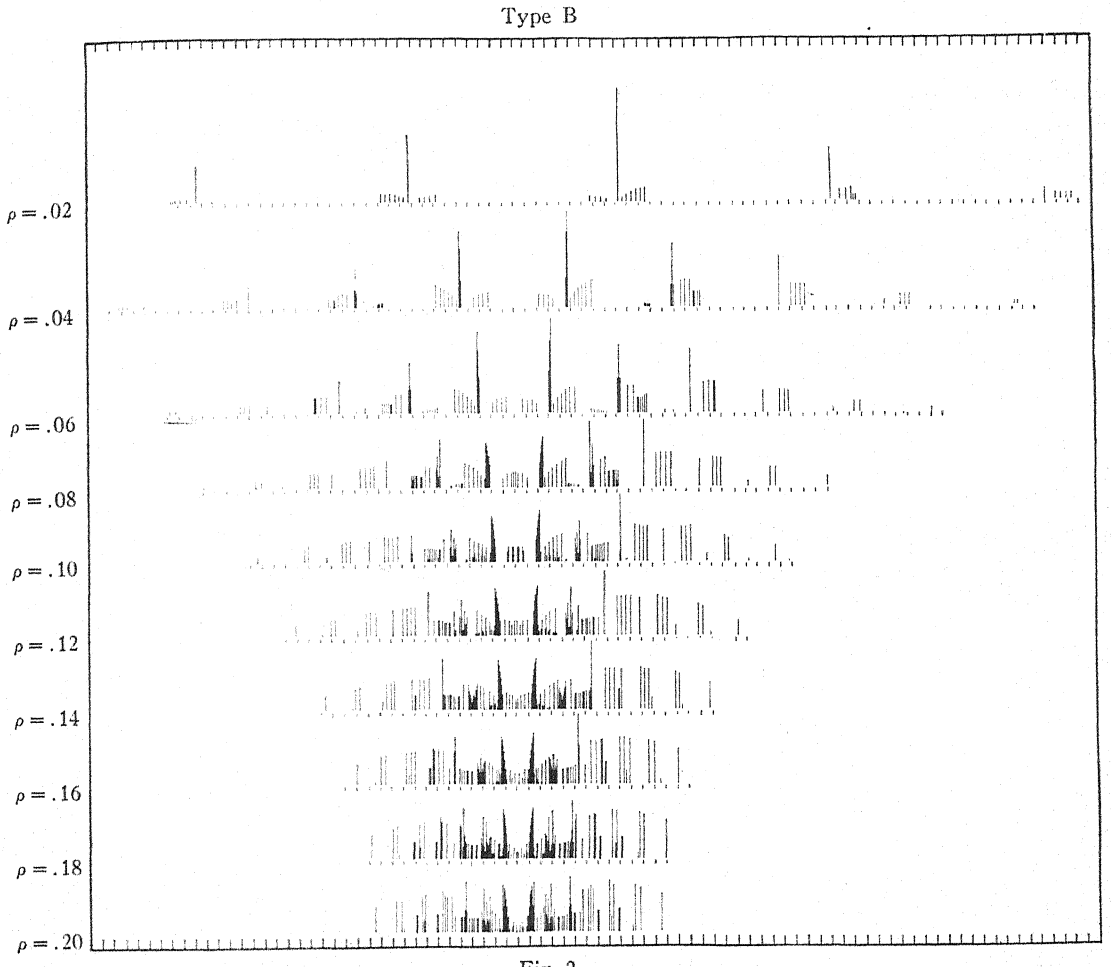


Fig. 2.

If now E'' represents increasingly more and more energy as ρ decreases than does E', then by (5) the ratio of intensities of these corresponding lines must become smaller and smaller. It is evident that the degree to which these differences in intensity of corresponding lines about the center take place depends entirely upon the values of the moments of inertia. As was earlier pointed out, these calculations have been made for a molecule for which $A_x = 2.0 \times 10^{-39}$ gm·cm², but for any other molecule where the moments of inertia are much different these intensities may be somewhat invalid.

As in type A, it is clear that more values of J would be required to give a complete description of these bands. Near the center, however, a fairly complete representation of the structure of the bands exists. The main difference in this region of adding more values of J would be to intensify line groups and to further fill in the background between such groups. It is believed that a fair representation of the lines is given out to about three lines from the center. As before when two lines lie too close together to be plotted separately they have been plotted as one line with their combined intensities.

Type C

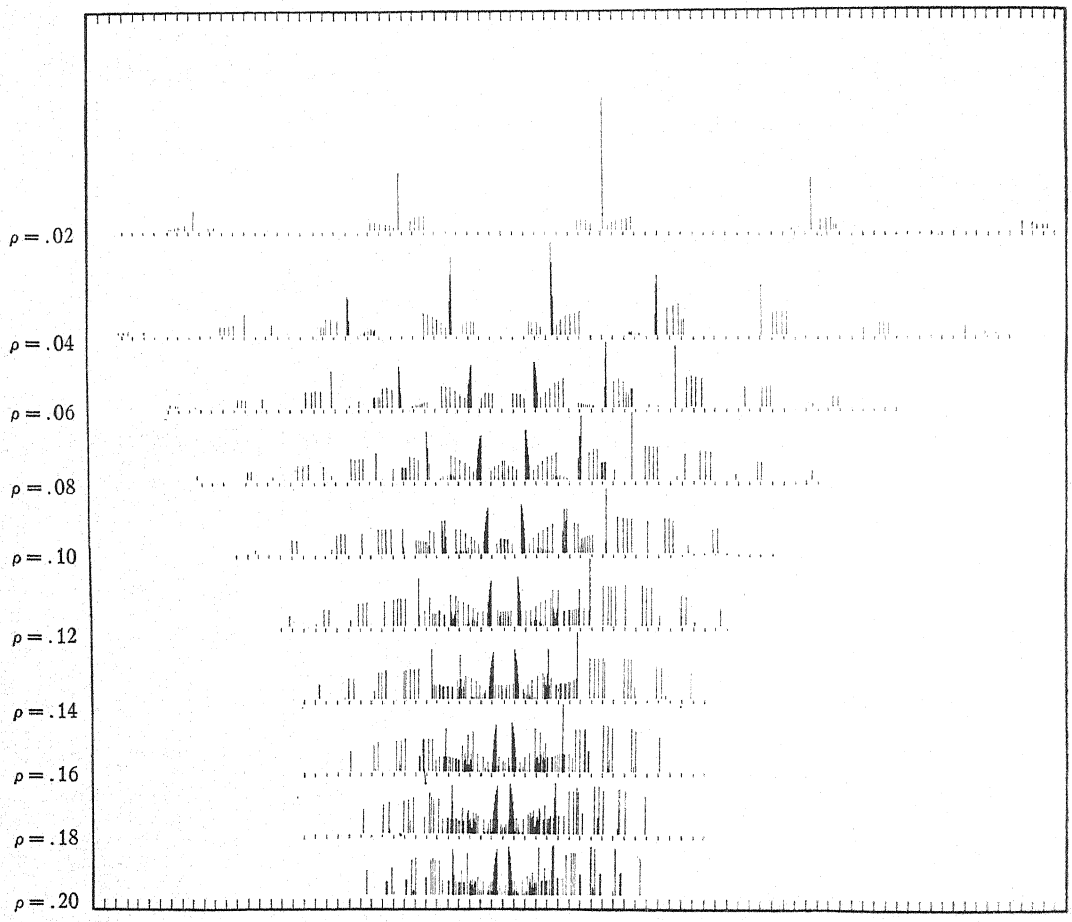


Fig. 3.

In Figure 3 is shown the third type of band which may occur and which has been designated as type C. This type of band originates with vibrations of the electric moment along the largest axis (x-axis) of inertia. Within the range of molecules with which we have been dealing this type of band much resembles type B, and for $\rho = 0$ they would become identical. The main differ-

[8] F. Hund, Zeits. f. Physik **43**, 805 (1927).

ence between the two may be seen from the diagram to be a tendency of the two lines nearest the center to form a Q branch while no such tendency exists in the type B band. In our case, however, what has been said about type B bands with respect to spacing and intensities is equally applicable to type C. Figure 3 is plotted to the same scale as Figure 2.

In such molecules where there are two or more identical atoms, each energy level must be classified as symmetric or antisymmetric. The symmetry properties of several kinds of molecules have been discussed by Hund[8] and more fully by Dennison,[5] but since the nature of this classification must depend upon the characteristic functions of the respective vibrations as well as upon those for the rotations and must consequently be considered especially for each individual molecule, this has not been taken into account. No generalization whatever can be made about the effect upon the appearance of the band except that it tends to make certain lines appear stronger than others.

By way of summary, it may be stated that as an aid in the interpretation of the infrared bands of the nearly linear slightly asymmetric rotators, calculations have been made on models of varying degree of asymmetry, each characterized by a parameter ρ defined as the ratio between the least to the intermediate moment of inertia. The further restriction that the atoms comprising the molecule shall lie in one plane has also been introduced. Three different types of bands were found to occur depending upon whether the electric moment vibrates along the least, the intermediate or the largest axis of inertia. Of these three types of bands, two were found to resemble one another to a great extent within the range of molecules that have been considered. Three charts summarizing the results of the calculations have been prepared which it is believed represent fairly accurately the general characteristics of the infrared bands of slightly asymmetric molecules,and it is hoped that these may prove themselves of value to the infrared spectroscopist as an aid in classifying and interpreting the spectra of such molecules.

AN ABSORPTION BAND IN ETHYLENE GAS IN THE NEAR INFRARED

By Richard M. Badger and John L. Binder
Gates Chemical Laboratory, California Institute of Technology
(Received August 12, 1931)

Abstract

The absorption spectra of gaseous ethane and ethylene have been investigated by photographic methods in the region λλ6500–9500. In the case of ethane no absorption was found. In ethylene a rather strong band was found at λ8720 which has a structure resembling that predicted by H. H. Nielsen for the oscillation-rotation bands of a molecule with moments of inertia in the ratio 1.4:1:0.14. The following very provisional values for the moments of inertia of the ethylene molecule are given: $A_x=31\times10^{-40}$, $A_y=27\times10^{-40}$, $A_z=3.8\times10^{-40}$.

Introduction

In the cases of some special polyatomic molecules where two of the moments are equal, either due to the symmetry of the molecule, as in ammonia,[1] or to a linear structure, as in acetylene[2] and hydrogen cyanide,[3] the vibration rotation spectra have submitted to a satisfactory analysis. But for the general case of a molecule with three unequal moments of inertia we have as yet no example which has been subjected to anything like a thorough treatment. In fact the spectrum of what might be expected to be a very simple case, the water molecule, has resisted many attempts at analysis.

One might expect the problem to be somewhat simplified in the case of a molecule which approximates a symmetrical rotator, in that two of the moments of inertia are nearly equal. A rather simple example of a molecule of this type is ethylene. The infrared spectrum of ethylene has been thoroughly investigated by Levin and Meyer[4] with thermocouple technique, but the resolving power employed was not quite sufficient to allow an analysis of the bands. Some time ago, during some preliminary work in the photographic infrared, an ethylene band was observed by one of the authors,[5] which was comparatively well resolved and which showed some interesting features in its structure. The present article describes further work, in which considerable improvement in the resolution of the band has been obtained.

Experimental Procedure

The ethylene gas used in this investigation was a commercial product prepared for anaesthetic purposes, guaranteed to be 99.2 percent pure. It was confined in a steel tube 280 cm in length, closed at one end with a plate glass

[1] R. M. Badger and R. Mecke, Zeits. f. phys. Chem. Abt. B, 5, 333 (1929).
[2] K. Hedfeld and R. Mecke, Zeits. f. Physik. 64, 151 (1930).
[3] R. M. Badger and J. L. Binder, Phys. Rev. 37, 800 (1931).
[4] A. Levin and C. F. Meyer, J. Opt. Soc. Am. 16, 137 (1928).
[5] R. M. Badger, Phys. Rev. 35, 1433 (1930).

window and at the other with a mirror. The light from the tungsten lamp source traversed the tube twice before entering the slit of the spectrograph. The latter contained a ten-foot grating in an Eagle mounting. The exposures were made in the first order using the iron arc spectrum in the second order for calibration. In most of the experiments the gas pressure employed was three atmospheres, in a few others about half an atmosphere. Eastman infrared sensitive plates hypersensitized in ammonia were used.

Since the absorption band observed is very complex, and since the resolving power of the photographic plate for absorption spectra is much less than for emission spectra, especially when the absorption is weak and the contrast poor, the following method was used in working up the results. A number of plates were exposed and from these the four best ones were chosen, and were enlarged about four times on fine-grained contrast plates. From these, horizontal regions free from pinholes and other blemishes were chosen and enlargements made on contrast film, using a weak cylindrical lens together with the camera lens to introduce astigmatism and get rid of grain. The four films which resulted were carefully superposed, and a reduced copy of this composite picture was made and photometered.

One has to be much more careful in introducing astigmatism to get rid of grain in absorption spectra than in emission spectra, since pin holes in the continuous background are likely to be mistaken for absorption lines. We believe that this difficulty has been avoided and the method worked very well as lines which were very doubtful on the original negatives came out quite definitely in the final picture. As can be seen on the photometer curve reproduced, the effect of grain has been almost eliminated and it is probable that even the small humps on the curve are significant.

In each of the several photographic procedures the contrast in the regions of weak absorption was improved, but with a corresponding loss of detail in the region of strong absorption, as can be seen on the photometer curve. The weak lines were consequently measured on the photometer curve, and the strong lines on another composite picture with less contrast, made from two other of the original negatives.

Experimental Results

A careful investigation of the region λλ6500–9500 resulted in the discovery of only one absorption region in ethylene gas. This is a very complex band, near the center of which are two strong maxima about 8 Angstrom units apart, which have the appearance of the Q branches found in the simpler oscillation-rotation bands. The absorption on the short wave-length side of these maxima seems to be greater than on the opposite side, but this may be due to the fact that this side of the band is better resolved. The band does not have very much resemblance to any of the ethylene bands found by Levin and Meyer[4] in the farther infrared. However, if the spacing between groups of closely neighboring lines is compared with the spacing of the maxima of the latter bands, the band at λ8720 is somewhat similar to the band at 3.2μ on the short wave-length side; and to the band at 2.3μ on the long wave-length side.

TABLE I. *The ethylene band at λ8720.*

line	λ	ν (cm^{-1})	line	λ	ν (cm^{-1})
+14	8672.0	11528.2	0	8719.9	11464.8
	74.3	25.2		20.4	64.2
+13	77.2	21.3		22.1	61.9
	78.6	19.4			
	79.9	17.6	−1	23.6	60.0
+12	80.7	16.7		24.5	58.8
	81.7	15.3	−2	26.6	56.1
	82.4	14.4			
			−3	28.6	53.5
+11	84.9	11.0		29.9	51.7
	86.5	08.9			
+10	91.7	02.1		32.3	48.6
+9	93.2	00.1		33.9	46.5
			−4	34.9	45.2
+8	94.8	11498.0		36.5	43.0
	95.8	96.7			
+7	870.33.	87.2	−5	39.9	38.6
				41.2	37.0
+6	05.0	84.6	−6	44.2	33.0
+5	07.8	80.9		45.3	31.5
+4	09.3	78.8		47.9	28.1
			−7	50.1	25.2
	10.5	77.2		51.0	24.0
+3	12.2	75.0			
+2	13.4	73.4	−8	54.6	19.4
				55.9	17.8
+1	15.2	71.0			
	16.4	69.4			
	18.1	67.2			

Brackets indicate definite regions of strong absorption which may, however, have a more complex structure than that indicated by the maxima given. The lines which are not numbered are doubtful.

The wave-length and frequency of absorption maxima, measured in the way described above under experimental procedure will be found in Table I, and a graphical representation of the band, together with a reproduction of a microphotometer curve, in Fig. 1. It is believed that all the maxima recorded are real with a few possible exceptions which are indicated in the table.

It should be mentioned at this point that ethane gas was also investigated in the same region as ethylene, but at pressures up to one atmosphere, in the absorption tube described above, no absorption was found. This is unfortunate since ethane has some points of special interest, especially the possibility of free rotation of the methyl groups relative to each other, about the carbon-carbon bond. However, in this investigation it was not possible to obtain enough pure gas to work at appreciably higher pressures. Ethane prepared from natural gas was found to contain methane in disturbing amounts, which could not be completely removed, and the gas used had to be prepared from ethylene bromide with the use of a zinc-copper couple.

Discussion of Results

The results of this investigation are here presented, though their complete analysis is as yet lacking, because of the rather striking similarity between the spectrum observed and that which has been predicted by quantum mechanics. The theory of the unsymmetrical rotator was worked out some time ago, but it is only recently that the results were put in a form such that they might readily be compared with experiment. In the last few months D. M. Dennison[6] and H. H. Nielsen[7] have calculated the vibration rotation band structure to be expected from plane, unsymmetrical rotators having moments of inertia in various ratios, and these results have beeen presented in diagrams which can readily be compared with observed spectra. In the present problem the diagrams of Nielsen are more useful, and copies of these were very kindly sent to the authors in advance of their publication.

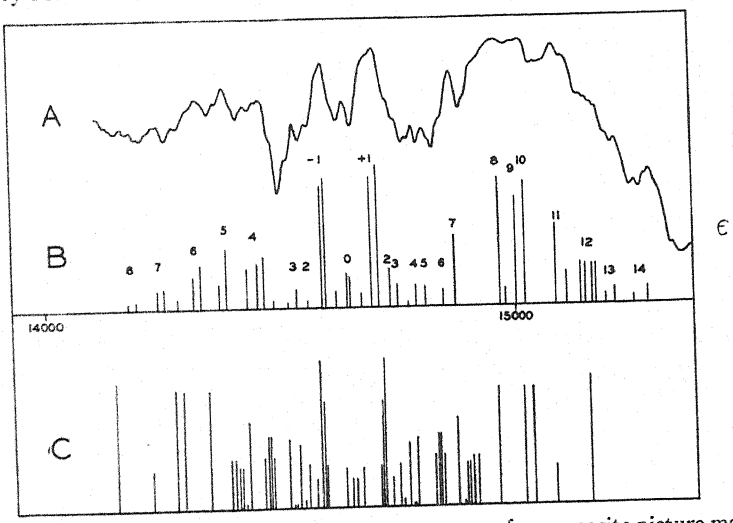


Fig. 1. The ethylene band at λ8720. *A*, Photometer curve of a composite picture made from four negatives. *B*, The principal maxima plotted on a frequency scale. *C*, Predicted spectrum for a molecule with constant moments of inertia in the ratio 1.14:1:0.14, when the change of electric moment due to vibration is along the intermediate axis. (Calculated by H. H. Nielsen).

The predicted spectra were necessarily calculated for a very much idealized case. A rigid molecule was assumed, the effect of special symmetry properties of the molecule on the intensities of the lines was not considered, and the Boltzmann factor was neglected. However, in Fig. 1, in which the observed ethylene band at λ8720 is compared with the spectrum predicted for an ideal molecule with moments of inertia in the ratio 1.14:1:0.14, a considerable similarity is evident. In particular one notes the two strong absorption regions which have the appearance of *Q* branches, and several of the more intense lines on the high frequency side of the band. On the low frequency side the similarity is less evident. One might of course expect a marked dissymmetry in the band due to the effect of symmetry properties, and due to the stretching of the molecule as it vibrates. The second effect is difficult to

[6] D. M. Dennison, Reviews of Modern Physics 3, 280 (1931).
[7] H. H. Nielsen, Phys. Rev. 38, 1432 (1931).

take into account at present since it is not quite certain what kind of oscillation gives rise to the band in question. It is rather probable that it is an overtone of a very active nonharmonic fundamental oscillation, since it is the only band observed in the photographic region. If so, it is probably the fourth harmonic of the fundamental at 3107 cm^{-1}, but the possibility is not entirely excluded that it may be a combination band. Further work in the intermediate infrared will probably be necessary to decide this point definitely.

If the correspondence between the observed ethylene band the predicted spectrum is real, it is possible from Nielsen's diagrams to estimate approximate moments of inertia of the ethylene molecule. These are $A_x = 31 \times 10^{-40}$, $A_y = 27. \times 10^{-40}$, and $A_z = 3.8 \times 10^{-40}$. These values are given provisionally. If one assumes that the angle between the bonds joining two hydrogen atoms to one carbon atom is the same as in methane, 109° 28′, one finds for the C–C separation 1.32A, and for the C–H separation 0.92A, which are certainly quite reasonable values.

Note added August 31, 1931. The authors have recently received from H. H. Nielsen copies of some of the new diagrams of predicted types of oscillation-rotation bands which appear in an article by him in this issue of the Physical Review.[7] These figures are more complete than the preliminary ones which were available at the time of writing of this article in that they include additional lines due to quantum levels for which J has the values 5 and 6, and that a correction has been made to the intensities which takes account of the Boltzmann factor. These changes slightly alter the general aspect of the figures and suggest a somewhat different interpretation of the ethylene band than that indicated above.

First of all the agreement between the experimental photometer curve and the predicted band now seems to be better for the "C" type of band; that is a band due to a vibration in which the change in electric moment is normal to the plane of the molecule. This is interesting since it indicates that the band under discussion is due to a combination of one of the deformation oscillations with a harmonic of one of the so-called valence frequencies. Further, a slight change in scale in comparing photometer curve and diagram seems desirable, which of course produces a corresponding change in the estimated moments of inertia. As before the maxima designated as $+1$ and -1 are to be interpreted as due to the first densely packed sets of lines on the two sides of the band origin, but it would appear that the maximum $+7$ (and probably -4) should be correlated with the second densely packed set of lines instead of with a single line.

If one draws from the diagrams a "predicted" photometer curve, by introducing factors to take account of the finite resolving power of the spectrometer and photographic plate, one finds a much greater correspondence between the observed and predicted curves than might be expected when one considers the possible influence of symmetry factors. The agreement is indeed very good in the central portion of the band. The outer portions of the calculated diagrams are less complete and it may be necessary to calculate additional lines for values of J up to about 10 before the final interpretation of the ethylene spectrum is made.

The authors are indebted to H. H. Nielsen for several helpful suggestions.

THE MAGNETIC ROTATION SPECTRUM AND HEAT OF DISSOCIATION OF THE LITHIUM MOLECULE

By F. W. Loomis and R. E. Nusbaum
The University of Illinois

(Received August 20, 1931)

Abstract

The magnetic rotation spectrum of the green, $^1\Pi - {}^1\Sigma$, band system of Li_2 has been observed and used to locate bands with high quantum numbers and so to obtain an accurate value for the heat of dissociation of the normal Li_2 molecule, yielding $D_0'' = 1.11 \pm 0.08$ volts. The spectrum is less simple than in Na_2, for instance, in that we observe not only a strong line at the head of each band, but also a few lines of the P and R, but not Q, branches. An improved method of plotting Franck-Condon diagrams is illustrated.

IT HAS been shown by Loomis[1] in the case of sodium that the magnetic rotation spectrum affords a very powerful method of attack on the analysis of the vibrational levels of a molecule, and particularly on the extension towards higher levels which is necessary for good estimation of the heat of dissociation. The reason for this is that the magnetic rotation spectrum is a much simplified version of the absorption spectrum with, consequently, much less overlapping of bands, so that the bands of high quantum numbers which are weak and, in this type of molecule at least, lie among stronger bands, can be identified and measured.

According to the simple theory of the magnetic rotation spectrum,[2] the intensities of lines in the P and R branches are proportional to the intensities of the corresponding absorption lines, times the Zeeman splitting, times some function of the Zeeman pattern. The Q branch should not appear in magnetic rotation. The Zeeman splitting falls off so rapidly as one proceeds from the origin, roughly as $1:J^2$, that only the lines nearest the origin appear at all. In fact, in sodium, each band appears as just one line, at the head, made up, in reality of a group of strong R lines. The corresponding P lines of low J are spread out and do not appear under the usual conditions. Roughly, it may be said that the magnetic rotation spectrum is rather like an absorption spectrum with an extremely low effective temperature as far as molecular rotation is concerned, but not as to vibration.

Now a vibrational analysis of the spectrum of Li_2 has already been made by Wurm,[3] on the basis of absorption measurements, and a value, 1.69 volts, deduced therefrom as the heat of dissociation: but the extrapolation is so long that no particular reliance can be placed on the result. The authors have therefore thought it desirable to study the magnetic rotation spectrum of

[1] Loomis, Phys. Rev. **31**, 323 (1928).
[2] Kemble, National Research Council Bulletin **57**, Chapter VII
[3] Wurm, Naturwiss. **16**, 1028 (1928).

take into account at present since it is not quite certain what kind of oscillation gives rise to the band in question. It is rather probable that it is an overtone of a very active nonharmonic fundamental oscillation, since it is the only band observed in the photographic region. If so, it is probably the fourth harmonic of the fundamental at 3107 cm^{-1}, but the possibility is not entirely excluded that it may be a combination band. Further work in the intermediate infrared will probably be necessary to decide this point definitely.

If the correspondence between the observed ethylene band the predicted spectrum is real, it is possible from Nielsen's diagrams to estimate approximate moments of inertia of the ethylene molecule. These are $A_x = 31 \times 10^{-40}$, $A_y = 27. \times 10^{-40}$, and $A_z = 3.8 \times 10^{-40}$. These values are given provisionally. If one assumes that the angle between the bonds joining two hydrogen atoms to one carbon atom is the same as in methane, 109° 28′, one finds for the C–C separation 1.32A, and for the C–H separation 0.92A, which are certainly quite reasonable values.

Note added August 31, 1931. The authors have recently received from H. H. Nielsen copies of some of the new diagrams of predicted types of oscillation-rotation bands which appear in an article by him in this issue of the Physical Review.[7] These figures are more complete than the preliminary ones which were available at the time of writing of this article in that they include additional lines due to quantum levels for which J has the values 5 and 6, and that a correction has been made to the intensities which takes account of the Boltzmann factor. These changes slightly alter the general aspect of the figures and suggest a somewhat different interpretation of the ethylene band than that indicated above.

First of all the agreement between the experimental photometer curve and the predicted band now seems to be better for the "*C*" type of band; that is a band due to a vibration in which the change in electric moment is normal to the plane of the molecule. This is interesting since it indicates that the band under discussion is due to a combination of one of the deformation oscillations with a harmonic of one of the so-called valence frequencies. Further, a slight change in scale in comparing photometer curve and diagram seems desirable, which of course produces a corresponding change in the estimated moments of inertia. As before the maxima designated as $+1$ and -1 are to be interpreted as due to the first densely packed sets of lines on the two sides of the band origin, but it would appear that the maximum $+7$ (and probably -4) should be correlated with the second densely packed set of lines instead of with a single line.

If one draws from the diagrams a "predicted" photometer curve, by introducing factors to take account of the finite resolving power of the spectrometer and photographic plate, one finds a much greater correspondence between the observed and predicted curves than might be expected when one considers the possible influence of symmetry factors. The agreement is indeed very good in the central portion of the band. The outer portions of the calculated diagrams are less complete and it may be necessary to calculate additional lines for values of J up to about 10 before the final interpretation of the ethylene spectrum is made.

The authors are indebted to H. H. Nielsen for several helpful suggestions.

THE MAGNETIC ROTATION SPECTRUM AND HEAT OF DISSOCIATION OF THE LITHIUM MOLECULE

By F. W. Loomis and R. E. Nusbaum
The University of Illinois

(Received August 20, 1931)

Abstract

The magnetic rotation spectrum of the green, $^1\Pi - {}^1\Sigma$, band system of Li_2 has been observed and used to locate bands with high quantum numbers and so to obtain an accurate value for the heat of dissociation of the normal Li_2 molecule, yielding $D_0'' = 1.14 \pm 0.03$ volts. The spectrum is less simple than in Na_2, for instance, in that we observe not only a strong line at the head of each band, but also a few lines of the P and R, but not Q, branches. An improved method of plotting Franck-Condon diagrams is illustrated.

IT HAS been shown by Loomis[1] in the case of sodium that the magnetic rotation spectrum affords a very powerful method of attack on the analysis of the vibrational levels of a molecule, and particularly on the extension towards higher levels which is necessary for good estimation of the heat of dissociation. The reason for this is that the magnetic rotation spectrum is a much simplified version of the absorption spectrum with, consequently, much less overlapping of bands, so that the bands of high quantum numbers which are weak and, in this type of molecule at least, lie among stronger bands, can be identified and measured.

According to the simple theory of the magnetic rotation spectrum,[2] the intensities of lines in the P and R branches are proportional to the intensities of the corresponding absorption lines, times the Zeeman splitting, times some function of the Zeeman pattern. The Q branch should not appear in magnetic rotation. The Zeeman splitting falls off so rapidly as one proceeds from the origin, roughly as $1 - J^2$, that only the lines nearest the origin appear at all. In fact, in sodium, each band appears as just one line, at the head, made up, in reality of a group of strong R lines. The corresponding P lines of low J are spread out and do not appear under the usual conditions. Roughly, it may be said that the magnetic rotation spectrum is rather like an absorption spectrum with an extremely low effective temperature as far as molecular rotation is concerned, but not as to vibration.

Now a vibrational analysis of the spectrum of Li_2 has already been made by Wurm,[3] on the basis of absorption measurements, and a value, 1.69 volts, deduced therefrom as the heat of dissociation; but the extrapolation is so long that no particular reliance can be placed on the result. The authors have therefore thought it desirable to study the magnetic rotation spectrum of

[1] Loomis, Phys. Rev. **31**, 323 (1928).
[2] Kemble, National Research Council Bulletin **57**, Chapter VII
[3] Wurm, Naturwiss. **16**, 1028 (1928).

take into account at present since it is not quite certain what kind of oscillation gives rise to the band in question. It is rather probable that it is an overtone of a very active nonharmonic fundamental oscillation, since it is the only band observed in the photographic region. If so, it is probably the fourth harmonic of the fundamental at 3107 cm^{-1}, but the possibility is not entirely excluded that it may be a combination band. Further work in the intermediate infrared will probably be necessary to decide this point definitely.

If the correspondence between the observed ethylene band the predicted spectrum is real, it is possible from Nielsen's diagrams to estimate approximate moments of inertia of the ethylene molecule. These are $A_x = 31 \times 10^{-40}$, $A_y = 27. \times 10^{-40}$, and $A_z = 3.8 \times 10^{-40}$. These values are given provisionally. If one assumes that the angle between the bonds joining two hydrogen atoms to one carbon atom is the same as in methane, 109° 28′, one finds for the C–C separation 1.32A, and for the C–H separation 0.92A, which are certainly quite reasonable values.

Note added August 31, 1931. The authors have recently received from H. H. Nielsen copies of some of the new diagrams of predicted types of oscillation-rotation bands which appear in an article by him in this issue of the Physical Review.[7] These figures are more complete than the preliminary ones which were available at the time of writing of this article in that they include additional lines due to quantum levels for which J has the values 5 and 6, and that a correction has been made to the intensities which takes account of the Boltzmann factor. These changes slightly alter the general aspect of the figures and suggest a somewhat different interpretation of the ethylene band than that indicated above.

First of all the agreement between the experimental photometer curve and the predicted band now seems to be better for the "C" type of band; that is a band due to a vibration in which the change in electric moment is normal to the plane of the molecule. This is interesting since it indicates that the band under discussion is due to a combination of one of the deformation oscillations with a harmonic of one of the so-called valence frequencies. Further, a slight change in scale in comparing photometer curve and diagram seems desirable, which of course produces a corresponding change in the estimated moments of inertia. As before the maxima designated as $+1$ and -1 are to be interpreted as due to the first densely packed sets of lines on the two sides of the band origin, but it would appear that the maximum $+7$ (and probably -4) should be correlated with the second densely packed set of lines instead of with a single line.

If one draws from the diagrams a "predicted" photometer curve, by introducing factors to take account of the finite resolving power of the spectrometer and photographic plate, one finds a much greater correspondence between the observed and predicted curves than might be expected when one considers the possible influence of symmetry factors. The agreement is indeed very good in the central portion of the band. The outer portions of the calculated diagrams are less complete and it may be necessary to calculate additional lines for values of J up to about 10 before the final interpretation of the ethylene spectrum is made.

The authors are indebted to H. H. Nielsen for several helpful suggestions.

THE MAGNETIC ROTATION SPECTRUM AND HEAT OF DISSOCIATION OF THE LITHIUM MOLECULE

By F. W. Loomis and R. E. Nusbaum
The University of Illinois

(Received August 20, 1931)

Abstract

The magnetic rotation spectrum of the green, $^1\Pi - ^1\Sigma$, band system of Li_2 has been observed and used to locate bands with high quantum numbers and so to obtain an accurate value for the heat of dissociation of the normal Li_2 molecule, yielding $D_0'' = 1.14 \pm 0.03$ volts. The spectrum is less simple than in Na_2, for instance, in that we observe not only a strong line at the head of each band, but also a few lines of the P and R, but not Q, branches. An improved method of plotting Franck-Condon diagrams is illustrated.

IT HAS been shown by Loomis[1] in the case of sodium that the magnetic rotation spectrum affords a very powerful method of attack on the analysis of the vibrational levels of a molecule, and particularly on the extension towards higher levels which is necessary for good estimation of the heat of dissociation. The reason for this is that the magnetic rotation spectrum is a much simplified version of the absorption spectrum with, consequently, much less overlapping of bands, so that the bands of high quantum numbers which are weak and, in this type of molecule at least, lie among stronger bands, can be identified and measured.

According to the simple theory of the magnetic rotation spectrum,[2] the intensities of lines in the P and R branches are proportional to the intensities of the corresponding absorption lines, times the Zeeman splitting, times some function of the Zeeman pattern. The Q branch should not appear in magnetic rotation. The Zeeman splitting falls off so rapidly as one proceeds from the origin, roughly as $1/J^2$, that only the lines nearest the origin appear at all. In fact, in sodium, each band appears as just one line, at the head, made up, in reality of a group of strong R lines. The corresponding P lines of low J are spread out and do not appear under the usual conditions. Roughly, it may be said that the magnetic rotation spectrum is rather like an absorption spectrum with an extremely low effective temperature as far as molecular rotation is concerned, but not as to vibration.

Now a vibrational analysis of the spectrum of Li_2 has already been made by Wurm,[3] on the basis of absorption measurements, and a value, 1.69 volts, deduced therefrom as the heat of dissociation; but the extrapolation is so long that no particular reliance can be placed on the result. The authors have therefore thought it desirable to study the magnetic rotation spectrum of

[1] Loomis, Phys. Rev. **31,** 323 (1928).
[2] Kemble, National Research Council Bulletin **57,** Chapter VII
[3] Wurm, Naturwiss. **16,** 1028 (1928).

Li_2, with a view to obtaining a dependable measurement of the heat of dissociation, and also of gaining further information about certain other points which will be discussed below.

While this research was in progress Professor Bartlett and Mr. Furry of this department carried through a computation of the heat of dissociation by quantum theoretical methods which are much more precise than that which had previously been used by Delbrück[4] for the same purpose. Delbrück had obtained the value 1.4 volts. Bartlett and Furry[5] found 1.12 volts.

Because of the high temperatures required to yield enough lithium vapor, it was necessary to use a somewhat modified experimental method. The lithium was contained in a nickel tube 100 cm long by 2.5 cm diameter, with a side tube fused on near one end for evacuation and with glass windows at the ends attached with sealing wax. As temperatures near the melting point of nickel were to be used, it was necessary to have a method of heating which

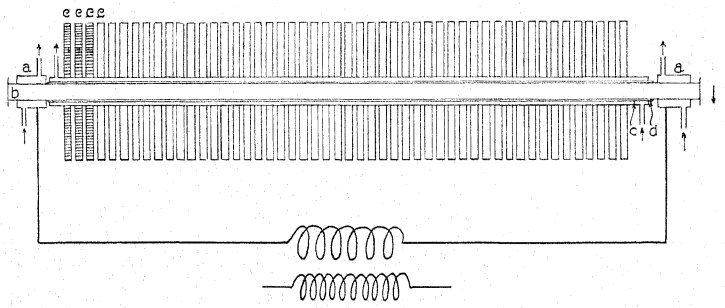


Fig. 1. Diagram of apparatus. *a*, *a:* cooling jackets. *b:* nickel absorption tube. *c:* water layer. *d*. asbestos layer, *e*, *e*, *e*. pancake coils.

allowed precise temperature control. For this purpose a large current (about 150 amperes) was sent along the nickel tube itself from a step down transformer governed by an induction regulator. Contacts were made to the tube by special water cooled electrodes which served the double purpose of preventing local heating at the contacts and of keeping the windows cool.

The magnetic field was produced by an air-cooled solenoid consisting of 50 coaxial pancake coils, each made of 90 turns of half-inch copper ribbon 0.05 cm thick and insulated by winding half-inch asbestos ribbon between the turns of the copper. The solenoid could carry a steady current of about 30 amperes and produced a field of some 1800 gauss. The nickel tube became saturated at low fields and did not act appreciably as a magnetic shield to the lithium vapor. The solenoid was protected from the heat of the nickel tube by a thin layer of water flowing between two coaxial brass tubes between the nickel tube and the solenoid. A diagram of the apparatus is shown in Fig. 1.

Usually sunlight was used as a source. It was reflected from a heliostat, through the first nicol, the tube of lithium vapor and the second nicol and focussed with a lens onto the slit of the spectrograph, a Hilger El with glass

[4] Delbrück, Ann. d. Physik **5**, 36 (1930).
[5] Bartlett and Furry, Phys. Rev. **37**, 1712A (1931).

optical system. Before the magnetic field was turned on, the nicols were set for extinction. This could only be done with success when the beam had been restricted by shields so that no part of the light was reflected from the walls of the tube. When the field was turned on, the spectrum appeared and could be photographed with exposures of from fifteen minutes to some ten hours, according to slit width, vapor density, etc.

There are two band systems of Li_2 in the visible, which have the $^1\Sigma$ ground state of the molecule in common.[6,7,8] The green system is a $^1\Pi - ^1\Sigma$ transition, the red one is $^1\Sigma - ^1\Sigma$, just as in the case of sodium. A photograph of almost the whole of the green system is reproduced in Fig. 2a; an enlarged portion of it, near the system origin, being shown in Fig. 2b. Attempts to find a magnetic rotation spectrum in the red have been unsuccessful. Unfortunately we are unable to say whether this is due to nonexistence of the spectrum or our inability, being limited by the melting point of nickel, to get sufficient

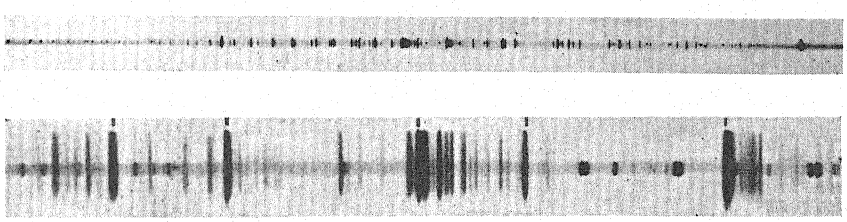


Fig. 2. a. Whole green magnetic rotation system of Li_2. b. Enlarged portion near origin. Short lines are iron comparison.

density of lithium molecules. It would be an interesting point to settle. There is a strong red magnetic rotation spectrum[9] of sodium in the region of the $^1\Sigma - ^1\Sigma$ system but all attempts to correlate it with the absorption system have hitherto failed. Moreover it is theoretically not to be expected that a $^1\Sigma - ^1\Sigma$ transition should have a magnetic rotation spectrum. We find that the magnetic rotation spectrum is stronger the lower the pressure of residual gas; and consequently we work with as low a pressure as is compatible with not fogging the windows. This is about 0.5 mm. The optimum temperature, or density of vapor, depends on the portion of the spectrum in which one is most interested. Too much vapor wipes out the spectrum by reabsorption.

On account of the favorable intensity distribution, discussed above, it was comparatively easy to extend the progressions of bands, in both directions, to where they completely disagreed with Wurm's[3] and with Harvey and Jenkins'[8] formulas. As convergence is approached however the process of measuring bands and assigning quantum numbers becomes difficult and it is necessary to proceed with caution. It is worth while to consider the reasons for this, as they constitute the essential limitations on the extent to which con-

[6] Wurm, Zeits. f. Physik **58,** 562 (1929).
[7] Wurm, Zeits. f. Physik **59,** 35 (1929).
[8] Harvey and Jenkins, Phys. Rev. **35,** 789 (1930).
[9] R. W. Wood, Proc. Am. Acad. **42,** 235 (1906); Astrophys. J. **30,** 339 (1909).

vergence can be approached, and hence on the accuracy with which heats of dissociation can be deduced from band spectra, at least of this type.

One difficulty is that, as convergence is approached, it ceases to be possible to represent the levels by any simple formula, so that extrapolation becomes difficult. If the spectrum is sufficiently sharp, however, this can be overcome with patience; since, when the correct assignments are found, the combination relations accurately check them.

Another difficulty is that we are not here dealing with a simple extreme case, such as iodine, where one can follow one single v' progression all the way to convergence because the Franck-Condon parabola lies along the axis of v' (or T'). Rather, in order to reach high values of v' we have to be able to assign the high numbered bands to the usual two dimensional array and moreover the weak bands with high v', in which we are most interested, lie among the strong bands near the system origin. That this is so can be readily seen by inspection of the improved Franck-Condon diagram in Fig. 7. Note that, as explained below, the frequency of each band is obtained by projecting it back at 45° onto the T' axis. This difficulty is the real limitation on the extent to which the absorption spectrum can be followed, as these weak bands are completely covered by the strong ones near the system origin. The principal advantage of the magnetic rotation method is that it localizes the strong bands so sharply that the weak ones can be picked out between them.

A more serious limitation is the rapidly diminishing intensity of the bands with increasing v'. The bands with highest v' lie on the left arm of the Franck-Condon parabola and correspond to transitions between the steep parts of the potential energy curves. Now with increasing v' the steep left side of a curve becomes steeper and the flat right side becomes very much flatter and correspondingly the time the vibrator spends in turning around at the left end becomes less while that spent at the right end becomes very much greater. The result is that the favoring of the right arm of the parabola over the left arm, which is present at all levels, becomes much accentuated at high quantum numbers and the transitions corresponding to the left arm of the parabola become very weak. This is often a controlling factor in intensity distribution, both in absorption and emission (fluorescence) spectra. This explanation can easily be restated in quantum mechanical form.

Contrary to what one might at first suppose, the Boltzmann factor is not the most important limitation on the intensities of the bands needed for estimation of the heat of dissociation. These bands have high v' but not particularly high v'', see Fig. 7, and it is v'' which, in absorption and magnetic rotation, is controlled by the Boltzmann factor. The right arm of the Franck-Condon parabola extends to much higher values of v'' than are found on the left arm.

Two further factors probably contribute to the difficulty of measuring bands with high v'. First, the heads of these bands tend to become somewhat diffuse, as B' decreases rapidly and $|C|$ increases, bringing the head to the origin where the line intensity is zero, and carrying the region of maximum intensity away from it. Second, there should be trouble due to an overlapping continuum which the Franck-Condon curve runs into. See Fig. 7.

The spectra in Fig. 2 are in one respect distinctly different from any previously observed. Whereas Wood's[9] magnetic rotation spectra of sodium consist of sharp lines, which have been interpreted, as explained above, as due to the piling up of strong R lines at the head of each band, here many of the strong lines show shading toward the red, or even series of lines running off to the red. Theoretically these should be the lines of the P branch and this we have confirmed by measuring them and comparing them with the absorption lines in the bands studied by Wurm[6] and by Harvey and Jenkins.[8] In each case we were able to show that the P and R lines were present and the Q lines absent; which is as it should be. It is interesting to see the theory of the formation of the line magnetic rotation spectrum confirmed in detail because, although it is intrinsically plausible, it has always seemed a little hard to reconcile with the sharpness of the lines. The present method of observation with a long tube of vapor tends to enhance these weak lines relatively to the strong ones because the strong ones are cut down by absorption.

All bands to which quantum numbers have been assigned are shown in Table I. The structure lines which shade off from these band heads are not included, nor are a number of weak heads which could not with certainty be distinguished from the structure lines. All distinct heads are included. Columns 1 and 2 give the quantum numbers assigned. Where a prime is attached the band is due to the isotopic molecule Li^7 Li^6. Column 3 shows the very roughly estimated photographic intensity. Column 4 shows the observed frequency; column 5 the frequency calculated by Eq. (1) and column 6 the difference, observed frequency minus calculated.

It will be noted that bands due to the molecule Li^7 Li^6 are present. In many cases they are strong enough so that their P branches show. Now Li^6 is about 1/16 as abundant as Li^7, so that these molecules should be about 1/8 as abundant as Li^7 Li^7. There is a slight, but very slight, hope that if we can later photograph this spectrum with higher dispersion we may be able to detect bands due to the molecules Li^6 Li^6 which are 1/256 as abundant as Li^7 Li^7, and possibly even detect the alternating intensities, or the absence of alternate lines which has been predicted on the basis of absence of hyperfine structure[10] of the atomic lines.

Since our measurements extend to bands with v' and v'' so high that Wurm's and Harvey and Jenkins' formulas completely fail, it was necessary for a good estimate of the heat of dissociation to construct a new formula to represent all the bands. Eq. (1)

$$\nu = 20439.40 + 269.69(v'+\tfrac{1}{2}) - 2.744(v'+\tfrac{1}{2})^2 - 0.0637(v'+\tfrac{1}{2})^3 - [351.60(v''+\tfrac{1}{2}) - 2.590(v''+\tfrac{1}{2})^2 - 0.0097(v''+\tfrac{1}{2})^3] \quad (1)$$

was found to fit all the bands with $v'<12$ rather well, and the residuals in Table I are calculated with reference to it. It appears however that bands with $v' \geqq 12$ show systematic and large deviations from this formula. Another third degree equation,

[10] Schüler, Zeits. f. Physik **66**, 431 (1930).

TABLE I.

v'	v''	Intensity	ν observed	ν calc. by (1)	observed-calculated
11	2	3	22218.92	22218.37	+0.55
7	0	0	22105.34	22105.69	−0.35
12	3	3	22056.62	22058.88	−2.26
10	2	6	22032.75	22032.20	+0.55
8	1	6	21973.67	21972.84	+0.83
13	4	3	21887.89	21894.49	−6.60
6	0	6	21882.43	21883.80	−1.37
11	3	6	21882.43	21882.58	−0.15
9	2	6	21837.64	21836.52	+1.12
7	1	15	21759.13	21759.30	−0.17
12	4	3	21726.92	21728.47	−1.55
14	5	0	21711.58	21724.91	−13.33
5	0	3	21652.90	21653.94	−1.04
8	2	6	21632.94	21631.73	+1.21
13	5	3	21563.84	21569.53	−5.69
11	4	6	21551.15	21552.17	−1.02
6	1	40	21538.15	21537.41	+0.74
9	3	6	21501.74	21500.73	+1.01
4	0	30	21418.22	21416.48	+1.74
7	2	30	21418.22	21418.19	+0.03
10	4	3	21367.13	21366.00	+1.13
5	1	40	21307.93	21307.55	+0.38
8	3	10	21295.48	21295.94	−0.46
11	5	6	21226.43	21227.21	−0.78
3′	0′	5	21198.91	21200.11	−1.20
6	2	8	21195.97	21196.30	−0.33
3	0	15	21171.42	21171.82	−0.40
4′	1′	20	21092.51	21092.86	−0.35
7	3	30	21081.68	21082.40	−0.72
12	6	30	21081.68	21084.05	−2.37
4	1	40	21069.55	21070.09	−0.54
10	5	0	21041.01	21041.04	−0.03
5	2	15	20966.64	20966.44	+0.20
8	4	15	20966.64	20965.53	+1.11
2′	0′	10	20939.54	20939.16	+0.38
2	0	100	20919.78	20920.33	−0.55
11	6	0	20907.05	20907.75	−0.70
6	3	5	20858.69	20860.51	−1.82
3′	1′	10	20839.65	20838.93	+0.72
3	1	100	20825.08	20825.43	−0.35
7	4	5	20751.12	20751.99	−0.87
4	2	10	20729.28	20728.98	+0.30
10	6	5	20722.40	20721.58	+0.82
1′	0′	15	20670.39	20671.21	−0.82
1	0	40	20663.32	20662.40	+0.92
8	5	30	20638.98	20640.57	−1.59
2′	1′	3	20576.40	20578.41	−2.01
2	1	50	20571.73	20573.94	−2.21
0	0	100	20397.79	20398.40	−0.61
0′	0′	50	20395.24	20396.68	−1.44
1	1	8	20315.32	20316.01	−0.69
2	2	3	20232.97	20232.83	+0.14
3	3	3	20149.02	20148.53	+0.49
4	4	0	20062.06	20062.78	−0.72
0	1	12	20052.24	20052.01	+0.23
1	2	12	19974.93	19974.90	+0.03
5	5	12	19974.93	19975.28	−0.35
3	4	0	19815.91	19818.12	−2.21
4	5	0	19738.10	19737.82	+0.28
0	2	12	19708.61	19710.90	−2.29
0′	2′	0	19678.51	19678.17	+0.34
1	3	6	19637.74	19639.11	−1.37
2	4	1	19567.22	19566.63	+0.59

TABLE I. (*Cont.*)

$v'-v''$		Intensity	ν observed	ν calc. by (1)	observed-calculated
0	3	12	19374.16	19375.11	−0.95
1	4	3	19308.58	19308.70	−0.12
6	8	1	19264.23	19263.49	+0.74
2	5	3	19242.18	19241.67	+0.51
3	6	3	19174.06	19173.70	+0.36
4	7	0	19104.23	19104.45	−0.22
1	5	1	18983.49	18983.74	−0.25
2	6	1	18922.34	18922.21	+0.13
3	7	6	18859.63	18859.79	−0.16
4	8	1	18797.24	18796.17	+1.07
5	9	1	18730.83	18731.02	−0.19
1	6	0	18664.50	18664.28	+0.22
6	10	0	18664.50	18664.00	+0.50
2	7	0	18607.85	18608.30	−0.45
3	8	0	18552.16	18551.51	+0.65
4	9	0	18493.76	18493.56	+0.20
5	10	0	18433.24	18434.14	−0.90
6	11	1	18372.81	18372.92	−0.11
7	12	1	18310.53	18309.57	+0.96
3	9	1	18249.82	18248.90	+0.92
8	13	1	18241.82	18243.79	−1.97
4	10	1	18196.20	18196.68	−0.48
5	11	1	18142.51	18143.06	−0.55
6	12	0	18087.04	18087.68	−0.64
7	13	0	18029.55	18030.25	−0.70
8	14	0	17969.74	17970.43	−0.69
9	15	0	17909.48	17907.88	+1.60

$$\nu = 20440.10 + 268.09(v' + \tfrac{1}{2}) - 2.341(v' + \tfrac{1}{2})^2 - 0.0879(v' + \tfrac{1}{2})^3 - [351.60(v'' + \tfrac{1}{2}) - 2.590(v'' + \tfrac{1}{2})^2 - 0.0097(v'' + \tfrac{1}{2})^3], \quad (2)$$

was found, by least squares, which represented the higher bands adequately but was definitely inferior for the lower ones. Fig. 3 illustrates the situation. The residuals from (1) are plotted against v' and can be compared with the curve which represents (2) − (1). The value of D_0', the energy of dissociation deduced from (1) is 3903 cm^{-1} = 0.48 volts. That deduced from (2) 3738 cm^{-1} = 0.46 volts. The latter should be distinctly better and may be accepted as having a probable error[11] of not over 0.03 volts. Hence

$$D_0'' = \nu(0, 0) + D_0' - \nu_A = 20398 + 3738 - 14904 = 9232 \text{ cm}^{-1} = 1.14 \pm 0.03 \text{ volts},^{12} \quad (3)$$

ν_A being the frequency of the resonance lines of the lithium atom. The value of D_0'' calculated from direct extrapolation of the lower levels is 1.20 volt, which agrees fairly well with (3) but is much less accurate, as the extrapolation is longer.

It will be noted that this new and accurate value of the heat of dissociation of the normal lithium molecule agrees surprisingly well with Bartlett and Furry's[5] quantum mechanical calculation, $D_0'' = 1.12$ volts, but differs con-

[11] That is, we believe the true value is at least as likely to be within the range 1.11 − 1.17 volts, as outside it.

[12] The corresponding value of the energy of dissociation reckoned from the bottom of the potential energy curve, D_e'', is 1.16 volts.

siderably, both from Wurm's[3] experimental value, 1.69 volts and from Delbrück's[4] calculated 1.4 volts.

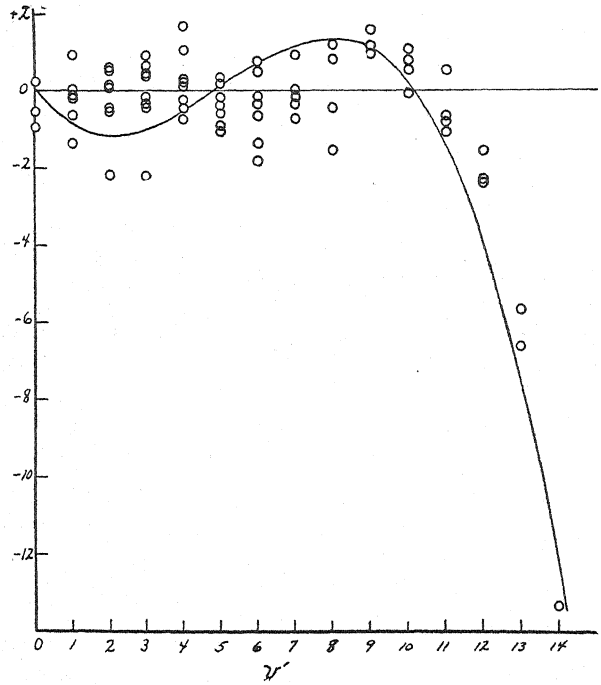


Fig. 3. Residuals of observed frequencies from Eq. (1). The curve represents Eq. (2).

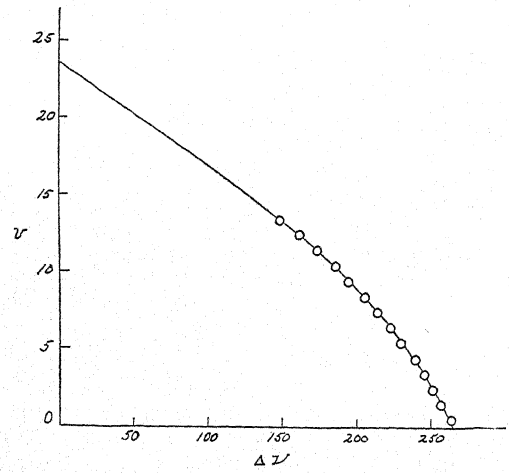


Fig. 4. v' vs. $\Delta\nu$ plotted for upper level of green system to allow extrapolation according to Birge and Sponer. The curve follows Eq. (2).

Figs. 4 and 5 show, in two ways, how little extrapolation for D' is necessary, and give some idea of the accuracy of the result. In Fig. 4, following Birge and Sponer[13] v' is plotted against $\Delta\nu$, or as they call it, ω, the energy

[13] Birge and Sponer, Phys. Rev. **28**, 259 (1926).

difference between successive vibrational levels, and D' is the area under the curve. In Fig. 5 $\Delta\nu$ is plotted against T' and the intercept on the T' axis is ν_0+D'. For convenience, a scale of the values of D_0'' which would correspond

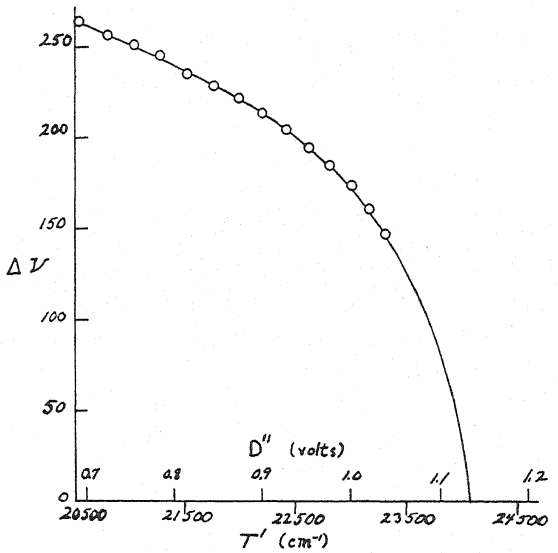


Fig. 5. $\Delta\nu$ vs. T' plotted and extrapolated to dissociation following Eq. (2). Upper scale of abscissae represents values of D_0'' which would be deduced from corresponding T' intercepts.

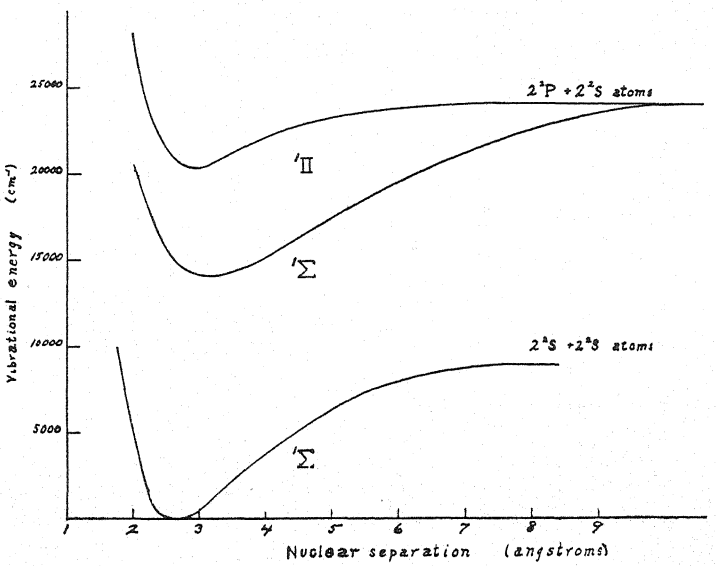


Fig. 6. Potential energy curves for the three accurately known levels of Li_2.

to various intercepts of the curve is inserted above the axis of T'. It is apparent that convergence has already been followed to within 0.1 volt of dissociation and that the value 1.14 volts can hardly be in error by more than about

0.03 volt. The curves shown in Figs. 4 and 5 are calculated on the basis of Eq. (2). The difference between Eqs. (1) and (2) would not show on the scale of these figures in the region where (1) is superior.

The potential energy curves in Fig. 6 were calculated, by the usual methods, on the basis of the data in Table II, which are the best now available for the constants of the lithium molecule.

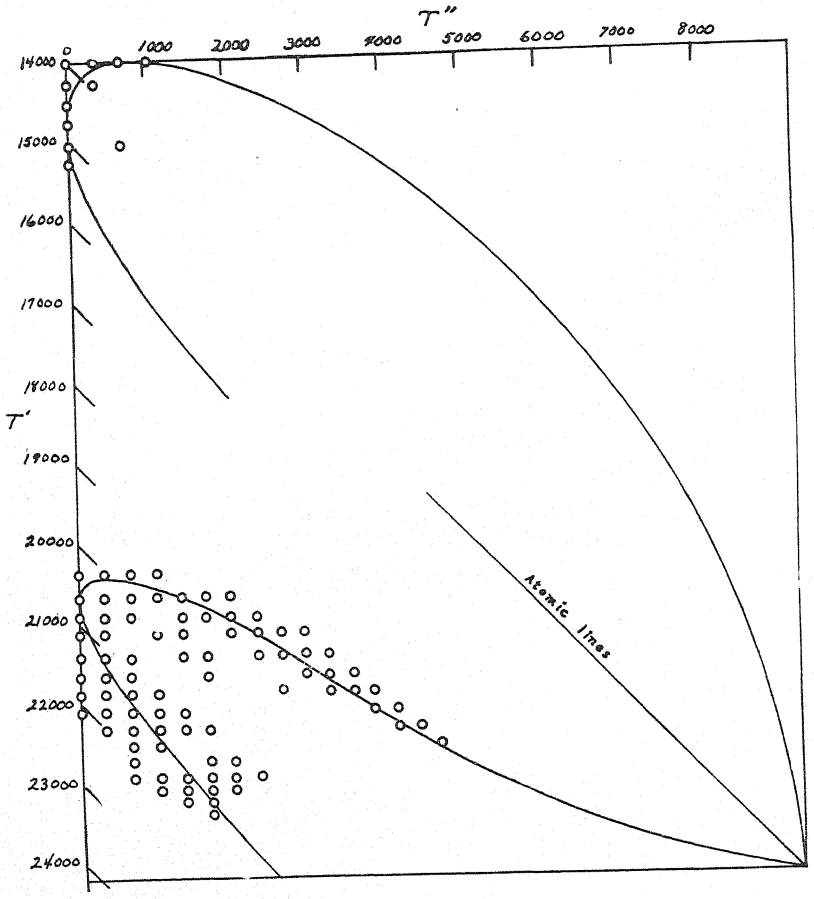


Fig. 7. Improved Franck-Condon diagram for the red and green systems. Circles represent observed bands; in the green system magnetic rotation, in the red system absorption bands. Lines of constant frequency are straight lines sloping at 45°.

TABLE II.

state	T_e	ω_e	$\omega_e x_e$	$\omega_e y_e$	B_0	$r_e \cdot 10^8$	$D_0(\text{cm}^{-1})$	$D_0(\text{volts})$
ground $^1\Sigma$	0	351.60	2.590	0.0097	0.66914[8]	2.67[8]	9232	1.14
upper $^1\Sigma$	14070[7]	253.2[7]	1.5[7]	—	0.495[7]	3.12[7]	10114	1.25
$^1\Pi$	20439.40	269.69	2.744	0.0637	0.55321[8]	2.93[8]	3738	0.46

All observed bands, and the calculated locus of maximum intensities are shown in Fig. 7 which is an improved form of Franck-Condon diagram. The

improvement consists in plotting T' and T'', the upper and lower energy terms, instead of v' and v'', the quantum numbers, as coordinates. There are several advantages to this method of plotting. In the first place, the frequency, $\nu = T' - T''$, of any band can be found by projecting the point representing it at 45° onto the T' axis. It also allows the representation of continua and of the atomic lines into which the systems converge and any number of systems can be plotted on one diagram. Moreover, the construction of the calculated locus of maximum intensities is much simpler as it involves merely plotting from two potential energy curves the heights of pairs of points with the same abcissae, and does not necessitate any calculation with vibrational quanta.

The bands of the red system as observed by Wurm[7] in absorption are also shown on Fig. 7, as is the calculated locus of maximum intensities for this system. The contrast between the richness of the magnetic rotation spectrum measurements and the meagreness of the absorption ones is very striking.

It will be noted that there must be an infrared edge to the absorption spectrum of Li_2 like that observed by Loomis and Nile[14] in Na_2. It should come at about 11000 $cm^{-1} = 9000$A. We looked for it there but failed to find it, almost certainly because we were not able to get sufficient density of vapor.

The agreement between the calculated locus and the observed bands, especially in the right arm of the green system, is unusually good. We are inclined to attribute it to our having been able to follow the levels so close to convergence, so that the extreme right hand portions of the potential energy curves are better than was the case of sodium, for instance.

[14] Loomis and Nile, Phys. Rev. **32,** 873 (1928).

THE SHOT EFFECT IN PHOTOELECTRIC CURRENTS

By B. A. Kingsbury
Bell Telephone Laboratories

(Received September 3, 1931)

Abstract

The shot effect, as it occurs in a photoelectric current, has been used to secure an evaluation of the electron charge. A new and original method of amplifier calibration, which involved the use of a modulated light beam, simplified the measurements and the computation of the result. In the absence of space charge, the experimental value of the electron charge was 1.61×10^{-19} coulombs for a thermionic current, and about 25 percent greater for a photoelectric current. It was found that the shot effect is enormously increased in photoelectric currents which are amplified by collision ionization. Statistical variations which might be expected to occur in a beam of radiant energy could not be detected, since, within the limits of experimental accuracy, the shot effect in photoelectric currents was found to be independent of the frequency of the light producing electron emission.

Introduction

THE escape of electrons from the illuminated cathode of a photoelectric cell is an irregular process which may be assumed to obey certain statistical laws. If the assumption is valid that the emergence or non-emergence of an electron has no effect on the probability of emergence of another electron, the number of electrons emitted in small equal time intervals follows a Poisson distribution. Variations in the light density are, for the time being, considered of second order, and the ratio of the number of electrons emitted to the number present is taken as very small. W. Schottky[1] has applied the above hypothesis to a thermionic current and accounted for the fluctuating voltage produced across the circuit through which the current flows. It is, of course, true that experiment has confirmed his supposition only for temperature-limited currents which flow through damped resonant circuits of high natural frequency.[2] For circuits of low natural frequency the observed result in general exceeds that expected from the theory. Johnson[3] attributes this to secular changes in the emissivity of the cathode, and Schottky[4] has worked out a mathematical expression for the effect. The shot effect, called by Schottky the "Schroteffekt," perhaps more properly translated the small

[1] W. Schottky, Über spontane Stromschwankungen in verschiedenen Elektrizitätsleitern, Ann. d. Physik. **57**, 541–567 (1918); W. Schottky, Zur Berechnung und Beurteilung des Schroteffektes, Ann. d. Physik **68**, 157–176 (1922).

[2] A. W. Hull and N. H. Williams, Determination of Elementary Charge from Measurements of Shot-effect, Phys. Rev. **25**, 147–173 (1925); N. H. Williams and H. B. Vincent, Determination of Electronic Charge from Measurements of Shot-effect in Aperiodic Circuits, Phys. Rev. **28**, 1250–1264 (1926).

[3] J. B. Johnson, Schottky Effect in Low Frequency Circuits, Phys. Rev. **26**, 71–85 (1925).

[4] W. Schottky, Small-Shot Effect and Flicker Effect, Phys. Rev. **28**, 75–103 (1926).

shot effect, has generally been found less in space charge controlled currents than the above assumption warrants.

At the present time there exists then a mathematical expression, developed in its most complete form by Fry[5] for the shot-voltage generated across the terminals of a circuit through which a temperature-limited current flows, in terms of the electron charge, e, the constants of the circuit, and the average space current.

It is to be expected that the shot effect in a photoelectric cell where no ionization occurs exactly parallels the effect for a temperature-limited current in a two electrode thermionic tube. The problem has thus far not been thoroughly investigated. Steinke[6] develops some data which he secured by measuring the time required for an electrometer to accumulate a definite charge, when the cathode of the photoelectric cell to which it was connected experienced constant illumination. His data include measurements on but one photoelectric cell, and the lack of sensitivity in the apparatus made measurements without ionization impossible.

The use of the photoelectric cell in measurements of the shot effect involves several advantages. The illumination of the cathode can be made to cover a considerable area, and so reduce secular changes in emission. The control of the cell current by modulation of the light reaching the cathode offers a simple means of securing the response curve of the amplifier and evaluating the result. Shot-voltages produced by ionization may be equally well studied in either device, but since, in practice, the photoelectric cell is usually adjusted so that collision ionization occasions considerable increase in cell current, measurements with it offer a more practical application. In this paper although shot-voltage measurements were made with ionization currents as well as pure electron currents no attempt has been made to treat the positive ion separately.

In addition to a somewhat approximate evaluation of the electronic charge, this article presents a comparison of the shot effect in thermionic and photoelectric currents where no ionization occurs, measurements of the effect in photoelectric cells where the cathodes are of different materials, and some data on shot-voltages in ionization-amplified currents. Finally, a comparison of shot-voltages is made when different sorts of radiation fall on the cathode of the photoelectric cell.

Experimental Arrangement

Fig. 1 shows the arrangement used to measure the shot effect in the photoelectric currents. The cell current was passed through a resistance and the voltage drop across this resistance was amplified by means of a specially designed high gain amplifier. The entirely resistance coupled amplifier employed nine three-electrode tubes. Coupling between stages due to feed-back through battery connections was avoided by inserting inductances in each plate lead

[5] T. C. Fry, The Theory of the Schroteffekt, J. Franklin Inst. **199**, 203–220 (1925).

[6] E. Steinke, Natürliche Schwankung Schwächster Photoströme, Zeits. f. Physik **38**, 378–403 (1926).

and connecting a condenser from the high side of each inductance to ground. The total voltage amplification was adjustable in known steps up to about 3×10^5 times, which was high enough to make the noise level of the amplifier itself easily measurable. This was done by means of interstage voltage dividers, which reduced the voltage applied to the grid of the tube to which they were connected. Two of these were provided. They operated without affecting the frequency characteristic. Care was taken to see that the amplifier did not overload, that is, the overload point of the amplifier was determined by calibration and all measurements made with less than $\frac{1}{3}$ of this output. The frequency response of the amplifier will be considered later.

To prevent interference from mechanical, acoustical, and electrical disturbances, special precautions were necessary. The photoelectric cell to be tested as well as the first four tubes of the amplifier were placed in a heavy copper box with a small glass window through which light was admitted to the cell. This box was supported on a spring suspension, and about the copper box with its spring suspension a heavy wooden box lined with hair felt was arranged.

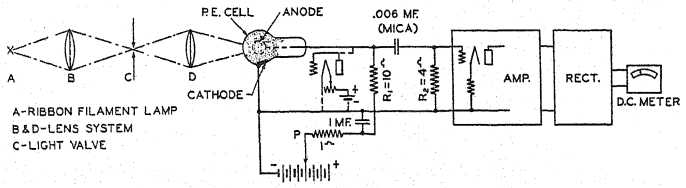


Fig. 1. Measuring apparatus.

During the summer months (1928) when these measurements were made, the high humidity which generally prevailed made the behavior of the amplifier somewhat erratic until a drying agent was introduced into the copper box which was tightly sealed, thus effectively reducing surface leakages in the photoelectric cell circuit and the first four tubes of the amplifier. The 10 megohm resistance, R_1 (Fig. 1) was a xylene resistance of liberal physical dimensions. Other types of grid leak resistances were tried but none was found which did not produce a pronounced disturbance at the output of the amplifier when carrying even the small current taken by the photoelectric cell. With this arrangement when the photoelectric cell was replaced by a xylene resistance of equal magnitude, that is the same d.c. resistance, the "noise voltage" generated by the amplifier was very steady and independent of the current flowing through R. These facts were taken as an indication that this residual "noise" was practically only that resulting from thermal electronic agitation[7] in the amplifier resistances.

The light source, a ribbon filament projection lamp, was operated from a large storage battery to insure constancy in its light output. The lamp used for the comparisons after a run at slightly above its rated current was em-

[7] J. B. Johnson, Thermal Agitation of Electricity in Conductors, Phys. Rev. **32**, 97–109 (1928).

ployed at a current 20 percent less than standard. Measurements made on successive days with the same cell checked very well and justified the belief that the light output was constant. The light source apparently has little effect on the shot effect if it remains constant during a series of measurements. In some of the earlier work several elaborate electrical filters were tried in the lamp circuit without in the least affecting the shot-voltage measured at the output of the amplifier.

The data which give the direct current flowing from the anode to the cathode of the photoelectric cell were obtained in two ways. The first method was to insert a galvanometer in the polarizing lead to the cell, directly before or after a shot-voltage measurement. In the second, the light valve indicated in Fig. 1 was employed. The light valve which is used extensively in the Western Electric system of recording sound on film is a loop of flat wire in an electromagnetic field so arranged that two opposite sides of the loop move toward one another when a current flows in one direction, and apart when the current reverses. The lightness of the moving parts makes possible tuning to frequencies above 10,000 p.p.s. The device is essentially a variable slit which can be used to control a light beam. A sinusoidal current of 1000 p.p.s. was passed through the valve so that the light reaching the cell changed from 0.5 normal to 1.5 times normal and back to 0.5 normal 1000 times per second. This can be spoken of as 50 percent modulation of the light reaching the cell at 1000 p.p.s. The calibration of the valve was made microscopically. The measurement of the voltage generated at the output of the amplifier was taken as proportional to the direct current flowing through the cell with the valve in normal position. One measurement with the galvanometer made possible the determination of all the other current values. This was done partly because of the greater rapidity with which the data could be taken, and partly because of the fact that by the second method disturbance of the set-up was avoided.

The output of the amplifier was measured by means of a d.c. meter in the plate circuit of a vacuum tube rectifier. Its response was uniform with frequency over the range involved in the measurements.

Experimental Procedure and Results

Figure 2 presents a static characteristic curve of the vacuum cell used in these tests. The direct current flowing through the cell is plotted as a function of the polarizing voltage. Care was taken to keep the illumination of the cell constant. The cell shows excellent saturation and a good vacuum appears probable.

After preliminary tests of various methods for securing a quantitative check on the magnitude of the shot effect in the photoelectric cell, a comparison with the effect in a thermionic tube with the grid and plate strapped together for anode, and the current entirely temperature-limited was adopted since Johnson[3] states that small thermionic currents controlled in this way yield values for the shot-voltage which the simple theory predicts.

A No. 239-A Western Electric Vacuum Tube was chosen which seemed to

be typical of several that were tested. The filament of this tube is oxide coated. The vacuum tube (the connections are indicated by the dotted lines

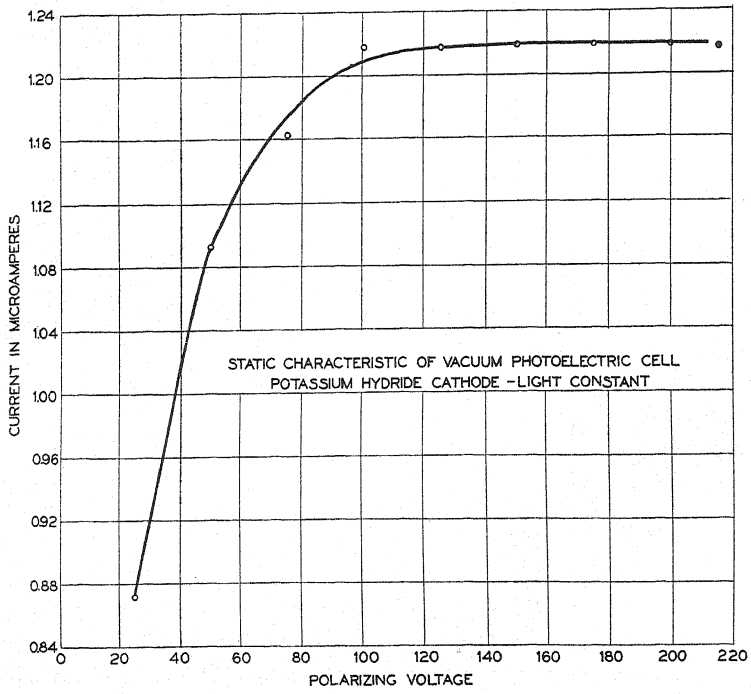


Fig. 2.

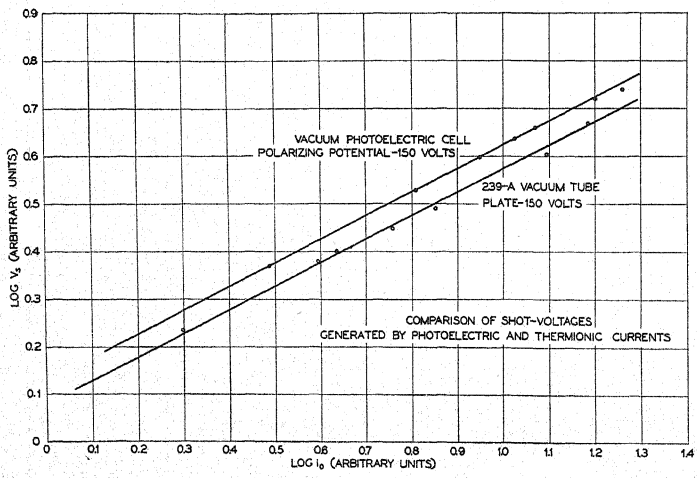


Fig. 3.

of Fig. 1) and the photoelectric cell connected in parallel were placed in the copper box and the box carefully sealed. The procedure was as follows: A polarizing potential of 150 volts was applied to the anodes. With zero cur-

rent in the filament of the vacuum tube the intensity of the light falling on the photoelectric cell was set at a certain value, and the space current measured with a galvanometer, the amplifier output was then noted. With the cell dark a voltage of measurable value at 1000 p.p.s. was impressed on the amplifier until the meter at the output of the amplifier gave the previous reading. This value of impressed voltage was taken as a measure of the shot-voltage at the input of the amplifier. A similar measurement was then made with the photoelectric cell dark and a current flowing through the filament of the vacuum tube, which produced approximately the same anode current.

The data are presented in Fig. 3. The maximum space current secured was about 2 microamperes. The logarithm of the space current i_0 is plotted as abscissa and the logarithm of the voltage $\bar{v}_s$ substituted at the input of the amplifier as ordinate. This method of plotting is used because the square of the shot-voltage $\bar{v}_i$ generated at the input of the amplifier is known to be proportional to the space current,[2] hence:

$$\bar{v}_i^2 = k i_0. \tag{1}$$

Now, the voltage $\bar{v}_s$ substituted at the input of the amplifier is considered proportional to $\bar{v}_i$ and the following relation may be assumed,

$$\bar{v}_s = k_1 i_0^{1/2} \tag{2}$$

where k_1 is a new constant. Or

$$\log \bar{v}_s = \tfrac{1}{2} \log i_0 + c \tag{3}$$

where $c = \log k_1$. Log $\bar{v}_s$ and log i_0 are the quantities plotted in Fig. 3. It will be seen that lines with the slope of $\frac{1}{2}$ fit the data very well, although the shot-voltages produced by the photoelectric current are about 12 percent larger than the corresponding shot-voltage in the thermionic current. The cause for this is not clear. It may be due to some sort of sputter action, or to residual ionization in the cell. The nature of the discrepancy tends to make the electron charge as calculated greater in the photoelectric than in the thermionic current. It should be mentioned, however, that the reading of the meter at the output of the amplifier was not quite as regular with the photoelectric cell as with the vacuum tube. The light does not seem to be the cause of this, since the heating current from the large storage battery was very steady and several types of lamps both vacuum and nitrogen-filled did not alter the effect. The lowest reading of the meter was always taken since extraneous disturbances would tend to increase the reading.

In ordinary use it is usually expedient to employ a photoelectric cell which contains a small quantity of gas, since ionization by collision considerably increases the space current. The anode potential at which ionization occurs in any cell is fixed by the gas pressure, i.e. at a sufficiently low accelerating voltage a gas-filled cell behaves like a vacuum cell.

Figure 4 presents data secured from measurements with a lamp current of 15 amperes on two typical photoelectric cells. Cell A is a gas-filled cell the cathode of which is a barium derivative. Cell B is a gas-filled cell with a

potassium-hydride surface and a central cathode. Twelve gas-filled cells were tested and these two were selected as typical of well made cells.

The curves give the logarithm of the shot-voltage, Volts $_N(\overline{V}_N)$, generated at the output of the amplifier as a function of the logarithm of the space current. The graphs really show the shot-voltages, which various polarizing potentials produce when the illumination reaching the cathode is kept constant. The shot-voltage at the output of the amplifier produced by a temperature limited thermionic current is included for the purpose of comparison. No ionization occurred in this current. The curves of Fig. 5 indicate the space current, i_0, which various polarizing potentials produce when the constant illumination used acted on the cell. This kind of plot is often spoken of as the static characteristic curve of a photoelectric cell.

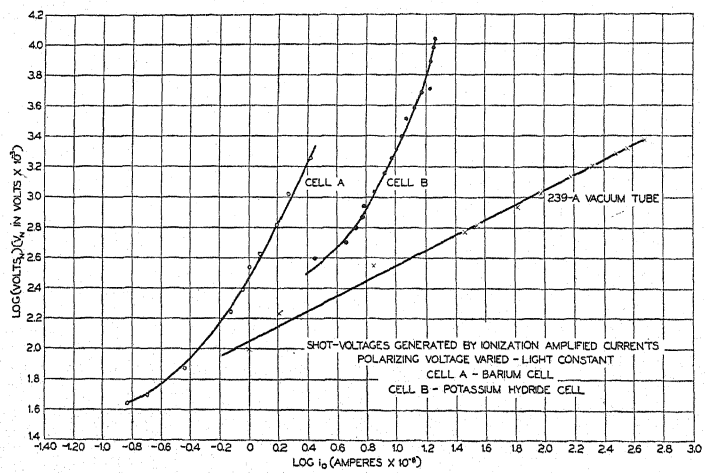


Fig. 4.

The Charge on the Elementary Carriers

In the previous discussion the shot-voltage at the input of the amplifier was found to be proportional to the square root of the electron current as measured by a d.c. ammeter. The mean of the square of the voltage at the output of the amplifier, due to the shot-voltage applied at the input, was the quantity measured, and hence it becomes desirable to have a mathematical expression for it.

Since the effect* of the mica condenser at the input of the amplifier is slight at most frequencies of importance, due to the magnitude of R_1 and R_2 (Fig. 1), the current i from the photoelectric cell is imagined to flow through an impedance made up of a capacity and resistance in parallel. If the resistance of R_1 and R_2 in shunt is called R_p†, the square of the absolute magni-

* The impedance of this condenser is about 1/4 megohm at 100 cycles which is only 1/16 of 4 megohms, and 1/40 of a megohm at 1000 cycles.

† If a complex impedance is introduced in place of R_p into the computations, the same final conclusion (Eq. 16) is reached. The method, here used, is employed in the interest of simplicity.

tude of this impedance Z_n is

$$|Z_n|^2 = \frac{R_p^2}{1 + R_p^2 C^2 \omega^2}. \tag{4}$$

Where C refers to the total shunt capacity at the input of the amplifier, and ω is 2π times the frequency.

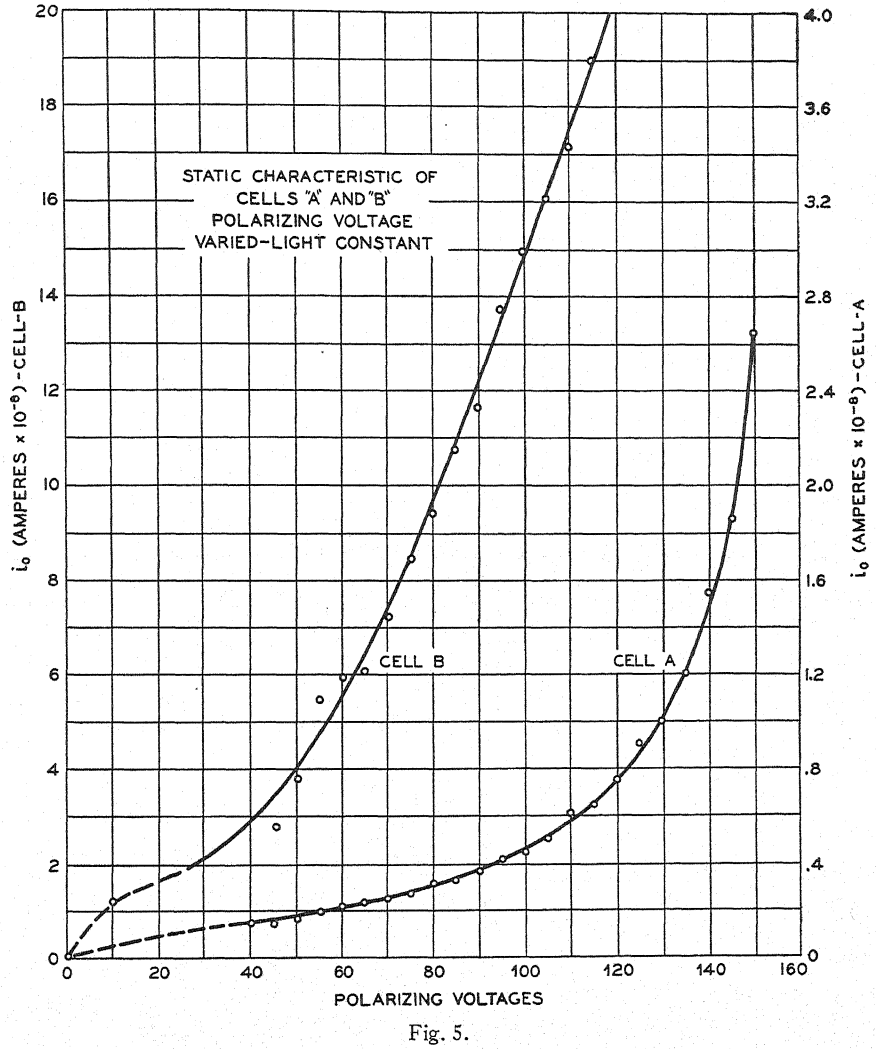


Fig. 5.

The lack of uniformity in the frequency response of the amplifier makes the following definition of amplification necessary

$$\overline{V}_n^2/\overline{v}_{i_n}^2 = A_0^2 f(n). \tag{5}$$

$\overline{V}_n$ is the r.m.s. value of voltage measured across the resistance, R_x, at the output of the amplifier, when a sine wave voltage of frequency n and r.m.s.

value $\bar{v}_{i_n}$ is applied to the input of the amplifier. A_0 represents the voltage amplification at the frequency n_0 of maximum response of the amplifier, and $f(n)$ expresses the square of the voltage amplification at frequency n relative to that occurring at n_0. At frequency n_0, $f(n)$ has the value unity. $\bar{I}_n$ is the current flowing through R_x when $\bar{V}_n$ is the voltage across it.

Equation (12) of Fry's solution[5] now can be applied to the conditions of the problem. For the case under consideration it reduces to

$$S = \frac{1}{2\pi} ei_0 \int_{-\infty}^{+\infty} \frac{R_x}{|\bar{Z}|^2} \frac{R_p^2}{1 + R_p^2 C^2 \omega^2} d\omega \tag{6}$$

S is the power expended in the resistance, R_x, i_0 the space current, and Z the transfer impedance to the measuring device. The other terms have the significance already assigned to them. Z may be defined as follows

$$\bar{Z} = \bar{v}_{i_n}/\bar{I}_n = \bar{v}_{i_n} R_x/\bar{V}_n$$

or

$$|\bar{Z}|^2 = \bar{v}_{i_n}^2 R_x^2/\bar{V}_n^2 = R_x^2/A_0^2 f(n). \tag{7}$$

Equation (6) now reduces to

$$S = \frac{1}{2\pi} ei_0 \int_{-\infty}^{+\infty} \frac{R_x A_0^2 f(n)}{R_x^2} |Z|_n^2 d\omega$$

or, when dn is substituted for $d\omega$ and the limits of integration altered

$$S = \frac{2A_0^2 ei_0}{R_x} \int_0^{\infty} |Z|_n^2 f(n) dn. \tag{8}$$

However, in view of the fact that the mean of the square of the voltage measured at the output is equal to $R_x S$, the working equation becomes

$$\bar{V}_N^2 = 2A_0^2 ei_0 \int_0^{\infty} |Z|_n^2 f(n) dn. \tag{9}$$

The photoelectric cell and light valve provide a simple method for evaluating the above integral. The current for a constant percentage of modulation of the valve can be readily determined microscopically. Suppose constant cell illumination and constant percentage modulation of the light reaching the cell is employed, then at each frequency the current flowing through Z_n will be constant. Equation (5) allows the following relation where the primes are used to designate voltages produced by the action of constant light modulation

$$\frac{\bar{V}_0'^2}{\bar{V}_n'^2} = \frac{\bar{v}_{i_0}'^2 A_0^2}{\bar{v}_{i_n}'^2 A_0^2 f(n)} = \frac{\bar{v}_{i_0}'^2}{\bar{v}_{i_n}'^2 f(n)}.$$

which since

$$\bar{v}_{i_0}'^2/\bar{v}_{i_n}'^2 = |Z|_0^2/|Z|_n^2$$

becomes

$$\bar{V}_0'^2/\bar{V}_n'^2 = |Z|_0^2/|Z|_n^2 f(n)$$

or

$$f(n) = |Z|_0^2 \bar{V}_n'^2/|Z|_n^2 \bar{V}_0'^2. \tag{10}$$

This value of $f(n)$ substituted in Eq. (9) gives

$$\bar{V}_N^2 = 2A_0^2 i_0 e \int_0^\infty \frac{|Z|_0^2 \bar{V}_n'^2}{|Z|_n^2 \bar{V}_0'^2} |Z|_n^2 dn \tag{11}$$

or

$$\bar{V}_N^2 = 2A_0^2 |Z|_0^2 i_0 e \int_0^\infty (\bar{V}_n'^2/\bar{V}_0'^2) dn. \tag{12}$$

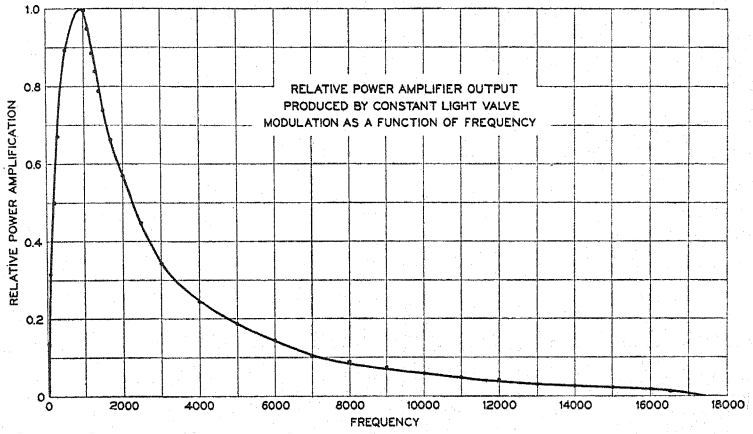


Fig. 6.

Measurements were made of $\bar{V}_n'^2$, for 50 percent modulation of the valve and a projection-lamp current of 15 amperes, at various frequencies and a curve (Fig. 6) plotted showing the value $\bar{V}_n'^2/\bar{V}_0'^2$ as a function of frequency. $\bar{V}_0'$, the maximum response occurred at 1000 p.p.s., due to the action of an inductance introduced in the battery lead to prevent disturbances there from affecting the photoelectric cell. The area under this curve is the value of the integral in Equation (12). It will be designated by A, and a summation of the area under the curve gives it the value 2.86×10^3.

Equation (12) will become then:

$$\bar{V}_N^2 = 2A_0^2 A |Z|_0^2 i_0 e. \tag{13}$$

If the light valve produces 50 percent sinusoidal modulation of the light reaching the cell at 1000 p.p.s. and i_0 is the space current flowing through the cell with the light valve in normal position, the mean square of the voltage at the output of the amplifier will be

$$\bar{E}_s^2 = |Z|_0^2 A_0^2 i_0^2/8 \tag{14}$$

where Z_0 is the input impedance of the amplifier at 1000 p.p.s.

If (14) is now divided by (13)

$$\frac{\overline{E_S}^2}{\overline{V_N}^2} = \frac{|Z|_0^2 A_0^2 i_0^2}{16|Z|_0^2 A_0^2 A i_0 e} \equiv R^2 \tag{15}$$

and e becomes

$$e = i_0/16AR^2. \tag{16}$$

The data for the No. 239-A Vacuum Tube, as shown in Figs. 3 and 4, yield on the basis of Equation (16), the value 1.61×10^{-19} coulombs for e while the data for the vacuum photoelectric cell give a value about 25 percent greater. It will be noted that two of the points on the curve for cell A in Fig. 4 nearly coincide with the vacuum tube curve, as well as one point for vacuum cell in Fig. 3.

Ionization-Amplified Currents

It is often convenient to think of each primary electron emitted from the cathode in an ionization amplified current as carrying a charge from cathode to anode, which is a constant times the magnitude of the electron charge. If this condition obtains, Equation (16) should give in place of e a value which would be increased by a factor representing the increase in cell current due to ionization. This is the same thing as saying that e, now called e' should be a linear function of the space current for the cells A and B. Fig. 7 exhibits the ratio of e/e' (e is the value secured from the vacuum tube data) as a function of the space current for these cells. The condition of linearity is not fulfilled although ionization is well under way at 40 volts polarizing potential where the measurements begin. The failure of e' to increase at low ionization amplification agrees with the data presented by Steinke,[6] although it apparently occurs here at lower ionization amplification. It should be understood that for all the values of e/e' given for one cell in Fig. 7, the number of electrons emitted from the cell cathode is approximately constant, that is, the condition of constant illumination and varied polarizing potential prevails.

The above equations were evolved on the basis of single electron emissions which involved the transfer independently from cathode to anode of a definite and constant charge. The data as cited above do not bear out the hypothesis that each primary electron experiences the same amplification, but make it clear that, if $\alpha_i e$ is the charge transported by the i-th electron emission, $\alpha_{i+1}e$ the charge transported by the $(i+1)$ electron emission will probably be different from $\alpha_i e$. The static characteristic curve of a photoelectric cell taken with constant illumination (Fig. 5) furnishes a method of determining the average value of α, $(\bar{\alpha})$, since $\bar{\alpha}$ is merely the ratio of the ionization-amplified current to the current when ionization begins. Probability theory makes the probability that α has the value n equal to:[8]

$$W(n) = e^{-\bar{\alpha}}\bar{\alpha}^n/n!. \tag{17}$$

[8] R. Fürth, Schwankungerscheinungen in der Physik, pp. 17–22.



By the application of Stirling's formula and differentiation the maximum value of $W(n)$ is found to be*

$$W(n)_{\max} = W(\bar{\alpha}) = e^{-\bar{\alpha}}\bar{\alpha}^{\alpha}/\bar{\alpha}! = 1/(2\pi\bar{\alpha})^{1/2} \tag{18}$$

Thus as $\bar{\alpha}$ increases the probability of its occurrence becomes continually less. This can perhaps be more clearly seen from the fact that, $\bar{\delta}^2$, the square of the average relative variation in α may be written

$$\bar{\delta}^2 = 1/\bar{\alpha} \tag{19}$$

which makes, according to Bateman,[9] the square of the absolute magnitude of the average variation

$$\bar{\nu}^2 = \bar{\alpha}. \tag{20}$$

The fluctuations which produce the shot-voltage, increase therefore not only in magnitude, but in irregularity as $\bar{\alpha}$ increases.**

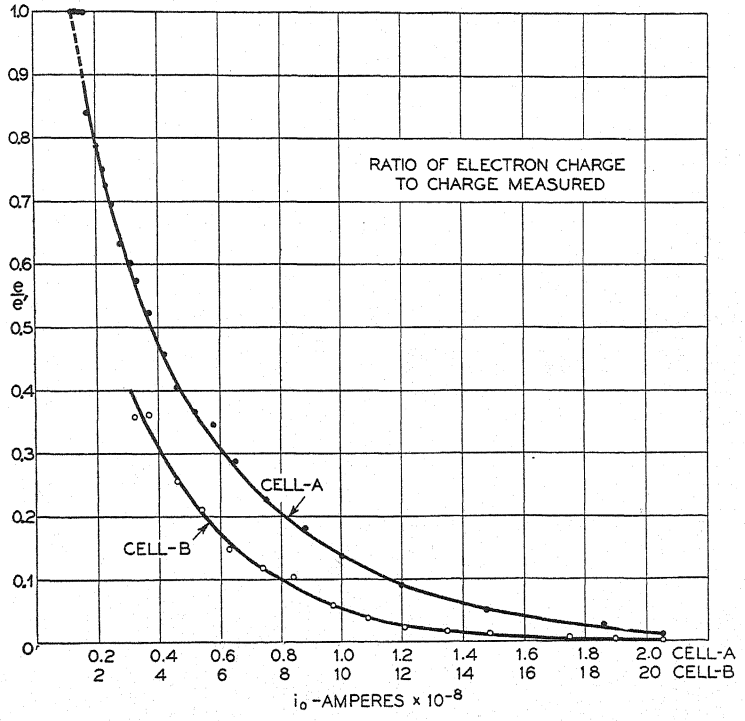


Fig. 7.

* This equation becomes less accurate as $\bar{\alpha}$ approaches unity. The case $\bar{\alpha}=0$ has no physical significance since the average charge can not be less than e which condition makes $\bar{\alpha}$ never less than one.

[9] H. Bateman, On the Probability Distribution of α Particles, Phil. Mag. **20**, 704 (1910).

** The equations (17) to (20) are rather general in form and apply with altered significance in the symbols to the emission of electrons from an illuminated cathode. Thus used, they are the basis for the derivation of equation (1). They are employed here to bring out the fact that ionization is a statistical process which acts on another statistical process, namely electron emission. The result can, of course, be thought of as a single process, but some gain in appreciation of what occurs may be found by considering the two steps.

The calculation of the average charge transmitted from a measurement of the shot-voltage, in this case, becomes clearly beyond the validity of Equation (16), since $W(\bar{\alpha})$ as well as $\bar{\alpha}$ has, when no ionization occurs, the value of unity. The development of an adequate equation to replace Equation (16) would involve the summation of the contribution of an infinity of primary electrons, each transmitting the charge $\alpha_i e$, to the shot-voltage generated at the input of the amplifier provided the amplified charge passed by each primary electron acts as the single electron in the absence of ionization. The securing of a result, which checks with experiment without several rather violent assumptions and special distributions, appears to be clearly beyond the bounds of the method.

Empirically it was found that Equation (16) becomes valid for all cases if e' is defined as

$$(e')^\beta = \bar{\alpha} e^\beta \exp 2(\bar{\alpha} - 1) \tag{21}$$

where β is a constant set by the cell-structure parameters and the gas content. e is the theoretical value of the electron charge and $\bar{\alpha}$ is as defined above. That is, for a current amplified by ionization the right hand side of Equation (16) may be replaced by

$$\bar{\alpha} e \bar{\alpha}^{(1/\beta-1)} \left(\exp \frac{2(\bar{\alpha} - 1)}{\beta} \right) = \frac{i_0}{16AR^2} . \tag{21a}$$

This is equivalent to multiplying the shot-voltage computed on the basis of $W(\bar{\alpha}) = 1$, by the factor $\bar{\alpha}^{(1/\beta-1)}$ $(\exp 2(\bar{\alpha}-1)/\beta)$. The factor reduces to unity when $\bar{\alpha}=1$ and the usual equation holds. An equation equivalent to (21) is

$$\beta \log (e'/e) = \log \bar{\alpha} + 2(\bar{\alpha} - 1) \log \epsilon. \tag{22}$$

Figure 8 shows the data of Fig. 7 plotted as suggested by Equation (22). The abscissa is $[\log \bar{\alpha} + 0.87\ (\bar{\alpha}-1)]$ and the ordinate $\log (e'/e)$. The factor β has no effect on the relationship except to alter the slope and hence it is not used. It is a factor peculiar to each cell and the determination of its value independent of Equation (22) seems impossible. $\bar{\alpha}$ was determined from the static characteristic curves as given in Fig. 5. The accuracy of the determination of $\bar{\alpha}$ is not as great as might be desired because the point at which ionization begins does not show up sharply. However, it seems as though the curves should pass through the origin and they have been drawn so. All the data taken apparently agree with this relationship, although data on cells A and B only have been included here. A slight error in $\bar{\alpha}$ would only occasion a change in slope.

Practical Considerations

The data secured in these measurements have a bearing on the employment of photoelectric cells to transform a modulated light beam into a varying electric current. If the electric current is amplified and used to operate a loud speaker, the shot-voltage generated by the photoelectric current at the input of the amplifier sets the level of the background "noise" in the system.

From the previous discussion and notation it will be evident that for 100 percent modulation of the light beam the ratio of signal to "noise" voltage across the terminals of the loud speaker will be $2R$. It is desirable to have $2R$ as great as possible but fidelity of reproduction requires that an ample frequency range be provided. The characteristics of the frequency response of the amplifier determines the term A in our equations.

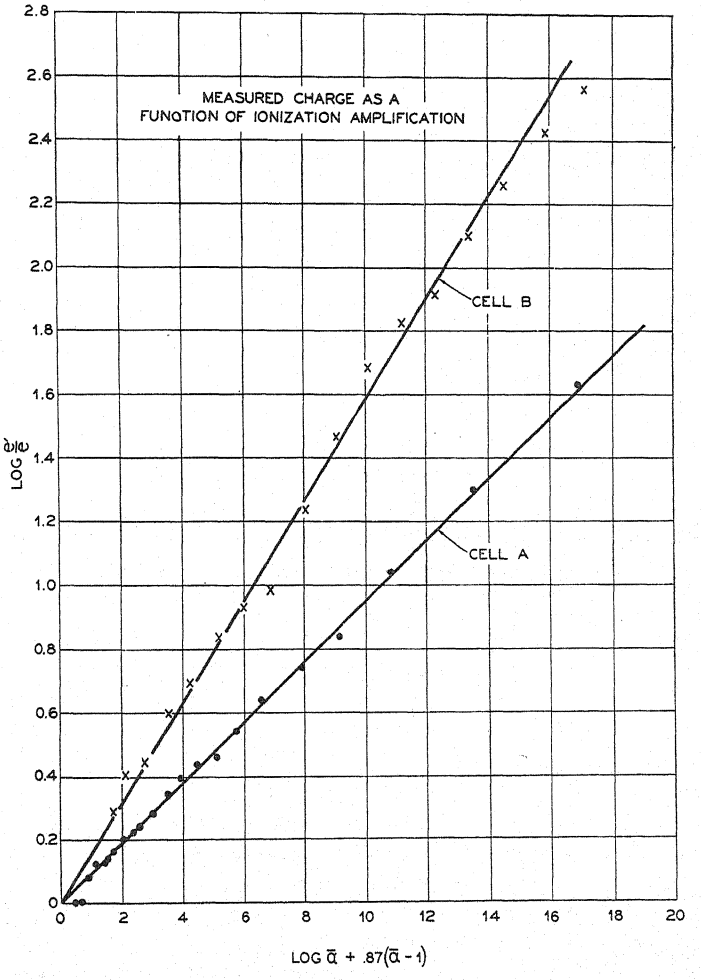


Fig. 8.

A combination of Equations (16) and (21) gives $2R$ the value

$$2R = \tfrac{1}{2}\left(\frac{i_0}{Ae\bar{\alpha}^{1/\beta}\exp\left[2(\bar{\alpha}-1)/\beta\right]}\right)^{1/2} \tag{23}$$

where the terms have the same significance as above. When $\bar{\alpha}$ equals unity, that is, in the absence of ionization the volume range increases as the square root of i_0, since A is constant. A small amount of ionization may produce a

slight increase in volume range although ionization which affects all electrons emitted alike might be expected to leave the volume range constant. Ultimately, and it usually occurs before the ionization is very great, the noise voltage as measured at the output of the amplifier increases more rapidly than the signal voltage, when the polarizing potential is made greater. Thus while the signal increases at the same rate as the average space current in the cell, the noise voltage has a larger rate.

Equation (23) can be transformed in the case where the number of electrons emitted per second is constant and equal to N, into a simpler equation

$$2R = \tfrac{1}{2}\left(\frac{N\bar{\alpha}e}{Ae\bar{\alpha}^{1/\beta}\exp\left[2(\bar{\alpha}-1)/\beta\right]}\right)^{1/2}$$

or

$$2R = K\frac{\bar{\alpha}^{(\beta-1)/2\beta}}{\exp\left[(\bar{\alpha}-1)/\beta\right]}. \tag{24}$$

where K is a constant. If the points as plotted for cell A in Fig. 4 are considered, the volume range that is the ratio of signal voltage to "noise" voltage is only about 2/5 as great at the last point as at the first. For this cell, with the illumination at which the measurements were made the polarizing voltage which yields the greatest volume range is about 90 volts, while for cell B it is about 45 volts. The equations as they are developed as well as the measurements themselves show that it is the best practice to use only slight ionization or no ionization in the cell and as intense a light source as possible. The required condition for an increase in volume range appears to be greater electron emission from the cathode. In this brief analysis the contribution of other effects to the "noise" voltage has been neglected. It is usually impossible to go to 100 percent modulation of the photoelectric cell current because of the curvature of the static characteristic curve, and the results given above therefore, represent the maximum which can be achieved under the most favorable circuit conditions.

The Action of the Exciting Radiation on the Shot Effect

Thus far the shot effect in photoelectric currents has been shown to arise only from the statistical variations in the rate of electron emission and the finite size of the elementary carriers, and to coincide approximately with the effect in the thermionic vacuum tube. The increased fluctuations introduced by ionization amplification have been analyzed in some detail. The agreement of the results secured in cells with potassium-hydride and barium cathodes makes the effect independent of the cathode material. It now remains to investigate the effect of the exciting radiation on the shot-voltages generated.

It is well known[10] that no matter how constant a light source, the instantaneous density of the light from it which reaches a small area undergoes certain density fluctuations. This should react on the shot-voltages. Two attempts were made to get at the effect of these variations on the shot-

[10] N. Campbell, Pro. Cambr. Phil. Soc. 15, 310 and 513 (1910).

voltages generated by the photoelectric current. The first, which was rather qualitative, rested on the fact that the radiation from the ribbon filament lamp would change both in quality and quantity as the lamp current was altered. The data are plotted in Fig. 9 which is similar to Fig. 4, except another potassium-hydridge cell (cell C) was employed and each of the three curves apply to the same cell. Each curve was taken with a constant lamp current, and, hence, constant illumination. The polarizing potential was varied in steps of 5 volts from 40 to 90 volts. Because of the different sensitivity

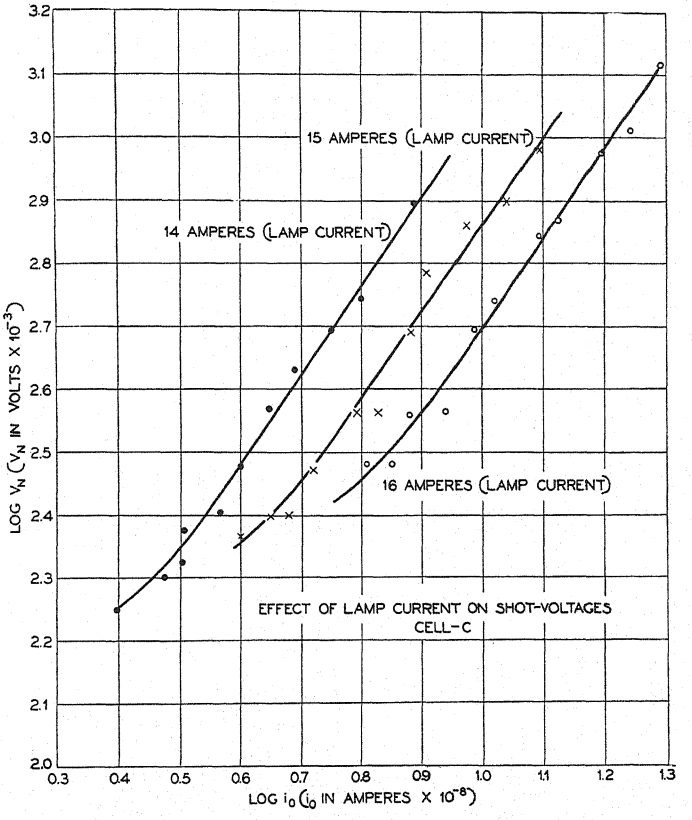


Fig. 9.

of the photoelectric cathode to various kinds of radiation, the relation between the number of electrons emitted and the number of incident light quanta should be different for each of the three curves. The variations in light density are roughly inversely proportional to the intensity of the light. Thus variations in light density might be expected to change the type of curve. This does not occur, the three curves within the limits of experimental accuracy are parallel. In other words, the change in curve is no more than occurs when cathodes of different sensitivity are employed.

The second test was of a more quantitative nature. In Fig. 10 is shown the relative transmission of two light filters as a function of the wave-length

of the light. The third curve presents the response of a potassium-hydride surface[11] to equal amounts of radiant energy of different wave-lengths. It will be seen that the filter No. 47 transmits in the region where the potassium-hydride surface is most sensitive, while with filter No. 62 the transmitted light causes a relatively slight photoelectric action. The total transmission of filter No. 47 was 2.9 percent and that of filter No. 62, 4 percent.

The procedure in the measurements was first to interpose the filter No. 62 in the path of the light reaching a potassium-hydride photoelectric cell con-

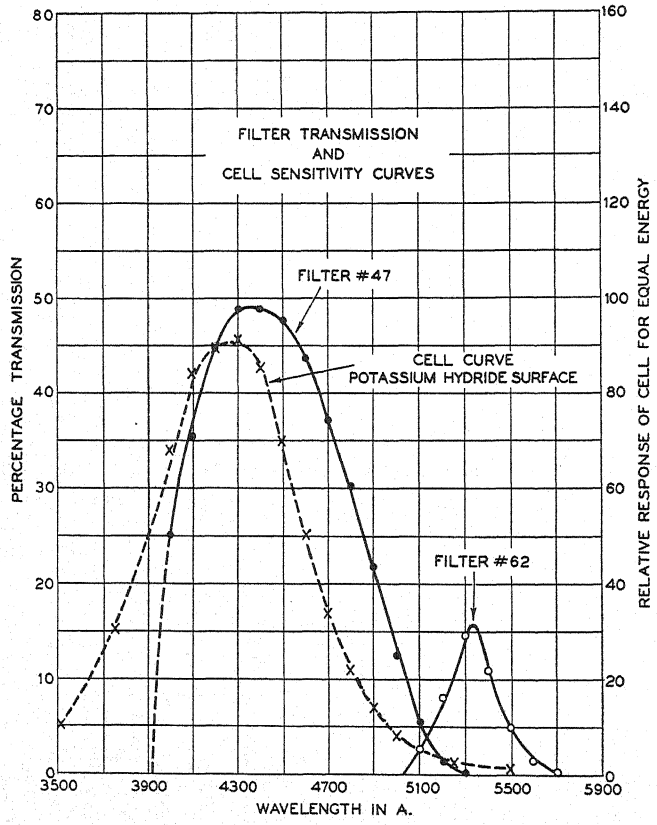


Fig. 10.

nected to the input of the amplifier. A measureable direct current was secured, and the shot-voltage generated measured by substituting a known small voltage at a 1000 p.p.s. on the input of the amplifier until the deflection of the meter at the output was the same as for the shot-voltage. This is the same procedure as employed in securing the data of Fig. 3. Then by adjusting the lamp current the same space current was secured with the other filter in the light beam and a shot-voltage measurement again made by substitution. The data secured from a series of measurements are shown in Table I. The ac-

[11] R. Pohl and P. Pringsheim, Die Lichtelektrischen Erscheinungen, p. 25.

TABLE I.

Shot-Voltage Measured (Relative Units) Green Filter No. 62	Blue Filter No. 47	i_0 amperes $\times 10^{-8}$
1.50	1.50	1.00
1.69	1.69	1.26
1.90	1.69	1.58
2.13	2.13	2.00
2.39	2.68	2.51
2.68	2.68	3.16

curacy here is not as good as in the previous measurements because only a small range of space currents could be secured and the ratio between successive voltage steps applied at the input of the amplifier was 1.12/1. However, even under these conditions, the shot-voltage at the same polarizing potential and cell current seems independent of the sort of illumination which produces the photoelectric action. The explanation of this phenomenon seems to come from the low efficiency of the photoelectric process. For instance, if the case is considered when the relative voltage input equals 2.13, the light emitted from the lamp, between the two conditions, as measured by the photoelectric cell increased 29 times. The cell sensitivity in the regions transmitted by the two filters differs by a ratio of about 15 to 1, which for the same current, signifies a ratio of almost 15 to 1 in the number of incident light quanta present.

This result confirms the work of Marx and Lichtenecker[12] who compared the output of two photoelectric cells when one experienced constant and the other intermittent illumination, applied in such a manner that over a certain time the amount of energy reaching each photoelectric cathode was the same. The filter method is much simpler and it would be very desirable if it could be carried out in such a way that the number of incident light quanta changed by a larger factor.

This problem of variations in the intensity of a beam of radiant energy is quite similar to the shot effect so far as the mathematical concepts are concerned. The light quanta play a role similar to that of the electrons which flow from the cathode to anode. This difference exists, however, every electron reaching the anode contributes to the shot-voltage, but every light quantum does not free an electron. A photoelectric cell of 100 percent efficiency would make the variations in the light measurable.

DISCUSSION

The work here presented tends to show that the evaluation of the electron charge by measurement of the shot effect in photoelectric currents in spite of serious difficulties when values of the charge which compare with those of other methods are required, is nevertheless capable of considerable accuracy

[12] E. Marx and K. Lichtenecker, Experimentelle Untersuchung des Einflusses der Unterteilung der Belichtungszeit auf die Electronenabgabe in Elster und Geitelschen Kaliumhydrurzellen bei sehr schwächer Lichtenergie, Ann. d. Physik **41**, 124–160 (1913).

and a large measure of simplicity. The chief difficulties, other than those of theory, arise from the large amount of amplification necessary and the extremely small space currents. However, the essentials of the theory are substantiated, although the case of ionization amplified currents is still somewhat of an enigma.

Measurements in this field, should be fruitful because ionization amplification merits a fuller understanding than is now available, while variations in light density as energy flows from a steady source require an experimental technique to confirm our present theories. This paper in itself can claim only to be a preliminary survey of a subject which merits fuller investigation.

The value for the electron charge secured here is in the neighborhood of the correct value. The identity of the shot effect in thermionic and photoelectric currents makes the cathode surface and the exciting radiation factors of second order in the phenomena.

THE PHOTOELECTRIC EFFECT FROM THIN FILMS OF ALKALI METAL ON SILVER

By Herbert E. Ives and H. B. Briggs
Bell Telephone Laboratories

(Received September 2, 1931)

Abstract

The thin films of alkali metals which spontaneously deposit in vacuo on other metals have long been known to exhibit photoelectric effects which vary in amount and character, depending on the underlying material, but the exact nature of this dependence has been obscure. Silver, because of its region of exceedingly low reflecting power in the ultraviolet and the accompanying variation of optical constants, is exceptionally well suited for studying the influence of the underlying metal. It is found that the region of low reflecting power profoundly affects the photoemission, but in a manner not to be explained simply by reduction of light reflected back through the alkali metal film or by the absorption of light by the silver. The results obtained are very satisfactorily explained upon computing, from the optical constants, the intensity at the surface, of the interference pattern formed by reflection just above the silver surface. The positions of the maxima and minima of photoemission, and their variations with angle of illumination and plane of polarization are accurately indicated.

SILVER, in the wave-length region 3200–3500A, exhibits a narrow band of low reflecting and high transmitting power. Measurements of reflecting power for light at normal incidence by Hagan and Rubens,[1] reproduced in Fig. 1, show a value at wave-length 3160A as low as that of glass, and the transmission is sufficiently high so that thin films of silver have been used as filters to transmit a narrow band of ultraviolet energy.

Thin films of alkali metals, spontaneously deposited in vacuo on specular surfaces of metals such as platinum, nickel or silver, give strong photoelectric currents, varying from metal to metal in a manner not heretofore understood.[2] The *vectorial effect* is pronounced, that is, the currents for light polarized with the electric vector parallel to the plane of incidence (symbolized by $\|$) are much greater than for light polarized with the electric vector at right angles to the plane of incidence (symbolized by $\perp$). The ratio of the $\|$ to the $\perp$ currents from a film of a given alkali metal differs with the underlying metal. It has been a fair presumption that these characterisics of the vectorial effect depend upon the optical properties of the metal beneath; but the nature of the dependence has been obscure.

The peculiar optical properties of silver have appeared to be admirably suited for throwing light on the influence of the underlying material on the photoelectric effect from thin films, for the optical properties of silver vary all the way from a typically metallic character in the visible region, through a region where the properties are similar to those of glass, to another region

[1] Hagen and Rubens, Ann. d. Physik **8**, 1, (1902).
[2] Ives, Astrophys. J. Nov., 1928, p. 60.

in the far ultraviolet where the metallic properties are quite as different as though another metal had been substituted.

The experimental work described below was initiated without any detailed theoretical picture of the results to be expected. One tentative picture would ascribe the photoemission to the silver as well as the alkali metal upon it; on this assumption the photoelectric effect might be expected to follow closely the absorbing power of the silver. Another picture would consider the thin layer of photosensitive alkali metal as lying sufficiently far above the silver reflecting surface so that light would pass through it twice and the photoeffect would be that due to an average of the incident and reflected energy from the silver; the region of low reflecting power of the silver would then again show as a region of reduced photoelectric emission, but the emis-

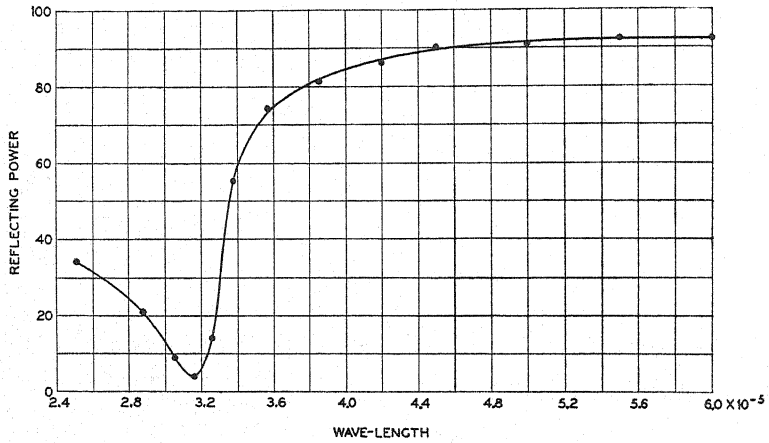


Fig. 1. Reflecting power of silver for perpendicularly incident light, as measured by Hagen and Rubens.

sion would not vary with wave-length in the same manner as on the first assumption. Acutally the experiments have shown that neither of these crude pictures is adequate and we have been led to an interpretation which depends upon a detailed analysis of the optical conditions at the silver surface. This interpolation has given a valuable clew to the nature of the vectorial effect itself, which has been discussed in a previous paper;[3] the present paper deals chiefly with the variation of photoelectric effect with wave-length, as determined by the optical properties of the silver base.

Apparatus and Experimental Procedure

The measuring apparatus used in this study consisted of a quartz-ultraviolet spectrometer, used either with a quartz mercury arc or with a quartz windowed tungsten ribbon lamp, to provide monochromatic light. A quartz Rochon prism in the path of the light energy from the spectrometer provided two beams, polarized at right angles to each other. Fused quartz wedges and

[3] Ives, "The Vectorial Photoelectric Effect," Phys. Rev. Sept. 15, 1931.

prisms were also introduced so that a quick shift could be made from one plane of polarization to the other without shifting the spot of light. The photoelectric currents were measured with a Compton electrometer by the steady deflection method, while the energy values of the radiation were recorded by a thermopile in conjunction with a high sensitivity moving coil galvanometer. With this apparatus it was possible to make reliable simultaneous measurements of photoelectric current and radiant intensity with the mercury arc lines. The tungsten lamp radiation, while sufficient for photoelectric excitation was too small to be satisfactorily measured by the thermopile in the ultraviolet region here in question. Comparison of photocurrents between several cells could, however, be readily made and this possibility was taken advantage of to secure important information.

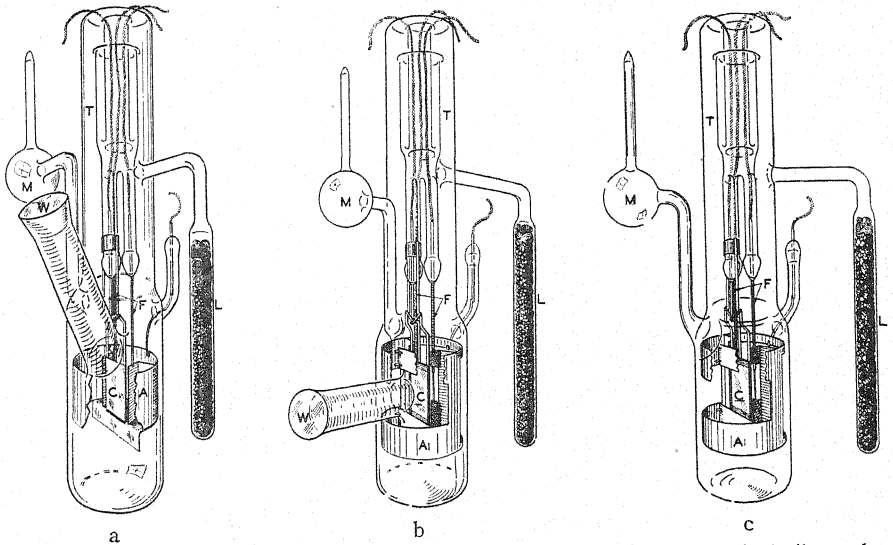


Fig. 2. (a) Quartz windowed cell for observation at 60° incidence. *C*, polished silver plate (cathode) on which thin film of alkali metal is spontaneously deposited. *A*, enclosing anode of nickel, with vanes to prevent scattered light from striking back of cathode. *W*, fused quartz window, attached to Pyrex tube by stepped glass seal. F, leads to tungsten filament used for degassing cathode by electronic bombardment. *M*, bulb into which alkali metal is introduced after multiple distillation. *L*, charcoal tube. *T*, reentrant tubulation to reduce leakage caused by formation of alkali metal films on glass parts.
(b) Quartz windowed cell for observation at perpendicular incidence. Parts lettered as in 2a.
(c) Pyrex glass cell for observations at a series of angles. Parts lettered as in 2a.

Several varieties of photoelectric cells were used, which may be listed and illustrated here:

I. Quartz windowed cells for observations at 60° incidence. Fig. 2a.
II. Quartz windowed cells for observations at perpendicular incidence. Fig. 2b.
III. Pyrex glass cells for observations at a series of angles, for the determination of "angle curves." Fig. 2c.

The structural details are sufficiently explained by the legends accompanying the figures.

All these types of cells provided together only what a single cell of type III made entirely of quartz would have given, but the technical difficulty of obtaining clear walled quartz cells forced the resort to several types of cells. These cells were all made up with tungsten filaments behind the plates to permit degassing by electronic bombardment. The alkali metals were introduced after multiple distillation, and were present in large quantities so that sufficient vapor pressure existed to cause photosensitive films to build up spontaneously in very brief periods.

The metal plates were in all cases given as high a polish as could be obtained. This was much higher in the case of the platinum plates used for

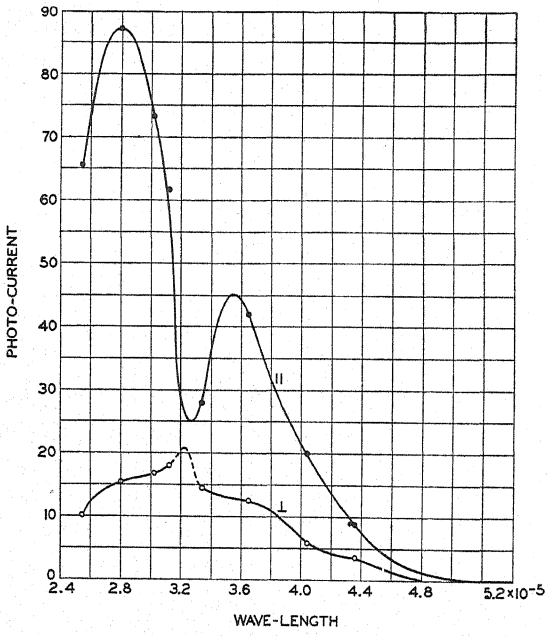


Fig. 3. Photoelectric currents per unit energy incident at 60°, plotted against wave-length, thin film of sodium or silver. Circles, electric vector perpendicular to plane of incidence; dots, electric vector parallel to plane of incidence.

reference purposes than in the case of the silver plates. Moreover the latter could not be raised to nearly as high a temperature for degassing, as could the platinum, without the surface disintegrating and becoming rough. For these reasons the results obtained with the silver plates are probably somewhat less clear-cut than would be desirable for exact quantitative check with any theory correlating photoeffect with optical properties.

Preliminary Experimental Results

In Fig. 3 are shown photoemission curves for sodium on silver, for light incident at 60°, for the $\parallel$ and $\perp$ cases; in Fig. 4 similar curves for potassium on silver, and in Fig. 5 for caesium on silver. In Fig. 4 is shown, in the dashed curve, the $\parallel$ emission from a thin film of potassium on platinum. It will be

seen at once that the films on silver exhibit a pronounced influence of the silver plate beneath. There is a deep cleft in the || curves for all cases shown.

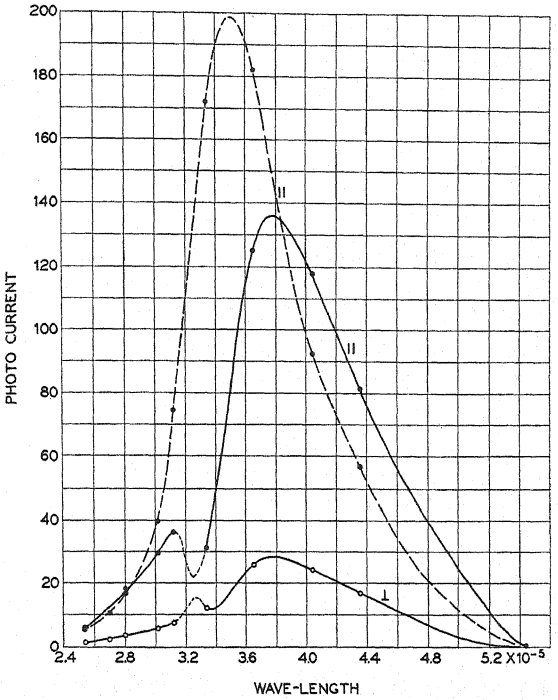


Fig. 4. Photoelectric currents per unit energy incident at 60° plotted against wave-length. Full lines, thin film of potassium on silver. Circles; electric vector perpendicular to plane of incidence; dots, electric vector parallel to plane of incidence. Dashed line, emission from thin film of potassium on platinum, electric vector parallel to plane of incidence.

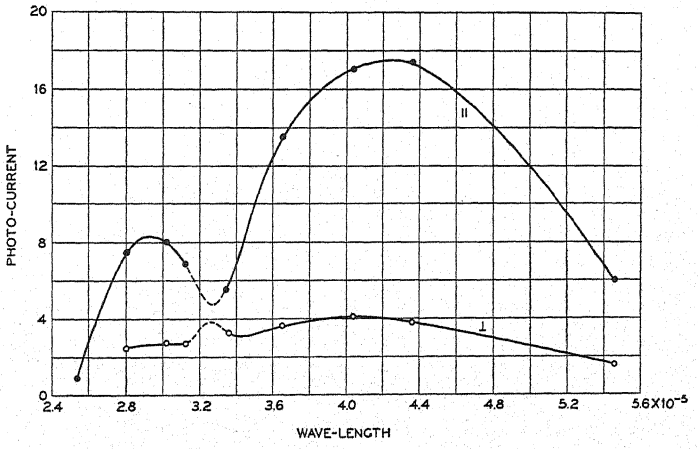


Fig. 5. Thin film of caesium on silver. Circles; electric vector perpendicular to plane of incidence dots, electric vector parallel to plane of incidence.

Comparing this cleft with the minimum of reflecting power for silver shown in Fig. 1 several questions are at once raised. First of all, the photoemission

curves show their depressions at about 3260A. while the reflection minimum is at 3160A. Second, the depression of photoemission appears to be absent for light polarized with the electric vector perpendicular to the plane of incidence. In the figures we have in fact dotted in an *increase* of emission for this case, the warrant for which we will give later.

It was immediately thought that these peculiarities might be explained when the reflecting power curves were computed for 60° incidence. This was accordingly done, using Minor's very full data[4] for the optical constants n and k, yielding the curves shown in Fig. 6, on which the computed reflecting power for perpendicular incidence is also plotted, agreeing quite well with Hagen and Rubens direct determination. It appears from these computations

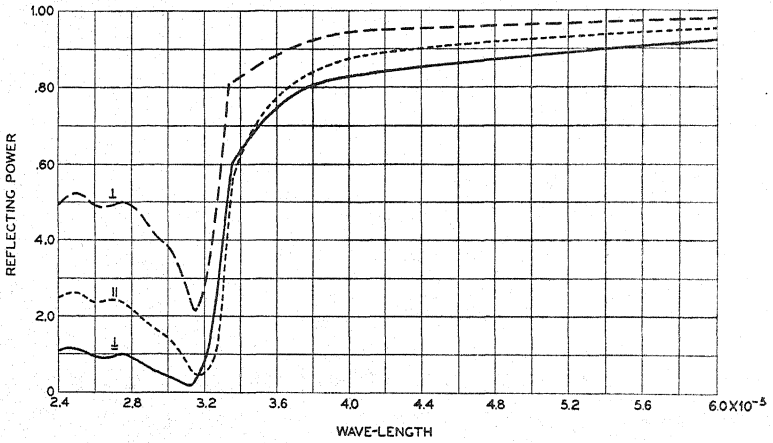


Fig. 6. Reflecting power of silver as computed from Minor's determination of optical constants. Full line; perpendicular incidence. Dotted and dashed lines, light incident at 60°; dots, electric vector parallel to plane of incidence; dashes, electric vector perpendicular to plane of incidence.

that at 60° the minimum of reflecting power is indeed shifted along the spectrum, but not nearly enough to agree in position with the photoemission minimum. Also it appears that the minimum is less for ⊥ light than for ||, but again the difference is not enough to account for the apparent absence of the ⊥ minimum found experimentally.

Theory for Trial

In order to explain our experimental results we have evolved a theory whose essential postulates are:

(a) That the photoelectrons come entirely from the thin film of alkali metal.

(b) That the effective light intensity is that at the metal-vacuum surface.

In order to test this theory it becomes necessary to determine the effective light intensity called for by (b). We are aided in this by an experimental result

[4] Minor, Ann. d. Physik **10**, 581 (1903).

previously obtained,[5] namely, that the *presence of the thin alkali metal film does not appreciably affect the condition of the light as reflected by the metal plate beneath.* In consequence of this fact, the determination of the light intensity at the metal-vacuum surface can be arrived at by computation, using the *refractive index and extinction coefficient of the metal underlying the photosensitive film.*

This theory has been discussed in some detail in a previous paper[3] where it is shown that the large differences in emission from thin films on platinum for illumination by light polarized in the two chief planes follow directly from the computed light intensities just above the platinum surface. That paper should be consulted for details of the theory and the computations.

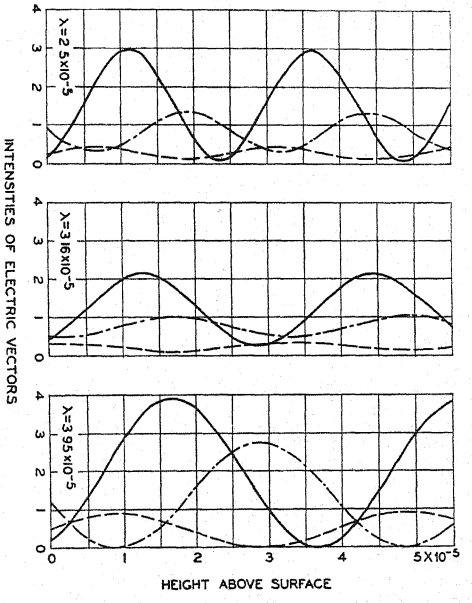


Fig. 7. Standing wave intensities above silver surface for light incident at 60°. Full line; the y component, electric vector perpendicular to plane of incidence. Dashed line, the x component; dot and dashed line, the z component, electric vector parallel to plane of incidence.

For the purposes of the present discussion the essential physical phenomenon is the formation, above the metallic reflecting surface, of an interference pattern whose phase and amplitude are dependent on the refractive index (N) and extinction coefficient (K_0) of the metal, and vary with the plane of polarization and angle of incidence.

In order to make this conception concrete, we show, in Fig. 7, the standing wave system as present over silver, for three wave-lengths in the neighborhood of its region of low reflection, as computed from the optical constants determined by Minor. In this are shown the electric intensities of the x and z components (dashed, dot-and-dashed lines) for light incident at 60°, polarized with the electric vector parallel to the plane of incidence ($\|$) and (full

[5] Ives and Johnsrud, J. Opt. Soc. **15**, 374 (1927).

lines) the y component (the only one in question) for light polarized with the electric vector perpendicular to the plane of incidence ($\perp$).

On inspecting these plots we note that while the $\perp$ standing wave system is very near a node at the metal surface for all three wave-lengths shown, the two components of the $\parallel$ standing wave system are well away from a node, except for the z component in the region of minimum reflection, which is near a node, but has considerable amplitude. On the scale of this plot the monatomic layer of alkali metal is too thin (circa 10^{-8} cm) to be indicated other than as a line coincident with the silver surface. For the purpose of the present study the intercepts of the standing wave systems, of which the three of Fig. 7 are samples, have been computed at short wave-length intervals throughout the low reflection region, and from these the electric intensities just above the silver surface have been computed for perpendicular incidence ($\perp$), and for

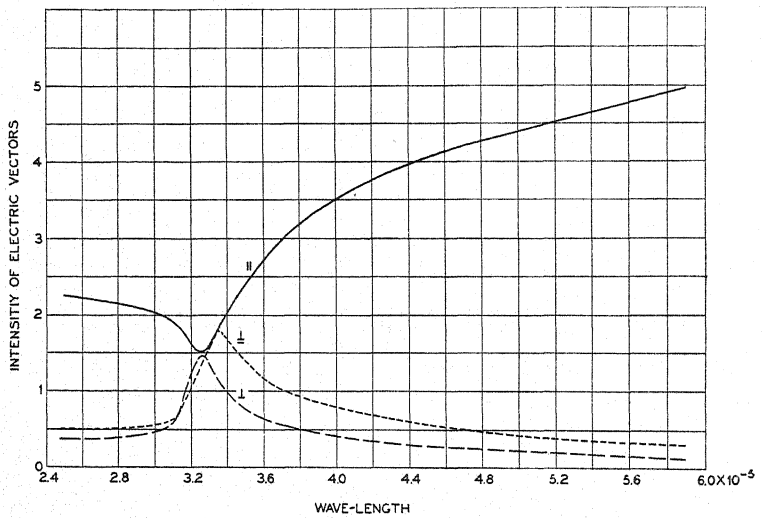


Fig. 8. Intensities of electric vectors just above silver surface, as computed from optical constants. Full line, light incident at 60°, electric vector parallel to plane of incidence. Dashed line, light incident at 60°, electric vector perpendicular to plane of incidence. Dotted line, perpendicularly incident light.

the two planes of polarization at 60° incidence, ($\parallel$ and $\perp$). These computations are potted in Fig. 8.

If now we could assume the photoemission to be proportional directly to the electric intensity in the alkali metal film, Fig. 8 gives the photoemission to be expected. We see at once that not only is the minimum of emission for the $\parallel$ case shifted by about 100 angstroms from the minimum of reflection, that is, from 3160A to 3260A, but for the $\perp$ case there should be a *maximum* of emission. Furthermore, for perpendicular incidence, in place of a strong minimum, as shown by the reflecting power, there is a very pronounced *maximum*. Considering further the variation of emission with angle of illumination, it appears that in the neighborhood of 3200A the $\perp$ angle curve should rise higher for 60° incidence than for perpendicular incidence, unlike the angle

curves ordinarily obtained from metals, which exhibit a steady decline in value toward the higher angles of incidence.

Before proceeding to describe the experimental tests of these findings it is important to recall, from the previous paper, just how far the theory, as developed, can be verified at the present time, and what limitations are imposed to its full application, principally through our ignorance of the optical constants of the alkali metals in the ultraviolet. It is important to note that the curves of Fig. 8 do not take account of the specific absorbing and emitting properties of the film. In other words, if the film absorbed energy equally well at all wave-lengths, and emitted the same photoelectric current for the same effective energy density at all wave-lengths, the emission by wave-length would be given at once by Fig. 8. Actually, however, the absorption of energy in a film is determined by the optical constants and thickness of the film;[6] and the photoemission per unit of absorbed energy is at present an unknown function of wave-length. When the optical constants of the alkali metals are completely known, the absorption of energy in a thin film will be capable of computation for all conditions of incidence and polarization of the light, all through the spectrum. It will then be possible to find the specific photoemission as a function of wave-length, and thus have all the factors necessary for the complete description of the thin film photoelectric phenomenon. At the present stage of the investigation, however, lacking the optical constants of the alkali metals, all the indication of the theory that we can expect to verify are:

(1) The occurrence of the several maxima and minima of emission shown by Fig. 8, at approximately their computed places (provided the alkali metal has no considerable singularity itself in its optical constants through this region).

(2) The shape of the $\perp$ angle curves for monochromatic light.

Experiments to Test Theory

Inspection of the curves plotted in Fig. 8 shows that *the most interesting and significant regions for testing the theory lie between the mercury arc lines which were used in the initial measurements.* What is required for an adequate test is a continuous light source of sufficient intensity to permit of accurate energy measurements at each point of interest. Such a source was not available. Instead a procedure was worked out which consists essentially in making relative photoelectric measurements by comparison with a photosensitive surface whose wave-length emission curve could be established beyond reasonable question all through the region in question. For this purpose a sodium-on-platinum cell was constructed of the type II, shown in Fig. 2b. This was measured with great care for light incident perpendicularly, using the mercury arc as a source of radiation, yielding the emission curve shown in Fig. 9 (circles). This curve shows a uniform slow rise in value through the wave-length region in which we are interested, and, since platinum has no

[6] A full treatment of the absorption of light in thin films will be given in a paper now in preparation by Mr. T. C. Fry.

singularities in its optical properties in this region, it is quite safe to interpolate the smooth curve shown between the mercury arc points. This curve constitutes our reference standard.

A second cell of the same type was then made up with a silver plate, and this was likewise filled with sodium. This alkali metal was chosen in part in order to use the same material as the reference standard, and in part because sodium is more suited to delicate measurements, due to the greater freedom of sodium cells from leakage currents. This second cell was mounted alongside the reference cell on a sliding carriage, so that they could be exposed alternately, in quick succession, to the light from the spectrometer, and the photocurrents measured. Measurements of this sort were made, using first the mercury arc, and then the tungsten ribbon lamp with a quartz window. In this way the whole region from 3200A to 4359A was covered at sufficiently small intervals to establish the perpendicular incidence emission curve with great accuracy. The curve so obtained is also shown in Fig. 9

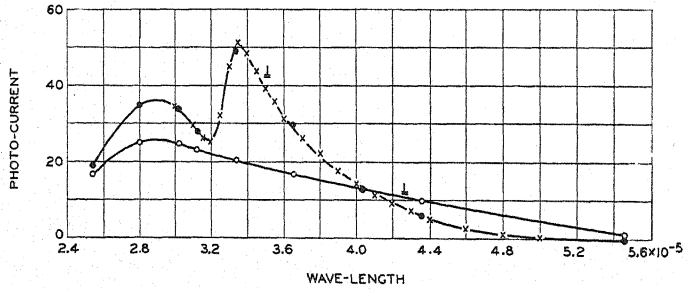


Fig. 9. Data from perpendicular incidence cells, type II. Circles, thin film of sodium on platinum, mercury arc lines. Dots, thin film of sodium on silver, mercury arc line. Crosses, points obtained by relative values of photocurrents in two cells, with tungsten ribbon source.

where the points interpolated by the use of the tungsten lamp are shown by the small crosses. It will be seen that it exhibits in striking fashion the maximum at 3350A predicted in Fig. 8.

The next step was to build up the 60° emission curves. This was done by obtaining "angle curves" for monochromatic light, using a cell of type III shown in Fig. 2c, and taking off from these angle curves the relative values for the 60° emission as compared with the 0°. Multiplying the perpendicular incidence curve of Fig. 9 by these ratios gave at once the 60° emission, the derived points being shown by the small crosses. Due to the absorption of the Pyrex glass in the angle-curve cells no measurements could be made below 3100A, but this fortunately was not an obstacle to obtaining data in just the region desired. Examples of the angle curves used for this purpose are shown in Fig. 10. Attention may be called to the dashed curve shown for 3260A, which is computed from the optical constants of silver, and agrees closely with the experimental finding, of curves rising with increasing angle of incidence.

The 60° emission curves for both planes of polarization are shown, together with the perpendicular incidence curve from which they are derived, in Fig. 11. Inspection of this figure shows that the predictions of the theory are strikingly confirmed. With light polarized with the electric vector parallel to the plane of incidence there is a *minimum* of emission at 3260A, as the curves for potassium and caesium thin films already indicated. With light polarized with the electric vector perpendicular to the plane of incidence there

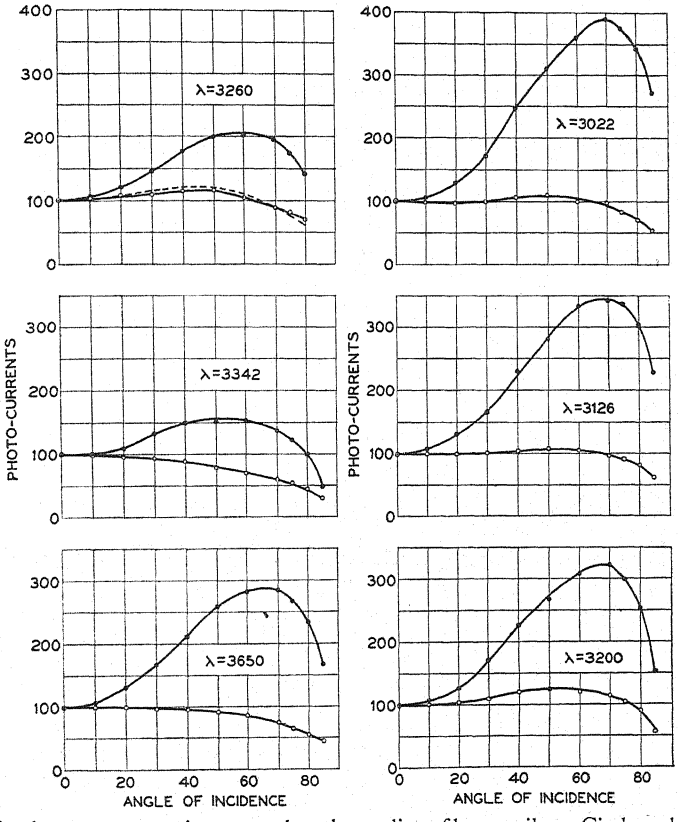


Fig. 10. Angle curves at various wave-lengths; sodium film on silver. Circles, electric vector perpendicular to plane of incidence; dots, electric vector parallel to plane of incidence. Dashed curve of 3260A, computed from optical constants of silver.

is a *maximum* of emission at the same wave-length. Around 3200A the currents for 60° angle of incidence, with the electric vector perpendicular to the plane of incidence, are greater than for perpendicular incidence.

The success of our substitution method of filling in the wave-length interval around 3200A, as just described, suggested its use with the 60° type of cell (Fig. 2a) as well to get a still further check on this important region. Accordingly a 60° cell[7] was mounted alongside the perpendicular-incidence platinum-plate cell and alternating measurements made, with both the mer-

[7] This is a different cell from that used to get the data of Fig. 3, and the actual angle was nearer 55° than 60°.

cury arc and the tungsten ribbon. The data so obtained are shown in Fig. 12, where the ∥ and ⊥ curves are for the silver plate 60° cell, and the ⊥ curves for the sodium on platinum normal incidence cell. These curves fully confirm the findings of Fig. 11, and agree well with the preliminary curve shown in

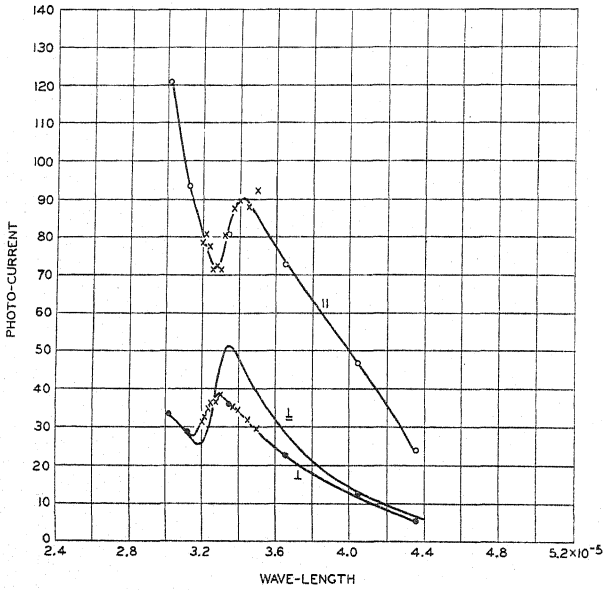


Fig. 11. Thin film of sodium on silver, photoemission at 60° and at 0° as derived from angle curves from perpendicular incidence data of Fig. 9.

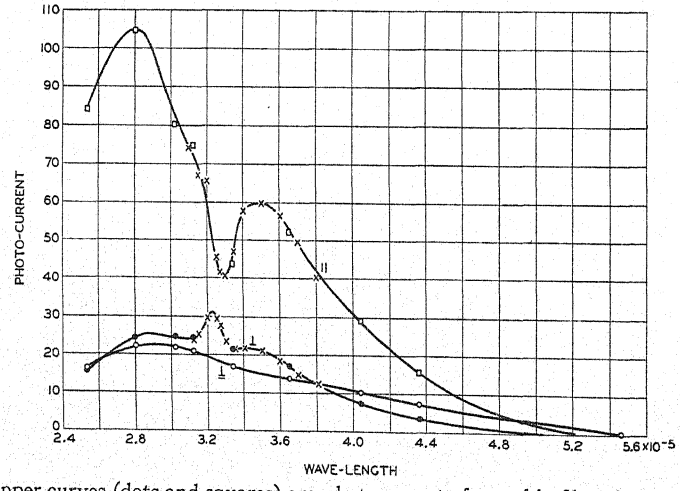


Fig. 12. Upper curves (dots and squares) are photocurrents from thin film of sodium on silver, light incident at 60°, as obtained by substitution measurements from thin film of sodium on platinum (perpendicular incidence) shown in lowest curve (circles).

Fig. 3. The agreement between the various sets of sodium data is considered excellent for this kind of work, remembering that measurements on four different sodium-on-silver cells are represented.

In the very satisfactory agreement with the essential predictions of our theory which is shown by the curves of Figures 11 and 12, for the case of light with the electric vector perpendicular to the plane of incidence, it will be noted that the peak of emission near 3260 is considerably smaller than would be expected if the values in the computed curves of Figure 8 were used as direct multiplying factors on an emission uniform or smoothly varying with wave-length. While this diminished prominence of the emission peaks may be real, and be explicable by further refinement of the theory, it is rather more likely to be due to a condition we have already pointed out, namely the lack of perfect polish of the silver surfaces, whereby some admixture of light polarized with the electric vector parallel to the plane of incidence occurs. Since excitation with this light shows a marked depression in the emission curve at this same point, a smoothing out of the peaks as found is exactly what would be expected in mixed light. In addition to this, the peaks in question are established entirely by measurements with a continuous spectrum source, for which the slits used in the spectrometer were of necessity of considerable width, which would have the effect of decreasing the measured magnitude of the peaks. In short, the agreement found with theory in the relative positions of the curves, and in the positions of their maxima and minima, can be interpreted, we believe, as a complete confirmation of the theory despite the apparent discrepancy in the magnitudes.

Discussion

The most important outcome of this study of alkali metal films on silver is the proof which it gives that the energy that must be considered in studying the photoelectric effect is not the incident, nor the absorbed energy, is ordinarily considered, but the *energy density at the surface.* While this has been demonstrated here only for the case of thin films, the fact that the photoemission from thin films is of the same order of magnitude as that from bulk alkali metals, is strong reason for believing that in the latter case the photoelectrons escaping all come from the top layer of atoms, so that the conclusion just drawn will be of general applicability. Speculations based on the positions of maxima of emission under excitation by an "equal energy" spectrum are, on this view, of little significance. Until the optical constants of the photoactive metals have been determined through the whole spectrum, and the absorptions in their surfaces computed there-from, the intrinsic emissivities cannot be considered known. The important question whether there is indeed any real difference in the emissive properties of the alkali metals with plane of polarization of the light ("normal" and "selective" effects) must be considered open until it is ascertained whether the apparent differences are not to be correlated with optical properties, along the lines here followed.

Acknowledgment

We are greatly indebted in this work to Mr. T. C. Fry for his mathematical studies of the optical properties of metals,[8] utilized extensively in the computations necessary for this paper, and to Miss C. L. Froelich for carrying through these computations.

[8] T. C. Fry, "Plane Waves of Light," J. Opt. Soc. 15, 137 (1927); 16, 1 (1928).

CONTACT POTENTIAL DIFFERENCE BETWEEN IRON AND NICKEL AND THEIR PHOTOELECTRIC WORK FUNCTIONS

By G. Norris Glasoe

University of Wisconsin

(Received September 5, 1931)

Abstract

Specimens of electrolytic iron and electrolytic nickel were outgassed by intensive heat treatment in high vacuum and the contact potential difference between them measured by the Kelvin null method. An apparatus is described by means of which the photoelectric long wave limits could be determined on the same specimens and under identical conditions as used for the contact potential measurements. The photoelectric long wave limits were determined in one case by using filters in the path of the light and in a second case by the method of plotting the photoelectric sensitivity curves obtained using monochromatic illumination of the metals. The results remained unchanged between 300 and 750 hours of heating in the first case and between 400 and 600 hours in the second. The equilibrium value of the contact potential difference was Fe-Ni$+0.21 \pm 0.01$ volt. The photoelectric long wave limits determined by the second method were 2620A $\pm$ 10A for the iron and 2500A $\pm$ 10A for the nickel. The corresponding work functions are 4.71 ± 0.02 volts for the iron and 4.93 ± 0.02 volts for the nickel. Using the method published by Fowler the work functions were 4.77 volts for the iron and 5.01 volts for the nickel. The difference in these work functions by either method is equal to the measured contact potential difference between the metals within the limits of error of the photoelectric measurements.

Introduction

A CONSIDERABLE amount of work has been done in the past few years in determining the contact potential difference existing between metals which have been more or less outgassed in high vacuum with greatly varying results. Somewhat more careful work has been done by several investigators on the determination of the photoelectric work functions for metals outgassed in the best obtainable vacua with more consistent results. On the basis of the results obtained for the contact potential difference and the difference in the photoelectric work functions for a given pair of metals the conclusion has been quite generally drawn that the Einstein photoelectric equation, giving an equality of these values, is satisfied although the agreement has never been very good. The lack of agreement has usually been attributed to the fact that conditions in the experiments on the contact potential and those on the photoelectric effect have not been the same which seems reasonable in view of the fact that both effects are very susceptible to the experimental procedure and technique. It therefore appeared desirable to perform an experiment in which both the contact potential difference and the photoelectric work functions could be obtained on the same specimens under identical conditions.

Apparatus and Procedure

The apparatus used in this work was designed so that measurements of the contact potential difference by the Kelvin null method and measurements of the photoelectric long wave limits could be made on the same specimens. The construction was of a type whereby the long wave limit determinations were made on the same surfaces as were used for the contact potential measurements. The metals used were electrolytic iron and electrolytic nickel. The construction which seemed best was such that the contact potential difference Fe-Ni was not directly measurable but was obtained from the difference of the values Pt-Fe and Pt-Ni obtained by using platinum as a reference metal.

The construction of the experimental tube and parts is shown in Fig. 1. All metal parts of the apparatus were of nickel, iron or tungsten, the nickel

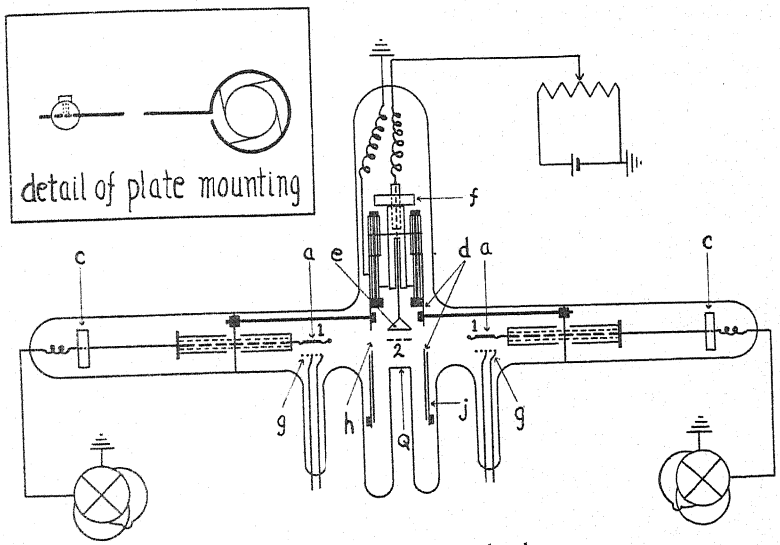


Fig. 1. The experimental tube.

being of German make, obtained from Baker and Co., free of magnesium. The electrolytic iron was obtained from Prof. O. P. Watts of the chemical engineering department of the University of Wisconsin and the electrolytic nickel from the International Nickel Co. Inc. through the courtesy of Dr. Paul D. Merica. The iron and nickel specimens were used in the form of plates (a) 1.5 cm in diameter and 0.1 mm thick. In order to minimize warping the edge of each plate was spun over perpendicular to the face. Each plate was mounted in a ring of 40 mil tungsten wire in such a way as to allow for differential expansion, as shown in the detail drawing of Fig. 1. The supporting tungsten wires were insulated from the rest of the metal parts of the apparatus by quartz tubes in which they fitted loosely enough to allow a sliding motion parallel to the length of the wire thus also serving as a mechanical bearing. These quartz tubes were held rigidly to the rest of the apparatus by small clamps and shielded from metallic vapors by sleeves in order to insure main-

taining good insulation. The movement of either plate was accomplished by means of a magnet, external to the tube, acting on an iron armature (c) fastened to the end of the tungsten wire.

All stationary parts of the apparatus were fixed rigidly to a nickel cylinder (d), 4 cm in diameter and 10 cm long, which served as an electrostatic shield during measurements. The reference plate of platinum (e) was mounted in this cylinder, insulated by Pyrex tubes, with its face perpendicular to the axis of the cylinder. This platinum plate was the movable plate necessary to the Kelvin null method of measuring contact potential difference, the movement being obtained by means of an external magnet acting on an iron armature (f). This piece of iron was threaded to the rod carrying the plate thus making the position of the plate adjustable with respect to the Fe or Ni plate for the contact potential measurement.

The Fe and Ni plates were heated in positions (1) by electron bombardment from filaments (g) of 10 mil tungsten wire wound in a spiral, with the center slightly convex toward the plate to avoid any focusing action of the filament which would result in nonuniform heating of the plate. The temperatures of the plates were very easily adjustable by this arrangement and they could be heated continuously for long periods of time. With an accelerating potential of 650 volts an electron current of 20–25 milliamperes heated the plates to a temperature at which they vaporized rapidly and the walls of the tube became covered with an opaque coating of evaporated metal in a very short time.

For a measurement of the contact potential difference Pt-Fe or Pt-Ni the Fe or Ni plate was moved through the opening (h) in the side of the nickel cylinder, into the position (2) directly in front of the Pt plate. The Fe and Ni plates were each connected to an electrometer and the Pt plate was connected to a potentiometer arrangement whereby its potential with respect to ground could be varied. The electrometer sensitivities ranged from 6000 mm/volt to 8000 mm/volt.

A photoelectric measurement was obtained by rotating the Fe or Ni plate through 180° in the position (2) thus having the same face as used for the contact potential measurement opposite a reentrant quartz window (Q) through which light from a quartz mercury arc could be focused on the plate. This quartz window and the Pt plate were protected from metallic vapors during the heating of the Fe and Ni specimens by drawing a short cylinder (j) over the openings in the large nickel cylinder thereby leaving no direct path from the hot metals to either the window or the Pt. The photoelectric currents were measured with the electrometers shunted with high resistances which gave current sensitivities of about 8×10^{-16} amp./mm.

In one run of the experiment the photoelectric long wave limits were determined by placing light filters in the path of the light from the arc to the plate. These filters were made by placing solutions of various concentrations in a cell 2 cm long having fluorite windows, the concentration being varied by small amounts until no measurable photoelectric current was obtained. Immediately after each trial on the photoelectric effect the light transmitted

by the filter was photographed by placing the cell between a quartz mercury arc and the slit of a quartz prism spectrograph. In order to check the results obtained by this method it was decided to use a monochromator instead of the filters and to plot the usual photoelectric sensitivity curves of the photoelectric current per unit of incident light intensity against the wave-length of the incident light and perform the extrapolation to zero current to determine the long wave limit. A second complete run of the experiment was thus made with a double monochromator formed by passing the light first through a Leiss single monochromator and then through a Hilger single monochromator. Using 0.6 mm slits this arrangement was found to give much greater intensity and purity of the light than could be obtained with 0.2 mm slits with either of the single monochromators alone. The intensity of the light was measured with a three junction Pt-Te vacuum thermopile designed according to the equations given by Firestone[1] and Cartwright.[2] The thermopile was mounted in front of the exit slit of the Hilger monochromator so that it could be moved in or out of the light path.

Before starting either run the metal parts of the apparatus were all baked out in an auxiliary system for several days at about 450°C before being assembled in the main experimental tube. The large nickel cylinder was put in a separate tube and heated by electron bombardment to 950°C for the same length of time. The parts were exposed to air for about a day while they were being put together and the main tube was being set up. The tube was connected, through two liquid-air cooled mercury vapor traps, to a mercury vapor pump backed by a Cenco rotary oil pump. All glass of the vacuum system was Pyrex so as to eliminate all necessity of wax joints, the one stopcock used being in the lead from the oil pump to the vapor pump. The apparatus was baked out at a temperature of 450°C–500°C for some 150 hours at the start of each run with the Fe and Ni plates being heated to about 850°C during most of this time. After baking out, the pressure in the system as indicated by an ionization gauge was of the order of 2×10^{-8} mm of mercury with the plates cold. The pressure increased to about 10^{-7} mm of mercury during the heating of the plates at first but with progressive heating the pressure with the plates hot or cold became very nearly the same and of the order of 1×10^{-8} mm of mercury.

Results

In the first run of the experiment the results obtained after the Fe and Ni had been heated for 300 hours were the same as those obtained after some 750 hours of heating. The plates were heated at an estimated temperature of 900°C a first and then the temperature of the Fe was raised to about 950°C and that of the Ni to about 1100°C. This increase in the temperature of heating resulted in no observable change in either the contact potential difference or in the photoelectric measurements for either specimen. The equilibrium value of the contact potential difference was Fe-Ni$+0.20\pm0.01$

[1] Firestone, Rev. Sci. Inst. **1**, 630 (1930).
[2] Cartwright, Rev. Sci. Inst. **1**, 592 (1930).

volt. The results obtained in the photoelectric measurements, using the light filters mentioned above, placed the long wave limit for the Fe at about 2650A and that for the Ni at or very near to 2537A. These wave-lengths expressed in equivalent volts give a work function of 4.65 volts for the Fe and 4.86 volts for the Ni. The difference in these work functions is 0.21 volt in the sense that the Fe is positive with respect to the Ni.

The only change made in the apparatus before starting the second run was the replacement of the original Fe plate, which had become badly warped due to the heating, by a new plate cut from the same piece of metal as the

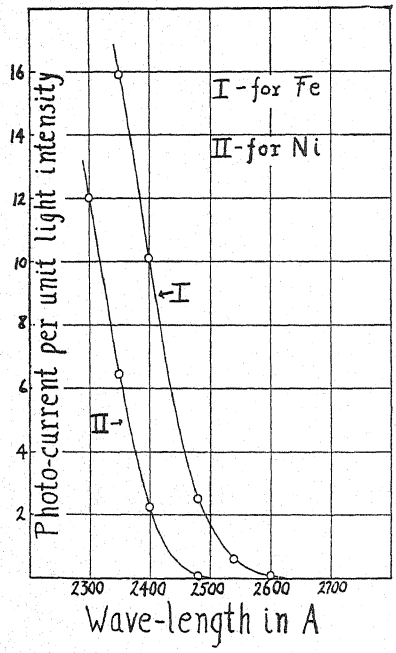


Fig. 2. Photoelectric sensitivity curves for iron and nickel.

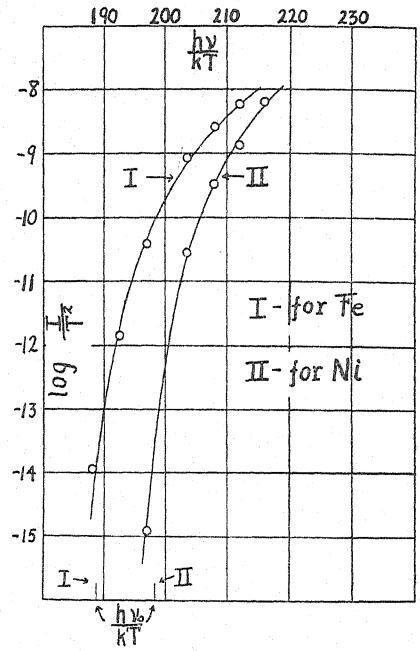


Fig. 3. Determination of threshold frequencies of iron and nickel from Fowler's theory.

original. The results obtained in this run after some 400 hours of heating were not changed by an additional 200 hours during which the temperatures of the plates were increased several times. As in the first run an accurate determination of the temperatures was not possible but some idea may be obtained by the fact that both the Fe and Ni vaporized readily enough so that at the end of the 600 hours of heating the walls of the tube in the vicinity of the plates were coated with a fairly thick metallic deposit. This deposit was opaque after about 200 hours of heating which was long before the highest temperature was reached and the last readings taken. The pressure as measured with the ionization gauge was of the order of 1×10^{-8} mm of mercury with the plates hot or cold after about 400 hours of heating.

The average value of the contact potential difference obtained after 400 hours of heating and up to 600 hours was Fe-Ni$+0.21\pm0.01$ volt, the ±0.01

volt being the spread of the measured values from the average. A typical set of the photoelectric sensitivity curves obtained for the two specimens is reproduced in Fig. 2, in which the curve for the Fe has been extrapolated to zero current at 2620A and that for the Ni to 2500A. The estimated variation of the position of this intercept is placed at ± 10A due to the fact that the one point on each curve comes so very close to the zero axis of photoelectric current. With increasing time of heating of the metals a number of such curves were obtained with the result that by this method the long wave limit for the Fe is placed at $2620\text{A} \pm 10\text{A}$ and that for the Ni at $2500\text{A} \pm 10\text{A}$. These wave-lengths expressed in equivalent volts give a work function of 4.71 ± 0.02 volts for the Fe and 4.93 ± 0.02 volts for the Ni. The difference in these work functions is 0.22 ± 0.04 volt in the sense that the Fe is positive with respect to the Ni.

The difference in the long wave limits obtained in the two separate runs may be reasonably explained by a consideration of the method of using light filters. Solution filters do not cut off the light sharply at any given wave-length but rather have a gradual cut-off on the short wave-length side. It is quite possible, therefore, that the light which was recorded photographically was accompanied by light of shorter wave-length which would be photoelectrically active but not of great enough intensity to be evidenced on the photographic plate. No significance is given to these differences as they seem well within the limits of error of the filter method.

The photoelectric work function found for iron in this work is in good agreement with that reported by Cardwell,[3] his value being 4.72 ± 0.07 volts. The iron specimens in the two cases were taken from the same piece of electrolytic metal. Roy[4] and Welch[5] give work functions for iron of 4.2 volts and 3.91 volts respectively but as stated by Cardwell such values are obtained in the early stages of a long outgassing process and can not be said to be characteristic of the well outgassed metal. Values of the work function for Ni given by Roy,[4] 4.12 volts, Welch,[5] 4.06 volts, and by Lukirsky and Prilezaev,[6] 3.67 volts, are all smaller than that obtained in this work and from a consideration of the experiments it may reasonably be said that they belong to the metal in the early stages of outgassing.

Fowler[7] has recently published a theoretical discussion of the manner in which the photoelectric sensitivity curves for a metal might be expected to behave with different temperatures of the specimen. According to Fowler the curve obtained by plotting $\log f(\mu)$ against μ [$f(\mu)$ being given by equation (9) of his paper and $\mu = (h\nu - \chi)/kT$, χ being the work function of the metal at $0°K$] should coincide with the experimental values of $h\nu/kT$ plotted to the same scale against $\log I/T^2$ if the origin of the theoretical curve is properly displaced. The amount of this shift along the $h\nu/kT$ axis gives the

[3] Cardwell, Proc. Nat. Acd. Sci. **14**, 439 (1928).
[4] Roy, Proc. Roy. Soc. London. **A112**, 599 (1926).
[5] Welch, Phy. Rev. **32**, 657 (1928).
[6] Lukirsky and Prilezaev, Zeits. f. Physik **49**, 236 (1928).
[7] Fowler, Phy. Rev. **38**, 45 (1931).

value for which $(h\nu-\chi)/kT=0$ and thus the value of $h\nu_0/kT$ since $\nu_0=\chi/h$. The data obtained in this experiment as given in the above photoelectric sensitivity curves were plotted according to this theory and a typical set of such points for the Fe and Ni specimens is reproduced in Fig. 3. The curve drawn through the points is the theoretical curve shifted by the amounts indicated at the bottom of the diagram. The values of these shifts, in units of $h\nu/kT$, obtained from a number of such plots ranged from 188 to 189 for the Fe and from 198 to 199.5 for the Ni. As all of the measurements were made at room temperature T was taken as 293° in the calculation of χ. The average values of χ expressed in equivalent volts gave a work function of 4.77 volts for the Fe and 5.01 volts for the Ni. The difference in these work functions is 0.24 volt with the Fe positive with respect to the Ni. This difference is slightly greater than that obtained in the other manner and also greater than the measured contact potential difference but it is doubtful whether much significance can be attached to this fact in as much as the variation lies within the limits of error of the photoelectric measurements and the theoretical curve is a first approximation to the theoretical equations.

Conclusion

The contact potential difference between specimens of iron and nickel after prolonged high temperature heating in a vacuum of the order of 1×10^{-8} mm of mercury is found to be Fe-Ni$+0.21\pm0.01$ volt. The photoelectric work functions of the same specimens determined by the method of plotting the photoelectric sensitivity curves are found to be 4.71 ± 0.02 volts for the iron and 4.93 ± 0.02 volts for the Ni. Using the method worked out by Fowler[7] the work functions are 4.77 volts for the iron and 5.01 volts for the Ni. Within the limits of error of the photoelectric measurements the difference in the photoelectric work functions may be said to be equal to the measured contact potential difference for metals subjected to an extensive outgassing program in high vacuum.

In conclusion, the author wishes to acknowledge his indebtedness to Dr. C. E. Mendenhall under whose direction this work was carried on and to the many members of the Physics department of the University of Wisconsin for their helpful cooperation during the progress of the work.

THE EQUILIBRIUM DISTRIBUTION OF POTENTIAL AND OF ELECTRONS OUTSIDE THE SURFACE OF A CONDUCTOR

By A. T. Waterman
Sloane Physics Laboratory, Yale University

(Received August 24, 1931)

Abstract

The potential distribution due to space charge in the neighborhood of a plane conducting surface is derived for the case of equilibrium under zero applied field and under retarding fields, by use of Poisson's equation and the Boltzmann distribution law, which is extended to include application to the Fermi-Dirac statistics. The electron density is likewise evaluated as a function of the distance from the surface. In both cases an applied electric field has no appreciable effect within a certain critical distance which is dependent upon the field. Assuming degeneracy within the conductor the electron atmosphere is also degenerate near the surface, becoming entirely classical at distances greater than 2 or 3×10^{-7} cm. Its density is independent of the nature of the conductor and at a given distance is directly proportional to the absolute temperature. The potential at a given distance is characteristic of the conductor and varies only slightly with temperature, while its magnitude is consistent with the Sommerfeld electron theory. The field intensity equals that computed from an image force law at distances in the neighborhood of 3×10^{-7} cm, depending upon temperature, and is increasingly greater than the latter at greater distances. The mean electron separation distance in a plane parallel to the surface is comparable with the distance of this plane from the surface.

IN A recent paper[1] R. S. Bartlett and the author pointed out that the conception of electrons within a conductor as a degenerate gas obeying the Fermi-Dirac statistics reopens the matter of the effect of space charge upon the thermionic work function. The general consequences were mentioned of an explanation of the work function based entirely upon space charge instead of the usual image force, and in a later paper Bartlett[2] has on this basis computed the potential distribution and the thermionic current density between plane parallel electrodes for the case of an applied field and for accelerating fields. The results show a work function of the correct order of magnitude and a variation of current with applied field of the correct general form, thus indicating that a space charge origin of the work function may be used to explain the Schottky effect. It is noteworthy that Bartlett is able from this point of view to derive a single curve for the thermionic current which is valid continuously from zero applied field through strong applied fields, and which therefore includes both the familiar Child's equation and the Schottky equation under one explanation.

It is the purpose of this paper to examine the equilibrium distribution of potential and electron concentration outside the surface of a plane elec-

[1] R. S. Bartlett and A. T. Waterman, Phys. Rev. 37, 279 (1931).
[2] R. S. Bartlett, Phys. Rev. 37, 959 (1931).

trode in the presence of retarding electric fields (including zero field). This is accomplished by solving Poisson's equation in conjunction with the Boltzmann distribution law (generalized to apply to the Fermi-Dirac statistics) after the manner in which this was done for the purely classical case by Langmuir.[3] The generalized distribution law referred to is

$$A = A_0 e^{-(V-V_0)\epsilon/kT} \tag{1}$$[4]

where A and A_0 are the Fermi A's[5] corresponding to two small regions about points P and P_0 in the electron gas where the potentials are V and V_0 respectively. In the present case P_0, A_0 and V_0 will refer to the interior of the conductor. A deviation of Eq. (1) follows from equality (in equilibrium) of the number of electrons per unit area per second proceeding from P_0 to P against the potential difference $V-V_0$, and of the electron current density leaving P in the opposite direction. Thus, taking u as the velocity component in the direction P_0P, the number of electrons reaching P per unit area per second, calculated in the usual kinetic theory manner, is

$$\nu_1 = \frac{\pi G}{a}\left(\frac{m}{h}\right)^3 \int_{u'}^{\infty} u(\log A_0 e^{-au^2} + 1)du$$

where $a = m/2kT$, $A_0 =$ Fermi A at P_0, $\frac{1}{2}mu'^2 = (V-V_0)\epsilon$, or

$$\nu_1 = \frac{\pi G}{2a^2}\left(\frac{m}{h}\right)^3 \int_0^{e^{-au'^2}} \frac{\log (A_0 y + 1)}{y}\, dy. \tag{2}$$

The number of electrons about P striking unit area per second is the similar expression integrated from 0 to ∞, or

$$\nu_2 = \frac{\pi G}{2a^2}\left(\frac{m}{h}\right)^3 \int_0^1 \frac{\log (Ay + 1)dy}{y} \tag{3}$$

where A refers to the region about P. Both (2) and (3) are valid whether the gas is classical or degenerate.

For equilibrium, $\nu_1 = \nu_2$ and

$$\int_0^{e^{-au'^2}} \frac{\log (A_0 y + 1)dy}{y} = \int_0^1 \frac{\log (Ay + 1)dy}{y}$$

If

$$f(A, y) = \int \frac{\log (Ay + 1)dy}{y},$$

this condition is satisfied when

$$f(A_0, e^{-au'^2}) = f(A, 1). \tag{4}$$

[3] Langmuir, Phys. Rev. **21**, 419 (1923).

[4] Cf. Waterman, Phys. Rev. **35**, 668 (1930); Bartlett: reference 2, p. 963.

[5] Defined by

$$n = \frac{2\pi G(2mkT)^{3/2}}{h^3} \int_0^{\infty} \frac{u^{1/2}du}{\frac{1}{A}e^u + 1}$$

$f(A, y)$ may be evaluated by series expansions both for $Ay<1$ and for $Ay>1$, when it is seen that (4) is satisfied in both cases, term for term, provided $A = A_0 e^{-au'^2} = A_0 e^{-(V-V_0)\epsilon/kT}$.

For both A and A_0 classical ($A = [nh^3/G(2\pi mkT)^{3/2}]$, n being the electron concentration), Eq. (1) becomes the familiar Boltzmann equation:

$$n = n_0 e^{-(V-V_0)\epsilon/kT}. \tag{1a}$$

For both A and A_0 degenerate ($\log A = \zeta/kT$, ζ being the thermodynamic potential):

$$\zeta = \zeta_0 - (V - V_0)\epsilon. \tag{1b}$$

For A classical and A_0 degenerate:

$$n = \frac{G(2\pi mkT)^{3/2}}{h^3} e^{\zeta_0 - (V-V_0)\epsilon/kT}. \tag{1c}$$

It may be noted in passing that Eq. (1) finds several labor-saving applications. Just as, in the form (1a) it has commonly been used to derive the thermionic saturation current density resulting in the $T^{1/2}$ equation, similarly in the form (1c) it results in the Sommerfeld T^2 law. In the form (1b) it gives directly the Volta P.D. between two metals or, as Becker has aptly named this quantity to distinguish it from the contact P.D., the junction P.D.

Potential Distribution

We proceed to the derivation of the equilibrium conditions in the neighborhood ($x>0$) of a metal whose surface lies in the plane $x=0$, in the presence of a uniform electric field in the x-direction which retards electron emission. Assuming the electron gas degenerate within the metals, then for points far enough from the surface so that the gas is effectively in the classical state, Eq. (1c) applies, whence by use of Poisson's equation,

$$\frac{d^2V}{dx^2} = \frac{4\pi G\epsilon(2\pi mkT)^{3/2}}{h^3} e^{\zeta_0 + (V-V_0)\epsilon/kT} \tag{5}$$

where $\epsilon = |\epsilon|$, the charge on an electron.

Performing the first integration subject to the boundary condition that at $x=\infty$, $V=-\infty$, $dV/dx = E$:

$$\left(\frac{dV}{dx}\right)^2 = \beta^2 e^{(V-V_0)\epsilon/kT} + E^2 \tag{6}$$

$$\text{where} \quad \beta^2 = \frac{8\pi G\epsilon(2\pi m)^{3/2}(kT)^{5/2}}{h^3} e^{\zeta_0/kT}. \tag{6}$$

The general solution of Eq. (6), subject to the boundary condition that at $x=0$, $V=V_0$,[6] is

[6] Strictly speaking on account of the penetration of surface, $x=0$ must be a plane a short distance within the conductor, if V_0 is to mean the normal intrinsic potential of the metal. The distance involved is of the order of atomic dimensions (cf. Waterman: Proc. Roy. Soc. **A121**, 28 (1928).

$$x = \frac{kT}{\epsilon E}\left(\log \frac{(y^2+\alpha^2)^{1/2}+\alpha}{(y^2+\alpha^2)^{1/2}-\alpha} - \log \frac{(1+\alpha^2)^{1/2}+\alpha}{(1+\alpha^2)^{1/2}-\alpha}\right)$$

where $\alpha = E/\beta$, $\log y = (V - V_0)\epsilon/kT$,
or

$$x = \frac{kT}{\epsilon E}[\log (1 + 2z^2 + 2z(1+z^2)^{1/2}) - \log (1 + 2\alpha^2 + 2\alpha(1+\alpha^2)^{1/2})] \quad (7)$$

where $z = \alpha/y$.

Since, assuming one electron per atom in the conductor, β is of order of magnitude 10^{10} or more for thermionic emitters, $\alpha \ll 1$ for all practicable applied fields, and the second logarithm in Eq. (7) may be expanded in powers of α. Similarly the first logarithm may be expanded in powers of z or of $1/z$, depending upon whether $\alpha <$ or $> y$. We have therefore as approximate solutions in a more usable form:

For

$$|V - V_0| > \frac{kT}{\epsilon} \log \frac{E}{\beta}, \quad (z > \alpha):$$

$$V - V_0 = -\frac{2kT}{\epsilon} \log \frac{\epsilon\beta}{2kT} x \quad (8)$$

for

$$\frac{\epsilon\beta}{2kT} x \gg 1$$

i.e. $x > 10^{-10}$ cm approx.

For

$$|V - V_0| < \frac{kT}{\epsilon} \log \frac{E}{\beta}, \quad (z < \alpha):$$

$$V - V_0 = -Ex + \frac{kT}{\epsilon} \log \frac{4E^2}{\beta^2}. \quad (9)$$

Thus in the region covered by Eq. (8) the applied field does not affect the potential distribution, while in the region where Eq. (9) is valid space charge effects are absent. The boundary between the two is quite narrow in range, and the critical distance from the surface is

$$x' = \frac{kT}{\epsilon E} \log (3 + 2(2)^{1/2}) = 1.52 \times 10^{-4} T/E \text{ cm } (E \text{ in } v/cm, T \text{ in } °K),$$

the distance at which

$$z = \alpha, \text{ or } |V - V_0| = kT/\epsilon \log E/\beta.$$

Fig. 1 shows the potential difference $(V_0 - V)$ between the interior of the metal and external points as a function of the distance x, for the case of tungsten at 2300°K. The solid line represents the case of no applied field, and agrees with that of Bartlett[7] derived in a different manner. The

[7] Bartlett, reference 2, Fig. 3.

broken lines show the effect of various applied fields, from 3v/cm to 3×10^7 v/cm. The main curve is not carried closer to the surface than about 3×10^{-7} cm, for within this region the electron gas begins to be degenerate and the premise of this calculation (Eq. 1c) is not applicable. It will be noted that at ordinary electrode distances the potential difference between interior and exterior is of an order of magnitude in agreement with the work function on the Sommerfeld theory. It is of interest further to remark that retarding fields of cold extraction magnitude affect the potential distribution at points so close to the surface that the electron gas becomes degenerate. If accelerating fields do likewise the conjecture may be ventured that herein lies a form of physical explanation for the slightness of temperature effect on cold extraction currents.

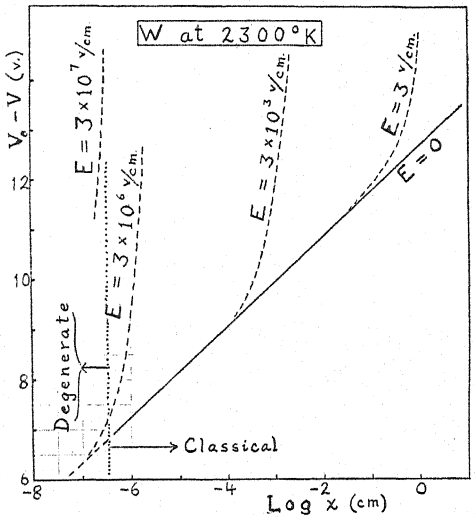


Fig. 1. Potential difference between conductor and points at distance x from surface.

Distribution of Electrons

The equilibrium distribution of electrons corresponding to this potential distribution, found by Eq. (1), is then given by

$$n = \frac{kT}{2\pi\epsilon^2 x^2}, \quad x \gg \frac{2kT}{\epsilon\beta} (\sim 10^{-10} \text{ cm}) \tag{10}$$

for zero applied field and for $x < x'$ for retarding fields.

For $x > x'$:

$$n = \frac{E^2}{2\pi kT} \cdot e^{-\epsilon E/kTx}. \tag{11}$$

It is seen that *the concentration of electrons at external points is independent of the nature of the emitting body*, and depends only upon the temperature, the distance from the surface, and the applied retarding field where effective,

i.e. outside the critical distance x'. This agrees with the result reached by Langmuir[8] for the completely classical case in the absence of applied field. Fig. 2 shows graphically the relation between n and x, covered by Eq. (9) and (10), the solid and broken lines having the same significance as before. The effect of an applied retarding field is to cut off the electron atmosphere quite sharply at the critical distance x', whereas inside the critical distance the density is not appreciably affected. For very high fields such as 10^6 v/cm, the electron atmosphere is effectively reduced to a layer about 10^{-6} cm in thickness within which the state is increasingly degenerate. Again attention may be called to the point that retarding fields of cold emission strength control the electron density down into the degenerate region.

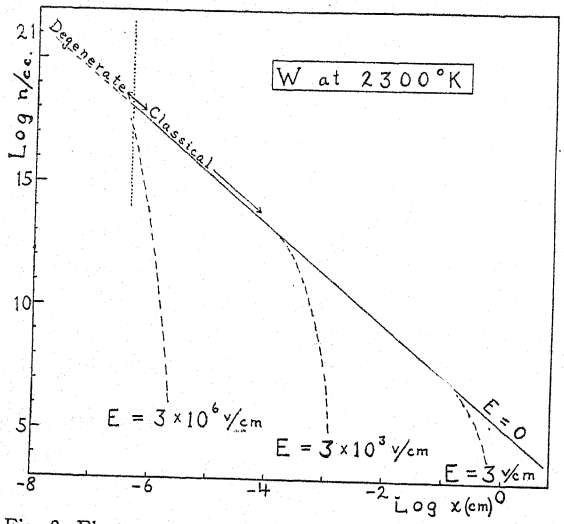


Fig. 2. Electron concentration vs. distance from surface.

The fact that the electron concentration is independent of the metal does not mean necessarily that according to this hypothesis all metals should yield the same thermionic currents in the absence of an applied field as the experiment would usually be performed. If the concentration given by Eq. (10) is used to derive the thermionic current density under these conditions, we have $I=(m/\epsilon)(kT/2\pi m)^{3/2}\ 1/x^2$. This would be the current density due to electrons striking an electrode at the distance x, assuming the current so small that equilibrium is maintained and assuming that the collecting electrode in no way affects the electron density or the potential distribution which would exist in its absence. At first sight it might appear that a suitable potential for this electrode could be computed by Eq. (7). Thus at a point 1 cm distant from a plane tungsten cathode at 2300°K the calculated potential is 12.7 v. with respect to the cathode. It does not follow directly however that the collecting anode will serve its purpose if set at this potential, since the anode, even though cold, has its own electron atmosphere and con-

[8] Langmuir, reference 3.

trols the potential in its neighborhood in a manner similar to the cathode. Clearly also any attempt to set the anode negative with respect to the cathode would put its own electron atmosphere under an accelerating field. It follows that, for a complete solution of the problem of thermionic currents between plane parallel electrodes from the present point of view, the electron atmosphere surrounding *both* electrodes should be taken into account, the one being subject to an accelerating field, the other to a retarding field.

A point of interest is that in equilibrium the electron concentration at any given distance from the surface is not so pronounced a function of temperature as one would judge from thermionic emission, since it is only directly proportional to the absolute temperature. Thus, on the hypothesis presented, a metal at room temperature should have an electron atmosphere whose density is of the order of one fifth to one seventh that at the same distance from the metal at thermionic temperatures. Over the same temperature range the equilibrium potential distribution is affected to a much less degree, by a factor of one-half to two-thirds at a distance of 1 cm, and and about five-sixths at 10^{-6} cm.

Although at the same temperature the electron density at a given distance from any plane metal surface should be the same (in equilibrium) in the absence of applied field, the potential should depend upon the nature of the metal. In fact the potentials at equal distances from two different metals at the same temperature should bear the ratio:

$$\frac{V_1}{V_2} = \frac{\log \beta_1}{\log \beta_2}.$$

If degeneracy is assumed within the metal $V_1/V_2 \sim \zeta_1/\zeta_2$ to a high degree of approximation and hence this ratio may differ from unity by a factor of two in extreme cases ($\zeta = (3n/4\pi G)^{2/3}h^2/2m$). Herein lies a possibility of a direct test as to the state of the electron gas within a metal, since if a classical state is assumed $\beta^2 = 8\pi n_0 kT$ where n_0 = electron concentration within the metal. Then, assuming the (classical) electron gas density within a metal proportional to the number of atoms *per cc.* V_1/V_2 would never differ from unity by more than about 5 percent. It may be possible to make this test by comparing the potentials required to produce equal currents from two different metals under otherwise identical conditions.[9]

The field intensity at external points in the absence of applied field, or within the critical distance x' with a retarding field is

$$\frac{dV}{dx} = -\frac{2kT}{\epsilon x} \tag{12}$$

The image force law gives an intensity $-\epsilon/4x^2$, and the ratio of the space charge intensity to the image force intensity is therefore $(dV/dx)_s : (dV/dx)_i = 8kTx/\epsilon^2$. At 300°K this ratio is $1.4\times10^6 x$; at 2300°K, $1.1\times10^7 x$. The two intensities are equal at $x = 7\times10^{-7}$ cm (300°K) and at $x = 9\times10^{-8}$ cm

[9] Cf. Bartlett and Waterman, reference 1.

(2300°K). Outside this distance the intensity reckoned on the space charge basis is greater than that due to the image force, increasingly so as the distance increases. Thus the former is 10^3 times the latter at a distance of 10^{-4} cm. Partial quantitative support for this conclusion is seen in experimental determinations by several investigators[10] of the field intensity close to a metal surface. In the most recent work Lawrence and Linford find the field intensity quite close to the surface (between 10^{-7} and 10^{-6} cm) to agree with the image force value, whereas at greater distances the intensity is consistently greater than that computed from the image force. This would be in general agreement with the present calculations.

Electron Separation Distance

Taking the mean distance between adjacent electrons as $n^{-1/3}$ this distance d compares with the distance x from the surface as follows:

$$\frac{d^3}{x^2} = \frac{2\pi\epsilon^2}{kT} = 4.5 \times 10^{-6} \text{ at } 2300°K.$$

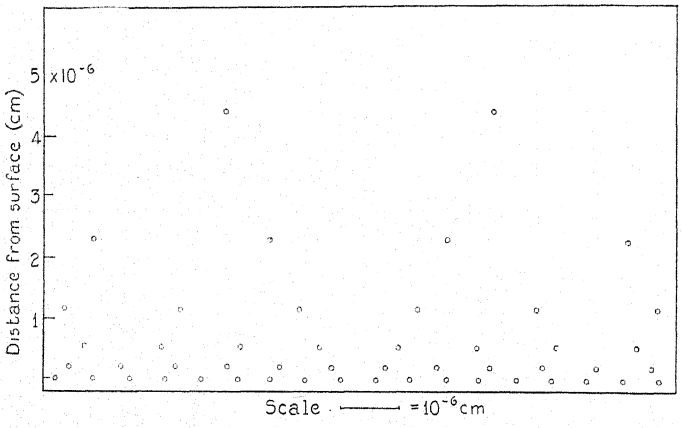


Fig. 3. Approximate indication of mean electron spacing.

Thus at 2300°K an electron 4.5×10^{-6} cm from the surface is at the same average distance from its neighbors. Closer to the surface it is farther from its neighbors than it is from the surface, and outside this distance the reverse is true. This calculation gives of course roughly the mean distance between electrons in a plane parallel to the surface and not in a direction perpendicular to this. Except at the closest distances an electron will always have a fairly dense atmosphere between it and the atoms of the metal. This is illustrated crudely by Fig. 3 where a rough picture is sketched in two dimensions to show the distribution of electrons between the surface and two electrons at the above distance of 4.5×10^{-6} cm. In this figure the horizontal distance between electrons has been computed from the above equa-

[10] Becker and Mueller, Phys. Rev. **31**, 431 (1928); Reynolds, Phys. Rev. **35**, 158 (1930); Lawrence and Linford, Phys. Rev. **36**, 482 (1930).

tion and the electrons are simply spaced symmetrically about a central vertical line. The range shown is that in which the image force action is utilized to explain the Schottky effect. The figure is illuminating in showing why according to the space charge analysis an image law may be used as an approximation *provided most electrons have been removed beyond a certain distance from the surface* (thus presumably for strong fields), though the plane to be used for image calculation would appear not to coincide with the surface atomic layer.

Space Charge vs. Image Force

The validity of space charge effects in the cases here treated (zero or retarding fields) is of course well known. The present analysis however brings out the fact that an applied retarding field has no appreciable influence on the potential or the electron density within a certain critical distance from the surface in question. This likewise appears to be not far from the truth for accelerating fields from Bartlett's calculations. That being the case a comparison of image force deductions with those of space charge inside this critical distance seems to be legitimate and desirable. When this is done the following conclusions may be drawn:

(1) The electric intensity due to space charge exceeds the image intensity at all distances from the surface beyond points so close that the surface structure should begin to play a part, where the two are equal. Experimental evidence on this point agrees better with the space charge intensity.

(2) The mean distance between adjacent electrons in a plane parallel to the surface is of the same order of magnitude as their distance from the surface, as calculated from space charge considerations. At the same time the calculation indicates the justification of an image force as an approximation, in the presence of strong fields.

Similar calculations based on the image law alone show it to be self-consistent, i.e. the mean distance between adjacent electrons is very much greater than the distance from the surface.

(3) The order of magnitude of the potential difference between the interior of the conductor and external points, as computed from space charge, is in agreement with the requirements of the Sommerfeld electron theory, thus giving directly the possibility of a work function of the correct magnitude. The value of the work function so obtained would depend upon the concentration of electrons available for thermionic emission ("thermelectrons"?) within the conductor, thus relating the work function with the thermodynamic potential.

The image force calculation of the work function can also be made consistent with the Sommerfeld theory by reducing (approximately by a factor of two) the distance from the surface at which the image law ceases.

The author is indebted to Professor R. S. Bartlett for many stimulating discussions, whose space charge analysis under accelerating fields was responsible for the present paper.

THE ELECTROOPTICAL SHUTTER—ITS THEORY AND TECHNIQUE

By Frank G. Dunnington
University of California

(Received August 25, 1931)

Abstract

This paper records a development in the design of the single cell type of electro-optical shutter together with a theory describing its action. Part I. gives a description of the shutter together with a method of observing simultaneously two stages of the phenomenon being studied. Part II gives the theory of shutter action. A condensed summary of the physical optics is followed by a development of the electric circuit theory which gives the manner of closing of the shutter when the leads to it are fairly short. The theory is illustrated by a series of numerical examples based on typical experimental conditions which show the effect of varying each controlling factor. The times required for closing (90 to 100 percent transmission) are of the order of 4×10^{-9} sec. under favorable conditions. The necessity for a Kerr cell of small electrostatic capacity is shown. Part III gives three groups of experimental data which were obtained with the shutter in a study of *spark breakdown:* one indicates the time resolution attainable; another gives the total time lag in closing; and a third gives the change in this lag with certain conditions. The information of the second group combined with the theory yields the rate of fall of voltage across the controlling spark gap (static breakdown), a typical value being 14×10^{-9} sec. to fall to 20 percent of the initial value (76 cm Hg, 5 mm gap). The theory and experimental data are found in complete agreement. An improved method is given for the determination of the correct damping resistance in the shutter circuit. Part IV gives a description and the factors considered in the design of the Kerr cells developed in the present study, also the essentials of the technique for their proper use.

Introduction

THIS paper is concerned with the Abraham and Lemoine type of electro-optical shutter, a single cell, "open-to-closed" type of shutter. The two cell, "closed-to-open-to-closed" type of shutter developed by Beams[1] will not be treated here. The principle of the Abraham and Lemoine electrooptical shutter has been known for some thirty years,[2] and use has been made of it by various experimenters when a device was needed to analyze the light of a rapidly varying phenomenon.[3,4,5,6] Thus it has been used to measure the time lag of fluorescence, the difference in times of appearence of the spectrum lines in a spark discharge and for a study of the early stages of spark discharges. The validity of the results obtained with it have been somewhat

[1] Beams, J.O.S.A. **5**, 597 (1926).
[2] Abrahan and Lemoine, C. R. **129**, 206 (1899).
[3] Gottling, Phys. Rev. **22**, 566 (1923).
[4] Beams, Phys. Rev. **28**, 475 (1926).
[5] Locher, J.O.S.A. **17**, 91 (1928).
[6] Lawrence and Dunnington, Phys. Rev. **35**, 396 (1930).

justly criticised.[7] It is in fact a long step from an understanding of its simple principles to its application in obtaining quantitative measurements when the times involved are of the order of 10^{-8} to 10^{-9} sec.

The information presented in the present paper is the result of a study which was initially undertaken to investigate spark breakdown phenomena. It was necessary to develop an apparatus which would make possible an optical analysis of a process moving from initiation to completion in a time of the order of 10^{-8} sec. The electrooptical shutter was chosen for this work as offering the only feasible means. It has been developed to the point of providing a satisfactory method for such a study, with the interpretation of the results reasonably quantitiative and the limitations of the shutter fairly well known.

During the later stages of the present study which has been in progress since the publication of a previous paper,[6] a paper appeared by von Hámos[8] recording the results of a somewhat similiar study. Since however the present study has been developed further, with the experimental method differing in several essentials, and the mathematical treatment considerably less approximate, no essential duplication results.

Part I. Description of the Electrooptical Shutter

The apparatus constituting the shutter proper is shown diagrammatically in Fig. 1. Light from the phenomenon at S which is to be analyzed is passed

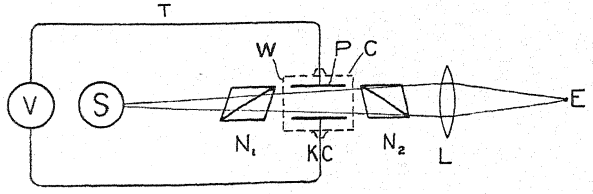


Fig. 1. Schematic representation of the electrooptical shutter.

through the nicol prism N_1, between the plates of the Kerr cell KC and then to the second nicol N_2 which is crossed with the first (i.e. set for total extinction of the light). A lens L which focuses the light on a photographic plate or an eyepiece at E completes the optical system. The Kerr cell consists of two parallel metal plates P (the size and spacing of which must be computed) placed in a glass cell C containing a liquid which possesses the property of becoming doubly refracting under the influence of an electric field. Electrical connections T are made from these two plates to the voltage V which is used to control the shutter. In the present study the optical source S, which was a spark gap, also provided the control voltage V through the voltage across the gap. This combining of S and V is not an unimportant detail as it provides the all important synchronization between the initiation of the phenomenon being studied and the closing of the shutter at some definite stage of the phenomenon.

[7] Gaviola, Phys. Rev. **33**, 1023 (1929).
[8] Von Hámos, Ann. d. Physik (5) **7**, 857 (1930).

The action of the shutter when controlled by a spark gap as shown in Fig. 2 is briefly as follows. Voltage from a direct current source is applied simultaneously to gap and Kerr cell. The existance of an electric field in the liquid of the Kerr cell causes it to become doubly refracting. Hence the plane polarized light incident upon the cell emerges elliptically polarized and a certain fraction of it passes through the second nicol prism. Thus when a potential exists across the plates of the Kerr cell the shutter may be considered open. When the applied voltage has reached a sufficient value the gap "breaks down." Two important characteristics of the breakdown are a rapid collapse of the voltage across the gap and the emission of light in the gap. Following the breakdown an electric wave is propagated out along the wires T toward the Kerr cell, while light is emitted and also travels toward the cell. The electric wave reaches the cell at a time after the beginning of the breakdown equal to the length of wire path between the gap and cell divided by the wave velocity (very nearly the speed of light), while the light reaches there after

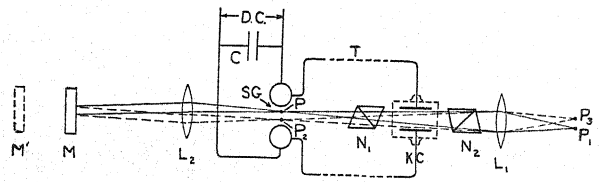


Fig. 2. Experimental arrangement of the shutter which provides a means of simultaneously observing two stages of development.

a time equal to the path traveled divided by the speed of light. Light arriving at the cell before the voltage wave passes on through, that arriving after is rejected due to the collapse of voltage and consequent vanishing of the double refraction.

Measuring times from the beginning of the break in the voltage across the gap, the length of time t_p which the shutter remains completely open after the breakdown is given by

$$t_p = \frac{L_w - L_l}{3 \times 10^{10}} \tag{1}$$

where L_w and L_l are respectively the lengths in centimeters of the wire path and light path from gap to cell. t_p will be referred to as the *path* time of cut-off. A study of the deviation of the actual or *effective* time of cut-off from this path time will constitute a large part of the paper.

It is evident from the expression for t_p that the time of cut-off can be varied by varying the length of either the wire or light paths. Normally the length of light path is fixed and the wire path is varied. However with this arrangement there is a limit to the quickness of cut-off since the wire path is always longer than the light path. To obtain still quicker cut-off times the light path must be lengthened without changing the wire path. This is conveniently accomplished by the second optical system devised in the present study and shown in Fig. 2. The lens L_2 produces a parallel beam of light which

is reflected back by the mirror M through the same lens and comes to focus at a position P_2 slightly to one side of the source P (spark). It then passes on through the shutter system and produces a second image at P_3 by the side of the direct one. Since this second image has a longer light path, it has a smaller time of cut-off, and therefore represents an earlier stage of the phenomenon. Indeed if L_l is made larger than L_w, negative times result (i.e. the shutter closes ahead of breakdown). This condition has been used frequently. *This double optical system hence makes possible the simultaneous observation of two stages of the phenomenon, the time difference between them, being known as accurately as one desires to measure the length of the additional light path of the second system.*

PART II. THEORY OF THE SHUTTER ACTION

(A) Physical optics.

A complete treatment of the physical optics of double refraction as applied to the Kerr effect has been summarized by Kingsbury.[9] The relation of use here is that giving the intensity I of light transmitted by the shutter system (neglecting absorption and loss by reflection) as a function of the electric field between the Kerr cell plates.

$$I = I_0 \sin^2 (\pi b L E^2) \tag{2}$$

Where I_0 is the incident intensity, b is Kerr constant of liquid used, L is length of plates in direction of optic axis, and E is field strength in e.s. volts /cm. This equation is valid only for the usual condition in which the electric field makes an angle of 45° with the plane of polarization of both nicol prisms.

In general the edge effect of the electric field at the ends of the Kerr cell plates will cause an appreciable error. This may be allowed for by replacing the L of Eq. (2) by the following relation given by Chaumont[10] for the effective length L'.

$$L' = L + \frac{a}{\pi}\left[1 + \frac{d}{a}\log\left(1 + \frac{a}{d}\right)\right]. \tag{3}$$

Where L is the length of plates in direction of light, a is their separation and d is their thickness. This relation is accurate only when the length and width of the plates is at least three times their separation, and when there is an appreciable body of liquid around the plates.

Since nitrobenzene has a much larger electrostatic Kerr constant than that of any other known liquid, it should be used. Many values have been published for the Kerr constant of nitrobenzene, the differences possibly being due among other causes to variations in purity, but that given by Möller[11] seems to be reliable for the very pure substance. It is $b = 3.46 \times 10^{-5}$ at 20°C and a wave-length of 5460A. The constant decreases rapidly with increasing temperature.[12]

[9] Kingsbury, Rev. of Sci. Inst. **1**, 22 (1930). For a general discussion of the electrooptical Kerr effect see Handb. d. Physik **21**, 724.

[10] Chaumont, Ann. d. Physik (9) **5**, 31 (1916).

[11] Möller, Phys. Zeits. **30**, 20 (1929).

[12] Hand. d. Physik **21**, 769–780.

Inspection of Eq. (2) shows maximum (i.e. 100 percent) transmission is attained for that value of the field (call it E_m) given by

$$E_m = (2bL)^{-1/2}. \tag{4}$$

It will be convenient to rewrite (2) in terms of this value.

$$\frac{I}{I_0} = \sin^2\left[\frac{\pi}{2}\left(\frac{E}{E_m}\right)^2\right]. \tag{5}$$

To give a visual picture of the behavior of intensity with field strength, Eq. (4) is shown graphically in Fig. 3. For small values of E/E_m the sine is approximately equal to the angle, so that the intensity is proportional to the fourth power of the field. As E increases to E_m the power in effect decreases from four to zero. This fact has led previous experimenters to the belief that

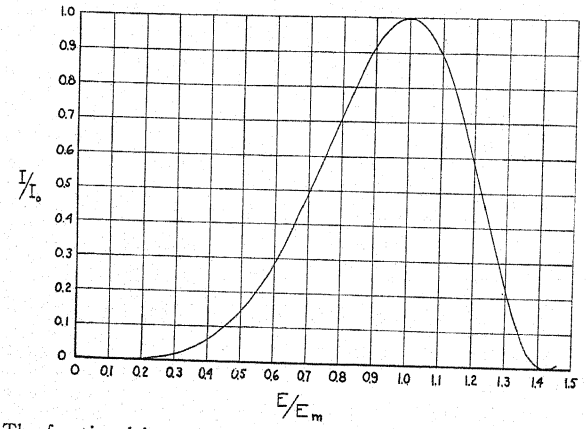


Fig. 3. The fractional intensity transmitted shown as a function of the field.

a "quicker" cut-off is obtained if smaller initial fields are used. On the contrary it will be shown in the following section that *quicker cut-offs are obtained with higher fields.*

(B) Electric circuit theory.

With this brief review of the optical behavior of the Kerr cell, let us consider the electric circuit of which it is a part. From this viewpoint, the Kerr cell is simply a small condenser. It is situated at the end of a transmission line (whose length may be a few centimeters or many meters) containing distributed inductance, capacity and resistance, and at the other end of which is a source of voltage V which decreases rapidly when the spark breaks down. We will assume that the drop of this control voltage can be represented by a function of the form

$$V = V_0 e^{-mt}(1 + mt) \tag{6}$$

where V_0 is the initial voltage, t the time and m a positive constant. This function was chosen because of the general resemblance of its form to oscillograph

curves of static spark breakdown.[13] Its slope at $t=0$ is zero. A nonoscillatory function was chosen since experimentally it is advantageous to have an aperiodic discharge. Further, the time involved in the actual spark breakdown, and hence in the voltage collapse, is small compared to the quarter period of the oscillation normally encountered in condensed discharges, so that any errors caused by erroneous voltage values at relatively late times are of secondary importance in the work at hand. We will also assume that the distributed inductance l and resistance r can be treated as lumped, and that the distributed capacity of the leads is considerably smaller than the capacity of the Kerr cell c so that it can be neglected. Experimentally these circuit assumptions are valid only for short transmission lines, say not more than 0.5 to 2 meters, since the distributed capacity soon approaches that of the Kerr cell. However, the study of the formation stages of spark breakdown requires such short leads so it is of considerable interest to obtain an analysis of the shutter action at these short times.

We have then, in effect (see Fig. 4) a condenser discharging through a symmetrically divided inductance and resistance during the time that the original impressed voltage is falling to zero.* The treatment of the spark gap

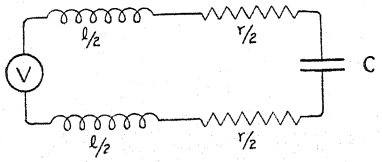


Fig. 4. Simplified shutter circuit.

as a voltage is advantageous not only because it makes possible the utilization of oscillograph data but also because it eliminates the necessity of dealing with the resistance of the spark. In addition it largely takes care of interaction between this shutter circuit and the reservoir condenser-gap circuit because the usual period of the latter is about a hundred times that of the former, and the only appreciable interaction would be the voltage appearing across the gap due to current flowing in the reservoir circuit. Considering, then, the circuit of Fig. 4, the following differential equation may be written:

$$l\frac{di}{dt} + ri + \frac{q}{c} = V_0 e^{-mt}(1 + mt) \tag{7}$$

where i is the current and q the charge on the condenser. With the ordinary circuit notation:

$$b = \frac{r}{2l}, \quad k = (lc)^{-1/2}, \quad i = \frac{dq}{dt}$$

[13] Rogowski and Klemper, Archiv. f. Elektrotechnik **24**, 127 (1930).

* In the treatment by von Hámos,[8] inductance as well as distributed capacity was neglected and the collapse of voltage across the gap was in effect assumed to be instantaneous, so that the problem reduced to the ordinary discharge of a condenser through a fixed resistance. In addition E_0/E_m was assumed to be less than 0.5, so that the transmission was proportional to the fourth power of E/E_m.

Eq. (7) may be rewritten:

$$\frac{d^2q}{dt^2} + 2b\frac{dq}{dt} + k^2q = \frac{V_0}{l}e^{-mt}(1 + mt). \tag{8}$$

The solution of this differential equation is

$$\boxed{\frac{q}{q_0} = \frac{E}{E_0} = Ce^{-bt}\cos\left[(k^2 - b^2)^{1/2}t - \theta)\right] + (f + gt)e^{-mt}} \tag{9}$$

where the constants are as follows:

$$f = \frac{k^2[m(3m - 4b) + k^2]}{(m^2 - 2bm + k^2)^2} \tag{10}$$

$$g = \frac{k^2m}{m^2 - 2bm + k^2} \tag{11}$$

$$\theta = \tan^{-1}\left[\frac{mf - g + b(1 - f)}{(k^2 - b^2)^{1/2}(1 - f)}\right] \tag{12}$$

$$C = \frac{1 - f}{\cos\theta}. \tag{13}$$

For convenience in reference, the other symbols will be redefined here in the units in which they will be used: r = resistance in ohms, c = capacity in farads (of Kerr cell), l = inductance in henries, $b = r/2l$, $k = (lc)^{-1/2}$, m = a positive constant, q/q_0 = fraction of charge remaining on condenser at time t (in seconds). The origin of time is the beginning of the break in the voltage across the spark gap. E/E_0 is the fraction of the initial field existing between the condenser plates at time t, E_0 being the initial field (volts/cm) as distinguised from E_m which is the field which gives maximum transmission.

The solution of the problem given by Eq. (9) is valid only for an oscillatory discharge but this is the condition of practical interest. The first term in the solution is of the same form as the ordinary solution for instantaneous voltage drop. The second term represents the effect of the gap voltage (see Eq. (6)). The results given by this solution can be best illustrated by a set of numerical examples using as a basis values from a typical experimental set-up. The values that will be used are: $r = 35$ ohms, $l = 0.75 \times 10^{-6}$ henries, $c = 14.7 \times 10^{-12}$ farads, $E_0 = E_m$ and $m = 0.21 \times 10.$[9] The first four are directly measured quantities, the last was obtained indirectly from experimental data as will be explained in Part III. The procedure will be to vary, one at a time, each of the five quantities, holding the other four constant, and to study the effect. Since what is finally desired is not the behavior of E/E_0 but of the transmission of the shutter, the values of E/E_0 obtained from (9) will be translated into I/I_0 by means of (5). The ratio I/I_0 will be referred to as the transmission.

Before proceeding to the example, the concept of time must be clearly understood. Since lumped constants were used in obtaining the above solution, no direct account is taken in it of the time t_w required for propagation of the wave from gap to shutter, (i.e. of $L_w/3\times10^{10}$, see Eq. (1)). Mr. H. W. Washburn[14] of this laboratory has made a derivation on the basis of distrib-

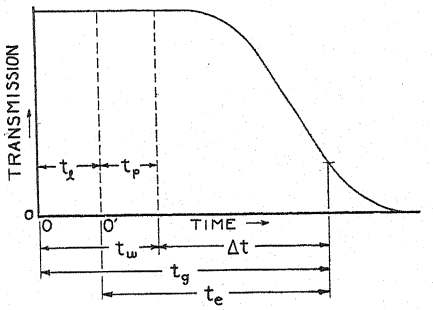


Fig. 5. Relation of various times to each other and to a typical computed transmission curve.

uted constants, which work will be published soon. For short lengths of leads to the Kerr cell, the two solutions give essentially the same results providing the time of propagation is neglected in the author's solutions. In effect then, lumping the constants, automatically allows for the time of propagation to a first approximation. Eq. (9) then gives directly the state of

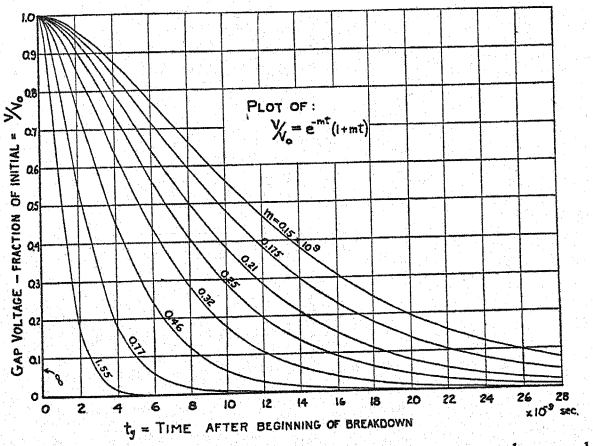


Fig. 6. Various assumed rates of voltage collapse across the spark gap.

transmission of the shutter at various times after breakdown. The t of this solution is the time scale given in all figures in this section and will be referred to *as* the gap time t_g. However, *to obtain the effective action of the shutter on the light the time t_l required for the light to travel from gap to shutter must be subtracted from the given times.* In the experimental set-up this amounted to 0.5×10^{-9} sec. This corrected time scale will be referred to as the effective

[14] Washburn, Phys. Rev. **38**, 584 (1931)—a preliminary report.

time t_e. Fig. 5 shows a typical transmission curve as obtained from Eq. (6) with the relation between the various times indicated. If the closing of the shutter were instantaneous the transmission curve would be coincident with the right hand dotted line. The interval designated as Δt represents the lag in the closing of the shutter to any given state of transmission and is numerically equal to $(t_g - t_w)$ or $(t_e - t_p)$.

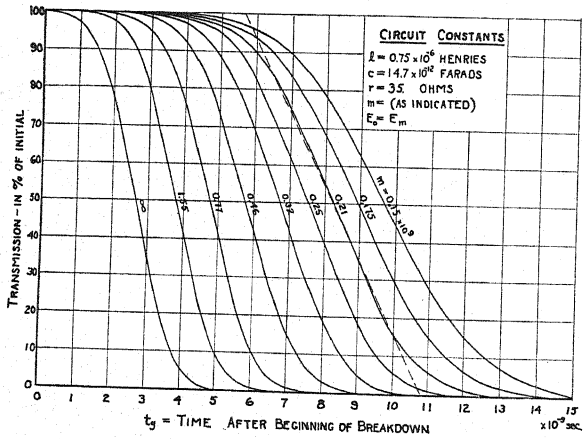


Fig. 7. Effect of varying the rate of collapse of spark gap voltage on the closing of the shutter.

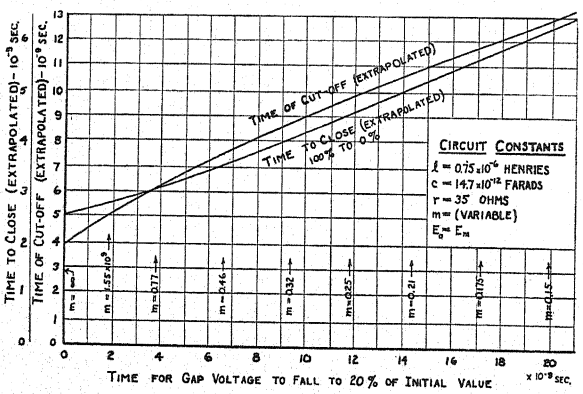


Fig. 8. Relation between rate of voltage fall and (a) time of cut-off of shutter (extrapolated), (b) time for shutter to close (extrapolated) from 100 to 0 percent transmission.

Since the value of m, that is of the rate of voltage collapse on the gap, has a large effect on the transmission curves, this will be studied first. Fig. 6 shows a plot of the voltage function (Eq. (6)) for various values of m from ∞ to 0.15×10^9. Thus if $m = 0.21 \times 10^9$, the gap voltage will fall to 20 percent in 14.3×10^{-9} sec. Fig. 7 gives the corresponding set of transmission curves. They are seen to be of quite different shape than the exponential curves assumed by previous experimenters. That for $m = 0.21 \times 10^9$ corresponds to the experimental condition. The path time of cut-off (Eq. (1)) for the

above example is $t_p = 0.7 \times 10^{-9}$ sec. If a straight line is drawn through the transmission curve for the above m, *the extrapolated time of cut-off is* $(10.8 - 0.5) \times 10^{-9} = 10.3 \times 10^{-9}$ sec. (*effective scale*) *as contrasted with the* t_p *of* 0.7×10^{-9} *sec.* Even with an instantaneous voltage drop ($m = \infty$), the extrapolated cut-off time is 4.0×10^{-9} sec. In drawing the above straight line, it is tipped slightly to allow for the rounding off of the transmission curve. The amount of tipping necessary was judged from some experimental data in Part III. As would be expected, the more slowly the voltage falls, the later the cut-off occurs. This is shown quantitatively in Fig. 8 which gives directly the relation between the rate of voltage fall as obtained from Fig. 6 and the corresponding extrapolated times of cut-off as obtained from Fig. 7. The times given in this and later tables are gap times. In addition the extrapolated time required for the shutter to close if its action were linear from start to finish instead of from about 90 to 10 percent is shown as a function of the rate of voltage fall. For example for $m = 0.21 \times 10^{-9}$ sec., the time to close is $(10.8 - 5.7) \times 10^{-9} = 5.1 \times 10^{-9}$ sec. This time to close is of interest since the time resolution of the shutter depends upon it. The other factor influencing the time resolution is the proportional rate of intensity increase of the light source being studied. This is considered later.

There is another quite important effect to be noted from the variation of the rate of voltage collapse, namely, the pronounced decrease in the oscillations (the damping resistance being held constant) with slower rates of voltage fall. This is shown in Table I in which the peak transmissions of the first

TABLE I. *Effect of rate of voltage collapse on magnitude of oscillations.*

m	Time for voltage to fall to 20 percent 10^{-9} sec.	1st Oscillation		2nd Oscillation	
		Time of peak 10^{-9} sec.	Maximum transmission (percent)	Time of peak 10^{-9} sec.	Maximum transmission (percent)
∞	0	10.7	66.9	21.2	30.3
0.46×10^9	6.6	14.6	17.9	25.0	7.20
0.21×10^9	14.4	18.0	0.100	27.5	0.407
0.15×10^9	19.8	—	—	27.8	0.0025

and second oscillations are given for a few values of m. The first oscillation (i.e. first reversal of voltage) is so suppressed with $m = 0.21 \times 10^9$ that it is less than the following (positive) oscillation, and with $m = 0.15 \times 10^9$ it is simply an undulation in the tail of the cut-off curve. A simple mechanical analogy is often helpful in visualizing the behavior of the shutter circuit, namely a simple pendulum suspended in a viscous fluid. The original displacing force can be thought of as being reduced in the same manner as the gap voltage. This force retards the motion of the pendulum toward the equilibrium position, hence the smaller oscillations and their nonsymmetrical character. It is apparent then that *the slower the rate of voltage collapse, the less damping resistance will be required for satisfactory operation.*

Before the shutter will function properly it is necessary to adjust the

damping resistance to the proper value. The effect of the damping resistance on the transmission curve is shown in Fig. 9. It is seen to be largely one of slowing down of the rate of closing with only a very slight displacement of the curve to later times. This is quantitatively shown by the extrapolated data given in the upper half of Table II. The effect of the oscillations can be judged from the data on the second oscillation given in the same table. The decrease of amplitude with resistance is so rapid that for a resistance

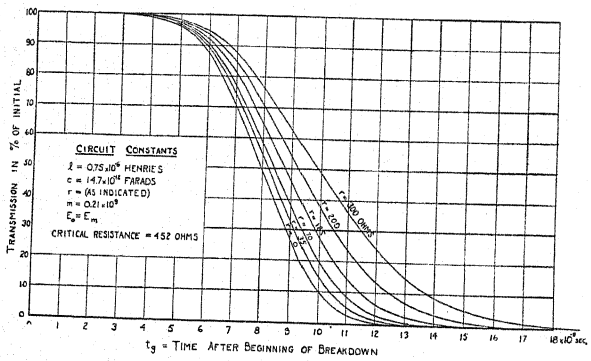


Fig. 9. Effect of varying the resistance in the Kerr cell circuit on the closing of the shutter.

TABLE II. *Data from Fig. 9 and 10 showing effect of varying the damping resistance and the initial field strength.*

	Variable	Time of cut-off (extrapolated) 10^{-9} sec.	Time to close (extrapolated) 10^{-9} sec.	2nd Oscillation		Initial transmission (percent)
				Time of peak 10^{-9} sec.	Maximum transmission (percent)	
	r					
Fig. 9	0	10.45	4.85	27.2	3.30	100
	35	10.8	5.1	27.5	0.407	"
	70	11.15	5.35	28.6	0.048	"
	125	11.8	5.9	30.5	0.0015	"
	200	12.7	6.7	(30.5)	(3.8×10^{-7})	"
	300	14.0	8.0	(30.5)	(2.9×10^{-7})	"
	E_0/E_m					
Fig. 10	0.4	10.0	6.4	27.5	0.010	6.19
	0.6	10.1	6.3	"	0.053	28.6
	0.8	10.4	6.15	"	0.235	71.0
	1.0	10.8	5.1	"	0.407	100.0
	1.2	11.2	3.7	"	0.845	58.9
	1.414	11.6	2.9	"	1.63	0.0

of 200 ohms or greater the second oscillation also becomes merely an undulation in the tail of the transmission curve. The critical resistance (aperiodic discharge) is 452 ohms. With increasing resistance the decrease of extraneous light passed by the oscillation is counteracted by the increase due to the rapid lengthening of the foot or tail of the transmission curve so that an optimum resistance value must be found (see Part III).

As has been mentioned before, the belief that a quicker cut-off is obtained if an initial field strength is used corresponding to a small ratio of E_0/E_m is not founded on fact. The effect of varying the initial field is shown

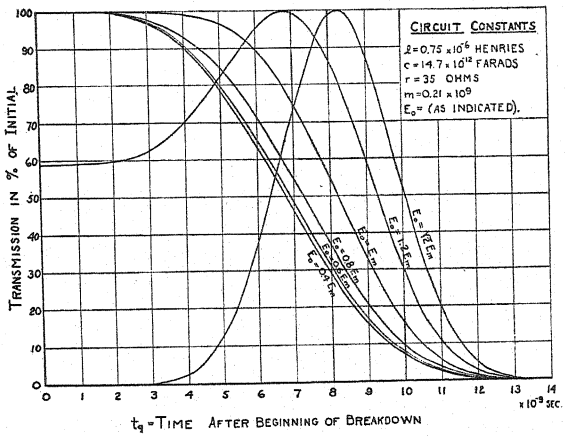


Fig. 10. Effect of varying the initial field (or voltage) in Kerr cell on the closing of the shutter.

in Fig. 10. It is apparent that more rapid cut-offs are obtained with *larger* E_0/E_m ratios, that is, the slope of the transmission curve is greater. This is especially true for values of $E_0 > 0.8\,E_m$. The extrapolated data are given in

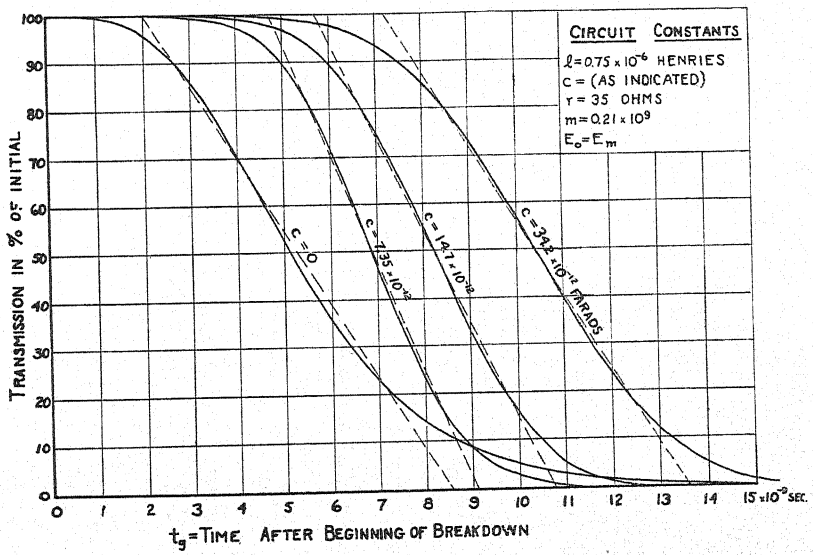


Fig. 11. Effect of varying the capacity of the Kerr cell on the closing of the shutter.

the lower half of Table II, together with that on the second oscillation and the initial transmission. The advantages of higher E_0/E_m ratios are: smaller times to close (which is of the greatest importance when very rapidly changing phenomena are being studied) and far greater light intensities; the dis-

advantage is the rapid increase of extraneous light due to the increased magnitude of the oscillations. Consideration of the curve $E_0 = 2^{1/2}E_m$ leads to the suggestion that the closed-open-closed action of the Beams[1] type of shutter could be attained with the single cell shutter being considered here. It can, but only with an approximately monochromatic light source, since the Kerr constant changes so rapidly with wave-length.

We now come to the important consideration of the effect of the capacity of the Kerr cell on the shutter action. The manner of closing is shown in Fig. 11 for three capacities, one larger and one smaller than that actually used in the experimental set-up. With increasing capacity there is both a displacement to later times and a decrease in the rate of closing. The former can be allowed for by shorter leads to the shutter but the latter is a disadvantage which can not be corrected, *hence the necessity of using a Kerr cell with as small a capacity as is experimentally feasible.* The extrapolated data are given in the upper half of Table III together with data on all the oscilla-

TABLE III. *Data from Fig. 11 and 12 showing effect of varying the capacity and inductance.*

	Variable	Time of cut-off (extrapolated) 10^{-9} sec.	Time to close (extrapolated) 10^{-9} sec.	Oscillation number	Time of peak 10^{-9} sec.	Maximum transmission percent	Relative energies passed by oscillations
	Capacity 10^{-12} farads						
Fig. 11	34.2	13.6	6.4	1	24.5	2.45	
				2	40.2	0.87	
				3	56.5	0.145	8.30
				4	73.0	0.063	
	14.7	10.8	5.1	1	18.0	0.100	
				2	27.5	0.407	
				3	38.5	0.103	1.00
				4	48.5	0.042	
				5	59.5	0.015	
	7.35	9.1	4.4	(1)	(14.2)	0.003	
				2	19.7	0.400	0.49
	(0)	(8.6)	(6.6)	3	28.0	0.016	
				—	—	—	0.01—
	Inductance 10^{-9} henries						
Fig. 12	1.80	14.0	6.7	1	25.5	1.18	
				2	41.3	0.184	3.19
	0.75	10.8	5.1	3	25.5	1.18	
	If $m = \infty$			(Same as above for $c = 14.7$)			1.00
	1.80	6.4	4.3				
	0.75	4.0	2.65				

tions of any appreciable magnitude. An increase in capacity is seen to cause a large increase in the oscillations, the damping resistance remaining constant. The last column of Table III gives an approximate idea of light energies (i.e. extraneous light) passed by the oscillations. The values are calculated on the basis of a constant intensity source. The extraneous light

is seen to decrease rapidly with decreasing capacity. The curve on Fig. 10 marked $c=0$ is the mathematical result obtained if the capacity of the cell is assumed zero. Actually, this is not a valid procedure since the basic assumption that the cell capacity is large with respect to the distributed capacity of the leads is no longer true. The curve, however, is of interest since it represents the manner of closing if the Kerr cell voltage exactly followed the gap voltage. Comparison with the other curves and a study of the behavior of the terms in Eq. (6) show the advantageous effect of the oscillatory condition of the circuit, namely that the oscillatory term *adds* to the upper part of the curve and, with sufficiently small capacities, *subtracts* from the lower part, thus doubly causing a quicker cut-off.

We will consider now the last of the five variables, namely inductance. Experimentally, changing the inductance is normally equivalent to chang-

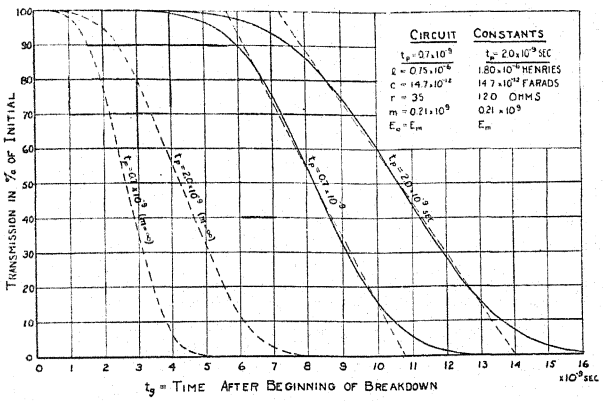


Fig. 12. Manner of shutter closing for two values of inductance (equivalent experimentally to the two path times $t_p=0.7$ and 2.0×10^{-9} sec.) Dotted curves give corresponding manner of closing if voltage drop were instantaneous.

ing the length of leads to the shutter, or in other words to changing the path time t_p. It is true that leads of a given length may be geometrically arranged to give different inductances, but if the requirement of low distributed capacity is met, there is little leeway for change in inductance of the short leads being considered in this paper. The previous statement that lumping the constants allows for the time of propagation to a *first approximation* is pertinent at this point. Fig. 12 shows the manner of closing for two inductances corresponding to the path times indicated. Similar to the change with increasing capacity there is to be observed both a displacement of the transmission curve to later times and a decrease in the rate of closing. A displacement equal to the increase in path times, namely (2.0–0.7) or 1.3×10^{-9} sec. is to be expected (see Fig. 5) but the calculated amount judged from the straight line intercepts at 100 percent is 1.6×10^{-9} sec. This, plus the increase in rate of closing results in a retardation in the time of cut-off of $(14-10.8)$ or 3.2×10^{-9} sec. (see lower half of Table III). This serves to emphasize a fundamental defect in the electrooptical shutter, namely, that

the rate of closing decreases as the path time of cut-off is increased. It is to be noted that only in this last case have two electric constants been varied in the same illustration. The resistance was varied as well as the inductance to correspond to the best experimental conditions, as these curves will be

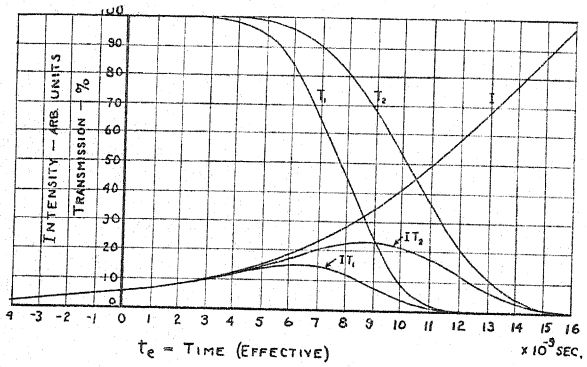


Fig. 13. Effectiveness of shutter closing when the light source is rapidly increasing in intensity. The areas under the IT curves represent the energies transmitted.

checked against experimental data in Part III. From the last column of Table III, it is seen that even under the best experimental conditions the amount of extraneous light passed by oscillations increases with inductance. The dotted curves of Fig. 12 give the manner of closing for the conditions discussed above except with $m = \infty$.

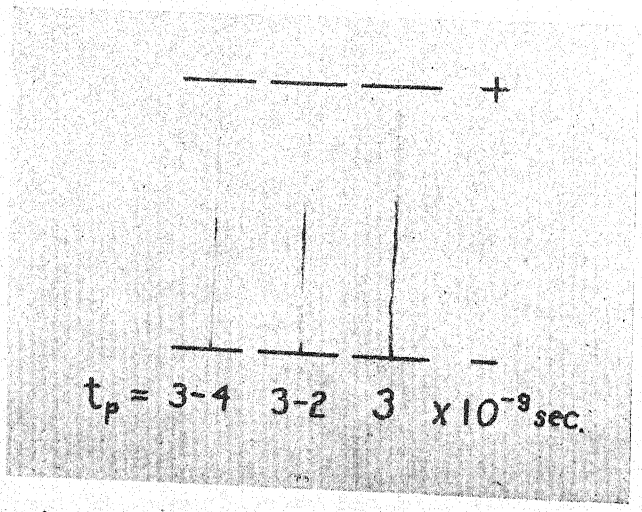


Fig. 14. Change in appearance of a spark in steps of 2×10^{-9} sec. Pressure = 76 cm of Hg, gap length = 5 mm.

The curve representing the light transmitted by the shutter will be similar in form to the transmission curves only if the light source is of constant intensity, a condition not usually found in practice. Fig. 13 illustrates

the conditions when the intensity is rapidly increasing. The time scale has been corrected for the light path. The two transmission curves T_1 and T_2 are the same as those in Fig. 12, while the intensity curve I has been estimated from experimental data and corresponds to the growth of the central bright region of the spark illustrated in Fig. 14. The intensity transmitted is represented for the two cases by the curves IT_1 and IT_2, and the energies of the transmitted pulses of light are proportional to the areas under the IT curves. It is seen that a majority of the energy is passed in a region near the peak of the IT curves, especially for later times of cut-off. Hence, to the eye or a photographic plate, what happens during a time interval of a few billionths of a second—the interval occurring somewhere along the upper half of the transmission curve—is predominant and what happens before and after is hardly seen. Thus, with a rapidly increasing intensity, the closed-open-closed effect of the Beams[1] type of shutter is approximated. An idea of the time resolution obtained under the foregoing conditions can be gained directly from the ordinates of the IT curves. Considering the IT_1 curve the transmitted energy representing the phenomenon at 11×10^{-9} sec. (consider say a time interval of 0.1×10^{-9} sec. duration) is only 17 percent of that at 8×10^{-9} sec., that at 12×10^{-9} sec. is only 4.5 percent of the same. *The theory thus indicates a time resolution of the order of 3 or 4×10^{-9} sec. with a rapidly increasing intensity, and about 5 to 6×10^{-9} sec. with a constant intensity source (see data on "times to close" in Table III for Fig. 12).*

Part III. Experimental Results Bearing on the Action of the Shutter

By use of the electrooptical shutter to study the early stages of spark breakdown, three classes of experimental data have been obtained which yield information of use in checking the foregoing theory: first, visual studies on the difference in appearance of sparks over intervals of a few billionths of a second, which give data on the time resolution; second, photographic data giving the time of the extrapolated cut-off; and third, measurements giving the change in the time of cut-off with certain shutter conditions. Unless otherwise stated all the experimental data were taken under the following set of conditions: air pressure in gap = 76 cm of Hg; gap length = 5 mm; time for reservoir condenser energy to begin to feed into gap $=5\times10^{-9}$ sec. (determined by distance of C, Fig. 2, from gap); capacity of Kerr cell $=14.7\times10^{-12}$ farads; for path time $t_p=0.7\times10^{-9}$ sec., inductance of shutter circuit $=0.75\times10^{-6}$ henries and resistance = 35 ohms; for $t_p=2.0\times10^{-9}$ sec., inductance $=1.80\times10^{-6}$ henries and resistance = 120 ohms. In all cases the spark breakdown occurred in completely dried air, the cathode was illuminated with ultraviolet light, and the reservoir condenser with a capacity of 0.008×10^{-6} farads was connected to the gap through a linear distributed resistance of 50 ohms.

First class.

A typical visual study of the change in appearance of a spark with time is shown in Fig. 14. The path times are given at the bottom, the first num-

ber (3) meaning the ordinary path time as computed by Eq. (1), while the subtracted number is the time required to travel the additional light path introduced by the second optical system (see Fig. 2). Thus the development is shown in steps of 2×10^{-9} sec. What is of interest here is not only the change in general appearance—the central region connecting with the cathode—but also the change in detail, small spurs and irregularities appearing both in the newly developed region in front of the cathode and also in the central region itself. A growth merely in length and brilliance of the central region would not necessarily yield any data on the time resolution since the displacement to later times of a very slowly falling transmission curve would allow more energy to pass and thereby increase the brilliance and observed length. *But the observed change in both form and detail certainly requires a time resolution of the order of 4×10^{-9} sec. or less. This agrees with the theoretical estimate of 3 to 4×10^{-9} sec. made from Fig. 13 for somewhat similar conditions.*

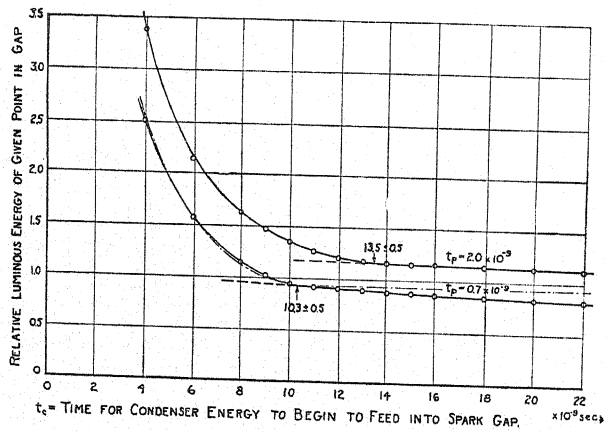


Fig. 15. Effect of variation of the distance of the reservoir condenser from the spark gap on observed luminous energy of the central region of breakdown. Shown for two times of cut-off: t_p=0.7 and 2.0×10^{-9} sec. (Chain curve is computed effect for $t_p=0.7\times10^{-9}$ sec.)

Second class.

The results of a photographic study giving directly the times of extrapolated cut-off for two path times are presented in Fig. 15. If the intensity of the central region of a spark such as in Fig. 14 is observed at a given path time it will be found to vary with the distance of the reservoir condenser (*C*, Fig. 2) from the gap. If this condenser is removed entirely the only electrical energy available to maintain a voltage across the gap is the charge stored on the electrodes and on the adjacent connecting wires. During breakdown this will feed into the gap, there resulting a certain rather rapidly falling voltage-time relation and a corresponding intensity-time curve for any given point in the gap. If the reservoir condenser is now placed at a moderate distance from the gap, everything during breakdown proceeds as before up the old time t_c at which the energy from the condenser begins to

feed into the gap. Assuming the speed of propagation along the connecting wires is that of light, t_c is given by

$$t_c = \frac{2 \times (\text{length of a connecting wire in cm})}{3 \times 10^{10}} \tag{14}$$

since the wave must go to the condenser and back. From this time on (at least for a certain period) the voltage on the gap is higher than formerly, there being more energy fed in, and as a consequence the light intensity at the given point is also greater. If t_c is greater than the extrapolated time of cut-off (effective time scale), there will still be no observed increase of intensity since the shutter is closed before the increase occurs; but if the condenser is now moved towards the gap a point will be found on the near side of which there is a continuous increase of intensity. This point corresponds to the condition of equality between t_c and the extrapolated cut-off time.

The procedure experimentally was to move the condenser step by step from a point as close as feasible to a distance as great at 10 or 11 meters, taking a composite photograph of the spark at each step. This series of photographs (negatives) was photometered and the density recorded of the given point in the gap (chosen as approximately the center of the central bright region, see Fig. 14). These densities were then translated into relative energies by a density energy curve, the latter being obtained from series of composite pictures taken through diaphragms of various sizes, the number of exposures on each composite being kept constant, to eliminate any intermittency effect. The averaged results of four runs for each t_p (two taken with the condenser moving away from gap, and two vice versa) are shown in Fig. 15. There is seen to be a definite point of inflection which point determines the effective time of cut-off.

That the shape and position of the transmission curve for $t_p = 0.7 \times 10^{-9}$ sec. given in Fig. 12 is substantially correct was proved in the following manner. A rate of voltage fall (i.e. a value of m) was chosen for this curve of Fig. 12 so that with the other constants corresponding to the condition $t_p = 0.7$, there resulted a theoretical transmission curve with an extrapolated cut-off time of 10.3×10^{-9} sec. (see Fig. 8). Then assuming that the *increase* in instantaneous intensity produced by the condenser energy beginning to feed into the gap is linear with time and is zero at the time t_c, a series of such ΔI curves was drawn, the curves being parallel with feet at times corresponding to various t_c times. The product of ordinates of any one ΔI curve with the transmission curve gives the transmitted ΔI curve, and the area under it is proportional to the transmitted increase in energy. The plot of these areas, reduced to a comparable scale, gives the chain curve of Fig. 15, which is seen to be almost coincident with the experimental curve including the location of the inflection point. This is a fairly good check on the steepness of the calculated transmission curve since a steeper cut-off would give a more rapidly rising chain curve and vice versa. The uncertainty in the check is the rate of increase in ΔI. It also constitutes a double check on the rate of fall

of voltage chosen in the foregoing manner, since not only does the rate of fall determine the location of the inflection point but also the steepness of the transmission curve (see Fig. 7 and "Time to Close," Fig. 8).

That the extrapolated time of cut-off obtained as previously described by drawing a straight line through the transmission curve at a slight angle to its front (see Fig. 12) corresponds to the effective time of cut-off as given experimentally by the point of inflection of the curves of Fig. 15 is proved as follows: a new computation of the relative energy increase is made exactly as before but using this straight line instead of the computed transmission curve. If the straight line is slightly tipped as shown in Fig. 12, the inflection point of this last energy increase curve can not be distinguished from the former (chain curve). This is to be expected from the fact that the *additional* energy passed by the tail of the transmission curve is proportional to the product of two small quantities and is therefore a quantity of the second order. However, this result is not to be interpreted as meaning that the tail of the transmission curve can be neglected in general, since the *total* energy passed by it is proportional to the product of a small and large quantity (the total intensity) and hence is of the first order, though usually small.

The possible existence of an error in the foregoing method for determining the effective time of cut-off should be mentioned. It is possible that an appreciable time lag exists between the *beginning* of the voltage change on the gap due to the condenser wave and the *beginning* of the intensity change due to it, the lag being due to a time interval between excitation and emission. However, the close agreement between the chain and experimental curves of Fig. 15 seems to indicate that the lag is small, that is, it would be of the order of 10^{-9} sec. rather than 10^{-8} sec. For example, if the lag amounted to even 5×10^{-9} sec. the time to close (calculated) would be increased to 1.6 times its former value, and the resulting chain curve would be much too straight to fit the experimental curve. It is still possible though that the shape of the actual ΔI curve would compensate for this. However, the reduced time resolution weighs against this, as does the change in the time of cut-off with inductance considered in the next paragraph. A second possible source of error is from the fact—as pointed out before—that the manner of the latter part of the voltage collapse is effected by the position of the reservoir condenser. The increase in voltage occurring when the condenser energy begins to feed in is probably temporary and followed by a more rapid drop due to the increased conductivity. This drop might even make the voltage less at later times than before, so that the net result on the shutter action is problematical. In any case the experimental data sets an approximate lower limit to the effective time of cut-off.

A further check on the theory is found in the movement of the effective cut-off (Fig. 15) with an increase in inductance, or t_p. The effective times of cut-off as obtained from Fig. 15 are 10.3×10^{-9} sec. at $t_p=0.7\times10^{-9}$ sec. and 13.5×10^{-9} sec. at $t_p=2.0\times10^{-9}$ sec. These are to be compared with the extrapolated times of cut-off of the curves of Fig. 12 which were computed for the same conditions. It is to be recalled that the rate of fall of voltage

for the given spark condition was determined in Fig. 12 by picking that rate for which the $t_p = 0.7$ curve gave an extrapolated cut-off time in agreement with the above experimental value of 10.3×10^{-9} sec. (see Fig. 8). Then using this rate of fall—the rate should be reasonably independent of the shutter adjustment—the curve for $t_p = 2.0 \times 10^{-9}$ sec. was computed and was found to have an extrapolated cut-off time of $(14.0 - 0.5)$ or 13.5×10^{-9} sec., in exact agreement with experimental data. This perfect agreement is probably accidental. All experimental results were completed before the theoretical calculations, and the accuracy of neither is sufficient to lead to quite such close agreement. However, the agreement constitutes another good check on the correctness of the theory and the rate of voltage fall used, for faster rates of fall give smaller changes in cut-off time and vice versa for slower rates. For example if the voltage required 28.5×10^{-9} sec. to fall to 20 percent, instead of 14.3×10^{-9} sec. as above, the *change* in the extrapolated cut-off time would be 3.7×10^{-9} sec. Further data from this example are of interest in considering the possible error discussed above. The extrapolated cut-off time for this example is 15.5×10^{-9} sec. instead of the former value of 10.3×10^{-9} sec. Hence the example corresponds to a possible excitation lag as discussed above of 5.2×10^{-9} sec. The extrapolated time to close is 8.4×10^{-9} sec. as compared with the former 5.1×10^{-9} sec., a 65 percent increase. This would increase the theoretical estimate of the time resolution to about 5 or 6×10^{-9} sec., which is to be compared with the experimental data indicating something less than 4×10^{-9} sec.

Third class.

Another check on the theory was made as follows: a change in the Kerr cell capacity was effected without changing the optical constants of the original cell by connecting a second cell across the first, using very short leads. The second cell thus functioned only as a capacity, providing an increase from 14.7×10^{-12} farads to 34.2×10^{-12}. The best damping resistance for the larger capacity proved to be the same as that for the smaller. The spark breakdown was observed visually first with the smaller capacity and with $t_p = (0.7 - 2.0) \times 10^{-9}$ sec., (i.e. using the longer or mirror optical system—see Fig. 2—with an additional light path of 2×10^{-9} sec.). With the larger capacity the light path had to be increased an equivalent of 2.4×10^{-9} sec. (average of 10 readings) to obtain the same stage of development as before, which means an increase in the effective time of closing of that amount. The increase measured in this manner is not exactly that of the extrapolated time of cut-off but a sort of mean displacement of the transmission curve (in this connection study the *IT* curves of Fig. 13). The calculated transmission curves for these two capacities are given in Fig. 11. The mean displacement between them is 2.2×10^{-9} sec., which agrees well with the measured value of 2.4×10^{-9} sec. At larger values of t_p, the measured increase in lag is much greater. For example at $t_p = 16 \times 10^{-9}$, it is 9×10^{-9} sec.

The best damping resistance for any given shutter arrangement must be determined experimentally. The experimental data on which it was deter-

mined for the two conditions $t_p = 0.7$ and 2.0×10^{-9} sec. are shown in Figs. 16, 17, and 18. For any given t_p, the photographic method is to take a series of composite pictures with various damping resistances. The photometered curves of a few of these at $t_p = 0.7 \times 10^{-9}$ sec. are given in Fig. 16. Visually

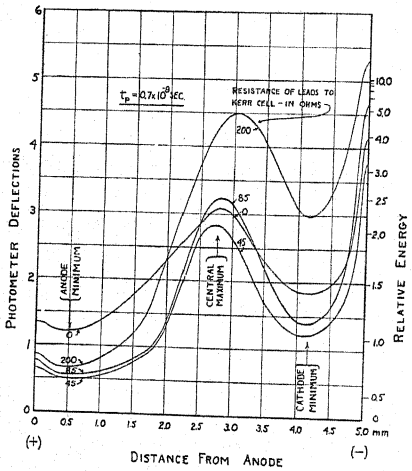


Fig. 16. Photometer curves showing energy distribution observed in gap at $t_p = 0.7 \times 10^{-9}$ sec. for various damping resistances.

this stage of development (with resistance around 35 ohms) appears about the same as the left figure in Fig. 14. It is to be noted that visually the bright regions (center and cathode) appear another order of magnitude brighter,

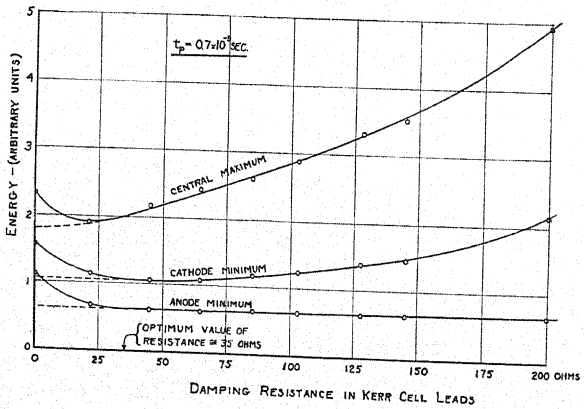


Fig. 17. Effect of varying the damping resistance on the luminous energy at three critical points in the gap (see Fig. 14). $t_p = 0.7 \times 10^{-9}$ sec.

relative to the anode region, than the energies as read from the photometer curves would indicate. Discussion of this with Professor R. S. Minor of the optometry department indicates that it is probably due to an overshooting of the brightness sensation, which phenomenon increases rapidly with

energy.[15] Considering the fact that in the development of this type of breakdown the central region first connects with the cathode and much later with the anode, or expressed differently, since the rate of intensity increase is rapid in the cathode minimum region and quite slow in the anode minimum region, it is possible to differentiate in Fig. 16 between variations due to changes in the oscillations and changes in the rate of cut-off. Thus the drop in transmitted energy between zero and 45 ohms resistance is approximately the same at all three critical points (see arrows), namely, about 0.4, and is due to a large decrease in oscillation (see Table II)—the decrease in the speed of cut-off being negligible (see Fig.9)—which oscillations pass light from the completely developed spark. Further increases in resistance cause rapid increases of energy at the cathode minimum but only very small increases at the anode minimum. This is due to the increasing slowness of cut-

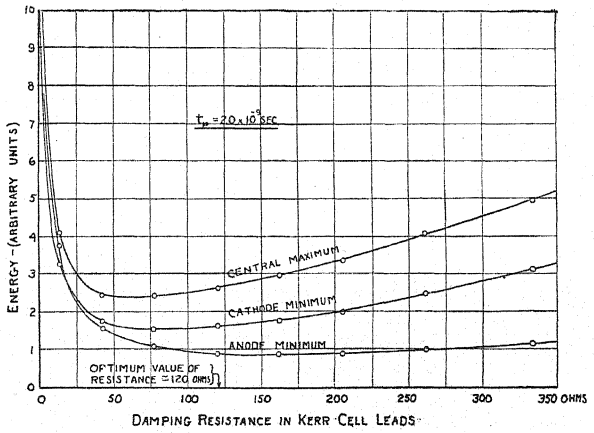


Fig. 18. Effect of varying the damping resistance on the luminous energy at three critical points in the gap (see Fig. 14). $t_p = 2.0 \times 10^{-9}$ sec.

off combined with the relative rates of intensity increase, the decrease from oscillations now being negligible. The behavior of the three critical regions is more clearly shown by plots of their ordinates as in Fig. 17 (averaged data from several runs). If the energy passed by oscillations—equal to the difference between the anode minimum curve and its extrapolated straight line (dotted)—is subtracted from the other two curves the results represent quite closely the effect from zero to 200 ohms of the slowing down of the speed of cut-off with resistance. It is apparent that the net result also depends on the rate of intensity increase. The optimum value of resistance was chosen as that at which the anode minimum curve first falls substantially to its minumum, namely 35 ohms. The visual effect of small energy changes in this anode region is more evident than several times the same energy change in the central region, due probably to a saturation effect from the brilliance of the latter.

[15] Broca and Sulzer, Jour. d. Physiol. et d. Path. Gen. No. 4, July 1902 quoted in "Light and Work" by Luckiesh, p. 167.

Fig. 18 shows a similar set of curves for $t_p = 2.0 \times 10^{-9}$ sec., the optimum resistance value was chosen as 120 ohms. This is 17.2 percent of the critical resistance while the 35 ohms at $t_p = 0.7 \times 10^{-9}$ sec. is only 7.7 percent of the corresponding critical resistance. If the period of the shutter circuit were infinitely short, the shutter would exactly follow the control voltage and there would be no oscillations, hence no need of any damping resistance. As the period is lengthened, the tendency to oscillate increases, hence the required percentage of the critical camping resistance $2(l/c)^{1/2}$ also increases.

Data can be obtained from Fig. 17 and 18 to check roughly the assumed intensity curve of Fig. 13. With the optimum damping resistance, the maximum energy of the central region is 2.00 for $t_p = 0.7$ and 2.65 for $t_p = 2.0$, the ratio of the first to the second being 1.33. The ratio of the energies represented by the IT curves of Fig. 13 is 1.64. This means that the intensity

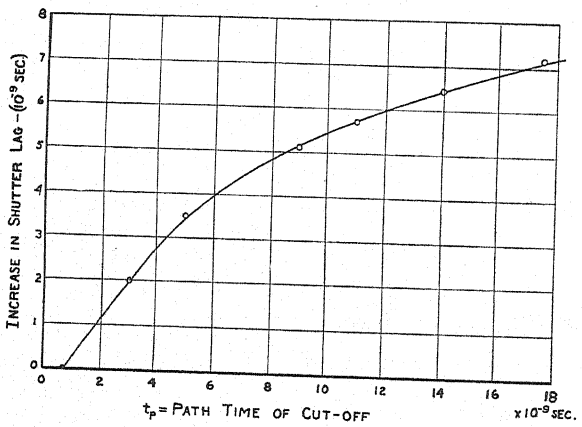


Fig. 19. Increase in shutter lag with path time of cut-off, relative to the lag at $t_p = 0.7 \times 10^{-9}$ sec. Data taken at a gap length of 5 mm and a pressure of 76 cm of Hg.

curve was assumed to rise a little too rapidly beyond say 5×10^{-9} sec., or that the part of the curve to the left of 5×10^{-9} sec. was assumed too low (i.e. the whole curve might be displaced upward a little).

Since the effective time of cut-off increases more rapidly than the path time of cut-off, a correction curve is needed which can be used to correct the path times for their *increase* in lag relative to an arbitrarily chosen time. Such a curve is given in Fig. 19 for the spark conditions given at the beginning of this section, that is for a pressure of 76 cm Hg and gap length of 5 mm. The curve gives the increase in the *effective* time of closing relative to that at $t_p = 0.7 \times 10^{-9}$ sec. Thus at $t_p = 2 \times 10^{-9}$ sec. the time of closing is $(2 - 0.7 + 1.2)$ or 2.5×10^{-9} sec. later than that at $t_p = 0.7 \times 10^{-9}$ sec. It is of interest to note the agreement of this value with that from the two corresponding theoretical curves of Fig. 12. The change in the effective time of closing as judged by their mean time displacement is 2.4×10^{-9} sec. The increase in the correction is seen to be rapid at first, then less rapid as the shutter circuit conditions go over into those which must be treated as a transmission line.

The curve was obtained through use of the second or longer optical system (see Fig. 2). For example, if t_p is made 6×10^{-9} sec., an increase of $(6-0.7)$ or 5.3×10^{-9} sec., and an increase in the light path equivalent to 9.3×10^{-9} sec. is required to compensate, then the increased lag at $t_p=6\times10^{-9}$ sec. is $(9.3-5.3)$ or 4.0×10^{-9} sec.

In summary it may be said that the experimental data given in the foregoing provide many interlocking checks on the theory presented in Part II. The most important of these are: the agreement between the theoretically estimated and experimentally determined time resolution; the correctness of the general shape and position of the calculated transmission curves as indicated by the agreement between the chain curve of Fig. 15 (based on one of these calculated transmission curves) and the corresponding experimental curve of the same figure, and also as indicated by the agreement between calculated and experimental data as to the time movement of these curves with changing inductance and capacity; the above agreements also provide a check on the rate of voltage collapse of the spark gap as determined by the method given which involves both experimental data and the theory.

Part IV. Design and Technique

The general form of the Kerr cell developed in the present study is shown in Fig. 20. The body T was made of Pyrex tubing, the brass plates P were supported by heavy tungsten leads L sealed into the glass. The windows W are described later. The reservoir chamber R provides a means of *completely* filling the cell proper with liquid as well as an air cushion to take care of temperature expansion.

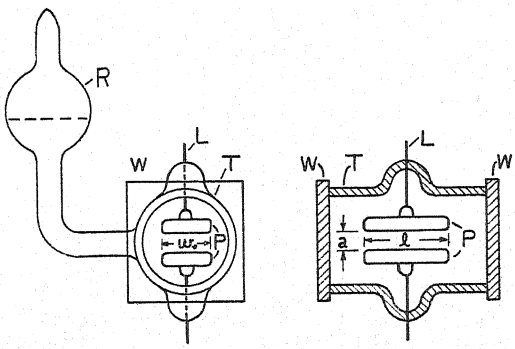


Fig. 20. Form of Kerr cell, showing end view and longitudinal cross section.

The size and spacing of the plates must first be determined. Both theory and experience indicate that the usable voltage range of a cell considering the factors of intensity, quickness of cut-off and extraneous light is that which gives an initial field of from 75 to 100 percent of E_m (i.e. the field which gives maximum transmission)—or certainly not more than 65 to 110 percent E_m. Knowing then the maximum voltage V_0 (e.s.u.) at which the cell is to be used and assuming a plate spacing a (in cm), Eq. (4) gives the necessary length l (in cm) to a first approximation:

$$l = \frac{a^2}{2bV_0^2} \cdot \tag{15}$$

The width w of the plates together with their separation, determines the aperture for light and the electrostatic capacity. A large aperture is desirable since greater intensity can be attained (providing the cross section of the nicol prisms is not the limiting factor) but this must be made secondary to reduction of the electrostatic capacity to a reasonable minimum, as this last determines the quickness of cut-off (see Table III). Neglecting the edge effect, which may be very large, the capacity mmf is given by

$$C = 0.0885k\frac{wl}{a} \tag{16}$$

where k = dielectric constant (about 37* for nitrobenzene), and all dimensions are in cm. Putting Eq. (15) in this gives

$$C = 0.0885\frac{k}{2bV_0^2}wa. \tag{17}$$

Thus the capacity can be *decreased* by decreasing the separation. This also decreases the length. *The determination of the size and spacing of the plates is therefore a compromise between obtaining the minimum electrostatic capacity and maximum usable aperture, and the limiting conditions are respectively the maximum field which the liquid will stand and the maximum length of cell which can be used without certain optical troubles, especially distortion, becoming pronounced.*

As an example the dimensions will be given of the cell used as an illustration in the present study. They are: plate length 1.0 cm, width 1.2 cm, separation 0.5 cm. This cell had a V_0 of approximately 16.4 kv and a measured capacity of 14.7 mmf.

If the mean electric field is in the region of the breakdown value (for nitrobenzene a variable depending on degree of purity but of the order of 45,000 volts/cm or higher) it is essential that the edges of the plates be rounded. However, rounding the edges of the plates destroys the accuracy of Eq. (3) so that E_0 can not be calculated.

The windows of the Kerr cell have presented more or less trouble. There are two essential requirements: the surfaces of the windows must have a *very* high degree of planeness and be parallel to the same degree; and second, the glass must be strain free. The first requirement results from the large prismatic action by the nitrobenzene on all irregularities in the outer window surfaces and the consequent blurring of detail in the image; the second requirement is apparent from the location of the cell between crossed nicols. The best solution found is the type of plate glass used in making shatterproof windshields. It can be obtained in $\frac{1}{8}$ inch sheets, and satisfies the first

* International Critical Tables, Vol. II, p. 89.

requirement perfectly. It is not strain free, but specimens can be found in which the degree of strain is very slight. The only other glass found that was of sufficient planeness was that in a selected lot of plano-ophthalmic lenses. The average plano lens produces a complete blurring of all detail due to the surface irregularities.

The windows are fastened to the body of the cell by water glass (sodium silicate). Before filling with the liquid the cell should be thoroughly baked out (at a temperature below that which will cause dehydration of the sodium silicate) to remove all the moisture possible. The cell should be sealed off after filling. The use of water glass has proved rather unsatisfactory due to its contamination by moisture of the liquid used. A search is being made for a better substance.

The most important part of the Kerr cell is the liquid used in it. Since nitrobenzene has a far greater Kerr constant than any other known substance, it alone will be considered. As purchased commercially, it is in an exceedingly impure state. To obtain a substance pure enough to function at all satisfactorily the liquid should be treated with a weak base such as aluminum or calcium oxide to remove acids and then distilled very slowly in vacuum (retaining the middle third), during which process the water vapor should be frozen out with liquid air. A far superior product results if the distillation is repeated a second time.

Experimentally the effect of impurities in the nitrobenzene are quite evident since they seem to cause a slowing down of the speed of closing of the electrooptical shutter. This is especially evident in the increase of the extraneous light when the early stages of a spark breakdown are being observed. The effect visually is striking. For example, with a gap of 5 mm at atmospheric pressure and $t_p = 1 \times 10^{-9}$ sec. the region consisting of the anode third of the gap appears almost dark in comparison to the bright central region when sufficiently pure nitrobenzene is used. With an impure sample, any degree of luminosity up to about a third or half that of the central region can be obtained depending on the amount of impurity. A very slight trace of moisture destroys the quickness of cut-off, hence the conductivity of a cell seems to be a fairly good indication of the performance that may be expected of it. The conductivity of pure nitrobenzene is given by Möller[11] as 7×10^{-11} mhos/cm^3. The conductivity of the nitrobenzene used in this study was not measured after its distillation. However, in a cell a year old that was still performing satisfactorily it was 2.5×10^{-10} mhos/cm^3 and in one passing a large amount of extraneous light it was 1.2×10^{-9}.

An electrolytic purifying action mentioned by Möller[11] has been noticed throughout the study. Upon the application of a direct current voltage there is a sudden rush of current. This will drop back to a steady value in a few seconds if the liquid is reasonably pure. If, however, it requires a minute to several minutes the cell will be found to have a poor cut-off. It has been found that even with a cell in which the nitrobenzene is reasonably pure there is considerable extraneous light passed if the cell is operated during the two or three seconds required for the electrolytic purification. This peculiarity

must be considered in photographic work. Erroneous results are avoided by first holding the potential slightly under the breakdown value for a sufficient time.

A factor of major importance is the adjustment of the damping resistance of the Kerr cell circuit to the optimum value. Since the correct value can not be exactly calculated with our present knowledge, the adjustment must be made experimentally. The adjustment is a compromise between the condition of no resistance which gives the quickest possible cut-off but large amounts of extraneous light and the condition of critical damping which eliminates all oscillations but causes a very slow cut-off. It can be made photographically in the manner described in Part III, or visually with somewhat less accuracy by studying the same intensity changes considered in Fig. 16 and 17.

The correct resistance must be obtained for each Kerr cell and for each length of leads to it, the value for short leads being normally between 5 and 25 percent of the critical resistance. For exact work, the adjustment should be made at the pressure and gap length to be subsequently used as the rate of fall of the spark gap voltage varies with gap length and pressure and hence the necessary damping resistance also varies (see Table II). It is hardly necessary to say that the damping resistances must be distributed linear resistances symmetrically spaced, a half on either side of the cell. An assortment of chromel high resistance wire was used in the present study with resistances as high as seven ohms per cm. At the frequencies encountered in the present work, the radio frequency resistance is almost identical with the direct current resistance.*

There remains to be mentioned one essential experimental condition which has apparently been neglected by all previous experimenters. To provide a path of variable length between spark gap and Kerr cell, a four wire "trolley" with two moveable jumpers is usually used. With such an arrangement there is normally a considerable length of the trolley system which, though not functioning as a part of the path between gap and shutter, is nevertheless electrically connected to the circuit. This unused section of the trolley causes a large delay in the closing of the shutter. The action is probably quite involved but the essential factor is the electrostatic capacity of the unused section. This constitutes in effect a condenser connected across the mid-point of the leads to the Kerr cell and which must be discharged before the shutter can close. An actual example will illustrate the magnitude of its effect. A four wire trolley with wires 4.5 meters long provided a 9 meter path from gap to shutter and hence gave a path time of cut-off 30×10^{-9} sec. (the light path was so small it can be neglected in this discussion). The connection of an additional 8 meter section of trolley onto the above without moving the trolley (i.e. leaving the path still 9 meters) caused a delay in the cut-off of about 12×10^{-9} sec., that is, caused an increase of

* The values of the ratio r.f./d.c. resistance found by von Hamos (reference 8) are apparently somewhat in error since what was actually measured was the r.f. resistance of the leads *plus* the effective spark resistance.

40 percent in the path cut-off time. A 4 meter section gave a retardation of about 6×10^{-9} sec. An obvious experimental way to avoid the difficulty is to divide the trolley into many short insulated sections, and connect with short jumpers as many sections as are needed.

Part V. Discussion

The nitrobenzene Kerr cell as developed in the present work has several important advantages over the carbon bisulphide cell used in previous work. The most important of these is probably the reduction in capacity with the consequent faster cut-off. Eq. (17) shows that cells designed for the same voltage V_0 and having the same aperture for light wa but using various liquids will have capacities proportional to the ratio k/b where k is the dielectric constant and b the Kerr constant. This ratio for nitrobenzene is 1.07×10^{6} and for carbon bisulphide 7.65×10^{6}, thus the capacity of the later would be approximately seven times that of the former. Further, the length of an equivalent carbon bisulphide cell is approximately 100 times that of a nitrobenzene cell since the Kerr constant of nitrobenzene is 100.7 times greater (see Eq. (15)). Thus the cell equivalent to the one illustrated in this paper would have a length of about 121 cm instead of 1.0 cm (the edge effect being allowed for). In other words, it is not feasible to build a carbon bisulphide cell which will give 100 percent initial transmission for voltages less than say 50,000 volts. If the length of the previous carbon bisulphide cell is reduced to the usual 12 cm, its initial transmission at the rated voltage is reduced by a factor of 1/665.

It should be mentioned that the results of the theoretical section, Part II, are strictly true only for light in a narrow band of wave-lengths near to that for which the Kerr constant was chosen (5460A). As seen from Eq. (4) the value of the field E_m which gives maximum (i.e. 100 percent) transmission is inversely proportional to the square root of the Kerr constant b. For longer wave-lengths the Kerr constant decreases, hence E_m would be larger. For example at 6000A, b has decreased to 3.04×10^{-5} and for the same voltage the E_0/E_m ratio becomes 0.94. Conversely for a shorter wave-length, say 4800A, b has increased to 4.17×10^{-5} and E_0/E_m becomes 1.10. The effect on the transmission curves can easily be estimated from Fig. 10. The justification for choosing b at a wave-length of about 5500A is that both the eye and the photographic plates used are most sensitive in the blue region, furthermore it is probable that a majority of the visible spark energy is also in the blue.[6]

It is noted that no account has been taken in this paper of a possible lag in the Kerr effect. The existence of such a lag has never been demonstrated and its magnitude is probably less than any of the time intervals dealt with in this paper.[16]

The complete agreement between the theory here presented as to the manner of closing of the shutter and all obtainable experimental data

[16] Beams and Lawrence, Jour. Frank. Inst. **206**, 169 (1928).

indicates convincingly the general correctness of the former. Further, since the shutter action can now be definitely determined, a tool is available for the *quantitative* analysis of the light from very rapidly varying phenomena. The electrooptical shutter is ideally adapted for the study of spark breakdown since the spark itself controls the shutter, but it will undoubtedly be adapted to other fields of study possibly by the use of impact instead of static breakdown as the source of the controlling voltage.

In conclusion I wish to thank Professor E. O. Lawrence for many helpful discussions and suggestions. I also wish to thank Mr. T. K. Kostko for his help in the somewhat lengthy computations involved in the theoretical section.

Note added in proof: Von Hámos[8] has made the ingenious suggestion that two shutters be connected electrically in parallel but arranged optically in series to obtain a faster cut-off. The capacity curves $c = 7.35$ and 14.7 of Fig. 11 provide a means of estimating how this arrangement would function. Assuming two cells with the smaller capacity, 7.35×10^{-12} farads, the square of the ordinates of the 14.7 curve would represent the net transmission. The time to close of this squared curve is 4.05×10^{-9} sec. as compared with 4.4×10^{-9} sec. for a single shutter, so that the improvement is small. However, the light passed by oscillations should be negligible. This last would be a decided improvement when making observations at early times.

AN OPTICAL STUDY OF THE FORMATION STAGES OF SPARK BREAKDOWN

By Frank G. Dunnington
University of California

(Received August 25, 1931)

Abstract

With the electrooptical shutter described in the preceding paper a visual and photographic study has been made of the manner in which a static breakdown occurs in an air gap with an approximately homogeneous initial field. The study covered a range of pressures P from 20 to 76 cm of Hg and gap lengths δ from 1.25 to 10 mm. The manner of breakdown for any condition can be told by the product $(P^{1/3}\delta)$: for values less than 11.9 the breakdown starts at the cathode; for values greater than 11.9 there are two initial breakdown regions, one at the cathode and one out in the gap. The exact manner in which the breakdown proceeds is shown and discussed in detail. The effect of space charges on the time required for the gap to completely breakdown is also shown and a possible arrangement of space charges is suggested which would explain the phenomena observed. Data on the rate of voltage fall of the gap are given.

Introduction

IN SPITE of the extensive amount of experimental work which has been done in the study of spark phenomena, the exact manner in which a gap breaks down, that is becomes conducting, has remained unknown. This is due not only to the complexity of the phenomena occurring but even more to the extremely short times required for this breakdown. Much theoretical work has also been done, most of which has been based on the theory of Townsend.[1] A fundamental difficulty encountered has been to explain how positive ions at the average fields existing at breakdown can supply a sufficient number of electrons in the vicinity of the cathode to maintain the discharge. As pointed out by Loeb[2] and others the difficulty is undoubtedly due to neglect of the distortion of the field caused by space charges. Several interesting attempts have been made to show more exactly how this distortion takes place. Von Hippel and Franck[3] in an attempt to explain the short times required for impact breakdown postulated a mechanism in which several successive electron bursts travelling the length of the gap produce an increase in field strength near the cathode sufficient to cause the positive ions to ionize. For the same problem Loeb[4] postulated a "chain" mechanism in which, under the action of a suddenly applied field, the ions existing in the gap from natural sources produce space charges in travelling 1 or 2 mm sufficient to cause *local* fields large enough to result in ionization by positive ions. Schumann,[5] considering static breakdown has made a more exact solu-

[1] Townsend, Electricity in Gases, Oxford, 1915.
[2] Loeb, Jour. Frank. Inst. **205**, 305 (1928); also Science **69**, 509 (1929).
[3] Von Hippel and Franck, Zeits. f. Physik **57**, 696 (1929).
[4] Loeb, Science **69**, 509 (1929).
[5] Schumann, Zeits. f. tech. Physik **11**, 58, 131 and 194 (1930).

tion of the differential equation connecting the ionization processes and has shown that the dark currents immediately preceding breakdown can produce large distortions of the field, the field at the cathode being increased and that at the anode reduced. This would lead one to expect the breakdown to start at the cathode and proceed toward the anode. Schumann also showed that the magnitude of the field distortion should increase with gap length and with pressure. A limitation to this, as well as other mathematical theories, is that they are valid only during the dark stage of the breakdown and do not apply to the stage in which an actual conducting filament is forming.

Realizing the lack of any experimental basis upon which a more complete theory could be built, this experimental investigation was undertaken to determine, if possible, the exact manner in which a gap does break down, that is, whether the conducting filament builds out from the cathode as indicated above, or proceeds in some other manner. The investigation was confined to a study of static breakdown in air. Simultaneously with it a

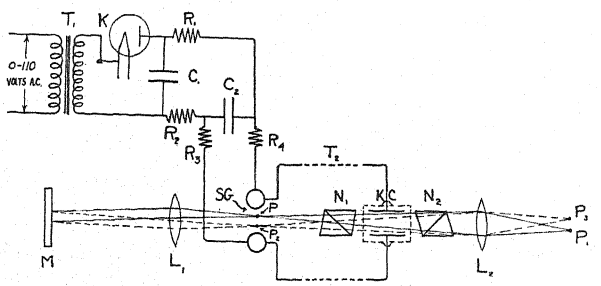


Fig. 1. Diagram showing electrooptical shutter with high voltage supply for spark gap.

study of impact breakdown has been made by von Hámos.[6] The present work has been in progress since the publication of a previous paper[7] which recorded the results of a study of both the form and spectrum of sparks during stages *after* a conducting filament has formed across the gap.

Apparatus

The only feasible method of experimental attack seemed to be the optical one using the electrooptical shutter. However, the electrooptical shutter as previously used by the author[7] and others did not yield results. It was seen that considerably more knowledge regarding its manner of action was needed before satisfactory results could be obtained. Such a development was undertaken, the results of which are given in the paper preceding this one. Reference is made to it for the theory and technique employed in utilizing the shutter in this study.

A diagram of the electrical and optical essentials of the apparatus is given in Fig. 1. The diagram shows the electrooptical shutter as described in the preceding paper together with the source of high voltage d.c. (0–20,000 volts). The alternating current supplied to the transformer T_1 (1 kw, 25,000

[6] Von Hámos, Ann. d. Physik 7, 857 (1930).
[7] Lawrence and Dunnington, Phys. Rev. 35, 396 (1930).

volts) was rectified by the kenetron K and filtered by the large filter condenser C_1 (0.024 mf). The spark gap SG was fed directly from the smaller condenser C_2 (0.008 mf). Upon breakdown, the discharge of the latter through the gap was aperiodic due to the slight overdamping of this circuit by the distributed linear resistances R_3 and R_4 (25 ohms each). The length of each lead connecting C_2 with SG was 75 cm, which means that the energy from the condenser began to feed into the gap 5×10^{-9} sec. after the beginning of the breakdown. The automatic recharging of C_2 from C_1 required possibly a tenth of a second due to the high resistances R_1 and R_2 (400,000 ohms each). The magnitude of the voltage impressed on the gap could be controlled by a potentiometer input to the primary of T_1 (not shown). The frequency of breakdown of the spark gap was controlled by a vernier adjustment of the voltage input, an increase in the voltage causing an increased frequency of breakdown, since the time lag is an inverse function of small overvoltages. All photographic work and part of the visual was done with essentially no overvoltage, the frequency of breakdown being quite erratic but averaging about 30 a minute. The other visual work was done with a frequency of about 60 to 120 a minute to give a fair persistance of vision, and required overvoltages less than a half of a percent. When possible such observations were checked at no overvoltage.

The spark gap SG consisted of two brass spheres of 4 cm diameter. These provided a fairly homogeneous field, the ratio of the maximum to the minimum field being 1.034 with a 2 mm gap and 1.173 with a 10 mm gap. The use of larger spheres to give a greater homogeneity made observation and photography difficult due to the large sidewise movement of the spark. The spheres were mounted in a glass chamber, the distance between them being varied by a screw feed working through metal bellows. The electrodes could be removed readily and were polished and cleaned with alcohol frequently. To provide constant experimental conditions, absolutely dry air was supplied to the spark chamber through a conventional drying system. Before each run, the system was pumped down for an hour or more at a pressure of about 10^{-5} mm of Hg. Liquid air traps on inlet and outlet sides of the spark chamber insured the absence of all vapors.

An essential auxiliary apparatus was a quartz mercury arc, the light from which was focused on the cathode of the spark gap to provide a continuous supply of photoelectrons. Since a perfectly black background is necessary for the observation of the faint early stages of the spark, all visible light from the arc was removed by use of a large quartz prism.

Another auxiliary apparatus was a specially constructed voltmeter to read the potential applied to the gap. A short period galvanometer, shunted to reduce its sensitivity to a full scale deflection (50 cm) at one milliampere, was placed in series with a twenty megohm resistance, the whole apparatus completely shielded and connected directly across C_2. Normally the voltmeter was disconnected after the breakdown potential had been measured. This allowed much better control of the voltage and left no steady current drain from C_1 and C_2 to cause a slight voltage ripple.

Experimental Results

Preliminary results giving the type of breakdown at various combinations of pressure and gap length indicated the necessity of a comprehensive survey of the manner of breakdown over a range of pressures and gap lengths in order that the way might be paved for a general understanding of the phenomena. Such a survey was undertaken over a range of pressures from 20 to 76 cm of Hg and for gap lengths from 1.25 to 10 mm. The range of the survey was also limited by the breakdown voltage, no condition being studied with a breakdown voltage below 3,500 volts or above 20,000 volts. The results are presented in Fig. 2. Each rectangle shows the step by step development of the spark at the pressure indicated at the left and the gap length below. The polarity is indicated at the right. The number at the top of each spark gives the time at which the shutter began to close as measured from the beginning of the voltage drop on the spark gap (i.e. these numbers are path times—see Part I of the preceding paper). At the time this survey was made it had not been found possible to photograph single sparks, hence the results shown are very carefully made pencil drawings. Each drawing was made directly after observation and was checked many times in order that it would accurately represent a typical spark. The length of each spark has been drawn the same, no matter what the actual gap length, so that the change in scale must be allowed for.

In general it is seen that the manner of breakdown varies continuously with both gap length and pressure. The expectation that the breakdown would start at the cathode and proceed across to the anode is seen to be fulfilled for sufficiently short gaps or sufficiently low pressures. The predominant role played by space charges is evident from the discrete regions of initial breakdown. The increasing effect of these space charges is noted as the gap is lengthened and the pressure increased, inasmuch as the initial breakdown region separates from the cathode and moves farther and farther out into the gap. Under such conditions there are two initial regions of breakdown: one out in the gap and one at the cathode. Still further increase of gap or pressure tends to subdue the cathode region. In all cases there is a third distinct region at the anode which appears during later stages of development. The central region always connects with the cathode first and with the anode last.

Before discussing these results further, some points should be mentioned which it has been impossible to show in Fig. 2, or which, though shown there, should be emphasized:

Multiple filament. One of the most interesting observations made in this study was the multiplicity of the filament frequently seen in the region between the cathode and central bright region as the two are connecting. The filament there, though frequently appearing single, is many times composed of a bundle of intertwined filaments, each apparently representing a different electron path. This was noted at all observed pressures at gap lengths of 7 mm and greater. Another multiplicity was sometimes observed immediately in front of the anode as the central region and the quite short anode region

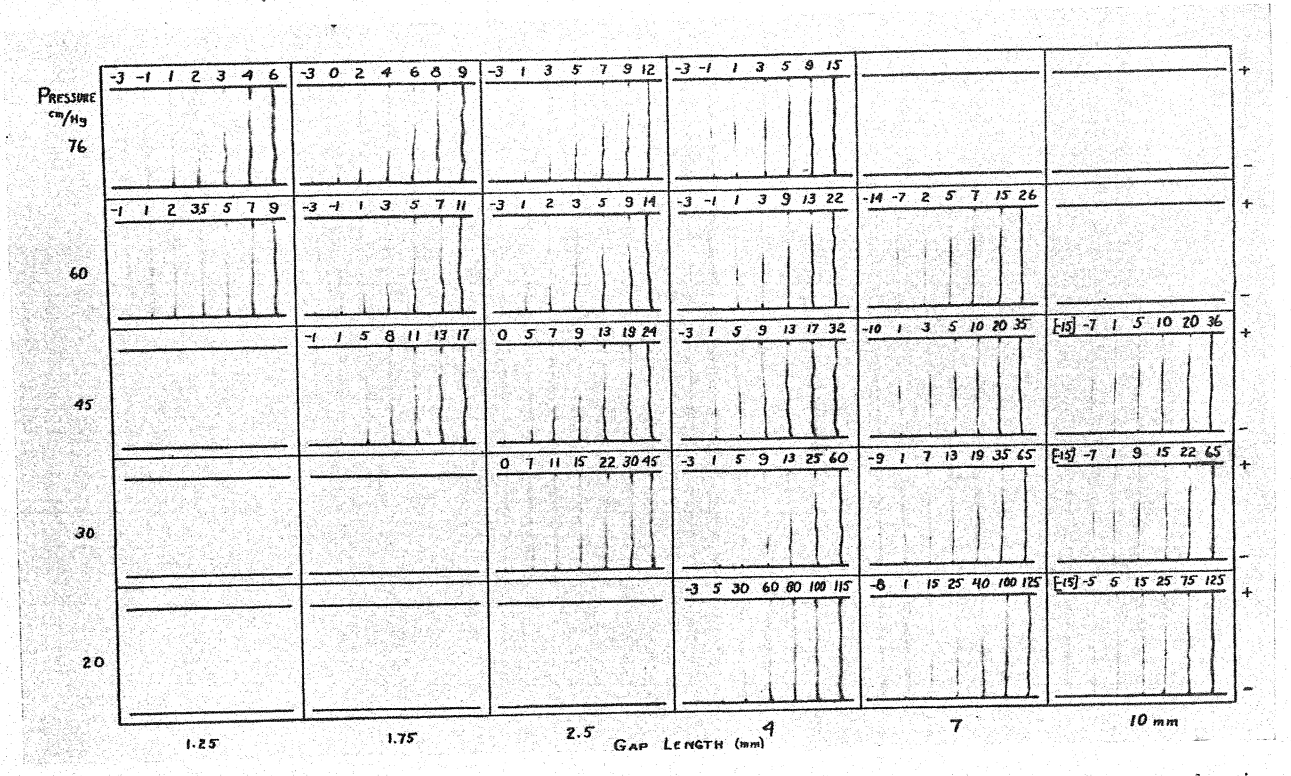


Fig. 2. Step by step development of the breakdown of a spark gap from an initially homogeneous field, shown as a function of pressure and gap length. Times given above each spark are in units of 10^{-9} sec.

began to connect. This multiple region was short and composed of two or three fairly well separated filaments. It was noted at medium to large gap lengths and pressures.

Fanning out of early haze. The hazy streak noted before the bright filament forms, and which extends from cathode (or the cathode region) to the anode, starts from a point at the cathode and widens out as it travels to the anode. This is probably due to the mutual repulsion of the electrons. Observed at medium to small gap lengths and pressures, especially at lower pressures.

Break in filament. A break or discontinuity in the filament was occasionally observed in the central part of the gap, or more frequently in the region between the center and the cathode. The break is probably due to two electron paths which have not quite joined together, and indicates that the *breakdown is not accomplished by electrons travelling the complete length of the gap but rather that it occurs in sections.* Observed under most all conditions but especially when space charges are large.

Irregularity of degree of development. No two sparks are ever exactly alike. Those shown in Fig. 2 are typical. Further the degree of development varies somewhat from breakdown to breakdown. Especially is this true for short gaps where the rate of development is rapid.

Intensity of image. The general intensity increases rapidly with increasing gap length (especially above 4 mm) and somewhat more slowly with pressure. This is entirely independent of the variation with voltage of the amount of light transmitted by the shutter. The intensity was *very high* for conditions corresponding to the upper right diagonal of Fig. 2 and *very low* along the lower left diagonal. There is a decided increase in sharpness of the image at longer gap lengths and higher pressures. Considering the relative intensity of various parts of the same image, there is undoubtedly an overshooting of the visual brilliance sensation, which overshooting increases with energy. This results in a greater apparent contrast (see Fig. 16 and discussion in preceding paper).

Since the completion of the survey given in Fig. 2, the photographic technique has been improved through the use of faster plates so that now single sparks can be photographed in a partially developed stage. Fig. 3 shows a series taken at a pressure of 76 cm of Hg and a gap length of 5 mm. The path times are given below each photograph. Two interesting breaks in the filament are recorded, one in the sixth picture where a short faint filament originates to the left of the end of the main filament and continues on to the anode and another in the next picture to the right where the break occurred earlier in the growth of the central region toward the anode and at the stage recorded has almost closed. It should be mentioned that no asymmetry has been observed in the present study in respect to the thickness of the filament at the cathode and anode in the later stages after the filament is completely across. The asymmetry reported in a previous paper[7] was apparently due to the shape of the electrodes used (parallel faces with sharp corners).

It is of interest to consider the relative effectiveness of pressure and gap length in increasing space charges and altering the manner of breakdown. The solid curve of Fig. 4 represents the condition in which the central region is just separating from the cathode region, that is, above the curve there are

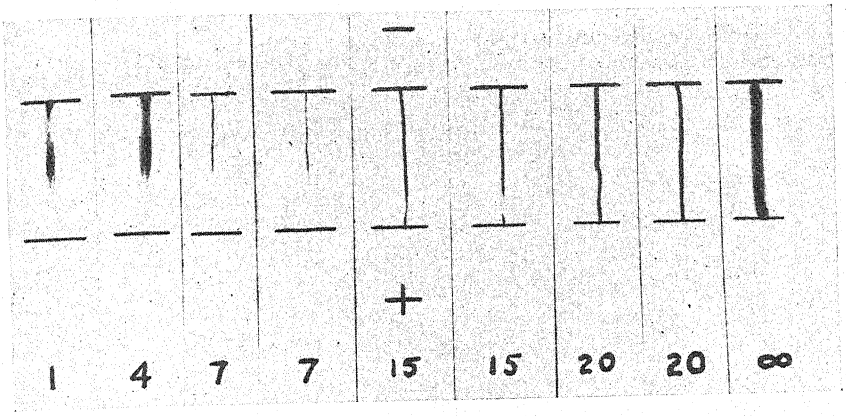


Fig. 3. Photographs of sparks showing the development of the breakdown. The first two are composite photographs, the remainder are single exposures. Pressure = 76 cm of Hg, gap length = 5 mm. Path times are indicated below in units of 10^{-9} sec.

two initial regions of breakdown and below only one. The curve is not a hyperbola since the product $(P\delta)$ is not a constant. However, as shown by the dotted line, the product $(P^{1/3}\delta)$ is very nearly a constant and equal to 11.9 if pressure is in cm of Hg and gap length in mm. Thus we may con-

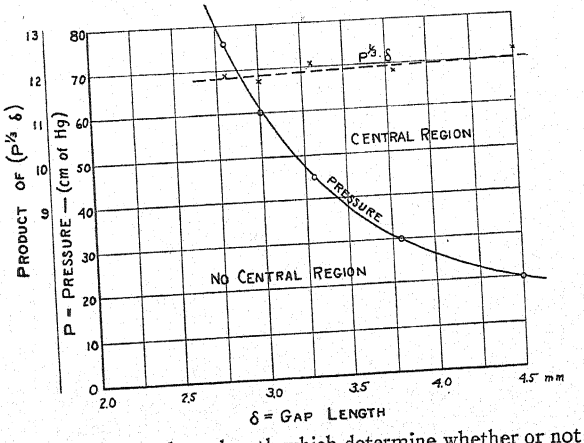


Fig. 4. Conditions of pressure and gap length which determine whether or not there is a separate central region of breakdown.

veniently say that if $(P^{1/3}\delta) < 11.9$ there is one initial breakdown region and if $(P^{1/3}\delta) > 11.9$ there are two such regions. *Pressure is therefore less effective than gap length in the production of space charges.* Space charges, however, increase with both, thus confirming Schumann's prediction.[5]

The movement of the central region (i.e. center of it) out from the cathode with increasing gap length is shown for various pressures in Fig. 5. The distance from the cathode is seen to increase almost linearly with increase in gap length but approximately only 0.6 as fast. The lower end of each curve stops at the gap length at which the union between the cathode and central region occurs (corresponding to the data of Fig. 4). The validity of the product rule determined above may now be further tested, for the $(P^{1/3}\delta)$ products of all combinations of pressure and gap length which give the same distance of the central region from the cathode should be the same. For example consider those which give a distance of 2 mm: the $(P^{1/3}\delta)$ products for the five pressures given on Fig. 4 are, in order of decreasing pressure, 19.1, 18.8, 18.9, 18.5, 18.2. The maximum deviation from the average of

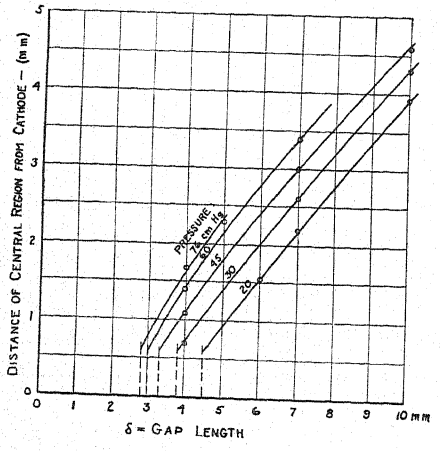


Fig. 5. Distance of the central breakdown region from the cathode, shown as a function of the length at various pressure.

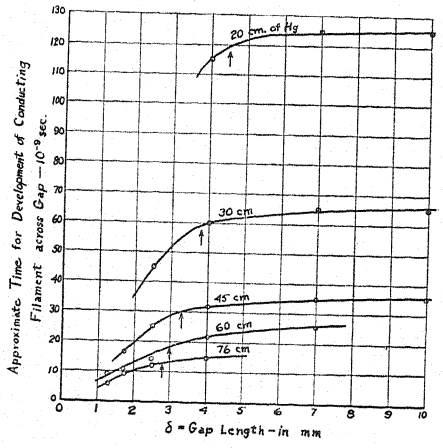


Fig. 6. Approximate time for development of conducting filament across the gap.

18.7 is only 2.7 percent. Hence the product $(P^{1/3}\delta)$ may be used as an indicator of the type of breakdown to be expected from any combination of pressure and gap length: if the product is less than 11.9 the initial breakdown is at the cathode, if equal to 15.5 there is in addition a central region 1 mm from the cathode, if 18.7 the latter is 2 mm from the cathode, if 24.0 it is 3 mm, if 29.4 it is 4 mm, etc.

The last time given in each rectangle of Fig. 2 represents the path time at which the filament first appears to be developed completely across the gap. A plot of these times as a function of the gap length is given in Fig. 6. The increase of time with increasing gap length is almost linear for short gaps, then there is a break, beyond which the time is nearly constant. The interesting fact is that this break occurs in each case at just that set of conditions at which the central region begins to separate from the cathode. That is, the break occurs at the conditions corresponding to any point on the curve of Fig. 4. These conditions have been indicated by arrows on Fig. 6.

This means that *for gap lengths beyond this break-point the increased space charges produce an increase in field strength just sufficient to speed up the breakdown so that, in spite of the longer gap, the breakdown is completed at about the same time.* The increase in time with decreasing pressure, the gap length being held constant, should also be noted, the increase being especially rapid below a pressure of 45 cm. This increase is to be expected both from the decrease of space charges with decreasing pressure and also the decrease in the ionization coefficients.

The effect of the distance of the reservoir condenser (C_2, Fig. 1) from the spark gap has a marked effect on the rate of development of the breakdown. Thus with a pressure of 76 cm of Hg and a 5 mm gap, the path time for development completely across with the condenser 75 cm away is 16×10^{-9} sec., while if the condenser is 300 cm away 22×10^{-9} sec. are required. Further the intensity of the filament is much less in the latter case in spite of the later time. In relation to the variation of the intensity at a given stage of development, see Fig. 15 of the preceding paper.

The effect of ultraviolet light on the cathode should be mentioned. No detailed study was made, but in general the breakdown without the ultraviolet light was very irregular in form. For instance, in a breakdown normally having a distinct cathode and central region at a certain stage, the two regions are frequently completely joined together and this single filament may extend beyond where the central region would normally be, or it may end short of where the normal central region would be. This indicates that *the space charges built up by the steady photoelectric current just prior to breakdown have a considerable influence on the manner of breakdown.* This is also shown in the well-known increase in breakdown potential when the ultraviolet light is removed. The results of Masch[8] on this point were checked in order of magnitude. Thus at atmospheric pressure the increase with a 3 mm gap was about 0.4 percent and with a 5 mm gap about 3 percent.

The effect of overvoltage is quite similar to that of the removal of the ultraviolet light in both the irregularity of the breakdown and the behavior of the central region. The development is usually somewhat more complete at any given time of cut-off.

Oxidation of the sparking surface of the electrodes which gradually occurs during a number of successive breakdowns produces almost exactly the same effect as removal of the ultraviolet light when the electrodes are clean. This is probably due to the fact that the photoelectric effect from the oxide surface is very small or nil. Hence when the spot on the cathode has become completely oxidized and of sufficient size there is no longer an appreciable number of photoelectrons crossing the gap in the region of the highest field strength. The breakdown then becomes both irregular in time as well as in form and requires a slightly higher potential.

There remains one important point, namely the interpretation of the path times given in Fig. 2 and 3 in terms of actual times at which the stage of development recorded took place. In Fig. 19 of the preceding paper an

[8] Masch, Archiv. f. Elektrotechnik **24**, 561 (1930).

experimentally determined correction curve was given for the increase in lag of the shutter relative to that at the time $t_p = 0.7 \times 10^{-9}$ sec. This curve applies for a pressure of 76 cm of Hg, a gap length of 5 mm and the particular Kerr cell used (capacity $= 14.7 \times 10^{-12}$ farads). In Fig. 15 of the same article the effective time of complete closing for the same set of conditions was found to be 10.3×10^{-9} sec. However, in Fig. 13 giving the computed closing curve T_1 for the same conditions and an assumed intensity increase I, it is seen from the transmitted light curve IT_1 that the stage of development would be about that at 7×10^{-9} sec. The actual time t_A corresponding to any path time t_p can now be computed as follows:

$$t_A = [7.0 + (t_p - 0.7) + L_p] \times 10^{-9} \text{ sec.}$$

where L_p is the increase in lag as obtained from Fig. 19. The accompanying table gives the results:

Path time $t_p =$	0.7	2	4	6	8	10	12	15	18 $\times 10^{-9}$ sec.
Actual time $t_A =$	7.0	9.5	13.0	16.2	19.1	21.8	24.3	27.9	31.5×10^{-9} sec.

As indicated before these results are for the set of conditions: pressure $= 76$ cm of Hg, gap length $= 5$ mm and Kerr cell capacity $= 14.7 \times 10^{-12}$ farads. A rough determination of the correction curve with the same Kerr cell but with a pressure of 37 cm and a 10 mm gap gave a curve substantially the same but lying slightly above. Time and the magnitude of the task prevented the obtaining of the actual times for other conditions. In general the actual time corresponding to any given path time will increase slowly with increasing length of time for completion of the filament across the gap (effect of rate of voltage fall on tap—see Fig. 8 of preceding article) and will increase more rapidly as the breakdown voltage is reduced (effect of increasing capacity of Kerr cell necessary at lower voltages—see Fig. 11 of preceding article). In making the survey a group of Kerr cells was used having capacities varying from 10 to 50×10^{-12} farads.

Discussion

The most outstanding feature of the results of this study is the demonstration of the predominant role played by space charges in influencing the manner of breakdown. No theoretical treatment or explanation of these space charges will be attempted here but the following simple and very approximate suggestion as to the probable distribution of charges in the gap may be of interest. Application of Gauss' theorem to a differential length of a tube of force in an electric field gives the well-known result that the field gradient dE/dx at any point x is proportional to the charge density ρ at the point. If now, the assumption is made that the field strength existing in the first stage of breakdown—that is, at the time the initial breakdown regions begin to appear—is approximately proportional to the luminous energy distribution, the upper curves of Fig. 7 are obtained. The group (1) corresponds to a breakdown such as that at a pressure of 76 cm and a gap of 4 mm, the group (2)

to a breakdown such as that at a pressure of 20 cm and a gap of 4 mm. The average field $\bar{E}$ is indicated by the dotted lines. Using these E curves and the mathematical relation stated above, the space charge curves given in the lower half of Fig. 7 result. In the two region type of breakdown there are seen to be three major space charge regions, two being positive and one negative, while in the one region (cathode) type of breakdown there is only one major region, it being positive and of irregular strength. In both cases there is probably a small negative charge in front of the anode. Comparison of the two density curves shows that the separation of the central breakdown region from the cathode region is due to the appearance of a negative charge in the middle of the original long region of positive charge. It is interesting to note that the multiplicity of filament frequently observed in later stages of the breakdown occurs in exactly the regions occupied by the negative charges in Fig. 7.

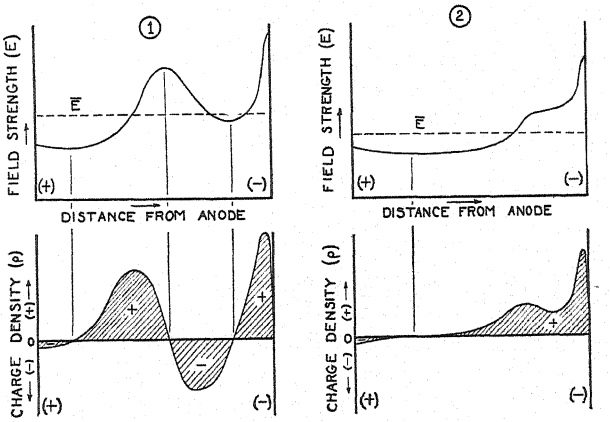


Fig. 7. Approximate field strength and distribution of space charges in the first stage of breakdown, (1) in type with cathode and central bright regions, (2) in type with cathode region only.

It is to be emphasized that the assumption on which the foregoing discussion is based may or may not be correct. It certainly would not be valid for any later stages when a partial filament has formed, for then the field would be highest just at the end of the filament (where the intensity is low) and lowest in the most completely developed (i.e. brightest) part of the filament. The above treatment, if valid, applies to the field and charges which *produce* the first section or sections of the filament.

Considerable work has been done with the cathode ray oscillograph in the study of the manner of voltage drop across the spark gap during an impact breakdown but as far as is known to the author only one picture has been obtained of a static breakdown. This picture, obtained by Rogowski and Klemper[9] indicated that at atmospheric pressure and a breakdown potential of 9000 volts (about a 2.5 mm gap) a time of 25×10^{-9} sec. was required for the voltage to fall to about 25 percent of its original value. As

[9] Rogowski and Klemper, Archiv. f. Elektrotechnik **24**, 127 (1930).

mentioned in the preceding paper, this present study gives further information on the rate of fall. At atmospheric pressure and a 5 mm gap, experimental data combined with theory indicate a voltage collapse to 20 percent of the initial value in 14.3×10^{-9} sec. (that at 2.5 mm would probably be smaller). An additional study at a 37 cm pressure and 10 mm gap gave a time of 28.5×10^{-9} sec. for the voltage to fall to 20 percent. A paper by Street and Beams[10] has just appeared giving potential collapse curves computed by a new method developed by them. In their results the exact location of the beginning of the voltage break on the gap is indefinite, but estimating it as closely as possible their results indicate a time of 21×10^{-9} sec. for the voltage to collapse to 20 percent at a pressure of 76 cm of Hg and a potential of 17.7 kv (about a 5.4 mm gap). Comparing their potential time curve for this condition with that of the author for the same pressure and a 5 mm gap (see Fig. 6 of preceding paper, $m=0.21\times10^{9}$), the slope is found to be almost the same for voltage values from 80 to 40 percent of the initial, but the curve falls more slowly for higher and lower values. Their results involve the assumption that the static and impact breakdown values are identical under the conditions of their experiment. Hence, the times obtained by them are equal to or greater than the true values. The time from Rogowski and Klemper's work can be similarly classified, while that obtained by the author is equal to or less than the true value. Hence, the only conclusion now possible is that, at atmospheric pressure and a gap of the order of 5 mm, the time for the voltage to collapse to 20 percent of its initial value lies somewhere between 14 and 25×10^{-9} sec. The author's results are incompatible with a value as large as the latter.

It should be emphasized that most of the experimental results of this paper were possible because it was discovered that the eye is a far more sensitive recorder of these extremely short pulses of light than any photographic plate. Even in the more recent photographic work, such as shown in Fig. 3, much of the detail is lost due to the present photographic limitations. Photographic studies, if feasible, would of course be far superior to visual observations.

The present study has hardly more than opened up a large field for investigation. The work will be continued, with a spectroscopic study of the light one of the immediate objectives.

It is again a pleasure to thank Professor E. O. Lawrence for many helpful suggestions.

[10] Street and Beams, Phys. Rev. **38**, 416 (1931).

THE STRUCTURE SENSITIVENESS OF MAGNETISM IN METALS

By F. E. Lowance and F. W. Constant
Duke University

(Received June 8, 1931)

Abstract

The magnetic susceptibility of copper, silver, platinum and bismuth was measured for the annealed state and after various degrees of cold work. The cold work consisted of twisting, stretching and pounding. In every case the cold work decreased the diamagnetism (Cu, Ag, Bi), or increased the paramagnetism (Pt). This probably explains the variation in the measured values of metallic susceptibilities as due to a structure sensitiveness. This is attributed to the increase in the paramagnetic contribution of the partly bound electrons of the metal due to the cold work; the electrical conductivity is usually decreased.

IT HAS recently been pointed out by Bitter[1] that there is considerable lack of agreement in the experimental values of the magnetic susceptibilities of certain metals as determined by different observers, and that the experimental errors are not nearly large enough to account for these discrepancies. Corrections have even been made for ferromagnetic impurities, without success. It is concluded that the susceptibility is a structure sensitive property.

The effect of internal strains on the magnetic susceptibility was first pointed out by Seeman and Vogt,[2] who investigated certain Cu-Au alloys in both the quenched and annealed states. Honda and Shimizu[3] have measured the effect of high pressures on the susceptibility of copper and silver, and Bitter and Foladare stretched wires of copper and silver. In every case the susceptibility has been found structure sensitive. This is not surprising, for we attribute magnetic properties to the conduction electrons in metals and we know that other properties attributed to these electrons, such as conductivity, are structure sensitive, and hence we should expect the susceptibilities to be too.

In order to investigate this matter further the experiments of Bitter and Foladare were extended. Wires of copper, silver, platinum and bismuth, guaranteed of high purity, were secured from Baker & Co. They were from 20 to 30 cm in length and from 0.77 mm, (in the case of platinum), to 2.00 mm in diameter. The susceptibility was measured by the Gouy method,[4] one and sometimes two wires being suspended from one arm of a delicate chainomatic balance, sensitive to 1/50 milligram for the light loads used. The scale

[1] F. Bitter, Phys. Rev. **36**, 978 (1930).
[2] H. J. Seemann and E. Vogt, Ann. d. Physik **2**, 976 (1929).
[3] K. Honda and Y. Shimizu, Nature **126**, 990 (1930).
[4] See E. C. Stoner, Magnetism and Atomic Structure, p. 40.

pans were removed and the weights placed on a paper pan suspended from the other arm. The lower end of the wires hung at the center of a solenoid 14 cm long, core diameter 1 cm, wound with 2900 turns of #19 copper wire. The solenoid carried a current of 8 amp., giving a field at its center of about 2100

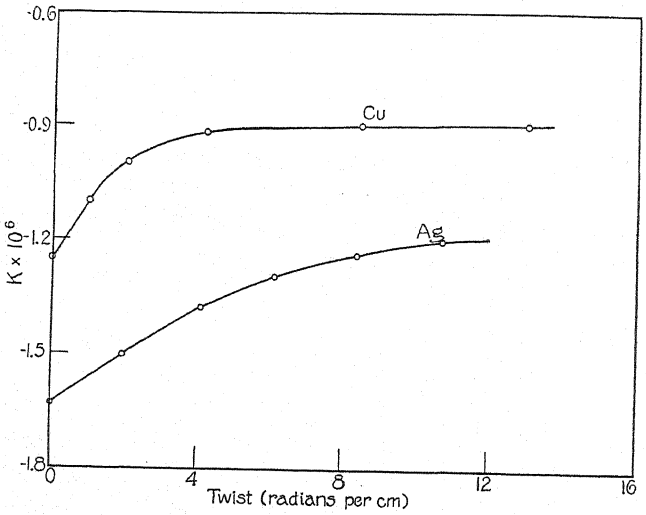


Fig. 1. Twisting-susceptibility curves for Cu and Ag.

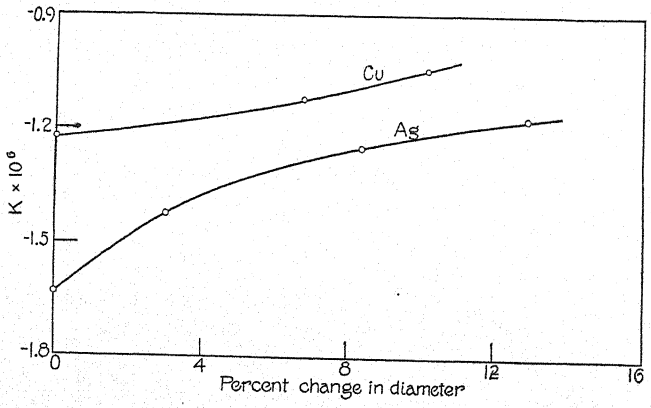


Fig. 2. Stretching-susceptibility curves for Cu and Ag.

gauss. The change in weight in grams due to the magnetization of the suspended wire is given by

$$\Delta w = kH^2A/2 \times 980$$

where k is the volume susceptibility, H the magnetic field and A the cross-sectional area of the wire. This amounted to about 0.2 milligrams in the case of the copper, which had the smallest numerical value of k. The average of six readings was always taken.

The mechanical treatment or cold work consisted of twisting, stretching and pounding. In every case care was taken not to contaminate the specimens with small impurities of iron. The twist was measured in radians per cm of length, the stretching by the percent change in the diameter. The twist-

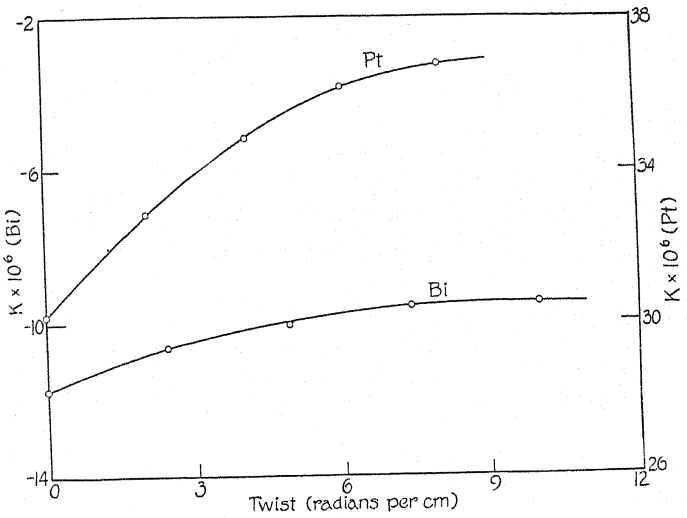


Fig. 3. Twisting-susceptibility curves for Pt and Bi.

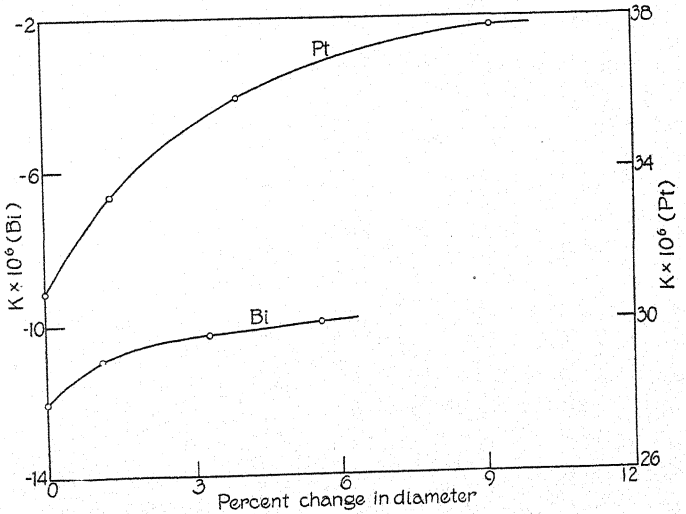


Fig. 4. Stretching-susceptibility curves for Pt and Bi.

ing or stretching was increased in successive steps, the latter usually up to the breaking point. Figs. 1 and 2 give the results of twisting and stretching for the copper and silver, and Figs. 3 and 4 the results for platinum and bismuth (plotted with reference to two different axes of ordinates). The results of the pounding are summarized in Table I.

TABLE I. *The effect of pounding on the magnetic susceptibility.*

Metal	$k\times10^6$ before pounding	$k\times10^6$ after pounding
Copper	− 1.22	−0.88
Silver	− 1.58	−1.15
Bismuth	−12.08	−9.13

In the case of the platinum one wire was twisted until an increase in k of 20 percent had been obtained, and the wire then annealed at a red heat, after which k was found to have decreased to within 2 percent of its former value.

It is evident then in every instance that cold work tends to make the susceptibility more positive, that is, to decrease the diamagnetism or increase the paramagnetism. This is in agreement with the results of Bitter, Honda and others. It was not possible to reverse the sign of k from negative to positive, but in each case where successive stages of strain were applied the change in the susceptibility approached a maximum or saturation value. This is not surprising, for cold work must be regarded as destroying the orderliness that exists in the lattices of the individual crystals of which the annealed metal is composed, and a certain amount of strain should be sufficient to make this lack of order almost complete.

It has been suggested by Bitter and also by W. de Haas[5] that the increase in k is due to the partly bound electrons. In general there are at least two contributions to the magnetism of a metal, (1) the diamagnetism of the ions or electrons completely bound to certain atoms, and (2) the predominating paramagnetism of the free electrons with their spins, which has been most successfully computed by Pauli.[6] Now it is probably doubtful if the free and bound electrons can be regarded as completely distinguishable, but rather the free electrons should be regarded as interchanging to some extent with the outermost "orbital" electrons, thus giving rise to the "partly bound" electrons. These latter will have both a diamagnetic and a paramagnetic effect. The former may account for the large diamagnetism of bismuth, where certain electrons are believed to describe large orbits about a group of atoms. The latter comes into play when the outermost orbital electrons come under the influence of the fields of electrons in neighboring atoms, and "interaction" occurs. This "interaction" has been calculated by Bloch,[7] and corresponds to Heisenberg's interaction in ferromagnetism, only when the interaction integral, J, is computed, instead of being positive, as is necessary for ferromagnetism, it will be negative for paramagnetism. The susceptibility k varies as $1/J$, from which it is seen that as the interaction of the partly bound electrons increases J becomes less negative, and hence k increases in the positive sense.

The effect of cold work is known to increase the mechanical hardness, which suggests greater binding or interaction between the atoms. It also gen-

[5] W. J. de Haas, Nature **127**, 335 (1931).
[6] W. Pauli, Zeits. f. Physik **41**, 100 (1927).
[7] F. Bloch, Leipziger Vortrage, Welleninterferenzen.

erally increases the resistance. Both phenomena indicate fewer free and more partly bound electrons. It therefore seems most logical to attribute the increase in the paramagnetism to the same cause.

It has been suggested[8] that the effect could be explained as due to a small amount of iron in solution in the annealed state, which is precipitated by cold work, becoming ferromagnetic. This is not likely in the present case because (1) the metals used were Baker and Company's purest, (2) the annealing was done slowly, and (3) the structure sensitiveness was observed similarly for metals in which iron is quite insoluble at room temperatures (Cu, Ag and Bi)[9] and for one in which iron is quite soluble (Pt); in fact iron, nickel and cobalt are all three soluble in platinum over a considerable range, alloys of 10% Ni-90% Pt and 10% Co-90% Pt having been studied microscopically by one of the authors[10] and found to be solid solutions. Hence no ferromagnetic element present in a small degree would be precipitated by cold work.

It seems therefore most acceptable to regard the structure sensitiviness of the magnetic susceptibility as due to the partly bound electrons, the free and completely bound electrons being structure insensitive.

[8] A. Kussmann and H. J. Seemann, Naturwissenschaften, **19**, 309, (1931).
[9] International Critical Tables, Vol. 2, pp 449–455.
[10] F. W. Constant, Phys. Rev. **36**, 1654 (1930).

THE ENTROPY OF POLYATOMIC MOLECULES[1]

By Donald Statler Villars
Research Laboratory, Standard Oil Co. (Indiana), Whiting, Indiana

(Received July 13, 1931)

Abstract

By counting the total number of completely antisymmetric eigenfunctions which can be formed from the rotational states, the *a priori* probabilities of the different symmetry varieties of ammonia (nuclear doublet and quadruplet) and of methane (nuclear singlet, triplet and quintet) are derived and used to compute the corresponding entropies at 298.1°K. The relative proportions of the different varieties at high temperatures are found to be equal for ammonia and in the ratio of 2:9:5 for methane (respectively). The absolute entropy of the mixture of the different forms of ammonia is calculated to be 51.5 cal. degree^{-1}, the virtual entropy (the absolute minus the nuclear spin minus the frozen rotational entropy) 44.1; the absolute entropy of methane, 50.1, and its virtual entropy 44.2 cal. degree^{-1}

THE entropy of diatomic molecules has been extensively discussed[2] but so far no values for polyatomic molecules have yet been calculated according to the newer quantum mechanical theories. In this article I shall carry out such calculations for two typical gases, ammonia and methane. In molecules such as these where there are two or more equal nuclei, symmetry characteristics in the latter arise in the eigenfunctions bringing about, since the coupling of the nuclear spins with the outer forces in the molecule is very weak, a state of affairs where it is impossible for those rotational states which are associated with one nuclear configuration to change (by radiation or collision) to states associated with another nuclear configuration by any but exceedingly low velocities unless catalyzed in a way involving complete separation of the similar nuclei and subsequent rearrangement (dissociation catalysts). The ordinary gas is thus a mixture of different varieties which are noncombining and rarely in true equilibrium except when in the presence of a dissociation catalyst or at a high temperature. The application of the considerations of Hund[3] concerning symmetry characters and electronic spins to the problem of rotational *a priori* probabilites and nuclear spins has already been discussed in detail[4] in this journal in connection with the specific heats of the different symmetry forms of methane and the reader is referred to that article as a pre-

[1] A preliminary announcement of the results contained herein was published in J. Am. Chem. Soc. **53**, L 2006 (1931). Unfortunately certain errors were made then, which are now corrected, cf. footnote 14.

[2] (a) Fowler, Proc. Roy. Soc. (London) **A118**, 52 (1928); (b) Giauque and Johnston, J. Am. Chem. Soc. **50**, 3221 (1928); (c) Rodebush, Proc. Nat. Acad. Sci. **15**, 678 (1929); (d) Villars, ibid. **15**, 705 (1929); **16**, 396 (1930); (e) Giauque and Johnston, Phys. Rev. **36**, 1592 (1930); (f) Giaque, J. Am. Chem. Soc. **52**, 4816 (1930); (g) MacGillavry, Phys. Rev. **36**, 1398 (1930); (h) Rodebush, Phys. Rev. **37**, 221 (1931); (i) Giauque, J. Am. Chem. Soc. **53**, 507 (1931).

[3] Hund, Zeits. f. Physik **43**, 788 (1927).

[4] Villars and Schultze, Phys. Rev. **38**, 998 (1931). Hereafter to be designated as V and S.

face to the present one. In that work it was decided that there must be two different symmetry forms of ammonia (the nuclear doublet and quartet) and three of methane (the nuclear singlet, triplet and quintet) just as there are two of hydrogen (nuclear singlet—"para"—and triplet—"ortho-hydrogen"). Basing the work on Hund's[5] symmetry character assignment of the rotational terms of ammonia and Elert's[6] of methane, we there deduced the *a priori* probabilities for each of the rotational states of methane. (Tabulated in V and S, Table III).

ENTROPY

The general formula[7] for the entropy of a substance is

$$S = R \ln \sum_i p_i e^{-\epsilon_i/kT} + E/T \tag{1}$$

where p_i is the *a priori* probability of state i of energy ϵ_i and the other symbols have their usual significance. It is convenient and customary to split the total entropy, S, up into its component parts[2d], in which case E represents the corresponding part of the whole energy.

$$S = S_t + S_r + S_v + S_{el} + S_{\text{mix}}. \tag{2}$$

S_t is the Sackur-Tetrode translational entropy[8]

$$\begin{aligned} S_t &= R \ln \left\{(2\pi mkT)^{3/2} h^{-3} V N^{-1} e^{5/2}\right\} \\ &= -2.2985 + R \ln M^{3/2} T^{5/2} P^{-1} \text{ cal. degree}^{-1} \end{aligned} \tag{3}$$

M being the molecular weight and P the pressure in atmospheres.

S_r is the rotational entropy and, for the polyatomic molecule of the symmetrical top form (three moments of inertia, two of which (A) are equal) is given by substituting for the rotational energy levels, ϵ_i

$$\epsilon_{j,\tau} = (h^2/8\pi^2)\left[j(j+1)/A + (1/C - 1/A)\tau^2\right] \qquad |\tau| \leqq j \tag{4}$$

and summing over all values of both τ and j.

S_v is the vibrational entropy, and is given by putting the energy level ϵ_i

$$\epsilon_v = vh\omega_k \tag{5}$$

(assuming harmonic oscillation—no appreciable error at room temperature) where ω_k is the frequency of the kth normal vibration of the molecule (in a diatomic molecule, there is only one such but in an n-atomic molecule there are $3n$–6 if it has three moments of inertia, or $3n$–5 if only two). The *a priori* probability p of each vibration is unity if one remembers to include an entropy for each of the $3n-\begin{cases}6\\5\end{cases}$ vibrations even though some happen to have the same frequency.

[5] Hund, Zeits. f. Physik **43**, 805 (1927). Tabulated in V and S, Table I.

[6] Elert, Zeits. f. Physik **51**, 6 (1928). Tabulated in V and S, Table II.

[7] Cf. any text book, for example, Taylor, Treatise on Physical Chemistry, 1st ed. Vol II, p. 1202 by Rodebush (D. Van Nostrand Co. 1925).

[8] Cf. Birge, Rev. Mod. Phys. **1**, 65 (1929).

The electronic entropy, S_{el}, is zero in the present[9] case of chemically saturated molecules (presumably $^1\Sigma$ ones with p_{el} consequently unity).

Finally the entropy of mixing, S_{mix}, must be included in those cases where one computes that of a mixture of different symmetry varieties by calculating the entropy of each separate kind and adding them together in their proportionate amounts. It is given by the familiar[10] equation

$$S_{mix} = -N_1R \ln N_1 - N_2R \ln N_2 - \cdots . \tag{6}$$

That this method leads to an identical result in calculations with diatomic molecules to that obtained by correctly treating the gas as only one substance and not a mixture has been demonstrated elsewhere[2d]. The first method is, in certain respects, simpler, and by its use one is less likely to make mistakes. I shall therefore employ it.

For the sake of convenience, it is desirable from this point on to make use of certain abbreviations customary in the literature

$$Q \equiv \sum_n p_n e^{-\epsilon_n/kT} = \sum_{j,\tau} p_{j,\tau} e^{-j(j+1)\sigma_1 - \tau^2\sigma_2} \tag{7}$$

$$\sigma_1 \equiv h^2/8\pi^2 A kT \tag{8}$$

$$\sigma_2 \equiv (h^2/8\pi^2)(1/C - 1/A)/kT. \tag{9}$$

By differentiating Q partially with respect to σ_1 and σ_2 it may be readily shown that

$$E_r/T = -R(\sigma_1 \partial \ln Q/\partial\sigma_1 + \sigma_2 \partial \ln Q/\partial\sigma_2) \tag{10}$$

and

$$S_r = R[\ln Q - \sigma_1 \partial \ln Q/\partial\sigma_1 - \sigma_2 \partial \ln Q/\partial\sigma_2]. \tag{11}$$

In the case of a rotator like methane where all three moments of inertia are the same, Eq. (11) still applies with just one term in σ ($\sigma_2 = 0$).

A similar equation may be derived for vibrational entropy

$$S_v = R[\ln Q_v - \sigma_v d \ln Q_v/d\sigma_v] \tag{12}$$

if one assumes the motion to be harmonic and understands

$$\left.\begin{aligned} \sigma_v &\equiv h\omega/kT = \Theta/T \\ \epsilon_v &= vh\omega. \end{aligned}\right\} \tag{13}$$

If σ_v is large this may be further simplified to

$$\begin{aligned} S_v &= R(1 + \sigma_v)e^{-\sigma_v} \\ &= R(1 + \Theta/T)e^{-\Theta/T} \end{aligned} \tag{14}$$

where Θ is the "characteristic" temperature.

In the subsequent calculations of the entropy of ammonia and of methane we shall concern ourselves with moderate temperatures (298.1°K) at which, on the one hand, the rotational energy is almost fully developed, but, on the

[9] A case where the electronic entropy must be considered was discussed in connection with hydroxyl[2d].

[10] Lewis and Randall, Thermodynamics, McGraw Hill Book Company (1923) p. 440.

other hand, very little vibrational energy has come into play (σ_v is large). For this reason, errors in assignment of fundamental vibrational frequencies will not affect the final result to any appreciable extent.

In order to compare our final results with experiment, one must subtract from them the entropy our gas would have at zero absolute, if it were not given time nor a catalyst to enable it to change over to its stable variety at that temperature. This is because most experimental low temperature measurements (for example, on specific heat) on which extrapolations to the absolute zero are based, are made under such conditions that true equilibrium never obtains, the proportion between the varieties remaining "frozen" in that obtaining at high temperature.

I shall now proceed to calculate the various types of entropy for ammonia and methane at 298.1°K.

The Entropy of Ammonia at 298.1°K

Translational

Substituting in Eq. (3) values for ammonia at 298.1°K and one atmosphere, I get

$$S_t^{298.1} = 34.45 \text{ cal. degree}^{-1}$$

Vibrational

For the fundamental vibrational frequencies of ammonia I take those derived from Dennison,[11] but corrected to agree with Badger and Mecke[12] from whose work I shall later use also the moments of inertia. Calculation gives (Table I)

$$S_v^{298.1} = 0.06 \text{ cal. degree}^{-1}$$

Table I. *Vibrational entropy of ammonia.*

k	$\tilde{\omega}_k$cm^{-1}	Θ B & M	(Dennison)	Θ/298.1	S_k
1	966	1380	(1346)	4.79	0.047
2, 3	1630	2330	(2330)	7.82	0.004 (×2)
4, 5	3336	4770	(4810)	16.0	0.000 (×2)
6	(4450)		(6370)		0.000
					0.055 = S_v

Rotational

The difficult part of the calculation of the entropy of ammonia lies in the evaluation of the rotational entropy. At room temperature where σ is small, the estimation of the double sum Q, may be carried out only by replacing it with a double integral, after which four steps are necessary to compare the calculated entropy with experiment; (1) decide upon the *a priori* probabilities, (2) compute the double integral, (3) determine the relative amounts of the different forms at high temperatures, and (4) subtract the "zero point" entropy.

[11] Dennison, Phil. Mag. **1**, 195 (1926).

[12] Badger and Mecke, Zeits. f. physik. Chem. **135**, 333 (1929). $A = 2.79 \times 10^{-40}$, $C = 3.40 \times 10^{-40}$ gm · cm^2.

The *a priori* probabilities of the different rotational energy states of ammonia are obtained by the following considerations.[4,5,6,13] There are four $S(3)$ (quadruplet) and two $S(2+1)$ (doublet) nuclear spin eigenfunctions, the latter type being doubly degenerate, making four in all. One may look upon this degeneracy as corresponding roughly to the case where more than one doublet of the same total L occurs in a supermultiplet in electronic spectra. The total of eight is thus exactly equal to the total *a priori* weight one would get from the hydrogen nuclei by dissociating the ammonia into its three hydrogen atoms. There is one $S(3)$ and one $S(1+1+1)$ vibrational eigenfunction for the ground vibrational level. Of the rotational levels, there are $(2j+1)$ eigenfunctions for $\tau=0$ which are alternately $S(3)$ for even j and $S(1+1+1)$ for odd j. When τ is divisible by three, there are $(2j+1)$ $S(3)$ and $(2j+1)$ $S(1+1+1)$ functions for each value of j. When τ is not divisible by three, there are $2(2j+1)$ degenerate $S(2+1)$ rotational functions for each value of j. By multiplying together all combinations and discarding any but those which come out completely antisymmetric, $S(1+1+1)$, (Pauli exclusion principle), and remembering that, according to Hund,[5] only one-fourth of the combinations of two degenerate functions, $S(2+1)$, will result in a completely antisymmetric one, $S(1+1+1)$, and another fourth will give a completely symmetric one, $S(3)$, we get the values given in Table II.

TABLE II. *Rotational weights of different varieties of ammonia.*

j	τ	Nuclear quartet $S(3)$	Nuclear doublet $S(2+1)$
0	0	4×1	4×0
1	0	3	0
1	1	0	3
2	0	5	0
2	1	0	5
2	2	0	5
3	0	7	0
3	1	0	7
3	2	0	7
3	3	7×2	0
4	0	9	0
4	1	0	9
4	2	0	9
4	3	9×2	0
4	4	0	9
		$4(2j+1)$ for $\tau=0$ $8(2j+1)$ for τ divisible by three	$4(2j+1)$ for τ indivisible by three

Generalizing the *a priori* probabilities, p, as is done at the end of Table II, one can write for the Q sums

$$ {}^4Q = \sum_{j=0}^{\infty} 4(2j+1)e^{-j(j+1)\sigma_1} + \sum_{j=0}^{\infty} \sum_{\tau\equiv 3}^{(\tau\equiv 3)\leq j} 8(2j+1)e^{-j(j+1)\sigma_1-\tau^2\sigma_2} \quad S(3) \quad (15) $$

$$ {}^2Q = \sum_{j=0}^{\infty} \sum_{\tau\equiv 1,2}^{(\tau\equiv 1,2)\leq j} 4(2j+1)e^{-j(j+1)\sigma_1-\tau^2\sigma_2} \quad S(2+1). \quad (16) $$

[13] Ludloff, Zeits. f. Physik 57, 227 (1929).

The double sum in (15) is to be taken only for values of $\tau = 3, 6, 9$ etc. up to one which may equal but not exceed the particular value of j assumed in the first summation. The double sum in (16) is taken for the remaining values of $\tau = 1, 2, 4, 5, 7, 8$, etc. up to j but not exceeding it. When the summations extend over a great many terms (σ small) these equations may be written in the integral form

$$ {}^4Q = 4\int_0^\infty (2j+1)e^{-j(j+1)\sigma_1}dj + \int_0^\infty (2j+1)e^{-j(j+1)\sigma_1}dj \int_{\tau\equiv 3}^{\tau\leq j} e^{\leq \tau^2\sigma_2}d\tau \quad (17) $$

$$ {}^2Q = 4\int_0^\infty (2j+1)e^{-j(j+1)\sigma_1}dj \int_{\tau\equiv 1,2}^{\tau\leq j} e^{-\tau^2\sigma_2}d\tau. \quad (18) $$

The first term of (17) is readily integrated. In order to compute the double integral in (17) one must introduce some simplifying approximation. Making use of Badger and Mecke's[12] data (which gives $\sigma_1 = 0.0476$; $\sigma_2 = -0.00854$) I find that the ratio $\sigma_1 : \sigma_2$ is -5.6. This suggests the possibility that σ_2 may be neglected with no appreciable error. Thus, the second integral in the second term of (17) could be taken as approximately $j/3$ as long as $j(j+1)\sigma_1$ is small; when the latter becomes large, the first exponential would have approached quite a small value before the second integral could have changed materially. The use of this approximation would give a lower limit to the sum Q(since σ_2 is negative). Likewise, the second integral in (18) might be taken as $2j/3$. Obviously, the next approximation is to be obtained by expanding the exponential in $\tau^2\sigma_2$ and integrating by parts. Carrying out this integration one gets the following, the last term in braces representing the second approximation.

$$ {}^4Q = (4/3)\pi^{1/2}\sigma_1^{-3/2}e^{\sigma_1/4}\left[\left\{1 - 4\pi^{-1/2}\sigma_1^{1/2} + (5/6)\pi^{-1/2}\sigma_1^{3/2}\right\} - (\sigma_2/2\sigma_1)\left\{1 - 2\pi^{-1/2}\sigma_1^{1/2} + \sigma_1/2\right\}\right] \quad (19) $$

$$ {}^2Q = (4/3)\pi^{1/2}\sigma_1^{-3/2}e^{\sigma_1/4}\left[\left\{1 - 4\pi^{-1/2}\sigma_1^{1/2} + (5/6)\pi^{-1/2}\sigma_1^{3/2}\right\} - (\sigma_2/2\sigma_1)\left\{1 - 3\pi^{-1/2}\sigma_1^{1/2} + \sigma_1/2\right\}\right] \quad (20) $$

This shows immediately that the proportions of the two forms at high temperature (σ small) are equal.

$$ {}^4Q : {}^2Q = 4/4. \quad (21) $$

Differentiating the natural logarithm of (19) and (20) and applying (11), one obtains for the absolute rotational entropies

$$ {}^4S_r = R[1.5 + \ln 4\pi^{1/2}/3 - 1.5\ln\sigma_1 - 2\pi^{-1/2}\sigma_1^{1/2} - \sigma_2/2\sigma_1 + \tfrac{1}{2}\sigma_2\pi^{-1/2}\sigma_1^{-1/2}] = 2.98 + 1.70 + 9.08 - 0.49 + 0.18 - 0.02 \quad (22) $$

$$ = 13.43 \text{ at } 298.1^\circ K $$

$$ {}^2S_r = R[1.5 + \ln 4\pi^{1/2}/3 - 1.5\ln\sigma_1 - 2\pi^{-1/2}\sigma_1^{1/2} - \sigma_2/2\sigma_1 + (3/4)\sigma_2\pi^{-1/2}\sigma_1^{-1/2}] = 13.42 \text{ at } 298.1^\circ K. \quad (23) $$

The total absolute rotational entropy is (cf 21)

$$\begin{aligned} S_r &= \tfrac{1}{2}{}^4S_r + \tfrac{1}{2}{}^2S_r - \tfrac{1}{2}R\ln\tfrac{1}{2} - \tfrac{1}{2}R\ln\tfrac{1}{2} \\ &= 13.425 + 1.377 \\ &= 14.80 \text{ cal. degree}^{-1} \text{ at } 298°K \end{aligned} \tag{24}$$

while the entropy of the gas at the absolute zero under conditions of "frozen" equilibrium would be

$$\begin{aligned} S_r' &= \tfrac{1}{2}R\ln 4 + \tfrac{1}{2}R\ln 12 + S_{\text{mix}} \\ &= 1.377 + 2.468 + 1.377 \\ &= 5.22 \text{ cal. degree}^{-1}. \end{aligned} \tag{25}$$

The latter must be subtracted from the absolute entropy to obtain what we shall call the "virtual" entropy, which corresponds to the calorimetrically measured quantity.†

$$\begin{aligned} S_r^* &= S_r - S_r' = 14.80 - 5.22 \\ &= 9.58 \text{ at } 298°. \end{aligned} \tag{26}$$

It is evident from the foregoing that the entropy of mixing does not enter into the final value of the virtual rotational entropy since it cancels out in the "zero point" correction, but that it is quite important to the value of the absolute entropy.

We are now ready to add together all our results in order to get the total entropy of ammonia.

$$\begin{aligned} S_{\text{NH}_3}^{298.1} &= 34.45 + 0.06 + 14.80 + 2.18 \\ &= 51.5 \text{ cal. degree}^{-1} \text{ absolute entropy}. \end{aligned}$$

(The entropy, $R\ln 3 = 2.18$, due to the nitrogen nucleus, hitherto neglected, is here included.)

$$\begin{aligned} S_{\text{NH}_3}^{298.1*} &= 34.45 + 0.06 + 9.58 \\ &= 44.1 \text{ cal. degree}^{-1} \text{ virtual entropy}^{14} \text{ at } 298.1°K. \end{aligned}$$

The absolute minus nuclear spin entropy ($R\ln 24 = 6.31$) is 45.2.

Comparison with experiment.

To compare these calculated values with experiment requires extreme caution. By using the equations of Lewis and Randall,[10] p. 557, for the heat and free energy of formation of ammonia, one may get the entropy change of the reaction

$$\Delta S_{\text{NH}_3}^{298.1} = -23.7.$$

† Cf. comments added in proof.

[14] The difference between these values and those announced in the preliminary statement (reference 1) arose from a discovery of certain fundamental errors which had been made in counting eigenfunctions.

It at first seemed justifiable to add to this the experimental (virtual) entropies of nitrogen and hydrogen to get an experimental value for the virtual entropy of ammonia (43.6) and it was on this basis that comparisons were made in the preliminary notice of this work.[1] Giauque, Blue and Overstreet,[15] in a letter to the Editor of this journal state that this calculation "is evidently in error," after giving theirs to be 46.1. This is a rather unfair statement, in that it implies an arithmetical error where in reality the difference lies in the manner of definition.††

Mature consideration shows that the entropy change of the reaction of formation which was obtained above is in reality the change in *absolute* entropy. Least confusion will therefore arise if one talks in terms of absolute entropy.

$$S_{NH_3} = \Delta S + \tfrac{1}{2}S_{N_2} + 1.5\, S_{H_2} \tag{27}$$

where the absolute entropy

$$\begin{aligned} S_{H_2} &= 33.98 \\ &= S_{H_2}{}^{*} + R \ln 4 + \tfrac{3}{4}R \ln 3 \end{aligned} \tag{28}$$

and similarly

$$\begin{aligned} S_{N_2} &= S_{N_2}{}^{*} + R \ln 9 \\ &= 2 \times 22.9 + 4.37 \\ &= 50.2. \end{aligned} \tag{29}$$

The term ($\frac{1}{3}R \ln 3 = 0.73$) corresponding to the odd rotating variety of nitrogen which I know to constitute one-third of the total from the intensity ratio of the band lines[16] and from the Raman effect,[17] I have stricken out (in proof) on the authority of a private communication from Giauque who states that experimental work by himself and Clayton has shown that the calorimetric value of the entropy of nitrogen is absolute entropy (as computed from band spectra) minus only the nuclear spin entropy. With (28) and (29) one gets as an "experimental" value for the absolute entropy of ammonia

$$\begin{aligned} S_{NH_3}^{298.1} &= -23.7 + 25.08 + 50.97 \\ &= 52.3 \text{ cal. degree}^{-1}. \end{aligned}$$

My calculated value of the absolute entropy, 51.5, thus agrees fairly well

[15] Giauque, Blue and Overstreet, Phys. Rev. **38**, 196-7 (1931). I wish to thank Professor Giauque for a copy of this letter which was furnished me while the present manuscript was being prepared. As far as I can tell, Giauque Blue and Overstreet have calculated the entropy of methane and ammonia by means of the old quantum theory involving the sometimes ambiguous symmetry number, to obviate the necessity for which was the especial virtue of the Gibson-Heitler[15a] theory. I shall show that the two methods are in agreement when the same data are used.

[15a] Gibson and Heitler, Zeits. f. Physik **49**, 465 (1928).

†† Added in Proof—This has been recognized by Bryant. J. Am. Chem. Soc. **53**, 3014 (1931).

[16] Mulliken, Trans. Farady Soc. **25**, 634 (1929).

[17] Rasetti, Nature **124**, 792 (1929).

with the above. Giauque, Blue and Overstreet[15] suggest that my choice of Badger and Mecke's[12] moments of inertia may have led to a small divergence in results for ammonia. One may readily calculate this effect from our Eqs. (22) and (23). They prefer the values of 5.47×10^{-40} and 2.792×10^{-40} gm cm^2 obtained by Barker.[18] This would give a ratio of $\sigma_1:\sigma_2$ of -2.04 instead of -5.6 as before. The terms in (22) and (23) corresponding to the second approximation are therefore 5.6/2.04 greater and this would give a greater entropy by 0.2 cal. degree.$^{-1}$ If their estimate of the vibrational entropy 0.3 prove to be better founded than that used above 0.06 (Table I), the remainder of the difference 0.3, might perhaps be largely that arising from neglect of the stretching effects of the rotation, although part of it is to be accounted for by the higher terms in the expansions (19) and (20).†††

The Entropy of Methane at 298.1°K

Translational

Substituting in Eq. (3) values for methane at 298.1°K and one atmosphere, I get

$$S_t^{298.1} = 34.27 \text{ cal. degree}^{-1}.$$

Vibrational

For the fundamental vibrational frequencies of methane I take those from Dennison.[19] Some doubt has been cast on the correctness of his assignment by Dickinson, Dillon and Rasetti[20] who find a very strong Raman line of frequency 2914.8 cm^{-1}, which is exactly equal to the difference between two of Dennison's fundamentals, 4217 and 1304 cm^{-1}. As they point out, this indicates that it either owes its origin to molecules in thermal vibration (highly improbable for the strongest line) or else that the choice of the fundamentals is wrong. For want of better information however, I shall use Dennison's data, with the assurance that the vibrational entropy at most only amounts to a small fraction of the whole. Calculation gives (Table III)

$$S_v^{298.1} = 0.11 \text{ cal. degree}^{-1}$$

Table III. *Vibrational entropy of methane.*

k	$\tilde{\omega}_k$cm^{-1}	Θ	$\Theta/298.1$	S_k
1, 2, 3	1304	1870	6.275	0.0274 (×3)
4, 5	1520	2180	7.31	.0112 (×2)
6, 7, 8	3014	4310	14.45	.0$_4$17 (×3)
9	4217	6040	20.3	—
				0.105 S_v

[18] Barker, Phys. Rev. **33**, 684 (1929).

††† Added in Proof—The remainder of the discrepancy between my value for the absolute entropy, 51.5, and theirs, 52.7, is probably to be ascribed to the fact that my series is carried out to the second approximation which is farther than theirs has been.

[19] Dennison, Astrophys J. **62**, 84 (1925).

[20] Dickinson, Dillon and Rasetti, Phys. Rev. **34**, 582 (1929).

Rotational

The rotational equations for the three different forms of methane have already been derived (V and S). Differentiating only once the natural logarithm of the expressions (25), (26) and (27) of that paper and applying (11) of the present article, one obtains for absolute rotational entropies

$$\begin{aligned} {}^5S_r &= R[-1.5\ln\sigma + \ln 5\pi^{1/2}/12 + 1.5 + 15\pi^{-1/2}\sigma^{3/2}\cdots] \\ &= 10.91 - 0.61 + 2.98 + 0.07 \\ &= 13.35 \text{ at } 298.1^\circ \end{aligned} \tag{30}$$

$$\begin{aligned} {}^3S_r &= R[-1.5\ln\sigma + \ln 9\pi^{1/2}/12 + 1.5 + 37\pi^{-1/2}\sigma^{3/2}\cdots] \\ &= 10.91 + 0.57 + 2.98 + 0.17 \\ &= 14.63 \text{ at } 298.1^\circ \end{aligned} \tag{31}$$

$$\begin{aligned} {}^1S_r &= R[-1.5\ln\sigma + \ln 2\pi^{1/2}/12 + 1.5 + 39\pi^{-1/2}\sigma^{3/2}\cdots] \\ &= 10.91 - 2.43 + 2.98 + 0.18 \\ &= 11.64 \text{ cal. degree}^{-1} \text{ at } 298.1^\circ K. \end{aligned} \tag{32}$$

As before, I shall use the Raman value of the moment of inertia which gives $\sigma = 0.0258$ at 298.1°K. The average absolute rotational entropy is, making use of the proportions found in (31) of V and S.

$$\begin{aligned} S_r &= (5/16){}^5S + (9/16){}^3S + (2/16){}^1S + S_{\text{mix}} \\ &= 4.17 + 8.23 + 1.46 + 1.89 \\ &= 15.75 \text{ cal. degree}^{-1}. \end{aligned} \tag{33}$$

The "zero point" entropy correction under conditions of frozen equilibrium would be

$$\begin{aligned} S_r' &= (5/16)R\ln 5 + (9/16)R\ln 9 + (2/16)R\ln 10 + S_{\text{mix}} \\ &= 1.00 + 2.45 + 0.57 + 1.89 \\ &= 5.91 \text{ cal. degree}^{-1}. \end{aligned} \tag{34}$$

Subtracting this from the absolute entropy, one gets the virtual entropy which may now be compared with experiment.†

$$\begin{aligned} S_r^* &= S_r - S_r' = 15.75 - 5.91 \\ &= 9.84 \text{ cal. degree}^{-1}. \end{aligned} \tag{35}$$

The total entropy is the sum of the foregoing amounts

$$\begin{aligned} S_{CH_4}^{298.1} &= 34.27 + 0.11 + 15.75 \\ &= 50.1 \text{ absolute entropy or} \\ S_{CH_4}^{298.1*} &= 34.27 + 0.11 + 9.84 \\ &= 44.2 \text{ cal. degree}^{-1} \text{ virtual entropy}^{14}. \end{aligned}$$

The absolute minus nuclear spin entropy ($R\ln 16 = 5.51$) is 44.6.

† Cf. comments added in proof.

Comparison with experiment.

The above value for the virtual entropy of methane (44.2) may be compared with an experimental entropy recently recalculated by Storch[21] from the specific heat measurements of Clusius[22] (43.39). Much better agreement of our calculated value is found when it is compared with the one computed by Giauque, Blue and Overstreet[15] (44.3) from the data of Clusius,[22] of Stock, Henning and Kuss[23] and of Keyes, Taylor and Smith.[24]

The reaction of formation may also be employed for comparison purposes. In this case, as before with ammonia one should compare absolute entropies, not experimental, if one is to avoid confusion. Storch[21] has recalculated the data of Randall and Mohammad[25] to agree with the later specific heat measurements of Eastman[26] and of Eucken and Luede[27] and gives us the values

$$\Delta H^{298.1}_{CH_4} = -18062 \text{ cal./mole}$$

$$\Delta F^{298.1}_{CH_4} = -12542 \text{ cal./mole.}$$

From these I compute

$$\Delta S^{298.1}_{CH_4} = -18.52 \text{ cal. degree}^{-1}$$

and add 2×33.98 (the absolute entropy of hydrogen) plus 1.39 (I. C. T. value for entropy of graphite) to get

$$S^{298.1}_{CH_4} = 50.8 \text{ cal. degree}^{-1}$$

which compares quite favorably with my calculated value of the absolute entropy of methane (50.1). This last estimate is uncertain in that we do not know whether the experimental entropy of graphite (1.39) differs from its absolute entropy. If it were a diatomic gas, one could say definitely that there would be no difference, since its nuclear spin entropy is zero and its lowest rotational level is the one of zero rotation (in C_2, the odd levels are missing).[16] It is quite probable that the lowest levels in the graphite crystal correspond to zero rotation, and if this is true, the above comparison is justified; if it is not true, then the corresponding entropy of rotation should be added to 50.8 and that value be compared with my theoretical one of 50.1

It may be noted in passing that 0.4 cal. degree^{-1} of the 1.9 units divergence noted by Storch as existing between the reaction of formation data and the specific heat data on methane has been removed in the above analysis, on the interpretation involving virtual entropies as I have defined them. This is not removed if the experimental entropies differ from their absolute values only

[21] Storch, J. Am. Chem. Soc. **53**, 2166 (1931).
[22] Clusius, Zeits. f. physik. Chem. **B3**, 41 (1929).
[23] Stock, Henning and Kuss, Ber. **54**, 1119 (1921).
[24] Keyes, Taylor and Smith, J. Math. Phys. Mass. Inst. Tech. **1**, 191 (1922).
[25] Randall and Mohammad, Ind. Eng. Chem. **21**, 1048 (1929).
[26] Eastman, Bureau of Mines Circular **6125**, May (1929).
[27] Eucken and Luede, Zeits. f. physik. Chem. **B5**, 436 (1929).

by their nuclear spin entropies. (The entropy indicated from the $CO_2 \rightarrow CH_4$ reaction is still in disagreement with the other values.)††

Conclusion

Before concluding, it might be briefly pointed out that the common factor multiplying all the *a priori* probabilities of a distinct symmetry variety affects the relative proportions (mole fraction) of the different varieties and their absolute entropies; not, however, the virtual entropy.

In conclusion I wish to emphasize my belief that comparisons between theory and experiment should be made, wherever possible, with the absolute entropies. If these are uncertain in symmetrical molecules, then this uncertainty will almost invariably be carried over to the calculated value which is being compared with experiment, except where the relative proportions of the different symmetry varieties are already known in advance. In only one case may the virtual theoretical value be compared with the actual calorimetric one and that is when the latter has been determined from specific heat measurements on that substance alone (not in connection with a reaction). In this case, the absolute entropy must be calculated beforehand, at any event. An important corollary of the conclusions developed above is that the experimental entropy change in a reaction (obtained from the free energy and heat change) is equal to the change in absolute entropy and in some cases may be distinctly different from that computed from the algebraic sum of the experimental entropies derived from specific heat measurements on the separate reactants.

Comments added in proof: (9/15/31)

The foregoing calculations of the absolute entropy by the application of quantum mechanics are seen to be in good agreement with those obtained from classical theory. In all fairness it should be stated however that the method of comparison with experiment is not at all certain. If calorimetric measurements were made on the *gas* all the way down to near the absolute zero, or if the liquid and crystal carry over the rotational states of the gas without material changes in the relative rotational and vibrational energy level spacings, the experimental calorimetric entropy should correspond to the virtual entropy (absolute minus nuclear spin minus frozen rotational entropy). This is true of hydrogen if too low temperatures are not attained. However, there is a second class of substances (Giauque, ref. 2f, p. 4825 believes all substances belong to this class except hydrogen) such as iodine[2i] in which the degenerate rotational levels become so widely separated (perturbed) by the crystal forces as the molecule passes into the crystalline state that the ratio, Σ/kT, is no longer negligible but becomes quite appreciable

†† Added in proof—The difference between my calculated value of the absolute entropy of methane, 50.13, and that of Giauque, Blue and Overstreet, 49.86, may be shown to be due to the fact that I have not neglected vibrational entropy (0.11) and have computed my series to a further degree of approximation than that used by these authors. My last approximation amounts to 0.15 and fully accounts for the difference between our results.

for all but the lowest of the resolved degenerate levels with the result that all molecules settle into the lowest state which is now of unit statistical weight. Under such conditions, the frozen rotational entropy is removed and the experimental value should correspond to the absolute minus nuclear spin entropy.

Finally, a third class has been proposed recently by Ludloff[28] in which even the entropy of nuclear spin is partially or wholly resolved, in solids of great crystal forces. He points out that even under such circumstances, the entropy of mixing will remain associated with the state of zero temperature. Of course substances may also belong to the in-between classes. Examples of class III given by him are N_2O, NH_3, Br_2 and Cl_2. In such a case, it will be necessary to know the relative amounts of the different symmetry forms in order to compute the entropy of mixing, and here the method of calculation I have chosen possesses distinct advantage over the one used by Gibson and Heitler [15a] and by Giauque, Blue and Overstreet.[15]

The calorimetric value of ammonia given by the latter, computed from data of Eucken and Karwat[29] and Henning and Stock[30] is 47.2. My four calculated values of entropy are summarized as follows: absolute, 51.5; absolute minus mixing (Ludloff, class III), 50.1; absolute minus nuclear spin (Giauque, class II) 45.2; absolute minus nuclear spin minus frozen rotational (virtual—class I), 44.1.

The same data for methane, which, according to Ludloff, belong to class II are: experimental calorimetric, 43.39 (Storch) or 44.3 (Giauque, Blue and Overstreet); absolute, 50.1; absolute minus mixing, (class III), 48.2; absolute minus nuclear spin (class II), 44.6; absolute minus nuclear spin minus frozen rotational (virtual—class I), 44.2

In this connection, Rodebush[2h] maintains that the only entropy worthy of consideration is that of the equilibrium mixture. To measure this, it is necessary to find a catalyst which establishes equilibrium at all temperatures down to near the absolute zero. I wish to point out that the discovery of such a catalyst serviceable at these low temperatures will probably be the exception rather than the rule in view of the recent proof by Taylor[31] that activation heats are associated with adsorption processes. While the equilibrium value of the entropy (absolute entropy) is the one which should be used in thermodynamic discussions, it seems to me more practicable, at least until such catalysts are universally assured to make the experimental measurements on the metastable mixture of the proportions existing at high temperature down to a temperature at which the resolution of the frozen rotational or the nuclear spin entropy just begins to become evident, extrapolate from there to the absolute zero and correct for the omission of this type of entropy by adding the suitable theoretical amount.

[28] Ludloff, Zeits. f. Physik **68**, 433–46 (1931).
[29] Eucken and Karwat, Zeits. f. phys. Chem. **112**, 467 (1924).
[30] Henning and Stock, Zeits. f. Physik **4**, 226 (1921).
[31] Taylor, J. Am. Chem. Soc. **53**, 578 (1931).

LETTERS TO THE EDITOR

Prompt publication of brief reports of important discoveries in physics may be secured by addressing them to this department. Closing dates for this department are, for the first issue of the month, the twenty-eighth of the preceding month; for the second issue, the thirteenth of the month. The Board of Editors does not hold itself responsible for the opinions expressed by the correspondents.

Ionization as a Function of Pressure and Temperature

Attention has been called by Swann,[1] Broxon[2] and others[3] to the fact that the residual ionization in an ionization chamber (due chiefly to cosmic rays) is not proportional to the pressure, but reaches a maximum value in the neighborhood of a hundred atmospheres. The proposed explanation has been that the ions are formed by high speed beta-particles ejected from the walls of the ionization chamber, and that these beta-rays are completely absorbed by the air if the pressure is sufficiently high.

An alternative explanation of the phenomenon is that a form of recombination may occur at high pressures, due to the fact that the electron ejected from a molecule by the ionizing beta-ray may lose its initial energy through molecular collisions before it has moved far enough from the parent positive ion to escape from the effect of its electrostatic attraction. In accord with the ideas underlying Thomson's theory of recombination,[4] we may suppose that if the initial energy of the electron carries it beyond a critical distance, molecular diffusion will probably carry it away, and a permanent ion will be formed. If i is the ionization per unit pressure when all ions remain permanent, p the pressure, and P is the probability that an ion will remain permanent, the ionization may be written as

$$i = i_1 p P. \qquad (1)$$

The probability P will approach unity for low pressures and zero for high pressures, and will have a greater value at high temperatures than at low temperatures, since diffusion will be more rapid. Kinetic theory calculations lead to rather complicated expressions for P, which will be presented in a later paper. They show, however, that the ionization i should reach a maximum as the pressure increases, and then fall gradually to zero for very high pressures. For the range of pressures studied by Broxon, the theoretical curve is similar to that observed, though the agreement is not exact.

A consequence of this recombination theory is that the variation of ionization with pressure should be nearly the same with gamma-rays as with cosmic rays, since neither are much absorbed by the air in the ionization chamber. On the beta-ray absorption theory, since the beta-rays excited by gamma-rays are presumably of much shorter range than those due to cosmic rays, the ionization should either reach its limit at a lower pressure, if the ionizing beta-rays come from the walls, or should increase without limit if the gamma-rays produce beta-rays within the gas. Experiments at Chicago with a spherical steel ionization chamber, 4 inches in diameter, and on Mt. Evans with a cylindrical steel chamber, gave pressure ionization curves with gamma-rays and cosmic rays which were closely similar to each other and to Broxon's pressure curve using a 10 (?) inch chamber

The 4 inch ionization chamber was also surrounded by a water bath so that its temperature could be varied from about 0°C to 35°C. With air at 100 atmospheres pressure the ionization was about 8 percent greater at the higher temperature, while at 20 atmospheres we were unable to detect any effect of temperature change. These results are in approximate quantitative agreement with the predictions

[1] W. F. G. Swann, J. Frank. Inst. **209**, 151 (1930).

[2] J. W. Broxon, Phys. Rev. **37**, 1321 (1931).

[3] K. M. Downey, Phys. Rev. **16**, 420 (1922). H. H. Fruth, Phys. Rev. **22**, 109 (1923).

[4] Thomson, Phil. Mag. **47**, 337 (1924); Conduction of Electricity Through Gases, 3 ed. pp. 44–57.

of the recombination theory, whereas the beta-ray range theory would predict no effect at either pressure.

Further support of the recombination theory of the limited ionization at high pressures comes from the observation that when nitrogen is used, the ionization remains proportional to the pressure up to pressures much higher than is the case with air. We have observed this to be the case using gamma-rays, and Broxon informs us that he finds the same difference with cosmic rays. The interpretation of this difference between nitrogen and air is apparently the fact that the energy lost by an electron per collision is much less in nitrogen than in air. Thus an electron ejected by a passing beta-particle should move farther from its parent positive ion in nitrogen than in air before losing its initial energy. This would make recombination less likely in nitrogen.

A. H. COMPTON
R. D. BENNETT
J. C. STEARNS

University of Chicago,
Ryerson Physical Laboratory,
September 23, 1931.

The Constancy of Cosmic Rays

In the preceding letter to the Physical Review we have called attention to the fact that the ionization of air traversed by gamma-rays from radium is a function of the pressure, and that this dependence upon the pressure is greater when the pressure is high. There have been from time to time important and careful experiments which have indicated a variation in the intensity of cosmic rays with the time of day. Those of Millikan have, for example, shown a maximum intensity in the afternoon and a minimum at night. This is the type of apparent variation that one should expect if the apparatus is not kept at a uniform temperature. Other observers have noted that the apparent variation in cosmic ray intensity is greater for the softer component of the cosmic rays. These softer components, however, can only be studied in very high altitudes where the temperature variation between day and night becomes relatively large. We, therefore, determined to study the variations in the intensity of cosmic rays in a high altitude in such a way that possible temperature variations would not influence our results.

The ionization chamber used in these experiments was a hollow steel sphere, 4 inches in diameter, filled with dry air at thirty atmospheres pressure. (The ionization was measured by means of a Lindemann electrometer. Hourly readings were taken of the ratio of the intensity of the cosmic ray entering this chamber when shielded with two inches of lead to the intensity of the gamma-rays from a milligram of radium placed in a fixed position about 30 centimeters from the chamber.) Any temperature variations should, under these conditions, affect equally the ionization produced by the cosmic rays and the gamma-rays.

This apparatus was taken to Summit Lake, near the top of Mount Evans, Colorado, at an altitude of 12,680 feet. A series of hourly readings taken for 240 consecutive hours showed no variations in the intensity greater than the variations to be expected from purely statistical considerations. (The probable error of the intensity for a four hour period was about 0.15 percent.) This series of readings appears to be as thorough a test of the diurnal variations of cosmic ray intensity as has yet been made, and since it shows no intensity changes, it would appear that probably some of the previous changes that have been recorded may be due merely to variations in the temperature of the apparatus employed.

The long, continuous series of readings necessary to make this test of diurnal variations could not have been completed without the cooperation of Messrs. V. J. Andrew, F. P. Longman, V. L. Ridenour, and A. A. Compton of Chicago; and W. J. Overbeck, P. M. Barth, and J. A. Headberg of Denver.

R. D. BENNETT
J. C. STEARNS
A. H. COMPTON

University of Chicago,
Ryerson Physical Laboratory,
September 23, 1931.

Thermionic Emission from a Plane Electrode

Being convinced of the importance of space charge in any theory of the thermionic work function, as Waterman and I have pointed out, I have sought explanations of the differences between experimental results and theoretical calculations along this line. In addi-

tion to any question of the validity of applying Poisson's equation, essentially as an equation of continuity, to an electron gas which perhaps cannot be considered as continuous, there is the difficulty that the calculations have been performed, for the sake of simplicity, for the case of parallel plane electrodes, whereas most of the experiments have used coaxial cylinders.

Supposing, erroneously I now believe, that it would be easier to revise the experiment than the theory, I have set up an arrangement for measuring the thermionic current between parallel electrodes of nickel. The emitter, so shaped that its temperature was reasonably uniform over the emitting surface, was heated by electron bombardment at a few thousand volts from a Coolidge filament. A surrounding cylinder separated from the emitter by a lavite insulator, served to focus the electron beam to secure uniform temperatures, and, in conjunction with an outer cylinder, insulated, stopped to a great extent the passage of electrons of the heating current to the collecting anode. Unfortunately this last could not be achieved completely, so that it was necessary to use a null method of measurement to balance out the stray current, and also to run a long series of control experiments.

Finally the temperature of the emitter was measured by an optical pyrometer through small holes in the collecting anode. This anode was about one millimeter distant from the hot cathode, though that distance depended on the temperature conditions in the tube and had to be measured frequently.

Currents were measurable only for a small range of temperatures, and with a rather large experimental error. Accelerating fields up to five thousand volts per cm were used, large enough to give Schottky effect curves since the currents were so small as to eliminate completely any of the space-charge effect that is usually considered.

The results show that, within the limits of my rather large experimental error, the dependence of current upon applied field and upon temperature is the same as in the cylindrical electrode case. I think that my results should be interpreted as failing to find any large departures from the Schottky image force rather than as confirming that theory.

It is possible that interesting results could be obtained with coated filaments, from which large currents could be drawn at moderate temperatures, thus greatly increasing the accuracy. On the other hand, I am now engaged in looking into the validity of my use of Poisson's equation, and trying to find a correction which will take into consideration the granular structure of the electron gas.

RUSSELL S. BARTLETT
Sloane Physics Laboratory,
Yale University,
September 15, 1931.

Radioactive Disintegration

In a previous discussion[1] of the properties of radioactive substances, we proposed the following equation

$$E=-\left(\frac{n}{Z}\right)^2\frac{\pi^2Mc^2}{(i)^2}$$

to represent the energy levels of the α-particles in the nucleus, where M is the mass of the helium nucleus, c the velocity of light, Z the atomic number of the element less two, and n and i are integers.

The long range particles from RaC'[2] can be assigned to energy levels which follow this law when we take for the value of E for $n=1$ and $i=22$, the value 1.00×10^4 el.-volts corresponding to the value 1.09×10^5 given by above equation for $i=7$. The following table compares the values for different values of n.

The comparison between the softest γ-rays emitted by the element and the energies of the normal α-particles is also fairly satisfactory. We should expect that the energy of the normal α-particle would be the same as the energy difference between the levels $n=0$ and $n=1$ of the preceding element in the series. In some cases, however, the values of i do not change in the disintegration process and we

[1] Bramley, Proc. Nat. Acad. Oct. 1931.

n	8	12	13	14	15	16	17	18
cal.	6.4	14.4	16.9	19.6	22.5	25.6	28.9	32.4
exp.	6.3	14.6	17.6	19.4	{22.0 / 23.5}	25.8	28.4	30.2

have good agreement with the α levels of the element as shown by the γ-rays emitted.

The other elements for which we have sufficient data, Pa and AcC do not fit this relationship. We have taken here the value of the softest γ-ray as corresponding to the transition $\Delta n^2=1$.

mum probability of occurrence. The data are given in the following table. We have calculated the constant of proportionality from the data for ThB.

If we divide the calculated values of $(1/\tau)$ of the second group by ten, and those of the third by one hundred, as we saw was necessary,[1] then the agreement is fair considering the difficulty of locating the maximum of the distribution function. The energy of the maximum is approximately $\frac{1}{3}$ of the energy of the hardest γ-ray. In the case of black-body radiation the energy of the maximum is nearly the same as that given by the temperature.

Element	Softest γ-ray	n	Energy of α-particle (cal.)	(exp.)
Ra	1.89	5	47.3	47.44
RdTh	0.848 0.841	8	54.3 53.8	53.47
AcX	1.435 1.53 1.57	6	51.66 55.08 56.52	56.59
RdAc	0.315	14	61.74	59.23

In the article,[1] we found that the reciprocal of the mean life $(1/\tau)$ for a β transition was proportional to the fourth power of the hardest γ-ray emitted by the element following the transition. We should also expect from the analogy to "black-body radiation" that $(1/\tau)$ should be proportional to the fourth power of the energy of the emitted β-particles which have the maximum probability of occurrence. If we plot the number of β-particles as a function of their energy, then we can find a value of the energy for which the distribution function has a maximum; this is the energy for which the emitted β-particles have a maxi-

Element	Energy		$1/\tau$ (cal.)	$1/\tau$ (exp.)
ThB	1.0×10^5		1.82×10^{-5}	1.82×10^{-5}
RaB	1.7×10^5		1.52×10^{-4}	4.31×10^{-4}
Ra	4.0×10^5	second group	4.65×10^{-3}	5.86×10^{-4}
RaE	2.7×10^5	third group	9.8×10^{-4}	1.6×10^{-6}

[2] Rutherford, Proc. Roy. Soc. **132,** 667. (1931).

Arthur Bramley

Bartol Research Foundation,
Swarthmore, Pa.,
September 19, 1931.

An Electrical Field Giving Uniform Deflecting Force on a Molecular Beam

The most desirable type of field distribution for use in molecular beam deflection experiments is evidently one in which the force is independent of the position of the molecule in the field. Any nonlinearity of the scale of deflection due to deflected molecules going through stronger or weaker parts of the field is thus avoided, as well as any spreading due to the original finite width of the beam. An electrical field having this property is described here.

This is a cylindrical or two-dimensional field, in which the molecular beam travels parallel to the generator of the cylinder (Normal to the plane of the accompanying figure). The magnitude of the deflection can be increased at will by increasing the length of the field. The correct form of the plates is found

by the method of conformal representation. Consider the transformation $W=z^{1+1/n}$, where $W=U+iV=Re^{i\phi}$, $z=x+iy=re^{i\theta}$. The absolute value of the field strength is given by $F=|dW/dz|=(1+1/n)\,|z^{1/n}|=(1+1/n)r^{1/n}$.

If now a molecule in the field has the Stark effect energy aF^n, the force on it, at least to a classical approximation, is given by $-\text{grad}\ aF^n=-a(1+1/n)^n\cdot\text{grad}\,r=-a(1+1/n)r_1$, where r_1 is a unit vector from the origin to the point in the field where the molecule is located. The force is thus constant in magnitude and always directed along the line joining the molecule and the origin.

The form of the equipotentials of the electrical field is found most easily by putting the transformation into the form

$$Re^{i\phi}=r^{1+1/n}e^{i(1+1/n)\theta},\ \text{or}$$

$$R=r^{1+1/n},\ \phi=(1+1/n)\theta.$$

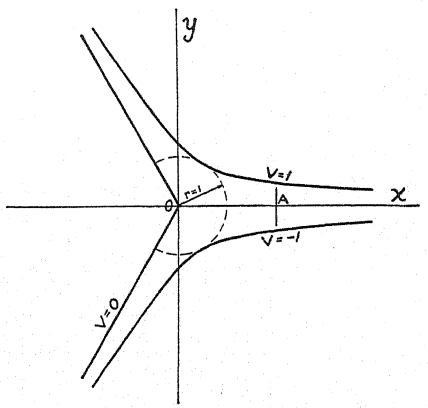


Fig. 1. Profile of condenser plates providing uniform deflecting force in the case of molecules with a quadratic Stark effect. The beam of molecules travels perpendicularly to the paper, in the region whose cross section is the line A.

The equipotentials $V=\pm1$ are represented in the W-plane by $R=\pm\text{cosec}\ \phi$, and in the z-plane by $r^{1+1/n}=\pm\text{cosec}(1+1/n)\theta$.

The case of greatest experimental interest is that in which $n=2$. Then the force is $-(9/4)ar_1$, and the equipotentials $V=\pm1$ are given by $r^{3/2}=\pm\text{cosec}\ (3/2\ \theta)$ In the realization of the field, electrodes are put at $V=1$ and $V=-1$. Also a third electrode in the form of a wedge with the dihedral angle 120° is placed as shown in the figure and put at zero potential. This is necessary because of the presence of a branch point at the origin, requiring a branch cut to infinity which can be considered to be in the part of the plane excluded from the field by the third electrode.

Since in the actual construction the plates cannot extend to infinity as required by the theory, an estimate must be made of the effect caused by cutting them off at a finite distance from the origin. This can be done by the method of successive transformations. Starting with the transformation giving the field at the edge of a plane parallel condenser, the application of the transformation used in this letter deforms the condenser plates into curves identical with those required by the simple theory given above, but now cut off at an arbitrary value of x. Calculation shows that when the plates are cut off at $r=4$, the modification in the force at $r=2$ is less than one part in a thousand.

When the potential on the plates is v, and the radius of the circle shown on the cut is r_0, the force is multiplied by the dimensional factor v^2/r^3_0.

This method is to be used in an experiment now in progress at Princeton.

EDWIN MCMILLAN
Palmer Physical Laboratory,
Princeton, New Jersey,
September 16, 1931.

The Metamagnetism in Bismuth Crystals

A fundamental problem of the constitution of a solid metal is the cause of the magnetic susceptibility due to its crystalline state, which property is for most crystals very different from the atomic susceptibility. Almost all measurements of susceptibilities of pure metals show an increase in the diamagnetic direction at the transition into the crystalline phase and also the recent investigations of Kapitza[1] and de Haas and van Alphen[2] in very large fields and at extreme low temperatures point towards the conclusion that the diamagnetic properties of a metal crystal depend on the action of "free" electrons caused by the coexistence of a large number of molecules (atoms) in a given geometric configuration.

[1] P. Kapitza, Proc. Royal Soc. **A131,** 243 (1931).

[2] W. J. de Haas and P. M. van Alphen. Comm. Phys. Lab. Univ. Leyden Nr. 212 a, 1931.

One experimental possibility of a closer approach to this problem seemed to be the study of the influence which foreign atoms, dissolved within a metal crystal, have on its diamagnetic susceptibility. The disturbing effect on the lattice caused by foreign atoms was very much larger than expected and a preliminary report of some of the results obtained will be given as follows.

amount of another metal was added to the original metal and a new crystal of the same orientation as the previous one was produced.

In this fashion a large number of crystals containing various concentrations of foreign atoms as well as different kinds of impurities were grown. The results obtained concerning the change of the magnetic properties of the crystal in different directions are the following:

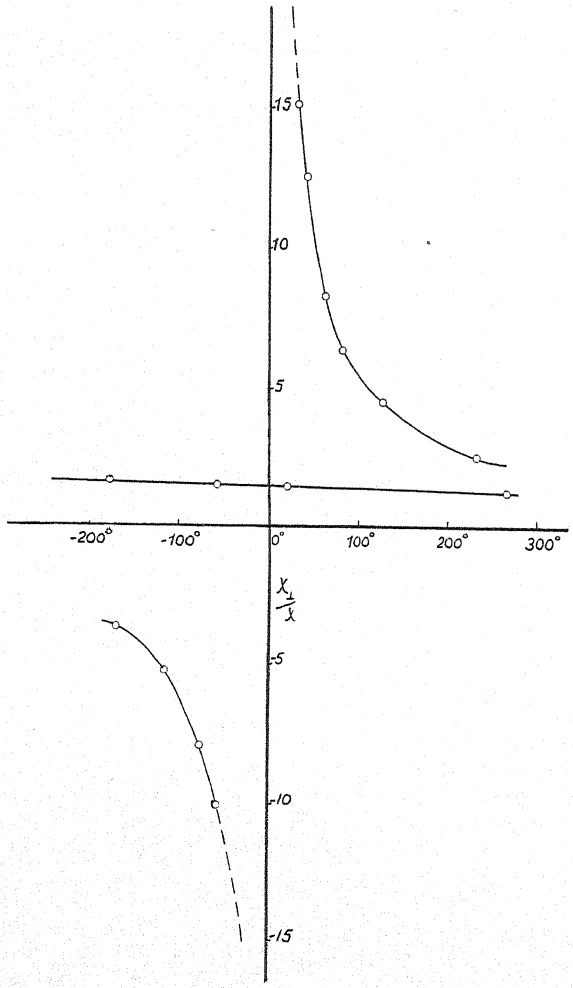


Fig. 1.

For most of the measurements Bi single crystals were used since their susceptibility is 15–20 times larger than the atomic diamagnetism. Bi is furthermore the most diamagnetic substance known. After the magnetic constants of a pure crystal had been determined[3] for different directions of the crystal, a small

a. The presence of foreign atoms affects the magnetic properties of the crystal only if the atom goes into a solid solution. Inclosures or occlusion of heterogeneous substances do not affect the susceptibility to a measurable ex-

[3] A. B. Focke, Phys. Rev. **36**, 319. (1930).

tent. Thus metals which cannot be dissolved in Bi (like Cu) do not change its magnetic properties.

b. If a soluble metal (Sn and Pb) is added in a quantity below the limit of saturation (which is very low (0.5 to 3 percent) for different enantiomorphic metals) the effect on the susceptibility is very large. Beyond the saturation (where it very soon becomes impossible to produce a single crystal) the effect due to enclosures of eutectic mixtures is negligible.

c. The effect of very small concentrations of foreign atoms is surprisingly large and affects the crystal differently in different directions. (An atomic concentration of only $1:10^4$ changes the susceptibility several percent.) The effect works, in all cases investigated, so as to *increase* the magnetic anisotropy of the crystal and to *decrease* the absolute values of the susceptibilities in all directions.

d. The coefficient of temperature of the magnetic anisotropy of the crystal is changed very much by foreign atoms so as to cause a large decrease with increasing temperature.

The effects c and d are illustrated by the diagrams 1 and 2. In Fig. 1 the anisotropy ($\chi_\perp/\chi_\parallel$) is plotted against temperature (C°). The straight line, representing the purest bismuth obtainable (0.005 percent Pb), decreases slightly with increasing temperatures. The two hyperbolic curves represent the anisotropy of a crystal saturated with Sn (*ca.* 3 at. percent). Close to 0°C $\chi_\perp/\chi_\parallel$ becomes infinite, for lower temperatures the anisotropy is negative indicating that the crystal is now *paramagnetic* in one direction (parallel to the principal axis) and *diamagnetic* in the other. As far as our knowledge goes this is the first time that such a phenomenon has been observed in a crystal.

The representation of the reciprocal anisotropy $\chi_\parallel/\chi_\perp$ as function of the temperature as chosen in Fig. 2 is much simpler. The values form a family of straight lines, each corresponding to a certain concentration of foreign atoms (given in atomic percents). It is remarkable that all intersect each other, if extrapolated beyond the melting temperature of Bi, in *one* point. The lines follow the relation:

$$\chi_\parallel/\chi_\perp = R = R_0 - \beta\,(T_0 - T),$$

where T is the absolute temperature, T_0 the "critical" temperature of the impurities, i.e. the temperature at which the presence of foreign atoms would no longer have influence

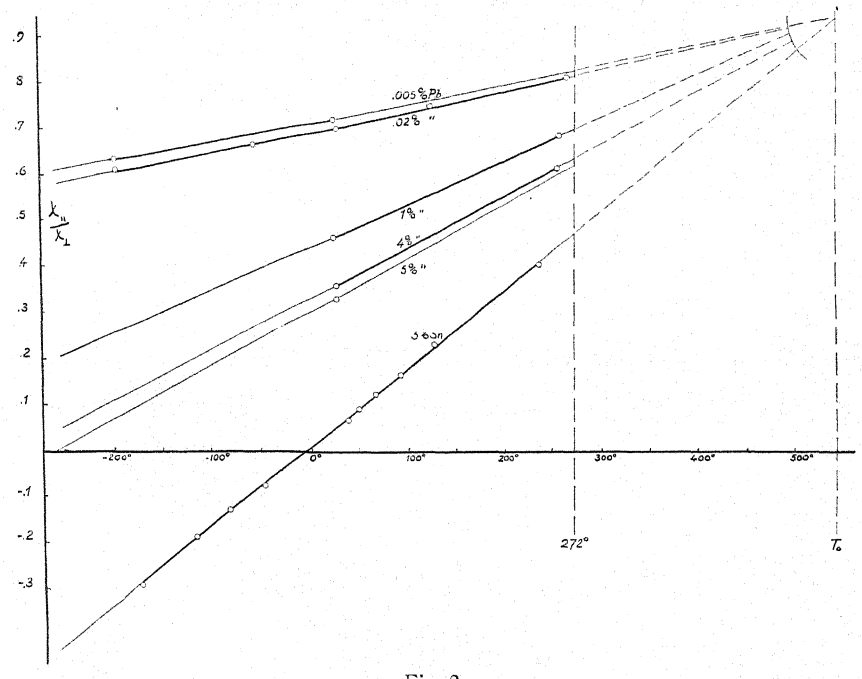


Fig. 2.

upon R (if the crystal had not already melted), R_0 is the reciprocal anisotropy at T_0, and β is the coefficient of temperature of R. At

$$T' = T_0 - R_0/\beta$$

the crystal diamagnetism parallel to the axis is destroyed to such an extent as to balance the atomic paramagnetism completely ($R=0$), below T' the crystal as a whole is metamagnetic.

It seems to be important that T_0 be independent of the type of impurity (as far as Pb and Sn are concerned), whereas β depends on the concentration as well as on the kind of the foreign atom. The values of the constants are:

$R_0 = 0.95 \pm 0.03$
$T_0 = 813° \pm 5°\text{K}$
$T' = 270°\text{K}$ for Bi saturated with Sn (ca. 3 at. percent).

β_{Pb} calculated per atom present in the crystal is smaller than β_{Sn}, hence a metamagnetic crystal could not be produced with Pb within the accessible range of temperature, though there is but little doubt that the inversion occurs at sufficiently low temperatures as well.

The investigation will be continued with special regard to the relation of the reported phenomena to the type of secondary structure observed in bismuth crystals.[4]

A. GOETZ AND
A. B. FOCKE

Norman Bridge Laboratory of Physics,
California Institute of Technology,
September 12, 1931.

[4] A. Goetz, Proc. Nat. Acad. **16**, 99. (1930).

BOOK REVIEWS

Grundlagen der Praktischen Optik. M. BEREK. Pp. 152, figs. 63. Walter de Gruyter and Company, Berlin, 1930. Price, R.M. 13.

The considerations of lens design which are of importance in practice are discussed in greater detail than in the usual treatise on geometrical optics, much of the material of purely academic interest being omitted. This has enabled the author to write a highly useful book without going into a bulky volume. A concise discussion of the general properties of optical systems, particularly the aberrations and their determination by ray tracing, is presented in the first four chapters. Following this, Seidel's theory of the third order aberrations is presented and applied to various problems in lens design. The properties of many of the well-known types of lenses are analyzed. It is noteworthy that the notation throughout is unambiguous and that a list of all the symbols used is given at the close of the book. This volume gives a splendid introduction to the subject of practical optics, a field in which the author has distinguished himself.

JOSEPH VALASEK
University of Minnesota

Der aufbau der Kupfer-Zinklegierungen. O. BAUER AND M. HANSEN. Cloth, pp. 150, 8 x 11″, 172 figs. Julius Springer, Berlin, 1927. Price 20 R.M.

This monograph is a very complete treatise on the copper-zinc alloys, particularly the constitution diagram of these alloys.

The first 83 pages are given to a very comprehensive review and critical discussion of the entire literature on the subject. Pages 84 to 140 report an investigation which is primarily concerned with the alloys containing more than 50 percent of zinc.

In writing up this research the authors have paid special attention to parts of the diagram which were not well established by previous investigations. Results are extensively illustrated by very good photomicrographs, numerous tables and drawings.

Their findings from their research and their interpretation of the researches of others have been used to draw a revised constitution diagram, which is described in detail as to the various fields, position of curves, and the reactions taking place at different temperatures and concentrations.

The collection of the bibliography of 156 references adds materially to the value of the monograph. . . .

OSCAR E. HARDER
Battelle Institute

Lehrbuch der Metallkunde des Eisens und der Nichteisenmetalle. Cloth, pp. 462, 9 x 6″, 399 figs. Julius Springer, Berlin, 1929. Price 29 R.M.

The author has divided the book into two parts; the first part of 288 pages is "general," and the second part of 162 pages is "special," of which 113 pages are given to ferrous materials and 50 pages to nonferrous. The first part may be described as the principles and methods of physical metallurgy, although more than the usual amount of attention is given to the mechanical properties, especially of the pure metals.

The first 153 pages discuss pure metals under the following general headings: state of metals 23 pages, x-ray crystallography 29, physical properties 12, and mechanical properties 89. Röntgenography and mechanical properties are given more than the usual amount of attention. These sections are treated in a more extensive and more fundamental way than in any English book which has come to the reviewer's attention. Apparatus, method of testing, and interpretation of results are discussed sufficiently to make this publication of special interest to workers in these fields.

Then follows 50 pages on constitution or equilibrium diagrams, 26 pages on methods of determining such diagrams, and 25 pages on the physical and mechanical properties of alloys as related to their constitution, and 11 pages on chemical properties and corrosion of alloys.

Pages 257 to 288 discuss technical processes, such as casting, working by rolling, pressing and machining, welding, soldering, coating, etc. This section is rather a departure from the general theme of the text.

In the second part pure iron, cast iron, plain carbon, and alloy steels and various steel treating processes are discussed, pages 289 to 401. Equilibrium diagrams and microstructures are used extensively and to good advantage. The material is well chosen and logically presented, and this section has much information in the limited amount of space.

The nonferrous metals—copper, aluminum, nickel, zinc, tungsten—and the alloys of copper-zinc, copper-tin, copper-aluminum, copper-nickel, noble metals and their alloys, pressure casting alloys, bearing metals, solders, amalgams, aluminum casting alloys, magnesium alloys, and age-hardening of alloys make the remainder of the text. This section is not up to the quality of the other sections, and some of the subjects are treated in a very sketchy and inadequate way, for example, noble metals and noble metal alloys, and especially copper-aluminum alloys.

The author has brought together in a single volume much valuable information and has furnished abundant references to original literature. This book should be a valuable reference as a starting point in a study of most of the subjects covered. Unfortunately for the American student, the German literature is cited more than the English. There is also some use of Landolt-Börnstein in cases where there are more recent researches, as for example, in Fig. 154. This treatise might lend itself well to use as a text for beginning students, providing they have a college education, but is rather difficult for undergraduates who are just beginning a study of metals and alloys. A translation of the book should have a good reception.

(See review by E. Fetz, **Metals and Alloys,** Vol. 1, No. 10, p. 484, April, 1930.)

OSCAR E. HARDER
Battelle Institute

Der Aktive Stickstoff. H. O. KNESER. A chapter of volume 8 of Ergebnisse der Exakten Naturwissenschaften. Pp. 229–257, figs. 12. Julius Springer, Berlin, 1929.

This chapter gives a complete and concise review of the subject of active nitrogen. It is divided into twelve parts, corresponding to different aspects of the problem, as for example, production of active nitrogen, chemical properties, spectrum, etc. This makes the review very readable and of value, not only to those readers who are interested in the physical properties of active nitrogen, but also to those who wish to use active nitrogen as a tool. There is also a bibliography containing 87 references, some as late as 1929.

JOSEPH KAPLAN
University of California at Los Angeles

Second Series *November 1, 1931* *Vol. 38, No. 9*

THE

PHYSICAL REVIEW

COMPARISON OF VISCOSITY AND MOLECULAR ARRANGEMENT IN TWENTY-TWO LIQUID OCTYL ALCOHOLS

By G. W. Stewart and R. L. Edwards

University of Iowa

(Received September 14, 1931)

Abstract

A comparison is made between the x-ray diffraction halos of 22 octyl alcohols and their corresponding viscosities and an unmistakable correlation found. The assumptions are that the halos indicate periodicities, that the periodicities may be interpreted as structural in the "cybotactic" groups, and that the relative diffraction intensity of the halos computed by assuming crystal structure may be used to estimate roughly the perfection of the liquid groups. It thus is shown that there is a correlation between the coefficient of viscosity and the perfection of grouping in the direction of the length of the chain molecules. This corresponds with the reasonable view that the viscosity within the liquid groups is caused by longitudinal slippage. Moreover, since the groups at any instant occupy a large fraction of the volume of the liquid, this viscosity is an important part of that measured. This interpretation accounts for the negative temperature coefficient of the viscosity, since the size of the groups decrease with temperature. The experiments and conclusions are in accord with Andrade's theory of momentary "crystallization" and with Ornstein's theory of the formation of liquid crystal groups, yet it is to be noted that these theories deal with different aspects and not the entire phenomenon.

THE x-ray diffraction study by the author[1] of 22 octyl alcohols prepared in the laboratory of Professor E. Emmet Reid of Johns Hopkins University has made possible an interesting comparison of x-ray findings with the coefficient of viscosity of the same compounds. The comparsion as herewith presented, leads to the conclusion that this coefficient does have a dependence upon differences in the space arrangement (cybotaxis) of the molecules of liquid isomers as determined by x-ray data.

In the discussions in Nature[2] the differences in the origin of viscosity in liquids and gases is emphasized. The picture of the phenomenon in liquids as given by Andrade is that there is "a temporary union of molecules in contiguous layers, the duration of this union not exceeding the very brief time required for the molecules to acquire a common velocity of translation." This union takes place under the action of the molecular fields. "The general pic-

[1] Stewart, Phys. Rev. **35**, 726 (1930).

[2] By E. N. da C. Andrade, J. Frenkel, D. H. Black ,E. W. Madge and Ambrose Fleming in issue of April 12, 1930, and by E. C. Sheppard, March 29, 1930.

ture is one of the liquid "crystallizing" in minute patches." It is evident that Andrade's view borders closely upon what the author has chosen to call the "cybotactic" condition of the liquid. The x-ray evidence by diffraction in liquids, both in this laboratory[3] and elsewhere,[4] has accumulatively stressed the correctness of the view that there are in a liquid minute groups[5] or bundles of molecules in each one of which there is sufficient periodicity to account for the diffraction halos obtained.

It is further evident that this periodicity is not caused merely by the effect of the volume of the molecules,[6] but also by all the forces arising in the molecular fields as well. The importance of the molecular fields may be obtained from a general comparison of the liquid and crystalline state, for example in density, compressibility and latent heat of evaporation. But as a specific illustration of the necessity of the introduction of these fields may be cited the difference in diffraction halos of 3-ethyl pentane[3] and diethyl carbinol.[3] Both molecules are admittedly of practically the same size and shape, yet with the former only one halo of importance appears, whereas with the latter there are two very prominent. The additional halo in the diethyl carbinol is caused by a periodicity in the direction of the molecular lengths, one which does not appear at all in the nonpolar compound. Moreoever, the periodicities indicated by the other diffraction maxima are not of the same magnitude. But it is the purpose of this article not to submit the large amount of evidence favoring the existence of minute well-ordered temporary regions or groups of molecules in a liquid, but rather to point out an interesting comparison of the coefficient of viscosity with the perfection of these molecular groups as shown by x-rays. The results have been hitherto unpublished, chiefly because they have appeared more suggestive than conclusive. But the discussion of liquid viscosity already mentioned and the current interest in obtaining the appropriate basis for a theory of that phenomenon would seem to require that the experimental evidence connecting the cybotactic view with the nature of viscosity be submitted. To this will be added a brief theoretical discussion of the cybotactic view.

[3] See Stewart and collaborators, Morrow, Skinner, in a series of papers in Phys. Rev. from September 1927 to September 1931, and Spangler, Radiology **16**, 346 (1931).

[4] For reveiws of literature see, for example, Good, Physica Acta, p. 305, 1930.

[5] It must be emphasized that the word "group" when describing molecular structure in a liquid, refers not to a minute crystal, to a region having a defined boundary, or to a permanent condition of the molecules involved. It refers to a region or spot of effective (at that instant) regularity of structure in a liquid. This condition of regularity of space arrangement fades off continuously into much less regularity. Hence there is no sharp boundary. These regions are very numerous occupying a large fraction of the total volume of liquid. A group does not retain its identity as determined by its constituent molecules. It is not a fragment of material, but it is a condition of position and potential energy which varies throughout the liquid. The existence of any group is temporary, yet the orderliness of the structure in more than one direction demands that its existence has a time duration.

[6] Debye in J. of Mathematics and Physics **4**, 133 (1925) and in Phys. Zeits. **28**, 315 (1927) has shown that even spherical atoms when occupying as much as one-half of the total volume, will produce an x-ray halo. Also Zernike and Prins, Zeits. f. Physik **41**, 184 (1927) emphasize the space effect.

EXPERIMENTAL

In order to make the discussion intelligible, the relative diffraction intensity curves for the 22 octyl alcohols are shown in Figs. 1, 2, and 3.[7] The angle θ is that read on the spectrometer. The radiation is essentially that of Mo$K\alpha$, but is not strictly monochromatic. Nevertheless its lack of homogeneity does not here lead to incorrect interpretations. Especially it should be remarked that any misleading effect of the continuous radiation is avoided by having a low voltage on the tube and by using thicknesses of samples that are less than the optimum for Mo$K\alpha$ radiation. The original article may be consulted

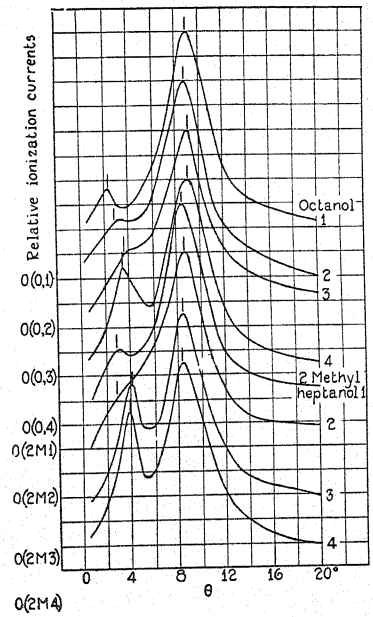


Fig. 1. X-ray diffraction; relative ionization currents of octyl alcohols.

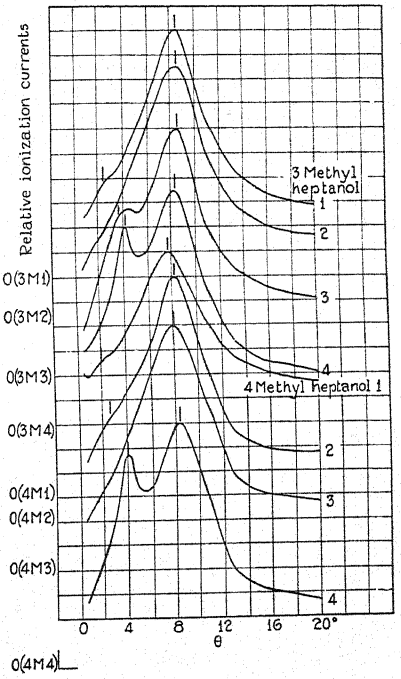


Fig. 2. X-ray diffraction; relative ionization currents of octyl alcohols

for the experimental details. It is assumed that these peaks indicate periodicity and that the most probable distance of separation of diffraction centers can be obtained by Bragg's law, $\lambda = 2d \sin \theta/2$. This assumption is warranted by the accepted view of crystal structure. The coherence in x-ray diffraction with crystals shows, by computation with Bragg's Law, the periodicities of the structure and in this interpretation both classical and quantum theories agree. Then for monochromatic radiation incident on a liquid, a band, instead of a line diffraction, may be interpreted as indicating not one periodicity but a number of them; as if one had powdered crystals with each set of planar separations varying over a small range in accord with a probability function. Some of the variation of periodicity, but much narrower in range,

[7] Stewart, Phys. Rev. **35**, 726–732 (1930).

may occur in the analogous single crystal also. The assumption of the correctness of Bragg's law for a liquid is thus based upon the straightforward conclusion that coherence indicates periodicity.

The periodicities obtained from the liquid are not sufficient to lead to a unique liquid structure. But it is in agreement with all the facts to assert that the molecules of n-alcohols, saturated normal fatty acids and n-paraffins[8] lie parallel in the so-called groups, with their long axes laterally equidistant and lying in two sets of parallel planes perpendicular to one another. This dimension is obtained from the major peak. On the other hand the position of the minor peak (not occurring with the paraffins) depends upon the length of the chain and is assumed to correspond to a periodicity having a direction or a component of a direction along the axes of the molecules. If the spacing of the molecules longitudinally is not orderly, permitting effective diffraction

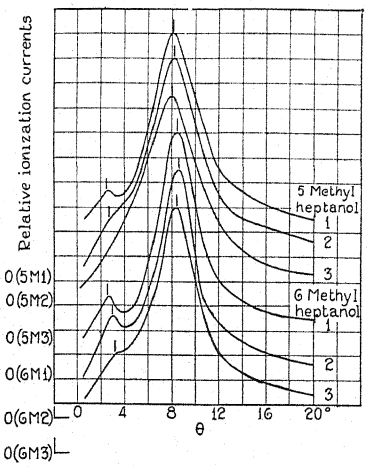


Fig. 3. X-ray diffraction; relative ionization currents of octyl alcohols.

centers to lie in parallel planes cutting the molecular axes, the minor peak will not be in evidence. These statements are consistent with all the facts and are discussed fully in the articles cited.

If one now considers the structure factor, F, of the molecules just as in the case of a crystal, it is easily seen[9] that the x-ray intensity from the lateral periodicity of these molecules will always be large and comparable with each other, while from the longitudinal periodicity the coherent scattering will be less and the variation among the compounds greater.

But as noted in x-ray diffraction experiments, these longitudinal periodicities appear (in chain compounds) only with polar molecules. The molecular field of a nonpolar chain compound is not sufficient to produce the longitudinal periodicity. One might thus expect that the slippage in the liquid groups may occur parallel to the molecular lengths and that there is a varia-

[8] Stewart and Morrow, Phys. Rev. **30**, 232 (1927); Morrow, Phys. Rev. **31**, 10 (1928); Stewart, Phys. Rev. **31**, 174 (1928).

[9] Spangler, Radiology **16**, 346 (1931).

tion in the intensities at the minor diffraction peaks not only because of structure factor but also because of the lack of perfection in the longitudinal periodicity.

One might thus anticipate that the viscosity would depend upon the perfection of the longitudinal periodicity, indeed, that the viscosity would increase with the perfection of grouping. This would be the case whether the groups occupied a large proportion of the volume or not. Clearly a comparison of the perfection of orderly longitudinal grouping with variation in viscosity would be advisable.

Degree of longitudinal periodicity in octyl alcohols compared with viscosity. The comparison just suggested must be of necessity crude, for one is not dealing with minute crystals wherein the structure factor of the molecules can be used with accuracy. Moreover, the structure of the liquid so-called groups is not definitely known. Reliance is placed merely upon a reasonable interpretation of diffraction curves.[9] The method of comparison is as follows.

TABLE I.

Compound	Heights of peaks	Computed relative heights	Col. 2–Col. 3 Ratio	Coefficient of viscosity
Octanol-1	11.0	24.9	0.433	0.204
Octanol-2	6.	12.4	.484	.218
Octanol-3	7.5	36.5	.206	.066
Octanol-4	27.2	69.0	.394	.154
2-methyl heptanol-1	11.0	49.5	.220	.083
2-methyl heptanol-2	6.0	40.0	.150	.091
2-methyl heptanol-3	28.0	104.	.270	.333
2-methyl heptanol-4	36.2	84.3	.430	.294
3-methyl heptanol-1	2.7	43.7	.062	.0361
3-methyl heptanol-2	0	29.1	0	.0311
3-methyl heptanol-3	16.5	140.	.118	.196
3-methyl heptanol-4	24.6	117.	.175	.042
4-methyl heptanol-1	1.0	53.2	.0188	.065
4-methyl heptanol-2	4.0	11.1	.364	.077
4-methyl heptanol-3	0.0	82.	0	.019
4-methyl heptanol-4	33.8	108.	.313	.322
5-methyl heptanol-1	6.0	13.6	.440	.137
5-methyl heptanol-2	4.0	4.46	.898	.047
5-methyl heptanol-3	0	84.5	0	.021
6-methyl heptanol-1	11.0	7.9	1.39	.227
6-methyl heptanol-2	17.8	3.92	4.54	.154
6-methyl heptanol-3	6.0	94.5	.0635	.026

In column two of Table I appear the relative heights of the secondary peaks as measured in Figs. 1, 2 and 3. In column 3 appear the relative heights these peaks should have if the diffraction occurred from powdered crystals having the structure mentioned. The computations for column 3 were made by Mr. Ross Spangler using the values of equivalent numbers of electrons as given by James and Brindley.[10] Column 3 then may be interpreted as indicating relative values of minor maxima in the diffraction curves which would occur if the groups were powdered crystals. Hence column 2 divided by column 3 would give a crude measure of the excellence or perfec-

[10] James and Brindley, Phil. Mag. **12**, 87 (1931).

tion of longitudinal periodicity which actually exists. This quotient is placed in column 4. In column 5 are given the observed coefficients of viscosity of these octyl alcohols as determined by Professor E. C. Bingham. The comparison is now made between column 4 and column 5 in Figs. 4 and 5. The values are plotted with change in molecular structure. With OH stationary and CH_3

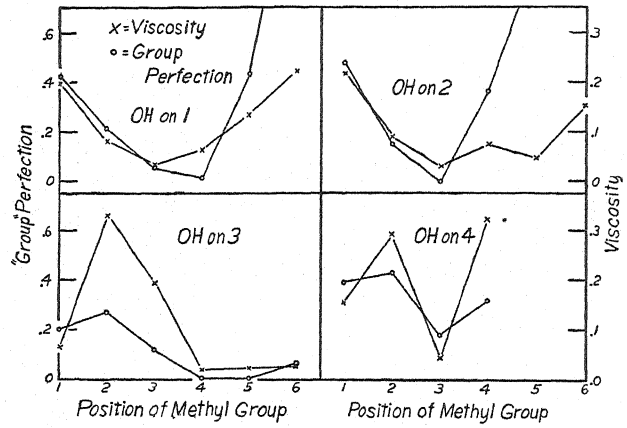


Fig. 4. Variation of "group" perfection and coefficient of viscosity.

attached as a branch to the different C atoms, the comparison is made in Fig. 4. It is to be noted that the range of the variables is large and therefore the correlation is striking. Only three compounds of the 22 in column four do not show a correlation. Similar comments may be made concerning Fig. 5 in which the position of the OH group is made the variable in the molecular

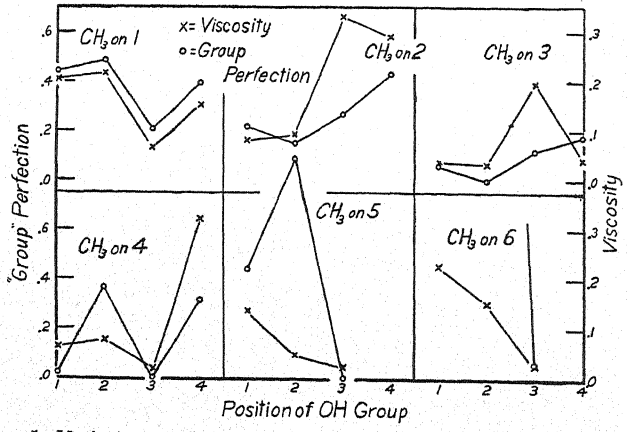


Fig. 5. Variation of "group" perfection and coefficient of viscosity.

structure. Incidentally, it may be pointed out that the three compounds with which the comparison is not favorable are those in which the molecule has OH near one end and CH_3 in a branch near the other. This indicates similar reasons for the disagreement, and the nature of the assumptions leaves ample room for such reasons. Speculations upon these disagreements are omitted

as having no purpose in this paper. That the correlation in Fig. 4 is noticeably better than in Fig. 5 is in harmony with the fact that in the former the polar group for any curve pair is stationary in the molecule. It should be pointed out that our assumptions take no consideration of the viscosity of the less regularly arranged molecules, which may depend on "shape." This is because, as mentioned below, these molecules are relatively few in number. Consequently the longitudinal slippage within the molecular groups is the chief factor in viscosity. From the foregoing evidence it now appears that the conditions producing the cybotactic condition in a liquid should be used as a basis for the consideration of the nature of liquid viscosity. This procedure is justified chiefly because of the evidence for cybotactic groups accumulated through x-ray diffraction experiments, but yet in part also because of the corroborative experiments here described.

The cybotactic view can be embodied in mathematical expressions only by very crude approximations, for the nature of the molecular fields is not understood. One such may be by the assumption of Andrade[11] as to a temporary union of molecules of one layer with another. This may be regarded as recognizing the existence of non-rigid somewhat orderly regions or groups in which, for example, molecules having a long axis will slip by one another in the direction of this axis. Andrade's theory has not been published so that it is impracticable to comment further on its conformity with the concept of groups advocated by the author.

A different approach to a theoretical consideration may be borrowed from Ornstein's[12] theory of liquid crystals. If the molecule is unsymmetrical, having a long axis, it is assumed that a molecule exerts a couple upon a neighboring one, the potential energy being proportional to the cosine of the angle between their axes and to a function of the distance of separation of the centers of mass of the molecules. Boltzmann's principle is applied. The theory finally leads to an expression which shows that the volume of the well-ordered regions decreases with an increase in temperature. From the experiments with x-rays it has become evident that, since the coherent diffraction with liquids is of the same order of magnitude[13] as that of the same mass in the form of crystal powder, the volume of the molecular groups is a large fraction of the total volume. Thus, if within the groups or well ordered regions the viscosity were greater than in the ungrouped molecules, the volume of the groups would be important in determining the measured value of the viscosity. An increase in temperature, decreasing this volume, would decrease the viscosity, which is in accord with experiments. In order to compute the effect, one would need to develop a theory for the dependence of viscosity upon the volume of the groups present when that volume is a large fraction of the whole.

The two theories are not contradictory, but refer to different aspects each without any claim of completeness. Andrade's theory emphasizes the effect of momentary group formation, which interferes with slippage. Ornstein's

[11] E. N. da C. Andrade, Nature, April 12, 1930.
[12] Ornstein, Zeits. f. Kristall. **79**, 90 (1931).
[13] Stewart, Phys. Rev. **37**, 9 (1931); See Fig. 1.

theory assumes a group which changes its size with temperature. In view of x-ray evidence concerning liquid diffraction it is reasonable to suppose that both conditions exist. It is significant that both causes lead to the correct sign of the change of viscosity with temperature and that both theories are in essential agreement with the cybotactic group view advocated by the author though as a matter of expediency they consider the conditions only in part.[14]

It is evident from the foregoing that a theory of viscosity which involves all the important aspects of the nature of a liquid is yet ahead, but that the theories of Andrade and of Ornstein are distinctly valuable. The cybotactic view would indicate the desirability of closer approximations in theory to the molecular fields existing in corresponding crystals. But until such fields are well understood the bases of theories proposed must of necessity be limited.

The reader is reminded that the correlation found between cybotactic group perfection and viscosity is presented because it seems opportune. The correlation is intrinsically not highly satisfactory. But the results do show an unmistakable relation, in spite of the various approximations that are of necessity made. This conclusion is however sufficient to emphasize the justification for the basis of viscosity theory similar to that given by Andrade. Not only does the temperature variation of viscosity point to an assumption of momentary union of molecules, but all x-ray diffraction experiments in liquids would urge the essential correctness of the assumption.

It is a pleasure to thank Professor E. Emmet Reid of Johns Hopkins University for the octyl alcohols used, Professor E. C. Bingham of Lafayette College for the viscosity data, and Dr. H. A. Zahl who, as a research assistant, took the x-ray data involved.

[14] There has just come to the attention of the author the earlier suggestions of Raman (Nature **111**, 532 and 600 (1923). He assumed two states of aggregation in the liquid "solid" and "vapor," and that the viscosity was proportional to the relative numbers of molecules in the two states. Raman's assumptions, while not those of the author, are closely similar. Raman's expression for the viscosity of a liquid is the same as Andrade, $\eta = Ae(b/T)$, where η is the viscosity coefficient, A and b are constants and T is the temperature. This formula agrees remarkably well with observed temperature variations. See also Iyer (Ind. J. of Physics, V Pt. IV, 371 (1930) for a discussion of the significance of A and b in Raman's suggestion.

THE BROWNIAN MOTION OF STRINGS AND ELASTIC RODS

G. A. VAN LEAR, JR. AND G. E. UHLENBECK
DEPARTMENT OF PHYSICS, UNIVERSITY OF MICHIGAN

(Received August 24, 1931)

ABSTRACT

The method introduced by Ornstein is applied to calculate the Brownian-motion mean-square deviation for strings and for elastic rods, the surrounding medium being a gas. For the string, a varying tension and elastic binding at the ends are supposed, and a formula is obtained for the mean-square deviation of any point at time t, having started with a given deviation of that point; the result contains infinite series. This result is specialized to the string with fixed ends and constant tension. For the mid-point, and for a limited time interval, the series are summed; for $t\to\infty$, the result is given for all points, agreeing with that given by Ornstein for the mid-point. Elastic rods are treated similarly, and similar results are obtained. The effect of gravity, when the rod is vertical, is introduced by a simple and consequent preturbation method, and a formula is obtained for the mean-square deviation of the lower end; this agrees closely with Houdijk's experimental results. The time dependence given by the complete formula cannot yet be tested, for Houdijk gives only long-time mean values in his publication.

INTRODUCTION

1. Most of the theoretical work on Brownian motion has been concerned with only one degree of freedom, and it is the purpose of this paper to apply the method first introduced by Ornstein[1] to cases in which there are more (in fact, an infinite number) of degrees of freedom. The systems to be treated are: I. the stretched string, and II. the elastic rod. The first has been treated by Ornstein[2] and the second by Houdijk,[3] but in each case results were obtained only for $t\to\infty$ (that is, only "equipartition" values were found); our extensions will consist principally in giving the dependence of the mean-square deviation on the initial deviation and on the time, but we also treat a more general string before specializing to a particular case, and give a better treatment of the effect of gravity in the case of the rod.

In general our treatment will follow the lines of that used by Uhlenbeck and Ornstein[4] in their second (exact) calculation for the mean-square deviation of a harmonically-bound particle in Brownian motion, where they use the method of Ornstein. In this method one starts from the equation of motion and certain assumptions about the influence of the surrounding medium on the particle, and calculates directly the mean values sought, making use of certain properties of a canonical ensemble (a large number of similar, but

[1] L. S. Ornstein, K. Akad. Amsterdam Proc. **21**, 96 (1919), (in English).
[2] L. S. Ornstein, Zeits. f. Physik **41**, 848 (1927).
[3] A. Houdijk, Archives Neerlandaises des Sciences Exactes et Naturelles, Series III A, **11**, 212 (1928).
[4] G. E. Uhlenbeck and L. S. Ornstein, Phys. Rev. **36**, 823 (1930).

independent, particles) in evaluating constants which appear in the calculation. It will be of interest to record their result here, for it is of the same type as those which we shall obtain; with a slight change of notation, it is:

$$\overline{s^2}^{s_0} = \frac{kT}{m\omega^2} + \left(s_0^2 - \frac{kT}{m\omega^2}\right)e^{-\beta t}\left(\cos\omega_1 t + \frac{\beta}{2\omega_1}\sin\omega_1 t\right)^2 \tag{1}$$

where s is the displacement from equilibrium position, t the time, m the mass, and ω the (undamped) natural frequency in 2π sec., $\beta = f/m$, where f is the damping force per unit velocity, and $\omega_1^2 = \omega^2 - \beta^2/4$. This result, like all those obtained by this method, is not subject to the restriction (which must be imposed on results obtained by certain other methods) that t must be large compared to β^{-1}, hence the term "exact."

Now it is well known that the vibrating string may be treated by means of its normal vibrations, and that each normal vibration obeys the equation of the harmonic oscillator; also, we shall show the same to be true of the rod. Thus we may, so to say, consider in each case the system to be an assembly of damped harmonic oscillators, each having for its frequency that of the corresponding normal vibration. The deviation of any point will then be determined by the displacements of all the component "oscillators," and similarly for the squared displacement, velocity, etc. Thus one can foresee that the treatment will not be essentially different from that for the harmonic oscillator itself, the additional elements necessary being: (1) the deduction from our assumptions (about the influence of the surrounding medium on the system) of results which will take the places of analogous assumptions for the individual "oscillators," (2) the treatment of the sums which result, and (3) a certain averaging process which is more complicated than that necessary for a single oscillator, and which will arise when we wish to make the known initial conditions apply to only one point of the string or rod.

I. The Brownian Motion of a Homogeneous String

2. We consider the Brownian motion of a homogeneous string (i.e., one with constant linear density ρ) of length L, surrounded by a gas. The string is bound elastically at its ends and is under a tension $\tau(x)$ which may vary with the distance x along it. The equation of motion of the string is:

$$\rho\frac{\partial^2 s}{\partial t^2} + f\frac{\partial s}{\partial t} = \frac{\partial}{\partial x}\left(\tau\frac{\partial s}{\partial x}\right) + F(x,t)$$

where f is the friction coefficient and $F(x,t)$ is the fluctuating force. This may be written:

$$\frac{\partial^2 s}{\partial t^2} + \beta\frac{\partial s}{\partial t} = p'\frac{\partial s}{\partial x} + p\frac{\partial^2 s}{\partial x^2} + A(x,t) \tag{2}$$

where $\beta = f/\rho$, $p = \tau/\rho$, $A = F/\rho$. The conditions to be satisfied at the ends are:

$$\begin{aligned} h_0 s(0, t) - \left(\frac{\partial s}{\partial x}\right)_{x=0} &= 0 \\ - h_L s(L, t) - \left(\frac{\partial s}{\partial x}\right)_{x=L} &= 0 \end{aligned} \tag{3}$$

where h_0 and h_L are the ratios of elastic constant of binding to tension at the two ends.

The assumptions which we make for this case are the natural generalizations of Ornstein's assumptions for the simpler cases, namely that the influence of the surrounding gas may be split up into two parts; (1) a systematic frictional force, $-f(\partial s/\partial t)$ per unit length, where f is a constant depending on the nature of the gas and its pressure, and (2) a fluctuating force, $F(x,t)$ per unit length, about which we make further assumptions in terms of $A(x,t)$:

$$\overline{A(x, t)} = 0 \tag{4}$$

$$\overline{A(x_1, t_1)A(x_2, t_2)} = \phi(x_1 - x_2, t_1 - t_2) \tag{5}$$

where $\phi(x,t)$ is even in both x and t and has a sharp maximum at (0,0). The mean is taken over a subensemble, each member of which started at $t=0$ with a given shape and distribution of velocity along it.

If we consider the homogeneous equation obtained by omitting the last term from (2), the usual treatment by separation of variables gives rise to two differential equations, of which the "space" one is a slightly-specialized case of the Sturm-Liouville equation. This equation, together with the boundary conditions, defines in the usual way the orthogonal eigenfunctions X_n, which we shall assume normalized, and which satisfy the following differential equation and boundary conditions:

$$pX_n'' + p'X_n' + \lambda_n X_n = 0 \tag{6}$$

and

$$\begin{aligned} h_0 X_n(0) - X_n'(0) &= 0 \\ - h_L X_n(L) - X_n'(L) &= 0 \end{aligned} \tag{7}$$

where λ_n is the corresponding eigenvalue.

We now return to Eq. (2), and expand $s(x,t)$ and $A(x,t)$ each in a series of eigenfunctions with coefficients which depend on the time:

$$s(x, t) = \sum_{n=1}^{\infty} S_n(t) X_n(x) \tag{8}$$

$$A(x, t) = \sum_{n=1}^{\infty} A_n(t) X_n(x). \tag{9}$$

Substituting these expansions into (2), equating to zero each term of the

sum which results if we transfer all terms to the left-hand member, and using (6), we obtain as the equation for $S_n(t)$:

$$S_n'' + \beta S_n' + \lambda_n S_n = A_n(t). \tag{10}$$

We can write down at once the general solution of this, which is:

$$\begin{aligned} S_n(t) = &\left[\frac{\beta S_n(0) + 2S_n'(0)}{2\omega_n} \sin \omega_n t + S_n(0) \cos \omega_n t\right] e^{-\beta t/2} \\ &+ \frac{1}{\omega_n}\int_0^t A_n(v) e^{-\beta(t-v)/2} \sin \omega_n(t-v)dv \end{aligned} \tag{11}$$

where

$$\omega_n^2 = \lambda_n - \tfrac{1}{4}\beta^2 \tag{12}$$

and we restrict ourselves to the case in which all the eigenvibrations are periodic by assuming

$$\lambda_n > \tfrac{1}{4}\beta^2.$$

$S_n(0)$ and $S_n'(0)$ are clearly the n-th coefficients of the expansions of the initial displacement and velocity, respectively.

3. As a preliminary step, which will furnish us with results to be needed later, we shall calculate the mean-square deviation of any point for simple initial conditions, supposing that at $t=0$ the string is at rest in its equilibrium position. This means that $S_n(0) = S_n'(0) = 0$, and denoting by $\overline{S^2}^0$ the mean-square deviation for these initial conditions, we obtain

$$\overline{s^2}^0 = \sum_1^\infty \frac{1}{\omega_n^2} \overline{I_n^2} X_n^2(x) \tag{13}$$

where

$$I_n = \int_0^t A_n(v) e^{-\beta(t-v)/2} \sin \omega_n(t-v)dv \tag{14}$$

because the double sum which results directly from (8) is reduced to a single sum by the fact (proved in Note 1, on the basis of assumption (5)) that $\overline{I_n I_m} = 0$ if $m \neq n$; this has the meaning that the different eigenvibrations are uncorrelated, in so far as they arise solely from the fluctuating force.

For $\overline{I_n^2}$ we get an integral similar to those occurring in the paper of Uhlenbeck and Ornstein;[4] using the results of Note 1, we find

$$\overline{I_n^2(t)} = \frac{\alpha_n}{2\beta}(1 - e^{-\beta t}) - \frac{\gamma_n}{4\lambda_n}\left\{\tfrac{1}{2}\beta + e^{-\beta t}(\omega_n \sin 2\omega_n t - \tfrac{1}{2}\beta \cos 2\omega_n t)\right\} \tag{15}$$

where

$$\gamma_n = \int_{-\infty}^{+\infty} \psi_n(v)dv, \quad \alpha_n = \int_{-\infty}^{+\infty} \psi_n(v) \cos \omega_n v dv,$$

$$\psi_n(v - w) = \overline{A_n(v)A_n(w)};$$

thus

$$\overline{I_n^2(\infty)} = \frac{\alpha_n}{2\beta} - \frac{\gamma_n \beta}{8\lambda_n}. \tag{16}$$

To determine the constants α_n and γ_n, we make use of the same devices as were used by Uhlenbeck and Ornstein for the harmonic oscillator; that is, we equate the mean potential energy of each eigenvibration (the mean being taken over a canonical ensemble) to $kT/2$, and the correlation between deviation and velocity to zero. In this way we obtain the result:

$$\alpha_n = \gamma_n = \frac{2\beta kT}{\rho}. \tag{17}$$

The calculations are given in Note 2.

One might fear that the assigning of the potential (and kinetic) energy $kT/2$ to each eigenvibration would give rise to convergence difficulties, since it makes the total energy of the system infinite, but this is not the case. We inquire only about the mean-square deviation, and the series which result are all amply convergent. However, there is a further point which may seem strange, namely that we found α_n and γ_n to be equal and independent of n. Their equality (which follows from only our initial assumptions and the lack of correlation between deviation and velocity, the use of the equipartition energy not being involved) would indicate that the correlation function, $\phi(x,t)$, is infinitely sharp in both x and t, and this one cannot believe.[5] However this difficulty becomes serious only at high frequencies, and seems to indicate that our assumptions must not be used where one is concerned with times that are too small, say of the order of magnitude of the time between successive molecular impacts on any small length considered. However, this limitation is much less stringent than that which had to be imposed on certain earlier work, where the results were not valid for times of the order of magnitude of β^{-1} or less, and on account of the convergence properties of our solutions, it brings in no difficulties here. The independence of n is to be understood in a similar way.

By substitution of (19), (17) becomes:

$$\overline{I_n}^2 = \frac{\omega_n{}^2 kT}{\rho\lambda_n} - \frac{kT}{2\rho\lambda_n} e^{-\beta t}\left\{\frac{4\lambda_n + \beta^2}{2\beta} + \omega_n \sin 2\omega_n t - \tfrac{1}{2}\beta \cos 2\omega_n t\right\} \tag{18}$$

and we obtain from (15):

$$\overline{s^2(x,t)}^0 = \frac{kT}{\rho}\sum_1^\infty \frac{X_n{}^2(x)}{\lambda_n}\left\{1 - \frac{\beta}{2\omega_n{}^2} e^{-\beta t}\left(\frac{4\lambda_n + \beta^2}{2\beta} + \omega_n \sin 2\omega_n t + \tfrac{1}{2}\beta \cos 2\omega_n t\right)\right\}. \tag{19}$$

Taking the limit of this expression for $t \to \infty$, we obtain for a canonical ensemble:

$$\overline{s^2} = \frac{kT}{\rho} F(x) \tag{20}$$

where:

$$F(x) = \sum_1^\infty \frac{X_n{}^2(x)}{\lambda_n}. \tag{21}$$

[5] Quite analogous questions must be raised in the case of the harmonic oscillator.

4. We are now ready to calculate a quantity which is more easily measured than that given by (21), namely the mean-square deviation of a given point of the string, after having started at $t=0$ with a given initial deflection of that point. Let this given value be C, so that:

$$s(x, 0) = C$$

for the particular value of x under consideration; this value will be taken to be the same throughout this discussion, so that in this section x is a constant. this means that:

$$\sum_1^\infty X_n(x)S_n(0) = C \tag{22}$$

and it is the value of this linear combination of the $S_n(0)$ which is to be given; otherwise we are to average over a canonical ensemble. That is to say, we consider a canonical ensemble of strings and, fixing on some particular numbers for x and C, pick out of it at $t=0$ a subensemble, all members of which have the deflections of the x-points equal to C. We then follow these strings in their motions, and it is the squared deflections of their x-points, averaged over this subensemble, which we wish to calculate.

To this end one may first calculate $\overline{s^2}^{s_0u_0}$, which is the mean-square deviation of a subensemble, each member of which has initially the same given shape and velocity distribution along it. This means that for each member, $S_n(0)$ and $S_n'(0)$ are the same; the difference in behavior of the different members arises only out of the fact that the fluctuating force, $F(x,t)$ varies from member to member. Next one calculates $\overline{\overline{s^2}}^{s_0}$, which is the mean-square deviation of a subensemble, each member of which has initially the same shape, and hence the same set of $S_n(0)$, no attention being paid to velocities. This is to be obtained by averaging $\overline{s^2}^{s_0u_0}$ over the $S_n'(0)$, using the facts that $\overline{S_n'(0)}=0$ (which follows from the lack of correlation between displacement and velocity in a canonical-ensemble) and that $\overline{S_n'^2(0)}$ has the value corresponding to equipartition of kinetic energy. The final result sought is to be obtained by averaging $\overline{\overline{s^2}}^{s_0}$ over the $S_n(0)$ with the restriction (22).

We find:

$$\overline{\overline{s^2}}^{s_0} = \sum_{n=1}^\infty \sum_{m=1}^\infty X_nX_m\left\{S_n(0)S_m(0)B_nB_m + \delta_{nm}\frac{kT}{\rho\lambda_n}(1 - B_n^2)\right\} \tag{23}$$

where

$$B_n(t) = e^{-\beta t/2}\left(\frac{\beta}{2\omega_n}\sin\omega_n t + \cos\omega_n t\right). \tag{24}$$

Now

$$\overline{\overline{s^2}}^{C} = \frac{\int_C \cdots \int \overline{\overline{s^2}}^{s_0} \exp(-V/kT)dS_1(0)dS_2(0)\cdots}{\int_C \cdots \int \exp(-V/kT)dS_1(0)dS_2(0)\cdots}$$

where V is the potential energy given in Note 2, and the C written under the integral-signs (an infinite number of them are implied) means that the integrations are to be performed with the condition (22). Using (23) and interchanging summations and integrations we obtain a result which contains the quotient of two integrals. This quotient is evaluated in Note 3, and using this, we obtain as the final result:

$$\frac{\overline{\equiv c}}{s^2} = \frac{kT}{\rho}F(x) + \left[C^2 - \frac{kT}{\rho}F(x)\right]e^{-\beta t}\left[\frac{1}{F(x)}\frac{\partial G}{\partial t} + \frac{\beta}{2F(x)}G\right]^2 \tag{25}$$

where

$$G(x, t) = \sum_{n=1}^{\infty} \frac{X_n^2 \sin \omega_n t}{\omega_n \lambda_n}. \tag{26}$$

This is in complete correspondence with Eq. (1) for the harmonic oscillator, in which $(\sin \omega_1 t)/\omega_1$ plays the same part as $G(x,t)/F(x)$, and $1/\omega^2$ corresponds to $F(x)$. It is interesting to observe (as can be shown to follow at once from the form of (25)) that this mean-square deviation never crosses the equipartition value, and further, that the curves corresponding to a given value of β, but to different values of C, differ only in scale, when referred to the equipartition line. These statements are true also for the harmonic oscillator.

5. As an example we consider the string with fixed ends and constant tension. For this case, we find:

$$F(x) = \frac{2L}{a^2\pi^2}\sum_{1}^{\infty}\frac{\sin^2 n\pi x/L}{n^2} = \frac{L}{a^2}\left(\frac{x}{L} - \frac{x^2}{L^2}\right)$$

where

$$a = \left(\frac{\tau}{m}\right)^{1/2} = \text{wave velocity}.$$

This gives us:[6]

$$\overline{s^2(x)} = \frac{kTL}{\tau}\left(\frac{x}{L} - \frac{x^2}{L^2}\right). \tag{27}$$

The other result to be specialized is (25). In this there appears, in addition to $F(x)$, the function $G(x,t)$ and its time derivative. The corresponding series contain both x and t as variables, and in this general form we have not been able to sum them. However, if we restrict our attention to the mid-point of the string, we can further simplify matters, for we shall show in Note 4 that for the interval $0 \leqq t \leqq L/a$, we may write:

$$G(L/2, t) = \frac{2L}{a^2\pi^2}\sum_{n\,\text{odd}}\frac{\sin (n^2a^2\pi^2/L^2 - \beta^2/4)^{1/2}t}{n^2(n^2a^2\pi^2/L^2 - \beta^2/4)^{1/2}}$$

$$= \frac{L}{2a^2}\left\{\sinh (\beta t/2) - \frac{2at}{L} I_1(\beta t/2)\right\}$$

$$\frac{dG(L/2, t)}{dt} = \frac{L}{4a^2}\left\{\cosh (\beta t/2) - \frac{2at}{L} I_0(\beta t/2)\right\}$$

[6] For the mid-point this gives the value $kTL/4\tau$, which has been given by Ornstein, reference 2.

where

$$I_n(z) = i^{-n}J_n(iz)$$

and $J_n(x)$ is the Bessel function of order n. Using these expressions and reducing, (25) becomes:

$$\overline{\overline{S^2(L/2,t)}}^C = \frac{kTL}{4\tau} + \left[C^2 - \frac{kTL}{4\tau}\right]\left\{1 - \frac{2at}{L}e^{-\beta t/2}[I_0(\beta t/2) + I_1(\beta t/2)]\right\}^2 \quad (28)$$

for:

$$0 \leqq t \leqq L/a.$$

In Fig. 1 we have plotted some curves showing how $\overline{\overline{S^2}}^C$ depends on the time. For these we have taken $a=L=1$, $\beta=1,2,3,4$, and $C^2=0$ and $=3kT/4\tau$. For $0\leqq t\leqq 1$ (28) was used; for later times it was necessary to use the series themselves, although it was found possible to replace β by zero in these

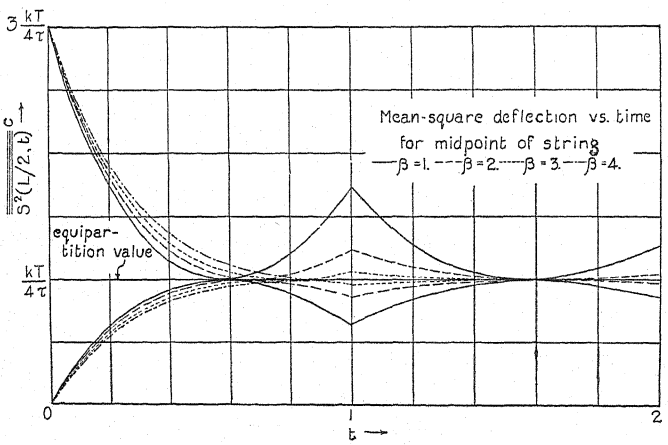


Fig. 1.

series without introducing too great an error. The apparent cusps in the curves at $t=1$ are curious; they are not in fact quite cusps if β is different from zero, but the difference is not apparent to the eye with the scale used.

II. The Brownian Motion of an Elastic Rod

6. We shall first treat, in the same manner as for the string, the problem of the Brownian motion of an elastic rod which has one end clamped and the other free, and later consider the effect of gravity. We take these end conditions because they are the ones most easily realized in experiments; the problem could as readily be carried through for any other combination of the usual conditions.

The equation of motion of an elastic rod under no forces is given by Rayleigh[7] as:

[7] Lord Rayleigh, Theory of Sound (London. Macmillan, 1894), vol. 1, p. 258.

$$\frac{\partial^2 S}{\partial t^2} + \frac{r^2 E}{4d}\frac{\partial^4 s}{\partial x^4} - \frac{r^2}{4}\frac{\partial^4 s}{\partial x^2 \partial t^2} = 0$$

where E = Young's modulus, r = radius of cross-section (assumed circular and constant), d = volume-density; other symbols are as for the string. The third term of the first member arises out of the kinetic energy of rotation of the cross-sectional laminae; it is neglected by Rayleigh in his further treatment, and we shall do likewise. Adding the damping and accidental-force terms, we obtain:

$$\frac{\partial^2 s}{\partial t^2} + \beta\frac{\partial s}{\partial t} + \frac{r^2 E}{4d}\frac{\partial^4 s}{\partial x^4} = A(x, t). \tag{29}$$

Taking the origin at the clamped end, and the end conditions (also given by Rayleigh) are:

$$\begin{aligned} s = 0, \quad \frac{\partial s}{\partial x} = 0 \quad &\text{for } x = 0 \\ \frac{\partial^2 s}{\partial x^2} = 0, \quad \frac{\partial^3 s}{\partial x^3} = 0 \quad &\text{for } x = L \end{aligned} \tag{30}$$

We make the same assumptions about $A(x, t)$ as for the string.

If we consider the homogeneous equation obtained by replacing the second member of (29) by zero and separate the variables as usual, the resulting "space" equation is:

$$\frac{d^4 X}{dx^4} = \frac{4\lambda d}{r^2 E} X$$

where λ is the separation parameter. The situation is the same as that obtaining for the Sturm-Liouville equation for, as Rayleigh shows, this equation, together with the boundary conditions arising out of (30), gives rise to a complete set of orthogonal eigenfunctions:

$$X_n = b_n[a_n(\cos m_n x/L - \cosh m_n x/L) + (\sin m_n x/L - \sinh m_n x/L)] \tag{31}$$

where m_n is the nth positive root of the equation:

$$\cos m \cdot \cosh m + 1 = 0 \tag{32}$$

$$a_n = \frac{\cos m_n + \cosh m_n}{\sin m_n - \sinh m_n} \tag{33}$$

$$\lambda_n = \frac{r^2 E m_n^4}{4dL^4} \tag{34}$$

and the coefficients b_n are chosen for normalization. Rayleigh discusses the roots of (32) and calculates the first few, giving formulas from which the rest can be found. In addition he shows that:

$$\sum_{n=1}^{\infty} \frac{1}{m_n^4} = \frac{1}{12} \tag{35}$$

and

$$X_n^2(L) = \frac{4}{L}. \tag{36}$$

We shall have occasion to use these results.

Returning to Eq. (29), we proceed just as for the string and expand $s(x, t)$ and $A(x, t)$ each in a series of eigenfunctions with coefficients which depend on the time; in the same way as before, we obtain Eq. (10) for $S_n(t)$, so that Eqs. (8)—(12) of article 2 apply as well as to this case as to the string.

7. The calculation of the mean-square deviation of any point, supposing that at $t=o$ the rod is at rest in its equilibrium position, follows here exactly as for the string; we may take all the equations of that article to apply to the present case. To obtain Eq. (17), however, we must use for the potential energy:

$$V = \frac{\pi r^4 E}{8} \int_0^L \frac{ds}{R^2}$$

where R is the radius of curvature of the rod at the point. In view of the approximate straightness we may replace this by:

$$V = \frac{\pi r^4 E}{8} \int_0^L \left(\frac{\partial^2 s}{\partial x^2}\right)^2 dx.$$

Using this, together with the differential equation and boundary conditions for the eigenfunctions, we again arrive at (*B*) of Note 2. The corresponding expression for the potential energy of the nth eigenvibration becomes, on using (36):

$$V_n = \frac{\pi r^4 E}{8L^4} m_n^4 S_n^2. \tag{37}$$

The further calculations are identical, and we again arrive at (17) where now $\rho = \pi r^2 d$. Hence results (18), (19) and (20) are valid for this case also; substituting for λ_n by (34) in (20) we obtain for the canonical-ensemble mean-square deviation of any point x:

$$\overline{s^2} = \frac{4L^4 kT}{\pi r^4 E} \sum_{n=1}^{\infty} \frac{X_n^2(x)}{m_n^4} \tag{38}$$

and for the free end, using (36) and (35) we obtain the result already given by Houdijk[3]:

$$\overline{s^2} = \frac{4L^3 kT}{3\pi r^4 E}. \tag{39}$$

The calculations of article 4 for the string, in which we found an expression (given by Eq. (25)) for the mean-square deviation of a given point x, after having started at $t=o$ with a given initial deviation C of that point, apply just as well to the rod. The general result becomes especially simple for the free end because the series converge quite strongly on account of the rapid increase of m_n. Taking only the first terms, and using *12* for m_1^4 instead of *12.4* (since this makes the value at $t=o$ strictly correct), we obtain:

$$\overline{\overline{s^2(L,t)}}^{C} \cong \frac{4L^3kT}{3\pi r^4E} + \left(C^2 - \frac{4L^3kT}{3\pi r^4E}\right)e^{-\beta t}\left(\cos\omega_1 t + \frac{\beta}{2\omega_1}\sin\omega_1 t\right)^2 \qquad (40)$$

where:

$$\omega_1^2 = \lambda_1 - \tfrac{1}{4}\beta^2 = \frac{3r^2E}{dL^4} - \tfrac{1}{4}\beta^2.$$

8. Houdijk[3] has observed the Brownian motion of the lower ends of thin filaments which were clamped vertically at their upper ends and were otherwise free, the surrounding medium being air. It is necessary in this case to take into account the effect of gravity, and we shall now modify the foregoing treatment in this regard. We shall assume that a rod under gravity executes the same eigenvibrations as without it and that their amplitudes will bear approximately the same ratios to each other, the effect of gravity being to increase the potential energy associated with each. We shall restrict our attention to the free (lower) end, and we may with good approximation assume that the form of the rod is given by the first eigenfunction.

To obtain the contribution, ΔV_1, of gravitation to the potential energy, we treat the rod as a string under the tension $\rho g(L-x)$, where we again use ρ for the linear density; thus we have:

$$\Delta V_1 = \frac{\rho g}{2}\int_0^L (L-x)\left(\frac{\partial s}{\partial x}\right)^2 dx; \qquad (41)$$

this is completely equivalent to multiplying the total mass by the distance through which its center of gravity is raised in bending it to a given shape. In accordance with the approximation mentioned above, we write:

$$s = S_1(t)X_1(x)$$

Substituting in (41), using the expression (31) for $X_1(x)$, and using the fact that to our present approximation, $s^2(L,\ t) = 4/L \cdot S_1^2(t)$ we obtain:

$$\Delta V_1 = \frac{0.98\rho g}{8}s^2(L,t)$$

To the same approximation,

$$V_1 = \frac{\pi r^4 E}{32L^3}m_1^4 s^2(L,t)$$

so that

$$V_1 + \Delta V_1 = \frac{\pi r^4 E m_1^4 + 3\cdot 96\rho g L^3}{32L^3}\, s^2(L, t) = \frac{kT}{2}.$$

Subsituting $\pi r^2 d$ for ρ and *12* for m_1^4, we obtain:

$$\overline{s^2(L)} = kT\frac{4L^3}{3\pi r^4 E + 0.98\pi r^2 dgL^3}. \tag{42}$$

This formula is practically identical with the one given by Houdijk, the only difference being that he has the number *1* where we have 0.98, and this difference is much too small to be significant in the comparison with experimental results. We have given the above derivation because we believe it to be more consequent then Houdijk's. His observations agree very well with the values predicted by this formula. The closeness of agreement is indicated by the fact that he uses it to determine Avogadro's number, N, (substituting R/N for k) from his observations, finding as the average of ten determinations the value 6.36×10^{23}, which differs from the accepted value of 6.06×10^{23} by only *5* percent.

Concerning the dependence of the mean-square deviation on the initial conditions and the time, to adapt formula (40) to this case we need only replace the equipartition value given there by the second member of (42). This formula cannot yet be tested, for Houdijk gives only limiting values in his publication.

NOTES

Note 1. We are to investigate the quantity $\overline{I_n I_m}$; it is clear that if we write it as a double integral, it will contain under the integral signs the quantity $\overline{A_n(v)A_m(w)}$, and by using (10) we obtain for this:

$$\overline{A_n(v)A_m(w)} = \int_0^L \int_0^L \overline{A(x, v)A(y, w)}X_n(x)X_m(y)dxdy.$$

Now let $x-y=u$ and $y=z$; using (5),

$$\overline{A_n(v)A_m(w)} = \int_0^L dz \int_{-\infty}^{+\infty} \phi(u, v-w)X_n(u+z)X_m(z)du.$$

But $\phi(u, v-w)$ differs from zero only for u very little different from zero, hence we replace $X_n(u+z)$ by $X_n(z)$ in the integrand, and by using the orthogonality property we obtain.

$$\overline{A_n(v)A_m(w)} = \delta_{nm}\psi_n(v-w)$$

where

$$\psi_n(v-w) = \int_{-\infty}^{+\infty} \phi(u, v-w)du$$

So that

$$\overline{I_n I_m} = 0 \quad \text{for} \quad n \neq m.$$

This procedure is of course not rigorous unless $\phi(u, v-w)$ is infinitely "sharp" in u, which we have not assumed.

For the string with fixed ends and constant tension, however, the eigenfunctions are sines, and in this case we may improve the argument. We have:

$$\overline{A_n(v)A_m(w)} = \frac{2}{L}\int_0^L dz \int_{-\infty}^{+\infty} \phi(u, v-w)\left[\sin\frac{n\pi u}{L}\cos\frac{n\pi z}{L} + \cos\frac{n\pi u}{L}\sin\frac{n\pi z}{L}\right]\sin\frac{m\pi z}{L}du.$$

When integrated, the first term of this gives zero because in the integration over u the integrand is an odd function, and the second term gives zero in the integration over z if $n \neq m$ because of the orthogonality of the sines. If $n=m$, however, we obtain:

$$\overline{A_n(v)A_m(w)} = \int_{-\infty}^{+\infty} \phi(u, v-w) \cos\frac{n\pi u}{L}\, du = \psi_n(v-w).$$

It is clear from this that for this case, ψ_n should be expected to depend on n, in that it will be diminished for very high values of n if ϕ is not infinitely sharp in its dependence on u, and therefore we have allowed for this also in the general case.

Note 2. We are to determine the constants α_n and γ_n. The potential energy of the system, which includes the potential energy of the binding at the ends is:

$$V = \tfrac{1}{2}\rho\left\{\int_0^L p(x)\left(\frac{\partial s}{\partial x}\right)^2 dx + h_0 p(0)s^2(0,t) + h_L p(L)s^2(L,t)\right\}.$$

When we substitute (8) into this, interchange summations and integration, and integrate by parts (using (7) and the orthogonality property), we find:

$$V = \tfrac{1}{2}\rho\sum_{n=1}^{\infty}\lambda_n S_n^2 \tag{A}$$

or

$$V_n = \frac{\rho\lambda_n}{2} S_n^2$$

where V_n is the potential energy of the n-th eigenvibration. In a similar manner, although much more simply, we find for the kinetic energy:

$$K = \tfrac{1}{2}\rho\sum S_n'^2$$
$$K_n = \tfrac{1}{2}\rho S_n'^2.$$

For $t\to\infty$, the subensemble which started at $t=0$ from rest and equilibrium position will become a canonical ensemble; thus:

$$\lim_{t\to\infty}\overline{V_n}^0 = \frac{\rho\lambda_n}{2}\overline{S_n^2(\infty)}^0 = \frac{\rho\lambda_n}{2\omega_n^2}\overline{I_n^2(\infty)} = \frac{kT}{2}.$$

Substituting (16) into this, we obtain the relation:

$$4\alpha_n\lambda_n - \gamma_n\beta^2 = \frac{8\omega_n^2\beta kT}{\rho}. \tag{B}$$

If we similarly equate the kinetic energy of the n-th eigenvibration to $kT/2$ we obtain, not another relation, but the same one again, as might have been expected from the results for the harmonic oscillator. To confirm this statement, one must calculate $S_n'^2(\infty)$ in the same way that we have calculated $S_n^2(\infty)$.

To get another relation we make use of the fact that in a canonical ensemble of strings there will be no correlation between the displacement and the velocity for any point. Thus, writing $u=ds/dt$:

$$\overline{su}^0 = \sum_{n=1}^{\infty}\sum_{m=1}^{\infty}\frac{1}{\omega_n\omega_m}\overline{I_nJ_m}X_nX_m$$

where J_m is an integral similar to I_m. Now it is clear that $\overline{I_nJ_m}$ will contain under the integral signs the quantity $\overline{A_n(v)A_m(w)}$, and we have shown that this vanishes unless $m=n$. Therefore, the double sum reduces to a single sum. Our requirement that $\mathrm{Lim}_{t\to\infty}\overline{su}^0=0$ gives the result $\alpha_n=\gamma_n$ and putting this into (B),

$$\alpha_n = \gamma_n = \frac{2\beta kT}{\rho}.$$

Note 3. The ratio of integrals to be calculated is.

$$L_{nm} = \frac{\int_C \cdots \int S_n(0)S_m(0) \exp\left\{-\rho \sum_1^\infty \lambda_i S_i^2(0)/2kT\right\} dS_1(0)dS_2(0) \cdots}{\int_C \cdots \int \exp\left[-\rho \sum_1^\infty \lambda_i S_i^2(0)/2kT\right] dS_1(0)dS_2(0) \cdots}$$

where the integration are to be carried out with the condition:

$$\sum_{n=1}^{\infty} X_n S_n(0) = C.$$

Let us first take the integrals to be only N-tuple, and the summations correspondingly to go only from 1 to N, afterward taking the limit for $N \to \infty$. Now introduce the new variables:

$$y_n = S_n(0)\left(\frac{\rho\lambda_n}{2kT}\right)^{1/2}.$$

The Jacobian of the transformation of course does not matter, being the same in the numerator and denominator; this gives us:

$$L_{nm,N} = \frac{2kT}{\rho(\lambda_n\lambda_m)^{1/2}} \frac{\int_{C_N} \cdots \int y_n y_m \exp\left(-\sum_1^N y_i^2\right) dy_1 dy_2 \cdots dy_N}{\int_{C_N} \cdots \int \exp\left(-\sum_1^N y_i^2\right) dy_1 dy_2 \cdots dy_N}$$

and the condition now becomes:

$$\sum_{n=1}^{N} a_n y_n = C_N$$

where

$$a_n = X_n\left(\frac{2kT}{\rho\lambda_n}\right)^{1/2}.$$

We now rewrite each integral so that the integrations over y_n and y_m are the last ones; these integrations are carried from $-\infty$ to $+\infty$, and the condition is satisfied by keeping constant

$$\sum_{j=1}^{N}{}'' a_j y_j = C_{nm} = C_N - a_n y_n - a_m y_m$$

in the integration over the remaining $N-2$ variables, where the double accent signifies that j does not take on the values n and m.

The integration over this hyperplane, whose distance from the origin is $C_{nm}D_{nm}^{-1/2}$, where $D_{nm} = \sum'' a_j^2$, is carried out by rotating our coordinate system so that one of the axes coincides with the normal; the condition is now satisfied by keeping this variable constant and integrating over the others from $-\infty$ to $+\infty$. This transformation involves no calculation because the variables appear in the integrand in an invariant form, and we obtain:

$$L_{nm,N} = \frac{2kT}{\rho(\lambda_n\lambda_m)^{1/2}} \frac{\int_{-\infty}^{+\infty}\int_{-\infty}^{+\infty} y_n y_m \exp(-y_n^2 - y_m^2 - C_{nm}^2/D_{nm}) dy_n dy_m}{\int_{-\infty}^{+\infty}\int_{-\infty}^{+\infty} \exp(-y_n^2 - y_m^2 - C_{nm}^2/D_{nm}) dy_n dy_m}.$$

We now take the limit for $N \to \infty$ by appropriately changing the definitions of C_{nm} and D_{nm}. The remaining integrations are carried out in a straight-forward manner by transforming the expression in the exponent onto its principle axes, etc. We obtain:

$$L_{nm} = \frac{X_n X_m}{F^2(x)\lambda_n\lambda_m}\left[C^2 - \frac{kT}{\rho}F(x)\right].$$

In the above discussion we have assumed $n \neq m$; a similar calculation for L_{nn} shows that the general result may be written:

$$L_{nm} = \frac{X_n X_m}{F^2(x)\lambda_n\lambda_m}\left[C^2 - \frac{kT}{\rho}F(x)\right] + \delta_{nm}\frac{kT}{\rho\lambda_n}.$$

Note 4. We have to consider:

$$\frac{\partial G(L/2, t)}{\partial t} = \frac{2L}{a^2\pi^2}\sum_{n\text{odd}}\frac{1}{n^2}\cos\left(n^2a^2\pi^2/L^2 - \beta^2/4\right)^{1/2}t.$$

Let

$$H(t) = \sum_{n\text{odd}}\frac{1}{n^2}\cos\left(k_n{}^2 - w^2\right)^{1/2}t$$

where

$$k_n = \frac{na\pi}{L}, \quad w = \tfrac{1}{2}\beta$$

thus,

$$\frac{\partial G}{\partial t} = \frac{2L}{a^2\pi^2}H(t)$$

$$G(L/2, t) = \frac{2L}{a^2\pi^2}\int H(t)dt + A.$$

We now make use of a method due to Versluys.[8] He shows by making a Taylor expansion that:

$$\begin{aligned}\cos\left(k_n{}^2 - w^2\right)^{1/2}t &= \cos k_n t - \frac{w^2t^2}{1!}\frac{d}{d(t^2)}\frac{\cos k_n t}{k_n{}^2} + \frac{w^4t^4}{2!}\frac{d^2}{d(t^2)^2}\frac{\cos k_n t}{k_n{}^4} + \cdots \\ &= \left\{1 + \frac{w^2t^2}{1!}\frac{d}{d(t^2)}\int_C^t\int_0^t dtdt + \frac{w^4t^4}{2!}\frac{d^2}{d(t^2)}\int_C^t\int_0^t\int_C^t\int_0^t(dt)^4 + \cdots\right\}\cos k_n t \\ &= V\cdot\cos k_n t\end{aligned}$$

where:

$$c = \frac{L}{2a}$$

and the operation V through which $\cos k_n t$ is transformed into $\cos\left(k_n{}^2 - w^2\right)^{1/2}t$ is independent of k_n; it may be written as follows:

$$V = \sum_{p=0}^{\infty}\frac{(w^2t^2)^p}{p!}\frac{d^p}{d(t^2)^p}\int_C^t\int_0^t\cdots\int_C^t\int_0^t(dt)^{2p}.$$

Thus we have:

$$H(t) = \sum_{n\text{odd}}\frac{1}{n^2}V\cdot\cos\frac{n\pi at}{L} = V\cdot\sum_{n\text{odd}}\frac{1}{n^2}\cos\frac{n\pi at}{L}$$

as it can be proved (according to Versluys) that here the operations V and Σ can be interchanged. Now:

$$\sum\frac{1}{n^2}\cos\frac{n\pi at}{L} = \frac{\pi^2}{4}(\tfrac{1}{2} - at/L) \quad \text{for} \quad 0 \leqq t \leqq L/a$$

$$\therefore H(t) = \frac{\pi^2}{4}\cdot\left(\tfrac{1}{2}V\cdot 1 - \frac{a}{L}V\cdot t\right).$$

We find:

$$V\cdot 1 = \sum_{p=0}^{\infty}\frac{(w^2t^2)^p}{(2p)!} = \cosh wt = \cosh\tfrac{1}{2}\beta t$$

and

$$V\cdot t = t\sum_{p=0}^{\infty}\frac{(wt)^{2p}}{2^{2p}(p!)^2} = tI_0(wt) = tI_0(\tfrac{1}{2}\beta t).$$

[8] W. A. Versluys, Proc. Acad. Amst. **31**, 670 (1928).

Therefore

$$\frac{\partial G}{\partial t} = \frac{L}{4a^2}\left[\cosh \tfrac{1}{2}\beta t - \frac{2at}{L} I_0(\tfrac{1}{2}\beta t)\right]$$

$$G = \frac{L}{2a^2\beta}\left[\sinh \tfrac{1}{2}\beta t - \frac{2at}{L} I_1(\tfrac{1}{2}\beta t)\right];$$

here we have used the fact that

$$\int z I_0(z) dz = z I_1(z)$$

and evaluated A so as to make $G(L/2, 0) = 0$, which gives $A = 0$.

For other intervals than the one used above, the series

$$\sum \frac{1}{n^2} \cos (n\pi at/L)$$

represents a "saw tooth" function having discontinuities in its first derivative at the points nL/a, $n = 1, 3, 5 \cdots$ and the attempt to extend the calculation past the point $t = L/a$ was not successful.

TRANSITION PROBABILITIES AND QUENCHING IN THE 3P STATE OF SODIUM

By N. E. Berry and G. K. Rollefson
Chemical Laboratory, University of California

(Received September 14, 1931)

Abstract

The effect of foreign gases upon the fluorescence of sodium vapor excited by the second line of the principal series has been investigated. The gases used were helium, nitrogen, and hydrogen and the intensities of both the 3303A line and the D light were observed. From the variation in intensity of the 3303A line as gas is added it is concluded that the presence of an inert gas has no appreciable effect upon the relative transition probabilities in the 3^2P state of sodium. With nitrogen or hydrogen as the added gas the D light intensity variation followed that of the 3303A line very closely but with helium a marked increase in intensity was produced by the first gas added with a decrease at higher pressures. This increase was explained as due to a transfer of sodium atoms from the 3^2P to the 3^2D state by collisions, thus increasing the number of atoms which radiate the D light. In addition to this increase in number the collisional transfers produced an increased "Doppler width" in the D light which persisted up to pressures well over 100 mm of helium and caused a decreased absorption of the fluorescence light. The bearing of this work on the difference in the intensity ratio of the 2^2S-3^2P and 1^2S-3^2P transitions as reported by Weiss for an arc and by Christensen and Rollefson in fluorescence is discussed. It is concluded on the basis of experimental evidence that any explanation of the difference which depends upon multiplicity of the 3^2P state is incorrect. An explanation of this difference based upon the assumption that the life period of an excited atom varies inversely as the transition probability of the radiation emitted is presented. It is shown that recent work on the life periods of atoms in the 2^3S_1 state of mercury at least partially supports this assumption. A new type of sodium arc with increased intensity and stability of operation is described.

WHEN transitions by radiation are possible from one energy level to two or more lower energy levels, the relative numbers of each of these possible transitions is designated by what is known as the transition probability. This transition probability has generally been assumed to be a constant, independent of the method of excitation or of the environment of the radiating atom.

Recent investigations concerning the transitions from the $3P$ state of sodium by Weiss,[1] by Christensen and Rollefson[2] and by Prokofjew[3] have seemed to indicate that the transition probabilities in this case are dependent upon either the method of excitation or the environment of the radiating atoms.

Figure 1 shows the different possible transitions from the $3P$ state of sodium. For convenience in discussion they are labelled (a), (b) and (c). The

[1] Weiss, Ann. d. Physik **1**, 565 (1929).
[2] Christensen and Rollefson, Phys. Rev. **34**, 1157 (1929).
[3] W. K. Prokofjew, Zeits. f. Physik **58**, 255 (1929).

fine structure of the terms is not shown. The investigation by Weiss[1] concerning the radiation in a low-voltage arc shows the ratio of the probabilities of transitions (b) and (a) to be 25 to 1. The results of the investigation of Christensen and Rollefson[2] on the fluorescence of sodium vapor excited by the 3303A radiation from a sodium arc show this ratio to be 1.7 to 1. R. Ladenburg has made the suggestion that the method of correction for absorption used by Christensen and Rollefson may be in error due to the change in absorption coefficient with wave-length over the breadth of the line. With the formulas and tables presented in a paper by Ladenburg and Levy[4] the theoretical correction has been calculated. It is found that for the measurements taken with the center of the exciting cone at a depth of 3 mm approximately 80 percent of the *D* light should be absorbed while the absorption of the 3303A is too small to have any appreciable effect upon the calculation. If the data obtained by Christensen and Rollefson are recalculated and the theoretical correction for absorption introduced, a value of 5.7 is obtained.

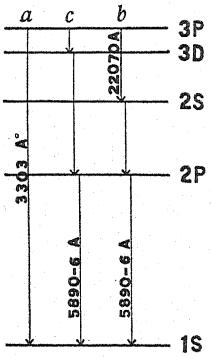


Fig. 1.

The calculation of this correction is, however, subject to serious errors due to the data upon which it was based. The experimental arrangement used by Christensen and Rollefson[2] was such that a fairly constant temperature could be maintained but no attempt was made to obtain an accurate measurement of the actual temperature of the fluorescence tube. A variation of approximately 15°C in the temperature produces a change of a factor of two in the vapor pressure of sodium. If the temperature used were fifteen degrees too high the correction for absorption would change to approximately 66 percent giving a ratio of 3.4. The data found for the vapor pressure of sodium itself do not agree within a factor of two.

That some error is involved is indicated by the fact that the ratios calculated from the data at two different depths differ by over twenty percent. The only experimental errors which might contribute to such a discrepancy are the photometric ones which do not exceed ten percent. If we assume that this discrepancy is due to an incorrect value for the vapor pressure of sodium and repeat the calculation for different pressures we find the same value for

[4] Ladenburg and Levy, Zeits. f. Physik 65, 189 (1930).

both depths if we select the conditions so that the corrected ratio is 3.4. We feel that this represents the best value which can be obtained from the data.

The results of the calculations carried out by Prokofjew[3] based upon the methods of wave mechanics, give a value of 2.1 for the ratio of these two transition probabilities.

The value of this ratio calculated by Christensen and Rollefson on the basis of their measurements of the relative intensities of the 5890A and 3303A radiation in fluorescence depends upon the assumption that the probability of transition (c) is negligible with respect to (b), Fig. 1, since both of these transitions must eventually result in the radiation of 5890A. In order to test the validity of this assumption the calculations carried out by Prokofjew[3] were extended to give an estimate of the relative probabilities of transitions (b) and (c) and it is found that this ratio is large enough (of the order of 50 to 1) that radiation due to transition (c) may be neglected.

In this investigation the effect of the addition of foreign gases upon the fluorescence of sodium, excited by 3303A, is studied. In order to carry out the investigation quantitatively it was found necessary to design a new type of arc of greater intensity and stability of operation than any of those thus far described in the literature.

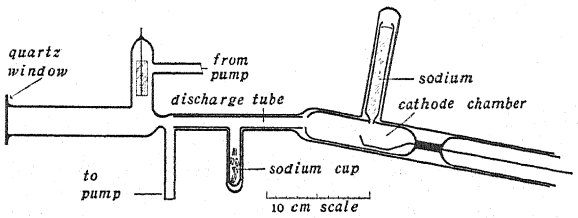


Fig. 2.

Figure 2, drawn to scale, gives the design of the arc. The quartz window and removable cathode are both sealed to the Pyrex with Dennison sealing wax. The electrical leads through the Pyrex are of tungsten and the anode is a cylinder of sheet nickel sealed to the tungsten wire with German silver. The cathode is of metallic sodium held in place by the cathode chamber, as shown in the diagram, with the electrical contact made directly to the tungsten wire.

The cathode chamber is made removable to facilitate refilling in case this becomes necessary. The sodium is introduced by placing a tube containing purified metal in the charging tube, as shown in the diagram, with one constricted end inserted in the small hole in the cathode chamber, sealing off the end of the charging tube, evacuating, and then heating the charging tube until the sodium melts and runs down. The discharge tube and sodium cup are placed inside a larger tube of the same shape to prevent the hot sodium from coming in contact with the wall which must remain vacuum tight. The sodium in the cup can be introduced in small tubes which are cut short enough to allow them to be inserted through the front of the arc before the quartz window is attached. The cup and discharge tube are equipped with heaters

and temperature controls, although the heat produced by the discharge is generally enough to maintain a sufficiently high temperature in the discharge tube. Argon is circulated through the arc as indicated, by means of a mercury pump with two liquid air traps filled with beads to remove the mercury vapor from the gas stream.

The sodium used is purified by first heating it for several hours, under vacuum, in such a way that it continually distills on to the sides of the flask and runs down again. This is done to expel occluded gases, especially hydrogen. When a very high vacuum is obtained the sodium is distilled through a side tube of large diameter and collected in tubes.

This arc is similar to that designed by Christensen and Rollefson[5] which we shall hereafter refer to as the "old type," but differs from it in several important respects. In the old type the cathode was heated and used as a part of the light source. In the new type it is not heated but is allowed to cool as much as possible and is not used as a part of the light source. The entire radiation, with appreciable intensity, is produced in the discharge tube in which the vapor pressure of sodium is controlled by the temperature of the sodium cup, the temperature of the discharge tube being always kept slightly higher. One advantage of this is the more accurate control of the vapor pressure of sodium which it affords, this being one of the chief factors involved in producing a discharge with constant intensity.

It is also found that the cool cathode eliminates a large degree of uncertainty of operation which was experienced with the old type. The trouble was undoubtedly connected with some sort of surface phenomenon, for it was always observed that whenever the "active point," usually visible on the surface of the cathode, was replaced by a diffused glow over the entire surface, the current dropped to a very small value with a corresponding decrease in intensity. This behavior was usually followed by complete failure. It was often found, however, that after allowing the cathode to cool, the arc could again be started at its normal current and also that heating the cathode to a higher temperature would result in breaking the discharge or reducing the current. It was further found that, whenever the $H\alpha$ line was present in the spectrum of the discharge, almost certain failure of the arc occurred. In view of this fact a tube of hot copper oxide was placed in the stream of circulating gas which reacted with the hydrogen changing it to water vapor which was removed in the same liquid air traps used to remove mercury vapor. This, of course, could remove only that portion of the hydrogen, present or produced in the back of the arc, which diffused into the circulating stream.

These difficulties are all eliminated in the new type of arc. The entire surface of the cathode chamber is usually found covered with sodium and the "active point" is seen to travel in a very devious path all over the surface. Even when the $H\alpha$ line is present in the spectrum of the discharge in appreciable amounts, this arc operates quite satisfactorily. In the old type whenever the cathode chamber was removed, after a few hours operation, it was always

[5] Christensen and Rollefson, Phys. Rev. **34**, 1154 (1929).

found to be cracked and had to be replaced. In the new type the cathode chamber does not crack and can be used again if refilling becomes necessary.

When the vapor pressure of sodium in the discharge tube is too low the arc will "flicker" but as the vapor pressure is increased the flickering ceases and a very steady discharge is maintained. As the vapor pressure is still further increased the intensity of the 3303A line gradually decreases. The optimum pressure is very easily obtained by increasing the temperature of the cup until the flickering just ceases.

The arc operates quite satisfactorily with about 0.5 cm of argon circulating through it. At lower pressures of argon the sodium diffuses out of the discharge tube quite rapidly, while increasing the pressure decreases the intensity of the 3303A line due to the quenching effect.

One of these arcs has been operated with 220 volts direct current at 2.5 amperes for about 150 hours and it seems in as good a condition as when new. This arc was operated with as low as 90 volts but some difficulty in starting it was encountered without the higher potential. A high frequency spark was used to start the arc.

This current of 2.5 amperes is by no means the maximum possible. By using less resistence in series with the arc the current can be increased to several times this value and one of these arcs was operated at 6 amperes for a period of one-half hour with perfectly satisfactory results.

For studying the fluorescence the apparatus assembly was identical with that described by Christensen and Rollefson with the addition of a small-diameter quartz tube, with a graded seal to Pyrex, leading from the fluorescence tube to the apparatus used to introduce varying pressures of foreign gases. The mean free path of sodium atoms in the pure vapor is so large, at the temperatures used, that the leak of sodium vapor through this tube is negligible. The foreign gas was always introduced while the fluorescence tube was cold, in order to prevent sodium vapor from being swept to the front and condensed on the window. It was found that addition of the foreign gases increased the necessary temperature of the hot air stream used to prevent condensation of sodium on the windows. An air stream of about 400°C was used with the fluorescence tube at 180–200°C. It was also found that with the air stream at this temperature, the temperature of the fluorescence tube necessary to cause "browning" was very much greater than when the air stream was kept at 280°C. This indicates that "browning" is preceded by condensation of sodium.

The assembly was constantly checked for stray light by making exposures for long periods with the fluorescence tube cold.

The helium gas used was passed through charcoal at both liquid air and liquid hydrogen temperatures. The nitrogen was passed through a tower filled with copper turnings and ammonium hydroxide to remove oxygen and then through a liquid air trap. The hydrogen was made electrolytically and was passed over hot copper to remove oxygen and then through charcoal at liquid air temperature.

The Wratten and Wainright panchromatic plate was used and a standard

developer and development procedure was adopted in order that blackenings on different plates might be compared. All the plates used were from the same box. All the photographs used to plot any one curve were taken on the same plate. The exposures of the fluorescence excited by 3303A radiation were taken over periods of one-half hour, one hour, two hours and three hours. The longer exposures were used in order to get blackenings of a density most accurately determinable, when the intensity was diminished by the addition of foreign gases. Photographs were also taken of the fluorescence when excited by *D* light. When a screen of approximately 10 percent transmission was inserted in the exciting beam, exposures of 10 seconds, 20 seconds, 40 seconds and 80 seconds gave satisfactory blackenings.

The photographic blackening densities were determined with a Zeiss microphotometer. All the photographs of the fluorescence and those taken to obtain the blackening—intensity calibration curves were photometered with the same adjustments of the instrument, and the readings were recorded on the same arbitrary scale. The blackening of any photograph could then be translated into intensity in terms of percent of an arbitrary standard.

The calibration curves were obtained with a direct current helium discharge operated by a 600 volt battery assembly at a current of 0.36 milliamperes in the case of the longer exposures and 0.8 milliamperes for the shorter exposures. The current was easily controlled to within 2 percent by gradually decreasing the resistance in series as the operating voltage of the battery decreased.

This discharge has strong lines at 5875A and 3187A as compared to 5890A and 3303A in the sodium fluorescence. A consideration of Harrison's work in spectral photometry, indicates that the use of these lines for calibration purposes is justified within a limit of 2 percent accuracy. For the longer-exposure calibrations a filter of $CrCl_3$ solution in a quartz vessel was placed between the discharge and the spectrograph. This absorbs a certain percentage of the 5875A radiation which is the more intense of the two and by varying the concentration of the solution the blackening produced by the two lines can be made approximately equal. This makes it possible to determine the calibration curves for both wave-lengths at the same time. For the calibration curves used with *D*-light excitation the $CrCl_3$ filter was not inserted since only the intensity of the 5875A line was needed.

Screens, calibrated for transmission with a thermopile, were used to reduce the intensity by a known fraction. The screens were kept moving and when two screens were used simultaneously they were moved in opposite directions at all times.

Photographs were obtained of the fluorescence excited by 3303A radiation and by *D* light with varying pressures of helium, nitrogen and hydrogen in the fluorescence tube and the resulting intensity curves are given below.

In Fig. 3, which shows the effect of helium on the fluorescence, curve *A* gives the variation in intensity of the 3303A line, the dots represent intensities with the fluorescent cone at a depth of 3 mm from the observer's side of the fluorescence vessel and the crosses are for a depth of 10 mm, the circles re-

present a theoretical quenching curve. Curve B gives the intensity of the "D" light when excited by 3303A the fluorescent cone being at a depth of 3 mm, curve C gives the intensity of "D" light with the cone at a depth of 10 mm. Curve D gives the intensity of D light excited by D light. In each case the intensities are in terms of the intensity with no helium present.

From the energy-level diagram for sodium, Fig. 1, it may be seen that the decrease in intensity of the 3303A line may be explained in two different ways. It may be due to transfers, by collisions of the second kind, of atoms in the $3P$ state to any one of the other four states designated. In other words it may be

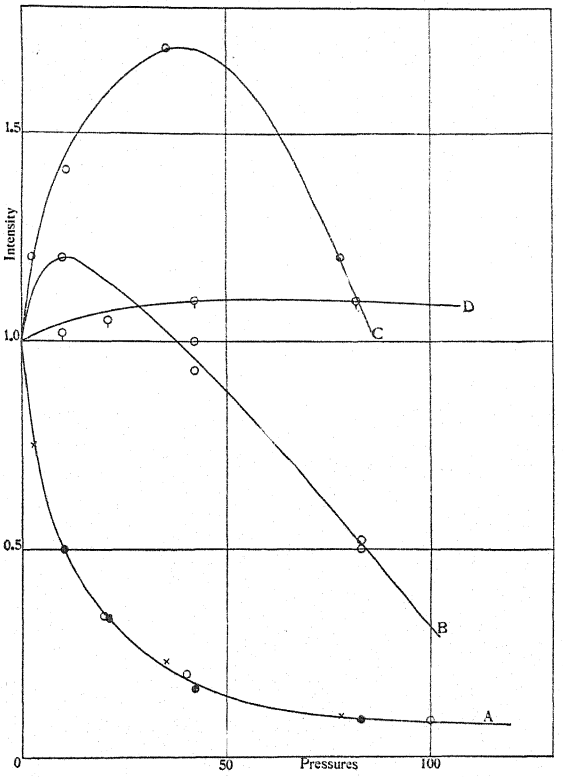


Fig. 3.

purely a quenching phenomenon. Also, it may be due to a change in the relative transition probabilities, effected by the presence of the helium, in favor of transitions "b" or "c". A combination of these two effects is also possible.

If the collisional transfers occur to either the $3D$, $2S$ or $2P$ state the effect upon the relative intensities of the 3303A and 5890A radiation is exactly the same as that produced by a change in the relative transition probabilities. However, the dependence of each of these effects upon the pressure of foreign gas may serve as a method of distinguishing them.

A theoretical quenching curve is determined by the expression for the fractional decrease in intensity

$$100 - I = \tau/(\tau + T),$$

where τ is the mean life of the excited atom, T is the mean time between effective collisions and I is the percent of the intensity of the unquenched radiation. At the pressure designated by $p_{1/2}$ at which the intensity has been reduced 50 percent it is evident that τ is equal to T, and we then have the following relations

$$T = k/p; \quad \tau = k/p_{1/2}$$

where p is the pressure at constant temperature and k is a proportionality factor. We may then write

$$100 - I = \frac{k/p_{1/2}}{k/p_{1/2} + k/p} = \frac{1}{1 + p_{1/2}/p}. \tag{1}$$

Replacing $p_{1/2}$ in Eq. (1) by the value obtained from any quenching curve gives the theoretical formula for that curve.

The small circles near curve A, Fig. 3, represent points on a theoretical quenching curve with the value for $p_{1/2}$ taken from curve A. The excellent agreement between the observed and calculated curves is evidence in favor of the supposition that the decrease in intensity of the 3303A radiation is due to a collisional effect and that the presence of helium has no apparent effect upon the relative transition probabilities.

Any effect upon the transition probability which depends upon the interaction of the excited sodium atom and a foreign gas molecule, at the instant of radiation, such as the effect of the electrostatic field, would be directly proportional to the pressure and independent of the life period of the excited atom since only its position at the instant of radiation is of importance. This straight-line relation might be slightly altered by the second order effect of multiple interaction. If the time required for the act of radiation is finite and if at any time during the act, interaction with a foreign gas molecule is effective in changing the transition probability the change in intensity will take the form of a quenching curve, but the value of τ will be different from that in the true quenching formula and the two effects cannot be superimposed. The two phenomena are indistinguishable only in case the effect of the foreign gas molecule is such that at any time during the normal life period of the excited atom, that interaction occurs, it may be caused to radiate or be so affected that when it does radiate its relative transition probabilities will have been changed. In case successive collisions are effective in changing the transition probability, the intensity variation will depend upon some higher power of the pressure.

Curve D, Fig. 3, gives the observed intensity for D light when excited by D light, and when compared with the data obtained by Mannkopff[6] using a resonance lamp for excitation it is evident that a considerable amount of increased absorption has occurred due to the pressure broadening of the absorption line. This is to be expected since the center of the incident D line is

[6] Mannkopff, Zeits.f. Physik **36**, 315 (1926).

very markedly absorbed and at the point of observation the excitation is due mainly to the remaining broadened portion. Consequently, the intensity is greatly affected by any broadening of the absorption line. In the case of the 3303A excitation, since the amount of absorption is very small there is still sufficient intensity in the center of the incident line at the point of observation to render the broadening effect negligible. This is verified by the close agreement between curve A and its theoretical quenching curve.

Curves B and C, Fig. 3, which give the intensity variation of D light when excited by 3303A, show the resultant of two effects—the increase in intensity due to collisional transfer of atoms from the $3P$ to the $3D$, $2S$ or $2P$ states, and the decrease in intensity due to complete quenching of atoms in any one of these states.

Boeckner[7] found that the probability of caesium atoms in the $4P$ state being transferred by collision to the $5D$ state was approximately twenty times that of being transferred to the $3S$ state. The energy difference in the first case is 0.043 volts and in the second case 0.18 volts, a factor of approximately 4. By analogy it seems certain that most of the collisional transfers from the $3P$ state of sodium will be to the $3D$ rather than to the $2S$ state, since the ratio of the energies involved is almost identical with that in the caesium atom, as are also the important quantum numbers. It may certainly be assumed that the number of atoms transferred to the $1S$ state, an energy difference of approximately 30 times as great as that between the $3P$ and $3D$ states, will be negligible. The increase in intensity due to the collisional transfers is not solely a matter of increasing the number of atoms radiating D light but also involves a decrease in the absorption because of an increased "Doppler width" of the fluorescence light. If it were not for the latter effect curves B and C should be identical, however, with this change in absorption the observed rise in intensity of the D light will be greater for the greater depths. The two curves will coincide when enough collisions occur between the time the atom is changed from the 3^2P state by a collision and the time at which the quantum of "D" light is emitted to restore the atoms to the normal distribution of velocities. From the results we have obtained it is obvious that this does not occur except at pressures well in excess of 100 mm of helium which means that the fast moving excited sodium atoms retain their high speeds for a large number of collisions. The fact that at high pressures the "D" light intensity drops below that which would be calculated from Mannkopff's data on quenching indicates that under these conditions some quenching to the 1^2S state occurs.

Figure 4 gives the results obtained when nitrogen and hydrogen were introduced into the fluorescence tube. In each case only the data for the 3303A line are plotted as the curves for the "D" light did not differ from these to any marked degree. The absence of any increase in the "D" light intensity such as was found with helium is taken to indicate that for these gases the quenching process involves returning the sodium atom to the 1^2S state. On the nitrogen

[7] Boeckner, Bur. Standards J. Res. 5, 13 (1930).

curve the dots represent the experimental points and the circles give the theoretical form for the quenching curve. From the close agreement between the two sets of points we may conclude that nitrogen has no pronounced effect upon the transition probabilities in the 3^2P state of sodium.

The data for the hydrogen curve are subject to some uncertainty due to the fact that the presence of hydrogen seems to accelerate the reaction between sodium and quartz causing a change in the transmission of 3303A through the windows. However, the observed points follow a theoretical quenching curve so well that it may be said that hydrogen has no effect on the transition probabilities.

The most probable source of error in the measurements is in the variation in the intensity of the arc and in the temperature controls throughout the

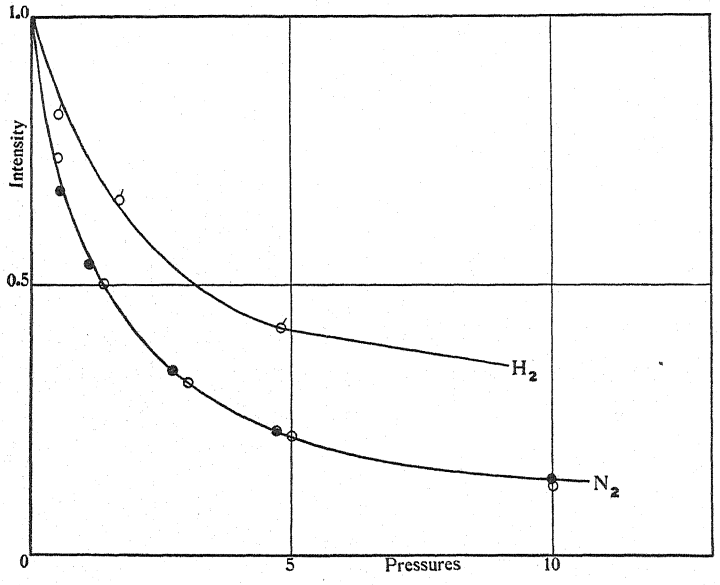


Fig. 4.

apparatus. This was checked by taking a series of consecutive photographs of the fluorescence, as used in the experiments. These were taken over a period of 4 hours and a deviation of not greater than 10 percent in the intensity was observed. The accuracy of the photometry was well within this limit. It seems, therefore, that an error of not greater than 10 percent is to be expected in the measurements.

The results of this investigation demonstrate that there is no apparent effect upon the transition probabilities in the $3P$ state of sodium when the excited atoms are subjected to the presence of an inert gas. Therefore, some other phenomenon must be responsible for the difference between the intensity ratio obtained by Weiss and that obtained by Christensen and Rollefson.

A separation of the $3P$ level into two or more levels having different transition probabilities and different populations might be assumed as a possible

explanation. This separation may or may not be the nuclear hyperfine structure. Let it be supposed that in the pure fluorescence the number of collisions during the mean life capable of transferring excited atoms from one of these states to the other is negligibly small. The radiation observed might be supposed to come largely from a state in which the ratio of the probabilities of transitions (b):(a) is small, with a smaller amount coming from a state in which this ratio is much higher. The high pressure of inert gas present in the arc as used by Weiss, due to transfers by collisions of the second kind, would tend to make the population in both states equal. It is then evident that the ratio of the intensities of these two transitions would be immediately increased.

This same effect, however, should be observed when inert gas is introduced into a fluorescence tube. It should appear in the investigation presented here as a decrease in the intensity of the 3303A radiation on the addition of helium. An obvious assumption would be that at least every kinetic theory collision would be effective in transferring atoms between states differing by so small an amount of energy as must be assumed between such states as those being considered here. At 10 mm pressure of helium, sodium atoms in the $2P$ state undergo on the average 4.5 kinetic theory collisions during the mean life of the excited atom. The figure for the $3P$ state should be at least as great. It is therefore to be expected that equilibrium between states within the $3P$ state should be reached at this pressure. A change in the ratio of the probabilities of transitions (b) and (a) from 1.7:1 to a ratio of 25:1 would result in a 90 percent decrease in the intensity of the 3303A radiation. From curve A, Fig. 3, it may be seen that at 10 mm pressure the intensity of the 3303A radiation has been decreased only 50 percent. This seems to be conclusive evidence that the explanation presented above is not valid.

The difference in the method of excitation has been suggested as a possible explanation, but if this difference is postulated as a method of putting atoms into different states within the $3P$ state, the argument is subject to the same objection presented in the preceding paragraph. In the arc there should be complete equilibrium and in the fluorescence equilibrium should be quickly established on the addition of inert gas, but this is found to be not the case. If it is assumed that the method of excitation causes some permanent change in the $3P$ state as an entity, the above objection no longer holds.

In general it may be said with some degree of certainty that the experimental evidence obtained in this investigation presents a very serious objection to any explanation of this disagreement in intensity ratios which depends upon a difference in transition probabilities of states within the $3P$ state.

Another possible explanation suggests itself when one makes an assumption concerning the actual mechanism of radiation of which so little is known. It seems not impossible to imagine that this mechanism is such that when more than one transition is possible, on the average that transition of greatest probability will occur in the shortest length of time; or, in other words, that the life period of the excited atom varies inversely as the transition probability of the radiation which occurs. This may be stated in another way: that

the chance of that radiation occurring which has the least probability increases with increasing life of the excited atom. It is doubtful that there is as yet any experimental evidence which can conclusively prove or disprove this assumption.

If this assumption is made, however, the explanation sought is immediately forthcoming. The measurements of Weiss were made by observing the radiation from sodium atoms in the $3P$ state in the presence of argon at a comparatively high pressure. It is then to be expected that something over 90 percent of the atoms in the $3P$ state were transferred to the $3D$ state before they could radiate and the relative intensities measured were of the radiations emitted by only those atoms which had survived this collision process. The number of collisions increases with increasing life period, consequently more of the atoms with shorter life periods than of those with longer life periods will survive the collision process. The relative intensities of the radiations will then change in favor of that one having the shorter life period; or on the basis of the assumption suggested above, the relative intensities would change in favor of the transition with greatest probability. In the case of the $3P$ state of sodium it would then be expected that the ratio of the intensities of the transitions (b):(a), Fig. 1 would be greater in the presence of a high pressure of argon than in the pure fluorescence, since transition (b) is the one of greatest probability.

The assumption suggested above is at least partially vindicated by the work of Randall[8] and of Richter[9] who found independently and by entirely different methods that the life periods of the atoms in the 2^3S_1 state of mercury appear approximately four times as great when the 5461A radiation is observed as when either the 4358 or 4047 line is observed. As an explanation of this it was suggested that the life periods and transition probabilities might be different for each hyperfine structure level, and Frisch and Pringsheim[10] attempted to demonstrate this by exciting mercury atoms to the 2^3S_1 state by different methods but found no variation in the relative intensity.

Mrozowski[11] gives some theoretical evidence against the possibility of any influence of nuclear moments on the life period but suggests that there is some sort of separation of the 2^3S_1 state into states with different life periods and different transition probabilities.

In the investigation carried out by Randall no complexity was observed in the constant k which was used in the formula C^{-kt} to describe the falling off of intensity with time after excitation. This indicates that all of the atoms radiating a particular wave-length had the same life period, and therefore probably existed in the same state. This prerequisite would be complied with if all the radiation was assumed to come from the same level but from atoms whose life periods depended upon the wave-length radiated.

Another very serious objection to any explanation of this difference in life

[8] Randall, Phys. Rev. 35, 1161 (1930).
[9] Richter, Ann. d. Physik 7, 293 (1930).
[10] Frisch and Pringsheim, Zeits. f. Physik 67, 169 (1930).
[11] Mrozowski, Zeits. f. Physik 68, 278 (1931).

periods which depends upon a multiplicity of the 2^3S_1 state is encountered when we consider the experiments which have been performed demonstrating the extremely large efficiencies or collisional radii for processes involving such small energy differences as there must be between such states.[12] It seems almost necessary to assume that in the experiments performed by Randall complete equilibrium between the populations of such states must necessarily have been established, and if this were the case a difference in life periods could not have been measured. It is also impossible that there could have been only a partial equilibrium since Randall found that varying the pressure had no effect upon the life periods measured. It seems therefore almost necessary to assume that either the life periods of atoms in any excited state may depend upon the wave-length radiated or else that there are states within the one state with different life periods and transition probabilities between which strong argument in favor of the explanation based upon a change in relative intensity due to quenching, which is presented above concerning the disagreement in the intensity ratios in the $3P$ state of sodium.

[12] Experiments by Wood and Mohler, Phys. Rev. **11**, 70 (1918), have shown that when Na vapor is excited by a single D line and the temperature of the fluorescence is above 220°C, both D_1 and D_2 appear in the fluorescence due to transfers by collision from one member of the doublet P state to the other. Datta, Zeits. f. Physik **37**, 625 (1926), in experiments on the depolarization in the resonance fluorescence of sodium finds an effective radius of approximately 10^{-4} cm, or approximately ten thousand times that of the normal kinetic theory radius.

A NOTE ON LOCAL MOMENTUM IN WAVE MECHANICS

By Lloyd A. Young*
Massachusetts Institute of Technology

(Received September 21, 1931)

Abstract

The present paper shows the exact relations between dynamical quantities of classical theory and their wave mechanical analogues. A new quantity *local momentum* is defined and discussed and the Bohr quantum condition is revived in a form compatible with modern theory.

1. THE one-dimensional Schrödinger equation for a particle moving in a force-free field is

$$\psi'' + p^2\psi = 0 \tag{1}$$

where p and p^2 are quantities proportional to the momentum and energy of the particle respectively.[1] This equation possesses the particular solutions

$$\begin{aligned} \psi^+ &= A^+ e^{+ipx} \\ \psi^- &= A^- e^{-ipx} \end{aligned} \tag{2}$$

representing the streaming of particles in the positive and negative directions of x. The constants A^+ and A^- are arbitrary and are used to normalize the intensity of the stream of particles to any desired quantity. The corresponding wave equation for a general scalar potential field $V(x)$ is

$$\psi'' + [E - V(x)]\psi = 0. \tag{3}$$

We may assume particular solutions of this equation of the form[2]

$$\psi^\pm = A^\pm(x) e^{\pm i\int P dx} \tag{4}$$

and adopt the terminology *local amplitude* for $A^\pm(x)$ and *local momentum* for $P(x)$. Both $A^\pm(x)$ and $P(x)$ may be taken as real quantities (since any complex number may be written in the form $ae^{i\theta}$ with a and θ real). Substitution of (4) into (3) leads, upon separately equating real and imaginary terms to zero, to the following differential equations for $A^\pm(x)$ and $P(x)$.

$$A^{\pm\prime\prime} - A^\pm P^2 + [E - V(x)]A^\pm = 0 \tag{5a}$$

$$2A^{\pm\prime}P + P'A^\pm = 0. \tag{5b}$$

* National Research Fellow.

[1] Throughout this note units are chosen in such a manner that all equations may be written in their simplest form. It is extremely easy to rewrite all results in the usual system of units.

[2] This substitution is well known in mathematics but its use in wave mechanics has been extremely limited.

The second of these gives an immediate relation between $A^{\pm}$ and P; namely

$$A^{\pm} = P^{-1/2} \tag{6}$$

Eq. (5a) may then be written in terms of $P(x)$ alone

$$P^2 + V - P^{1/2}\frac{d^2}{dx^2}P^{-1/2} = E \tag{7}$$

or if we define the quantity *local kinetic energy* by the relation $T^* = P^2$ we have

$$T^* + V - T^{*1/4}\frac{d^2}{dx^2}T^{*-1/4} = E. \tag{7a}$$

This equation is exact and is the wave mechanical analogue of the classical conservation of energy law.

Now we have as particular solutions of the wave equation corresponding to pure travelling waves in the case of free motion[3]

$$\begin{aligned}\psi^+ &= a^+P^{-1/2}e^{i\int P\,dx}\\ \psi^- &= a^-P^{-1/2}e^{-i\int P\,dx}.\end{aligned} \tag{8}$$

For the corresponding probability densities we have

$$\begin{aligned}\bar{\psi}^+\psi^+ &= \overline{a^+}a^+/P\\ \bar{\psi}^-\psi^- &= \overline{a^-}a^-/P.\end{aligned} \tag{9}$$

The most general real solution of (3) representing the wave solution for a discrete state of the system may be written

$$\psi = aP^{-1/2}\cos\left[\int_{x0}^{x} P\,dx + \text{phase factor}\right]. \tag{10}$$

If the range of x is, for example, from $-\infty$ to ∞ we may show that in order that ψ satisfy the usual boundary conditions we must have

$$\int_{-\infty}^{\infty} P\,dx = n\pi \tag{11}$$

where n is a positive integer. Since ψ_n is the n-th characteristic solution of a Sturm-Liouville differential equation it must possess n-1 roots in the finite region of x. This is just the number of roots possessed by $\cos\int P dx$. It is easy to show that $P(x)$ does not vanish for finite x by a simple study of Eq. (7).

2. The comparison of the preceding equations with classical equations is extremely interesting. Eq. (7a) is to be compared with the classical equation

$$T + V = E$$

in which T is the ordinary kinetic energy. The probability densities (9) become identical with the classical expressions when the *local momentum* is re-

[3] With A and P depending on x either of the Eqs. (8) is capable of describing combinations of progressive and standing waves. As an example write $ae^{ipx}+be^{-ipx}$ in the form $A(x)e^{i\int Pdx}$.

placed by the ordinary momentum. $\int Pdx$ is the wave mechanical action integral and Eq. (11) is the analogue of the most fruitful equation of modern physics—the Bohr-Sommerfeld quantum condition

$$\oint pdx = nh.$$

The local momentum P becomes in the limit (in the sense of the correspondence principle) equal to the classical momentum.

3. As an example the *local momentum* for the two lowest states of the harmonic oscillator is plotted (Fig. 1) as a function of x along with curves of the classical momentum $p(x)$. The scale of x has been so chosen that the $p(x)$ curves which are usually pictured as ellipses are here shown as circles. For all

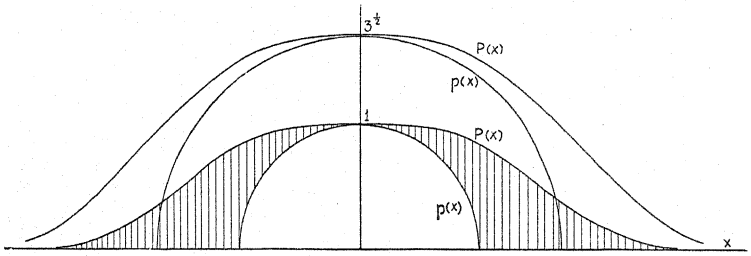


Fig. 1. Comparison of local and classical momentum for the first two states of the harmonic oscillator.

states the area corresponding to the shaded area for the lowest state is $\pi/2$. This alone will show that $P(x)$ and $p(x)$ must approach one another for high quantum states.

4. The present note is not intended to be complete and further investigations are in progress 1*st* on the fundamental nature of P and 2*nd* the application of the results of this paper to various quantum theory problems. In conclusion the writer wishes to express his appreciation to Professor G. E. Uhlenbeck who aroused his interest in the problem of the relation between quantum and classical physics and to Professors J. C. Slater, P. M. Morse and N. H. Frank, of the Massachusetts Institute of Technology, and to M. H. Johnson, Jr., of Harvard University, for their comments and criticism of the manuscript of this note.

Author's Note Added in Proof: Attention should be called to two articles which are related to this note namely H. A. Wilson, Phys. Rev. **35**, p. 948 and W. E. Milne, Phys. Rev. **35**, p. 863. Neither of these writers, it is apparent, realized the rich physical content of their equations.

VALENCE FORCES IN LITHIUM AND BERYLLIUM

By J. H. Bartlett, Jr. and W. H. Furry
University of Illinois

(Received September 2, 1931)

Abstract

With the nodeless wave functions of Guillemin and Zener, the method of Heitler and London is applied to determine how two normal lithium atoms, and also two normal beryllium atoms, influence each other (as a function of the distance). For the diatomic lithium molecule in the ground state, the equilibrium distance is calculated to be 2.4A, and the heat of dissociation to be 1.09 volts. The experimental values are 2.67A (Harvey and Jenkins) and 1.14 volts (Loomis and Nusbaum), respectively. Two normal beryllium atoms repel each other.

AN ACCURATE determination of the heat of dissociation and of the equilibrium separation of the nuclei in a diatomic molecule demands, if one uses the method of Heitler and London,[1] that the eigenfunctions of the individual atoms be known to a high degree of precision. Guillemin and Zener,[2] and later Zener[3] have succeeded in finding eigenfunctions for the atoms in the second row of the periodic table (starting with lithium), which are simple in form and give a quite accurate value for the ionization potential. This indicates that the valence electron is represented quite well, and that one should expect these eigenfunctions to be suitable for use in calculating the molecular constants.

In the present paper, we have made use of such functions. The first part is devoted to a revision of a calculation made by Delbrück,[4] who used atomic functions which gave a value of 3.9 volts for the ionization potential of lithium, as against the experimental value of 5.37 volts. In the second part, we investigate the interaction of two beryllium atoms, each in the normal state at infinite separation.

I. Molecular Constants of Li_2

Since Delbrück[4] has shown that the K-shells make only a very small contribution, we shall neglect them entirely. Accordingly, the lithium problem reduces to one which is analogous to that treated by Heitler and London,[1] the only difference being in the form of the atomic wave functions. We shall calculate (a) strictly along the lines of Heitler and London, using "nonpolar" wave functions, i.e., those which allow only one electron on each atom at infinite separation, and (b) according to the modification made by Slater,[5] which admits wave functions with two electrons on one atom and none on the other (corresponding to Li^- and Li^+, respectively).

[1] W. Heitler u. F. London, Zeits. f. Physik **44**, 455 (1927).
[2] V. Guillemin u. C. Zener, Zeits. f. Physik **61**, 199 (1930).
[3] C. Zener, Phys. Rev. **36**, 51 (1930).
[4] M. Delbrück, Ann. d. Physik **5**, 36 (1930).
[5] J. C. Slater, Phys. Rev. **35**, 509 (1930).

Unless otherwise stated, the notation used throughout this paper will be the same as that used by one of the writers previously.[6] For s electrons, a (1) will denote the wave function describing electron 1 on nucleus a.

We shall use the nodeless functions, namely

$$a(1) = ca_1 e^{-\kappa a_1/2}, \text{ etc.}$$

(a) Calculation with nonpolar wave functions only

The zeroth approximation functions are:

$$^1\Sigma(S^N):\psi = a(1)b(2) + a(2)b(1)$$
$$^3\Sigma(A^N):\psi = a(1)b(2) - a(2)b(1).$$

The energies are:

$$^1\Sigma(S^N):E = \frac{J+K}{1+S}$$
$$^3\Sigma(A^N):E = \frac{J-K}{1-S}$$

where

$$J = \int H'[a(1)]^2[b(2)]^2 dv_1 dv_2$$
$$K = \int H' a(1)b(1)a(2)b(2)dv_1 dv_2$$
$$S^{1/2} = \int a(1)b(1)dv_1$$
$$H' = \frac{2}{R} + \frac{2}{r} - \frac{2}{a_2} - \frac{2}{b_1}.$$

These energies are relative to the energy at infinite separation.

Writing

$$j = \int \frac{2}{r}[a(1)]^2[b(2)]^2 dv$$
$$k = \int \frac{2}{r} a(1)b(1)a(2)b(2)dv$$
$$I = \int \frac{2}{b_1}[a(1)]^2 dv_1$$
$$I' = \int \frac{2}{b_1} a(1)b(1)dv_1$$

[6] J. H. Bartlett, Jr., Phys. Rev. 37, 507 (1931).

we have

$$J = \frac{2}{R} - 2I + j$$

$$K = \frac{2}{R}S - 2S^{1/2}I' + k.$$

For the normalization, $2\pi c^2/\kappa^5 = 1/48$. From the previous paper,[6]

$$j = (4/9)(i_1 + i_3) + i_9/9.$$

Making the transformation

$$a = (R/2)(\lambda + \mu), \quad b = (R/2)(\lambda - \mu),$$

and using Neumann's expansion,

$$k = \int \frac{2}{r} c^4 a_1 a_2 b_1 b_2 e^{-(\kappa/2)(a_1+b_1+a_2+b_2)} dv_1 dv_2$$

$$= \frac{4}{R} \cdot 2\pi \int \sum_{\tau=0}^{\infty} D_{\tau 0} P_\tau \begin{pmatrix} \lambda_1 \\ \lambda_2 \end{pmatrix} Q_\tau \begin{pmatrix} \lambda_2 \\ \lambda_1 \end{pmatrix} P_\tau(\mu_1) P_\tau(\mu_2) \cdot c^4 (R/2)^{10} (\lambda_1^2 - \mu_1^2)^2 (\lambda_2^2 - \mu_2^2)^2 \cdot e^{-\alpha(\lambda_1+\lambda_2)/2} d\lambda_1 d\lambda_2 d\mu_1 d\mu_2.$$

The possible values of τ are 0, 2, and 4.

$$k^{(0)} = (\alpha/2)^9 (\kappa/288) \int Q_0 \begin{pmatrix} \lambda_2 \\ \lambda_1 \end{pmatrix} (\lambda_1^4 - 2\lambda_1^2/3 + \tfrac{1}{5})(\lambda_2^4 - 2\lambda_2^2/3 + \tfrac{1}{5}) e^{-\alpha(\lambda_1+\lambda_2)/2} d\lambda_1 \, d\lambda_2$$

$$= (\alpha/2)^9 (\kappa/144) \{ s_0(44) - (\tfrac{2}{3})[s_0(24) + s_0(42)] + (\tfrac{1}{5})[s_0(04) + s_0(40)]$$
$$- (2/15)[s_0(02) + s_0(20)] + (4/9) s_0(22) + (1/25) s_0(00) \}$$

where[6]

$$s_\tau(m, n) = \int_1^\infty Q_\tau(\lambda_1) e^{-\alpha\lambda_1/2} \lambda_1^m d\lambda_1 \cdot \int_1^{\lambda_1} e^{-\alpha\lambda_2/2} \lambda_2^n d\lambda_2$$

and

$$\alpha = \kappa R.$$

Now let

$$v_\tau(m, n) = \int_1^\infty d\lambda_1 \int_1^\infty d\lambda_2 Q_\tau \begin{pmatrix} \lambda_2 \\ \lambda_1 \end{pmatrix} P_\tau \begin{pmatrix} \lambda_1 \\ \lambda_2 \end{pmatrix} \lambda_1^m \lambda_2^n e^{-\alpha(\lambda_1+\lambda_2)/2}.$$

In particular,

$$v_2(m, n) = (3/2)[s_2(m, n+2) + s_2(n, m+2)]$$
$$- (\tfrac{1}{2})[s_2(m, n) + s_2(n, m)].$$

Then

$$k^{(2)} = (\alpha/2)^9 (\kappa/90) \{ (1/9) v_2(22) - (2/21) v_2(20) + (1/49) v_2(00) \}.$$

For $\alpha=5$, one finds $k^{(0)}=0.1876\kappa$ and $k^{(2)}=0.0012\kappa$, so that the latter contribution is almost negligible.

We shall omit the further details of the calculation, which is quite easy, and give the results.

TABLE I. *Integrals and energies.*

α	$\alpha=3$	4	5	6	7	8	9	10
s	0.7916	0.6642	0.5316	0.4061	0.2968	0.2081	0.1405	0.0914
I/κ	.4468	.4022	.3564	.3138	.2772	.2463	.2206	.1995
I'/κ	.4324	.3835	.3289	.2738	.2221	.1761	.1368	.1045
j/κ	.3367	.3177	.2969	.2746	.2527	.2316	.2121	.1948
k/κ	.2856	.2379	.1888	.1432	.1022	.0714	.0477	.0302
${}^1\Sigma/\kappa$	.0858	−.0251	−.0614	−.0641	−.0548	−.0400	−.0267	−.0173
${}^3\Sigma/\kappa$	.316	.203	.133	.0854	.0555	.0332	.0194	.0116

With a value[2] of $\kappa=1.26$, the equilibrium distance is found to be 2.4A and the heat of dissociation is 1.09 volts. This is to be compared with the experimental values of 2.67A and 1.14 volts, respectively.[7,8] Delbrück obtained values of 4.6A and 1.4 volts, which indicates that the atomic wave functions did not describe the behavior of the valence electron over a sufficient range. This is traceable to the fact that he used a wave function with a large radial node, while we have used a nodeless function.

(b) Calculation with polar wave functions included

When we allow the possibility of two electrons being on one atom, then we have four possible resulting states. The wave functions are

$$
\begin{aligned}
{}^1\Sigma,\ S^N \quad \psi_1 &= \begin{vmatrix} a_\alpha(1)+b_\alpha(1) & a_\beta(1)+b_\beta(1) \\ a_\alpha(2)+b_\alpha(2) & a_\beta(2)+b_\beta(2) \end{vmatrix} \\
A^N \quad \psi_4 &= \begin{vmatrix} a_\alpha(1)+b_\alpha(1) & a_\beta(1)-b_\beta(1) \\ a_\alpha(2)+b_\alpha(2) & a_\beta(2)-b_\beta(2) \end{vmatrix} \\
A^N \quad \psi_3 &= \begin{vmatrix} a_\alpha(1)-b_\alpha(1) & a_\beta(1)+b_\beta(1) \\ a_\alpha(2)-b_\alpha(2) & a_\beta(2)+b_\beta(2) \end{vmatrix} \\
{}^1\Sigma,\ S^N \quad \psi_2 &= \begin{vmatrix} a_\alpha(1)-b_\alpha(1) & a_\beta(1)-b_\beta(1) \\ a_\alpha(2)-b_\alpha(2) & a_\beta(2)-b_\beta(2) \end{vmatrix}
\end{aligned}
$$

where α and β specify the two possible spin orientations.

The function ψ_1 will give an approximation to the normal state, but the state represented by ψ_2 can exert a perturbing effect, so that the correct zeroth approximation to the wave function of the normal state is a certain linear combination of ψ_1 and ψ_2.

The secular equation is

$$
\begin{vmatrix} H_{11}-E & H_{12} \\ H_{12} & H_{22}-E \end{vmatrix} = 0
$$

[7] A. Harvey and F. A. Jenkins, Phys. Rev. **35**, 789 (1930).
[8] F. W. Loomis and R. E. Nusbaum, Phys. Rev. **37**, 1712 (1931).

where

$$H_{11} = \frac{\int \psi_1^* H \psi_1 dv}{\int |\psi_1|^2 dv}, \qquad H_{22} = \frac{\int \psi_2^* H \psi_2 dv}{\int |\psi_2|^2 dv}$$

and

$$H_{12} = \frac{\int \psi_1^* H \psi_2 dv}{\left[\int |\psi_1|^2 dv \cdot \int |\psi_2|^2 dv\right]^{1/2}}$$

there being no off-diagonal term containing E as a factor, because the wave function $a+b$ is orthogonal to $a-b$.

Let us now abbreviate as follows:

$$i = \int [a(1)]^2 [a(2)]^2 (2/r) dv$$

$$j'' = \int [a(1)]^2 a(2) b(2) (2/r) dv$$

$$H' c(1) d(2) = \left(\frac{2}{R} + \frac{2}{r_{12}} - \frac{2}{a_1} - \frac{2}{a_2} - \frac{2}{b_1} - \frac{2}{b_2} + \frac{2}{c_1} + \frac{2}{d_2}\right) c(1) d(2)$$

$$L = \int H' [a(1)]^2 [a(2)]^2 dv = \frac{2}{R} - 2I + i$$

$$J'' = \int a(1) a(2) H' a(1) b(2) dv = \frac{2}{R} S^{1/2} - S^{1/2} I - I' + j''$$

$$H_{11} = 2E_0 + \frac{2L + 2J + 4K + 8J''}{(2 + 2S^{1/2})^2}$$

$$H_{22} = 2E_0 + \frac{2L + 2J + 4K - 8J''}{(2 - 2S^{1/2})^2}$$

$$H_{12} = \frac{i - j}{2(1 - S)}.$$

It is to be noticed that in addition to the "coulomb" and "exchange" integrals we have a new integral typified by J''. This keeps appearing in the subsequent calculations, and is in general of the same order of magnitude as the other integrals.

$$i = \int [a(1)]^2 [a(2)]^2 (2/r) dv = \lim_{R \to 0} \int [a(1)]^2 [b(2)]^2 (2/r) dv$$

$$= c^4\left\{\frac{8\pi}{\kappa^4}\int a^2e^{-\kappa a}[\gamma_5(\kappa a)/\kappa a + \Gamma_4(\kappa a)]dv\right\}$$
$$= (\kappa/288)\{24\Gamma_4 - 24\Gamma_4/2^4 - 18\Gamma_5/2^5 - 6\Gamma_6/2^6 - \Gamma_7/2^7\}$$
$$= .3633\kappa.$$

If $\kappa = 1.26$, $\quad i = 6.2$ volts.

This value of i is larger than the ionization potential of lithium, which would indicate a negative electron affinity. No accurate calculations of the electron affinity of lithium have been made.

Calculation of j''

We may calculate j'' in two different ways, and thus obtain a check. The first way is direct, and the second requires the Neumann expansion. Here we give only the first method.

$$j'' = \int (2/r)a(1)b(1)[a(2)]^2dv$$
$$= (8\pi c^4/\kappa^4)\int abe^{-\kappa(a+b)/2}\{\gamma_5(\kappa a)/\kappa a + \Gamma_4(\kappa a)\}\cdot(2\pi/R)adadbdb.$$

Setting $y = \kappa a$,

$$\int_{|R-a|}^{R+a} b^2dbe^{-\kappa b/2} = (2/\kappa)^3\left\{\Gamma_3\left|\frac{\alpha-y}{2}\right| - \Gamma_3\left(\frac{\alpha+y}{2}\right)\right\}$$

$$j'' = (128\pi^2c^4/\alpha\kappa^9)\int_0^\infty y^2dye^{-y/2}\{\gamma_5(y)/y + \Gamma_4(y)\}\left\{\Gamma_3\left|\frac{\alpha-y}{2}\right| - \Gamma_3\left(\frac{\alpha+y}{2}\right)\right\}$$
$$= (128\pi^2c^4/\alpha\kappa^9)\Big[\int_0^\alpha ydy\{\gamma_5(y) + y\Gamma_4(y)\}e^{-\alpha/2}\cdot\{a_0 - a_1y + a_2y^2\}$$
$$+ \int_\alpha^\infty ydye^{-y}\{\gamma_5(y) + y\Gamma_4(y)\}e^{\alpha/2}\cdot\{b_0 + b_1y + b_2y^2\}$$
$$- \int_0^\infty ydye^{-y}\{\gamma_5(y) + y\Gamma_4(y)\}e^{-\alpha/2}\{a_0 + a_1y + a_2y^2\}\Big]$$

where

$$a_0 = 2 + \alpha + \alpha^2/4 \quad a_1 = 1 + \alpha/2 \quad a_2 = b_2 = \tfrac{1}{4}$$
$$b_0 = 2 - \alpha + \alpha^2/4 \quad b_1 = 1 - \alpha/2.$$

The calculation gives:

$$j'' - I' = -(\kappa/72\alpha)\{2e^{-\alpha/2}(134.01 - 56.531\alpha + 13.3125\alpha^2)$$
$$- 32e^{-\alpha/2}[(\alpha/2)^7(A_6 - 2A_5 + A_4) + (\alpha/2)^6(A_5 - 4A_4 + 3A_3)$$
$$+ (\alpha/2)^5(A_4/2 - 3A_3 + 9A_2/2) + (\alpha/2)^4(3A_3 + 3A_1)$$
$$+ (\alpha/2)^3(3A_2 + 6A_1) + (\alpha/2)^2\cdot 6A_1]_\alpha$$
$$+ 32e^{\alpha/2}[(\alpha/2)^7(A_6 - 2A_5 + A_4) + (\alpha/2)^6(5A_5 - 8A_4 + 3A_3)$$
$$+ (\alpha/2)^5(12.5A_4 - 15A_3 + 4.5A_2) + (\alpha/2)^4(18A_3 - 15A_2 + 3A_1)$$
$$+ (\alpha/2)^3(15A_2 - 6A_1) + (\alpha/2)^2\cdot 6A_1]_{2\alpha}\}$$

where the subscript α after the bracket indicates that the A's inside have α as an argument.

TABLE II.

α	$\alpha=3$	4	5	6	7	8	9	10
j''/κ	0.3155	0.2834	0.2482	0.2124	0.1762	0.1426	0.1132	0.0876
L/κ	.1364	.0589	.0505	.0690	.0946	.1207	.1443	.1643
J''/κ	.0787	−.0204	−.0489	−.0490	−.0413	−.0318	−.0230	−.0167
J/κ	.1098	.0133	−.0159	−.0197	−.0160	−.0110	−.0069	−.0042
K/κ	.0439	−.0550	−.0782	−.0704	−.0550	−.0373	−.0236	−.0147
$(H_{11}-2E_0)/\kappa$	.0908	−.0181	−.0531	−.0536	−.0412	−.0217	−.0004	+.0188
$(H_{22}-2E_0)/\kappa$	.7888	.6392	.5028	.3972	.3229	.2745	.2331	.2029
H_{12}/κ	.0639	.0679	.0708	.0747	.0786	.0832	.0880	.0928
$^1\Sigma/\kappa$	.0850	−.0250	−.0620	−.0657	−.0574	−.0435	−.0298	−.0194

The $^1\Sigma$ state referred to in Table II is the nonpolar one. It is seen that the two methods (a) and (b) of calculating the molecular constants lead to practically the same results. In what follows, we shall calculate by method (a).

II. INTERACTION OF TWO NORMAL BERYLLIUM ATOMS

There is but one possible state for the molecule when the two atoms are each in a ^1S state, and that is the $^1\Sigma$ state. We assume the wave function to be

$$\psi = \sum_P (-)^{\sigma_p} P a_\alpha(1) a_\beta(2) b_\alpha(3) b_\beta(4)$$

where P refers to a permutation of 1, 2, 3, 4 and σ_p is the order of P. The energy is

$$E = \frac{\int \psi^* H \psi dv}{\int \psi^* \psi dv}$$

where

$$H = \sum_{i=1}^{4} \Delta_i + \frac{8}{R} - \sum_{i=1}^{4} \left(\frac{4}{a_i} + \frac{4}{b_i} \right) + \sum_{i<j} \frac{2}{r_{ij}} .$$

Then

$$E = \frac{\int \left[\sum_{P'} (-)^{\sigma_{P'}} P' a_\alpha^*(1) a_\beta^*(2) b_\alpha^*(3) b_\beta^*(4) \right] H \left[\sum_{P''} (-)^{\sigma_{P''}} P'' a_\alpha(1) a_\beta(2) b_\alpha(3) b_\beta(4) \right] dv}{\int \left[\sum_{P'} (-)^{\sigma_{P'}} P' a_\alpha^*(1) a_\beta^*(2) b_\alpha^*(3) b_\beta^*(4) \right] \cdot \left[\sum_{P''} (-)^{\sigma_{P''}} P'' a_\alpha(1) a_\beta(2) b_\alpha(3) b_\beta(4) \right] dv} .$$

Summing over P'', and setting $P = P'P''^{-1}$:

$$E = \frac{\int \left[\sum_{P} (-)^{\sigma_p} P a_\alpha^*(1) a_\beta^*(2) b_\alpha^*(3) b_\beta^*(4) \right] H \left[a_\alpha(1) a_\beta(2) b_\alpha(3) b_\beta(4) \right] dv}{\int \left[\sum_{P} (-)^{\sigma_p} P a_\alpha^*(1) a_\beta^*(2) b_\alpha^*(3) b_\beta^*(4) \right] \cdot \left[a_\alpha(1) a_\beta(2) b_\alpha(3) b_\beta(4) \right] dv} .$$

Splitting off the unperturbed energy,

$$E-E_0=\frac{\int\left[\sum_P(-)^{\sigma_P}Pa_\alpha^*(1)a_\beta^*(2)b_\alpha^*(3)b_\beta^*(4)\right]\cdot H'[a_\alpha(1)a_\beta(2)b_\alpha(3)b_\beta(4)]dv}{\int\left[\sum_P(-)^{\sigma_P}Pa_\alpha^*(1)a_\beta^*(2)b_\alpha^*(3)b_\beta^*(4)\right]\cdot[a_\alpha(1)a_\beta(2)b_\alpha(3)b_\beta(4)]dv}$$

where

$$H'=\frac{8}{R}-\frac{4}{b_1}-\frac{4}{b_2}-\frac{4}{a_3}-\frac{4}{a_4}+\frac{2}{r_{13}}+\frac{2}{r_{14}}+\frac{2}{r_{23}}+\frac{2}{r_{24}}$$
$$=H'(13)+H'(14)+H'(23)+H'(24)$$
$$H'(ij)=\frac{2}{R}-\frac{2}{b_i}-\frac{2}{a_j}+\frac{2}{r_{ij}}.$$

The condition of spin orthogonality gives nonvanishing contributions from $P=1$, (13), (24), (13)(24) only. The contributions to numerator and denominator of the expression for $E-E_0$ are:

P	Numerator	Denominator
1	$4J$	1
$(13)=(24)$	$-K-2S^{1/2}J''-SJ$	$-S$
$(13)(24)$	$4SK$	S^2.

Then

$$E-E_0=\frac{4(J+SK)-2(K+SJ)-4S^{1/2}J''}{(1-S)^2}.$$

α	$\alpha=3$	4	5	6	7	8	9	10
$^1\Sigma/\kappa$	0.840	0.584	0.392	0.251	0.162	0.099	0.058	0.028

The $^1\Sigma$ state is seen to be a repulsive one.

Discussion

The calculations for lithium show that good results may be obtained with simple wave functions. The success here justifies, we believe, the use of similar functions in the more complicated problems.

One would expect that two normal beryllium atoms would behave toward each other as do two normal helium atoms. This expectation is given support by our calculations, which show that the resulting molecular state is repulsive.

However, it is not at all obvious that two beryllium atoms, one of which is in the normal state, and the other of which is in the first excited state, should repel each other. The character of the states resulting from this configuration will be determined in the concluding installment of this paper, which is to follow shortly.

MANY-ELECTRON WAVE FUNCTIONS

By James H. Bartlett, Jr.
Department of Physics, University of Illinois

(Received August 14, 1931)

Abstract

If it is possible to describe the state of an atom by the addition of several vectors, and if one assumes the wave function for any state of a configuration to be a linear combination of product functions for that configuration, then one can determine the coefficients in the linear combination by a simple method. Examples are given. The usual interval formula is not applicable for $2p^3$, where nonsplitting is the case.

Introduction

In a previous paper,[1] the writer has investigated, for two equivalent $2p$ electrons, the stages between (ls), or Russell-Saunders, coupling and (jj) coupling. As a zeroth approximation, the wave functions for the intermediate case were assumed to be linear combinations of product functions associated with $2p^2$. The secular equation could be solved rather readily when the functions used to determined its matrix elements were those linear combinations associated with the various terms (such as $^3P_2$) of Russell-Saunders coupling. Such linear combinations were found by solving an appropriate secular equation. The purpose of the present paper is to call attention to an apparently little-known method which enables one to write down these linear combinations directly.

1. If there exist two independent states $\psi_{m_A}{}^A$ and $\psi_{m_B}{}^B$, which may be represented by vectors A and B with projections m_A and m_B respectively, then the total system may be written as $\psi_{m_A}{}^A\psi_{m_B}{}^B$. If the two vectors combine to form a resultant vector C with projection m_C, then this state will have the form $\psi_{m_C}{}^C=\Sigma_{m_Am_B}S_{Cm_Am_B}{}^{AB}\psi_{m_A}{}^A\psi_{m_B}{}^B$, where $m_A+m_B=m_C$. The coefficients $S_{Cm_Am_B}{}^{AB}$ are known,[2] at least if we restrict the quantum numbers to integral and half-integral values. If $\psi_{m_A}{}^A$ refer to electrons 1 and 2, and $\psi_{m_B}{}^B$ to electron 3, the resulting function will not be antisymmetric with respect to interchange of any two electrons, in general, and determinant wave functions must be constructed.

For convenience, the coefficients for $B=\frac{1}{2}$ and $B=1$ are listed.

Table I. $S_{Cm_Am_B}^{A\frac{1}{2}}$

C	$m_B=-\frac{1}{2}$	$m_B=\frac{1}{2}$
$A-\frac{1}{2}$	$\left(\frac{A+m_C+\frac{1}{2}}{2A+1}\right)^{1/2}$	$-\left(\frac{A-m_C+\frac{1}{2}}{2A+1}\right)^{1/2}$
$A+\frac{1}{2}$	$\left(\frac{A-m_C+\frac{1}{2}}{2A+1}\right)^{1/2}$	$\left(\frac{A+m_C+\frac{1}{2}}{2A+1}\right)^{1/2}$

[1] J. H. Bartlett, Jr., Phys. Rev. **34**, 1252 (1929). See also Phys. Rev. **35**, 229 (1930).
[2] E. Wigner, Gruppentheorie (Vieweg, 1931) S. 206.

TABLE II. $S^{A1}_{Cm_Am_B}$

C	$m_B=-1$	$m_B=0$	$m_B=1$
$A-1$	$\left[\frac{(A+m_C)(A+m_C+1)}{2A(2A+1)}\right]^{1/2}$	$-\left[\frac{(A+m_C)(A-m_C)}{A(2A+1)}\right]^{1/2}$	$\left[\frac{(A-m_C+1)(A-m_C)}{2A(2A+1)}\right]^{1/2}$
A	$\left[\frac{(A-m_C)(A+m_C+1)}{2A(A+1)}\right]^{1/2}$	$\frac{m_C}{[A(A+1)]^{1/2}}$	$-\left[\frac{(A-m_C+1)(A+m_C)}{2A(A+1)}\right]^{1/2}$
$A+1$	$\left[\frac{(A-m_C)(A-m_C+1)}{(2A+1)(2A+2)}\right]^{1/2}$	$\left[\frac{(A+m_C+1)(A-m_C+1)}{(2A+1)(A+1)}\right]^{1/2}$	$\left[\frac{(A+m_C+1)(A+m_C)}{(2A+1)(2A+2)}\right]^{1/2}$

Table II has been given in a different form by Wigner.[3] The form above seems to be handier and more symmetrical.

2. A simple example is that of two equivalent p electrons. Let the wave function $\psi_{m_A}{}^{(1)}\psi_{m_B}{}^{(2)}$ be denoted by (m_A, m_B). We shall determine the space function by combining the l-vectors, and the spin function by combining the s-vectors. The product of these two functions will then be represented by a vector L and a vector S, together with their projections m_L and m_S. It will be a linear combination of individual product functions and need not have the required antisymmetry property. If, however, we replace each individual product function by the corresponding determinant, the linear combination of these determinants will be our required function. In the case of two electrons, $S_1=\frac{1}{2}$ and $S_2=\frac{1}{2}$, resulting in wave functions symmetric or antisymmetric in the spins. The space factor turns out likewise, and so we do not need to introduce determinant functions. This is only a special case, however.

The space factors for $2p^2$, $m_l=0$ follow:[4]

$$S:(\tfrac{1}{3})^{1/2}\{(1,-1)-(0,0)+(-1,1)\}$$
$$D:(\tfrac{1}{6})^{1/2}\{(1,-1)+2(0,0)+(-1,1)\}$$
$$P:(\tfrac{1}{2})^{1/2}\{(1,-1)-(-1,1)\}.$$

Since these are either symmetric or antisymmetric in the two electrons, it is only necessary to multiply by the appropriate spin factor to obtain a wave function which is antisymmetric.

For $m_l=1$, $P:(\tfrac{1}{2})^{1/2}\{(1,0)-(0,1)\}$
$D:(\tfrac{1}{2})^{1/2}\{(1,0)+(0,1)\}$.

For $m_l=-1$, $P:(\tfrac{1}{2})^{1/2}\{(0,-1)-(-1,0)\}$
$D:(\tfrac{1}{2})^{1/2}\{(0,-1)+(-1,0)\}$.

The spin functions are:

$$s=0:(\tfrac{1}{2})^{1/2}\{\alpha(1)\beta(2)-\alpha(2)\beta(1)\}$$

[3] E. Wigner, Gruppentheorie, p. 208.

[4] These functions agree with those in the previous paper, reference 1.

$$s = 1 \begin{cases} m_s = 1 : \alpha(1)\alpha(2) \\ m_s = 0 : (\tfrac{1}{2})^{1/2}\{\alpha(1)\beta(2) + \alpha(2)\beta(1)\} \\ m_s = -1 : \beta(1)\beta(2). \end{cases}$$

$\alpha(1)$ denotes that function of electron 1 corresponding to $m_s = \frac{1}{2}$, and $\beta(1)$ corresponds to $m_s = -\frac{1}{2}$.

If now, we wish the functions for ^3P, $j = 0$, 1, and 2, then the coefficients $S^{1\,1}{}_{j\,m_l m_s}$ are what are required. For $m = 0$ (and for the other values of m also) the form of the wave function is the same as for $m_l = 0$ above,[4] i.e.:

$$^3P_0 : (\tfrac{1}{3})^{1/2}\{(1, -1) - (0, 0) + (-1, 1)\}.$$

The parentheses refer here to m_l and m_s however, instead of to m_{l_1} and m_{l_2}.

3. A more complicated example is furnished by the configuration $2p^3$ which has for terms ^2P, ^2D, and ^4S. When there are three electrons described by vectors l_1, l_2, l_3 and s_1, s_2, s_3 then we may suppose the resultant of l_1 and l_2 to be $\bar{l}$ and that of s_1 and s_2 to be $\bar{s}$. The total wave function characteristic of a state (l, s, m_l, m_s) may be written as

$$\sum_p (-)^{i_p} P \psi^{l}_{m_l} \psi^{s}_{m_s} = \sum s_{\bar{l}}(\bar{l} l_3; \bar{m}_l m_{l_3}) s_{\bar{s}}(\bar{s} s_3; \bar{m}_s m_{s_3}) \sum (-)^{i_p} P$$
$$[s_{\bar{l}}(l_1 l_2; m_{l_1} m_{l_2}) s_{\bar{s}}(s_1 s_2; m_{s_1} m_{s_1}) \psi(l_1 s_1; m_{l_1} m_{s_1}/1)$$
$$\psi(l_2 s_2; m_{l_2} m_{s_2}/2)]\psi(l_3 s_3; m_{l_3} m_{s_3}/3)$$

where P is a permutation of (123) and i_p its order. Thus we may proceed from determinant wave functions for two electrons, if it proves to be convenient. If we try to build up the $^2D_{5/2}$, $m_l = 2$ from $2p^2\ ^1D_2$ and $2p$ then the functions for ^1D are:

$$m_l = 2 \qquad (\tfrac{1}{2})^{1/2} \left| \alpha^1(1)\beta^1(2) \right|$$
$$m_l = 1 \qquad (\tfrac{1}{2}) \left\{ \left| \alpha^1(1)\beta^0(2) \right| - \left| \alpha^0(1)\beta^1(2) \right| \right\}.$$

For $2p$,

$$m_l = 0 \qquad \alpha^0(3)$$
$$m_l = 1 \qquad \alpha^1(3)$$

(where the superscripts now denote the magnetic quantum number).

The only possible function for $^2D_{5/2}$, $m_l = 2$ is then $(1/6)^{1/2} |\alpha^1(1)\beta^1(2)\alpha^0(3)|$. One does not need to resort to the vector addition method to deduce this result.

For $j = 3/2$, $m = 3/2$ there are three possible states, namely ^2D, ^2P, and ^4S. The ^2D may be considered as arising from $2p\ ^3P$ and $2p$, or else from $2p^2\ ^1D$ and $2p$. The same wave function is obtained in either case, which seems at first surprising because the ^1D and ^3P terms have not the same energy. But if we consider that the added electron is equivalent to the other two, the reason is apparent. If a nonequivalent p electron should be added, then we should obtain two ^2D terms with different energies.

For $2p^3$ some of the wave functions follow:

$$
\begin{aligned}
^2D{:}m_l = 1,\ m_s &= \tfrac{1}{2}{:}(1/12)^{1/2}\{\,|\,\beta^1(1)\alpha^{-1}(2)\alpha'(3)\,| - |\,\beta^0(1)\alpha^1(2)\alpha^0(3)\,|\,\}\\
m_l = 0,\ m_s &= \tfrac{1}{2}{:}(1/6)\{\,|\,\beta^1(1)\alpha^{-1}(2)\alpha^0(3)\,| + 2\,|\,\beta^0(1)\alpha^{-1}(2)\alpha^1(3)\,|\\
&\quad + |\,\beta^{-1}(1)\alpha^0(2)\alpha^1(3)\,|\,\}\\
^2P{:}m_l = 1\ \ m_s &= \tfrac{1}{2}{:}(1/12)^{1/2}\{\,|\,\beta^1(1)\alpha^{-1}(2)\alpha^1(3)\,| + |\,\beta^0(1)\alpha^1(2)\alpha^0(3)\,|\,\}\\
m_l = 0\ \ m_s &= \tfrac{1}{2}{:}(1/12)^{1/2}\{\,|\,\beta^1(1)\alpha^{-1}(2)\alpha^0(3)\,| + |\,\beta^{-1}(1)\alpha^1(2)\alpha^0(3)\,|\,\}\\
^4S{:}m_l = 0\ \ m_s &= 3/2{:}(1/6)^{1/2}|\,\alpha^1(1)\alpha^0(2)\alpha^{-1}(3)\,|\\
m_l = 0\ \ m_s &= \tfrac{1}{2}{:}(1/18)^{1/2}\{\,|\,\beta^{-1}(1)\alpha^1(2)\alpha^0(3)\,| + |\,\beta^0(1)\alpha^{-1}(2)\alpha^1(3)\,|\\
&\quad + |\,\beta^1(1)\alpha^0(2)\alpha^{-1}(3)\,|\,\}\\
^2D_{3/2}, m = 3/2{:}&(1/6)^{1/2}\{(4/5)^{1/2}|\,\alpha^1(1)\beta^1(2)\beta^0(3)\,| - (1/10)^{1/2}|\,\alpha^1(1)\beta^1(2)\alpha^{-1}(3)\,|\\
&+ (1/10)^{1/2}|\,\beta^0(1)\alpha^1(2)\alpha^0(3)\,|\,\}\\
^2P_{3/2},\ m = 3/2{:}&(1/12)^{1/2}\{\,|\,\alpha^1(1)\beta^1(2)\alpha^{-1}(3)\,| + |\,\alpha^0(1)\beta^0(2)\alpha^1(3)\,|\,\}.
\end{aligned}
$$

4. Suppose now, to verify the correctness of the linear combinations, that we calculate the energy levels of $2p^3$, $j=3/2$, for (jj) coupling. This necessitates finding the matrix elements of $(l\cdot s)_1+(l\cdot s)_2+(l\cdot s)_3$. Given two determinantal wave functions $|n_1(1)\ n_2(2)\ n_3(3)|$ and $|n_1'(1)\ n_2'(2)\ n_3'(3)|$, then the matrix elements will not vanish only when not more than one of the n's is different from an n'. If $n_1=n_1'$, $n_2=n_2'$ and $n_3\neq n_3'$, the matrix element is $(n_3|l\cdot s|n_3')$. If $n_3=n_3'$, the matrix element is $(n_1|l\cdot s|n_1')+(n_2|l\cdot s|n_2')+(n_3|l\cdot s|n_3')$.

The matrix elements of $(l\cdot s)$ are:[5]

$$
\begin{aligned}
(m_s, m_l|\ l\cdot s\ |m_s, m_l) &= \lambda m_s m_l\\
(\alpha, m_l|\ l\cdot s\ |\beta, m_l+1) &= (\lambda/2)[l(l+1) - m_l(m_l+1)]^{1/2}\\
(\beta, m_l|\ l\cdot s\ |\alpha, m_l-1) &= (\lambda/2)[l(l+1) - m_l(m_l-1)]^{1/2}.
\end{aligned}
$$

The secular equation is then:

$$
\begin{vmatrix} -\epsilon & (5/4)^{1/2} & 0\\ (5/4)^{1/2} & -\epsilon & 1\\ 0 & 1 & -\epsilon \end{vmatrix} = 0.
$$

The roots are $\epsilon=0$ and $\pm 3/2$, agreeing with what one would expect from elementary considerations. When the electrostatic interaction is not negligible, then one must solve the cubic equation by applying the well-known formulae.

It is seen that the diagonal terms in the matrix of (l.s) are zero, which means that the ^2P and ^2D of $2p^3$ do not split up, as is the case[1] with $2s2p^3$. This is not what one should expect from the formula $\Delta E=$ const. $[j(j+1)-l(l+1)-s(s+1)]$, showing that the range of applicability of this formula is limited. One can verify the fact that no splitting occurs by a consideration of $^2D_{5/2}$ and $^2P_{1/2}$. The displacement must be the same for (ls) coupling as for (jj)

[5] W. Heisenberg u. P. Jordan, Zeits. f. Physik **37**, 268 (1926).

coupling, where it is zero, a result that one can obtain without using wave functions.

Discussion

The vectorial method of finding correct linear combinations seems to be quite general, but does not, of course, apply when the resulting state cannot be represented as a vector which is the sum of several component vectors. For instance, the transition from (ls) to (jj) coupling involves a disturbance of symmetry so that one cannot find the wave functions for the intermediate cases by the above method. But it becomes much easier to find these functions if one knows the proper functions for (ls) coupling. The problem reduces to that of solving a secular equation for a given j and m, the degree of this equation being the only practical limitation, instead of the number of electrons.

Note added Sept. 8, 1931: The correct linear combinations can also be found by a method due to N. M. Gray and N. A. Wills (Phys. Rev. **38,** 248, 1931). The present writer believes, however, that the vectorial method, due to Wigner, is the simpler.

SPECTRA OF TWO ELECTRON SYSTEMS

By M. H. Johnson, Jr.
University of Michigan and Harvard University

(Received September 23, 1931)

Abstract

Following the method of Güttinger and Pauli[1] four angular momentum vectors are treated in matrix mechanics. Analytic formulas are obtained for the matrix components of the spin-orbit interaction of two electrons in LS coupling. Since the electrostatic energy in LS coupling is a diagonal matrix whose elements may be calculated by Slater's method, this gives the complete energy matrix. Then for any two electron configuration one easily obtains the secular equations whose roots give the energy levels in intermediate coupling. In this manner the secular equations are worked out for the configurations p^2, $p \cdot p$, d^2, $d \cdot d$, and $d \cdot p$.

Introduction

IN THE theory of complex spectra the effect of the electrostatic repulsion of the electrons on the energy levels of an atom has been reduced in many cases to the calculation of a few radial integrals.[2] By this method it is always possible to calculate the multiplet separations for two electron configurations with such accuracy as is afforded by a first order perturbation theory. In order to obtain more detailed information about the energy levels it is necessary to include in the perturbation problem the interaction of the spin each electron with its own orbital motion. This has been done for two electrons when one is in an s state.[3] Also partial information (in some simple cases complete) about the secular equations has been obtained by Goudsmit.[4]

It is easy to see why the spin-orbit interaction has not been dealt with by Slater's method. In this method it is not necessary to find the wave function for a given state of the atom. For due to the high degree of degeneracy remaining in the problem after the application of the perturbation, it is possible to find all the energy levels from the invariance of diagonal sums. When the spin-orbit interaction is included, much of this degeneracy is removed so the diagonal sum method loses its effectiveness.

The essential difficulty with Slater's wave functions is that the square of the total angular momentum, J^2, which is an integral of the equations of motion, is not diagonal when these wave functions are used. Consequently the secular determinant when computed with these functions, is not factored according to J values as it should be. The proper linear combination of Slater's functions to make J^2 diagonal may be found by studying the angular momentum operators.[5] With these proper functions as a basis the matrix of the spin-

[1] Güttinger and Pauli, Zeits. f. Physik **67**, 743 (1931). This will be referred to as 1.
[2] J. C. Slater, Phys. Rev. **34**, 1293 (1929).
[3] Houston, Phys. Rev. **33**, 297 (1929).
[4] Goudsmit, Phys. Rev. **35**, 1325 (1930). This method has recently been extended by D.R Inglis, Phys. Rev. **38**, 862 (1931).
[5] Gray and Wills, Phys. Rev. **38**, 248 (1931).

orbit interaction would be factored according to J values. However for the general two electron configuration this appears to be a lengthy process. So in this paper we attempt to calculate the spin-orbit interaction in LS coupling directly from the matrix equations.[6]

Elimination of the Quantum Number M_J

If $\boldsymbol{L}$ is the total orbital angular momentum, $\boldsymbol{S}$ is the total spin angular momentum and $\boldsymbol{J}$ their resultant, then

$$\begin{aligned} \boldsymbol{J} &= \boldsymbol{L} + \boldsymbol{S} \\ \boldsymbol{L} &= \boldsymbol{l}_1 + \boldsymbol{l}_2 \\ \boldsymbol{S} &= \boldsymbol{s}_1 + \boldsymbol{s}_2 \end{aligned} \tag{1}$$

where $\boldsymbol{l}_1$ and $\boldsymbol{l}_2$ are the orbital and $\boldsymbol{s}_1$ and $\boldsymbol{s}_2$ are the spin angular momenta of electrons 1 and 2 respectively. Then the following commutation relations are valid

$$\begin{aligned} [J_x, A_x] &= 0 \\ [J_x, A_y] &= [A_x, J_y] = iA_z \\ [J_x, B] &= 0 \end{aligned} \tag{2}$$

where A is any vector which is a function of the spin and orbital momentum vectors and B is any scalar formed from these vectors. In these equations angular momentum is measured in units of $h/2\pi$. In particular Eqs. (2) hold for $\boldsymbol{l}_1$, $\boldsymbol{l}_2$, $\boldsymbol{s}_1$ and $\boldsymbol{s}_2$. Now we suppose that J^2 is diagonal with the characteristic values $J(J+I)$ and J_z is a diagonal with the characteristic values M_J, $|M_J| \leqq J$. Then from reference 1 we find that the solutions of Eqs. (2) are

$$\begin{aligned} (A_x \pm iA_y)^{JM_J}_{JM_J\mp 1} &= A^J_J\{(J \pm M_J)(J \mp M_J + 1)\}^{1/2} \\ A^{JM_J}_{zJM_J} &= A^J_J M_J \\ (A_x \pm iA_y)^{J\ M_J}_{J+1M_J\mp 1} &= A^J_{J+1}(\pm 1)\{(J \mp M_J + 1)(J \mp M_J + 2)\}^{1/2} \\ A^{J\ M_J}_{zJ+1M_J} &= A^J_{J+1}\{(J+1)^2 - M_J{}^2\}^{1/2} \\ (A_x \pm iA_y)^{J\ M_J}_{J-1M_J\mp 1} &= A^J_{J-1}(\mp 1)\{(J \pm M_J)(J \pm M_J - 1)\}^{1/2} \\ A^{J\ MJ}_{zJ+1M_J} &= A^J_{J-1}(J^2 - M_J{}^2)^{1/2}. \end{aligned} \tag{3}$$

In particular if $A = J$, then $A^J_J = 1$ and $A^J_{J+1} = 0$.

Calculation of L and S

The calculation of $\boldsymbol{S}$ is exactly the same as in reference 1. We now suppose that L^2 and S^2 are also diagonal with the characteristic values $L(L+I)$ and

[6] We should also note another possible method of obtaining the matrix of the spin-orbit interaction by those famous ξ's and η's, which may be simple for one experienced in their peculiarities. H. Weyl, Gruppentheorie und Quantenmechanick Kap. III; H. A. Kramers, Amst. Akad. 33, 953 (1930).

$S(S+I)$. This is possible since the matrices L^2, S^2, J^2 and J_z all commute with one another. Then from reference 1 we find for $\mathbf{S}$

$$S_J^J = \frac{J(J+1)+S(S+1)-L(L+1)}{2J(J+1)}$$

$$S_{J-1}^J = \left(\frac{(L+S+1-J)(L+S+1+J)(J-L+S)(J-S+L)}{4J^2(2J-1)(2J+1)}\right)^{1/2} \tag{4}$$

$$S_{J-1}^J = S_J^{J-1}.$$

The last equation follows from the Hermitean character of the components of $\mathbf{S}$.

The results for $\mathbf{L}$ may be obtained from the above by interchanging L and S. This gives

$$L_J^J = \frac{J(J+1)+L(L+1)-S(S+1)}{2J(J+1)}$$

$$L_{J-1}^J = -\left(\frac{(S+L+1-J)(S+L+1+J)(J-S+L)(J-L+S)}{4J^2(2J-1)(2J+1)}\right)^{1/2} \tag{5}$$

$$L_{J-1}^J = L_J^{J-1}.$$

The minus sign before the component nondiagonal in J occurs in extracting a square root. The minus sign must be used in order that $(L_x+S_x)^{LSJ}_{LSJ\pm1}{}^{M}_{M}I=0$ as is required by the fact that J^2 commutes with all components of $\mathbf{J}$. Of course all components of $\mathbf{L}$ and $\mathbf{S}$ are diagonal in L and S as all components of both $\mathbf{L}$ and $\mathbf{S}$ commute with L^2 and S^2.

Dependence of l_1, l_2, s_1 and s_2 on the Quantum Number J

In the following formulas we use l for l_1 and l_2 and s for s_1 and s_2 whenever the formulas apply for both subscripts. We find the dependence of I on J from the equation

$$[S_x - iS_y, l_z]^{L\,SJ'\,M_J}_{L'SJ''M_J+1} = 0.$$

The calculation is exactly the same as the calculation of the coordinate matrix in reference 1. Hence we have the result

$$l^{LSJ}_{LSJ} = l^{LS}_{LS}\frac{J(J+1)+L(L+1)-S(S+1)}{2J(J+1)}$$

$$l^{LSJ}_{LSJ+1} = -l^{LS}_{LS}\left(\frac{(L+S+J+2)(L+S-J)(J+1+L-S)(J+1-L+S)}{4(J+1)^2(2J+1)(2J+3)}\right)^{1/2}$$

$$l^{L\ SJ}_{L-1SJ+1} = -l^{L\ S}_{L-1S}\left(\frac{(J-L+S+2)(J-L+S+1)(L+S-1-J)(L+S-J)}{4(J+1)^2(2J+1)(2J+3)}\right)^{1/2} \tag{6}$$

$$l^{L\ SJ}_{L-1SJ} = l^{L\ S}_{L-1S}\left(\frac{(J+L-S)(J-L+S+1)(L+S+1+J)(L+S-J)}{4J^2(J+1)^2}\right)^{1/2}$$

$$l^{L\ SJ}_{L-1SJ-1} = l^{L\ S}_{L-1S}\left(\frac{(J+L-S-1)(J+L-S)(L+S+1+J)(L+S+J)}{4J^2(2J-1)(2J+1)}\right)^{1/2}.$$

The remaining terms may be obtained by interchanging the upper and lower indices.

For the dependence of s on J we use the equation

$$[L_x - iL_y, s_z]^{LS\,J'\,M_J}_{LS'J''M_J+1} = 0.$$

With $J'=J-1$ and $J''=J+1$ we have

$$L^{LSJ-1}_{LSJ}\quad {}^{LS\,J}s_{LS'J+1} = {}^{LSJ-1}s_{LS'J}\,L^{LS'J}_{LS'J+1}. \tag{7}$$

With $J'=J$, $J''=J+1$ and with $J'=J$, $J''=J-1$ we obtain the following two equations in exactly the same manner as Eqs. (15′) and (16′) are obtained in reference 1.

$$\{(J+1)L^{LSJ}_{LSJ} - (J+2)L^{LS'J+1}_{LS'J+1}\}\,{}^{LS\,J}s_{LS'J+1} - L^{LS'J}_{LS'J+1}\,{}^{LS\,J}s_{LS'J} = 0 \tag{8}$$

$$\{JL^{LSJ}_{LSJ} - (J-1)L^{LS'J-1}_{LS'J-1}\}\,{}^{LS\,J}s_{LS'J-1} + L^{LS'J}_{LS'J-1}\,{}^{LS\,J}s_{LS'J} = 0. \tag{9}$$

With $S'=S$ in Eq. (7) we obtain

$${}^{LSJ}s_{LSJ+1} = -\,{}^{LS}s_{LS}\,L^{LSJ}_{LSJ+1}$$

$$= {}^{LS}s_{LS}\left(\frac{(L+S-J)(L+S+J+2)(J+1+L-S)(J+1+S-L)}{4(J+1)^2(2J-1)(2J+1)}\right)^{1/2} \tag{10a}$$

From Eq. (8) with $S'=S$ we have

$$L^{LSJ}_{LSJ}\,{}^{LSJ}s_{LSJ+1} = {}^{LSJ}s_{LSJ+1}\{(J+1)L^{LSJ}_{LSJ} - (J+2)L^{LSJ+1}_{LSJ+1}\}$$

$${}^{LSJ}s_{LSJ} = {}^{LS}s_{LS}\frac{J(J+1)+S(S+1)-L(L+1)}{2J(J+1)}. \tag{10b}$$

From Eq. (7) with $S'=S-1$ we have

$$L^{LSJ-1}_{LSJ}\;{}^{LS\;\;J}s_{LS-1J+1} = {}^{LS\;\;J-1}s_{LS-1J}\quad L^{LS-1J}_{LS-1J+1}$$

or

$$\left(\frac{(L+S+1-J)(J-S+L)}{4J^2(2J-1)(2J+1)}\right)^{1/2}{}^{LS\;\;J}s_{LS-1J+1}$$

$$= \left(\frac{(L+S-J-1)(J-S+L+2)}{4(J+1)^2(2J+1)(2J+3)}\right)^{1/2}{}^{LS\;\;J-1}s_{LS-1J}$$

$${}^{LS\;\;J}s_{LS-1J+1} = -\,{}^{LS}s_{LS-1}\left(\frac{(L+S-J-1)(L+S-J)(J-S+L+2)(J-S+L+1)}{4(J+1)^2(2J+1)(2J+3)}\right)^{1/2} \tag{10c}$$

From Eq. (8) with $S'=S-1$ we have

$${}^{LS\;\;J}s_{LS-1J}\,L^{LS-1J}_{LS-1J+1} = {}^{LS\;\;J}s_{LS-1J+1}\{(J+1)L^{LSJ}_{LSJ} - (J+2)L^{LS-1J+1}_{LS-1J+1}\}$$

$${}^{LS\;\;J}s_{LS-1J} = -\,{}^{LS}s_{LS-1}\left(\frac{(L+S-J)(J-S+L+1)(J+S\mp L)(L+S+J+1)}{4J^2(J+1)^2}\right)^{1/2} \tag{10d}$$

Finally from Eq. (9) with $S'=S-1$ we obtain

$$s^{LS\ J}_{LS-1J-1} = s^{LS}_{LS-1}\left(\frac{(L+S+J)(J-L+S-1)(J+S-L)(L+S+J+1)}{4J^2(2J-1)(2J+1)}\right)^{1/2}. \quad (10e)$$

The remaining components may be obtained by interchanging the upper and lower indices. Formulas (10a) to (10e) can, except for sign, be obtained from Eqs. (6) by interchanging L and S.

Determination of l^{LS}_{LS} etc.

If we suppose that L^2, S^2, L_z and S_z are diagonal, then $\boldsymbol{L}$, $\boldsymbol{l}_1$ and $\boldsymbol{l}_2$ will be related to each other in the same manner as $\boldsymbol{J}$, $\boldsymbol{L}$ and $\boldsymbol{S}$ in the above calculation. $\boldsymbol{S}$, $\mathbf{s}_1$, and $\mathbf{s}_2$ will also be related in this manner. Then we can obtain the components of $\boldsymbol{l}_1$ and $\boldsymbol{l}_2$ and of $\mathbf{s}_1$ and $\mathbf{s}_2$ in this representation by a substitution of the appropriate quantum numbers in Eqs. (4) and (5). Now suppose we make a unitary transformation to a representation in which J^2, L^2, S^2 and J_z are diagonal. Such a transformation leaves L^2, S^2 and J_z invariant and so can only have components between states of the same L, S and M_J values. Between two sets of L, S and M_J values, the matrix components of $\boldsymbol{l}$ and $\mathbf{s}$ will have a constant factor $l^{LS}_{L'S'}$ and $s^{LS}_{LS'}$. This factor which is determined by the substitution of the appropriate quantum numbers in Eqs. (4) and (5), will not depend on J and will remain after the transformation. The other factor will depend on J and is just the factor we have determined above. Hence we have

$$\begin{aligned}
l^{LS}_{1LS} &= \frac{L(L+1)+l_1(l_1+1)-l_2(l_2+1)}{2L(L+1)} \\
l^{LS}_{2LS} &= \frac{L(L+1)+l_2(l_2+1)-l_1(l_1+1)}{2L(L+1)} \\
l^{L\ S}_{1L-1S} &= \left(\frac{(l_1+l_2-L+1)(l_1+l_2+L+1)(L-l_1+l_2)(L-l_2+l_1)}{4L^2(2L-1)(2L+1)}\right)^{1/2} = -\,l^{L\ S}_{2L-1S} \\
s^{LS}_{1LS} &= \frac{S(S+1)+s_1(s_1+1)-s_2(s_2+1)}{2S(S+1)} \\
s^{LS}_{2LS} &= \frac{S(S+1)+s_2(s_2+1)-s_1(s_1+1)}{2S(S+1)} \\
s^{LS}_{1LS-1} &= \left(\frac{(s_1+s_2-S+1)(s_1+s_2+S+1)(S-s_1+s_2)(S-s_2+s_1)}{4S^2(2S-1)(2S+1)}\right)^{1/2} = -\,s^{LS}_{2LS-1}.
\end{aligned} \quad (11)$$

Remembering that in our case $s_1=s_2=\frac{1}{2}$, the formulas for s_1 and s_2 reduce to

$$\begin{aligned}
s^{LS}_{1LS} &= s^{LS}_{2LS} = \tfrac{1}{2} \\
s^{LS}_{1LS-1} &= -\,s^{LS}_{2LS-1} = \tfrac{1}{2}\left(\frac{(2+S)(2-S)}{(2S-1)(2S+1)}\right)^{1/2}.
\end{aligned}$$

Summary of Formulas

$$(l_x \pm il_y)^{L\ S\ JM_J}_{L'S'JM_J\mp1}/l^{L\ S\ J}_{L'S'J} = (s_x \pm is_y)^{L\ S\ JM_J}_{L'S'JM_J\mp1}/s^{L\ S\ J}_{L'S'J}$$
$$= \{(J \pm M_J)(J \mp M_J + 1)\}^{1/2}$$
$$l_{zL'S'JM_J}/l^{L\ S\ J}_{L'S'J} = s_{zL'S'JM_J}/s^{L\ S\ J}_{L'S'J} = M_J$$
$$(l_x \pm il_y)^{L\ S\ J\ M_J}_{L'S'J+1M_J\mp1}/l^{L\ S\ J}_{L'S'J+1} = (s_x \pm is_y)^{L\ S\ J\ M_J}_{L'S'J+1M_J\mp1}/s^{L\ S\ J}_{L'S'J+1}$$
$$= \pm\{(J \mp M_J + 1)(J \mp M_J + 2)\}^{1/2}$$
$$l_{zL'S'J+1M_J}/l^{L\ S\ J}_{L'S'J+1} = s_{zL'S'J+1M_J}/s^{L\ S\ J}_{L'S'J+1} = \{(J+1)^2 - M_J^2\}^{1/2}$$
$$(l_x \pm il_y)^{L\ S\ J\ M_J}_{L'S'J-1M_J\mp1}/l^{L\ S\ J}_{L'S'J-1} = (s_x \pm is_y)^{L\ S\ J\ M_J}_{L'S'J-1M_J\mp1}/s^{L\ S\ J}_{L'S'J-1}$$
$$= \mp\{(J \pm M_J)(J \pm M_J - 1)\}^{1/2}$$
$$l_{zL'S'J-1M_J}/l^{L\ S\ J}_{L'S'J-1} = s_{zL'S'J-1M_J}/s^{L\ S\ J}_{L'S'J-1} = (J^2 - M_J^2)^{1/2}$$

$$l^{LSJ}_{LSJ+1}/l^{LS}_{LS} = -\left(\frac{(L+S+J+2)(L+S-J)(J+1+L-S)(J+1+S-L)}{4(J+1)^2(2J+1)(2J+3)}\right)^{1/2}$$

$$l^{LSJ}_{LSJ}/l^{LS}_{LS} = \frac{J(J+1) - S(S+1) + L(L+1)}{2J(J+1)}$$

$$l^{LSJ}_{LSJ-1}/l^{LS}_{LS} = -\left(\frac{(L+S+J+1)(L+S+1-J)(J+L-S)(J+S-L)}{4J^2(2J-1)(2J+1)}\right)^{1/2}$$

$$l^{L\ SJ}_{L-1SJ+1}/l^{L\ S}_{L-1S} = -\left(\frac{(L+S-J-1)(L+S-J)(J-L+S+2)(J-L+S+1)}{4(J+1)^2(2J+1)(2J+3)}\right)^{1/2}$$

$$l^{L\ SJ}_{L-1SJ}/l^{L\ S}_{L-1S} = \left(\frac{(L+S-J)(J-L+S+1)(J+L-S)(L+S+J+1)}{4J^2(J+1)^2}\right)^{1/2}$$

$$l^{L\ SJ}_{L-1SJ-1}/l^{L\ S}_{L-1S} = \left(\frac{(L+S+J)(J+L-S-1)(J+L-S)(L+S+J+1)}{4J^2(2J-1)(2J+1)}\right)^{1/2}$$

$$l^{L\ SJ}_{L+1SJ+1}/l^{L\ S}_{L+1S} = \left(\frac{(L+S+J+2)(J+L-S+1)(J+L-S+2)(L+S+J+3)}{4(J+1)^2(2J+1)(2J+3)}\right)^{1/2}$$

$$l^{L\ SJ}_{L+1SJ}/l^{L\ S}_{L+1S} = \left(\frac{(L+S-J+1)(J-L+S)(J+L-S+1)(L+S+J+2)}{4J^2(J+1)^2}\right)^{1/2}$$

$$l^{L\ SJ}_{L+1SJ-1}/l^{L\ S}_{L+1S} = -\left(\frac{(L+S-J+1)(L+S-J+2)(J-L+S)(J-L+S-1)}{4J^2(2J-1)(2J+1)}\right)^{1/2}$$

$$s^{LSJ}_{LSJ+1}/s^{LS}_{LS} = \left(\frac{(L+S-J)(L+S+J+2)(J+1+L-S)(J+1-L+S)}{4(J+1)^2(2J+1)(2J+3)}\right)^{1/2}$$

$$s^{LSJ}_{LSJ}/s^{LS}_{LS} = \frac{J(J+1) - L(L+1) + S(S+1)}{2J(J+1)}$$

$$s^{LSJ}_{LSJ-1}/s^{LS}_{LS} = \left(\frac{(L+S-J+1)(L+S+J+1)(J+L-S)(J-L+S)}{4J^2(2J-1)(2J+1)}\right)^{1/2}$$

$$s^{LS\ J}_{LS-1J+1}/s^{LS}_{LS-1} = -\left(\frac{(L+S-J-1)(L+S-J)(J-S+L+2)(J-S+L+1)}{4(J+1)^2(2J+1)(2J+3)}\right)^{1/2}$$

$$s^{LS\ J}_{LS-1J}/s^{LS}_{LS-1} = -\left(\frac{(L+S-J)(J-S+L+1)(J+S-L)(L+S+J+1)}{4J^2(J+1)^2}\right)^{1/2}$$

$$s^{LS\ J}_{LS-1J-1}/s^{LS}_{LS-1} = \left(\frac{(L+S+J)(J-L+S-1)(J+S-L)(L+S+J+1)}{4J^2(2J-1)(2J+1)}\right)^{1/2}$$

$$s^{LS\ J}_{LS+1J+1}/s^{LS}_{LS+1} = \left(\frac{(L+S+J+2)(J-L+S+1)(J+S-L+2)(L+S+J+3)}{4(J+1)^2(2J+1)(2J+3)}\right)^{1/2}$$

$$s^{LS\ J}_{LS+1J}/s^{LS}_{LS+1} = -\left(\frac{(L+S-J+1)(J-S+L)(J+S-L+1)(L+S+J+2)}{4J^2(J+1)^2}\right)^{1/2}$$

$$s^{LS\ J}_{LS+1J-1}/s^{LS}_{LS+1} = -\left(\frac{(L+S-J+1)(L+S-J+2)(J-S+L)(J-S+L-1)}{4J^2(2J-1)(2J+1)}\right)^{1/2}$$

$$l^{LS}_{1LS} = \frac{L(L+1)+l_1(l_1+1)-l_2(l_2+1)}{2L(L+1)} \qquad l^{LS}_{2LS} = \frac{L(L+1)+l_2(l_2+1)-l_1(l_1+1)}{2L(L+1)}$$

$$l^{L\ S}_{1L-1S} = -\,l^{L\ S}_{2L-1S} = \left(\frac{(l_1+l_2-L+1)(l_1+l_2+L+1)(L-l_1+l_2)(L-l_2+l_1)}{4L^2(2L-1)(2L+1)}\right)^{1/2}$$

$$l^{L\ S}_{1L+1S} = -\,l^{L\ S}_{2L+1S} = \left(\frac{(l_1+l_2-L)(l_1+l_2+L+2)(L+1-l_1+l_2)(L+1-l_2+l_1)}{4(L+1)^2(2L+1)(2L+3)}\right)^{1/2}$$

$$s^{LS}_{1LS}\ s^{LS}_{2LS} = \tfrac{1}{2}$$

$$s^{LS}_{1LS-1} = -\,s^{LS}_{2LS-1} = \tfrac{1}{2}\left(\frac{(2-S)(2+S)}{(2S-1)(2S+1)}\right)^{1/2}$$

$$s^{LS}_{1LS+1} = -\,s^{LS}_{2LS+1} = \tfrac{1}{2}\left(\frac{(1-S)(3+S)}{(2S+1)(2S+3)}\right)^{1/2}$$

The Matrix of the Spin-Orbit Interaction

We wish to obtain the matrix of $a_1(l_1\cdot s_1)+a_2(l_2\cdot s_2)$. From Eqs. (2) we know that this expression commutes with J^2 and J_z. It will therefore be diagonal with respect to the quantum numbers J and M_J. By matrix multiplication we have

$$\begin{aligned}(l\cdot s)^{L\ S\ JM_J}_{L'S'JM_J} &= \sum_{J''}\tfrac{1}{2}(l_x-il_y)^{L\ SJ\ \ M_J}_{L'SJ''M_J+1}(s_x+is_y)^{L'S\ J''M_J+1}_{L'S'J\ \ M_J}\\ &\quad+\tfrac{1}{2}(l_x+il_y)^{LSJ\ \ M_J}_{L'SJ''M_J-1}(s_x-is_y)^{L'S\ J''M_J-1}_{L'S'J\ \ M_J}+l_{zL'SJ''M_J}{}^{L\ SJ\ \ M_J}\ {}^{L'S\ J''M_J}_{\ \ s_zL'S'J\ \ M_J}\\ &= (J+1)(2J+3)l^{L\ SJ}_{L'SJ+1}{}^{L'S\ J+1}_{\ \ s_L'S'J}+J(J+1)l^{L\ SJ}_{L'SJ}{}^{L'S\ J}_{\ \ s_L'S'J}\end{aligned}$$

$$+J(2J-1)l^{L\,SJ}_{L'SJ-1}s^{L'S\,J-1}_{L'S'J}.$$

Substitution from our previous formulas into the above equation yields the following result for the matrix components of the spin-orbit interaction.

$$(l\cdot s)^{L\ \ S\ \ JM_J}_{L-1S-1JM_J}$$
$$=-\tfrac{1}{2}(l^{L\ \ S}_{L-1S})(s^{L-1S}_{L-1S-1})\{(L+S-J)(L+S-J-1)(L+S+J)(L+S+J+1)\}^{1/2}$$

$$(l\cdot s)^{L\ \ SJM_J}_{L-1SJM_J}$$
$$=\tfrac{1}{2}(l^{L\ \ S}_{L-1S})(s^{L-1S}_{L-1S})\{(L+S-J)(J-L+S+1)(J+L-S)(L+S+J+1)\}^{1/2}$$

$$(l\cdot s)^{L\ \ S\ \ JM_J}_{L-1S+1JM_J}$$
$$=\tfrac{1}{2}(l^{L\ \ S}_{L-1S})(s^{L-1S}_{L-1S+1})\{(J-L+S+2)(J-L+S+1)(J-S+L)(J-S+L-1)\}^{1/2}$$

$$(l\cdot s)^{LS\ \ JM_J}_{LS-1JM_J}$$
$$=-\tfrac{1}{2}(l^{LS}_{LS})(s^{LS}_{LS-1})\{(L+S-J)(J+L-S+1)(L+S+J+1)(J-L+S)\}^{1/2}$$

$$(l\cdot s)^{LSJM_J}_{LSJM_J}$$
$$=\tfrac{1}{2}(l^{LS}_{LS})(s^{LS}_{LS})\{J(J+1)-L(L+1)-S(S+1)\}$$

$$(l\cdot s)^{LS\ \ JM_J}_{LS+1JM_J}$$
$$=-\tfrac{1}{2}(l^{LS}_{LS})(s^{LS}_{LS+1})\{(L+S-J+1)(J+L-S)(L+S+J+2)(J-L+S+1)\}^{1/2}$$

$$(l\cdot s)^{L\ \ S\ \ JM_J}_{L+1S-1JM_J}$$
$$=\tfrac{1}{2}(l^{L\ \ S}_{L+1S})(s^{L+1S}_{L+1S-1})\{(J-L+S)(J-L+S-1)(J+L-S+1)(J+L-S+2)\}^{1/2}$$

$$(l\cdot s)^{L\ \ SJM_J}_{L+1SJM_J}$$
$$=\tfrac{1}{2}(l^{L\ \ S}_{L+1S})(s^{L+1S}_{L+1S})\{(L+S-J+1)(J-L+S)(J+L-S+1)(L+S+J+2)\}^{1/2}$$

$$(l\cdot s)^{L\ \ S\ \ JM_J}_{L+1S+1JM_J}$$
$$=-\tfrac{1}{2}(l^{L\ \ S}_{L+1S})(s^{L+1S}_{L+1S+1})\{(L+S-J+1)(L+S-J+2)(L+S+J+2)(L+S+J+3)\}^{1/2}$$

These formulas apply for both electrons. In conjunction with the expressions given above for $l^{LS}_{L'S}$ and $s^{LS}_{LS'}$ they completely determine the matrix of the spin-orbit interaction.

The Configuration p^2

In this case $l_1=l_2=1$ and $a_1=a_2=a$. The multiplets are ^1D, ^3P and ^1S. The energy matrix calculated from the above formulas is given below. It is sufficient to give separate matrices for each J value as there are no components between states of different J value.

$J=2$

	$^1D_2$	$^3P_2$
$^1D_2$	0	$(\frac{1}{2})^{1/2}a$
$^3P_2$	$(\frac{1}{2})^{1/2}a$	$a/2$

		$^3P_1$
$J=1$	$^3P_1$	$-a/2$

		$^3P_0$	$^1S_0$
$J=0$	$^3P_0$	$-a$	$-(2)^{1/2}a$
	$^1S_0$	$-(2)^{1/2}a$	0

From Slater's paper we find for the electrostatic energies in terms of his radial integrals

$$^1D: \quad F^0 + 1/25F^2$$
$$^3P: \quad F^0 - 5/25F^2$$
$$^1S: \quad F^0 + 10/25F^2.$$

We now measure energies from the $^3P_1$ level. Then adding the electrostatic energies to the diagonal terms and setting the determinant of the energy matrix equal to zero, we obtain the following secular equations.

$$J=2 \quad W^2 - W(3/2a + 6/25F^2) + 6/25F^2a = 0$$
$$J=1 \quad W = 0$$
$$J=0 \quad W^2 - W(15/25F^2) - 9/4a^2 - 15/50F^2a = 0.$$

These equations determine the energy levels in intermediate coupling in terms of the coupling parameters a and F^2. They have been previously obtained and discussed by Goudsmit.[7]

The Configuration $p \cdot p$

In this case also $l_1 = l_2$ but now $a_1 \neq a_2$. The multiplets are singlet and triplet D, P and S. From our formulas, the energy matrix is

		$^3D_3$
$J=3$	$^3D_3$	$\frac{1}{2}(a_1 + a_2)$

		$^3D_2$	$^1D_2$	$^3P_2$
$J=2$	$^3D_2$*	$-\frac{1}{4}(a_1 + a_2)$	$-\frac{1}{2}(3/2)^{1/2}(a_1 - a_2)$	$\frac{1}{4}(3)^{1/2}(a_1 - a_2)$
	$^1D_2$	$-\frac{1}{2}(3/2)^{1/2}(a_1 - a_2)$	0	$\frac{1}{4}(2)^{1/2}(a_1 + a_2)$
	$^3P_2$	$\frac{1}{4}(3)^{1/2}(a_1 - a_2)$	$\frac{1}{4}(2)^{1/2}(a_1 + a_2)$	$\frac{1}{4}(a_1 + a_2)$

		$^3D_1$	$^3P_1$	$^1P_1$	$^3S_1$
$J=1$	$^3D_1$	$-\frac{3}{4}(a_1+a_2)$	$\frac{1}{4}(5/3)^{1/2}(a_1-a_2)$	$-\frac{1}{4}(10/3)^{1/2}(a_1+a_2)$	0
	$^3P_1$	$\frac{1}{4}(5/3)^{1/2}(a_1 - a_2)$	$-\frac{1}{4}(a_1+a_2)$	$-\frac{1}{4}(2)^{1/2}(a_1-a_2)$	$(\frac{1}{3})^{1/2}(a_1-a_2)$
	$^1P_1$	$-\frac{1}{4}(10/3)^{1/2}(a_1+a_2)$	$-\frac{1}{4}(2)^{1/2}(a_1-a_2)$	0	$\frac{1}{2}(\frac{2}{3})^{1/2}(a_1+a_2)$
	$^3S_1$	0	$(\frac{1}{3})^{1/2}(a_1-a_2)$	$\frac{1}{2}(\frac{2}{3})^{1/2}(a_1 + a_2)$	0

[7] Reference 4. To agree with Goudsmit's results we must set $a/2 = A$ and $3/25\ F^2 = X$ in the above equations.

* In the secular equations the parameters never appear in the denominators of fractions. An expression such as $6/25\ F^2$ must always be taken to mean $(6/25)\ F^2$.

$J=0$

	$^3P_0$	$^1S_0$
$^3P_0$	$-\frac{1}{2}(a_1+a_2)$	$-\frac{1}{2}(2)^{1/2}(a_1-a_2)$
$^1S_0$	$-\frac{1}{2}(2)^{1/2}(a_1-a_2)$	0

For the electrostatic energies referred to the ^3D multiplet we find by Slater's method[8]

$$
\begin{aligned}
^3D&: \quad 0\\
^1D&: \quad 2G^0+2/25G^2=\alpha\\
^3P&: \quad -6/25F^2+2G^0-4/25G^2=\beta\\
^1P&: \quad -6/25F^2+6/25G^2=\gamma\\
^3S&: \quad 9/25F^2-9/25G^2=-3/2\gamma\\
^1S&: \quad 9/25F^2+2G^0+11/25G^2=\delta.
\end{aligned}
$$

Measuring the energy levels from the $^3D_3$ we obtain the following secular equations

$$
\begin{aligned}
J=3\quad & W=0\\
J=2\quad & -W^3+W^2\{\alpha+\beta-3/2(a_1+a_2)\}-W\{\alpha\beta-\tfrac{1}{4}(a_1+a_2)(4\alpha+5\beta)\\
& +9/4a_1a_2\}-3/4(a_1+a_2)\alpha\beta+\tfrac{3}{4}a_1a_2(\alpha+2\beta)=0\\
J=1\quad & W^4-W^3\{\beta-\tfrac{1}{2}\gamma-3(a_1+a_2)\}+W^2\{-\tfrac{1}{2}\gamma(\beta+3\gamma)\\
& +\tfrac{1}{4}(a_1+a_2)(-9\beta+5\gamma)+9/4(a_1^2+a_2^2+3a_1a_2)\}\\
& -W\{-3/2\beta\gamma^2+\tfrac{1}{8}(a_1+a_2)(7\beta+24\gamma)+3/32(a_1+a_2)^2(12\beta-7\gamma)\\
& -3/32(a_1-a_2^2)\gamma-27/8a_1a_2(a_1+a_2)\}+15/8(a_1+a_2)\beta\gamma^2-5/8(2a_1^2\\
& +29_2^2+5a_1a_2)\gamma^2=0\\
J=0\quad & W^2-W\{\beta+\delta-3/2(a_1+a_2)\}+\beta\delta-\tfrac{1}{2}(a_1+a_2)(\beta+2\delta)+2a_1a_2=0.
\end{aligned}
$$

The Configuration d^2

In this case $l_1=l_2=2$ and $a_1=a_2=a$. The multiplets are ^1G, ^3F, ^1D, ^3P and ^1S. From our formulas the magnetic energy matrix is

$J=4$

	$^1G_4$	$^3F_4$
$^1G_4$	0	a
$^3F_4$	a	$3/2a$

$J=3$

	$^3F_3$
$^3F_3$	$-\frac{1}{2}a$

$J=2$

	$^3F_2$	$^1D_2$	$^3P_2$
$^3F_2$	$-2a$	$-2(3/5)^{1/2}a$	0
$^1D_2$	$-2(3/5)^{1/2}a$	0	$(21/10)^{1/2}a$
$^3P_2$	0	$(21/10)^{1/2}a$	$\frac{1}{2}a$

[8] E. U. Condon and G. H. Shortley, Phys. Rev. **37**, 1025 (1931).

		$^3P_1$
$J=1$	$^3P_1$	$-\frac{1}{2}a$

		$^3P_0$	$^1S_0$
$J=0$	$^3P_0$	$-a$	$-(6)^{1/2}a$.
	$^1S_0$	$-(6)^{1/2}a$	0

By Slater's method[8] we find for the electrostatic energies referred to the ^3F multiplet

$$^1G: \quad 12/49F^2 + 10/441F^4 = \alpha$$
$$^3F: \quad 0$$
$$^1D: \quad 5/49F^2 + 45/441F^4 = \beta$$
$$^3P: \quad 15/49F^2 - 75/441F^4 = \gamma$$
$$^1S: \quad 22/49F^2 + 135/441F^4 = \delta.$$

Measuring energies from the $^3F_3$ level, we find the following secular equations.

$$J=4 \quad W^2 - W(\alpha + 5/2a) + 2a\alpha = 0$$
$$J=3 \quad -W = 0$$
$$J=2 \quad -W^3 + W^2(\beta+\gamma) - W\{\beta\gamma - \tfrac{1}{2}a(\beta+2\gamma) - 25/4a^2\} - 3/2a\beta\gamma - 3/20a^2(10\beta+21\gamma) = 0$$
$$J=1 \quad -W + \gamma = 0$$
$$J=0 \quad W^2 - W(\gamma+\delta) + \gamma\delta + \tfrac{1}{2}a(\gamma-\delta) - 25/4a^2 = 0.$$

The Configuration $d \cdot d$

In this case $l_1 = l_2 = 2$ but $a_1 \neq a_2$. The multiplets are singlet and triplet S, P, D, F and G. From our formulas the magnetic energy matrix is

		$^3G_5$
$J=5$	$^3G_5$	a_1+a_2

		$^3G_4$	$^1G_4$	$^3F_4$
$J=4$	$^3G_4$	$-\frac{1}{4}(a_1+a_2)$	$-\frac{1}{2}(5)^{1/2}(a_1-a_2)$	$\frac{1}{4}(5)^{1/2}(a_1-a_2)$
	$^1G_4$	$-\frac{1}{2}(5)^{1/2}(a_1-a_2)$	0	$\frac{1}{2}(a_1+a_2)$
	$^3F_4$	$\frac{1}{4}(5)^{1/2}(a_1-a_2)$	$\frac{1}{2}(a_1+a_2)$	$\frac{3}{4}(a_1+a_2)$

		$^3G_3$	$^3F_3$	$^1F_3$	$^3D_3$
$J=3$	$^3G_3$	$-5/4(a_1+a_2)$	$\frac{1}{4}(3/7)^{1/2}(a_1-a_2)$	$-3/2(1/7)^{1/2}(a_1+a_2)$	0
	$^3F_3$	$\frac{3}{4}(3/7)^{1/2}(a_1-a_2)$	$-\frac{1}{4}(a_1+a_2)$	$-\frac{1}{2}(3)^{1/2}(a_1-a_2)$	$2(1/7)^{1/2}(a_1-a_2)$
	$^1F_3$	$-3/2(1/7)^{1/2}(a_1+a_2)$	$-\frac{1}{2}(3)^{1/2}(a_1-a_2)$	0	$(3/7)^{1/2}(a_1+a_2)$
	$^3D_3$	0	$2(1/7)^{1/2}(a_1-a_2)$	$(3/7)^{1/2}(a_1+a_2)$	$\frac{1}{2}(a_1+a_2)$

		$^3F_2$	$^3D_2$	$^1D_2$	$^3P_2$
$J=2$	$^3F_2$	$-(a_1+a_2)$	$(2/5)^{1/2}(a_1-a_2)$	$-(3/5)^{1/2}(a_1+a_2)$	0
	$^3D_2$	$(2/5)^{1/2}(a_1-a_2)$	$-\frac{1}{4}(a_1+a_2)$	$-\frac{1}{4}(6)^{1/2}(a_1-a_2)$	$\frac{3}{4}(7/5)^{1/2}(a_1-a_2)$
	$^1D_2$	$-(3/5)^{1/2}(a_1+a_2)$	$-\frac{1}{4}(6)^{1/2}(a_1-a_2)$	0	$\frac{1}{2}(21/10)^{1/2}(a_1+a_2)$
	$^3P_2$	0	$\frac{3}{4}(7/5)^{1/2}(a_1-a_2)$	$\frac{1}{2}(21/10)^{1/2}(a_1+a_2)$	$\frac{1}{4}(a_1+a_2)$

$J = 1$

	$^3D_1$	$^3P_1$	$^1P_1$	$^3S_1$
$^3D_1$	$-\frac{3}{4}(a_1+a_2)$	$\frac{1}{4}(7)^{1/2}(a_1-a_2)$	$-\frac{1}{4}(14)^{1/2}(a_1+a_2)$	0.
$^3P_1$	$\frac{1}{4}(7)^{1/2}(a_1-a_2)$	$-\frac{1}{4}(a_1+a_2)$	$-\frac{1}{4}(2)^{1/2}(a_1-a_2)$	a_1-a_2
$^1P_1$	$-\frac{1}{4}(14)^{1/2}(a_1+a_2)$	$-\frac{1}{4}(2)^{1/2}(a_1-a_2)$	0	$\frac{1}{2}(2)^{1/2}(a_1+a_2)$
$^3S_1$	0	a_1-a_2	$\frac{1}{2}(2)^{1/2}(a_1+a_2)$	0

$J = 0$

	$^3P_0$	$^1S_0$
$^3P_0$	$-\frac{1}{2}(a_1+a_2)$	$-\frac{1}{2}(6)^{1/2}(a_1+a_2)$
$^1S_0$	$-\frac{1}{2}(6)^{1/2}(a_1+a_2)$	0

Now we could proceed as before, that is add the electrostatic energies to the diagonal terms of the above matrix and then expand the determinant of the matrix in order to obtain the secular equations. But in this case the expanded fourth order equations are so complicated that it seems preferable to leave them in the form of fourth order determinants, as the determinants are probably easier than the expanded form to handle numerically. For this reason we do not give the expanded form for the secular equations.

The Configuration $d \cdot p$

In this case we have $l_1 = 2$ and $l_2 = 1$. The multiplets are singlet and triplet P, D and F. From our formulas the magnetic energy matrix is

$J = 4$

	$^3F_4$
$^3F_4$	$\frac{1}{2}(2a_1+a_2)$

$J = 3$

	$^3F_3$	$^1F_3$	$^3D_3$
$^3F_3$	$-1/6(2a_1+a_2)$	$-(\frac{1}{3})^{1/2}(2a_1-a_2)$	$\frac{1}{3}(2)^{1/2}(a_1-a_2)$
$^1F_3$	$-(\frac{1}{3})^{1/2}(2a_1-a_2)$	0	$(1/6)^{1/2}(a_1+a_2)$
$^3D_3$	$\frac{1}{3}(2)^{1/2}(a_1-a_2)$	$(1/6)^{1/2}(a_1+a_2)$	$1/6(5a_1+a_2)$

$J = 2$

	$^3F_2$	$^3D_2$	$^1D_2$	$^3P_2$
$^3F_2$	$-\frac{2}{3}(2a_1+a_2)$	$\frac{1}{3}(7/5)^{1/2}(a_1-a_2)$	$-\frac{1}{3}(21/10)^{1/2}(a_1+a_2)$	0
$^3D_2$	$\frac{1}{3}(7/5)^{1/2}(a_1-a_2)$	$-1/12(5a_1+a_2)$	$-\frac{1}{2}(1/6)^{1/2}(5a_1-a_2)$	$\frac{3}{4}(3/5)^{1/2}(a_1-a_2)$
$^1D_2$	$-\frac{1}{3}(21/10)^{1/2}(a_1+a_2)$	$-\frac{1}{2}(1/6)^{1/2}(5a_1-a_2)$	0	$\frac{3}{4}(2/5)^{1/2}(a_1+a_2)$
$^3P_2$	0	$\frac{3}{4}(3/5)^{1/2}(a_1-a_2)$	$\frac{3}{4}(2/5)^{1/2}(a_1+a_2)$	$\frac{1}{4}(3a_1-a_2)$

$J = 1$

	$^3D_1$	$^3P_1$	$^1P_1$
$^3D_1$	$-\frac{1}{4}(5a_1+a_2)$	$\frac{1}{4}(3)^{1/2}(a_1-a_2)$	$-\frac{1}{4}(6)^{1/2}(a_1+a_2)$
$^3P_1$	$\frac{1}{4}(3)^{1/2}(a_1-a_2)$	$-\frac{1}{4}(3a_1-a_2)$	$-\frac{1}{4}(2)^{1/2}(3a_1+a_2)$
$^1P_1$	$-\frac{1}{4}(6)^{1/2}(a_1+a_2)$	$-\frac{1}{4}(2)^{1/2}(3a_1+a_2)$	0

$J = 0$

	$^3P_0$
$^3P_0$	$-\frac{1}{2}(3a_1-a_2)$

For the same reason as the previous case we do not give the expanded form of the secular equations.

Many Electron Configurations

Our formulas for four vectors may be applied to give the secular equations relating the levels arising from a common parent term. We take l_1 and s_1 for the orbital and spin momentum of the ion and l_2 and s_2 for the orbital and spin momentum of the added electron. Then the formulas for the matrix of

the spin-orbit interaction apply directly when we remember that s_1 is no longer restricted to the value 1/2. We must use Eqs. (11) for $s_{1LS'}^{LS}$.

We consider first the addition of an s electron to a ^3P multiplet, a case already treated by Goudsmit.[4] The multiplets are ^4P and ^2P. Remembering that $l_1=l=L$, $s_1=l$, $l_2=0$ and $s_2=1/2$ we have from Eqs. (11)

$$l_{1LS}^{LS} = 1$$

$$l_{2LS}^{LS} = 0$$

$$s_{1LS}^{LS} = \frac{S(S+1)+5/4}{2S(S+1)} = \begin{cases} 2/3 \text{ for } {}^4P \\ 4/3 \text{ for } {}^2P \end{cases}$$

$$s_{1LS-1}^{LS} = \left(\frac{(25/4-S^2)(S^2-\frac{1}{4})}{4S^2(4S^2-1)}\right)^{1/2}.$$

Our formulas for the matrix of the spin-orbit interaction give

$J = 5/2$

	$^4P_{5/2}$
$^4P_{5/2}$	a_1

$J = 3/2$

	$^4P_{3/2}$	$^2P_{3/2}$
$^4P_{3/2}$	$-\frac{2}{3}a_1$	$-\frac{1}{3}(5)^{1/2}a_1$
$^2P_{3/2}$	$-\frac{1}{3}(5)^{1/2}a_1$	$\frac{2}{3}a_1$

$J = \frac{1}{2}$

	$^4P_{1/2}$	$^2P_{1/2}$
$^4P_{1/2}$	$-5/3a_1$	$-\frac{1}{3}(2)^{1/2}a_1$
$^2P_{1/2}$	$-\frac{1}{3}(2)^{1/2}a_1$	$-\frac{4}{3}a_1$

Let α be the electrostatic energy of the ^2P multiplet referred to the ^4P. Then measuring energies from the $^4P_{5/2}$ level we obtain the following secular equations

$$J = 5/2 \qquad -W = 0$$

$$J = 3/2 \qquad W^2 - (\alpha - 2a_1)W - 5/3\alpha a_1 = 0$$

$$J = \tfrac{1}{2} \qquad W^2 - (\alpha - 5a_1)W - 8/3\alpha a_1 + 6a_1^2 = 0.$$

As another example we consider the addition of a p electron to a ^1P multiplet. The multiplets are ^2S, ^2P and ^2D. From Eqs. (11), remembering that $l_1=1$, $s_1=0$, $l_2=1$, $s_2=1/2=S$, we have

$$s_{1LS}^{LS} = 0$$

$$s_{2LS}^{LS} = 1$$

$$l_{2LS}^{LS} = \tfrac{1}{2}$$

$$l_{2L-1S}^{L\ S} = \tfrac{1}{2}\left(\frac{9-L^2}{4L^2-1}\right)^{1/2}.$$

Then we find for the matrix of the spin-orbit interaction

$J = 5/2$

	$^2D_{5/2}$
$^2D_{5/2}$	$\frac{1}{2}a_2$

$J = 3/2$

	$^2D_{3/2}$	$^2P_{3/2}$
$^2D_{3/2}$	$-\frac{3}{4}a_2$	$\frac{1}{4}(5)^{1/2}a_2$
$^2P_{3/2}$	$\frac{1}{4}(5)^{1/2}a_2$	$\frac{1}{4}a_2$

$J = \frac{1}{2}$

	$^2P_{1/2}$	$^2S_{1/2}$
$^2P_{1/2}$	$-\frac{1}{2}a_2$	$\frac{1}{2}(2/5)^{1/2}a_2$
$^2S_{1/2}$	$\frac{1}{2}(2/5)^{1/2}a_2$	0

Let α be the electrostatic energy of the ^2P multiplet referred to the ^2D and β be the electrostatic energy of the ^2S referred to the ^2D. Measuring energies from the $^2D_{5/2}$ level we obtain the following secular equations.

$J = 5/2 \qquad -W = 0$

$J = 3/2 \qquad W^2 - (\alpha - 2a_2)W + 5/8a_2(a_2 - 2\alpha) = 0$

$J = \frac{1}{2} \qquad W^2 - (\alpha + \beta - 3/2a_2)W + \alpha\beta - \frac{1}{2}a_2(\alpha + 2\beta) + 2/5a_2^2 = 0$

The Adjustment of the Parameters

In the secular equations that we have given the coefficients are functions of the radial integrals F^k, G^k and a_1 and a_2. Until these integrals can be calculated they must be treated as parameters which may be adjusted to fit the experimental data. In simple cases this may be accomplished easily by using the sums of energies for each J value. These sums are always linear in the parameters so that if we set the various sums equal to their experimental values, we obtain a linear set of equations for the parameters. In more complicated cases we will not obtain enough equations to determine the parameters in this way and more laborious calculations will have to be made. However these calculations will be useful for other quantities besides the energy levels may be found in terms of the same parameters. Thus in the following paper the g values for intermediate coupling are calculated in terms of these parameters and in a later paper the writer will treat the question of intensities in intermediate coupling.

In conclusion the writer wishes to thank Professor Pauli for suggesting the method of treating this problem.

ZEEMAN EFFECT IN INTERMEDIATE COUPLING

By D. R. Inglis and M. H. Johnson, Jr.
University of Michigan and Harvard University

(Received September 4, 1931)

Abstract

A method is given for calculating g-values in intermediate coupling when the matrix of internal energy of the atom (spin-orbit plus electrostatic interaction) is known in LS coupling. The transformation from the states of LS coupling to the states of intermediate coupling, in which the internal energy matrix is diagonal, is then readily determined in terms of the parameters expressing the relative magnitudes of the interactions. The coupling parameters are ascertained from the measured energy levels. The transformation so determined is applied to the matrix of the energy due to an external magnetic field, as known for LS coupling. The diagonal terms of the transformed matrix contain the g-values of the states of the atom in intermediate coupling. Application of the method is made to the configurations p^2, p^3 and d^2. Agreement with the available experimental g-values is satisfactory, being as good as the agreement of energy levels to be had from a first order calculation.

THE "anomalous" Zeeman effect for two-electron configurations with one s-electron has been treated by Houston.[1] Goudsmit[2] has extended the treatment to another special type of configuration, p^2 and p^4. The energy level problem for general two-electron configurations has been treated in the preceding paper in a manner which makes possible an easy method for calculating g-values in intermediate coupling. The method applies to any atom of which the matrix of the perturbing energy of the electrons is known in LS coupling.

Zeeman effect (as distinguished from Paschen-Back effect) is concerned with an external magnetic field sufficiently weak that the magnitude of the total angular momentum is a constant of the motion. Then the components of the energy matrix between states of different values of J may be neglected. In LS coupling L^2, S^2 and J_z are diagonal matrices (being constants of the motion), and they commute with L_z and S_z. Thus the energy due to the external field, $(L_z+2S_z)H$, has matrix elements only between states with the same quantum numbers L, S and M_J. As we neglect the elements between states of different J value, this Zeeman energy is a diagonal matrix in LS coupling. From Eqs. (3), (4) and (5) of the preceding paper, we have the familiar result

$$\begin{aligned} H(L_z + 2S_z)^{LSJMJ}_{LSJM_J} &= HM_J(L^{LSJ}_{LSJ} + 2S^{LSJ}_{LSJ}) \\ &= HM_J \frac{3J(J+1) + S(S+1) - L(L+1)}{2J(J+1)} \\ &= HM_J g_{LSJ} \end{aligned} \tag{1}$$

giving the Landé g-values in LS coupling.

[1] W. V. Houston, Phys. Rev. **33**, 297 (1929).
[2] S. Goudsmit, Phys. Rev. **35**, 1325 (1930).

If we know the matrix of the internal energy of the atom in LS coupling, we can find the transformation, R, which carries it to diagonal form. R will have no components between states of different J and M_J, as the internal energy commutes with J^2 and J_z. Hence it is sufficient to consider together states with the same J and M_J.

The matrix of the energy due to the external field is diagonal in LS coupling, and has the elements HM_Jg_k, where g_k is the g-value of a state specified by the quantum numbers $L_kS_kJ_k$. This matrix may be transformed to intermediate coupling:

$$HM_Jg' = HM_JRgR^{-1}.$$

We treat the energy due to the external field as a perturbation of the atom in intermediate coupling, expanding in powers of the perturbation parameter H. The first order corrections to the energies are the diagonal elements of the perturbing energy matrix. The g-values are defined by the coefficients of the first power of H in the energies,[3] so they are the diagonal terms

$$g_k' = \sum_l R(kl)g_lR^{-1}(lk) = \sum_l R(kl)g_lR^*(kl). \tag{2}$$

Applications

The configuration p^2. Here the levels with $J=0$ are not split up by the field and the level with $J=1$, $^3P_1$, has $g=3/2$ for all couplings. For the levels with $J=2$ the matrix of the g-values in LS coupling is

	$^1D_2$	$^3P_2$
$^1D_2$	1	0
$^3P_2$	0	3/2

Using the energy matrix from the preceding paper (with $^3P_1$ as reference level), we find for the transformation matrix,

$$R(k1) = \frac{2^{1/2}(\epsilon_k - 1)}{[2(\epsilon_k - 1)^2 + 1]^{1/2}}$$

$$R(k2) = \frac{1}{[2(\epsilon_k - 1)^2 + 1]^{1/2}}.$$

In these equations $\epsilon_k = W_k/a$, where W_k is the energy of a state in intermediate coupling (a solution of the secular equation for $J=2$ in the preceding paper) and a is the parameter of spin-orbit interaction. We find for the g-values in intermediate coupling[4]

[3] The g-values are thus independent of the nondiagonal elements of the transformed matrix, and therefore small elements of the matrix that are nondiagonal with respect to J^2 in LS coupling do not affect the g-values.

[4] With Goudsmit's method,[2] which applies especially to this case, we obtain the formula

$$g_k' = \frac{5}{4} + \frac{1/4 - X/a}{2(\epsilon_k - \epsilon_e)}$$

$$g_k' = \frac{2(\epsilon_k - 1)^2 + 3/2}{2(\epsilon_k - 1)^2 + 1}.$$

This formula has been applied in calculating the values listed in Table I. The parameters have been determined simply from their relations to the energy

TABLE I. *Energies and g-values of the configuration p^2.*

	Sn I $5p^2$					Pb I $6p^2$				
	$J=0$	2	2	1	0	$J=0$	2	2	1	0
ν obs.	15471	6921	1736	0	−1692	21639	13639	2831	0	−7817
ϵ_k obs.	7.39	3.31	0.83	0	−0.81	2.96	1.87	0.39	0	−1.07
ϵ_k calc.	7.34	3.35	0.78	0	−0.76	2.97	1.85	0.41	0	−1.08
g (LS)		1.00	1.50	1.50			1.00	1.50	1.50	
g_k' calc.		1.042	1.458	1.50			1.205	1.295	1.50	
g_k' obs.*		1.050	1.420	1.501			1.230	1.269	1.501	

* E. Back, Zeits. f. Physik **43**, 309 (1927). The g-values for Sn I observed by Green and Loring (Phys. Rev. **30**, 574, 1927) agree with Back's, except that they have 1.46 instead of 1.420, in better agreement with the theoretical value and with the g-sum rule.

sums. The energy values calculated from these parameters are also listed, and are seen to agree with the observed levels as well as is to be expected from a first order calculation.

The configuration p^3. For this case the multiplets are ^2D, ^2P, and ^4S. The g-values for $^2D_{5/2}$ and $^2P_{1/2}$ are independent of the coupling. For the levels with $J=3/2$ the equation for the energies has been given by one of us[5] as

$$W^3 + W^2X - W(9a^2/4 + 6X^2) - 15Xa^2/4 = 0.$$

The energies of the states in LS coupling are known, and contain no term in the first power of a. This and the selection rule that $\Delta L = 0, \pm 1$ and $\Delta S = 0$, ± 1 for the matrix components of the spin-orbit interaction limit the energy matrix to the form

	$^2D_{3/2}$	$^2P_{3/2}$	$^4S_{3/2}$
$^2D_{3/2}$	0	α_1	0
$^2P_{3/2}$	α_1	$2X$	α_2
$^4S_{3/2}$	0	α_2	$-3X$

with $^2D_{5/2}$ taken as reference level. This yields the secular equation

$$W^3 + W^2X - W(\alpha_1^2 + \alpha_2^2 + 6X^2) - 3X\alpha_1^2 = 0.$$

(his equation 13). Application of this formula also gives the results of Table I. It differs from ours in form, since his method is a solution of a secular equation directly for energies, and involves no transformation coefficients. It is equivalent to solving the equation

$$\begin{vmatrix} e_{11} + g_1H - \epsilon_0 - g'H & e_{12} \\ e_{21} & e_{22} + g_0H - \epsilon_0 - g'H \end{vmatrix} = 0$$

where the terms without H vanish, ϵ_0 being a solution for zero field. When we go to determinants of higher order, the coefficient of H involves nondiagonal elements. A direct solution of the determinant becomes increasingly unwieldy, and Goudsmit's method fails with too few relations to determine the coefficients.

[5] D. R. Inglis, Phys. Rev. **38**, 377 (1931).

Comparison with the above determines[6]

$$\alpha_1^2 = 5a^2/4$$
$$\alpha_2^2 = a^2$$

For the transformation matrix we find

$$R(k1) = \frac{5^{1/2}}{2}\,\frac{\epsilon_k + 3X/a}{\epsilon_k}\,R(k3)$$
$$R(k2) = (\epsilon_k + 3X/a)R(k3)$$
$$R(k3) = \frac{1}{[1 + (5/4\epsilon_k + 1)(\epsilon_k + 3X/a)]^{1/2}}.$$

In LS coupling

$$g = \begin{array}{c|ccc} & {}^2D_{3/2} & {}^2P_{3/2} & {}^4S_{3/2} \\ \hline {}^2D_{3/2} & 4/5 & 0 & 0 \\ {}^2P_{3/2} & 0 & 4/3 & 0 \\ {}^4S_{3/2} & 0 & 0 & 2 \end{array}$$

Hence for the g-values in intermediate coupling we have

$$g_k' = \frac{\epsilon_k^2 + (4\epsilon_k^2/3 + 1)(\epsilon_k + 3X/a)}{\epsilon_k^2 + (\epsilon_k^2 + 5)(\epsilon_k + 3X/a)}.$$

The comparison with experimental data[7] is indicated in Table II.

TABLE II. *Energies and g-values of Bi I. $6p^3$.*

	$J=1\frac{1}{2}$	$\frac{1}{2}$	$2\frac{1}{2}$	$1\frac{1}{2}$	$1\frac{1}{2}$
ν obs.	17728	6223	0	−4018	−15437
ϵ_k obs.	1.81	0.637	0	−0.41	−1.58
ϵ_k calc.[5]	1.73	0.637	0	−0.44	−1.62
g (LS)	4/3	2/3	6/5	4/5	2
g_k' calc.	1.25			1.25	1.66
g_k' obs.	(1.26)			1.225	1.65*

* A tentative value kindly communicated to us by R. F. Bacher. The other measured value is taken from his dissertation (Michigan, 1930). The value in parentheses is known only from the measurements of the others through the sum rule.

The configuration d^2. In this case the levels with $J=4$ and with $J=2$ are of interest. For the levels with $J=4$, we find the following transformation matrix when the energy matrix of the preceding paper is used and ${}^3F_3$ is taken as reference level:

[6] A similar determination is possible in other very simple cases where we know the secular equation from consideration of extreme couplings. In these few cases we are not dependent upon the preceding paper, or the method of Gray and Wills, for the energy matrix.

[7] The only further measurements of "anomalous" g-values for interesting configurations of which we are aware are for Ne I, $2p^53p$. Here the magnetic parameters may be estimated from the doublet separations of Ne II and Na I, but we have found no satisfactory fit for the energies, so no g-values could be calculated.

$$R(k1) = \frac{\epsilon_k - 2}{[(\epsilon_k - 2)^2 + 1]^{1/2}} \qquad R(k2) = \frac{1}{[(\epsilon_k - 2)^2 + 1]^{1/2}}$$

In LS coupling we have

$$g = \begin{array}{c|cc} & {}^1G_4 & {}^3F_4 \\ \hline {}^1G_4 & 1 & 0 \\ {}^3F_4 & 0 & 5/4 \end{array}$$

Then, in intermediate coupling,

$$g_k' = \frac{(\epsilon_k - 2)^2 + 5/4}{(\epsilon_k - 2)^2 + 1}.$$

For the levels with $J=2$ the transformation coefficients are

$$R(k1) = -\frac{2(3/5)^{1/2}}{\epsilon_k + 3/2} R(k2)$$

$$R(k2) = \left[\frac{12}{5(\epsilon_k + 3/2)^2} + \frac{21}{10(\epsilon_k - \gamma/a - 1)^2} + 1\right]^{-1/2}$$

$$R(k3) = \frac{(21/10)^{1/2}}{\epsilon_k - \gamma/a - 1} R(k2)$$

where $\gamma = (15/49)F^2 - (75/441)F^4$. From the matrix

$$g = \begin{array}{c|ccc} & {}^3F_2 & {}^1D_2 & {}^3P_2 \\ \hline {}^3F_2 & 2/3 & 0 & 0 \\ {}^1D_2 & 0 & 1 & 0 \\ {}^3P_2 & 0 & 0 & 3/2 \end{array}$$

we get the g-values in intermediate coupling,

$$g_k' = \frac{\{32 + 20(\epsilon_k + 3/2)^2\}(\epsilon_k - \gamma/a - 1)^2 + 63(\epsilon_k + 3/2)^2}{\{48 + 20(\epsilon_k + 3/2)^2\}(\epsilon_k - \gamma/a - 1)^2 + 42(\epsilon_k + 3/2)^2}.$$

Conclusion

The agreement of calculated Zeeman effect with experiment, judged by percentage discrepancy, is usually[8] considerably better than the agreement of observed and calculated energy levels, after adjustment of the radial-integral parameters. In judging calculations of g-values, however, one must bear in mind that they vary between quite narrow limits while the parameters of energy vary all the way from the parameters of LS to those of (jj) coupling. A fairer criterion of agreement of an intermediate-coupling g-value is then the relative error in the deviation from the extreme-coupling g-value. One cannot expect greater accuracy in the calculation of g-values than in the

[8] See also reference 1; Laporte and Inglis, Phys. Rev. **35**, 1337 (1930); J. Bakker, Naturwiss., **18**, 1100 (1930).

calculation of energy separations in a first-order treatment of this sort. A disagreement of energy levels with theoretical values causes a maladjustment of parameters, which makes an error in the g-value calculated in terms of the parameters. In addition, there are errors due to second-order contributions of the states of other configurations to the g-values directly. In Tables I and II, the agreement of the g-values with experiment is entirely satisfactory.

Application of the method has here been made to only a few of the simplest cases.[9] Calculation of g-values of other two-electron configurations should be of interest with extension of the experimental data. For more than two electrons, the calculations are also possible, but are limited by the difficulty in determining the energy matrix for configurations in which the same multiplet appears more than once.

[9] *Footnote added in proof, October 14*: Calculations for p^2 by the method of Goudsmit, corresponding to and agreeing with Table I, are given by Green and Loring (Phys. Rev. in print). In the preparation of Table II, the magnetic data for Sb I (H. Löwenthal, Zeits. f. Physik **57**, 828 (1929); Green and Loring, Phys. Rev. **31**, 707 (1928) were overlooked. They agree satisfactorily with the theory:

TABLE II, *A. g-values of Sb I, $5p^3$.*

J	$1\frac{1}{2}$	$\frac{1}{2}$	$2\frac{1}{2}$	$1\frac{1}{2}$	$1\frac{1}{2}$
ϵ_k obs.	2.72	1.86	0	−0.38	−2.79
ϵ_k calc.	2.51	1.86	0	−0.46	−3.02
g_k calc.	1.267	2/3	6/5	0.908	1.955
g_k obs.	1.280	0.668	1.205	0.898	1.967

For this configuration, $a=3520$, $X=3270$. For As I, $4p^3$, which is near (LS) coupling, the predicted g-values are 1.319, 2/3, 6/5, 0.825, and 1.988.

It has been remarked (Green and Loring, Phys. Rev. in print; L. A. Young, W. V. Houston, in conversation) that much of the disagreement between theoretical and experimental energy levels may be due to our neglect in the Hamiltonian of those terms corresponding to coupling of the spin of one electron to the orbit of the other, and to spin-spin interaction, which assume importance in the triplets of He and Li^+. These neglected terms become relatively small linearly with increasing *effective* nuclear charge. They are thus expected to be smaller for the configurations p^5s and d^9s than for ps, ds, p^5p, etc. It has been apparent (reference 8) that the agreement is indeed more satisfactory in the former cases, provided there be no overlapping of configurations.

ABSORPTION SPECTRA OF SALTS IN LIQUID AMMONIA

By R. W. Wood
Johns Hopkins University
(Received September 21, 1931)

Abstract

A preliminary investigation of the modifications in appearance and position of absorption bands of colored metallic salts and organic compounds dissolved in anhydrous liquid ammonia.

THE absorption spectra of solutions of metallic salts, having narrow absorption bands, in anhydrous liquid ammonia have not been studied so far as I have been able to discover.

The bands are modified in a very striking manner, due chiefly, I believe, to the nature of the solvent rather than to its low temperature, which is only −38 degrees, scarcely low enough to account for the observed changes.

The first experiments were made with solutions of salts of the rare earths, not all of which were soluble, however. The most striking results were ob-

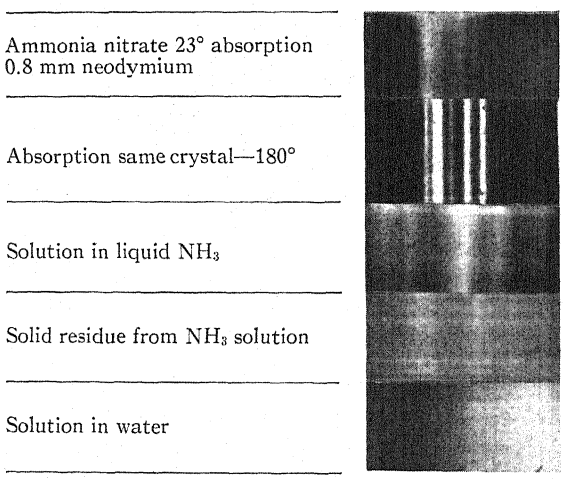


Fig. 1. The absorption band in the yellow.

tained with neodymium ammonium nitrate, the rather broad double bands in the yellow, shown by water solutions, breaking up in five rather narrow and completely separated bands. The ammonia was drawn from an inverted iron tank directly into a Dewar flask, the operation being performed in the open air, of course. The liquid can then be handled in the same way as liquid air. Incidentally, it may be mentioned that the liquid forms a convenient constant low temperature bath.

The solutions were contained in a small cylindrical Dewar flask of fused quartz placed in front of the slit of the spectrograph, at such a distance as to focus the source on the slit.

The absorption band in the yellow is shown in its various modifications in Fig. 1, reproduced as a negative, i.e., the dark absorption bands are shown white. The upper spectrum is that of a crystal of the double salt, 0.8 mm in thickness at room temperature. The next below that of the same crystal at −180 degrees, the crystal in this case being mounted just above the surface of liquid air, which was boiling quietly in the Dewar flask. Here we find ex-

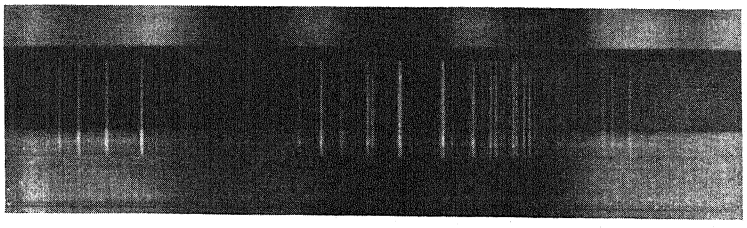


Fig. 2.

tremely narrow absorption lines. Below this is the absorption of a solution of the salt in liquid ammonia, a group of five rather narrow bands well separated but much expanded.

On evaporation the ammonia solution deposits a glassy crust on the floor of the Dewar flask, this substance being insoluble both in ammonia and in water. This seems to be a somewhat unique case, a solid residue by evapora-

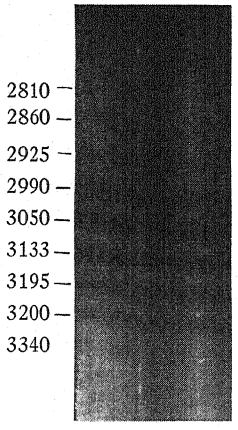


Fig. 3.

tion, which is insoluble in the solvent. I have not yet tried evaporation in vacuo or in a hydrogen atmosphere, which I suppose is the next logical proceeding to see whether a chemical change has resulted from contact with the air. The absorption spectrum of this solid residue is shown below that of the ammonia solution.

Below this is given the spectrum of a water solution, the band being very broad and shifted towards the red. All five spectra are in exact coincidence. Potassium permanganate dissolves readily in ammonia giving a purple solu-

tion similar in color to the water solution. The absorption bands in the green are, however, much less diffuse, and the contrast between the bright and dark regions of the spectrum is much greater than in the case of an aqueous solution. The upper spectrum of Fig. 2 is that of the ammonia solution, the lower that of a solution in water, the iron spectrum dividing the two for comparison.

A previously unrecorded set of bands was found in the ultraviolet, but they appear only with a very dilute solution, showing a bare trace of purple color by transmitted light. These bands are shown in Fig. 3, with their wave-lengths indicated. Continuous absorption is given for this region in all references that have come to my knowledge. I have observed a very faint trace of them in photographs made of a dilute water solution, though I doubt if I should have noticed them, if their presence had not been indicated by the ammonia solution. Both photographs are reproduced as positives, the absorption bands being dark. The wave-lengths of the ultraviolet bands were determined from the very narrow spectrum of the cadmium spark superposed on the absorption spectrum.

Many aniline dyes, and other fluorescent and nonfluorescent compounds are soluble in liquid ammonia, the absorption bands being modified in an analogous manner, and it appears probable that useful filters for suppressing certain spectrum regions may result from a further investigation of these solutions. The work is to be continued.

THE APPEARANCES OF THE FORBIDDEN LINES AND THE INTENSITY MODIFICATIONS OF THE SPECTRA OF MERCURY, CADMIUM AND ZINC UNDER HIGH FREQUENCY EXCITATION

By J. Okubo and E. Matuyama
Tohuku Imperial University

(Received July 27, 1931)

Abstract

With an oscillator of frequency 3×10^7 cycles per sec. the intensity modifications of the spectra of mercury, cadmium and zinc were studied. The singlet series and the intercombination lines which begin on the singlet levels were strengthened as has been observed by previous investigators in the case of mercury and the results were extended to the case of cadmium and zinc. Further, the intensity relations of the forbidden line $1S-2p_1$ of mercury were studied under this condition of excitation and also $1S-2p_{1,3}$ of cadmium were observed. The relations between the lines and the bands are discussed. Some consideration is also given to the conditions of excitation from the intensity modifications of lines.

IN RECENT years, many experimenters have drawn attention to the luminous phenomena produced in gases at very low pressures by a high frequency electrical oscillation with comparatively low potentials. Many efforts have been made to investigate the exciting and the ionizing processes of gases under these circumstances. However many unsolved questions still remain. The results of the spectroscopic observations of mercury show that the intensities of the lines show remarkable differences compared with those in the arc. The results generally may be summarized as follows; all the singlet series and the lines which begin on the singlet levels are strengthened while the triplet series and the lines which begin on the triplet levels are weakened or remain unaltered. Obviously, under these circumstances, the atoms or molecules are excited or ionized under conditions noticeably different from those in the usual arcs, or in Geissler tubes and it is very desirable to study this more fully and to extend the spectroscopic observations to other gases and vapors.

The present paper is a report of some experimental work in this field extending it to the vapors of cadmium and zinc as well. It also describes the appearance of forbidden lines in addition to the intensity modifications of the series lines that were observed.

The arrangement of the apparatus used, as is shown in Fig. 1, is quite similar to that used by S. Tolansky[1] in his investigation of mercury. The discharge tube was made of transparent fused silica 15 cm long with a 2 cm bore around which were wrapped two thin strips of tin, 2 cm wide, that served as electrodes which connected it with a secondary circuit coupled with

[1] S. Tolansky, Proc. Phys. Soc. A42, 556 (1930).

Lecher wires of a 10 meter oscillator arranged after the manner of E. W. Gill and R. H. Donaldson. The discharge is brightest for a given length of the secondary circuit, and the light from this tube was observed always in an end-on view. The plate voltages applied to the valve were from 300 up to 600 volts while the plate current was about 20 m.a. The vapors were evaporated from the metals placed in the middle of the tube, which was coaxially heated by a cylindrical electric resistance furnace 30 cm long and 9 cm in diameter.

Experimental Results

1. **Mercury.** Since the first observation of J. R. Clark,[2] and M. Ponte* many investigations of the intensity modifications of the spectra in mercury have been carried out. Recently S. Tolansky,[1] using an electrodeless discharge and extending the region of observations from λ7000A to λ2400A, obtained the general results on the intensity modifications already referred to. He also examined the fine structures of lines λ5461A and λ4916A.

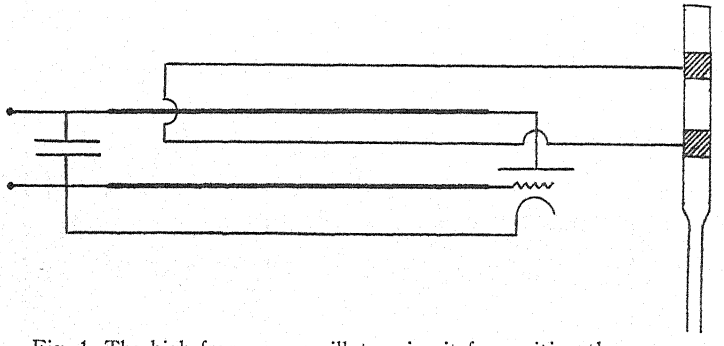


Fig. 1. The high frequency oscillator circuit for exciting the vapors.

In the present experiment, the spectra were photographed in the region from λ7000A to λ2000A. The observations of Tolansky on the strengthening and the weakening of the singlet and the triplet lines are confirmed and in addition it was observed that the forbidden line $1S-2p_1$ is emitted in this discharge and also that the intensities of some unclassified lines are markedly reduced with rise of temperature.

The forbidden line $1S-2p_1$ is observed weakly in the spectra emitted from the vapor at room temperature. Heating the tube caused the discharge to become brighter and the line $1S-2p_1$ was much more strengthened than the neighboring diffuse triplet lines $2p_2-12d$ and $2p_2-13d$ as is shown in Figs. 2a and 2b which are reproductions of the photometric curves of spectra emitted from the vapor at 70°C and at the room temperature respectively. From the figure, it is also observable that the vapor at 70°C is able to emit only lines classified in the sharp and the diffuse triplet series with remarkable regularities of intensities while there are found, at room temperature, some spark lines λλ2224A, 2260A, and 2262A in addition to the triplet lines with an irregular distribution of intensities. It is very interesting that a change of tem-

[2] J. R. Clark, Nature **120**, 727 (1927).
* M. Ponte, Nature **121**, 243 (1928).

perature of some fifty degrees has such a considerable influence on the intensities of the lines.

T. Takamine[3] has already, in the case of the so-called branched arc, investigated the dependence of the intensities of the forbidden line $1S-2p_1$, and

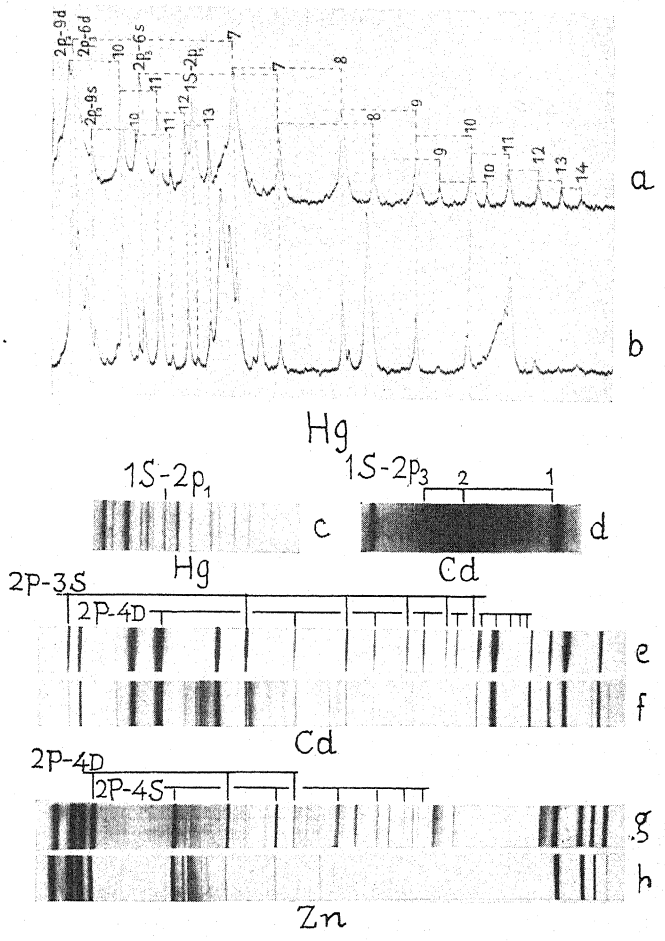


Fig. 2. (a) The photometric curve of the forbidden line $1S$-$2p_1$ and its neighbouring lines of mercury at 70°C. (b) The same, at room temperature (at about 20°C). (c) The spectra of mercury, the photometric curve of which has shown in (a). (d) The appearances of the forbidden lines of cadmium ($2p_3$ was missed in the reproducing process). (e) The spectra of cadmium showing the development of higher members of the singlet series under the high frequency excitation. (f) The spectra in the same region in a vacuum arc with a hot cathode. (g) The spectra of zinc showing the developments of higher members of the singlet series under the high frequency excitation. (h) The spectra in the same region in a vacuum arc with a hot cathode.

the neighboring classified and unclassified lines on the current density. He found that, except in observations at the part near the main arc, the forbidden line is strengthened very rapidly at first and, after attaining a maximum, decreases again slowly with increase of the current density. All other neigh-

[3] T. Takamine, Zeits. f. Physik **37**, 72 (1926).

boring lines gradually are enhanced with the current density. With this observation on the branched arc in mind, the enhancement of the forbidden line in the case given in Fig. 2a may be accounted for as being due to the increase of the current density with rise of temperature. However, as the vapors are, in both cases, under quite different conditions of excitation, the spectra emitted are not similar and therefore it will be adequate to seek for other reasons that the forbidden lines in this experimental condition are much more strengthened than other neighboring lines. Probably the main causes are the increase in number of low speed electrons and in the frequency of collisions between atoms and electrons resulting from the increase of pressure.

It is very interesting to observe that the band at 2345A is lacking in the spectra in the high frequency excitations, in spite of the fact that it is strongly emitted in the branched and the distilled arcs. T. Takamine[3] has already found that the band enhances hand in hand with the forbidden line and has suggested that the conditions favorable to exciting the forbidden line are also the conditions favorable to forming the molecules emitting the band at 2345A. However, in the high frequency excitation, it was found that the forbidden line was observable independent of the band and it seems that there are, at least in this case of excitation, no intimate connections between the line and the band. On the contrary the band at 2482A seems to have some relation with the forbidden line, as only this band has appeared strongly in the vapor at about 70°C at which the line enhances, while it disappeared at room temperature.

This band has been explained by Condon as the nuclear diffraction band, and suggested that it is emitted by the Hg_2 molecules excited in the initial state from which the molecule separates into the normal and the metastable p_1 atoms. The above mentioned relations between the band and the forbidden line seem to favor his suggestion regarding the initial level of the band.

2. **Cadmium.** The vapor was evaporated from Kahlbaum cadmium placed in the tube which was heated coaxially with a cylindrical electric furnace. The pressure of the vapor was estimated as about 0.05 mm Hg.

Careful examination of the spectra obtained showed that the singlet series especially the singlet diffuse series, are strengthened and were observed with moderate exposures up to the line $1P-12D$.

In consequence of the fact that atoms excited in D-levels are strongly concentrated, the intercombination lines which begin on D-levels are also strengthened and 7 members in the p-D combination are easily observed. The p-S combination lines are also strengthened as are the P-D combinations. Similar to the observations of Tolansky in mercury, the intercombination lines beginning on the triplet levels undergo generally slight intensity modifications.

It is worthy of notice that four intense lines of pp' combinations in the arc are lacking in this case of excitation. As the lines, according to the classification of R. A. Sawyer,[4] begin on the triplet levels, the intensity reductions

[4] R. A. Sawyer, Jour. Opt. Soc. Amer. **13**, 431 (1926).

will be due to the decreasing of the number of atoms excited to the initial levels.

The forbidden lines $1S$–$2P_1$ and $1S$–$2p_3$ were clearly observed as in the case of mercury and they are reproduced in Fig. 2d.

3. **Zinc.** Similar observations were made on the vapor of zinc. Just as in the case of the former two metals, the singlet series, especially the singlet sharp series lines enhanced while triplet lines remained unaltered. Ten members of the singlet sharp series and 4 members of the singlet diffuse series were observed. The intercombination lines were not so well excited as in the case of cadmium and the resonance line was markedly strengthened.

It is also to be regretted that the forbidden lines were not found in this case.

Under the conditions involved in high frequency discharges, the vapors are excited at very low pressures with comparatively low voltages and it is to be expected that the spectra of comparatively high potentials will be emitted because of the increase of mean free path of electrons. The excitation functions of spectral lines has been studied by R. Seeliger and his coworkers and recently more carefully and quantitatively by W. Hanle.[5,6] He has shown that, in the cases of helium, neon and mercury, the maximum of the excitation functions of triplet lines are sharp while those of singlet lines are flat and lie about thirty or more volts higher than the former. Considering that the electrons having velocities corresponding to about twenty volts predominate in this discharge and that the excitation functions of the lines are determinable with the initial levels, the strengthening of the singlet lines and of the intercombination lines beginning on the singlet levels and the reductions of the triplet lines and the intercombination lines which begin on the triplet levels are well accounted for.

In the branched arcs, the forbidden lines vanish when the current density through the tube is increased to the point at which the p-d lines show sensible broadening. Since the vapors in this experimental condition are at very low pressures and the current density is small, the interatomic field will certainly be very weak and this will also be one of the favorable conditions for the appearance of the forbidden lines. It is also true that a slight rise of temperature in the case of mercury brings the vapor to a more favorable condition as the result of the increase in pressure and in the numbers of electrons.

The assumption that the atoms are, in the high frequency discharge, more uniformly excited with electrons having higher velocities than in the case of arcs, accounts for the intensity modifications of spectra in this discharge. In the cases of mercury and helium we have many detailed studies by many authors on the excitation function and the influence of pressure on the spectral intensity. From this point of view further photometric studies of the spectra of mercury and helium under this excitation condition will be very interesting. The experiment is now in progress and will be reported on another occasion.

[5] W. Hanle, Zeits. f. Physik **56**, 94 (1929).
[6] W. Hanle, Phys. Zeits. **30**, 902 (1929).

DIFFUSION OF ELECTRONS BACK TO AN EMITTING ELECTRODE IN A GAS

By Irving Langmuir
General Electric Company, Schenectady, N. Y.

(Received September 23, 1931)

Abstract

An expression is derived for the current i between two electrodes, one of which emits (with uniform current density I_0) electrons with an initial volt velocity, V_0, when the electrodes are placed in a gas at such a pressure that the electrons suffer only elastic collisions. If V is the voltage between the electrodes, λ the mean free path of an electron, the current is given by

$$i = (16\pi/3)I_0\lambda C\phi$$

where C is the electrostatic capacitance between the electrodes and

$$\phi = (V/V_0)\ln(1 + V/V_0).$$

If the emitted electrons have a Maxwellian velocity distribution, this equation is applicable with slightly modified values of ϕ, V_0 now being replaced by $T/11600$ volts.

IN SOME recent investigations[1] it was observed that the electron current from a negatively charged electron-emitting electrode in neon at 1 mm pressure did not reach a saturation value, but continued to increase with increasing applied potential, although the currents were so small that space charge effects could be neglected. The conditions of the experiment were such that the electrons, which were probably emitted with a uniform initial velocity, suffered elastic collisions with gas atoms, and the mean free path was so short that the energy gained from the field between collisions was small compared to the initial velocity of electrons. It was thought that under these conditions, electrons leaving the electrode would, as a result of the elastic collisions, diffuse back to the cathode. The following paper contains the derivation of an expression for the current from an electron-emitting electrode as a function of voltage under these conditions.

The motion of slow electrons moving in a gas under the influence of an electric field has been considered theoretically by Hertz[2] for conditions similar to those stated above except that the electrons were assumed to have zero initial velocity. In these investigations he obtained the following expression for the drift velocity of an electron

$$v_x = \frac{1}{3}\frac{\gamma\lambda}{v} - \frac{v\lambda}{3}\frac{1}{n}\frac{dn}{dx} \tag{1}$$

where v is the velocity of an electron along its path; v_x the drift velocity of an electron in direction of the field; $\gamma = (e/m)(dV/dx)$ is the acceleration of an electron in the direction of the electric field; and λ is the electronic mean free

[1] See a recent letter to the editor. I. Langmuir and C. G. Found, Phys. Rev. **36**, 604 (1930).
[2] Hertz, Zeits. f. Physik **32**, 278 (1925).

path. In this equation the 2nd term in the right member represents the effect of diffusion, the diffusion coefficient D being

$$D = (\tfrac{1}{3})v\lambda.$$

If the electron velocities were everywhere uniform throughout the gas as has often previously been assumed in considering the mobility of electrons, the effect of the field would be to cause a drift with velocity $v_x = \gamma\lambda/v$.

The 1st term in the right member of Eq. (1), however, is only 1/3 as great as this expression for the mobility. This is due to the fact that in Hertz's derivation the electrons were assumed to make only elastic collisions with gas molecules and thus their velocities increase as they move into regions of more positive potential. There is thus a *thermal effusion* effect by which the electrons tend to move back against the field. The result is that the net drift is only 1/3 as great as if no increase of electron velocity occurred.

Assuming that the electrons start from the electrode (0) with a uniform velocity corresponding to V_0 volts, and that they suffer only elastic collisions with gas atoms, their velocity at any point is given by

$$(\tfrac{1}{2})mv^2 = (V + V_0)e \tag{2}$$

where V is the potential at the point relative to that of the emitting electrode.

Differentiating, we obtain

$$vdv = \frac{e}{m}\frac{dV}{dx}dx = \gamma dx$$

and the concentration gradient is thus

$$\frac{dn}{dx} = \frac{\gamma}{v}\frac{dn}{dv}. \tag{3}$$

Combining Eqs. (1) and (3), the drift velocity is

$$v_x = \frac{\gamma\lambda}{3}\left(\frac{1}{v} - \frac{1}{n}\frac{dn}{dv}\right) \tag{4}$$

It is not, in general, necessary that the maximum concentration gradient should lie in a direction coinciding with that of the maximum potential gradient. For the sake of simplicity, however, let us consider those cases in which at each point these two directions do coincide. The equipotential surfaces are then also surfaces of equal concentration n, and n is thus a single-valued function of V. We shall also restrict ourselves to cases in which the currents are so small that space charge effects are negligible, i.e., the potential distribution is given by integration of Laplace's equation.

Consider now a tube of force of small cross-section reaching from the emitting electrode (0) to a second electrode (1) which is at potential V_1. Let A be the cross-sectional area of the tube at any distance s measured along the tube and let L be the number of lines of force ($\int E_s dA$) contained in the tube.

Then

$$dV/ds = L/A. \tag{5}$$

The acceleration is then

$$\gamma = \frac{e}{m}\cdot\frac{L}{A}. \tag{6}$$

The drift current i_A along the tube of force is

$$i_A = Anev_s. \tag{7}$$

Therefore, combining Eqs. (6) and (7)

$$\frac{v_s}{\gamma} = \frac{i_A m}{ne^2 L}. \tag{8}$$

Substituting in Eq. (4) we obtain

$$\frac{3i_A m}{e^2 \lambda L} = \frac{n}{V} - \frac{dn}{dv}. \tag{9}$$

Assuming that the free path λ is the same throughout the length of the tube of force, then since i_A is also constant Eq. (9) may be integrated giving

$$n = \frac{3i_A mv}{e^2 \lambda L} \ln\left(\frac{c}{v}\right) \tag{10}$$

where c is a constant of integration.

To determine the integration constant we can insert the boundary condition that the concentration at the electrode 1 (anode) is zero.

Putting $n=0$ for $v=v_1$ we find $c=v_1$ and Eq. (10) becomes

$$n = \frac{3i_A mv}{e^2 L\lambda} \ln\left(\frac{v_1}{v}\right). \tag{11}$$

At any point in the gas the random current density[3] is

$$I_e = (\tfrac{1}{4})nev. \tag{12}$$

Inserting the value of n from Eq. (11) and expressing v in terms of V in accord with Eq. (2) we obtain

$$I_e = \frac{3}{4}\,\frac{i_A(V+V_0)}{L\lambda} \ln\left(\frac{V_1+V_0}{V+V_0}\right). \tag{13}$$

In Eq. (9), i_A and L are constant along the tube of force. We have, however, postulated that the equipotential surfaces lying between the two electrodes are identical with the surfaces of equal concentration and therefore n, v and dn/dv are constant over any equipotential surface. We see then by Eq. (9) that the ratio i_A/L, which is constant along any tube, must also have the

[3] See I. Langmuir and K. T. Compton, Rev. Mod. Phys. 3, 221 (1931).

same value for all tubes in the field and thus must be equal to i/L_t where i is the total current between the electrodes and L_t is the total number of lines of force passing between the electrodes.

If all the lines of force which emanate from one electrode pass to the other, i.e., if the algebraic sum of the charges of the two electrodes is zero, then

$$L_t = 4\pi V_1 C \tag{14}$$

where C is the electrostatic capacitance between the electrodes in cm.

Replacing i_A and L in Eq. (13) by i and L_t we thus obtain the result

$$I_e = \frac{3}{16\pi}\cdot\frac{i}{\lambda C}\cdot\left(\frac{V+V_0}{V_1}\right)\ln\left(\frac{V_1+V_0}{V+V_0}\right). \tag{15}$$

Let us denote by I_0 the random current density at the surface of the cathode as calculated from this equation, by placing $V=0$. In order that the presence of the electrode shall be compatible with the conditions that we have assumed in the neighboring gas it is clearly necessary that the electrode should emit electrons (of uniform velocity corresponding to V_0 volts) with a *uniform current density* I_0 which thus corresponds to the saturation current density. The electrons must also be emitted in random directions, i.e., according to Lambert's cosine law.

If we have an emitting electrode which fulfils these conditions, we may thus calculate the current i that passes to the anode:

$$i = \frac{16\pi}{3} I_0 \lambda C \phi \tag{16}$$

where the function ϕ is defined by

$$\phi = \frac{V_1/V_0}{\ln\left(\frac{V_0+V_1}{V_0}\right)} \tag{17}$$

Values of ϕ for various values of V_1/V_0 are given in Table I.

TABLE I. *Currents produced by electrons emitted with uniform velocity. ϕ is defined by Eqs. (16) and (17).*

V_1/V_0	ϕ	V_1/V_0	ϕ	V_1/V_0	ϕ
−1.0	0	0.1	1.049	3	2.165
−0.99	0.206	0.2	1.097	4	2.480
−0.9	0.390	0.3	1.140	5	2.79
−0.8	0.496	0.4	1.189	6	3.08
−0.6	0.655	0.6	1.276	8	3.64
−0.4	0.784	0.8	1.360	10	4.16
−0.2	0.895	1.0	1.445	15	5.42
−0.1	0.949	1.5	1.637	20	6.58
0	1.000	2.0	1.820	30	8.75

As the anode voltage is raised the current increases in proportion to ϕ. Since the electrons are emitted with velocities corresponding to V_0 volts, the

anode current falls to zero only when a *retarding* voltage of V_0 volts is applied. With accelerating voltages the current increases slowly but continuously.

If both electrodes emit electrons with velocity V_0 and if the potential of one with respect to the other lies between $-V_0$ and $+V_0$, the current must flow both ways so that the net current is to be obtained by applying Eq. (16) for each electrode in turn and taking the difference of these two currents (or algebraic sum). When the voltage lies outside of the range $-V_0$ to $+V_0$, one or the other of the currents becomes zero so that a single application of Eq. (16) suffices.

It should be kept in mind that Eq. (16) is strictly applicable only at such high pressures that the electron free path is small compared to the distance between the electrodes. Otherwise the boundary conditions which we have used, such as $n=0$ at the anode, are not valid.

We have seen that it was necessary for us to assume that I_0 is uniform over the cathode surface. If this condition is not fulfilled the surfaces of equal concentration no longer coincide with the equipotential surfaces and the problem of the current flow is then far more complicated than for the case we have treated.

It is also clear for the same reason that the foregoing method is not applicable when there are *two anodes* at different potentials. This difficulty is apparent when we consider that according to our procedure n must be placed equal to zero at each of these surfaces, although they are at different potentials. This violates our postulate that n is a single valued function of V. Two anodes at the same potential may, of course, be regarded as a single anode and Eqs. (16) and (17) are then applicable.

Practical applications of Eq. (16) will usually be made with electrodes of simple shapes. Substituting the well-known expressions for the capacitance[4] in Eq. (16) we obtain:

For *parallel planes*, the net current per unit area flowing between the electrodes is

$$I_x = (4/3)I_0\phi\lambda/a. \tag{18}$$

The current that flows is thus inversely proportional to the pressure and at high pressures may be very small compared to the saturation electron emission I_0.

For *coaxial cylinders* the net current per unit length is

$$i_L = (8\pi/3)I_0\phi\lambda/\ln(r_1/r_0). \tag{19}$$

Here I_0 is the current density of the electron emission corresponding to saturation from the *emitting electrode* regardless of whether this is the outer or the inner cylinder. The radii of the cylinders are r_1 and r_0.

For *concentric spheres* the total current is

$$i = (16\pi/3)I_0\phi\lambda r_0 r_1/(r_1 - r_0). \tag{20}$$

[4] See p. 198 of reference 3.

It should be noted that if the *saturation current density* I_0 from the inner and the outer cylindrical (or spherical) electrodes are equal, the actual currents remain unchanged if the relative polarity of the electrodes is reversed, although the total saturation currents, if they could be obtained, would be proportional to the areas of the emitting electrodes. This conclusion can readily be tested by experiment.

The source of the electrons from the emitting electrode may be one of many kinds, for example, photoelectric or thermionic. A case of particular interest in connection with a study of the un-ionized (or weakly ionized) regions beyond the end of a neon arc[4] is the liberation of high velocity electrons (*ca.* 10 volts) from the surfaces of electrodes by the action of metastable atoms which diffuse to these electrodes. The metastable atoms are generated throughout the gas by the action of ultraviolet light (broadened resonance lines) from the arc, at a rate proportional to the inverse cube of the distance from the end of the arc. Let us calculate the relative current densities I_0 of emitted electrons from the inner and outer cylinders under these conditions.

If the electrodes are at a considerable distance from the end of the arc and the radiation passes parallel to the axis, then within the space between two cylindrical electrodes of short lengths we may assume a uniform rate of production of metastable atoms. The diffusion of these to the two electrodes is a problem essentially similar to that[5] of the potential distribution between cylinders if the space contains a uniform space charge ρ.

Imposing the boundary conditions $V=0$ at the surface of both cylinders, we find that the potential gradient at any point of radius r is

$$\frac{dV}{dr} = \pi\rho\left[\frac{(r_2^2 - r_1^2)}{r \ln (r_2/r_1)} - 2r\right] \tag{21}$$

where r_2 and r_1 are the radii of the outer and inner cylinders respectively. By substituting first $r=r_1$ and then $r=r_2$ we find the potential gradients at the surfaces of the two electrodes. The ratio of these two gradients is equal to the ratio of the corresponding rates of arrival of metastable atoms *per unit area* and therefore should be proportional to the ratio I_1/I_2 of the saturation current densities (I_0) of the emitted electrons from the two electrodes. In this way we find

$$\frac{I_1}{I_2} = \frac{r_2[r_2^2 - r_1^2 - 2r_1^2 \ln (r_2/r_1)]}{r_1[r_2^2 - r_1^2 - 2r_2^2 \ln (r_2/r_1)]}. \tag{22}$$

For example, if $r_2/r_1=10$ this gives $I_1/I_2=-2.62$ (the negative sign merely indicates that the currents flow in opposite directions).

The corresponding equation for concentric spheres is

$$\frac{I_1}{I_2} = -\frac{r_2(r_2 + 2r_1)}{r_1(r_1 + 2r_2)} \tag{23}$$

which gives $I_1/I_2=-5.72$ when $r_2/r_1=10$.

[5] See p. 213 of reference 3.

Thus we see that the current density I_0 at the inner electrode is greater than at the outer electrode if the electrons owe their origin to metastable atoms produced uniformly throughout the gas. It therefore follows from Eq. (19) that the net current will be greater (2.62 fold for $r_2/r_1=10$) when the small inner cylindrical electrode is cathode than when the larger electrode is cathode, although if the currents were saturated the current in the former case would be smaller instead of larger (0.26 instead of 2.6 fold).

We have thus far assumed that all the electrons are emitted with the same velocity V_0 volts. Although this may be roughly true for electrons emitted under the influence of metastable atoms, it will certainly not be a satisfactory approximation for thermal emission of electrons. By summation of the currents from each velocity group, we may calculate the net current produced by a Maxwellian velocity distribution.

The total number of electrons per unit volume which have speeds (irrespective of direction) lying between c and $c+dc$ is given by[6]

$$4\pi n(m/2\pi kT)^{3/2} \exp(-mc^2/2kT)c^2dc.$$

Because of the relation expressed by Eq. (12) it follows that the contribution of these electrons to the random current density crossing any given plane is

$$dI = \pi en(m/2\pi kT)^{3/2} \exp(-mc^2/2kT)c^3dc. \tag{24}$$

Applying this to the surface of an electrode which emits electrons with a Maxwellian velocity ditribution corresponding to temperature T and current density I_0, and integrating from $c=0$ to $c=\infty$ we find

$$I_0 = ne(kT/2\pi m)^{1/2} \tag{25}$$

Eliminating n between Eqs. (24) and (25) we obtain

$$dI = I_0\epsilon^{-\eta_0}\eta_0 d\eta_0 \tag{26}$$

where

$$\eta_0 = mc^2/2kT = V_0e/kT = 11600V_0/T \tag{27}$$

if V_0 is the emission velocity in volts.

To calculate the net current between the two electrodes, we may insert the value of dI in place of I_0 in Eq. (16) and integrate from $\eta_0=0$ to $\eta_0=\infty$.

In this integration the value of ϕ is obtained from Eq. (17) by placing

$$V_1/V_0 = \eta/\eta_0$$

which by Eq. (27) is equivalent to

$$\eta = V_1e/kT = 11600V_1/T \tag{28}$$

if V_1 is in volts.

[6] This is obtained from Eq. (71) of Compton and Langmuir's article, Rev. Mod. Phys. **2**, 205 (1930), by replacing h by $1/2kT$.

In this way we find

$$i = (16\pi/3) I_0 \lambda c \phi_T \tag{29}$$

where

$$\left.\begin{aligned} \phi_T &= \eta \int_0^\infty \frac{\epsilon^{-x} dx}{\ln (1 + \eta/x)} \quad \text{if } \eta > 0 \\ \text{or} \qquad \phi_T &= \eta \int_{-\eta}^\infty \frac{\epsilon^{-x} dx}{\ln (1 + \eta/x)} \quad \text{if } \eta < 0 \end{aligned}\right\} \tag{30}$$

The reason that the lower limit of integration must be changed when η is negative is that electrons whose initial velocities give $\eta_0 < -\eta$ cannot reach the collector.

TABLE II. *Currents produced by electrons emitted with Maxwellian velocities at temperature T; ϕ_T is defined by Eqs. (29) and (30); η is given by Eq. (28).*

η	ϕ_T	η	ϕ_T	η	ϕ_T
−4	0.042	−0.2	0.892	4	2.358
−3	0.100	0	1.000	6	2.908
−2	0.236	+0.1	1.034	8	3.421
−1	0.516	0.5	1.217	10	3.913
−0.8	0.600	1	1.408	20	5.895
−0.6	0.688	2	1.748	30	8.170
−0.4	0.787	3	2.051	50	11.892

The values of η given in Table II have been calculated from Eqs. (30) by Simpson's rule or by series expansion. They are believed to be accurate within one or two units in the last figure. Comparison with Table I shows that for values of η and V_1/V_0 which are equal, the values of ϕ_T and ϕ are very nearly equal when η is greater than about -0.6. By Eq. (28) we see that this means that, except for large negative voltages, no great error is made if the thermally emitted electrons are considered to have a uniform energy corresponding to $T/11600$ volts.

Experiments which will probably be described in a paper by C. G. Found and the writer have given results which are explicable in terms of the theories here presented. The writer is much indebted to Mr. Found for assistance in the preparation of this paper.

THE AVERAGE LIFE OF THE IONIZED HELIUM ATOM

By Louis R. Maxwell
Bartol Research Foundation, Swarthmore, Pennsylvania
(Received August 19, 1931)

Abstract

Review of the theory in relationship to ionized helium:—From the results of previous workers it is shown that the theoretical values for the average life of energy levels of ionized helium are 1/16th as long as the life-time of the same levels of hydrogen. A table of average lives for ionized helium is given which shows that the average life becomes progressively greater for higher quantum states.

Experimental method for measuring the average life:—Electrons in helium at low pressure were confined into a narrow beam by a longitudinal magnetic field. A transverse electric field drew out the ions formed in the beam. The light was projected on the slit of a spectrograph with the direction of motion of the ions parallel to the slit. Formulas giving the intensity of the displaced spark line as a function of its distance from the center of the electron beam have been derived previously. The average life can be obtained from the measurements of the amount of the displacements of the region of maximum intensity of the spark line from the center of the beam.

Experimental results and comparison with the theory:—(1) A comparison of displacements for the first four lines of the "4686" series of He^+ show that the average life becomes progressively greater for the higher quantum states in agreement with the theory. (2) Results obtained for the line 2733A $6\rightarrow 3$ give an average life of $1.1\pm 0.2 \times 10^{-8}$ sec. for the sixth quantum state in good agreement with 1.17×10^{-8} sec. the theoretical value for the mean average life of this level. (3) As the voltage of the electrons in the beam was increased the measured average life became greater which showed the presence of transitions into the sixth state from the higher quantum levels. (4) An alternative method for interpretating the experimental results is given which does not assume a free interchange among the sublevels. The theoretical intensity distribution of each of the five fine structure lines which make up the unresolved line 2733A is calculated. It is found that the resultant intensity distribution is almost exactly the same as the intensity distribution calculated for the case of free interchange or in other words for the case of a single exponential decay law. The experimental intensity curve agrees with the theoretical curve.

Discrepancies existing among authors for values of the matrix amplitude squared for hydrogen:—On comparing the values for the matrix amplitudes squared for hydrogen obtained by different authors, it is found that the values obtained by Slack and Kupper are in disagreement for the following transitions: $5_1\rightarrow 4_2$, $6_1\rightarrow 4_2$, $5_0\rightarrow 4_1$, $6_0\rightarrow 4_1$, $6_5\rightarrow 5_4$, $6_0\rightarrow 5_1$, $6_3\rightarrow 5_4$, $6_2\rightarrow 4_3$. These discrepancies do not greatly affect the theoretical value for the mean average life of the sixth quantum state, or the alternative method for interpretating the experimental results.

Effect of electron spin:—It is proved that the electron spin corrections do not alter the theoretical interpretation of the experimental results, because it is shown that the average life of the n, l, j, m state is independent of j, and m, and equal to the average life in the nonspin theory of the n, l, m state, independent of m, and also that the mean average life is independent of spin.

ONE of the important quantities which can be calculated from the quantum theory is the average rate of radiation of energy produced by transitions occurring in atoms. Theoretical considerations give directly the prob-

ability of transition and consequently the average lifetime in the initial states. It becomes possible, therefore, to test the theory by comparison with experiments which give numerical results for the average lives of excited states. The present work deals with the measurement of the average life for ionized helium. It is possible to obtain a direct comparison between the absolute values of the average life as obtained from the experiment and from the theory.

PART I. THE THEORY

Since the experimental method used for determining the average life is limited to those emitters which are ions, it is advisable to deal with ionized helium which is the simplest type of ion and one which can be treated theoretically in the same manner as hydrogen.

The average life of an excited state is equal numerically to the reciprocal of the sum of the transition probabilities corresponding to all of the possible transitions which can take place from the level concerned. Expressed analytically, the average life $T(n, l, m)$ of the state n, l, m is given by

$$T(n, l, m) = \frac{1}{\sum_{n', l', m'} A^{n', l', m'}_{n, l, m}}$$

where $A^{n', l', m'}_{n, l, m}$ is the probability of a transition from state n, l, m to state n', l', m'. This summation is extended over all of the lower states. We see from this equation that in order to obtain a numerical value for the average life a knowledge of the numerical values of all the transition probabilities is essential. Schrödinger[1] quotes a formula for the total intensities of the lines in the Lyman and Balmer series given to him by Pauli, and capable of giving the transition probabilities. Sugiura[2] has calculated the transition probabilities for a number of the lines of the Paschen, Balmer and Lyman series lines of hydrogen. In a later paper[3] he also considered the more general case of the transition probability between two states in a field with a central charge Ze. Slack,[4] using a formula obtained by Sommerfeld and Unsöld, has prepared a table of transition probabilities for a large number of transitions for hydrogen. Kupper,[5] also, has calculated the values for the matrix amplitudes squared for many transitions in hydrogen.

It is well known that from the classical theory the average energy radiated per unit time is given by

$$-\overline{\frac{dE}{dt}} = \frac{64\pi^4\nu^4}{3c^3} \left| P_1 \right|^2$$

[1] Schrödinger, Ann. d. Physik **80**, 437 (1926) for the formula of W. Pauli.

[2] Sugiura, Jour. d. Physique **8**, 113 (1927).

[3] Sugiura, Scientific Papers of the Institute of Physical and Chemical Research (Tokyo) No. 193, June 25, 1929.

[4] Slack, Phys. Rev. **31**, 527 (1928).

[5] Kupper, Ann. d. Physik **86**, 511 (1928).

where the electrical moment P of the classical vibration is written in the exponential form $P=P_1e^{2\pi i\nu t}+P_{-1}e^{-2\pi i\nu t}$. Utilizing this expression directly in the quantum theory, we have the following for the value of the transition probability,[6]

$$A^{n',l',m'}_{n,l,m}=\frac{64\pi^4e^2\nu^3_{n,l,m}{}^{n',l',m'}\left|J^{n',l',m'}_{n,l,m}\right|^2}{3c^3h} \tag{1}$$

where $J^{n',l',m'}_{n,l,m}$ is the vector matrix amplitude given by

$$\left|J^{n',l',m'}_{n,l,m}\right|^2=\left|x^{n',l',m'}_{n,l,m}\right|^2+\left|y^{n',l',m'}_{n,l,m}\right|^2+\left|z^{n',l',m'}_{n,l,m}\right|^2$$

with the matrix elements $(x, y, z)^{n',l',m'}_{n,l,m}$ expressed in terms of the normalized wave functions $\psi_{n,l,m}\psi_{n',l',m'}$ in the following form:

$$\left.\begin{matrix}x\\y\\z\end{matrix}\right\}^{n',l',m'}_{n,l,m}=\int_\tau\begin{matrix}x\\y\\z\end{matrix}\psi_{n,l,m}\,\psi^*_{n',l',m'}d\tau.$$

Since we are not interested in each matrix element component for different magnetic quantum numbers m the expression $\sum_m\sum_{m'}\left|J^{n',l',m'}_{n,l,m}\right|^2$ is evaluated. From (1) we obtain

$$\sum_m\sum_{m'}A^{n',l',m'}_{n,l,m}=\frac{64\pi^4\nu^3_{n,l}{}^{n',l'}e^2\sum_m\sum_{m'}\left|J^{n',l',m'}_{n,l,m}\right|^2}{3c^3h}.$$

Sugiura defines the quantity $A^{n',l'}_{n,l}$, as the mean probability of a transition by the following formula;

$$A^{n',l'}_{n,l}=\frac{\sum_m\sum_{m'}A^{n',l',m'}_{n,l,m}}{g_l} \tag{2}$$

where $g_l=2l+1$ is the number of magnetic levels or the statistical weight of the lth level. This equation can be thought of as defining the transition probability which determines the rate at which energy is radiated from the magnetic levels of the initial states. It is the reciprocal of this expression which gives the average life, and also the quantity which when multiplied by g_l will give the total rate at which energy is radiated from all the magnetic levels and consequently give the intensity of the spectrum line. From the summation-rule for the Zeeman components we see that $A^{n',l'}_{n,l}$ is also equal to $\sum_{m'}A^{n',l',m'}_{n,l,m}$ independent of m.

From Eqs. (1) and (2) we have the final expression for the transition probability $A^{n',l'}_{n,l}$ as defined above,

$$A^{n',l'}_{n,l}=\frac{64\pi^4\nu^3_{n,l}{}^{n',l'}e^2\sum_m\sum_{m'}\left|J^{n',l',m'}_{n,l,m}\right|^2}{3c^3hg_l}. \tag{3}$$

[6] See for instance, Sugiura, reference 2.

Sugiura has evaluated this quantity by obtaining the following expression for the matrix amplitude squared for the case of a central charge Ze and for a transition from state n, l to n', l'

$$\sum_{m}\sum_{m'}|J_{n,l,m}^{n',l',m'}|^2 = \left(\frac{a_0}{4Z}\right)^2 l''\frac{(n-l-1)!(n'-l'-1)![(l+l'+3)!]^2}{(n+l)!(n'+l')!} \left(\frac{2n}{n+n'}\right)^{2(l'+2)}\left(\frac{2n'}{n+n'}\right)^{2(l+2)}(C_{n,l}^{n',l'})^2 \tag{4}$$

where $C_{n,l}^{n',l'}$ is the coefficient of $y_1^{n-l-1}y_2^{n'-l'-1}$ in the expansion of

$$\frac{(1-y_1)^{l'-l+2}(1-y_2)^{l-l'+2}}{\left(1-y_1y_2-\frac{n-n'}{n+n'}y_1+\frac{n-n'}{n+n'}y_2\right)^{l+l'+4}}$$

and l'' is the greater value of l and l', $a_0=h^2/4\pi^2me^2$. Therefore we see from this equation that the matrix amplitude squared is inversely proportional to Z^2 for any given transition. Taking into account that ν^3 is directly proportional to Z^6 we see from Eq. (3) that $A_{n,l}^{n',l'}$ is directly proportional to Z^4.[7] Thus, in the case of ionized helium the values of the transition probabilities are 16 times greater than the values for the same transitions in hydrogen. This means that the average life of the levels in ionized helium will be 1/16th as long as the average life-time of the same levels in hydrogen. Consequently, for the purpose of calculating the average life for ionized helium we can use directly numerical values for the transition probabilities for hydrogen.

The mean average life.

The substates corresponding to different l values for a given value of n have for the relativistic case, energies which differ from each other only by a very small amount, so that it is impractical to separate the different fine structure lines in the measurements of the average life.

Sugiura has calculated a mean average life $T(n)=1/\sum_{n'}A_n^{n'}$ which can be used for comparison with experiments provided that there exists free interchange or statistical equilibrium among the various sublevels of the nth state. $A_n^{n'}$ is the average rate of transition from the state n to n' and is given by

$$A_n^{n'}=\frac{\sum_{l,l'}g_lA_{n,l}^{n',l'}}{\sum_l g_l}$$

[7] See also Sommerfeld, Atombau and Spektrallinen (Wellenmechanischer Ergänzungsfand) p. 96.

and is called by Slack the total probability of line emission from n to n'. The intensity of the unresolved line will diminish *exponentially** with the time, and the decay time $T(n)$ will be given by

$$T(n) = \frac{\sum_l g_l}{\sum_l \sum_{n',l'} g_l A_{n,l}^{n',l'}} . \tag{5}$$

* Although it is perhaps obvious that the unresolved line will diminish exponentially with the time on account of averaging the rates of transitions, however it can be shown analytically to be true in the following manner:

Let $n_{n,l}(t)$ be the number of electrons in the n, l, state. We shall assume that

$$n_{n,l}(t) = f_n(t) g_l \tag{A}$$

where as before $g_l = 2l+1$ (the number of magnetic levels) and $f_n(t)$ a factor of proportionality which is independent of l. Therefore, $N_n(t)$ the total number of electrons in the nth state is given by

$$N_n(t) = \sum_l n_{n,l}(t) = f_n(t) \sum_l g_l . \tag{B}$$

The rate at which electrons leave the n, lth state to go to lower states n', l' is given by

$$\frac{dn_{n,l}(t)}{dt} = - \sum_{n',l'} A_{n,l}^{n',l'} n_{n,l}(t) .$$

$$\therefore \frac{dN_n(t)}{dt} = \sum_l \frac{dn_{n,l}(t)}{dt} = - \sum_l \sum_{n',l'} A_{n,l}^{n',l'} n_{n,l}(t)$$

By virtue of (A) we see that

$$\frac{dN_n(t)}{dt} = - \frac{\left(f_n(t) \sum_l g_l \right) \sum_l \sum_{n',l'} A_{n,l}^{n',l'} g_l}{\sum_l g_l} .$$

Utilizing Eq. (B), leaves

$$\frac{dN_n(t)}{dt} = - \frac{N_n(t) \sum_l \sum_{n',l'} A_{n,l}^{n',l'} g_l}{\sum_l g_l} .$$

Therefore, we have on integrating, the following

$$N_n(t) = N_n(0) e \exp - \left(\frac{\sum_l \sum_{n',l'} A_{n,l}^{n',l'} g_l}{\sum_l g_l} \right) t .$$

From Eqs. (A), (B), and (C) we find that

$$n_{nl}(t) = \frac{N_n(0) g_l}{\sum_l g_l} e \exp - \left(\frac{\sum_l \sum_{n',l'} A_{n,l}^{n',l'} g_l}{\sum_l g_l} \right) t .$$

Therefore, the intensity of the spectrum line corresponding to a transition from state n to n' is given by

$$I_n^n(t) = \sum_l \sum_{l'} I_{n,l}^{n',l'}(t) = \left[\sum_l \sum_{l'} \frac{g_l A_{n,l}^{n',l'} h\nu_{n,l}^{n',l'} N_n(0)}{\sum g_l} \right] e \exp - \left[\frac{\sum_l \sum_{n',l'} A_{n,l}^{n',l'} g_l}{\sum_l g_l} \right] t$$

We see, from this equation, that the intensity of the unresolved line willl diminish exponentially with the time, having a decay time the same as that given above for $T(n)$.

Effect of electron spin.

A similar expression for the mean average life $T'(n)$ can be written at once taking into account electron spin.

$$T'(n) = \frac{\sum_{l,j} g_{l,j}}{\sum_{l,j} \sum_{n',l',j'} g_{l,j} A^{n',l',j'}_{n,l,j}}. \tag{6}$$

To determine the effect of electron spin on the values of the average lives, let us consider the general proof that the spin corrections will not effect the intensity.[8] From the general theorem of spectroscopic stability[9]

$$\sum_{j,m,j'm'} \left| J^{n',l',j'm'}_{n,l,j,m} \right|^2 = \sum_{m_s,m_l,m_s',m_l'} \left| J^{n',l',m_s',m_l'}_{n,l,m_s,m_l} \right|^2.$$

The left hand side has the usual spin coupling while the amplitudes on the right hand side result when the spin is completely decoupled and has separate spacial quantization. The matrix elements on the right side are completely independent of m_s i.e.

$$X^{n',l',m_s'm_l'}_{n,l,m_s,m_l} = \delta^{m_s'}_{m_s} X^{n',l',m_l'}_{n,l,m_l},$$

similarly for the y and z components, where

$$\left| X^{n'l'j'm'}_{n,l,j,m} \right|^2 + \left| Y^{n',l',j'm'}_{n,l,j,m} \right|^2 + \left| Z^{n'l'j'm'}_{n,l,j,m} \right|^2 = \left| J^{n',l',j'm'}_{n,l,j,m} \right|^2$$

The sum-rule assures that $\sum_{j'm'} \left| J^{n',l',j',m'}_{n,l,j,m} \right|^2$ is independent of j, m, and $\sum_{m'l} J^{n',l',m'l}_{n,l,m_l}$ of m_l. Since there are $(2L+1)(2S+1)$ values of j, m, or m_l, m_s we have

$$(2S+1)(2L+1) \sum_{j'm'} \left| J^{n',l',j',m'}_{n,l,j,m} \right|^2 = (2S+1)(2L+1) \sum_{m_l'} \left| J^{n',l',m_l'}_{n,l,m_l} \right|^2.$$

On cancelling out the factor $(2L+1)(2S+1)$ we have the desired result. In addition, if we sum over n' and l' then it is proved at once that the *average life of the n, l, j, m state is independent of j, and m, and equal to the average life in the nonspin theory of the n, l, m state independent of m.***

By virtue of the above theorem we can write at once that

$$A^{n',l'}_{n,l} = \frac{\sum_{j,j'} g_{l,j} A^{n',l',j'}_{n,l,j}}{\sum_j g_{l,j}}$$

also

$$g_l = \tfrac{1}{2} \sum_j g_{l,j}.$$

[8] The writer is indebted to Professor J. H. Van Vleck for this proof.

[9] Cf. for instance Van Vleck, Phys. Rev. 29, 740 (1927).

** In this connection Sugiura has previously mentioned that the decay constants or average lives for the n, l terms are necessarily independent of j as long as the sum-rule holds.

By use of these equations it is seen at once from (5) and (6) that $T(n) = T'(n)$. Therefore, *the mean average life is independent of the spin corrections.*

In Table I are given theoretical values for the average lives and the mean average lives for levels up to and including the seventh state of ionized

TABLE I. *Theoretical values of the average life of ionized helium.*

Level	Average life	Mean average life
n_l	$T(n, l)$, (sec.)	$T(n)$, (sec.)
1_0		
2_0		
2_1	1.02×10^{-10}	1.36×10^{-10}
3_0	1.01×10^{-8}	
3_1	3.38×10^{-10}	6.4×10^{-10}
3_2	9.93×10^{-10}	
4_0	1.456×10^{-8}	
4_1	7.89×10^{-10}	2.127×10^{-9}
4_2	2.320×10^{-9}	
4_3	4.66×10^{-9}	
5_0	1.82×10^{-8}	
5_1	1.49×10^{-9}	
5_2	4.33×10^{-9}	5.38×10^{-9}
5_3	8.73×10^{-9}	
5_4	1.45×10^{-8}	
6_0	2.576×10^{-8}	
6_1	2.443×10^{-9}	
6_2	7.196×10^{-9}	1.178×10^{-8}
6_3	1.471×10^{-8}	
6_4	2.682×10^{-8}	
6_5	3.906×10^{-8}	
7_0	3.286×10^{-8}	
7_1	3.647×10^{-9}	
7_2	1.175×10^{-8}	
7_3	2.141×10^{-8}	2.237×10^{-8}
7_4	3.373×10^{-8}	
7_5	6.449×10^{-8}	
7_6	8.802×10^{-8}	

helium. These values for levels up to and including the fourth state were taken from a similar table prepared by Sugiura for hydrogen. The present values for ionized helium differ by a factor of 16 from those for hydrogen for the reason given above. Since Sugiura's table does not include levels higher than the fourth, the values of the average lives for the fifth, sixth and seventh states were obtained from Slack's table of transition probabilities for hydrogen. These transition probabilities as obtained by Slack were multiplied by 16 to give the average life for ionized helium as listed in the table.

Discrepancies existing among the values of the matrix amplitude squared for hydrogen obtained by different authors.

A comparison has been made between the values of the matrix amplitude squared as obtained by Sugiura,[2] Slack[4] and Kupper.[5] For all the transitions

from the second, third and fourth quantum states, the values obtained by the different authors are in good agreement.

For the case of the transitions from the fifth state, Slack's and Kupper's values are in agreement with the exception of the transitions $5_1 \rightarrow 4_2$ and $5_0 \rightarrow 4_1$. For the transitions from the sixth quantum state, Slack's and Kupper's results disagree for the following transitions: $6_1 \rightarrow 4_2$, $6_0 \rightarrow 4_1$, $6_5 \rightarrow 5_4$, $6_0 \rightarrow 5_1$, $6_3 \rightarrow 5_4$, and $6_2 \rightarrow 4_3$. Table II has been prepared showing the values of the matrix amplitudes squared for the above transitions.

In the third column are given values calculated from Kupper's "Spezielle Serien" formulae. For example, Kupper gives for the $n_0 \rightarrow 4_1$. $(4P-nS)$ transition the following formula:

$$\frac{2^{21}n^9(n-4)^{2n-10}(57n^4-38n^2+80)^2}{3(n+4)^{2n+10}}.$$

If we use the more general formula given by Kupper, called the "Allgemeine Formeln der Seriengruppen $n-l-1=D'$ $(n'>n)$" we obtain for the $n_0 \rightarrow 4_1$ transition a different quantity:

$$\frac{2^{21}n^9(n-4)^{2n-10}(57n^4-608n^2+1280)^2}{5\times 3(n+4)^{2n+10}}$$

which is evaluated numerically in the fourth column in Table II. For the $6_0 \rightarrow 4_1$ transition this formula gives 1.59 which is the same value that is obtained from Sugiura's formula. Also it agrees well with Slack's values of 1.88 but is in disagreement with 14.8 the value obtained by Kupper's special series formula. For the $5_0 \rightarrow 4_1$ transition the agreement is not as good, as illustrated in Table II.

TABLE II. *Comparison of values for the matrix amplitude squared for hydrogen.*[10]

Transition	Kupper's table	Calculated from Kupper's special series formula	Calculated from Kupper's general formula	Calculated from Sugiura's formula	Calculated from Slack's table
$5_1 \rightarrow 4_2$	9.1				0.094
$6_1 \rightarrow 4_2$	1.21	1.26			0.013
$5_0 \rightarrow 4_1$	105.	135.	10.58		21.0
$6_0 \rightarrow 4_1$	14.8	14.8	1.59	1.59	1.88
$6_5 \rightarrow 5_4$	201.	1851.		1851.	1822.
$6_0 \rightarrow 5_1$	247.				77.60
$6_3 \rightarrow 5_4$	8.2				12.3
$6_2 \rightarrow 4_3$	0.48				0.284

These discrepancies do not appreciably effect the theoretical value for the mean average life of the sixth quantum state.

PART II. THE EXPERIMENT

The experimental method used in the present work for measuring the average life is similar to that previously described by the writer[11] for the case

[10] The values here are $\frac{1}{2}$ the values given by Sugiura's formula of Eq. (4).

[11] Maxwell, Phys. Rev. **32**, 721 (1928).

of an election beam of nonuniform current density. It is necessary to modify slightly the derivation used previously by taking into account the more general case where there are a large number of levels involved instead of the simple case of two levels as treated before.

On referring to the previous work we see that if δn is the number of excited ions per second leaving the volume element dv lying between ξ and $\xi+d\xi$ then $\delta n e^{-\beta t(x,\xi)}$ is the number of these which will arrive at a distance x from the lower edge of the beam without becoming deexcited, where $t(x, \xi) = [2m(x-\xi)/Xe]^{1/2}$ is the time required for the ion to go from ξ to x. β is the reciprocal of the average life of the level n_l given by

$$1/\beta = T(n, l) = 1/\sum_{n',l'} A_{n,l}^{n'l'}.$$

Now the number of transitions which take place from state n, l to n', l' in volume element dA lying between x and $x+dx$ in time dt while the ions move the distance dx is

$$-d_{n,l}^{n',l'}(\delta n e^{-\beta(n,l)t(x,\xi)}) = A_{n,l}^{n',l'}\delta n e^{-\beta(n,l)t(x,\xi)}\frac{\partial t}{\partial x}dx.$$

This corresponds to a similar expression for the number of transitions occurring per second in dA obtained previously in which β has now been replaced by $A_{n,l}^{n',l'}$. The subsequent integration is unchanged so that the intensity formulas remain the same, except that they must now be multiplied by $g_l A_{n,l}^{n',l'}/\beta(n, l)$. For the previous case, this factor was obviously equal to unity. The introduction of the statistical weight g_l takes into account the case in which all the magnetic levels for a given n term have the same probability of excitation. The equation locating the maximum of the intensity curve is given by

$$2e^{-[(1/T(n,l))][2mx'/Xe]^{1/2}} - e^{-[1/T(n,l)][2m(a+x')/Xe]^{1/2}} - 1 = 0 \qquad (7)$$

This is the equation from which it is possible to determine the average life $T(n, l)$ after measuring experimentally the displacement x' of the maximum of the intensity curve.

Experimental arrangement.

The experimental arrangement used, showing the electrodes, and the electrical diagram are given in Fig. 1. The electrodes were mounted in a tube through which helium was circulated at a low pressure. The parts were made of molybdenum because it has nonmagnetic properties and because it does not give out occluded gases. The source of electrons was a 7 mil diameter tungsten filament whose cross section is indicated at F in the figure. Placed directly in front of the filament was the circular electrode 1 with a rectangular opening at its center of dimensions 0.6 mm by 4 mm. The filament 18 mm long, was in alignment with this opening, so that only electrons produced over 4 mm of its central portion were capable of being accelerated through the electrode 2 by potential V_1. The opening in electrode 2 was 2.75 mm by

6.0 mm. The electrons did not touch the edges of this opening because they were collimated into a narrow beam by an external magnetic field H of 2520 gauss applied in the direction of the accelerating electric field. The electrons passed between the electrodes 3 and 4 between which was applied an electric field which served to draw the ions out of the beam. The ions moved in a direction perpendicular to the direction of the electron beam. The magnetic field maintained the electron beam in spite of the cross electric field. The electrons then passed through electrodes 5 and were finally collected by 6 after receiving an additional amount of energy from the battery D. This procedure prevented secondary electrons from returning into the region between 3 and 4.

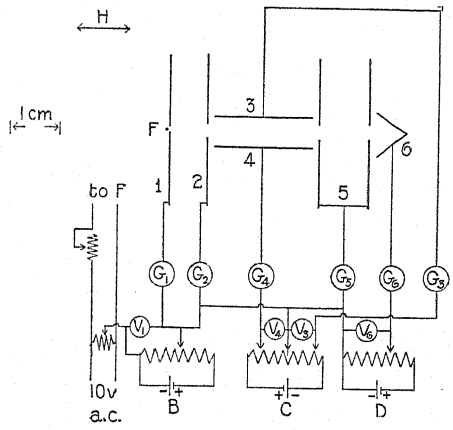


Fig. 1. Arrangement of electrodes and electric circuit.

The electrical circuit shows how the various potentials were applied. Battery B with its resistances produced the accelerating potentials while C served to maintain the transverse electric field. The potentials V_3 and V_4 could be arranged so that the space between 3 and 4 occupied by the electron beam was kept at any potential desired relative to the potential of 2. The filament was heated by a 60 cycle alternating current, so that it was not distorted by the force exerted on it by the magnetic field.

The light emitted from the region between 3 and 4 was projected on to the slit of the spectrograph with the image of the beam perpendicular to the slit. The direction of motion of the ions was then parallel to the slit. The distribution of density of the lines of ionized helium would be displaced in the direction of the motion of the emitters. The arc lines on the other hand would be undisplaced and furnished a reference point locating the center of the beam.

Fig. 2 shows the arrangement of the parts in the tube relative to the position of the spectrograph. The filament F was held firmly in position by large clamps made of tantalum. This prevented any large vibrations of the filament due to interaction of the alternating heating current and the external magnetic field. The shape of the electron beam is determined largely

by the size of the filament. The actual beam was 4 mm deep and approximately 0.4 mm wide. The light emitted from the region between 3 and 4 passed through the quartz window Q and was projected by the quartz lens L on to the slit S of the Hilger E_4 quartz spectrograph, in the manner described above. The lens was focused with respect to the center of the electron beam. This produced, with a magnification of 1.26 times, an image of depth 6.32 mm whose center lay in the plane of S. The spectrograph used was capable of bringing to focus the parts of the image of the beam outside of this plane. The magnification of the spectrograph for the wave-length 2733A for example, was practically unity, so that the total magnification in this case was 1.26 times.

The helium was purified by a glow discharge between iron and misch metal electrodes. It was then drawn through an adjustable leak and a liquid

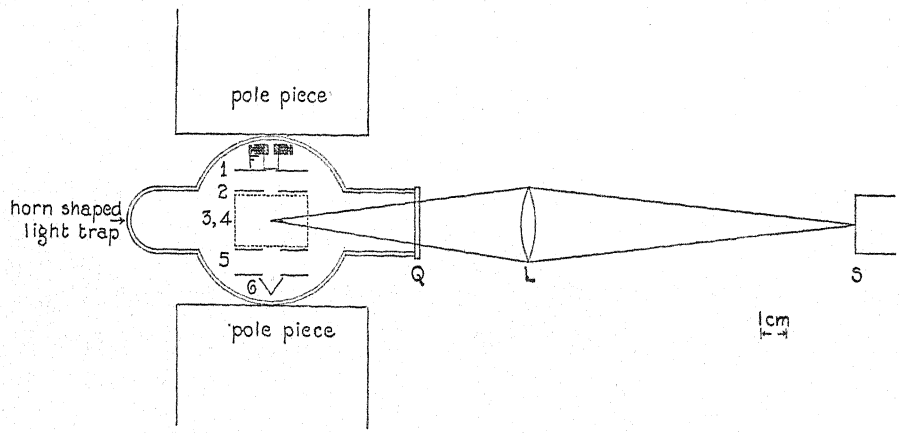


Fig. 2. A cross section showing arrangement of electrodes with respect to the position of the spectrograph.

air trap into the experimental tube and pumped finally back again into the purifier. The pressure in the experimental tube was generally maintained at 0.01 mm of Hg which means that the mean free path at this pressure was 2 cm for the atoms and about 10 cm for the electrons. This pressure was sufficient to produce enough excitation for simultaneous ionization and excitation. The mean free path of the helium ions was great enough so that they suffered practically no collisions before radiating. Thus de-excitation by collisions was prevented.

Results and Discussion

The dependence of the average life upon the state of excitation.

Fig. 3 shows results for the first four lines of the "4686" series of ionized helium obtained in some preliminary experiments in which a different type of filament and slit system were used than were illustrated in Fig. 1. Fig. 3 represents curves made from densitometer records taken along the lengths of the lines. With each of these lines there is an arc line which gives the posi-

tion of the electron beam. All the lines were obtained on one plate at a single exposure. The pressure of helium in the tube was 1.2×10^{-2} mm of Hg, the electron voltage was 500 volts and the transverse electric field was 305 volts/cm, while the magnetic field was 2520 gauss. The electron current collected to 6 was 0.5 milliamperes and the positive ion current to electrode 3 was 0.025 milliampere.

The shape of the electron beam in this case was so irregular that it was impossible to obtain values for the average life, but it sufficed for the purpose of comparing the average lives for the different lines. From Fig. 3 we see that for the lines 4686A (4→3) and 3203A (5→3) the displacements in the direction of motion of the helium ions are small. However, the line 2733A (6→3) shows clearly a displacement in the direction in which the positive ions are moving. The next line of this series 2511A, (7→3) exhibits a greater shift than the previous line 2733A. From Eq. (7) we see that the lines which

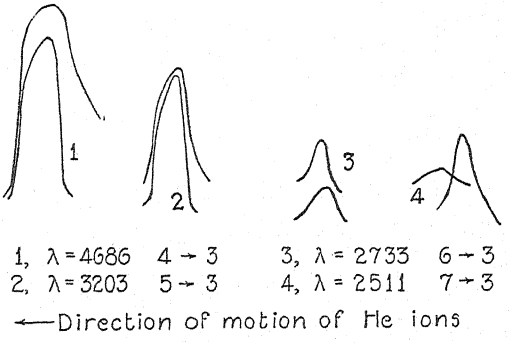


Fig. 3. Experimental results obtained illustrating the relative displacements of the first four lines of the "4686" series of He^+.

have the greatest displacements must originate from levels which have the longest mean lives. *Therefore, these experimental results show that the average life becomes progressively greater for levels with larger total quantum numbers.* This is in agreement with the theoretical values for the average life as shown in Table I.

Simultaneous ionization and excitation by electron impact.

In the derivation of the intensity formulas, it was assumed that at the time of collision the atom is ionized and excited. Compton and Boyce[12] have shown that the spark lines of helium can be formed only by single electron impacts when the electron current densities and gas pressures are low. This was proven by the fact that electrons with 65 volts energy excited only the arc lines of helium whereas the spark spectrum was fully developed at 85 volts. The spark spectrum would have appeared at 55 volts if it had been caused by cumulative action. This has been later confirmed by Elenbass[13]

[12] Compton and Boyce, Jour. Frank. Inst. 205, 497 (1928). See also Compton and Lilly, Astrophys. J. 52, 1 (1920).

[13] Elenbass, Zeits. f. Physik 59, 289 (1930).

who found that the 4686A line of ionized helium did not appear until about 80 volts.

It was found in the present experiment that with the cross field applied, the line 2733A became very weak as the voltage was decreased until at about 80 volts it remained only strong enough to be measured. In order more accurately to determine the initial potential for the appearance of this line, the transverse electric field was removed so that the electron velooities would be more uniform. It was found that the line was entirely absent at 65 volts whereas it was visible at 82 volts. This confirms the results obtained by the above workers.

We see from the previous work that the intensity of the displaced spark line at any given position along its length is proportional to the electron cur-

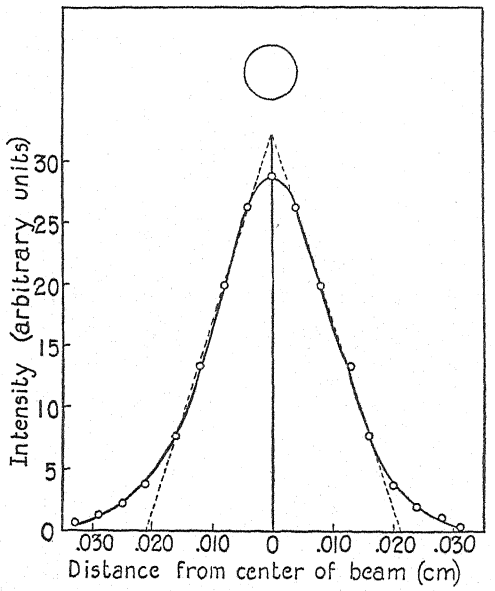


Fig. 4. Intensity distribution of line 2733A without the transverse field. The circle represents the cross section of the filament drawn to scale illustrating the size of the beam in comparison with the diameter of the filament.

rent if the excitation is produced at a single collision, whereas if it is due to a double collision the intensity will be proportional to the square of the electron current. Measurements of the relative intensity of both the 4686A and 2733A lines have been made as a function of the electron current with the transverse field applied and the intensity was found always to be directly proportional to the electron current showing therefore again, that the excitation occurs at a single collision.

Shape of the electron beam.

In the derivation of the intensity formulas it was assumed that the intensity of the electrons in the beam increased uniformly up to the center of the beam and then decreased uniformly to the upper edge of the beam. Fig. 4 shows how the intensity of the line 2733A varies along its length for the case of

no transverse field. This illustrates that the distribution of electrons is nearly the same as the assumed distribution. The dotted lines forming a triangle represent the distribution of electrons which give a width of the beam equal to 0.041 cm. The circle in the upper part of the figure represents the cross section of the 7 mil diameter tungsten filament drawn to scale with respect to the rest of the figure.

When the electric field is applied this distribution is not appreciably changed as long as the velocity of the exciting electrons is greater than the minimum speed for ionization and excitation. This fact is demonstrated by measuring the intensity distribution of a suitable arc line of helium. A line must be selected which is not lengthened by absorption and reemission of the light in leaving the tube. This line must also be excited by approximately the same speed electrons which are capable of ionizing and exciting the helium atom. The helium arc line 4437A was selected because for the case of no transverse field it had practically the same distribution of intensity as the helium spark lines. When the field was applied the shape of the line indicated that the distribution in intensity was practically unaltered for the beam used here. The assumption of the distribution of intensity for the subsequent calculation of the mean life is thereby justified.

Average life for sixth quantum state.

Fig. 5 shows enlargements made from the actual negatives obtained with the experimental arrangement as given in Fig. 1. Negatives are reproduced here for cases with and without the transverse electric field. The line 2733A of ionized helium is drawn up in the direction of motion of the positive ions when

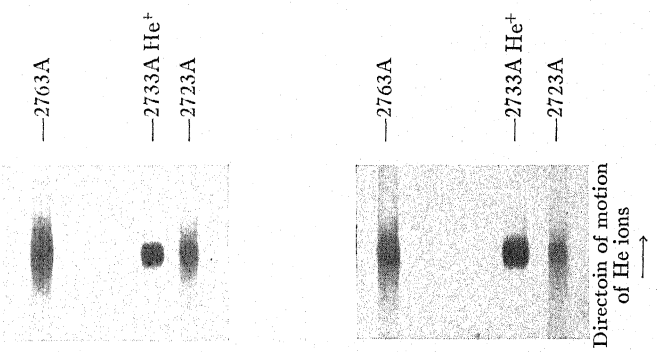


Fig. 5. Enlargements (magnification, five times) made from original negatives obtained for (1) without transverse field and (2) without transverse field showing effect of motion of helium ions for line 2733A. The adjoining arc lines located the center of the electron beam.

the field is applied. The lines 2763A and 2723A are two principal series lines of the orthohelium system. They are unaffected by the electric field and their densest portion locates the center of the electron beam. In exposure 2 the electrons had approximately 210 volts velocity, while the cross electric field was 740 volts/cm. The currents and pressure were the same as for the pre-

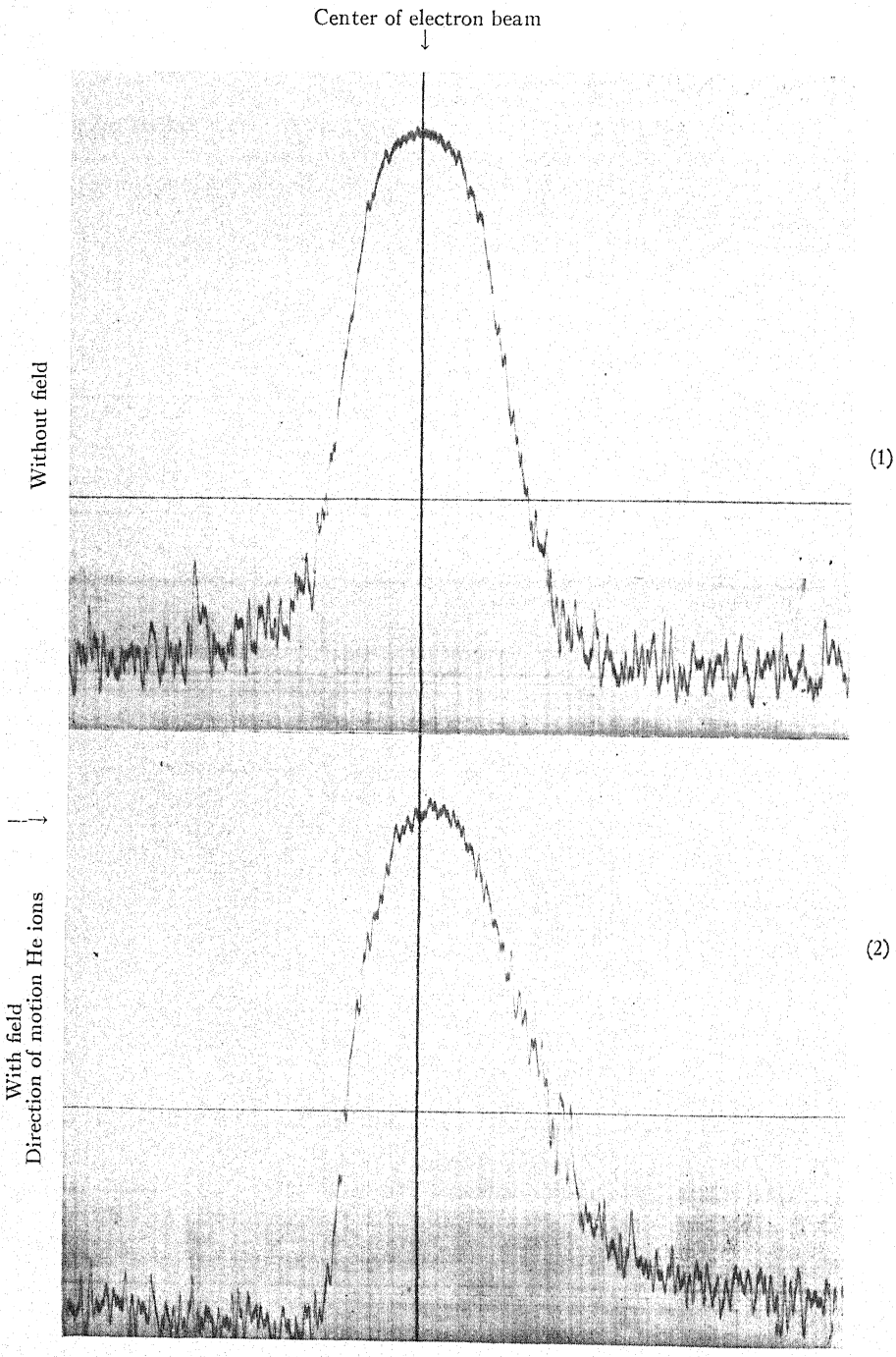


Fig. 6. Microphotometer records of line 2733A for (1) without cross field, and (2) with cross field. Vertical line marks center of electron beam located by helium arc lines 2723A and 2763A.

vious experiment described above. The magnetic field was 2520 gauss. The spectrum was photographed on an Eastman speedway plate with an exposure of twelve hours. The experimental conditions for exposure 1 were similar to 2 except that the cross field was zero and the voltage of the electrons was 350 volts.

Fig. 6 shows two records made by a Goos and Koch microphotometer taken along the length of the line 2733A, (1) with and (2) without the transverse electric field. The vertical line locates the center of the beam as determined by the center of the two adjoining arc lines shown in Fig. 5. This is accomplished by making microphotometer records for these two arc lines which lie on opposite sides of the line 2733A. By this means it is possible to correct for error produced by improper alignment of the direction of motion of the spectrum plate in the microphotometer. From Fig. 6 we see that for record (2) the line is displaced in the direction of motion of the helium ions. Record (1) is made from the plate shown in exposure 1 of Fig. 5. (2) is taken from an exposure in which the accelerating potential was about 120 volts, the cross field 650 volts/cm, the other conditions were the same as given above.

In Table III are given the experimental values obtained for the average life determined for different energies of the exciting electrons. *It is seen that*

TABLE III.

Energy of electrons in beam (volts)	Average life experimental values for sixth quantum state (sec.)	Mean average life theoretical value sixth quantum state
260	$1.6\pm0.2\times10^{-8}$	
120	$1.5\pm0.2\times10^{-8}$	
112	$1.3\pm0.2\times10^{-8}$	
100	$1.1\pm0.2\times10^{-8}$	
80	$1.1\pm0.2\times10^{-8}$	1.17×10^{-8} sec.

the experimental values for the average life decrease as the energy of the electrons is diminished, and approaches the theoretical value for the mean average life. As the energy of the exciting electrons is decreased there will be less excitation to the levels higher than the sixth. The number of transitions downward into the sixth state will thus decrease and cause the average life to become shorter. This conclusion is substantiated by the fact that as the voltage is lowered the intensity of the line 2511A coming from the seventh state diminishes faster than does the intensity of the line 2733A coming from the sixth state. Thus the ratio of the number of electrons in the sixth state to the number in the seventh becomes greater as the voltage is decreased. This will produce fewer transitions into the sixth state and consequently the average life of the sixth state will become shorter. Because of the small energy differences between the sixth and seventh levels it is practically impossible to excite to the sixth state with enough intensity to produce lines which can be photographed, while at the same time produce no excitations to the seventh state.

The values obtained at 100 volts and 80 volts differ from the theoretical value for the mean average life by less than 0.10×10^{-8} sec. which is consider-

ably less than the experimental error. The agreement obtained here is better than is found by other workers for the case of hydrogen. For example, the theoretical values for the mean average life of the 2nd, 3rd, and 4th quantum states of hydrogen are 2.18×10^{-9} sec., 1.03×10^{-8} sec. and 3.4×10^{-8} sec. respectively. Wien's[14] canal-ray measurements on H_α of the Lyman series give 6.7×10^{-9} sec. for the average life of the second quantum state. Slack[15] obtains experimentally the value of 1.2×10^{-8} sec. for this state. For the third quantum state Wien again obtains 6.7×10^{-9} sec. from measurements on H_b of the Lyman series while Wien and Kerschbaum[14] obtain 1.85×10^{-8} sec. from H_α of the Balmer series. Their results for the fourth state as determined by H_β give the same value of 1.85×10^{-8} sec.

Curve 1 in Fig. 7 gives the intensity distribution of the line 2733A with respect to the center of the beam, while curve 2 represented by the dotted line gives the theroretical intensity distribution calculated by the use of the

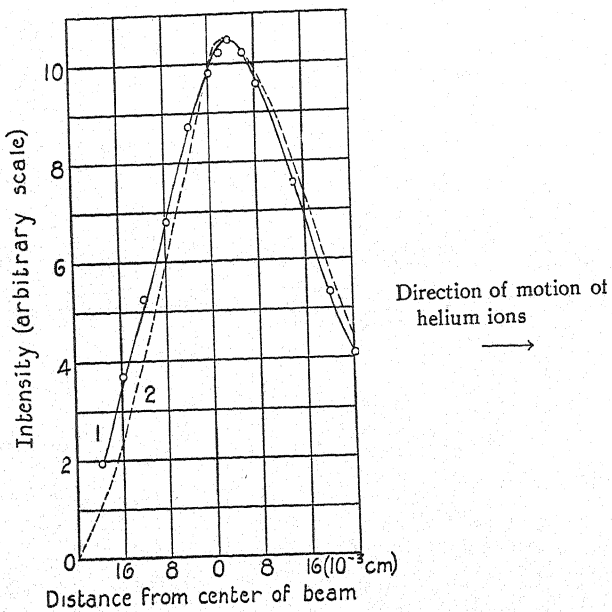


Fig. 7. Intensity distribution of line 2733A found experimentally, given by curve 1 while curve 2 shows a similar distribution calculated from intensity formulas using the theoretical value for mean average life.

intensity formulas (7) and (8)[16] for the average life of 1.17×10^{-8} sec., the value given in Table III for the mean average life. The two curves show approximately the same distribution of intensity, which gives an agreement between the experiment and the theory. It is noticed that the width of the beam is 0.048 cm as compared to 0.041 cm as is given in Fig. 4. This slight increase

[14] Wien, Ann. d. Physik **83**, 1 (1927); See also table of values for average lives from canal ray experiments of Wien and Kerschbaum, prepared by Kerschbaum, Ann. d. Physik **83**, 294 (1927).

[15] Slack, Phys. Rev. **28**, 1 (1926).

[16] These numbers refer to equations on page 725, Phys. Rev. **32**, (1928).

in the width of the beam is probably caused by the action of the transverse electric field.

In order to compare the average life measured experimentally with the theoretical value for the mean average life, there must be a continuous interchange between the sublevels so that the number of electrons in any sublevel is proportional to its quantum weight. Sugiura has pointed out in connection with the interpretation of Wien's canal-ray experiments, that the perturba-

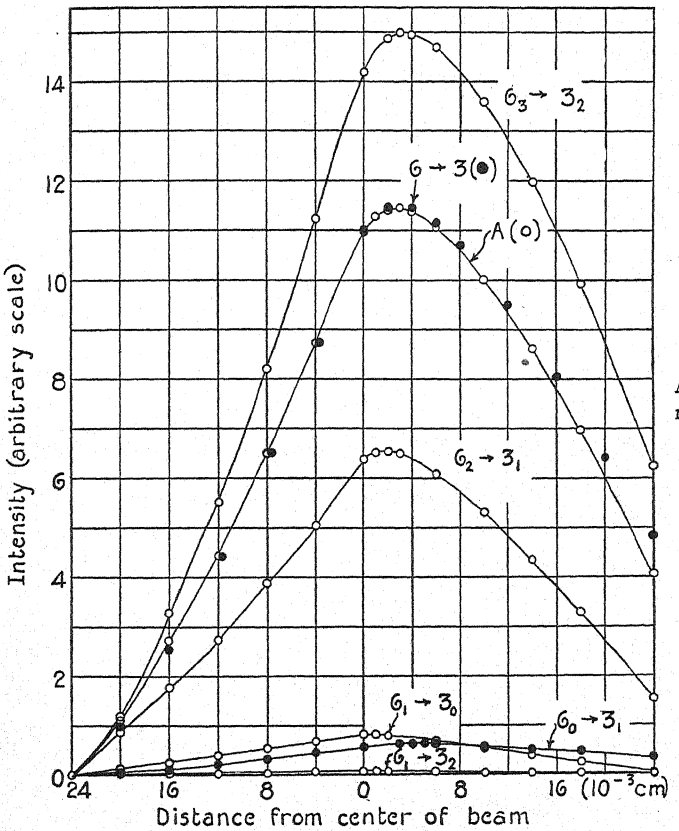


Fig. 8. Theoretical intensity distribution for the five fine structure lines of the line 2733A. Curve *A* represented by the circles is the resultant intensity curve plotted on a reduced scale. Curve 6→3 indicated by full dots gives the intensity distribution for the case of free interchange among the *l* values (or for the case of a single exponential decay law). The values for the average life used were taken from Table I, and 658 volts/cm was the strength of field used.

tions to which the hydrogen atoms were subjected were large compared with the component separations due to relativity, so that free interchange existed among the various sub-divisions of a term. In the present work the helium ions radiate in the presence of crossed electric and magnetic fields which further complicates the perturbations of the quantum states. However Elenbass[17] has found that the line 4686A of ionized helium is polarized when ex-

[17] Reference 13.

cited by unidirectional electrons. To interpret these results one must assume that free-interchange did not take place, otherwise the light could not be polarized.

In the present work we cannot prove the existence of statistical equilibrium so that it is considered a postulate for comparing the results of experiments with the mean average life.

Alternative interpretation of the experimental results.

It is, however, possible to obtain a comparison with the theory by considering the decay time of each of the fine structure lines which make up the single line 2733A, without the assumption of statistical equilibrium. A theoretical intensity curve is obtained for each line individually and then a resultant intensity curve is plotted and compared with the theoretical intensity curve obtained above for the case of free interchange. This method requires a knowledge of the relative population of the substates at the time of excitation.

The results of these computations are illustrated in Fig. 8. The theoretical intensity distribution for the five fine structure lines is plotted with respect to the distance from the center of the beam. The relative intensities of these curves for a given position depends upon the transition probability $A^{n',l'}_{n,l}$ the quantum weight g_l, and the average life $1/\beta(n,l)$ as given in the formulas for the intensity distribution.[18] It is noticed that the two lines $6_3 \rightarrow 3_2$ and $6_2 \rightarrow 3_1$ predominate and determine approximately the intensity distribution of the resultant intensity curve A which is plotted on a reduced scale. Thus the curve A represented by the circles gives the theoretical intensity distribution for the case of *no interchange* between the l values. There is also plotted in this figure the values of the intensity for the case of *free interchange* or (in other words for the case of a single exponential decay law), taken from curve 2 in Fig. 7 and is represented by $6 \rightarrow 3$ located by the full dots. It is seen that these two sets of points lie almost identically on the same curve which shows that the theoretical distribution is the same for the two cases. Thus we have shown that we cannot distinguish between the two methods of interpreting the experimental results. Both are in good agreement with the experimental intensity distribution obtained.

If we take into account electron spin correction we find that each of the above five lines split up into groups of lines. Since we have proved above that the average life of the n,l,j,th state is equal to the average life of the n,l,th state, therefore, these lines resulting from spin will have the same average life as the line from which they originated. This means that in this case we shall have five groups of lines with average lives corresponding to the average lives of the five lines given above. Also the sum of the intensity of the lines in any particular group is proportional to the intensity of the parent relativistic line independent of l.[19] Therefore, the relative intensity of the sum of the intensities of the lines in a group will be the same as the relative inten-

[18] The values for $A^{n,'l'}_{n,l}$ and the average life used here are obtained from Slack's table although Kupper's values could be used without greatly changing the results obtained.

[19] This has been proved above. See also Sommerfeld and Unsöld, Zeits. f. Physik **38**, 237 (1926).

sity of the five single lines for the relativistic case. Thus we see that the *distribution of intensity of the resultant line calculated by considering all the additional fine-structure lines due to spin will be exactly the same as for the relativistic case.*

ERRORS

(1) Approximate solution.

The most fundamental error is caused by the fact that the shape of the electron beam is never actually the ideal case in which the distribution is triangular as assumed in the calculation of the intensity of the displaced lines. A more exact treatment could be obtained by a numerical integration performed by introducing experimental values for the electron distribution func-

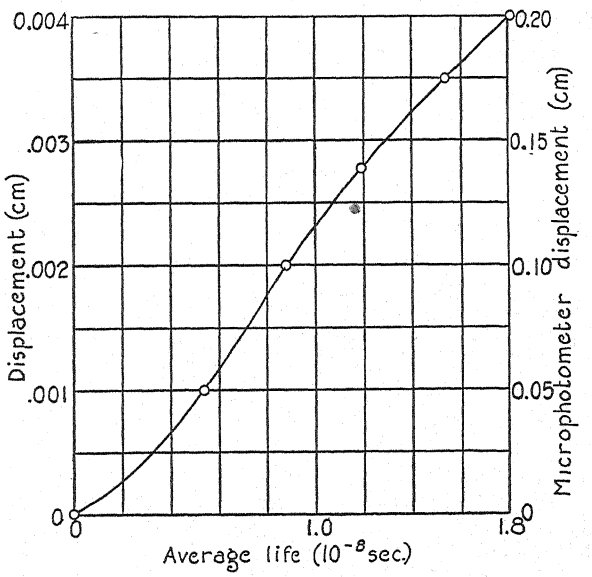


Fig. 9. Relationship between the displacements and the average life for a field of 658 volts/cm, and beam width 0.048 cm.

tion $N(\xi)$. However, Fig. 4 shows that the distribution obtained is approximately triangular so that the results are sufficiently accurate to compare satisfactorily with the theory.

(2) Center and shape of the electron beam.

In the present experimental conditions there exists a cross field of approximately 660 volts/cm. Since the width of the beam is approximately 0.04 cm there is a drop of potential of about 26 volts across the electron beam itself. This means that there will be a distribution of velocities across the beam within this amount. This will alter the effective distribution curve and will be more pronounced in the case where the speed of the exciting electrons is only a small amount in excess of the minimum velocity required for excitation. This error will become practically negligible for higher velocities of the order of 150 volts or more. It is very difficult to determine the amount of this

error for the lower velocities without knowing the probability of excitation function for both the arc lines and the spark lines.

(3) Measurements of displacements.

Fig. 9 shows the relationship between the average life and the displacement of the maximum of the shifted spark line for a cross field of 658 volts/cm. On the ordinate axis there is plotted at the left of the figure the displacements, while at the right is plotted the corresponding distances which are actually measured on the microphotometer record. On the abscissae is plotted the average life for a beam of width 0.048 cm. These are the constants used in obtaining the results given in Table III. The error in reading the displacements on the microphotometer record was not greater than 0.2 mm. Therefore we see from Fig. 9 that the corresponding error for the average life is 0.20×10^{-8} sec. This is the error given in Table III.

(4) Effect of the thermal velocities of the helium ions.

In the above calculations of the average life it is assumed that when the excited ion is formed it is initially at rest. This, of course, is never actually the case on account of the thermal velocities possessed by the ions. A helium atom or ion at a temperature of 20°C has a root mean square velocity of 1.38×10^{5} cm/sec. Under the action of a transverse electric field of 732 volt/cm the ion, initially at rest, would obtain this velocity of 1.38×10^{5} cm/sec. after being accelerated through a distance of 5.33×10^{-5} cm. This distance is small compared to the distances considered in the present experiment. Thus the initial velocity due to thermal agitation of the ion can be neglected.

(5) Space charge.

To reduce the effect of space charge in these experiments, the electron current in the beam was decreased until it required about 12 hours exposure to photograph the line 2733A. The electron currents in the beam were not greater than 0.5 milliampere and the positive ion current was less than 0.06 milliampere. *It was found that the displacements of the spark line 2733A were not appreciably altered when the currents were reduced to about one-half the above values.* This indicates that the distribution of space charge in the presence of the strong transverse field does not disturb appreciably the velocities of the helium ions.

(6) Shape of emitting portion of the filament.

Although the displacements measured are of the order of 0.002 cm it is unnecessary for the filament to be straight and in proper alignment to less than this amount. The filament however, was not actually straight for its central portion sagged about 0.002 cm. This part of the filament would be out of alignment with the other portions by an amount comparable to the experimentally measured displacements. However, the intensity photographed by the spectrograph is the resultant of the radiation coming from different depths of the beam. Although each radiating segment is not in alignment with the optic axis of the spectrograph and the projecting lens, nevertheless the displacement recorded by the photographic plate will be

exactly the same as if the segments were in very accurate alignment. This is true provided that all segments radiate with the same intensity, which is practically the case. Therefore, any sagging or improper alignment of the filament will produce no error in the measured displacements, but it will obviously produce an error in the value for the width of the beam and in the intensity distribution curves. These errors of 0.002 cm are so small that they are unimportant in determining the width of the beam, however they became more important in the measurement of the intensity distribution.

(7) Vibrations of the filament.

The maximum amplitude of vibration of the filament due to the interaction between the alternating heating current and the magnetic field was about 0.001 cm which is small compared to the width of the beam so that it caused no appreciable errors.

In conclusion the writer desires to express his thanks to Dr. A. Bramley for helpful discussions of the work.

Note added in proof, October 2, 1931:

In view of the discrepancies given above for the matrix amplitude squared, Professor Slack has recalculated his values for the intensities and transition probabilities for hydrogen and has kindly furnished the data for Table IV.

With Slack's corrected values for the transition probabilities we find that the average life of the 5_0, 6_0, 7_0, 7_3 and 7_4 states are changed to 2.2×10^{-8}

TABLE IV. *Summary of corrected intensities in the 4th, 5th, and 6th series of hydrogen* (Prepared by Slack).

Component	Previously published*		Corrected		Matrix amplitude squared	Kupper's matrix amplitude squared
	Intensity ergs/sec.	Probability sec.$^{-1}$	Intensity ergs/sec.	Probability sec.$^{-1}$		
5_4-4_3	20.8×10^{-7}	43.0×10^{5}	20.8×10^{-7}	43.0×10^{5}	628	630
5_3-4_2	12.6	26.1	12.6	26.1	297	291
5_2-4_1	7.26	15.0	7.26	15.0	122	125
5_2-4_3	0.246	0.507	0.246	0.507	4.13	4.4
5_1-4_0	3.60	7.43	3.60	7.43	36.3	36
5_1-4_2	0.0092	0.019	0.92	1.9	9.3	9.1
5_0-4_1	6.09	12.54	3.15	6.49	10.58	105
6_4-4_3	9.94×10^{-7}	13.3×10^{5}	9.94×10^{-7}	13.3×10^{5}	53.3	55
6_3-4_2	9.85	13.2	9.85	13.2	41.1	40
6_2-4_1	6.58	8.81	6.58	8.81	19.6	22.5
6_2-4_3	0.094	0.126	0.161	0.215	0.48	0.48
6_1-4_0	3.88	5.19	3.88	5.19	6.88	6.0
6_1-4_2	0.0075	0.010	0.75	1.0	1.30	1.21
6_0-4_1	3.11	4.16	2.44	3.25	1.45	14.8
7_4-4_3	7.94×10^{-7}	8.75×10^{5}	3.97×10^{-7}	4.37×10^{5}	14.6	14.7
7_3-4_2	8.65	9.55	4.57	5.04	12.9	12.9
7_3-4_1	4.28	4.73	4.28	4.73	8.6	6.7
7_2-4_3	0.057	0.063	0.057	0.063	0.115	0.137
7_1-4_0	2.38	2.63	2.38	2.63	2.88	2.15
7_1-4_2	0.0041	0.0045	0.41	0.45	0.49	0.41
7_0-4_1	1.98	2.19	1.77	1.95	0.71	4.2

* Slack, reference 4.

TABLE IV. (*continued*)

Component	Previously published Intensity ergs/sec.	Previously published Probability sec.$^{-1}$	Corrected Intensity ergs/sec.	Corrected Probability sec.$^{-1}$	Matrix amplitude squared	Kupper's matrix amplitude squared
6_5-5_4	4.20×10^{-7}	16.0×10^{5}	4.33×10^{-7}	16.4×10^{5}	1852.	201.
6_4-5_3	2.63	10.0	2.63	10.0	921.	1020.
6_3-5_2	1.97	7.50	1.97	7.50	538.	520.
6_3-5_4	0.045	0.17	0.030	0.114	8.15	8.2
6_2-5_1	1.14	4.32	1.14	4.32	226.	203.
6_2-5_3	—	—	0.078	0.295	15.1	20.
6_1-5_0	0.617	2.35	0.617	2.35	72.3	67.
6_1-5_2	—	—	0.268	1.02	31.3	15.3
6_0-5_1	1.97	7.50	0.69	2.63	26.9	247.
7_5-5_4	2.40×10^{-7}	5.69×10^{5}	2.40×10^{-7}	5.69×10^{5}	154.	139.
7_4-5_3	2.46	5.82	2.46	5.82	128.	122.
7_3-5_2	1.97	4.66	1.97	4.66	80.	75.
7_3-5_4	0.0093	0.022	0.20	0.48	0.82	0.81
7_2-5_1	1.27	3.01	1.27	3.01	37.	36.
7_2-5_3	—	—	0.808	1.91	2.35	2.37
7_1-5_0	1.01	2.40	1.01	2.40	17.6	20.7
7_1-5_2	—	—	0.258	0.66	4.8	3.9
7_0-5_1	1.10	2.60	0.583	1.38	3.4	35.
7_6-6_5	1.13×10^{-7}	7.10×10^{5}	1.20×10^{-7}	7.5×10^{5}	4500.	4497.
7_5-6_4	0.635	4.00	0.635	4.0	2020.	2734.
7_4-6_3	0.617	3.89	0.545	3.43	1420.	1582.
7_4-6_5	0.0113	0.071	0.0057	0.036	15.0	14.1
7_3-6_2	0.421	2.65	0.421	2.65	850.	848.
7_3-6_4	—	—	0.016	0.10	32.4	36.3
7_2-6_1	0.235	1.48	0.246	1.55	356.	
7_2-6_3	—	—	0.030	0.19	43.7	58.9
7_1-6_0	0.051	0.32	0.159	1.0	138.	
7_1-6_2	—	—	0.098	0.62	85.	
7_0-6_1	1.04	6.53	0.20	1.26	58.	

sec., 3.3×10^{-8} sec., 5.0×10^{-8} sec., 2.4×10^{-8} sec., and 4.5×10^{-8} sec., respectively. The values for the average life of the other states and the mean average lives remain practically the same. The only lines illustrated in Fig. 8 affected by these corrections is the transition $6_0\rightarrow3_1$. Since this component is weak in comparison with the other transitions, the resultant intensity curve *A* is not appreciably changed.

MASS SPECTROGRAPH ANALYSES, AND CRITICAL POTENTIALS FOR THE PRODUCTION OF IONS BY ELECTRON IMPACT, IN NITROGEN AND CARBON MONOXIDE

By Alfred L. Vaughan
Department of Physics, University of Minnesota

(Received August 11, 1931)

Abstract

The dissociation products formed by bombarding nitrogen and carbon monoxide with electrons of a definite velocity have been studied with a mass spectrograph.

Nitrogen.—N_2^+ and N^+ ions appear at 15.8 ± 0.1 and 24.5 ± 0.1 volts respectively. The N^+ ion has kinetic energy and is attributed to $N_2 \rightarrow N^+ + N + e$. Increases in the efficiency of production of the N^+ ion appear at 40.0 ± 1.0 and 47.0 ± 1.0 volts. The largest percentage of the total positive ion current carried by kinetic energy ions is approximately 28 percent at 140–160 volts. Efficiency curves of total ionization and of N_2^+ exhibit maxima at 100.0 ± 5.0 and 60.0 ± 5.0 volts respectively.

Carbon monoxide.—CO^+, C^+ and CO^{++} ions appear at 13.9 ± 0.2, 22.5 ± 0.2, and 43.0 ± 1.0 volts respectively. Maximum numbers of CO^+, C^+, and CO^{++} ions formed per electron per cm path per mm pressure at 0°C are 10.13, 0.50, and 0.14 at 102, 105, and 125 volts respectively. The C^+ ion possesses kinetic energy and is probably due to $CO \rightarrow C^+ + O + e$. Assuming that the CO^{++} ion would dissociate into $C^{++} + O$ the energy of dissociation cannot be less than from 2 to 3 volts. O^- ions are formed between 9.5 ± 1.0 and 16.5 ± 1.0 volts, and again beginning at 22.5 ± 1.0 volts and reach a maximum at 33 volts. The first group is evidently due to the attachment of an electron to the CO molecule followed by a dissociation $CO^- \rightarrow C + O^-$. The second group may be due to $CO \rightarrow C^+ + O^-$. O^- ions are only 2.7 percent as numerous as C^+ ions at 30 volts.

Introduction

THE material presented in this paper is an extension of the work done by Bleakney[1] on multiply charged ions produced by electron impact in gases at low pressures. The purpose of this paper is to describe the results of a similar study of the ionization products in the diatomic molecular gases—nitrogen and carbon monoxide. Smyth[2] and Hogness and Lunn[3] have made mass spectrograph analyses of the ions produced in nitrogen by electron impact while Hogness and Harkness[4] have made a similar study of carbon monoxide. The present method confirms some of the results of these previous investigations and presents some new data, particularly in the experiments on carbon monoxide.

[1] W. Bleakney, Phys. Rev. **34**, 157 (1929); **35**, 139 (1930); **35**, 1180 (1930); **36**, 1303 (1930)
[2] H. D. Smyth, Proc. Roy. Soc. **104A**, 121 (1923).
[3] T. R. Hogness and E. G. Lunn, Phys. Rev. **26**, 786 (1925).
[4] T. R. Hogness and R. W. Harkness, Phys. Rev. **32**, 936 (1928).

Apparatus and Procedure

The apparatus employed in this experiment was the same as that used by Bleakney[1] in the study of helium, neon, and argon. The nitrogen and carbon monoxide used were prepared by Smith.[5] The gases were admitted to the apparatus through a fine capillary at the end of the tube opposite the electron gun and were pumped through the ionization chamber and out past the filament. Effects of dissociation by the filament were thus reduced to a minimum. The pressures used were from 5 to 10×10^{-5} mm Hg. The gases used were found to be very pure. Water vapor and a trace of carbon monoxide existed as impurities in the tube before the gas to be studied was admitted. If liquid oxygen were kept on the mercury trap continuously for about 80 hours the water vapor impurity was so reduced as not to interfere appreciably. The carbon monoxide impurity was never large enough to be troublesome except in determining ionization potentials.

Results

Nitrogen

A typical e/m analysis curve of the products obtained by bombarding nitrogen with electrons of definite velocity is shown in Fig. 1. The positive ion current to the analyzer is plotted as a function of the analyzing field, E, in

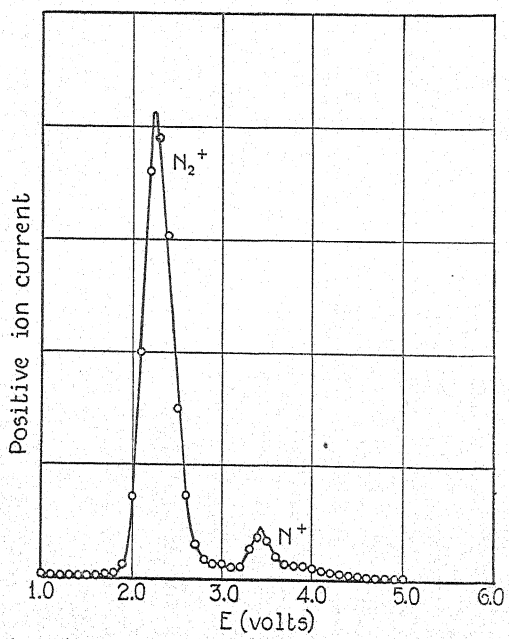


Fig. 1. A typical e/m analysis curve of nitrogen. Electron velocity = 100 volts.

volts. This curve shows the N_2^+ and the N^+ ions. A background of H_2O^+ shows between the two peaks. The trailing off to the right of the N^+ ion may be attributed to those N^+ ions which have considerable kinetic energy.

[5] John T. Tate and P. T. Smith, unpublished.

The ionization potentials of the N_2^+ and N^+ ions were determined by plotting the maximum heights of the peaks as a function of the electron velocity

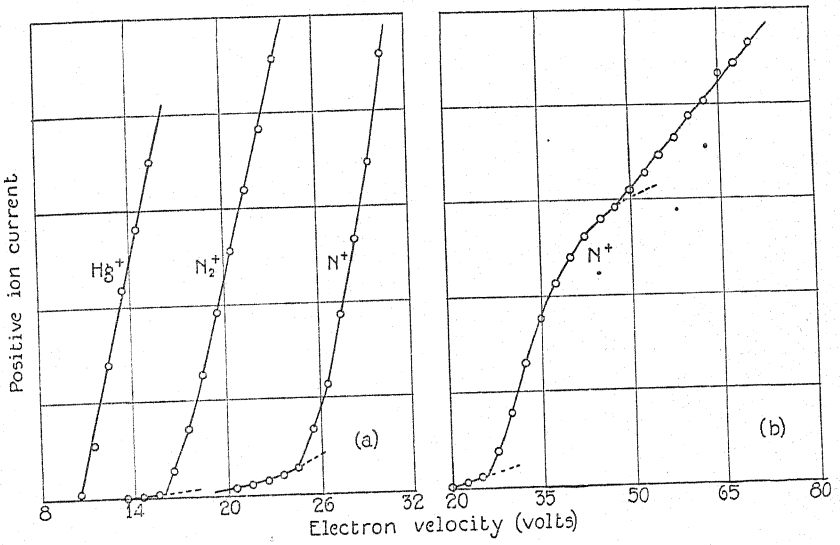


Fig. 2. (a) Curves showing the ionization potentials in nitrogen. (b) Ionization potential curves of N^+ showing a break at 47 volts.

in volts. When the liquid oxygen on the mercury trap was replaced by solid carbon dioxide there was a sufficient amount of mercury vapor present in the

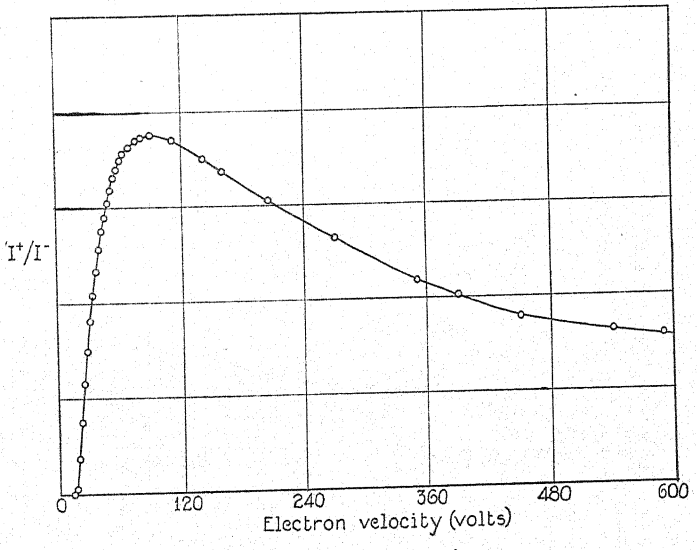


Fig. 3. Efficiency curve for nitrogen.

tube for calibration purposes. The results are shown in Fig. 2 (a). The impurity under the curve for N_2^+ is CO^+ whereas that under the N^+ curve is

H_2O^+. This method shows N_2^+ and N^+ appearing at an electron velocity of 15.8 and 24.5 volts respectively with an estimated probable error of ± 0.1 volts. Fig. 2 (b) shows an increase in the efficiency of production of the N^+ ion at 47.0 ± 1.0 volts. A similar but considerably smaller increase was noticed at 40.0 ± 1.0 volts. These breaks have also been found by Lozier.[6]

By plotting the ratios of the areas under the N_2^+ peak to the electron current as a function of the electron velocity in volts the maximum efficiency of formation of the N_2^+ ion was found to occur at an electron velocity of 60.0 ± 5.0 volts. The total efficiency of ionization as plotted in Fig. 3 shows a maximum at 100.0 ± 5.0 volts. This curve was obtained by plotting the ratio of the total positive ion current collected at the upper plate of the ionization chamber to the electron current as a function of the electron velocity in volts. The efficiency curve of total ionization in N_2 given in Fig. 3 is almost identical with the one obtained by Smith.[5]

A rough measure of the percentage of the current carried by those ions possessing kinetic energy was obtained by the method outlined by Bleakney,[7] and was shown to reach a maximum of 28 percent at 140–160 volts electron velocity. The assumptions made in obtaining this result make it impossible to consider it as other than an indication of the order of magnitude.

Discussion of results in nitrogen.

The value given in this paper of 15.8 ± 0.1 volts as the ionization potential of N_2, although lower than the generally accepted value, agrees with that given by Samson and Turner[8] and the earlier results obtained by Boucher[9] and by Found.[10] The appearance of N^+ at 24.5 ± 0.1 volts has been attributed to a single impact resulting in $N_2 \rightarrow N^+ + N + e$. The value given is in good agreement with that of 24.6 volts given by Hogness and Lunn[3] who, however, attributed the formation to a different process. According to data given by Samson and Turner[8] together with a correction by Birge[11] the minimum value at which N^+ can appear from the above process is 22.7 ± 0.1 volts. From this the N^+ ion should have at least 0.9 volts kinetic energy. These conclusions have been verified by Lozier.[6] There was no means of determining whether or not any N_2^{++} ions were formed since their m/e is the same as that of the N^+ ion. No N^{++} ions were found below 400 volts. No search was made for negative ions.

Carbon monoxide

Fig. 4 is a typcial e/m analysis curve of the positive ions formed by bombarding CO with electrons. Ions having an m/e of 28, 14, and 12 were found which correspond to CO^+, CO^{++}, and C^+ and have ionization potentials of 13.9 ± 0.2, 43 ± 1.0, and 22.5 ± 0.2 volts respectively as obtained from Fig. 5.

[6] W. W. Lozier, unpublished.
[7] W. Bleakney, Phys. Rev. **35**, 1185 (1930).
[8] L. A. Turner and E. W. Samson, Phys. Rev. **34**, 747 (1929).
[9] P. E. Boucher, Phys. Rev. **19**, 189 (1922).
[10] C. G. Found, Phys. Rev. **16**, 41 (1920).
[11] R. T. Birge, Phys. Rev. **34**, 1062 (1929).

The second peak from the left in Fig. 4 is due to an ion having an m/e of 18 and an ionization potential of 13.2 volts and so has been attributed to H_2O^+. Solid carbon dioxide instead of liquid oxygen was used on the mercury trap in this experiment. The O^+ ion, if formed, was entirely masked by the H_2O^+ ion.

The two e/m analysis curves in Fig. 4 were taken at electron velocities of 35 and 210 volts. They show the resolving power of the apparatus as well as the relative magnitudes of the ions formed at those velocities. Attention is called to the complete absence of an ion having an m/e of 14 at 35 volts electron velocity. The determination of the ionization potential of CO may not be accurate since the positive ion current due to the Hg^+ ion which was used

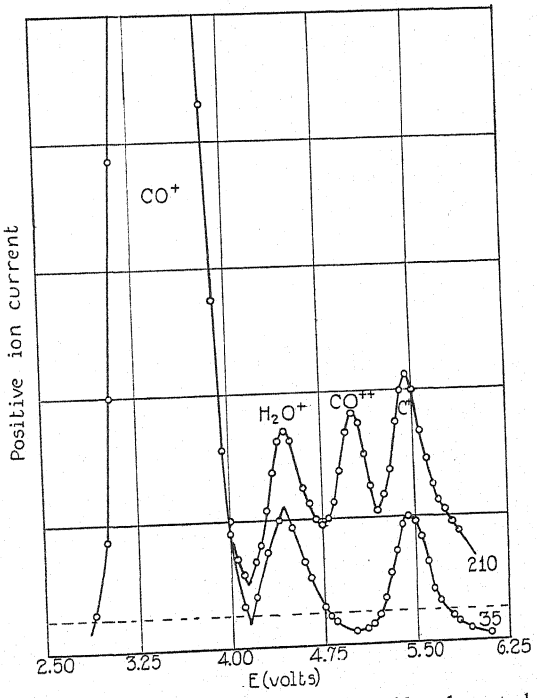


Fig. 4. e/m analysis curves of carbon monoxide taken at electron velocities of 35 and 210 volts.

to calibrate the voltage scale was very small compared to the positive ion current due to the CO^+ ion. The impurity shown under the C^+ curve in Fig. 5 was H_2O^+ while that under the CO^{++} was C^+ and H_2O^+. It was found that by decreasing the drawing out field in the ionization chamber the C^+ peak shown in Fig. 4 decreased considerably in size. This was an indication that the C^+ ion was formed with kinetic energy. This also afforded a means whereby more accurate measurements could be made of the CO^{++} ion inasmuch as decreasing the size of the C^+ peak made the CO^{++} peak stand out more distinctly. An increase in the efficiency of formation of the C^+ ion was consistently evident at about 30 volts.

Fig. 6 shows the percent of positive ion current carried by the different

ions. These curves were obtained by plotting the ratios of the areas under the peaks to the electron current as a function of the volt velocity of the impinging electrons. Multiplying the total number of ions formed as given by Smith[5] by the percent of current carried by a particular ion and dividing by the

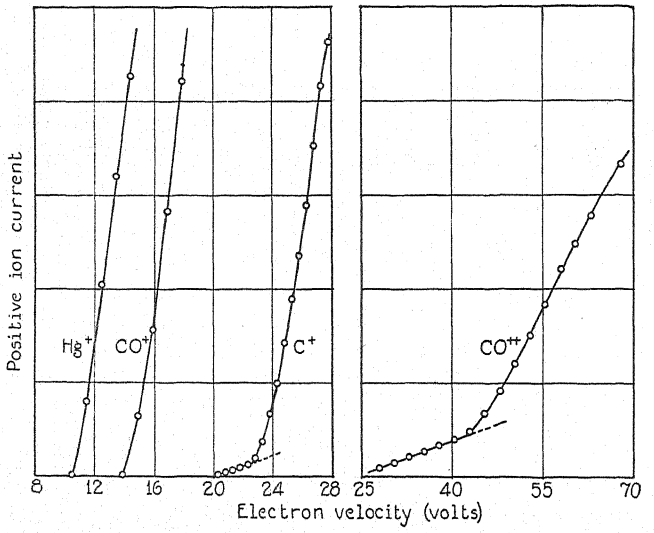


Fig. 5. Curves showing the ionization potentials in carbon monoxide.

charge on the ion gives the number of that type of ion formed per electron per cm path reduced to 1 mm pressure at 0°C. These results are shown in Fig. 7. The numbers of CO^+, C^+, and CO^{++} ions formed reach maxima of 10.13, 0.50, and 0.14 at 102, 105, and 125 volts respectively. An independent determina-

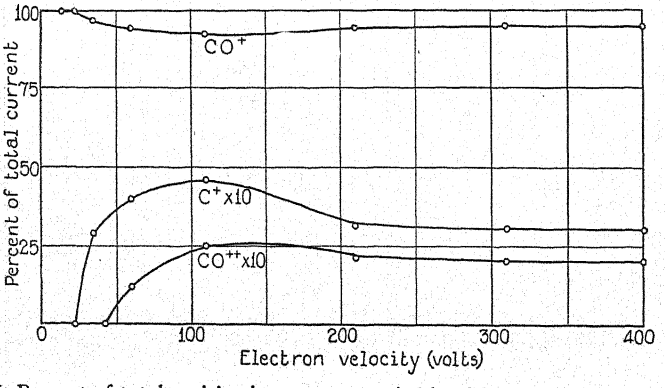


Fig. 6. Percent of total positive ion current carried by CO^+, C^+, and CO^{++} ions.

tion of the efficiency of formation of the CO^+ ion obtained by plotting the area under the peak yielded a maximum at 100 volts.

Negative ions having an m/e of 16 were found in carbon monoxide. These negative ions which are undoubtedly O^- first appeared at 9.5 volts, reached a

sharp maximum at 12 volts and had completely disappeared at 16.5 volts as shown in Fig. 8. The same type of negative ions reappeared at 22.5 volts

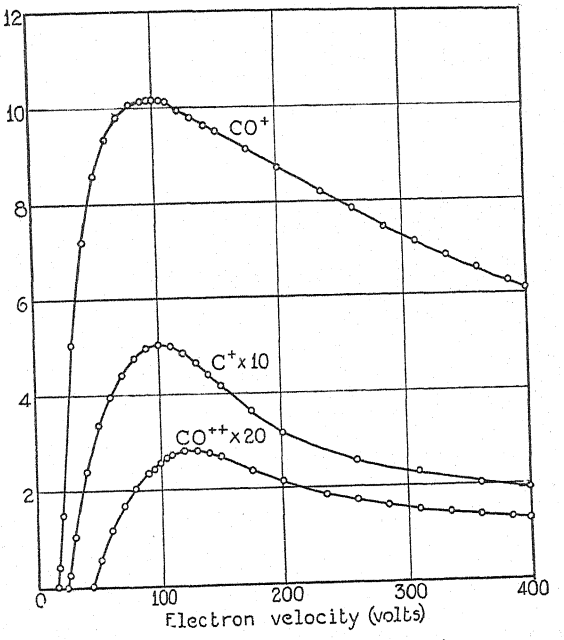


Fig. 7. Number of ions, N, formed per electron per cm path per mm pressure at 0°C.

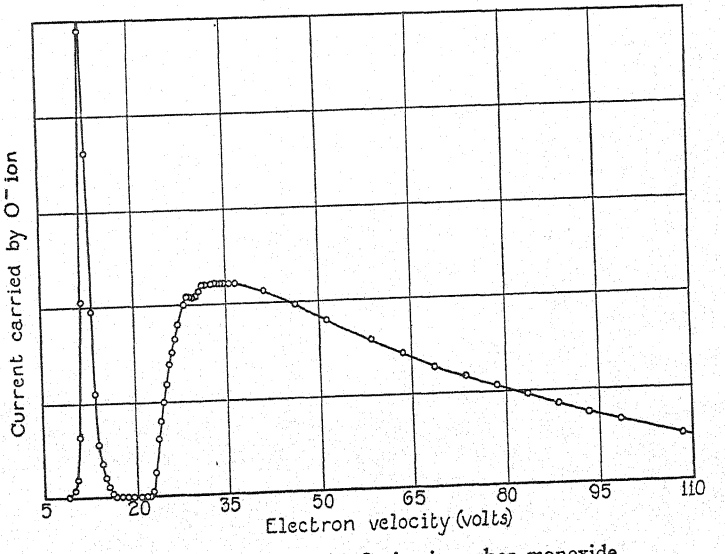


Fig. 8. Current carried by O^- ion in carbon monoxide.

and increased to a maximum at 33 volts and then dropped off gradually as the electron velocity was increased. These voltages given are accurate only to

within a volt since the correction had to be calculated rather than determined experimentally. Fig. 8 was obtained by plotting the maximum height of the O^- peak in the analyzer as a function of the electron velocity. If the O^- ion formed at 9.5−16.5 volts has no kinetic energy and if the one starting in at 22.5 volts does have kinetic energy then the relative heights of the two parts of the curve are not accurate. In this case the second part would be too small. The dip in the curve at 29 volts appeared consistently. This break was also detected by another method[6] in this laboratory. It may be that this dip is associated with the break found at 30 volts in the C^+ ionization potential curve. The O^- ion was found to be only 2.7 percent as numerous as the C^+ ion at an electron velocity of 30 volts.

Discussion of results in carbon monoxide.

The value of 13.9 ± 0.2 volts as given in this paper as the ionization potential of CO agrees with that given by Hogness and Harkness[4] but may be in error as mentioned before. Birge[12] gives a calculated value of 14.2 volts. In a private communication Mulliken gives the most probable value of the heat of dissociation of CO as 9.8 volts. With the value given by Hopfield[13] of 11.2 volts as the ionization potential of the carbon atom the minimum electron velocity at which the C^+ ion could appear by the single process $CO \rightarrow C^+ + O + e$ is 21 volts. The appearance of C^+ at 22.5 ± 0.2 volts indicates 1.5 volts kinetic energy to be divided between the dissociation products. The value of 22.5 ± 0.2 volts is also in good agreement with the value of 22.8 volts given by Hogness and Harkness.[4]

The CO^{++} ion appearing at 43.0 ± 1.0 volts is, so far as the author knows, the first multiply charged polyatomic molecule whose ionization potential has been determined. J. J. Thomson[14] found a doubly charged molecular ion having an m/e of 28 and attributed it to either N_2^{++} or CO^{++}. R. Conrad[15] has identified several doubly charged molecules in the glow discharge of mixtures of methane, oxygen, and water vapor.

The experimental value of 43.0 ± 1.0 volts for the critical potential of $CO \rightarrow CO^{++} + 2e$ indicates that the dissociation products of the doubly charged ion are most likely to be $C^{++} + O$ rather than $C^+ + O^+$ or $C + O^{++}$. If one combines the energy necessary to dissociate CO into C+O which is 9.8 volts as given above with the ionization potentials of 11.2[12] and 13.5[16] volts for atomic carbon and oxygen respectively 34.5 volts is obtained for an assumed dissociation of CO into $C^+ + O^+$. As this is much less than the observed value of 43 volts it does not seem possible that $C^+ + O^+$ can be the correct dissociation products. In a similar way with the 35[17] volts energy necessary to remove the second electron from atomic oxygen one gets 58.3 volts

[12] R. T. Birge, Nature **117**, 229 (1926).
[13] J. J. Hopfield, Phys. Rev. **35**, 1586 (1930).
[14] J. J. Thomson, "Rays of Positive Electricity," 2nd Ed., p. 84 (1921).
[15] R. Conrad, Phys. Zeits. **31**, 888 (1930).
[16] J. J. Hopfield, Astrophys. J. **59**, 114 (1924).
[17] R. A. Millikan and I. S. Bowen, Proc. Nat. Acad. Sci. **13**, 531 (1927).

for the energy necessary to dissociate CO into $C+O^{++}$. Since it seems unlikely that the dissociation energy of CO^{++} can be as high as $58.3-43\backsimeq 15$ volts, and since in the formation of CO^{+} the dissociation products were found to be $C^{+}+O$ and not $C+O^{+}$, the dissociation of CO^{++} into $C+O^{++}$ is very improbable. The dissociation into $C^{++}+O$ requires 9.8 $(CO\rightarrow C+O)+11.2(C+O\rightarrow C^{+}+O+e)$[12] $+24.3(C^{+}+O\rightarrow C^{++}+O+e)$[17] $=45.3$ volts which shows that the heat of dissociation of the CO^{++} ion cannot be less than from 2 to 3 volts.

The only thing to be said about the O^{-} ion at the present time is that its first appearance is probably due to an attachment of an electron to a CO molecule followed by the dissociation $CO^{-}\rightarrow C+O^{-}$. The fact that it appears only over a small range of electron velocities lends support to the above interpretation. The second appearance may be due to a splitting up of $CO\rightarrow C^{+}+O^{-}$. The negative ion will be discussed by Lozier.[6]

It is a pleasure to acknowledge the constant interest and timely suggestions of Professor John T. Tate and the many helpful discussions with Drs. W. W. Lozier and P. T. Smith.

THE EMISSION OF NEGATIVE IONS UNDER THE BOMBARDMENT OF POSITIVE IONS

By K. S. Woodcock
Ryerson Physical Laboratory
University of Chicago

(Received September 11, 1931)

Abstract

The results which Sawyer obtained from the reflection of lithium ions from reflectors of platinum foil and nickel crystal deposited on tungsten, indicated two distinct angles at which reflection occurs more strongly than at other angles, one coming nearly at the angle of specular reflection as found by Read and Gurney, and the other which appeared only at relatively high voltages, at an angle approximately normal to the reflecting surface. Experiments made by reflecting the lithium ions from a metal surface in a field free space gave the bundle at the specular angle as before, but no trace of a bundle at the normal to the surface could be found. When a field is applied so as to retard reflected positive ions there was evidence of negative emission coming from the target under the bombardment of lithium ions. A magnetic analysis system was set up to determine the nature of the negative charges. Negative fluorine, chlorine, oxygen and sulphur ions were obtained by bombarding NaF, CaF_2; NaCl, CaO, PbS and oxide-coated vacuum tube filaments. Clean metal targets of platinum, gold, aluminum, tantalum, nickel, and tungsten were found to emit electrons and the negative ions H_1^-, H_2^-, OH^-, and Cl^- with traces of what is probably N^- and $LiOH^-$. The strongest bundles were the first four which indicate that water-vapor molecules were broken up into their components.

Introduction

THE results which Sawyer[1] obtained from the reflection of lithium ions reflected from reflectors of platinum foil and nickel crystals deposited on tungsten, indicated two distinct angles at which reflection occurs more strongly than at other angles, one coming nearly at the angle of specular reflection as observed by Read[2] and Gurney[3] and the other, which appeared only at relatively high voltages, at an angle approximately normal to the surface of the reflector. This latter beam was observed when the reflection took place in strong electrostatic field. The present investigation developed out of a further study of this normally reflected beam. It was suspected from these experiments that the observations were complicated by a new type of emission, namely the emission of negative ions from metal surfaces under the bombardment of positive ions. The second part of the paper describes a direct investigation of this new phenomenon and gives an analysis, by the methods used for positive rays, of the types of negative ions obtained in this way.

Part I

The tube used in the first experiments on reflection of positive ions by metals was the one described by Sawyer modified somewhat as shown in Fig.

[1] R. B. Sawyer, Phys. Rev. **35**, 1090 (1930).
[2] G. E. Read, Phys. Rev. **31**, 629 (1928).
[3] R. W. Gurney, Phys. Rev. **32**, 467 (1928).

1. In this a strip of platinum foil F carrying a small crystal of spodumene on a constricted portion served as a source of positive ions when heated electrically. After heating to a yellow heat for several minutes the emission is practically all lithium ions. These ions are drawn to the drum D by a potential applied from the outside of the tube. The collector C was a small Faraday chamber subtending an angle of about 9 degrees from the target T. It was supported by a stiff wire insulated from the rest of the apparatus. Connection to the electrometer was made through very flexible nickel ribbon wound like a clock spring. The whole collector system was very carefully shielded from any possible ions escaping from the filament by enclosing the collector in a hood, and by a disk which covered the end of the cylinder H and extended beyond the guard ring G. The collector and cylinder were rotated on a common axis by means of an electromagnet applied from the outside to the arm-

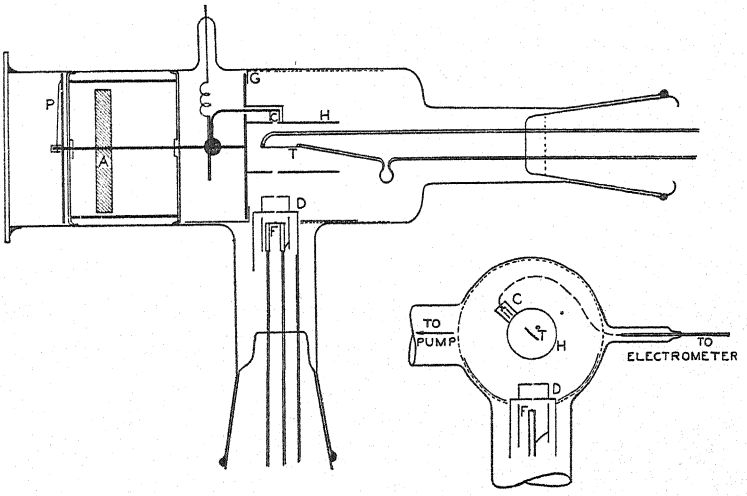


Fig. 1.

ature A. The angle reading could be made through the Pyrex window with the pointer P on the scale.

The target T on which the lithium ions fell, was a strip of platinum foil about 0.3 cm wide and 1 cm long. It was held in place by two leads, one of which was flattened and bent to serve as a spring to keep the target taut. The other was placed behind the target to reduce field distortion. A piece of nickel gauze was put over the slit in the cylinder H in the region of the collector in order to reduce the distortion of the field.

As the target and filament had to be changed frequently two ground joints were used, that were sealed by a ring of picein cement about the outer edge. No difficulty was experienced with contamination of the target, as it was kept at a low red heat throughout the observations.

To examine the reflection in its simplest form the ions were allowed to strike the target in a field free space. This was done by applying an accelerating potential between the filament and drum, and the retarding potential be-

tween the cylinder and collector. When the positive ions were reflected in a field free space the peak at the angle corresponding to specular reflection appeared as before, but no trace of a peak at the normal could be found. This was true in the apparatus used by Sawyer, and also in the modified form which differed only in the use of a Faraday chamber as a collector, which was shielded in front by a nickel gauze in order to avoid all electric fields in the reflecting chamber. In the case of Sawyer's experiments the potential was applied partly between the filament F and the drum D and partly between the cylinder H and target T, the drum and cylinder being at the same potential. The cylinder to target potential served as an accelerating voltage for the incident ions, and at the same time as a retarding potential for the same ions after reflection.

It was also found that when the gauze was put over the slot in the cylinder, and a retarding field for positive ions was applied between the target and cylinder, there was evidence of negative charges coming to the collector when it was nearly normal to the target. In one instance a negative potential of 28 volts had to be applied to the collector to prevent it from collecting negative charges which are then presumably deflected into the gauze. Since the specular bundle remained positive as before, it is reasonable to assume that the negative ions were formed on the target and accelerated to the cylinder by the field that retarded the reflected positive ions.

To compare the sharpness in angle of a beam of ions liberated at the target with the negative beam actually observed, a bit of spodumene was put on the target and heated. With no accelerating voltage some of the positive ions found their way to the collector, but with a few volts accelerating potential a very narrow intense beam was observed. This indicates that the field at the surface of the target is normal to it and is strong enough to form a beam strongly concentrated in the normal direction.

Attempts to eliminate the negative charges, obtained by bombardment of the target, by putting an electromagnet around the tube in such a way as to deflect them away from the collector were unsucessful. The nickel shields may have weakened the magnetic fields to a certain extent but the insensitiveness of the negative charges points to the emission being ionic rather than electronic in nature.

Although we may explain the negative charges observed near the normal to the target as due to secondary negative ions set free by bombarding positive ions, the reflected positive ion bundle which Sawyer observed is more difficult to explain. Since the beam occurs only when the field is strong inside the cylinder the concentration of the ions at the normal is probably due to the field itself. It may be that, since the target is wide in comparison to the diameter of the cylinder, the lines of force are in such a direction that ions reflected from the center of the target would be reflected specularly, while those striking the target nearer the edges would be drawn toward the normal, after reflection, by the field.

PART II

To identify the negative charges freed from a metal surface by positive ion bombardment and to see whether they are electrons or ions a Dempster[4] magnetic analysis system was set up as shown in Figs. 2 and 3. A filament F coated with spodumene was made positive with respect to the target T supported above it. Any negative ions formed at the target would be accelerated downward by this same potential. Some of them would go by the edge of the filament and pass through the slit S into the magnetic field. With a stream of ions of the same mass and the same velocity a value of the magnetic field

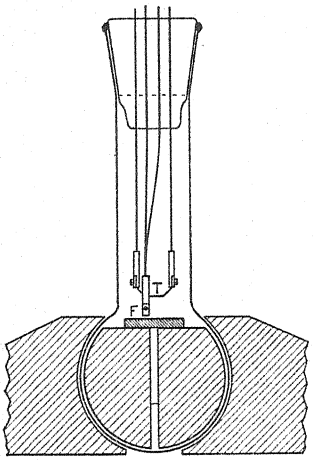


Fig. 2.

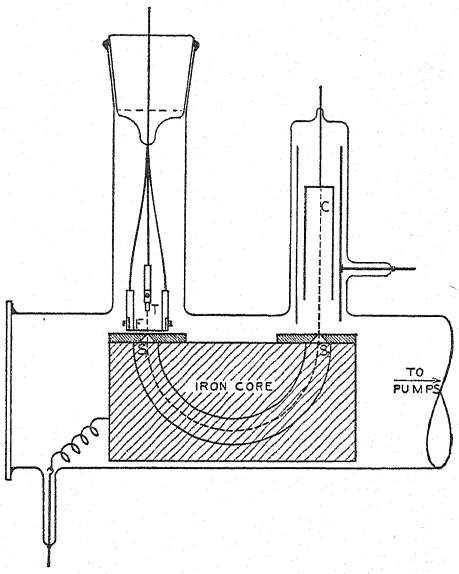


Fig. 3.

could be found that would deflect them through a semi-circle and allow them to pass out through the other slit S to the collector C.

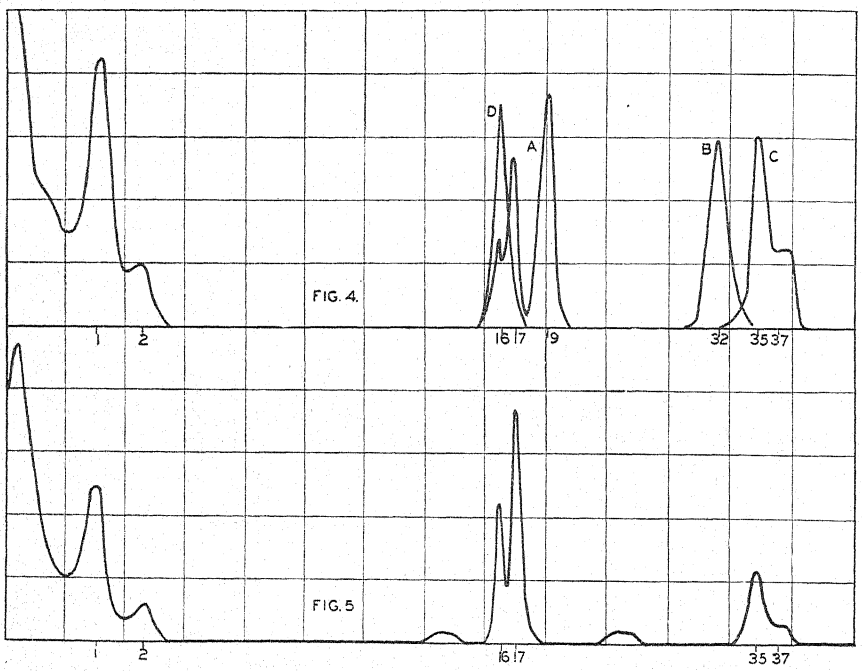
The first results with the apparatus gave a considerable negative ion emission, but the resolution was not good enough to separate definite ion bundles. At this time the experiments were interrupted, but Dr. J. S. Thompson kindly undertook to carry out the analysis of the ions. He introduced some improvements in the apparatus, such as the shield about the collector, which greatly improved the resolving power. With the improved apparatus he was able to demonstrate the emission of negative ions and to identify several distinct negative ion bundles.[5]

Experiments were later resumed by the author with the same apparatus to study further the different kinds of ions that may be obtained in this way. To avoid uncertanty in identifying the ions the slits were narrowed to 0.8 mm and the apparatus calibrated by means of positive ions that were accelerated

[4] A. J. Dempster, Phil. Mag. 7 Series 13, 115 (1926).
[5] J. S. Thompson, Phys. Rev. **38**, 1389 (1931).

at various potentials. When heated, spodumene liberates positive ions of lithium, and traces of sodium, and potassium according to other investigators[6] and these ions are brought to the collector successively as the field strength in the iron armature is increased. Assuming the magnetic field to be symmetrical when the magnetizing current is reversed, the mass of the negative ions may be deduced. Later the calibration was checked by the use of negative fluorine ions.

Richardson[7] finds that negative ions are obtained from iodides, chlorides, bromides, and fluorides by heating their salts. Barton[8] found negative ions of mass 33 to be liberated from the oxides of strontiun and barium when heated.



Figs. 4 and 5.

This suggested that electronegative ions might be obtained from the bombardment of their salts by positive ions. The negative ions obtained by bombarding various salts are shown in Fig. 4. The ion intensity is plotted against the magnetizing current. Fig. 4A shows the negative ions obtained by bombarding NaF or CaF_2 with 500 volt lithium ions. The ion at 19 does not appear at all when the platinum target is clean, but appears with great intensity when the target is covered with the fused fluoride salt, thus definitely associating the peak with the negative fluorine ion. The method of applying consists of wetting the surface of the target with a solution of the salt. As the target is

[6] J. L. Hundley, Phys. Rev. **30**, 864 (1926).
[7] O. W. Richardson, Emission of Electricity from Hot Bodies. p. 107.
[8] H. A. Barton, Phys. Rev. **26**, 360 (1930).

slowly heated the water evaporates leaving a fine layer of salt on the target, which can be fused by further heating. CaF_2 could not be dissolved in water but was powdered and the powder dusted on the target with a bit of cotton, then fused by heating. A thick film is undesirable as there may be considerable voltage drop through it. No negative ion emission was obtained by simply heating the target, that was strong enough to observe by the methods used in these experiments.

The ions obtained by bombardment of NaCl fused to the target are shown in Fig. 4C. Considerable intensity was obtained when the target was cold, but in common with other salts, the emission was stronger when it was heated. The ions show the doubling to be expected from the isotopic nature of chlorine and the agreement with 35 and 37 is very good. No chlorine ions were observed when the bombarding ion current was cut off and the target heated only. The method of applying this salt to the target by evaporating a solution of it on the target surface does not work out well in this case, since the salt crystals explode when they lose their water of crystalization. A small hood held over the target effectively holds the escaping crystals until they have been fused. Richardson[7] found that negative ions were obtained by heating manganous chloride that had molecular weights between 59 and 88, showing that the ions were of atomic or molecular magnitude and possibly molecular chlorine. Barton[9] found a few negative chlorine ions from HCl formed either by bombardment with low velocity electrons or from thermal dissociation at a hot filament.

In Richardson's experiments there are no records of negative ions of the elements in the sixth column of the periodic table. Barton[8] thought his ion of mass 33, which was obtained from heating barium and strontium oxides, might be due to molecular oxygen. He found no negative atomic oxygen however as might have been expected. The question as to whether negative atomic oxygen is freed from its compounds under positive ion bombardment was investigated by depositing calcium oxide on a platinum target. On bombarding it with lithium ions the negative ion bundle shown in Fig. 4D was obtained. It could be identified definitely from the calibration curve as having a mass 16. Although molecular oxygen (32) was looked for, no trace of it could be found. The impacting ion evidently frees atomic oxygen which is drawn to the collector before it has a chance to combine with another atom to form a molecule.

When a commercial oxide-coated vacuum tube filament was used as a target, negative ions of atomic oxygen gave a strong peak when the filament was bombarded with lithium ions. Before it had been heated it gave in addition a more intense bundle at mass 17, but this disappeared when the target was heated, leaving only the peak at 16. The oxide coated strip was then activated by heating to a yellow heat for several minutes an applying a potential until a strong emission of electrons was obtained. The negative ion emission from it, by bombardment, then gave the two peaks at 16 and 17 in the same pro-

[9] H. A. Barton, Phys. Rev. 30, 614 (1927).

portions as before it had been heated. This indicates that moisture remains in the oxide coated filaments even after they have been heated to a bright yellow heat and "activated" by drawing electrons from them for some time.

The emission of negative oxygen ions from oxides, by bombardment, suggested that sulphur ions might be obtained from sulphides. PbS was powdered and fused to a clean platinum target, great care being taken not to decompose the substance. When bombarded with the positive lithium ions no effect was produced until the target was heated, then the peak shown in Fig. 4B appeared with a mass 32. No negative ions are emitted when the bombarding ion current is cut off even through the target is hot. Schmidt[10] finds no ions up to a temperature of 450°C by the heating of PbS. We conclude then that the bombardment of lithium ions dissociates the hot sulphide and frees negative ions of sulphur.

When ever any of the substances examined were bombarded with positive ions we get in addition to their characteristic ion bundles several distinct peaks as shown in Fig. 4 to the left. The peak nearest the axis is due to electrons and varied in intensity somewhat. The peak at mass 1 was very strong and a much weaker peak appeared at mass 2. These are evidently H_1^- and H_2^- that have been knocked out by the impinging positive ions, probably from water vapor contained in the salts.

From the negative ions, produced as described above, a calibration of the magnet was made which checked approximately with the positive ion calibration, but showed that the magnetic field was not absolutely symmetrical on reversal.

In addition to the clean platinum target used by Thompson targets of aluminum, gold, tantalum, nickel and tungsten were bombarded with positive ions. The negative ion beams emitted by these various metals resemble each other closely, indicating that the emission is independent of the metal of the target. A typical negative ion "spectrum" is shown in Fig. 5. The strong emission near the axis occurs at a field too weak to deflect anything more massive than electrons. The most prominent peaks occur at exactly 16 and 17 and are unquestionably due to O^-, and OH^-. Another strong bundle occurs at mass 1, with a much weaker one at mass 2. Since these two are probably H_1^- and H_2^- and they occur with O_1^- and OH^- in such large quantities in all metals observed, it appears that the lithium ions must strike water vapor molecules on the surface of the target, breaking them up into their components which are drawn to the collector. The fact that the H_1^- and OH^- bundles are stronger than the H_2^- and O^- bundles seems to support such an hypothesis.

The next strongest negative ion beam comes at 35 and 37 and is unquestionably chlorine since the position and shape of the curve is exactly the same as that obtained when the target is coated with NaCl. Just as any fresh metal will give the characteristic yellow color of sodium when first put in a Bunsen flame, so these negatively charged chlorine atoms appear to be present in all

[10] G. C. Schmidt, Ann. d. Physik 75, 337 (1924).

metals tested. Prolonged bombardment however makes them disappear. The smaller peaks at 13 and 24 to 25 are much less intense. They do not occur at all in metals that are exceedingly pure and have clean surfaces. After the metal has been bombarded for some time they disappear. Probably they are N_1^- and $LiOH^-$.

The negative ions produced by bombardment of metal surfaces are evidently due to contamination of the target or to adsorbed gases. Cl^-, O_1^- and OH^- ions nearly all disappear from targets such as platinum and tungsten when they are heated to a bright yellow heat for five minutes or more. In distinction to this behavior the emission of ions from oxides, chlorides, fluorides and sulphides persists as long as the salt remains on the target.

In the experiments described above the potential between the target and the filament was 500 volts. An attempt was made to find a critical voltage below which the negative ions were not freed from the target by bombardment, but no critical lower potential could be observed. The intensity of the negative ion beam decreased rapidly as the voltage was reduced, but some negative ions were observed as low as 50 volts.

In conclusion the writer wishes to acknowledge his indebtedness and express his appreciation to Professor A. J. Dempster who proposed the problem and whose suggestions for its development have been invaluable. The writer also wishes to thank Dr. R. B. Sawyer and Dr. J. S. Thompson for their cooperation and valuable assistance.

THE RESIDUAL IONIZATION IN NITROGEN AT HIGH PRESSURES

By James W. Broxon
University of Colorado

(Received September 22, 1931)

Abstract

The residual ionization in nitrogen at high pressures was measured under conditions existing during a recent investigation of the residual ionization in air, with lead and water shields. As in earlier investigations, the residual ionization in nitrogen was found to be greater than that in air at all pressures. However, at the new high pressures the ionization-pressure curve becomes parallel to the pressure axis, as do the air curves. The explanation in terms of subsidiary radiations excited by the cosmic penetrating radiation in the walls of the ionization chamber serves as well for nitrogen as for air. The new work is discussed in relation to earlier investigations of the residual ionization in air, oxygen, nitrogen and carbon dioxide.

RECENTLY the writer[1] investigated the ionization produced by the cosmic penetrating radiation in aged, dry air contained in a large spherical ionization chamber at pressures up to 170 atmospheres. Earlier investigations[2] of the residual ionization in four gases, air, oxygen, nitrogen and carbon dioxide, over a pressure range extending from 1 to 70 or 80 atmospheres, had shown that within this range the ionization in the former two gases was very nearly the same under corresponding conditions. The latter two gases also yielded nearly identical ionization values, but in these gases the absolute values of the ionization and also the final slopes of the ionization-pressure curves were decidedly greater than in the cases of air and oxygen. Further, the forms of the ionization-pressure curves obtained with nitrogen and carbon dioxide were such as to arouse a suspicion that constant slopes of appreciable magnitude might have been attained. In view of these observations and the essentially constant values of the residual ionization in air measured at the higher pressures in the more recent work, it appeared that a special investigation of the residual ionization in nitrogen at the new high pressures would be of value.

Equipment and Procedure

The nitrogen used was obtained from a commercial concern. It would seem that in the process of purification of the nitrogen by evaporation from liquid air, any radium emanation would be retained in the oxygen and the nitrogen would be particularly free from radioactive contamination. However, in view of the high ionization values formerly observed, the nitrogen was kept stored in cylinders for a period of six months before being admitted into the chamber in which the ionization was measured.

[1] J. W. Broxon, Phys. Rev. **37**, 1320 (1931).
[2] H. F. Fruth, Phys. Rev. **22**, 109 (1923); J. W. Broxon, Phys. Rev. **27**, 542 (1926).

According to a statement by the company manufacturing it, the nitrogen was 99.8 percent pure, with 0.2 percent argon and oxygen. The gas was passed through a long tube containing phosphorus pentoxide and also plugs of glass wool and cotton to remove moisture and dust, precisely as in the case of the high pressure measurements in air. The chamber was washed by admitting and then releasing the gas until, as calculated on the basis of fractional removal, less than 10^{-6} percent of the gas finally investigated should have consisted of air originally in the ionization chamber. However, the gas as it was released from the ionization chamber was analyzed by Mr. K. A. Gagos of the University Department of Chemistry, and was found to contain 0.72 percent oxygen, with no observable carbon dioxide or water vapor. No test was made for argon. Mr. Gagos used a Bureau of Mines[3] apparatus, and estimated his accuracy at 0.02 percent. Subsequent analysis of gas obtained directly from the commercial cylinders, incidentally, showed that some of these had an even greater oxygen content.

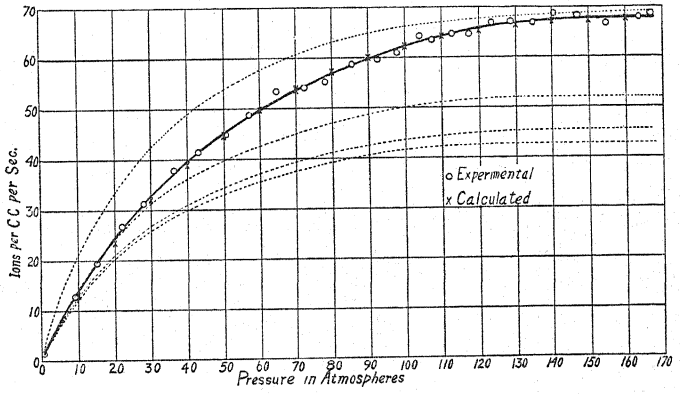


Fig. 1. Residual ionization in nitrogen.

The ionization was measured with precisely the same equipment used in the investigation of air,[1] the location of the apparatus and the method of measurement remaining unchanged. Because of the expense involved, only one series of pressure observations could be made. These were made[4] with the ionization chamber surrounded both by the two-inch lead shield and by the water shield formed by filling the fourteen-foot water tank in the center of which the ionization chamber was located. The series of readings extended over a five-day interval, June 15–19, 1931.

Observations

The observed ionization values are shown plotted against the pressures in Fig. 1. The actual temperatures during the observations varied between 15.35°C and 17.5°C. In order to facilitate comparison with the ionization-pressure curves previously found for air, the pressures were changed to cor-

[3] Bull. Bur. of Mines **42**, 17 (1913)

[4] Measurements of the dielectric constant of the nitrogen at the high pressures were made, also, and will be presented in a later paper.

responding pressures at 18°C, and these are the pressures designated in the diagram. In order further to facilitate comparison, the four curves formerly[1] obtained with air with various conditions as to shielding are represented in the diagram by dotted lines.

Discussion

Notwithstanding the long aging of the nitrogen, the ionization in this gas was again observed to be very considerably higher than that in air under the same conditions. The lowest of the dotted curves represents the ionization in the air under corresponding conditions, with both shields about the ionization chamber. At all pressures at which observations were made, extending from 0.82 to 167 atmospheres, the ionization in the nitrogen was greater than that in the air at corresponding pressures. In fact, the relation between the new high pressure nitrogen and air curves is nearly the same, in the region of the earlier investigation, as the relation between the nitrogen and air curves obtained by the writer[2] at sea level in 1925, these measurements having been made with entirely separate equipment, but with ionization chambers of about the same size and shape. If the ionization in excess of that at atmospheric pressure as observed with the present equipment with both lead and water shields is divided by the corresponding values obtained in the 1925 work with the unlined twelve-inch sphere, the ratio obtained in the case of air increases from 0.29 at 20 atmospheres to 0.30+ at 70 atmospheres, while the corresponding ratio in the case of nitrogen increases from 0.32 to 0.35 in the same region. The ionization in the nitrogen does not appear to have been decreased quite as much as that in air by the heavy shielding, but perhaps this may be accounted for by the fact that the nitrogen used in the earlier investigation was also commercial nitrogen, and no test of its purity was made.

A very significant characteristic of the new nitrogen curve is the very small slope at the high pressure end. Although the ionization at first increases with increase of pressure more rapidly than does that in air, so that the curve approaches that obtained with air with no special shielding, yet the slope continues to decrease with pressure and appears to be quite definitely zero (not exceeding 0.02 or 0.03 ion/cc·sec·atm.) at the high pressure end, precisely as in the case of the curves obtained with air. The region of constant ionization values does not begin at quite as low pressures as do those obtained with air, but it is sufficiently extended to establish definitely the very small value of the final slope. Therefore, on the basis of the explanation of the ionization-pressure relation previously suggested, in terms of secondary radiations excited by the cosmic penetrating radiation in the walls of the container, the ionization measurements made with the two gases now agree in showing an exceedingly small primary ionization due directly to the penetrating radiation. On this basis, however, it would appear that the secondary radiations with nitrogen in the chamber must be somewhat more penetrating and ionize more copiously than in the case of air. The form of the nitrogen curve is better represented by the simple relation derived by the writer[1] in explanation of the observations made in air, than is the case with the air curves. The calculated

values designated in the diagram were obtained by the use of this relation and the assumption that 90 percent of the final maximum ionization was due to radiations of range corresponding to 180 atmospheres in the bomb (roughly 180 diameters of the bomb in nitrogen at atmospheric pressure) and 10 percent to radiations of range corresponding to 50 atmospheres. The final slope of the curve found by differentiating the theoretical expression thus obtained and evaluating the derivative at 170 atmospheres is $dI/dP = 0.003$ ion per cc per sec. per atmosphere.

In the opinion of the writer, the chief discrepancy between the residual ionization measurements in the different gases investigated has been removed by the discovery that at the very high pressures practically no increase of ionization with pressure is observed in either air or nitrogen. The greater absolute values[5] of the ionization in nitrogen are quite striking, however, and deserve consideration. This difference between the magnitudes of the ionization in these gases appears to be well established. As mentioned before, the difference was observed both by Fruth[2] and by the writer in the earlier experiments. Moreover, Fruth separated nitrogen from air and found that the ionization-pressure relation was practically the same as in commercial nitrogen, although the nitrogen he prepared contained 4 percent of oxygen. However, when he mixed nitrogen and oxygen in the proper proportions to form air, he observed the same ionization-pressure relation as in air (and oxygen), with the exception of the sharp breaks and the horizontal portions of the curves which he observed at about 53 atmospheres and which have not been verified by the later experiments. Very recently, Professor A. H. Compton discussed with the writer some unpublished work which he has been carrying on. He, also, has observed the constancy of the residual ionization at high pressures, and that the ionization in nitrogen is greater than that in air.

That the difference in absolute values might be due to a radioactive gas in the nitrogen seems very unlikely in view of the precautions taken. Moreover, that it might be due either to this cause or to a spontaneous disintegration of the nitrogen seems unlikely in view of the forms of the ionization-pressure curves. In such a case the ionization would be expected to increase with the density of the gas. Not only does the ionization in each gas fail to increase beyond a certain amount, but the pressure-rate of divergence between the corresponding curves for nitrogen and air, although nearly constant up to about 70 atmospheres, gradually decreases at higher pressures, and the two curves become practically parallel and horizontal at pressures above 140 atmospheres. If the explanation of observations in terms of subsidiary radia-

[5] An observation contributing to the establishment of the fact that the differences among the curves obtained with different conditions as to shielding in the recent investigation of the residual ionization in air at high pressures were due solely to the differences in shielding, was unintentionally omitted from the report (reference 1) of that investigation. The air remaining in the chamber at atmospheric pressure after a series of observations with a particular shield was kept enclosed until the succeeding shielding had been arranged. In each instance the ionization measured under these circumstances was the same as that measured in the new supply of air at atmospheric pressure at the end of the succeeding series of observations.

tions from the walls of the chamber is accepted, the differences among the residual ionization values in the four gases investigated suggest the possibility of the production, whenever sufficient free oxygen is present, of some surface condition causing an appreciable absorption of the subsidiary radiations.

Although the difference between the final values of the ionization in air and nitrogen is very considerable in comparison with either of these, being 59 percent of the maximum ionization in air, it is perhaps worth remarking that the difference is after all a rather small quantity in view of the high pressures; a little more than 25 ions per cc per sec. at 167 atmospheres, the difference amounts only to about 0.15 ion per cc per sec. per atmosphere. At the local atmospheric pressure, the difference between the ionization values is of the order of 0.1 ion per cc per sec.

Grateful acknowledgment is made of the assistance provided by Professor S. L. Simmering and Mr. C. A. Wagner who carefully compressed a portion of the nitrogen to twice the commercial pressures, and by Mr. Louis Strait and Mr. Raymond Jordan who assisted with the recording of observations.

THE DOPPLER EFFECT IN THE CANAL RAYS IN NEON

W. ROMIG
RYERSON PHYSICAL LABORATORY, UNIVERSITY OF CHICAGO

(Received September 21, 1931)

ABSTRACT

The neon spectrum in the ultraviolet between 2500A and 4000A from a canal-ray tube was examined for Doppler effects. Potentials up to 24,000 volts were applied to excite the discharge. Doppler effects were found to be present among the stronger lines in the first and second spark spectra of neon and, with only two exceptions, were absent from the arc spectrum lines. About fifty strong and faint lines showing Doppler effects were observed. The canal-ray stream consists of rapidly moving neon atoms which radiate only when in the ionized state. Neon behaves similarly to argon at high voltages and differs from most gases in that the radiation from the canal rays is almost entirely from atoms in the ionized state.

INTRODUCTION

DOPPLER effects among optical frequencies have been well known to exist in certain lines of the line spectra of various gases since Stark's[1] discovery of the effect in 1905. Dorn,[2] working with neon in 1908 obtained several Doppler effects among the strongest lines in the region of the spectrum between 6000A and 7000A. It was thought of interest to photograph the neon discharge in the ultraviolet to find if Doppler effects exist in the region from 2500A to 4000A, and if possible, to find some correlation among the lines showing the effect.

The observations of Friedersdorff[3] with argon show that with potentials above 36,000 volts only the lines of the blue spectrum show Doppler effects, while below that voltage the lines of the red spectrum show small Doppler effects. The neon spark spectra have recently been discovered[4,5] and analyzed[6] and it is of interest to find out the state of ionization of the luminous neon atoms in the canal-ray beam.

APPARATUS AND PROCEDURE

The essential feature of the apparatus consisted of a discharge tube constructed as shown in Fig. 1. The main tube was of Pyrex glass about fifty centimeters long. The cathode, for which the purest commercial aluminum obtainable was used, was made in the shape of a thin disk perforated by a small hole at the center. The anode, also of aluminum, was in the form of a hol-

[1] J. Stark, Phys. Zeits. **6**, 892 (1905).
[2] E. Dorn, Phys. Zeits. **10**, 614 (1909).
[3] K. Friedersdorff, Ann. d. Physik **47**, 737 (1915).
[4] T. R. Merton, Proc. Roy. Soc. **A89**, 447 (1913).
[5] L. Bloch, E. Bloch, and G. Déjardin, Journal de Physique et le Radium **7**, 129 (1926).
[6] T. L. de Bruin, C. J. Bakker, Zeits. f. Physik **69**, 19 (1931).

low cylinder welded to tungsten for sealing through the Pyrex. The main tube extended about seven centimeters beyond the cathode where it was ground flat to accomodate a fused quartz window for end on exposures. Midway between this end window and the cathode a side tube projected normally two centimeters beyond the main tube. A fused quartz window covered this side tube permitting photographs to be taken of the canal rays in a direction at right angles to their motion. A moistened cotton pack around the window seals served to prevent the sealing wax from softening during operation of the tube.

To prevent sputtering beyond the cathode in the region of the windows, a perforated glass disk slightly smaller than the inside diameter of the main tube was slipped into position about five millimeters from the cathode and held there by projections from a phosphor bronze strip encasing the disk. The canal rays passed through the coaxial holes in the cathode and disk and impinged upon the end window. With this arrangement there was very little sputtering beyond the cathode.

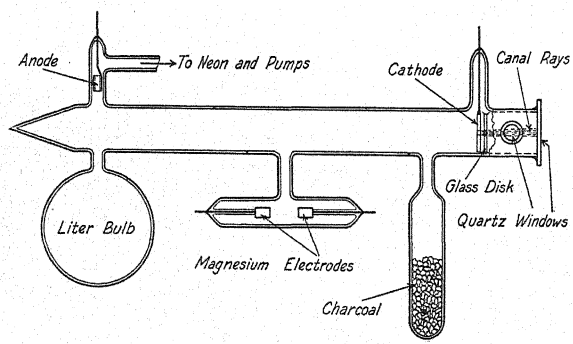


Fig. 1. Discharge tube used for observation of canal rays in neon.

The main tube was connected near the anode to the pumps and to the neon supply. The pumps were operated while the glass walls, electrodes, and charcoal trap were being outgassed. To aid in purification, magnesium electrodes in a side tube were heated until some of the metal evaporated. With the deposition of a magnesium coating upon the walls around the electrodes, the whole tube system became very "hard." The charcoal trap which had previously been heated dull red was next cooled and immersed in liquid air. Neon was then admitted into the tube. After several flushings with the discharge passing between the aluminum electrodes the neon was found to be very pure and could be maintained so for five or six hours provided liquid air was kept constantly around the charcoal trap.

At the low pressure most desirable for operation, the neon "cleaned up" rather rapidly requiring renewal from the supply. A liter bulb sealed to the main tube served to increase the amount present at any one time. With the tube connected always to the pumps and neon supply it was possible to add neon as desired. Small amounts, after having the mercury vapor condensed in the trap shown in Fig. 2, were let into the discharge tube.

The pressure most favorable for producing a sharply defined canal ray-stream was found to be just slightly higher than that pressure at which the discharge failed to pass with a potential of twenty-four thousand volts. To maintain this pressure neon was added at about hourly intervals.

The electrical circuits external to the discharge tube and the positions occupied by the spectrograph with respect to the tube are shown in Fig. 2. The high voltage necessary for operation at low pressures was supplied by a transformer in conjunction with a kenotron tube for rectification. The cathode was grounded. A calibrated spark gap was placed in shunt across the electrodes, and during exposures this was set so that the highest tube voltage would be twenty-four thousand. Except by observation of the discharge during exposure, no provision was made to prevent the potential difference across the tube from falling below any definite minimum value. Previous observations at various low pressures showed how the appearance of the discharge and particularly of the canal ray stream varied with the potential difference across

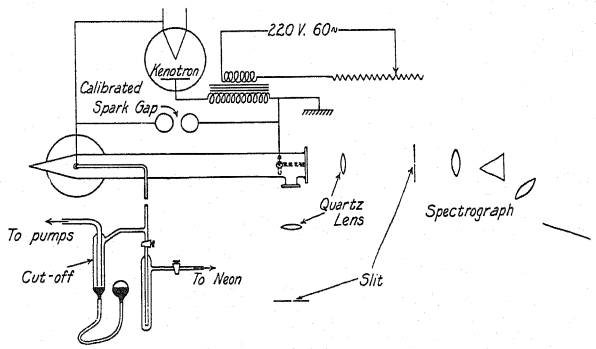


Fig. 2. Diagram showing electrical circuits, method of admitting mercury-free neon, and the spectrograph.

the electrodes, and during operation only such a small amount of gas was allowed in the tube as to produce an appearance corresponding to a voltage nearly twenty-four thousand. At this voltage the velocity of neon atoms calculated from the relation $Ve=\frac{1}{2}mv^2$ is about 5×10^7 cm per second.

Photographs were made with the type E 3 Hilger spectrograph. This instrument is fitted with a quartz lens and prism system throughout, and gives a dispersion of about ten Angstroms per mm at 2600A, and thirty-five angstroms per mm at 4000A. The spectrograph slit width was between two and three hundredths mm, being slightly wider for the side exposures where the intensity upon the slit was less.

For end on exposures a quartz lens focussed the image of the hole in the cathode upon the slit. Exposure times of three hours in this position produced on the plates all except the faintest neon lines throughout the portion of the spectrum under investigation. Side exposures required double this time. Eastman 40 plates were used for all exposures.

RESULTS

Both the end on and side photographs were made on the same plate with the spectrograms close together for comparison. The spectrograph was

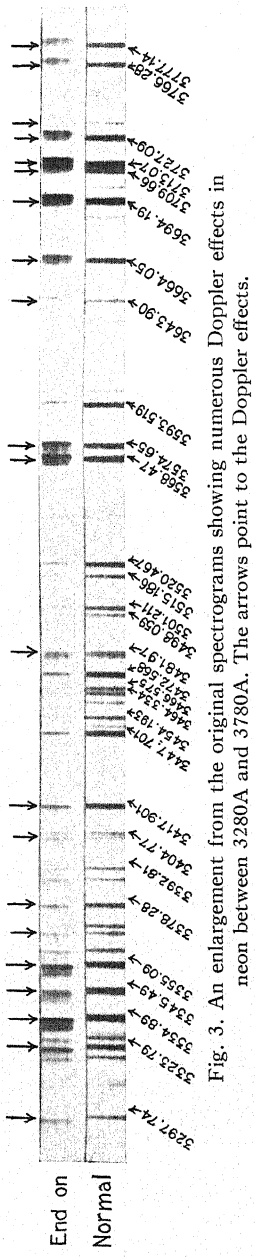


Fig. 3. An enlargement from the original spectrograms showing numerous Doppler effects in neon between 3280A and 3780A. The arrows point to the Doppler effects.

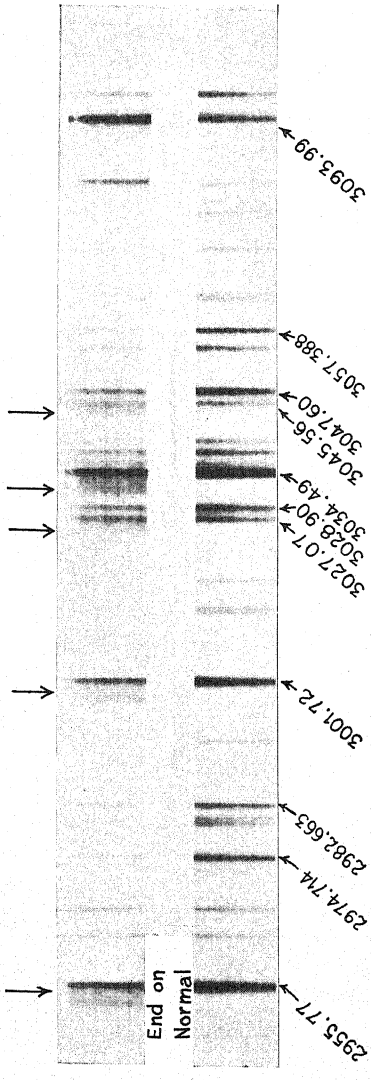


Fig. 4. An enlargement from the original spectrograms showing several Doppler effects in neon between 2950A and 3100A.

equipped with a scale which gave approximate wave-lengths and facilitated identification of the lines.

Fig. 3 shows an enlarged portion of the original spectrograms with numerous Doppler effects indicated by arrows. The broadening in the end on spectrogram is toward the violet since the canal rays were moving toward the slit. In the end on spectrogram of Fig. 3. there are a number of rather sharply defined arc lines indicated (3447.701, 3454.193, 3464.334, 3466.575, 3472.568, 3498.059, 3501.211, 3515.186, 3520.467), for which the effect is clearly absent. Other Doppler lines exist in the end on spectrogram with less intensity than some of these arc lines. It is apparent also that overriding of the Doppler intensity upon other lines occurs where several lines are very close together. In such cases one can generally tell by microscopic examination which of the lines display Doppler effects.

A second enlargement of the original spectrograms between 2950A and 3100A is shown in Fig. 4. The diffuse broadening toward the violet which is quite noticeable in several lines extend over about three and one half Ang-

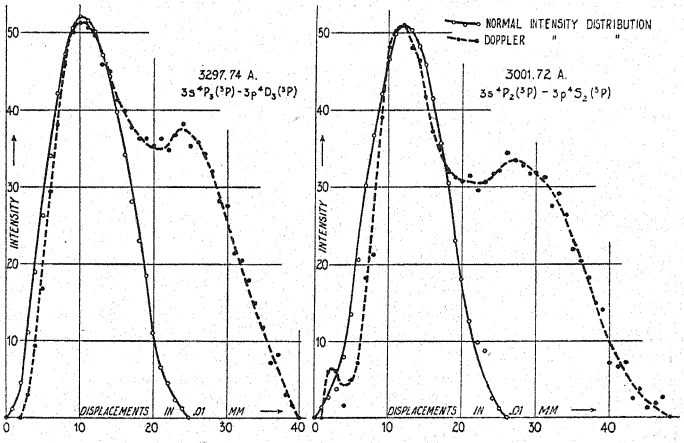


Fig. 5. Curves showing intensity distribution in two Doppler lines as measured by a photoelectric photometer.

stroms. The observed maximum shift is thus only about two thirds the shift one would expect for particles traveling with a velocity of 5×10^7 cm per second, as calculated from the Doppler relation. This discrepancy is commonly observed with ordinary canal rays as the particles fall through only part of the potential applied to the tube.

Photometric measurement of the intensity distribution in several lines was made and the results illustrated in Fig. 5. The photoelectric photometer used was built by Dr. Elmer Dershem, who intends to publish a description of the instrument. A narrow slit about 0.02 mm was moved transversely across a line in steps of 0.01 mm. Intensities were measured by time intervals required for an electrometer gold leaf to move across a fixed portion of eye piece scale. The dashed lines which represent the Doppler lines in Fig. 5 indicate the general trend of Doppler intensity distribution and display the minima which usually exist between the Doppler effects and their undisplaced lines.

The wave-lengths of the lines were identified from Paschen's tables and the tables for the spark spectra of neon given by L. Bloch, E. Bloch, and G. Déjardin. It was at once apparent that, almost without exception, the lines in the first table were accompanied by no Doppler effect lines, while the lines of the spark spectra all showed Doppler effects. The complete list of Doppler effects in neon between 2500A and 4000A is given in Table I. The lines showing the strongest Doppler effects are put in the first column and the lines with

TABLE I. *Doppler lines.*

Strong definite Doppler effects			Faint Doppler effects			Doubtful on account of faintness (F) or overriding (R)		
2792.04	(4)	II	2590.01	(7)	III	2593.57	(6)	III F
2955.77	(7)	II	2610.04	(5)	III	2595.66	(6)	III R
3001.72	(7)	II	2613.41	(4)	III	2615.86	(4)	III F
3027.07	(4)	II	2677.90	(5)	III	2678.65	(3)	III R
3034.49	(5)	II	2756.68	(3)	II	2785.28	(3)	III F
3198.58	(6)	II	2762.97	(3)	II	2794.22	(3)	II R
3218.22	(8)	II	2809.51	(4)	II	3028.90	(4)	II R
3229.58	(3)	II	2835.233	(3)	I	3047.60	(6)	II R
3230.13	(5)		2866.60	(6)	III	3093.99	(4)	II R
3244.15	(5)	II	2910.11	(2)	II	3232.38	(3)	II R
3297.74	(8)	II	2910.44	(2)		3311.32	(4)	II R
3323.79	(7)	II	3045.56	(3)	II	3357.89	(12)	II R
3334.89	(10)	II	3054.70	(5)	II	3360.63	(5)	II R
3344.44	(5)	II	3070.99	(2)	II	3406.88	(5)	II R
3345.49	(3)		3118.00	(4)	II			
3355.09	(7)	II	3164.42	(3)	II			
3367.25	(6)	II	3213.77	(3)	II			
3378.28	(5)	II	3214.33	(5)				
3417.901	(10)	I	3224.84	(5)	II			
3418.002	(6)		3309.78	(3)	II			
3481.97	(6)	II	3319.76	(3)	II			
3568.47	(6)	II	3327.22	(5)	II			
3574.65	(5)	II	3388.47	(5)	II			
3643.90	(5)	II	3392.81	(7)	II			
3644.87	(3)		3404.77	(4)	II			
3664.05	(9)	II	3542.89	(7)	II			
3694.19	(10)	II	3734.94	(17)	II			
3709.66	(7)	II	3751.25	(4)	II			
3713.07	(10)	II						
3727.09	(9)	II						
3766.28	(8)	II						
3777.14	(8)	II						

faint Doppler effects in the second. The third column contains lines where existence of a displaced line is probable but not absolutely certain because of the faintness of the lines or from overlapping of the lines. The number in brackets after each wave-length indicates the intensity of the line and the Roman numerals II, III indicate the first and second spark spectra. Only two strong arc lines were found to show any Doppler effect. These appeared on all plates. In argon it has been shown by Friedersdorff that with potentials greater than 36,000 volts only the lines of the blue spectrum show Doppler effects, while at lower voltages, Doppler effects also appear with the lines of the red spectrum. It is possible that at low voltages Doppler effects might be observed with the arc lines of neon. The analysis of the neon spectrum into

arc and spark lines shows that at the voltages used in these experiments the canal ray bundle in equilibrium consists almost exclusively of singly or doubly charged particles and does not consist of a mixture of positive and neutral particles as in most gases.

No certain indications of several maxima were observed as found in argon by Stark and Kirschbaum[7] and by Friedersdorff. In neon Aston[8] observes singly and doubly charged neon atoms but does not give the relative intensity of the doubly charged atoms. It is probable that there is an equilibrium established between the doubly and singly charged atoms, so that in each displaced spark line there is superimposed a faint intensity from some atoms moving with a higher speed due to their original acceleration as doubly charged atoms.

The author respectfully acknowledges his indebtedness to Dr. A. J. Dempster, under whose direction the work was carried on.

[7] Stark and Kirschbaum, Ann. d. Physik **42**, 266 (1913).
[8] F. W. Aston, Isotopes, 66.

THE VELOCITY SPECTRUM OF NORMAL GASEOUS IONS IN AIR AND THE PROBLEM OF IONIC STRUCTURE

By Leonard B. Loeb and Norris E. Bradbury
Department of Physics, University of California

(Received September 12, 1930)

Abstract

A consideration of the evidence as to the existence of the so called spectra of ion mobilities recently reported by various observers combined with experimental results of the writers indicate that while ions at ages of from 0.5 to 2.0 seconds show marked ranges of mobilities this is not necessarily the case for the normal ions studied over shorter time intervals. It is shown from the recent work of Loeb and the more recent results of Luhr that ions probably consist of one or two molecular addition products of an active type of molecule which pick up the original charged carrier as a result of electrochemical forces depending on the molecular constitution and the sign of the charge. Such products may be present in traces as impurities or may be produced in air by the ionizing agent. The rate of formation of the velocity spectrum therefore will depend on the relative stability of the various ion addition products and the relative and absolute concentrations of the active molecules. Hence the appearance of such a spectrum will vary with the age of the ions and the experimental conditions. It is believed that the greater portion of the lowering of the mobility of the ions below the theoretical value deduced by the assumption that the neutral molecules are not attracted by the ions is due to the usually assumed force of dielectric polarization as utilized in the complete Langevin equation. While the law utilized is not accurate for close approach of ion and molecule (i.e. to one or two atomic radii) it suffices at greater distances. The effect of the electrochemical combinations mentioned above are superposed on this general attraction and lead to an explanation of the differences of positive and negative mobilities and to the three fold lowering of the recombination coefficient on long aging without a very significant (10 percent) change in the ionic mobility recently observed by Luhr and Bradbury.

Introduction

IN A recent article one of the writers (Loeb)[1]* pointed out the necessity for a decision on the question of the reality of the existence of what might be termed a spectrum of mobility among the normal positive and negative gaseous ions. In recent years there have been many papers which on various grounds indicated the possibility that the gaseous ions usually measured had instead of a unique mobility a sort of distribution curve of mobilities confined between narrow limits and centered about some more probable value.[2,10] The *critical* study of the problem has however been confined to but a few observers.[11,12] The diverse results obtained and conclusions drawn, (extending from the notion of a large number of separately resolved mobilities[3,5] through the notion of a continuous band or spectrum of mobilities[6,7,8,10,11,12,13] down to that of a unique mobility,[1] have indicated the existence of a lack of

* Numbered references appear in bibliography on page 1728.

critical control in some cases. They have further indicated a rather wide range of experimental conditions sometimes offering obstacles to any careful critical investigation and at other times causing such a real difference in physical conditions as to make a comparison of conclusions impossible.

In view of the fact that the experimental work of the writers' appeared at least in part to be in conflict with the very careful work of Zeleny[11] and of Fontell[12] a critique of the writers' work was undertaken with results which will constitute a portion of this paper. The conclusions reached from this analysis together with other recent results including those of Luhr[14] make possible a general interpretation of the nature of gaseous ions which serves to clarify a number of hitherto obscure points. It is the purpose of this paper to present these results and conclusions.

The Existence of a Mobility Spectrum

A. Previous investigations

The first notion as to the existence of mobility spectra among the ions doubtless arose in the study of the slow or Langevin ions whose heterogeneous nature led to the observation of such spectra.[2,3,4] The application of this concept to the case of normal ions in air doubtless began as a result of more recent modifications of the air blast methods to normal ions,[2,3,17,18] although as early as 1915 Haines[13] reported to have observed separate groups of normal ions in H_2. The air blast methods utilized what was assumed to be a narrow slab of ionized air and this when caught on a collector of narrow but finite extent as a result of a transverse electrical field led at once to current-potential, or current-down stream distance curves of such shape and width that the assumption of a spectrum of mobilities was inevitable. No critical study of these curves, however, was made and little significance was placed on such curves until the experiments of La Porte[6] using a sort of Fizeau toothed wheel method. This study which was a pioneer investigation in which a critique of the various sources of error was made gave a continuous spectrum of a wide scope of mobilities in air for both ions. In the method ions generated by alpha particles from an intense polonium source were driven through a region between two plates with constant field and received at the other end by an ion collector. The entrance of the ions into the measuring field and their reception at the collector after the lapse of a given time was regulated by a rotating disk in the apparatus having slits which passed the slits in the entrance and exit ends of the constant field. The variation of ion current to the collector as a function of speed of rotation, or as a function of the constant field, gave curves starting at zero rising to a maximum and falling again to zero. The method in itself was bound to give curves of this sort. The extent of the velocity, and hence mobility, range of ions studied was however such as to indicate that there was a real range of mobilities present. In view of the fact that the range observed by La Porte was markedly greater than that observed by the later observers[11,12] using methods in which the control of disturbing variables is simpler; in view of the impurities present due to large quantities of ebonite and the circulating action of the rotating

shutters on the gas; finally owing to what appears to have been an inadequate correction for diffusion it is doubtful whether too much reliance can be placed on this apparent spread as evidence of a spectrum, although the results appear to point significantly towards the existence of such a spectrum.

Following La Porte's work there have been published two further papers utilizing what is essentially a Fizeau method. In these cases, however, the shutters were electrical instead of mechanical. These are the experiments of R. I. Van de Graaf[19] and of Tyndall, Starr and Powell.[8] Both groups of workers admitted the ions to the constant field and from it to the collecting chamber by means of properly timed alternating potentials, actuated by commutators or transformers. Unfortunately in both these experiments the sharpness of the boundaries of the ionized groups of gases entering the field were limited by the fact that the auxiliary alternating fields used interacted with the fixed driving field through gauzes. Despite certain criticisms leveled at the explanation[21] it is an experimental fact that two fields of opposing sign so interpentrate through the meshes of a gauze, (in ion mobility work large mesh gauzes are generally used because of the high absorption coefficient of finer gauzes for the ions), that the equipotential surfaces may well bulge considerably in one sense or the other through the gauzes. Hence at the zero of time when the ions start moving they do not start at the same level but may have a distribution extending a mm or two ahead of or behind the gauze, depending on whether auxiliary or driving field is the greater. The ions are only able to reach to the equipotential surface during the retarding field and are allowed to accumulate there during that period except for diffusion. Such nonplanar distributions of ions act materially to distort and enlarge the extent of the velocity spectra observed. This difficulty was unquestionably recognized by Tyndall, Starr and Powell, who did not attempt to ascribe too much significance to the width of their ion spectrum.

More recently Fontell[12] in his doctor's dissertation has made a most careful study of the reality of the existence of a mobility spectrum among the ions in air. His work was exceedingly carefully controlled and in principle constitutes a method which is perhaps one of the most sensitive used. In this method a thin beam of x-rays ionizes the air near one plate of a condenser system for a short time interval, the ions being in a field. Thereafter the ionized air is driven by the field to a collecting electrode where the current due to the ions is measured as a function of the time by an amplifying system and galvanometer devised for other purposes by Wassastjerna. Under these conditions the ion group is spread apart by the field in transit so that at first only the fastest ions reach the collector but gradually the slower ones and some faster ones liberated later in the cycle reach the collector. From the record of the galvanometer deflection as a function of time by means of a complicated reduction system, Fontell obtains the actual mobility spectrum of the ions caught. The work carefully corrects for diffusion, self repulsion, width of x-ray beam and similar effects. It covers ages of ions ranging from 0.3 to 4.0 seconds and in this sense coincides well with the ionic age range involved in Zeleny's work.

Another most careful and critical of the recent investigations is that of John Zeleny,[11] using ions in air from the room with water vapor present, an age range of the order of 1 second and an air blast method. In this investigation most sources of error have been critically analyzed with the possible exception of the action of the moving air stream in aspirating more ions (and perhaps a larger spatial extent of ionization) into his chamber than is evident from the measurements. When the spectrum obtained using mobilities is compared to that due to the geometrical considerations and corrections are made for diffusion there is in these ions an unexplained spectral width indicating ions existing in air with mobilities spread from 1.03 to 1.48 for the positive and 1.68 to 2.18 for the negative ions. In view of the fact that the corrections are as great as the observed differences perhaps too much emphasis cannot be placed on the *exact* values of the spread of the spectrum. That there definitely appears to be a spectrum is, however, most significant and it coincides in general extent and for the same ion age with that inferred by Fontell from his data.

B. Investigations of the writers

One of the writers (Loeb) has in the past been one of those who have remained somewhat skeptical of the reality of a mobility spectrum. The recent results of this writer[22] on the change of the mobilities of Na^+ ions with time and certain results in this laboratory to be mentioned have led to a more critical analysis of all the evidence at hand, with the result that this article has been written. The reason for the skepticism lay in the observations of Loeb[23] on mobilities of photoelectrically generated negative ions using the original Rutherford A.C. method under carefully controlled conditions. In this method if ions of a unique mobility k exist the ratio of the A.C. ion current i to the half saturation current i_0 can be deduced by theory to be given by $i/i_0=(V-V_0)/V$, where V is the potential applied to the condenser and $V_0=D/kT$, where T is the half period of the square wave and D is the plate distance. The actual i/i_0 curves obtained experimentally on ordinary dried air in 0.1 second or less, under these conditions agreed so closely with theory that the possibility of the existence of more than a single mobility seemed rather remote. The recent work of Fontell and Zeleny led, however, to an investigation of the resolving power of this method with the following results.

One can assume that ions are generated with mobilities ranging from k_1 to k_2 distributed equally over this range of mobilities. An alternating potential of amplitude V is placed across the plane parallel plates separated by D cm. Ultraviolet light is liberating ions continuously from the one plate at a rate of i_0 ions of all sorts per second. The field driving the ions across D is on for a time T, after which ions liberated too late in the phase, or of mobility too low to reach D are swept out of the space by a strong reverse field. It is now necessary to see how many ions the upper collecting plate will collect as a function of V, T and D. The current i relative to the saturation current i_0 in this case compared with that given for a single class of ions will then give an idea of the resolving power of the method. To make such a comparison one may reason as follows.

If ions are uniformly distributed in a band between k_1 and k_2 (an assumption probably contrary to fact but producing negligible errors as far as this question is concerned) the i_0dt ions emitted in dt seconds will in a time t be distributed over an area $V(k_1-k_2)\ t\ dt$ in the x, t diagram of Fig. 1. Here V is the field strength across the plate S. The fast ions k_1 will be at $x_1=Vk_1t$ and the slowest ions at $x_2=Vk_2t$. The density ρ of ions in this strip dt wide will then be $\rho=i_0dt/V(k_1-k_2)t\ dt$. In the ensuing intervals dt beginning at $t=t$ and going back to $t=0$ the successive areas containing the ions in the $x-t$ plane will present the appearance of the shaded triangle AOB indicated in the Fig. 1. From $x_1=Vk_1t$ to $x_2=Vk_2t$ the ions will be contained in a triangular

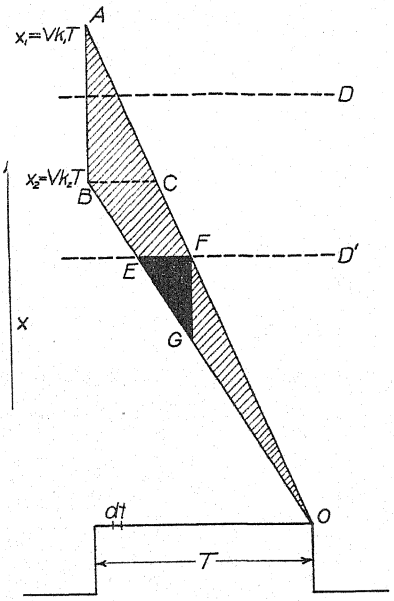


Fig. 1.

element. ABC. Within this element the number of ions reaching a certain distance D will be given by the area of the triangle intercepted between $x_1=Vk_1T$ and $D=x=k_1Vt$. Hence the *initial* increase of charge received by a plate at a point D will be parabolic beginning at a mobility k_1. At a time such that $D=Vk_2T$ all the ions in ABC will have reached D. From then on the number of ions is distributed in the space time diagram inside the triangle bounded by OBC. At any value of x below $x_2=Vk_2T$ the number of ions is constant and equal to i_0. The curve for the quantity reaching D as a function of t between $D=Vk_1T$ and $D=Vk_2T$ is then given by the integral

$$Q=\int_{D/Vk_1}^{T}\frac{i_0(Vk_1t-D)dt}{V(k_1-k_2)t}$$

which includes the density of ions as a function of t.

$$Q=\frac{i_0}{V(k_1-k_2)}\left[(Vk_1T-D)-D\log\frac{k_1VT}{D}\right].$$

As $Q/T=i$ and calling $k=D/VT$ between limits $k_1>k>k_2$ we have

$$i/i_0 = \frac{1}{k_1 - k_2}\left[k_1 - k\left\{1 + \log\frac{k_1}{k_2}\right\}\right] \tag{1}$$

This gives i/i_0 as a function of the variable k between the limits k_1 and k_2. Here k can be espressed as a f (D, V or T) and for each k the i/i_0 can be expressed as a f (V) by calculating the value of k corresponding to each V for D and T constant. Beyond time intervals for which ions of mobility k_1 and k_2 reach D we can express the quantity Q in terms of the area $ABEF$ represented by the smaller distance D' in the figure. This area is the area of the whole triangle ABO less the area of triangle OEF, or better the area of triangle ABO less the area of triangles OFG and GEF. Hence we can write that for a plate D' the quantity is given by

$$\text{Area } ABO = i_0T$$

$$\text{Area } OFG = i_0(D'/k_1V)$$

$$\text{Area } EFG = \int_{D'/Vk_1}^{D'/k_2V} \frac{i_0(D' - Vk_2t)dt}{V(k_1 - k_2)t} = \frac{i_0}{V(k_1 - k_2)}\left(D\log\frac{k_1}{k_2} - D - D\frac{k_2}{k_1}\right).$$

Whence the quantity Q received by D' under these conditions is

$$\begin{aligned} Q &= i_0T - \frac{i_0D}{k_1V} - \frac{i_0}{V(k_1 - k_2)}\left(D\log\frac{k_1}{k_2} - D - D\frac{k_2}{k_1}\right) \\ &= i_0T - \frac{i_0D}{V(k_1 - k_2)}\log\frac{k_1}{k_2}, \text{ whence } i = Q/T, \\ i &= i_0\left(1 - \frac{D}{VT(k_1 - k_2)}\log\frac{k_1}{k_2}\right). \end{aligned} \tag{2}$$

Putting $k=D/VT$ between the limits $k_2>k>0$ we get for the current ratio after the slower ions begin to cross the relation

$$i/i_0 = 1 - \frac{k}{k_1 - k_2}\log\frac{k_1}{k_2}.$$

At $k=k_2$ the Eqs. (1) and (2) are the same. As k_1 approaches k_2 the Eq. (2) becomes $i/i_0=1-D/kTV$ which is the simple equation $i/i_0=(V-V_0)/V$ given above for a unique mobility.

An idea of the resolving power of this Rutherford A.C. method as applied to the case of ions with mobilities lying between $k_1=2.2$ and $k_2=1.6$, as observed by Fontell for negative ions is shown in Fig. 2. There i/i_0 as computed from the above is compared with the curve i/i_0 computed for ions of a single $k=1.9$, the average value. It is seen that the difference is not very marked and the resolving power is small. In Fig. 3 is a typical result, previously published[23] obtained by Loeb for nearly identical conditions for dry air $T=0.0275$ at atmospheric pressure. D was 1.41 cm. in this case and

negative ions from a plane photoelectric source were used. The observed curve in this case shows no asymptotic foot within the limits of accuracy of the method.

As Zeleny[11] correctly points out, these results should have been corrected for diffusion. However, the correction becomes small in time intervals of 0.02

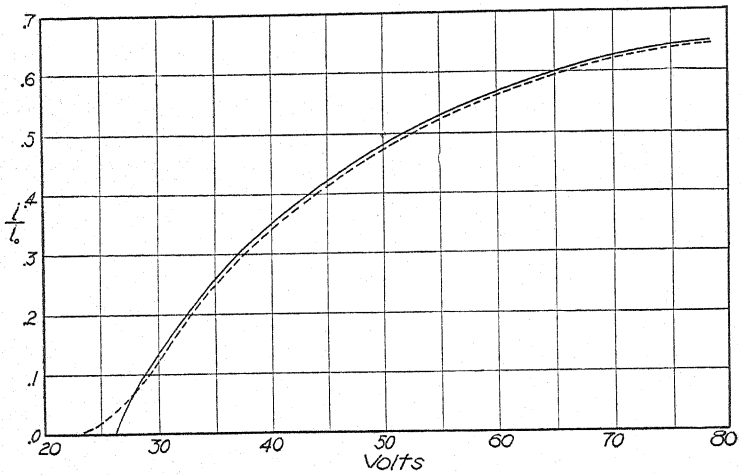


Fig. 2.

seconds and in any case the presence of notable diffusion would have yielded asymptotic feet. This may in part account for such feet at longer times of passage as observed.

It appears from the above that the method as used is a highly insensitive one for indicating the existence of mobilities spread over a more limited range

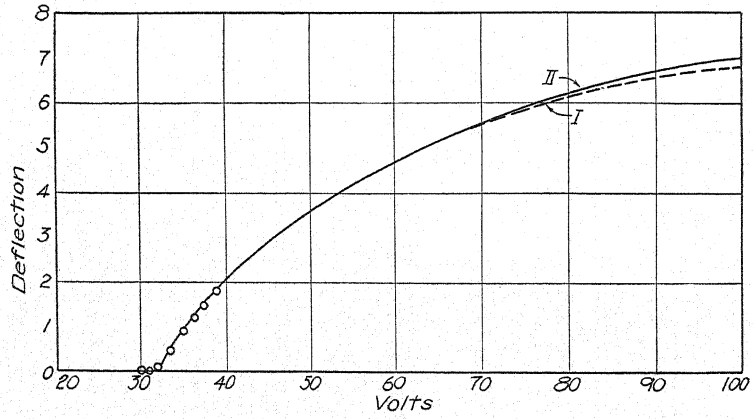


Fig. 3.

of values. Perhaps the best conclusion that can be drawn on the basis of this work is that with *dry air, photoelectric ions* (no great amount of chemical products e.g., ozone and nitric oxides are formed by the ionizing agent) and in *shorter time intervals* the spread of the mobility spectrum is even without

corrections for diffusion distinctly less than that observed by Zeleny and Fontell at *longer* intervals of time and under different conditions.

There is a chance that by using a differential method, i.e., measuring the *current at each instant* during the cycle instead of the *integrated current*, as was done by Fontell, a much more significant result might be obtained. This is, however, at present experimentally impossible. A better result than the one above could be obtained by using an ionizing flash of ultraviolet light which is short in duration compared to T. Such a curve could be analyzed to get the form of the distribution if with very sensitive measurements the derivative of the curves obtained in this fashion were determined graphically. Such an experiment is to be undertaken in the near future.

An almost exact analogue of this proposed method has been carried out by J. L. Hamshere[10] in an admirable investigation. Hamshere used ions generated by polonium and driven into the measuring field by means of an auxiliary gauze and plate in the generating chamber. The apparatus was so arranged that the auxiliary field as used in the Franck modification of the Rutherford A.C. method was put on so that just at the beginning of the phase driving the ions from the origin towards the collecting plate this auxiliary field was put on for but a short time. This gave a burst of ions through the gauze into the measuring field which then was spread into a velocity spectrum by the field. The current reaching the upper plate then depends on the distance D, the duration T of the positive or driving field acting on the ions before the field reversed, and the field V applied. The process is then repeated. This method except for the use of polonium as an ionizing agent and the gauze, instead of a photoelectric source is the one suggested above. However, in spite of Hamshere's use of the high auxiliary field, as had been suggested by the writer,[23] to avoid the effects of the initial displacement of the ions due to interpenetration, (his gauzes had wide meshes of 1 mm) it is most probable that much scattering of the origin of the ions at the beginning of T must have resulted from this procedure. Further the intense polonium ionization as we shall see produces ideal conditions for formation of products which are active on the ions. Again no attempt at correction for diffusion was made. Finally one of the writers in all his work with methods of this type never observed the type of intercepts obtained by Hamshere on the high mobility side of his curves which are neither intercepts of the abrupt type to be expected from unique mobilities, nor intercepts of a truly asymptotic character which would be expected. It appears as if some spurious effect must have subvened to cause these curves. Perhaps this was due to accumulations of ions at the equipotential barriers in the meshes while the reverse field was on. The curves obtained by Hamshere were then graphically differentiated to give the mobility spectrum. In general they agree with the type of curves of Zeleny and Fontell. They appertain, however, to ions of much shorter life than the ions of the latter observers. In view of the conditions mentioned and in view of Bradbury's results to be discussed it appears to the writers that while Hamshere has devised an ideal method in principle, the work should be carried out with the photoelectric

method before too much credence can be placed in an interpretation of these curves as representing a true velocity spectrum of ions over short time intervals.

While the results of Loeb on the absence of a broad mobility spectrum over short time intervals are not entirely convincing, even admitting the possible sources of difficulty in Hamshere's work, the conclusions arrived at are substantially borne out by recent work of Bradburg[16] using the method of Tyndall and Grindley.[24]

The mobility of gaseous ions in dry air of considerable purity and also of normal purity has recently been investigated by one of the authors (Bradbury). In these experiments the alternating current method devised by Tyndall and Grindley[24] with intense x-ray ionization was employed. This is a

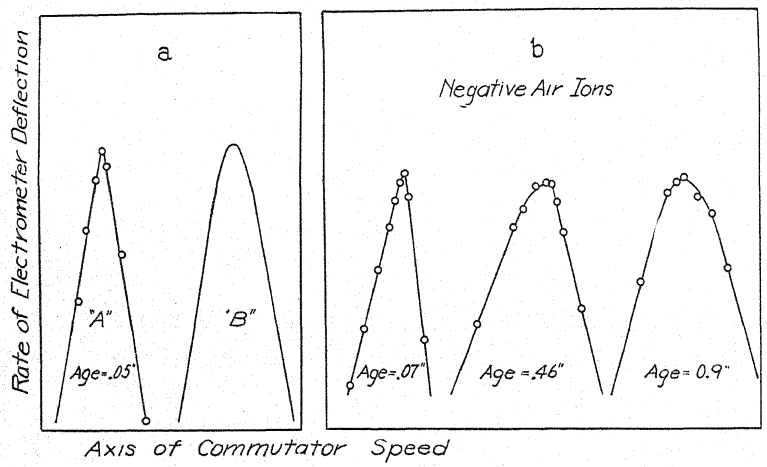


Fig. 4. (a) Curve A is a typical curve for positive ions of age equal to 0.05'' giving a value for the mobility of 1.60. Curve B is the theoretical curve to be expected if the mobilities were distributed over a ten percent range on either side of the accepted value. (b) A series of typical curves for negative air ions of increasing age, showing the change to a type of curve corresponding to B in Fig. 1 and giving evidence of a spread of mobilities.

"peak" method, and the mobility is calculated from the position of the maximum in the ion current curve as the time of alternation of the field is varied. The mathematical theory of this method has been developed by Tyndall and Grindley. It appears from the integrals relating the ion current to the time of one complete cycle that the sides of the peak should be straight lines, intersecting at a point, by the position of which a mobility is uniquely determined. In practice this is not always the case. Even when new ions are studied, the sharp peak will be slightly rounded off by diffusion, self-repulsion, and other factors arising from the measuring instruments themselves. In addition to this if the time, the time $(\delta-\gamma)T$, of retardation of the ions being measured towards the lower plate is too great, or the position of ionized band between the plates is too near the upper plate, at the higher and lower frequencies of alternation, ions of the opposite sign will begin to reach the upper plate. This causes the measured current to decrease more rapidly than

that predicted by the simple Tyndall and Grindley equations and an outward curvature of the sides of the peak results. Since the curving was never found to influence the position of the maximum, no great care was taken to avoid this condition in the effort to obtain ion currents of measurable intensity. However, by varying the conditions of δT, V_r, and the slit width (width of ionized beam) the sides of the curve could be made quite satisfactorily straight as seen in Fig. 4. It seems in view of such curves of interest to consider the resultant shape of the Tyndall-Grindley curve should there be a distribution of mobilities between certain limits. In other words, it is important to see what the effect of a continuous distribution of mobilities will be on these curves. This can be accomplished by testing the effect of a range of mobilities on the curve shape; a result which can most easily be accomplished, in view of the integrals involved, by a graphical method which sums the ordinates of a series of individual curves over the range of mobilities involved. When this is done we obtain a curve of the shape shown in Fig. 4 a curve B. Curve A is an experimental curve recently obtained in pure air with x-ray ionization for positive ions of age equal to 0.05 seconds. By combining a series of curves of this shape distributed uniformly over a range ten percent greater and ten percent less than the accepted value (a smaller range than was found by Zeleny) curve B was obtained. With sides of the same slope, the rounded top is very apparent. Fig. 4b shows a series of experimental curves for negative ions in less pure gas taken on ions of increasing age, as shown. Comparing these curves with that of Fig. 4a it seems very apparent that ions of age less than 0.08 do not have a spread of mobilities as great as that chosen.

The curves shown indicate quite strikingly two facts. First the ions of shorter life in pure air *do not appear to show any certain indications of a velocity spectrum of any great extent*, (certainly the range is smaller than 10 percent. Secondly at ages greater than 0.1 second the appearance of a range of velocities is quite definite and becomes more pronounced as time goes on. Again as in all methods the resolving power is too small to indicate the nature of the changes occurring but it is clear that such a real spectrum exists. These results strikingly confirm the conclusions to be drawn from the photoelectric method for newer ions and the results of Fontell and Zeleny on older ions. They disagree definitely with those of Hamshere and the results at shorter time intervals of LaPorte.*

Theoretical Conclusions

That this confirmation should occur is not surprising in view of certain theoretical considerations concerning ions together with recent results obtained by Luhr[14] in this laboratory. Luhr has been studying the ions produced in air, O_2, N_2, and SO_2 and other gases by a Geissler discharge after sorting the somewhat aged ions by means of the method of molecular beams and a positive ray analyzer of the Dempster type. While he has as yet not achieved a

* In a recent paper Zeleny (Phys. Rev. **38**, 969 (1931)) has confirmed the absence of a mobility spectrum in air over the shorter time intervals using an air blast method.

study of the really older ions the facts found in air with *high concentrations of the ionization products of discharge* indicate that as the pressure of the gas increases, especially in air, the ions are predominantly of a higher molecular weight than those at low pressures which consist of O^+, O_2^+ and N_2^+ and O^{3+}, etc. These older ions have molecular weights ranging up to 200. They are not in a continuous group of all masses, but *largely consist of single charged molecules of the reaction products of the discharge*, i.e., oxides of nitrogen, nitric acid and where SO_2 is present even H_2SO_4.

It is clear that in any ionized complex gas such as air all sorts of chemical products must be formed in quantities depending on the nature of the ionizing process. Depending on their electrochemical affinity as shown from studies of mixtures[34] certain of these molecules are strongly attracted to ions of one sign or the other. These compounds or attached molecular ions are formed not by the inverse fifth power law attractions but forces between the charged portions of single molecules due to structural characteristics as worked out by researches analogous to those of H. A. Stuart,[25] C. P. Smyth,[26] C. T. Zahn[27] and others. For example the O atom in ethyl ether is highly negative and should strongly attract and attach positive ions, or the positive atom or molecule can combine with an NH_3 molecule to give an ammonium like ion, while the strongly positive H in the OH group attracts negative ions. Now there must be formed a number of such ion complexes *with not more than one or two molecules attached*, in any gas ionized by x-rays or α-rays, in the measure that active molecules are present, and that probability of reaction and number of impacts of ions with these lead to formation of such complexes. The lower the concentrations of these substances the longer times of sojourn in the gas must transpire for such attachments. In gases as ordinarily studied there will even be competition among various molecules for the ions of a given sign. At first a less strongly attracted but more frequent impurity will win, but with age the more strongly attracted but rarer substances will get a large share of the remaining charged atoms. This action is beautifully illustrated in the aging effects observed by one of the writers' for Na^+ ions in N_2 and H_2, and by the aging effects observed by Erikson[17,31] and the action of water vapor, alcohol and ozone on ions in air as observed by Tyndall[24,28] and his collaborators, Mahoney,[30] Valasek,[29], Hamshere[10] and others.

Thus it is to be expected that while the earlier ions are more uniform in structure, and thus of uniform mobility, aging particularly in gases with many chemical products will lead to the predominance of a greater diversity of the ion structures present, with a consequent spread of mobilities. Hence it is not surprising that in gases like those used by Fontell, Zeleny and one of us over long time intervals with the selective action of recombination in some cases removing the lighter complexes, to find quite a velocity spectrum among the ions. With greater resolving powers of our measuring equipment of course the separation of the ion groups should appear, if the spectrum has not too many components, as in Luhr's apparatus. It is also clear that the distribution of mobilities in such a group must be rather more like that found by Zeleny and others than the uniform velocity band utilized in calculations in this paper.

The Difference between Positive and Negative Mobilities

This assumption of the nature of ions at once clarifies many heretofore disturbing phenomena which have been very hard to understand. To utilize this concept let us first restate the situation. It must, and will be maintained throughout, that the *ions are essentially simple in structure* one charged molecule O_2, N_2, O_3, etc., attached to possibly one and perhaps two, but not more, other molecules of appropriate structure. More than one or two attached molecules would so weaken the bonds, with the space limitations imposed by the attached molecules that they would cease to be effective. These attachments must be considered in the nature of loose chemical combinations caused by structural effects, and *not primarily caused by the inverse fifth power law attractions*. In some active organic molecules of high molecular weight, i.e., with large inactive chains of CH_2 groups the effect of this attachment alone will cause marked diminution of the mobility owing to great increase in ion radius. This has been observed by Tyndall[28] and his collaborators with the alcohols and by Loeb and Dyk[32] with the amines.

In the main, however, the very great lowering of the mobilities, to one-fifth the simple kinetic theory value,[35] are due not to this compound formation but to the *apparent increase of the ionic radius due to the attractive forces of the ionic charges on neutral gas molecules*. The main lowering will therefore be ascribable to dielectric attractive forces of the inverse fifth power law type which must hold fairly well at distances of 10^{-7} cm and greater. For closer approach doubtless the dielectric forces are less and this with our understanding of repulsive forces show why the influence of the actual kinetic theory radius as it appears in Langevin's equation may not be as critical as it appears.[1] That these dielectric forces must be the main factor in reducing ionic mobilities to the observed low values is definitely attested by the fact that this Langevin law alone or even the Loeb-Thomson modification and the Wellisch equation as modified by Loeb,[33] give the correct order of magnitude and nearly correct values for the mobilities of the ordinary ions. Hence the mobilities observed are produced by (1) the dielectric attractions which have superposed on them and (2) the increases in mass and actual physical diameter caused by the one or two electrochemically bound molecules.

Granted this postulate we can at once see that the effect of the sign of the charge on mobilities is not in any way to be ascribed to a difference in the dielectric constant for positive and negative ionic force fields.[36] It must be ascribed to the specific electrochemical combinations which result by reaction of positive and negative ions with molecules present in some gases, the negative ion adding the larger molecule in some gases in others the positive ion doing so. If this is true the whole question of the difference of positive and negative mobilities is simplified and may be even extended to the C. T. R. Wilson cloud chamber experiments. The fact that negatively charged droplets condense to visible size much more readily than do the positively charged drops may not need to be ascribed to more intense dielectric forces on the water droplets in the intense radial fields of the small negative drops than on small positive drops. They can now be ascribed to the fact that the

droplet that has picked up a negative ion has also picked up from the negative ion a more hygroscopic addition product than there exist about the positive ions. Thus a droplet such as Thomson postulates, containing 1000 water molecules, that cannot grow at a given supersaturation because of surface tension forces, in picking up a negative $O_2^-(2\ SO_2)$ ion has besides the compensating charge the vapor tension of 20 N H_2SO_3 solution. This may cause more ready condensation on the negative ion than on the positive ion which has no such addition product.

The Recombination Coefficient

Another problem which is clarified by this viewpoint is the apparent difficulty in the different effects of aging on mobilities and recombination coefficients as observed by Luhr[15] and Bradbury.[16] In the intense x-ray ionization reactive substances are formed in the gas in progressively greater amounts on aging. The faster ions owing to lighter mass recombine quickly and leave the slower ions. Now since those reaction products picked up by ions in air are, as Luhr[14] has observed, atoms not of atomic and molecular weights 16 and 32, but some molecules of molecular weights as high as 200, we can see how the value of the recombination coefficient which is inversely proportional to the square root of the mass of the ion can be reduced without materially changing the mobility of the ions. Thus the reduction of the recombination coefficient with time is not due to the formation of a very large cluster ion which is incompatible with a 10–20 percent mobility decrease, but is due to the attachment of a molecule of greater mass without a very much greater radius: Thus the increase in radius of an O_2^+ ion to that of an $(HNO_3)_2O_2^+$ ion is not as drastic an increase in radius as would be that due to an addition of 8 to 12 O_2 molecules in a monomolecular cluster which are loosely bound by dielectric forces.

It is therefore seen that the recent studies of the velocity spectrum of ions together with other recent work leads to a comparatively simple picture of ionic structure and behavior which from its nature and its simplicity cannot be far from true. It is hoped that the clarification due to this analysis will guide future workers to a means of more quickly and completely establishing the obvious conclusions here made.

In conclusion the writers wish to acknowledge their thanks to Dr. H. A. Stuart for the valuable information which he gave concerning molecular structure as it affects this problem, and to Dr. O. Luhr for permission to anticipate the publication of his results.

Bibliography

[1] L. B. Loeb, Phys. Rev. **38,** 568 (1931).
[2] J. J. Nolan, Proc. Roy. Irish Acad. **35,** 38 (1920).
[3] J. J. Nolan and I. T. Harris, Proc. Roy. Irish Acad. **36,** 31 (1922).
[4] O. Blackwood, Phys. Rev. **20,** 499 (1922).
[5] H. B. Wahlin, Phil. Mag. **49,** 566 (1925).
[6] Marcel, La Porte, Ann. de Physique **8,** 466, 711 (1927).
[7] J. S. Rogers, Phil. Mag. **5,** 881 (1928).
[8] Tyndall, Starr and Powell, Proc. Roy. Soc. **A121,** 172 (1928).

[9] Tyndall and Powell, Proc. Roy. Soc. **A129,** 162 (1930).
[10] J. L. Hamshere, Proc. Camb. Phil. Soc. **25,** 205 (1929); Proc. Roy. Soc. **A127,** 298 (1930).
[11] John Zeleny, Phys. Rev. **34,** 310 (1929).
[12] Nils Fontell, Commen. Physico Mathematicae Soc. Scientiarum Fennica **23,** 7 (1931).
[13] W. B. Haines, Phil. Mag. **30,** 503 (1915); **31,** 339 (1916).
[14] O. Luhr, Phys. Rev. **38,** 1730 (1931).
[15] O. Luhr, Phys. Rev. **35,** 1394 (1930).
[16] N. E. Bradbury, Phys. Rev. **37,** 1311 (1931).
[17] H. A. Erickson, Phys. Rev. **20,** 117 (1922).
[18] W. Busse, Ann. d. Physik **81,** 262 (1926); **82,** 697 (1927).
[19] R. I. Van der Graaf, Phil. Mag. **6,** 210 (1929).
[20] P. Langevin, Ann. Chim. Phys. **8,** 238 (1905).
[21] Morton, Phil. Mag. **6,** 795 (1928).
[22] L. B. Loeb, Phys. Rev. **38,** 549 (1931).
[23] L. B. Loeb, Journal Franklin Inst. **196,** 537, 771 (1923).
[24] Tyndall and Grindley, Proc. Roy. Soc. **A110,** 341 (1926).
[25] H. A. Stuart, Zeits. f. Physik **63,** 533 (1930); **55,** 358 (1929).
[26] C. P. Smyth, Dielectric Constant and Molecular Structure, Chemical Catalog Co., New York, 1931.
[27] C. T. Zahn and J. B. Miles, Phys. Rev. **27,** 455 (1926); **32,** 497 (1928); **35,** 484(1920); **37,** 1516 (1930).
[28] Tyndall and others, Proc. Roy. Soc. **A110,** 358 (1926); **A111,** 577 (1926); **A121,** 185 (1928).
[29] L. M. Valasek, Phys. Rev. **29,** 542 (1927).
[30] J. J. Mahoney, Phys. Rev. **33,** 217 (1929).
[31] H. A. Erikson, Phys. Rev. **33,** 403 (1929).
[32] L. B. Loeb and K. Dyk, Proc. Nat. Acad. Sci. **15,** 146 (1929).
[33] L. B. Loeb, "Kinetic Theory of Gases," McGraw-Hill, New York, 1927, p. 467.
[34] L. B. Loeb, Phys. Rev. **32,** 81 (1928); **33,** 267 (1929).
[35] L. B. Loeb, "Kinetic Theory of Gases," McGraw-Hill, New York, 1927, p. 451 ff.
[36] L. B. Loeb, Phys. Rev. **32,** 94 (1928).

THE MASS OF POSITIVE IONS IN A GLOW DISCHARGE

By Overton Luhr
University of California, Berkeley

(Received September 19, 1931)

Abstract

Preliminary results are presented here in an attempt to determine directly the mass of gas ions in air, N_2, O_2, and SO_2. The ions were formed in a glow discharge, allowed to drift at low velocity through a distance of 2.5 cm, and passed as a molecular beam through a slit 0.01 mm by 5.0 mm where the mass spectrum was analyzed with a positive ray analysis apparatus of the Dempster type. The pressure in the discharge and drift spaces was maintained at 0.1 to 0.5 mm of mercury. The following ions appeared in relatively large quantities: N^+, N_2^+, O^+, N_2^+, O_2^+, O_3^+, SO_2^+, and $H_2SO_3^+$. In addition a smear of heavier ions appeared in smaller numbers, though the intensity was greater in air than in the pure gases and, in air, became relatively larger at high pressures. Peaks corresponding to molecular weights of 56–64, 76, 80, 96, 108, 138, 140, 168 and 200 were the most prominent indicating the presence of such ions as $2N_2^+$, $N_2O_2^+$, $2O_2^+$, $N_2O_3^+$ and heavier combinations. N_3^+ and O_3^+ ions apparently play an important role in gas ion phenomena though the N_3^+ is relatively unstable since it breaks up in the magnetic field into $N_2^+ + N$. In view of the results it seems likely that air ions aged over a considerable period of time are of a complex and heterogeneous nature, due probably to the formation of nitric oxides, while the ions in pure gases remain monatomic, diatomic and triatomic except for attachment to impurities.

Introduction

THE most perplexing problem in the field of gas ions to-day concerns the nature of the ions. As a result of extensive and thorough measurements of such quantities as mobility, coefficient of recombination, and attachment coefficient of electrons the behaviour of ions under various conditions is fairly well known. However, it is often difficult to interpret this behaviour correctly as such measurements do not give any direct or definite answer to the question of the mass and composition of the ions. In some cases gas ions may consist of single atoms and molecules, but it seems likely that in most gases as the ions age they become more complex in nature. This supposition is born out by many mobility experiments such as those of Erickson on the aging of the positive ion, those of Loeb on mobility in mixtures, and more recently the work of Loeb[1] on Na positive ions in H_2 and N_2, and that of Bradbury[2] on aging. Such investigators as Zeleny and Fontell in their recent work on the spread of mobilities have shown quite definitely that at any rate after aging about a second, there must be ions of various sizes and kinds present. The possibility that ions of a molecular weight of several hundred occur after aging a second or more was indicated by the recombination experiments of the writer.[3]

[1] L. B. Loeb, Phys. Rev. **38**, 549 (1931).
[2] N. E. Bradbury, Phys. Rev. **37**, 1311 (1931).
[3] O. Luhr, Phys. Rev. **35**, 1394 (1930); **36**, 24 (1930).

Since all angles of approach to the mobility problem have failed to determine definitely the real constitution of the ions it appears imperative that the mass be measured by a direct method. It occurred to Professor L. B. Loeb that the problem might be solved by forming the ions in a glow discharge and employing the Stern method to determine the velocity spectrum in a molecular beam. After consultation with Professor Stern on the feasibility of the method it was decided that accurate measurement with velocities of the order of a fortieth of a volt would be impossible owing to the presence of unknown contact potentials. Professor Stern suggested however, that the problem might be approached by forming a molecular beam as suggested by Professor Loeb and measuring the distribution of masses with a Dempster type of positive ray analysis apparatus. Since the chance of a collision in a molecular beam is very remote the ions should not break up in the analyzing chamber and the masses present could be determined directly. In all previous positive ray analyses the normal ions would be broken up by low pressures and high fields before entering the analyzing chamber. The conditions in a glow discharge cannot of course be strictly compared to those in a gas at high pressures where the ionization is produced by x-rays, polonium or some similar method. However, the intensity of ionization obtained by such means is entirely too small to be measured by a positive ray analysis method when one considers that the ion current must diffuse through a slit of the order of 0.01 by 5.0 mm in size. Normal gas ion conditions can be approximated in the glow discharge if the pressure is kept as high as possible and the ions after formation are allowed to drift through some cm of gas with a velocity so small that any aggregates which might be formed would not be likely to break up on collision with neutral molecules; that is, the result would be the same as though the ions were formed by any other method at high pressures and aged over a very short period of time. It was felt in undertaking the experiment that even if normal gas ion conditions could not be attained useful knowledge would result from the determination of the ionization products formed in a discharge tube operating between 0.1 and 1.0 mm of mercury pressure.

The present results are preliminary in nature and probably give a better idea of the ionization products as formed in the discharge than the nature of normal gas ions. However, particularly at the higher pressures where the effective aging is greater, positive ions of mass larger than a single molecule begin to appear in quantities comparable with the number of charged atoms and molecules. So far no negative ions have been observed even in gases such as oxygen and sulfur dioxide which have considerable electron affinity; but this is not surprising considering the low pressures and hence relatively few collisions which the electrons would make with neutral molecules before being swept out of the volume.

Apparatus and Method

The form of apparatus finally adopted after considerable experiment is shown in Fig. 1. A discharge was maintained between the electrodes *A* by means of a sixty cycle neon sign transformer with a potential of about 4000

volts or as high as could be employed without overheating the tube. About 2.5 cm below the electrodes was a nickel cap G with a tungsten wire grid in the center through which some of the ions formed in the discharge could pass. The grid G and the first slit of the analyzing chamber S_1 were separated a distance of 2.5 cm, the ions drifting through the gas in this space with a field of five volts per cm. The slit S_1 was 0.01 mm wide and 5.0 mm long; so the pressure in the discharge and drift spaces could be maintained at 0.1 to 0.5 mm of mercury while the pressure in the analyzing chamber could be kept down to 10^{-4} mm by continuous pumping.

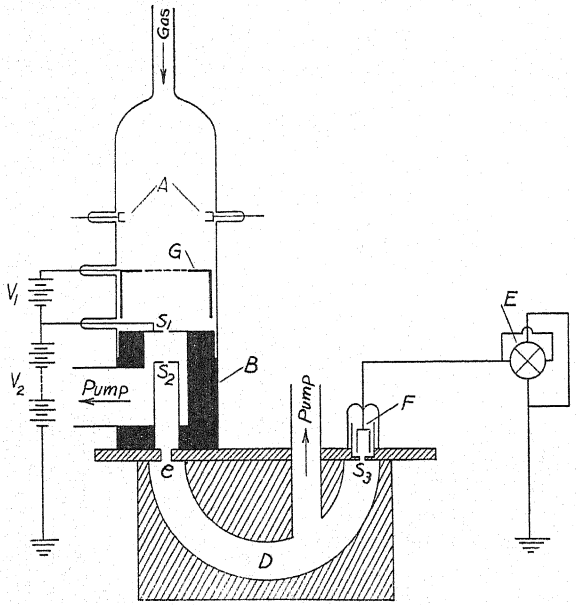


Fig. 1. Diagram of apparatus.

The analyzing chamber, made of brass, was of the standard Dempster type kindly loaned to the writer by Dr. R. E. Holzer and recently described by him.[4] The ions passed through the slit S_1 with a velocity of only a small fraction of a volt, were accelerated by the potential V_2 (100 to 200 volts), bent into a semicircle of 5.0 cm radius by a magnetic field at the point C and collected in the Faraday cylinder F where the charge was measured by the electrometer E. S_1 was insulated from the grounded analyzing chamber by mica and picein wax. B was a soft iron cylinder for magnetic shielding. The slit S_2 was 0.5 mm wide and S_3 about 1.5 mm wide.

The first attempts at measurement were made with an all glass apparatus having the inside walls silvered for electrostatic shielding. The metal cap and grid G were omitted and although some ion current was obtained through the slits S_1 and S_2, the velocities were so heterogeneous due to the high potential discharge that no appreciable current was obtained through the slit S_3. The

[4] R. E. Holzer, Phys. Rev. **36**, 1204 (1930).

glass apparatus was finally abandoned in favor of the metal chamber and a brass plate with a cm hole in the center was used in place of the grid and cap *G*. Still no ions were obtained in the Faraday cylinder as the metal plate did not sufficiently shield the drift space from the high potential discharge. Large ion currents were later obtained by placing a single electrode above the brass plate, the plate itself acting as the other electrode; but in this case the ions were projected through the slit S_1 with a velocity of about 300 volts and the conditions of drift were obviously not fulfilled. Next a filament and grid of the type employed by Smyth,[5] Hogness and Lunn[6] and others was tried and worked very well at pressures up to 0.05 mm, but above that the intensity of ionization dropped to a negligible amount. As it was necessary to work at pressures of at least 0.1 mm and preferably near 1.0 mm this method had to be abandoned. Finally the apparatus shown in Fig. 1 and described above was adopted and gave satisfactory results at pressures of 0.1 to 0.5 mm, though the ion current, especially at higher pressures was relatively small. It is hoped by means of a more intense discharge, faster pumping (hence a wider slit S_1) and more sensitive methods of detection that in the future much higher pressures, longer aging and at the same time larger currents may be attained. Negative ion currents of sufficient intensity to be measured should also be obtained under such favorable conditions.

The gases employed in the experiment were purified by passage through tubes of $CaCl_2$, NaOH, and P_2O_5; and in addition in the case of pure nitrogen through a tube of hot copper to remove the oxygen. The gas then flowed through a capillary, passed through two liquid air traps and into the discharge tube. The liquid air traps precluded the possibility of the presence of any large amount of mercury, water vapor or organic material from stopcock grease, gauges and walls of the tube.

In taking measurements it was found most satisfactory in view of the large range of masses to be covered, to keep the accelerating potential V_2 constant and vary the magnetic field by changing the current through the coils of the electromagnet. The electromagnet was calibrated by means of a flipcoil and Grassot fluxmeter, and the calibration later checked with ions of known mass. A rate of deflection method was employed in measuring the ion currents to the electrometer.

Results

Results were obtained in a number of pure gases and mixtures including N_2, O_2, SO_2, air, SO_2-N_2 mixtures and N_2-ether mixtures. The intensity of ionization in pure SO_2 and N_2-ether mixtures was too small to be measured satisfactorily. Typical results obtained for the other gases are shown in Figs. 2 to 7 inclusive. As the relative intensities of the various ions were extremely sensitive to small changes in the pressure of the discharge it was difficult to check the curves accurately, especially at higher pressures. There was such a smear of ions or larger mass and the intensity was so small that it was difficult

[5] H. D. Smyth, Phys. Rev. **25**, 452 (1925).
[6] T. R. Hogness and E. G. Lunn, Proc. Nat. Acad. Sci. **10**, 398 (1924).

even to check the position of many of the peaks. However, peaks corresponding to certain of the masses appeared so consistently that there can be no doubt of their existence.

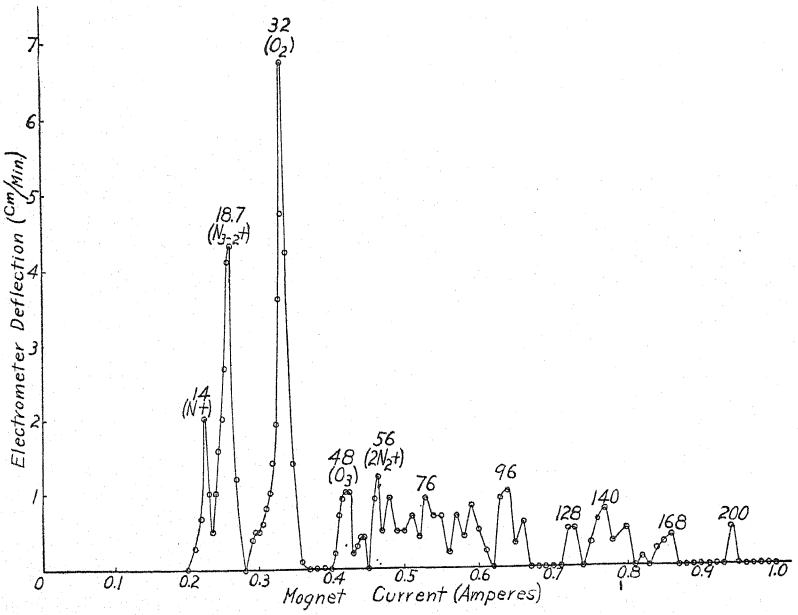


Fig. 2. Results in air with pressure in the discharge tube of 0.075 mm of mercury and accelerating potential V_2 of 150 volts. Numbers above the peaks indicate the molecular weights of the ions.

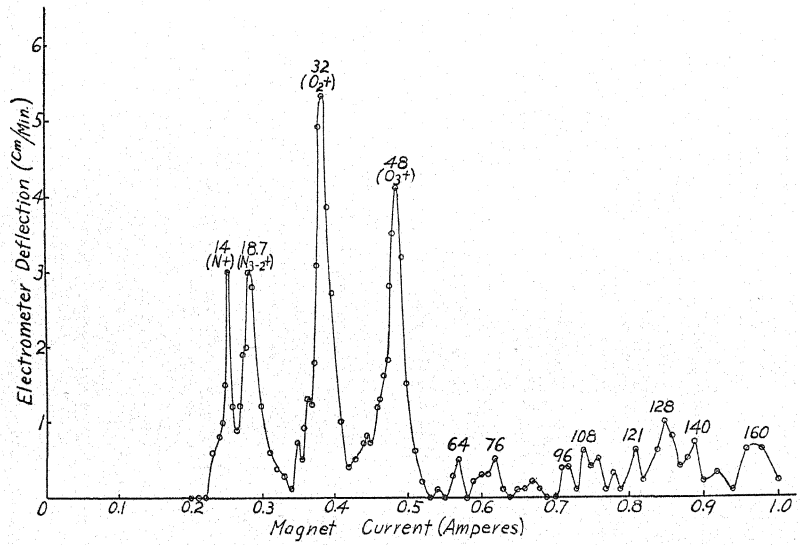


Fig. 3. Results in air with pressure in the discharge tube of 0.10 mm and accelerating potential V_2 of 150 volts. Numbers above the peaks indicate the molecular weights of the ions.

Fig. 2 shows a curve taken in air at 0.075 mm pressure in the discharge tube with an accelerating potential V_2 of 150 volts. The first mass which appears is 14.0 corresponding to N^+. O^+ is absent in measurable quantities, but a strong peak appears at a mass of about 18.7 which can only be accounted for by assuming an N_{3-2}^+ ion which is accelerated in the electric field as N_3^+ and

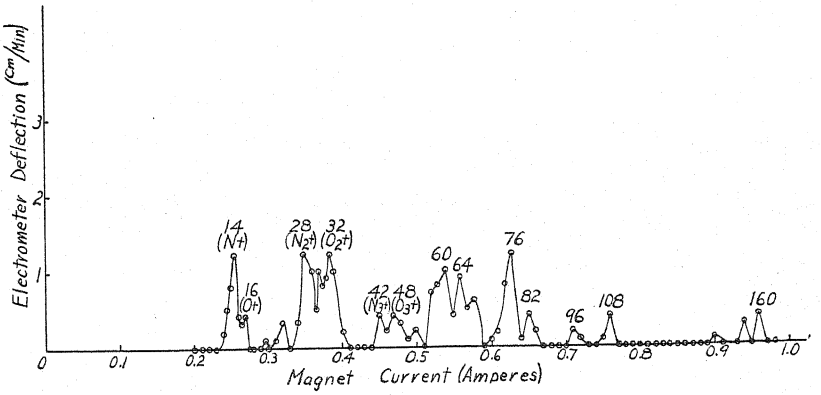


Fig. 4. Results in air with pressure in the discharge tube of 0.400 mm and accelerating potential V_2 of 191 volts. Numbers above the peaks indicate the molecular weights of the ions.

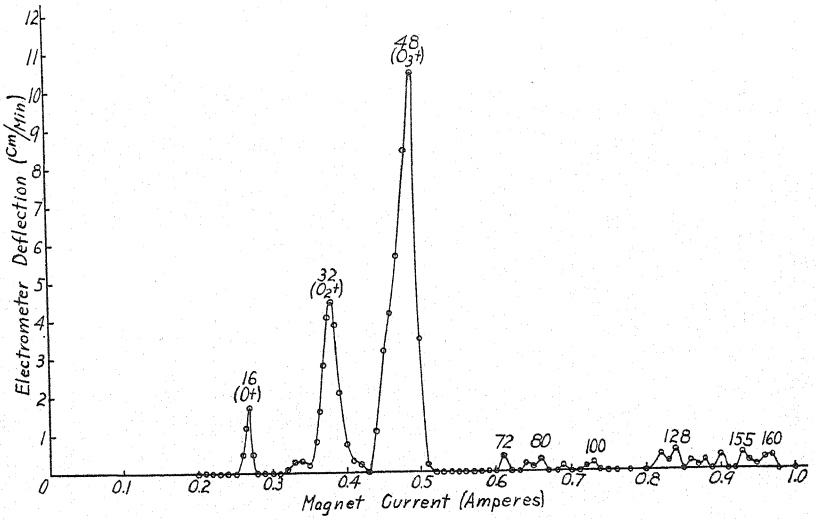


Fig. 5. Results in pure oxygen with pressure in the discharge tube of 0.10 mm and accelerating potential V_2 of 193 volts. Numbers above the peaks indicate the molecular weights of the ions.

breaks up in the magnetic field into N_2^+. This ion may have been observed by Smyth[7] working at low pressures but he attributed the corresponding peak to an impurity, presumably water. In the present work however, the peak occurs at a point corresponding to a mass which is consistently greater than 18. It disappears completely in pure O_2 or other pure gases but is always rela-

[7] H. D. Smyth, Proc. Roy. Soc. **104A**, 121 (1923)

tively strong in pure N_2 or in nitrogen mixtures. In view of the careful drying of the gases and the presence of the liquid air traps there could hardly be suffi-

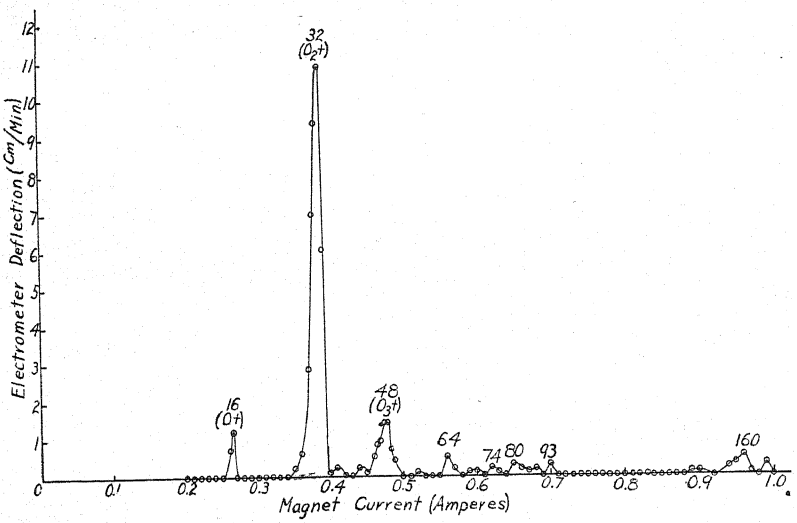


Fig. 6. Results in pure oxygen with pressure in the discharge tube of 0.30 mm and accelerating potential of 193 volts. Numbers above the peaks indicate the molecular weights of the ions.

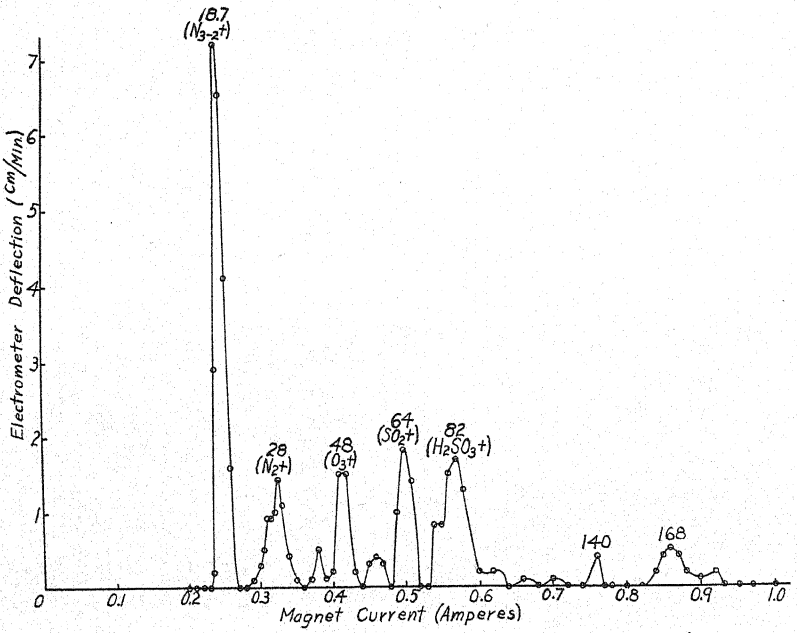


Fig. 7. Results in mixture of fifty percent N_2 and fifty percent SO_2 at a pressure of 0.30 mm and accelerating potential of 150 volts.

cient water vapor remaining to give such intense ionization. The next peak is due to O_2^+, N_2^+ being absent or too weak to measure. O_3^+ appears next as

a definite peak, with masses of approximately 56, 60, 76, 96, 128, 140, 168, and 200 following. These peaks do not stand out very definitely against a smear of ionization in the background, but peaks corresponding to these masses have a tendency to appear again and again in air.

Fig. 3 shows another curve taken in air at slightly higher pressure (0.10 mm). In this case O_3^+ is very pronounced with O_2^+ still the strongest, N^+ and N_{3-2}^+ quite strong and a smear of heavier ions.

Fig. 4 is a typical curve taken in air at higher pressures (0.40 mm). As the pressure increases the intensity of the ions of smaller mass decreases markedly while the intensity of the heavier ions, particularly of masses around 60 and 76 tends to increase. This is of course to be expected as the ions are now aged somewhat longer having made about 400 collisions with neutral molecules before entering the analyzing chamber.

Figs. 5 and 6 show two runs in pure oxygen taken at 0.10 and 0.30 mm pressure respectively. In both cases the number of heavy ions is relatively small, but it is interesting to note that at the lower pressure the O_3^+ peak is much the strongest while at the higher pressure O_2^+ appears to be the principle product of ionization.

Fig. 7 shows the results for a mixture of fifty percent N_2 and fifty percent SO_2. N_{3-2}^+ appears the most intense while N_2^+, O_3^+, SO_2^+ and $H_2SO_3^+$ show up as definite peaks of relatively large intensity. In this case the SO_2 was taken directly from a tank without drying or purifying; so water vapor was undoubtedly present in considerable quantity and may have contributed partially to the N_{3-2}^+ peak.

Measurements in pure N_2 showed N_{3-2}^+ to be the most intense with considerable N^+ and N_2^+ but no appreciable number of heavier ions. As has been indicated previously, no negative ions could be found in any of the gases but this is not surprising since even at the higher pressures of about 0.5 mm the electrons would make only about five hundred collisions in the drift space and only a negligible number could attach to neutral molecules. Small quantities of negative ions formed in the discharge at lower pressures have been observed by J. J. Thomson and Smyth but would probably escape detection in the present experiments due to the relatively low intensity of ionization. No multiply charged ions were found in the work reported here, but it was to be expected that the few doubly charged ions formed in the discharge would lose one of their charges to a neutral molecule while passing through the drift space.

Summary and Conclusions

The results may be summed up as follows: (1) In air, N_2, O_2, and SO_2 the following positive ions give strong definite peaks varying in intensity under varying conditions of pressure of the gases but easily obtainable from a glow discharge of the kind employed in this experiment: N^+, N_{3-2}^+, O^+, N_2^+, O_2^+, O_3^+, SO_2^+ and $H_2SO_3^+$. (2) In addition to the simple ions noted above there appears a smear of complex ions of larger mass up to a molecular weight of 200. The number of these heavy ions is small but is greater in air than in the pure gases and becomes relatively larger at higher pressures where the ions

make several hundred collisions with neutral molecules in the drift space. The peaks which appear most often and most prominently correspond to ions of the following molecular weights: 56–64, 76, 80, 96, 108, 128, 140, 160, 168 and 200. (3) Negative ions do not appear in measureable quantities.

It seems likely that the heavier ions consist of such combinations of atoms and molecules as $2N_2^+$, $N_2O_2^+$, $2O_2^+$, $N_2O_3^+$, $O_2O_3^+$, $N_2O_5^+$ etc. The preliminary results obtained in these experiments do not definitely answer the question of the nature of gaseous ions. However, the fact that in air at higher pressures the heavier ions become nearly equal in number to the lighter ions indicates that after some aging air ions at least do not consist of simple atoms and molecules of nitrogen and oxygen, or even of ozone and N_3. In particular, nitric oxides probably play an important role in the formation of the heavier molecular aggregates. On the other hand, in pure oxygen and nitrogen, the relative number of heavy ions is much smaller even at high pressures and it is probable that aside from attachment to impurities the ions remain essentially of a simple nature. Undoubtedly O_3^+ and N_3^+ ions play considerable role in gas ion phenomena and apparently the O_3^+ ion is very stable while N_3^+ is less stable since it breaks up into $N_2^+ + N$ in the magnetic field. It is interesting to compare the behaviour of nitrogen and hydrogen. The writer as well as other observers employing a filament at low pressures (the order of 0.01 mm) has observed a considerable quantity of H_{3-1}^+ as well as H^+, H_2^+ and H_3^+. Apparently H_3^+ breaks up in the magnetic field into $H^+ + H_2$ while N_3^+ breaks up into $N_2^+ + N$.

There remains a point to be discussed regarding the possibility that certain heavy ions, if formed, would break up in the analyzing chamber where they are rapidly accelerated in electric and magnetic fields. If the ions are relatively stable it should be impossible for a breakup to occur as long as there is no collision with neutral molecules or other ions. Since this condition is fulfilled in a molecular beam of the type employed in these experiments, and a certain number of heavy ions have actually been observed, some of the ions at least are able apparently to withstand the shock of acceleration in the fields. On the other hand a breakup in the magnetic field is certainly observed in the case of N_3^+ and H_3^+. It seems doubtful however that this effect is due directly to the magnetic forces. An ion of this sort may be stable only when in an excited state and if radiation takes place a breakup may follow. The possibility remains that other less stable heavy ions may be present which have not been observed owing to a change of mass in the analyzing chamber. Perhaps the more or less irregular smear of heavy ions observed is due in part to an effect of this sort; but the important fact remains that ions up to a molecular weight of 200 have been observed, indicating that aged ions in air are of a complex and probably heterogeneous nature.

In conclusion, the writer wishes to take this opportunity for expressing his gratitude to Professor L. B. Loeb whose advice and help have been an inspiration throughout the course of these and previous experiments at the University of California. He also wishes to thank Professor Otto Stern of Hamburg for valuable suggestions in regard to the technique of molecular beams, and Commander T. Lucci of the Italian Navy, retired, who aided in taking some of the readings.

THE MOLECULAR SCATTERING OF LIGHT FROM AMORPHOUS AND CRYSTALLINE SOLIDS

By Alexander Hollaender and John Warren Williams
Laboratory of Physical Chemistry, University of Wisconsin

(Received September 22, 1931)

Abstract

There have been photographed the Raman spectra of several specimens of plate glass and of certain crystalline sulphates and their water solutions. In the case of the plate glass it is shown that at least most of the lines owe their origin to the silica content. The data for the crystalline sulphates are of interest because of the appearance of lines corresponding to both the active and inactive frequencies of the sulphate ion. These lines also make their appearance when the crystals are dissolved in water. With the data now available in the literature it is difficult to describe exactly the shifts of the Raman lines produced by the solution process because these shifts frequently depend upon the concentration of the ions and because for a given concentration different lines may be shifted by different amounts.

THE theoretical and experimental study of the Raman effect has justified the vast amount of work devoted to it, both as a means of demonstrating the quantum laws and as an analytical tool in probing the internal structure of chemical compounds. For the latter purpose it serves to study the structure of molecules either in the pure or dissolved state. In the hands of Kohlrausch[1] and of Andrews[2] and their associates there has been accumulated considerable information concerning the frequencies of and modes of vibration about the various kinds of chemical bonds in pure organic compounds. The Raman effect has also been used in a number of instances to study the structure of inorganic crystals and amorphous materials. Nisi,[3] Woodward,[4] Rao,[5] and a number of other investigators have used its study to indicate the changes taking place when an inorganic electrolyte is dissolved in water, it being predicted that in this manner there may eventually be obtained a quantitative measure of the degree of dissociation of the salt into ions. In general the work with inorganic substances and their solutions has not been as successful as that with the organic liquids and there remain many difficulties to be overcome.

The work to be reported in this article has to do with the molecular scattering of light from inorganic solids and from their water solutions in the cases where they are sufficiently soluble. The substances are in most cases crystalline in nature. Data for certain of these systems were presented more than two years ago as preliminary communications to this Journal.[6] It has just now

[1] Kohlrausch, "Der Smekal-Raman Effekt," Springer, Berlin, 1931.
[2] Andrews, *et al*, Phys. Rev. **36**, 531 (1930).
[3] Nisi, Jap. Jour. Phys. **5**, 119 (1929).
[4] Woodward, Phys. Zeits. **32**, 212 (1931).
[5] Rao, Proc. Roy. Soc., **A127**, 279 (1930).
[6] Hollaender and Williams, Phys. Rev. **34**, 380, 994 (1929).

been possible to improve the early results in accuracy and to make the proper identification of the excited line with its exciting line in several cases, where errors could not at that time be avoided, by means of improved apparatus and experimental methods which have since become available to us.

The experimental procedure differed scarcely if at all from that described by Kohlrausch[1] and by Schaefer and Matossi.[7] The salt solutions were placed in a long tube, illuminated along its length with a commercial mercury arc, and the spectrum of the light scattered at right angles was photographed by means of a large glass spectrograph through a plane window in the end of the tube. The tubes were cooled by means of a water jacket and the lamps were cooled by an electric fan. The measurements reported here were made with instruments manufactured by Steinheil. The tube containing the solutions was replaced by smooth flat sections of the solid when exposures of glasses and crystalline substances were made. A system of filter solutions was developed so that either of the exciting lines used (Hg 4047 or Hg 4358) and all other strong lines of the mercury arc could be so reduced in intensity that the systems were exposed to a radiation which was practically monochromatic. The filters used were acid solutions of quinine sulphate for the 4047 group and solutions of iodine in carbon tetrachloride for the 4358 group or for lines of longer wave-length. The plates were photometered with a Moll recording microphotometer, kindly placed at our disposal by the Department of Physics. The position of the Raman lines was also determined directly from the plates with a Gaertner comparator.

I. Raman Effect in Amorphous Solids

Infrared studies with crystalline materials have led to such interesting theoretical conclusions[8] that it is only natural for the Raman effect to have been discovered in these substances very shortly after the original announcement of Raman. Crystalline quartz has given a number of scattered lines whose frequency differences, but not intensities, agree quite well with those of infrared absorption and reflection maxima. The large number of observed frequencies is somewhat surprising because a single SiO_2 molecule can have not more than three characteristic frequencies and it can be explained only by assuming the crystal to have a very complicated lattice. One might expect to find even more scattered lines in fused quartz or in a glass containing a large percentage of silica because of a still more complicated structure. Furthermore, at the time of our original experiments it was believed that the Raman effect could not be observed in a fused quartz.[9] Exposures have been made with a number of samples of plate glass, the results of a typical experiment being given in Table I.

Gross and Romanova[10] and very recently Bhagavantam[11] have also reported successful exposures of fused quartz and various glasses. Their results

[7] Schaefer and Matossi, Fortschritte der Chemie, Physik u. phys. Chem. **20**, No. 6 (1930).
[8] See, for example, Schaefer and Matossi, "Das Ultrarote Spektrum," Springer, Berlin, 1930
[9] Pringsheim and Rosen, Zeits. f. Physik **50**, 741 (1928).
[10] Gross and Romanova, Zeits. f. Physik **55**, 744 (1929).
[11] Bhagavantam, Ind. Jour. of Phys. **6**. 1 (1931).

TABLE I. *Data for plate glass.*

Exciting line	Excited line	$\Delta\nu$	λ
4358	4718	1748	5.7
	4682	1585	6.3
	4619	1293	7.7
	4572*	1071	9.3
	4513	785	12.7
	4485	647	15.5
	4463	537	18.6
	4450	471	21.2
	4408	259	38.6

* This is the most intense band. The microphotograph indicates that it may possibly be resolved into three lines, with the most intense one in the center.

(in part) are compared with those of the authors in Table II. As far as the data now available in the literature are concerned the Raman spectra for both crystalline and fused quartz and for the various glasses are almost identical. Therefore, it is impossible to draw any conclusions with regard to the crystal structure, or lack of it, in these materials.

TABLE II. *Data for quartz and the glasses.*

Material	Reference	Frequency differences							
Crystalline quartz	10	125	264	463	526	633	800	1075	1220
Amorphous quartz	10	—	263	440	500	670	800 to 830	1030 to 1090	1240
Flint glass	11	119*	—	460 to 500	—	640	780	1080	1320
Crown glass	11	115*	340	460	—	650	800	1070	1320
Plate glass	†	—	259	471	537	647	785	1071	1293

† This article.
* Observed by Gross and Romanova.

In the glasses the scattering was extremely faint, and even when mirrors were used to concentrate the incident light upon the sample, exposures of from 3 to 10 days, depending upon the color of the sample, were required. The Raman lines were always more or less diffuse, rather than sharp as in the case of crystalline quartz, and it has been necessary to estimate the position of maximum intensity in order to measure their position. The comparison table indicates that at least most of the lines owed their origin to the silica content (SiO_2), in other words they were due to molecular vibrations characteristic of the constitutent materials.

The presence of the frequency differences 1748 and 1585 was somewhat surprising. These differences, corresponding to shorter wave-lengths, have not been observed in quartz. It is considered possible they may have resulted from the other constituents of the glass. To be certain of the existence of these larger frequency differences all mercury lines between 4358A and 5300A have been filtered out. For different samples of glass these larger frequency differences appear to change their position.

II. Raman Effect in Crystalline Sulphates and their Water Solutions

Two types of crystals may be distinguished, those with simple ions at the lattice points, and those containing complex ions. In the simple ion lattice one mode of vibration is possible, but in the complex crystals two kinds of vibration are known, a lattice or "outer" vibration in which, for example, the complex anion vibrates with respect to the metal ion, and an atomic or "inner" vibration in which the complex ion remains fixed in position and its individual atoms vibrate with respect to each other. Roughly speaking the frequencies of the inner vibrations will be independent of the particular cation present. They will also correspond to shorter infrared wave-lengths than those of the outer vibrations. It has been possible only in exceptional cases to find Raman lines corresponding to the outer vibrations, but this may be in part due to difficulty in obtaining optically clear crystals. Information concerning the inner vibrations of an ion may be obtained either from the crystals themselves or from their water solutions because only the lattice bonds are destroyed by the solvent.

There has been much discussion with respect to this particular point. Is there a shift in the characteristic frequency differences given by an ion when it is dissolved or are they unchanged? It is claimed by some investigators that smaller frequency differences (corresponding to longer wave-lengths) are found in solution while such shifts have not been evident in the data of others. From a theoretical point of view one can certainly expect to find these shifts. The experimental data now available in the literature seem hardly adequate to settle this point, the most important reason being that shifts due simply to changes in the concentration of the solutions have hardly been considered. In most cases the concentrations of the solutions studied have not been given. Recent data of Embirikos[12] are of interest in this connection because they show that in passing from a 1 normal solution to a 2 normal solution the frequency difference for Li_2SO_4 changed from 989 to 999 and for $MgSO_4$ it changed from 986 to 996. The presence of water of crystallization may also modify any changes in frequency difference due to the solution process.

Of the crystals containing complex ions the carbonates and sulphates have been most completely studied, but there still remain many difficulties to be overcome. In the case of the SO_4 ion infrared reflection maxima at 9μ and 16μ, corresponding to active frequencies, are known. There are also two inactive frequencies, one of which is, in all probability, given by the Raman frequency difference 980, corresponding to 10.2μ. The other has been calculated from these three to be about 26μ by Schaefer.[13]

Data, presented in Table III, have been obtained for the molecular scattering of light from crystalline gypsum, barium sulphate and copper sulphate, and from water solutions of copper sulphate, magnesium sulphate and potassium alum. The crystals used contained smaller amounts of impurities and

[12] Embirikos. Zeits. f. Physik 65, 266 (1930).

[13] Schaefer, Zeits. f. Physik 60, 586 (1930). See also reference 8, page 352.

TABLE III. *Data for crystalline sulphates and their water solutions.*

Exciting line	Excited line	$\Delta\nu$	λ	Remarks
	Gypsum ($CaSO_4 \cdot 2H_2O$)			
4358	4584	1128	8.9	
	4553	980	10.2	
	4495	696	14.3	
4047	4701	3437	2.9	Water band
	4613	3031	3.3	Water band
	4213	980	10.2	
	Barite ($BaSO_4$)			
4358	4553	980	10.2	
	4496	702	14.3	
	4448	461	21.6	
4047	4213	980	10.2	
	Copper sulphate ($CuSO_4 \cdot 5H_2O$)			
4358	4553	980	10.2	
4047	4701	3437	2.9	Water band
	4213	980	10.2	
	Copper sulphate, 1 normal water solution			
4358	4553	980	10.2	
	4477	607	16.5	
4047	4701	3437	2.9	Water band
	4651	3208	3.1	Water band
	4213	980	10.2	
	4169	723	13.7	
	Magnesium sulphate, 1 normal water solution			
	4584	1128	8.9	
4358	4553	980	10.2	
	4497	706	14.3	
	4477	607	16.5	
	4452	482	20.8	
	Potassium alum, saturated water solution at 25°C			
4358	4553	980	10.2	
	4477	607	16.5	
	4451	477	21.0	
4047	4213	980	10.2	

were imperfect in structure. The scattering produced by these imperfections made it impossible for us to observe some of the weaker lines reported by others.

Lines were found corresponding to the active frequencies 9μ and 16μ, and to the inactive frequencies 10μ and 26μ. The agreement with the longest wave-length, a calculated position, was not good. Thus for this wave-length, Schaefer, Matossi and Aderhold reported a Raman line corresponding to 24.5μ,[7] but later corrected it to 21.7μ. This Raman line in the work of Dickinson and

TABLE IV. *Data for substances containing SO_4 radical.*

Substance	Author	Frequency differences								
Sulphuric acid 100%	N	414	564	740	911	—	1043	1170	1366	1517
Sulphuric acid 100%	W	430	580	—	908	—	—	1143	1359	—
Ammonium sulphate solution	D-D	458	624	—	—	987	—	—	—	—
Copper sulphate	J-D	429	602	—	—	980	—	1091	—	—
Gypsum	S-M-A	460	620	—	—	985	—	1139	—	—
Gypsum	H-W	—	—	696	—	980	—	1128	—	—
Barite	H-W	461	—	702	—	980	—	—	—	—
Copper sulphate 1 N solution	H-W	—	607	723	—	980	—	—	—	—
Magnesium sulphate 1 N solution	H-W	482	607	706	—	980	—	1128	—	—
Alum solution	H-W	477	607	—	—	980	—	—	—	—

N Nisi, reference 3.
W Woodward, reference 4.
D-D Dickinson and Dillon, Proc. Nat. Acad. Sci. **15**, 334 (1929).
S-M-A Schaefer, Matossi and Aderhold, Zeits. f. Physik **65**, 289 (1930).
J-D Joos and Damaschun, Phys. Zeits. **32**, 553 (1931).
H-W This article.

Dillon corresponds to 21.8μ, that of Joos and Damaschun to 23.3μ, and those of the present authors average 21.0μ.

There have been collected in Table IV data for substances containing the SO_4 radical. No attempt has been made to include all the available data, its chief purpose is to show the order of agreement between values reported from different laboratories and to compare the interesting data of Nisi and of Woodward for pure sulphuric acid with those of the crystalline sulphates. In the data for pure sulphuric acid the frequency difference 980 does not appear, but when the solution has been diluted to 50 percent by volume with water there is no doubt concerning its presence. Woodward does not find the difference 1043 until a small amount of water is present and believes this frequency to be due to the HSO_4^- ion. The 980 frequency difference is assigned to the SO_4^{--} ion.

The effect of the presence of increasing amounts of water in the sulphuric acid is interesting in connection with a point already mentioned. Certain of the frequency differences are, within the limits of experimental error, perfectly constant throughout the whole range of concentration 100 percent sulphuric acid to 10 percent sulphuric acid by volume, several increase with dilution, and others decrease with dilution. These and other data indicate that no simple general statement will describe the effect of the solution process upon a characteristic frequency difference, they also explain why in certain cases no shift has appeared while in others there may be appreciable changes. The data of this article cannot be claimed to be sufficient to contribute to the solution of this particular problem. We have, however, been able to verify the magnitude of the shift of the line corresponding to the frequency difference 980 reported by Embirikos in the case of one and two normal water solutions of magnesium sulphate.

The frequency difference, approximately 700, has been found by us in gypsum, barite, and solutions of copper and magnesium sulphates, but has not been reported by other investigators, studying these same systems. Nisi has reported 740 for pure sulphuric acid. This difference corresponds to approximately 14μ, the position of a known infrared reflection maximum for water, but it is difficult to see how this Raman shift can be accounted for on the basis of the presence of water. We are at present unable to assign a definite significance to it.

As indicated in Table III frequency differences corresponding to wavelengths of the order of magnitude 3μ are to be associated either with the water of crystallization or with the solvent water. The water bands were also present in the spectrum of the magnesium sulphate solution but no attempt was made to locate their maximum intensities. The very exact study of the Raman effect in such systems as have been reported here promises to give information not only with regard to the dissociation process but also to clear up some of the difficulties which have been met in the study of the water bands themselves. There seems to be a tendency for the individual components of the latter to become sharper and more distinct as the concentration of the added electrolyte is increased.

AN INTERPRETATION OF THE SELECTIVE PHOTOELECTRIC EFFECT FROM TWO-COMPONENT CATHODES

By A. R. Olpin
Bell Telephone Laboratories

(Received September 11, 1931)

Abstract

Evidence is produced to support the view that photoelectrically selective, two component cathodic surfaces are crystalline in nature. Then, assuming that Fowler's equation for the energy of electrons selectively transmitted through a single potential valley $[W=(n^2h^2/8md^2)]$ is equally valid for the energy of electrons selectively transmitted through the periodic sequence of valleys characteristic of the potential field within a crystal, and that all of the energy of photoelectrons is acquired from the incident light quanta, the wave-lengths of light to which such a surface should respond selectively can be computed. Such computations have been made with d equal to the internuclear distance between electro-positive ions in the lattice structure of alkali metal hydride, oxide and sulphide crystals. The hydride crystals belong to the sodium chloride type and the oxide and sulphide crystals are supposedly of the calcium-fluoride type. The correlation between these computed values and the positions of the observed selective maxima is exceptionally good. Moreover, the fact that the alkali metal hydrides exhibit but one selective maximum and the oxides two or three maxima is in keeping with the geometry of their respective crystalline types.

ONE of the most significant characteristics of the photoelectric emission from two-component cathode surfaces, such as those of the alkali metal hydrides and oxides, is the selective response to light of specific frequencies. This results in the appearance of definitely located maxima in the spectral response curves for these compounds. To avoid the necessity of repeated reference to other publications, I have assembled a group of typical curves and present them in Fig. 1.

A number of ideas have been advanced to account for a selective response to light, but heretofore no theory has adequately explained why: (1) A single specifically located maximum is always observed in the spectral response curve of any given alkali metal hydride surface; (2) One, two or three definitely located maxima may appear in the spectral response curve of an alkali metal oxide cathode, depending presumably upon the relative proportions of metal and oxygen, and the technique involved in the preparation of the compound; (3) The wave-length of the light to which a two-component surface responds selectively is a direct function of the size of the components.

In this paper I propose an interpretation of the composition of two-component cathode surfaces, and an explanation of the selective photoelectric emission therefrom which accounts for all the above observations with striking precision.

Preparation of Two-Component Selective Photoelectric Surfaces

The preparation of light sensitive alkali metal hydride photoelectric cells,[1,2] as is quite generally known, consists in ionizing hydrogen by means of an electrical brush discharge, on a coating of freshly distilled metal. Possibly

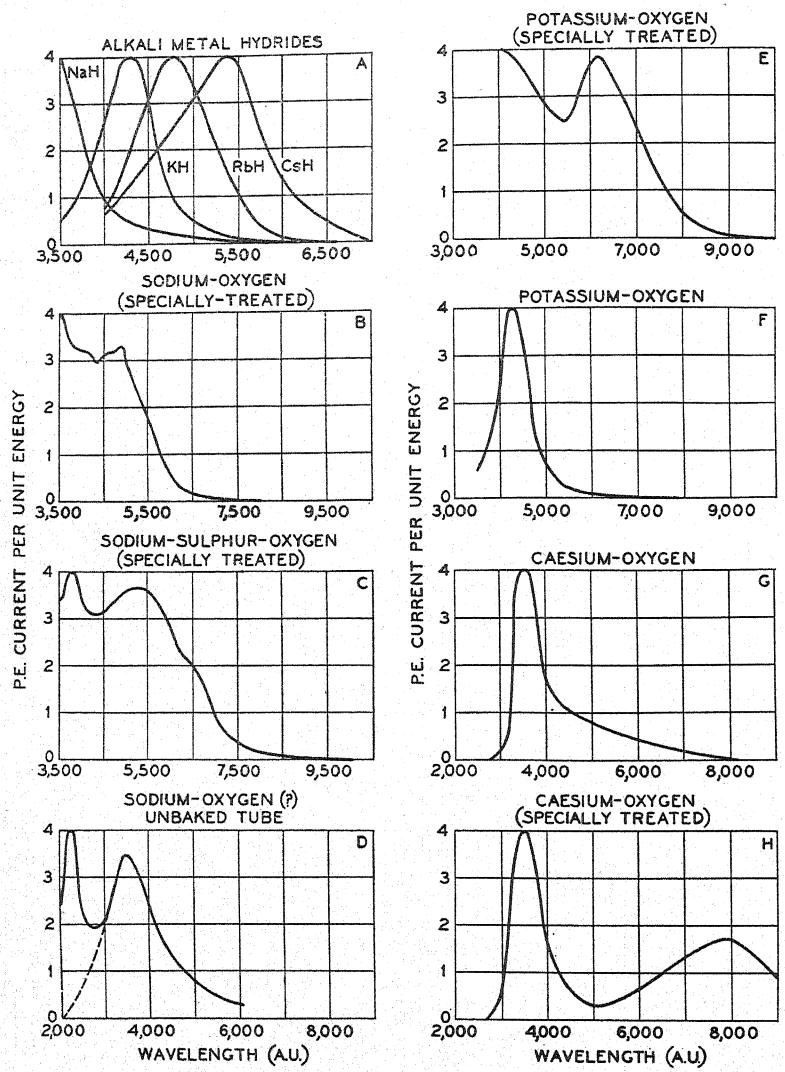


Fig. 1. Groups of typical spectral response curves for various gas-treated alkali metal photoelectric cells.

better results are obtained when the metal is made the cathode during the discharge, but this is not absolutely essential. Typical spectral response characteristics of such cells for visible light are shown in Fig. 1A.

[1] H. E. Ives, Bell System Tech. J. 5, 320 (1926).
[2] E. F. Seiler, Astrophys. J. 52, 3, 129 (1920).

The method of preparing selectively emitting cathodes of the alkali metals by the use of oxygen has been the subject of considerable experimentation in recent years. The mere introduction of small amounts of this gas onto an alkali metal surface is sufficient to greatly enhance the photoelectric sensitivity,[3] but in these cases the pronounced selective maxima in the spectral response curves appear, in general, at practically the same wave-lengths as those for the pure metals or the hydrides, as illustrated for the cases of sodium and potassium by the curves in Fig. 1D and 1F. However, if after oxidizing the surface of a sodium cathode, a limited area is heated to create a vapor of sodium and oxygen, a coating is formed on the cool portions of the cathode which is very much more sensitive to light and exhibits a quite different spectral response characteristic, with a new selective maximum at longer wave-lengths (Fig. 1B). Moreover, if on a silver plate which has been oxidized under control, caesium in the proper proportions is deposited and the whole sub-

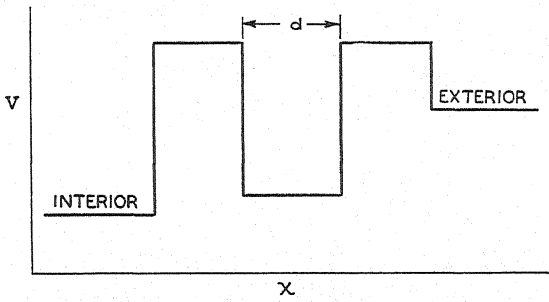


Fig. 2. Conventional representation of the work done by an electron in passing through a surface consisting of alternate layers of electropositive and electronegative elements, as Ag–O–Cs–O–Cs.

jected to a heat treatment which includes as a final step, heating to a temperature just under that at which caesium monoxide volatilizes (250°C),[4] a cathode strikingly sensitive to red and near infrared light is obtained (Fig. 1H).[5] By means of a similar process, red sensitive potassium-oxide photoelectric cells can also be made (Fig. 1E).[6] Obviously, the processes described above produce a complex surface structure, physically favorable to the emission of electrons by light. The nature of this structure and an explanation of these pronounced maxima are the subjects of this discussion.

Campbell-Fowler Theory

Campbell,[7] in an attempt to account for the selective response of caesium-oxide cells to red light, suggested that the surfaces of their cathodes consist of alternate layers of oxygen and caesium. The structure he mentioned as most

[3] A. R. Olpin, Phys. Rev. **36**, 251 (1930).

[4] J. W. Mellor—"A Comprehensive Treatise on Inorganic and Theoretical Chemistry." Vol. II p. 486. Longmans, Green and Co., Ltd., London (1927).

[5] L. R. Koller, Phys. Rev. **36**, 1639 (1930).

[6] N. R. Campbell, Phil. Mag. **6**, 633 (1928).

[7] N. R. Campbell, p. 10 "A Discussion on Photoelectric Cells and their Application"—The Physical and Optical Societies, London (1930).

likely was Ag–O–Cs–O–Cs. The potential energy of an electron moving through such a sequence of atomic or molecular layers was conventionally represented by a diagram similar to the one in Fig. 2, wherein the abscissa is the distance normal to the surface and the ordinate, the potential energy of a electron moving in this direction. Fowler[8] then showed, by means of the wave mechanics, that, to a first approximation, the transmission of electrons through such a surface structure will be greatest provided the waves associated with their motion are of such length that they will form stationary waves in the potential valley.

If the width of the valley is d, the condition for standing waves to form, obviously, is that

$$\lambda = \frac{2d}{n} \ (n = \text{an integer}). \tag{1}$$

But since the wave-length associated with a moving electron is

$$\lambda = h/mv, \tag{2}$$

according to Campbell and Fowler's theory, the speed of electrons most readily transmitted should be

$$v = \frac{nh}{2md}. \tag{3}$$

Consequently, the kinetic energy of such electrons will be

$$w = \tfrac{1}{2}mv^2 = \frac{n^2h^2}{8md^2}, \tag{4}$$

which is the expression Fowler obtained from a rigorous solution of Schroedinger's wave equation.

If all the energy possessed by the electron is acquired from the incident light quanta, then

$$w = \tfrac{1}{2}mv^2 = h\nu = \frac{n^2h^2}{8md^2} \tag{5}$$

and

$$\nu = \frac{n^2h}{8md^2}. \tag{6}$$

A hasty computation of this energy value when d is of atomic or molecular dimensions indicates that if it is to correspond to that of a quantum of visible or near infrared light, n must be unity. Eq. (6) is thus a simple relationship between the frequency of light ν for which maximum emission should occur and the width of the potential valley d responsible for this selectivity. Replacing ν by c/λ and simplifying, we get

$$d = 0.0551(\lambda_{max})^{1/2} \tag{7}$$

or

$$\lambda_{max} = 330.d^2, \tag{8}$$

where both λ_{max} and d are expressed in Angstrom units.

[8] R. H. Fowler, Roy. Soc. Lond. Proc. **A128,** 123 (1930).

More recently Frenkel,[9] while adhering to Fowler's idea of selective transmission, announced that a "selective transparence must exist for any type of surface field involving a transition of the potential energy from one (constant) level inside the metal to another constant level outside it irrespective of the presence or absence of local maxima or minima".

Nature of Compounds on Two-Component Cathode Surfaces

On account of the simplicity of the relationships expressed by Eq. (8), it would be easy to check Fowler's theory, were it possible to determine the proper value of d to use. Physically, the conventional distribution of potential showing a valley as diagrammed in Fig. 2 does not exist. Even though we concede the actual presence of alternate layers of electropositive and electronegative atoms or ions on the cathode surface, as postulated by Campbell, the potential energy of an electron passing through such a configuration must more nearly resemble that represented by the diagram in Fig. 3. Here

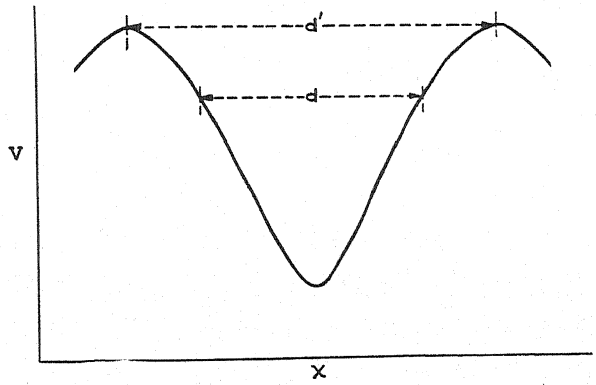


Fig. 3. Potential energy of an electron passing through a structure consising of a layer of electropositive ions sandwiched between layers of electronegative ions.

the width of the valley is a function of its depth, and consequently it is not easy to obtain a quantitative correlation between λ_{max} and d. We can, however, insert the observed values of λ_{max} in Eq. (7) and see whether or not the values of d called for, are of the order of magnitude of atomic dimensions. Actually, they are found to lie between 3 and 5 Angstroms, which suggests a very rough correlation with the atomic diameters of the alkali metals.

The values of d obtained by Eq. (7) when the observed values of λ_{max} for alkali metal surfaces sensitized with hydrogen are used, have been tabulated in Table I, and those obtained when the observed values of λ_{max} for alkali metal surfaces sensitized with oxygen are used are listed in Table II.

It will be noted that the values in the first table are very nearly equal to the sum of the diameters of the positive metal and negative hydrogen ions multiplied by $\frac{1}{2}(2)^{1/2}$, and those in the latter table are approximately equal to the sum of the diameters of the positive metal and negative oxygen ions multiplied by either $\frac{1}{3}(3)^{1/2}$, $\frac{1}{2}(2)^{1/2}$, or $\frac{1}{3}(6)^{1/2}$.

[9] J. Frenkel, Phys. Rev. **38**, 309 (1931).

TABLE I.

Cathode material	λ_{max} (observed)	$d=0.0551(\lambda_{max})^{1/2}$	d' = sum of diameters of positive metal and negative H ions[10]	$\frac{d}{d'}$
LiH	2800A	2.92A	4.10A	0.712
NaH	3300	3.17	4.50	.704
KH	4350	3.63	5.20	.698
RbH	4800	3.82	5.52	.692
CsH	5400	4.05	5.84	.694
				$[\frac{1}{2}(2)^{1/2}=0.707]$

TABLE II.

Cathode material	λ_{max} (observed)	$d=0.0551(\lambda_{max})^{1/2}$	d' = sum of diameters of positive metal and negative O ions[10]	$\frac{d}{d'}$
Sodium oxide	2270A	2.62A	4.60A	0.570
"	3500	3.26	4.60	.709
"	4700	3.78	4.60	.822
Potassium oxide	3130	3.08	5.30	.582
"	4260	3.57	5.30	.674
"	6200	4.34	5.30	.819
Caesium oxide	3500	3.26	5.94	.549
"	5500	4.09	5.94	.689
"	8000	4.93	5.94	.830
				$[\frac{1}{3}(3)^{1/2}=0.578;\ \frac{1}{2}(2)^{1/2}=0.707;\ \frac{1}{3}(6)^{1/2}=0.818]$

Obviously, these factors suggest a definite configuration or alignment of molecules on the surface in some form of cubical arrangement, which, in turn, suggests the presence of a crystalline formation on the gas-treated alkali metal cathodes of photoelectric cells, and the existence of selective maxima because of selective transmission of electrons through the periodic fields of potential characteristic of such structures. The nature and dimensions of the respective crystalline forms will be considered in greater detail in succeeding paragraphs.

An interpretation of the cathode surface as a crystalline arrangement of the component ions impresses us as a very reasonable picture, for the amount of material used in forming some of the best photoelectric cells indicates that the surface coatings of the cathode might be as thick as 1,000 atom diameters. Certainly, they are sufficiently thick to be plainly visible and they contribute a definite coloration to the surface. Now, the fact that it is the ratio of alkali metal to oxygen (approx. 3 to 1) and not the total amount of each that determines the selective characteristic of a surface,[11] together with the fact that the final heat treatment previously described is of such a nature that the molecules deposited on the cathode will be thermally agitated but not evaporated, suggest strongly the likelihood of a crystalline formation. At the same time

[10] See Table of Ionic Radii, V. M. Goldschmidt, Far. Soc. Trans. **25**, 6, 253 (1929).

[11] This is based on an unpublished report by Dr. C. H. Prescott of the Bell Telephone Laboratories after considerable experimentation. A recent paper by N. R. Campbell [Phil. Mag. **12**, 75, 173 (1931)] further substantiates this ratio.

any excess free alkali metal, having a lower boiling point than the salt, will deposit on the top surface of the crystal and greatly reduce the work function.

A crystalline surface structure will exhibit a periodic succession of potential valleys instead of a single potential valley as postulated by Campbell and Fowler. Just how this condition will affect the validity of Eqs. (4) to (8) has not yet been investigated. However, I shall proceed to point out a striking correlation between observed positions of selective maxima and those computed by means of Eq. (8) when values of d associated with the period of the potential field in a crystal are used.

Alkali Metal Hydrides

All of the alkali metal hydrides are known to crystallize with the sodium chloride structure.[12] The arrangement of ions in a unit cell of this type is diagrammatically shown in Fig. 4.

The most likely path for an electron to follow in passing through such a crystal is one normal to the 110 plane and quite close to the positive metal

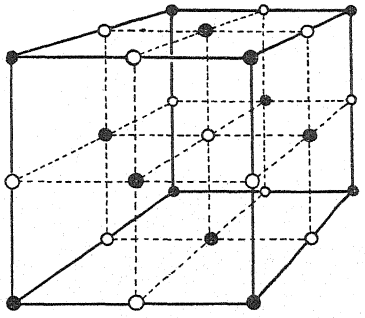


Fig. 4. Arrangement of ions in alkali metal hydride crystals (NaCl structure). The circles represent the metal and the dots the hydrogen ions.

ions. In any other direction through the crystal, an electron will encounter more powerful retarding potentials because of the presence of negative hydrogen ions along its path. The nature of the potential field normal to the 110 plane, that is, the work an electron must do in passing through a hydride crystal in this direction, has been computed by Mr. L. A. MacColl of these laboratories on the basis of certain simple assumptions as to the nature of the potential fields of atoms and ions. His results are illustrated by the curve in Fig. 5. The potential is periodic and the period is $\frac{1}{2}(2)^{1/2}$ $(=0.707)$ times the sum of the diameters of the positive alkali metal and negative hydrogen ions. As illustrated in Table I, this is very close to the value of d, which when used in Eq. (8) gives values of λ_{max} in striking agreement with those observed. The fact that small deviations from the value 0.707 are noted for the hydrides of the more electropositive metals is likely due to the fact that Goldschmidt's values for ionic radii may not be altogether proper, since, as Bode[12] points out, the hydrogen ion is probably greatly deformed in the alkali metal hydrides, as indicated by the large refractive indices.

[12] H. Bode, Zeits. f. phys. Chem. (B) 6, 251 (1930).

Alkali Metal Oxides

Whenever small amounts of oxygen or air come in contact with a clean alkali metal surface in an evacuated tube, the photoelectric sensitivity is greatly enhanced and a selective response to light of certain specific wavelengths produced.[13] In such cases a chemical reaction almost invariably occurs and it is usually of sufficient intensity that the heat of reaction might conceivably create a vapor pressure of the metal, so that a thin metallic film will deposit on the surface. Presumably, the compound formed by the chemical reaction and deposited underneath the metallic film is either the monoxide or peroxide of the metal. Similar compounds might be obtained by heating to high temperatures an oxidized silver or copper plate in the presence of the more reactive alkali metals, like caesium.

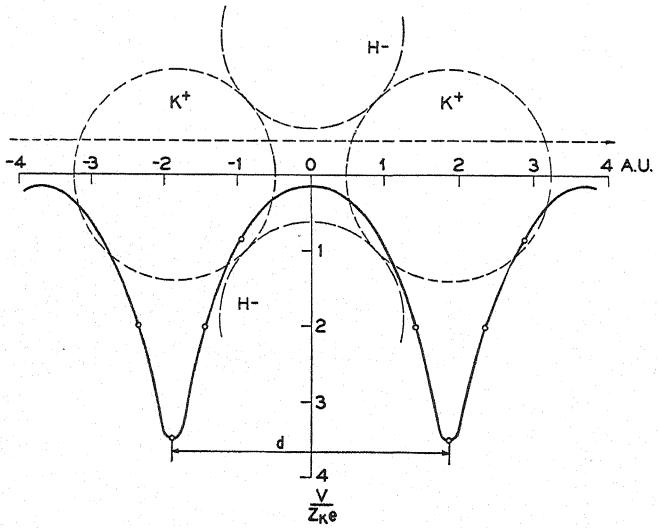


Fig. 5. The potential energy of an electron moving through a potassium-hydride crystal in a direction normal to the 110 plane, and at a distance from the nuclei of the potassium ions indicated by the dotted line with the arrowhead, can be represented by a periodic sequence of hills and valleys like the one shown here.

The selective transmission of electrons through surfaces coated with oxide films will be dependent upon the arrangement of ions in the individual molecules to a large extent. Adopting Slater's conclusions[14] that the valence bonds of the oxygen atom are mutually perpendicular, the diagrams in Fig. 6 representing caesium monoxide and sodium and caesium peroxide have been prepared. Obviously, an electron passing through such a surface structure will encounter a periodic field of potential and the period in the case of the monoxide will be $\frac{1}{2}(2)^{1/2}$ times the sum of the diameters of the metal and oxygen ions. In the case of the peroxide, the period is equal to the diameter of the larger ion in the molecule. More specifically, it is the diameter of the alkali

[13] A. R. Olpin, reference 3.
[14] J. C. Slater, Phys. Rev. 37, 481 (1931).

metal ion in all cases excepting those of sodium and lithium cells; in the latter cases it must be the diameter of the negative oxygen ion.

These dimensions correlate closely with the value of d demanded by Eq. (8). The chief discrepancy comes in the case of the monoxide of the heavier metals, and this may result from the fact that the angle between the valence bonds in alkali metal monoxides is slightly greater than 90°. As a matter of fact Pauling[15] said it should be between 90° and 109°28′ but closer to the former value. Actually 95° will give the proper value of d to correlate the calculated and observed positions of the selective maxima. Or, this slight discrepancy may result from a number of other causes, such for example, as ionic deformation or selective light absorption. It is not the fact that there are slight discrepancies that is surprising, but rather the fact that they are so few and small.

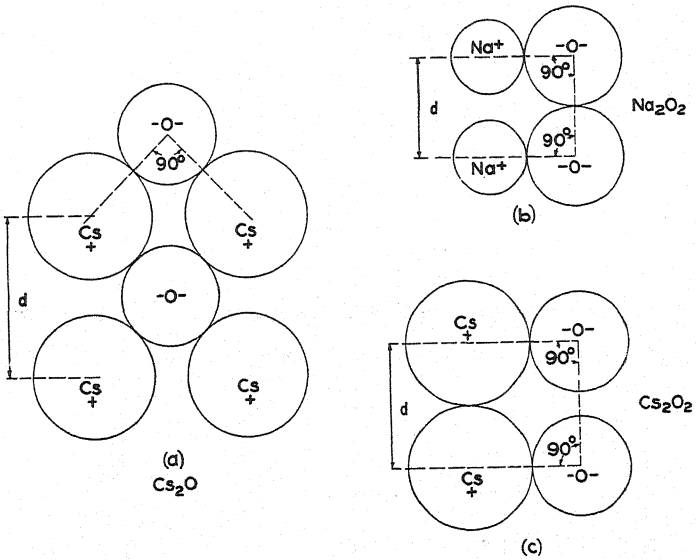


Fig. 6. Diagrams of molecular configurations illustrating distance of closest approach of component positive ions. (a) caesium monoxide, (b) sodium peroxide, and (c) caesium peroxide.

Whenever, as described previously, a cathode coated with an alkali metal oxide is heated under control in such a way that the surface molecules are agitated but not evaporated, and then the surface cooled rather quickly, the characteristic spectral response of the surface changes decidedly. Where there was a spectral maximum previously ,there now appears a minimum, and new maxima appear at other wave-lengths. Presumably this is due to a rearrangement of the ions or molecules on the surface into a crystalline structure.

The crystalline structure of the oxides of the alkali metals of large radii

[15] L. Pauling, J. A. C. S. **53**, 1356 (1931).
[16] Bijvoet and Karssen, Recueil des Travaux Chimiques des Pays—Bas **43**, 680 (1924).
[17] Claasen, Recueil des Travaux Chimiques des Pays—Bas **44**, 790 (1925).

has not been reported, but I have assumed that the monoxides have structures identical with those of Li_2O[16] and Na_2S.[17] In Fig. 7 the arrangement of ions in such a crystal is diagrammatically illustrated. Because of the nature of electrostatic forces within such a crystal, an electron transmitted through it will tend to follow a path close to the nuclei of the positive metal ions and normal to the 100 or 110 planes. The work it must do at various points along either of these paths can be represented by curves similar to the one in Fig. 5, which means that the electron encounters a periodic field of potential within the crystal. In the direction normal to the 100 plane the period is $\frac{1}{3}(3)^{1/2}$ times the sum of the diameters of the positive metal and negative oxygen ions, and in the direction normal to the 110 plane, the period is $\frac{1}{3}(6)^{1/2}$ times this sum. These are the values which must be used for d to satisfy Eq. (8) when the observed positions of the selective maxima are used, as shown in Table II.

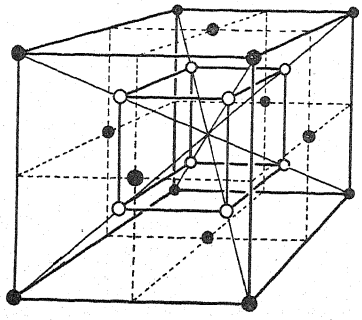


Fig. 7. Arrangement of ions in alkali metal monoxide crystals (CaF_2 structure). The circles represent the metal and the dots the oxygen ions.

Alkali Metal Sulphides and Other Compounds

In the light of the foregoing discussion, it is natural to expect that the wave-lengths of light to which an alkali metal sulphide responds selectively should be longer than for the corresponding oxide. Similarly, the selective maximum might be expected to appear at longer wave-lengths for selenides than for sulphides, and at still longer wave-lengths for tellurides as compared with selenides. Actually this condition has been qualitively observed in the cases of potassium-oxides, sulphides, selenides and tellurides,[18] and to some extent in the case of corresponding sodium compounds.[19] Also, I have recently obtained a good set of curves showing that the position of the selective maximum for the potassium halides is a function of the size of the halogen ion.

Since, in the preparation of the potassium sulphide photoelectric cells referred to in the preceding paragraph, no attempt is made to produce a crystalline arrangement of the surface ions, the separation of the positive ions undoubtedly is that determined by their positions in separate sulphide molecules; and the determination of this value will be similar to that used for the noncrystalline oxides. If the angle between the valence bonds in alkali metal

[18] W. Kluge, Zeits. f. Physik 67, 497 (1931).
[19] A. R. Olpin, reference 3.

sulphides be taken as 90° and the surface coating be similar to that illustrated in Fig. 6 (a), the period of the resulting periodic field of potential is almost exactly the value of d called for by Eq. (8) in the light of experimental data.

When a sulphur-treated sodium photoelectric cell is subjected to treatment similar to that which supposedly forms a crystalline oxide surface, the selective maximum in the spectral response curve always appears at longer wave-lengths than is the case without the sulphur. Moreover, a small hump or irregularity is frequently observed in the spectral response curve at λ6500, where a maximum should appear for crystalline sodium sulphide, if it crystallizes with the calcium-fluoride structure (see Fig. 1C).

TABLE III.

Cathode material		d' Sum of diameters of metal and gas ions	d $(=\frac{1}{2}(2)^{1/2}d')$	λ_{max} $(=330.d^2)$	λ_{max} (observed)	Observer
LiH		4.10A	2.9A	2770	2800	Pohl and Pringsheim[20]
					3400	Pohl and Pringsheim[20]
NaH		4.50	3.18	3340	3300	Olpin and Briggs[21]
KH		5.20	3.68	4470	4350	Pohl and Pringsheim[20]
RbH		5.52	3.9	5020	4800	Pohl and Pringsheim[20]
CsH		5.84	4.13	5630	5400	Seiler[22]
Na_2O	non-crystalline	4.60	3.25	3480	3500	Olpin[23] Richardson and Compton[24]
K_2O	non-crystalline	5.30	3.75	4640	4000–4600	Kluge[25] Olpin[23]
Cs_2O	non-crystalline	5.94	4.20	5820	5400	Pohl and Pringsheim[20] Olpin[23]
			d(=diameter of O ion)			
Na_2O_2	non-crystalline		2.64	2300	2270	Richardson and Compton[24]
			d(=diameter of metal ion)			
Cs_2O_2	non-crystalline		3.30	3590	3500	Koller[26]
			$d(=\frac{1}{3}(3)^{1/2}d')$			
Na_2O	crystalline	4.60	2.65	2320	2270	Richardson and Compton[24]
K_2O	crystalline	5.30	3.06	3090	3130	Wiedmann[27]
Co_2O	crystalline	5.94	3.43	3880	3500	Koller[26]
			$d(=\frac{1}{3}(6)^{1/2}d')$			
Na_2O	crystalline	4.60	3.76	4670	4700	Olpin[23]
K_2O	crystalline	5.30	4.33	6190	6200	Olpin[23]
Cs_2O	crystalline	5.94	4.85	7760	7500–8000	Koller[26] Zworykin[28] Olpin[23] Ballard[29]
			$d(=\frac{1}{2}(2)^{1/2}d')$			
Na_2S	non-crystalline	5.44	3.84	4860	4900	Olpin[23]
K_2S	non-crystalline	6.14	4.34	6200	6000–6200	Olpin[23]
			d(=diameter of sulphur ion)			
Na_2S_2	non-crystalline		3.48	4000	3800	Olpin[23]
K_2S_2	non-crystalline		3.48	4000	4100	Kluge[25] Olpin[23]
			$d(=\frac{1}{3}(6)^{1/2}d')$			
Na_2S (Crystalline)		5.44	4.44	6500	6500	Olpin[23]

[20] R. Pohl and P. Pringsheim, "Die Liehtelektrischen Eischeinungen" Sammlung Viewig, Berlin (1914).

[21] A. R. Olpin and H. B. Briggs, unpublished.

[22] E. F. Seiler, reference 2.

[23] A. R. Olpin, reference 3.

[24] O. W. Richardson and K. T. Compton, Phil. Mag. **26,** 549 (1913).

[25] W. Kluge, reference 18.

[26] L. R. Koller, reference 5.

[27] G. Wiedmann and W. Hallwachs, Verh. d. D. phys. Ges. **16,** 107 (1914).

[28] V. K. Zworykin and E. D. Wilson, "Photocells and Their Application," p. 57.—John Wiley and Sons, N. Y. (1930).

[29] J. W. Ballard, J. O. S. A. **20,** 11, 618 (1930).

It appears, then, that the secret of making selective cathodes in photoelectric cells is that of forming a surface structure in which there is a periodic field of potential. If the selective reponse is desired at long wave-lengths, a large period is required; if at short wave-lengths, a small period. Of course, the surface work function is the limiting factor, however, for it is important that electrons transmitted or conducted through the periodic potential field can be emitted from the surface. In order to keep the work function as low as possible, a monoatomic film of electropositive metal is deposited on the surface.

In Table III are listed the values of d computed from the postulated surface structures described above, and the positions of the selective maxima given by Eq. (8) when these values are used. Opposite these computed values of λ_{max} are recorded the observed values and the observer.

The Lindemann Formula

In 1911 F. A. Lindemann[30] derived the following expression for the natural period of a vibrating system composed of two interpenetrating spheres of radius r and continuously distributed charge $\pm ne$ and $\pm e$ respectively:

$$\nu = \frac{1}{2\pi}\left(\frac{ne^2}{mr^3}\right)^{1/2} \tag{9}$$

This frequency, which is also the frequency of an electron revolving around a central body of charge $+ne$, was identified with that of the selective photoelectric maximum. Putting n equal to unity, the valence of the normal alkali metal atom, and r equal to the radius of each monovalent alkali metal atom in turn, values of ν are obtained in striking agreement with the observed frequencies for the metals and their hydrides.

More recently I pointed out[31] that if the several maxima, characteristic of oxide cells, result from the formation of different compounds, then all that is necessary to obtain values of ν by the Lindemann formula equivalent to the observed selective maximum is to assign to n the valence of the metal in those compounds. In this way the ultraviolet peaks in the response curves were ascribed to the peroxides (as Na_2O_2) of valence 2 and the maxima at long wave-lengths were ascribed to suboxides of valence 1/2 (as Na_4O). Although it is inconsistent with modern theory to think of a nuclear charge equal to $\frac{1}{2}e$ it was suggested that the force exerted on an electron by surrounding atoms might give that net effect.

By the Lindemann formula

$$\nu = \frac{1}{2\pi}\left(\frac{ne^2}{mr^3}\right)^{1/2}$$

and by the Fowler equation,

$$\nu = \frac{h}{8md^2}. \tag{10}$$

[30] F. A. Lindemann, Verh. d. D. phys. Ges. **13**, 482 (1911); ibid. **13**, 1107 (1911).
[31] A. R. Olpin, reference 3.

Equating these two expressions for the natural frequency of electronic systems,

$$\frac{1}{2\pi}(ne^2/mr^3)^{1/2} = \frac{h}{8md^2}, \tag{11}$$

or, simplifying,

$$d^2n^{1/2} = kr^{3/2} \quad (k = \text{const.}) \tag{12}$$

Now for any given metal atom r is constant, so that

$$d^2n^{1/2} = \text{a constant} \tag{13}$$

and d^2 varies inversely as $n^{1/2}$ or the square root of the valency.

As a specific case of this, take the case of the oxides of potassium. Eq. (13) becomes

$$d^2n^{1/2} = 9.12A^2, \tag{14}$$

when the radius of the potassium atom for coordination number 12 is used. By substituting the values of d computed from the structure of the surface compounds as described above [i.e. the sum of the diameters of the positive potassium and negative oxygen ions multiplied by $\frac{1}{3}(3)^{1/2}$, $\frac{1}{2}(2)^{1/2}$, and $\frac{1}{3}(6)^{1/2}$ respectively], the following values of n are obtained: $n=1.98$; $n=0.88$; $n=0.49$.

Similar values are found for the other alkali metals. These compare favorably with the values 2, 1 and 0.5 used as the valence of the alkali metal as mentioned above, and account for the generally close correlation between the experimentally observed positions of the selective maxima and those computed by either the Lindemann formula or the wave mechanics.

Summary and Conclusions

A theory of the selective photoelectric effect for gas-treated alkali metal cells is presented, based on the calculations of wave mechanics, the main features of which are: (1) A two-component cathodic surface structure within which there is a periodic field of potential; (2) Selective transmission of electrons through this field provided their energy bears a definite, fixed relation to its period; (3) Emission of electrons arriving at the surface provided the surface work function is sufficiently low.

A periodic field of potential is shown to be typical of that within a crystal, and a microcrystalline surface structure is postulated for all red-sensitive photoelectric cathodes.

Data are presented correlating the positions of selective maxima in observed photoelectric response curve for the alkali metal hydrides with the sodium chloride arrangement of ions, and the alkali metal oxides and sulphides with the calcium fluoride structure.

The single selective maximum observed in the spectral response of each hydride cell, and the several maxima characteristic of oxides and sulphides are shown to be the natural consequences of these structures.

A correlation between data heretofore obtained by the modified Lindemann formula and those obtained by the wave mechanics is explained.

ON THE THEORETICAL REQUIREMENTS FOR A PERIODIC BEHAVIOUR OF THE UNIVERSE

By Richard C. Tolman
California Institute of Technology, Pasadena
(Received September 18, 1931)

Abstract

This article investigates, on the basis of relativistic mechanics and relativistic thermodynamics, the theoretical requirements for nonstatic models of the universe to exhibit a behaviour which is periodic in time. The discussion is limited to models which can be regarded from a large-scale point of view as filled with a uniform distribution of fluid, and the time coordinate is purposely chosen so as to agree with the proper time that would be used by local observers at rest in this fluid. It is first shown that the analytical requirements which would correspond to the continuous expansion and contraction of such models between definite maximum and minimum limits, together with the thermodynamic requirement that the expansion and contraction must be reversible, could not both be simultaneously satisfied with any fluid for filling the model which has reasonable properties. Attention is then turned to models of the universe having line elements which would be quasi-periodic in the time. A wide range of possibilities is found for models which would expand from zero proper volume to a maximum and then return, the treatment failing however to provide the analytical conditions for a minimum at the lower limit. It is pointed out, nevertheless, that from a physical point of view contraction to zero proper volume could only be followed by renewed expansion, so that we might expect for such models a continued series of expansions and contractions. Furthermore, it is found possible to satisfy the analytical requirements for such quasi-periodic behaviour by models which would expand and contract at a finite rate reversibly without increase in entropy, so that we might then expect a continued series of *identical* expansions and contractions. It is pointed out that Einstein's recent model of a nonstatic universe filled with incoherent matter, exerting no pressure and unaccompanied by radiation, would satisfy the thermodynamic as well as the analytical requirements for such a series of identical repetitions, and models filled solely with black-body radiation and with an equilibrium mixture of radiation and perfect gas are discussed which also satisfy these requirements. In conclusion some remarks are made concerning the bearing of such findings on the behaviour of the actual universe.

§1. Introduction

THE problem of the ultimate fate of our physical surroundings has long been the subject of human thought and speculation. *A priori*, three general types of future behaviour of the universe as a whole would appear to be possible. First, the universe might permanently remain in an approximately steady state; second, it might be subject to progressive change in some particular direction; and third, it might undergo a periodic change in properties, returning at definite intervals at least approximately to an earlier condition.[1]

[1] Different combinations of these general types of behaviour would of course also be possible. Thus we might have periodic happenings taking place simultaneously in different parts of the universe so related as to assure a steady state for the universe looked at as a whole. Or we might have a quasi-periodic behaviour superimposed on a general progressive change in a particular direction.

The possibility for the universe to be in an approximately steady state has usually been regarded as untenable, on account of the implications of the second law of thermodynamics and the actual observation of such important unidirectional phenomena as the flow of radiation from the stars. But interesting suggestions as to compensatory processes, which might really be maintaining the universe in a steady state, have sometimes been made.[2]

The second possibility of a progressive change in the properties of the universe in a particular direction, that of maximum entropy, has usually been regarded in the past as a necessary consequence of the second law of thermodynamics and has furnished what may be called the orthodox view of physics. This view might carry with it, however, the unsatisfactory implication that the universe was created with a supply of available energy at a finite time in the past. Moreover, the apparent inevitability of the view as a necessary consequence of the second law is diminished both by the possibility of fluctuations away from the maximum of entropy discovered many years ago by Boltzmann,[3] and by the previously unsuspected possibility for thermodynamic changes to take place at a finite rate without increase in entropy, which I have recently shown[4,5] to be allowed by the second law of thermodynamics in the form which it assumes in the extension of thermodynamics to general relativity.[6]

The third possibility, that the universe might be subject to a regular periodic change in properties, will be discussed in the present paper. This alternative has been discarded in the past since the classical form of the second law of thermodynamics would permit thermodynamic changes to take place in the universe at a finite rate only in the direction of increasing entropy, thus preventing any return of the universe to an earlier condition. It has now been demonstrated, however, that the relativistic form of the second law of thermodynamics would permit important changes to take place at a finite rate entirely reversibly without any increase in entropy at all. Thus in the case of a model of the universe filled solely with radiation, I have shown[4] that a reversible expansion of the universe could take place at a finite rate without increase in entropy, and that this expansion would be accompanied by a number of phenomena, such as the flow of radiation away from any given observer out into space, which would previously have been regarded as necessarily irreversible. And in the case of a model filled with a mixture of perfect gas and radiation, under the subsidiary assumption that the matter maintains

[2] See for example MacMillan, Astrophys. J. **48**, 35 (1919); Science **62**, 63, 96, 121 (1925); Millikan and Cameron, Proc. Nat. Acad. **14**, 637 (1928); Millikan, Nature **126**, 14 (1930).

[3] Boltzmann, Wied. Ann. **60**, 392 (1897).

[4] Tolman, Phys. Rev. **37**, 1639 (1931).

[5] Tolman, Phys. Rev. **38**, 797 (1931).

[6] The principles for extending thermodynamics to general relativity were developed in previous papers:—Tolman, Proc. Nat. Acad. **14**, 268 (1928); ibid. **14**, 701 (1928); Phys. Rev. **35**, 875 (1930); ibid. **35**, 896 (1930); and have been applied to problems of a different character than the present in other papers:—Tolman, Proc. Nat. Acad. **14**, 348 (1928); ibid. **14**, 353 (1928); ibid. **17**, 153 (1931); Phys. Rev. **35**, 904 (1930); Tolman and Ehrenfest, Phys. Rev. **36**, 1791 (1930).

itself in equilibrium with the radiation, I have been able to show[5] that a reversible transformation of matter into radiation could take place, and would be accompanied by a reversible expansion and reversible flow of radiation out into space.

Such examples of reversible changes make it very interesting to investigate the occurrence of models of the universe which would exhibit periodic behaviour, since such would now appear thermodynamically possible. It was pointed out, nevertheless, in the articles cited that neither of the above models would actually furnish a strictly periodic solution of the equations of motion, and this will be confirmed by more general considerations in the present article. Recently, however, a simple model of the universe has been discussed by Einstein[7] which exhibits a possibility for quasi-periodic solutions of a type which must now also be considered.

§2. Outline of Present Article

The discussion in the present article will be limited to models in which the universe can be regarded from a large-scale point of view as filled with a perfect fluid, having properties which change with the time but are independent of position. Furthermore, the time coordinate will be chosen so as to agree with the proper time as used by local observers at rest with respect to the material in the model, since it is evident that equations periodic in form with respect to an arbitrarily chosen time coordinate might have no special physical interest.

The possibilities for change with time in such models consist in an expansion or contraction in the proper volume of the universe. The equations of motion for such changes will first be obtained from the principles of relativistic mechanics, and the analytical requirement for these equations to correspond to a periodic expansion and contraction will be exhibited. Combining this analytical requirement with the thermodynamic requirement for periodic behaviour, namely that the motion should be reversible in the sense of relativistic thermodynamics, it will then be shown that no strictly periodic solution for the equations of motion would be possible for a model of this kind filled with any combination of incoherent matter and radiation. This general result confirms the conclusion already found for the two special models mentioned above, and also has the consequence of ruling out as physically probable the very interesting periodic line element recently proposed by Takéuchi.[8]

At first sight the result would appear to prove conclusively that no model whatever of the kind considered could exhibit a continued sequence of identical expansions and contractions. It will next be shown, however, that a new method of attack can be undertaken, by abandoning the attempt to find strictly periodic solutions of the equations of motion and considering instead quasi-periodic solutions which correspond to an expansion of the universe from zero proper volume to an upper limit and contraction again to the

[7] Einstein, Berl. Ber. (1931) p. 235. See also de Sitter, Bull. Astron. Inst. Netherlands **6**, 141 (1931).

[8] Takéuchi, Proc. Phys. Math. Soc. Japan **13**, 166 (1931).

starting point, the analytical treatment failing however outside the range between these points of zero volume.

A wide range of possibilities for solutions of this type will be found to exist. Furthermore, cases will be found where the analytical requirements for these quasi-periodic solutions can be satisfied by systems which expand and contract reversibly without increase in entropy. In such cases, since the only physical possibility after contraction to zero volume would be another expansion, and since the system arrives at the point of zero volume after contraction with unchanged entropy, it would seem allowable to expect a continued sequence of identical expansions and contractions, even though the mathematical analysis fails to carry us through the exceptional point of zero volume.

As mentioned above, one quasi-periodic solution corresponding to expansion from zero volume to an upper limit and return has already been given by Einstein.[7] It corresponds to a model in which the contents of the universe are taken as incoherent matter exerting zero pressure and unaccompanied by radiation. In this article it will be specially pointed out that the expansion and contraction of the Einstein model would not be accompanied by increase in entropy and hence could presumably be repeated over and over again.

Since the actual universe presumably contains radiation as well as matter, it will also be interesting to consider a model filled solely with black-body radiation which is the opposite extreme to the Einstein model containing nothing but matter. The form of line element for such a model will be exhibited, and it will be shown that this model would also expand and contract reversibly. Attention will then be turned to a more complicated model containing an equilibrium mixture of black-body radiation and perfect monatomic gas, and it will be shown that such a model could also furnish quasi-periodic solutions corresponding to reversible expansions and contractions. Finally in conclusion, a few remarks will be made concerning the possible bearing of such considerations on the problem of the behaviour of the actual universe.

§ 3. The Mechanics of the Nonstatic Universe

The line element for a nonstatic universe filled with a uniform distribution of matter and energy can be derived,[9] by treating the contents of the universe for the purposes of large-scale considerations as a perfect fluid, and written in the form

$$ds^2 = -\frac{e^{g(t)}}{[1 + r^2/4R^2]^2}(dr^2 + r^2 d\theta^2 + r^2 \sin^2\theta d\phi^2) + dt^2 \qquad (1)$$

where r, θ and ϕ are the spatial coordinates, t is the time coordinate, R is a constant, and the dependence of the line element on the time is given by the exponent $g(t)$.

With this choice of coordinates, particles which are at rest in the coordinate system will not be subject to acceleration but will remain perman-

[9] See Tolman, Proc. Nat. Acad. **16**, 320 (1930).

ently at rest, and it will be noted that the time coordinate t will agree with the proper time as used by local observers at rest with respect to such particles.

The proper pressure p_0 and proper macroscopic density ρ_{00} of the fluid corresponding to this line element are given by the equations[10]

$$8\pi p_0 = -\frac{1}{R^2}e^{-g} - \ddot{g} - \tfrac{3}{4}\dot{g}^2 + \Lambda \tag{2}$$

$$8\pi\rho_{00} = \frac{3}{R^2}e^{-g} + \tfrac{3}{4}\dot{g}^2 - \Lambda \tag{3}$$

where Λ is the cosmological constant. The pressure and density are independent of position, and are dependent as shown on the exponent g and its time derivatives $\dot{g}$ and $\ddot{g}$, and thus on the time itself.

The proper volume associated with the coordinate range $\delta r\ \delta\theta\ \delta\phi$ in accordance with the above line element, is evidently

$$\delta V_0 = \frac{r^2 \sin\theta\, e^{3g/2}}{[1 + r^2/4R^2]^3}\,\delta r\,\delta\theta\,\delta\phi \tag{4}$$

and since the dependence of the line element on the time occurs solely because of the functional dependence of the exponent g on t, it is evident that changes in the state of the universe with time can be characterized as expansions or contractions in proper volume, according as g is increasing or decreasing with the time.

In accordance with the expressions for pressure and density given by (2) and (3), this change in volume of the universe is governed by the simple equation[11]

$$\frac{d}{dt}(\rho_{00}\, e^{3g/2}) + p_0 \frac{d}{dt}(e^{3g/2}) = 0. \tag{5}$$

Or noting Eq. (4), we can write

$$\frac{d}{dt}(\rho_{00}\,\delta V_0) + p_0 \frac{d}{dt}(\delta V_0) = 0 \tag{6}$$

which shows that the change in the energy content associated with any small element of fluid is equal to the negative of the work performed on the surroundings.

§ 4. The Analytical Requirements for a Strictly Periodic Solution

Since changes in the line element with time occur because of the dependence of g on t, it is evident that the conditions for a strictly periodic behaviour of the model can be met only if g passes periodically through its minimum and maximum values. Using the subscripts 1 and 2 to denote the values assumed by different quantities when g has its minimum and maximum values, we can write as the analytical condition for the minimum

[10] See preceding reference, Eqs. (34).

[11] See Tolman, Proc. Nat. Acad. **16**, 409 (1930); Eq. (4).

$$g = g_1 \qquad \dot{g}_1 = 0 \qquad \ddot{g}_1 \geqq 0 \tag{7}$$

and as the condition for the maximum

$$g = g_2 \qquad \dot{g}_2 = 0 \qquad \ddot{g}_2 \leqq 0 \tag{8}$$

and by intercombination these expressions give as a necessary requirement for a strictly periodic solution

$$g_1 < g_2 \qquad \dot{g}_1 = \dot{g}_2 = 0 \qquad \ddot{g}_1 \geqq \ddot{g}_2 \tag{9}$$

§ 5. The Thermodynamic Requirements for a Strictly Periodic Solution

As the thermodynamic requirement for a strictly periodic solution, it is evident that the changes taking place in our model of the universe must be thermodynamically reversible, since otherwise it would not be possible for the model to return to an earlier state. As previously shown[12] in accordance with the principles of relativistic thermodynamics, the condition for reversibility will be met in a system of the kind considered if we have the equation

$$\frac{d}{dt}(\phi_0 \ \delta V_0) = 0 \tag{10}$$

holding at each point in the fluid, where ϕ_0 is the proper density of entropy as measured by a local observer at rest with respect to the fluid, and δV_0 is the proper volume of a small element of the fluid.

Since the proper volume in accordance with the principles of general relativity is dependent on the gravitational potentials $g_{\mu\nu}$, this condition for reversibility permits a mutual change in entropy density and gravitational field which was not contemplated in the classical thermodynamics. The equation states that the total entropy for each small element of fluid shall be constant as measured by a local observer, and this can evidently be met if the change in proper volume for the element occurs without flow of heat into the element, with exact balance between the internal and external pressures acting at the boundary of the element, and without irreversible processes taking place inside the element. In the case of the systems we are discussing the condition for no flow of heat into the element is evidently met in general on account of Eq. (6), and the exact balance between internal and external pressures is assured by the uniformity of pressure throughout the whole model as shown by Eq. (2); so that the avoidance of irreversible changes within the element is the only part of the requirement that must be specifically watched. If the requirement for reversibility is met, it will be noted that the changes taking place in the properties of the fluid filling our model of the universe would be those which would result from a reversible adiabatic change in volume of that kind of fluid.

[12] See reference 4, Eq. (18).

§ 6. Impossibility of a Strictly Periodic Solution

It can now be shown that the two separate sets of requirements for a strictly periodic solution could not both be satisfied by any fluid for filling the model of the universe which has reasonable physical properties.

On the one hand in accordance with the general expressions for density and pressure given by (2) and (3), and the necessary analytical requirement for a strictly periodic solution given by (9), we can evidently write

$$8\pi(\rho_1 - \rho_2) = \frac{3}{R^2}(e^{-g_1} - e^{-g_2}) \tag{11}$$

$$8\pi(p_1 - p_2) = -\frac{1}{R^2}(e^{-g_1} - e^{-g_2}) - (\ddot{g}_1 - \ddot{g}_2) \tag{12}$$

$$g_1 < g_2 \quad (13a) \qquad \text{and} \quad \ddot{g}_1 \geqq \ddot{g}_2 \tag{13b}$$

where $(\rho_1 - \rho_2)$ is the difference in energy density when the universe has its minimum and maximum volumes, and $(p_1 - p_2)$ is the difference in pressure.

On the other hand in accordance with the thermodynamic requirement for a periodic solution given in § 5, the changes in density and pressure when the universe passes from its minimum to its maximum volume must be those which would result from a reversible adiabatic expansion of the fluid, which would evidently give us

$$\rho_1 > \rho_2 \quad (14a) \qquad \text{and} \quad p_1 \geqq p_2 \tag{14b}$$

for any kind of fluid with which we might wish to regard the universe as filled.

All of the above relations, however, cannot be simultaneously satisfied. If the density is to decrease on expansion, then in accordance with (11) and (13a), it is evident that R must be real and R^2 positive. And with R^2 positive it will then be seen from (12), (13a) and (13b) that the pressure would increase on expansion, in contradiction to (14b).

It is evident that the relations (14a) and (14b) on which this reasoning is based would hold for any combination of incoherent matter and radiation which we might take as the fluid for filling the universe. By a special assignment of assumed properties, it might of course be possible to obtain strictly periodic solutions, but it does not appear probable that they would have actual physical interest. Thus a fluid which would correspond to the assumption made by Takéuchi,[13]

$$g = \sin kt \tag{15}$$

would appear to have very arbitrary properties.

§ 7. Analytical Requirements for a Quasi-Periodic Solution

In view of the above result we may now turn our attention to the possibility of quasi-periodic solutions, in which the proper volume of the universe increases from zero to an upper limit and returns, the mathematical analysis, however, failing to carry us through the exceptional point of zero volume. A

[13] See reference 8.

wide variety of possibilities presents itself for such solutions, and we may confine our attention for the present to those in which we take the constant R as real, and the cosmological constant Λ equal to zero as in Einstein's original simple form of the equations of relativistic mechanics.[14]

We can then obtain an expansion from zero proper volume $g_1 = -\infty$ to an upper limit $g_2 > g_1$ and return again to $g_3 = -\infty$, with reasonable values for density and pressure, if we place the following restrictions on g and its derivatives,

$$g_1 = -\infty \qquad \dot{g}_1 > 0 \qquad \ddot{g}_1 = -\infty \tag{16}$$

$$g_2 > g_1 \qquad \dot{g}_2 = 0 \qquad \ddot{g}_2 \leqq -\frac{1}{R^2} e^{-g} \tag{17}$$

$$g_3 = -\infty \qquad \dot{g}_3 < 0 \qquad \ddot{g}_3 = -\infty \tag{18}$$

In accordance with these restrictions, the model will evidently pass through a maximum volume at $g = g_2$. Furthermore, making use of the general expressions for proper density and pressure given by (2) and (3), the model will exhibit at the limits of the expansion, with $\Lambda = 0$, the densities

$$8\pi\rho_1 = \infty \qquad \text{and} \quad 8\pi\rho_2 \geqq 0 \tag{19}$$

and the pressures

$$8\pi p_1 = -\infty + \infty \qquad \text{and} \quad 8\pi p_2 \geqq 0 \tag{20}$$

and these expressions evidently place no undue restrictions on the physical properties of the fluid with which we fill the model.

It is evident that solutions which agree with the conditions imposed by (16), (17) and (18) could not be regarded analytically as strictly periodic, since the value of $\ddot{g}$ is necessarily minus infinity at the lower limit of zero volume in order to prevent the pressure from becoming negative, and this is incompatible with the analytical conditions for a minimum. Nevertheless, it is evident physically that contraction to zero volume could only be followed by another expansion, and in addition, as noted by Einstein[7] in a similar connection, the idealization on which our considerations have been based can be regarded as failing in the neighborhood of zero volume. Hence from a physical point of view it seems reasonable to consider that solutions of the kind which we are considering could correspond to a series of successive expansions and contractions.

[14] The introduction of the cosmological term $\Lambda g_{\mu\nu}$ into the field equations of relativity was necessary for Einstein's static model of the universe. The term is not inevitably necessary, however, for nonstatic models, and Einstein (reference 7) now welcomes the opportunity to set it equal to zero. There are several arguments in favor of giving Λ the definite value zero. The equations of the theory are thereby simplified; the conclusions drawn from them are rendered less indeterminate; and it no longer becomes necessary to inquire into the significance and magnitude of what would otherwise be a new constant of nature. On the other hand, since the introduction of the Λ-term provides the most general possible expression of the second order which could be used for the energy momentum tensor, a definite assignment of the value $\Lambda = 0$ must be regarded as somewhat arbitrary and not necessarily correct.

§ 8. Thermodynamic Requirements for a Series of Identical Expansions and Contractions

Since the foregoing indicates the possibility of a series of expansions and contractions, we may next inquire into the further possibility that the successive expansions and contractions could have the character of identical repetitions. For this to be possible, it is evident that each expansion and contraction would have to be reversible from the point of view of relativistic thermodynamics, since any increase in entropy would prevent the return to an earlier condition.

If, however, the condition for thermodynamic reversibility

$$\frac{d}{dt}(\phi_0 \delta V_0) = 0 \tag{21}$$

already discussed in § 5 should be satisfied, a series of identical expansions and contractions would seem possible.

We may now discuss some quasi-periodic solutions fulfilling these requirements.

§ 9. Einstein's Quasi-Periodic Solution

As already mentioned one quasi-periodic model has already been suggested by Einstein. For simplicity denoting the "radius" of the universe by P where

$$P = Re^{g/2} \tag{22}$$

the general behaviour of the Einstein model can be most readily appreciated by solving the differential equation for P which he gives. We obtain

$$\sqrt{\frac{P}{P_0}} = \sin\left(\frac{t}{P_0} + \sqrt{\frac{P}{P_0}}\sqrt{1 - \frac{P}{P_0}}\right) \tag{23}$$

where P_0 is a constant, and note that the radius of the universe would expand from the value zero at $t=0$, to the upper limit $P=P_0$ at $t=\pi P_0/2$, and then return once more to zero at $t=\pi P_0$, the solution failing, however, to make P an analytical minimum at the lower limit.

The values of $\dot{g}$ and $\ddot{g}$ which correspond to (22) and (23) can be written in the form

$$\frac{\dot{g}^2}{4} = \frac{P_0}{P^3} - \frac{1}{P^2} \tag{24}$$

and

$$\ddot{g} = -3\frac{P_0}{P^3} + \frac{2}{P^2} \tag{25}$$

and substituting in the general expressions for pressure and density given by (2) and (3), with $\Lambda = 0$ we obtain,

$$8\pi p_0 = 0 \tag{26}$$

$$8\pi\rho_{00} = \frac{3P_0}{P^3} = \frac{3P_0}{R^3 e^{3g/2}}. \tag{27}$$

The model thus corresponds to a universe filled with incoherent particles of matter, exerting no pressure, and unaccompanied by radiation.

From the point of view of the present paper, our interest lies in the entropy of the model. In accordance with the expressions for proper volume and density given by (4) and (27), it is evident that we shall have in the case of this model

$$\frac{d}{dt}(\rho_{00}\,\delta V_0) = 0 \tag{28}$$

owing to the fact that the only quantity g, which depends on the time, cancels from the product. For particles of matter exerting no pressure, it is evident, however, that the proper entropy $\phi_0\,\delta V_0$ will be proportional to the proper mass $\rho_{00}\,\delta V_0$ so that we must also have

$$\frac{d}{dt}(\phi_0\,\delta V_0) = 0 \tag{29}$$

which is the thermodynamic condition for reversibility already discussed in § 5. We may hence conclude that the model expands and contracts reversibly, which is perhaps an obvious conclusion in the case of this simple system. Since the behaviour of the model is thermodynamically reversible, there would be no thermodynamic hindrance which would prevent a continuous sequence of identical expansions and contractions.

§ 10. Quasi-Periodic Solution for a Universe Filled with Radiation

The real universe undoubtedly contains radiation as well as matter. The actual amount of this radiation is unknown. Nevertheless, it may be noted that as low a temperature as 12° absolute would correspond to a density of radiation of 1.7×10^{-31} gm/cm^3 which is approximately the same as Hubble's estimate[15] of the averaged-out density of visible matter in the universe. In any case it will be interesting to consider the extreme example of a model containing nothing but black-body radiation, even if we regard this merely as an intellectual exercise.

As mentioned above[16] I have already considered this model, without making any assumptions as to the value of the cosmological constant Λ, and come to the conclusion that no strictly periodic solution of the equations of motion could be found. The possibility of quasi-periodic solutions presents itself nevertheless, and setting $\Lambda=0$, it can readily be shown that the line element for such a model then has the form

$$ds^2 = -\frac{At - t^2/R^2}{[1 + r^2/4R^2]^2}(dr^2 + r^2d\theta^2 + r^2\sin^2\theta d\phi^2) + dt^2 \tag{30}$$

where A is a positive constant.

[15] Hubble, Astrophys. J. **64**, 369 (1926).

[16] See reference 4.

In accordance with this form of the line element, the universe would start from zero proper volume at $t=0$, expand to a maximum at $t=AR^2/2$ and contract to zero again at $t=AR^2$, and the behaviour would be symmetrical on the two sides of the maximum as can easily be seen by transforming so that the zero of time comes at that point. Outside the range $t=0$ to $t=AR^2$, the treatment fails since the analytical expression would then correspond to negative volumes which are physically impossible.

The values of g and its differential coefficients corresponding to this line element are

$$e^g = At - t^2/R^2 \tag{31}$$

$$\dot{g} = \frac{1}{t} - \frac{1}{AR^2 - t} \tag{32}$$

and

$$\ddot{g} = -\frac{1}{t^2} - \frac{1}{(AR^2 - t)^2}. \tag{33}$$

Substituting these values into the general expressions for proper pressure and density given by (2) and (3), with Λ set equal to zero, we obtain

$$8\pi p_0 = \frac{1}{4}\,\frac{A^2}{(At - t^2/R^2)^2} \tag{34}$$

and

$$8\pi \rho_{00} = \frac{3}{4}\,\frac{A^2}{(At - t^2/R^2)^2} \tag{35}$$

We note at once that the energy density is always three times the pressure, so that the line element does correspond to a universe filled solely with black-body radiation, It is also interesting to observe that the energy density would be infinite at the times $t=0$ and $t=AR^2$ when the volume of the model is zero, and would drop to $3/R^2$ at $t=AR^2/2$ when the volume is at its maximum.

As in the case of the preceding model, our main interest for the present lies in the entropy of the system. In accordance with the known properties of black-body radiation, it is evident that we may write

$$\rho_{00} = aT_0^4 \quad \text{and} \quad \phi_0 = \frac{4}{3}\,aT_0^3 \tag{36}$$

for the proper (macroscopic) energy density ρ_{00} and proper entropy density ϕ_0 in terms of the Stefan-Boltzmann constant a and the proper temperature T_0. And by combination we can write

$$\phi_0 = \frac{4}{3}\,a^{1/4}\rho_{00}^{3/4}. \tag{37}$$

Substituting the values given by (35) and (31) we can then obtain for the entropy density

$$\phi_0 = \left(\frac{4}{3}\,a\right)^{1/4}\left(\frac{A^2}{8\pi}\right)^{3/4} e^{-3g/2} \tag{38}$$

and comparing with the general expression for proper volume given by Eq. (4), we at once see that we shall have the relation

$$\frac{d}{dt}(\phi_0 \delta V_0) = 0 \tag{39}$$

owing to the fact that the only quantity g, which depends on the time cancels from the product. This, however, is the condition for thermodynamic reversibility already discussed in § 5. Hence we may also conclude in the case of this model that there would be no thermodynamic hindrance which would prevent a continuous sequence of identical expansions and contractions.

§ 11. Quasi-Periodic Solution for a Universe Containing an Equilibrium Mixture of Matter and Radiation

It will also be interesting to consider the possibility for a quasi-periodic solution in the case of the model, which I have previously treated, of a universe containing a perfect monatomic gas in equilibrium with black-body radiation. If we set the cosmological constant Λ equal to zero, the equations of motion previously obtained[17] for this model become

$$8\pi p_0 = -\frac{1}{R^2}e^{-g} - \ddot{g} - \tfrac{3}{4}\dot{g}^2 = 8\pi(N_0 k T_0 + \tfrac{1}{3}aT_0^4) \tag{40}$$

$$8\pi\rho_{00} = \frac{3}{R^2}e^{-g} + \tfrac{3}{4}\dot{g}^2 = 8\pi(N_0 mc^2 + \tfrac{3}{2}N_0 k T_0 + aT_0^4) \tag{41}$$

$$N_0 = bT_0^{3/2}e^{-mc^2/kT_0} \tag{42}$$

where N_0 is the proper concentration of the gas in number of molecules per unit volume, T_0 the proper temperature, m the mass of one atom, and the constants k, a, c and b have their customary significance.

As demonstrated in the previous article these differential equations show no possibility for a strictly periodic solution of physical significance. To investigate the possibility for a quasi-periodic behaviour of the model, we shall not try to integrate the equations owing to their great complexity, but instead shall content ourselves with a demonstration of the existence of quasi-periodic solutions without obtaining their explicit form.

In accordance with Eq. (40) it is evident that the pressure p_0 is necessarily a positive quantity

$$p_0 \geqq 0 \tag{43}$$

since the concentration N_0 and temperature T_0 are both quantities which physically cannot be negative. Hence from (40), taking R as real, it is evident that we must also have

$$\ddot{g} \leqq -\frac{1}{R^2}e^{-g} \tag{44}$$

So that $\ddot{g}$ will always be negative if the volume of the universe is finite (i.e. $g < \infty$).

[17] See reference 5.

It appears evident, however, that this provides the possibility of choosing conditions so that models of the kind under discussion would pass through a point of maximum expansion. To prove this it is only necessary to admit the possibility of setting up a model of the universe with an equilibrium mixture of the gas and radiation contained in a finite volume which at the moment is not changing with the time. This set-up, with $\dot{g}$ put equal to zero and $\ddot{g}$ as seen above necessarily negative, evidently corresponds to the condition at the maximum point of expansion of a model which starts at zero volume with $\ddot{g}$ equal to $-\infty$ passes through a maximum with $\ddot{g}$ still negative and returns again to zero volume with $\ddot{g}$ again equal to $-\infty$. So that the conceivability of the proposed set-up shows the possibility of quasi-periodic solutions for models of the universe containing an equilibrium mixture of perfect monatomic gas and black body radiation.

It is also interesting to note that this method of showing the possibility for quasi-periodic solutions would apply to any model in which the fluid must be regarded as always exerting a positive pressure.

Since my previous work on this model showed that its expansion or contraction would be thermodynamically reversible, provided we make the somewhat arbitrary assumption that the matter in the model always immediately adjusts itself so as to remain in equilibrium with the radiation, it is evident in this case too that there would be no thermodynamic hindrance to a continuous succession of identical expansions and contractions.

§ 12. Conclusion

The result of the foregoing investigation of the theoretical requirements for the periodic behaviour of a certain class of nonstatic models of the universe has been threefold. In the first place, it has been shown that we cannot expect a strictly periodic solution of the equations of motion for such models, which would correspond to an oscillation in proper volume between a minimum and maximum value, unless indeed we should assign properties to the material filling the universe of a kind which would presumably not be of actual interest. It has been shown in the second place, however, that we might expect a wide variety of quasi-periodic solutions, which would correspond to an expansion of the model from zero proper volme to a maximum and return, —the solutions failing, however, to provide the analytical conditions for a minimum at the lower limit, even though physically contraction to this limit could only be followed by renewed expansion. Finally, it has been shown in accordance with the principles of relativistic thermodynamics that the conditions necessary for such quasi-periodic solutions could be met by systems which expand and contract reversibly without increase in entropy, so that there would be no thermodynamic hindrance to a continued series of identical expansions and contractions, and this conclusion has been illustrated by three examples.

The three models, which were chosen as examples to illustrate the possibility of a continued series of identical expansions and contractions, were,— first, a universe filled with incoherent matter exerting no pressure and unac-

companied by radiation,—second, a universe filled solely with black-body radiation,—and third, a universe filled with a mixture of perfect monatomic gas in equilibrium with black-body radiation. It is of interest, in connection with speculations as to the possibility that the actual universe might undergo a series of identical expansions and contractions, to find that so wide a range of models show such behaviour. This interest is increased, moreover, by the fact that my previous studies[18] of the second and third of these two models have shown that an ordinary observer would find a number of phenomena during the expansion of these models, such as the flow of radiation out into space and the annihilation of matter, which he would interpret as necessarily irreversible, in spite of the fact that all the processes taking place in such universes would really be reversible when analyzed from the legitimate point of view of relativistic thermodynamics.

In conclusion, however, we must not fail to emphasize that all our specific considerations have dealt with highly idealized models and not with the actual universe. These models have, moreover, some quite unsatisfying properties. In the first place, the models are all limited to a restricted class in which the properties of the contents of the universe, looked at from a large-scale point of view, are assumed to be the same throughout the whole universe at a given instant, and in justification of this assumption we merely have the data obtained from astronomical observations on the nebulae out to a limit of only about 10^8 light years. In the second place, moreover, the models do not concern themselves with many questions which may be very important for a satisfactory cosmological picture, such as the tendency of matter to conglomerate in stars and stellar systems,[19] the relative abundance of the different elements,[20] the relative concentration of matter and radiation,[21] and the rate at which matter and radiation adjust themselves to mutual equilibrium.[22] For these reasons we must not overestimate any insight that we obtain into the possible behaviour of the actual universe as a result of calculations on highly idealized models. Nevertheless, the principles of relativistic thermodynamics seem to have made a real contribution to cosmology, in showing that reversible models can at least be conceived which could exhibit a succession of identical expansions and contractions taking place at a finite rate.

[18] See references 4 and 5.

[19] The treatments which I have given to the flow of radiation in a universe, which is expanding reversibly, show that an ordinary observer in such a model would find a general outward flow of radiation from his region, but do not concern themselves with the more special problem of a directed outward flow from individual stars.

[20] I have shown, Jour. Am. Chem. Soc. **44**, 1902 (1922), that the relative abundance of hydrogen and helium appears to be very different from that demanded by thermodynamic equilibrium and similar findings have been obtained for the relative abundance of isotopes by Urey and Bradley, Phys. Rev. **38**, 718 (1931).

[21] The constant b in Eq. (42) would have to be enormous to secure appreciable concentrations of matter.

[22] The model of a universe containing an equilibrium mixture of gas and radiation would behave reversibly only if the mutual equilibrium were maintained. See reference 5.

PERMANENT ELECTRIC AND MAGNETIC MOMENTS OF CRYSTALS

By F. Zwicky
Norman Bridge Laboratory, California Institute of Technology, Pasadena

(Received September 19, 1931)

Abstract

In the first part of this paper the conditions for the existence of self-perpetuating electric moments in crystals are discussed. If these conditions are satisfied, the crystals must either show macroscopic electric moments or they will necessarily possess a definite type of a secondary structure. Certain complications may come in, however, if one is dealing with metals. Finally, the analogous magnetic case is qualitatively discussed.

§1. Introduction

THE theory of the ideal crystal lattices must be regarded as a complete failure as far as the treatment of structure sensitive properties is concerned. I have recently endeavored to show that a satisfactory theory of the physics of solids can be developed by introducing a secondary structure of crystal lattices.[1] This structure in general may be described as a periodic, very slight variation in density. I arrived at the conception of a secondary structure from purely theoretical arguments which threw doubt on the current conception of ideal crystals being thermally stable. Although many important conclusions of this theory were verified experimentally, its foundations are not very satisfactory for the following reasons.

In the first place, the procedure which I followed did not supply any unambiguous way of determining the exact nature of the deviations which transform an ideal lattice into a real and thermally stable crystal.

In the second place, it was very difficult to account for dimensions of the secondary lattice larger than a few hundred Angstroms, such as we have been finding in single crystals of metals. Although the theory does not really enable one to derive accurate values for the lattice constant D of the secondary structure there are strong reasons for assuming that approximately

$$D = d/(1 - d_P/d) \tag{1}$$

Here d is the ordinary lattice constant and d_p the corresponding spacing of a single plane of atoms which in itself is assumed to be in equilibrium under its own forces. The relative change from d to d_p can be estimated to be of the order of one percent, which according to (1) makes values of D larger than $100d$ very improbable. It also has been objected that it would be very hard to understand how actions over such large distances come about.

In the third place, experimental investigations carried out on single crystals suggest that there are secondary lattices of very different types. The theory therefore is confronted with the task of finding as many effects as

[1] F. Zwicky, Proc. Nat. Acad. Sci. **15**, 816 (1929); Helvetica Physica Acta **3**, 269 (1930); and **4**, 49 (1931).

possible which will render an ideal crystal thermally unstable. In addition, one has to try to find, if possible, a common denominator for all these effects. In a recent publication[2] I have advanced a tentative solution of this latter problem. The essence of my proposal was that those effects which are mainly responsible for the formation of a crystal at the same time necessitate a secondary structure. Those effects were recognized to be simultaneous cooperative actions between many particles. It seems therefore desirable to investigate more closely the characteristics of such actions. In this paper one very special phenomenon which depends on the cooperation of many particles will be considered. Its character will be best understood by studying some of its essential features in relation to a simple lattice.

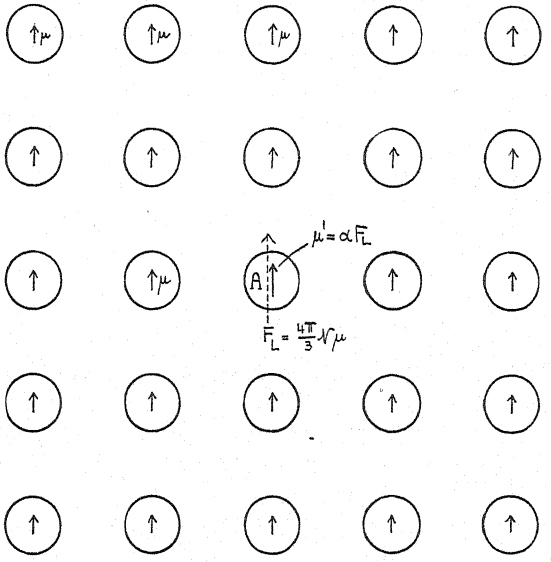


Fig. 1. Lattice of self-perpetuating dipoles.

§2. General Remarks on Self-Perpetuating Electric Moments

The essential part of this paper is devoted to a generalization of K. F. Herzfeld's considerations concerning the characteristics of metals. Herzfeld derives a criterion which decides whether or not an element will occur as a metal. His argument is roughly as follows:[3]

Consider a simple cubic lattice occupied by atoms whose dielectric constant is α. (See Fig. 1.) Suppose that all the atoms except A are endowed with an infinitely small electric dipole μ. Then because of the action of the μ's there will be an electric field at A which is equal to $F_L = 4\pi P/3 = 4\pi N\mu/3$, where N is the number of atoms per unit volume and P the polarization per unit volume.[4] The average field throughout the crystal of course is zero,

[2] F. Zwicky, Proc. Nat. Acad. Sci. September, 1931.
[3] H. F. Herzfeld, Phys. Rev. 29, 701 (1926).
[4] See for instance P. Debye in Handbuch d. Radiologie, Vol. VI, p. 600.

provided that the lattice is infinitely extended. The so-called Lorentz field deforms the atom A and endows it with a moment μ'

$$\mu' = 4\pi N\mu\alpha/3. \tag{2}$$

Suppose now that

$$4\pi N\alpha/3 = 4\pi \mathrm{N}\alpha\rho/3M = R\rho/M > 1 \tag{3}$$

where R is the molar refractivity, ρ the density, M the molecular weight, and $\mathrm{N} = 6.06 \times 10^{23}$. It then follows that

$$\mu' > \mu.$$

This means that the assembly of the induced dipoles is a self perpetuating configuration of ever increasing moment. The process stops, of course, as soon as all the atoms are stripped of their loosest electrons. Condition (3) therefore is a condition for the element to be a metal.

It is very important to notice that the conclusions drawn above are valid only if α either increases or at least stays constant with increasing μ. This is probably generally true if α is the polarizability of an atom. We may, however, generalize Herzfeld's theory to systems with elementary units other than atoms, as will be shown in the next section. It then happens that the respective dielectric constant decreases with increasing polarization. The system involved may then jump into a configuration of permanent electric polarization without this process resulting in a collapse of the elementary particles, such as the stripping of atoms of their electrons. The permanent electric polarization need not be apparent in macroscopic dimensions, as will be shown later. In the case of a resulting macroscopic moment we are dealing with a crystal which possesses the characteristics of an electret. If only microscopic regions are electrically polar, they may compensate each other over large distances. We then obtain a peculiar type of a secondary structure.

In the next section we shall discuss the properties of a definite simple lattice which, however, is chosen so as to exhibit all the general features in which we are interested in our discussion.

§3. Permanent Electric Polarization in Cubic Face Centered Ionic Lattices

We investigate the properties of a lattice which is built up of positive and negative ions. We assume that for the mutual potential energy of two ions i and k we may write, as usually adopted for a first approximation,

$$\epsilon_{ik} = e_i e_k/r_{ik} + A/r_{ik}^{p} \tag{4}$$

where A and p for simplicity are taken to be the same for all the three possible combinations of the two ions.

The average energy ϵ of an ion in the face centered cubic lattice can be shown to be

$$\epsilon = -1.747e^2/r + \gamma A/r^{p} \tag{5}$$

with r designating the usual lattice constant. Numerical values of γ for different p's are tabulated in Table I.

TABLE I.

p	5	6	7	8	9	10
γ	166	269	478	888	1700	3287

Now for this lattice to be in equilibrium we must require

$$\frac{\delta\epsilon}{\delta r} = 0 \text{ for } r = d \tag{6}$$

or

$$A = 1.747e^2d^{p-1}/p\gamma. \tag{6'}$$

It is usually assumed that this condition is all that is required in order to make a lattice of the described type dynamically stable. Indeed, in all the cases dealt with in the literature it was found that a lattice of the above type, with A equal to (6') is also stable against a linear extension, shearing, or against a displacement of the whole negative lattice relative to the positive lattice, etc. However, there was known no general proof that condition (6) insures the complete dynamic stability of the lattice. In fact, it can be shown that this is not at all the case. For this purpose we shall investigate more closely the stability of our model with regard to relative displacements of the negative and the positive lattice. Such displacements evidently may be caused by external electric fields. It is well known that the characteristic frequencies involved correspond to the frequencies of the residual rays.

Suppose that the lattice of the positive ions is given a uniform infinitesimal displacement ξ in the direction of the [100] axis. At the location of each ion a Lorentz field

$$F_L = 4\pi P/3 \tag{7}$$

is created, with (7') $P = Ne\xi/2$ and $N = 8/d^3$

$$F_L = 16\pi e\xi/3d^3. \tag{8}$$

The energy per molecule (negative and positive ion) is equal to

$$\Delta u^- = -e\xi F_L/2 = -8\pi e^2\xi^2/3d^3. \tag{9}$$

There is also a change of energy Δu^+ due to the forces of repulsion. Summing up the individual contributions of all the neighboring atoms one finds for Δu^+ per molecule

$$\Delta u^+ = 4p(p-1)\left[2^p + \frac{4}{9}\left(\frac{2}{3^{1/2}}\right)^p + \frac{4}{5}\left(\frac{2}{5^{1/2}}\right)^p + \frac{4}{9}\left(\frac{2}{3}\right)^p + \cdots\right]\frac{A}{d^{p+2}}\xi^2. \tag{10}$$

Values of the numerical factor (h) for different p's are tabulated in Table II.

TABLE II.

p	5	5	7	8	9	10
h	2680	7860	21800	57700	148000	369000

For the total change of energy per molecule we obtain, therefore,

$$\begin{aligned}\Delta u &= [-8.4e^2/d^3 + hA/d^{p+2}]\xi^2 \\ &= 1.75e^2/d^3 \times [-4.8 + h/p\gamma]\xi^2.\end{aligned} \tag{11}$$

The numerical values of $h/p\gamma$ are given in Table III.

TABLE III.

p	5	6	7	8	9	10
$h/p\gamma$	3.23	4.87	6.51	8.10	9.67	11.2

From this table we derive the remarkable conclusion that Δu for p slightly smaller than 6 becomes negative. This is a very remarkable result indeed. It means that a cubic crystal of the described kind will voluntarily jump into a state of permanent electric polarization. Unlike the analogous case of atoms, no destruction of the lattice will take place because of the fact that it becomes

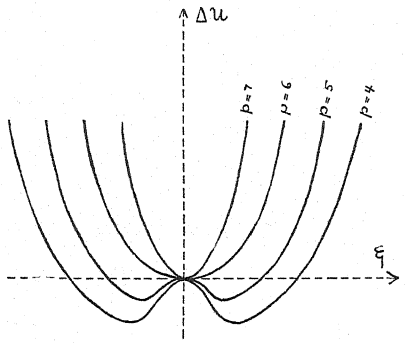


Fig. 2.

more and more difficult to move the two lattices apart as ξ increases. The self-perpetuating movement of the two lattices will therefore stop at some definite value ξ_e of ξ. Fig. 2 shows the energies Δu plotted schematically as a function of ξ for different values of p. The ideal crystal is dynamically stable with regard to a variation ξ only if $p>6$. For $p<6$ it is dynamically unstable. The equilibrium position in this case is given by the minimum of Δu. It corresponds to a state of permanent electric polarization.

The most important result of the above investigation is this. Suppose that we build up a model of a crystal lattice by assuming a certain potential energy function for the mutual interaction of the two particles in the lattice. This energy function may contain certain parameters, A and p in our case. If A and p are determined by adjusting certain characteristics of our model to certain given experimental data (lattice constant, compressibility), one cannot be assured that the model is dynamically stable. Indeed, the particular model discussed above is stable against a uniform pressure because of A having been properly adjusted by (6′). The model also turns out to be stable if a linear extension or a shear is considered. However, for $p<6$ it is unstable against a relative motion of the positive and negative partial lattices.

§4. Generalization of the Model Used in the Previous Section

It is obvious that the computations given in the previous section need to be generalized in various ways.

In the first place, our calculation involves implicitly the assumption that no change of dimensions normal to the relative displacement ξ of the two partial lattices is involved. This is certainly not correct, and additional terms must be introduced. For the present discussion it is sufficient to notice that this lateral effect can only increase the initial instability of the lattice.

In the second place, it will be necessary to compute Δu to higher order terms in ξ in order to determine the final equilibrium position ξ_e. It will, however, be of interest to do so only if one is sure that a certain model actually is a good approximation of the real crystal. More about this will be said in section 5.

In the third place, we must take into account that the ions themselves are deformable. The Lorentz field is as before $F_L = 4\pi P/3$. The expression (7′) for the total moment P per cm³ is changed to

$$P = N\mu/2 + N\mu_0 \tag{12}$$

with

$$\mu = e\xi \quad \mu_0 = \alpha F_L \tag{13}$$

if we use the same notation as in the previous section. Therefore

$$F_L = 4\pi N/3[e\xi/2 + \alpha F_L] \tag{14}$$

or

$$F_L = 2\pi N e\xi/(3 - 4\pi N\alpha). \tag{15}$$

It is evident from the order of magnitudes of $N \sim 10^{23}\text{cm}^{-3}$ and $\alpha \sim 10^{-24}\text{cm}^3$ that the denominator may be considerably smaller than 3, or F_L considerably larger than the corresponding expression with α equal to zero.

In order to get an idea about the magnitude of the Lorentz fields and the corresponding energies involved, we assume that our model has a lattice constant equal to that of rock salt, $d = 5.6 \times 10^{-8}$ cm. For $\xi_e = 10^{-10}$cm we obtain $F_L = 1.36 \times 10^6$volts. The energy per molecule due to this field is

$$\Delta u^- = \Delta u_1^- + \Delta u_2^- = -e\xi/2 - \alpha F_L^2/2 \tag{16}$$

or in our case $\Delta u_1^- = -1.06 \times 10^{-16}$ergs. The energy Δu^- is proportional to ξ^2. It therefore can easily assume values equal to kT say near to the melting point, with ξ amounting to only a few percent of the lattice constant. This is very important because of the fact that certain phenomena may be observed calorimetrically without being easily detectable by a structure investigation with x-rays.

§5. On a New Type of a Secondary Structure

We are now coming back to some of the ideas which have already been mentioned in the introduction.

Suppose that we are dealing with an ionic cubic face centered lattice whose equilibrium configuration is characterized by a permanent electric polarization, due to a value $p < 6$ in relation (4). It is obvious that there are

forces operative during the growth of the crystal which tend to prevent its building up an electric moment. These forces originate on the necessarily existing surfaces. If, for instance, the crystal grows as a large plate a depolarizing field equal to $4\pi P$ will be set up by the surfaces if P is directed normal to the plate. This because of the bound surface charges originated by the electric polarization itself. If the external shape is a sphere or a cube the depolarizing field will be $4\pi P/3$, which still is sufficient to compensate for the Lorentz field. The neutralizing action of the surfaces can be disregarded only if the crystal grows in form of a long needle or if there are charges present which compensate for the action of the surfaces by covering them with charged layers. The bound and the real charges on a surface in this case form double layers with no corresponding external fields. It seems very artificial and unsatisfactory to introduce accidental conditions of this kind. If possible the crystal will favor some kind of an arrangement which allows it to assume

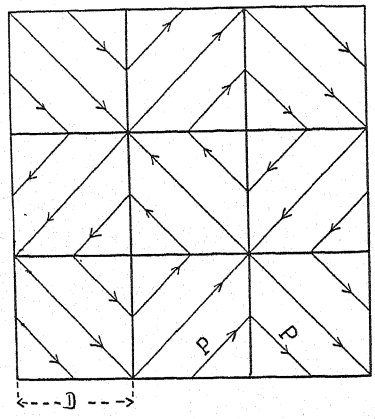


Fig. 3. Permanent electric polarization in crystals.

the configuration of lowest energy without making use of any special external condition. Arrangements of this kind probably must possess the same symmetry character as the primary structure. Fig. 3 gives an illustration of a possible arrangement. It is based on the idea of avoiding neutralizing surfaces by arranging the Lorentz field vectors in circles or in squares conforming with the cubic character of the primary structure as nearly as possible.

In a three-dimensional lattice the secondary structure resulting from a self-perpetuating polarization may be derived by the following simple method, which has been suggested to me by Dr. H. M. Evjen. First think of the crystal being subdivided into identical square needles which are parallel to the [100] direction. Polarize these needles alternately in the [100] and [100] directions. This process is now repeated for the [010] and the [001] direction in such a way that each intersection of three needles is a cube. The resulting vectors representing the polarization evidently will lie in one of the four space diagonals of the cube.

From Fig. 3 it is evident that the crystal will exhibit a certain peculiar type of secondary structure. In the thermodynamically stable state this

structure may be expected to be an absolutely regular one characterized by a greater lattice constant D. An approximate relation between D and the usual smaller lattice constant d may be derived as follows:

The permanent electric polarization causes a relative change Δ in dimension lateral to it. We consider two adjacent regions whose vectors P are at right angles to each other. These two regions can be approximately in phase with each other only over a distance smaller than $D = d/\Delta$. In fact, if a positive and negative ion face each other at A, then at a distance $D/2$ away from A, two ions of the same sign are in opposition, provided that the dividing line between the two parts of the crystal is of the type [100]. We therefore have to keep our regions in Fig. 3 smaller than D or we will begin to loose energy along their boundaries. This means that the new type of a secondary structure proposed in this section is characterized by a greater lattice constant approximately equal to

$$D = d/\Delta. \tag{17}$$

We have seen in section 4 that values of ξ_e equal to 10^{-9} cm lead to reasonable moments such as have been observed in certain crystals, Rochelle salt, for instance. The quantity Δ will of course depend on ξ_e and therefore have a very wide spread. In general Δ will be very small. Therefore

$$D \gg d.$$

This is a very satisfactory result, inasmuch as it may provide an understanding of such remarkably large spacings of the order of 1μ as we have observed for the secondary structure of certain metals. It is a very interesting problem to find out whether the observed secondary structure of metal single crystals can be traced back to the origin proposed here. Although I cannot offer a complete solution of this problem, I should like to advance some tentative suggestions which might prove valuable.

According to the theory of Herzfeld which I have sketched in section 2, electrons are stripped from sufficiently dielectric atoms embedded in solid matter. If the polarizability is increasing with increasing moment, we must conclude that the electrons try to get away from the remaining ions as far as possible. This behaviour, which seems very strange at first sight, is due to the existence of a self perpetuating polarization. We therefore arrive at the following picture of a metal with say one stripped or free electron per atom. We suppose these atoms to be arranged in a face centered cubic lattice. The electrons will exhibit a tendency to arrange themselves in a similar lattice which, however, is displaced by half the lattice constant in one of the principal directions say [100]. Electrons and ions are thus in the same relative position to each other as the ions in NaCl. This is the picture of a simple metal which F. Haber has advanced many years ago. Of course one must not think of such an arrangement as a static one. If it were static the lattice formed by the electrons could be detected with x-rays, which is not the case. The problem to be solved is to find the interaction between the electron lattice or electron gas and the remaining ions. From the fact that a static arrangement

of charges is unstable (law of Earnshaw), it seems probable that the interaction between the two lattices is such that a simplified expression for the mutual energy of an electron and an ion would require an exponent $p<6$. This suggests that metals form crystals whose equilibrium configurations are characterized by permanent electric moments. The formation of macroscopic moments would again be prevented by the building up of a secondary structure. From this viewpoint the large lattice constants $D=5000$–20000A which we have observed in different metals appear comprehensible.

Finally, a few words about the alkali-halides. For most of them $p>6$. Therefore they do not fall within the range of our present considerations, unless a combination of a relatively small p together with a large polarizability α makes them eligible for a secondary structure of the type described above. This may be the case, for instance, for PbS. According to (15) F_L must be multiplied by a factor

$$f = 3/(3 - 2\pi/\Gamma)$$

if α is not neglected. Here $\Gamma=a^3/2\alpha$ and $a=d/2$. Now for PbS we have $\Gamma=2.54$ and therefore $f\sim 6$. This would put PbS into the category of crystals with permanent moments in microscopic regions, for almost any value of p, which may be the explanation of why PbS and PbTe behave so differently from the other alkali-halides.

§6. Permanent Magnetic Moments of Crystals

A ferromagnetic crystal may in some respects be regarded as the magnetic analogue to a crystal possessing a permanent electric moment. However, there are some conspicuous differences between the two cases. In the electric case the back coupling of the induced dipoles in established by the Lorentz field $F_L=4\pi P/3$. To account for the ferromagnetism in Fe, Ni, Co, etc. according to P. Weiss back-coupling fields of the order 10000 M must be introduced, where M is the magnetic polarization per unit volume. In spite of this enormous back-coupling factor, namely 10000 instead of $4\pi/3$, a single crystal of iron is not magnetic as a whole. This is a very puzzling fact. Indeed it is hard to understand why the crystal should not be uniformly magnetized, as the largest possible demagnetizing factor 4π falls far too short from compensating the enormous factor 10000. This problem has not found a satisfactory solution so far. Whatever this solution may be, it seems safe to conclude that it must involve the existence of a secondary structure of magnetic origin. For, although an iron crystal is not magnetized as a whole it must be magnetized in parts, because of the magnetization betraying itself in the caloric behavior of the crystal (rise of the specific heat below the Curie point, etc.). A magnetic secondary structure therefore exists. Off hand it is impossible to say whether the elementary regions are fibers or cubic blocks or of some other shape. However considerations analogous to those leading to Fig. 3 make it possible to determine the exact shape. Assuming them to be cubic, F. Bitter[5] has suggested various ways for estimating their size. He finds that they contain

[5] F. Bitter, Phys. Rev. **37**, 91 (1931).

approximately 350000 atoms each. If we wish to make a theoretical estimate we must apply some relation similar to the one used in the electric case (17)

$$D = d/\Delta$$

where Δ now stands for the relative change in length due to magnetostriction caused by the magnetic saturation. Unfortunately there is no way so far to obtain Δ. If Bitter's estimates are correct, then Δ must be of the order of 1 percent.

It is very interesting to notice that ferromagnetic crystals behave abnormally in regard to plastic deformation. Single crystals ordinarily glide along certain planes belonging to a discrete crystallographically determined set. In iron, however, only the [111] direction is distinguished, but any plane through it may be a slip plane.[6] This becomes comprehensible if one considers that the elementary parts of the magnetic secondary structure of iron are slightly tetragonal. Adjacent blocks are in phase only for distances less than 200A making use of Bitter's estimate. Iron is therefore, in a way, much more similar to an amorphous substance than to other metal crystals whose secondary structures are characterized by spacings of the order of 1μ. It is to be hoped that if iron single crystals are annealed and distorted in a magnetic field that they also will exhibit definite crystallographic slip planes. Experiments to check this are being carried out at this Institute.

§7. Concluding Remarks

I have recently proposed a scheme which was intended to provide a general working basis for the physics of crystals. I showed that those phenomena which essentially characterize the crystalline state are due to the simultaneous cooperation of many particles in regard to a line-up in space. There are different types of such cooperative effects. The main purpose of this paper is to point out two of them which are related to the formation of permanent electric and magnetic moments in crystals. I also attempted to show in which way these two effects may be the cause of a secondary structure of crystals.

[6] G. I. Taylor and C. F. Elam, Proc. Roy. Soc. **A112**, 337 (1926).

LETTERS TO THE EDITOR

Prompt publication of brief reports of important discoveries in physics may be secured by addressing them to this department. Closing dates for this department are, for the first issue of the month, the twenty-eighth of the preceding month; for the second issue, the thirteenth of the month. The Board of Editors does not hold itself responsible for the opinions expressed by the correspondents.

The Magnetization of Colloidal Suspensions

If one assumes the Weiss-Heisenberg postulate of spontaneously magnetized "domains," then it is difficult to see how it is possible to demagnetize a ferromagnetic body. The recent work of Akulov,[1] Powell,[2] and Bitter[3] has done much to resolve this difficulty, but it would still be desirable to obtain more direct experimental evidence of the existence of these domains, as all investigators in this field are not yet fully convinced of their reality. An estimate of the size of these domains can be made from the rate of the approach to saturation of the material in high fields. Such a calculation has recently been made by Bitter,[3] with the result that a group containing approximately 10^5 atoms would constitute a domain. This corresponds to a linear dimension of the order of 150 mμ. Hence if we could divide a ferromagnetic body into particles this small, we should expect each particle to be magnetically saturated.

Colloidal suspensions of nickel or iron can be obtained with this order of particle size, and an investigation of their magnetic properties should be interesting. In suspensions of this character, the concentration of the particles would be so small that the effect of one particle on another could be neglected. The suspension would thus be equivalent to a gas composed of large molecules, and its magnetic moment would be given by the Langevin formula

$$N\mu = N\mu\left(\coth\frac{\mu H}{kT} - \frac{kT}{\mu H}\right)$$

where N is the number of particles per cc, and μ the magnetic moment of each particle. For a particle of nickel of diameter 150 mμ, we have a saturated magnetic moment of 7.0×10^{-12} c.g.s. m per particle, and if we take a field of 1000 gauss and $T=300°$K, then $\mu H/KT$ has the value 1.7×10^5. Under these conditions, the suspension as a whole will have a magnetization within 10^{-3} percent of that possible at this temperature. If, however, we decrease the magnetic moment of the particle by reducing its size, the Brownian rotations of the colloidal particles will become important, since the magnetic moment will assume directions determinate with respect to the directions of the crystal axes, and $\bar{\mu}$ will become smaller than μ. We might thus trace out a Langevin curve. The same result can, of course, be accomplished by varying either the field of the temperature, but the feasible range of variation of H or T, especially of the latter, is much less than that of μ.

Such evidence would, of course, constitute a very direct proof of spontaneous magnetization of small particles. A suspension of particles of this character would also show other interesting properties. It should exhibit a magnetic viscosity which would be directly dependent on the viscosity of the medium in which the particles are suspended, and there should be no hysteresis of the ordinary kind.

CAROL G. MONTGOMERY
Sloane Physics Laboratory,
Yale University,
October 3, 1931.

[1] Akulov, Zeits. f. Physik **69**, 78–99 (1931) and earlier papers.

[2] Powell, Proc. Roy. Soc. **A130**, 167–181 (1930).

[3] Bitter, Phys. Rev. (2) **38**, 528–548 (1931).

Equivalent Electrical Networks

In a recent article [Phys. Rev. **37**, 1583 (1931)] N. Howitt discusses a method of deriving networks equivalent to a given structure. This method depends on the preservation of the positive-definite (or semi-definite) character of three quadratic forms associated with the network, in an affine transformation of these forms. If this transformation be written $i_s=\sum_r c_{sr}i_r'$, then for equivalence with respect to driving point impedance in the jth mesh it is necessary only that all c_{sr} be real, $c_{jj}=1$ and $c_{jk}=0$ when $j\neq k$.

Certain subsidiary conditions leading to further restrictions on the coefficients are mentioned by Howitt, *viz* that "the self-parameter of every mesh be greater than its total mutual parameters with respect to other meshes." The latter condition is unnecessary if a generalized conception of mutual parameters be admitted. For inductances this is nothing more than the usual conception of mutual inductance; the property of being positive-definite is sufficient for a quadratic form to represent a physical system of self and mutual inductances. Such a system may, however, be replaced by an equivalent system of self-inductances and ideal transformers whence it is at once evident that positive-definite forms associated with resistances and capacitances can also be represented with the aid of ideal transformers. From the practical point of view such ideal transformers may be objectionable but from the theoretical standpoint we must accord them the same privileges as pure inductances, pure capacitances, or pure resistances. No other restrictions on the c_{sr} than those mentioned in the first paragraph are therefore necessary for physical realizability.

Howitt notes the possibility of extending the method of affine transformation to equivalence with respect to driving point impedance in more than one mesh. It should be observed, however, that equivalence with respect to driving point impedance in any two meshes necessarily entails equivalence with respect to the mutual impedance between these meshes. Conversely no equivalence with respect to mutual impedance can be obtained by this method without having equivalence with respect to the corresponding self-impedances.

While the method of affine transformation gives a large class of equivalent networks, it can be shown that it does not always lead to *all* equivalent networks. By use of Howitt's notation a network may be characterized by the matrix $\|a_{rs}\|$ where $a_{rs}=\lambda_{rs}p+\rho_{rs}+\sigma_{rs}p^{-1}$. The affine transformation which leaves invariant the driving point impedance $Z^{-1}(p)=\delta\log|\delta_{rs}|/\delta a_{ii}$ will also leave invariant the derivatives $\partial\log|\lambda_{rs}|/\partial\lambda_{ii}$, $\partial\log|\rho_{rs}|/\partial\rho_{ii}$, $\partial\log|\sigma_{rs}|/\partial\sigma_{ii}$. The latter are not necessarily invariant at the same time as $Z(p)$. In particular it can be shown that several values of $\partial\log|\rho_{rs}|/\partial\rho_{ii}$ are sometimes possible for networks with a given $Z(p)$, the number of possible values depending on the particular $Z(p)$ prescribed. Moreover, the number of meshes in such networks is not necessarily fixed (not counting the trivial case where additional meshes arise from proportional impedences in parallel). This point has been discussed at greater length in a paper by the present writer in a forthcoming issue of the Journal of Mathematics and Physics entitled: "Synthesis of a Finite Two-terminal Network whose Driving-point impedance is a Prescribed Function of frequency."

The problem of finding *all* equivalent networks has not yet been completely solved.

O. BRUNE

Massachusetts Institute of Technology,
Cambridge, Mass.,
September 28, 1931.

Reaction Due to Gas Molecules Leaving the Cathode of an Arc

Wellman[1] has suggested recently that the evolution of gas from the cathode of a vacuum arc may account for the large reaction upon the cathode observed by Tanberg.[2] As Mr. Tanberg is no longer in these Laboratories, the writers have examined Tanberg's original results for additional data, not contained in his paper, which may be of value in calculating the effect of the gas coming from the cathode.

Unfortunately, due to a typographical er-

[1] Wellman, Phys. Rev. **38**, 1077 (1931).
[2] Tanberg, Phys. Rev. **35**, 1080 (1930).

ror, the value of current in Table III of Tanberg's paper[2] appears as 2.3 amps. instead of 23 amps. as it should. The value for the force pressure rise from 5×10^{-3} to 100×10^{-3} mm For a series of tests, Mr. Tanberg recorded the following results:

Current	Arcing time	Pressure before test	Pressure after test
23 amps.	6.4 sec.	0.6×10^{-3} mm	15×10^{-3} mm
23	7.6	0.1×10^{-3}	55×10^{-3}
23	3.0	0.1×10^{-3}	20×10^{-3}
23	4.4	0.8×10^{-3}	20×10^{-3}
23	3.3	0.6×10^{-3}	11×10^{-3}

of the evolved gas calculated by Mr. Wellman, which for a current of 2.3 amps. came to the same magnitude as the measured force on the cathode, must therefore be reduced by a factor of 10.

Actually, in comparing the reaction of the escaping gas with the total force on the cathode, one should use the total weight of gas liberated, the arcing time, and the measured force for the same test. Such complete data for any one test are not available. The arcing time varied from 3 to 15 seconds, and the

The volume of the vessel used in the experiment was 5750 cm³; with the associated vacuum system, the total volume was approximately 7000 cm³. The pressure was read upon a McLeod gauge, within perhaps a minute after the arcing ceased.

R. C. Mason
W. E. Berkey

Research Laboratories,
W. E. & M. Co.,
East Pittsburgh, Pa.,
September 23, 1931.

The Structure of the Water Vapor Molecule

The fine structure of water vapor in the more intense bands has been studied recently by Plyler and Sleator.[1] The work on the band at 1.87μ has been repeated by the writer, using higher resolution. Also the region of 1.40μ has been studied and about 100 lines were observed in the harmonic of the strong band at 2.67μ. This band has the appearance of a double type band with much more absorption on the longer wave-length side. Or it may be a zero branch type much distorted. If of the double type, the center is at 1.3765μ, and if of zero type, the center is at 1.3842μ.

In the band at 1.87μ a region has been found which has the appearance of the 6.26μ band. The first three lines on each side of the center have about the same spacing and intensity variation as found in the 6.26μ band. Some of the other lines also correspond but not completely as two bands overlap somewhat in this region. This region appears more like a definite band when small amounts of water vapor are used. The center is at 1.8835μ. If this value is used as a fundamental frequency with that at 2.67μ and 6.26μ, we find the half angle $\alpha=57\ 30'$, or the total angle is 115° between the lines connecting the oxygen atom to the two hydrogen atoms. The calculated intensities for the three fundamentals check well with the observed intensities. Also all the smaller bands which have been observed for water vapor correspond to combination or overtones of these three bands.

It is interesting to note that this value of the angle for water vapor is of the order of magnitude as predicted by Slater[2] in his theory of directed valence.

E. K. Plyler

Physics Department,
University of North Carolina,
October 10, 1931.

[1] E. K. Plyler and W. W. Sleator, Phys. Rev. **37**, 1493 (1931).

[2] J. C. Slater, Phys. Rev. **38**, 1109 (1931).

Diamagnetic Susceptibility of the Rare Gas Atoms According to Slater's Method

Diamagnetic susceptibility of a symmetrical atom is given by $\chi=-(-e^2)/(6mc^2)\Sigma\bar{r^2}$ where $\bar{r^2}$ is the mean square distance of an electron from the nucleus, Σ means that the summation extends over all the electrons in the atom. By evaluation of an approximate

TABLE I. *Susceptibilities and charge distributions of electron shells according to Slater.*

Electron groups	Kr $Z-S$	Kr $-\chi.10^6$	Xe $Z-S$	Xe $-\chi.10^6$	Nt $Z-S$	Nt $-\chi.10^6$
$2s, p$	31′855	0′19	51′85	0′07	81′85	0′03
$3s, p$	24′7	1′33	42′7	0′45	74′7	0′15
$3d$	14′8	4′61	32′8	0′95	65′5	0′26
$4s, p$	8′2	31′75	26′2	2′54	58′2	0′49
$4d$		37′88	14′8	9′89	46′8	0′99
$5s, p$			8′2	34′94	40′2	1′44
$4f$				48′84	27′4	4′05
$5d$,					14′8	13′17
$6s, p$					10′3	25′98
						46′56

wave function, Slater (Phys. Rev. **36**, 57, 1930) has given a method of calculating Σr^2 in terms of the effective principal quantum number n^* and of the effective nuclear charge $(Z-S)$ for any one electron in a group by an equation

$$\Sigma r^2 = [(n^*)^2(n^* + \tfrac{1}{2})(n^* + 1)]/(Z - S)^2$$

According to Slater, n^* is assigned values of 1, 2, 3, 3′7, 4′0, and 4′2 in place of $n=1$, 2, 3, 4, 5, and 6, for the successive electron shells from K to P. $(Z-S)$ is evaluated for different groups of electrons $1s$; $2s, p$; $3s, p$; $3d$; $4s, p$; $4d$; $4f$, $5s, p$; $5d$; $6s, p$; etc.—in such a way that s and p electrons of a group are taken together but d and f are separated. Susceptibilities calculated by this method seem to be in better accord than by Pauling's or by Hartee's distribution of charge method. Hence it is proposed to give in Table I the susceptibilities and the charge distributions of the corresponding electron groups of the rare gas atoms Kr, Xe, and Nt for which experimental values are not known.

SUSIL CHANDRA BISWAS

Physics Department,
Dacca University,
Bengal, India,
October 3, 1931.

The Equation of State of Real Gases

The usual theoretical equations of state are derived by the use of phase integrals extended over the entire phase space of the system, i.e. the integrations performed are carried out over all possible velocities of all molecules. Such treatment is defective for the following reason: If there exists between all pairs of molecules a potential energy $\epsilon(r)$ which has a minimum, then there are discrete energy states, and all phase space is no longer accessible in the classical sense. For light gases the part of phase space thus excluded is appreciable and must be corrected for in the equation of state.

We obtain the pressure of a gas from the relation

$$p = kT(\partial/\partial V) \log Z, \qquad (1)$$

where Z is the complete partition function (Zustandssumme) of the gas. The gas will be considered as a mixture of n pairs of molecules in quantized collision states, whose interaction with similar pairs and with "free" molecules may be neglected. Z then consists of two factors, S^n, associated with the first mentioned pairs, and Z_p, belonging to the free molecules. S in turn is represented by

$$\left(\sum_i e^{-E_i/kT}\right)\left[\frac{(2\pi mkT)^{3/2}V}{h^3}\right] \qquad (2)$$

where the first factor, in which E_i denotes the discrete energies, results from the internal motions, the second being due to the classical motion.

Z_p is the ordinary phase integral for the gas, but the integrations are to be carried out only over the accessible domain: for all pairs of molecules in collision the velocities in the integrand of Z_p must be integrated from sets of values corresponding to a kinetic energy ϵ to $\pm\infty$. ϵ depends on the relative coordinates of the molecules, hence the result of the velocity integration appears as a variable in the volume integration.

As does the complete phase integral in the usual theory, Z_p decomposes into products of integrals over the phase space of pairs of molecules, if only binary collisions are considered. We obtain a result formally similar to

the ordinary one:

$$Z_p = \left(\frac{m^3}{h^3} gV\right)^N (1+z)^N. \qquad (3)$$

Here $g=(2\pi kT/m)^{3/2}$, N is the number of "free" molecules, and

$$z = \frac{N}{2g^2V^2}\left\{\int_{\text{all ph. sp.}} I d\omega - \int_{\text{excluded ph. sp.}} I d\omega\right\} \qquad (4)$$

The integrand I is

$$e^{-m/2kT(v_1^2+v_2^2)}(e^{-\epsilon(r_1-r_2)/kT}-1).$$

The first integral in (4) can be evaluated easily and gives the classical result $4\pi g^2 V\int(e^{-\epsilon/kT}-1)\,r^2dr$, while the second can be expanded into a series which converges rapidly for most cases of physical interest:

$$4\pi g^2 V\int \phi\left(\frac{-\epsilon}{kT}\right)(e^{-\epsilon/kT}-1)r^2dr.$$

$$\phi(x)\begin{cases} = 0.273x^{3/2} - 0.085x^{5/2} + 0.019x^{7/2} \\ \quad - 0.001x^{9/2} + \cdots, \\ = 0 \text{ for } x < 0. \end{cases}$$

Combining 1, 2, 3, 4 we notice that the first factor of S contributes nothing to p since it does not depend on V. The second, of course, produces the partial pressure nkT/V, which, because n is always very small compared with N, needs not be considered. Since $z \ll 1$, $\log(1+z)$ is simply z, and we are led to

$$p = \frac{NkT}{V}\left\{1 - \frac{2\pi N}{V}\int\left[1-\phi\left(\frac{-\epsilon}{kT}\right)\right](e^{-\epsilon/kT}-1)r^2dr\right\}. \qquad (5)$$

The coefficient of $1/V$ in $\{\}$ is known as the second virial coefficient B. (Eq. (5) does not agree with an expression published in this column by Kirkwood and Keyes, August 1, which I have been unable to verify.)

A numerical application of (5) to gases like He or H_2 shows that the correction which is to be made on the classical B values even at low temperatures is not as large as has frequently been supposed. For helium in particular, all theoretical data for a calculation of B are now available, but it is only fair to say that, while things agree well at high temperatures, the result at low temperatures is quite embarrassing. If in the expression for ϵ only the part of the mutual energy arising from dipole forces is used, and in (5) only the classical part ($\phi=0$) is retained, as was done by Kirkwood and Keyes (Phys. Rev. **37**, 832, 1931) then the agreement at low temperatures of B with experimental data is fair. Moreover, if the correction given by (5) is applied, the agreement becomes very satisfactory indeed. However, the inclusion in ϵ of quadrupole forces, recently calculated (Margenau, Phys. Rev. **38**, 747, 1931), destroys the agreement completely. The best experimental value for B_{He} at 20°K is about -4. The theoretical value, computed classically, turns out to be about -24, and the use of (5) reduces it only to -21. This state of affairs offers a strong temptation to ignore the quadrupole forces completely and to look for reasons why they should be ineffective; but we find it impossible to entertain any doubt regarding the necessity of their inclusion. We are unable at present to offer an explanation of this discordance.

HENRY MARGENAU
Sloane Physics Laboratory,
Yale University,
October 12, 1931.

Auto-Ionization in the Noble Gases and Alkaline Earths

The recent explanation by Shenstone (Phys. Rev. **38**, 873, 1931) that the "*ultra-ionization potentials*" observed for mercury vapor are due to an "*auto-ionization*" process of the atom appears to be correct since it accounts very beautifully for certain well-known anomalies in the spectra of many elements. One of these anomalies, as pointed out by Shenstone and to be given later, is the well-known diffuseness of certain lines in the arc spectrum of Cu.

In the inert gases all observed series approach the inverted $^2P_{\frac{1}{2}}$, $1\frac{1}{2}$ level of the corresponding ions. With almost perfect *jj*-coupling in krypton and xenon each series of energy levels arising from p^5ms, p^5mp, p^5md, and p^5mf, consists of two distinct groups of series, one of which approaches the lower limit $^2P_{1\frac{1}{2}}$, and the other of which approaches the upper limit $^2P_{\frac{1}{2}}$ (some 5000 and 9000 cm^{-1} away for Kr and Xe respectively). From six to eleven members each of some twenty or more series are found, from observed lines, to approach the lower limit $^2P_{1\frac{1}{2}}$, whereas only one or two members each of ten or more series approaching the upper limit $^2P_{1/2}$ are observed. The apparent reason is that succeeding members of these latter series lie above

the $^2P_{1\frac{1}{2}}$ limit. Electrons excited to any of these states are in the *continuum* of the lower set of levels having the same quantum numbers and parity, but approaching the lower limit. The result is, the ejection of an electron, (i.e. *auto-ionization*) and the return of the atom to the lower limit $^2P_{1\frac{1}{2}}$.

Three members of the $^3P^e$ (*3dmd*) series in calcium, made famous through the work of Russell and Saunders, lie above the series limit, $4^2S_{\frac{1}{2}}$, of the four chief series of singlets and triplets. The continuum above these four chief series corresponds to *even* S and D terms and to *odd* P and F terms. The *mean-life* of the three negative $^3P^0$ states is sufficiently great therefore to combine normally with lower *odd* terms and give respectable spectrum lines. The observed $^3S^3$ term, attributed to (*3d4d*) by Russell, in combination with other terms gives, as would be expected from a short mean-life, diffuse lines.

In strontium a negative $^3F^0$ term (*4d5p*) lies above the $5^2S_{\frac{1}{2}}$ limit and in a continuum of $^3F^0$ terms (*5s4f*). These negative $^3F^0$ (*4d6p*) terms, because they are observed at all, would be expected to have a very short *mean-life* and should therefore give rise to diffuse lines, as observed. These same $^3F^0$ terms in barium lie below the first limit $6^2S_{\frac{1}{2}}$ and give rise to sharp lines, as expected.

H. E. WHITE

Department of Physics,
University of California,
Berkeley, California,
September 9, 1931.

On the Range of Fast Electrons and Neutrons

Recent experiments on the stopping of cosmic rays raise again the question of the energy losses of electrons and protons with velocity very close to that of light. On the one hand we have a good deal of evidence that there are, associated with the cosmic rays, rays which are certainly not gamma-radiation, and which behave in some respects like beta-rays, since they produce a large number of ions in their passage through matter. This conclusion, which was reached originally by experiments with Geiger counters in series, has been beautifully confirmed by Mott-Smith,[1] who was able to show that the cosmic rays are accompanied by particles which produce definite cloud-chamber tracks, tracks rather thinner than those of an ordinary radioactive beta-particle. These ionizing rays are, according to Rossi, at least as penetrating as the cosmic rays themselves, and perhaps more so. On the other hand the independence of cosmic-ray intensities of terrestrial latitude makes it hard to believe that the rays enter the earth's atmosphere as charged particles. We should then want to know the theoretical answer to the question: Can a gamma-ray produce secondary beta-particles more penetrating than itself?

Numerous calculations have been made of the range of particles moving with velocities not too near that of light. Thus quantum-theoretical formulae have been obtained by Gaunt and Bethe, which in essential points confirm the classical formula of Bohr. But no quantum theoretical calculations have been made for particles of very high energy; and the classical result of Bohr for this case is based on a derivation which is not quite free from objection. Now it would seem at first that no adequate calculation could here be made, since we have at present no complete theory of the interaction of particles of very high relative velocity. That such a calculation is, nevertheless, possible rests on the fact that the processes chiefly responsible for the stopping of a beta-particle involve relatively insignificant energy losses, and that the mean energy loss of a beta-particle on collision with an atom is very small. This preponderance of relatively small energy losses becomes even more marked for particles whose velocity approaches that of light, and makes it possible to calculate the range of the particles without neglecting the retardation of the forces between them and the atomic electrons. Such a calculation has in fact been made by Møller for the collision of two free electrons; we have made it for the collision of electrons and protons with electrons bound in an atom. The results are very simple. If the energy of the particle (rest mass M, and charge E) is

$$\epsilon Mc^2$$

then for *very* large ϵ the number of ions produced per cm path increases with $\ln\epsilon$, and the energy loss per cm path through a gas in which there are N electrons per cc is

$$[4\pi e^2E^2N/mc^2]\cdot\ln\epsilon. \qquad (1)$$

[1] We want here to thank Dr. Mott-Smith for telling us at a Berkeley seminar of his recent very beautiful experiments.

Here e and m are the electronic charge and rest mass. For large but not very large ϵ this formula must be modified: to $\ln\epsilon$ must be added

$$\ln mc^2/kh\nu$$

where m is the electronic rest mass, ν a mean ionization frequency for the atomic electrons, and $1.1 \leqq k \leqq 1.2$. This term is just the one found by Bethe for slow electrons, and in every case reduces the range of the particle below the value given by (2). The formula (1) gives for the range R of the particle

$$R = [mMc^4/4\pi e^2E^2N] \cdot [\epsilon/\ln\epsilon] \qquad (2)$$

This range is just twice that given by Bohr's relativistic formula. Our result gives equal ranges to electrons and protons of equal energy, and makes this range just one fourth of the mean distance, which, according to the Klein-Nishina formula, a gamma-ray of this same energy travels before its first Compton scattering.

The result (1) makes it hard to believe that the particles observed with cosmic rays are electrons or protons, since they are observed to ionize less than slower beta-particles. And if we believe in the approximate validity of the Klein-Nishina formula, then (2) shows that the particles cannot be secondary electrons. We have therefore thought it of interest to investigate the ionizing power of the neutrons, which were suggested by Pauli to salvage the theory of the nucleus. These neutrons,[2] it will be remembered, are particles of finite proper mass, carrying no charge, but having a small magnetic moment. Although the full calculations of the collision of such a neutron with an electron have not yet been completed, we have carried them far enough to see that there are characteristic differences between the ionizing power of a neutron and that of an electron, differences which rest ultimately upon the fact that the field of the neutron falls off more rapidly with distance than the Coulomb field. (The field of a neutron may, of course, be derived from its wave equation; and this has been given by Pauli.) In particular, the number of ions produced by a neutron is, for energies large compared to the electronic proper energy mc^2, sensibly independent of the velocity of the neutron, and of its mass, and does not increase, like (1), with increasing velocity. Thus even a very fast neutron would, if its magnetic moment were of the order of that of the proton, produce ion tracks perceptibly thinner than those of a beta-particle. It will be remembered that, according to Pauli, it is one of the functions of the neutron to carry off the apparently lost energy in a radioactive beta-ray disintegration. It would be of extreme interest to see whether, in such a disintegration, thin tracks, of the kind observed by Mott-Smith, could be found. If they were found, we should be certain that the neutrons not only played a part in the building of nuclei, but that they also formed the cosmic rays; if no such tracks were found, we should know that the neutrons, if they exist at all, have nothing to do with cosmic radiation.

The theory of the collision of neutrons and electrons, and the detailed calculation of the ranges of neutrons and fast electrons, will be published very shortly.

J. F. CARLSON
J. R. OPPENHEIMER

LeConte Hall,
Berkeley, California,
October 9, 1931.

[2] We are much indebted to Dr. Pauli for telling us, at a theoretical seminar in Ann Arbor last summer, the elements of the theory of the neutron, its functions and its properties.

The Calculation of the Characteristic Frequency from the Coefficient of Compressibility

A number of years ago Einstein[1] derived an expression for the characteristic frequency of a monatomic solid which is as follows

$$\nu = 2.8 \times 10^7 A^{-1/3}\rho^{-1/6}\kappa^{-1/2} \qquad (1)$$

where κ is the coefficient of compressibility, A is the atomic weight and ρ is the density of the solid. This relation was derived from dimensional considerations, and the constant was evaluated by considering the effect on a given atom of its 26 immediate neighbors in a lattice which we now call the simple cubic or rock salt type. The result must be regarded as an approximation yet it is a useful one and therefore deserves further consideration. A reexamination of the derivation in the light of present knowledge reveals that several ambiguities and restrictions inherent in the original work now may be removed.

[1] Einstein, Ann. d. Physik **34**, 170 (1911); **35**, 879 (1911).

First, it would appear from the discussion as given by Einstein that it applies only to the lattice postulated and is limited by the number of neighboring atoms taken into account. This is not entirely true. A careful study of the calculations shows that the number of atoms considered may be cancelled out and need not appear in Eq. (2) of his second paper. This may be more easily seen if the generalized number n is substituted for 26. The only way the lattice enters into this result is through d, the equilibrium distance between atoms.

This brings us to the second point, namely, the device by which Einstein eliminates v, the atomic volume, in terms of d. This is accomplished by assuming that d is equal to the radius of a sphere of volume equivalent to that of 8 atoms, the number contained in the unit cube of the lattice he considered. A moment's reflection will show that this method does not give the true distance between the atoms, as recognized today but introduces a small error; hence some more exact and more general scheme of eliminating v is desirable.

The simplest way to do this is to express d, as determined by x-ray measurements, as an empirical function of v. This is easily done. In Fig. 1 values of d for a number of metals, as given by Ewald[2] are plotted against $(v)^{1/3}$ as calculated from the data of Vol. I of the International Critical Tables. The variation is linear and since elements possessing both face-centered and body-centered cubic structures are included the constant may be taken as identical for both systems without appreciable error. It may even be assumed as a first approximation that it holds for other types of lattice. The analytical expression for the curve of Fig. 1 is $d=1.35\times10^{-8}\ (v)^{1/3}$. By use of this in Eq. (2) of Einstein's second paper we get

$$\nu = 2.9 \times 10^{7} A^{-1/3}\rho^{-1/6}\kappa^{-1/2}. \qquad (2)$$

This is practically the same as the result given by him except that it is less restricted and may be safely given more general application.

It is interesting to note in this connection that if we give temperature the dimensions of energy, ml^2t^{-2}, as may be done[3] the coefficient of thermal expansion has the same dimensions as the coefficient of compressibility. This suggests that the expression

$$\nu = \text{const}\ A^{-1/3}\rho^{-1/6}\kappa^{-1/2} \qquad (3)$$

might yield useful information. A study of a number of metals shows that if the value 2.4×10^{8} is assigned to the constant, Eq. (3) leads to values of ν which are approximately correct except in the case of the alkali metals. This relation obviously has not the theoretical foundation which supports Eq. (1) since the symmetrical law of force assumed in the derivation of the latter leads to an expansion coefficient of zero. It is, however, an interesting empirical formula.

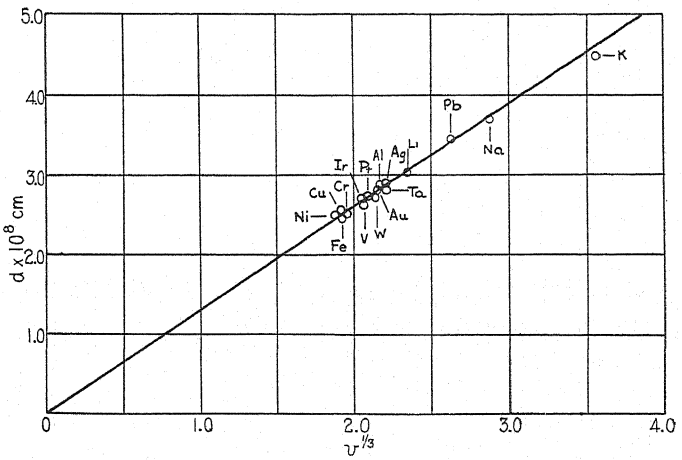


Fig. 1. The calculation of characteristic frequencies.

[2] Ewald, Handbuch der Physik, 24, Chap. 4. Springer, Berlin, 1927.

[3] Cf. Bridgman, Dimensional Analysis, Yale Univ. Press. 1922, p. 71.

TABLE I. *Comparison of values of ν for metals calculated by different methods.*

	Debye (Elastic constants)	Debye (Specific heat)	Grüneisen (Expans. coeff.)	Lindemann (Melting temp.)	Haber (Ultra-violet spectra)	Austin (Compressibility coeff.)	Austin (Expansion coeff.)
Ag	4.4	4.5	4.6	4.4	4.6	4.2	4.4
Al	8.3	8.3	7.7	7.8	8.2	7.0	8.1
Cd	3.5	3.5	3.7	2.8	—	2.8	3.5
Cu	6.8	6.6	7.1	6.8	7.2	6.0	6.0
Fe	9.7	9.5	8.5	8.3	—	7.0	7.5
Pb	1.5	1.8	2.2	1.9	2.5	2.1	1.8

In Table I values of ν for a few metals as calculated by Eqs. (2) and (3) are compared with those obtained by other methods as given by Rawlins and Taylor.[4] It will be observed that the agreement is satisfactory even in the case of cadmium, which possesses an hexagonal lattice.

J. B. AUSTIN

Research Laboratory,
U. S. Steel Corporation,
Kearny, N. J.,
October 7, 1931.

[4] Rawlins and Taylor, Infrared Analysis of Molecular Structure, Cambridge Univ. Press, Cambridge p. 86, 1929.

Crystalline Rubber Hydrocarbon

Substantially all of the chemical and physical evidence concerning the nature of rubber is consistent with the chemical formula $(C_5H_8)x$, and this is the generally accepted formula for "rubber hydrocarbon." An examination of the evidence discloses, however, that the above formula is not the only one which is consistent with this evidence. The difficulty of establishing beyond question the chemical composition of "rubber hydrocarbon" has been due largely to the lack of efficient physical methods for fractionating the "hydrocarbon," of proving that the final fractions are one-component systems, and of chemically identifying these fractions. If, as seems not improbable, "rubber hydrocarbon" is a mixture of closely related hydrocarbons not all of which can be represented by the formula $(C_5H_8)x$, no single method of fractionation can be relied upon to separate this mixture into its constituents. The only methods heretofore available for this purpose have been those based upon extraction with different liquids and fractional precipitation. One of the most powerful methods for fractionating a mixture of this character is systematic crystallization, and a laboratory technic for applying this method to "rubber hydrocarbon" has recently been developed at this Bureau. The conditions which must be met in order to induce crystallization in such a typically colloidal material as rubber can be predicted. These conditions have been met and are embodied in the following procedure.

The "rubber hydrocarbon," previously purified from all nonhydrocarbon materials, is dissolved to form a dilute solution in a suitable solvent. This solution is cooled to the temperature necessary to induce crystallization and then held at the desired temperature until crystallization is completed. The excess solution can then be removed and the crystals dried in vacuo for examination.

The accompanying photograph illustrates one type of crystal clusters which are obtained in this way. These crystals were grown at -55°C from a 0.05 percent solution of the hydrocarbon in pure dry ether.

The Bureau is now engaged in a determination of the melting point of these crystals, which point lies somewhere between -35 and 0°C. The melted crystals are typically rubber-like in nature, and a preliminary combustion analysis indicates a hydrogen-carbon atomic ratio close to 8/5, thus proving beyond any question that the crystals are rubber crystals. It is planned to carry out a systematic fractionation of "rubber hydrocarbon" by repeated crystallizations and to make accurate combustion analyses and molecular weight determinations of the final fractions.

This investigation has been carried out in the Section of Organic Chemistry of this Division under the direction of C. E. Waters.

The purification of the "rubber hydrocarbon" and the growing of the crystals were conducted by W. H. Smith, and the combustion analyses were made by H. J. Wing. The photomicrographic technic offered great difficulties, since the crystals had to be photographed in the solution at a temperature of −55°C. The development of this technic was started by F. W. Ashton and brought to successful completion by Charles P. Saylor.

In addition to the crystallization technic described above, it has also been found possible to distill the "rubber hydrocarbon," but fractionation by this procedure is very slow and of value only for confirmation purposes.

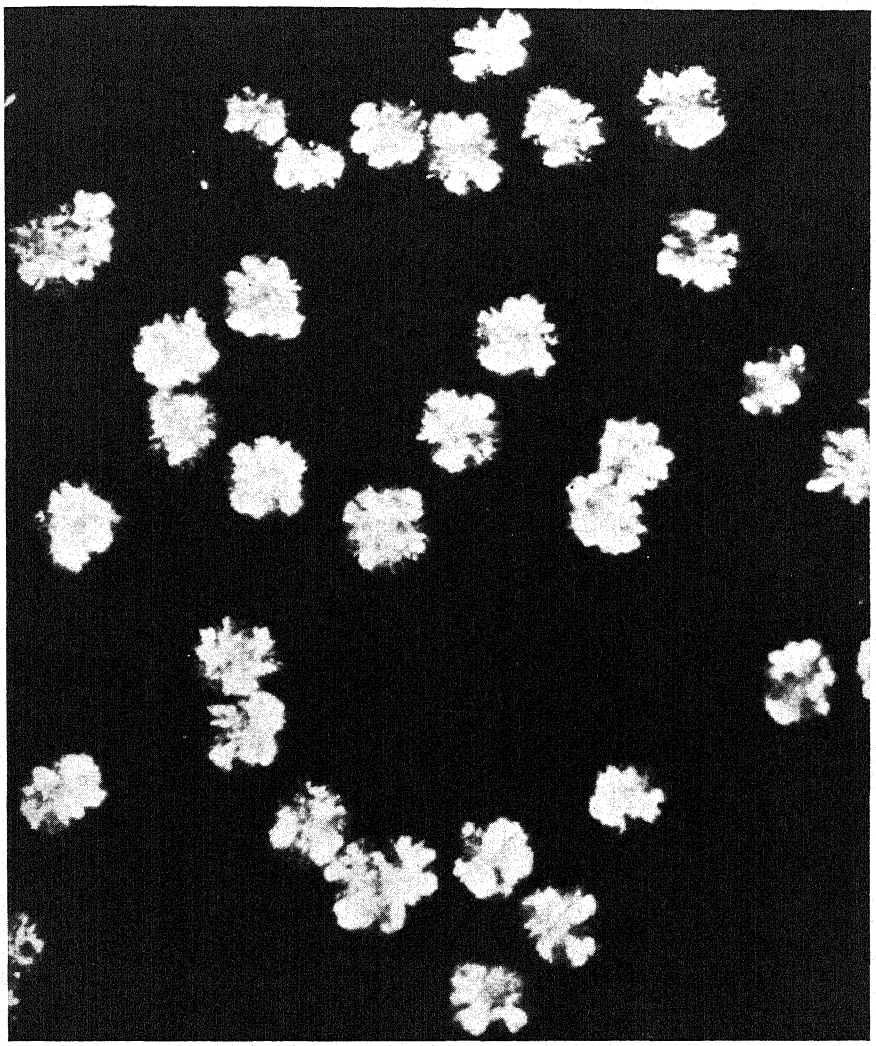


Fig. 1. Crystals of rubber hydrocarbon photographed between crossed nicols at a temperature of −55°C. Magnification—200 diams.

E. W. WASHBURN, CHIEF,
CHEMISTRY DIVISION
Bureau of Standards,
Washington, D. C.,
October 3, 1931.

Note on the Crystal Structure of Arsenic Triodide

In my paper (Phys. Rev. **38,** 351 (1931)) exact reference should have been made to correspondance between Dr. Braekken and myself (Zeits. f. Krist. **75,** 574 (1930)).

In Fig. 1, p. 355 "projection $\perp C$ axis" should have been a 60° rhombus and not a 60° parallelogram with unequal sides.

There are several misprints: T_{Th} should read T_{rh} in the abstract; parentheses are missing in the fifth line below Fig. 2 and $a°$ at the end of the ninth line below Fig. 2 should read A. In the "Discussion of the Structure" the distance of closest approach of iodine in layers perpendicular to the trigonal axis is given as "about 4.13A." There are really two interiodine distances in these planes, one a little smaller and one a little larger than 4.13A. Also in the final structure the iodine ions are not exactly in hexagonal close packing.

DOROTHY HEYWORTH

Ryerson Physical Laboratory,
Chicago, Illinois,
October 2, 1931.

Periodic System of Atomic Nuclei and the Principle of Regularity and Continuity of Series. A Correction

Since this paper [Phys. Rev. **38,** 1270 (1931)] was completed four new species have been found by Aston: Sr 11 (Fig. 9), Te 21 (Fig. 10), Ba 23 (Fig. 9), and Ba 25 (Fig. 10). The numbers given are the isotopic numbers. These species should be added to the known isotopes of Fig. 2. The first three are already listed as predicted by the principle of continuity and regularity of series in the figures of the given numbers. The fourth (Ba 25) belongs to the beryllium series and its existence is entirely in accord with the principle. Its existence points to the presence of a double level in the beryllium series at this point. The paper cites the earlier composition given for strontium and barium as "entirely inadequate."

WILLIAM D. HARKINS

Department of Chemistry,
University of Chicago,
October 3, 1931.

A New Criterion for Predissociation. A Correction

In a Letter to the Editor of the above title (Phys. Rev. **38,** 1079, 1931) line 14, the beginning of the sentence should read, "Transitions will occur not only" instead of "Transitions will not occur not only."

JOSEPH KAPLAN

University of California
at Los Angeles,
September 28, 1931.

BOOK REVIEWS

Periodisches System. EUGEN RABINOWITSCH AND DR. ERICH THILO. Pp. 302, Figs. 50. Verlag von Ferdinand Enke in Stuttgart, 1930.

A distinguished physicist once made a remark that all facts understood by chemistry belong to physics and that the mysteries left belong to chemistry. True or not, it must be admitted that wherever the carriage of chemistry got stuck, physics was generous enough to pull her out. In the book of Rabinowitsch and Thilo, published under the modest title "Periodic System" dealing with subjects on the border line between physics and chemistry, many modern and historical examples are given of the progress of chemistry by the advanced views in physics. The first fifty pages give a historical review of the history and development of the periodic system beginning with the fifteenth century B.C. It is interesting to note that the history of the basic unit weight of matter is not yet finished although the writers state (page 16) that, "das auf Sanerstoff gleich 16 basierend Atomgewichtssystem ist bis jetzt allgemein beibehalten." Recently after the discovery of the isotopes of oxygen, Aristide von Grosse (1930) proposed to refer the atomic weight to $He^4=4.000$; Aston (Nature 1931) on the other hand concludes that neither helium nor the proton, etc. are units free from objection!

Since the periodic properties of the atom have in recent times been so closely related to its structure, the authors appropriately devote Part II to the structure of the nucleus, Part III to the spectroscopic evidence for its electronic structure as developed by Bohr and later modified by the principles of wave mechanics, Part IV to a detailed consideration of the properties of each element and their relation to the position of each element in the periodic system. Finally, the fifth part of the book (fifty pages) deals with the periodicity of chemical properties and is of special importance to chemists. The possibility of existence of ionic (heteropolar) compounds is calculated from the heat of formation; the theory on the existence of atomic (homopolar) compounds cannot be presented in such a general form at the present time; the book, however, is stimulative to continued studies on this field.

Quite generally, it may be stated that the writers give a critical survey of our knowledge of the properties of the atom and they are quite honest in stating where the theories are not complete enough for a good understanding of all facts. This text can be recommended to any physicist or chemist interested in the development of the story of the atom and its importance for physics and chemistry. The book should be very useful in the hand of advanced students although it still would be more helpful to them if references to monographs and the literature had been made.

Print and appearance are excellent.

I. M. KOLTHOFF
University of Minnesota

Experimental Physical Chemistry. DANIELS, MATHEWS, AND WILLIAMS, Pp. 475, figs. 132. McGraw-Hill Publishing Company. New York, 1929. Price $3.50.

The book is divided into three parts. The first contains specific instructions for performing a large number of experiments; the second describes some of the standard apparatus of physical chemistry; the third describes some of the operations used in the practice. Altogether the amount of information compressed into the book is very great. It would seem to be both an excellent laboratory manual and a useful handbook for the more mature student.

In the first part are many experiments besides the classical ones of the older physical chemistry. The later chapters include experiments on radioactivity, photochemistry and electrochemistry of gases. Seventy-eight experiments in all are given; they cover so wide a field that if so large a number of experiments could actually be performed it would form an ideal background for the coming physical chemist. In fact, this can hardly be done in the usual elementary course; the book is the result of many years laboratory experience at the University of Wisconsin and there about half of the material embraced in the book is covered. The instruc-

tions are clear and each experiment is concluded with practical applications and suggestions for further work. The treatment is always interesting and suggestive.

The second part of the book covers a large field and though it cannot treat the various methods exhaustively it gives references which make it a suitable starting point for one looking up the technique in a not familiar field.

The book appears to be excellent as a laboratory manual and as a reference book it could well be on the shelf of any physical chemist or physicist. Much of the material is definitely physical and material is collected here which it is difficult to find elsewhere.

JOHN A. ELDRIDGE
University of Iowa

Electricity and Magnetism, an Advanced Textbook for Colleges. CHARLES A. CULVER, Macmillan Company, Publishers.

The book is based upon a three hour semester course which the author has given for junior and seniors in a College of Liberal Arts. The book takes up the fundamental principles from the usual point of view. By means of frequent tables of values and diagrams, frequent reference to recent work, and mention of apparatus used in current practice, the author keeps close to actual laboratory technique and gives the treatment of the theory a concreteness which it might not otherwise have possessed. It would seem an admirable text for a second course in electricity.

It is a notable fact that the names of Einstein and of Maxwell are not mentioned in the index. The first omission is not surprising since it is not yet customary to consider the close relation between electricity and the relativity theory even in quite advanced textbooks on electricity. It is rather more surprising that such a book could be written without referring to Clerk Maxwell.

JOHN A. ELDRIDGE
University of Iowa

Lehrbuch der Experimentalphysik für Studierende. DR. EMIL WARBURG, 21 and 22 Edition. Pp. 482, figs. 451. Theodore Steinkopff, Dresden and Leipzig, 1929. Price. Rm 15.80.

This is a textbook corresponding approximately to American first-year college texts. Judging by the large number of revised editions printed since the first edition in 1893, this book has been widely used.

O. M. STEWART
University of Missouri

Gruppentheorie und ihre Anwendung auf die Quantenmechanik der Atomspektren EUGEN WIGNER. Pp. 332, figs. 12. Friedr. Vieweg and Sohn Akt-Ges., Braunschweig, 1931. Price Rm 29.60.

"Dieses Buch ist aus dem Wunsche entstanden, die Anwendung gruppentheoretischer Methoden in der Quantenmechanik einem weiteren Leserkreis zugänglich zu machen."

Theoretical physicists seem to be pretty well divided into two camps, one of which has championed the theory of groups while the other has consistently refused to use it. As one physicist put it, papers on atomic structure can be divided into two classes—those which quote Schur and those which don't! This situation has been possible only because the results obtained from group theory in the problems of atomic structure have been largely duplicated and in some cases extended by use of more elementary methods. Coupling this with the fact that it is a real task to become in any sense familiar with the technique of group theory, it is small wonder that many do not consider the game worth the candle.

On the other hand, there are definite arguments to be advanced in favor of a wider study of the theory. While elementary methods can be used at present in atomic structure problems, the purely computational difficulties involved are becoming enormous. It seems that one must develop, if possible, some way of improving the starting point; i.e. the initial statement of the problem. How to do this is a question, but it does seem that group theory should be a good culture medium for the germs of thought on this problem because of the very power and generality of its methods.

Then too, one is well aware that the present quantum mechanics is no longer considered to be an adequate *general* theory of matter. Without attempting to be dogmatic, one may say that one of the most important advances which quantum mechanics has brought with it has been the emphasis on the symbolic method, as developed particularly by Dirac. While its real meaning seems by no means obvious, and while it is a double-edged tool to be used with caution, one can't help feeling that this symbolism really has great possibilities. Abstract group theory is, of course, a perfect example of the symbolic method, and one is encouraged to hope that the suggestiveness of its ideas will give valuable aid in the future development of a more correct quantum mechanics. On the basis of such ideas as these one can feel very favorably inclined towards a work such as this of Professor Wigner.

The first fifth of the book (62 pages) is devoted to preliminary material. Vectors and matrices in many dimensional complex space give the formal approach to the subject. The preliminary sections on the postulates of quantum mechanics, perturbation theory, and the statistical interpretation of quantum mechanics are naturally only brief reviews and summaries of these topics, but are ample for the purpose. Some may prefer to read these sections before the material on matrices in order to become oriented to Professor Wigner's style and viewpoint. The more elementary facts about abstract finite groups are developed in the next two sections—sub-groups, the separation of the elements into classes, the factor group, etc. The main theorems on the theory of representations of a group by matrices are contained in Secs. 9–12. Of particular interest is Sec. 10 on the treatment of continuous groups.

With Sec. 13 begins the problem of studying the groups of special interest to quantum mechanics—the symmetric (permutation) group and the group of rotations and reflections in three dimensional space. The last half of the book is devoted to the problems of atomic structure. Here one can find all of the important features of the *mathematical* theory. No attempt is made, of course, to include any experimental data. Attention may be called particularly to the treatment of the vector model and the development of the rules for the addition of vectors (p. 196).

The last section gives the group theory treatment of Slater's method for finding atomic wave functions. Developed originally by means of the most direct and elementary mathematical methods suited to the problem, one finds it here in a refined and spiritualized form.

The reviewer has found the treatment clear and precise throughout, but by no means always easy to follow. This is probably unavoidable since the subject matter is intrinsically difficult. The material is logically developed and shows evidence of great care in choice and arrangement. The printing has been done very carefully. The reviewer joins the author in expressing the hope that the book may help to diffuse knowledge of the theory among physicists.

E. L. HILL
University of Minnesota

Photochemical Processes, a General Discussion held by the Faraday Society. Pp. 573. Gurney and Jackson, London 1931. Price 10s 6d.

This report on photochemical processes, which is the fifty-fifth General Discussion of the Faraday Society, presents in a clear and interesting fashion the striking progress which has been made in this field since 1925. Its interest and value is considerably increased by the inclusion of the general discussions which followed all of the more important papers.

The first part of the report is devoted to a consideration of molecular spectra in relation to photochemical change. The subject is introduced with a clear and worthwhile review by R. Mecke, who also contributes a paper on the calculation of the ozone equilibrium in the atmosphere. The ultraviolet absorption spectra of acetylene and formaldehyde are discussed by G. Herzberg, and those of hydrogen sulfide, hydrogen selenide, and hydrogen telluride by C. F. Goodeve and N. O. Stein. The physical and chemical evidence in regard to the ultraviolet absorbtion of aldehyde and ketone vapors is reviewed by F. W. Kirkbride and R. G. W. Norish.

The second part, which is introduced by Max Bodenstein, consists of a series of papers on photochemical kinetics in gaseous systems. These papers deal chiefly with photochemical secondary processes; i.e., the chemical reactions which follow the initial excitation on dissociation.

The third part, which is devoted to photochemical changes in liquid and solid systems, is

introduced by A. Berthoud. In addition to several papers on photochemical reactions in liquid systems, there are in this group two papers on photographic processes and an interesting discussion of the temperature coefficient of photochemical reactions by K. W. Young and D. W. G. Style.

The fourth part, on Photosynthesis, is introduced by E. C. C. Baly, with a detailed account of some recent experiments on artificial photosynthesis. In addition to the papers on photosynthesis, this section includes a description, by Edith Weyde and W. Frankenburger, of a new actinometer for ultraviolet light.

ROBERT LIVINGSTON
University of Minnesota

Second Series *November 15, 1931* *Vol. 38, No. 10*

THE
PHYSICAL REVIEW

THE STRUCTURE OF SOFT X-RAY LINES

By William V. Houston
California Institute of Technology

(Received October 1, 1931)

Abstract

The experimental work on soft x-rays has shown that the lines produced by the bombardment of a solid target are much broader than those emitted by a vapor. This is due to the fact that the upper level is not sharp. The breadth and the shape can be calculated from the various models which have been used for describing the behavior of electrons in metals. The free electron model gives a line which has a sharp edge on the short wave-length side. This is not observed in Be. The calculated width, however, agrees well with the observed. The bound electron model gives a more satisfactory shape for Be, but the width cannot be exactly determined. The comparison of the line shapes calculated on the basis of these two models with that observed in Be shows that, although the free electron model gives a good approximation to the zero point energy, the distribution of energy levels is strongly affected by the periodic potential in the crystal.

THE experimental work on very soft x-rays and on far ultraviolet spectra has shown that although there is a correlation between the lines of these two types, there are also outstanding differences. The lines emitted by an excited vapor, such as is produced by a hot spark discharge, are sharp lines of the type ordinarily found in optical spectra. On the other hand, lines in the same region, when produced by bombardment of a solid target, are found to have a very considerable width, and to be displaced from their position as observed in the hot spark.[1] To give an explanation of this fact one must remember that the x-radiation is emitted during a transition between stationary states of the solid body, while with the source in the vapor state, the transition is between states of a single atom. That this can be neglected in the treatment of the ordinary x-ray spectra is due to the fact that the very low levels of an atom are practically undisturbed when the atom becomes part of a crystal.

In terms of the model in which the interaction between electrons is not explicitly considered, and in which each electron moves in a potential field due to the nuclei and all the other electrons, the process of excitation and emission of a soft x-ray line may be described as follows. The excitation con-

[1] Ericson and Edlen, Zeits. f. Physik 59, 656 (1930); M. Soderman, Zeits. f. Physik 65, 656 (1930).

sists in the removal, by the bombarding electron, of another electron from one of the low levels of the target. In the case of low levels it may equally well be said that the electron is removed from one of the low levels of a particular atom in the target. This electron may be put into one of the unoccupied upper states of the crystal, or it may be entirely ejected. The emission of the x-ray then takes place when an electron from an upper state falls into the vacant lower state. If this electron comes from one of the highest group of ordinarily occupied states, that is from the group of states occupied by the valence electrons, it may have had any one of a large number of energies in this initial state. On this account the observed line will consist of a large number of superposed lines which blend together to give a wide band. The width and the shape of this band are determined by the distribution in energy of the upper levels as well as the distribution of transition probabilities. In case the lower state is one of a group of levels whose energies differ somewhat among themselves, this too must be taken into account. In most cases accessible to observation this is probably negligible. These observations, then, furnish a convenient means of checking experimentally the energy level distribution required by the various models for the behavior of electrons in metals.

The work of Söderman on Be furnishes a good example of what may be done in this direction.

The Free Electron Model

The model used by Pauli, Sommerfeld,[2] and others assumes that the outstanding characteristic of the valence electrons is their ability to move more or less freely through the crystal. The wave functions given by this model, as well as the distribution of energy values are given by Sommerfeld. The total number of stationary states whose energies lie between E and $E+dE$ is proportional to $E^{1/2}dE$. For ordinary temperatures, the temperature energy is so small compared with the zero point energy that it may be neglected. In this case, all of the energy levels up to those having the critical energy $\overline{E}=(h^2/2m)(3n/8\pi)^{2/3}$ will be occupied, and all those states having higher energy will be empty. In this expression for the critical energy, h is Planck's constant, m is the mass of an electron, and n is the number of free electrons per cubic centimeter.

In Be the electrons which occupy the L levels in the atoms will form the group of free electrons in the metal. It is then necessary to find the transition probability between one of these "free" states and an unoccupied K state. This can be found in the usual way from the knowledge of the functions. When averaged over all possible relative positions of the K function and the "free" function, the square of the amplitude of the electric moment turns out to be

$$M^2 = DE/(h^2Z^2/8\pi^2ma_0^2 + E)^6 \qquad (1)$$

D is a constant whose value is not essential, since only the dependence on E

[2] W. Pauli, Zeits. f. Physik **41**, 81 (1927); A. Sommerfeld, Zeits. f. Physik **47**, 1 (1928).

affects the shape of the x-ray line. The fact that the transition probability depends only on E and not on the direction of motion of the free electron is due to the spherical symmetry of the K function. In Eq. (1) Z is the effective nuclear charge which determines the extent of the K function, a_0 is the radius of the first Bohr orbit, while the other symbols have their usual significance. The combination of the transition probabilities with the distribution of energy levels gives for the shape of the emitted line

$$I \sim E^{3/2}/(h^2Z^2/8\pi^2ma_0^2 + E)^6 \qquad (2)$$

from $E=0$ to $E=\overline{E}$. In this expression the ν^4 factor is neglected since the width of the line is only a small part of its total frequency.

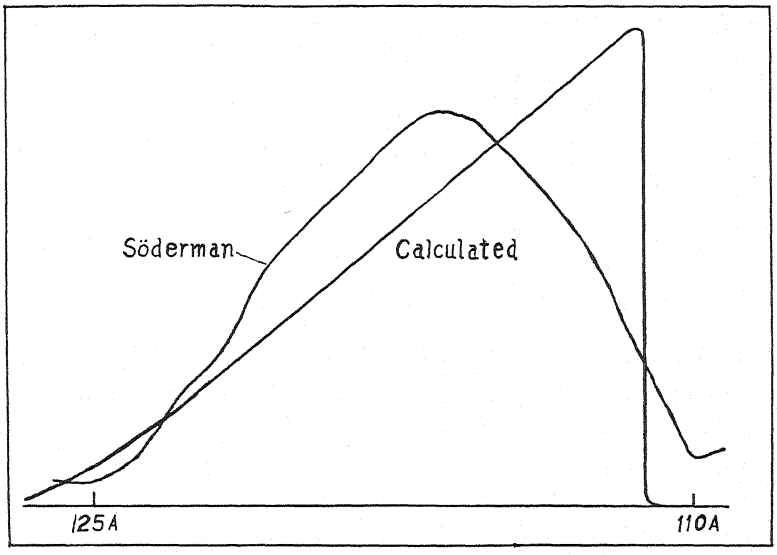


Fig. 1. Comparison of line observed in Be with that calculated from the free electron model.

Fig. 1 shows the agreement of this calculated curve with the observations of Söderman for Be. The width is calculated on the basis of two free electrons per atom. The height of both curves is of course arbitrary. The distinctive feature of the free electron model is the sharp edge on the short wave-length side. This does not appear in the observations, although there is a certain amount of asymmetry to be seen. The calculated width agrees very well, however, with that observed.

The Bound Electron Model

The other model for which calculations can readily be made is that introduced by Bloch.[3] From this point of view each electron is initially attached to a particular atom, but can easily jump to an adjacent atom under the influence of an external field. In this case the spread of the energy levels is pro-

[3] F. Bloch, Zeits. f. Physik **52**, 555 (1928).

duced by the perturbation of the electron by the surrounding atoms. The energy of a stationary state is given by Bloch to be

$$E_{lmn} = E_0 + \alpha - 2\beta\{\cos(2\pi l/G_1) + \cos(2\pi m/G_2) + \cos(2\pi n/G_3)\} \quad (3)$$

E_0 is the energy of the electron in the field of its own nucleus only. α is the electrostatic perturbation of the adjacent nuclei and electrons, while β is the exchange integral. l, m, and n are integers which designate the state and may have values such that the arguments of the cosines range between $-\pi$ and $+\pi$.

The number of energy levels lying between E and $E+dE$ is very difficult to evaluate analytically, but a rough graphical integration gives the form indicated in Fig. 2. The width of the group of levels depends upon the value of the integral β. For the curve shown in Fig. 2 the functions suggested by Slater[4] were used in evaluating this integral. Each atom was assumed to have six effective neighbors, and their distance was determined from the density as if the crystal had a simple cubic lattice. In this model the transition probability is about the same for all states since it is essentially the transition probability from an L state to a K state. Although the theoretical determination of the width is subject to a number of uncertainties, the figure shows that it is of the right order of magnitude. The shape of the curve agrees roughly with the observations.

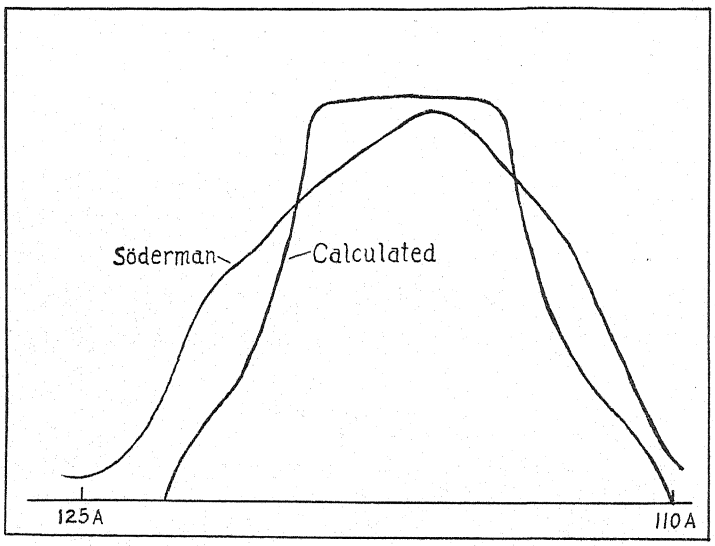


Fig. 2. Comparison of line observed in Be with that calculated from the bound electron model of Bloch.

[4] J. C. Slater, Phys. Rev. **36**, 57 (1930).

Discussion

The distinctive difference between the two theoretical curves lies in the sharpness at the short wave-length edge. In each case the Pauli exclusion principle, or the Fermi statistics, causes all of the states whose energy is less than a certain critical amount to be occupied, and all others to be empty. In the free electron model the density of states increases continually with the energy, so that there is a sharp edge. The other model, which takes some account of the periodic variations of potential within the crystal, indicates that the density of the states is not a monotonic function of the energy, but consists of a series of maxima which roughly correspond to the various types of state in the free atom. In case the outer shell of the atom is closed, as is the case with Be, the end of the occupied states falls at a minimum and does not produce a sharp break. On the other hand, an element such as Li should have a sharp edge on its lines, since there are only enough electrons to fill up half of the states in the first group. The observed shape of the curve indicates that in Be the potential variations do produce a considerable effect on the distribution of the energy levels.

In all of these calculations the lower level has been treated as single since a rough calculation shows that it will be much narrower than the upper level.

The operation of the Pauli exclusion principle is clearly seen in the fact that the lines have any width at all. If the classical statistics were applicable all of the electrons would be in states at or near the lowest value of the energy.

UPPER ATOMIC-NUMBER LIMITS FOR SATELLITES OF THE X-RAY LINE $L\beta_2$*

By R. D. Richtmyer**
Department of Physics, Cornell University

(Received October 5, 1931)

Abstract

The region of the x-ray spectrum in the immediate neighborhood of the line $L\beta_2$ has been photographically studied for the elements of atomic number 50, 51, 52, 53, 56, 58, and 60, with a view to determining more precisely the atomic number ranges of the satellites (five in number) of $L\beta_2$. It appears that these ranges have clearly defined upper limits in the cases of all but one of the satellites of $L\beta_2$, and that the previously supposed presence of these satellites beyond these limits, approximately atomic number 53, can be traced in some cases to certain diagram lines which had not heretofore been thoroughly investigated, and that the presence of the satellites beyond these limits is in general to be doubted, at least as far as present accuracy and sensitivity of observation are concerned. The existence and sharpness of these limits seems to be in conflict with the Wentzel-Druyvesteyn double-ionization theory of the origin of the satellites. A table of new wave-lengths is included.

THE purpose of this investigation of the satellites of the x-ray line $L\beta_2$ was to determine with greater certainty, if possible, the range (apparently restricted at both ends) of atomic numbers of the elements for which these satellites can be observed.

$L\beta_2$ has five satellites, which appear as shown in Fig. 1. The two more prominent ones, numbered 4 and 6 in the figure, were early observed by Siegbahn, and are recorded in his *Spectroscopy of X-rays*. Siegbahn calls these $L\beta_{11}$ and $L\beta_{12}$, but they are perhaps most frequently called $L\beta_2'$ and $L\beta_2''$. They are clearly resolved for the elements of atomic number from 40 to 50, inclusive, and are listed unresolved by Siegbahn for several additional scattered elements. When unresolved he sometimes also calls them $L\beta_8$. Three more satellites were reported in 1929 by F. K. and R. D. Richtmyer[1] for the atomic number range 40 to 50, inclusive, and are called by them $L\beta_2$(a), $L\beta_2$(b), and $L\beta_2$(c).

A Siegbahn vacuum spectrometer was used, with a calcite crystal, and was found to be very satisfactory. The usual photographic method of procedure was followed, the crystal being oscillated slowly through a small angle during the exposure, to eliminate false lines due to crystal imperfections. The voltage used in the case of each element was five times the excitation voltage of the parent line $L\beta_2$, for reasons to be discussed later, and the high-voltage, direct-current generating outfit used made it possible to measure and control the voltage with considerable assurance. The copper anode of the tube con-

* Presented at the December, 1930 meeting of the American Physical Society in Cleveland.

** The author wishes to make grateful acknowledgment for the privilege of using certain pieces of apparatus purchased for the use of F. K. Richtmyer by the Heckscher Research Council of Cornell University.

[1] F. K. and R. D. Richtmyer, Phys. Rev. **34**, 574 (1929).

tained a bevelled slot into which a copper wedge would fit. The element in question, in the most convenient, sufficiently stable form or compound was placed on this wedge.

The angle of diffraction of the various satellites was determined by measuring, by means of a comparator, their positions on the photographic plate relative to the position of the parent line, whose wave-length is accurately known. The wave-length of the satellites could then be determined by means of the expression

$$\Delta\lambda = 2d\left\{\cos\left(\theta - \frac{\Delta\theta}{2}\right)\right\}\Delta\theta$$

where θ is the Bragg angle for $L\beta_2$. The error in the wave-length difference brought about by the approximations involved in this expression was determined as of the order of magnitude of one part in 100,000 in the narrow region

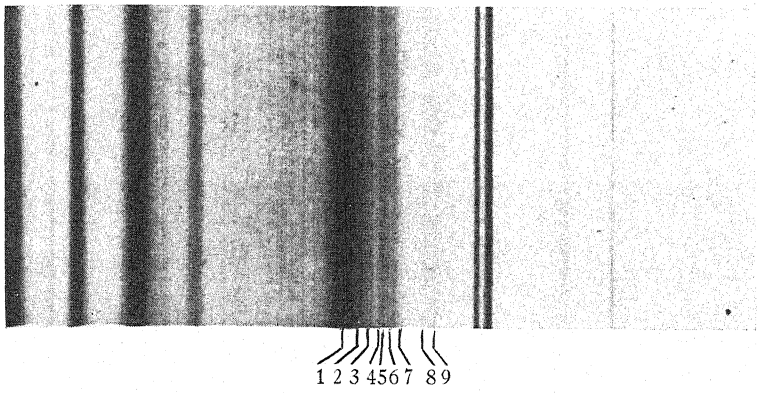


Fig. 1. A portion of the x-ray spectrum for Sn. The numbered lines are: 1, $L\beta_2$; 2, $L\beta_2$(a); 3, $L\beta_7$; 4, $L\beta_2'$; 5, $L\beta_2$(b); 6, $L\beta_2''$; 7, $L\beta_2$(c); 8, $L\beta_{10}$; 9, $L\beta_9$. On the original plate, which has more depth of contrast than the reproduction, all these lines are clearly visible.

of the plate at the center where the satellites are found. The lighting conditions and magnification of the comparator had to be carefully controlled to render the very faint lines visible. The exposure of the plates in the spectrometer was so regulated by trial and error to give maximum visibility of the satellites, and ranged from two to eight hours, depending upon the element.

TABLE I. *Wave-lengths (x-units).*

	Sn (50)	Sb (51)	Te (52)	I (53)	Ba(56)	Ce (58)	Nd (60)
$L\beta_2$	3167.9*	3016.6*	2876.1*	2746.08*	2399.3*	2204.1*	2031.4*
$L\beta_2$(a)	3162.2	3010.9†	2870.9†	2740.45†	2395.8†	2200.1†	2028.4†
$L\beta_2'$	3142.3	2992.9	2852.7†	2724.35†			
$L\beta_2$(b)	3138.9						
$L\beta_2''$	3134.6	2985.4	2845.2†	2718.5†			
$L\beta_2$(c)	3129.9						
$L\beta_7$	3149.4	2998.5†	2857.4†	2724.35†	2375.4	2176.4	2004.9
$L\beta_9$	3106.6	2964.7	2832.35†	2709.05†	2371.5	2183.7	2012.2
$L\beta_{10}$	3113.1	2971.7	2839.0†	2715.1†	2382.0	2190.66	2019.1
?				2731.8†			

* Values taken from M. Siegbahn, *The Spectroscopy of X-Rays.*

† Lines not previously reported.

TABLE II. *Difference in frequency between $L\beta_2$ and satellites (in ν/R units).*

	Sn (50)	Sb (51)	Te (52)	I (53)
$L\beta_2$ (a)	0.521	0.592	0.566	0.684
$L\beta_2'$	2.33	2.34	2.595	2.63
$L\beta_2$ (b)	2.66			
$L\beta_2''$	3.06	3.08	3.432	3.365
$L\beta_2$ (c)	3.49			
	Ba(56)	Ce (58)	Nd (60)	
$L\beta_2$ (a)	0.552	0.746	0.664	

The results of the experiments are shown in Tables I and II and Figs. 2 and 3. Many lines, other than those given in Table II, were found on the plates, and a rough check up of their wave-lengths showed them to be lines previously reported, other than satellites of $L\beta_2$. Fig. 2 is the "differential Moseley graph" introduced by F. K. Richtmyer for dealing with satellites,

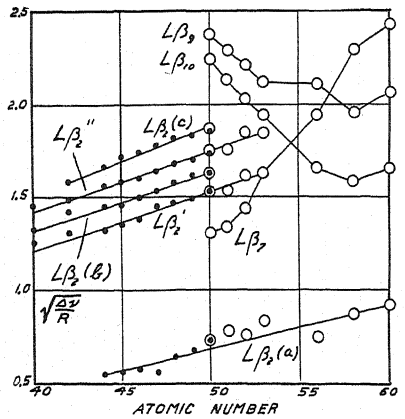


Fig. 2. For the ordinates, $\Delta\nu$ is the frequency difference between the line in question and $L\beta_2$. R is Rydberg's constant. Note that for the satellites the square root of this frequency difference is a linear function of the atomic number of the emitter. Black dots, F. K. Richtmyer and R. D. Richtmyer, Phys. Rev. **34,** 574 (1929); circles, R. D. Richtmyer, present work.

and it is seen that the straight-line law is still followed by the new points of this work. Fig. 3 is essentially an ordinary Moseley graph which has undergone a certain linear transformation. A Moseley graph is of course obtained by plotting the values of $(\nu/R)^{1/2}$ for a given x-ray line, as a function of atomic number, where ν is the frequency of the line, and R is Rydberg's constant. The points so plotted lie so nearly on a straight line that an ordinary drawing of them does not show any deviations. But if one subtracts from the ordinates of these points the corresponding ordinates of a straight line passing roughly through the points, and then plots these differences, on a magnified ordinate scale, as a function of atomic number, slight deviations can be made to show up. In other words, the ordinates of Fig. 3 are $(\nu/R)^{1/2}-f(Z)$, where $f(Z)$ is a particular linear function of atomic number. The straight line which was chosen for that purpose in this case was the straight line passing through the values of $(\nu/R)^{1/2}$ of the parent line, $L\beta_2$, for elements of atomic number 50 and 60.

All the lines shown are satellites of $L\beta_2$ except $L\beta_7$, $L\beta_9$, $L\beta_{10}$, and the single, unidentified line for iodine. As is shown by the graphs, one of the lines for iodine may be interpreted as either $L\beta_7$, $L\beta_2'$, or both. Those of Siegbahn's points for Cs(55) and Ba(56) which have been interpreted on the graphs as $L\beta_{10}$ (the lines which are marked by an asterisk in Fig. 3) are listed by him as the unresolved doublet $L\beta_2'$ and $L\beta_2''$, or, in his notation, $L\beta_{11}$ and $L\beta_{12}$. The present interpretation of them as $L\beta_{10}$ seems preferable for three reasons: in the first place, the satellites $L\beta_2'$ and $L\beta_2''$ decrease very rapidly in intensity in the atomic number range 50 to 53, and are barely visible at all for iodine. The line in question as observed for Ba(56) was rather intense. Secondly, Siegbahn's points fit in admirably with the previously unreported values for $L\beta_{10}$ for the intervening elements Te(52) and I(53). Thirdly, the lines in question, as also all other diagram lines, are slightly narrower and more

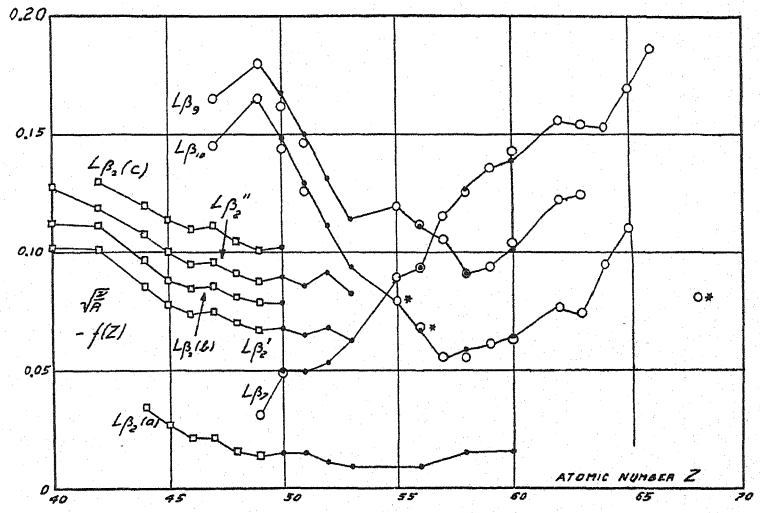


Fig. 3. The lines marked with an asterisk are listed by Siegbahn as $L\beta_{11}$ and $L\beta_{12}$ ($L\beta_2'$ and $L\beta_2''$ in the notation used in this article). Circles, M. Siegbahn; squares, F. K. and R. D. Richtmyer, Phys. Rev. **34**, 574 (1929); black dots, present work. See text.

distinct than any of the satellites, and are not overlaid with a faint continuous background, as are the satellites. The point for atomic number 68, and a similar one for 71, Siegbahn calls also the unresolved doublet $L\beta_2'$ and $L\beta_2''$. In view of the behaviour of the satellites in the region studied, it seems probable that Siegbahn's interpretation is open to question.

In the case of lines which have been measured before (see Fig. 3), the present values for their wave-lengths check, for the most part, to within one or two tenths of an x-unit with previous values.

The abruptness with which the satellites[2] disappear with increasing atomic number at their upper limit merits some attention. In 1927 Druyvesteyn,[3]

[2] Throughout this paragraph, discussion is restricted to the satellites $L\beta_2'$, $L\beta_2$(b), $L\beta_2''$, and $L\beta_2$(c).

[3] Druyvesteyn, Zeits. f. Physik **43**, 707 (1927).

following classical quantum mechanics, derived a relation for the ratio of the number of KL ionizations to the number of K ionizations which should take place under given circumstances. With Druyvesteyn's relation we can predict how the intensity of the satellites should vary with atomic number if we expose our plates in such a way that the parent line has always the same intensity. Druyvesteyn's formula is

$$\frac{\text{No. } KL}{\text{No. } K} = A\left(\frac{Z-\alpha_L}{Z-\gamma_L}\right)^2 \frac{\alpha_L}{(Z-\gamma_L)^2}$$

where α_L and γ_L are the partial and total screening constants of the L shell, q_L is the number of electrons in the L shell, and A is a factor which is constant for a given ratio of the initial energy of the cathode electrons to the binding energy of the K shell. This ratio remains constant, if, as in the case of the present experiments, the ratio of the voltage used to the K excitation voltage is maintained at a constant value. In applying Druyvesteyn's relations to the present case, the question is raised whether a similar formula holds for the ratio of the number of LM ionizations to the number of L ionizations. It seems that this is the case under the experimental conditions used. There are, following Druyvesteyn in part, six methods of importance by which LM ionization can be brought about: (1). The cathode particle expells first an L electron and then an M electron. (2). The cathode particle expells first an M electron and then an L electron. (3). The cathode particle expells an L electron with sufficient energy that it can ionize the M shell. (4). The K shell is initially ionized, and LM comes as a result of a radiationless rearrangement. (5). From the transition KL to LM. (6). From the transition KM to LM. The distinctions between the first three methods may not be sharp, depending upon our pictures of subatomic processes, but at least these three methods are the exact analogues of the ones Druyvesteyn considered for his case of KL ionization, while the last three methods above are excluded in the present case, because the voltage used was less than half the K excitation voltage. Therefore the above formula should apply to the present case by writing everywhere L for K and M for L. This formula may be trusted to give us a rough idea of the intensity relations we should expect. It predicts a gradual falling off of intensity with increasing atomic number; a falling off which would be barely perceptible within a small range of atomic numbers. For instance, assuming α_M and γ_M to be of the order of 10, the intensity of the satellites for 56(Ba) should be only about fifty percent less than the intensity of the satellites for 47(Ag), and only about twenty-five percent less than for 50(Sn). For 53(I) it should be about ten or twelve percent less than for 50(Sn). Quantitative determination of the intensities of these satellites as they appear on the photographic plates close to the strong parent line is very difficult and uncertain, and was therefore not attempted. But judging from comparison with the familiar example of the $K\alpha$ doublet, where the intensity ratio is 2:1, the rate at which the intensity of the satellites falls off is of a much larger order of magnitude than would be expected from Druyvesteyn's

relation. For both 47(Ag) and 50(Sn) the satellites are really quite intense lines, though of course very much less intense than the parent line. For 53(I) the satellites are extremely faint; only two of them show at all. For 56(Ba) they could not be made to show under any conditions or length of exposure, provided that the aforementioned reinterpretation of Siegbahn's previously reported lines is correct.

No alteration of the intensity of the line $L\beta_2$(a) from 50(Sn) to 60(Nd) was noticed. This line apparently differs fundamentally from the other satellites.

Possibly contemporary quantum mechanics will predict new intensity relations for the satellites.

The results of the experiments may be summed up as follows. There are definite upper limits for the atomic-number ranges of four of the five satellites of $L\beta_2$. At its upper limit, each of these satellites disappears abruptly with increasing atomic number, in a way which cannot be accounted for on the double-ionization theory of the origin of satellites. These limits are, respectively; $L\beta_2'$, 53(I); $L\beta_2$(b), 50(Sn); $L\beta_2''$, 53(I); and $L\beta_2$(c), 50(Sn). I feel that not without much more sensitive methods can they be observed for elements beyond the limits here set. The first and third of these satellites had not previously been reported for elements beyond 51(Sb). For a fifth satellite, $L\beta_2$(a), which is very close to the parent line, no such upper limit was found. This satellite was found for all the elements investigated.

For some of the elements investigated there are several faint diagram lines in the frequency range where the satellites occur, and considerable confusion has been caused by them, because they are of the same order of intensity as the satellites, and because information about them is incomplete. It was possible to observe them and measure their wave-lengths for the elements studied, and therefore to clear up this confusion to some extent. In many cases previous wave-lengths and interpretations are corroborated, but in one or two cases new interpretations are made necessary.

The author wishes to express thanks to Professor F. K. Richtmyer for valuable aid in conducting this research and in preparing this manuscript.

DISPERSION OF X-RAYS IN CALCITE

By Louis A. Pardue
Yale University

(Received September 23, 1931)

Abstract

The dispersion of x-rays in calcite has been investigated. The total radiation and the $K\alpha_1$ line from a molybdenum target tube operated at about 44,000 volts were used in different experiments. The decrement of unity in the index of refraction for the $K\alpha_1$ wave-length was found to be $(2.001 \pm 0.009) \times 10^{-6}$. This does not agree with the value computed on the Drude-Lorentz theory. The specimen was a right prism with the optic axis parallel to the 90° refracting edge. No evidence was found for double refraction. The intensities of Mo$K\alpha_1$ radiation reflected from calcite mirrors were measured for angles in the neighborhood of the critical angle. These experimental values were compared with the values computed on the basis of Thibaud's modification of Fresnel's equation and found to be in fair agreement.

OPTICAL terminology and theory may be applied to x-rays if due account is taken of their higher frequency. Since the different theories of the dispersion of x-rays agree in the limiting case where the frequency of the radiation is much greater than the natural frequency of the electrons in the dispersing medium, the results (Table I) for the refractive index of calcite for Mo$K\alpha_1$ are suggestive. The values reported for δ are considerably larger than the value resulting from all theories in the limiting case for higher frequencies. The theoretical value is

$$\delta \equiv 1 - \mu = ne^2/2\pi m\nu^2$$

where μ is the index of refraction, n the number of electrons per cm^3 in the dispersing medium, e the charge on an electron, m the electronic mass, and ν the frequency of the radiation. Table I gives the results of the various investigators and their methods.

Table I.

	$(1-\mu)\ (10)^6$ Theor.	Exper.	Method
Davis and Hatley[1]	1.84	2.0	Crystal wedge
Hatley[2]	1.84	2.03 ± 0.09	Crystal wedge
Compton[3]	1.84	2.10 ± 0.15	Deviation

[1] C. C. Hatley, B. Davis, Phys. Rev. [2] **23**, 290 (1924).
[2] C. C. Hatley, Phys. Rev. [2] **24**, 486 (1924).
[3] A. H. Compton, Phys. Rev. [2] **37**, 1694 (1931).

While the probable errors are large there is a definite lack of correspondence between theory and experiment. It was deemed desirable to make a very careful study of dispersion of Mo$K\alpha_1$ x-rays in calcite, having in mind the possibility of double refraction, about the only phenomenon in optics

whose counterpart in x-rays has escaped detection. The specimen of calcite chosen was a right prism with the optic axis parallel to the 90° refracting edge. To have the optic axis so directed is a logical choice in seeking double refraction in x-rays but one without strong support. An investigation was made of the energy reflected from polished and cleaved faces of calcite at angles in the neighborhood of the critical angle.

Arrangement and Adjustment of Apparatus

In these experiments the Société[3] Genevoise spectrometer was used. The various adaptations of it to the different needs will be pointed out with reference to Fig. 1. X is the x-ray tube (a water-cooled molybdenum target tube of the Coolidge type), S_1, S_2, S_3 and S_4 are slits. C_1 and C_2 are calcite crystals, and P is the 90° calcite prism with the optic axis parallel to the 90° edge. P was mounted on a specially designed holder which permitted the

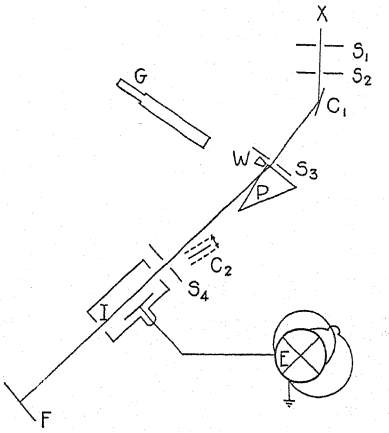


Fig.. 1

prism to be rotated about both horizontal and vertical axes in steps so small that any desired angular setting could be made easily. The holder also permitted the prism to be moved into and out of the beam laterally, keeping the faces of the prism accurately parallel to themselves. The 90° edge was in the axis of rotation of the prism mounting. The beam passed through this axis and nearly normal to one face of the prism. I is an ionization chamber and F is a photographic plate. The ionization currents were compared with a quadrant electrometer or a pliotron tube mounted over C_2. Methyl bromide (CH_3Br) vapor was used in the chamber to increase the absorption and ionization. The gain is due to the greater density of methyl bromide vapor as compared with air and to the higher K absorption of bromine for molybdenum rays. The angular positions of the prism were determined by means of an autocollimating telescope G, while the angular positions of C_1 and C_2 were determined by means of divided circles attached to the instrument. The divided circle attached to C_2 is presumably very good, being marked by the makers in 10 minute intervals which could be subdivided to 1 second by means of reading microscopes.

The slits, crystals and prisms were made parallel to the axis which supported C_2. This was accomplished by setting the axis of the autocollimating telescope perpendicular to the axis carrying C_2. To attain this a mirror with accurately parallel sides was placed on the table supporting C_2 and the autocollimating telescope and table were adjusted until the elevation of the beam reflected into the telescope did not change when the mirror was turned through 180°. The axis had previously been made vertical by means of a level. Since the telescope carried an accurate cathetometer level, the crystals on the mountings could be made parallel to the axis. Also by means of a steel mirror with accurately parallel sides placed between the jaws of the slits, the slits were made parallel to the axis. In the refraction experiments a lead wedge, W, was placed very close to the edge of the prism to stop as much as possible of the beam from getting by. The photographic plate was screened with lead from the direct beam practically all of the time during which a refraction photograph was being taken. This screen was removed during the last few minutes in order to obtain the direct beam from which to measure for the displacement of the refracted line.

To fix the angular position of the prism with respect to the beam, total reflection was used. P was rotated to different angular positions and the changes in intensity were noted by means of the electrometer readings. Having found the critical angle in this manner, the prism was turned into such a position that it would give total reflection. A photograph of the reflected line and the direct line on a plate at a known distance gave reliable data from which to compute the angle which the reflecting surface made with the beam. With this knowledge P could be turned to any desired angular position for refraction. The angles through which P was turned were measured by the autocollimating telescope, G, which had been calibrated previously against the circle attached to C_2. This telescope consisted of an object lens of 43 cm focal length and an eye combination which was the microscope of the Gaertner comparator used to measure the plates taken in this work. The microscope had a magnification of 28. When the reflector was turned through 1 second, the reflected image moved through 5.37 microscope divisions. The image reflected from the prism was such that the angles through which the prism was turned could easily be measured to 1 second.

Reflection and refraction were obtained for the heterogeneous radiation direct from the tube and for monochromatic radiation. When direct radiation was used, the arm carrying S_1, S_2 and C_1 was removed and the two slits were placed between P and the tube X. The double crystal arrangement permitted the determination of rocking curves and reflecting power of the crystals.

The measurement of the deviation of the refracted beam can be found in terms of the distance of the photographic plate from the refracting edge and the displacement on the plate of the refracted line from the undeviated line. Fig. 2 shows the rays and suggests how the measurements were taken.

The distance from F to A' was measured by pressing the end of a brass rod which had been squared in a lathe against the plate F and marking the point opposite A' with a sharp knife blade. This length was then measured

by comparison with a standard meter bar. The length AA' was measured with a traveling microscope. In the total reflection experiments the distance FA' was needed, while in the refraction experiments FA was needed. The edges of the lines measured to are clearly indicated in the diagram. Distances on the photographic plates were measured with a Gaertner traveling microscope reading to 0.001 mm. The calibration of the screw on the microscope was checked against a Zeiss scale and found to have no error larger than the errors of reading. That the plate (19 cm long) was satisfactorily perpendicular to the beam was checked by sighting along the arm of chamber I which was parallel to the beam.

The fact that the optic axis was parallel to the 90° edge of the prism was confirmed by a measurement of the indices of refraction of the ordinary and extraordinary rays on an optical spectrometer.

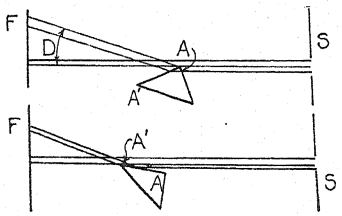


Fig. 2.

Experimental Results and Conclusions

As already mentioned, the specimen used in these experiments on total reflection and refraction was a 90° calcite prism having the optic axis parallel to the 90° edge. At first the two faces forming the 90° angle were highly polished. Later the polish on one face was removed by grinding in order to obtain a sharper edge, since the one left by the makers was a few hundredths of a millimeter thick. With the blunt edge it was impossible to obtain refraction at small angles of incidence on the emergent face. Total reflection from this edge was a disturbing feature. The dimensions of the faces forming the 90° angle were 10 mm×8 mm. A measurement of the ordinary and extraordinary indices of refraction for the Hg 5461 line gave 1.66169 and 1.4880 respectively as compared with the values 1.661647 and 1.487890 given by Baly[4] showing that the optic axis was very closely parallel to the 90° edge.

The experiments on total reflection, besides being useful in setting the prism for refraction, give some very interesting results. They give a determination of the index of refraction of calcite for the $K\alpha_1$ line of molybdenum as accurate at least as that obtained by the deviation method used by Davis-Hatley[1] and Hatley[2], who have determined the now accepted value. The broken curve, Fig. 3, shows the variation of the intensity of the reflected radiation in passing through the critical angle and the lack of any definite break shows there is no appreciable double refraction.

The prism was turned back to a point corresponding to a point on the

[4] E. C. C. Baly, Spectroscopy, Third Ed., Vol. 1, p. 83.

curve of maximum reflected intensity. A total reflection photograph gave 1.66×10^{-3} radians for the angle between the prism and the beam. Taking the mid-point of descent of the curve for the critical angle, we obtain for the critical angle 1.95×10^{-3} radians. The accuracy of this determination is limited in part by the choice of the critical angle from Fig. 3. Since the steep portion of the descent has an angular width of about 0.2×10^{-3} radians, the method has necessarily a possible error of 5 percent. Fig. 3 shows also in full line the theoretical curve for calcite. This was computed from the expression

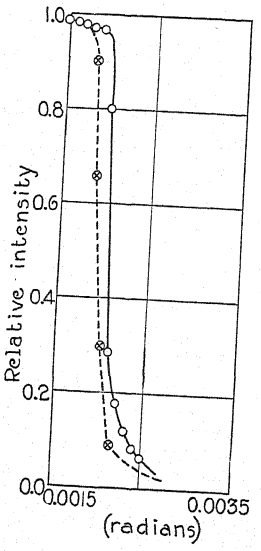


Fig. 3.

derived by Thibaud[5] for the ratio of the intensity of the reflected beam to that of the incident beam:

$$A = \frac{(1+m)^2 + 2(m^2+a^2)^{1/2} + 2(1+m)\left[2(m^2+a^2)^{1/2}\right]^{1/2}\cos\phi/2}{(1+m)^2 + 2(m^2+a^2)^{1/2} - 2(1+m)\left[2(m^2+a^2)^{1/2}\right]^{1/2}\cos\phi/2}$$

in which $\pi<\phi<2\pi$ and m is defined by the equation $\theta=(1+m)\theta_c$ where θ is the glancing angle of incidence and θ_c is the critical angle. The remaining quantities are defined in terms of the following relations:

$$K = k\lambda/4\pi;\quad a = K/2\delta;\quad \theta_c^2 = 2\delta;\quad \tan\phi = [-a(1-\delta)]/(m-a^2\delta);$$

$k\equiv$absorption coefficient; and $1-\delta\equiv$index of refraction. Table II gives the values of the constants used.

TABLE II.

k	20.6
a	2.91×10^{-3}
θ_c (radians)	2.00×10^{-3}
$\delta\times10^{6}$	2.00
$\lambda\times10^{8}$	0.709

[5] J. Thibaud, Jour. de Physique [7] 1, 37 (1930).

k and δ were measured in these experiments, k being determined by the absorption in a plate of calcite 1 mm thick. The faces of the plate were parallel to cleavage planes. The curve shown is typical of several that were taken for monochromatic radiation. Curves were also taken for the direct radiation from the molybdenum tube. These had a descent somewhat broader than those obtained with monochromatic radiation. The tube, however, was operated at a voltage somewhat higher than the excitation voltage of the K-series of molybdenum. The voltage varied slightly in different experiments but was always approximately 40,000 peak. Total reflection was also obtained from a cleavage face of a calcite crystal at C_2. Here the descent of the intensity curve was very broad. A total reflection photograph from this cleavage face, which was a very good one as evidenced by its x-ray reflection of the Bragg type, gave a very broad and diffuse line. In fact it had several components. This crystal reflected 18.7 percent of the incident monochromatic radiation when crystals were in the antiparallel position. The tolerance angle was also measured for this position and was found to be 12 seconds in the first order.

The first experiments on refraction were performed with the direct radiation from the molybdenum target tube. The prism was set in the reflecting position by the process mentioned above. The prism was then turned to such a position that the angle ρ between the beam and the emerging face had the desired value, 9 minutes in the first experiment. A 5 hour exposure gave the refracted lines on a plate 166.6 cm from the refracting edge. The target of the tube was about 40 cm from this edge. ρ was made less in succeeding experiments until it was impossible to get refraction at 2 minutes. The edge was found not to be sharp. The edge was made sharp by grinding the entering face which had been highly polished. After the grinding it was not polished again. The refraction experiments were repeated, and it was found that good refracted lines could be obtained at values of ρ less than one minute. The lines were as sharp as they were before the entering face was ground, showing that the condition of the entering face has little part in refraction. The photographs showed a line due to the $K\alpha$ doublet and one due to the $K\beta$ doublet. Also there was radiation due to shorter wave-lengths. The fact that this refracted band of shorter wave-lengths came to a fairly sharp edge and did not reach the lines suggests that the short wave-lengths coming from the general radiation from the tube included considerable radiation from tungsten which had been deposited on the target. A study of the intensity curves,[6] due to A. W. Hull, for a molybdenum tube operating at the voltage used here (around 44,000 but not held constant) would not lead one to expect this edge if molybdenum radiation alone were present. On the other hand a comparison with the energy curve for a tungsten target[6] would lead one to expect this edge. A rough calculation (this could not be made precise because of the overexposure of the central line) confirmed the view that the band was due to general radiation.

[6] B. Davis, Phys. Rev. [2] 9, 64 (1917).

Refraction was also obtained for an edge formed by two good cleavage faces from one of which total reflection was obtained as mentioned above. The refracted lines were very diffuse. Since the entering face does not effect refraction, then the emerging cleavage face is not suitable for refraction experiments. The fault could not be with the edge since the cleavage edge was much better than the edge on the 90° prism even after the grinding of the latter. These experiments on refraction with the direct radiation were not made very quantitative since the object was to get refraction with monochromatic radiation.

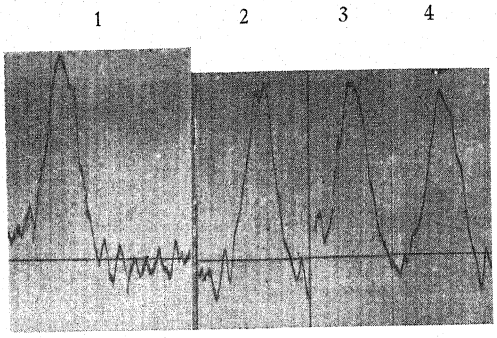


Fig. 4.

To obtain refraction with the $K\alpha_1$ line of molybdenum, C_1 was set to reflect $K\alpha_1$ at the best intensity. A good reflected line was obtained from C_1 in 2 seconds when the peak voltage was 45,000 volts and the current through the tube was 25 m.a. The angle ρ was made 7 minutes in the usual way. A good $K\alpha_1$ refracted line was obtained in 24 hours but on too dark a background to permit a close examination to be made of it. The wedge, W, was readjusted and ρ was made 1.45 minutes. The refracted line was good on a clear background. It was 0.077 mm broad and was free from a regular structure when examined under a microscope and by means of densitometer photographs (Fig. 4). Curves 1, 2, 3, and 4 were taken across different positions of this refracted line with a magnification of 40. Other refracted lines, less broad, obtained for smaller values of ρ and at longer exposures (up to 36 hours) also failed to show any fine structure which could be attributed to double refraction.

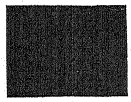


Fig. 5.

Fig. 5 shows the refracted line on the right and at the left the undeviated line from another of the good plates.

An attempt was made to find a possible fine structure by reflecting the refracted beam from C_2, but the beam was too weak to give an ionization cur-

rent measurable with an electrometer sensitivity such that the normal ionization did not mask the increase due to the refracted beam.

The refraction photographs permit a determination of the index of refraction of calcite for the $K\alpha_1$ line which has a smaller probable error than the now accepted value which was determined by the deviation from Bragg's formula. From the theory worked out by Stauss[7]

$$D + \rho = (\rho^2 + 2\delta)^{1/2}$$

in which D is the deviation due to refraction and δ is the dimensionless decrement of unity in the index of refraction. ρ has already been defined. In this equation the angles are to be expressed in radians.

Table III gives the data and results on the 11 plates taken. The distance FA' was 169.7 cm, AA' was 0.8 cm.

From the critical angle (1.95×10^{-3} radians) we get $\delta=1.90\times10^{-6}$. This value is subject to greater uncertainty than the others and is not averaged with them.

TABLE III.

Plate	d (mm)	ρ (radians)$\times10^3$	$\delta K\alpha_1\times10^6$
1.	3.096	0.192	1.993
2.	2.900	0.298	1.950
3.	2.743	0.432	1.941
4.	2.845	0.380	2.021
5.	2.838	0.380	2.012
6.	2.988	0.316	2.084
7.	2.227	0.920	2.050
8.	2.805	0.389	1.989
9.	2.313	0.791	1.989
10.	2.514	0.615	1.989
11.	2.840	0.360	1.995
		Mean	2.001 ± 0.009

It is the author's pleasure to acknowledge his indebtedness to Professor C. D. Cooksey for initiating this work, and to him, Professor L. W. McKeehan, and Mr. Donald Cooksey for much helpful advice throughout the course of the investigation. Also to Professor L. W. McKeehan the writer wishes to express his thanks for placing at his disposal the necessary facilities for doing the work.

[7] H. E. Stauss, J.O.S.A. **19**, 167 (1929).

FAINT BRANCHES IN THE OH BANDS

By G. M. Almy and G. D. Rahrer
University of Illinois

(Received October 3, 1931)

Abstract

Intense photographs of the OH bands in the near ultraviolet reveal a number of weak branches of the ${}^{0}P$ and ${}^{S}R$ types. The identification of these branches is made by a comparison of the observed wave numbers of the faint lines with their calculated wave numbers. No lines due to the molecule $O^{18}H$ were found, although under the conditions of the experiment they were to be expected.

INTENSE photographs of the group of OH bands in the near ultraviolet have been made primarily for the purpose of obtaining, in emission, bands due to $O^{18}H$. This object has not been realized but a study of the plates has disclosed a number of faint branches due to weak transitions (for which $\Delta K = \pm 2$) which have not been previously reported.

The spectrum of a heavy uncondensed discharge through water vapor was photographed with an E-1 Hilger quartz spectrograph. The water vapor was pumped rapidly through the 2 mm capillary (about 15 cm in length) of the discharge tube, which was viewed end-on. The continous spectrum of hydrogen was troublesome but its intensity was greatly reduced by increasing the rate of flow through the discharge tube with the use of a liquid air condenser placed between the tube and the pump.

The weak branches which have been identified are those of the type designated by the symbols ${}^{0}P_{12}$ ($\Delta K = +2$) and ${}^{S}R_{21}$($\Delta K = -2$). ${}^{S}R_{21}$ branches have been reported for the (0, 0) band at λ3064 by Watson,[1] for the (1, 0) band at λ2811 by Jack,[2] and the ${}^{0}P_{12}$ branch of the (0, 0) band has been identified by Almy.[3] The positions of the lines of these branches can be calculated by the following formulas, based on combination principles:[4]

$$ {}^{0}R_{21}(J) = Q_1(J) + \Delta_2F_2'(J) - 0.216(J - \tfrac{1}{2}) $$
$$ {}^{S}P_{12}(J) = Q_2(J) - \Delta_2F_2'(J - 1) + 0.216(J - \tfrac{1}{2}). $$

The comparison of the measured and the calculated wave numbers of five unreported branches in three different bands is given in the following tables. The agreement in wave numbers, together with the intensities, leaves little doubt as to the correct assignment of these lines.

As to the isotope effect, no lines due to $O^{18}H$ have been found. The relative abundance of O^{16} to O^{18} has been variously estimated at 630 to 1,[5] 1075

[1] W. W. Watson, Astrophys. J. **60**, 145 (1924).
[2] D. Jack, Proc. Roy. Soc. **A115**, 375 (1927).
[3] G. M. Almy, Phys. Rev. **35**, 1495 (1930).
[4] Cf. R. S. Mulliken, Phys. Rev. **32**, 388 (1928) and Almy, reference 3.
[5] R. Mecke and W. H. J. Childs, Zeits. f. Physik **68**, 362 (1931).

to 1,[6] and 1250 to 1.[7] The strongest $O^{16}H$ band (0, 0) was photographed in a region favorable for observation of the isotope effect in about five seconds. Thus the corresponding lines due to $O^{18}H$ should have appeared in one or two hours. Exposures up to four hours showed no lines which could have been properly assigned to $O^{18}H$. It is possible that they were masked by the hydrogen continuum.

TABLE I. $^{S}R_{21}$ *branch of the* $\lambda 2608$ *(2, 0) band.*

$J+1/2$	Intensity	Calculated wave number	Observed wave number
2	0	38404.35	38404.50
3	1	38442.07	38442.90
4	0	38475.83	38476.61
5	0	38504.76	38504.72
6	0	38526.18	38526.74
7	0	38542.23	38542.85
8	0	38551.61	38552.18
9	0	38553.32	38552.18
10	0	38550.94	38552.18

TABLE II. $^{S}R_{21}$ *branch of the* $\lambda 3428$ *(0, 1) band.*

$J+1/2$	Intensity	Calculated wave number	Observed wave number
2	3	29073.9	R_1(6-1/2)
3	5	29128.4	R_2(13-1/2)
4		29182.7	Not observed
5	1	29237.7	29236.9
6	1	29286.7	29285.8
7	1	29340.3	29341.2
8	0	29390.4	29390.6
9	0	29437.7	29437.4
10	0	29482.8	29493.8

TABLE III. $^{O}P_{12}$ *branch of the* $\lambda 2608$ *(2, 0) band.*

$J+1/2$	Intensity	Calculated wave number	Observed wave number
2	5	38036.77	Q_2(5-1/2)
3	1	37965.07	37964.73
4	5	37885.61	Q_2(8-1/2)
5	1	37798.02	37797.73
6	3	37702.41	P_2(7-1/2)
7	0	37601.62	37601.35
8	2	37492.88	Q_2(13-1/2)
9	0	37377.95	37378.08

TABLE IV. $^{O}P_{12}$ *branch of the* $\lambda 2811$ *(1, 0) band.*

$J+1/2$	Intensity	Calculated wave number	Observed wave number
2	1	35241.92	35240.94
3	1	35173.07	35172.65
4	2	35097.45	35097.03
5	2	35015.10	35014.69
6	2	34926.73	34927.13
7	10	34833.29	Q_2(14-1/2)
8	2	34735.64	34735.21
9	1	34632.21	34632.51
10	5	34524.74	P_2(1-1/2) of (2, 1) band
11	1	34412.25	34411.85
12	1	34296.05	34295.58
13	1	34175.53	34176.52
14	1	34050.94	34050.77
15	1	33926.50	33927.18
16	0	33787.97	33787.86
17	6	33652.27	P_2(21-1/2)
18	0	33511.00	33510.91
19	0	33366.05	33365.51

TABLE V. $^{O}P_{12}$ *branch of the* $\lambda 3428$ *(0, 1) band.*

$J+1/2$	Intensity	Calculated wave number	Observed wave number
2	4	28691.5	P_2(3-1/2)
3	3	28624.2	P_2(5-1/2)
4	1	28556.1	28555.8
5	1	28485.8	28487.5
6	1	28412.0	28413.1
7	2	28339.8	P_1(13-1/2)
8	0	28260.3	28261.3
9	0	28182.0	28182.4
10		28102.0	Not observed
11	0	28018.2	28018.3

[6] S. M. Naudé, Phys. Rev. **36**, 333 (1930).
[7] H. D. Babcock, Proc. Nat. Acad. Sci. **15**, 471 (1929).

INVESTIGATIONS IN THE FAR INFRARED

By John Strong*
California Institute of Technology

(Received September 22, 1931)

Abstract

An instrument is described for investigations of the reflectivity, transmissivity and emission of various materials over the spectral range 20 to 150μ. The following measurements are reported: Reflectivities of rough surfaces, galena, β-magnesia, zincite, stibinite, corundum, sphalerite, molybdenite and cuprite. Transmissivities of KBr, KI a layer of KCl evaporated on a lacquer film, a thin film of amorphous quartz, liquid CCl_4, and powdered Al and Cu. Emission of liquid and solid NaCl near the melting temperature.

Introduction

In the near infrared a prism spectrometer is useful for preliminary investigations when high resolving power is not required. It is the purpose of this paper to describe an instrument to play a similar role in the far infrared and to present the results of investigations carried out with this instrument.

This new instrument employs the reststrahlen method of obtaining monchromatic bands of radiation. The instrument is so designed that investigations on the reflectivity, transmissivity and emission of various materials may be expeditiously carried on over the spectral range 20 to 150μ. In order to see that the results obtained by the reststrahlen method may be equivalent to those obtained in the near infrared with a prism spectrometer it is necessary to bear in mind that the practice of representing position in the infrared spectrum by wave-length is less natural than representation by frequency. This is because the width of absorption lines, the distance between lines and the extension of an absorption band, are, when plotted against frequency, approximately the same in all regions of the spectrum, that is to say, they do not depend on wave-length. For filters the sharpness of transition from opacity to transparency will be the same. In order to get an equally accurate picture of a spectrum in any region of the infrared the number of observations per unit spectral range, on a frequency scale, is the same. The so-called far infrared, i.e. wave-lengths greater than 20μ, is not very wide when frequencies are considered. The importance of this region is due to the character of its spectra rather than their quantity. In fact the far infrared from 20–150μ corresponds, in frequency range, to approximately $\frac{1}{2}\mu$ at 3μ. This means that the twelve rather uniformly distributed wave-lengths which were employed for the present investigation correspond to about 24 points per μ at 3μ. This is about five times the frequency of points taken by Coblentz[1] in his classical studies with a prism spectrometer.

* National Research Fellow.

[1] W. W. Coblentz, Investigations of Infrared Spectra, 1908.

The Restrahlen

Table I, taken in part from "Das Ultrarote Spektrum" by Schaefer and Matossi, describes the twelve reststrahlen bands used in the present investigation.

Table I.

Number of reflections	Crystal mirrors	Filter (3 mm paraffin in each case)	Wave-length in μ	Frequency in $\sim$/cm	Energy in cm of deflection (scale at 3 meters)
4	Quartz	1 cm KCl	20.7	483	44
3 1	Fluorite Metal	5 mm KCl	23	435	18
2 2	Fluorite Calcite	3 mm KBr	27.3	366	42
4	Calcite	none	29.4	340	95
3 1	Fluorite Metal	0.4 mm quartz 1.2 mm KBr	32.8	305	2.6
3 1	Aragonite Metal	0.4 mm quartz	41	244	1.6
4	NaCl	2 mm quartz	52	192	5.2
4	KCl	"	63	159	2.0
4	KBr	"	83	120	1.6
4	KI	"	94	106	1.0
4	TlBr	"	117	85	1.7
4	TlI	"	152	66	1.0

The use of a paraffin window for the thermocouple (about 3 mm in thickness) has the advantage that it does not transmit the short wave-length reststrahlen of quartz at 8.7μ and calcite at 6.7μ to the receiver. With this filter the use of the 20.7 and 29.4μ reststrahlen is exactly the same as the other reststrahlen.

The substitution of a 1 cm KCl filter for the 2.5 mm AgCl filter recommended by Rubens and Nichols[2] for the 20.7μ reststrahlen is justified by transmission curves given by Rubens and Trowbridge[3] for AgCl and KCl.

Regarding the 41μ reststrahlen, Rubens[4] states, "Die Reststrahlen von Arrogonit waren, wie ihre Zerlegung im Gitterspektrum erkennen liess, ziemlich inhomogen und zeigten zwei Maxima, ein schwächeres bei 35, ein stärkeres bei 41μ."

In the present experiments, the 27.3μ rays were not polarized as specified by Liebisch and Rubens.[5]

Four calcite mirrors gave radiations which were transmitted by quartz. These were the 94μ radiations observed by Rubens. The fraction of the cal-

[2] H. Rubens and E. F. Nichols, Wied. Ann. **60**, 418 (1897).
[3] H. Rubens and A. Trowbridge, Wied. Ann. **60**, 724 (1897).
[4] H. Rubens, Berliner Berichte, p. 199, (1919).
[5] H. Liebisch and H. Rubens, Berliner Berichte 1919, p. 876.

cite reststrahlen transmitted by 2 mm quartz was 0.0136. In the data which follow in this paper this lack of homogeneity in the 29.4μ reststrahlen was disregarded.

The Apparatus

The apparatus has been described in an earlier paper.[6] However, there have been several alterations of the earlier form of the apparatus. These are shown in Fig. 1 and are described below;—The Welschbach mantle, used previously, was replaced by a Globar heater. The use of a Kahlbaum paraffin window with a Globar heater gives the advantages of the Welschbach mantle, namely a scarcity of near infrared radiations without the disadvantages of its fluctuations. The Globar heater (3/8″×8″) was mounted in a cooled brass cylinder—the radiations emerging through a circular hole in the center of the

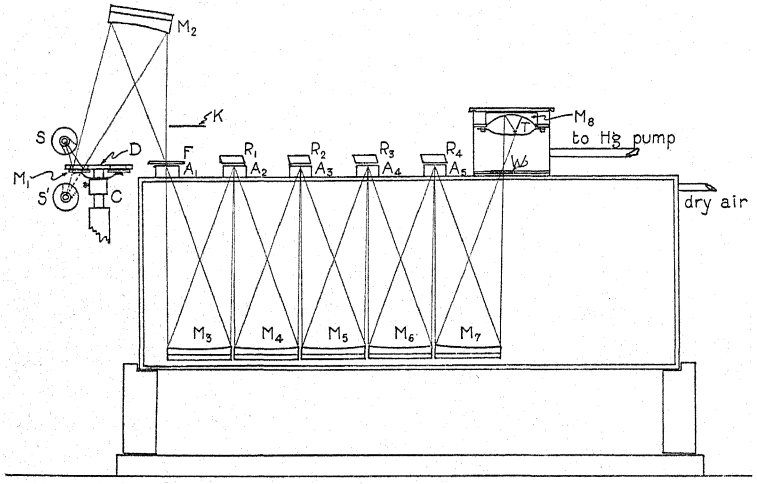


Fig. 1. Diagram of apparatus.

cylinder. For reflectivitives this source was placed in the position S (see Fig. 1) the emitted radiations being reflected to M_2 by means of the mirror M_1. By revolving the disk D the mirror M_1 may be either of the three samples being investigated or a silver mirror. These are clamped under the four symmetrical holes in the disk by the collar and spring washer C. For measuring transmissions the Globar heater takes the position S'. One of the holes in the disk is open in this case and the other three are covered with samples.

When the silver mirror reflects the energy from the heater to M_2 the reststrahlen energy may be determined by observing the galvanometer deflection as the metal shutter, K, is successively placed in and out of the radiation path. For transmission, the reststrahlen energy is determined with the radiation passing through the empty hole. The ratio of the reflected or transmitted energy to the reststrahlen energy gives respectively the reflectivity or transmissivity of the sample. In practice, the reflection or the transmission of three samples was determined each time the reststrahlen energy was determined.

[6] John Strong, Phys. Rev. **37**, 1565 (1931).

The radiations collected by M_2 are passed through the filter F and then through the aperture A_1. M_3 collects this energy to reflect it to the first reststrahlen mirror R_1. After four successive reflections R_1 to R_4 the mirrors M_7 and M_8 focus the radiation onto the thermocouple receiver. The thermocouple window, W, is 3 mm paraffin (Kahlbaum M.P. 68–70°C). The advantage of using the auxiliary mirror, M_8, to give a small focus on the thermocouple receiver is represented by a factor of 4.

The air in the apparatus was dried by passing it over $CaCl_2$ and P_2O_5. A continuous stream of dry air made diffusion of moisture into the apparatus through the holes A_1 to A_5 impossible. These holes were each covered with a lacquer membrane. The reststrahlen crystals and filters were painted with very thin colorless lacquer to protect them from attack by atmospheric moisture.

The apparatus was protected from thermal fluctuation by a felt jacket. The restrahlen crystals R_3 and R_4 were covered with a metal housing so the thermocouple could not "see out." This practice adds to the steadiness of the galvanometer.

The galvanometer used with the thermocouple was a L. and N. type H.S. and was mounted on a vibrationless support. The scale, placed at 6 meters from the galvanometer, was read with a 24 power telescope to 1/10 mm.

The galvanometer was given 15 seconds to come to equilibrium between readings. This time was accurately measured with a metronome to facilitate the cancellation of drift. The reflectivities or transmissivities of three samples may be determined four times at each of the twelve wave-lengths in an afternoon if the apparatus is kept working constantly.

The advantages of this apparatus for making preliminary spectral investigations by the reststrahlen method may be summarized as follows; (1) The reststrahlen crystals required are small, making them more easily obtainable. (2) The change from one set of crystals to another may be made quickly without disturbing the dry air in the radiation path. (3) The use of a paraffin filter facilitates measurement at 20.7 and 29.4μ.

The following measurements illustrate the applicability of this instrument for preliminary investigations in the far infrared.

Reflectivities

Rough surfaces

Lord Rayleigh[7] showed, by qualitative experiments, that rough surfaces reflect long infrared waves almost as well as polished surfaces. The practice of using a rough mirror to isolate the near infrared from the far infrared makes the quantitative investigation of the reflectivity of rough surfaces desirable. In order to study this, three rough mirrors were prepared by grinding brass on brass with 400, 200 and 60 carborundum. The reflectivities of these mirrors in the far infrared are shown in Fig. 2. The large variations of the observed points from the curves are probably due to some interference effects rather than to experimental error.

[7] Lord Rayleigh, Proc. of the Royal Inst. XVI, p. 563, 1901.

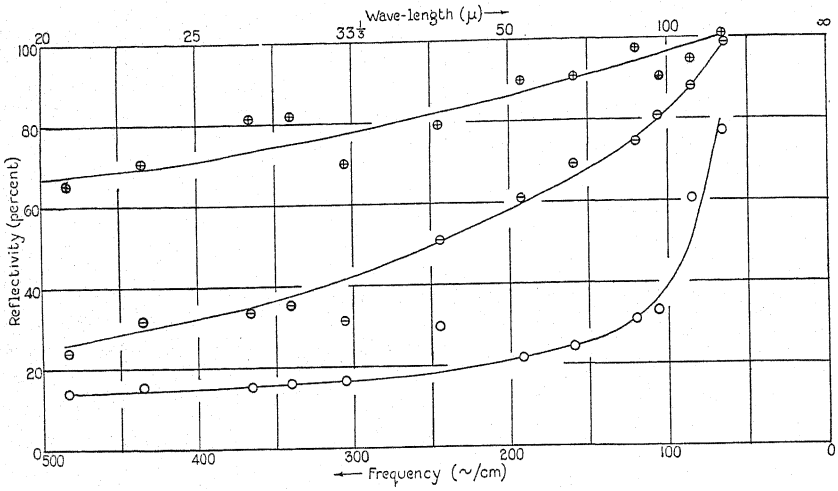


Fig. 2. Reflectivities of brass ground with 400 carborundum, crosses; 220 carborundum, thetas; and 60 carborundum, circles.

Galena

The measurements of the reflectivity of galena are shown in Fig. 3. It will be observed there are two maxima, one near 80μ and the other near 120μ. The sample was polished to a high luster except at places where small pieces of the crystal chipped out. The surface used was parallel to a cleavage plane.

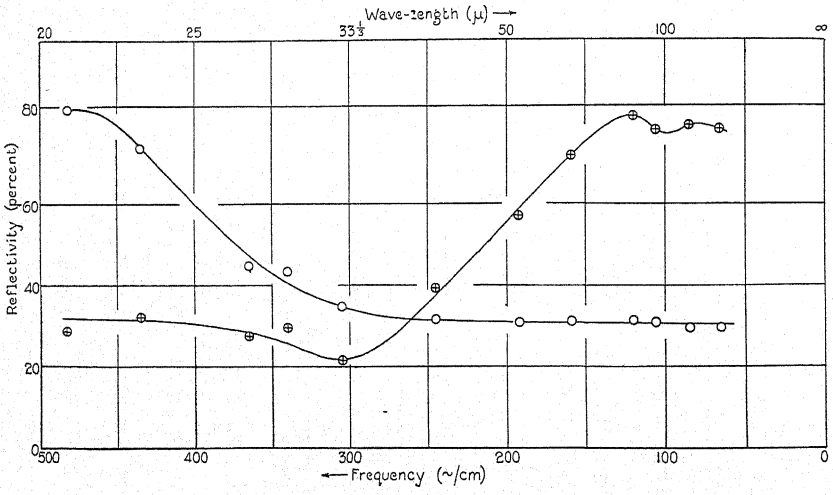


Fig. 3. Reflectivity of beta-magnesia, circles, and galena, crosses.

Four galena reflectors gave a reststrahlen whose intensity when filtered by 2 mm of quartz was 1.3 times that of the rocksalt reststrahlen. The reflection of galena for these radiations was 72 percent. The transmissivity of 0.1 mm black paper was 22 percent. For 152μ the transmissivity of the paper was 38 percent.

Magnesia

The reflectivities of magnesia for the far infrared are shown in Fig. 3. The sample was from a dense polycrystalline mass fused in an electric furnace. The exact position of the reflection maximum can only be determined with higher resolving power than was here obtainable.

Zincite

The reflection of a natural zincite crystal is shown in Fig. 4. The reflectivity is not to be considered as accurate in absolute value because the zincite was not sufficiently uniform to take a good polish. The surface was, however, much less rough than the 440 brass shown in Fig. 2. The curve is drawn with maxima at 22 and 28μ to agree with the predictions of S. Tolksdorf.[8]

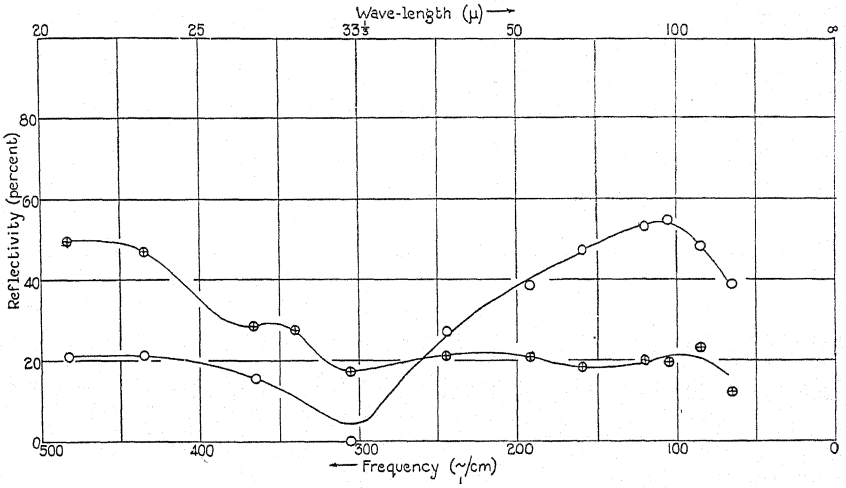


Fig. 4. Reflectivities of zincite, crosses and stibinite, circles.

Stibinite

The sample of stibinite was cleaved from a small crystal. It was neither flat nor large enough for the hole in the plate D (see Fig. 1). Nevertheless the results plotted in Fig. 4 indicate a maximum of reflectivity at 94μ.

Sphalerite

Because of nonuniformity this crystal did not take a good polish. As a consequence of this, the reflectivities are not to be considered quantitatively correct. The results (Fig. 5) agree with those of Rubens for (ZnFe)S in having a maximum at 30.9μ.

Corundum

The sample was not large enough to afford quantitative investigations. The results (Fig. 5) show maxima at 23μ and 27μ which may possibly be the fundamental bands whose overtones were observed by Coblentz[9] at 11.8 and

[8] S. Tolksdorf, Zeits. f. phys. Chem. **132**, 161 (1928).
[9] W. W. Coblentz, Investigations, part V, p. 18, 1908.

13.5μ. It will be observed there is a third and weaker maximum at 52μ. In Fig. 6 the reflectivities of cuprite and molybdenite are shown. Neither of these substances showed very remarkable spectra in the infrared. The samples were not perfect, so a quantitative interpretation of the results is not justified.

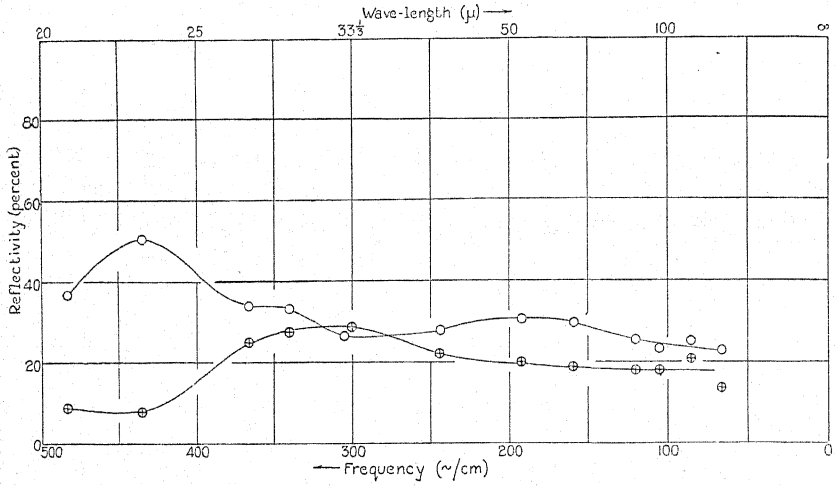


Fig. 5. Reflectivities of corundum, circles, and sphalerite, crosses.

Transmissivities

KBr and KI

The transmission of 3.19 mm of KBr and 0.83 mm of KI is plotted in Fig. 7. It is well to keep in mind the result reported in an earlier paper,[6] namely that 2 cm of KI transmits 50 percent of the 32.8μ reststrahlen. These results do not distinguish between loss of light due to surface reflection and that due to body absorption.

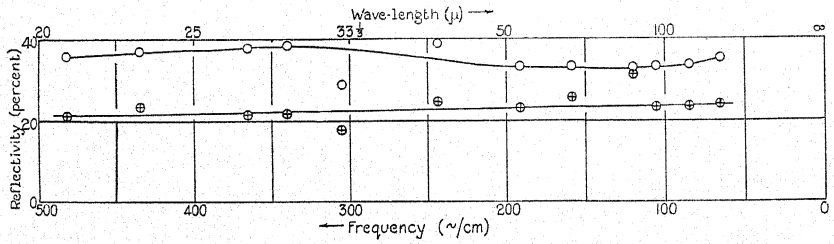


Fig. 6. Reflectivities of cuprite, circles; and molybdenite, crosses.

KCl evaporated on a lacquer film

This experiment was made to see if an evaporated film would not be free of the anomaly reported by Hirsekorn[10] for the lacquer films on which KCl smoke was deposited. The evaporated film gave only a single absorption at the expected position. The sample was prepared by evaporation of KCl onto a lacquer film in vacuum. Hirsekorn evaporated at atmospheric pressure and

[10] H. G. Hirsekorn, Ann. d. Physik **6**, 985 (1930).

observed two maxima of absorption on either side of the region of metallic reflection for KCl.

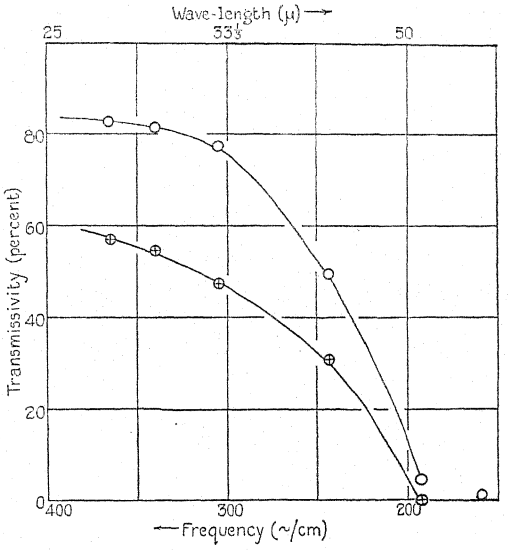


Fig. 7. Transmissivities of 3.19 mm KBr, crosses; and 0.83 mm of KI, circles.

Quartz film

Thin films of amorphous quartz have been used as absorption cell windows in the far infrared by Czerny.[11] For such purposes it is useful to know their transmission. This is shown in Fig. 8 for a film, about 10μ thickness, of

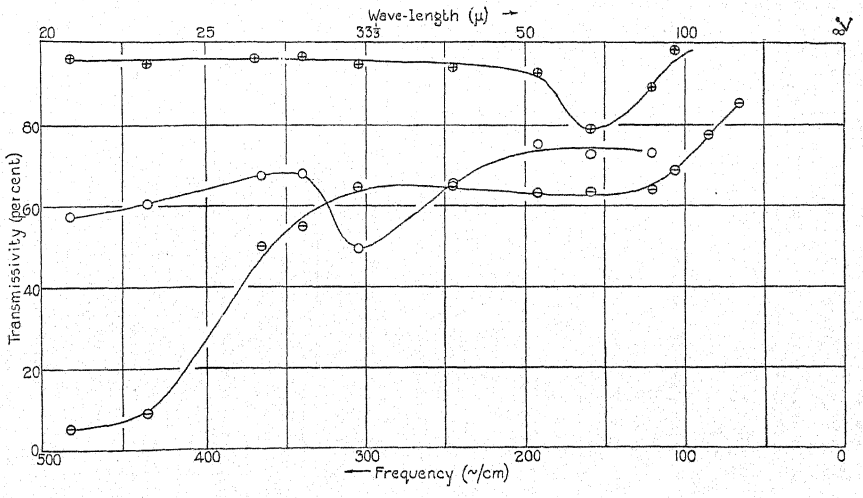


Fig. 8. Transmissivities of 10μ film of amorphous quartz, thetas; liquid CCl_4, circles; KCl evaporated on lacquer film, crosses.

[11] M. Czerny, Zeits. f. Physik **44**, 235 (1927).

amorphous quartz. The increase in transmission beyond 83μ may be ascribed to the destructive interference between the light reflected from the front and back surfaces of the quartz film.

CCl_4

CCl_4 has a band system analogous to CH_4. Trumpy[12] has predicted for CCl_4 an active frequency at 311$\sim$/cm. This is the only active frequency in the far infrared. In order to test for the presence of this band a solution of CCl_4 in paraffin was placed between two thin paraffin sheets. This was chosen in preference to the gas method because of the low vapor pressure of CCl_4. The transmission of this sample showed a minimum at the predicted position in the spectrum (see Fig. 8).

I believe this method of studying the transmission of liquids in the far infrared to be superior to the use of a thin cell bounded by windows because it is free from objectionable interference effects. These effects may be particularly annoying in the far infrared where (if the windows are quartz) the reflectivities are high and the Bragg reflection consequently more troublesome.

Copper and aluminum powders

These powders were suspended in Kahlbaum paraffin and sheets as thin as 0.15 mm proved to be opaque although this was not to be expected since the particles were small as compared with the wave-length of the radiation.[13]

Emission

NaCl

The emission of NaCl on a platinum ribbon was investigated just below and just above the melting temperature. The results are given in Table II.

Table II. *Ratio of emission of NaCl on Pt ribbon above melting temperature to emission below melting temperature.*

63μ	52μ	41μ
1.24	1.01	1.20

The results are unfortunately not decisive because at the lower temperature very little NaCl volitalized whereas the molten salt sent up a little curl of smoke which may have absorbed some of the radiations as it was partially in the radiation path. However, it is probable that the characteristic frequency of NaCl at 52μ disappears on melting.

[12] B. Trumpy, Zeits. f. Physik **66**, 790 (1930).

[13] In this connection the result of another experiment is of interest. The fluorite reststrahlen was not transmitted through a tube 10 feet long filled with the smoke from burning phosphorus.

THE INFRARED SPECTRUM AND THE MOLECULAR CONFIGURATION OF N_2O

By E. K. Plyler and E. F. Barker
University of Michigan

(Received October 8, 1931)

Abstract

Vibration spectrum. The three normal vibrations of N_2O are all active. The fundamental bands at 17.0μ, 7.78μ and 4.50μ, and the three harmonics have all been observed; also six combination bands at wave-lengths greater than 2μ. The 17.0μ fundamental and two combination bands involving this fundamental have strong zero branches, while the harmonic and two combination bands involving the harmonic transition have no zero branches. All other bands are doublets.

Rotational analysis. Three bands at 17.0μ, 7.78μ and 8.60μ have been resolved under high dispersion. All show rotation lines with continuously varying intensities (no alternation) and almost uniform spacing, the same for each band, viz. 0.84 cm^{-1}. The corresponding value of the moment of inertia, 59.4×10^{-40}, is practically equivalent to that computed from the doublet separations of the various bands.

Form of the molecule. The molecule is apparently linear but not symmetrical. The observations are not consistent with a triangular configuration, nor with the symmetrical linear configuration N—O—N, but they may be correlated precisely by means of the model N≡N=O.

THE infrared vibration spectrum of the N_2O molecule has been studied by Warburg and Leithauser[1], by E. v. Bahr[2], and more recently by Snow[3] but none of these observations were extended to wave-lengths sufficiently great to include all of the bands, nor was the available resolution adequate to reveal the rotational structure. Snow presented arguments based upon the physical properties of the gas which suggest that the molecule is linear in form, and believed that his results indicated the symmetrical arrangement N-O-N. Since the total number of electrons is the same as for CO_2 which is certainly linear and symmetrical[4] this would require that both in properties and spectrum the two gases should be very much alike. The observations indicate, however, a much richer spectrum for N_2O, with many more bands of appreciable intensity and without the restrictions as to combination frequencies which apply to CO_2.

The observations to be described below extend to about 20μ and include a number of bands not previously reported. The rotational structure is clearly resolved in several typical cases, and suggests at once a linear model, but certainly not a symmetrical one. The three fundamental frequencies are all active, as would have been expected for a triangular configuration of the atoms; they are however numerically inconsistent with the mechanical solu-

[1] Warburg and Leithauser, Ber. D. phys. Ges. **1**, 148 (1908).
[2] E. v. Bahr, Verh. D. phys. Ges. **15**, 710 (1913).
[3] Snow, Proc. Roy. Soc. **A128**, 294 (1930).
[4] Martin and Barker, Phys. Rev. **37**, 1708 (1931).

tion for this case,[5] on the assumption of central force fields, yielding for the apex angle an imaginary value. It is quite apparent that the asymmetry must involve a difference in the distances from the oxygen atom to the two nitrogen atoms, rather than a departure from linearity. Such a situation seems probable only if the oxygen atom occurs at one end rather than at the middle of the group, the molecular form being $N \equiv N = 0$.* In this case the vibration corresponding to ν_1, the inactive frequency for symmetrical molecules, would be represented in the absorption spectrum by fundamental and harmonic bands of the doublet type. The same would be true of ν_3, while ν_2 should exhibit zero branches in the fundamental and odd numbered harmonic bands, but none in even numbered harmonics. This follows immediately from the correspondence principle, and has been derived rigorously by Dennison.[6]

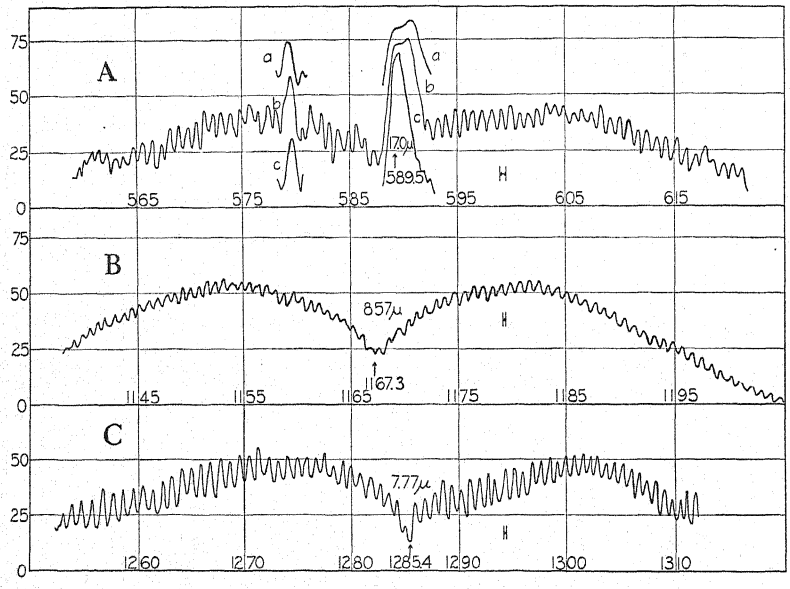


Fig. 1. Bands of N_2O showing rotational structure.
A. The fundamental ν_2, 26 cm cell, pressures 4, 16 and 30 cm.
B. The harmonic $2\nu_2$, 6 cm cell, 24 cm pressure.
C. The fundamental ν_1, 6 cm cell, 10 cm pressure.

The Observed Fundamental Bands

The lowest frequency fundamental band occurs at 17.0μ and arises from a change in electric moment perpendicular to the linear axis of the molecule, i.e. from the vibration ν_2. It has been resolved by means of a grating with a 7″×9″ surface ruled 1200 lines per inch, which was so effective that slits 0.6

[5] Dennison, Phil. Mag. **1**, 203 (1926).

* During the course of the investigation our observations were submitted to Professor Dennison, and he first suggested this interpretation, which is apparently the only completely consistent one. We understand that the idea originated in a discussion between Dennison and Snow on the subject of the N_2O spectrum.

[6] Dennison, Rev. Mod. Phys. **3**, 280 (1931).

mm wide (including a frequency range of about 0.4 cm^{-1}) were adequate. The outline of this band is shown in Fig. 1A, upon a scale too small to indicate the individual readings which were taken at intervals of about 0.2 cm^{-1}. There is a strong zero branch at about 590 cm^{-1} with positive and negative branches consisting of lines appearing single at this resolution, which are

TABLE I. *Observed frequencies for the fundamental ν_2 at 17.0μ, and residuals from the computed values.*

Positive branch			*Negative branch*	
wave numbers	residuals	m	wave numbers	residuals
		2	587.3	+.03
		3	6.4	+.10
592.4	−.04	4	5.6	+.06
3.3	−.10	5	4.9	−.08
4.0	+.05	6	3.9	+.07
4.9	−.01	7	3.1	+.03
5.7	+.04	8	2.4	−.09
6.5	+.07	9	1.4	+.07
7.4	+.01	10	0.6	+.03
8.3	−.05	11		
9.1	−.01	12		
600.0	−.07	13	78.1	+.03
0.8	−.03	14	7.4	−.11
1.6	+.01	15	6.5	−.05
2.4	+.07	16	5.7	−.09
3.3	+.01	17	4.8	−.03
4.1	+.04	18	3.9	+.04
4.9	+.09	19	3.0	+.11
5.7	+.13	20	2.2	+.07
6.5	+.17	21	1.4	+.03
7.4	+.12	22	0.6	.00
8.3	+.05	23	69.9	−.11
9.1	+.10	24	9.0	−.06
10.0	+.04	25	8.1	.00
0.8	+.10	26	7.3	−.04
1.7	+.04	27	6.5	−.08
2.5	+.08	28	5.6	.00
3.4	+.02	29	4.7	+.06
4.2	+.07	30	3.8	+.13
5.2	−.09	31	3.0	+.10
6.1	−.14	32	2.3	−.04
7.0	−.20	33	1.5	−.16
7.8	−.16	34		
8.6	−.11	35		
9.5	−.15	36		
20.4	−.20	37		
1.2	−.17	38		

spaced about 0.84 cm^{-1} apart. There is practically no convergence, as indicated in Table I, and the positions of the lines are well represented by the equation

$$\nu_2 = 589.01 \pm 0.839m + 0.0001m^2 \qquad (1)$$

m being merely an ordinal number, not equal to the quantum number J. The residuals in the table are differences between values from this equation and the observed frequencies; in only a few cases are they greater than 0.10 cm^{-1}, which is about the limit of accuracy in measurement. The maximum of the curve observed with 4 cm pressure in the cell, lies at 589.5 cm^{-1}, but this frequency would certainly be reduced somewhat if still less absorbing material were used.

In addition to the rotation lines there also appear secondary maxima at 590.6 and 579.6 which must be zero branches for the absorption due to molecules already possessing one or more quanta of vibrational energy. The former results in a curious broadening of the zero branch on its high frequency side as the amount of absorbing gas is increased, finally developing a double peak. Clearly this is not the result of a parabolic displacement of successive lines in the zero branch, since the convergence is so small. The proportion of molecules in the first excited state at ordinary temperatures is fairly large, in fact about 13.6 percent due to the low frequency and also to the fact that this state has a weight of two. For the first excited state the motion is isotropic in a plane normal to the molecular axis, and hence involves one quantum of rotational energy about this axis.[7] It may be represented by $1_{\pm 1}$, the normal state being 0_0, where the principal quantum number designates the vibrational state, and the subscript indicates angular momentum about the figure axis. From this state two transitions are possible, one to the double

TABLE II. *Observed frequencies for the fundamental ν_1 at 7.78μ, and residuals from the computed values.*

Positive branch wave numbers	residuals	m	*Negative branch* wave numbers	residuals
1286.1	+.11	1	1284.5	+.03
7.0	+.03	2	3.8	−.11
7.9	−.03	3	2.9	−.05
8.7	−.02	4	2.0	+.00
9.5	+.01	5	1.1	+.05
90.3	+.04	6	2.0	+.09
1.2	−.06	7	79.4	+.02
2.0	−.04	8	8.6	−.04
2.8	−.04	9	7.7	.00
3.6	−.03	10	6.8	+.03
4.4	−.02	11	6.0	−.04
5.2	−.03	12	5.1	−.01
6.0	−.04	13	4.2	.00
6.9	−.15	14	3.4	−.07
7.6	−.06	15	2.5	−.06
8.4	−.07	16	1.5	+.03
9.2	−.09	17	0.6	+.05
1300.0	−.11	18	69.7	+.05
0.7	−.04	19	8.8	+.04
1.5	−.07	20	8.0	−.05
2.2	+.00	21	7.0	+.06
2.9	+.06	22	6.1	+.04
3.7	+.02	23	5.2	+.02
4.5	−.06	24	4.3	−.02
5.2	+.03	25	3.3	+.09
6.0	+.01	26	2.4	+.05
6.7	+.03	27	1.5	+.03
7.4	+.08	28	0.6	.00
8.2	+.01	29	59.7	−.03
8.9	+.05	30	8.7	+.03
9.7	−.02	31	7.8	−.02
10.4	+.02	32	6.9	−.04
1.0	+.14	33	5.8	+.10
1.8	+.07	34	4.9	+.04
		35	4.0	.00
		36	3.1	−.03

[7] Dennison, Rev. Mod. Phys. 3, 296 (1931), particularly Fig. 6.

level $2_{\pm 2}$, and one to the single level 2_0. These may be assigned the frequencies 590.6 and 579.6 respectively, corresponding to the two subsidiary zero branches. The rotation lines of these bands cannot be seen, of course, but they doubtless are responsible for slight displacements of observed maxima, making the residuals larger than they would otherwise be.

The band at 7.78μ, Fig. 1C was analysed with a 7″×9″ grating having 2400 lines per inch. The slit widths were 0.20 mm equivalent to about 0.27 cm^{-1}, and observations were made at intervals of 0.20 cm^{-1}. There is no zero branch, although a very weak line appears at the center, probably belonging to one of the bands originating in molecules already excited to the first vibration state of ν_2. The positive and negative branches have almost exactly the same spacing as in the lower frequency band, but there is some convergence toward smaller wave-lengths. The positions of the lines are given in Table II,

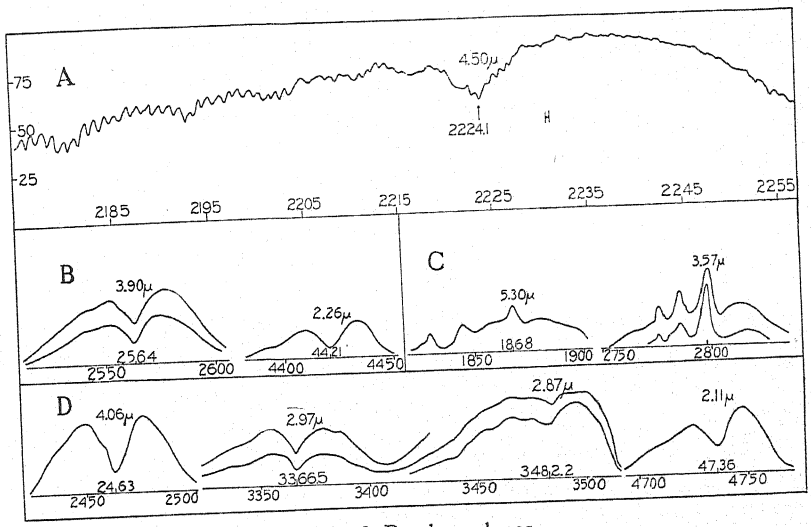


Fig. 2. Band envelopes.

A. The fundamental ν_3, partially resolved.
B. The harmonics $2\nu_1$ at 3.90μ and $2\nu_3$ at 2.26μ.
C. Combination bands $\nu_1+\nu_2$ at 5.30μ and $\nu_2+\nu_3$ at 3.57μ.
D. Combination bands $\nu_1+2\nu_2$ at 4.06μ, $2\nu_2+\nu_3$ at 2.97μ, $\nu_1+\nu_3$ at 2.87μ and $2\nu_1+\nu_3$ at 2.11μ.

together with the residuals (computed values minus observed values) obtained from the equation

$$\nu_1 = 1285.37 \pm 0.837m - 0.0017m^2. \qquad (2)$$

Although ν_1 and ν_2 are vibrations of essentially different character, the coefficients of the linear terms in both Eqs. (1) and (2) are practically equal, the corresponding difference in moment of inertia being no greater than would be expected as a result of deformations involved in the vibrations themselves. If the molecule had been in the form of a triangle with one atom at each vertex, thus constituting an asymmetrical rotator, the rotation lines would have been very irregular both in spacing and intensity: or, as a special case, the

rotator might have been symmetrical, with moments of inertia $A=B=C/2$, but none of the bands would then exhibit a single strong zero branch as ν_2 does here, for no change in electric moment parallel to the symmetry axis could occur.

The third fundamental band lies at 4.50μ. It has been mapped with a grating having 7200 lines per inch and is shown in Fig 2A. The slit included 0.33 cm^{-1}. Although many trials were made to determine the optimum conditions for resolution, no clear cut rotation series could be obtained. From certain sections of the band it is evident that the line spacing is the same as in the other fundamentals, but the envelope shows a scalloped appearance for all gas pressures, indicating superposed bands of appreciable intensity. As before, these are probably due to absorption by molecules already vibrating in the lowest frequency mode. The interaction between ν_2 and ν_3 is apparently large, so that the maximum of the positive branch for the first upper stage band falls very near the center of the primary band, which is so obscured that an accurate determination os its position is impossible. The fact that the 7.8μ band is not so distorted indicates relatively less interaction between ν_1 and ν_2. The frequency indicated as the center, 2224.1 cm^{-1}, is that of the lowest point of this portion of the curve.

The relative intensities of the fundamentals ν_2 (17.0μ), ν_1 (7.8μ), and ν_3 (4.5μ) may be estimated as approximately 4:7:10.

The Harmonic and Combination Bands

The harmonic of the 17.0μ band, located at 8.6μ, is shown in Fig. 1B, as mapped with the 2400 line grating. If the molecule were linear and symmetrical this transition would yield zero intensity of absorption;[6] if linear but unsymmetrical the component of the electric moment normal to the axis would still remain constant, but there would be a varying component along the axis, giving rise to a band with positive and negative branches but no zero branch. This is exactly as observed. The line spacing is about 0.84 cm^{-1} as before, and the intensity is about one fifth as great as that of the fundamental. The observed wave numbers shown in Table III are fairly well represented by the equation

$$\nu = 1167.31 \pm 0.835m + 0.0009m^2. \quad (3)$$

Beginning from the first excited state only one absorption band occurs in this region, instead of two as in the fundamental. It corresponds to the double transition $1_{\pm 1} \rightarrow 3_{\pm 1}$, but the suppression of the zero branch makes its position difficult to determine. The fact that the depressions between the lines are not nearly so marked as in the neighboring band at 7.8μ, indicates the disturbing effect of this superposition, which probably also explains the large residuals for small values of m.

Harmonics of the other two fundamentals are shown in Fig. 2B without high resolution. These are doublets, as would be expected. Six combination bands have been observed in the same manner. Of these two involve the fundamental transition in ν_2, and exhibit zero branches (λ5.3 and λ3.57, Fig. 2C)

TABLE III. *Observed frequencies for the harmonic $2\nu_2$ at 8.60μ, and residuals from the computed values.*

Positive branch wave numbers	residuals	m	*Negative branch* wave numbers	residuals
1167.8	+.34	1	1166.4	+.08
8.8	+.18	2	5.5	+.14
9.7	+.12	3	4.6	+.22
70.7	−.03	4	4.0	−.01
1.4	+.11	5	3.1	+.07
2.2	+.15	6	2.3	+.03
3.2	.00	7	1.6	−.06
4.0	+.05	8	0.7	−.01
4.9	−.01	9	59.9	−.03
5.8	−.05	10	9.1	−.05
6.7	−.05	11	8.3	−.05
7.5	−.04	12	7.4	+.02
8.4	−.09	13	6.6	+.01
9.2	−.03	14	5.8	−.01
80.0	+.04	15	5.0	.00
0.9	.00	16	4.2	−.02
1.8	−.04	17	3.3	+.08
2.7	−.06	18	2.6	−.04
3.6	−.11	19	1.8	−.03
4.4	−.03	20	1.0	−.03
5.3	−.13	21	0.2	−.02
6.1	−.04	22	49.5	−.05
7.0	−.06	23	8.7	−.11
7.9	−.03	24	8.0	−.18
8.7	+.03	25	7.1	−.09
9.6	+.03	26	6.3	−.09
90.5	+.02	27	5.4	+.02
1.4	+.03	28	4.7	−.09
2.3	+.03	29	4.0	+.02
3.2	+.04	30	3.1	−.03
4.1	−.05	31	2.2	+.09
4.9	+.05	32	1.5	+.01
5.8	+.04	33	0.7	+.04
6.7	+.04	34	0.0	−.04
7.6	+.04	35	39.2	.00
8.5	+.03	36		
9.3	+.13	37		
1200.3	+.06	38		
1.1	+.14	39		
2.1	+.05	40		
3.0	+.06	41		

while two others involve the first harmonic of ν_2 and are doublets (λ4.05 and λ2.97, Fig. 2D). The zero branch bands each show three maxima corresponding to transitions $0_0 \rightarrow 1_1$, $1_1 \rightarrow 2_0$, and $1_1 \rightarrow 2_2$ for the ν_2 component.

The positions and approximate intensities for all of the observed bands are assembled in Table IV, with the assigned interpretations indicated. From the equation given by Dennison* for the positions of the various vibration levels it is possible to determine in first approximation the anharmonic correction terms. Aside from a common constant the levels are given in frequency units by the expression

$$V_1\nu_1 + V_2\nu_2 + V_3\nu_3 + x_{11}V_1^2 + x_{22}(V_2^2 - \tfrac{1}{3}l^2) + x_{33}V_3^2 + x_{12}V_1V_2 + x_{13}V_1V_3 + x_{23}V_2V_3$$

* Reference 6, p. 296. Although written for the linear symmetrical molecule, this equation is equally applicable to the unsymmetrical group of three colinear atoms, as may easily be seen.

TABLE IV. *Positions and relative intensities of observed bands.*

	λ	ν (obs.)	int.	ν^0	transition in V_2
ν_2	17.0	579.5	4		$1_1 \rightarrow 2_2$
		589.0	40	593.0	$0_0 \rightarrow 1_1$
		590.5	4		$1_1 \rightarrow 2_0$
ν_1	7.78	1285.4	70	1288.7	
ν_3	4.50	2224.1	100	2237.9	
$2\nu_2$	8.60	1167.3	20		
$2\nu_1$	3.90	2564.2	16		
$2\nu_3$	2.26	4420.7	2		
$\nu_1+\nu_2$	5.30	1868.0	0.5		$0_0 \rightarrow 1_1$
		1845	0.1		$1_1 \rightarrow 2_2$
		1829	0.1		$1_1 \rightarrow 2_0$
$\nu_1+2\nu_2$	4.06	2462.2	6		
$\nu_2+\nu_3$	3.57	2799.1	1.2		$0_0 \rightarrow 1_1$
		2786	0.3		1_1+2_2
		2777	0.3		1_1+2_0
$2\nu_2+\nu_3$	2.97	3366.5	1.6		
$\nu_1+\nu_3$	2.87	3482.2	10		
$2\nu_1+\nu_3$	2.11	4736.0	0.8		

where l measures angular momentum about the axis, in units of $h/2\pi$. By taking differences between the appropriate expressions of this sort for different observed bands, sets of equations are obtained from which the values of the x's may be determined, and hence the frequencies ν^0 corresponding to infinitesimal amplitudes. Table V shows the values of these coefficients, with the transitions from which they are obtained. The values of ν^0 appear in

TABLE V. *Anharmonic correction coefficients.*

coefficient	value	transitions employed
x_{11}	−3.3	$(0\rightarrow 2)V_1-(0\rightarrow 1)V_1$
x_{22}	−4.0	$(0_2\rightarrow 2_0)V_2-(0_0\rightarrow 1_1)V_2$
	−4.0	$(1_1\rightarrow 2_0)V_2$
	−1.25	$(1_1\rightarrow 2_2)V_2$
x_{33}	−13.8	$(0\rightarrow 2)V_3-(0\rightarrow 1)V_3$
x_{12}	−7.7	$(0\rightarrow 1)V_1+(0_0\rightarrow 1_1)V_2$
	−6.3	$(0\rightarrow 1)V_1+(0_0\rightarrow 2_0)V_2$
	−15.4	$(0\rightarrow 1)V_1+(1_1\rightarrow 2_2)V_2$
	−10.0	$(0\rightarrow 1)V_1+(1_1\rightarrow 2_0)V_2$
x_{13}	−27.3	$(0\rightarrow 1)V_1+(0\rightarrow 1)V_3$
	−26.1	$(0\rightarrow 2)V_1+(0\rightarrow 1)V_3$
x_{23}	−14.0	$(0_0\rightarrow 1_1)V_2+(0\rightarrow 1)V_3$
	−14.3	$(1_1\rightarrow 2_2)V_2+(0\rightarrow 1)V_3$
	−13.3	$(1_1\rightarrow 2_0)V_2+(0\rightarrow 1)V_3$
	−12.5	$(0_0\rightarrow 2_0)V_2+(0\rightarrow 1)V_3$

Table IV, column 5. The above expression is, of course, a first approximation only: with our interpretation of the bands it gives consistent values whenever l is not greater than unity. It does not, however, fit very well the assignments $(2_2\rightarrow 1_1)V_2=590.5$ and $(1\rightarrow 0)V_1+(2_2\rightarrow 1_1)V_2=1845$.

Form of the Molecule

The considerations bearing upon the question of geometric arrangement of the atoms in the molecule of N_2O may be summarized as follows: (1) The observed bands are of two types, one with an intense zero branch and one without, but in each case the rotation lines of the positive and negative branches form simple series with the same spacing. This excludes the possibility of a triangular configuration, which would result either in an asymmetrical rotator with very irregular lines, or in a symmetrical rotator with two different line spacings. (2) The moment of inertia as computed from the fine structure using the formula $B=h/4\pi^2I$, is 59.4×10^{-40}, which is of the same order of magnitude as the value obtained from the doublet differences of the band envelopes. This doublet difference is practically the same in all bands and averages 29 cm^{-1}, corresponding to $I=55\times10^{-40}$, a value somewhat smaller than the previous one because of slight broadening of the bands due to the large proportion of the molecules already excited vibrationally at room temperature. This numerical agreement also indicates the linear arrangement of atoms in the molecule. (3). The uniformly varying intensities in fine structure lines indicates that the molecule is not of the form N–O–N, since nuclear spin in the N atoms would then lead to alternating intensities, as in the bands of N_2. (4) The absence of any restriction upon vibrational transitions also excludes the possibility of the symmetrical arrangement. All combinations of ΔV_1, ΔV_2 and ΔV_3 appear, with zero branches only when ΔV_2 is odd. (5) The variation of specific heat with temperature is a further indication that the molecule is linear. Snow has kindly informed us that his computations using our three fundamental frequencies reproduce the specific heat curve very accurately.

A very rough comparison of the relative strengths of the two chemical bonds may be obtained by assuming infinitesimal harmonic vibrations as of mass points fastened together by two weightless springs, and vibrating along the line of centers. Let the force constants be K_1 and K_2 for the N–N and the N–O linkages respectively, the interaction between the two extreme atoms being neglected. From the character and the frequencies (ν_1 and ν_3) of the two normal vibrations, and the known masses of the atoms, it follows at once that $K_1=2.4\times10^6$ and $K_2=2.2\times10^6$ dynes/cm.

Raman Lines

The observed Raman spectrum of N_2O consists of a single line[8] at 1281 cm^{-1}, in fairly good agreement with our value for ν_1. For linear molecules ν_2 would not appear in the Raman scattering, due to the symmetry of the vibration.[9] Neither would ν_3 appear if the configuration were symmetrical. However, it should be observed, though possibly with low intensity, for the unsymmetrical arrangement indicated above.

[8] Dickinson, Dillon and Rasetti, Phys. Rev. **34**, 582 (1929).

[9] Placzek, Zeits. f. Physik **70**, 84 (1931).

Permanent Electric Moment

The electric moment of N_2O is apparently very small[10] which at first glance seems to favor the hypothesis of a symmetrical molecule. It is probably not zero, however. In the absence of definite information concerning the electron distribution and the interatomic distances, it is impossible to estimate precisely what value would be expected for an unsymmetrical linear configuration. It is clear, however, that the position of the electrical center for the positive nuclei is very sensitive to changes in the relative distances from central to extreme atoms, and it might happen to fall very close to the corresponding center for the electron shell. Hence our model is not necessarily inconsistent with the observed dipole value.

[10] Braunmuhl, Phys. Zeits. **28**, 141 (1927).

THE RAMAN EFFECT IN CERTAIN ORGANIC COMPOUNDS

By M. E. High
Mendenhall Laboratory of Physics, Ohio State University

(Received August 31, 1931)

Abstract

The Raman spectra of the normal and iso forms of propyl ether, amyl ether, propyl propionate, butyl propionate, amyl propionate, and also methyl propionate have been measured. Certain characteristic frequencies remain unchanged throughout the series but other frequencies which appear singly in the normal forms are split into several frequencies in the iso forms, due to the rearrangement of the atomic groups. The Raman spectra have also been observed in the ortho, meta and para forms of chlorotoluene, cresyl methyl ether, nitrochlorobenzene and nitrotoluene. In addition to the characteristic frequencies which remain unchanged there are certain frequencies which consistently increase from the ortho to meta to para forms. Similar increases are noted in the infrared absorption spectra of the xylenes.

Introduction

DATA on the incoherent scattering of light, as first observed by Raman,[1] should give important information about the different modes of vibration and rotation of molecules and the energies associated with each of these modes of vibration and rotation. Hence a study of the Raman effect in organic molecules gives a means of advancing our knowledge of these molecules. Dadieu and Kohlrausch[2] and others have already shown that certain atomic groupings in organic molecules are definitely associated with frequency shifts observed in the Raman effect.

It is the purpose of this investigation to compare the Raman effect in certain normal forms of organic compounds with the Raman effect in the iso forms of these same compounds and to investigate the influence on the Raman effect of shifting the substituents from the ortho to the meta and to the para position in organic compounds.

Experimental

The design of the apparatus used follows that suggested by Wood[3] and modified by Morris,[4] except that four mercury arcs were used instead of one. The arcs were vertical, as was also the tube which contained the substance to be examined. The scattered light, after passing through a totally reflecting prism was focused on the slit of the spectrograph. The tube containing the liquid was about 25 mm in diameter and 12 cm long. A blast of air kept the liquid and the arcs cool. The spectrograph was a specially constructed, high-speed instrument, with lenses of 6 inch focal length and 2.5 inch aperture. There were two 60 degree glass prisms with faces 2.5 by 4 inches.

[1] Raman, Ind. J. Phys. **2**, 387 (1928).
[2] Dadieu and Kohlrausch, Ber. **63**, 251 (1930); J. O. S. A. **21**, 286 (1931).
[3] Wood, Phil. Mag. **6**, 729 (1928).
[4] Morris, Phys. Rev. **38**, 141 (1931).

TABLE I.

Substance Formula	$\Delta\nu$	$\Delta\nu$	$\Delta\nu$	$\Delta\nu$	$\Delta\nu$	$\Delta\nu$	$\Delta\nu$
n-propyl ether C_3H_7–O–C_3H_7	874(2) (ea)	1091(2) (ade)	1282(3) (ae)	1446(4) (ae)	2864(3) (adeg)	2931(3) (egh)	
iso-propyl ether $(CH_3)_2CH$–O–$CH(CH_3)_2$	791(6) (ade)	848(2) (ae)	903(5) (ae)	930(1) (de)	1453(8) (ae)	2872(9) (ef)	2916(2) (afh)
n-amyl ether CH_{11}–O–C_5H_{11}	764(2) (ae)	1292(4) (ae)	1447(7) (ae)	2853(5) (ae)	2904(5) (aeh)	2957(5) (aegh)	
iso-amyl ether $(CH_3)_4(CH)_2(CH_3)_4O$	765(4) (ae)	815(1) (ade)	908(1) (ae)	950(3) (ade)	1144(4) (ade)	1449(9) (ae)	2862(7) (ae)
n-propyl n-propionate C_2H_5–COO–C_3H_7	490(1) (ae)	889(1) (ade)	1033(2) (de)	1076(1) (de)	1450(9) (ae)	1735(4) (a)	2874(6) (defg)
iso-propyl propionate C_2H_5–COO–$CH(CH_3)_2$	431(5) (ade)	482(2) (ae)	597(5) (ae)	825(8) (ade)	875(3) (ade)	926(8) (ae)	1109(2) (ae)
n-butyl propionate C_2H_5–COO–C_4H_9	281(5) (ae)	1288(3) (ae)	1450(8) (ae)	1737(5) (a)	2917(band) (aeh)		
iso-butyl propionate C_2H_5–COO–$CH_2CH(CH_3)_2$	282(5) (ae)	821(3) (ae)	889(2) (ae)	1456(7) (ae)	1737(4) (a)	2920(band) (aeh)	
n-amyl propionate C_2H_5–COO–C_5H_{11}	956(4) (ae)	1080(2) (ae)	1292(3) (ae)	1446(8) (ae)	1732(4) (a)	2918(band) (aeh)	
iso-amyl propionate C_2H_5–COO–$(CH_3)_2CH(CH_3)_2$	770(2) (ae)	822(3) (ae)	1449(7) (ae)	1731(3) (a)	2910(band) (aeh)		
methyl propionate C_2H_5–COO–CH_3	435(4) (ae)	593(2) (ae)	838(7) (ade)	1072(3) (ae)	1442(4) (ae)	1735(4) (a)	2941(5) (aegh)
o-chlorotoluene C_6H_4–Cl–CH_3	160(8) (a)	*246*(7) (a)	356(4) (a)	442(6) (a)	543(9) (a)	673(9) (a)	797(7) (ab)
m-chlorotoluene C_6H_4–Cl–CH_3	*186*(3) (ae)	*233*(3) (ae)	414(5) (ae)	515(6) (ae)	682(7) (ade)	995(10) (ae)	1081(4) (ae)
p-chlorotoluene C_6H_4–Cl–CH_3	*304*(3) (ae)	373(4) (ad)	631(5) (ade)	794(10) (ade)	1085(8) (ade)	1205(5) (ae)	1378(2) (ae)
o-cresyl methyl ether C_6H_4–CH_3–OCH_3	*174*(4) (ae)	*235*(2) (ae)	491(6) (ae)	580(4) (ae)	743(9) (ade)	982(0) (ae)	1044(7) (ae)
m-cresyl methyl ether C_6H_4–CH_3–OCH_3	209(2) (a)	284(1) (a)	457(2) (a)	721(4) (ae)	784(4) (ae)	995(6) (a)	1271(4) (a)
p-cresyl methyl ether C_6H_4–CH_3–OCH_3	233(2) (ae)	334(4) (ae)	415(5) (ae)	515(5) (ade)	637(5) (de)	814(10) (ade)	1175(4) (de)
For the remaining compounds all Raman lines were excited by Hg 4358							
o-nitrochlorobenzene C_6H_4–NO_2–Cl	147(3)	470(2)	665(3)	749(3)	874(3)	1057(7)	1160(8)
m-nitrochlorobenzene $C_6H_4NO_2$–Cl	178(2)	670(3)	896(1)	1014(5)	1143(5)	1369(10)	1604(5)
p-nitrochlorobenzene C_6H_4–NO_2–Cl	217(1)	366(0)	401(1)	635(3)	859(3)	1122(8)	1360(10)
o-nitrotoluene C_6H_4–NO_2–CH_3	150(3)	555(4)	673(1)	1062(4)	1098(1)	1167(2)	1214(3)
m-nitrotoluene C_6H_4–NO_2–CH_3	1011(2)	1103(2)	1231(2)	1364(10)	1602(3)	2920(0)	3057(2)
p-nitrotoluene C_6H_4–NO_2–CH_3	281(2)	643(3)	682(1)	806(2)	869(5)	1117(8)	1217(3)

TABLE I. (*Cont.*)

Substance Formula	$\Delta\nu$	$\Delta\nu$	$\Delta\nu$	$\Delta\nu$	$\Delta\nu$	$\Delta\nu$	$\Delta\nu$
n-propyl ether C_3H_7–O–C_3H_7							
iso-propyl ether $(CH_3)_2CH$–O–$CH(CH_3)_2$	2929(9) (deh)	2975(9) (adefh)	3073(1) (fh)				
n-amyl ether C_5H_{11}–O–C_5H_{11}							
iso-amyl ether $(CH_3)_4(CH)_2(CH_2)_4O$	2906(7) (aeh)	2958(7) (aegh)	3145($\frac{1}{2}$) (ef)				
n-propyl n-propionate C_2H_5–COO–C_3H_7	2933(9) (aeh)	2975(4) (eh)					
iso-propyl propionate C_2H_5–COO–$CH(CH_3)_2$	1138(1) (de)	1172(2) (ae)	1456(9) (ae)	1737(7) (a)	2933(7) (aeh)	2980(7) (afh)	3115(1) (ah)
n-butyl propionate C_2H_5–COO–C_4H_9							
iso-butyl propionate C_2H_5–COO–$CH_2CH(CH_3)_2$							
n-amyl propionate C_2H_5–COO–C_5H_{11}							
iso-amyl propionate C_2H_5–COO–$(CH_2)_2CH(CH_3)_2$							
methyl propionate C_2H_5–COO–CH_3							
o-chlorotoluene C_6H_4–Cl–CH_3	1041(10) (abe)	1201(4) (ae)	1379(3) (ae)	1592(8) (ae)	2914(6) (ae)	3056(8) (ae)	
m-chlorotoluene C_6H_4–Cl–CH_3	1208(4) (ae)	1369(2) (ae)	1581(3) (ae)	2920(4) (ae)	3057(7) (aegh)		
p-chlorotoluene C_6H_4–Cl–CH_3	1596(6) (ae)	2921(2) (aeh)	3059(5) (adefg)				
o-cresyl methyl ether C_6H_4–CH_3–OCH_3	1156(4) (ae)	1185(2) (de)	1236(7) (ade)	1296(5) (ae)	1441(2) (ae)	1595(7) (ae)	2909(2) (af)
m-cresyl methyl ether C_6H_4–CH_3–OCH_3	1445(4) (a)	1613(5) (a)	2920(5) (a)				
p-cresyl methyl ether C_6H_4–CH_3–OCH_3	1207(3) (ae)	1287(5) (ae)	1370(1) (ae)	1448(4) (ae)	1605(4) (ae)	2917(2) (aefgh)	
For the remaining compounds all Raman lines were excited by Hg 4358							
o-nitrochlorobenzene C_6H_4–NO_2–Cl	1374(10)	1604(5)	3052(2)				
m-nitrochlorobenzene C_6H_4–NO_2–Cl	3055(2)						
p-nitrochlorobenzene C_6H_4–NO_2–Cl	1604(6)	3054(3)					
o-nitrotoluene C_6H_4–NO_2–CH_3	1360(10)	1592(4)	2918(1)	3051(2)			
m-nitrotoluene C_6H_4–NO_2–CH_3							
p-nitrotoluene C_6H_4–NO_2–CH_3	1360(10)	1613(7)	2915(1)	3053(3)			

Results

In Table I data are given for the compounds studied. The frequency shifts are given in wave numbers. If a frequency is *underscored* it means that that frequency appeared as an anti-Stokes line as well as a Stokes line. The number in parenthesis after each frequency is the intensity, estimated visually from the plates. The letters in parenthesis following the intensity indicate the mercury lines which gave rise to a Raman line corresponding to the particular frequency. The letters signify mercury lines as follows:

	Wave-length in A.U.	Wave number in cm^{-1}		Wave-length in A.U.	Wave number in cm^{-1}
a	4358	22938	e	4047	24705
b	4348	22994	f	3663	27290
c	4339	23038	g	3654	27354
d	4078	24516	h	3650	27388

Discussion of Results

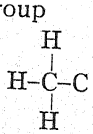
There are certain frequencies which remain unchanged throughout each of the series. These are the frequencies which are defined by Dadieu and Kohlrausch[2] as "inner" frequencies, and are due to molecular configurations which are present in each molecule. The vibration, which occurs in this configuration, is, therefore, very little affected by the remaining part of the molecule.

In the ethers and propionates under consideration, one of these constant frequencies is about 1450 cm^{-1}. This frequency has been assigned by Dadieu and Kohlrausch[2] and by Trumpy to the vibration of the group.



which occurs in each of the compounds. The C–H bond ordinarily gives frequencies in the neighborhood of 3000 cm^{-1}. That the CH_2 group can produce such a low frequency as 1450 cm^{-1} is explained by Dadieu and Kohlrausch by assuming that the hydrogen atoms vibrate at right angles to the direction of the linkage.

Another frequency, common to all the propionates, is 1735 cm^{-1}, approximately. Dadieu and Kohlrausch[2] have assigned this frequency to the C=O bond. The frequencies 2865 and 2929 cm^{-1} have been assigned by Dadieu and Kohlrausch to vibration of the group



and the frequency 2967 cm^{-1} to the linkage type



In the amyl and butyl propionates these three frequencies are not resolved but appear as a band.

TABLE II.

Substance	H –C– H	C=O	H H C–C H		H X–C–X H	NO_2	C=C	C–H ali-phatic	C–H aro-matic
n-propyl ether	1446	—	2864	2931	—	—	—	—	—
iso-propyl ether	1453	—	2872	2929	2975	—	—	—	—
n-amyl ether	1447	—	2853	—	2957	—	—	—	—
iso-amyl ether	1449	—	2862	—	2958	—	—	—	—
n-propyl propionate	1450	1737	2874	2933	2975	—	—	—	—
iso-propyl propionate	1456	1737	—	2937	2980	—	—	—	—
n-amyl propionate	1446	1732	—	—	—	—	—	—	—
iso-amyl propionate	1449	1731	—	—	—	—	—	—	—
n-butyl propionate	1450	1737	—	—	—	—	—	—	—
iso-butyl propionate	1456	1737	—	—	—	—	—	—	—
methyl propionate	1442	1735	—	2941	—	—	—	—	—
o-chlorotoluene	—	—	—	—	—	—	1592	2914	3056
m-chlorotoluene	—	—	—	—	—	—	1581	2920	3057
p-chlorotoluene	—	—	—	—	—	—	1596	2921	3059
o-dichlorobenzene*	—	—	—	—	—	—	1569	—	3066
m-dichlorobenzene*	—	—	—	—	—	—	1575	—	3072
p-dichlorobenzene*	—	—	—	—	—	—	1572	—	3061
o-xylene*	—	—	—	—	—	—	1594	2916	3043
m-xylene*	—	—	—	—	—	—	1597	2917	3042
p-xylene*	—	—	—	—	—	—	1618	2917	3040
o-cresyl methyl ether	—	—	—	—	—	—	1595	2909	—
m-cresyl methyl ether	—	—	—	—	—	—	1613	2920	—
p-cresyl methyl ether	—	—	—	—	—	—	1605	2917	—
o-nitrochlorobenzene	—	—	—	—	—	1374	1604	—	3052
m-nitrochlorobenzene	—	—	—	—	—	1369	1604	—	3055
p-nitrochlorobenzene	—	—	—	—	—	1360	1604	—	3054
o-nitrotoluene	—	—	—	—	—	1360	1592	2918	3051
m-nitrotoluene	—	—	—	—	—	1364	1602	2920	3057
p-nitrotoluene	—	—	—	—	—	1360	1613	2915	3053
Average Values	1450	1735	2865	2932	2969	1364	1590	2918	3054

* From Dadieu and Kohlrausch, J.O.S.A. **21,** 286 (1931).

In the ortho, meta and para group there is a frequency 3050 cm^{-1} which is present in each substance except cresyl methyl ether and which has been assigned by Dadieu and Kohlrausch[2] to the aromatic C–H bond. They have assigned the frequency 2918 cm^{-1} to the aliphatic C–H bond and the frequency 1600 cm^{-1} to the C=C bond. Ganesan and Venkateswaran,[6] as well as Dadieu and Kohlrausch, have assigned the frequency 1364 cm^{-1} to the nitro group, NO_2.

Comparison of normal and iso forms

The molecules of the normal forms of ethers and propionates are supposed to consist of chains and in the iso forms these chains are split at one or both ends. Any difference in the Raman spectra ought to be explained, therefore, in terms of this rearrangement of the parts of the molecules.

In n-propyl ether there is a frequency 874 cm^{-1} which may be due to vibration of the group CH_3-CH_2. In the iso form this frequency is split into four frequencies: 791, 848, 903 and 930 cm^{-1}. This splitting must come from

[5] Trumpy, Zeits. f. Physik **62,** 806 (1930).

[6] Ganesan and Venkateswaran, Ind. J. Phys. **4,** 195 (1929).

the rearrangement of the groups in the split chain. A possible source of these frequencies is the group

$$\begin{matrix} CH_3 \\ CH_3 \end{matrix} > CH$$

This more complex arrangement would be expected to have a greater number of possible vibration frequencies than the simpler group CH_3-CH_2. There is also a corresponding increase in the number of frequencies in the iso form as compared to the normal form in amyl ether and propyl propionate. (Fig. 1.) The results for amyl and butyl propionate are not satisfactory because of the large amount of continuous spectrum and the weakness of the lines.

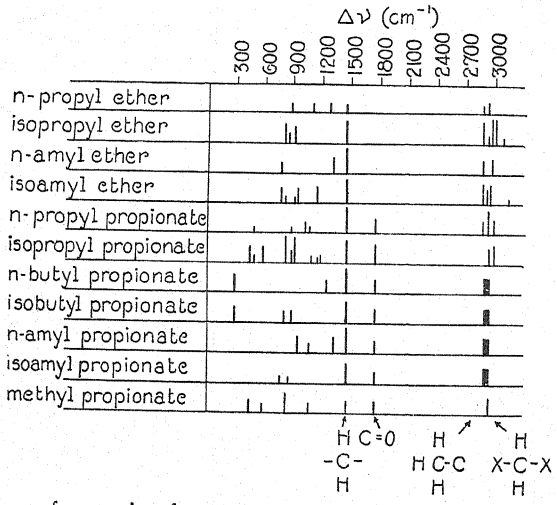


Fig. 1. Raman frequencies of normal and iso forms, showing the more complex spectra of the iso forms.

Comparison of ortho, meta and para forms

In these compounds there is a large number of frequencies, between approximately 150 and 1300 cm^{-1}, which have not been assigned to a particular vibrator. While these frequencies do not remain constant from one compound to another, yet there is a regularity in the shifts of some of them. (Fig. 2). In each case the smallest, and usually the two smallest frequencies increase progressively from the ortho to the para forms of the compound. But in addition to these smallest frequencies there are larger frequencies which have this same regular increase. Fig. 3 shows the frequencies which thus shift.

It is important to notice that these same shifts occur in the infrared spectra of ortho, meta and para-xylene. Coblentz[7] calls attention to the regular shifting of two infrared bands in o, m and p-xylene. These two bands, at about 9.7 and 13.4 μ are shown in Fig. 3 under *infrared*. It will be seen from Fig. 3 that there is a Raman frequency which corresponds to each of these particular infrared frequencies. (The dotted Raman frequencies were not observed by Dadieu and Kohlrausch). There are also two additional Raman frequencies

[7] Coblentz, "Investigations of Infrared Spectra," Carnegie Institution of Washington Publication 35 (1905).

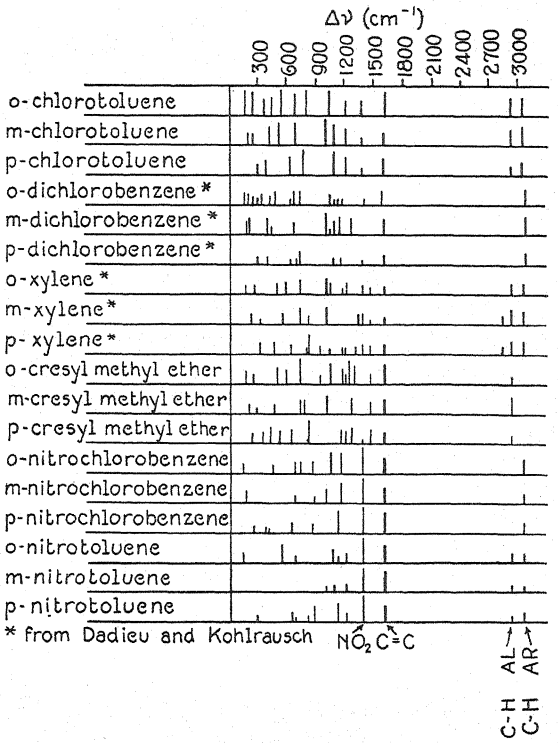


Fig. 2. Raman frequencies of ortho, meta and para forms, showing characteristic frequencies and shifting of certain other frequencies.

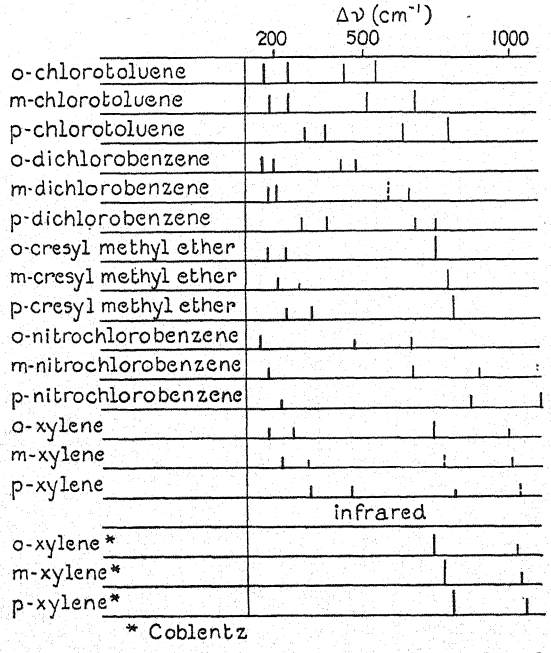


Fig. 3. Increase in frequencies from ortho to meta to para forms.

which show the same sort of shift but which lie outside the region studied by Coblentz. For xylene, then, the Raman spectra show the same shifts which occur in the infrared spectra, but in addition the Raman spectra show this same sort of shift in other frequencies which have not yet been observed by infrared methods.

In Fig. 3 the frequencies which show shifts similar to those of the xylene frequencies are plotted. Nitrotoluene is not included because of the failure to observe the smaller frequencies in m-nitrotoluene.

Comparison with infrared data

A comparison between the Raman spectrum and infrared spectrum of a substance shows in general that there are certain frequencies common to both spectra and other frequencies which appear only in the Raman spectrum or only in the infrared spectrum. In Table III the wave-lengths common to both

TABLE III.

	Wave-length in μ			Wave-length in μ	
Substance	Raman	Infrared*	Substance	Raman	Infrared**
o-nitrotoluene	3.43 6.26 7.35 8.56 9.4	3.42 6.25 7.5 8.4 9.36	methyl propionate	3.40 5.76 6.94 9.3 12.0	3.4 5.8 6.9 9.2 11.9
p-nitrotoluene	3.28 3.43 7.35 8.88	3.23 3.43 7.5 8.65	iso-amyl propionate	5.76 6.94 12.2 13.0	5.9 7.0 12.5 13.1

* Coblentz, "Investigations of Infrared Spectra," Carnegie Institution of Washington Publication 35 (1905).

** Weniger, Phys. Rev. **31**, 388 (1910).

spectra are given for the four compounds for which infrared data were available. There are other frequencies in each spectrum which are found only in that spectrum. These results are in accord with the theoretical treatment of Ganesan and Venkateswaran.[6] They have pointed out that an infrared absorption band involves only two energy levels and a transition must be permissible between these two levels, while a Raman frequency involves three levels, the initial and final and a third level. Hence the presence of an infrared band depends on the possibility of a transition between two given levels, while the occurrence of a Raman frequency depends on the presence of a suitable third level, and these two conditions may be quite independent.

Continuous spectrum

Every Raman spectrum contains a certain amount of continuous background. One method for removing most of this continuous background in certain cases has been reported in the Physical Review **38,** 374 (1931).

In conclusion the author wishes to express his appreciation to Professor Alpheus W. Smith for suggesting the problem and for his advice and assistance in the work. He is also indebted to Dr. M. L. Pool for valuable suggestions and criticism throughout the course of the work.

THE RAMAN EFFECT AND THE CARBON-HALOGEN BOND

By William D. Harkins and Harold E. Bowers
George Herbert Jones Chemical Laboratory,
University of Chicago

(Received September 14, 1931)

Abstract

By far the most intense line in the Raman spectra of (organic) aliphatic bromides exhibits a Raman wave number ($\Delta\bar{\nu}$) of about 600 cm^{-1} in the methyl derivative, of 564 cm^{-1} if from two to five carbon atoms are present in the normal chain, and of about 539 cm^{-1} if the chain is branched sufficiently close to the bromine atom. These frequencies are the most characteristic of the carbon-bromine bond. It is assumed that these Raman lines, and the corresponding most intense lines in the spectra of the chlorides and of the iodides, are produced by a decrease (or increase in anti-stokes lines) by unity in the vibrational quantum number. On the basis of this assumption the use in the calculations of this paper of only the first term in the brackets of the more general equation

$$\epsilon^v = hc[\overline{w}_e(v+\tfrac{1}{2}) - x_2(v+\tfrac{1}{2})^2 + \cdots]$$

may be considered to give only a small error, possibly of the order of one percent. Here w is the wave number, but the w used elsewhere in this paper gives the frequency, since for simplicity it includes the hc term. Although the fundamental frequency associated with the carbon-halogen bond in normal aliphatic compounds decreases by about 8 percent if the number of carbon atoms in the molecule is increased from one to two, a further increase in the length of the molecule up to 5 carbon atoms does not give any further decrease; that is, the frequency is independent of the length of the molecule. The fundamental frequencies which for the methyl halides are associated with this bond are 2.13×10^{13} for the chloride, 1.81×10^{13} for the bromide, and 1.60×10^{13} per second for the iodide. The value 1.81×10^{13} for the bromide with one carbon atom, is reduced to 1.69×10^{13} if three, four or five carbon atoms are present in the molecule. If it is assumed that the mechanical frequency (w_0) is, for a value of $\Delta v = \pm 1$, related approximately by the equation

$$\Delta\nu = w_0(v'-v'') = \frac{1}{2\pi}\left(\frac{f}{\mu}\right)^{1/2}(v'-v'')$$

to the Raman frequency ($\Delta\epsilon$) which is associated with this bond, then the vibration of the bromine atom with respect to the adjacent part of the hydrocarbon chain, has a frequency which is independent of the length of the molecule, provided more than one carbon atom is present. The conclusion from these results is that the force constant which corresponds to the carbon-bromine bond, and therefore, presumably, the strength of the bond, either remains constant, or else increases only slightly as the length of the molecule increases. However, the force constant for methyl halides may be appreciably higher than those for the longer chain compounds. This indicates that the characteristic frequency of this bond corresponds to an inner vibration: that is, in general only a part of the rest of the organic molecule vibrates with respect to the halogen atom to give this frequency. The force constant characteristic of the carbon-halogen bond is found to have, for the methyl halides, values of about 3.0 for the chloride, 2.6 for the bromide, and 2.2×10^{-5} dynes per cm for the iodide. Thus the values decrease in the same order as the corresponding heats of dissociation. The values are much less than that (5×10^{-5} dynes per cm) previously found for single bonds (C:C, C·O, and C·N) in organic compounds. Another frequency, about 53

percent of that more distinctly characteristic, and with a value of about 300 cm^{-1} for the wave number, seems to be also associated with carbon-bromine bond, possibly with some type of transverse vibration. A not too distant branching of the chain of the aliphatic hydrocarbon causes a decrease of about 5 percent in the characteristic frequency associated with the carbon-bromine bond, and probably indicates a decrease in the strength of the bond. The value 1638 cm^{-1} is obtained for the wave number which is associated with the double bond of allyl bromide, while Dadieu and Kahlausch obtain 1639 cm^{-1} for the chloride and 1645 cm^{-1} for the alcohol. This illustrates the smallness of the effect of the change of mass of the substituted group upon the frequency at the double bond, which seems to indicate an inner and not an outer vibration. Experimental data are presented for the Raman spectra of nine (organic) aliphatic bromides. The spectra were taken by a large three prism Steinheil G.H. glass spectrograph, by the use of two constricted quartz mercury arcs. The ultraviolet light from these arcs was filtered out by special glass filters in order to prevent the appearance of a brown color in the liquid, and the resultant continuous fluorescence spectrum.

1. Introduction

WHILE very extensive researches have been carried out to determine the Raman frequencies most closely associated with various substituted radicals in organic compounds, there have been no investigations which show in a satisfactory way the effect of a change of length of the organic molecule upon any such frequency.[1] The work reported here was begun in 1929 to remedy this deficiency. In order to prevent the extra complication which arises when several atoms are present in the radical, it was decided to study the frequencies associated with a single halogen atom in the molecule.

2. Experimental Method

The Raman spectra were taken by the use of a large Steinheil three prism glass spectrograph. The Pyrex tube used to hold the liquid is similar in shape to that designed by Wood. The liquid, after purification by distillation, is put into a glass bulb (Fig. 1) which is kept sealed to the Raman tube. After evacuation of the tube, the liquid is distilled over into the Raman tube. This liquid is then poured back into the tube, and this process repeated several times to give an "optically empty" liquid.

The source of light was a set of vertical constricted 220 volt quartz mercury arcs. It was found that these arcs work smoothly if started on a 220 volt D.C. circuit, but the quartz of the capillary deteriorates rapidly when the arc is in operation. Thus the best Raman spectra are obtained if the capillary is replaced by a new one after each day of operation.

Organic bromides are changed chemically and colored brown by the action of ultraviolet light. The colored liquid thus produced gives rise in such work to a continuous fluorescence spectrum which obscures the Raman lines to some extent. To prevent this photochemical action various Corning glass filters were used to absorb wave-lengths below λ3650A.

When two 220 volt constricted arcs were used it was found that in the presence of the filters it was necessary to give an exposure of 10 to 12 hours

[1] A. Dadieu and K. W. F. Kohlrausch, however, have (J. Opt. Soc. Am. **21**, 298 (1931)) published values for molecules up to 4 carbon atoms in length.

to obtain an entirely satisfactory Raman spectra. Without the filters the time is greatly reduced, but many lines are partly obscured by the continuous spectrum. With chlorides or hydrocarbons, the filters are not in general necessary.

3. Wave-Lengths and Shift of Frequency

The approximate wave-length of each line was obtained by direct comparison with the spectrum of an iron arc, but the final values were calculated by the use of the Hartmann formula, from the wave-lengths of adjacent well-known lines in the mercury spectrum.

Many of the Raman lines are broad and diffuse. This seems to be due in some cases to the overlapping of Raman lines, excited by two or more lines of the incident spectrum. The shift of frequency ($\Delta\nu$) was obtained by calcu-

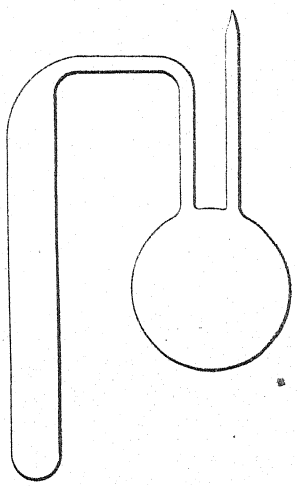


Fig. 1. Raman tube of the Wood type as modified by Langer and Meggers.

lating all of the possible frequency shifts with reference to the strong mercury lines in the adjacent spectrum. The shifts selected as real were those which gave the same value if the Raman lines were caused by two or more exciting lines. In the relatively few cases in which there was no such coincidence in the values, the scattered line was assigned to the nearest mercury line of high intensity. A few doubtful selections are indicated by question marks. This is the usual method employed when the mercury arc, with its great number of lines, is used as the exciting source. Without doubt this method gives rise to the inclusion in tables of data, of frequency shifts which are not real, and to the omission of certain true shifts.

This is illustrated by Table I, which gives the Raman frequencies as determined by the writers (H.B.), by Dadieu and Kohlrausch[2] (D.K.), by Bhagavantam and Venkateswaren[3] (C.D.), and by Cleeton and Dufford[4]

[2] A. Dadieu and K. W. F. Kohlrausch, J. Opt. Soc. Am. 5, 286–322 (1931).
[3] S. Bhagavantam and S. Venkateswaren, Proc. Roy. Soc. A127, 360 (1930).
[4] Cleeton and Dufford, Phys. Rev.

(C.D.) for allyl bromide ($CH_2=CHCH_2Br$), and for n-propyl bromide ($CH_3CH_2CH_2Br$).

TABLE I. *Wave numbers of bromides.*

Allyl bromide			Propyl bromide		
H.B.	D.K.	B.V.	H.B.	D.K.	C.D.
254 (3)	252	259	312 (2)	314	308
—	385	—	—	397	—
535 (2)	526	535	459 (2)	—	—
695 (2)	687	690	563 (1)	564	566
—	926	—	648 (2)	647	—
1000 (2)	—	—	778 (1)	773	—
1193 (2)	1190	—	—	836	—
1215 (2)	1212	1209	—	885	—
1296 (4)	1292	1301	—	—	968
1320 (2)	—	1321	1023 (2)	1024	—
1378 (2)	—	—	—	—	1079
1410 (2)	1406	1414	1143 (2)	1131	—
1638 (2)	1633	1641	1165 (2)	—	—
2157 (2)	—	—	1185 (2)	—	—
2986 (2)	2966	2975	1229 (2)	—	1254
—	3011	—	1435 (1)	1430	1456
—	3085	—	—	—	2736
			2896 (2)	2862	2875
			2933 (2)	2935	2923
			2965 (2)	2959	2976
			2993 (3)	3000	—

TABLE II. *Raman wave numbers for bromides. Average $\Delta\bar{\nu}$ values.*

iso-propyl bromide	n-butyl bromide		Secondary butyl bromide	iso-butyl bromide	Tertiary butyl bromide	n-amyl bromide	iso-amyl bromide
	H.B.	D.K.					
172 (1)	280 (2)	279	291 (4)	303 (4)	301 (6)	219 (1)	288 (2)
297 (3)	457 (2)		317 (1)	421 (2)	515 (5)	436 (1)	564 (2)
353 (2)	563 (2)	557	347 (2)	470 (2)	538 (2)	473 (1)	619 (2)
409 (2)	642 (3)	637	455 (2)	495 (2)	615 (2)	564 (3)	636 (2)
423 (1)	702 (2)	—	482 (2)	517 (2)	803 (2)	642 (3)	648 (2)
540 (4)	745 (2)	—	533 (2)	572 (2)	954 (2)	703 (2)	749 (2)
882 (2)	798 (3)	794	612 (1)	622 (3)	1141 (2)	747 (2)	822 (2)
964 (1)	867 (3)	853	635 (2)	653 (4)	1260 (2)	780 (2)	1297 (2)
1040 (3)	893 (2)	—	840 (2)	796 (1)	1456 (1)	1057 (2)	2872 (2)
	—	1057					
1096 (2)	1103 (3)		956 (1)	812 (2)	2923 (3)	1113 (2)	2932 (3)
	—	1139					
1227 (3)	1170 (2)		1077 (1)	1144 (2)	2970 (2)	1208 (2)	2962 (2)
	—	1257					
1284 (2)	1299 (2)	—	1103 (1)	1198 (2)	3025 (2)	1248 (3)	
1441 (2)	1362 (2)	—	1212 (2)	1234 (2)		1302 (3)	
	—	1440					
2927 (2)	1491 (2)	—	1263 (2)	1313 (1)		1436 (2)	
2958 (3)	2874 (2)	2865	1451 (2)	1454 (1)		1491 (2)	
2983 (2)	2935 (4)	2930	2877 (2)	2871 (2)		2824 (2)	
2993 (2)	2964 (4)	2962	2922 (3)	2962 (3)		2877 (2)	
			2974 (2)			2936 (2)	
						2968 (4)	
						3013 (2)	
						3068 (2)	

NOTE: The figures in parentheses give the number of values from which the average value was obtained.

For allyl bromide the values of Dadieu and Kohlrausch are from 2 to 9 wave numbers smaller than ours, while those of Bhagavantam and Venkateswaren vary from ours by from +5 to −6. Where the differences are much greater it is possible that the same lines were not measured.

The Raman wave number 459 for n-propyl bromide was found only by ourselves, and not by the two other workers. That it may correspond to a real frequency is indicated by its occurrence with the value 457 in n-butyl bromide and 455 in secondary butyl bromide. A vibration of about this wave number is attributed by Andrews to a transverse vibration in the -C-C-C- chain.

The wave numbers which correspond to the Raman shifts for other organic bromides are listed in Table II and Fig. 2. It may be seen that n-amyl bromide gives a surprisingly large number of values, but it is possible

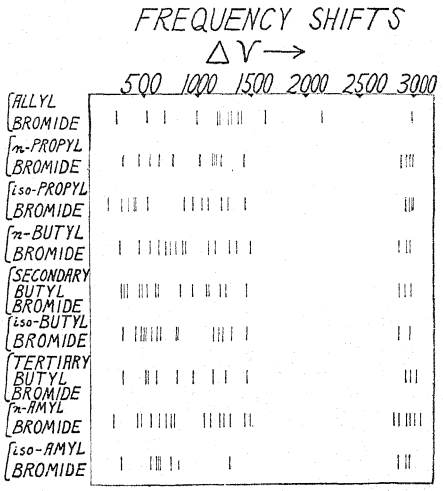


Fig. 2.

that some of them do not correspond to real shifts. One difficulty, which is not sufficiently recognized in connection with the Raman spectra of such compounds, is that it is exceedingly difficult to obtain such organic liquids free from isomers or other compounds similar in properties.

The data from which the mean values of the Raman shifts given in Tables I and II have been obtained, are given in Table III. The few anti-Stokes lines are designated by a negative $\Delta\bar{\nu}$. In general the variation in the value of $\Delta\bar{\nu}$ for what seems to be the same Raman shift is not more than 3 units.

4. The Carbon-Halogen Bond with a Single Carbon Atom

As is indicated in Table IV the frequency which corresponds to the carbon-chlorine bond is 2.13×10^{13}, to the carbon-bromine bond, 1.81×10^{13}, and to the carbon-iodine bond 1.60×10^{13} per second, when only one carbon atom is present. If more than one carbon atom is in the molecule these

characteristic frequencies are reduced by from 6 to 11 percent for bromides and probably somewhat more for chlorides, as is shown in the next section.

The equation for the Raman frequency ($\Delta\nu$) may be written in a simple approximate form as

$$\Delta\nu = \omega_0(v' - v'') = \frac{1}{2\pi}\left(\frac{f}{\mu}\right)^{1/2}(v' - v'')$$

TABLE III. *Wave-lengths of Raman and exciting lines.*

Raman line $\bar{\nu}$	Exciting line λ	Exciting line $\bar{\nu}$	$\Delta\bar{\nu}$	Raman line $\bar{\nu}$	Exciting line λ	Exciting line $\bar{\nu}$	$\Delta\bar{\nu}$
			Allyl bromide				
24451	4046.56	24705	254	21997	4347.50	22995	998
24174	4046.56	24705	531	21744	4339.24	23039	1295
24010	4046.56	24705	695	21744	4358.34	22938	1194
23514	4046.56	24705	1191	21721	4046.56	24705	2984
23514	4077.84	24516	1002	21721	4339.24	23039	1318
23492	4046.56	24705	1213	21721	4358.34	22938	1217
23408	4046.56	24705	1297	21699	4347.50	22995	1296
23328	4046.56	24705	1377	21642	4358.34	22938	1296
23296	4046.56	24705	1409	21617	4358.34	22938	1321
23068	4046.56	24705	1637	21617	4347.50	22995	1378
22786	4339.24	23039	253	21528	4077.84	24516	2988
22682	4358.34	22938	256	21528	4358.34	22938	1410
22546	4046.56?	24705	2159	21299	4358.34	22938	1639
22400	4358.34	22938	538	20885	4339.24?	23039	2154
22243	4358.34	22938	695				
			n-propyl bromide				
24394	3663.27	27290	2896	21830	4347.50	22995	1165
24394	3650.14	27388	2994	21809	4046.56	24705	2896
24394	4046.56	24705	311	21809	4339.24	23039	1230
24057	4046.56	24705	648	21809	4347.50	22995	1186
24057	4077.84	24516	459	21793	4358.34	22938	1145
22626	4358.34	22938	312	21774	4046.56	24705	2931
22536	4347.50	22995	459	21774	4358.34	22938	1164
22375	4358.34	22938	563	21742	4046.56	24705	2963
22291	4358.34	22938	647	21711	4046.56	24705	2994
22160	4358.34	22938	778	21711	4358.34	22938	1227
21970	4347.50	22995	1025	21503	4358.34	22938	1435
21918	4358.34	22938	1020	20003	4347.50	22995	2992
21855	4339.24	23039	1184	20003	4358.34	22938	2935
21855	4347.50	22995	1140	19972	4358.34	22938	2966
			iso-propyl bromide				
24407	3650.14	27388	2981	21897	4358.34	22938	1041
24407	4046.56	24705	298	21844	4358.34	22938	1094
24298	3663.27	27290	2992	21812	4339.24	23039	1227
24298	4046.56	24705	407	21778	4046.56	24705	2927
24165	4046.56	24705	540	21749	4046.56	24705	2956
24165	4077.84	24516	351	21711	4046.56	24705	2994
23975	4077.84	24516	541	21711	4347.50	22995	1284
23824	4046.56	24705	881	21711	4358.34	22938	1227
23664	4046.56	24705	1041	21556	4077.84	24516	2960
23477	4046.56	24705	1228	21556	4347.50	22995	1439
23477	4077.84	24516	1039	21495	4358.34	22938	1443
23232	4077.84	24516	1284	20011	4347.50	22995	2984
22641	4347.50	22995	354	20011	4358.34	22938	2927
22641	4358.34	22938	297	19980	4358.34	22938	2958
22528	4358.34	22938	410	18135	5460.74	18307	172
22399	4358.34	22938	539	18010	5460.74	18307	297
22056	4358.34	22938	882	17884	5460.74	18307	423
21974	4358.34	22938	964	17768	5460.74	18307	539
21897	4347 50	22995	1098				

TABLE III. (*Continued*)

Raman line $\bar{\nu}$	Exciting line λ	Exciting line $\bar{\nu}$	$\Delta\bar{\nu}$	Raman line $\bar{\nu}$	Exciting line λ	Exciting line $\bar{\nu}$	$\Delta\bar{\nu}$
			n-butyl bromide				
24425	3650.14	27388	2963	22197	4347.50	22995	798
24425	4046.56	24705	280	22139	4358.34	22938	799
24143	4046.56	24705	562	22070	4358.34	22938	868
24061	4046.56	24705	644	22045	4358.34	22938	893
24061	4077.84	24516	455	21891	4347.50	22995	1104
23961	4046.56	24705	744	21870	4339.24	23039	1169
23907	4046.56	24705	798	21836	4358.34	22938	1102
23877	4077 84	24516	639	21768	4046.56	24705	2937
23838	4046.56	24705	867	21768	4358.34	22938	1170
23813	4046.56	24705	892	21741	4046.56	24705	2964
23813	4077.84	24516	703	21741	4339.24	23039	1298
23650	4077.84	24516	866	21676	4339.24	23039	1363
23603	4046.56	24705	1102	21643	4077.84	24516	2873
23216	4046.56	24705	1489	21577	4077.84	24516	2939
23216	4077.84	24516	1300	21577	4358.34	22938	1361
22659	4358.34	22938	279	21553	4077.84	24516	2963
22480	4358.34	22938	458	21503	4347.50	22995	1492
22375	4358.34	22938	563	20064	4347.50	22995	2931
22294	4339.24	23039	745	20064	4358.34	22938	2874
22294	4347.50	22995	701	20004	4358.34	22938	2934
22294	4358.34	22938	644	19974	4358.34	22938	2964
			Secondary butyl bromide				
24414	3650.14	27388	2974	22406	4358.34	22938	532
24414	3663.27	27290	2876	22359	4347.50	22995	636
24414	4046.56	24705	291	22326	4358.34	22938	612
24224	4046.56	24705	481	22154	4347.50	22995	841
24224	4077.84	24516	292	22099	4358.34	22938	839
24171	4046.56	24705	534	21982	4358.34	22938	956
24171	4077.84	24516	345	21892	4347.50	22995	1103
23253	4046.56	24705	1452	21861	4358.34	22938	1077
23253	4077.84	24516	1263	21828	4046.56	24705	2877
23229	4358.34	22938	−291	21828	4339.24	23039	1211
22647	4347.50	22995	348	21783	4046.56	24705	2922
22647	4358.34	22938	291	21783	4347.50	22995	1212
22621	4358.34	2293	317	21732	4046.56	24705	2973
22586	4339.24	23039	453	21732	4347.50	22995	1263
22482	4358.34	22938	456	21593	4077.84	24516	2923
22455	4358.34	22938	483	21488	4358.34	22938	1450
22406	4339.24	23039	633	20018	4358.34	22938	2920
			iso-butyl bromide				
24401	4046.56	24705	304	22518	4358.34	22938	420
24283	4046.56	24705	422	22469	4339.24	23039	570
24235	4046.56	24705	470	22469	4358.34	22938	469
24212	4046.56	24705	493	22421	4347.50	22995	574
24212	4077.84	24516	304	22421	4358.34	22938	517
24189	4046.56	24705	516	22316	4358.34	22938	622
24083	4046.56	24705	622	22285	4358.34	22938	653
24052	4046.56	24705	653	22142	4358.34	22938	796
23893	4046.56	24705	812	22126	4358.34	22938	812
23893	4077.84	24516	623	21833	4046.56	24705	2872
23861	4077.84	24516	655	21796	4347.50	22995	1199
23590	4358.34	22938	−652	21796	4358.34	22938	1142
23560	4046.56	24705	1145	21741	4046.56	24705	2964
23470	4046.56	24705	1235	21741	4358.34	22938	1197
23392	4046.56	24705	1313	21705	4358.34	22938	1233
23239	4358.34	22938	−301	21555	4077.84	24516	2961
22634	4358.34	22938	304	21484	4358.34	22938	1454
22542	4339.24	23039	497	20068	4358.34	22938	2870
				19976	4358.34	22938	2962

TABLE III. (*Continued*).

Raman line $\bar{\nu}$	Exciting line λ	Exciting line $\bar{\nu}$	$\Delta\bar{\nu}$	Raman line $\bar{\nu}$	Exciting line λ	Exciting line $\bar{\nu}$	$\Delta\bar{\nu}$
			Tertiary butyl bromide				
25005	4046.56	24705	−300	22134	4358.34	22938	804
24403	4046.56	24705	302	21982	4358.34	22938	956
24214	4077.84	24516	302	21797	4358.34	22938	1141
24189	4046.56	24705	516	21781	4046.56	24705	2924
24167	4046.56	24705	538	21781	4339.24	23039	1258
24000	4077.84	24516	516	21734	4046.56	24705	2971
23903	4046.56	24705	802	21734	4347.50	22995	1261
23903	4077.84	24516	613	21594	4077.84	24516	2922
23564	4046.56	24705	1141	21482	4358.34	22938	1456
23564	4077.84	24516	952	20015	4339.24	23039	3024
23453	4358.34	22938	−515	20015	4358.34	22938	2923
23240	4358.34	22938	−302	19970	4347.50	22995	3025
22635	4358.34	22938	303	19970	4358.34	22938	2968
22422	4339.24	23039	617	18008	5460.74	18307	299
22422	4358.34	22938	516	17793	5460.74	18307	514
22400	4358.34	22938	538				
			n-amyl bromide				
24141	4046.56	24705	564	21882	4347.50	22995	1113
24062	4046.56	24705	643	21882	4358.34	22938	1056
23956	4046.56	24705	749	21830	4046.56	24705	2875
23923	4046.56	24705	782	21830	4339.24	23039	1209
23877	4077.84	24516	639	21768	4046.56	24705	2937
23811	4077.84	24516	705	21739	4046.56	24705	2966
23739	4077.84	24516	777	21739	4339.24	23039	1300
23647	4046.56	24705	1058	21692	4046.56	24705	3013
23499	4046.56	24705	1206	21692	4077.84	24516	2824
23454	4046.56	24705	1251	21692	4347.50	22995	1303
23403	4046.56	24705	1302	21692	4358.34	22938	1246
23403	4077.84	24516	1113	21637	4046.56	24705	3068
23269	4046.56	24705	1436	21637	4077.84	24516	2879
23269	4077.84	24516	1247	21637	4358.34	22938	1301
22719	4358.34	22938	219	21549	4077.84	24516	2967
22502	4358.34	22938	436	21549	4339.24	23039	1490
22465	4358.34	22938	473	21503	4077.84	24516	3013
22430	4347.50	22995	565	21503	4347.50	22995	1492
22375	4358.34	22938	563	21503	4358.34	22938	1435
22294	4339.24	23039	745	20068	4339.24	23039	2971
22294	4347.50	22995	701	20004	4358.34	22938	2934
22294	4358.34	22938	644	19971	4339.24	23039	3068
21882	4046.56	24705	2823	19971	4358.34	22938	2967
			iso-amyl bromide				
24142	4046.56	24705	563	22190	4358.34	22938	748
24055	4046.56	24705	650	22116	4358.34	22938	822
23955	4046.56	24705	750	21834	4046.56	24705	2871
23883	4046.56	24705	822	21768	4046.56	24705	2937
23883	4077.84	24516	633	21743	4046.56	24705	2962
22707	4347.50	22995	288	21743	4339.24	23039	1296
22651	4358.34	22938	287	21641	4358.34	22938	1297
22400	4339.24	23039	639	20065	4347.50	22995	2930
22374	4347.50	22995	621	20065	4358.34	22938	2873
22374	4358.34	22938	564	20008	4358.34	22938	2930
223 2	4358.34	22938	616	19976	4358.34	22938	2962
22292	4358.34	22938	646				

in which v represents a quantum number, μ the mutual mass, w_0 is sometimes considered as the fundamental mechanical frequency, and f as the force con-

stant. The values of f for the methyl halides are given in Table IV. It is assumed that in the emission of these intense Raman lines $v'-v''=\pm 1$.

The force constant (a) is calculated in the ordinary way, and it is considered that the methyl group vibrates as a unit with respect to the halogen atom. In (b) a slight, somewhat arbitrary allowance has been made for the fact that this is not strictly true.

TABLE IV. *Values for the carbon-halogen bond.*

Compound	Wave Number cm^{-1}	ν Frequency per Second $\times 10^{-13}$	Force Constant f dynes $\times 10^5$ a	b	Amplitude $\times 10$ cm $v=\frac{1}{2}$	$v=1\frac{1}{2}$	$\frac{1}{2}fa\times 10$ $v=\frac{1}{2}$	$v=1\frac{1}{2}$
CH_3Cl	712	2.135	3.136	3.02	6.7	11.6	2.0	3.5
CH_3Br	603	1.808	2.695	2.60	6.65	11.5	1.7	3.0
CH_3I	534	1.601	2.246	2.17	6.9	11.9	1.5	2.6

The force constant decreases from the chloride to the iodide. The values are much smaller than those of the single bonds listed by Dadieu and Kohlrausch which are, in 10^5 dynes per cm, equal to 4.31 for C·C in ethane, 4.96 for C·C in methyl alcohol, and 4.89 for C·N in methyl amine.

Thus if f represents the strength of the bond, the carbon-halogen bond seems to be much weaker than the most common of the other single bonds found in organic compounds. That the strength of the bond decreases rapidly from chloride to bromide to iodide, is in agreement, not only with the heats of dissociation, but also with the other known relations.

The meaning of the amplitude a' is definite in the classical quantum theory, but loses this definiteness in the newer quantum mechanics.

Since $\epsilon=fa^2/2=(v+\frac{1}{2})w_0h$

$$a=\left(\frac{2\epsilon}{f}\right)^{1/2}=\left(\frac{(2v+1)hw_0}{f}\right)^{1/2}$$

in which (ϵ) is the energy and w_0 is the mechanical frequency. The values for this amplitude for $v=\frac{1}{2}$ and $v=3/2$ are given in Table IV.

Dadieu and Kohlrausch give the mean value of the force as $\frac{1}{2}fa$, and consider this to be more characteristic of the bond than the force constant.

For $v=\frac{1}{2}$ the values of $\frac{1}{2}fa$ in 10^{-4} dyne cm are 2.0, 1.7, and 1.5 for methyl chloride, bromide, and iodide, respectively, while Dadieu and Kohlrausch give 2.04 for the C·C bond in methane, 2.27 for the C·O bond in methyl alcohol, 2.23 for the C·N bond in methyl amine, 4.13 for the double bond in ethylene, 4.4 for the carbonyl C·O bond, 4.14 for the oxygen bond in O_2, and 6.28 for the bond in carbon monoxide.

5. The Effect of a Lengthening of the Chain Upon the Carbon-Halogen Bond

The effect of a lengthening of the hydrocarbon chain upon the characteristic carbon-bromine frequency is exhibited in Table V.

This is the most intense line in the Raman spectrum of the bromides.

The remarkable fact revealed by our data is that while the carbon-bromine frequency is reduced by about 6 percent if the number of carbon atoms in the chain is increased from one to two, a further increase from two to five carbon atoms produces no appreciable effect.

TABLE V. *Characteristic wave numbers for the carbon-bromine bond in organic bromides*.

CH_3Br	603 (C.D.)	594 (D.K.)
C_2H_5Br	566 (C.D.)	557 (D.K.)
n$-C_3H_7Br$	563 (H.B.)	564 (D.K.)
n C_4H_9Br	563 (H.B.)	557 (D.K.)
$C_5H_{11}Br$	564 (H.B.)	
$(CH_3)_2CH\ (CH_2)_2Br$	564 (H.B.)	

If an attempt is now made to apply Eq. (1) to determine the value of the force constant f and thus, presumably, the strength of the bond, it is apparent that the equation cannot be solved without additional knowledge or an additional assumption. It seems to have been customary to assume that all of the hydrocarbon chain vibrates with respect to the bromine atom: —or more complicated equations are used which indicate a change of the single fundamental frequency into two values.

The constancy of the fundamental carbon-bromine frequency seems to suggest that neither of these assumptions is valid in this case.

Thus it seems apparent from the constant value of the frequency for normal compounds that *the organic radical cannot vibrate as a whole with respect to the bromine atom*, for such an assumption leads to an absurd value of the force constant for very long chains.

Thus, on the basis of the assumption that the effective mass of the methyl group with respect to the vibration toward bromine is 14.4 atomic weight units, the force constant for methyl bromide is 2.60×10^5 dyne/cm (or 2.70 if CH_3 vibrates as a single unit of mass 15). If now the amyl group vibrates as a unit the force constant for amyl bromide would be 7.0×10^5 dyne/cm, or more than two and a half times larger than for methyl bromide. This is much too large.

If the force constant in all of the normal bromides is assumed to be constant and equal to 2.60×10^5 dyne/cm, the effective mass of the portion of the hydrocarbon chain of two or more carbon atoms, which vibrates (with respect to the bromine) is 17. This indicates that the CH_2 group adjacent to the bromine possesses most of the mass which is effective. That is the CH_2 group vibrates, but its effective mass is increased by the constraint due to its union with the rest of the hydrocarbon chain.

If it is assumed that the force constant decreases with the length of the chain, then the amount of mass in the radical R which vibrates, also decreases with increase of mass of the radical, which seems to be improbable, except for the increase from one to two carbon atoms. Thus these facts, together with the equation $\nu=1/2\pi(f/\mu)^{1/2}(v'-v'')$, lead to the idea that (1) the force constant remains constant as the length of the chain increases, or

(2) the force constant increases as the length of the chain increases, and at the same rate as the mutual mass (μ) of the vibrating parts increases.

From what is known from the standpoint of organic chemistry, it seems that the strength of the carbon-halogen bond does not increase rapidly with the length of the chain.

Thus the final conclusions reached are: (1) The force constant either remains constant, or else it increases only slightly with an increase in length and mass of the normal hydrocarbon chain. (2) As indicated before, only a part of the radical R vibrates with respect to the halogen atom in the process in which the characteristic frequency is emitted.

The values of Dadieu and Kohlrausch suggest that the characteristic frequency of this bond may be higher if an odd number of carbon atoms is present in the molecule than if this number is even. The variation in value is, however, very small, and is not exhibited by our data.

The data of a recent paper by West and Farnsworth[5] indicates the probability that the chlorides exhibit the same relations as the bromides. Unfortunately for the purpose of the present paper, their work does not extend to chains of more than 3 carbon atoms.

TABLE VI. *Characteristic wave numbers for the carbon-halogen bond.*

1.	2. Cl	3. Br	4. I	5. Cl-Br	6. Br-I	7. Cl^2-Br^2 $\times 10^{-3}$	8. Br^2-I^2 $\times 10^{-3}$	9. $\frac{Br^2-I^2}{Cl^2-Br^2}$
Methyl	711 (W.F.)	603 (C.D.)	522 (D.K.)	108	81	142	91	.64
Ethyl	655 (W.F.)	536 (C.D.)	499 (D.K.)	89	67	109	71	.65
n-Propyl	650 (W.F.)	563 (H.B.)	—	87	—	105	—	—
n-Butyl		563 (H.B.)						
n-Amyl		564 (H.B.)						

Since, with a constant mutual mass, the force constant varies as the square of the frequency, it is apparent from column 9 of Table VI, that the decrease in the value of the force constant is only 65 percent as great between the bromide and iodide as it is between the chloride and bromide.

6. THE EFFECT OF A BRANCHING OF THE CHAIN UPON THE FUNDAMENTAL FREQUENCY ASSOCIATED WITH THE CARBON-HALOGEN BOND

The branching of the hydrocarbon chain seems to have no effect upon the fundamental frequency associated with the carbon-halogen bond, provided the branching occurs sufficiently distant from the halogen atom. Thus iso-amyl bromide ($(CH_3)_2 \cdot CH \cdot CH_2 \cdot CH_2 \cdot Br$) gives the wave number 564, which is the same as that associated with n-amyl, n-butyl, and n-propyl bromides. However, if the branching is considerably less distant, the frequency is reduced considerably. Thus with iso-compounds, or if the halogen atom is attached to a secondary or tertiary carbon atom, the wave number is reduced from 564 to about 537 cm^{-1} (Table VII).

[5] W. West and M. Farnsworth, Trans. Faraday Soc. **27**, 145 (1931).

Thus a branching of the chain sufficiently close to the substituted halogen atom either lowers the force constant and presumably weakens the bond, or else it lowers the effective mass of the part of the hydrocarbon chain which vibrates. The former of these seems the more probable.

The frequency for iso-butyl bromide (wave number 572 cm^{-1}) seems exceptional in that it is higher than for the normal compound. However, a lower frequency also appears.

TABLE VII. *Characteristic wave numbers for the carbon-halogen bond with branched chains.*

(Normal)	711	(564)
ISO propyl $(CH_3)_2$ CH X	616 (W.F.)	540
Secondary butyl CH_3CH_2CHX CH_3	—	537
Tertiary butyl $(CH_3)_3$ C X	564 (D.K.)	538
ISO amyl $(CH_3)_2$ CH CH_2CH_2 X		(564)
ISO butyl $(CH_3)_2$ CH CH_2 Br		(572) and (517)

7. A Lower Characteristic Frequency Seemingly Associated with the Carbon-Bromide Bond

A wave number of about 300 cm^{-1} has been found for all of the organic monobromides investigated by us, with the exception of allyl bromide, in which a double carbon bond is present. A similar value of about 330 cm^{-1} has been found for chlorides by West and Farnsworth, and with ethyl iodide a value of 260 cm^{-1} was found by Dadieu and Kohlrausch.

Table VIII gives a list of these wave numbers for different chlorides and bromides, and a single value for an iodide.

The values for the bromides (in the upper part of Table VIII) may be associated with some type of transverse vibration at the carbon-bromine bond. Unlike the frequency which the writers have associated with a longitudinal vibration at this bond, the values for iso- or secondary compounds do not exhibit any general differentiation from those of the normal compounds. A few examples are listed to show that if two or more halogen atoms are present the frequencies due to carbon-halogen bonds are greatly modified. Thus, according to Dadieu and Kohlrausch, carbon tetrachloride is represented by the wave numbers 216 (4), 313 (4), 455 (4), 755 (2), 782 (2), in which the numbers in parenthesis represent the intensities. The more intense lines have wave numbers which are smaller than the most characteristic of the carbon-halogen bond in aliphatic compounds. This is probably due in part at least to a greater mutual mass of the vibrating parts of the molecule.

8. Wave Numbers between 1400 and 1460 cm^{-1}

Almost all of the hydrocarbons of the paraffin series and their derivatives exhibit a Raman wave number between 1400 and 1460 cm^{-1}.

This has been attributed by Dadieu and Kohlrausch to a transverse vibration of the hydrogen atoms in the CH_2 group, and by Daure to the single carbon-carbon bond. There seems to be much evidence which indicates the probability that one of these points of view is correct, and certain different

details of evidence which seem to speak against each of these ideas. Present opinion seems on the whole more in favor of the former of these conclusions. Table IX lists frequencies in this range as found in monobromides.

TABLE VIII. *Lower wave numbers presumably characteristic of the carbon-halogen bond.*

	Cl	Br	I
Methyl	372 (W.F.)		
Ethyl	327 (W.F.)	290	260 (D.K.)
n-propyl	333 (W.F.)	312	
n-butyl	—	280	
Isopropyl	330 (W.F.)	297	
Isobutyl	—	303	
Isoamyl	—	288	
Secondary butyl	—	291	
β Chloropropylene	337 (W.F.)		
The above values are changed considerably if more than one halogen atom is present.			
CX_4	216–313 (D.K.)		
CHX_3	259–364 (D.K.)	154–221 (D.K.)	
CH_2X_2	283 (D.K.)	178 (D.K.)	119 (D.K.)
XH_2C-CH_2X	295 (D.K.)	188 (D.K.)	
$X_2HC-CHX_2$	287–351 (D.K.)	218 (D.K.)	
1–3 dibromopropane		371 (D.K.)	

TABLE IX. *Wave numbers of about 1450 cm^{-1} for monobromides.*

ethyl bromide	1439 (D.K.)		
n-propyl bromide	1435 (H.B.)	isopropyl bromide	1441
n-butyl bromide	1440 (D.K.)	isobutyl bromide	1454
	1491 (H.B.)	secondary butyl bromide	1451
n-amyl bromide	1436 (H.B.)	tertiary butyl bromide	1456
	1491 (H.B.)	allyl bromide	1410

9. FREQUENCY CHARACTERISTIC OF THE DOUBLE BOND BETWEEN CARBON ATOMS

Dadieu and Kohlrausch have found 1639 cm^{-1} as the wave number characteristic of the double carbon bond in allyl chloride. The writers obtain the value 1638 for the bromide, so the increase of mass of the halogen has little effect upon the frequency. Dadieu and Kohlrausch point out that the frequency, characteristic of the double bond, is moderately constant. Thus their values for di-chlor, tri-chlor, and tetra-chlor ethylene indicate values of 1583, 1585, and 1569, respectively.

The writers are indebted to a Grant-in-Aid of the National Research Council which was used for the purchase of the spectrograph used in this work.

THE EMISSION OF SECONDARY ELECTRONS FROM TUNGSTEN

By A. J. Ahearn
Bell Telephone Laboratories, New York

(Received September 28, 1931)

Abstract

An apparatus is described for investigating critical potentials in the emission of secondary electrons from tungsten. Measurements on the velocity distribution in the primary beam show that secondary electrons from the electron gun are absent. Tube characteristics which might introduce spurious critical potentials in the secondary emission from tungsten appear to be absent. By heat treating the tungsten and cleaning up residual gases, maxima and critical slope changes were developed below 40 volts. With sensitive methods of measuring and plotting the data, critical potentials within the range from 40 to 500 volts were observed only at the following uncorrected voltages; 70, 108, 208, 297 volts. All but the 70 volt effect disappeared eventually after heat treatments of the tungsten target. Thus when the tungsten surface is most free from contamination, critical potentials persisted only at the following uncorrected voltages; maxima at about 3.5 and 8 volts and slope increases at 24, 33 and 70 volts. The phenomena may be associated with the diffraction of electrons or the production and absorption of characteristic soft x-rays. Regardless of the mechanism operating at the critical potentials, their decrease or elimination beyond 40 volts points strongly to effects of surface contamination rather than to characteristics of tungsten.

Introduction

MANY investigations[1] have been made on the secondary electron characteristics of metals. Critical potentials[2] have been observed in some of these researches. The most recent work on critical potentials in the secondary electron emission of tungsten is that of Krefft[3]. The present work was undertaken to investigate the reality of these as characteristic of clean tungsten.

The Experimental Tube

A beam of electrons was projected from an electron gun and struck a tungsten target. The secondary electrons emitted by the tungsten under bombardment were received on a collector. By measuring I_p the primary current which bombarded the target and I_s the secondary electron current emitted, the secondary electron emission I_s/I_p was obtained.

The essential details of the experimental tube which was used are drawn to scale in Fig. 1. The elements F, S, A and B constitute an electron gun. The filament F is a tungsten ribbon $27\times0.5\times0.06$ mm operated at about 4.5

[1] Soller, Phys. Rev. **36**, 1212 (1930); Rudberg, Roy. Soc. Proc. **A127**, 111 (1930); Farnsworth, Phys. Rev. **31**, 405 (1928); Brinsmade, Phys. Rev. **30**, 494 (1927).

[2] Stuhlman, Phys. Rev. **25**, 234A (1925); Petry, Phys. Rev. **28**, 362 (1926); Rao, Roy. Soc. Proc. **A128**, 57 (1930); Rao, Roy. Soc. Proc. **A128**, 41 (1930); Hyatt and Smith, Phys. Rev. **32**, 929 (1928); Farnsworth, Phys. Rev. **34**, 679 (1929).

[3] Krefft, Phys. Rev. **31**, 199 (1928); Krefft, Ann. d. Physik **84**, 639 (1927).

amperes. D_1 is a square aperture 3.0 mm on each side. D_2, D_3, D_4, D_5 are circular apertures of diameters 1.5, 1.0, 1.0 and 2.0 mm respectively. The target T, which is the source of the secondary electrons is of tungsten sheet 0.06 mm thick supported on tungsten rods. The filament H is a flat spiral of tungsten ribbon supported on tungsten rods. It serves to heat the target T by bombardment and radiation. The element C serves to collect the secondary electrons emitted by T. The aperture D_6 is 4.5 mm in diameter. The elements S, A, B and C are of nickel sheet 0.3 mm thick. An ionization gauge is attached to the experimental tube. A 6 cm length of 4 mil thoriated tungsten filament is included for use as a getter to clean up residual gases after removal of the tube from the pumps. Guard rings prevent electrical leakage over short glass paths between the electron gun and the element C.

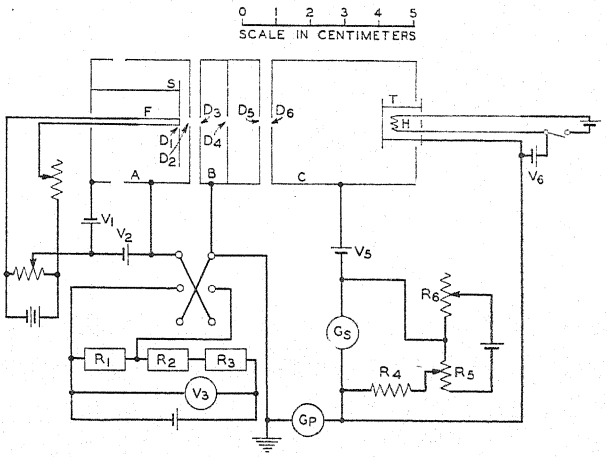


Fig. 1. Apparatus and electrical circuit.

The experimental tube was exhausted by a four-stage mercury diffusion pump. There were two liquid air traps between the diffusion pumps and the tube. Liquid air was maintained continuously on the one next to the pumps. During the twenty four hours preceding the seal off, the trap next to the tube was immersed in liquid air. The entire tube up to its seal off constriction was maintained at about 450°C in an electric furnace until the pressure was reduced to about 1×10^{-6} mm Hg. The elements, S, A, B and C were then maintained at a bright red heat by high frequency induction for several hours until in this condition the pressure was again reduced to about 1×10^{-6} mm Hg. The filament F, and the "getter" were then outgassed, and the target T heated at a bright red heat until again the pressure was about 1×10^{-6} mm Hg. This entire outgassing process was then repeated. Thus the condition was finally reached where the target could be heated to a temperature (yellow color) sufficient to heat the element C to a visible red color without increasing the pressure of about 1×10^{-7} mm Hg. After this condition was established with the filaments and target glowing, the glass was torched for about one hour and then the tube was sealed off from its pumps. During the course

of the pumping of the tube some measurements were made and so it was on the pumps continuously for about three weeks.

Method of Measurements

Fig. 1 shows the circuit used. V_p, the potential of T and C with respect to F, was varied by adjusting the value of R_1, keeping $R_1+R_2=10{,}000$ ohms and having $R_1+R_2+R_3=100$ V_3. In this way, potential changes can be made and reproduced easily and accurately.

G_S and G_P were galvanometers each of 10,000 megohms sensitivity. During most of the measurements, both the primary and the secondary currents were measured with the galvanometers at full sensitivity by means of annulling current circuits one of which is shown in Fig. 1. R_4 had a constant value of 100,000 ohms. The annulling current was adjusted by varying R_5 and R_6 whose maximum values were 10 and 10,000 ohms respectively.

In order to use the galvanometers as described above, it is essential that the filament F be maintained at a constant temperature. To this end, all connections in the filament heating circuit were either welded, soldered or tightly clamped and the rheostat was water cooled.

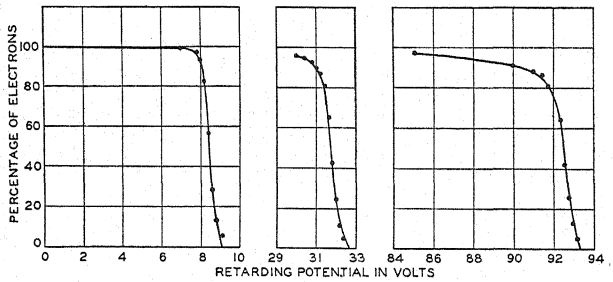


Fig. 2. Electron velocity distribution in primary beam.

In critical potential measurements it is important that the primary beam of electrons have a uniform velocity distribution not only to secure sharp slope changes but also to avoid spurious ones. With this in view the electron gun shown in Fig. 1 was patterned after that of Davisson and Germer[4] in order to obtain a beam of electrons in which secondary emission from the metal of the electron gun was absent. Fig. 2 shows velocity distribution curves for the primary electrons for bombarding potentials of 7, 30 and 90 volts. In the 90 volt case 91 percent and 97 percent of the original beam are present with a retarding potential of 90 volts and 85 volts respectively. If secondary electrons were present they would be largely eliminated by a retarding potential of a few volts. Therefore it seems reasonable that secondary electrons are absent in all three cases and that the differences between the three curves of Fig. 2 are probably due to the distribution of the retarding field.

During some early measurements with S 15 volts negative and A 50 volts

[4] Davisson and Germer, Phys. Rev. **30**, 705 (1927).

positive with respect to F, a sharp increase in the measured value of the secondary emission was observed as the potential V_p of the primary beam passed through that of A. The value of V_p at which this slope increase occurred varied along with variations in the potential of A. The effect, although a small one, was quite clearly a characteristic of the tube rather than of the tungsten target. It may have been caused either by a sudden spreading of the primary beam or by a migration of electrons to C from the rear of the electron gun as the electric field between A and B was reversed. To avoid this difficulty, the electron gun was operated as follows. The element S was a few volts negative with respect to the center of F while A was a few volts positive to F. The velocity of the electrons emerging from B was adjusted by an electric field of the proper value between A and B.

When the experimental tube was first constructed, a Faraday cylinder about 5 cm long and slightly smaller in diameter than the target was mounted in the place of the target. Measurements then made showed that the ratio of currents measured by the G_S and G_P galvanometers was as small as could be expected from the dimensions of the Faraday cylinder. Thus with the target mounted in the tube, the current measured by the G_S galvanometer consisted of secondary electrons from tungsten.

Varying the potential V_5 from zero to 3 volts had no influence on the appearance or magnitude of critical potential effects and produced a negligible increase in the emission coefficient. For part of the results shown $V_5=0$ and for the rest $V_5=3$ volts.

Results

The results presented are divided into four states according to the temperature, heat treatment and gas content of the target and general vacuum conditions in the tube. State 1 denotes the condition which existed after the tube had been removed from the pumps for one month with no treatment of any kind since its removal. The pressure was about 1×10^{-7} mm Hg. The measurements were made with the target at tube temperature. State 2 represents the following conditions. By means of the thoriated tungsten getter the pressure was reduced to about 3×10^{-8} mm Hg. The target was heated at about 1450°K for ten or fifteen hours. All temperatures given in this paper are based on pyrometer measurements made on the outer end of the element T. Being farthest from H this is the coldest part of T. No correction was made for the absorption by the glass walls of the tube. The actual temperatures reached will therefore be higher than the values given. The measurements were made with the target at about 1200°K. It is assumed that the tungsten is more free from surface contamination than in state 1. State 3 designates the following conditions. The target was heated to about 1700°K for an hour. This temperature did not increase the tube pressure of about 2×10^{-8}mm Hg. The tube then remained undisturbed for one month. The measurements were made with the target at tube temperature. State 4 represents the following conditions. After the measurements corresponding to state 3 were obtained, the target was heated at about 1400°K continuously for fifty hours. Then each

day before measurements were made at about 1300°K, the target was heated intermittently for a total of one hour at about 1800°K. After the day's measurements were over, the target was operated at about 1400°K until the 1800°K heat treatment preceding further measurements was given. It is thought in this work that the tungsten target is most free from contamination in state 4. In Figs. 3 to 16 the curves are marked 1, 2, 3, 4 corresponding to the above states.

The curves of Fig. 3 show the general secondary emission characteristics of tungsten, details of which are shown in Figs. 4–16. Curve *A* was obtained during the pumping of the tube described in section 2 before the target had been heated beyond about 900°K, while curve *B* resulted just after the target was first heated to about 1300°K for one hour. Both curves *A* and *B* were obtained with the target at tube temperature. Curves 1, 2, 3 correspond to

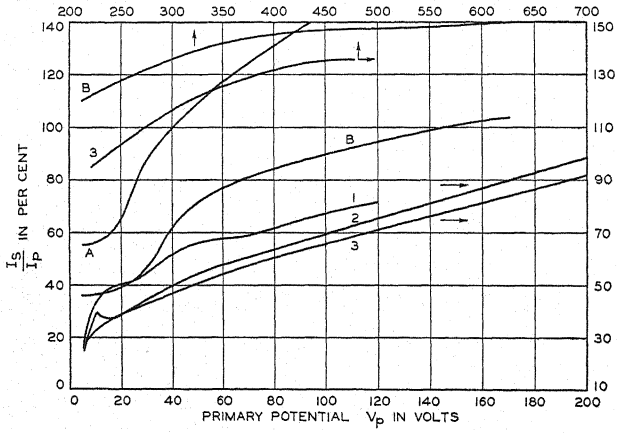


Fig. 3. General secondary electron characteristics of tungsten. The arrows indicate the special scales for the curves.

states 1, 2, 3 respectively. The curve corresponding to state 4 agreed well with curve 3. It is to be noted that on curve *A* the emission factor reaches 100 percent at 40 volts compared to 230 volts on curve 3. Fig. 4 contains curves 1, 2, 4 corresponding to states 1, 2 and 4. Curves corresponding to state 3 agree well with those of state 4. The nature of the changes which occur from state to state is obvious. During state 1 no measurements below 5 volts were made.

Fig. 5 shows the experimental curves between 20 and 40 volts corresponding to states 1, 2, 3, 4. Beyond the low voltage range of Fig. 4, with the exception of state 1 it was not satisfactory to determine slope changes by plotting the data as in Fig. 5. The following method due to Thomas[5] was used to magnify small slope changes. Straight lines were selected whose slopes were approximately that of the first portion of the curves of Fig. 5. A derived curve was then drawn whose ordinates were the differences between the ordinates of the experimental curve and those of the straight line. In this way slope changes of the experimental curve appear either magnified or as a minimum

[5] Thomas, Phys. Rev. **26**, 739 (1925).

on the derived curve. The lower half of Fig. 6 contains these derived curves corresponding to the experimental data of Fig. 5. These differences are

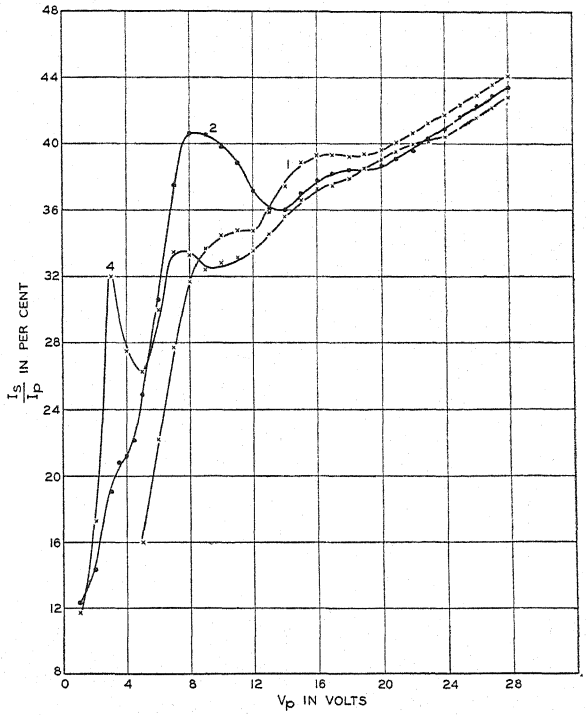


Fig. 4. Secondary electron characteristics of tungsten from 0 to 28 volts.

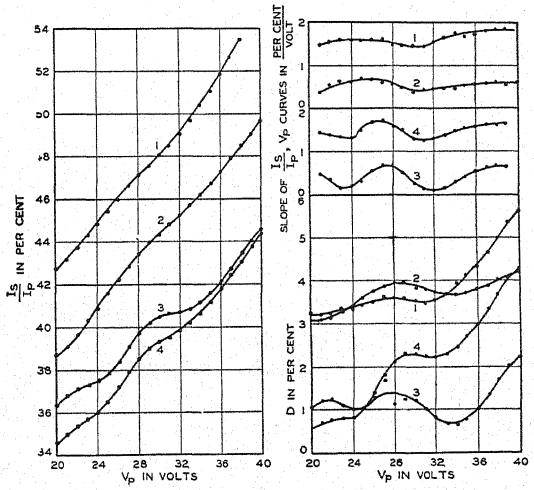


Fig. 5. Secondary electron characteristics of tungsten from 20 to 40 volts. Curve 1: Subtract 3 from ordinate. Curve 3: Add 2 to ordinate. Curve 4: Add 5 to ordinate.

Fig. 6. Secondary electron characteristics of tungsten from 20 to 40 volts. For slope curves: Curve 1: Subtract 1 from ordinate. Curve 4: Subtract 1 from ordinate.

marked D, the ordinates being expressed in the same units as in the experimental curves. For convenience in plotting, the derived curves have been separated from each other so that their relative ordinates are without significance. One sees for example that the small slope change near 33 volts in curve 1, Fig. 5, readily appears in derived curve 1 of Fig. 6 as a maximum and minimum. For comparison with the derived curves, the slopes of the experimental curves are given at the top of Fig. 6. An inspection of Figs. 5 and 6 shows that the slope change near 33 volts is greater in state 1 than in state 2, and that the slope changes near 24 and 33 volts are larger in state 3 than in state 4.

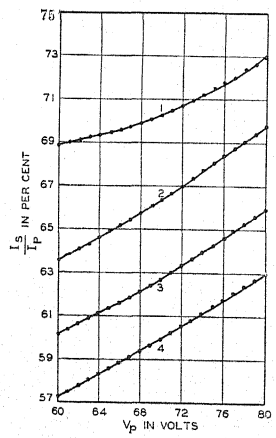


Fig. 7. Secondary electron characteristics of tungsten from 60 to 80 volts. Curve 1: Subtract 11 from ordinate. Curve 2: Subtract 6 from ordinate. Curve 3: Subtract 6 from ordinate.

Figs. 7 and 8 contain the experimental curves, their slopes, and the corresponding derived curves from 60 to 80 volts. With the possible exception of curve 1, the data of Fig. 7 are ambiguous as to the presence of critical changes of slope. However, the derived curves in Fig. 8 clearly reveal a critical slope increase at about 70 volts. Again as in Figs. 5 and 6, the curves of Fig. 8 show that the slope increases for states 1 and 3 are much longer than for states 2 and 4 respectively. By comparison with curve 1 the slope change in curve 4 has almost disappeared. No slope changes were observed from 40 to 60 volts, nor from 80 to 90 volts.

Fig. 9 reveals very little whereas curves 1, 2 and 3 of Fig. 10 reveal a definite slope increase at about 108 volts. Again the change of slope is larger in states 1 and 3 than in states 2 and 4 respectively. In fact in curve 4 of Fig. 10 the change of slope at 108 volts seems definitely to be absent.

Fig. 11 contains derived curves of two runs from 120 to 190 volts. In comparing the magnitude of the changes of slope in Fig. 10 with the variations between $4A$ and $4B$, the differences in the scale factors should be noted. These curves show no significant critical changes of slope in state 4. In Figs. 12 and 13, the slope change which appeared at about 207 volts in state 3 has disappeared in state 4.

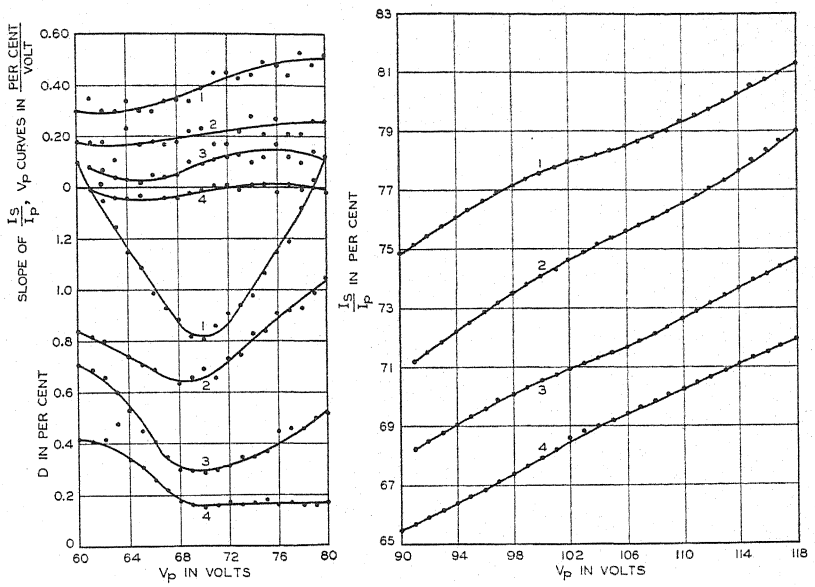


Fig. 8. Secondary electron characteristics of tungsten from 60 to 80 volts. Slope curves: Curve 1: Subtract 0.2 from ordinate. Curve 2: Add 0.1 to ordinate. Curve 3: Add 0.2 to ordinate. Curve 4: Add 0.3 to ordinate.

Fig. 9. Secondary electron characteristics of tungsten from 90 to 118 volts. Curve 1: Subtract 10 from ordinate. Curve 2: Subtract 4 from ordinate. Curve 3: Subtract 2 from ordinate.

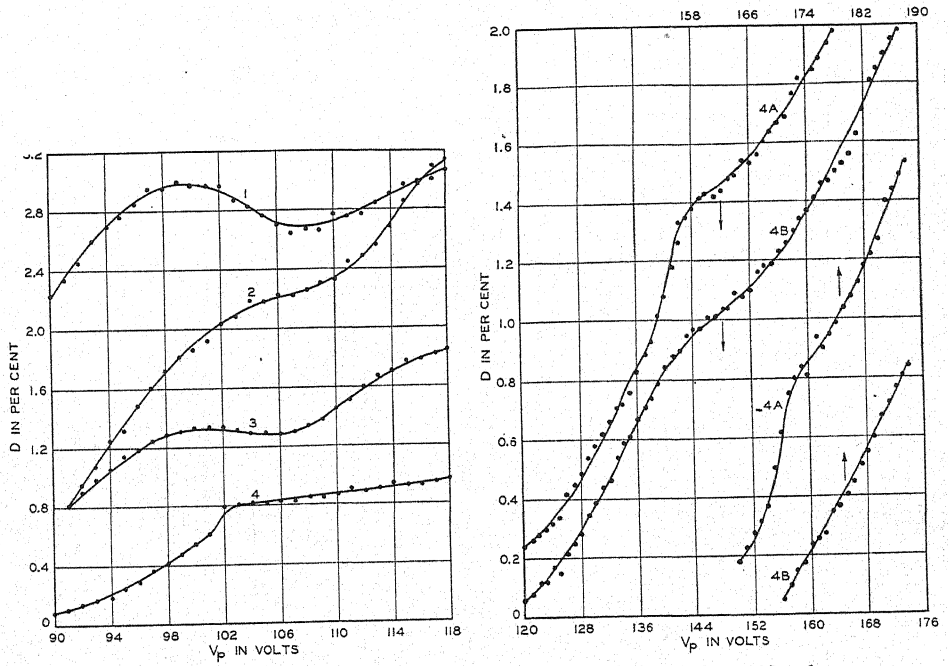


Fig. 10. Secondary electron characteristics of tungsten from 90 to 118 volts.
Fig. 11. Secondary electron chacteracteristi s of tungsten from 120 to 190 volts.

Fig. 14 contains derived curves for two runs in the state 4 from 220 to 276 volts and from 310 to 364 volts. In Figs. 13, 14, 15 and 16, there are some places where different portions of the curves do not fit together. As shown in the curves, these discontinuities are not reproduced in the same place when the scale is shifted. The points on the voltage axis at which the galvanometer readings were shifted by means of the annulling current circuit of Fig. 1 from one end of the galvanometer scale to the other are marked on the curves with short vertical lines. They agree nicely with the discontinuities in the curves and it therefore seems reasonable that the latter are the result of slight de-

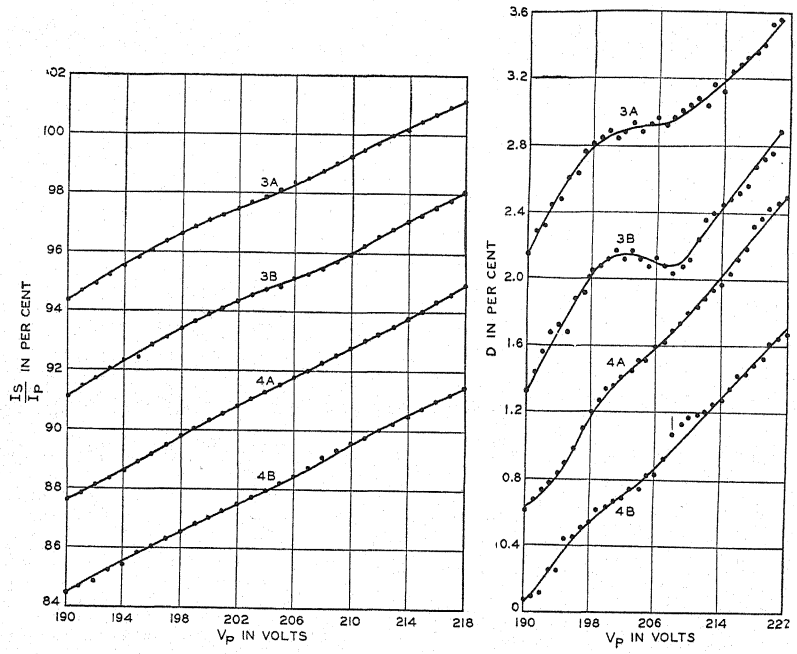


Fig. 12. Secondary electron characteristics of tungsten from 190 to 218 volts. Curve 3A: Subtract 7 from ordinate. Curve 4B: Add 3 to ordinate.

Fig. 13. Secondary electron characteristics of tungsten from 190 to 218 volts.

partures from linearity between galvanometer deflection and current at the extreme ends of the scale. The curves of Fig. 14 show no significant critical potentials. Fig. 15 shows a change of slope at about 297 volts in state 3, but it is absent in state 4.

The curves of Fig. 16 show no significant changes of slope between 360 and 490 volts. The measurements given in Fig. 16 were made with the target at tube temperature. The filament *H* burned out in giving the 1800° heat treatment of state 4 as described at the beginning of section 4. However, the measurements were completed within six hours after the target was reduced to tube temperature.

As discussed early in this section, in states 1 and 3 the measurements were made with the target at tube temperature and after it had stood for a long

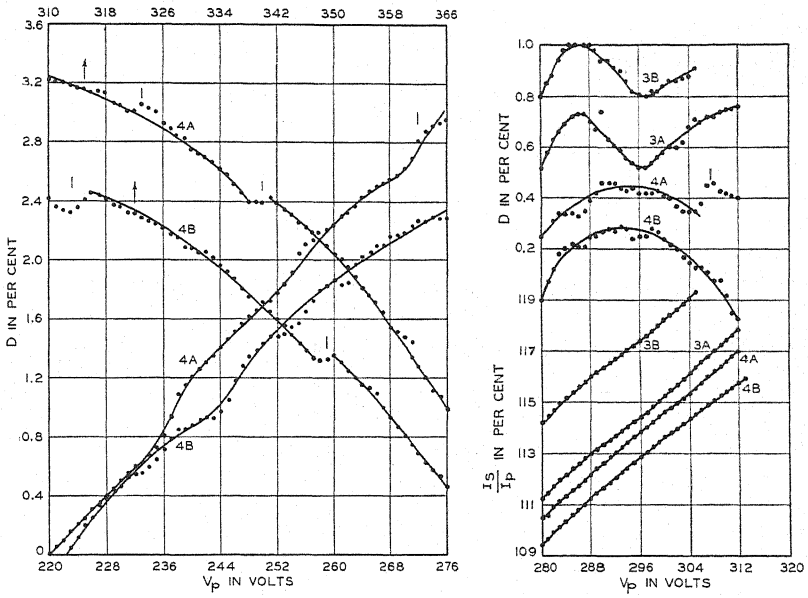


Fig. 14. Secondary electron characteristics of tungsten from 220 to 276 and from 310 to 364volts. See discussion of Fig. 14 in section on results for meaning of short vertical lines.
Fig. 15. Secondary electron characteristics of tungsten from 280 to 312 volts.

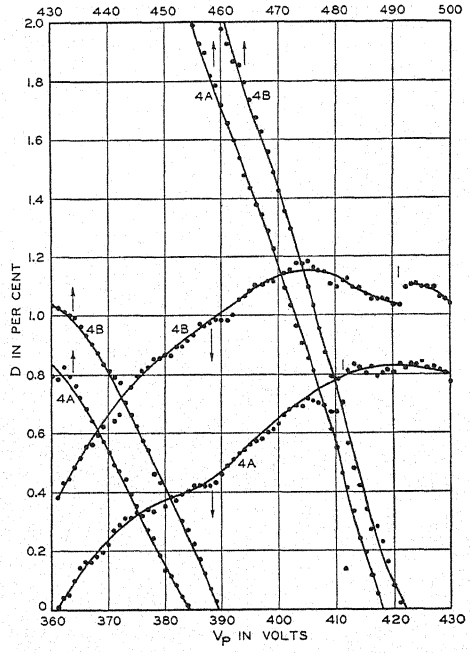


Fig. 16. Secondary electron characteristics of tungsten from 360 to 490 volts.

time without any heat treatment whatever. On the other hand, in states 2 and 4 the measurements were made with the tungsten target at about 1200 and 1300°K after certain heat treatments had been given. It seems most probable that states 1 and 3 correspond to a relatively contaminated surface as compared with states 2 and 4, and that the tungsten surface is most free from contamination in state 4.

In summarizing the observed effects, their variation from state to state is to be emphasized. In the low voltage region, as we progress from state 1 to state 2 and likewise from state 2 to state 4 (state 3 agreeing well with state 4) maxima are observed near former slope changes.

Proceeding from states 1 and 3 to states 2 and 4 respectively, the magnitude of the slope change at about 33 volts decreased as shown by Fig. 6. Also, the transition from state 2 to state 3 has increased the change of slope of curve 3 over curve 1 as well as curve 4 over curve 2. It is to be noted that in the transition from state 2 to state 3 the increase in slope at about 20 volts disappears and another appears at about 24 volts.

The data from 40 to 500 volts may be generalized as follows. In going from state 1 to state 2 and also from state 3 to state 4 the magnitude of the slope changes were always decreased. In this region only 4 critical potentials were observed even with the sensitive methods of measuring and graphing the data, and all but one of these disappeared in state 4.

Thus critical increases of slope at 70, 108, 208 and 297 volts were the only ones ever observed beyond 40 volts. Of these, only the 70 volt one persisted in state 4, and it was greatly weakened in intensity.

Thus in state 4, the state in which the tungsten surface is most free from contamination, only the following critical potentials have persisted; maxima at about 3.5 and 8 volts and slope increases at 24, 33 and 70 volts. These values are merely the applied voltages uncorrected for contact potential, etc

Discussion

It seems reasonable that the critical potentials observed in this work are characteristic of the tungsten target and are not caused by peculiarities of the tube. If in the primary beam there were secondary electrons which were emitted from the nickel of the electron gun, any critical potentials for nickel would introduce critical potentials in the measurements which would not be characteristic of tungsten. The curves of Fig. 2 indicate that the primary beam is free of secondary electrons from the nickel and therefore this possibility seems eliminated.

In contrast to these results, in the work of Krefft[3] on the secondary electron emission of tungsten between 25 and 500 volts, 25 critical potentials are indicated on his curves, 16 of which are indicated as remaining in measurements with the tungsten target at 1450°K. He used only one galvanometer to measure both the primary and secondary current. It was not operated at maximum sensitivity in the measurements. His slope changes were indicated on the experimental curves rather than on derived curves which are more

sensitive to slope changes. Thus, due to the more sensitive methods of measuring and plotting the data, slope changes, which in Krefft's curves are just noticeable would be quite prominent in the present work if they occurred. Moreover slope changes would have to be considerably smaller than in Krefft's work in order to escape detection.

Krefft states that secondary electrons from the metal of the electron gun were present in the primary beam. As pointed out at the beginning of this section, these might introduce spurious critical potentials.

Critical potentials in the emission of secondary electrons have been associated with the diffraction of electrons and the production of characteristic soft x-rays. The most recent measurements on the production of characteristic soft x-rays of tungsten are those of Richardson and Rao.[6] The characteristic soft x-rays were detected photoelectrically. The experimental arrangements were such that the x-rays were produced by electrons some of which had the distribution in velocity characteristic of the electrons coming from the thermionic source and the others the distribution which is characteristic of secondary electron emission of the x-ray target. Thus any critical potentials in the emission of secondary electrons, in reflection of electrons with or without energy losses, or in the diffraction of electrons by the x-ray target would produce slope changes in the excitation of continuous x-rays which might be observable. These in turn would be interpreted as critical potentials for the production of characteristic x-rays. It would seem that before a relation between secondary electron and soft x-ray critical potentials could be established, these ambiguities must be eliminated. Unfortunately there are as yet little spectroscopic data on soft x-rays of tungsten to compare with these photoelectric measurements on soft x-rays.

From about 25 to 500 volts, Richardson and Rao report about 60 critical potentials for the production of soft x-rays in tungsten. Over the same voltage range Krefft reported 25 critical potentials for the production of secondary electrons 9 of which disappeared after certain heat treatments. In the present work only 6 critical potentials were observed in this range and only three of these survived the heat treatment described in section 4. So far as the number of critical potentials is concerned, the marked difference between the three experiments makes any connection between them improbable.

Data on the diffraction of electrons from polycrystalline tungsten are not yet known. It may be that in state 4 the maxima at 3.5 and 8 volts and the critical increases of slope at 24 and 33 volts as well as other low voltage effects are diffraction phenomena.

Regardless of the mechanism producing the slope changes, their diminution or elimination beyond 40 volts points strongly to effects of surface contamination rather than to characteristics of tungsten.

This work was begun at the University of Minnesota. With an experimental tube which was kept on the pumps, consistent results were not ob-

[6] Richardson and Rao, Roy. Soc. Proc. **A128**, 16 (1930).

tained. Time did not allow the improvement in vacuum technique which was thought necessary.

The author is indebted to Drs. M. J. Kelly and H. E. Mendenhall for the opportunity and facilities to continue the work at Bell Telephone Laboratories and for helpful discussions of the work and to Dr. C. J. Davisson for suggestions and criticisms. The general problem was suggested by Professor John T. Tate to whom the author is grateful for suggestions and criticisms given during the progress of the experiments.

THE DETERMINATION OF THE PHOTOELECTRIC THRESHOLD FOR TUNGSTEN BY FOWLER'S METHOD

By A. H. Warner
University of California at Los Angeles

(Received October 12, 1931)

Abstract

The photocurrent per unit intensity curves for two different tungsten surfaces have been replotted by means of the method suggested by R. H. Fowler. The points all fit the theoretical curve very well, although the thresholds for the two surfaces are different. For one surface the data were obtained at temperatures of 1100, 900 and 790°K. The average value of the threshold at 0°K was 2632A, or 4.69 volts, with a greatest difference between individual values of 1.3 percent. The thermionic work function of this surface was 4.71 volts. The second surface was investigated at room temperature, and was formed by evaporation after very careful outgassing. The threshold for this surface was 2720A or 4.54 volts at 0°K, which agrees with Dushman's value of 4.54 volts for the thermionic work function at the same temperature. This should be regarded as the most reliable value.

IN AN earlier paper by the author[1] a value of the photoelectric threshold for tungsten was reported, based upon photocurrent per unit intensity curves made at various temperatures up to 1100°K. The value there given was 2575A, or 4.79 volts.

This value was of necessity based upon the measurements made at temperatures above 700°K, since below this the currents were too small to be determined accurately. This increase in current with temperature was apparently not accompanied by a shift in threshold, and was ascribed to the elimination of a contaminating gas layer from the surface.

In order to obtain larger currents at room temperatures, a tube was constructed with two central tungsten filaments, from one of which tungsten was evaporated upon the wall of the tube after the utmost precautions had been taken to eliminate all traces of gas, and the tube had been sealed off from the pump. The evaporation acted as a further clean up and it is felt that any contamination that may exist must be due to impurities contained in the tungsten itself.

The second filament and the evaporated coating are both illuminated through a quartz window, which is fastened to the Pyrex tube by means of a graded seal. The reaction of the filament which is of small area is too small to be detected at any temperature by a Dolazalek electrometer. Excellent results are obtained from the coating on the walls, which is maintained at room temperature. A more sensitive electrometer has been obtained and further work with the filament should be possible.

[1] A. H. Warner, Phys. Rev. **33**, 815 (1929).

It is the purpose of this paper to reexamine the data from both tubes by means of the method suggested by Fowler,[2] and to compare the results obtained.

Tungsten Filament

The current per unit intensity curves for the first tube are shown in Fig. 1. A Hilger quartz monochromator was used, with 0.05 inch slit width. This did not provide as monochromatic a beam as is desirable, but smaller slits gave too small currents. Readings taken at ten Angstrom intervals between 2350A and 2600A show that there was considerable overlapping of the lines.

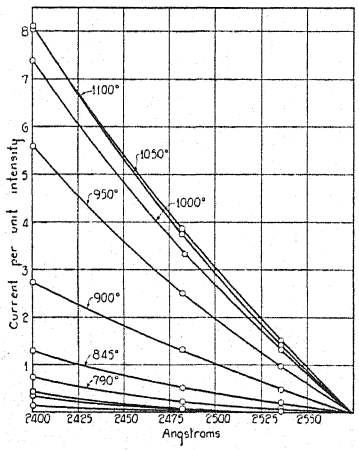


Fig. 1.

The intensities of the lines were governed by adjusting the current, voltage and temperature of the arc to agree with conditions under which Kazda[3] made a careful determination of relative line intensities. This method is subject to error unless the optical path is also identical with the one used by Kazda. While the same type of monochromator was used, there undoubtedly were small differences in the quartz windows of the cell, and the quartz of the arc itself.

In accordance with Fowler's method log I/T^2 has been plotted against $h\nu/kT$ for 1100°K, 900°K and 790°K. (Fig. 2.) The horizontal shifts necessary to bring the experimental curves into concidence with the theoretical are given in Table I.

Table I.

°K	$h\nu_0/kT$	$\lambda_0 A$	ϕ_0 (volts)	Average
1100	49.8	2619	4.71	$\lambda_0=2632$
900	60.0	2650	4.65	$\phi_0=4.69$
790	69.0	2626	4.70	

[2] R. H. Fowler, Phys. Rev. **38**, 45 (1931).
[3] C. B. Kazda, Phys. Rev. **26**, 643 (1925).

It can be seen that the points agree very well with the theoretical curve, and that the variation in λ_0 is small.

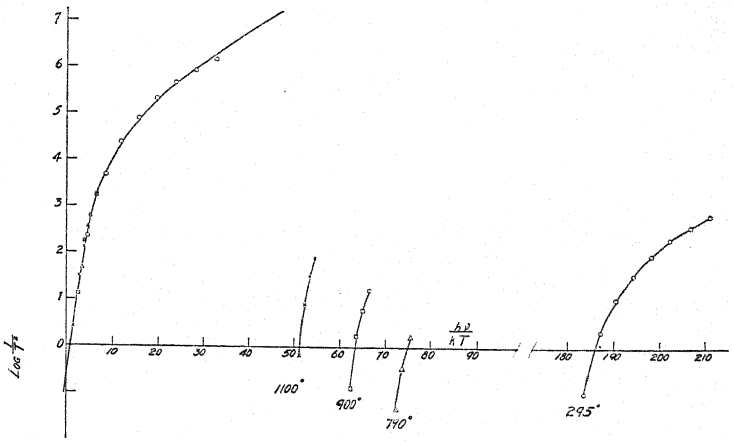


Fig. 2.

Evaporated Surface

The current per unit intensity curve for the evaporated surface in the second tube is shown in Fig. 3, which also shows the photoelectric response of

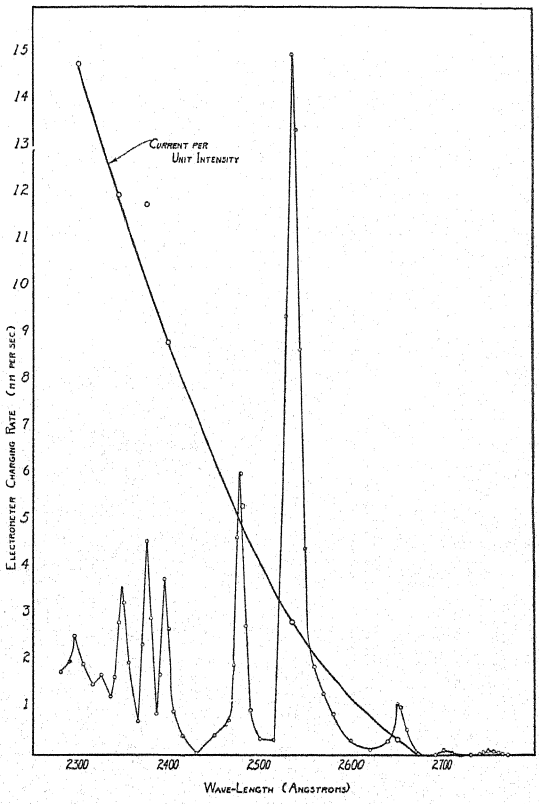


Fig. 3.

the surface as a function of wave-length. A Bausch and Lomb monochromator was used, with both entrance and exit slits set at 0.002 inch. As a result a very monochromatic beam was obtained, as is shown by the resolution of the lines of the mercury arc.

The intensities of the lines were determined by using Kazda's technique. The use of fine slits to obtain a highly monochromatic beam reduces the energy in the transmitted beam to such a low value that some method of extrapolation from a determination with wider slits is necessary. The use of Kazda's values, uncorrected for the change in type of monochromator introduces some uncertainty in the values of the intensities. The points of the current per unit intensity are quite consistent in spite of this.

The plot of these data according to Fowler's method is also shown in Fig. 2. The points fall very nicely upon the theoretical curve, and the $h\nu/kT$ shift gives the value of the threshold as 2720A, or 4.54 volts. The value from the current per unit intensity curve is between 2675A, or 4.61 volts, and 2750A, or 4.49 volts.

There was still a measurable current at 2700A, and investigation revealed that the surface was slightly sensitive to wave-lengths as long as 5600A. This is to be ascribed to traces of thorium. A sample of the wire used for the filament was mounted in a tube in which its thermionic properties could be investigated. It was found possible to activate it so that the work function agreed with the values given by Kingdon for a tungsten wire covered with thorium. (2.76 volts, 4470A.) The threshold for thorium on a tungsten surface is being studied and will be reported in a later paper.

It is to be expected from theoretical grounds that the photoelectric and thermionic work functions are equal. Dushman's[4] very careful thermionic work gave a value of 4.54 volts for pure tungsten. The photoelectric value (4.54 volts) for the evaporated surface, calculated by Fowler's method, is in complete agreement with this. The value given by Dushman is b_0 and should be independent of temperature. The photoelectric value obtained by Fowler's method should also be independent of temperature. These values then may be considered to be the work function at 0°K, and are found to be equal where the photoelectric measurements were made upon a tungsten surface formed by evaporation in a high vacuum.

The accuracy of the photoelectric determination depends upon the measurement of the current and the line intensities, upon the precision with which the $h\nu/kT$ shift can be determined when the experimental curve is superimposed upon the theoretical one, and upon the measurement of the temperature.

The positions of the points on the curve showing the photoelectric response as a function of wave-length were determined by taking several readings for each wave-length used and averaging. The readings never differed by more than a few percent. The values of the currents for the various lines were taken from the maxima exhibited by the final curve. The sharpness of

[4] S. Dushman, Phys. Rev. **25**, 338 (1925).

these peaks introduces some uncertainty, but it is thought their heights can be determined within two percent.

The determination of line intensities introduces an uncertain error. Two points of the current per unit intensity curve fall off the best curve through the other points. A redetermination of the intensities is being made.

The $h\nu/kT$ shift can be made quite accurately. In this case the shift is large (178.8), and should be accurate to better than one percent. The temperature was also determined quite accurately.

The accuracy of the current per unit intensity determination of the threshold depends largely upon the points in the vicinity of the intercept. If the small currents for 2700A and 2750A are included, the curve becomes parallel with the axis. The presence of the sensitive impurity is largely responsible for these currents, but it is probable that the tungsten also contributes slightly to the current at 2700A. From these considerations it would seem that the threshold should lie in the region between 2675A and 2750A with its most probable value at 2720A, as given by the Fowler method.

Conclusions

The value given by the work at higher temperatures (2630A, 4.69 volts) must be considered as less reliable, due to the presence of a contamination that inhibited the activity of the surface. This threshold was undoubtedly characteristic of the surface, as the thermionic work function agreed very closely. The variance of the latter from the commonly accepted value may be accepted as conclusive evidence that the surface was not perfectly clean.

The data from both tubes are seen to fit the Fowler theoretical curve. The threshold for the evaporated surface of tungsten at 0°K calculated by Fowler's method agrees extremely well with the value to be expected from the thermionic work function at the same temperature as determined by Dushman. This value is 4.54 volts, or 2720A.

The author is greatly indebted to Dr. R. A. Millikan for his generosity in placing the facilities of the Norman Bridge Laboratory of the California Institute of Technology at his disposal.

THE TEMPERATURE OF THE LOWER ATMOSPHERE OF THE EARTH*

By E. O. Hulburt
Naval Research Laboratory

(Received October 9, 1931)

Abstract

From the known amounts of the various gases of the atmosphere from sea level to about 20 km, from the observed light absorption coefficients of the gases and from the albedo of the earth's surface the temperature of the atmosphere in radiative equilibrium is calculated on the assumption that the sunlight is the only source of energy. The calculation is perhaps more rigorous than has hitherto been attempted, although it contains a number of approximations. The sea level temperature comes out to be about 19° above the observed world-wide average value 287°K, and the temperature above about 3 km falls many degrees below the observed temperatures. The temperature gradient in levels from 3 to 6 km is greater than that of convective equilibrium and hence the atmosphere would not be dynamically stable if radiation equilibrium prevailed. Therefore air currents take place to bring about convective equilibrium. Continuing the calculation it is found that only when the convective region extends to about 12 km (as is observed), with radiative equilibrium above 12 km (as is observed), does the atmosphere satisfy the conditions of dynamic stability and thermal equilibrium with the received solar energy. For this case the calculated sea level temperature is 290°K in good agreement with the observed value 287°K. Calculation shows that doubling or tripling the amount of the carbon dioxide of the atmosphere increases the average sea level temperature by about 4° and 7°K, respectively; halving or reducing to zero the carbon dioxide decreases the temperature by similar amounts. Such changes in temperature are about the same as those which occur when the earth passes from an ice age to a warm age, or *vice versa*. Thus the calculation indicates that the carbon dioxide theory of the ice ages, originally proposed by Tyndall, is a possible theory.

Introduction

1. IT IS generally accepted that the most important source of heat energy on the surface of the earth is the light of the sun. The only other known source of possible importance, namely, the leakage of heat to the surface by conduction from the interior of the earth, is relatively small, being less than one ten-thousandth of the energy of sunlight. It should therefore be possible to calculate the surface temperature of the earth and the temperature of the atmosphere to various heights above sea level on the assumption that the earth and the atmosphere radiate away to space an amount of energy equal to that received from the sun. Such a calculation requires a knowledge of the amounts of the gases of the atmosphere at all levels from sea level upward, the absorption coefficients of the gases throughout the optical spectrum, the reflecting power of the surface of the earth, the mixing action of winds, and other quantities. The problem has never been worked out completely. In the present paper an attempt at a fairly rigorous solution is presented, although

* Published with the permission of the Navy Department. Read before the National Academy of Sciences April 27, 1931.

it contains a number of approximations, and fair agreement is found with the observed temperatures of the earth and the atmosphere. In the process of working out the problem one is led to an understanding of the effects of radiation and convection on the values of the temperatures. In important papers on the subject Gold[1] discussed types of atmospheres which could be in convective and radiative equilibrium and Maris[2] derived conclusions about the temperatures, mainly of the high atmosphere, from calculations of the rates of energy absorption and radiation in various levels of the atmosphere.

The Observed Temperatures of the Atmosphere

2. The sea level temperature averaged over the earth is 287°Kelvin, or 14° Centigrade. The average temperatures t°K of the atmosphere are plotted as abscissas against the height z above sea level in the dotted curves 1′ and 1″, Fig. 1, which refer to summer and winter conditions, respectively. The

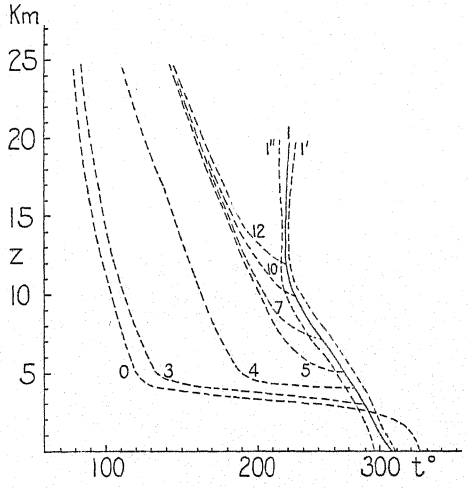


Fig. 1. Curves 1′ and 1″ give the observed temperatures t of the atmosphere at various heights z above sea level, for summer and winter, respectively, curve 1 is the average of 1′ and 1″ and the other curves are theoretical.

data[3] were obtained from 416 souding balloon flights in the years 1900 to 1912 in Europe and hence refer to a north latitude of about 50°. Curve 1, Fig. 1, is the average of the abscissas of curves 1′ and 1″ with the exception of the point at sea level which was plotted at 287°. We assume that curve 1 represents the world-wide average temperatures of the atmosphere, a questionable assumption, but perhaps not far wrong.

It is seen from curve 1, Fig. 1, that t falls off rapidly to about 220°K at $z=10$ or 12 km and is roughly constant from $z=12$ to 20 km. From $z=0$ to about 12 km the winds are relatively swift; this is known as the "convective

[1] Gold, Proc. Roy. Soc. **82,** 43 (1909); later discussed by Emden, Sitz. d. K. Akad. Wiss. zu München, page 55 (1913), and by Milne, Phil. Mag. **44,** 872 (1922).

[2] Maris, Terr. Mag. and Atmos. Elec. **33,** 233 (1928); **34,** 45 (1929).

[3] Humphreys, "Physics of the Air," 2nd Ed., 55 (1929).

region" (or the "troposphere"). From $z=12$ to 20 km, spoken of as the "isothermal region" (or the "stratosphere"), the winds are relatively slow. The temperature of the isothermal region over the equator is usually around 200° K and over polar regions is around 230°K. The height where the isothermal region sets in is about 15 km at the equator and decreases with increasing latitude. At any locality it may vary up and down 5 km or so with weather or other conditions, in polar regions it may descend to the surface of the earth.

In the convective region the atmosphere is in adiabatic equilibrium, but only approximately so. The theoretical adiabatic temperature gradient[4] is about 10 degrees km^{-1}, which gives a temperature of 187° at 10 km for a sea level temperature 287°. The observed value at 10 km is about 220° so that the atmosphere is warmer than it would be if adiabatic equilibrium prevailed. There are a number of factors which together are probably adequate to account for this,[2] such as the heat carried upward by water vapor, the effect of winds blowing from warm to cold regions, the direct absorption of the incoming sunlight by the atmosphere, etc. Hereafter we shall use the portion of curve 1, Fig. 1, from $z=0$ to 12 km as the curve of adiabatic or convective equilibrium. In so doing we take into account after a fashion the transport of heat energy by moisture and the other factors.

The present paper grew out of an attempt to find the answer to three inter-related questions, (1) why is the average sea level temperature about 287°K, (2) why does convection hold sway to about 10 or 12 km and not above, and (3) why is the temperature constant with height from about 12 to 20 km? In their pioneer papers Humphreys[5] and Gold[1] from considerations of radiation equilibrium showed that the average-in-height temperature of the absorbing layers of the atmosphere would not be below 212°K. Gold went a step farther and showed that if the atmosphere consists of two shells, the inner in the adiabatic and the outer in the isothermal state, the inner must extend to a level above 0.5 km but not greatly above 1 km. No detailed answers to the three questions were presented; the answers arrived at in the present paper are given in sections 11 and 12.

The Light Absorption Coefficients of the Gases of the Atmosphere

3. The absorption coefficient α of a gas for light of wave-length λ is defined by

$$I = I_0 \epsilon^{-\alpha x},$$

where I_0 is the original intensity of the light and I is the intensity after passing through x cm of the gas at standard conditions, i.e. 0°C and atmospheric pressure. In the present calculations we are interested primarily in the infrared region of the spectrum and the only gases of the atmosphere which are known to have important absorption bands in this region are water vapor, carbon dioxide and ozone. The values of α for these gases, taken from the tabulations of Maris[2], are plotted in Fig. 2 as ordinates against λ in μ as abscissas. Maris obtained the values of α for water vapor and carbon dioxide by

[4] See, for example, Jeans "The Dynamical Theory of Gases," page 336 (1925).
[5] Humphreys, Astrophys. J. 29, 14 (1909).

calculation from the tables of Gold[1] who summarized the measurements of Paschen, Rubens and Aschkinass, Angström, Langley and others, made over 30 years ago. In the case of carbon dioxide only the average values of α across the various absorption bands are known, hence the flat tops of the carbon dioxide curve of Fig. 2. The shape of the absorption curve across several of the carbon dioxide bands has been observed, for example the 12.5 to 16μ band is given[6] roughly by the dotted curve a, Fig. 2, but the data are not sufficient to enable one to calculate with any certainty the exact values of α across the bands. Maris calculated the values of α for ozone given in Fig. 2 from rather

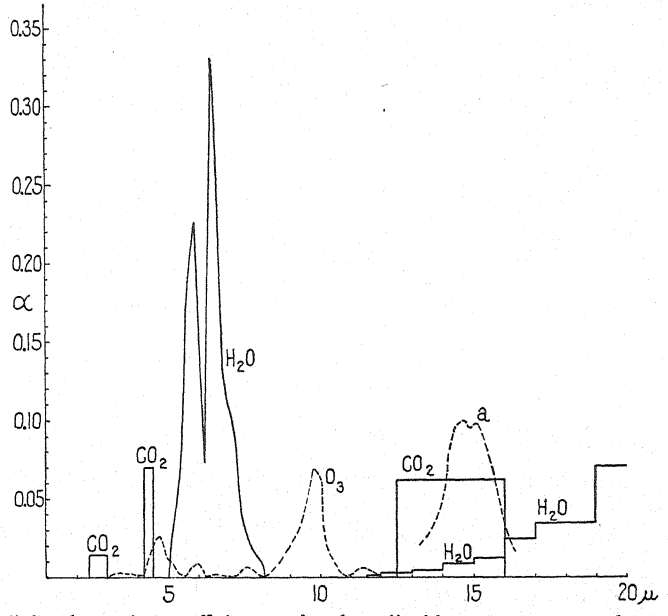


Fig. 2. The light absorption coeffieicnt α of carbon dioxide, water vapor and ozone; for ozone the scale of ordinates must be multiplied by 10.

conflicting measurements of Fabry[7] and of Ladenburg and Lehmann.[8] In general recent investigators have been interested in determining the fine structure, etc., of the bands and not in getting accurate absorption coefficients. It may be hoped that more exact values of α will be obtained with modern infrared spectrographic technique. This would enable the calculations of this paper to be improved, not however very easily. Several approximations, perhaps permissible under the present circumstances, would no longer be so, and to carry out the mathematical analysis without the approximations will be a matter of some labor.

The Distribution of Carbon Dioxide, Water Vapor, and Ozone Up Through the Atmosphere

4. Denote by x cm the equivalent thickness, reduced to standard condi-

[6] Burmeister, Verh. d. Deutsch. Phys. Gesell. **15**, 589 (1913).
[7] Fabry, Proc. Phys. Soc. London **39**, 1 (1926).
[8] Ladenburg and Lehmann **21**, 305 (1906).

tions, of a gas in the atmosphere from sea level to a height z. Let x_b cm be the thickness from sea level to infinity, i.e. outside of the atmosphere; x_b may be spoken of as the thickness to the "top" of the atmosphere. Then $x_b - x$ is the thickness of the gas from any level to infinity. The values of x and $x_b - x$ for carbon dioxide and water vapor are given in Table I. The values for carbon dioxide were calculated from standard tables, e.g. those of Maris[2], of the partial pressures of the gases of the atmosphere; the tables were of course based on direct observations. The values for water vapor were calculated from the pressures of saturated water vapor at the temperatures of the atmosphere given by curve 1, Fig. 1. $x_b = 3300$ cm, which amounts to 2.56 grams of water in a 1 cm vertical column of the atmosphere; this is in agreement with the value 2.6 grams deducible from Arrhenius' values of average humidity.[9] It is assumed that the values of Table I represent world-wide averages. This is satisfactory for carbon dioxide, which is very constant over the earth, but is perhaps questionable for water vapor, which varies tremendously with the weather, etc.

TABLE I.

	Carbon dioxide		Water vapor		Average
z	x	$x_b - x$	x	$x_b - x$	$\alpha(x_b - x)$
0 km	0 cm	252 cm	0 cm	3300 cm	145
3	102	150	2590	410	60
5	142	110	3080	220	5.2
7	164	88	3250	50	3.8
10	192	60	3276	24	2.3
12	207	45	3285	15	1.67
15	225	27	3291	9	1.00
20	239	13	3295	5	0.44
∞	252	0	3300	0	0

For ozone x_b is about 0.3 cm. Ozone exists in the levels above about 50 km[7]. Its distribution with height is not known, but we do not need to know the distribution, for in the present paper we are content to deal with the effects of ozone in a very simple way, as described in section 13.

THE TEMPERATURE OF THE SURFACE OF THE EARTH WARMED BY THE SUN AND ASSUMED TO HAVE NO ABSORBING ATMOSPHERE

5. The solar constant S, i.e. the energy of the sunlight falling on the outside of the atmosphere in the spectrum region from 0.3 to about 3μ, is 1.35×10^6 erg cm^{-2} sec.$^{-1}$. Of this energy about 30 percent is absorbed in the atmosphere[10], mainly in the levels below 10 km, so that only about 70 percent reaches sea level. However, for reasons given in section 10, we assume that the atmosphere is perfectly transparent to the incoming solar radiation and thus treat the 30 percent on the same basis as the 70 percent. The clouds and surface of the earth reflect away to space about 32 percent of the sunlight (reference 3, page 84). Therefore a fraction 68 percent, denoted by A, of the solar energy is absorbed by the earth.

[9] Arrhenius, Phil. Mag. **41**, 264 (1896).

[10] Abbott and Fowle, Annals Astrophys. Obs., Smithsonian Inst., **2**, 173 (1908).

The Stefan-Boltzmann law for the energy E erg cm^{-2} sec.$^{-1}$ radiated by a black body at a temperature t°K is

$$E = \sigma t^4, \tag{1}$$

where $\sigma = 5.71 \times 10^{-5}$ erg deg.$^{-4}$. If the earth had no atmosphere and were in thermal equilibrium with the sun's radiation we have, since the earth receives the sunlight as a disk and radiates as a sphere,

$$4\pi r^2 \sigma t_0^4 = \pi r^2 SA, \tag{2}$$

where r is the radius of the earth, t_0 the temperature of the surface and A is 68 percent. This gives

$$t_0^4 = SA/4\sigma, \tag{3}$$

or

$$t_0 = 252°.$$

t_0 is the black-body temperature. The true temperature t_0' of the earth's surface is given by

$$at_0'^4 = t_0^4, \tag{4}$$

where a is the fraction of the radiation of a black body at temperature t_0 absorbed by the surface (a is also known as the "emissive power"). If $a = 1$ the surface is a black body and $t_0' = t_0$; if $a < 1$ the surface is not a black body and $t'_0 > t_0$. Although a for the surface of the earth, including the clouds, is about 0.68 for radiation from 0.2 to 3μ, the value of a for radiation of longer wave-lengths is not known. The longer wave-lengths are of importance because t_0 is actually about 287°K and a black body at this temperature radiates mainly in the range from 3 to 30μ (see Fig. 4). We shall assume that $a = 1$, so that $t_0' = t_0$. The assumption is probably not far from the truth because 7/8 of the earth's surface is water and water is absorbent to the longer infrared radiations. The variation of a for the land with changes in climate may be important (see section 14).

The Temperature of the Atmosphere and of the Surface of the Earth in Radiative Equilibrium

6. It is assumed that heat energy is transferred through the atmosphere only by radiative processes. This amounts to assuming that convection is absent, for conduction is on the whole negligibly small compared to radiation or convection. Take the pressures of the atmosphere and the amounts of the component gases at various heights to be those observed, i.e., as given in Table I. Assume, as in section 5, that the atmosphere is transparent to the incoming solar radiation of which 32 percent is reflected out to space by the surface of the earth and the clouds. Thus on the average each cm^2 of the earth's surface absorbs $SA/4$ erg sec.$^{-1}$, where A is 68 percent. The surface is assumed to radiate this energy in the form of black-body radiation (see section 5) upward to the atmosphere which transmits some of the radiation and absorbs some of it. The atmosphere is heated by the radiation which it absorbs and reradiates the energy upward and downward, the downward radia-

tion warming the earth. Thus each layer of the atmosphere is subjected to an upward and a downward stream of radiation. The condition of radiative equilibrium is that the temperature distribution out through the atmosphere be such that each level of the atmosphere radiate as much energy as it absorb and that the energy leaving the top of the atmosphere be equal to $SA/4$.

The first step in expressing the foregoing ideas in mathematical terms is to make an approximation by replacing the complicated absorption bands of Fig. 2 by a single equivalent absorption band of average absorption coefficient α across the band. This simplifies the equations very much. The conclusions which we reach are not appreciably troubled by the approximation. A more exact treatment is hardly justified at the present time in view of the uncertainties in the values of the absorption coefficients and other quantities.

Let the energy emitted from the surface of the earth be E erg cm^{-2} sec.$^{-1}$. Let ϕ be a fraction such that ϕE be the portion of E comprised in those wave-lengths of the spectrum to which the atmosphere is perfectly transparent. Then $(1-\phi)\,E$ is the energy in the wave-lengths absorbed by the atmosphere. The quanities are shown diagrammatically in Fig. 3a, in which the area under the black body curve is E and the shaded portion is $(1-\phi)E$. The earth receives and absorbs $SA/4$ erg cm^{-2} sec.$^{-1}$ from the sun and a certain amount of energy sent down by the atmosphere, and radiates ϕE directly to space and $(1-\phi)E$ which is absorbed by the atmosphere (see Fig. 3).

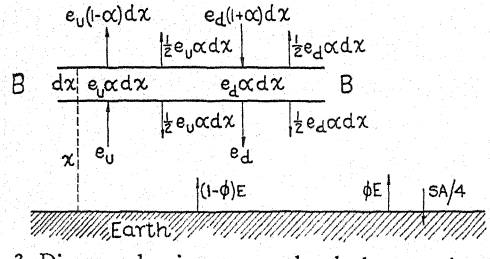


Fig. 3. Diagram showing energy absorbed, transmitted and emitted by an elementary layer BB of the atmosphere.

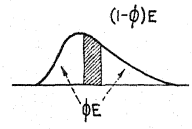


Fig. 3a.

Consider a horizontal layer of the atmosphere at a height x or z cm above sea level, shown by BB, Fig. 3. Let the thickness of the layer be dx. At the layer there is an upward stream of radiation e_u erg cm^{-2} sec.$^{-1}$ and a downward stream e_d, the streams of radiation comprising only the wave-lengths in the single equivalent absorption band of the atmosphere. Of e_u an amount $e_u\alpha dx$ is absorbed by the layer, and an amount $e_u(1-\alpha dx)$ passes through. The absorbed energy is reradiated, $e_u\alpha dx/2$ upward and an equal amount downward (see Fig. 3); similarly for e_d. For radiation equilibrium the temperature t of the layer is expressed by the relation, obtained from the Stefan laws of radiation embodied in (1) and (4),

$$\tfrac{1}{2}(e_u + e_d)\alpha dx = f\sigma t^4 \alpha dx, \tag{5}$$

or

$$e_u + e_d = 2f\sigma t^4,$$

where f is the fraction of the energy of a black body at temperature t in the

region of the absorbed wave-lengths. In general f, e_u and e_d are functions of x.

Since the atmosphere can radiate only in the spectrum region of the absorption bands, the difference between the upward and downward radiation streams is constant at all heights. Hence

$$e_u - e_d = \text{constant} = SA/4 - \phi E. \tag{6}$$

Denote by de_u the change in e_u in the distance dx measured positively upward. Then de_u is equal to the upward radiation leaving the top side of the layer minus the upward radiation entering the lower side of the layer. Therefore, referring to Fig. 3,

$$\begin{aligned} de_u &= \tfrac{1}{2}e_u\alpha dx + e_u(1 - \alpha dx) + \tfrac{1}{2}e_d\alpha dx - e_u, \\ &= -\tfrac{1}{2}\alpha(e_u - e_d)dx. \end{aligned}$$

Substituting (6)

$$= -\tfrac{1}{2}\alpha(SA/4 - \phi E)dx.$$

Integrating

$$e_u = -\tfrac{1}{2}\alpha(SA/4 - \phi E)x + C, \tag{7}$$

where C is a constant of integration. At the top of the atmosphere $x = x_b$ and $e_u = SA/4 - \phi E$. Hence $C = (1 + \alpha x_b/2)(SA/4 - \phi E)$ and (7) becomes

$$e_u = (SA/4 - \phi E)[1 + \alpha(x_b - x)/2]. \tag{8}$$

Either by a similar derivation, or directly from (6) and (8), we find

$$e_d = (SA/4 - \phi E)[\alpha(x_b - x)/2]. \tag{9}$$

From (5), (8) and (9)

$$2f\sigma t^4 = (SA/4 - \phi E)[1 + \alpha(x_b - x)]. \tag{10}$$

Equation (10) gives t in terms of quantities all of which are known except E. To find E we make use of the fact that at sea level $x = 0$ and $e_u = (1 - \phi)E$. Substituting these values into (8) gives

$$E = \frac{SA}{4}\,\frac{1 + \alpha x_b/2}{1 + \phi\alpha x_b/2}. \tag{11}$$

From (1) $E = \sigma t_0^4$, where t_0 is the temperature of the surface of the earth, and (11) becomes

$$t_0^4 = \frac{SA}{4\sigma}\,\frac{1 + \alpha x_b/2}{1 + \phi\alpha x_b/2}. \tag{12}$$

Introducing (11) into (10) yields

$$t^4 = \frac{SA}{8\sigma f}\,\frac{1 - \phi}{1 + \phi\alpha x_b/2}[1 + \alpha(x_b - x)]. \tag{13}$$

Equations (13) and (12) are the desired relations which give the temperatures of the atmosphere and of the surface of the earth for the condition of radiation equilibrium. In the foregoing derivation we have neglected the curvature

of the earth, which introduces no appreciable error, and have regarded the atmosphere as sufficiently homogeneous so that reflection or scattering of the radiation does not occur, which is probably permissible above the cloud region. Further, we have dealt with the streams of radiation as though they flowed only in the vertical direction. Actually, the radiation is everywhere diffuse radiation, but the case of diffuse radiation is very closely given by the vertical radiation derivation for relatively great absorption such as occurs in the infrared bands of the water vapor and the carbon dioxide of the atmosphere. Maris (reference 2, page 245) proved this by a calculation using Gold's evaluation of a certain integral (reference 1, page 62).

7. We must distinguish between the temperatures of the bottom of the atmosphere and the surface of the earth; these of course are not necessarily the same when the energy exchanges occur only by radiation as is assumed in the present case. The temperature t_0 of the surface of the earth is given by (12), which, when the numerical values are substituted for S and A, reduces to

$$t_0 = 252\left(\frac{1+\alpha x_b/2}{1+\phi\alpha x_b/2}\right)^{1/4}. \tag{14}$$

The temperature of the bottom of the atmosphere, denoted by t_0'', is found by putting $x=0$ and $f=1-\phi$ in (13). This gives

$$t_0'' = 252\left(\frac{1}{2}\,\frac{1+\alpha x_b}{1+\phi\alpha x_b/2}\right)^{1/4}. \tag{15}$$

For an atmosphere which does not absorb at all, this being the same as the case of no atmosphere as far as radiation processes are concerned, $\phi=1$ and from (14) $t_0=252°\text{K}$. This agrees, as it should, with (3). For a weakly absorbing atmosphere αx_b and $\phi\alpha x_b$ are small compared to unity and (14) and (15) yield approximately

$$t_0 = t_0''(2)^{1/4}, \tag{16}$$

which is the well-known Schwartzchild[11] relation. For an atmosphere which absorbs strongly in its bands, as is the case of the water vapor and the carbon dioxide of the atmosphere, αx_b and $\phi\alpha x_b$ are large compared to unity, being of the order 10^2, and (14) and (15) give approximately

$$t_0 = t_0'' = 252(1/\phi)^{1/4}. \tag{17}$$

8. To determine ϕ and f of (12) and (13) the black-body energy curves for a number of temperatures were plotted in Fig. 4. Referring to Fig. 2 we see that there are three important regions of absorption, the first from about 5 to 8μ due to water vapor, the second from about 12 to 16μ due both to carbon dioxide and water vapor, and the third from about 16 to 20μ due to water vapor. In the curves of Fig. 4 these regions are shaded. The ratio of the shaded areas to the total area under the black-body curve, denoted by f_1, f_2 and f_3, respectively, are plotted as ordinates in Fig. 5 against the temperature t as

[11] Schwartzchild, Gött, Nach. page 41 (1906).

abscissa. The three absorption areas together make up the assumed equivalent single absorption band and hence from the definition of f (section 6) we have $f=f_1+f_2+f_3$. f is also plotted in Fig. 5. ϕ is one minus the value of f at sea level.

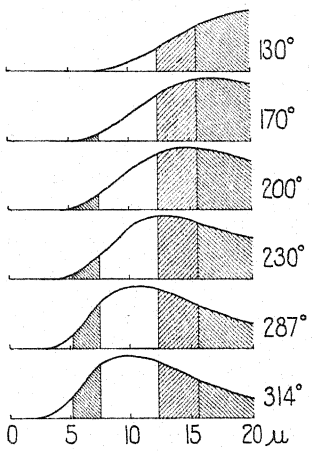


Fig. 4. Spectral energy curves of a black body at various temperatures.

We have left out of account the region of wave-lengths beyond 20μ simply because there are no observations of the absorption coefficients for this range of the spectrum. For example, it is not known whether water vapor is opaque or transparent to these wave-lengths. The method of calculating f

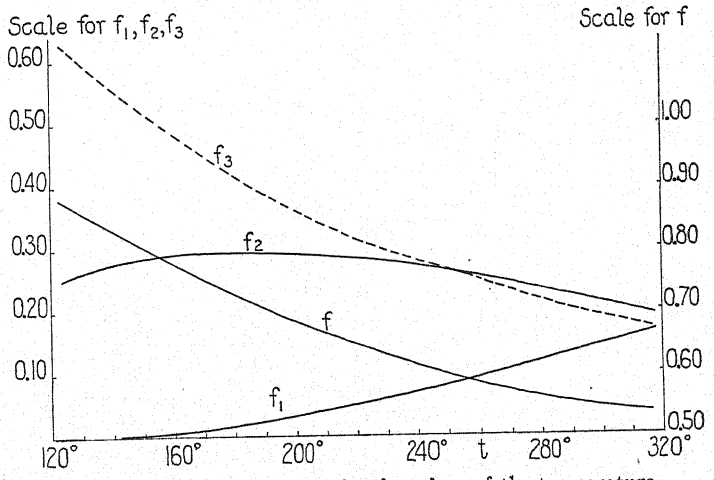


Fig. 5. Values of f_1, f_2, f_3 and f as functions of the temperature.

from the curves up to 20μ amounts to assuming that the atmospheric gases absorb in the region above 20μ to about the same extent as they do below 20μ; it is a sort of compromise between assuming that the atmosphere is either completely transparent or completely opaque to the longer wave-lengths.

The average values of the quantity $\alpha(x_b-x)$ which occurs in (13) were calculated approximately at each height z by combining the values for water vapor and carbon dioxide of Fig. 2. and Table I, weighing them according to the relative amounts of the two gases, the widths of the absorption bands and the average values of α across the bands. The values of $\alpha(x_b-x)$ are given in the last column of Table I. The "top" of the atmosphere is the region above which there is not enough atmosphere to cause appreciable absorption. From the values of α (x_b-x) it is seen that light in the wavelengths absorbed by the single equivalent absorption band is reduced to about 1/5, 1/2.7 and 1/1.5 of its original intensity in getting out to space from 12, 15 and 20 km levels, respectively. Therefore the "top" of the atmosphere is around 25 km.

From the values of $\alpha(x_b-x)$ and from (12) and (13) t and t_0 were calculated in the following way: t_0 was guessed and $1-\phi$ corresponding to t_0 was read off the f curve of Fig. 5. The values of t_0 and ϕ were substituted in (12) (or in (14) or (15)) and if the equation was satisfied t_0 was correct. If not, t_0 was guessed again and the procedure repeated until the correct values of t_0 and ϕ were obtained. These were put into (13) and the same method of successive approximations was used to determine t and f for each height z. The values of t are plotted in curve 0, Fig. 1, which gives the temperatures which would exist in the atmosphere if radiation equilibrium prevailed. The curve does not agree with the observed temperatures of curve 1, Fig. 1, giving a sea level temperature of 306° which is 19° above the observed value, and at levels above 5 km giving temperatures many degrees below those observed.

9. We digress for the moment to consider the effect on t_0 of changes in the carbon dioxide content of the atmosphere. From (14) it is found that doubling, or tripling, or reducing to zero the carbon dioxide of the atmosphere changes t_0 by less than 1° Centigrade. This same conlusion was reached by Angström,[12] Abbott,[13] Humphreys,[3] and others, as the result of qualitative discussions of terrestrial radiation which were perfectly correct as far as they went. However, the assumption of radiation equilibrium has led to atmospheric temperatures at variance with those observed. And we conclude, what was perhaps obvious from the start, that the physics of the atmosphere is not governed by radiation processes alone. So that any calculation of the possible effects on climate of changes in the carbon dioxide of the atmosphere must be left to a later section (section 14) after convection has been considered.

The Temperature of the Atmosphere Taking Into Account Convection and Radiation

10. If the temperature of the atmosphere were that of the radiation equilibrium curve 0, Fig. 1, the atmosphere would be dynamically unstable. The air above 3 km would be so dense, because of its low temperature, that it would descend rapidly; convective equilibrium would be brought about and the t, z curve would approach curve 1, Fig. 1. In general, if the t, z curve at

[12] Angström, Ann. d. Phys. 6, 173 (1901).
[13] Abbott, reference 10, page 173.

any point is less steep than the convective equilibrium curve at that point, the atmosphere is dynamically unstable and a flow of air occurs in such a direction as to bring about convective equilibrium more or less completely. The t, z curve may of course be steeper than the adiabatic curve in a dynamically stable atmosphere. Convection is of course, also promoted by horizontal winds blowing from night to day areas, from warm to cold regions, etc.

Therefore curve 0, Fig. 1, shows that radiation equilibrium cannot exist in the atmosphere below about 5 km; it might, however, exist at greater heights, for above 5 km curve 0 is steeper than curve 1, Fig. 1. Assume that below a level, denoted by z_1, convective equilibrium exists, as given by curve 1, Fig. 1, and that above z_1 radiation equilibrium prevails. The two states will merge into each other through a region of transition, but for simplicity we regard the transition as abrupt. The assumption means that the energy leaving the earth advances upward through the atmosphere by the process of convection until a level z_1 is reached above which it advances by the process of radiation. We take various values of z_1 and investigate the stability of the atmosphere by calculating t_0 and the t, z curve above z_1 for each value.

Let the equivalent thickness of the absorbing gases, reduced to standard conditions, from z_1 to a higher level z be x_1 and to infinity be x_{b1}. At z_1 the temperature is t_1 as given by curve 1, Fig. 1, and the upward energy stream is e_{u1} where

$$e_{u1} = f\sigma t_1^4. \tag{18}$$

In the region above z_1 we have corresponding to (8) and (9), putting in (1),

$$e_u = (SA/4 - \phi\sigma t_0^4)[1 + \alpha(x_{b1} - x_1)/2], \tag{19}$$

and

$$e_d = (SA/4 - \phi\sigma t_0^4)[\alpha(x_{b1} - x_1)/2]. \tag{20}$$

Substituting $x_1 = 0$ and (18) into (19) and solving for t_0 gives

$$\phi t_0^4 = \frac{SA}{4\sigma} - \frac{f\sigma t_1^4}{1 + \alpha x_{b1}/2}. \tag{21}$$

From (5), (19), (20) and (21) we obtain

$$2f\sigma t^4 = (SA/4 - \phi\sigma t_0^4)[1 + \alpha(x_{b1} - x_1)]. \tag{22}$$

$x_{b1} - x_1$ is the same as $x_b - x$ so that the last column of Table I can be used in calculations from (22). In passing it may be noted that the temperature of the bottom of the part of the atmosphere in radiation equilibrium, obtained by putting $x_1 = 0$ in (22) and using (21), is not exactly equal to t_1 the temperature of the top of the part of the atmosphere in convective equilibrium. This is not an inconsistency, but merely results from the assumption that the convective region merges abruptly into the radiative region. A similar case was discussed in section 7.

For the case $z_1 = 3$ km, t_1 from curve 1, Fig. 1, is 269° and from (21) t_0 comes out to be 305°. With this value for t_0, t was calculated from (22) for z

above 3 km and is plotted in curve 3, Fig. 1. Just as in the case for curve 0, the atmosphere is dynamically unstable for the lower part of curve 3. Further, the value $t_0 = 305°$ is inconsistent with the assumption of $z_1 = 3$ km. For the assumption that t below 3 km be given by curve 1, Fig. 1, requires that t_0 be about 287°. Whereas the radiation equilibrium requirements laid down in (21) call for $t_0 = 305°$. Thus the assumption that $z_1 = 3$ km leads to an atmosphere dynamically unstable and one for which the radiation of energy to space is less than the energy received from the sun.

In a similar manner curves 4, 5, 7, 10 and 12, Fig. 1, were obtained corresponding to the cases $z_1 = 4$, 5, 7, 10 and 12 km, respectively. The respective values of t_0 were 301, 294, 293, 291 and 290°. For $z_1 = 15$ km t_0 was 296°. It is seen that only for z_1 between 7 and 14 km, and better still for z_1 between 9 and 12 km, does the atmosphere satisfy the conditions of dynamic stability and equilibrium with solar radiation. Such an atmosphere agrees closely with the observed atmosphere, for example, the calculated and observed values of t_0 are 290° and 287°, respectively. The agreement is no doubt better than is warranted by the accuracy of the data on which the calculations are based. Apparently the uncertainties and omissions have conspired to counteract each other to some extent.

The reason for treating the 30 percent of the incoming solar radiation, which is mostly absorbed in the levels below 10 km, (see section 5) as though it actually reached sea level is now clear. Since the thermal energy received from the sun by the surface of the earth and the atmospheric levels to about 12 km is spread around and transferred upward by convection, it makes little difference whether the energy is supplied to the earth's surface or to some level in the convective region.

Summary

11. We may summarize the conclusions thus far reached and in so doing give the answers to the first two questions in section 2. If the atmosphere were in radiative equilibrium at all heights the average temperature at sea level would be 306°K, or about 19° hotter, and at levels above 3 km more than 100° colder than it is. Such an atmosphere would be dynamically unstable and vertical convection currents would be set up. These would stir up the atmosphere in the lower levels to give the temperatures of convective equilibrium, thereby cooling the atmosphere at sea level and warming it above. If the convective region extended only to, say, 5 km we find that the atmosphere again is dynamically unstable and in addition that the total radiation emitted from the earth and the atmosphere is less than the energy received from the sun. When the convective region extends to 10 or 12 km (as is observed) the atmosphere is found to be stable, the calculated sea level temperature is about 290° (close to the observed value 287°) and the total radiation emitted from the earth and the atmosphere is equal to the received solar energy. If the convective region extended to a level greater than 12 or 15 km the outgoing radiation is less than the incoming solar radiation. Thus we have proved that the only type of atmosphere, of the types considered, which satisfies the

conditions of dynamic stability and thermal permanence is the type of atmosphere which is observed.

12. Nothing in the foregoing analysis has led to the answer to the third question of section 2, namely, why is the temperature of the atmosphere approximately constant with height from 12 to 20 km? True, it has been shown that, in agreement with the observed lack of winds, the conditions in this region are those of radiative and not of convective equilibrium. But equilibrium with outgoing terrestrial radiation calls for a decreasing temperature with increasing height. The constancy of t with z therefore requires some additional hypothesis. The obvious hypothesis, emphasized by Maris,[2] is that the incoming solar radiation is absorbed in the isothermal region in such a way that, together with the absorbed outgoing terrestrial radiation, t is constant with z. The constancy of t with z instead of being commonplace is in reality strange and unexpected and probably to be explained as the result of the combined action of two or more causes.

The Effect of Ozone

13. A simple calculation shows that the ozone, which exists in levels above about 50 km, has a slight effect on the temperature of the earth; it cools the earth about 1°. Ozone has two general regions of absorption, one in the ultraviolet extending from about λ2300 to 2900A and one in the infrared of which the most important portion is the band from about λ8.5 to 10.5μ, see Fig. 2. The solar energy curve in the ultraviolet below 2900A is of course not known, but if it be extrapolated into the ultraviolet on the assumption that the sun radiates as a black body at 6000°K the energy from 2300 to 2900A is about 4 percent of the solar constant S. The 3 mm of ozone is sufficiently thick to absorb completely this ultraviolet energy. If the ozone were not present and the ultraviolet energy came through to the earth S would be increased by 4 percent and t_0, instead of being 287°, would be $287\times(1.04)^{1/4}=289.8°$.

If the ozone is present in the atmosphere it absorbs the 4 percent ultraviolet energy and reradiates it equally upward and downward. Because the ozone is not very hot, probably not above 500°K, the reradiation is almost entirely in the infrared and mainly in the 8.5 to 9.5μ band. This band happens to be in a region which is little absorbed by water vapor and carbon dioxide, see Fig. 2. Therefore the ozone energy either reaches the surface of the earth or at least enters well into the convective region of the atmosphere, and adds 2 percent to S. The earth radiation at 287° passes out to the ozone where 2 percent is absorbed. The 2 percent is got by calculation from the values of α of Fig. 2 (or see Fig. 4, ref. 2). Of this 1 percent, which amounts to 0.3 percent of S, is reradiated downward to the earth. Thus the radiation received by the earth is equal to S increased by 2.3 percent, and t_0 becomes $287\times(1.023)^{1/4}=288.6°$, which is 1.2° less than 289.8°. Therefore the earth is about 1° cooler, *ceteris paribus*, than it would be if the ozone were removed from the atmosphere.

The Carbon Dioxide Theory of the Ice Ages

14. The sea level temperature t_0 was calculated in section 10 to be 290° by means of (21) with $z_1=12$ km, $t_1=219°$ and $\alpha x_{b1}=1.67$ from Table I. To determine the changes in t_0 with changes in the amount of carbon dioxide in the atmosphere we may, to a first approximation, assume that αx_{b1} varies, the other quantities remaining constant. The value $\alpha x_{b1}=1.67$ was the arithmetical average of $\alpha x_{b1}=2.83$ for the 12.5 to 16μ band of carbon dioxide and $\alpha x_{b1}=0.52$ for the 14 to 20μ band of water vapor, the 5 to 8μ band of water vapor being of no importance for 219° radiation (see the 200° curve of Fig. 4). If the carbon dioxide of the atmosphere were doubled $\alpha x_{b1}=(2\times 2.83+0.52)/2=2.59$; if the carbon dixide were halved, $\alpha x_{b1}=(2.83/2+0.52)/2=0.92$. With these values in (21) t_0 comes out 294° and 286°, respectively. Thus doubling or halving the carbon dioxide in the atmosphere changes t_0 by 4°. Similarly, tripling or reducing to zero the carbon dioxide increases or decreases t_0 by 7°. Such changes as these in the world-wide average surface temperature of the earth are of about the same amount as occurred during the ice ages.[14] The calculation is thus in support of the carbon dioxide theory of the ice ages advanced long ago by Tyndall.[15] It is perhaps well to mention the essence of the physics underlying the calculation. In the convective region of the atmosphere the outgoing thermal energy is passed upward by convection to the radiative region above 12 km. So that the radiative region controls to a considerable extent the temperatures in the lower lying convective region. And the radiative region owes its optical properties more to the carbon dioxide than to the water vapor there.

Further, an increase or decrease in the world-wide average atmospheric temperatures of a few degrees would give rise to other changes. The water vapor in the atmosphere would be increased or decreased, this would accentuate the temperature changes. At the same time changes in the areas covered by vegetation and snow fields would take place, thus changing the optical properties, that is, the emissive power a, section 5, of the surface of the earth. Whether a would increase or decrease can not be said at the present time, for the reflecting powers, etc., of snow, sand, vegetation, etc. in the infrared to 40μ are not known. In general so many other changes may be thought of, such as a change in the carbon dioxide content of the sea, etc., that speculation as to the exact consequences of an increase or decrease in the average world-wide temperatures of a few degrees seems fruitless.

About all we can conclude is that the carbon dioxide theory of the ice ages is at least a possible one, and that objections which have been raised against it by some physicists[9,12,13] are not valid. We can not conclude that objections may not crop up in the future. Geologists[14] apparently have come upon no evidence, and have no unanimous opinion to offer, as to the fundamental causes of the ice ages. And we let it go at that.

[14] See any treatise on geology, for example, Coleman, "Ice Ages, Recent and Ancient," MacMillan (1926), or the excellent article on glacial periods by Howe, Encyclopaedia Brittanica, 13th ed., 12, 56 (1926).

[15] Tyndall, Phil. Mag. **22**, 277 (1861).

SPARKING POTENTIAL AND ELECTRODE MATERIAL

By Leonard B. Loeb
Department of Physics, University of California

(Received September 19, 1931)

Abstract

A consideration of the character of the normal spark breakdown in air with external ionization and involving time lags of greater than 10^{-4} seconds indicates that with the assumption of space charges the original Townsend theory of sparking can be maintained and that the spark mechanism as is experimentally found will be independent of electrode material. It is shown that the results of Duffendack, Wolfe and Randolph in which they find a dependence of sparking potential on the work function of the electrodes is due to their special experimental arrangement and in no sense contradicts the Townsend theory as asserted by them. It is shown that short time (less than 10^{-5} seconds) surge impulse breakdown in gaps of small area with insufficient ionization necessitates a new breakdown mechanism involving probable impact ionization at the cathode by positive ions to replace the deficient ionization. On the basis of this point of view further much needed investigations are indicated.

Introduction

THE countless investigations on the sparking potentials in air and other gases at atmospheric pressures and above have all been unanimous in ascribing a relatively unimportant role to the electrode material [1,21] and considerable importance to the nature of the gas and the gas density. This of course assumes the absence of thick nonconducting oxide films or water films on the electrodes. It also applies largely to conditions where the *potential of the gap is gradually raised to the sparking potential* so that overvoltages are not involved. If the cathode is illuminated by ultraviolet light or the gas in the gap is ionized these *sparking potentials are closely the same* for a given shape of electrodes and are remarkable constant. If no ionization is provided the results may be erratic and average possibly one or two percent above the values for the same gaps when electrons or ions are present, the variation depending on how the potentials are raised. In fact the constancy of these phenomena is such that this method is a *standard* method for measurement of high potentials *without any specification as to electrode material.*

Recent investigations of Duffendack, Wolfe and Randolph[2] using spark plugs and an induction coil or magneto discharge led these observers to

[1] J. J. Thomson, Conduction of Electricity through Gases, 2nd Edition, Cambridge Press' 1906, Chapter 15, especially p. 437; W. O. Schumann, Elektrische Durchbruchsfeldstärke von Gasen, Julius Springer, Berlin, 1923, pp. 17, 20, 156, 159; J. S. Townsend, Electricity in Gases, Oxford Press, 1914, Chapter X; E. Warburg, Handbuch der Physik (Geiger and Scheel) Vol. XIV, Chapter 7, page 367; R. Seeliger, Einführung in die Physik der Gasentladung, Barth, Leipzig, 1927, p. 85.

[2] O. S. Duffendack, R. A. Wolfe and D. W. Randolph, Development of an Electron Emitting Alloy, paper delivered before the Electrochemical Society April 23-25, 1931, printed in preprint form only.

results which appear to disagree with the above common observation. They found by an oscillographic study of the spark between wires in a spark plug that the sparking potential at breakdown, measured over short time intervals was high and very variable with ordinary spark plug wires of nickel alloy. When, however, alloys were used with about 0.04 percent of Ba or Mg present these sparking potentials became uniform and as much as 30 percent lower than before. At the same time they found that the work function of the metal was materially lowered, and in fact that the sparking potentials *as measured by them* were definitely connected with the work function. They therefore asserted that the work function of the metal does influence the sparking potential of the metal and that the overwhelming mass of previous data must be in error.

That an *apparent* contradiction exists in unquestionably correct. However, *this contradiction is in reality only apparent* and inasmuch as it involves questions of considerable importance in theory it may not be amiss to point out the obvious cause for the discrepancy, which in itself is not uninteresting.

Effect of Electrode Material on Sparking

The previous investigations have all been carried out as stated by slowly raising the potential until a spark occurred and by measuring the potential. The lack of dependence on electrode material indicated, as Townsend[3] had long ago shown, that the essential spark mechanism depended on the production near the cathode of electrons through ionization of the gas molecules by some mechanism, presumably by positive ions.[21] At very low pressures (less than 1 cm) in inert gases Holst[4] and Oosterhuis and also James Taylor[5] had shown a dependence on electrode material, the sparking potential being the lower the lower the work function. Neuman[6] in this laboratory confirmed these findings but found that between 1 and 2 cm pressure in argon the mechanism changed and the potential became independent of the electrode material. He there pointed out the obvious conclusion that when the gas density is so low that the electron formation near the cathode essential to a self-sustaining discharge can only come from bombardment of the cathode by positive ions the work function of the cathode must play an important role. As the pressure reaches a point where the probability of ionization of the gas in the high space charge near the cathode by positive ions becomes commensurate with that at the cathode surface, the discharge mechanism changes to one independent of cathode material. This view is doubtless correct. All these experiments were performed by the gradual raising of the potential up to sparkover.

[3] J. S. Townsend, Electricity in gases, Oxford Press, 1914, Chap. IX, pp. 322 and 30; Phil Mag. **45**, 444 (1923); Marx: "Handbuch der Radiologie" Vol. I, p. 241.

[4] G. Holst and E. Oosterhuis, Phil. Mag. **46**, 1117 (1923); Physica **1**, 78 (1921); C. R. **175**, 577 (1922).

[5] J. Taylor, Phil. Mag. **3**, 753 (1927); **4**, 505 (1927); Proc. Roy. Soc. **A114**, 73 (1927); also H. G. L. Huxley, Phil. Mag. **3**, 1056 (1927).

[6] L. J. Neuman, Proc. Nat. Acad. Sci. **15**, 259 (1929).

The Time Lag in Spark Discharge

In the work of Duffendack, Wolfe and Randolph the potential was raised in a small fraction of a second (the time scale was in 10^{-5} of a second) and the breakdown potential was measured by oscillograph. Further no source of ionization was furnished at the cathode, unless in some experiments the cathode was at red heat due to gasoline explosion.* Hence their experimental procedure constitutes an obviously new approach to the problem, which involves as its chief feature the rate of rise of potential. In other words, a time element is introduced into this investigation which was absent in other investigations. This time element brings into consideration a different aspect of spark discharge, i.e. that of the well-known time lag. This is a factor which has been little studied and still less discussed in its bearing on the breakdown potential. Since the time element has certain interesting features it will repay one to consider the role of time in spark discharge.

A study of the effect of time on the breakdown of spark gaps reviewing past literature was made by Zuber[7] in 1925 and was mathematically discussed by Laue.[8] Since Zuber's work some new features have been added in the work of Rogowski[9] and others using the high speed cathode-ray oscillograph, and by others, essentially Lawrence and Dunnington[12] and Beams [10,11] using the Kerr cell shutter. Zuber studied the spark lag, i.e. the time between the point where the potential reaches the sparking value, or some small overvoltage of one or two percent, and the time at which the spark passes. He finds that down to about 0.1 second the number of time intervals, between arriving at the sparking potential and the passage of the spark, which exceed t seconds is given by $n_t = n_0 e^{-p\beta t}$. Here β is the chance that an electron is formed in the gap by ultraviolet light, radiation from radium or by natural processes and p is the chance that such an electron can in the gap lead to a spark discharge. Thus the average time lag of the spark is $\bar{t} = 1/p\beta$. The quantity p depends on overvoltage, the nature of the gas and the spark gap. Zuber did not go to shorter time intervals because of the physical limitations of his measuring circuit. He also found that $\bar{t}$ was in reality a function of β, and for *very small* overvoltages that it was about proportional to the intensity of ionization. He further found that overvoltages also reduced $\bar{t}$ and that moist air acted in a similar fashion. The interpretation of these results in terms of later knowledge is of considerable importance.

* In their paper before the Electrochemical Society no accurate description of the spark chamber was given, an omission which makes discussion somewhat difficult.

[7] K. Zuber, Ann. d. Physik **76**, 231 (1925).

[8] M. von Laue, Ann. d. Physik **76**, 261 (1925).

[9] W. Rogowski, Archiv. f. Elektrotechnik **20**, 19 (1928); and O. Beyerle, Archiv. f. Elektrotechnik **25**, 267 (1931); P. O. Pedersen, Ann. d. Physik **71**, 317 (1923); R. Tamm, Archiv. f. Elektrotechnik **20** (1928); Burroway, Archiv. f. Elektrotechnik **16**, 14 (1926); J. J. Torok, Trans. A.I.E.E. **47**, 177 (1928); **48**, 46 (1930).

[10] J. W. Beams, Jour. Franklin Inst. **206**, 809, 1928; Phys. Rev. **28**, 475 (1926); Phys Rev. **35**, 24 (1930).

[11] J. C. Street and J. W. Beams, Phys. Rev. **38**, 416 (1931); L. von Hamos, Ann. d. Physik **7**, 857 (1930).

[12] E. O. Lawrence and F. G. Dunnington, Phys. Rev. **35**, 396 (1930).

With the limitations of his apparatus Zuber could not determine whether there was *a real lower limit to the time t* at which a spark could occur. The writer[13,17] had in 1928 postulated that a space charge mechanism was required to cause a spark to occur according to the Townsend theory; and assuming the charge due to positive ion migrations in a long gap he indicated that below $t=10^{-5}$ to 10^{-4} seconds such a mechanism could not take place. It was accordingly predicted that *the minimum spark lag must lie at time intervals of this order of magnitude.* This point in fact has never been investigated. It is the writer's belief that the space charge mechanism is probably correct for what will be termed the *normal spark breakdown.* Shortly thereafter the work on *surge impulse breakdown* of spark gaps of Pedersen,[9] Rogowski, Tamm, Burroway, Torock and Beams[10,11] indicated that for considerable overvoltages the time lag lay in periods of 10^{-8} or even 5×10^{-9} seconds. The later researches of Lawrence and Dunnington,[12] and Dunnington[14] show, however, that for actual breakdown without overvoltage and the electrodes illuminated with ultraviolet light the time lag is always finite and large, as observed by Zuber. Once, however, breakdown started it was found to be accomplished in time intervals of the order of 5×10^{-9} seconds up to 10^{-7} seconds. The results of Pedersen, Rogowski, *et al* led the writer[15] to abandon the positive ion mechanism for the space charge accumulation *especially in the case of surge impulse breakdown* and to formulate a mechanism of space charge formation based *entirely on the movement of mobile electrons.* Independently Franck and von Hippel[16] formulated a similar theory using a slightly different idea requiring longer time intervals. Schumann[17,18] later developed the Franck and von Hippel idea quantitatively by equations which in the main agree well with Dunnington's[14] observations concerning the mechanism of breakdown. Both the Franck and von Hippel and the Schumann theory apply beautifully to the case of *normal breakdown with time lag*, although they are probably not completely essential. It is further probable that the *electron ionization mechanism* as postulated by the writer and Franck and von Hippel may not be *completely adequate for short time surge breakdown* of spark gaps and that an *added factor to be discussed later may enter with inadequate ionization.*[21]

The Mechanism of the Normal Spark Breakdown

The new developments lead one to the following conclusions. Spark discharge in gases in the atmospheric pressure range, when occurring near the minimum sparking potential, occur essentially on the basis of the mechanism assumed by Townsend. That is electrons must be generated by *positive ion impact on gas molecules* near the cathode in such numbers that the discharge becomes self-sustaining. *This mechanism only can account for the independence of the work function of the electrode surfaces universally observed* for spark dis-

[13] L. B. Loeb, Jour. Franklin Inst. **205**, 305 (1928).
[14] F. G. Dunnington, Phys. Rev. **38**, 1535 (1931).
[15] L. B. Loeb, Science **69**, 509 (1929), also Jour. Franklin Inst. 1930.
[16] J. Franck and A. von Hippel, Zeits. f. Physik **57**, 696 (1929).
[17] W. O. Schumann, Zeits. f. Technische Physik **11**, 131 (1930).
[18] W. O. Schumann, Zeits. f. Technische Physik **11**, 194 (1930).

charge of this character. In order, however, that the Townsend mechanism can occur space charges must be produced near the cathode of such magnitudes that the Townsend mechanism can take place (i.e. space charges giving gradients of the order of five to ten times the initial uniform sparking potential gradient). The consequences of the existence of space charges have actually been observed in the early periods of spark discharge under minimum sparking potential conditions by Dunnington.[14]

The space charges require for their formation 10^{-4} to 10^{-5} seconds if they are to be produced by positive ions and 2×10^{-8} to 10^{-7} seconds if they are to be formed by electron movement only, provided they can be and are so produced. It is quite possible that to form the space charges by electron movement only, overvoltages are required.[17,18,19] It is in fact only in surge impulse breakdown with overvoltages that we have any definite knowledges of time lags less than 10^{-4} seconds. It may therefore be that for space charges and breakdown in less than 10^{-4} seconds considerable overvoltages, electron ionization and possibly a new mechanism for causing this process may be required, especially in the absence of ultraviolet light, while this is not essential for normal breakdown. Consequently while the time lags in spark breakdown measurements for the minimum sparking potential are such as to always insure the space charge formation and the Townsend mechanism,[21] this may in no sense hold for shorter time intervals.[17,18,19]

Returning to the question of space charge formation in longer time intervals, it is clear that under the conditions of minimum spark potential investigations the actual limit for space charge formation and for breakdown is of the order of 10^{-4} seconds or a bit less. The question then arises as to what causes the observed statistical lags of Zuber extending in some cases into minutes. The essential feature that affects the time lag and makes classical sparking potential measurements differ from the overvoltages breakdown *must depend on some rare fortuitous combinations of circumstances whose occurrence ends in the building of a space charge under the minimum potential conditions*. Since high fields exist across the gap any ionization occurring in such a fashion as not to lead to an appropriate space charge will be swept away and one must await the occurrence of the right combination of events to give a spark. As Zuber showed, the occurrence of appropriate conditions is a most complex phenomenon. It depends first on the occurrence of at least one electron in the gap where the then undistorted field is highest. In addition it must depend on whether this electron is near enough to the cathode to be effective in building up a space charge. This is influenced by the sort of gas, by the small overvoltage, by gap design and by the pressure of the gas. It may as postulated by Franck and von Hippel and by Schumann not depend on *one electron, but on a succession of electrons liberated in proper time sequence near the cathode*. It may again depend on a proper spatial orientation of electrons in the gap as postulated by the writer's chain mechanism; or it may depend on a proper space time sequence. In the limit if no artificial ionization is present such a fortuitous combination of events may on the average occur very rarely

[19] W. O. Schumann, Zeits. f. Technische Physik **11**, 58 (1930).

and we observe time lags which preclude any accurate approach to the true sparking potential (i.e. such lags that owing to human impatience the potentials appear 2 percent high). With ionization at the cathode the results are more uniform, the time lags are shorter and conditions are much improved so that the potentials are slightly lower. In spite of this, however, there are time lags of a finite amount (exceeding 0.1 of a second) indicating definitely a spatial, or temporal spatial, succession of electronic events which is not too common. Once, however, these occur the space charges are built up, the ionization by positive ions begins and the spark takes place in a very short time.

The Surge Impulse Breakdown Mechanism

One may now turn to the problem presented by Duffendack, Wolfe and Randolph's method. These observers measure the actual potential at breakdown of presumably an *un*illuminated spark plug gap whose actual minimum breakdown potential as it occurs in air is not measured by the static method. Such gaps have so small a volume of air to be ionized by the normal atmospheric processes that the chance of a proper occurrence of circumstances leading to a normal spark is most remote. In addition the fields between spark plug terminals are far from uniform and it can occur that, with considerable overvoltages, fields far greater than those causing sparking under ordinary conditions obtain. These observers measure at what potential in a rapidly rising potential wave the gap actually breaks down. The time between that when the true minimum potential on the spark coil wave is reached and that when due to a considerable overvoltage (of the order of several tens of percent) the spark passes at the observed potential is of the order of 10^{-5} seconds. Hence they observe a phenomenon that depends on just the type of surge breakdown mechanism in which the electronic space charge mechanism is completely unknown and has at best only been conjectured. There is in this operation no time for the *fortuitous and apparently efficient set of occurrences* which give the true minimum sparking potential. Instead on a rapidly rising potential wave the field strength at the points on the electrodes rises to absolutely unknown values. It continues to rise until conditions of ionization in the gap are such that perhaps just any one electron or ion located anywhere in or near the gap can start a space charge building mechanism. The impulse may even pass without a spark. It is most probable that the intense fields near points on the cathode catch the first positive ion appearing due to natural ionization, and if this when accelerated can produce on *impact with the cathode* a new electron, a mechanism for space charge formation of the Franck and von Hippel type is set up. It is unlikely that in such intense radial fields the field at any distance from the minute point on the cathode would be great enough to generate ions by collision of the positive ion and gas molecule. This is emphasized first by the fact that for ionization of a gas by positive ions with any efficiency much higher fields are needed than those for liberation of electrons from the cathode surface by positive ions; and secondly by the fact that the high fields probably lie about *rough points* on the cathode and are not of sufficient intensity at several ion free paths to give the positive ion a chance to ionize other gas molecules. It therefore appears not unreasonable to assume

that in this *forced discharge at very high fields* the space charge mechanism is built up by electrons from the positive ion bombardment of the electrode surface. This mechanism then replaces the adequate ionization obtaining in other sparks. Such an electron and space charge source must depend on the work function of a particular spot on the cathode. A similar conclusion was also reached independently in one of Schumann's splendid papers.[21] If the work function for this spot is low the potential needed for a spark will be lower than for a point of high work function. By making electrodes of uniformly low work function the surge impulse breakdown potential will be markedly lower and more uniform. It will, however, never be really uniform (as can be seen by the photographs of Duffendack, Wolfe and Randolph) for the potential rises quickly and the points are not uniform. It is most probable that considerable uniformity could be introduced into such experiments with perhaps even lower potentials, if really intense ionization at the cathode is introduced by an external agent (e.g. ultraviolet light on the cathode). In this case the potential should be independent of work function, except insofar as the photoelectric efficiency of the source varies markedly with this quantity. This condition has been studied to some extent by Rogowski and Tamm[20] and is in accord with the above.

It thus appears that the work of Duffendack, Wolfe and Randolph in no sense invalidates the generally accepted theory of the ordinary spark breakdown mechanism, nor does it cause us to revise it in the least. Their work deals with conditions radically different from the ones used in classical studies. In fact they have discovered that *by removing almost all natural chances of ion formation between the electrodes* by short time intervals and small electrode area *it takes a new mechanism requiring much higher fields to produce a space charge and a spark.* In the absence of ionization and under their special conditions as to electrode form it is probable that the most efficient mechanism depends on electron emission from the cathode by positive ion bombardment.[21] This is definitely dependent for its effectiveness on the work function of the metal. It is conceivable by still further altering conditions in shortening time intervals and using smaller electrodes that one might be able to suppress sparking entirely until one reached field strengths leading to the well-known field currents. This would also depend on work functions and yield still another spark mechanism. It may be that recent results of Street and Beams[11] apply to just this situation. This phenomenon would hardly, however, disprove the Townsend interpretation of the spark under entirely different conditions.

It is imperative as seen from this discussion that experiments be made to really measure the shortest time limit in normal spark discharge. It would also be of great interest to find for what time intervals and fields the new electrode-material dependent mechanism begins to manifest itself. It should also be of interest to see whether in all short time surge impulse breakdown the nature of cathode material does not play a role, and to determine the effect of intense external ionization on such breakdown.

[20] W. Rogowski and R. Tamm, Archiv. f. Elektrotechnik **20**, 107 (1928).
[21] W. O. Schumann, Zeits, f. Technische Physik **11**, 143 (1930).

THOMAS-FERMI EQUATION SOLUTION BY THE DIFFERENTIAL ANALYZER

By V. Bush and S. H. Caldwell
Massachusetts Institute of Technology

(Received September 25, 1931)

Abstract

A numerical solution of the Thomas-Fermi equation $d^2\phi/dx^2=\phi^{3/2}/x^{1/2}$, with the boundary conditions $\phi(0)=1$ and $\phi(\infty)=0$, is presented, as obtained mechanically by means of the Differential Analyzer. This device for solving ordinary differential equations is described in a separate paper in the Journal of the Franklin Institute. The results are given for larger values of argument than have previously been reported, and at high values of argument precision has been improved. Over a part of the range, previously published results are checked, and the entire range is checked by an independent integration.

A MACHINE recently developed at the Massachusetts Institute of Technology is capable of the solution of many forms of ordinary differential equations.[1] This paper presents the results obtained by its use in the solution of the Thomas-Fermi[2,3] equation, which was picked as one of the first problems for attack largely because it brought out certain interesting points in connection with the operation of the machine.

The equation with dimensionless variables introduced is

$$\frac{d^2\phi}{dx^2}=\frac{\phi^{3/2}}{x^{1/2}} \tag{1}$$

and the boundary conditions are

$$\phi(0)=1 \tag{2.0}$$

$$\phi(\infty)=0. \tag{2.1}$$

An equation of this type, with boundary conditions as given, is inherently difficult to solve by any method. It is nonlinear and involves a singularity at $x=0$. Moreover, the boundary conditions are such that they cannot be satisfied directly; one must be satisfied at the point of singularity at $x=0$, and the other at infinity. It is also characteristic of this equation that small errors introduced when solving with x increasing have a cumulative effect as the solution proceeds.

The second derivative in Eq. (1) becomes infinite for $x=0$, so the solution for the region from $x=0$ to $x=0.2$ was taken from an expansion given by Baker.[4] The remainder of the problem was divided for solution into two parts,

[1] V. Bush, Jour. Franklin Inst. **212**, 447 (1931).
[2] L. H. Thomas, Proc. Camb. Phil. Soc. **23**, 542 (1927).
[3] E. Fermi, Zeits. f. Physik **48**, 73 (1928).
[4] E. B. Baker, Phys. Rev. **36**, 630 (1930).

corresponding to the regions from $x=0.2$ to $x=10$ and from $x=10$ to $x=\infty$.

In the region from $x=0.2$ to $x=10$, in order to keep the ordinates in the result large and hence maintain precision, there was introduced in Eq. (1) a new variable

$$\psi = \phi\epsilon^{x/2} \tag{3}$$

which gave the equation

$$\frac{d^2\psi}{dx^2} = \frac{d\psi}{dx} - \frac{\psi}{4} + \frac{\psi^{3/2}}{x^{1/2}\epsilon^{x/4}} \tag{4}$$

Moreover, it was found advisable to operate the machine with x decreasing in order to minimize the effect of casual errors, which in this region produced a cumulative effect with increasing x. The required starting conditions at $x=10$ were obtained by running a family of solutions in the region from $x=10$ to $x=\infty$, using a range of values for $\phi(10)$ within which the correct value was known to lie. Each of these solutions satisfied Eqs. (1) and (2.1), and was extended back by means of Eq. (4) to $x=0.2$. At that point the values of ϕ and ϕ' were read and plotted, together with points computed from Baker's expansion for different values of $\phi'(0)$. The intersection of the two curves established by interpolation the values of $\phi(10)$ and $\phi'(10)$ for which the solution satisfied the original equation and both boundary conditions.

In the region from $x=10$ to $x=\infty$, a change of variables was made, introducing

$$u = \frac{1}{x}, \quad q = \phi u \tag{5}$$

after which Eqs. (1) and (2.1) became

$$\frac{d^2q}{du^2} = \frac{q^{3/2}}{u^4} \tag{6}$$

and

$$q(0) = 0. \tag{7}$$

The procedure here was to assume a value of q at $u=0.1$ and to adjust by trial the corresponding values of q' so that Eq. (7) was satisfied when the machine was run with q decreasing. This was repeated for a number of values of q covering the desired range. This procedure, while exceedingly laborious when using formal methods, is not unduly time consuming on the analyzer, for a single solution can be run in a few minutes when once the machine is set up.

For the solution of Eqs. (4) and (6), the differential analyzer was connected as shown in Figs. 1 and 2 respectively.[5] In these diagrams scales, signs

[5] For explanation of symbols used, see reference 1.

and gear ratios are disregarded. The revolutions of each shaft are proportional to the quantities indicated.

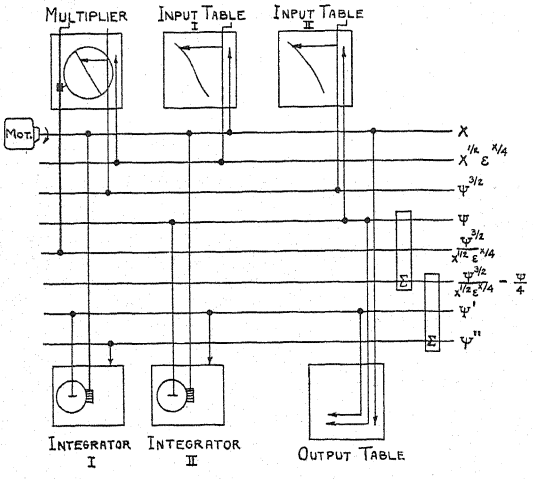


Fig. 1. Connections of the Differential Analyzer to solve the equation

$$\frac{d^2\psi}{dx^2} = \frac{d\psi}{dx} - \frac{\psi}{4} + \frac{\psi^{3/2}}{x^{1/2}\epsilon^{x/4}}.$$

Table I shows the numerical solution obtained for the region from $x=0.2$ to $x=36.92$. These values agree to within less than one percent with those re-

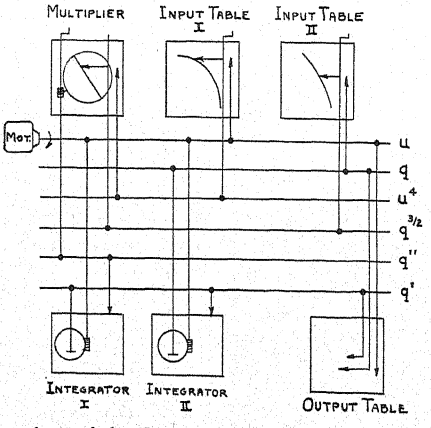


Fig. 2. Connections of the Differential Analyzer to solve the equation

$$\frac{d^2q}{du^2} = \frac{q^{3/2}}{u^4}.$$

ported by Baker,[4] whose table covers the range up to $x=14.88$. In the region from $x=15$ to $x=20$, Fermi[3] gives values of one significant figure; the present

table gives two significant figures for all values beyond $x=16$. The initial slope was found to be -1.589 and thus agrees with Baker's value.

TABLE I.

x	ϕ	x	ϕ	x	ϕ
0	1.000*	2.500	0.193	10.44	0.0225
0.010	0.985*	2.708	0.176	10.67	0.0216
0.030	0.959*	2.918	0.162	10.92	0.0206
0.060	0.924*	3.125	0.150	11.16	0.0198
0.080	0.902*	3.333	0.138	11.43	0.0189
0.100	0.882*	3.542	0.127	11.72	0.0180
0.150	0.835*	3.750	0.118	12.01	0.0171
0.200	0.793	3.960	0.110	12.31	0.0163
0.250	0.755	4.167	0.102	12.63	0.0155
0.292	0.727	4.375	0.0956	12.97	0.0147
0.333	0.700	4.583	0.0895	13.33	0.0139
0.375	0.675	4.792	0.0837	13.72	0.0131
0.417	0.651	5.000	0.0788	14.12	0.0123
0.458	0.627	5.209	0.0739	14.55	0.0116
0.500	0.607	5.418	0.0695	15.01	0.0109
0.542	0.582	5.625	0.0656	15.48	0.0102
0.584	0.569	5.834	0.0619	16.00	0.0094
0.625	0.552	6.042	0.0587	16.56	0.0088
0.667	0.535	6.250	0.0554	17.14	0.0081
0.709	0.518	6.458	0.0526	17.78	0.0075
0.750	0.502	6.667	0.0500	18.46	0.0069
0.792	0.488	6.875	0.0473	19.20	0.0064
0.833	0.475	7.083	0.0450	20.00	0.0058
0.875	0.461	7.292	0.0430	20.87	0.0053
0.917	0.449	7.500	0.0408	21.82	0.0048
0.958	0.436	7.708	0.0389	22.85	0.0043
1.000	0.425	7.917	0.0371	24.00	0.0038
1.042	0.414	8.125	0.0355	25.26	0.0034
1.083	0.406	8.333	0.0340	26.67	0.0030
1.125	0.393	8.542	0.0321	28.24	0.0026
1.167	0.382	8.750	0.0310	30.00	0.0022
1.208	0.374	8.958	0.0298	32.00	0.0019
1.250	0.364	9.167	0.0287	34.29	0.0016
1.458	0.322	9.375	0.0275	36.92	0.0011
1.667	0.287	9.583	0.0265		
1.875	0.259	9.792	0.0255		
2.083	0.234	10.000	0.0244		
2.292	0.212	10.22	0.0235		

* Computed points.

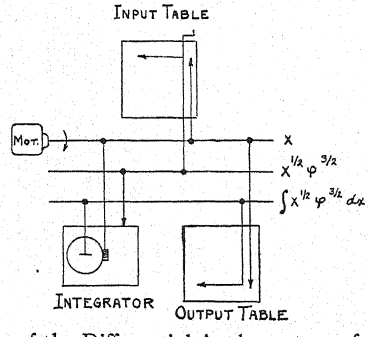


Fig. 3. Connections of the Differential Analyzer to perform the integration

$$\int x^{1/2}\phi^{3/2}dx.$$

A condition which ϕ must satisfy and which was not used in making the solution is given by

$$\int_0^\infty \phi^{3/2} x^{1/2} dx = 1. \tag{7}$$

This was used as a final check on the work, with the machine connected as in Fig. 3. The integral between the limits $x=0$ to $x=30$ had the value 0.994.

This problem was suggested by Professor R. M. Langer of the Department of Physics, and we are greatly indebted to him for his many suggestions and the active interest he took in the solution. Messrs. S. E. Caldwell, G. B. Hoadley, and J. R. Outt assisted in the operation of the machine and the measurement of final results.

LETTERS TO THE EDITOR

Prompt publication of brief reports of important discoveries in physics may be secured by addressing them to this department. Closing dates for this department are, for the first issue of the month, the twenty-eighth of the preceding month; for the second issue, the thirteenth of the month. The Board of Editors does not hold itself responsible for the opinions expressed by the correspondents.

On Inhomogeneities in the Magnetization of Ferromagnetic Materials

For some time work has been in progress on a method for detecting slight inhomogeneities in the magnetization of ferromagnetic materials and as a result of a good deal of experimenting the conclusion has been reached that qualitative observations are best made with small magnetized particles in suspension in a liquid. If such a suspension is allowed to settle on a magnetized surface, the pattern of the deposit reveals those points at which irregularities in the magnetic flux occur. The first successful attempts were made with finely divided iron obtained by sparking between iron electrodes under alcohol. This material was, however, very poor, and revealed only one pattern, namely, that obtained near saturation, as in Fig. 1, and that only with some uncertainty. Since starting this investigation Hámos and Thiessen[1] have published observations similar to those mentioned above.



Fig. 1. Patterns obtained on an iron-silicon alloy in large fields. Magnification ×16.

[1] L. v. Hámos and P. A. Thiessen, Zeits. f. Physik **71**, 422 (1931).

The technique for observing inhomogeneities has, however, been carried considerably farther, and though the procedure may still be regarded as a crude first attempt, very pretty results have been obtained. The essential improvement results from using particles having a larger permanent moment. So far the best have been small Fe_2O_3 particles, and I am greatly indebted to Mr. L. McCulloch of these Laboratories for preparing the suspension with which the following results were obtained.

The first observations were made on crystals of iron and of an iron-silicon alloy having large grains. The samples had been ground and annealed. For large magnetizations the deposits found were like that shown in Fig. 1, the field being perpendicular to the striations. The markings do not show any relationship to the grain structure. For somewhat smaller magnetizations, however, various systems of evenly spaced straight parallel lines appear, as in Fig. 2, the lines being usually more or less perpendicular to the magnetization, but varying slightly in direction and spacing from grain to grain. As the sample is rotated in the field, the lines gradually disappear, and new sets of lines having a new orientation take their place. At very low magnetizations no detectable patterns have been found. Similar results have been observed on an iron-silicon alloy melted in H_2. Its surface was quite smooth and clean, and as free from strains as is possible in material having more than one grain.

Observations were made on the untouched surface of samples of nickel and cobalt melted in H_2 with similar results, except that in nickel a new aspect of the phenomenon manifested itself. Instead of showing single parallel lines of like intensity, the microscope revealed

rather complicated patterns whose detail changed with the degree of magnetization. Three representative deposits are shown in Figs. 3 to 5. The last two differ only in intensity of magnetization. Many cases have been observed in which both the periodicity of the

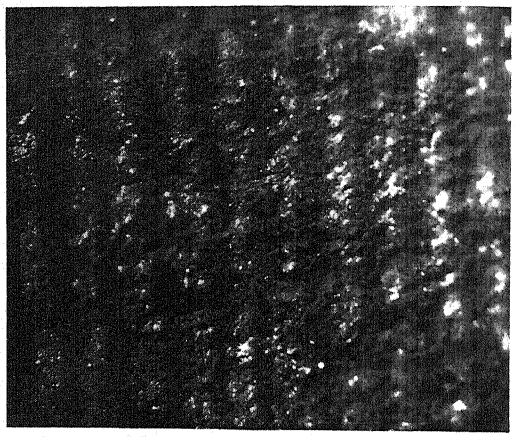


Fig. 2. Pattern obtained on the same sample as that shown in Fig. 1, but at smaller magnetizations. The width of the lines is probably due to surface irregularities. Magnification ×47.

intensity and the spacing of the lines made various complex but regular patterns. There are indications that the regularity of the patterns depends on the homogeneity of the mag-



Fig. 3. Pattern obtained on a sample of nickel. Magnification ×47. On the original photograph some of the lines are distinctly seen to be double, while others are single.

netization, and that inhomogeneous magnetization gives rise to several superimposed patterns.

As to the interpretation of these results, little can be said at present with any confidence. The periodicity of the patterns makes it convenient to describe them in terms of periodic functions. It is of some interest to observe that the energies J associated with the spin-spin interactions would give rise to a wave phenomenon of the observed order of magnitude if the usual relations $J=h\nu$, and $\lambda\nu=c$ are applicable. If z is the number of nearest neighbors that an atom has, then zJ is of the order of $2\ \theta K$, θ being the Curie temperature and K the Boltzmann constant. This gives for iron with $z=8$ and $\theta=1060°$K, and for nickel with $z=12$ and $\theta=630°$K, the following wave-lengths:

Fe	Ni
0.055 mm	0.14 mm



Fig. 4. The narrow lines are the deposit obtained on a crystal of nickel. Magnification ×16.

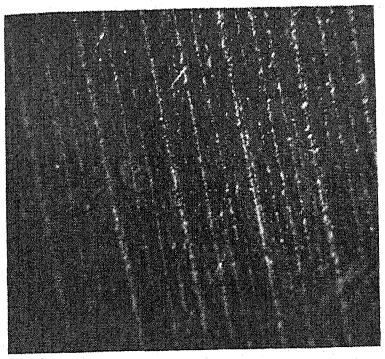


Fig. 5. Pattern obtained on the same grain as that shown in Fig. 4, but at a slightly higher magnetization. Magnification ×16.

In all figures the magnetic field is in this → direction.

In addition, the work of Wolf[2] indicates that iron is a comparatively homogeneous material in which almost all the atoms are in the same state, whereas nickel is made up of two states in the ratio of 3 : 1. In a qualitative way, therefore, if standing waves of some sort, such as Bloch's spin-waves for instance, are associated with magnetization, one would expect them to be more simple in a uniform material like iron than in a material like nickel in which at least three values of J are present.

A more detailed report will appear shortly in this journal.

F. BITTER

Research Laboratories,
Westinghouse Elec. and Mfg. Co.,
East Pittsburgh, Pa.

[2] A. Wolf, Zeits. f. Physik, **70**, 519 (1931).

The Absolute Values of the Mobilities of Gaseous Ions

The necessity of establishing the absolute values of the mobilities of gaseous ions under conditions of high purity and exact control of experimental conditions has long been recognized. The marked effect of extremely minute traces of impurities on the observed mobilities, as well as the unknown complications introduced in those methods which employ gauzes, air streams of possible turbulence and volumes of ionization vaguely defined make it imperative that a method be employed which is free from all these objections. Prior to the development by Tydall and Grindley (Proc. Roy. Soc. **A110,** 341, 1926) of a mobility method of considerable resolving power, the only method for studying ion mobilities free from experimental uncertainties was that employing ultraviolet light for the production of negative ions. By use of this method Loeb has obtained 2.21 as the absolute value of the mobility of the negative ion in air. The method of Tyndall and Grindley, however, permits ions of both signs to be studied, is free from all the objections mentioned above, and can be adapted to studies where high gaseous purity is maintained. It is, therefore, being employed in these measurements of the absolute mobilities of ions in pure gases.

In the experiments which are at present being carried out, the ionization is produced by intense, hard x-rays from a Coolidge tube under a potential of 80 kv pure D.C. The ionization chamber is of glass, with all metal parts reduced as far as possible in dimensions. The whole may be baked out under vacuum before filling with the gas to be studied which has been passed through a carefully constructed purifying train. A slight adaptation made in the potential cycle applied to the plates of the ionization chamber permits the study of positive ions in gases where free electrons exist.

Under these conditions of purity, the absolute values of the mobility of the positive and negative ions in air have been determined and found to be the same as those obtained by Loeb, Tyndall and Grindley. At normal temperature and pressure, the values obtained are 2.21 cm/sec. per volt/cm for the negative ion and 1.60 cm/sec. per volt/cm for the positive ion, the average age of the ions being 0.05 seconds.

A study of the mobility of the positive ion in hydrogen is of particular interest in view of the results of Loeb (Phys. Rev. **38,** 549, 1931). For Na^+ ions of extremely short age (10^{-5} seconds) he has found an initial mobility of 17.5, which after 10^{-4} seconds, changes abruptly to a value of 13.5. A subsequent change reduces the mobility to 8.4 at which value it becomes independent of the age of the ion. The correctness of these observations, as well as a slight refinement of the absolute values obtained, is most interestingly obtained from experiments made under the conditions described above. A typical curve showing the existence of two distinct classes of ions in hydrogen is shown in Fig. 1. The age of the

slower ion is approximately 0.07 seconds. It is the normal ion in hydrogen and has an absolute mobility of 8.25 cm/sec. per volt/cm. The hump on the high mobility side of the curve is definite evidence of the presence of an ion of age equal to 0.04 seconds and mobility 13.1 cm/sec. per volt/cm. While this latter value is not exact owing to the lack of resolving power of the method under such conditions, particularly with the low current intensity obtained in hydrogen ionized by x-rays, the agreement with the value obtained by Loeb is extremely good in view of the uncertain temperature correction in his calculations. These experiments thus obtain a slightly more accurate absolute value for the mobility of the normal ion in hydrogen, and entirely substantiate the existence of one ion of much higher mobility as observed by Loeb. The detection of the 17.5 mobility ion is beyond the limits of this method.

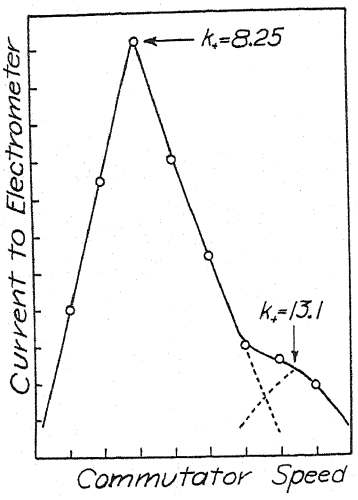


Fig. 1.

The experiments are being continued for ions in other gases.

NORRIS BRADBURY

Department of Physics,
University of California,
Berkeley, California,
October 19, 1931.

The Nuclear Moments of Indium and Gallium

The nuclear moment of indium was reported about a year ago by Jackson (Proc. Roy. Soc. **128,** 508, 1930) to be 1 from a study of the hyperfine structure of the resonance lines. Almost simultaneously McLennan and Allin (Proc. Roy. Soc. **129,** 208, 1930) reported it to be $\frac{1}{2}$ by studying practically the same lines. A more recent communication by Jackson (Nature **127,** 924, 1931) pointed out that the difference between his results and those of McLennan and Allin is just what one would expect from the difference in the resolving powers of their analyzing apparatus. A still more recent paper by McLennan, Allin, and Hall (Proc. Roy. Soc. **133,** 333, 1931) which continues their former investigation, again arrives at the conclusion that the nuclear moment is $\frac{1}{2}$. We have studied the resonance lines of indium using a Fabry-Perot interferometer and find indeed that λ4101 ($5p\ ^2P_{\frac{1}{2}}-6s\ ^2S_{\frac{1}{2}}$) has four distinct components as reported by Jackson, which, while it does not determine the nuclear moment, requires that it be greater than $\frac{1}{2}$. Microphotometer curves of this line show that the outside components are of equal intensity (which would be expected for any value of the nuclear moment) and that the inner components are both of smaller intensity. From the intensity rules this latter would be expected only if the nuclear moment were greater than $1\frac{1}{2}$. The line λ4511 ($5p\ ^2P_{1\frac{1}{2}}-6s\ ^2S_{\frac{1}{2}}$) was reported by Jackson to have four components but as the lines could not be fitted to a level scheme where both initial and final states were split into two, he concluded that he did not have the complete pattern and that one more line existed which he did not resolve. We have found a fifth component which is present very weakly and furthermore a strong indication of broadening in one of the more intense components, showing that the pattern consists of six lines, again in agreement with only those values for the nuclear moment which are greater than 1. The measured intervals are somewhat different from those reported by Jackson and these also point to the higher nuclear moment, the value $2\frac{1}{2}$ giving good agreement with the interval rule. The hyperfine-structure components of this line fall into two groups of three each and it must be that McLennan, Allin and Hall in observing only two lines have not separated the members of the groups. While it does not seem possible to say with certainty at present what the value of the nuclear moment for indium is, it

seems quite certain that it is greater than $1\frac{1}{2}$.

The resonance lines of gallium were examined with the same apparatus and the line $\lambda 4032$ ($4p\,^2P_{\frac{1}{2}} - 5s\,^2S_{\frac{1}{2}}$) was found to consist of three components at -0.083, 0, $+0.098$ cm^{-1}. In order to make certain that the central component was single the interferometer plates were separated 3.6 cm, causing the outside, components of adjacent orders to overlap, but the central component showed no signs of broadening, and one may conclude that the gallium nucleus has a spin moment $\frac{1}{2}$ as this is the only value which would give three components. The intensities as estimated visually are also in good agreement with the expected ratio of 2 to 1 for the central component with respect to either of the outer ones. The other resonance line is more difficult to resolve and we have succeeded in obtaining only partial resolution. There does not seem to be any doubt, however, that the same difficulty exists for gallium that also exists for thallium and indium regarding the relative hyperfine structure separations of the two members of the doublet arising from a single p electron. Here again the separation of the state with $J=\frac{1}{2}$ is comparable to the S state with which it combines but the state with $J=1\frac{1}{2}$ has a much smaller separation than that to be expected theoretically.

J. S. CAMPBELL
R. F. BACHER

National Research Fellows,
California Institute,
October 15, 1931.

Current-Intensity Relation of the λ600 Band of Helium

Sommer (Nat. Acad. Sci. Proc. **13**, 213, 1927) identified as a helium band a diffuse line occurring at λ600 on some of Lyman's plates. This identification has been confirmed by subsequent investigators but its relation to the rest of the helium molecular spectrum has remained undetermined. An investigation has been carried on at Princeton University in an attempt to determine the origin of the band. The extreme ultraviolet spectra of low voltage arc, Schuler cathode, and uncondensed capillary discharged have been obtained with a vacuum spectrograph. The band at λ600 appeared strongly only under such conditions of pressure and purity of the helium as permitted the appearance of the visible bands of helium. It has a distinctly sharp edge at the short wave-length side and shades away to the red. By using an approximate method of photometry it was found that in the uncondensed capillary discharge the intensity of λ600 varied directly with the current, whereas Weizel (Zeits. f. Physik **95**, 320, 1930) has observed that the visible bands of helium vary in intensity as the square of the current. An intensity varying as the first power of the current has generally been interpreted as signifying a primary, or one-stage process, while an intensity varying as the square of the current has been interpreted as a secondary, or two stage process, such as excitation by an electron of an atom which has been excited by a preceding electron. This suggests the possibility of a difference in the mechanism of excitation between the λ600 band and the visible bands. A more detailed discussion will be published later. Grateful acknowledgement is made to the Carnegie Institution of Washington for financial assistance.

JOHN L. NICKERSON

Mount Allison University,
Sackville, New Brunswick, Canada,
October 17, 1931.

Production of Second and Third Spark Spectra in a Hollow Cathode Lamp

The normal operation of a hollow cathode discharge tube with argon gas usually excites only the arc and a portion of the first spark spectra of the cathode material, while its operation with helium gas gives the arc and first spark spectra, and usually no more, the limit being approximately the energy available from the singly ionized gas. The introduction of a spark gap in series with the lamp removes this limitation and lines from higher stages of ionization are obtained. Lines of doubly ionized carbon and copper and of doubly and triply ionized germanium have been identified in spectrograms thus produced. Pulsating direct current was supplied to the Schuler Lamp by a full-wave rectifier consisting of two hot cathode mercury rectifier tubes, a filter choke and a 3 mfd condenser shunting the output. The lamp was normally operated at 0.4 to 1.2 amperes and at 500 to 2000 volts.

In normal operation with helium as the circulating gas the Ge II spectrum was strongly

excited when the carbon cathode containing about ½ gram of metallic germanium was operated at red heat. Ge I and C II lines were moderately strong, and lines of C I and gaseous impurities were rather weak, while a few of the most easily excited Ge III lines were present weakly.

After the adjustable spark gap had been placed in series with the lamp and closed, the lamp was operated normally until the Ge II was strongly excited. The spark gap was then opened slightly so that sparking occurred and the condenser gave an oscillatory discharge. An air blast on the spark gap reduced the tendency to arc. When sparking was taking place the lines appeared as follows: Ge I was little affected, Ge II was considerably intensified, Ge III and C III were brought out strongly and Ge IV only weakly excited. A spectrogram of the usual high potential hot spark without inductance usually shows certain Ge IV lines as the strongest lines in all of the Ge spectra. With the series spark gap bands, near 4000A, due to gaseous impurities, were much reduced in intensity. The helium bands 5500A to 6500A apparently were unaffected. When copper was used as the cathode the spark gap produced many strong lines that do not belong to the spectra of Cu I and Cu II, among these being the lines so far attributed to Cu III. Exposures of 15 minutes to 2 hours have been used for the region 500 to 2500A in a 1½ meter vacuum spectrograph.

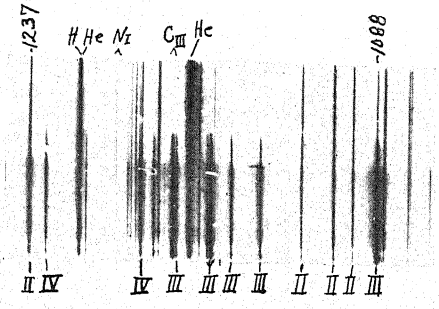


Fig. 1

The reproduction, Fig. 1, shows a portion of the germanium-helium spectrum taken with and without the use of the series spark gap. At the top two wave-lengths are indicated along with some impurities present. The stage of ionization of some of the germanium lines is indicated at the lower edge. Fig. 2 shows two germanium-helium spectra in the 4200A region. The wave-lengths and identifications are indicated at the top. It should be noted that when the spark gap is used the Ge III lines appear while the band *B* disappears.

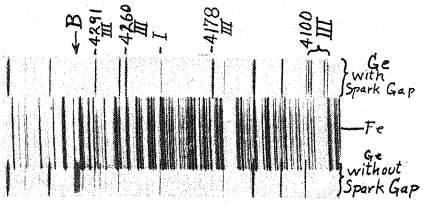


Fig. 2

This method of using a Schuler lamp is described because it provides a convenient method of exciting (apparently) all of the first and second spark spectra with scarcely any lines from higher stages of ionization present. By using argon to excite the arc spectrum, then helium with and without the spark gap all the lines may be identified as to stage of ionization. In addition the lines produced are very sharp, the source can be made sufficiently large to fill the angle subtended by any grating, and the sputtering is much less than with the hot spark. Since it is difficult to prevent arcing at the spark gap it is possible that a quenched gap of few sections, a make-and-break spark gap, or a magnetic blow-out might be employed to advantage. The spark gap must dissipate a large amount of heat.

It may be possible to excite still higher stages of ionization by a high potential condenser discharge through the lamp during an interruption of the direct current.

This technique has resulted from a suggestion by Dr. P. G. Kruger that a spark gap be employed to reduce the intensity of bands which had been troublesome.

C. W. GARTLEIN
R. C. GIBBS

Physics Department,
Cornell University,
Ithaca, N. Y.
October 26, 1931.

BOOK REVIEWS

Counting and Measuring. H. VON HELMHOLTZ, translated by CHARLOTTE LOWE BRYAN, with an introduction and notes by HAROLD T. DAVIS. Pp. xxxiv+39. D. Van Nostrand, New York, 1930. Price $2.50.

This little book contains a translation, with introduction and notes of Helmholtz' "Zählen und Messen," a paper which first appeared in the jubilee volume of philosophical papers dedicated to Eduard Zeller in 1887. More recently it has been reissued in the collection of Helmholtz' "Schriften zur Erkenntnistheorie" edited by P. Hertz and M. Schlick and published by Springer (Berlin 1921) to commemorate the hundredth birthday of Helmholtz. Through a strange oversight the volume under review nowhere gives an explicit reference to the original paper.

It is interesting to have this essay brought to attention at a time when physicists are devoting so much thought to the method of mathematical physics and its philosophical implications. That geometry, as referring to the actual space in which physical observations are made, is an empirical science, is now well recognized everywhere. Helmholtz takes us back even farther and shows how even the axioms of arithmetic are grounded in a physical empiricism. An illuminating quotation in this connection is:

"The first axiom, 'If two magnitudes are equal to a third, they are equal to each other,' is therefore not a law of objective significance, but it determines only what physical relations we can recognize as relations of equality."

In the introduction Professor Davis has traced the main course of thought on the problem of number and continuity from the Zeno paradoxes, through Cantor and Dedekind to the modern conflict between the schools of Hilbert and Brouwer. Unforuntately the space allotted to this task is too small for the fullest clarity to be attained in dealing with such a range of topics.

E. U. CONDON
Princeton University

Physics for Students of Pharmacy. C. J. SMITH. Pp. 287, figs. 194. Edward Arnold and Company, London, 1929. Price, $3.50.

A small book of two hundred and eighty-seven pages, with subject matter very highly selected from the standpoint of pharmacy students. The treatment is mainly with reference to the properties of matter, and classical apparatus encountered in laboratory experience. No attempt is made to discuss any of the so-called "modern physics," or modern mechanical devices. The properties of fluids occupy about one half of the section on mechanics. Sound is omitted. Heat and geometrical optics are treated quite fully. Bar magnets (the positions of Gauss are discussed at length) are given undue prominence, being allotted eighteen pages, while electromagnetic induction, x-rays, and radioactivity are covered in seven pages. Very few of the illustrations are taken directly from pharmaceutical experience. The author writes accurately and concisely, occasionally injecting practical details in manipulation, and frequently inserting historical statements.

R. C. WILLIAMSON
University of Florida

Physics of the Home. F. A. OSBORN. Pp. 391. figs. 221. McGraw-Hill Book Company, New York City, 1929, Second edition. Price $3.00.

The title of the book is apt. The book is written from the standpoint of students in Home Economy. The topics are selected with reference to their bearing in the home. Principles are stated briefly and concisely, and applications, (with numerous illustrations appealing to feminine experience) are discussed. Because of limitations in time, little space is devoted by the author to theoretical developments, or modern physics. One occasionally finds errors such as,

"tensile strength of steel wire equals 0.175 lbs. per square inch," or awkward expressions such as, "some notes have been sharped and flattened," or, "a vacuum of not less than one inch of mercury." But on the whole, the book should fill its place very well, and one will find much of interest in turning through its pages and noting the author's illustrations.

R. C. WILLIAMSON
University of Florida

Soap Films. A. C. S. LAURENCE. Pp. 141, figs. 61. G. Bell and Sons, Ltd., London. 1929. Price 12s 6d.

This book gives a good picture of the investigations which have been conducted on soap films. The author for several years assisted Sir James Dewar in his studies of soap films and later carried out independent investigations in this field. There are seven chapters to the book. Chapter I briefly discusses surface tension. Chapter II considers the characteristics of soap solutions and the preparation of soap and soap solutions to be used in making films and bubbles. Chapter III takes up the subject of soap films, their preparation and life history. Abnormal development, critical fall of soap films, and stratified films are also discussed in this chapter. Chapter IV is devoted to the black film. Chapters V, VI, and VII respectively discuss the subjects of soap solutions, soap molecules and the composition and structure of the soap film. Appendix I is devoted to the subject of oleic acid while appendix II deals with the color and thickness of soap films.

The author has presented the subject in a clear and pleasing manner. Students and investigators will obtain from this book a good picture of the subject of soap films and the physical behavior of soap solutions. Sixteen plates as well as other figures excellently illustrate the subject matter.

L. H. REYERSON
University of Minnesota

Analytical Mechanics. H. M. DADOURIAN, Pp. 427, figs. 148, D. Van Nostrand Company, New York, 1931. Price $4.00.

In this edition, as the author points out in the preface, much has been rewritten and one whole chapter almost entirely revised. This review, however, is not a comparison of the present edition with the previous ones but a consideration of the book as it now stands.

The scope of work covered is that of a good introductory course. In mode of development the author has first treated the mechanics of equilibrium and then proceeded to dynamics. In this choice he has been guided by the laudable aim, as he says, of introducing as few new concepts at a time as possible and of leading the student from the simpler to the more complex. There is too the advantage that if a student is taking a first course in calculus simultaneously the first portions of this text contain little calculus and so he should not be much called upon to anticipate results from the calculus course.

On the other hand there are, in the opinion of the reviewer, some real weaknesses. The concept of force is introduced on page 15, but without any statement there or elsewhere of how it is to be measured (by definition). Our ideas of its nature from muscular effort can surely not supply this need. Again on page 17 the kinetic reaction of a particle is defined as the product of its mass by its acceleration, although mass itself has not been previously mentioned. The mass idea is not discussed until page 122 and its nature and measurement are not treated until page 150. When this treatment is finally given it is based on force measurement which remains undefined. Surely such procedure cannot be conducive to clarity of ideas. Moreover, the experiments described on pages 151, 153 and 162 to clarify the ideas of mass and force are ideal, and incapable of verification to a degree that would afford reasonable confirmation. That on 162 is even theoretically unsatisfactory in that the motion is unstable. Would it not be preferable to have the evidence underlying fundamental ideas presented in such a form that the student could convice himself if he desired by trying the experiments out, or by reading the accounts of experiments that have actually been performed?

In the matter of notation the usual black face type for vectors is used. There is inconsistency however in many of the figures. Thus, in Fig. 98, page 242, the two arrows labelled $\boldsymbol{T}$ are

not the same force, the directions being different. If both are to be labelled by the same letter that letter can only denote magnitude and so should not be in bold face type. Again, in the figure on page 178 the arrow labelled $m\dot{v}$ should be labelled $-m\dot{v}$; and the same is true of every figure in which the kinetic reaction is represented.

There is no mention made of significant figures and some results imply an accuracy which is not obtainable. Thus, on pages 254 and 256, the answers are given to four figures while in each case the last digit has no significance.

On the other hand it is refreshing to find a text that is really consistent in the matter of units. Symbols everywhere represent physical quantities, units included. This consistence is a pleasant contrast with the practice of so many books where, in the same problem, the same letter is indifferently used to denote both an abstract number and a physical quantity.

The author also makes a good point in stressing that every force is associated with the action of some body. Such association is very helpful in the drawing of adequate figures for the solutions of problems.

The figures are well drawn and the type is good.

J. W. CAMPBELL
University of Alberta

Scientific Inference. HAROLD JEFFREYS. Pp. 247. The Macmillan Company, New York, 1931. Price $3.25.

Where all physical laws describing and explaining phenomen whose observation or appreciation lies within the ken of human experience are being reduced from the firm, "exact" basis of old to a system of probabilities, it is coming to be of more and more importance that the methods of derivation of such laws be subjected to rigorous analysis,—logical as well as mathematical. This is especially so because of the misconception, still somewhat prevalent, that results, derived by reasoning from probabilities, are therefore, *ipso facto* of an inferior nature to those obtained by using more "exact" methods.

Jeffrey's book forms indeed a most welcome addition in this rather neglected field, and its thorough treatment of the major and fundamental concepts at the basis of all scientific endeavor should make it a valuable aid to many of us who have been taking the ways and means of nature a little too much for granted. The author's primitive postulate is that it is possible to learn from experience, and that from this assumption and its logical consequences alone, there can be developed a justification for the adoption of *simple* quantitative laws, a justification which proves to be, plainly, that the *simple* law has a vastly greater inherent probability of being "true" than a more complicated one.

As one might expect from the author the treatment throughout is not only rigorous, but at the same time illuminating and stimulating. It does seem to this reviewer, however, that in some instances the rigor is too much on the side of the mathematical analysis, and he feels also that where so many of the fundamentals of Science involved have been subjected to the most careful and painstaking scrutiny, other, equally important fundamental concepts or results of observation have been passed over by *ex-cathedra* statements. One might mention: "But when the error arises as the resultant of a large number of independent errors of comparable importance, the normal law (of error) *is* right," and "We *know* . . . that light *is* a wave motion." As far as the former statement goes, one might, perhaps with more justification, say that if the normal law of error is found to hold in practice, then it would appear reasonably probable that the assumption concerning the existence of a large number of independent errors might have been right. Furthermore, this reviewer is not convinced that the question of the rejection of observations is quite as simple as it can be made to appear mathematically.

W. J. LUYTEN
University of Minnesota

Standard Four-Figure Mathematical Tables. L. M. MILNE-THOMSON, and L. J. COMRIE. Pp. 245. Macmillan and Company, England, 1931. Price 10/6 net.

This new volume of four-figure mathematical tables is not only one of the most useful books of its kind that has come to the reviewer's notice in recent years, but its form of presenta-

tion and general appearance make it a delight to the eye as well,—perhaps too obvious a thing to say where it concerns a work by such experienced calculators as Messrs. Milne-Thomson and Comrie. In addition to the usual tables of logarithms, antilogarithms, roots, powers, and reciprocals of numbers, and the natural and logarithmic tables of the trigonometric functions, natural logarithms, the gamma—and the error function, there are many others, such as those for trigonometric functions in radians, and for the inverse trigonometric and hyperbolic functions. The addition, at the end, of a table of integrals, both definite and indefinite, a revision of practically all the important formulae which occur in practical work, and a table of frequently used constants, gives the work a completeness as to render it almost indispensable to any research worker who ever has occasion to indulge in computations.

In choosing a type in which some figures extend above, and others below the general horizontal level of the majority, these new tables continue a practice which publishers of mathematical tables in this country would do well to follow—there can be no question but that the newer type is much easier on the eyes.

The work is available in two editions. In edition A the logarithms of numbers less than unity have been increased by 10. In edition B the logarithms of numbers less than unity are printed with negative characteristics.

W. J. LUYTEN
University of Minnesota

Astrophysik. (No. XI of **Strucktur der Materie.**) SVEIN ROSSELAND. Pp. 252, figs. 25. Julius Springer, Berlin 1931. Price RM 21.20.

The great advances made, as well as the revolutionary ideas introduced into astrophysics in the last decade or so, have made the want of an up-to-date, comprehensive survey of this important field felt very acutely in recent years. The appearance of Rosseland's Astrophysik, as No XI in the series: Struktur der Materie, edited by Born and Franck, fills this lacuna admirably.

After a short introductory review of the observational data of astrophysics and a thorough treatment of the fundamental physical and concepts underlying modern astrophysics, and with a view especially to their application to stellar interiors, the author divides the field in four main divisions. The first of these stellar hydrodynamics, includes Eddington's theory and the pulsation hypothesis. Energy problems, and stellar evolution, covering the problem of the source of stellar energy and the cosmogonic evolution of the universe forms the next part. The following division treats of the constitution of the atmospheres of the stars, and the problems arising in the interpretation of stellar specta. The last part considers the problems of the gaseous nebulae and the identification of "nebulium."

Considering the small amount of space at his disposal the author has succeeded remarkably well in presenting his subject in a manner at once comprehensive, authoritative, and well-documented, and for these reasons the book should appeal to a large class of physicists and astronomers. Owing to the limitations of space, no doubt, there are several points which are not as fully treated as they deserve,—at least from this reviewer's point of view. One might wish, e.g. that the spectral differences between giants and dwarfs and their relation to absolute magnitude determination had been given a more adequate space, and that the fundamental facts of observation had been given a less hurried survey. This applies to the first section as well as to the introductory parts to later discussions, where e.g. all irregular variable stars and novae together are dismised in one sentence, and the casual reader might well get the impression that the main division of all nebulae is in galactic nebulae and planetaries, while no mention is made of a possible observed change of period of the Cepheids beyond the fact that the lengthening demanded by Eddington has not been confirmed.

Another ciriticism might be levelled at the editorial make-up of the book, and its general appearance. It is particularly disconcerting to find that the entire book has been written as one chapter; and to have the first section of a new main division being in the middle of the same page where the last section of the previous main division left off. Furthermore, the index which is rather incomplete, does not differentiate between subjects and authors.

W. J. LUYTEN
University of Minnesota

Die elliptischen Funktionen von Jacobi. MILNE-THOMSON. Pp. 69, figs. 3. Julius Springer, Berlin 1931. Price RM 10.50.

The subtitle of the book, "Five-place Tables, with differences, of *sn u, cn u, dn u*, with the natural numbers as argument, arranged according to values of $m(-k^2)$, together with formulas and curves" gives a concise statement of the purpose and scope of the work. It is to be emphasized that these are *direct* tables of the functions *sn u, cn u, dn u*, in contrast to the ten-place tables of the elliptic integrals given by Legendre, *Traité des fonctions elliptiques*, Paris, 1825, Vol. II, and to the shorter five place tables such as in Hancock, *Elliptic Integrals*, New York, 1917, taken from Legendre's work. From Legendre's table the values of *sn u, cn u*, and *dn u* can be obtained only indirectly.

Each of the functions $sn(u, k)$, $cn(u, k)$, $dn(u, k)$ is tabulated to five places for real values of the variable u at intervals of 0.01, ranging from $u=0$ to $u=2$ or to $u>K$ if $K>2$. The largest value of u required is $u=6.5$ for $sn(u, 1)$. Instead of k, the quantity $k^2=m$ is used as the parameter, and the functions are tabulated for eleven values of m, at intervals of 0.1 ranging from $m=0$ to $m=1$. The first differences with respect to u are given in small type between the corresponding entries. Interpolation with respect to u requires the use of second differences, which are all small and easily obtained. Interpolation with respect to m is linear provided $u<\frac{1}{2}K$, while if $u>\frac{1}{2}K$ the function may be expressed in terms of functions of $K-u$ by appropriate formulas.

In addition to the tables just described a supplementary table gives the values of K, K', E, E', and $q(=e-\pi K'/K)$ to eight significant figures for values of $m=k^2$ ranging from $m=0$ to $m=1$ at intervals of 0.01. Altogether the tables, which occupy 66 pages, are well printed, conveniently arranged, and easily legible.

The introduction of eight pages consists of numerical examples illustrating the use of the tables; a list of the periods, zeros, poles, and residues; a group of fundamental formulas, including the trigonometric series, the power series, the addition formulas and the like; a table of some thirty integrals involving elliptic functions or their inverses; and finally a paragraph on the Weierstrass θ-function. It is to be regretted that formulas involving the theta-functions were not included, and that the list of integrals is not more complete.

Nevertheless the book satisfies a long-felt want on the part of many who have desired direct tables for the elliptic functions, and the author is to be complimented on having undertaken the work and on the excellent manner in which he has accomplished it.

W. E. MILNE
University of Oregon

Vorlesungen über Differential—und Integralrechnung. R. COURANT. Erster Band: **Funktionen einer Veränderlichen.** Pp. xiv+140, figs. 127. Berlin, Julius Springer, 1927. Price, RM 18.60.

This book, by one of the foremost of German mathematical scholars, is a first course in the differential and integral calculus—for students of suitable preparation and maturity. For readers trained under American conditions, and already acquainted with the essentials of the calculus, it is a valuable supplementary treatise, presenting familiar principles in a new light, and offering much additional material for which it would ordinarily be necessary to refer to more advanced texts.

Such chapter headings as differential and integral calculus of the elementary functions, Further development of the integral calculus, applications, Taylor's formula and the approximation of functions by polynomials, digression on numerical methods, infinite series and other limiting processes, call for no special comment. Partial differentiation and multiple integrals are reserved for a second volume, on functions of more than one variable; the subject of differential equations, as a separate major topic, is represented only by a short chapter on "The differential equations of the simplest oscillatory phenomena," with a note to the effect that the differential equations of more general phenomena of this sort will be taken up in the second volume.

Passages going beyond the minimum content of an ordinary course in the calculus are the chapter on Fourier series and trigonometric interpolation, and sections on polynomial interpolation, with special reference to the formulas of Newton and Lagrange, Wallis's infinite prod-

uct for π, Stirling's formula for the factorial, special functions illustrating peculiarities of continuity and differentiability, the multiplication and division of power series, the evaluation of the probability integral, the Bernoulli numbers, etc. A section on applications of the exponential function discusses continuously compounded interest, radioactive disintegration, the cooling or heating of a body in a surrounding medium, the dependence of atmospheric pressure on height above the earth's surface, the progress of chemical reactions, and the switching on and off of an electric current.

There are noteworthy differences between this course and those with which the American student is familiar. Exercises are not provided, except for an occasional statement in the frank and informal language of direct address that "I can leave it to you to prove so-and-so." The chapter on the "differential and integral calculus of the elementary functions" begins on page 109, being preceded by a 50-page chapter on "fundamental concepts of the integral and differential calculus," in which the definite integral is introduced first, then the derivative, and then the indefinite integral as inverse of the derivative; and this in turn is preceded by an introductory chapter of approximately equal length, discussing in some detail the notions of number, function, limit, and continuity. The reader will find much here which he has ordinarily thought of as belonging in a course in the theory of functions; but he will find the essential significance of this material, as an explanation of the fundamental principles of the calculus, more apparent than it sometimes is when the theory of functions is presented as a separate subject. The calculus is treated throughout as an analysis of relations of number and quantity, rather than as a technique for the manipulation of formulas.

The book is admirably printed and neatly bound, convenient to the hand and to the eye. To the American student who is under the necessity of preparing for an examination in mathematical German it gives an excellent opportunity for self-instruction in the language through the study of material which is familiar enough to be readily intelligible, and at the same time novel enough to be worthy of careful attention on its own account.

DUNHAM JACKSON
University of Minnesota

PROCEEDINGS
of the
AMERICAN PHYSICAL SOCIETY

Minutes of the Schenectady Meeting
September 10, 11 and 12, 1931

The 172nd meeting of the American Physical Society was held in Schenectady, New York, on Thursday, Friday and Saturday, September 10, 11 and 12, 1931 upon invitation from Union College and the General Electric Company.

The scientific sessions were held in the Physics Building of Union College and in Rice Hall in the Research Laboratory of the General Electric Company. The presiding officers were the Vice-president, Paul D. Foote, P. I. Wold and Herbert E. Ives.

On Thursday morning at 10 o'clock the Society convened in Rice Hall where the program consisted of two invited papers commemorating the one hundredth anniversary of the notable experiments of Michael Faraday and Joseph Henry in the field of electro-magnetic induction. The paper on "Faraday's Diary" was written by Sir William Bragg, Director of the Royal Institution and read by Professor John Zeleny of Yale University. Professor W. F. Magie of Princeton University gave an address on the life and scientific work of Joseph Henry. This session was attended by 230 persons.

At noon on Thursday the members of the Society, 232 in number, were the guests of the General Electric Company at the Works Restaurant. At the same hour the ladies who came to the meeting, 76 in number, were guests at a luncheon at the beautiful Riverwood Inn on the Mohawk River.

On Thursday afternoon about 180 persons were taken through the General Electric Research Laboratory in groups of fifteen each making thirteen stops, where men in charge of the problems were present to explain with experimental demonstrations their particular research.

The Physical Society dinner was held at the Mohawk Golf Club on Thursday evening with 254 in attendance. The Vice-president, Paul D. Foote, presided calling for a few remarks from President Frank P. Day of Union College, President Karl T. Compton of the Massachusetts Institute of Technology, Dr. W. R. Whitney and Dr. Irving Langmuir of the General Electric Company, and Dr. Henry A. Barton, the newly appointed Director of the American Institute of Physics. The guests were further entertained by one of the employees of the General Electric Company who was a very clever magician.

On Friday morning at 9 o'clock the Society convened in two sections at the Physics Building of Union College for the reading of the twenty-five contributed papers. After these sessions discussion groups met to consider the following subjects:

(1) x-rays and crystal structure with Bergen Davis presiding.
(2) teaching of physics—P. I. Wold.
(3) electric discharge through gases—Irving Langmuir.
(4) acoustics—C. W. Hewlett.

After the close of the morning program the Society was invited to be the guests of Union College at luncheon in the rose garden on the Union College grounds. There were 302 present at this delightful occasion. After the luncheon 183 went to a picnic at Indian Ladder, the procession of about fifty automobiles being led by police escort all the way out and back.

Saturday morning was devoted to a symposium on magnetism. There were two invited papers, one by Professor S. L. Quimby of Columbia University on "New Experimental Methods in Ferro-Magnetism" and one by Dr. Francis Bitter of the Westinghouse Electric and Manufacturing Company on "Interpretation of Ferromagnetic Phenomena."

After this program discussion groups met again on
(1) molecular spectra, presided over by W. W. Watson.
(2) engineering physics—G. B. Pegram.
(3) electric discharge through gases—Irving Langmuir.

In the afternoon a carefully prepared program of short papers was presented for a discussion group on magnetism. The leader of this group was Lewi Tonks.

At the close of the Saturday morning session in Rice Hall the following motion presented to the Society by Professor John Zeleny was voted unanimously:

Resolved: that the American Physical Society and all those attending this session express their heartiest thanks to the General Electric Company, Union College, the local committee, President Day, Professor Wold, Dr. Whitney and Dr. Jesse and all those connected with them for the facilities afforded us for our meeting and for the magnificent entertainment they have provided during this Schenectady meeting.

Meeting of the Council. At its meeting held on Thursday morning, September 10, 1931, two persons were elected to fellowship, thirty-two were transferred from membership to fellowship and twenty-nine were elected to membership. *Elected to Fellowship:* Erik G. Rudberg and Yoshikatsu Sugiura. *Transferred from Membership to Fellowship:* Carl A. F. Benedicks, P. M. S. Blackett, Arthur A. Bless, W. E. Curtis, N. A. de Bruyne, E. Gilbert Dymond, C. Drummond Ellis, K. George Eméleus, James Franck, August Hagenbach, Sunao Imanishi, Raynor C. Johnson, Robert W. King, H. A. Kramers, Henry Margenau, A. B. McLay, Yoshio Nishina, T. Peczalski, J. Alingh Prins, G. M. Shrum, Manne Siegbahn, Herbert W. Skinner, Masamichi So, Herta Sponer, Hildegard Stücklen, Tutomu Tanaka, C. C. Van Voorhis, Shou Chin Wang, William W. Watson, Max Wehrli, Trygve D. Yensen and Usaburo Yoshida. *Elected to Membership:* E. W. Anderson, Loring B. Andrews, David W. Armstrong, L. H. Bailey, Richard F. Baker, William S. Benedict, Elmer R. Binkley, Donald S. Bond, Carl C. Chambers, J.

Hollie Cross, A. H. Croup, Roger W. Curtis, Einosuke Fukushima, Leo G. Hall, Wendell F. Kinsey, J. E. Lennard-Jones, K. V. Pestrecov, Esme E. Rosaire, William W. Shirley, H. M. Smallwood, Scott W. Smith, William O. Smith, Arthur B. Stanely, Demetrius Tarris, D. D. Taylor, Walter Weizel, M. L. Wiedmann, Albert J. Williams Jr., and Robley C. Williams.

K. T. Compton reported for the American Institute of Physics that H. A. Barton had been elected Director of the Institute and that John T. Tate had been appointed adviser on publications. Dr. Barton was introduced to the Council and it was voted that he be invited to attend the meetings of the Council ex-officio as a non-voting member.

Editor John T. Tate reported the new journal "Physics" to be developing rapidly, with plenty of material for publication and about 900 subscriptions.

The regular scientific program of the Society consisted of twenty-five papers, numbers 8, 13 and 18 being read by title. The abstracts of these papers are given in the following pages. An Author Index will be found at the end.

W. L. SEVERINGHAUS, *Secretary*

1. The vectorial photoelectric effect in thin films of alkali metals. HERBERT E. IVES *Bell Telephone Laboratories.*—It is assumed that the photoelectric effect exhibited by thin films of alkali metals on specular platinum surfaces is proportional at any wave-length to the electric intensity just above the platinum. This electric intensity is found, using the optical constants of platinum, by computing the intensities of the wave patterns formed by the interference of the reflected and incident beams. These computations are made for various angles of incidence and for light polarized in and at right angles to the plane of incidence. The intensities thus found exhibit very large ratios of value for the two planes of polarization, in striking agreement with the characteristics of the vectorial photoelectric effect. The changes of amplitude of the perpendicular electric vector on entering the alkali metal film, as computed from the optical constants of the alkali metal, account for the experimentally found low values of the emission ratios at long, and their high values, at short wave-lengths.

2. The photoelectric effect from thin films of alkali metal on silver. HERBERT E. IVES, AND H. B. BRIGGS, *Bell Telephone Laboratories.*—The thin films of alkali metals which spontaneously deposit in vacuo on other metals have long been known to exhibit photoelectric effects which vary in amount and character, depending on the underlying material, but the exact nature of this dependence has been obscure. Silver, because of its region of exceedingly low reflecting power in the ultraviolet and the accompanying variation of optical constants is exceptionally well suited for studying the influence of the underlying metal. It is found that the region of low reflecting power profoundly affects the photoemission, but in a manner not to be explained simply by reduction of light reflected back through the alkali metal film. The results obtained are very satisfactorily explained upon computing, from the optical constants, the intensity of the standing waves formed by reflection just above the silver surface. The positions of the maxima and minima of photoemission, and their variations with angle of illumination and plane of polarization are accurately indicated.

3. Correlating the selective photoelectric effect with the selective transmission of electrons through crystalline surface structures. A. R. OLPIN, *Bell Telephone Laboratories.*—Evidence is produced to support the view that photoelectrically selective, two-component cathodic surfaces are crystalline in nature. Then, assuming that Fowler's equation for the energy of electrons selectively transmitted through a single potential valley, $W=(n^2h^2)/(8md^2)$, is equally valid for the energy of electrons selectively transmitted through the periodic sequence of valleys characteristic of the potential field within a crystal, and that all of the energy of photoelectrons is acquired from the incident light quanta, the wave-lengths of light to which such a surface should

respond selectively can be computed. Such computations have been made with d equal to the internuclear distance between electropositive ions in the lattice structure of alkali metal hydride, oxide and sulphide crystals. The hydride crystals belong to the sodium chloride type and the oxide and sulphide crystals are supposedly of the calcium fluoride type. The correlation between these computed values and the positions of the observed selective maxima is exceptionally good. Moreover, the fact that the alkali metal hydrides exhibit but one selective maximum and the oxides two or three maxima is in keeping with the geometry of their respective crystalline types.

4. Thermionic emission in caesium-oxide photocells at room temperatures. E. F. KINGSBURY, *Bell Telephone Laboratories.*—The measurements on these cells recently reported (Kingsbury and Stilwell, Physical Review **37**, 1549, June 1, 1931) have been extended to a number of cells of a wide variety of treatment during construction. A relation between the thermionic constants, log A and b_0, has been obtained which approximates in slope the relation obtained by Richardson and Young (Proc. Royal Society **A107**, 377, 1925) for potassium cells sensitized with oxygen. The caesium cells, however, give from 100 to 1000 more emission at corresponding temperatures. The variation in overall photo sensitivity to tungsten light seems to be independent of the thermionic constants. In general the photoresponse decreases with increasing temperature but the behavior is complex, some cells increasing with rise of temperature and some showing an erratic superposition of the two effects.

5. The emission of secondary electrons from tungsten. A. J. AHEARN, *Bell Telephone Laboratories.*—An apparatus is described for investigating critical potentials in the emission of secondary electrons from tungsten. Measurements on the velocity distribution in the primary beam show that secondary electrons from the electron gun are absent. Tube characteristics which might introduce spurious critical potentials in the secondary emission from tungsten appear to be absent. By heat treating the tungsten and cleaning up residual gases, maxima and critical slope changes were developed below 40 volts. From 40 to 500 volts, only 4 critical potentials were observed even with the sensitive methods of measuring and plotting the data, and all but one of these disappeared eventually after heat treatments of the tungsten target. The phenomena may be associated with the diffraction of electrons or the production and absorption of characteristic soft x-rays. Regardless of the mechanism operating at the critical potentials, their decrease or elimination beyond 40 volts points strongly to effects of surface contamination rather than to characteristics of tungsten.

6. Transmission of electrons through potential barrier of thoriated filament. W. B. NOTTINGHAM, *Bartol Research Foundation.*—Thermionic measurements on a thoriated filament showed the electron velocity distribution to be accurately Maxwellian at the temperature of the filament for values of applied potential negative of V_0. At V_0 thus determined, the work function was 3.2 to 3.5 volts. With small accelerating potentials, referred to V_0, the current increased rapidly and reached a fair saturation value at 1.5 to 2.0 volts. Electron velocity distributions from a *deactivated* or pure tungsten filament were Maxwellian at the temperature of the filament. Comparing curves for activated and deactivated filaments heated to give the same "saturation" emission, showed that the velocity distribution from the pure tungsten was accurately reproduced with the activated filament over the range of accelerating potential mentioned above. This result can be ascribed to the transmission of electrons *through* a potential barrier ($B-C=1.4$ volts), 4.5×10^{-8} cm wide at one volt under the top. The transmission coefficient $D(W)$ of the Nordheim-Fowler theory must be a function of the energy of the impinging electrons. Therefore the emerging electrons will certainly not have a Maxwellian distribution at the temperature of the filament. Experimentally the barrier transmits the faster electrons easily, as would be expected, with the result that those transmitted happen to have practically a Maxwellian distribution with a temperature $48\%\pm3$ higher than the filament.

7. On the theory of thermionic emission. N. H. FRANK, *Massachusetts Institute of Technology.*—A theory of thermionic emission between plane parallel electrodes including space charge effects is developed to include the modifications introduced by quantum mechanics. Two modifications appear; (a) the use of the Fermi-Dirac statistics instead of the classical

statistics, and (b) the introduction of a probability of emergence of electrons within the metal which is a continuous function of the electron energies. The effect of (a) alone is to change the expression for saturation current. Expressed in terms of saturation current, all results of classical theory remain unchanged. The introduction of (b) modifies all these results. For the case of accelerating anode potentials high enough to prevent the formation of a potential minimum, the charge density and potential distributions are but slightly altered. For high retarding anode potentials (no potential minimum), the current voltage characteristic is

$$i = i_s \epsilon^{-e\phi/kT} \cdot f$$

ϕ is anode potential, i_s saturation current. Classically $f = 1\lambda$ quantum-mechanically it is a slowly varying function of ϕ. The charge density and potential distributions for this case are essentially different than the classical expressions. The case of a potential minimum is handled as a combination of the above two cases. Just as in the classical case numerical or graphical integrations are necessary before numerical results can be obtained.

8. Determination of e/m by the refraction of x-rays. J. A. BEARDEN, *Johns Hopkins University.*—Since the usual dispersion theory has been so thoroughly established we may, by measuring the index of refraction of x-rays, use the theory as a means of determining e/m. Measurements of the index of refraction of the copper K series in a 90° quartz prism have been made by two methods. In the first method the incident beam struck the first face of the prism at a glancing angle larger than the critical angle of total reflection. In the second method the incident beam struck the second face at a very small angle. The alignment of the prism, slits, and plateholder was made as described by the writer in a previous paper (Phys. Rev. **37**, 1210 (1931)). Twenty-nine measurable exposures have been obtained under various conditions. The dispersion formula

$$\delta = 1 - \mu = \frac{e^2}{2\pi m} \sum_i \frac{N_i}{\nu^2 - \nu_i^2}$$

was used for determining e/m. The value of ν was obtained from the writer's grating wave-length measurements. e/m was thus found to be

$$e/m = 1.764 \times 10^7 \text{ e.m.u./g.}$$

This is in good agreement with the results obtained by Stauss (Phys. Rev. **36**, 1101 (1930)) but differs from either of the accepted values of e/m. Calculations of e/m have also been made using the complete dispersion formula which includes the absorption in the prism.

9. An x-ray study of the nature of solid solutions. ROBERT T. PHELPS AND WHEELER P. DAVEY, *Pennsylvania State College.*—(1). The solid solution of pure Al in pure Ag lowers the lattice parameter of the Ag by an amount which is proportional to the Al content of the solution. Saturation of Al in Ag is reached at 5.4 percent Al by weight. Further addition of Al gives aggregates of Ag_3Al of sufficient size to give x-ray diffraction patterns. (2). The experimental values for the densities of the solid solutions of Al in Ag are somewhat lower than those calculated on the basis of a direct substitution of Al atoms for Ag in the Ag lattice. This discrepancy is greater than the combined error in the two values. (3). Systematic examination of the various possible types of explanation for this discrepancy leaves us with only one tenable theory, namely that the Al in the solid solution is chemically combined with the adjacent Ag. If this explanation is used as a basis for a general theory of the nature of solid solutions, the picture is found to be consistent with the known facts for both solid solutions and liquid solutions. So far, it has not been found inconsistent with any known fact.

10. A 1,500,000 volt electrostatic generator. ROBERT J. VAN DE GRAAFF, *National Research Fellow, Princeton University.*—The application of extremely high potentials to discharge tubes affords a powerful means for the investigation of the atomic nucleus and other fundamental problems. The electrostatic generator here described was developed to supply suitable potentials for such investigations. In recent preliminary trials, spark-gap measurements showed a potential of approximately 1,500,000 volts, the only apparent limit being brush discharge from the whole surface of the 24-inch spherical electrodes. The generator has the basic advantage of supplying a direct steady potential, thus eliminating certain difficulties inherent in the applica-

tion of non-steady high potentials. The machine is simple, inexpensive, and portable. An ordinary lamp socket furnishes the only power needed. The apparatus is composed of two identical units, generating opposite potentials. The high potential electrode of each unit consists of a 24-inch hollow copper sphere mounted upon a 7 foot upright Pyrex rod. Each sphere is charged by a silk belt running between a pulley in its interior and a grounded motor driven pulley at the base of the rod. The ascending surface of the belt is charged near the lower pulley by a brush discharge, maintained by a 10,000 volt transformer kenotron set, and is subsequently discharged by points inside the sphere.

11. Negative hydrogen ions from H_2O by electrons of a critical velocity. DONALD W. MUELLER AND H. D. SMYTH, *Princeton University.*—Lozier and Bleakney have observed negative hydrogen ions appearing over a small range of electron velocities in apparatus containing water vapor. Their result has been qualitatively confirmed using a mass spectrograph. Hydrogen negative ion intensity falls off above and below 8 volts incident electron velocity. Oxygen and hydroxyl negative ions were also observed but increasing in amount above about twenty volts incident electron velocity.

12. On the absolute determination of gravity. A. C. LONGDEN, *Knox College, Galesburg, Ill.*—The importance of a new determination is discussed. In the work here described, a reversible pendulum is used in which roller bearings are substituted for knife-edges and quartz suspension rods or tubes are used instead of metal. Invar is disqualified on account of its magnetic qualities. The period of the pendulum is determined to within 1 or 2 parts in a million by a very direct method which involves no corrections and which can be performed in a few minutes, while the pendulum is swinging through a very small amplitude and while the *change* of amplitude is quite negligible. The author points out the errors of the "Coincidence Method" as it is generally used, and shows that it may either be improved, or abandoned as unnecessary. He also cites some of the results on record, which are accepted as highly exact, but which in reality include rather large errors. The method includes a number of refinements in comparing the length of the pendulum with that of a standardized invar rod.

13. Entropy of polyatomic molecules. D. S. VILLARS, *Research Laboratory, Standard Oil Co. (Ind.)*—By applying the data of Hund on ammonia and of Elert on methane to obtain the total number of completely antisymmetric eigenfunctions which can be formed from the different rotational states, one can get the *a priori* probabilities of the different non-combining symmetry varieties (nuclear doublet and quadruplet for ammonia and nuclear singlet, triplet and quintet for methane) and from them the entropies. The relative proportions at high temperature of the different varieties are one to one for ammonia and 2:9:5 for methane (resp.). The absolute entropy of the ammonia mixture is 51.5 cal. degree^{-1} at 298.1°K and of the methane mixture, 50.1 at the same temperature.

14. Some physical properties of compressed carbon monoxide. W. EDWARDS DEMING AND LOLA E. SHUPE, *Bureau of Chemistry and Soils, U. S. Department of Agriculture, Washington, D. C.*—Compressibility data obtained by Bartlett on carbon monoxide have been adjusted and extrapolated so that p, v, T data from −70°C to 400°C and from 25 to 1200 atm. are available. Using the graphical scheme for obtaining derivatives, previously described in similar calculations for nitrogen, the following physical properties have been computed, and are available in tables and curves at eleven temperatures and fourteen pressures, over the range noted above: specific volume, density, expansion coefficients, fugacity, C_p, $C_p - C_v$, C_v, μ. The C_v vs. t isobars for 300 to 1200 atm. show a minimum at about 100°. On the low temperature side of this minimum the curves are very steep; for 1200 atm. C_v drops from 4.4 R at −70° to 2.57 R at 100°. Above 100°, C_v is only a few hundredths cal./mole deg. higher than C_v^* (zero pressure) for pressures to 400 atm.; further increase in pressure raises C_v only a few tenths. Below 25°, C_v for $p = 25$ is slightly less than C_v^*; for $p = 100$, 150, 200, C_v falls considerably below C_v^* as t falls to −70°. The C_p vs. p isotherms show that above 500 atm. C_p does not change much with further increase in pressure. Below 0°, decrease in temperature is accompanied by considerable increase in C_p, when $p > 200$.

15. An optical study of heat transfer by convection from solid surfaces to air. R. B. KENNARD. *Bureau of Standards.*—A hot body is placed in one arm of a Jamin interferometer which is built about an open well so as to permit the free circulation of air about the body. The temperature distribution in the air is obtained without the introduction of any material thermometric apparatus. An equation relating the fringe shift to the air temperature is developed. Photographs are shown of the fringes near horizontal and vertical plane surfaces. The transition from laminar flow to turbulent flow is shown by a change in the direction of the fringes. The temperature gradient for laminar flow is constant for the temperature range used. If the temperature gradient were constant throughout and the same as for laminar flow, the "equivalent" film would be 5.5 mm thick and independent of the temperature of the hot plate. The interference fringes were photographed about a wire of 3/10 mm diameter, and about cylinders of 5 mm, 12.7 mm and 30 mm diameter. From these photographs the isothermals about these cylinders were plotted, and the relative heat emission along different radii estimated. The relation between the thickness of the layer of heated air and the diameter of the cylinder is noted.

16. Some evidence indicating the existence of Ba isotopes 136 and 137. R. C. GIBBS, AND P. G. KRUGER, *Cornell University.*—In 1925 Aston reported the chief isotope of Ba to be 138, with the possibility that isotopes 136 and 137 might exist in extremely small quantities. From such data one would expect the Ba lines to show no hyperfine structure, since elements with an even atomic weight in general have a nuclear spin of zero. The Ba II lines λ's 4554A and 4934A ($6s^2S_{1/2}-6p\ ^2P_{3/2,\ 1/2}$) show structure when photographed with a Fabry-Perot interferometer, the satellites combined having roughly one tenth the intensity of the parent line. This leads one to think that the satellites are probably due to an odd isotope (137) and that the parent line is due to the even isotopes (136 and 138). A mixture of 27 percent of isotope 136, 9 percent of isotope 137 and 64 percent of isotope 138 gives 137.37 for the average atomic weight, which agrees with the chemical atomic weight of Ba. This gives an even to odd ratio of isotopes of about 10:1, and so roughly checks with the intensity relation in the structure of the lines.

17. Quantitative intensity determinations in the spectra of normal and of singly ionized vanadium, V I and V II. GEORGE R. HARRISON, *Massachusetts Institute of Technology.*—The relative intensities of all lines of V I and V II stronger than 1/2 of 1 percent of the intensity of the principal lines and lying between λλ5200 and 2500A. have been determined under various conditions of excitation in the vacuum arc, using the first and second orders of a 35 ft. concave grating and standard methods of photographic photometry. The proportionate number of anomalous lines found is somewhat greater than in Ti I and II, and less than in Cr I and II, as is to be expected from the multiplet separations and the number of terms of similar J value which can perturb one another. The spectral analysis used is a fairly complete one kindly furnished in advance of publication by Dr. W. F. Meggers. The data obtained are being used to test the excitation conditions in the vacuum arc, the J-group sum rule of Johnson and the writer (Phys. Rev. **37**, 1702, 1931 and issue for Aug. 15, 1931), and the role played by quantum numbers and the magnetic and electrostatic term separations in determining the intensity perturbations produced in a given line. Attempts are now being made to extend these data to both longer and shorter wave-lengths.

18. Band spectrum intensities by graphical methods. ELMER HUTCHISSON, *University of Pittsburgh.*—In order to facilitate the comparison of experimentally determined band intensities with those predicted by theory, an easy and rapid method of determining the theoretical results is desirable. Making use of the author's previous calculations (Phys. Rev. **36**, 410 (1930); **37**, 45 (1931)), based upon the Franck-Condon principle, charts have been prepared which permit a graphical determination of the intensities of vibrational bands in electronic transitions. Transition probabilities associated with the lowest energy levels are given by means of contour lines on a chart in which the changes in the equilibrium distances between the atoms during the transitions are plotted as ordinates and the square roots of the ratios of the vibrational frequencies in the lower and upper states are plotted as abscissas. Besides the squares of the transition probabilities, the complete expression for the intensities in absorption involves the fourth powers of the frequencies of the bands and the populations of the initial states which

are also obtained graphically as a function of the temperature of the absorbing gas. The use of these charts allows a rapid estimation of the band intensities in any particular electronic transition. As an example of the use of these charts, the band intensities of the $^1\Sigma - ^1\Sigma$ transition of AgH are calculated. The computed values are found to be in fairly good agreement with the experimental results of Hulthèn and Zumstein (Phys. Rev. **28,** 13 (1928)).

19. The Kerr-effect in Rochelle salt. HANS MÜLLER, *Massachusetts Institute of Technology.*—An electric field parallel to the *a*-axes of Rochelle salt produces a large electro-optical effect which does not reverse with the direction of the field. This effect has been measured for temperatures between 0 and 35°C and fields up to 30 kv/cm. The effect exists in the entire temperature region but has a sharp maximum at about 23°C. The change of the difference between the indices of refraction $n_a - n_b$ resp. $n_a - n_c$ is not proportional to the square of the field strength but increases almost linearly up to 15 kv/cm. At higher fields the effect tends towards saturation. The effect is not due to temperature change due to conduction. It is much too large to be accounted for by electrostriction. The observations support the hypothesis that the anomalous dielectric and piezoelectric properties of Rochelle salt are due to the fact that the electric dipoles of the H_2O molecules of the water of crystalization behave similarly to the magnetic dipoles in the case of ferromagnetism.

20. The Hall effect in solid mercury. JAMES T. SERDUKE AND THOMAS F. FISHER, *Union College.* (*Introduced by P. I. Wold.*)—Various investigators have studied the Hall effect in Hg, especially in the liquid form. In the liquid form the results are uncertain and subject to doubt. In the solid form Fenninger in 1914 found the Hall constant to be not larger than 0.000011. The present investigators developed a method of obtaining a Hg strip 14 cm long, 2 cm wide and of various thickness down to 0.006 cm and have measured the Hall effect and resistivity in solid mercury at a temperature of about −60°C. The conclusions are that in this case the Hall effect is negative and the constant has a value of -0.00078 ± 10 percent. The Hall constant is independent of field strength, current density and thickness of specimen. No definitely measurable longitudinal effect, i.e. change in resistivity with magnetic field was found.

21. Exhibition of parallax panoramagrams made with a large diameter concave mirror. HERBERT E. IVES, *New York City.*—The general methods by which relief pictures may be made by a single exposure, using a large lens or mirror, have been described previously (J.O.S. A. 20, 597(1930)). The pictures exhibited were made by means of a strip of spherical concave mirror of 48 inch diameter and 48 inch radius, built up out of three 16 inch sections. The light from the object after leaving the concave mirror is reflected to one side by means of a 45° half silvered mirror. An opaque line grating of 20 lines to the inch, with clear spaces 1/50 the width of the opaque is placed slightly in front of the sensitive plate, and a similar grating, slightly behind a positive print on glass converts this into a relief picture. Details of the "camera," which consists of a dark room with a large window, are given. The pictures are notable, as compared with pictures previously exhibited, made with a large lens, for the larger angle (60°) through which relief is observed.

22. The small shot effect in photoelectric currents. B. A. KINGSBURY, *Bell Telephone Laboratories.*—The small shot effect, as it occurs in a photoelectric current, has been used to secure an evaluation of the electron charge. A new and original method of amplifier calibration, which involved the use of a modulated light beam, simplified the measurements and the computation of the result. In the absence of space charge, the experimental value of the electron charge was 1.61×10^{-19} coulombs for a thermionic current, and about 25 percent greater for a photoelectric current. It was found that the small shot effect is enormously increased in photoelectric currents which are amplified by collision ionization. Statistical variations which might be expected to occur in a beam of radiant energy could not be detected, since, within the limits of experimental accuracy, the small shot effect in photoelectric currents was found to be independent of the frequency of the light producing electron emission.

23. Force relations in drawing copper wire. R. L. DOAN AND J. L. BETSILL, *Western Electric Company, Hawthorne Station.*—An empirical relationship has been derived between the draw-

ing force and percent reduction in drawing copper wire through successive chilled iron dies which takes into consideration the progressive hardening of the metal with cold work. This is: $\log F/\Delta = A - B \log X$. Where F is the drawing force, Δ the reduction in cross section and X the percent reduction at any particular die. A and B are factors which depend on the total reduction from the initial soft rod. The effect of varying the die angle has been investigated for 5°, 10°, 20°, 30° and 40° single angle dies. The drawing force was found to be a minimum and the tensile strength of the product wire a maximum for the 10° angle although more detailed experiments will be required to locate the optimum angle. The fall in tensile strength of the wire when drawn through large angle dies is associated with the development of internal ruptures which widen out and give rise to typical cup and cone fractures.

24. A three-dimensional vibrograph. J. E. SHRADER, *Drexel Institute, Philadelphia.*—A new vibrograph has been devised which indicates and records simultaneously in the same plane vibrations of a body in each of three directions mutually perpendicular. This vibrograph operates on the seismographic principle. A cubic mass of lead is suspended from a frame by a system of springs. The mass and its frame are enclosed in a case which is placed upon the vibrating body. Relative motions between the mass and its frame are shown by the deflection of beams of light from mirrors mounted on spindles attached to the suspended mass. Motion of rotation is communicated to the spindles by flexible strings. One end of each string is fastened to the frame and is then wrapped about the spindle and then passes to a light spiral spring which is attached to the opposite side of the frame. The record is made on double width moving-picture film. A timing record on the same film is made by the use of a small synchronous motor. The instrument shows amplitude of vibration, wave form, phase relations and frequency of three components of vibration simultaneously on the same plane.

25. The emission spectrum of metallic silver under electron bombardment and its relation to the absorption spectrum. F. L. MOHLER, *Bureau of Standards.*—In previous communications, Mohler and Boeckner have shown that the visible and near ultraviolet spectra emitted by metals bombared by low speed electrons are generally nearly equal energy continuous spectra of comparable intensity but silver is an exception. The intensity rises from 3200A to a value near 3600A, over 10 times the intensity at shorter wave-lengths. The shape of the intensity curve between 3200 and 3600A, when corrected for internal reflection, resembles a Fermi distribution of energy and an exact fit is obtained by assuming a reasonable value for the temperature of the metal. The result suggests that the emission process involves ionization of a discrete underlying level and the fall of one of the continuum of conduction electrons into the ionized level. The absorption spectrum of the underlying level should be a band extending to shorter wave-lengths with the shape of the long wave-length edge influenced by the Fermi distribution. The absorption rises from a low value near 3200 to a maximum near 2500A, and preliminary experiments indicate that the slope of this branch of the absorption curve does indeed change with temperature in a manner consistent with this interpretation.

AUTHOR INDEX TO ABSTRACTS OF SCHENECTADY MEETING

Ahearn, A. J.—No. 5

Bearden, J. A.—No. 8
Betsill, J. L.—see Doan
Briggs, H. B.—see Ives

Davey, Wheeler P.—see Phelps
Deming, W. Edwards and Lola E. Shupe—No. 14
Doan, R. L. and J. L. Betsill,—No. 23

Fisher, Thomas F.—see Serduke
Frank, N. H.—No. 7

Gibbs, R. C. and P. G. Kruger—No. 16

Harrison, George R.—No. 17
Hutchisson, Elmer—No. 18

Ives, Herbert E.—Nos. 1, 21
——— **and H. B. Briggs**—No. 2

Kennard, R. B.—No. 15
Kingsbury, B. A.—No. 22
Kingsbury, E. F.—No. 4
Kruger, P. G.—see Gibbs

Longden, A. C.—No. 12

Mohler, F. L.—No. 25
Mueller, Donald W. and H. D. Smyth—No. 11
Müller, Hans—No. 19

Nottingham, W. B.—No. 6

Olpin, A. R.—No. 3

Phelps, Robert T. and Wheeler P. Davey—No. 9

Serduke, James T. and Thomas F. Fisher—No. 20
Shrader, J. E.—No. 24
Smyth, H. D.—see Mueller
Shupe, Lola E.—see Deming

Van De Graaff, Robert J.—No. 10
Villars, D. S.—No. 13

Second Series *December 1, 1931* *Vol. 38, No. 11*

THE
PHYSICAL REVIEW

DIFFUSE SCATTERING OF X-RAYS FROM SYLVINE AT LOW TEMPERATURE

By G. E. M. Jauncey* and G. G. Harvey
Washington University, St. Louis, Mo.

(Received October 26, 1931)

Abstract

By use of a modification of the photographic method described by Claus the authors have compared the intensities of x-rays of wave-length 0.43A diffusely scattered from sylvine at angles in the range 25° to 90° at a temperature of 90°K with the intensities at these same angles at a temperature of 300°K. Jauncey and Harvey have shown that the intensity of the diffusely scattered rays should be given by $S=S'-F^2/Z$, where S' is independent of the temperature and F is the atomic structure factor containing the effect of thermal agitation. With James and Brindley's F values at 90°K and 300°K theoretical values of S for 90°K have been calculated. The experimental S values at 90°K are lower than the theoretical S values. This result is in accord with that found by Claus for rocksalt. Plotting $\log (S'-S_1)/(S'-S_2)$, where the subscripts refer to the two temperatures, against $(\sin^2\phi/2)/\lambda^2$ a straight line is obtained whose slope agrees with that required by the Waller and not the Debye formula for the temperature effect. It is impossible by means of this experiment to show whether or not there is zero point energy. In order to do this an assumption concerning the electron distribution in the atom must be made.

I. Introduction

Compton[1] has shown theoretically that the intensity of x-rays diffusely scattered by a monatomic gas is given by

$$S = 1 + (Z - 1)f'^2/Z^2 \qquad (1)$$

where S is the scattering per electron in terms of the Thomson[2] value in the same direction, Z the atomic number of the gas and f' an average atomic structure factor for the atom at rest. The difference between f, the true atomic structure factor, and f' has been discussed by Jauncey[3] and Herzog.[4] Jauncey and Harvey[5,6] have subsequently shown theoretically that the in-

* The senior author has been aided in this research by a grant from the Washington University Science Research Fund.

[1] A. H. Compton, Phys. Rev. **35**, 925 (1930).
[2] J. J. Thomson, Conduction of Electricity through Gases, 2nd Edition, p. 325.
[3] G. E. M. Jauncey, Phys. Rev. **38**, 1 (1931).
[4] G. Herzog, Zeits. f. Physik **69**, 207 (1931).
[5] G. E. M. Jauncey, Phys. Rev. **37**, 1193 (1931).
[6] G. E. M. Jauncey and G. G. Harvey, Phys. Rev. **37**, 1203 (1931).

tensity of the diffuse scattering from simple cubic crystals consisting of atoms of one kind is given by

$$S = 1 + (Z - 1)f'^2/Z^2 - F^2/Z \tag{2}$$

where F is the atomic structure factor, including the effect of thermal agitation, as obtained from crystal reflection. Independently Woo[7] has obtained the formula

$$S = \frac{1 - f'^2/Z^2}{(1 + \alpha \text{ vers } \phi)^3} + \frac{f'^2 - F^2}{Z} \tag{3}$$

where $\alpha = h/mc\lambda$ and ϕ is the angle of scattering. Woo's formula reduces to ours for small values of α. In Eq. (2) f' and Z are independent of the temperature while F for sylvine is a function of the temperature as found by James and Brindley.[8] Hence S should be a function of the temperature. With rocksalt Claus[9] has shown that at low temperatures the values of S are below their corresponding values at room temperature. However, the values of S found by Claus at low temperature did not agree with the values calculated from the room temperature values of S and James and Firth's values[10] of F at room and liquid air temperatures. It was thought that this disagreement might be due to the fact that Eq. (2) is valid only for simple cubic crystals consisting of atoms of one kind whereas rocksalt consists of atoms of two kinds. It was suggested that the diffuse scattering from sylvine, which may be considered as consisting of atoms of one kind, should be measured at low temperatures. Accordingly this research was undertaken to determine the intensity of diffuse scattering of x-rays from sylvine at low temperatures.

II. Method of Experiment

A photographic method similar to that described by Claus[9] was used. However, instead of scattering the x-rays from the front face of a thick crystal, as done by Claus, we have caused a beam of x-rays to penetrate through a thin sliver of crystal and have measured the photographic effect of the diffusely scattered x-rays which penetrate through the crystal. The arrangement is shown in Fig. 1. The crystal was enclosed in a thick copper cylinder, the lower portion of which dipped into a Dewar flask which could be filled with liquid air at will. This flask was itself enclosed in an outer case which sits on the table of a Bragg ionization spectrometer and which is of double-walled brass packed with asbestos between the walls as is shown in Fig. 2 of Claus' paper.[9] The rays entered the cavity in the copper cylinder through a thin mica window and the scattered rays emerged through a similar window. The scattered rays passed through wide windows both in the copper cylinder and outer brass case, so that with one exposure the diffuse scattering over a large range of angles could be obtained. This procedure was suggested to the authors by Dr. Claus. The outer window was covered with thin mica. Around the boundary of the window was placed a heating coil in order to prevent

[7] Y. H. Woo, Phys. Rev. **38**, 6 (1931).
[8] R. W. James and G. W. Brindley, Proc. Roy. Soc. **A121**, 155 (1928).
[9] W. D. Claus, Phys. Rev. **38**, 604 (1931).
[10] R. W. James and Elsie M. Firth, Proc. Roy. Soc. **A117**, 62 (1928).

moisture from being deposited on the window. There was no tendency for moisture to collect upon the mica windows of the copper cylinder because these windows were continually bathed in a draft of dry air rising from the reservoir of liquid air. In order to produce fiducial marks upon the developed film lead strips were placed vertically across the window in the outer casing at known angles.

Following the method developed by Claus[9] exposures of 1, 2, and 3 hours were run at room temperature; then liquid air was poured into the Dewar flask and after the sylvine crystal had come to an equilibrium temperature (90°K) as registered by a copper-iron thermocouple an exposure of 4 hours was run; during this exposure the level of the liquid air in the Dewar flask was kept constant as described by Claus.[9] Next, the liquid air was allowed to evaporate off and the crystal to come to room temperature after which a set

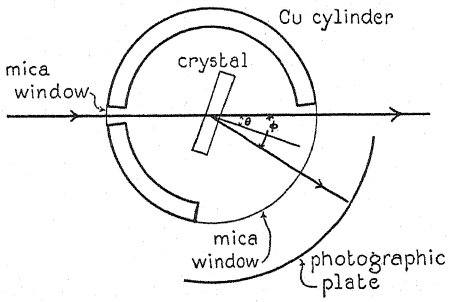


Fig. 1. Diagram of apparatus.

of 3, 2 and 1 hour exposures was run. All seven exposures were obtained on the same film. The film was then developed and run through a microphotometer and the relative intensities of the diffuse scattering at room temperature (300°K) and 90°K obtained for scattering angles between 25° and 90°.

The wave-length was obtained by measuring the absorption in aluminum of the scattered beam. This was done photographically and the wave-length could be obtained at all angles on the same film. However, the absorption coefficient was found not to vary in any definite way with the angle within the limits of measurement possible and so the mean value for several angles was used. This corresponds to a wave-length of 0.43A which we take to be the average wave-length.

TABLE I.

$x=(\sin\phi/2)/\lambda$	Intensity at 90°K / Intensity at 300°K				$S_{300°K}$	$S_{90°K}$	
	A	*B*	*C*	Ave.		Exp.	Th.
0.503	0.41	0.55	0.53	0.50	2.88	1.44	1.96
0.603	0.48	0.53	0.55	0.52	2.63	1.37	1.87
0.700	0.51	0.58	0.58	0.56	2.42	1.36	1.79
0.795	0.61	0.59	0.61	0.60	2.27	1.36	1.74
0.880	0.69	0.68	0.64	0.67	2.14	1.43	1.75
0.985	0.75	0.71	0.69	0.72	2.00	1.44	1.75
1.075	0.75	0.78	0.75	0.76	1.90	1.45	1.73
1.162	0.81	0.88	0.83	0.84	1.80	1.51	1.70

III. Experimental Results

Three separate runs were made for three settings of the crystal angle θ (see Fig. 1) and three films were obtained. The results of the photometric measurements of these films are shown in columns A, B and C of Table I, the average value being shown in the fifth column.

IV. Comparison with Theory

In the sixth column of Table I are shown the S values for sylvine at room temperature as obtained by Harvey.[11] In the seventh column are shown the S values at 90°K obtained by multiplying Harvey's experimental S values for room temperature by the respective ratios shown in column five. Wollan[12]

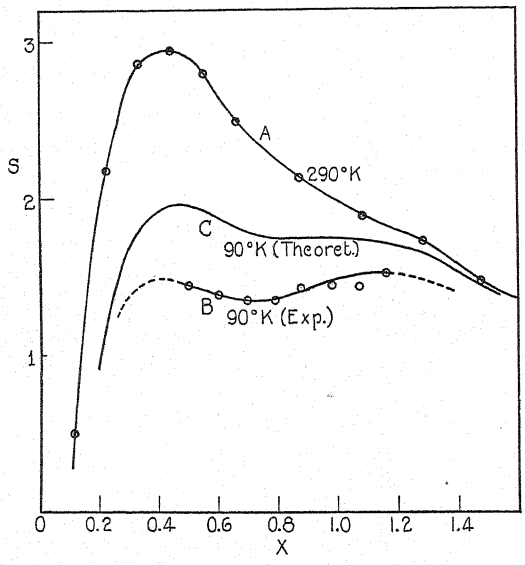


Fig. 2. Curves A and B show experimental S values for sylvine at room and liquid air temperatures. Curve C shows theoretical values at liquid air temperature.

and Harvey[11] have respectively shown that the experimental S values for argon and sylvine give f' values which are identical when calculated from Eqs. (1) and (2). Since the S values for a monatomic gas cannot vary with the temperature and since the f' values for sylvine are equal to those for argon, the f' values for sylvine are independent of the temperature. Jauncey and Harvey[13] have recently discussed this and have shown the experimental relation

$$S_{\text{gas}} = (S + F^2/Z)_{\text{crystal}}. \tag{4}$$

We may rewrite the equation for a crystal in the form

$$S = S' - F^2/Z \tag{5}$$

[11] G. G. Harvey, Phys. Rev. **38**, 593 (1931).
[12] E. O. Wollan, Phys. Rev. **37**, 862 (1931).
[13] G. E. M. Jauncey and G. G. Harvey, Phys. Rev. **38**, 1071 (1931).

where $S'=1+(Z-1)\,f'^2/Z^2$ is the S value for the atoms of sylvine when in the gaseous form. S' is independent of the temperature and so S varies with the temperature in virtue of the variation of F with the temperature. James and Bridley[8] have obtained F values for sylvine at liquid air temperature and from these F values the theoretical S values shown in the eighth column of Table I have been obtained. It is immediately seen that the experimental S values are all lower than the theoretical S values. The disagreement between the S values shown in columns seven and eight of Table I may be due to experimental error in the average ratios shown in column five or it may be due to experimental error in James and Brindley's F values at liquid air temperature or the disagreement may be real. The authors are at present unwilling to decide among these various possibilities. However, this disagreement in the case of sylvine is in accord with the disagreement found by Claus[9] for rocksalt. The experimental S values for sylvine at room and liquid air temperatures are shown as curves A and B in Fig. 2. The theoretical values at liquid air temperature are shown as curve C in this figure.

The experimental S curve for room temperature contains a hump at $x=0.45$ and a suspicion of a hump at $x=1.25$. The theoretical curve at 90°K definitely has two humps. Our experimental curve at 90°K has humps at $x=0.40$ and $x=1.15$ so that although there is disagreement between the absolute values of the ordinates of the theoretical and experimental S curves for 90°K, yet the two curves do have the same general shape.

Eq. (5) may be written

$$S' - S = F^2/Z \tag{6}$$

and assuming Debye's formula[14] for the temperature effect we have

$$F^2 = f^2 e^{-M} \tag{7}$$

where

$$M = \frac{6h^2}{\Theta mk}\,\frac{\Phi(z)}{z}\,\frac{\sin^2\phi/2}{\lambda^2} \tag{8}$$

or

$$M = \frac{6h^2}{\Theta mk}\left\{\frac{\Phi(z)}{z}+\frac{1}{4}\right\}\frac{\sin^2\phi/2}{\lambda^2}. \tag{9}$$

Eq. (8) holds for the absence and Eq. (9) for the presence of zero point energy. In these equations Θ is the characteristic temperature of the crystal as occurs in the Debye theory of specific heats, $z=\Theta/T$, $\Phi(z)=1/z\int_0^z(y\,dy/e^y-1)$, ϕ is the scattering angle and the other quantities have their usual significance. We shall write

$$\frac{6h^2}{\Theta mk}\,\frac{\Phi(z)}{z}\,\frac{\sin^2\phi/2}{\lambda^2} \equiv Bx^2 \tag{10}$$

where $x=(\sin\phi/2)/\lambda$. According to Waller[15] M in Eq. (7) should be replaced by $2M$. Hence, if the value of x is kept constant and the temperature varied,

$$S' - S \propto e^{-Bx^2} \text{ or } e^{-2Bx^2} \tag{11}$$

[14] P. Debye, Ann. d. Physik **43**, 49 (1914).
[15] I. Waller, Zeits. f. Physik **17**, 398 (1923).

according as to which formula is used. The value of S and the value of B depend upon the temperature so that if S_1 and B_1 are the values of S and B respectively at temperature T_1 and S_2 and B_2 the values at T_2 we have

$$\log \frac{S' - S_1}{S' - S_2} = (B_2 - B_1)x^2 \text{ or } 2(B_2 - B_1)x^2 \tag{12}$$

so that if $\log (S'-S_1)/(S'-S_2)$ is plotted against x^2 a straight line should be obtained whose slope is either (B_2-B_1) or $2(B_2-B_1)$ according as the Debye or Waller formula is correct. For the range of temperatures used in our experiment these values are 1.15 and 2.30 respectively. It is important to note in Eq. (12) that because only the difference (B_2-B_1) is involved this method tells us nothing regarding the presence or absence of zero point energy. Plot-

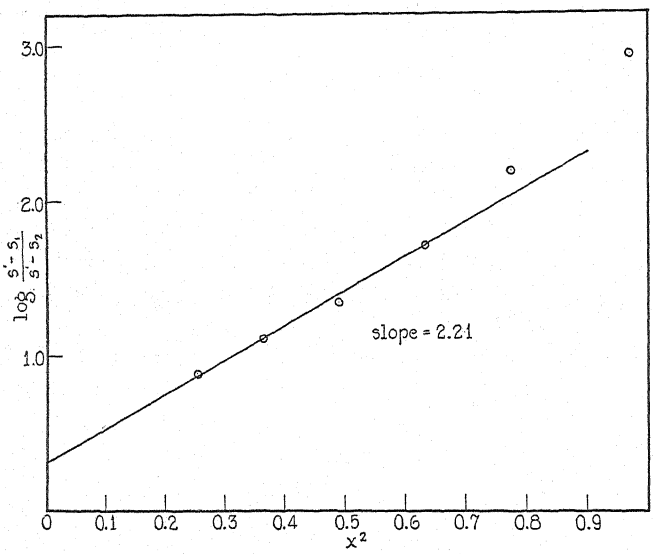


Fig. 3. Plot of experimental values.

ting our experimental values we obtain the curve as shown in Fig. 3. It is seen that between $x=0.5$ and $x=0.8$ the curve is a straight line whose slope is 2.21. For values of x beyond 0.8 no reliance can be placed on the points since the ordinate depends on the ratio of two differences each of which is subject to considerable uncertainty due to the fact that S' approaches S for large values of x. This explains why the last two points in Fig. 3 do not fall on the curve. It might be objected that this slope depends somewhat on the wave-length which we have assumed and also upon the correctness of the angle of scattering. Actually, of course, the wave-length and scattering angle are averages. We therefore supposed a possible variation of $\pm 2°$ in the scattering angle and ± 0.02A in the wave-length. We then constructed nine different curves similar to Fig. 3 and obtained nine different values of the slope. With the exception of one value all the slopes came out between 2.00 and 2.35. We therefore feel considerable confidence in our value of 2.21 which is distinctly in agreement with Waller's value of 2.30 and not with Debye's value.

Eq. (6) may be written.

$$Z(S' - S) = f^2 e^{-2Kx^2} e^{-2Bx^2} \tag{13}$$

where $K \equiv (3h^2/2\Theta mk)$ is due to zero point energy and is independent of the temperature. The slope of the curve in Fig. 3 shows that B has the Waller value but indicates nothing as regards the existence or non-existence of zero point energy. In Eq. (13) both f and e^{-Kx^2} are independent of the temperature but are functions of x. Information concerning K can be obtained only if an assumption is made concerning the values of f. Three possibilities have been considered. First, if a model of the atom of argon is assumed, values of the true atomic structure factor, or f values, can be calculated for this model. If these values are substituted in the values of the product above mentioned the value of K can be determined. Second, we may assume that f is equal to f', as is done by Compton[1] and Wollan[12]. Third, we may assume zero point energy according to the Waller theory[15] and calculate f values. All of these methods require a high degree of accuracy in the experimental values. Instead of attempting to perform these calculations we have preferred to take the values of S at 300°K and 90°K together with F values at 300°K and from these to calculate F values at 90°K from the relation

$$Z(S_{300°} - S_{90°}) = F^2_{90°} - F^2_{300°}. \tag{14}$$

The values so calculated are shown in the second column of Table II. James and Brindley's values are shown in column three for comparison.

TABLE II.

x	$F_{90°K}$		x	$F_{90°K}$	
	J and H	J and B		J and H	J and B
0.503	6.71	6.00	0.880	3.79	2.95
0.603	5.76	5.04	0.985	3.79	2.35
0.700	5.01	4.24	1.075	2.91	1.94
0.795	4.42	3.53	1.162	2.30	1.54

James and Brindley's F values for sylvine at room temperature fitted our theory most excellently because when combined with Harvey's S values[11] for sylvine at room temperature the resulting f' values agree remarkably well with Wollan's f' values for argon.[12] It seems peculiar that James and Brindley's F values for sylvine at liquid air temperature when combined with the results of this present paper do not fit the theory so well.

V. Conclusion

We have shown that the diffuse scattering of x-rays from sylvine decreases with decrease of temperature. For temperatures of 300°K and 90°K the decrease is a function of x such that it supports Waller's formula[15] as opposed to Debye's formula[14] for the temperature effect. However, the decrease is greater than that required by the theory of Jauncey and Harvey[6] for the diffuse scattering from crystals if the F values of James and Brindley[10] at liquid air temperature are used. It is suggested that more work is needed on the effect of temperature both on the diffuse scattering and regular reflection from crystals before more definite conclusions can be drawn.

ABSORPTION OF SOFT X-RAYS IN GASES

By R. G. Spencer
Ryerson Physical Laboratory
The University of Chicago

(Received October 16, 1931)

Abstract

A crystal spectrograph for measuring absorption coefficients of soft x-rays in gases has been constructed, and with it absorption coefficients of air, argon and oxygen have been measured for spectral lines of wave-lengths 1.537, 2.284, 4.145 and 6.973A. Absorption coefficients in the regions immediately adjacent to the K absorption limit of argon have been measured with general radiation. No departure from the ordinary absorption law greater than experimental error was found in these regions. The magnitude of the K absorption discontinuity of argon was measured by a method which is not dependent upon the extrapolation of curves to the absorption limit, and also by a method which is independent of the absolute magnitude of the absorption coefficients on either side of the absorption limit.

NOT many measurements of absorption coefficients in the range of wave-lengths from 1.5 to 10A have been made. Growther[1] has reported absorption coefficients of a few gases for the copper $K\alpha$ line. Woernle[2] has made absorption measurements for several gases over a range of wave-lengths from 2.287 to 9.868A. Jonnson[3] has done quite extensive work in measuring absorption coefficients for metals in the same wave-length region. Jonnson used a photographic method. Crowther and Woernle used ionization methods. Dershem and Schein,[4] with the aid of a ruled grating, have used the photographic method to measure absorption coefficients for the $K\alpha$ line of carbon in various gases. It was thought desirable to extend this method to the region in which crystals could be used with the view of making possible the investigation of absorption discontinuities.

Apparatus and Experimental Procedure

The apparatus was designed so as to have a very small volume and a high resolving power. The distance from the crystal to the plate holder is about 59 cm. Although expensive gases have not been used, the small volume of the spectrograph and the long path of the x-ray beam would make it possible to work with them with a minimum expense. The high resolving power of the instrument makes it possible to distinguish between adjacent wave-lengths with good accuracy and to work in regions very close to an absorption limit. Figure 1 is a schematic diagram of the spectrograph, including a top view and a side view. The copper tubes A and B, the cylinder C, and the photographic

[1] Crowther, Phil. Mag. 10, 329 (1930).
[2] Woernle, Ann. d. Physik 5, 475 (1930).
[3] Jonnson, Dissertation, Uppsala, 1928.
[4] Dershem and Schein, Phys. Rev. 37, 1238 (1931).

plate holder D form a gas tight compartment. C contains a crystal mounting attached to a divided circle. The brass plate which covers it can be removed for the purpose of adjusting the crystal. M_1 and M_2 are electromagnets which are screwed into the walls of the plate holder. They are screwed into the walls far enough to make good magnetic contact with the inside, but enough wall is left to make the plate holder gas tight. M_2 operates a mechanism, contained inside the plate holder but not shown in the diagram, which drives the slide q back and forth. Thus S_3 which is a wide slit can be opened or closed at any time. The magnet M_1 operates a mechanism which pulls the plate p past the slit S_3. Every time that M_1 is energized p moves a definite distance. The distances l_1 and l_2 are equal, so that Bragg focusing is obtained.

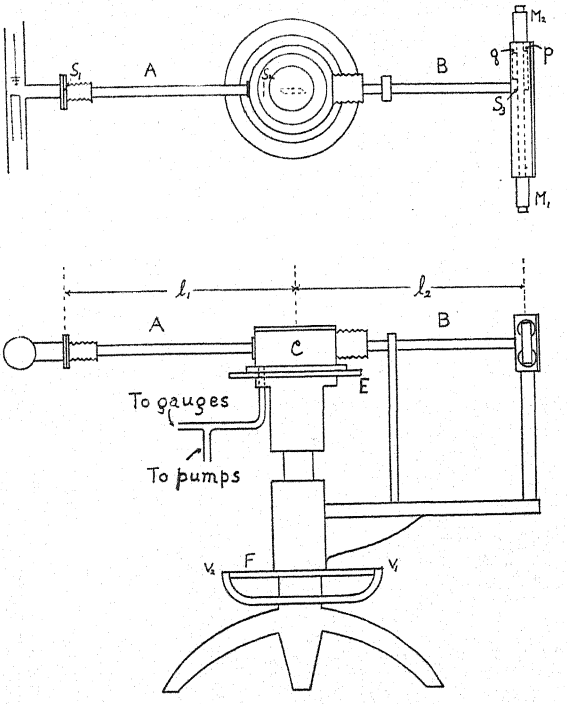


Fig. 1. Diagram of apparatus.

The tube B is fastened to the cylinder C by means of a piece of silphon tubing. The silphon tubing bends enough to permit the plate holder to be turned through an angle of eighteen degrees without rotating C. C is fastened to the plate E by means of twenty screws equally spaced around its circumference. It can thus be turned in steps of eighteen degrees, so that the plate holder can be set at any desired angle. Several faces are milled on the side of C as indicated in the diagram. Each face subtends an angle of eighteen degrees at the center of C. A wide slit is cut through each face. One end of the tube A is soldered to a small plate which can be screwed on to any one of these faces. The remaining faces are covered with interchangeable blanks. When one wishes to rotate C the tube A is simply attached to a different face.

F is an accurately divided circle which is rigidly attached to the arm which carries the plate holder. It is fitted with two verniers v_1 and v_2. S_1 and S_2 are two slits of suitable width for collimating the x-ray beam. S_1 is covered with a thin celluloid window which separates the x-ray tube from the spectrograph. All metal joints in the spectrograph were either soldered or sealed with sulphur-free rubber. A metal x-ray tube designed by Dershem[5] was used.

The spectrograph was pumped out to a pressure of less than 10^{-5} cm of mercury and the photographic plate was exposed to the radiation for a certain interval. The plate was then moved to a new position by energizing the magnet M_1 and exposed for a longer interval. In this way four or five lines of increasing density were obtained on the plate. Sufficient gas to absorb between one half and three fourths of the x-ray energy was then admitted into the spectrograph. Several lines of different times of exposure were then obtained with the x-ray beam passing through the gas. A plate thus obtained yields sufficient data, when photometered, to determine the ratio I_0/I, where I_0 is the intensity of the x-ray beam before absorption and I its intensity after absorption.

From the absorption law $I=I_0e^{-\mu x}$ and the gas law $P_sV_s/T_s=PV/T$ one obtains the following expression for the mass absorption coefficient:

$$\frac{\mu}{\rho}=\frac{1}{\rho_s x}\frac{P_sT}{PT_s}\log\frac{I_0}{I} \tag{1}$$

where μ/ρ is the mass absorption coefficient, x the length of path, P the pressure of the gas, T its temperature, ρ its density and the subscript s refers to standard conditions of temperature and pressure.

I_0/I was found by photometering the plate. The instrument used was a photoelectric photometer designed by Dershem. A detailed description of this instrument will appear soon in the Review of Scientific Instruments. In this photometer a beam of light is allowed to pass through the plate, through a fine slit, and then impinge upon a photoelectric cell. The cell is connected to a string electrometer. To obtain the relative densities of a number of lines one merely finds the time necessary for the string of the electrometer to pass a certain number of divisions on its scale when the light is passing through the line and the time necessary for the string to pass the same number of divisions when the light is passing through the plate adjacent to the line. The difference between these two times, (photometer time), gives a number which represents the relative density of the line. A graph in which photometer time is plotted against exposure time is made for the lines that were obtained when the spectrograph was evacuated. From this graph and the number which represents the relative density of one of the absorption lines one can find the time of exposure which would have been necessary to produce the same density of the line if the absorbing gas had not been present. From the reciprocity law the ratio of the time of exposure when the x-ray beam is passing through the absorber to the time necessary to produce the same density when the beam is passing through a vacuum is equal to I_0/I.

[5] Dershem, J.O.S.A. **18**, 127 (1929).

Eastman x-ray plates were used. Care was taken to obtain uniform development over the entire plate, and overdevelopment, which would have produced chemical fog, was avoided.

The gases were dried by passing them through a liquid air trap before they entered the spectrograph. The oxygen used contained less than 0.4 percent of impurities most of which was nitrogen. The argon used contained less than 0.1 percent of impurities.

Results

Absorption measurements were made for air, oxygen, and argon for four spectral lines of wave-lengths 1.537, 2.284, 4.145, and 6.973A. By use of general radiation, absorption coefficients were measured in the regions immediately adjacent to the argon absorption limit for the purpose of determining whether or not there was any anomalous absorption in these regions. The wave-lengths of general radiation given in Table I are extrapolated from the argon absorption limit assuming that it occurs at 3.8657A. This value was

Table I. *Mass absorption coefficients in air, oxygen and argon.*

Spectral line	Wave-length	Author	W or C*	Author	W or C	Author	W or C
CuK	1.537A	9.54	9.49C	11.6	11.1C	112.	
CrK	2.284	29.3	31.8W	35.5	36.4W	344.	354.W
	3.716					1320.	
	3.8637					1465.	
	3.8677					147.	
	3.946					151.	
AgL	4.145	168.	163.4W	221.	222.W	171.	174.W
WM	6.973	747.	740.W	971.	976.W	762.	748.W

* The values marked C are values published by Crowther, and those marked W are values published by Woernle.

taken from a table given in Compton's 'X-rays and Electrons'. Absorption coefficients were measured for wave-lengths within 0.002A of the absorption limit on each side of it. Table I gives the values obtained for both spectral lines and general radiation, and compares them where the wave-lengths are the same with values obtained by Crowther and Woernle.

In working with general radiation care was taken to keep the voltage low enough so that second or higher order radiation was not excited. The times of exposure varied from one to five hours. Consequently, ten to fifteen hours were required to obtain a plate.

The magnitude, δ, of the K absorption discontinuity of argon, where δ is defined as the ratio of μ/ρ on the short wave-length side, (the scattering coefficient in this region is small enough to be neglected), to μ/ρ on the long wave-length side of the absorption limit, can be determined by simply dividing μ/ρ for $\lambda = 3.8637$ by μ/ρ for $\lambda = 3.8677$. This gives the value $\delta = 9.96$.

It was also found to be possible to evaluate δ by a method which is independent of the absolute magnitude of μ/ρ on either side of the absorption limit. If on the same plate one measures I_0/I on each side of the absorption limit he obtains from the definition of δ and Eq. (1)

$$\delta = \frac{\log (I_0/I)_K}{\log (I_0/I)_L}$$

where K refers to the short and L to the long wave-length side of the absorption limit. This can easily be done if a band of general radiation is reflected from the crystal so that the absorption limit falls approximately in the middle of it. The average value of δ found by this method is 10.

Figure 2 is a reproduction of one of the plates. The first two images were obtained when the x-ray beam was passing through a vacuum, and the third shows the K absorption limit of argon.

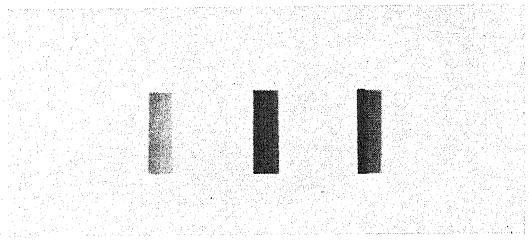


Fig. 2.

Discussion of Errors and Results

The quantities which were measured and used to determine absorption coefficients are the temperature of the gas, its pressure, and the ratio I_0/I. The temperature could easily be measured with an accuracy which would make negligible any error which it might cause. The McLeod gauges were so designed and calibrated that the measurements of the pressure were less than one half percent in error. Most of the error is thus due to measuring I_0/I. The more important factors which contribute to the error in its measurements, such as variation in intensity of the x-ray beam, irregularities in the emulsion on the photographic plate, irregularities in development, etc., introduce only random errors and should be minimized by repeated measurements. Small consistent errors might be introduced by lack of homogeneity of the x-rays and inaccuracy of the reciprocity law. But, under the conditions of the experiment such errors are probably negligible. Each plate gives several values of I_0/I and each absorption coefficient given in the table is the average of three or more plates. The probable error in most cases is less than two percent.

It is found that equations of the type $\mu/\rho = C\lambda^x$ can be made to fit the data within experimental error. C and x are constant for a given substance over a range that does not contain an absorption discontinuity. If $\log \lambda$ is plotted against $\log \mu/\rho$, the following equations are found from the slopes and the intercepts of the respective lines:

$$\mu/\rho = 33.9\lambda^{2.79} \text{ for argon } \lambda < \lambda_K \tag{2}$$

$$\mu/\rho = 3.39\lambda^{2.79} \text{ for argon } \lambda_k < \lambda < \lambda_L \tag{3}$$

$$\mu/\rho = 3.39\lambda^{2.91} \text{ for oxygen.} \tag{4}$$

From Fig. 3 one can see that there is no anomalous absorption greater than experimental error in the regions near the argon absorption limit. Eqs. (2) and (3) are valid at least to within 0.002A of the absorption limit.

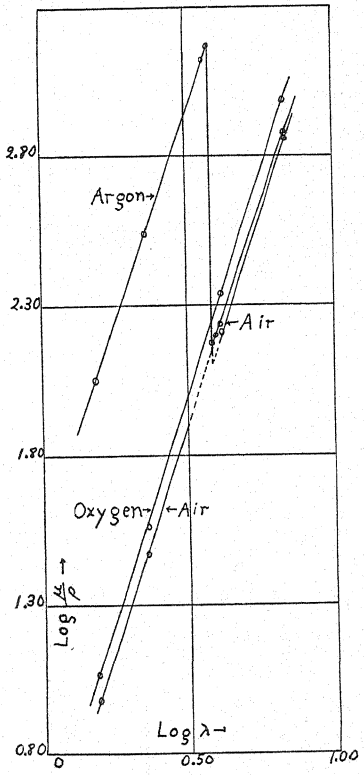


Fig. 3.

It is a pleasure to acknowledge the valuable suggestions received from various members of the staff of the department of physics of the University of Chicago. I am especially indebted to Professor A. H. Compton and Dr. Elmer Dershem who suggested the problem and cooperated in directing the work.

LATERAL SPACE DISTRIBUTION OF X-RAY PHOTOELECTRONS

By Paul Kirkpatrick
University of Hawaii, Honolulu

(Received September 29, 1931)

Abstract

The lateral distribution in space of the directions of emission of photoelectrons ejected from argon atoms by partially polarized x-rays having the mean wave-length 0.53A was determined by examination of photographs of 2008 condensation tracks produced in a C. T. R. Wilson expansion apparatus. Discarding by a definite analytical procedure the isotropically distributed emissions, which are ascribed to unpolarized radiation, the distribution of the remaining 752 tracks is found to be in excellent agreement with the indications of quantum mechanics that (for K electrons) the probability of emission is proportional to the square of the cosine of the angle between the electric vector of the absorbed radiation and the projection of the direction of emission upon a plane normal to the direction of incidence.

THE longitudinal distribution of the directions of emission of photoelectrons ejected by x-rays from the atoms of a gas has been the subject of many experimental investigations. The lateral distribution, that is, the distribution referred to a plane perpendicular to the direction of incidence of the radiation, although it has often been treated by theorists, has received the direct attention of only two experimenters.

The general form of the experimental distribution was discovered by Bubb,[1] who, following C. T. R. Wilson's[2] qualitative observation on the subject, disclosed the existence of the two very pronounced emission maxima in the general directions of the electric vector. Bubb's data, however, do not permit us to assign the precise functional representation without ambiguity. Auger and Perrin[3] considered that Bubb's data were in fairly satisfactory agreement with their own prediction that the probability of emission would be found proportional to the square of the cosine of the angle between the electric vector of the absorbed radiation and the projection of the direction of emission upon a plane normal to the direction of incidence. Kirchner[4] criticized this statement and showed that a better, though still approximate, fit might be obtained by increasing the exponent of the cosine to at least three. Upon studying several hundred tracks produced and photographed in his own laboratory Kirchner first considered the evidence to favor a $\cos^3$ or $\cos^4$ distribution, but revised this conclusion later, after a penetrating study of the errors of the experiment, concluding that his data supported the $\cos^2$ hypothesis as well as any other. The discrepancies in this case, however, were stated to be somewhat larger than the average errors of experiment. It thus appears

[1] F. W. Bubb, Phys. Rev. **23**, 137 (1924).
[2] C. T. R. Wilson, Roy. Soc. Proc. **A104**, 11 (1923).
[3] P. Auger and F. Perrin, Jour. d. Physique **8**, 93 (1927).
[4] F. Kirchner, Phys. Zeits. **27**, 799 (1926); Ann. d. Physik **83**, 521 (1927).

that the observations, to date, do not furnish decisive tests of the theoretically predicted distributions.

The lateral distribution is necessarily isotropic for unpolarized x-rays, and any observed lateral distribution will be a function of the degree of polarization of the radiation employed. It was the desire to use this relationship in the measurement of the polarization of faint x-radiations which prompted the studies embodied in the present paper, in which an attempt has been made to place our knowledge of this distribution upon a broader experimental basis.

Data were obtained by the expansion method of C. T. R. Wilson.[5] The expansion equipment followed rather closely the plans originated by Wilson about twenty years ago, substantially the original design being adopted, after several futile attempts at improvement. X-rays were produced by a Universal Coolidge tube, operated at constant potentials of the order of 30 kv. The x-rays from the tube impinged upon a crystal so adjusted as to select and reflect to the expansion chamber a narrow band of general radiation from the highly polarized portion of the continuous spectrum near the short wave-length limit. The mean wave-length thus employed was 0.53A.

The large number of tracks required were photographed upon panchromatic motion picture film by means of a Leitz Leica camera with its lens mounted far enough forward to produce approximately natural-sized images. The camera was mounted on the opposite side of the expansion chamber from the x-ray source, and the axis of its lens coincided with the extension of the axis of the entrant beam. A window of plane parallel lead glass in the side wall of the expansion chamber facilitated the photography of the tracks, while preventing the x-ray beam from proceeding through the chamber and entering the camera. The expansion chamber was filled with argon gas, stated to be 95 percent pure.

Probably the chief novelty in the matter of technique was the illumination of the tracks for photography by an ordinary incandescent bulb. For this purpose a 1000 watt projection bulb and reflector were mounted about two feet above the glass top of the expansion chamber. The light passed successively through a condensing lens, a water cell, a simple shutter and the chamber top. The lamp was operated at about 140 percent of its normal voltage and was automatically turned on for about a second at each photographic exposure. Overloading the lamp in this way increased its photographic efficiency very greatly, yet the lamp remained apparently uninjured after the completion of over 1500 exposures. The shutter above the expansion chamber was automatically opened, admitting light to the chamber, immediately *after* the expansion, and the camera shutter was then electrically operated, allowing an exposure of 1/20 second. The illumination was sufficient to permit stopping the camera lens to $f/9$. This simple and convenient method of illumination was suggested by Mr. Arne Wikstrom, who also assisted in its development, contributing freely of his interest and time to the investigation.

The x-ray tube was inclined at 45° to the horizontal to avoid a conceivably

[5] C. T. R. Wilson, Roy. Soc. Proc. **A85**, 285 (1911); Roy. Soc. Proc. **A87**, 277 (1912).

undesirable coincidence of the axis of polarization with any of the obvious geometrical dimensions of the expansion chamber. Many hundreds of successful exposures were examined and the directions of the initial portions of 2008 tracks were measured directly upon the films by the use of a special protractor. These 2008 tracks included all photoelectron tracks which were sharply focused and adequately illuminated and which possessed clearly marked origins within that part of the film which corresponded to the known locus of the x-ray beam.

The integral curve of these tracks is plotted in Fig. 1, where the abscissas represent δ, the angle on the film from the line containing the directions of minimum emission. This line is normal to the plane of the predominant elec-

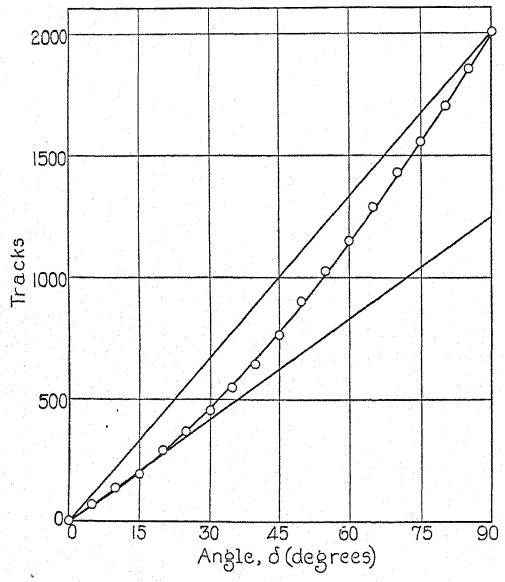


Fig. 1. Integral curve representing lateral space distribution of photoelectrons ejected by partially polarized x-rays.

tric vector of the x-ray beam. All four equivalent quadrants have been combined into one in constructing this curve. The meaning of the integral curve is made clear by the statement that any circled point along this curve indicates that the number of tracks denoted by its ordinate was found to have initial directions deviating from the direction of minimum emission by an angle not greater than that specified by the abscissa. The steep rise of this curve toward the right end indicates the concentration of emissions about the direction of the predominant electric vector.

Since nearly all theories of the photoelectric effect for plane-polarized x-rays have agreed in predicting a probability of emission varying as the square of the cosine of the angle between the electric vector of the absorbed radiation and the projection of the direction of emission upon a plane normal to the direction of incidence it is logical to proceed at once to a test of this hypothesis, rather than to attempt the general problem of determining, with-

out preconception, the equation of the curve which best fits the experimental points of Fig. 1. A curve through these points may be regarded as the sum of the integral curves of the isotropic and the anisotropic electron distributions. The former, chiefly caused by unpolarized x-rays, is the straight line depicted, whose equation is $n=k\delta$, while the latter, upon the basis of the $\cos^2$ hypothesis, may be shown to be represented by the equation $n'=k'(\delta-\sin\delta\cos\delta)$. In these equations n and n' are the numbers of tracks involved, k and k' are constants. It may be noted that δ, previously defined, is the complement of the angle involved wherever the expression "$\cos^2$" has been used.

The slope of the straight line $n=k\delta$ is found as follows. An integration shows that the area inclosed between the curve of Fig. 1 and its chord is $4/\pi^2$ times the triangular area of which the chord and the line $n=k\delta$ form two sides. Therefore if the former area be planimetered the straight line of the

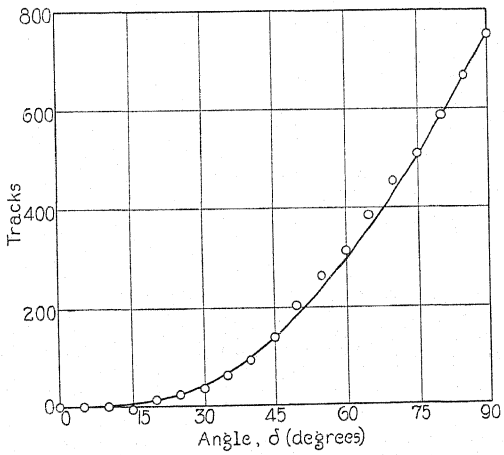


Fig. 2. Integral curve reprresenting lateral space distribution of photoelectrons ejected by completely polarized x-rays.

isotropic integral curve may be inserted in an entirely definite manner, subject always to the validity of the $\cos^2$ hypothesis.

The tracks representing unpolarized radiations may now be discarded and the remaining 752 tracks replotted as in Fig. 2, where the ordinates of the circled points are those of Fig. 1 diminished by the corresponding ordinates of the unpolarized integral curve. The solid curve of Fig. 2 is a plot of the theoretical equation $n'=k'(\delta-\sin\delta\cos\delta)$. The very close agreement between the curve and the experimental points appears fully to substantiate the $\cos^2$ distribution assumed. For most of the points the fit may be considered perfect. The slight discrepancy between fifty and seventy degrees, while unexplained, is not regarded as significant.

Recent quantum mechanical theories are in general agreement with earlier treatments of this subject in their prediction of a $\cos^2$ lateral distribution. A. Sommerfeld and G. Schur[6] find precisely this relation for the K photo-

[6] A. Sommerfeld and G. Schur, Ann. d. Physik **4**, 409 (1930).

electrons, while for the L photoelectrons Schur[7] shows the probability of ejection to be proportional to $A\sin^2\delta+B$, where A and B are constants depending upon the frequency of the incident radiation and the binding energy of the electron. Though no detectable effects of the L distribution as distinct from the K would be expected in the present data because of the minute difference between these distributions, as calculated from Schur's equations, and also because of the relatively small number of L photoelectrons, it is nevertheless worth pointing out that in any case the method adopted above could not make this distinction, since the isotropic part of the L distribution is indistinguishable from the unpolarized distribution. Indeed, neither these experiments nor any others to date are capable of logically ruling out the possibility that the lateral K electron distribution may have also an isotropic portion, though no theoretical reasons for supposing this to be the case have been advanced.

The experimental work described above was performed in the Department of Physics at Cornell University. These lines are all too brief adequately to express their writer's appreciation of the cordial hospitality of this department, and the generous interest and assistance of Professor F. K. Richtmyer.

[7] G. Schur, Ann. d. Physik **4**, 433 (1930).

ON COLLISION PROBLEMS INVOLVING LARGE INTERACTIONS

By Oscar Knefler Rice
Chemical Laboratory, Harvard University

(Received September 8, 1931)

Abstract

Many collisions, particularly those in which there is an exchange of electronic energy from one atom or molecule to another, involve interactions between the colliding bodies, which (being treated as perturbations) are too large to be handled by the ordinary Born method. A method is given for the treatment of such problems. Two cases must be distinguished, that of good and that of poor resonance, resonance being good if the transition which takes place at the collision does not involve the transfer of much energy from internal energy to relative translational energy, or *vice versa*. The case of good resonance is handled by Dirac's perturbation method (variation of constants), and the probability that a transition take place at a collision of given distance of closest approach found in terms of the perturbation (interaction) matrix component for that collision. In the case of poor resonance, we first assume the two atoms or molecules are held at a fixed distance from each other, and apply the perturbation due to the interaction between them constructing potential energy curves as a function of the distance, as if the whole system were a large molecule. We then allow the translational motion to take place. This introduces further perturbations, which in the case of poor resonance are always small, so that relatively few transitions will occur. Since the amount of energy which we may have transferred from internal to translational, or *vice versa*, and still have the case of good resonance may be determined in special cases as a function of the distance of closest approach, we may tell in any special case how close the two molecules or atoms must come to each other in order for there to be a transition at the collision. Thus a radius of action can be found. In general it is concluded that if the transition is to take place with a large radius of action (compared with kinetic theory radii), then less energy can be transferred from internal to translational, or *vice versa*, than has hitherto been supposed.

§1. Introduction

MANY collision problems, particularly those in which the transition at collision involves the exchange of electronic energy from one atom or molecule to another, bring in interactions between the atoms or molecules, which (being treated as perturbations in a wave-mechanical perturbation theory) are so large that the ordinary Born method for handling such problems breaks down.[1] The first attempt to treat a case of this kind was made by Kallmann and London.[2] As their treatment was not entirely free from objections, I made an attack on the problem in another way,[3] as did also Zener,[4] but these attempts still leave much to be desired.

It will be the object of this communication to describe a method which I believe may be made the basis for a satisfactory solution of the problem. I

[1] Kallmann and London, Zeits. f. Physik **60**, 417 (1930).
[2] Kallmann and London, Zeits. f. phys. Chem. **2B**, 207 (1929).
[3] Rice, Proc. Nat. Acad. Sci. **17**, 34 (1931).
[4] Zener, Phys. Rev. **38**, 277 (1931).

have not as yet completed the application to any particular case, but certain conclusions of a rather general nature seem possible, and it appears desirable to describe the procedure in as simple and general a way as possible, without the encumbrance of the special notation necessary for a special problem. The results also have an application of general interest with respect to the question of distinguishing between adiabatic and nonadiabatic processes, which we will not enter into in detail, but which the reader may readily see for himself.

§2. Statement of the Problem

We suppose that we have two molecules or atoms. Neglecting at first any interaction between them, the state of this pair of molecules or atoms may be designated by an eigenfunction ψ which may be written in the form

$$\psi = XR \tag{1}$$

where R depends on r, the distance between the centers of gravity of the two molecules and X depends on all other coordinates, to be designated as the internal coordinates. We assume that there are two eigenfunctions X which need to be considered, X_1 and X_2. Taking the initial state of the system to be that designated by the subscript 1, we require the probability that on collision it should go over (due to the action of the mutual attractions or repulsions neglected in setting up (1)) to the state designated by subscript 2.

The assumption that there are only these two states X_1 and X_2 to be considered constitutes the chief limitation on our method, because we know that, on account of the rotational degeneracy, it is always necessary to consider many states at a time.[3] Nevertheless I believe that the general character of the results will not be altered, though this must be investigated in the treatment of special cases.

The physical meaning of the transition from the state 1 to the state 2 may be illustrated by a typical example, in which X_1 represents one of the atoms in an excited electronic state, the other atom being unexcited, while with X_2 it is reversed. The transition considered then represents an exchange from one atom to the other of electronic excitation energy.

Corresponding to the two states X_1 and X_2 are two internal energies E_1 and E_2, respectively. Corresponding to the initial and final translational eigenfunctions R_1 and R_2 we have the translational energies T_1 and T_2, respectively. The total energies we shall designate as W_1 and W_2. Naturally we must have

$$W_1 = W_2. \tag{2}$$

If

$$E_1 = E_2 \tag{3}$$

we speak of a condition of exact resonance. This corresponds to no change of translational into internal energy, or *vice versa*, at collision. If $E_1 \neq E_2$ and $E_2 - E_1$ is fairly great[4a] we say the resonance is poor. As is to be expected the

[4a] When statements of the size of quantities are made we shall always have reference to their *absolute magnitudes.*

probability of transition at a collision depends greatly on whether the resonance is good or poor. We shall find it necessary to use two different methods of attack for "good" and "poor" resonance, and shall have occasion to define these terms more exactly later.

In either case our first step is to set up an unperturbed wave equation, neglecting any mutual interaction between the two atoms or molecules. ψ_1 and ψ_2 obey the wave equations,

$$\begin{aligned}(H - W_1)\psi_1 &= 0\\ (H - W_2)\psi_2 &= 0\end{aligned} \tag{4}$$

where H is the unperturbed Hamiltonian operator for the system. X_1 and X_2 obey the equations

$$\begin{aligned}(H_0 - E_1 - l_1(l_1+1)/\kappa^2 r^2)X_1 &= 0\\ (H_0 - E_2 - l_2(l_2+1)/\kappa^2 r^2)X_2 &= 0\end{aligned} \tag{5}$$

where H_0 is the part of the Hamiltonian operator which contains derivatives with respect to the internal coordinates; l_1 and l_2 are the quantum numbers which give the angular momentum which is connected with the free motion of the two atoms or molecules in the states 1 and 2 respectively; and $\kappa^2 = 8\pi^2 M/h^2$ where h is Planck's constant and M the reduced mass. The terms involving the l's enter into the equation in the ordinary process of separating the variables.[5]

R_1 and R_2 can be expressed in terms of quantities F_1 and F_2 defined in accord with the equation

$$R = F/r \tag{6}$$

the F's obeying the equation (subscripts 1 or 2 to be inserted)

$$d^2F/dr^2 + (\kappa^2 T - l(l+1)/r^2)F = 0. \tag{7}$$

The quantity l_1 plays an important role in our calculations. For it is seen that F_1 decreases very rapidly for values of r less than r_0, where

$$r_0 = l_1(l_1+1)/\kappa^2 T_1. \tag{8}$$

This distance is the distance of closest approach (or at least what would be the closest approach if there were no forces between the atom or molecules) of two molecules or atoms with the given relative kinetic energy and angular momentum in the classical theory, and the same interpretation retains most of its significance in the quantum theory.

It is evident that in the transition l will be subject to selection rules, and we shall now assume

$$l_1 = l_2 \tag{9}$$

for only in this way can we remain consistent with our original assumption that only one final state exists which combines with the given state 1. This condition also demands certain selection rules among the other rotational quantum numbers. These we will not need, however, to consider further.

[5] As in Frenkel, "Wellenmechanik," Springer, Berlin, 1929, pp. 245–6.

We now take into account the interaction between the two atoms or molecules, that is, the energy in excess of that they would have if they were an infinite distance apart. This can be expressed as a function, V, of the internal coordinates of the two atoms and the distance r. The problem is treated as a perturbation problem, with V the perturbation function. Corresponding to V will be a matrix

$$v_{11} \quad v_{12}$$

$$v_{21} \quad v_{22}.$$

(In the matrix as written the exponential time factor is assumed not to be included.) First we shall consider the case where[6] $v_{11}=v_{22}=0$. The matrix must of course be Hermitian so that $v_{21}=v_{12}^*$, where the asterisk means conjugate complex.

v_{12} will be a function of r_0, E_1, and E_2-E_1, and it may readily be seen that it will be larger in absolute value the smaller[7] r_0 and $|E_2-E_1|$. The fact that large values of v_{12} are associated with small values of $|E_2-E_1|$ is due to the fact that when $|E_2-E_1|$ is small $|T_2-T_1|$ will be small also, since the total energy cannot change in the collision. If T_1 and T_2 are the same the eigenfunctions F_1 and F_2 of Eq. (7) will be the same, and the integral by which v_{12} is determined, the integrand of which contains the factor F_1F_2dr, will be large. But if F_1 and F_2 are different, and since they are oscillating functions of r, the factor F_1F_2 will then have positive and negative parts when considered as a function of r; in the integration these will tend to cancel, giving small values for the integral. The situation is not greatly different from that described by Condon in his well-known explanation of the intensities in band spectra.

§3. Case of Good Resonance

We shall at first assume that E_2-E_1 is so small that v_{12} is not less than, say, $\frac{1}{2}$ of the value it would have if $E_2-E_1=0$. We shall define this as "good" or "exact" resonance. We may then find the probability of transition per collision in terms of v_{12}. To simplify the notation we shall assume $v_{12}^*=v_{12}$. The results will hold if this is not the case.

We substitute $-(h/2\pi i)\partial/\partial t$ for W_1 or W_2 in Eq. (4), put in a more general function ψ, and bring in the mutual energy, so that

$$\left(H+V+\frac{h}{2\pi i}\frac{\partial}{\partial t}\right)\psi=0. \tag{10}$$

We proceed, according to the Dirac method of variation of constants,[8] to

[6] This is true if the interaction is the dipole interaction described in my preliminary article. These are probably the only forces we need to consider if we merely wish to discover whether radii of action larger than kinetic theory radii can occur. (See Kallmann and London, reference 2.) And, of course, as soon as we have to consider radii of the order of kinetic theory radii we cannot neglect v_{11} and v_{22}.

[7] See, e.g., the calculation in reference 3. The maximum may not occur *exactly* at $E_2-E_1=0$, and some modification of the statement is necessary if Eq. (9) does not hold.

[8] Dirac, Proc. Roy. Soc. **112A**, 673–5 (1926).

find ψ in terms of the original eigenfunctions, which satisfy the equations of the type (4). In so doing it is of course to be noted that due to the free motion of the two atoms or molecules with respect to each other there will be a continuous series of eigenfunctions and eigenvalues for Eq. (4). It will therefore be necessary to integrate over the energy, though naturally only states in the immediate neighborhood of W_1 will make any appreciable contribution. For purposes of normalization it is most convenient to introduce a largest value, r_1, for r, the ψ's then being normalized so that, for example,

$$\int \psi_1^2 d\tau = 1 \tag{11}$$

where $d\tau$ is the volume element, and where the integration is taken over all allowable values of the coordinates (r goes from 0 to r_1). The introduction of the largest value, r_1, will cause the continuous set of eigenfunctions to become a very close-spaced set of discrete ones. We will designate the difference between successive eigenvalues as ϵ (ϵ_1 or ϵ_2 corresponding to the initial or final states, respectively). ϵ will be given in terms of r_1 and T by the following expression

$$\epsilon = hT^{1/2}/r_1(2M)^{1/2} = 2\pi T^{1/2}/r_1\kappa. \tag{12}$$

It is seen that there will be a group of eigenfunctions with the internal part X_1 and a group with the internal part X_2. Any one of the former group we designate as ψ_i, of the latter as ψ_f, the corresponding energy values will be E_i and E_f, W_i and W_f, T_i and T_f. The particular ψ's with energies W_1 and W_2 will still be ψ_1 and ψ_2.

We set

$$\psi = \Sigma_i a_i \psi_i \exp(-2\pi i W_i t/h) + \Sigma_f a_f \psi_f \exp(-2\pi i W_f t/h) \tag{13}$$

where the a's are coefficients which will be functions of the time, and follow Dirac by substituting ψ in Eq. (10), and using relations like (4):

$$\begin{aligned}(H - W_i)\psi_i &= 0\\ (H - W_f)\psi_f &= 0.\end{aligned} \tag{14}$$

we remember that[9] $v_{ff} = v_{ii} = 0$ getting thus the following equations:

$$-(h/2\pi i)da_f/dt = \Sigma_i a_i v_{fi} \exp\{2\pi i(W_f - W_i)t/h\} \tag{15}$$

$$-(h/2\pi i)da_i/dt = \Sigma_f a_f v_{fi} \exp\{2\pi i(W_i - W_f)t/h\}. \tag{16}$$

We begin with the system in a given state, which means that, at time $t=0$, all the a_f's are zero and all the a_i's are zero except a_1, which may be taken as 1. The solution which we get must be consistent with this condition. We start now by trying, as a solution,

[9] This means, of course, that states with the same internal state do not interact with each other, and that the only transitions which occur directly are transitions which involve a change from one internal state to another. This, of course, considerably simplifies our problem, but the method of avoiding the difficulty which one runs into if this is not the case, has been given by Morse and Stueckelberg, reference 22. See §7.

$$a_f = k_f[1 - \exp\{2\pi i(W_f - W_1)t/h\}/(W_f - W_1) \tag{17}$$

where k_f is a function of f. In the case in which the perturbation is small $k_f = v_{f1}$ as was shown by Dirac. We are interested in the case of large perturbations, but it will be seen later that k_f nevertheless remains proportional to v_{f1} if resonance is good. We proceed by substituting (17) into (16) and evaluating (16) by changing the sum into an integration. (This is done by simply replacing the summation sign by $\int dW_f/\epsilon_f$.) (16) then goes over, after a slight transformation, into the form:

$$-\frac{h}{2\pi i}\frac{da_i}{dt} \tag{18}$$
$$= \int_0^\infty \frac{k_f v_{fi}[\cos\{2\pi(W_1-W_f)t/h\}+i\sin\{2\pi(W_1-W_f)t/h\}-1]e^{2\pi i(W_i-W_1)t/h}}{W_f - W_1}\frac{dW_f}{\epsilon_f}.$$

If t is large enough there is no contribution from the sine term in the integrand of (18) except in the immediate neighborhood of $W_f = W_1$; that part of the integral reduces practically to

$$-(ik_2 v_{2i}/\epsilon_2)\int_{-\infty}^{\infty}\frac{\sin(W_f - W_1)}{W_f - W_1}d(W_f - W_1),$$

a known form.[10] (k_2 is the value of k_f when $W_f = W_2 = W_1$) The contribution from the cosine term is negligible. (Any difficulty which might arise from the singularity at $W_f - W_1$ is automatically taken care of by the fact that the cosine term is equal to 1 at this point, hence the two terms cancel each other.) Eq. (18) thus reduces to

$$\frac{h}{2\pi i}\frac{da_i}{dt} = \left(\frac{i\pi k_2 v_{2i}}{\epsilon_2} + \int_0^\infty \frac{k_f v_{fi}}{W_f - W_1}\frac{dW_f}{\epsilon_f}\right)e^{2\pi i(W_i - W_1)t/h}. \tag{19}$$

The remaining integral in (19) can be evaluated roughly. v_{fi}, taken as a function of W_f, (holding i constant) may be expected in general to have a rather sharp maximum at or near the point where $T_f = T_i$. In the case of exact resonance this is also where $W_f = W_i$. In general we may designate the W_f which goes with $T_f = T_i$ as W_{fi}. If W_{fi} is not equal or nearly equal to W_1 the integral may be considered to have its greatest contribution in the neighborhood of $W_f = W_{fi}$. It will be approximately

$$\int_0^\infty \frac{k_f v_{fi}}{W_f - W_1}\frac{dW_f}{\epsilon_f} = \frac{k_{f_i} v_{f_i i}}{W_{f_i} - W_1}\frac{\Delta W_{f_i}}{\epsilon_{f_i}} \tag{20}$$

where ΔW_{f_i} is such a quantity that

$$\int_0^\infty v_{fi}dW_f = v_{f_i i}\Delta W_{f_i}, \tag{21}$$

and may be called the effective width of the curve v_{fi} plotted against W_f. But as W_{f_i} approaches W_1 that is to say, putting the matter the other way

[10] Peirce, "A Short Table of Integrals," Ginn and Co., Boston, 1910, Formula 484.

round, as W_i approaches W_{i_2} the value of the integral will eventually become zero at some point where the positive and negative parts cancel. It may be seen that roughly its value should not exceed such a value as would be obtained by putting $\Delta W_{f_i} = W_{f_i} - W_i$. Since ΔW_{f_i} will be small this means that W_{f_i} is nearly equal to W_1 which is equal to W_2, hence that we may substitute the subscript 2 for f_i. Then, putting the matter the other way round, we see that the i subscript will be roughly i_2. Thus

$$\text{Max} \int_0^\infty \frac{k_f v_{f_i}}{W_f - W_1} \frac{dW_f}{d\epsilon_f} \sim \frac{k_2 v_{2i_2}}{\epsilon_2} . \tag{22}$$

If now the state i_2 chances to be close to the state 1, that is, if T_2 is nearly equal to T_1 (the case of good resonance) the value of (22) becomes $k_2 v_{21}/\epsilon_2$ while for i near 1 in (19) it is seen that the right hand side of (19) will be of the order of its first term. If we assume as a first approximation that we may neglect the second term in (19) we may write (for W_i near W_1)

$$(h/2\pi i) da_i/dt = (i\pi k_2 v_{21}/\epsilon_2) \exp \{2\pi i(W_i - W_1)t/h\} . \tag{23}$$

The word "near" means: "Defined about as closely as good resonance is defined."

Eq. (23) will not hold unless we have good resonance, for when i is 1 the second term in the parentheses in (19) becomes by (20):

$$[k_{f_1} v_{f_1 1}/(W_{f_1} - W_1)] \Delta W_{f_1}/\epsilon_{f_1} . \tag{24}$$

This is to be compared with the first term, $i\pi k_2 v_{21}/\epsilon_2$. Now if resonance is not good v_{21} will be small compared with $v_{f_1 1}$ which is, of course, the maximum value of v_{f_1}. Furthermore, we may in general expect that v_{f_1} will fall off more rapidly than $1/(W_f - W_1)$ as $W_f - W_1$ becomes greater than ΔW_{f_1}. So the second term of (19) becomes then predominant unless k_{f_1} is sufficiently smaller than k_2 which it will not be (23) was derived on the assumption that the first term predominated. Since we shall base our subsequent deductions in this part of the paper on (23), they will hold roughly for the case of good resonance, that is T_2 must be near enough T_1 so v_{21} is within a factor of 2 or so of the maximum value.

Integrating (23) and making $a_i = 0$ at $t = 0$ we get (note $v_{21} = v_{12}$)

$$a_i = ik_2 \pi v_{12} [\exp \{2\pi i(W_i - W_1)t/h\} - 1]/\epsilon_2 (W_i - W_1) . \tag{25}$$

We can substitute this into Eq. (15) and proceed in the same way that we have just done. We must note, however, that at $t = 0$ we have $a_1 = 1$. As $i \to 1$ the value of (25) becomes $-2\pi^2 k_2 v_{12} t/\epsilon_2 h$. It seems, therefore, entirely natural to set[11]

$$a_1 = 1 + \lim_{i \to 1} ik_2 \pi v_{12} [\exp \{2\pi i(W_i - W_1)t/h\} - 1]/\epsilon_2 (W_i - W_1) . \tag{26}$$

When we evaluate (15) and integrate we get (for W_f near W_2)

[11] It is necessary to retain a_1 in this form in order to get reasonable results in our subsequent calculations.

$$a_f = (v_{12} - k_2\pi^2 v_{12}^2/\epsilon_1\epsilon_2)[1 - \exp\{2\pi i(W_f - W_1)t/h\}]/(W_f - W_1). \quad (27)$$

But this must coincide with the expression (17) for a_f. Equating these two for a_2 we get an equation for k_2, which yields

$$k_2 = v_{12}/(1 + \pi^2 v_{12}^2/\epsilon_1\epsilon_2). \quad (28)$$

In order to find the total number of systems in the second state we must evaluate $\sum_f a_f a_f^*$. With the aid of (17) and (28) we find by turning the summation into an integration

$$\Sigma_f a_f a_f^* = 4\pi^2 v_{12}^2 t/h(1 + \pi^2 v_{12}^2/\epsilon_1\epsilon_2)^2\epsilon_2. \quad (29)$$

Thus the rate of transfer from the state 1 to all the states f, which rate we may call γ_{12} is given by

$$\gamma_{12} = 4\pi^2 v_{12}^2/h(1 + \pi^2 v_{12}^2/\epsilon_1\epsilon_2)^2\epsilon_2. \quad (30)$$

Now the eigenfunction ψ_1 represents a system in a certain internal condition with translational energy T_1, moving hence from r_0 to r_1 and back again with velocity $(2T_1/M)^{1/2}$. In unit time it will go from r_0 to r_1 and back again approximately $(2T_1/M)^{1/2}/2r_1$ times which may be taken as the number of collisions per unit time of a system in the state 1. This is equal to ϵ_1/h, by (12), hence the probability of transition per collision may be obtained by dividing (30) by ϵ_1/h and is given by [12]

$$N_{12} = 4\pi^2 v_{12}^2/(1 + \pi^2 v_{12}^2/\epsilon_1\epsilon_2)^2\epsilon_1\epsilon_2. \quad (31)$$

It is seen that N_{12} first increases then decreases as v_{12} increases and hence as r_0 the distance of closest approach, decreases. When

$$\pi^2 v_{12}^2/\epsilon_1\epsilon_2 = 1 \quad (32)$$

$N_{12}=1$. It never becomes greater than this, as of course it must not. The value of r_0 for which (32) holds may be taken as a rough measure of the effective radius of action in any case of exact resonance, since v_{12} will usually increase very rapidly as r_0 increases. This gives a rough justification for the method used in my preliminary article, as far as that is concerned with exact resonance, and, therefore, a justification, except for a numerical factor, of Kallmann and London's result for that case. Eq. (31) is of course not an absolutely exact equation and depends on the validity of the approximations which have been made.

It may be remarked that the quantity on the left hand side of (32) is independent of r_1 as it must be. Since the parts of the integration at great distances r contribute nothing to v_{12}, the latter quantity will depend inversely on r_1, due to the normalization of ψ_1 and ψ_2, while the same dependence is true for ϵ_1 and ϵ_2, as is seen from (12).

Eq. (31) solves the transition problem for the case of exact resonance, whether the perturbation is large or small. It reduces, of course, to the usual result for small perturbations if $v_{12}^2 \ll \epsilon_1\epsilon_2$. It has been pointed out that there

[12] Because we have the case of exact resonance, $\epsilon_1 = \epsilon_2$.

will be obstacles in the way of obtaining a similar result if the resonance is not exact. We might, however, expect that we could at least treat the cases where $v_{12}^2 \ll \epsilon_1\epsilon_2$ by the usual formula for small perturbations. Unfortunately this is not true, however. The difficulty arises from the fact that, in the case of poor resonance, v_{12} is not as large as v_{1f_1}, so that though v_{12}^2 is small compared to $\epsilon_1\epsilon_2$ it may not be true that $v_{1f_1}^2$ will be, so we really do not have the case of small perturbations after all. The criterion for small perturbations is that the second term of (13) should always and for all values of r, but particularly such values as are of importance in the integral which defines a perturbation matrix component, v_{if}, be small compared with the first term. At time $t=0$ the r-factor of the first term is simply F_1. The r-factor of the second term should never approach this in magnitude. To find the conditions under which this will be true, let us evaluate $\Sigma_f a_f F_f \exp(-2\pi i W_f t/h)$. Since if the perturbation is small we have $k_f = v_{f1}$ we shall simply substitute this value in (17) and use this expression. In a manner similar to that in which we obtained Eq. (19) we get (t large)

$$\Sigma_f a_f F_f(\exp(-2\pi i W_f t/h) = -\left(i\pi F_2 v_{21}/\epsilon_2 + \int_0^\infty \frac{v_{f1}F_f}{W_f - W_1}\frac{dW_f}{\epsilon_f}\right) \exp(-2\pi i W_1 t/h).$$

It is seen that if v_{21}/ϵ_2 is small the first term will always be small, but we must evaluate the integral. Now the range of W_f over which v_{f1} has a large value is just that range over which F_f does not get appreciably out of phase in those regions (the important regions) of r which contribute to the integral giving v_{f1}. Thus we set $F_f = F_{f_1}$ for that region of r, and evaluate the integral as we did the integral in (19), obtaining as a rough value $v_{f_1 1}F_{f_1}\Delta W_{f_1}/\epsilon_{f_1}(W_{f_1} - W_1)$. If this is small we can use the small perturbation approximation. Since, if resonance is poor, $\Delta W_{f_1} \ll W_{f_1} - W_1$ it is always safe to use the approximation if $v_{f_1 1}/\epsilon_{f_1}$ is not greater than about 1. That is, we may surely use the approximation for small perturbations provided this approximation would be correct, even if we had exact resonance. Any attempt to carry the small perturbation case up toward the region where $v_{12}^2/\epsilon_1\epsilon_2$ itself is large, as was done in our preliminary article[3] will be inadmissible except for getting an upper limit, as, indeed, we stated to be the case at the time. (though, due to the rapid decrease of v_{12} as $|E_2 - E_1|$ increases, this may nevertheless turn out to be a pretty good approximation). The method of §5 allows us to show that in the case of poor resonance the transition probability at collision will always be small (except, perhaps, at the very boundary of good resonance, i.e. not very poor resonance). If we have to contrast this with cases where the probability of transition approaches unity, this is entirely satisfactory—transition probabilities, if resonance is poor, are negligible. In many cases, however, transition probabilities of the order of 1 never occur—we are interested in comparing very much smaller probabilities. Here the calculations for small perturbations hold, and no further analysis is required.

§4. Discussion of §3

Since in §3 we have really given only an outline of the derivation of (28), it may be well to discuss further some of the points involved, as well as give an interpretation of the results in terms of an incoming wave and outgoing waves of particles.

In the first place our deductions are based on the assumption that (for state f very far from 2)

$$k_2/k_f = v_{12}/v_{1f} \tag{33}$$

and more or less implicitly on the assumption that (for state i very far from 1)

$$k_1/k_i = v_{21}/v_{2i}. \tag{34}$$

But are these assumptions consistent with each other and with Eq. (19) and with the equation similar to (19) but involving da_f/dt instead of da_i/dt, for all values of i and f? The answer is yes. For Eq. (34) follows from (19) provided the first term on the right-hand side of (19) is large compared with the second, and this condition is fulfilled provided (33) is true. Using (33) we have to show that

$$\left| i\pi k_2 v_{2i}/\epsilon_2 \right| \gg \left| k_2 v_{1f_i} v_{f_i i} \Delta W_{f_i}/v_{12}(W_{f_i} - W_1)\epsilon_{f_i} \right|. \tag{35}$$

Since $v_{f_i i} \sim v_{12}$ and $v_{1f_i} \sim v_{2i}$ and $\epsilon_2 \sim \epsilon_{f_i}$ and $\Delta W_{f_i} \ll W_{f_i} - W_1$ this is seen to be true.[13] Similarly (33) follows from (19) and (34). They are therefore consistent, and so we have gone a step further in the construction of the complete consistent solution of the Dirac equations (15) and (16), at least within the limits which the approximations for i and f not far from 1 and 2, respectively, allow.

We may next consider the question of the constant of integration in the expressions for a_f and a_i. This has been chosen to make the quantities have the proper values, in general zero, at $t=0$. But it will have been noted that the evaluation of da_i/dt from (18) depends upon the assumption that t is great. Specifically it may be seen from (18) that it must be so great that $\exp 2\pi i \Delta W_f t/h$ has gone through a considerable number of periods. This being the case, the expression (19) for da_i/dt does not hold from the moment $t=0$, and the same may be said for the similar expression for da_f/dt. This will affect the constant of integration. However, if i is near enough to 1, it is obvious that $\exp 2\pi i(W_i - W_1)t/h$ will (because $|W_i - W_1| \ll \Delta W_{f_1}$) have gone through but a fraction of a period after the expression (19) has begun to hold. Therefore, the constant of integration must be approximately correct if i is near 1 (and similarly if f is near 2), which is all that is necessary. In fact, the exact value of the constant of integration is not important so long as it does not vary rapidly with i when i is in the neighborhood of 1 (or with f when f is in the neighborhood of 2), for it would not matter, for example, if the last term in (19) were multiplied by a factor, which might be complex, but in all events would of the order of 1 in absolute value.

One of the most satisfactory checks of the general correctness of the procedure in §3 will be afforded by the ability to express the results in terms of ingoing and outgoing waves of pairs of atoms or molecules. We may now consider how this may be done.

Consider first the eigenfunctions F_f. At great distances, they are of the form,

$$F_f = \sin \kappa T_f^{1/2} r \tag{36}$$

ignoring a possible phase constant and the normalization factor. The part of the complete eigenfunction with the final internal state which depends on r is given by

$$\Sigma_f a_f F_f e^{-2\pi i T_f t/h} = e^{-2\pi i T_2 t/h} \int_{-\infty}^{\infty} \frac{k_f (e^{-2\pi i (T_f - T_2)t/h} - 1) \sin (\kappa T_f^{1/2} r)}{T_f - T_2} \frac{d(T_f - T_2)}{\epsilon_f}. \tag{37}$$

We have substituted from (17) for a_f, since we have decided that (17) will hold if W_f is near enough to W_2 or W_1 and as we may see only such states contribute appreciably to the integral[14]

[13] Actually some of our deductions are based on the assumption that T_1, T_2, and all T_i and T_f are of the same order of magnitude. This will include a range of values very much greater than such a difference $T_1 - T_2$ as would be necessary in order for resonance to be poor, and cannot invalidate our conclusions.

[14] Since this is true, it is permissible to take the limits from $-\infty$ to ∞, when we change over to the variable $T_f - T_2$ instead of T_f.

in (37). Also we have made the obviously correct substitution $T_f - T_2$ for $W_f - W_2$. We can also substitute sin $\{\kappa T_2^{1/2} r + \kappa r(T_f - T_2)/2T_2^{1/2}\}$ for sin $(\kappa T_f^{1/2} r)$ and then perform the integration. We obtain[15]

$$\Sigma_f a_f F_f e^{-2\pi i T_f t/h} = -\frac{\pi k_2}{\epsilon_2} e^{i\kappa T_2^{1/2} r} \quad \text{if} \quad \frac{\kappa r}{2T_2^{1/2}} < \frac{2\pi t}{h} \tag{38}$$

$$= 0 \quad \text{if} \quad \frac{\kappa r}{2T_2^{1/2}} > \frac{2\pi t}{h}.$$

This represents a wave of pairs of particles traveling outward from each other with a relative particle velocity equal to $(2T_2/M)^{1/2}$ and with a definite wave front which moves out with the relative particle velocity. Now, in similar fashion, using (25) and (26), we find

$$\begin{aligned} &\Sigma_i a_i F_i \exp(-2\pi i T_i t/h) \\ &= (i\pi^2 v_{12} b_2/\epsilon_1\epsilon_2) \exp(i\kappa T_1^{1/2} r) + \sin(\kappa T_1 r) \text{ if } \kappa r/2T_1^{1/2} < 2\pi t/h \\ &= \sin(\kappa T_1 r) \qquad \text{if } \kappa r/2T_1^{1/2} > 2\pi t/h. \end{aligned} \tag{39}$$

This may be interpreted as the original stationary state with index 1, represented by the sine term, plus a *negative* wave of pairs of particles, with relative particle velocity equal to $(2T_1/M)^{1/2}$ and a definite wave front with the relative particle velocity, corresponding to those which have been removed and are going out in the wave represented by (38). To show that this is true note that sin $(\kappa T_1^{1/2} r) = -\frac{1}{2}i$ [exp $(i\kappa T_1^{1/2} r) - \exp(-i\kappa T_1^{1/2} r)$] so that the first equation of (39) becomes

$$\begin{aligned} &\Sigma_i a_i F_i \exp(-2\pi i T_i t/h) \\ &= -i(\tfrac{1}{2} - \pi^2 v_{12} b_2/\epsilon_1\epsilon_2) \exp(i\kappa T_1^{1/2} r) + \tfrac{1}{2} i \exp(-i\kappa T_1^{1/2} r). \end{aligned} \tag{40}$$

It may readily be shown (with the aid of (28)) that the square of the absolute value of the coefficient of exp $(i\kappa T_1^{1/2} r)$ in (40) plus the square of the absolute value of the coefficient of exp $(i\kappa T_2^{1/2} r)$ in (38) is equal to the square of the absolute value of the coefficient of exp $(-i\kappa T_1^{1/2} r)$ in (40). Thus we see that our solution represents a groups of pairs of particles coming inward in the state represented by the index 1, and two groups of pairs of particles going outward (i.e., pairs of particles in which a collision has occurred), one of which groups represents pairs of particles in which the transition in which we are interested has occurred, the other pairs of particles in which the transition has not occurred, and that we have conservation of matter. We must remember that we are considering the case of exact resonance so $T_1 = T_2$, and $\epsilon_1 = \epsilon_2$.

§5. Case of Poor Resonance

For the case of poor resonance we shall need a different method of attack. In effect, we shall treat the two atoms as an unstable molecule. We first find the internal eigenfunctions when we hold r fixed but take the interaction between the two atoms into account. There will, of course, be two of these eigenfunctions, which we designate as χ_1 and χ_2. If we divide the Hamiltonian H into the two parts, H_0, which contains the derivatives with respect to all the internal coordinates, and H_r which contains the derivatives with respect to r then χ_1 and χ_2 will satisfy the equations[16]

$$\begin{aligned} (H_0 + V - U_1 - l_1(l_1+1)/\kappa^2 r^2)\chi_1 &= 0 \\ (H_0 + V - U_2 - l_1(l_1+1)/\kappa^2 r^2)\chi_2 &= 0 \end{aligned} \tag{41}$$

where U_1 and U_2 are the eigenvalues (which will of course be functions of r).

[15] We change the exponentials into the sine-cosine form, and expand the expression for sin $\{\kappa T_2^{1/2} r + \kappa r(T_f - T_2)/2T_2^{1/2}\}$, using the formula for the sine of the sum of two angles. The integral finally reduces to integrals of the form of Formula 484 in Peirce, reference 10.

[16] See Eq. (9).

So by ordinary perturbation methods we can find χ_1 and χ_2 in terms of X_1 and X_2 (which obey Eqs. (5)) and U_1 and U_2 in terms of E_1 and E_2. We will have

$$\begin{aligned}\chi_1 &= a_{11}X_1 + a_{21}X_2 \\ \chi_2 &= a_{12}X_1 + a_{22}X_2\end{aligned} \tag{42}$$

where the coefficients a_{11}, a_{12}, a_{21} and a_{22} will be functions of r, though X_1 and X_2 are, of course, not. In setting up the perturbation matrix components (matrix components of V) for this problem we integrate with respect to all variables but r and the matrix components, which we call

$$\begin{matrix} u_{11} & u_{12} \\ u_{21} & u_{22} \end{matrix}$$

will be functions of r. We take $u_{11}=u_{22}=0$. (This is the only way, in general, that it is possible to have $v_{11}=v_{22}=0$). The solution of the perturbation problem gives us[17] (assuming $E_1>E_2$ and $U_1>U_2$)

$$\begin{aligned}U_1 &= (E_1 + E_2 + ((E_1 - E_2)^2 + 4u_{12}^2)^{1/2})/2 \\ U_2 &= (E_1 + E_2 - ((E_1 - E_2)^2 + 4u_{12}^2)^{1/2})/2\end{aligned} \tag{43}$$

$$-a_{21}/a_{11} = a_{12}/a_{22} = u_{12}/(E_2 - U_1) = u_{12}/(U_2 - E_1). \tag{44}$$

The actual values of the a's can be obtained from the normalization of the χ's but are not necessary for our purposes. It is only necessary to note (a) that the ratio in (44) changes from 0 to 1 as u_{12} becomes large, which means as r becomes small; and (b) that this change takes place in the neighborhood of such a value of r that $u_{12}\sim E_1-E_2$. On account of the normalization a_{11} and a_{22} change from 1 to $2^{1/2}$ and a_{12} and a_{21} from 0 to $2^{1/2}$.

Now in considering the result of a collision we are not really interested in what happens during the collision itself, but only in the difference in the condition of the system before and after the collision. Since for large r we see that χ_1 coincides with X_1 and χ_2 with X_2, a change from χ_1 to χ_2 is essentially the same thing as a change from X_1 to X_2, and if we can find the probability of such a change at a collision we have solved the problem.

Thus far we have not talked about the relative translational motion in this case. Now we can use the energies U_1 and U_2 as effective potential energies (the usual thing in the treatment of molecules) and set up wave equations of the form

$$\begin{aligned}(H_r + U_1 + l_1(l_1+1)/r^2 - W_1)S_1 &= 0 \\ (H_r + U_2 + l_1(l_1+1)/r^2 - W_2)S_2 &= 0\end{aligned} \tag{45}$$

where S_1 and S_2 are to be the translational eigenfunctions and W_1 and W_2 the total energies. Naturally, as before, $W_1=W_2$ and we must remember that the Eqs. (45) have continuous sets of eigenfunctions. As before we use the subscripts i and f to designate functions of the initial and final types.

[17] This method of calculating energy curves was suggested by London, Zeits. f. phys. Chem. **11B**, 222 (1930). It was also suggested to me by Dr. Clarence Zener before the appearance of London's article. The subsequent handling of the transition problem is, as far as I am aware, new.

The procedure which is ordinarily used in the case of molecules, and which we follow here, is as follows. We try for eigenfunctions expressions of the form $\chi_1 S_1$ and $\chi_2 S_2$ and substitute them into the exact wave equation, which is of the form (4). Such functions do not fit the wave equation exactly, and we have certain terms left over which may be treated, following Slater,[18] as a perturbation. We have a perturbation matrix, which we write out:

$$p_{11} \quad p_{12}$$
$$p_{21} \quad p_{22}.$$

We may now use these matrix components and attempt to solve with them the problem of the transition from state χ_1 to state χ_2 as we solved the problem of the transition from X_1 to X_2 in §3 by the use of the perturbation matrix components v_{12}, etc. One might expect to run into difficulties in this attempt, but we shall now show that in the case of poor resonance the matrix components must always be small, so that the possibility of transition can be entirely neglected.

As in analogous cases[19] we may write these matrix components (we take a general one which we call p_{mn}) as follows:

$$p_{mn} = -\kappa^{-2}\int (\chi_m G_m/r)\left[(G_n/r)(\partial^2\chi_n/\partial r^2) + (2/r)(dG_n/dr)(\partial\chi_n/\partial r)\right]d\tau' r^2 dr \quad (46)$$

where $G_m = rS_m$, etc., $d\tau'$ is the volume element, excluding dr, and the integration is taken over all allowed values of the coordinates. Now G_m will roughly be a sinusoidal function of the argument $\kappa T_m^{1/2} r$ (where T_m is the translational energy) and amplitude of $(2/r_1)^{1/2}$ (on account of the normalization), and similarly for G_n. The value of the derivatives of the χ's will depend upon the derivatives of the a's in terms of which the χ's are expressed (Eq. (42)). Now a_{11} will change practically from $2^{1/2}$ to 1 in some distance, equal, say to Δr with an average da_{11}/dr of roughly $1-2^{1/2}$, and similarly for the other a's. Then it is seen that the integral with respect to r need be carried over a region equal to only Δr. We can say roughly that

$$\begin{aligned} \chi_m &\lesssim X_1 \\ \partial\chi_n/\partial r &\lesssim X_1/\Delta r \\ \partial^2\chi_n/\partial r^2 &\lesssim X_1/(\Delta r)^2. \end{aligned} \quad (47)$$

(The choosing of the subscript 1 for these expressions rather than 2 is purely arbitrary—either would give the order of magnitude satisfactorily.)

Also we may write

$$dG_n/dr \sim \kappa T_n^{1/2} G_n' \quad (48)$$

where G_n' is the derivative of G_n with respect to its argument. Using (47) and (48) in (46) we see that[4a]

[18] Slater, Proc. Nat. Acad. Sci. **13**, 423 (1927).
[19] See Rice, Phys. Rev. **35**, 1552 ff (1930).

$$p_{mn} \lesssim -\kappa^{-2} \int (X_1 G_m/r)\left[(G_n/r)(X_1/(\Delta r)^2) + (2/r)(\kappa T_n^{1/2} G_n')(X_1/\Delta r)\right] d\tau' r^2 dr$$

and noting that $\int X_1^2 d\tau' = 1$ we have

$$p_{mn} \lesssim -\kappa^{-2} \int (G_m G_n/(\Delta r)^2 + 2\kappa T_n^{1/2} G_m G_n'/\Delta r) dr. \tag{49}$$

If the two sinusoidal functions G_m and G_n (or G_m and G_n') are in phase p_{mn} will have its largest possible value. Remembering then what we have said about extending the integration with respect to r over a region equal to Δr and our statement about the amplitude of G_m of G_n we may write

$$p_{mn} \lesssim 1/\kappa^2 r_1 \Delta r + 2T_n^{1/2}/\kappa r_1. \tag{50}$$

Now if T_n is of the order of the translational energy of an atom or molecule at room temperature $1/T_n^{1/2}\kappa$ will be of the order of 10^{-9} cm. It is not to be expected that any interaction between the atoms will cause the a's to change appreciably in much less than this distance, so we may write $\Delta r > 10^{-9}$ cm, so the right hand side of (50) will be of the order of its second term. Thus we may write

$$p_{mn} \lesssim 2T_n^{1/2}/\kappa r_1. \tag{51}$$

By Eq. (12) we may write

$$p_{mn} \lesssim \epsilon_n/\pi. \tag{52}$$

Now this is just large enough, (assuming $\epsilon_1 \sim \epsilon_2$) so that if we substitute p_{12} for v_{12} in Eq. (31), N_{12} becomes of the order of 1. But the right hand side of (52) gives the maximum value that p_{mn} can take. In the case of poor resonance p_{mn} will be much less because then the sinusoidal functions in (49) will be out of phase[20] and have different periods, if $n \neq m$. We rapidly get into the regions of small perturbations and negligible transition probabilities (see end §3). This situation will be only accentuated by the original effect of the perturbation u_{12} on the potential energy between the atoms, as indicated in (43) inasmuch as it pushes the energy curves away from each other. We must also consider the case where $m = n$. It may be shown that the second term on the right of (46) is zero when integrated if[21] $m = n$—this leaves only the first term to consider. It may be taken into account by simply adding increments[22] to U_1 and U_2, and solving this new problem (that is, we use the new eigenfunctions for Eqs. (45). The cross terms of the matrix component will be changed, and the diagonal ones will then be zero). The increment to be added is the part of the integral which is integrated with respect to all variables except r, that is $-\kappa^{-2}\int \chi_m(\partial^2\chi_m/\partial r^2) d\tau'$. It may be shown to have the same

[20] The fact that we have to deal with G_n' instead of G_n makes a little change in what we will define as good or exact resonance, but not enough to make much difference, especially for the rather rough considerations we have in mind.

[21] Similar to Rice, Phys. Rev. 35, 1555 (1930).

[22] Morse and Stueckelberg, Ann. d. Physik 9, 579 (1931).

value whether m is 1 or 2, by the use of (44) and the relations $a_{11}^2+a_{21}^2=a_{12}^2+a_{22}^2=1$. Since U_1 and U_2 are affected in the same way, the question of whether resonance occurs or not is not greatly affected, especially as the size of the term added to the U's will usually be small. It will be of the order $1/\kappa^2(\Delta r)^2$ at the value of r where it is greatest and even if the colliding atoms were hydrogen, for which κ is smallest Δr would have to be as small as 3×10^{-9} cm for the additional energy term to be equal to the average translational energy of an atom at room temperature.

The question may arise as to why it is that we can assume that poor resonance for the matrix components v_{11}, etc., is also poor resonance for the matrix components p_{11}, etc. This can be seen from the Eq. (44) and for the expression for p_{mn}, which is to be compared to the expression $v_{mn}=\int F_m F_n u_{mn} dr$. ($u_{mn}$ already contains the integration for all variables besides r.) If we go from large to small values of r, it will be seen from (44) that u_{mn} will at first have the same general characteristics as a function of r as the nonoscillating part of the integrand of (46), but the latter eventually approaches zero as r decreases (at the point where the a's become practically all equal) while u_{mn} continues to increase. If the nonoscillating part of the integrand of (46) decreases (as $r\rightarrow0$) at a point $r<r_0$ (where r_0 is defined in (8) $-r_0$ gives the point where the oscillating part decreases) then it is obvious that the properties of p_{mn} will be similar to those of v_{mn}. If the decrease takes place at a greater value of r this means that the contributions to the integral for p_{mn} occur at greater values of r than those for v_{mn}, and consequently at a point where the integrand will be changing more gradually. Thus the relatively important contributions to p_{mn} will be spread over a relatively greater range of r than those of v_{mn} and this means that the two oscillating factors in the integration will more quickly get out of phase with each other in the case of p_{mn} than in the case of v_{mn}. Thus poor resonance for v_{mn} will certainly be poor resonance for p_{mn}.

One may also question why the method of this section could not be used for cases of exact resonance, as well. It might of course, theoretically at least, be used, but complications will arise. As may be seen from (43) and (44) the change in the values of the a's would take place at greater and greater values of r the less E_2-E_1 became.[4a] This would introduce great complications both in the calculation and its interpretation. It seems best, therefore, to stick to the easily worked out and easily interpreted method of §3.

§6. Summary of the Results

It thus appears that we may say that, if resonance is good, transitions will take place provided the atoms or molecules come roughly within a certain minimum distance of each other. Outside that distance no appreciable exchange of energy will take place.

But, exact resonance, as it is defined in §3, depends upon how closely the atoms do approach, because the matrix components depend on this. Hence, provided they approach within the maximum distance described in the above paragraph, we may say that they will or will not exchange energy, depending

on how closely the energies E_1 and E_2 match. Conversely, we may say, given E_2-E_1, exchange of energy will take place provided the distance of approach is less than a certain critical distance. This distance may be found as a function of E_2-E_1. In general it will be greater the smaller[4a] E_2-E_1.

It is not my desire to enter into particular cases here. But it may not be amiss to mention that cases 2 and 3 of my preliminary article are roughly the cases of poor resonance. An unfortunate typographical error occurred in the definition of these cases.[23] In both instances the expression $(r_0\eta E_{k_1})^{-1/2}$ should have been $(r_0\eta E_{k_1}{}^{1/2})^{-1}$. The present result, if it may be applied directly to the case where many final and initial states are involved, says that practically no transfer of energy will take place if the resonance is poor. It would be difficult to imagine the possibility of radii of action larger than kinetic theory of radii if the resonance difference were greater than a millivolt, a case which practically does not occur unless the exchange is between identical atoms. As far as our results go they thus say that abnormally large radii of action do not occur. Zemansky has recently shown that, in the cases of interaction of mercury atoms with other atoms, many of the large radii of action formerly believed to exist are due to misinterpretation of the experimental data. A careful evaluation of the quantities involved, even if resonance is exact, shows that a reasonably favorable situation is required in order to give exceptionally large radii, and the present results at least strongly indicate that such an evaluation will usually be much too sanguine. I believe therefore, that all cases (except some in which resonance is exact) in which experimental results are reported which give large radii of action that they should be very carefully scrutinized. In many cases, I believe, it will be found that a reinterpretation of the data does away with the necessity of assuming that large radii of action actually exist.

§7. Case of Nonzero Diagonal Matrix Components

The case where the components u_{11} and u_{22} of the matrix of §5 and therefore v_{11} and v_{22} of the matrix of §3 are not zero may probably be dealt with by use of the two methods described above. u_{11} and u_{22} may simply be added in the Eq. (7) or (45) as potential energies[22] (u_{11} in the first equation in either case, u_{22} in the second). Then we proceed to take care of the cross terms in the matrix as above.

The corrected potential energy curves may have various complex forms. In particular the curves for the two states may cross. We may expect the case in which transitions may be probable to be that in which the relative translational energy in the initial state is such that the two atoms or molecules would just come to rest with respect to each other at the point where the curves cross. The results of this expectation have been discussed in a recent

[23] Due to an error in V, the expression for r_c in Case 1 should be increased by about 40 percent a change which is, however, about canceled by the substitution of the expression in the Eq. (32) for that of Eq. (4) of the earlier article. The r_c's for cases 2 and 3 will also be slightly modified, but these results are no longer of so much interest being superceded by the present results.

note.[24] It is hoped, however, that it will be possible to take some definite, though hypothetical case, and work it through in some detail, so further discussion of this case will be left for a future communication.

As mentioned above in a footnote[6] the case of zero diagonal matrix components can hold only when the collisions which need to be considered have a distance or closest approach greater than kinetic theory radii. This means that either the radius of action is so large that such close collisions do not contribute an appreciable amount to the total number of transitions, or else we are only interested in seeing whether large radii of action occur or not. But in many cases the radii of action are of the order of kinetic theory radii, and this means that undoubtedly the interactions are too large to be considered by the ordinary Born collision method or the modifications of it which have thus far appeared. Such cases require the treatment indicated by the present section, and they probably occur more often than the cases where the diagonal matrix components can be neglected. The discussion in the previous sections of this paper, therefore, must be considered as illustrative of the type of thing one must expect where large interactions occur, and not as something to be compared directly with much of the experimental data which is at hand. It is, however, of particular interest, as indicating the entirely different treatment of the case of poor resonance necessary when the interactions are large, and the relatively low probabilities of transition in this case as compared with the probabilities when resonance is good.

§8. Discussion

It may be of interest to compare my results with those of the recent article by Zener,[4] in which the problem of inelastic collisions is attacked by a method based partly on classical theory and partly on quantum theory. While I feel that the correctness of his Eq. (1), on which his conclusions are based, is not entirely self-evident, I believe that it should give good results as long as the interactions are small. By this, I mean that the interaction (called here u_{12} and by Zener $V_{n'n''}$) must everywhere be so small that the probability of energy exchange would be small if the resonance were exact, and this definition holds even in the case where resonance is poor (see end §3). I do not believe that Zener would concur in this definition, but I use it as the basis for discussion. If the interaction is small, then the probability of transition may be found by the Born or the Dirac method. This consists in the evaluation of Eq. (3) of my preliminary article,[3] and Zener has shown that this method gives essentially identical results in the particular case discussed in my article. The transition probabilities thus considered are always so small we would neglect them in the case of large interactions. In the case where the interaction is large Zener proposes to use and generalize the method I suggested,[3] except that he is going to substitute the probability he calculates by his method for the probability I calculate by mine. This can give only an upper limit, as it gave in my case; as stated above (end §3) this may

[24] Rice, Phys. Rev. **37**, 1187, 1551 (1931); see also Jabłoński, Zeits. f. Physik **70**, 730 (1931).

be a good approximation, but it is harder to judge how good in Zener's treatment than in mine. The advantage of Zener's method, in those cases in which it can be applied, lies in the case with which the calculations can be made and the results envisioned.

The recent paper of Morse and Stueckelberg[22] does not attempt to treat the case of large interactions, but introduces a device which prevents large interactions from artificially appearing where they really do not belong. The general results obtained are very interesting, but before even the theory of small perturbations can be said to be in final form it will need very considerable modifications. Their theory bears the same relation to the true theory of small perturbations, as the main part of this paper bears to the more general problem outlined in §7.

THE EVALUATION OF THE MATRIX COMPONENTS FOR HELIUM

By Lloyd P. Smith*
California Institute of Technology
(Received September 5, 1931)

Abstract

An expression involving a certain number of differentiations has been obtained for the matrix components involved when the first order correction to the wave function is desired starting from the product of hydrogen-like wave functions and treating the electrostatic interaction energy between the two electrons as the perturbation energy. The result given holds for all discrete states.

WHEN one attempts to calculate the first order approximation to the wave function for helium for any discrete state using perturbation methods and starting from the product of hydrogen wave functions and using the electrostatic interaction energy as the perturbation energy one encounters matrix components of the following type:

$$H = \int R_{n_1 l_1}(r_1) R_{\nu_1 \lambda_1}(r_1) \frac{1}{r} R_{n_2 l_2}(r_2) R_{\nu_2 \lambda_2}(r_2) P_{l_1}^{m_1}(\cos\theta_1) P_{\lambda_1}^{\mu_1}(\cos\theta_1) P_{l_2}^{m_2}(\cos\theta_2) P_{\lambda_2}^{\mu_2}(\cos\theta_2) e^{i(m_1-\mu_1)\phi_1} e^{i(m_2-\mu_2)\phi_2} dV \quad (1)$$

the integration being taken over all of the six dimensional space. The polar coordinates with subscript one denote the position of electron one and similarly the subscript two refers to the coordinates of the second electron. The letters n, l, m, denote the quantum numbers for the initial state of electron one or two as indicated by the corresponding subscript.

Similarly the Greek letters ν, λ, μ denote the quantum numbers of the final states. All normalizing factors have been omitted in (1). The radial part of the wave function for electron one in the initial state $n_1 l_1$ is given by

$$R_{n_1 l_1}(r_1) = \left(\frac{2r_1}{n_1 a}\right)^{l_1} e^{-r_1/n_1 a} L_{n_1+l_1}^{2l_1+1}\left(\frac{2r_1}{n_1 a}\right)$$

where $a = h^2/Me^2Z$ and $L_{n_1+l_1}^{2l_1+1}(2\nu_1/n_1 a)$ is the usual Laguerre polynomial. The distance between the two electrons is denoted by r which in terms of the coordinates is given by

$$r = (r_1^2 + r_2^2 - 2r_1 r_2 \cos\gamma)^{1/2} \quad (2)$$

where γ is the angle between the two radius vectors r_1 and r_2. The term $1/r$ which occurs in Eq. (1) makes a general evaluation of the integral quite difficult. The usual expansion in powers of the ratio of r_1 and r_2 and spherical harmonics, namely

$$\frac{1}{r} = \sum_{t=0}^{\infty} x^t P_t(\cos\gamma)$$

* National Research Fellow.

where $x = r_1/r_2$ or r_2/r_1 the ratio being chosen so that $|x| < 1$, is not desirable in this case since the domain of both r_1 and r_2 is from 0 to ∞. This would require the evaluation of indefinite integrals. We therefore seek an expansion valid for all r_1 and r_2.

In order to obtain such an expansion we make use of the expansion[1]

$$\frac{\sin kr}{kr} = \pi \sum_{p=0}^{\infty} (p + \tfrac{1}{2}) \frac{J_{p+1/2}(kr_1)}{(kr_1)^{1/2}} \frac{J_{p+1/2}(kr_2)}{(kr_2)^{1/2}} P_p(\cos\gamma) \tag{3}$$

where r is defined by (2). Integrating both sides of this expression with respect to k from 0 to ∞ we obtain the desired expansion

$$\frac{1}{r} = \sum_{p=0}^{\infty} (2p+1) P_p(\cos\gamma) \int_0^{\infty} \frac{J_{p+1/2}(kr_1)}{(kr_1)^{1/2}} \frac{J_{p+1/2}(kr_2)}{(kr_2)^{1/2}} dk. \tag{3a}$$

When this expression is substituted in Eq. (1) and the order of summation and integration interchanged, the integrals appearing in each term of the sum may be separated into two integrals of the form

$$K_p(n_1 l_1, n_2 l_2, \nu_1 \lambda_1, \nu_2 \lambda_2) = \int_0^{\infty}\int_0^{\infty}\int_0^{\infty} R_{n_1 l_1}(r_1) R_{\nu_1 \lambda_1}(r_1) \frac{J_{p+1/2}(kr_1)}{(kr_1)^{1/2}} R_{n_2 l_2}(r_2) R_{\nu_2 \lambda_2}(r_2) \frac{J_{p+1/2}(kr_2)}{(kr_2)^{1/2}} r_1^2 r_2^2 dk dr_1 dr_2 \tag{4}$$

and

$$\int_0^{\pi}\int_0^{\pi}\int_0^{2\pi}\int_0^{2\pi} P_{l_1}^{m_1}(\cos\theta_1) P_{\lambda_1}^{\mu_1}(\cos\theta_1) P_{l_2}^{m_2}(\cos\theta_2) P_{\lambda_2}^{\mu_2}(\cos\theta_2) P_p(\cos\gamma) e^{i(m_1-\mu_1)\phi_1} e^{i(m_2-\mu_2)\phi_2} \cdot \sin\theta_1 \sin\theta_2 d\phi_1 d\phi_2 d\theta_1 d\theta_2. \tag{5}$$

The integral (4) is separable in r_1 and r_2 and the resulting integrals being of the Gegenbauer type can be evaluated in terms of a hypergeometric function or a generalized Legendre function of the second kind but then the product of two such functions would have to be integrated with respect to k from 0 to ∞ and the writer was unable to evaluate the integral in this form or to find its evaluation in the literature.

The integral (5) can be made separable in all of the angles by applying the addition theorem for Legendre polynomials to $P_p(\cos\gamma)$ i.e.

$$P_p(\cos\gamma) = \sum_{q=-p}^{q=+p} \frac{(p-|q|)!}{(p+|q|)!} P_p^{|q|}(\cos\theta_1) P_p^{|q|}(\cos\theta_2) e^{iq(\phi_1-\phi_2)}.$$

When this expression for $P_p(\cos\gamma)$ is substituted in (5) and the integrations with respect to ϕ_1 and ϕ_2 are carried out it is evident that there exists only one value of q for which the integral will be different from zero, namely $q = \mu_1 - m_1 = m_2 - \mu_2$. The above sum is therefore reduced to the one term

$$P_p(\cos\gamma) = \frac{(p-|\mu_1-m_1|)!}{(p-|\mu_1-m_1|)!} P_p^{|\mu_1-m_1|}(\cos\theta_1) P_p^{|m_2-\mu_2|}(\cos\theta_2) e^{i(\mu_1-m_1)\phi_1} e^{i(m_2-\mu_2)\phi_2}$$

[1] Watson, Theory of Bessel Functions, p. 363.

and upon substituting this in (5) and carrying out the integrations with respect to ϕ_1 and ϕ_2, the result is

$$4\pi^2 \frac{(p - |\mu_1 - m_1|)!}{(p + |\mu_1 - m_1|)!} \Theta^{\mu_1 m_1}(l_1 p \lambda_1) \Theta^{\mu_2 m_2}(l_2 p \lambda_2) \tag{6}$$

where

$$\Theta^{\mu_1 m_1}(l_1 p \lambda_1) = \int_0^\pi P_{l_1}^{m_1}(\cos\theta_1) P_p^{|\mu_1 - m_1|}(\cos\theta_1) P_{\lambda_1}^{\mu_1}(\cos\theta_1) \sin\theta_1 d\theta_1 \tag{7}$$

and

$$\Theta^{\mu_2 m_2}(l_2 p \lambda_2) = \int_0^\pi P_{l_2}^{m_2}(\cos\theta_2) P_p^{|m_2 - \mu_2|}(\cos\theta_2) P_{\lambda_2}^{\mu_2}(\cos\theta_2) \sin\theta_2 d\theta_2 . \tag{8}$$

J. A. Gaunt[2] has evaluated integrals of the form

$$\int_{-1}^{+1} P_l^u(x) P_m^v(x) P_n^w(x) dx \tag{9}$$

for the case when $u \geqq 0$, $v \geqq 0$, $w \geqq 0$, and $u = v + w$. In Gaunt's work a slightly different definition of $P_k^u(x)$ has been used, namely

$$P_k^u(x) = (k - u)!(1 - x^2)^{u/2} D_x^{k+u} \frac{(x^2 - 1)^k}{2^k k!} .$$

The definition used throughout this paper is the one given above after removing the factor $(k-u)!$, and the necessary changes will be made in Gaunt's results to conform with the definition used here. The integrals (7) and (8) can always be put in the form (9) by recalling the relation

$$P_k^{-u}(x) = (-1)^u \frac{(k - u)!}{(k + u)!} P_k^u(x) .$$

The integral (9) yields a value different from zero only when the following conditions are satisfied:

$$m + n \geqq l \geqq m - n; \quad l \geqq u; \quad l \geqq n - m \tag{10}$$

and also

$$l + m + n = 2s$$

where s is a positive integer. The analogous conditions that must be satisfied simultaneously in order that both (7) and (8) will yield a value different from zero are

$$\begin{gathered} |\lambda_1 - l_1| \leqq p \leqq \lambda_1 + l_1; \quad \lambda_1 \geqq \mu_1; \quad l_1 \geqq m_1; \quad \lambda_1 + p + l_1 = 2s_1 \\ |\lambda_2 - l_2| \leqq p \leqq \lambda_2 + l_2; \quad \lambda_2 \geqq \mu_2; \quad l_2 \geqq m_2; \quad \lambda_2 + p + l_2 = 2s_2 \\ \mu_1 - m_1 = m_2 - \mu_2 \end{gathered} \tag{11}$$

where s_1 and s_2 are any positive integers. The last condition comes of course from integration over ϕ_1 and ϕ_2. The above conditions therefore lead to a re-

[2] Gaunt, Royal Soc. of London Phil. Trans. **228**, 194 (1929).

striction on the possible values of p and thereby reduces the sum in (3a) to a finite number of terms.

The explicit expressions for (7) and (8) when the above selection rules are satisfied will not be given here but they may be obtained in any case from the general expression for (9) which according to Gaunt is

$$\int_{-1}^{+1} P_l^u(x) P_m^v(x) P_n^w(x)\,dx = (-)^{s-m-w} 2 \frac{(m+v)!(n+w)!(2s-2n)!s!}{(m-v)!(s-l)!(s-m)!(s-n)!(2s+1)!} \sum_t (-)^t \frac{(l+u+t)!(m+n-u-t)!}{(l-u-t)!(m-n+u+t)!(n-w-t)!t!}. \quad (12)$$

The range of values for t in the above sum is sufficiently indicated by the factorials.

Evaluation of the Radial Integrals

The more difficult integrations over the radial functions must now be carried out. When the expressions for the radial functions are substituted in (4), the integral becomes

$$K_p(n_1 l_1 \cdots) = \int_0^\infty \int_0^\infty \int_0^\infty \left(\frac{2r_1}{n_1 a}\right)^{l_1} \left(\frac{2r_1}{\nu_1 a}\right)^{\lambda_1} \left(\frac{2r_2}{n_2 a}\right)^{l_2} \left(\frac{2r_2}{\nu_2 a}\right)^{\lambda_2} e^{-(1/n_1+1/\nu_1)r_1/a} e^{-(1/n_2+1/\nu_2)r_2/a} \cdot L_{n_1+l_1}^{2l_1+1}\left(\frac{2r_1}{n_1 a}\right) L_{\nu_1+\lambda_1}^{2\lambda_1+1}\left(\frac{2r_1}{\nu_1 a}\right) L_{n_2+l_2}^{2l_2+1}\left(\frac{2r_2}{n_2 a}\right) L_{\nu_2+\lambda_2}^{2\lambda_2+1}\left(\frac{2r_2}{\nu_2 a}\right) \cdot \frac{J_{p+1/2}(kr_1)}{(kr_1)^{1/2}} \cdot \frac{J_{p+1/2}(kr_2)}{(kr_2)^{1/2}} r_1^2 r_2^2 dk dr_1 dr_2. \quad (13)$$

Before proceding further it is desirable to obtain a convenient representation for the Laguerre polynomials. This can be done by making use of the usual generating function for these polynomials, namely

$$\sum_{\beta=0}^{\infty} L_{\alpha+\beta}^{\alpha}(x) \frac{h^\beta}{(\alpha+\beta)!} = \frac{(-)^\alpha e^{-xh/1-h}}{(1-h)^{\alpha+1}}; \quad |h| < 1.$$

It is not convenient, however, to use this form of the generating function but one obtained from it by making the transformation $h = u/1+u$. The above expression then becomes,

$$\sum_{\beta=0}^{\infty} \frac{L_{\alpha+\beta}^{\alpha}(x)}{(\alpha+\beta)!} \left(\frac{u}{1+u}\right)^\beta = (-)^\alpha e^{-xu}(1+u)^{\alpha+1}.$$

From this it is seen that the Laguerre polynomials are just the coefficients in the expansion of the function on the right according to powers of $u/1+u$. These coefficients can be determined in the well known way and we have,

$$\frac{L_{\alpha+\beta}^{\alpha}(x)}{(\alpha+\beta)!} = \frac{(-)^\alpha}{\alpha!} \frac{d^\beta}{du^\beta} \left[e^{-xu}(1+u)^{\alpha+\beta}\right]_{u=0}.$$

Making use of this representation for each of the Laguerre polynomials in

(13) and making the changes in the variables indicated by the relation $s_1 = kv_1$ and $s_2 = kv_2$, the expression for K becomes

$$K_p(n_1 l_1 \cdots) = \frac{B\left(\frac{2}{a}\right)^{l_1+l_2+\lambda_1+\lambda_2}}{{n_1}^{l_1} {n_2}^{l_2} {\nu_1}^{\lambda_1} {\nu_2}^{\lambda_2}} D_{v_2}{}^{\nu_2-\lambda_2-1} D_{v_1}{}^{\nu_1-\lambda_1-1} D_{u_2}{}^{n_2-l_2-1} D_{u_1}{}^{n_1-l_1-1}$$
$$(1+v_2)^{\nu_2+\lambda_2}(1+v_1)^{\nu_1+\lambda_1}(1+u_2)^{n_2+l_2}(1+u_1)^{n_1+l_1}$$
$$\cdot \int_0^\infty \int_0^\infty \int_0^\infty {s_1}^{l_1+\lambda_1+3/2} {s_2}^{l_2+\lambda_2+3/2} J_{p+1/2}(s_1) J_{p+1/2}(s_2)$$
$$k^{-(l_1+l_2+\lambda_1+\lambda_2+6)} e^{-\left\{(1+2u_1/n_1+1+2v_1/\nu_1)s_1+(1+2u_2/n_2+1+2v_2/\nu_2)s_2\right\} 1/ak} dk\, ds_1 ds_2 \tag{14}$$

where

$$B = \frac{(n_1+l_1)!(n_2+l_2)!(\nu_1+\lambda_1)!(\nu_2+\lambda_2)!}{(n_1-l_1-1)!(n_2-l_2-1)!(\nu_1-\lambda_1-1)!(\nu_2-\lambda_2-1)!} \tag{15}$$

and

$$D_{v_2}{}^{\nu_2-\lambda_2-1} = \frac{d^{\nu_2-\lambda_2-1}}{dv_2{}^{\nu_2-\lambda_2-1}}.$$

The integration with respect to k can now be carried out by elementary methods and we have,

$$\int_0^\infty k^{-(\eta_1+\eta_2+2)} e^{-(\xi_1 s_1+\xi_2 s_2)1/ak} dk = \frac{(\eta_1+\eta_2)!\, a^{\eta_1+\eta_2}}{(\xi_1 s_1+\xi_2 s_2)^{\eta_1+\eta_2+1}} \tag{16}$$

where the following symbols have been introduced for the sake of shortness

$$\xi_1 = \frac{1+2u_1}{n_1} + \frac{1+2v_1}{\nu_1}; \quad \xi_2 = \frac{1+2u_2}{n_2} + \frac{1+2v_2}{\nu_2}$$
$$\eta_1 = l_1+\lambda_1+2; \qquad \eta_2 = l_2+\lambda_2+2. \tag{16a}$$

In order to proceed with the evaluation of the remaining integral

$$a^{\eta_1+\eta_2}(\eta_1+\eta_2)! \int_0^\infty \int_0^\infty J_{p+1/2}(s_1) J_{p+1/2}(s_2) \frac{{s_1}^{\eta_1-1/2} {s_2}^{\eta_2-1/2} ds_1 ds_2}{(\xi_1 s_1+\xi_2 s_2)^{\eta_1+\eta_2+1}} \tag{17}$$

we again make use of the expansion (3) for the particular case when $k=1$, i.e.

$$\frac{\sin({s_1}^2+{s_2}^2-2s_1s_2x)^{1/2}}{({s_1}^2+{s_2}^2-2s_1s_2x)^{1/2}} = \pi \sum_{p=0}^{\infty} (p+\tfrac{1}{2}) \frac{J_{p+1/2}(s_1)}{(s_1)^{1/2}} \frac{J_{p+1/2}(s_2)}{(s_2)^{1/2}} P_p(x).$$

Multiplying this expression through by $P_p(x)$ and integrating both sides from -1 to $+1$, we have a convenient representation for the product of two Bessel functions, namely

$$J_{p+1/2}(s_1) J_{p+1/2}(s_2) = {s_1}^{1/2} {s_2}^{1/2} \frac{1}{\pi} \int_{-1}^{+1} \frac{\sin({s_1}^2+{s_2}^2-2s_1s_2x)^{1/2}}{({s_1}^2+{s_2}^2-2s_1s_2x)^{1/2}} P_p(x) dx.$$

With this representation for the Bessel functions in 17, we have,

$$(\eta_1+\eta_2)!a^{\eta_1+\eta_2}\frac{1}{\pi}\int_0^\infty\int_0^\infty\int_{-1}^{+1}\frac{s_1^{\eta_1}s_2^{\eta_2}}{(\xi_1 s_1+\xi_2 s_2)^{\eta_1+\eta_2+1}}\frac{\sin(s_1^2+s_2^2-2s_1s_2x)^{1/2}}{(s_1^2+s_2^2-2s_1s_2x)^{1/2}}P_p(x)dxds_1ds_2. \quad (18)$$

It is useful to make two further changes of variable as defined by the relations

$$s=r\cos\theta \quad \text{and} \quad s=r\sin\theta.$$

The above integral then becomes

$$(\eta_1+\eta_2)!a^{\eta_1+\eta_2}\frac{1}{\pi}\int_0^\infty\int_0^{\pi/2}\int_{-1}^{+1}\frac{(\cos\theta)^{\eta_1}(\sin\theta)^{\eta_2}}{(\xi_1\cos\theta+\xi_2\sin\theta)^{\eta_1+\eta_2+1}}\frac{\sin r(1-x\sin 2\theta)^{1/2}}{r(1-x\sin 2\theta)^{1/2}}P_p(x)dxd\theta dr. \quad (19)$$

Changing the order of integration, the integration with respect to r can be performed since,

$$\int_0^\infty\frac{\sin r(1-x\sin 2\theta)^{1/2}}{r(1-x\sin 2\theta)^{1/2}}dr=\frac{\pi}{2(1-x\sin 2\theta)^{1/2}} \quad \text{and} \quad 1-x\sin 2\theta\geqq 0.$$

The expression (19) now becomes

$$(\eta_1+\eta_2)!a^{\eta_1+\eta_2}\tfrac{1}{2}\int_0^{\pi/2}\int_{-1}^{+1}\frac{(\cos\theta)^{\eta_1}(\sin\theta)^{\eta_2}}{(\xi_1\cos\theta+\xi_2\sin\theta)^{\eta_1+\eta_2+1}}\frac{P_p(x)dxd\theta}{(1-x\sin 2\theta)^{1/2}}. \quad (20)$$

The integration with respect to x can be accomplished by making use of the generating function for the spherical harmonics, namely

$$\frac{1}{(1-2xh+h^2)^{1/2}}=\sum_{p=0}^{\infty}P_p(x)h^p;\ |h|<1.$$

Multiplying both sides of this equation by $P_p(x)$ and integrating from -1 to $+1$, we have

$$\int_{-1}^{+1}\frac{P_p(x)dx}{(1-2xh+h^2)^{1/2}}=\frac{2}{2p+1}h^p.$$

This resembles the integral in question namely,

$$\int_{-1}^{+1}\frac{P_p(x)dx}{(1-x\sin 2\theta)^{1/2}} \quad (21)$$

especially when it is written in the form

$$\int_{-1}^{+1}\frac{P_p(x)dx}{\left(1-x\dfrac{2h}{1+h^2}\right)^{1/2}}=\frac{2}{2p+1}h^p(1+h^2)^{1/2}.$$

This will be identical with (21) provided $2h/1+h^2=\sin 2\theta$. This relation is satisfied for both $h=\tan\theta$ and $h=\cot\theta$. The first expression must be used for

$0 \leqq \theta \leqq \pi/4$ and the second for $\pi/4 \leqq \theta \leqq \pi/2$ since $|h|$ must remain less than 1. The value of (21) then becomes

$$\int_{-1}^{+1} \frac{P_p(x)dx}{(1 - x \sin 2\theta)^{1/2}} = \begin{matrix} \dfrac{2}{2p+1} \sin^p \theta \cos^{-(p+1)}\theta \text{ for } 0 \leqq \theta \leqq \dfrac{\pi}{4} \\ \dfrac{2}{2p+1} \cos^p \theta \sin^{-(p+1)}\theta \text{ for } \dfrac{\pi}{4} \leqq \theta \leqq \dfrac{\pi}{2}. \end{matrix} \tag{22}$$

After dividing up the range of integration of θ and using the appropriate expression from (22) the integral (20) becomes

$$\frac{(\eta_1 + \eta_2)!a^{\eta_1+\eta_2}}{2p+1}\left[\int_0^{\pi/4} \frac{(\cos\theta)^{\eta_1-p-1}(\sin\theta)^{\eta_2+p}d\theta}{(\xi_1\cos\theta + \xi_2\sin\theta)^{\eta_1+\eta_2+1}} + \int_{\pi/4}^{\pi/2} \frac{(\cos)^{\eta_1+p}(\sin\theta)^{\eta_2-p-1}d\theta}{(\xi_1\cos\theta + \xi_2\sin\theta)^{\eta_1+\eta_2+1}}\right]$$

or

$$\frac{(\eta_1 + \eta_2)!a^{\eta_1+\eta_2}}{2p+1}\left[\int_0^{\pi/4} \frac{(\tan\theta)^{\eta_2+p}\sec^2\theta d\theta}{(\xi_1 + \xi_2\tan\theta)^{\eta_1+\eta_2+1}} + \int_{\pi/4}^{\pi/2} \frac{(\cot\theta)^{\eta_1+p}\csc^2\theta d\theta}{(\xi_1\cot\theta + \xi_2)^{\eta_1+\eta_2+1}}\right].$$

These integrals can be made to assume a simpler form by letting $t = \tan\theta$ in the first integral and $t = \cot\theta$ in the second. The result is

$$\frac{(\eta_1 + \eta_2)!a^{\eta_1+\eta_2}}{2p+1}\left[\int_0^1 \frac{t^{\eta_2+p}dt}{(\xi_1 + \xi_2 t)^{\eta_1+\eta_2+1}} + \int_0^1 \frac{t^{\eta_1+p}dt}{(\xi_1 t + \xi_2)^{\eta_1+\eta_2+1}}\right]. \tag{23}$$

Unfortunately the above integrals can not in general be evaluated in closed form since they are the integral representations for a certain class of hypergeometric functions and may be represented as such but it seems more practical to proceed in a different manner. We shall make use of the fact that the exponent in the denominators of the integrands always exceeds that in the numerators due to the restrictions imposed on p. It is also to be noted that the above type of integrals can be evaluated in closed form for the special case when the exponent of the denominator is greater by two than the exponent of t in the numerator. If, for example, such a special case of the first integral in (23), is considered, we have,

$$\int_0^1 \frac{t^{\eta_2+p}dt}{(\xi_1 + \xi_2 t)^{\eta_2+p+2}} = \frac{1}{(\eta_2 + p + 1)\xi_1(\xi_1 + \xi_2)^{\eta_2+p+1}}. \tag{24}$$

The above integral can be made equal to the first integral in (23) by performing a certain number of differentiations thus:

$$\int_0^1 \frac{t^{\eta_2+p}dt}{(\xi_1 + \xi_2 t)^{\eta_1+\eta_2+1}} = (-)^{\eta_1-p-1}\frac{(\eta_2 + p + 1)!}{(\eta_1 + \eta_2)!}\int_0^1 D_{\epsilon_1}{}^{\eta_1-p-1}\left\{\frac{t^{\eta_2+p}dt}{(\xi_1 + \epsilon_1 + \xi_2 t)^{\eta_2+p+2}}\right\}_{\epsilon_1=0}$$

$$= (-)^{\eta_1-p-1}\frac{(\eta_2 + p + 1)!}{(\eta_1 + \eta_2)!}D_{\epsilon_1}{}^{\eta_1-p-1}\left\{\int_0^1 \frac{t^{\eta_2+p}dt}{(\xi_1 + \epsilon_1 + \xi_2 t)^{\eta_2+p+2}}\right\}_{\epsilon_1=0}.$$

After the indicated differentiations have been performed ϵ_1 is placed equal to zero. The integral thus obtained may be evaluated by means of (24) and we then have,

$$\int_0^1 \frac{t^{\eta_2+p}dt}{(\xi_1+\xi_2 t)^{\eta_1+\eta_2+1}} = (-)^{\eta_1-p-1}\frac{(\eta_2+p)!}{(\eta_1+\eta_2)!}D_{\epsilon_1}{}^{\eta_1-p-1}\left\{\frac{1}{(\xi_1+\epsilon_1)(\xi_1+\epsilon_1+\xi_2)^{\eta_2+p+1}}\right\}_{\epsilon_1=0} \cdot \quad (25)$$

In a similar manner, the second integral of (23) becomes,

$$\int_0^1 \frac{t^{\eta_1+p}dt}{(\xi_1 t+\xi_2)^{\eta_1+\eta_2+1}} = (-)^{\eta_2-p-1}\frac{(\eta_1+p)!}{(\eta_1+\eta_2)!}D_{\epsilon_2}{}^{\eta_2-p-1}\left\{\frac{1}{(\xi_2+\epsilon_2)(\xi_1+\epsilon_2+\xi_2)^{\eta_1+p+1}}\right\}_{\epsilon_2=0} \cdot \quad (26)$$

Because of the restrictions on p, the indicated number of differentiations can never become negative since $\eta_1-p-1>0$ and $\eta_2-p-1>0$. With the help of (23), (25), and (26) the expression for K from (14) assumes the form,

$$K_p(n_1l_1,\ n_2l_2,\ \nu_1\lambda_1,\ \nu_2\lambda_2) = \frac{B}{2p+1}\frac{2^{l_1+l_2+\lambda_1+\lambda_2}a^4}{n_1{}^{l_1}n_2{}^{l_2}\nu_1{}^{\lambda_1}\nu_2{}^{\lambda_2}}D_{v_2}{}^{\nu_2-\lambda_2-1}D_{v_1}{}^{\nu_1-\lambda_1-1}D_{u_2}{}^{n_2-l_2-1}D_{u_1}{}^{n_1-l_1-1}D_{\epsilon_1}{}^{l_1+\lambda_1+1-p}D_{\epsilon_2}{}^{l_2+\lambda_2+1-p}$$

$$\left[(1+v_2)^{\nu_2+\lambda_2}(1+v_1)^{\nu_1+\lambda_1}(1+u_2)^{n_2+l_2}(1+u_1)^{n_1+l_1}\right. \quad (27)$$

$$\left.\left\{\frac{(-1)^{l_1+\lambda_1+1-p}(l_2+\lambda_2+p+2)!}{(\xi_1+\epsilon_1)(\xi_1+\epsilon_1+\xi_2)^{l_2+\lambda_2+p+3}}+\frac{(-1)^{l_2+\lambda_2+1-p}(l_1+\lambda_1+p+2)!}{(\xi_2+\epsilon_2)(\xi_1+\epsilon_2+\xi_2)^{l_1+\lambda_1+p+3}}\right\}\right]$$

$$v_2=v_1=u_2=u_1=\epsilon_1=\epsilon_2=0.$$

In the above expression it must be remembered that ξ_1 and ξ_2 are linear functions of the u's and v's defined by the expressions (16a) and that B is defined by (15).

The troublesome integration of the radial functions for arbitrary discrete quantum numbers has thus been reduced to a certain number of differentiations and although the indicated differentiations may become complicated and tedious it is always possible to perform them and for a great many choices of the quantum numbers only a few differentiations need be performed especially when one remembers the restrictions imposed on p and in some cases on the quantum numbers themselves by the relations (11).

The complete matrix components may be expressed in the form,

$$H = 4\pi^2\sum_p \frac{(p-|\mu_1-m_1|)!}{(p+|\mu_1-m_1|)!}K_p(n_1l_1,\ n_2l_2,\ \nu_1\lambda_1,\ \nu_2\lambda_2)\Theta^{\mu_1m_1}(l_1p\lambda_1)\Theta^{\mu_2m_2}(l_2p\lambda_2)$$

where the quantum numbers and p are to take on values consistent with (11).

The writer wishes to thank Professor H. Bateman for suggestions and discussions in connection with the above work.

THE VIBRATIONS OF PENTATONIC TETRAHEDRAL MOLECULES*

By Harold C. Urey and Charles A. Bradley, Jr.
Department of Chemistry, Columbia University

(Received September 30, 1931)

Abstract

Andrews has suggested that the restoring forces in polyatomic molecules can best be chosen as harmonic restoring forces along the directions of the chemical bonds and perpendicular to them. In order to test the suggestion, we have calculated the vibrational frequencies of tetrahedral molecules with this choice of forces. The agreement between calculated and observed values is unsatisfactory. It seems that there may be repulsive forces between the corner atoms of the type between ions of crystals or the inert gas atoms. The introduction of terms in the potential energy proportional to $1/r_j^n$, where r_j is the distance between two corner atoms, makes it possible to secure very good agreement between calculated and observed frequencies, in the case of CCl_4, $SiCl_4$, $SnCl_4$, CBr_4, and $SnBr_4$ but not such close agreement in that of $TiCl_4$. The calculated frequencies are not very sensitive to the value of n which may be anywhere from 5 to 9. The repulsive forces necessary are of the same order of magnitude as those calculated from crystal properties and the viscosities of the inert gases. In the case of the $SO_4^=$ and ClO_4^-, the inverse high power repulsive force is not sufficient, but the addition of terms, e^2/r_j, e being the electronic charge, as well as an inverse higher power term does give very good agreement between calculated and observed frequencies of these molecules.

ANDREWS[1] has made the suggestion that the most promising assumption to make in regard to the restoring forces in molecules is that these forces to a first approximation consist of harmonic forces along the directions of the chemical bonds and perpendicular to them. Kettering, Shutts and Andrews[2] have constructed ingenious molecular models on the basis of this suggestion, which duplicate many details of the vibrational frequencies of molecules. A number of years ago Bjerrum[3] considered the same choice of forces in discussing triatomic molecules of the CO_2 type, as well as the assumption of central forces, but was unable to decide definitely between them.[4] The recent theoretical investigations of Slater[5] and Pauling[6] on the nature of the chemical bond also suggest the presence of valency forces acting along and perpendicular to the chemical bond.

* Contribution 680 from the Department of Chemistry, Columbia University. This paper is part of a dissertation presented by C. A. Bradley, Jr. to Columbia University in partial fulfillment of the requirement for the doctor's degree.

[1] D. H. Andrews, Phys. Rev. **36**, 544 (1930).

[2] C. F. Kettering, L. W. Shutts, and D. H. Andrews, Phys. Rev. **36**, 531 (1930).

[3] N. Bjerrum, D. physik. Ges. Ber. **16**, 737 (1914).

[4] A study of the vibrational frequencies of the ClO_2 molecule has been made in this laboratory by Miss Helen Johnston and one of the writers (H. C. U.) which definitely favors the valence type forces.

[5] J. C. Slater, **37**, 481 (1931).

[6] L. Pauling, J.A.C.S. **53**, 1367, 3225 (1931).

Dennison[7] has solved the problem for the vibrations of the tetrahedral pentatomic molecule assuming that the forces act along the lines joining the atoms and Schaeffer[8] has given the dependence on the mass of the central atom. Trumpy[9] applied these formulae to several molecules of this type and showed that the three arbitrary constants required can be adjusted so as to give fair agreement with observation.

This type of molecule is particularly well suited to a test of the choice of restoring forces because the angles can be assumed to be known. Only two arbitrary constants are postulated and four frequencies expected, so that two can be used to calculated the constants and the calculated and observed values of the other two compared. Satisfactory agreement is not secured in this case. However, we find that the presence of repelling forces between the like atoms at the corners of the tetrahedron having the order of magnitude of known repulsive forces between inert gas atoms or ions in crystals make agreement between calculated and observed values very satisfactory for all, but one molecule, to which the calculations have been applied.

The Dynamical Problem

The potential energy function which includes forces along the bonds, perpendicular to them, and along the lines joining the like atoms is,

$$V = V_0 + \sum_1^4 \frac{\partial V}{\partial r_i}\Delta r_i + \tfrac{1}{2}\sum_1^4 \frac{\partial^2 V}{\partial r_i^2}\Delta r_i^2 + \tfrac{1}{2}\sum_1^4 k_2 r_0^2 \Delta\theta_i^2 + \sum_1^6 \frac{\partial V}{\partial r_j}\Delta r_j + \tfrac{1}{2}\sum_1^6 \frac{\partial^2 V}{\partial r_j^2}\Delta r_j^2, \tag{1}$$

where r_i is the distance from the central atom to the ith corner atom, r_j is the distance between two corner atoms, r_0 is the equilibrium value of each r_i and $\Delta\theta_i$ is an angular displacement perpendicular to the bond direction.[10] The central force potential energy function does not include the fourth term and the valence force potential energy function does not include the second and last two terms on the right of Eq. (1). If the potential energy contributed by the interaction of the corner atoms depends on an inverse power of the distance (a usual assumption) as

$$V_j = \frac{k_3}{r_j^n}, \tag{2}$$

the last two terms may be replaced by

$$-\sum_1^6 \frac{nk_3}{a^{n+1}}\Delta r_j + \tfrac{1}{2}\sum_1^6 \frac{n(n+1)k_3}{a^{n+2}}\Delta r_j^2, \tag{3}$$

[7] D. M. Dennison, Astrophys. J. **62**, 84 (1925).

[8] Cl. Schaeffer, Zeits. f. Physik **60**, 586 (1930).

[9] B. Trumpy, Zeits. f. Physik **66**, 790 (1930).

[10] The term containing $\Delta\theta$ is defined as the sum of four terms depending on the displacement of the bond direction from its equilibrium direction. Another way of defining this would be that this consists of the sum of six terms, $\frac{1}{2}k_2'\Sigma r_0^2\Delta\theta_j^2$, where $\Delta\theta_j$ is the change in angle between two pairs of corner atoms and the central atom. The two definitions are identical, however, for $k_2' = \frac{1}{2}k_2$ and thus only a redefinition of an empirically chosen constant is involved.

where a equals the equilibrium distance between corner atoms. If the undisplaced configuration is to be stable, the forces acting along the bonds must be balanced by forces acting between the corner atoms and this leads to a relation between $\partial V/\partial r_i$ and $\partial V/\partial r_j$, namely,

$$\frac{\partial V}{\partial r_i} = -6^{1/2}\frac{\partial V}{\partial r_j} = 6^{1/2}\frac{nk_3}{a^{n+1}}. \tag{4}$$

Our potential energy function is then

$$\begin{aligned} V = V_0 + 6^{1/2}\sum_1^4 \frac{nk_3}{a^{n+1}}\Delta r_i + \tfrac{1}{2}\sum_1^4 \frac{\partial^2 V}{\partial r_i^2}\Delta r_i^2 + \tfrac{1}{2}\sum_1^4 k_2 r_0^2 \Delta\theta_i^2 \\ - \sum_1^6 \frac{nk_3}{a^{n+1}}\Delta r_j + \tfrac{1}{2}\sum_1^6 \frac{n(n+1)k_3}{a^{n+2}}\Delta r_j^2. \end{aligned} \tag{5}$$

The kinetic energy can easily be written in terms of the velocities using suitable coordinates and the problem can be solved by usual methods.[11]

The frequencies in terms of the force constants are found to be as follows,

$$\nu_1 = \frac{1}{2\pi}\left\{\frac{k_1 + (n+1)\gamma_3}{m}\right\}^{1/2}, \tag{6}$$

$$\nu_2 = \frac{1}{2\pi}\left\{\frac{k_2 + \frac{n+2}{4}\gamma_3}{m}\right\}^{1/2},$$

$$\begin{aligned} \nu_{3,4} = \frac{1}{2\pi}\Bigg\{\left(\frac{3n+2}{2}\gamma_3 + 2k_1 + k_2\right)\frac{1}{6m} + \left(\frac{2\gamma_3 + k_1 + 2k_2}{m}\right)\frac{m}{6\mu} \\ \pm \Bigg(\Bigg[\left(\frac{3n+2}{2}\gamma_3 + 2k_1 + k_2\right)\frac{1}{6m} - \left(\frac{2\gamma_3 + k_1 + 2k_2}{m}\right)\frac{m}{6\mu}\Bigg]^2 \\ + \frac{2m}{9\mu}\left(\frac{\gamma_3 + k_2 - k_1}{m}\right)^2\Bigg)^{1/2}\Bigg\}^{1/2}, \end{aligned}$$

where

$$k_1 = \left(\frac{\partial^2 V}{\partial r_i^2}\right)_0, \qquad \gamma_3 = \frac{4nk_3}{a^{n+2}}, \qquad \mu = \frac{mM}{4m+M},$$

and m and M are the masses of the corner and central atoms respectively.[12]

[11] We have found that the simplest method for securing the frequencies is that used by Lorentz, The Electron, pp. 294–297, for a similar problem. We have checked our results by setting up the determinamental equation and solving by the general method.

[12] The dependence of these formulae on γ^3 and k_1 should be derivable from the formulae of Schaeffer by using the proper values of his α and β in terms of our assumed inverse power function. This is not possible, however, unless the sign of β in all his formulae is changed or what is the same thing, unless the β is redefined with opposite sign. This error appears in Dennison's original formulae, in Schaeffer's formulae and also in Trumpy's work (see below) and in Ruark and Urey, Atoms Molecules and Quanta, McGraw-Hill, 1930, p. 441. The latter authors have also made some algebraic error in deriving formulae for ν_3 and ν_4. The error in the sign of the β does not invalidate previous numerical calculations for only the sign of an empirical constant is involved. It means that Trumpy has really assumed attracting forces instead of repelling forces between the corner atoms.

Application to Experimental Data

The experimental data consist of the Raman spectra and infrared spectra of molecules of this type. The experimental errors in these data may amount to a few wave numbers. In addition the data deal with transitions between the normal level of the molecule and levels having one of the vibrational quantum numbers equal to 1. The energy change for this transition is (in wave numbers)

$$\Delta\tilde{\nu} = \tilde{\nu}_0 - 2x\tilde{\nu}_0,$$

if the energy is of the form

$$\tilde{\nu} = \tilde{\nu}_0(v + \tfrac{1}{2}) - x\tilde{\nu}_0(v + \tfrac{1}{2})^2.$$

The quantity which we have attempted to calculate is $\tilde{\nu}_0$ and thus the theoretical formulae do not refer exactly to the observed quantities. Thus even if the theory were exact, which we do not maintain, and the experimental data very precise, which they are not, exact agreement could not be expected. Also conclusions based on agreement closer than a percent or two would be unjustified.

We first applied the formula assuming pure valency forces so that γ_3 is first assumed to be zero. The constants were calculated from the frequencies ν_1 and ν_2 and then the frequencies ν_3 and ν_4 calculated by using these constants. The results are given in Table I. The agreement between calculated and observed is not satisfactory so that the assumption of pure valency forces is not sufficient.

TABLE I

Compound	Inactive frequencies		$\tilde{\nu}_3$			$\tilde{\nu}_4$		
	$\tilde{\nu}_1$	$\tilde{\nu}_2$	Obs.	Calc.	% Diff.	Obs.	Calc.	% Diff.
(1) CCl_4	460	214	760–790	1168	+49.7	311	299	−3.8
(1) $SiCl_4$	422	149	608	724	+19.0	220	210	−4.5
(2) $TiCl_4$	386	119	491	552	+12.4	139	164	+17.9
(2) $SnCl_4$	367	104	401	437	+8.9	136	132	−2.9
(3) CBr_4	265	125	667	864.6	+14.7	183	156.2	−14.8
(2) $SnBr_4$	220	64	279	309.0	+10.7	88	87.4	−0.7
(4) $SO_4^{=}$	980	451	1113	1315	+18.1	620	579	−5.7
(5) ClO_4^{-}	935	467	1121	1241	+10.8	634	591.4	−6.7

(1) Cl. Schaeffer, Zeits. f. Physik **60**, 586 (1930).
(2) B. Trumpy, Zeits. f. Physik **66**, 790 (1930); P. Daure, Ann. de. Physique **12**, 26 (1929).
(3) A. Dadieu and K. W. F. Kohlrausch, Monat. **57**, 488 (1931).
(4) R. G. Dickinson and R. T. Dillon, Proc. Nat. Acad. Sci. **15**, 695 (1929).
(5) H. Nisi, Jap. Jour. Physik **5**, 119 (1929); R. G. Dickinson and R. T. Dillon, Proc. Nat. Acad. Sci. **15**, 695 (1929).

If γ_3 is assumed not equal to zero, we have formulae which depend on four constants which may be fixed arbitrarily and thus exact agreement between calculated and observed values should be secured. However, we are somewhat limited in our choice of the value of n. We picture the molecule $SiCl_4$ for example, to consist of the central atom and four chlorine atoms sur-

rounded by fields of force similar to the field of force about an argon atom and in general the corner atoms to be similar in this respect to inert gas atoms generally. The general character and magnitude of the forces between atoms and ions having inert gas configurations are known from the study of crystals and the properties of the inert gases. It is found that high inverse power potential energy functions fit these data in a highly satisfactory way. We have found that a potential energy function of the form, k_3/r_j^n, with n equal to any number between about 5 and 9 would be satisfactory for the calculation of the frequencies within a few percent so that within the limits which we regard as significant as explained above any choice of n between these two would be permissible. We have found that the choice of $n=6$ or 7 gives better agreement in general than larger or smaller values.

The constants k_1, k_2 and γ_3 were determined by solving the following three linear equations in these quantities,

$$x_1 = \tilde{\nu}_1^2 = k_1' + (n+1)\gamma_3'$$

$$x_2 = \tilde{\nu}_2^2 = k_2' + \frac{n+2}{4}\gamma_3' \tag{7}$$

$$x_3 = \tilde{\nu}_3^2 + \tilde{\nu}_4^2 = \left(\frac{3n+2}{2}\gamma_3' + 2k_1' + k_2'\right)\tfrac{1}{3} + (2\gamma_3' + k_1' + 2k_2')\frac{m}{3\mu},$$

where k_1', k_2' and γ_3' are equal to k_1, k_2, and γ_3 respectively multiplied by the factor $1/4\pi^2c^2m$. The comparison with the fourth quantity $\nu_3^2-\nu_4^2$ could have been made directly, but we have chosen to calculate both ν_3 and ν_4 and compare each of these with the experimental value, since these are the observed quantities and a better judgment of the closeness of agreement can be made. Table II lists the results together with the values of k_1, k_2 and γ_3, using $n=7$.

TABLE II.

	$\tilde{\nu}_1$	$\tilde{\nu}_2$	$\tilde{\nu}_3$			$\tilde{\nu}_4$			k_1	k_2	γ_3
			Obs.	Calc.	dev. %	Obs.	Obs.	dev. %			
CCl_4	460	214	760–790	771.2	?	311	316.6	+2.12	173,771	20,735	32,553
$SiCl_4$	422	148	608	609.5	+0.2	220	216.0	+0.82	258,321	14,818	13,387
$TiCl_4$	386	119	491	482.0	−1.83	139	166.2	+19.4	227,998	7,194	9,717
$SnCl_4$	367	104	401	403.4	+0.6	136	128.7	−5.4	230,638	9,337	5,718
CBr_4	265	123	667	666.7	+0.1	183	183.8	+0.4	139,954	17,684	23,677
$SnBr_4$	220	64	279	279.0	0.0	88	88.0	0	183,407	6,949	5,450

The agreement between calculated and observed values is as close as can be expected except in the case of $TiCl_4$. (The disagreement between the calculated and observed values of $\tilde{\nu}_4$ for $SnCl_4$ is rather great but probably not significant.) Trumpy[9] also found the poorest agreement in the case of $TiCl_4$. A comparison of our percent deviations between calculated and observed and those secured by Trumpy using the central force formulae is given in Table III. The superiority of the valence type forces is immediately evident.

In order to justify our assumption of repelling forces between the corner atoms, it is necessary to show that these forces are of the same order of magnitude as those found from the properties of crystals and the inert gases. Ex-

TABLE III. *Deviations between calculated and observed frequencies as given by Trumpy and by this paper.*

Compound	$\tilde{\nu}_1$		$\tilde{\nu}_2$		$\tilde{\nu}_3$		$\tilde{\nu}_4$	
	U. & B.	T.	U. & B.	T.	U. & B.	T.	U. & B.	T
CCl_4	0	0	0	−9.3	?	?	+2.12	−3.5
$SiCl_4$	0	0	0	−4.7	+0.2	−2.3	−1.82	+4.5
$TiCl_4$	0	0	0	−7.6	−1.83	−4.8	19.4	+13.0
$SnCl_4$	0	0	0	0	+0.6	−4.3	−5.4	−5.1
CBr_4	0	—	0	—	+0.1	—	0.4	—
$SnBr_4$	0	0	0	−4.7	0.0	−2.9	0.0	+3.4

act agreement cannot be expected because atoms, such as the chlorine atoms of CCl_4, bound by nonpolar bands to a central atom can hardly have the same potential energy relative to each other as free inert gas atoms or ions of crystals. Calculations show that agreement between calculated and observed values of $\tilde{\nu}_3$ and $\tilde{\nu}_4$ is not greatly changed by using different values of n, and also that the constants k_1 and k_2 are not greatly changed, and γ_3 changes somewhat more but remains of the same order of magnitude. In the case of $SiCl_4$ best agreement between calculated and observed is secured with $n=6$. Table IV shows the results of such calculations for $SiCl_4$.

TABLE IV.

n	$\tilde{\nu}_3$	$\tilde{\nu}_4$	k_1	k_2	γ_3
5	607.3	222.1	253,926	12,420	18,581
6	608.3	219.1	256,494	13,815	15.563
7	609.5	216.0	258,321	14,818	13,387
8	610.0	214.5	259,705	15,574	11,745
10	610.9	211.9	261,670	16,644	9,431
	608 (obs.)	220 (obs.)			

It is evident to us from these calculations and others of a similar kind that values of n from 5 to 9 are about equally satisfactory so far as this calculation is concerned and thus only order of magnitude of $\partial V/\partial r_j$ and $\partial^2 V/\partial r_j^2$ used by us and those used by others can be compared. We have calculated the values of γ_3 for CCl_4, $SiCl_4$ and $SnCl_4$ assuming $n=8$, which is the value used by Lennard-Jones and Dent[13] and calculated the value of $\partial V/\partial r_j$ from it, $\partial V/\partial r_j = -(\gamma_3 a/4)$. The values of the a's are those determined by Wierl[14] using the electron diffraction method. The values of γ_3 for CBr_4 and $SnBr_4$ have been calculated by using $n=9$, which is Lennard-Jones and Dent's value. In this case we have estimated the values of the a's from the ionic radii of Goldschmidt and Pauling,[15] reducing these values by 7 percent as was found necessary in the chlorine compounds by Wierl. The values of $-(\partial V/\partial r_j)$ so calculated are compared with Lennard-Jones and Dent's values in Table V. The two agree in order of magnitude, but our values do not follow a formula nk_3/a^{n+1} with the same k_3 for CCl_4, $SiCl_4$ and $SnCl_4$ or

[13] J. E. Lennard-Jones and B. M. Dent, Proc. Roy. Soc. **A112**, 230 (1926).
[14] R. Wierl, Ann. d. Physik **8**, 521 (1931).
[15] L. Pauling, J.A.C.S. **49**, 765 (1927); V. M. Goldschmidt, Trans. Far. Soc. **25**, 253 (1929).

for CBr_4 and $SnBr_4$. If we take $n=6$, values for the $-(\partial V/\partial r_j)$ not greatly different for those given in Table V, are secured and they follow fairly closely a formula, nk_3/a^{n+1}.

TABLE V.

Compound	a	γ_3	$-\partial V/\partial r_j$ (dynes)	
			U. and B.	L-J. and D.
CCl_4	2.98	28530	21.25×10^{-5}	24.22×10^{-5}
$SiCl_4$	3.29	11746	9.66	9.94
$SnCl_4$	3.81	5034.9	4.80	2.65
CBr_4	3.19	18436	14.70	28.14
$SnBr_4$	4.05	4274	4.33	2.59

However it is quite evident that any discussion of the value of n, based on the frequencies of these molecules, is futile for data and calculation here given cannot give a decisive answer. We can only conclude that the assumption of valency forces and an inverse power repulsive force between the corner atoms of the correct order of magnitude is able to account for the vibrational frequencies of these molecules with the exception of $TiCl_4$. At present we cannot explain this discrepancy.

The constant, k_2, decreases regularly in the compounds CCl_4, $SiCl_4$ and $SnCl_4$, but the value for $TiCl_4$ is somewhat irregular. The constant, k_1, is smaller in the case of CCl_4 than in that of $SiCl_4$ and $SnCl_4$ and also smaller in the case of CBr_4 than in that of $SnBr_4$. This seems, at first sight, to be unlikely and not to be in agreement with an intuitive judgement based on chemical evidence.[16] By the strength of the nonpolar bond, we may refer to two properties; (1) the dissociation energy associated with the bond; and (2) the restoring force constant for small displacements from the equilibrium position, namely, $\partial^2 V/\partial r_i^2$. It is this latter idea, which appears here.

Morse[17] has shown that the following function will fit the potential energy functions of diatomic molecules with a high approximation:

$$V(r) = -2De^{-A(r-r_0')} + De^{-2A(r-r_0')}.$$

We shall take the potential energy of the tetrahedral molecule in so far as it depends on the distance, r_i, between corner and central atom as this function with r_0' as the equilibrium distance between the central and corner atoms in the absence of the repelling forces between the corner atoms. Then the potential energy is, when $r=r_0$, the equilibrium distance with the repulsive forces present

$$V = 4[-2De^{-A(r_0-r_0')} + De^{-2A(r_0-r_0')}] + 6\frac{k_3}{a^n} = -Q, \qquad (8)$$

and using Eq. (4)

[16] See Pauling's 6th property of the electron-pair band, J.A.C.S. **53**, 1369 (1931).
[17] P. M. Morse, Phys. Rev. **34**, 57 (1929).

$$\left(\frac{\partial V}{\partial r_i}\right)_{r_i=r_0} = 2DAe^{-A(r_0-r_0')} - 2DAe^{-2A(r_0-r_0')} = 6^{1/2}\frac{nk_3}{a^{n+1}}, \tag{9}$$

and

$$\left(\frac{\partial^2 V}{\partial r_i^2}\right)_{r_i=r_0} = -2DA^2e^{-A(r_0-r_0')} + 4DA^2e^{-2A(r_0-r_0')} = k_1. \tag{10}$$

It seems to us that we should expect $(\partial^2 V/\partial r_i^2)_{r=r'_0} = 2DA^2$ to fit Pauling's rule rather than the quantity k_1. The quantity $2DA^2$, equal to k_1' say, can be calculated roughly in the case of CCl_4 and is larger than the k_1's for $SiCl_4$ and $SnCl_4$.

Letting $e^{-A(r_0-r_0')} = x$, Eqs. (8), (9), and (10) become

$$2x - x^2 = \frac{Q + 6\dfrac{\gamma_3 a^2}{4n}}{4D}, \qquad x - x^2 = \frac{6^{1/2}}{8}\frac{\gamma_3 a}{DA}, \qquad x - 2x^2 = -\frac{k_1}{2DA^2}.$$

It is possible to solve these three equations for x, D, and A in terms of Q, the heat of formation, and the constants γ_3 and k_1. When this is done, we find that $2DA^2 = k_1' = 385{,}000$, $r_0 - r_0' = 0.22$A, and $A = 1.12 \times 10^8$. This value for k_1' is of the order of magnitude of the restoring force constants in the case of SiF in which one atom belongs in the first period of eight and the other in the second period of eight of the periodic system. Thus,

$$CC1_4, k_1' = 385{,}000, \qquad SiF, k = 491{,}400.$$

Thus k_1' is larger than the k_1 for $SiCl_4$ and for $SnCl_4$ and it seems likely that it is larger than the k_1''s of these molecules which unfortunately cannot be calculated. We expect a similar relation to hold for the k_1''s of CBr_4 and $SnBr_4$ which also cannot be calculated.

The $SO_4^=$ and ClO_4^- Ions

The assumption that there is no central force between the oxygen atoms of these ions, and the assumption that there is a high inverse power central force between them both fail to give agreement between the observed and calculated frequencies of $SO_4^=$ and ClO_4^-. This might be expected for the bonds of these ions may be partly ionic. Two possible ways of forming the $SO_4^=$ ion would be (1) from S^{6+} and $4O^=$; (2) from $S^{2+}+4O^-$. The latter according to the theories of Slater[5] and Pauling[6] should be tetrahedral. The actual ion may be a combination of both these and perhaps of other possible configurations. Therefore it occurred to us to try the addition of a term $\Sigma(e^2/r_j)$ to the potential energy as well as a high inverse power term. With this assumption very good agreement can be secured in the case of $SO_4^=$, and fair agreement in the case of ClO_4^-. The frequencies for this case are easily secured from Eqs. (6) by using two γ terms, one with $n=1$ and the other with $n=7$. The value of the $\gamma_4 (=4e^2/a^3)$ was calculated using Vegard and

Maurstad's[18] values for the O−O distance in the case of $SO_4^=$, 1.63×10^{-8}cm, and a distance estimated from Goldschmidt and Pauling's ionic values for ClO_4^- of 1.60×10^{-8} cm. The results of these calculations are given in Table VI.

TABLE VI

Ion	$\tilde{\nu}_1$	$\tilde{\nu}_2$	$\tilde{\nu}_3$			$\tilde{\nu}_4$			k_1	k_2	γ_3	γ_4	Number of charge oxygen
			Obs.	Calc.	% dev.	Obs.	Calc.	% dev.					
$SO_4^=$	980	451	1113	1127.8	+1.4	620	592.4	−4.5	634,805	115,960	33,262	0	0
$SO_4^=$	980	451	1113	1113.6	+0.05	620	618.9	−0.2	606,406	98,922	24,742	48,278	1
$SO_4^=$	980	451	1113	1079.4	−3.0	620	676.4	+9.0	521,209	47,803	−816	193,111	2
ClO_4^-	935	467	1121	1140.8	+1.8	631	594.4	−5.9	674,150	163,539	18,239	0	0
ClO_4^-	935	467	1121	1125.4	+0.4	631	623.3	−1.1	644,802	145,714	9,147	51,044	1
ClO_4^-	935	467	1121	1096.3	−2.2	631	672.7	+6.8	556,757	92,240	−18,131	204,176	2

The assumption that each oxygen atom of $SO_4^=$ and ClO_4^- carries one unit of negative charge is consistent with the observed frequencies; the calculated frequencies are not changed greatly by a considerable change in γ_4, for γ_4 must be taken equal to about 70,000 in order to get exact agreement between the calculated and observed values of $\tilde{\nu}_3$ and $\tilde{\nu}_4$ of ClO_4^-, i.e., the effective charge on an oxygen must be $\sim1.15\ e$; however, the observed frequencies are *not* at all consistent with the assumption of either zero or two negative charges on each oxygen atom as can be seen from the table. We expected k_1, k_2 and γ_3 to be larger for ClO_4^- than for $SO_4^=$ because of the greater charge on the central atom, and this proves to be true for k_1 and k_2, but not for γ_3. Neither changing the value of n nor changing the value of γ_4 changes the relative values of γ_3 for the two ions appreciably. The inverse 7th power repulsion forces between the oxygens in the equilibrium position are 1.66×10^{-4} and 0.599×10^{-4} dynes in the case of $SO_4^=$ and ClO_4^- respectively. These forces calculated from the tables of Lennard-Jones and Dent assuming the forces are the same as those of F^- ions are 0.737×10^{-4} and 0.951×10^{-4} dynes respectively and again assuming the repulsive forces to be the same as those between $O^=$ ions are 3.393×10^{-4} and 4.393×10^{-4} dynes respectively. In the case of sulfate our calculated force falls between the two values calculated according to these authors as we should expect it to do considering the trends of values in their tables; however, our value for the ClO_4^- case does not follow these expectations.

A possible explanation for this difficulty, which immediately comes to mind, is our neglect of polarization forces. Such forces should be small in the case of bonds of the nonpolar type as in the chlorides and bromides considered, but, as a simple calculation shows, should be of appreciable magnitude in the case of these partially ionic bonds. The central charged atom should induce a dipole in the corner oxygens and, if these are charged, the mutual energy of these ions and dipoles should be of appreciable magnitude, thus introducing a term depending on both the r_i's and r_i's. Our agreement between calculated and observed frequencies is as good as can be expected neglecting such forces and therefore the introduction of further empirical constants could not be checked against our data. Further, an estimate of such

[18] L. Vegard, and A. Maurstad, Zeits. f. Kristallographie **69**, 519 (1929).

a term from other data would be unreliable, for the polarizability of singly charged oxygen atoms bound by nonpolar linkages to sulphur or chlorine would be difficult to estimate.

The calculations for these ions as they stand are in accord with the assignment of single nonpolar electron-pair bonds between the sulphur and oxygens or the chlorine and oxygens in sulphate and perchlorate ions respectively as suggested by G. N. Lewis.[19]

[19] G. N. Lewis, J.A.C.S. **38**, 762 (1916). "Valence and the Structure of Atoms and Molecules," Chem. Cat. Co., New York, 1923.

ON QUANTUM-MECHANICAL REFLECTION COEFFICIENTS AND THEIR NUMERICAL DETERMINATION

By V. Rojansky* and W. Wetzel
Physical Laboratory, University of Minnesota

(Received September 26, 1931)

Abstract

A method, based on the use of Milne's function w, for the numerical determination of quantum-mechanical reflection coefficients in one-dimensional problems to any preassigned degree of accuracy is outlined. The case in which a "barrier" is both preceded and followed by a field-free space is considered in detail, sections 2–4, and a numerical example is worked out, section 5. The procedure in the case in which a "barrier" is preceded by a field-free space and is followed by a potential for which Schroedinger's equation can be solved analytically is outlined, sections 6–7, and the special case in which a "barrier" is followed by a uniform field is considered in some detail, section 8. The case in which a "barrier" is both preceded and followed by potentials for which Schroedinger's equation can be solved analytically is mentioned, section 8. Formulas are given for the evaluation in terms of ψ and its first derivative, of the respective densities of the dextral and of the sinistral current flowing past any point x in regions where the total energy is greater than the potential energy, section 6. A procedure is given for finding solutions representing unidirectional beams at infinity, section 6.

1. THE purpose of this paper is to outline a method, based on the use of Milne's function[1] w, by which quantum-mechanical reflection coefficients can be evaluated numerically to any preassigned degree of accuracy. The method is straightforward, and should be useful whenever the determination of reflection coefficients to a desired degree of accuracy by analytical methods is sufficiently laborious, or whenever a numerical check on an analytical calculation is advisable.[2] In the course of development certain relations are derived which may be of interest in other connections. No approximations of either mathematical or physical nature are made here, but such approximations may be found justifiable and convenient in applying the method to specific physical problems.

2. The general solution of Schroedinger's equation set up for electrons of energy E moving in a field-free one-dimensional space described by the potential V = a constant ($V<E$) is

$$\psi = \psi(x) = De^{i\alpha x} + Se^{-i\alpha x}, \quad \alpha = \kappa(E - V)^{1/2}, \quad \kappa = (8\pi^2 m/h^2)^{1/2}, \quad (1)$$

where D and S are arbitrary constants, and where $(\quad)^{1/2}$, as throughout this paper, represents the positive square root. Writing the momentum opera-

* National Research Fellow.

[1] W. E. Milne, Phys. Rev. **35**, 863 (1930).

[2] This method was originally devised to check the calculations of W. Wetzel, Phys. Rev. **38**, 1205 (1931) on the reflection coefficient of an electric condenser.

tor as $p=-ih/2\pi\cdot\partial/\partial x$, we interpret the first and second term of (1) as representing, respectively, a beam of electrons of density $|D|^2$ moving from left to right, and a beam of electrons of density $|S|^2$ moving from right to left. We shall call these beams the dextral and sinistral, respectively. It is readily shown by the use of (1) that

$$4\alpha^2|D|^2=|\psi'+i\alpha\psi|^2, \text{ and } 4\alpha^2|S|^2=|\psi'-i\alpha\psi|^2, \tag{2}$$

so that

$$\frac{|D|^2}{|S|^2}=\frac{|\psi'+i\alpha\psi|^2}{|\psi'-i\alpha\psi|^2}, \tag{3}$$

where, as in what follows, a dash denotes differentiation with respect to x. A generalization of (2) and (3) to the case when $V=V(x)$ will be given in section 6.

Consider electrons of energy E moving in one dimension in a field given by a potential $V(x)$ of the form:

$$\begin{aligned} &V(x)=V_l=\text{const. for } x\leqq 0;\ V(x)=v(x) \text{ for } 0\leqq x\leqq a;\\ &V(x)=V_r=\text{const. for } x\geqq a, \end{aligned} \tag{4}$$

and let $E>V_l$, $E>V_r$. The general solution ψ of Schroedinger's equation is then conveniently divided into three sections: $\psi=\psi_l$ for $x\leqq 0$, $\psi=\psi_b$ for $0\leqq x\leqq a$, and $\psi=\psi_r$ for $x\geqq a$, where the subscripts l, b, and r connote "left", "barrier", and "right", and where

$$\psi_l(0)=\psi_b(0),\ \psi_l'(0)=\psi_b'(0);\ \psi_b(a)=\psi_r(a),\ \psi_b'(a)=\psi_r'(a). \tag{5}$$

In particular

$$\psi_l=D_l\epsilon^{i\alpha_l x}+S_l\epsilon^{-i\alpha_l x},\quad \alpha_l=\kappa(E-V_l)^{1/2}, \tag{6}$$

and

$$\psi_r=D_r\epsilon^{i\alpha_r x}+S_r\epsilon^{-i\alpha_r x},\quad \alpha_r=\kappa(E-V_r)^{1/2}. \tag{7}$$

If ψ is a particular solution for which $D_l=0$, i.e., if it represents the special case in which there is only sinistral flow on the left of $x=0$ then the reflection coefficient R appropriate to $V(x)$ and E is $|D_r|^2/|S_r|^2$. Thus, from (3):

$$\textit{if } D_l=0,\ \textit{then } R=\frac{|\psi_r'+i\alpha_r\psi_r|^2}{|\psi_r'-i\alpha_r\psi_r|^2}, \tag{8}$$

the fraction to be evaluated anywhere in the region $x\geqq a$. If we choose $x=a$, we have

$$\textit{if } D_l=0,\ \textit{then } R=\frac{|\psi'(a)+i\alpha_r\psi(a)|^2}{|\psi'(a)-i\alpha_r\psi(a)|^2} \tag{9}$$

where the ψ's are not subscripted because in view of (5) it is immaterial whether ψ_b or ψ_r is used at $x=a$. Eq. (9) is useful because it allows the evaluation of R without the explicit use of the second pair of Eqs. (5), i.e., without

evaluating the coefficients in (7).[3] To illustrate; if $a=0$, so that $V(x)$ has simply a discontinuity at $x=0$ we write (6) in the form $\psi_l=\exp(-i\alpha_l x)$ and obtain directly from (9) the relation $R=(\alpha_r-\alpha_l)^2/(\alpha_r+\alpha_l)^2$.

3. If R is to be determined by numerical integration of Schroedinger's equation two integrations, one for the real and one for the imaginary part of ψ, are necessary.[3a] (R cannot be determined from a real or a pure imaginary ψ, i.e. from a ψ representing zero current.) Integrating twice can, however, be obviated by using Milne's function w.

In his paper on the numerical determination of characteristic numbers[1] Milne proved a theorem a special case of which can be stated for our purpose as follows: If $w=w(x)$ is the particular solution of the equation

$$w'' + \kappa^2[E - V(x)]w = \beta^2 w^{-3}, \quad \beta \neq 0, \tag{10}$$

satisfying the conditions

$$w(x_0) = 1, \text{ and } w'(x_0) = 0 \tag{11}$$

where x_0 and $\beta(\beta\neq 0)$ are arbitrarily fixed constants, then the exact general solution of Schroedinger's equation

$$\psi'' + \kappa^2[E - V(x)]\psi = 0 \tag{12}$$

is

$$\psi = c_1 w \exp\left(i\beta \int_{x_0}^{x} w^{-2}dx\right) + c_2 w \exp\left(-i\beta \int_{x_0}^{x} w^{-2}dx\right), \tag{13}$$

where c_1 and c_2 are arbitrary constants. Thus the general solution of Schroedinger's Eq. (12) can be expressed in terms of *one* particular solution of Milne's Eq. (10).

4. We write $w=w_l$ for $x\leqq 0$, $w=w_b$ for $0\leqq x\leqq a$, and $w=w_r$ for $x\geqq a$, and to fix the adjustable constants we consider Milne's equation for the region $x\leqq 0$:

$$w_l'' + \alpha_l^2 w_l = \beta^2 w_l^{-3}. \tag{14}$$

The choice of constants $\beta=\alpha_l$ and $x_0=0$ is seen to be advisable because it leads to a simple solution of (14),

$$w_l(x) = 1, \tag{15}$$

which satisfies conditions (11) everywhere in the region, and because it superficially simplifies (13). The integrals in (13) now integrate to x for $x\leqq 0$ and the first and second terms of (13) are recognizable (for $x\leqq 0$) as representing, respectively, a dextral and a sinistral beam with $D_l=c_1$ and $S_l=c_2$. To use (9) we set D_l, i.e., c_1 equal to zero. Thus if Milne's Eq. (10) is written

$$w'' + \kappa^2[E - V(x)]w = \alpha_l^2 w^{-3}, \quad \alpha_l = \kappa(E - V_l)^{1/2} \tag{16}$$

[3] Eq. (9) can also be used when R is being evaluated approximately by using approximate ψ's, for example, by the method suggested by N. H. Frank and L. A. Young, Phys. Rev. **38**, 80 (1931).

[3a] One integration of the differential equation being carried out, the other can be reduced to quadratures. Cf. Condon and Morse, *Quantum Mechanics*, (1929), p. 34.

and w is its particular solution such that

$$w(0) = 1, \quad w'(0) = 0, \tag{17}$$

and if

$$\psi = c_2 w \exp\left(-i\alpha_l \int_0^x w^{-2} dx\right), \tag{18}$$

then R is given by (9); elimination of ψ from (9) by means of (18) yields the relation[4]

$$R = \frac{[w'(a)]^2 + [\alpha_r w(a) - \alpha_l / w(a)]^2}{[w'(a)]^2 + [\alpha_r w(a) + \alpha_l / w(a)]^2}, \quad \alpha_r = \kappa(E - V_r)^{1/2}, E > V_r. \tag{19}$$

It will be noticed that while both E and V_l must be fixed to determine $w(a)$ and $w'(a)$ numerically, V_r remains arbitrary to the end.[5]

Discontinuities in $V(x)$ or in its derivatives may occur at some points in the region $0 < x < a$. If $x = \xi$ is such a point the requirement of continuity of ψ and ψ' at ξ becomes, in view of (5) and (13): $w(\xi_-) = w(\xi_+)$ and $w'(\xi_-) = w'(\xi_+)$. The example below refers to a case in which a discontinuity in $V(x)$ occurs.

5. The procedure for the numerical evaluation of R by means of (19) will now be illustrated by an example (to which the writers attach no physical

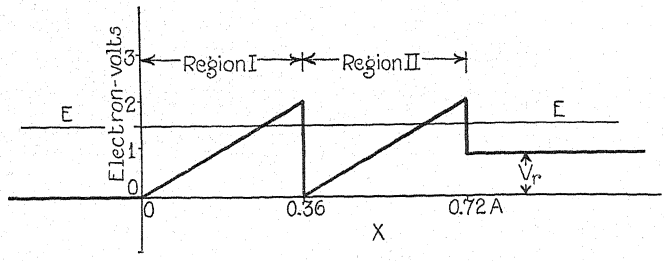


Fig. 1. Graph of $V(x)$ and E used in the example of section 5. The heavy line represents $V(x)$.

significance) so chosen as to demonstrate the main points of the calculation, while avoiding trivial complications, such as interpolation, etc. Let $E = 1.5$ electron volts, $V_l = 0$, $v(x) = eFx = 5.5556 \times 10^8\, x$ electron volts in "region I": $0 \leqq x \leqq 0.36$A, $v(x) = eF(x - 0.36 \times 10^{-8}) = 5.5556 \times 10^8\ (x - 0.36 \times 10^{-8})$ electron volts in "region II": $0.36\text{A} \leqq x \leqq 0.72\text{A}$, and let V_r remain arbitrary, though less than 1.5 electron volts. Fig. 1 is a graph of E and $V(x)$, and the last columns in Tables I and II give the numerical values of $v(x)$. Substituting the numerical values, and expressing x in Angstrom units to avoid high powers of 10, we convert Milne's Eq. (16) into Eqs. (20) and (21) for regions I and II, respectively. The numerical integration, including "starting", was done by Milne's method of numerical integration of ordinary differential equations.[6]

[4] It follows from (5) and (13) that $w_l(0) = w_b(0)$, $w_l'(0) = w_b'(0)$, $w_b(a) = w_r(a)$, and $w_b'(a) = w_r'(a)$, so that w need not be subscripted in (19).

[5] To return to the example at the end of section 2: if $a = 0$ we get the value of R directly from (19) in view of (17).

[6] W. E. Milne, Am. Math. Monthly **33,** 455 (1926). The method is also described in J. B.

Tables I and II show the appearance of the writers' calculations, with minor additions and omissions. The numbers which can be written down prior to the integration are printed in bold-faced type. The "initial conditions" for each table are printed in italics. Note the use of (17) at $x=0$, and the "fitting" of the two sections of w at $x=0.36$A, accomplished by taking the values of w and w' at $x=0.36$A in Table II to be the same as those at $x=0.36$A in Table I. Also note the discontinuity of w'' at $x=0.36$A (0.5156 in Table I, -0.0176 in Table II).[7]

$$w'' = 0.3954w^{-3} - 1.4645(0.2700 - x)w = Pw^{-3} - Qw \qquad (20)$$

TABLE I: $0 \leqq x \leqq 0.36A$.

x	w	w'	w''	Pw^{-3}	Qw	Q	$v(x)$
−.06	(1.0000)	(.0026)	(−.0879)	(.3954)	(.4833)	(.4833)	
.00	*1.0000*	*.0000*	.0000	.3954	.3954	**.3954**	**.0000**
.06	1.0001	.0026	.0878	.3953	.3075	**.3075**	**.3333**
.12	1.0004	.0105	.1751	.3949	,2198	**.2197**	**.6667**
.18	1.0014	.0236	.2617	.3937	.1320	**.1318**	**1.0000**
.24	1.0033	.0419	.3475	.3915	.0440	**.0439**	**1.3333**
.30	1.0065	.0653	.4320	.3878	−.0442	**−.0439**	**1.6667**
.36	1.0113	.0937	.5156	.3823	−.1333	**−.1318**	**2.0000**

$$w'' = 0.3954w^{-3} - 1.4645(0.6300 - x)w = Pw^{-3} - Q'w \qquad (21)$$

TABLE II: $0.36A \leqq x \leqq 0.72A$.

x	w	w'	w''	Pw^{-3}	$Q'w$	Q'	$v(x)$
0.30	(1.0056)	(0.0972)	(−0.0972)	(0.3888)	(0.4860)	(0.4833)	
.36	*1.0113*	*.0937*	−.0176	.3823	.3999	**.3954**	**0.0000**
.42	1.0169	.0951	.0633	.3760	.3127	**.3075**	**.3333**
.48	1.0228	.1013	.1448	.3695	.2247	**.2197**	**.6667**
.54	1.0292	.1125	.2271	.3627	.1356	**.1318**	**1.0000**
.60	1.0364	.1286	.3097	.3552	.0455	**.0439**	**1.3333**
.66	1.0447	.1497	.3927	.3468	−.0459	**−.0439**	**1.6667**
.72	1.0545	.1757	.4762	.3372	−.1390	**−.1318**	**2.0000**

Attention should be called to the entries in parentheses at $x=-0.06$A. These are incidental to the starting of the integration by Milne's method, are calculated on the assumption that w satisfies Eq. (20) also for $x<0$, and are discarded after the integration has been started. The use of these entries can be avoided by adopting some other method of starting, for example a Taylor's expansion, but the writers found Milne's arithmetical method very straightforward and rapidly convergent. Similar remarks apply to the entries in parentheses at $x=0.30$ A in Table II—these are calculated on the assumption that w satisfies Eq. (21) for $x<0.36$A. The present calculation went so smoothly that the use of an interval greater than 0.06A would have been justifiable.

Scarborough's "*Numerical Mathematical Analysis*," Johns Hopkins Press, (1930), but Scarborough does not give Milne's method of "starting," or the use of formula (14) of Milne's paper just quoted. The use of this formula is quite important in preventing oscillations, and in early detection of the computer's errors.

[7] If $V(x)$, rather than $V'(x)$, had a discontinuity at $x=0$, the entries for w and w' at $x=0$ in Table I would be 1.0000, and 0.0000, respectively, but the entry for w'' would differ from 0.0000.

The numerical integration thus yields the values:

$$w(a) = 1.0545, \quad w'(a) = 0.1757, \quad (a = 0.72\text{A}), \tag{22}$$

and using $\alpha_l = \kappa E^{1/2} = .6288$ (Angstrom units^{-1}) we have from (19):

$$R = \frac{[0.1757]^2 + [1.0545\alpha_r - 0.6288/1.0545]^2}{[0.1757]^2 + [1.0545\alpha_r + 0.6288/1.0545]^2},$$

where α_r remains arbitrary. Taking, for example, $V_r = 0$ so that $\alpha_r = \alpha_l$ we get

$$R = 0.0219.$$

A few remarks may be added: (1) Every line in Tables I and II allows the evaluation of R (for $E = 1.5$ electron volts) as a function of V_r for a certain kind of a barrier. For example, the entries at $x = 0.54$A allow the evaluation of R from (19) for a barrier which at, and to the left of, $x = 0.54$A is precisely like the barrier described above, but for which $V(x)$ becomes the constant V_r at, and to the right of, $x = 0.54$A. (2) It is not necessary that the functional form of $v(x)$ be known—the method can be applied equally well when $v(x)$ is given numerically, provided that the data are "smooth", except for isolated discontinuities. (3) The numerical values of w and w' being available, any particular solution of Schroedinger's equation, for the $V(x)$ and E used in the calculation of w and w', can be constructed by means of (13). Eq. (18) should be used for this purpose only if a solution representing a purely sinistral beam for $x \leqq 0$ is desired. (4) If for some interval within $0 \leqq x \leqq a$ a simple analytical expression is available for ψ or for w, it may be convenient to bridge the numerical integration across this interval analytically.

6. Our next problem is to consider the case in which $V(x)$ is not constant for $x \geqq a$, but is some function of x, say $V_r(x)$, for which the general solution of Schroedinger's equation is available. In this connection it will be necessary to set up a method for finding particular solutions which represent, respectively, purely dextral and purely sinistral flow for infinitely large values of x. We shall denote these solutions by $\psi_{D\infty}$ and $\psi_{S\infty}$, respectively, the arbitrary multiplicative constants being supposed to be absorbed in these symbols.[8]

Let ψ (not identically zero) be a particular solution of Schroedinger's equation for a potential $V(x)$ and total energy E. When the state of affairs is described by this ψ electrons flow in general, in both directions past any point x, and we can speak of the dextral and of the sinistral current flowing past x. The difference between these, the resultant current, is independent of x, but each of the two component currents in general varies from point to point, because, in general, partial reflection of the electron waves takes place at every point. Now, let us consider a region in which $E > V(x)$, set $\alpha(x) = \kappa[E - V(x)]^{1/2}$, and define two functions of x, $|D(x)|^2$, and $|S(x)|^2$, by the relations:[8a]

[8] The functions $\psi_{D\infty}$ and $\psi_{S\infty}$ need not exist for any given $V(x)$ or for any given combination of $V(x)$ and E.

[8a] The notation on the right-hand sides of (25) and (26) is ambiguous. The two outside bars are meant to form one pair, and the two inside bars the other pair.

$$4|\alpha(x)|^2|D(x)|^2=|\psi'+i|\alpha(x)|\psi|^2;$$
$$4|\alpha(x)|^2|S(x)|^2=|\psi'-i|\alpha(x)|\psi|^2. \tag{25}$$

Comparison of (25) with (2) suggests that $|D(x)|^2$ and $|S(x)|^2$ may possibly be interpreted as representing the respective densities of the dextral and the sinistral current flowing past x. That this interpretation is justified is shown most easily by a reference to the work of Hill,[9] who writes the general solution of the one-dimensional Schroedinger's equation as a sum of two terms (neither satisfying Schroedinger's equation independently) one of which represents purely dextral and the other purely sinistral flow. [Substitution of Hill's ψ into the right-hand sides of (25) shows that when α is real our $|D(x)|^2$ and $|S(x)|^2$ are equal, respectively, to Hill's $|C_1(x)|^2$ and $|C_2(x)|^2$, which proves the point in question. (Note the distinction between Hill's and our α's). The proof can also be based on a consideration of the identities[9a]

$$\psi=[(\psi'+i|\alpha|\psi)\epsilon^{-i|\alpha|x}/2i|\alpha|]\epsilon^{i|\alpha|x}-[(\psi'-i|\alpha|\psi)\epsilon^{i|\alpha|x}/2i|\alpha|]\epsilon^{-i|\alpha|x},$$

and

$$\psi'\bar{\psi}-\psi\bar{\psi}'=2i|\alpha|[|D(x)|^2-|S(x)|^2],$$

where

$$2i|\alpha|D(x)=(\psi'+i|\alpha|\psi)\epsilon^{-i|\alpha|x},\ 2i|\alpha|S(x)=-(\psi'-i|\alpha|\psi)\epsilon^{i|\alpha|x},\text{and}\alpha=\alpha(x).$$

It will be noticed that although we restricted ourselves to positive values of α, we write $|\alpha|$ for α. We do this because this allows the equations above to be formally satisfied in regions where $\alpha^2<0$. It is not necessary to make this generalization for the purpose of the present paper, nor is it necessary here to seek any physical interpretation for $|D(x)|^2$ and $|S(x)|^2$ for $\alpha^2<0$.]

In view of this physical interpretation the ratio of the density of the dextral to that of the sinistral current flowing past x is[8a]

$$\frac{|D(x)|^2}{|S(x)|^2}=\frac{|\psi'+i|\alpha(x)|\psi|^2}{|\psi'-i|\alpha(x)|\psi|^2},\quad(\alpha^2>0). \tag{26}$$

Therefore the functions $\psi_{D\infty}$ and $\psi_{S\infty}$ referred to above can be defined by the relations:

$$\textit{if } \psi'-i|\alpha(x)|\psi\to 0 \textit{ as } x\to+\infty, \textit{ then } \psi \textit{ is a } \psi_{D\infty} \tag{27}$$

and

$$+i|\textit{if } \psi'\alpha(x)|\psi\to 0 \textit{ as } x\to+\infty, \textit{ then } \psi \textit{ is a } \psi_{S\infty} \tag{28}$$

and whenever they exist it should be possible to find them as follows:[10] let

[9] E. L. Hill, Phys. Rev. **38**, 1258 (1931).

[9a] It now appears to the writers that the consideration of these identities may not constitute a rigorous proof even when the time dependence of ψ is taken into account, and that the argument should be based directly on Hill's work.

[10] The work of R. H. Fowler and L. Nordheim, Proc. Roy. Soc. A119, 173 (1928), may be quoted as an instance in which the necessity of finding $\psi_{D\infty}$ arises. These writers test the unidirectionality of flow by evaluating $\psi\bar{\psi}$. The present method has the slight advantage in the fact that it tests not only for unidirectionality but also for the direction of flow.

ψ_1 and ψ_2 be two known, linearly independent ψ's; we write $\psi_{D\infty}=A_1\psi_1+A_2\psi_2$ and determine, say, A_2 in terms of A_1, so as to satisfy (27); evaluation of $\psi_{S\infty}$ is done in a similar way, using (28). Now, Eq. (28) is satisfied by the complex conjugate of $\psi_{D\infty}$. (The matter of writing $|\alpha|$ for α is trivial in this connection, because the only case of interest to us here is that in which α becomes real as $x\rightarrow\infty$). Therefore $\psi_{D\infty}$ and $\psi_{S\infty}$ are linearly independent, and, furthermore, we can make the matter of multiplicative constants more definite by requiring that

$$\psi_{D\infty}\rightarrow\bar{\psi}_{S\infty},\ \text{as}\ x\rightarrow+\infty. \tag{29}$$

7. A method of determining a $\psi_{D\infty}$ and a $\psi_{S\infty}$ for the region $x\geqq a$ being available, we proceed to find the formula for R. In view of the linear independence of $\psi_{D\infty}$ and $\psi_{S\infty}$ we can write $\psi_r=D\psi_{D\infty}+S\psi_{S\infty}$, where D and S are to be determined so as to satisfy the second pair of Eqs. (5). If, furthermore, $\psi_l=S_l\exp(-i\alpha_l x)$, then $R=|D|^2/|S|^2$, provided (29) is satisfied. Now, the ψ given by (18) is of the required form for $x\leqq 0$, and we proceed to join ψ_b and ψ_r at $x=a$

$$\psi(a)=c_2w(a)\exp\left(-i\alpha_l\int_0^a w^{-2}dx\right)=D\psi_{D\infty}(a)+S\psi_{S\infty}(a) \tag{30}$$

$$\psi'(a)=c_2[w'(a)-i\alpha_l w^{-1}(a)]\exp\left(-i\alpha_l\int_0^a w^{-2}dx\right)=D\psi_{D\infty}'(a)+S\psi_{S\infty}'(a). \tag{31}$$

Solving (30) and (31) for D and S, and substituting into $R=|D|^2/|S|^2$ we get the result:

$$R=\frac{|[w'(a)-i\alpha_l/w(a)]\psi_{S\infty}(a)-w(a)\psi_{S\infty}'(a)|^2}{|[w'(a)-i\alpha_l/w(a)]\psi_{D\infty}(a)-w(a)\psi_{D\infty}'(a)|^2} \tag{32}$$

where $w(a)$ and $w'(a)$ are to be found by numerical integration of (16) without the necessity of specifying any of the ψ's.

8. One of the most interesting physical situations in which the problem of evaluating R arises is the case in which a constant potential for $x\leqq 0$ is followed by a potential barrier in the region $0\leqq x\leqq a$, which, in turn, is followed by a constant field in the region $x\geqq a$, and we shall now consider this case to illustrate the procedure outlined above. We have:

$$V_r(x)=C-Fe(x-a), \tag{33}$$

and the available linearly independent solutions for this region are $\psi_1=y^{1/2}J_{1/3}(Z)$ and $\psi_2=y^{1/2}J_{-1/3}(Z)$, where $y=(\kappa^2Fe)^{1/3}[(E-C)/Fe+x]$, $Z=2/3y^{3/2}$, and where the J's denote Bessel's functions. We set $\psi_{D\infty}=A_1\psi_1+A_2\psi_2$, use the asymptotic expansions of the J's for large values of x, and find that to satisfy (27) it is necessary that $A_2=-A_1\exp(i\pi/3)$, so that $\psi_{D\infty}$ is a constant times $y^{1/2}H_{1/3}^{(1)}(Z)$, $H^{(1)}$ denoting the Hankel's function of the first kind.[11] We find in a similar way that $\psi_{S\infty}$ is a constant times $y^{1/2}H_{1/3}^{(2)}(Z)$ so that (29) is satisfied if we take, for example

[11] The difference in the sign of i between this result and that of Fowler and Nordheim, reference 10, is due to a difference in the definition of the momentum operator.

$$\psi_{D\infty} = y^{1/2}H_{1/3}^{(1)}(z), \quad \psi_{S\infty} = y^{1/2}H_{1/3}^{(2)}(z). \tag{34}$$

We now use these functions and their derivatives, evaluated at $x=a$, to eliminate the ψ's and their derivatives in (32).

A completely worked out numerical example would be out of place here, because it appears that the most laborious part of the calculation in a simple example is the evaluation of the functions (34) and of their derivatives at $x=a$, the evaluation which is intimately connected with the case of a constant field, and which cannot be avoided by the use of other *exact* methods than that outlined here. Suffice it to say that, for example, using the numerical values of w and w' at $x=0.72$A given in Table II, we can calculate R for a potential of the form given in Fig. 2, where the potential for $x \leqq a$ is exactly like that in Fig. 1, but where it is of the form (33) for $x \geqq a$, the dotted lines representing two of the various possibilities. In the case $E<C$ one must be careful to use properly the functions J, I, H, as outlined by Fowler and Nordheim.[10,11] If $a=0$, i.e., if the constant field follows the constant potential with-

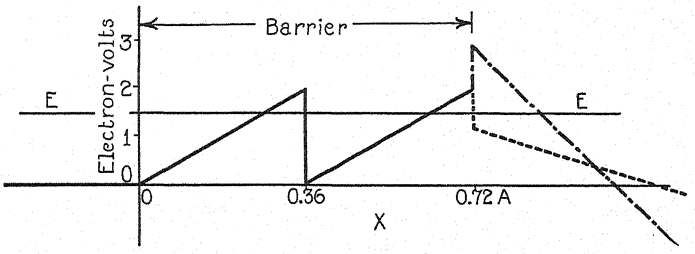


Fig. 2. Graph of $V(x)$ and E referred to in section 8. The heavy line represents $V(x)$ for $x \leqq a$, the dotted lines represent two of the possibilities for $V(x)$ for $x \geqq a$.

out the intervention of a "barrier", we put in (32) $w(0)=1$, and $w'(0)=0$ from (11), and the writers verified that then (32) yields the equation at the top of page 178 of Fowler and Nordheim's paper.

It may be added that the present methods are readily extended to the case in which $V(x)$ is not constant for $x \leqq 0$, but is some function of x for which the general solution of Schroedinger's equation is available. In this case one would start with a ψ representing purely sinistral flow at $-\infty$, and determine c_1 and c_2 in (13) so as to satisfy the requirements of continuity at $x=0$. From then on the procedure would be exactly that of section 7, although the formula for R would be more complicated because now both c_1 and c_2 would appear in the equations corresponding to (30) and (31). The numerical integration of Milne's equation, however, would proceed exactly as in the simpler cases.

The writers wish to acknowledge the benefits they derived from discusssions with Professor E. L. Hill.

Note added to proof. In this paper we adapted the method of fitting the ψ's, at points where $V(x)$ or $V'(x)$ is discontinuous, by means of fitting the w's, because this method appears simpler from the numerical standpoint, as, for example, it permits the calculation of R without a reference to the numerical values of ψ and ψ' anywhere in the region, and, since it preserves the form

(18), it allows expressing R by (19), in which no exponentials occur. However, the ψ's can also be fitted by the more familiar procedure of readjusting the coefficients c_1 and c_2 in (13). In fact, one is at liberty to change w, w', and β, in any way consistent with Milne's theory, at any stage of the calculation even if $V(x)$ and $V'(x)$ are continuous, provided that the c's are readjusted. When this paper was being written it was overlooked that if $v(x)$ is periodic this alternative procedure may in certain cases be simpler than the one described, because the additional labor involved in the calculation of the c's may be outweighed by the fact that the numerical integration is shortened. To illustrate, let us return to the example of section 5, in which $v(x)$ is periodic. We can carry out the calculation in that case as follows: we find ψ and ψ' at 0.36A using (19) and the last line of Table I, write ψ in the form (13) for region II, assume the values $w=1$, $w'=0$ at 0.36A for this region, and determine c_1 and c_2 by fitting the ψ's. We then calculate ψ and ψ' at 0.72A from the last line of Table I, using (13) and c_1 and c_2, and finally find R from (9). In this example the method of fitting the w's turns out to be simpler than this alternative method, even though in the latter one need not calculate Table II at all, but if $v(x)$ has several periods within the barrier, or if the numerical integration over a period is long, the latter method is likely to be advantageous. This alternative method is readily extended to the case in which $v(x)$ consists of periodic and nonperiodic sections, and as was already mentioned can be used equally well when $v(x)$ and $v'(x)$ are continuous.

It will be noticed that if this alternative method be adopted in a given problem, then the quadrature in (13) must be carried out. The question therefore arises as to whether it may not be advisable then to integrate Schroedinger's rather than Milne's equation. The writers tend to the opinion that, in general, the integration of Milne's equation is to be preferred even in this case, because it appears that systematic numerical readjustment of the c's can be carried out more easily when ψ is given in the form (13). (The footnotes marked a were also added in proof.)

THE STRUCTURE OF THE NUCLEUS AND ITS TOTAL MOMENT OF MOMENTUM

By Samuel D. Bryden, Jr.
Massachusetts Institute of Technology

(Received August 17, 1931)

Abstract

The known values of the nuclear moment are classified in four divisions according to even and odd nuclear number and even and odd atomic number. All of the 31 cases are consistent with, and 12 cases in two divisions definitely support the hypotheses that: 1st, The electrons in the nucleus have no spin; 2nd, The protons have a spin of 1/2 in units of $h/2\pi$. These hypotheses are applied to the building up of the nuclei of equivalent protons, and the results indicate that: (1). There is an analogy between the construction of the nucleus of equivalent protons and the construction of the extranuclear portion of the atom of equivalent electrons. (2). Five quantum numbers are associated with the proton, corresponding to the five quantum numbers of the electron. (3). The rules of Pauli and Hund may be applied to the protons. (4). (*ii*) coupling predominates for the protons. (5). The nuclear moment is to be identified with the inner protonic quantum number of the normal nuclear state. (6). The nuclear moment I is in general the smallest I of the lowest I-group. (7). The order of filling of the protonic subgroups is somewhat similar, especially for small nuclear numbers, to the order of filling of the electronic subgroups of an atom.

THE total nuclear moment of momentum is determined from observations on the hyperfine structure of line spectra and the intensity alternation in band spectra. Its value is known for about 21 elements, not including about 8 which are at present doubtful.

The available values of the nuclear moment I are classified in four divisions and listed in Tables I and II according to even and odd atomic number Z, and even and odd nuclear number P. The nuclear number P is a number equal to the total, not net, positive nuclear charge; it is also equal to the number of protons in the nucleus.

Inspection of the values in Table II proves that the integral and fractional values of the nuclear moment in the four Z-P classes are consistent with the hypotheses that: (1). The electrons in the nucleus have no spin.[1] (2). The protons have a spin of $\frac{1}{2}$ in units of $h/2\pi$.

It is the fact that the electrons have a spin of $\frac{1}{2}$ in units of $h/2\pi$ in atoms, ions, and molecules which gives rise to the rules of Pauli and Hund for determining the electronic configuration of a given number of equivalent electrons and the spectroscopic term of the normal state. But it is apparently the protons in the nucleus, not the electrons, which have a spin of $\frac{1}{2}$. Therefore, we may assume that it is to these nuclear building blocks that the rules of Pauli and Hund must be applied. Thus by an adaption of the rules used in atomic spectra, the protonic configuration of the nucleus and its normal spectrosco-

[1] R. de L. Kronig, Naturwiss. **16**, 335 (1928).

TABLE I. *Classification of nuclear moments observed values.*

	Z Odd	P Odd	I Obs.
H	1	1	1/2
Li	3	7	3/2
F	9	19	1/2
Na	11	23	≧1/2
Cl	17	35	5/2
K	19	39	0?
		41	
Mn	25	55	5/2
Br	35	79	3/2?
		81	
Rb	37	85	≧1/2
		87	
Cu	29	63	
		65	0?
Ag	47	107	
		109	0?
In	49	115	1/2
Sb	51	121	
		123	3/2?
I	53	127	large
Cs	55	133	≧1/2
La	57	139	5/2
Pr	59	141	5/2
Tl	81	203	1/2
		205	1/2
Bi	83	209	9/2

	Z Odd	P Even	I Obs.
Li	3	6	0
N	7	14	1

	Z Even	P Even	I Obs.
He	2	4	0
C	6	12	0
S	16	32	0
Ca	20	40	0
		44	0?
Fe	26	54	0?
		56	0
Kr	36	78	0?
		80	0?
		82	0?
		84	0
		86	0
Sr	38	86	0?
		88	0
Cd	48	110	0?
		112	0
		114	0
		116	0?
Ba	56	138	0
Hg	80	196	0?
		198	0
		200	0
		202	0
		204	0?
Pb	82	206	0
		208	0

	Z Even	P Odd	I Obs.
Cd	48	111	1/2
		113	1/2
Hg	80	199	>1/2
		201	>1/2
Pb	82	207	1/2

The nuclear moments of H, He, Li, C, N, O, F, S, Cl, I, are given by R. S. Mulliken, Reviews of Modern Physics **3**, 154 (1931). For Li, Na, Rb, Cs, Cd, Pr, La, Tl, Bi, see Chapter XI of The Structure of Line Spectra by Pauling and Goudsmit; in addition there may be mentioned:

Li—P. Guttinger, W. Pauli, Zeits. f. Physik **67**, 743 (1931).
K, Cu, Ag, Sr, Ba—S. Frisch, R. de L. Kronig, Naturwiss. **21**, 444 (1931).
Mn—H. E. White, N. Ritschl, Phys. Rev. **35**, 1146 (1931).
In—J. C. McLennan, E. J. Allin, Proc. Roy. Soc. ***A*129**, 208 (1930).
Pb—H. Hopfermann, Naturwiss. **19**, 400 (1931).
Kr—C. J. Humphrey, B. S. J. R. **5**, 1041 (1931).
Hg—S. Tolansky, Proc. Roy. Soc. ***A*130**, 558 (1931); H. Schuler, Naturwiss. **43**, 895 (1930).
Tl—H. Schuler, J. E. Keyston, Naturwiss. **15**, 320 (1931).

The isotopes in Tables I and VI are principally from the data of F. W. Aston, Phil. Mag. **49**, 1199 (1925), and

S—Proc. Roy. Soc. ***A*115**, 509 (1927).
Kr, Xe, Hg—*ibid.* ***A*126**, 521 (1930).
Cr, Zn, Mo, Sn—*ibid.* **130**, 307 (1931).
Ru, Os—Nature Feb. 14, 1931.

W—Nature Dec. 13, 1930.
The isotopes determined from band spectra are:
Be—W. W. Watson, A. E. Parker, Phys. Rev. **37**, 167 (1931).
C—A. S. King, R. T. Birge, Phys. Rev. **34**, 379 (1929).
N—S. M. Naude, Phys. Rev. **36**, 333 (1930).
O—H. D. Babcock, Phys. Rev. **37**, 227 (1931).

TABLE II. *Origin of nuclear moment.*

Atomic No. Z	Nuclear No. P	Observed nuclear moment	No. of certain cases	Proton spin	Electron spin	Proton plus electron spin
Odd	Odd	Fractional	11	Frac.	Integ.	Frac.
Odd	Even	Integral	1	Integ.	Frac.	Frac.
Even	Even	Integral	16	Integ.	Integ.	Integ.
Even	Odd	Fractional	3	Frac.	Frac.	Integ.

pic state may be determined. The inner quantum number I of the normal nuclear state is identified with the total moment of momentum of the nucleus in units of $h/2\pi$, just as the inner quantum number J of the normal electronic state of the atom is proportional to the total moment of momentum of the electrons in that configuration.

The first step in the application of these rules is to assume that associated with the proton in the nucleus are five quantum numbers analogous to the five quantum numbers of an electron in an atom, namely:

TABLE III.

Quantum number of	Electron	Proton
Total quantum number	n	t
Azimuthal quantum number	l	k
Inner quantum number	j	i
Magnetic quantum number	m	q
Spin quantum number	s	r

Also it is assumed that these five protonic quantum numbers obey the same rules of composition and selection as the corresponding electronic quantum numbers.

The second step is the building up of the nuclei with successive subgroups and shells of equivalent protons. According to the exclusion principle of Pauli, there are $2(2k+1)$ equivalent protons in a complete subgroup and $2t^2$ equivalent protons in a complete shell.

The construction of the Periodic System of the Isotopes is the third step. For this a knowledge of the order in which the protonic subgroups are filled is indispensable. Precisely as in the case of the Periodic System of the Elements, it appears one must rely, in the final analysis, upon spectroscopic evidence. There are more than 200 isotopes. The necessary spectroscopic evidence (nuclear moments) is known for about 30 isotopes, an insufficient number to determine uniquely the order of the protonic subgroups in the Periodic System of the Isotopes. Therefore we will proceed by analogy and assume for trial an order of filling of the protonic subgroups similar to that of the electronic subgroups. The nuclear number P increases slightly more than twice as

fast as the atomic number Z, so the Periodic System of the Elements can be used as a guide for only the first half of the Periodic System of the Isotopes. The last half is completed by extropolating the dominant regularities of the first half. The resulting tentative order of the protonic subgroups is given in Table IV.

TABLE IV. *Tentative order of filling protonic subgroups.*

Equiv. protons	No. per subgroup	Total No. protons	Equiv. protons	No. per subgroup	Total No. protons
$1s$	2	2	$7s$	2	88
			$5f$	14	102
$2s$	2	4	$6d$	10	112
$2p$	6	10	$7p$	6	118
$3s$	2	12	$8s$	2	120
$3p$	6	18	$5g$	18	138
			$6f$	14	152
$4s$	2	20	$7d$	10	162
$3d$	10	30	$8p$	6	168
$4p$	6	36			
			$9s$	2	170
$5s$	2	38	$6g$	18	188
$4d$	10	48	$7f$	14	202
$5p$	6	54	$8d$	10	212
			$9p$	6	218
$6s$	2	56			
$4f$	14	70	$10s$	2	220
$5d$	10	80	$6h$	22	242
$6p$	6	86	$7g$	18	260

The fourth step is the determination of the predominating interaction or "coupling scheme" for the protons. Consider (kr), (ls) in atomic spectra, and (ii), (jj) in atomic spectra, as two representative extremes. It will be recalled that there is a tendency in atomic spectra, particularly for atoms of large atomic number Z, especially if the atom is ionized, to depart from (ls) coup-

TABLE V. *Theoretically lowest I value or group with (kr) and (ii) coupling.*

Proton config.	I for (kr) coupling	I for (ii) coupling
g 1	7/2	7/2
2	6	0 2 4 6
3	15/2	3/2 5/2 7/2 9/2 11/2 15/2
4	8	0 $(2)^2$ $(4)^2$ 5 6 8
5	15/2	3/2 5/2 7/2 9/2 11/2 15/2
6	6	0 2 4 6
7	7/2	7/2
8	0	0
9	9/2	9/2
10	8	0 2 4 6 8
11	21/2	3/2 5/2 7/2 $(9/2)^2$ 11/2 13/2 15/2 17/2 21/2
12	12	$(0)^2$ $(2)^2$ 3 $(4)^3$ 5 $(6)^3$ 7 $(8)^2$ 9 10 12
13	25/2	1/2 3/2 $(5/2)^2$ $(7/2)^2$ $(9/2)^3$ $(11/2)^2$ $(13/2)^2$ $(15/2)^2$ $(17/2)^2$ 19/2 21/2 25/2
14	12	$(0)^2$ $(2)^2$ 3 $(4)^3$ 5 $(6)^2$ 7 $(8)^2$ 9 10 12
15	21/2	3/2 5/2 7/2 $(9/2)^2$ 11/2 13/2 15/2 17/2 21/2
16	8	0 2 4 6 8
17	9/2	9/2
18	0	0

ling and to approach closely (*jj*) coupling. Thus it would appear reasonable for (*ii*) coupling to predominate in the nucleus, for all nuclei are ionized and the nuclear number P may attain a value twice that of the atomic number Z. Deviations from (*ii*) coupling in the nucleus would be expected to occur primarily for the lighter nuclei which are composed of equivalent s and p protons. In these cases, however, the lowest protonic inner quantum number I is, with one exception, the same for both coupling schemes.

The theoretically lowest I value or group for equivalent g protons[2] with (*kr*) and (*ii*) coupling are listed in Table V.

The observed and theoretical values of the nuclear moment have been compared for all the known isotopes as indicated in Table VI which lists the

TABLE VI. *Comparison of observed and theoretical nuclear moments.*

Atomic No.	Nuclear No.	Isotope percent	Equiv. protons	Theo. nuclear moment I	Obs. nuclear moment I_0
1 H	1	100	$1s$ 1	1/2	1/2
	2		2	0	
	3		$2s$ 1	1/2	
2 He	4	100	2	0	0
	5		$2p$ 1	1/2	
3 Li	6	3	2	0	0
3 Li	7	97	3	3/2	3/2
4 Be	8	0.0	4	0	
4 Be	9	99.9	5	3/2	
5 B	10	46	6	0	
5 B	11	54	$3s$ 1	1/2	
6 C	12	99.9	2	0	0
6 C	13	0.0	$3p$ 1	1/2	
7 N	14	99.9	2	0	1 ($3s^1$, $3p^3$?)
7 N	15	0.1	3	3/2	
8 O	16	99.9	4	0	0
8 O	17	0.0	5	3/2	
8 O	18	0.0	6	0	
9 F	19	100	$4s$ 1	1/2	1/2
10 Ne	20	90	2	0	0

first 20 isotopes. This comparison shows that:

A. Alternation rule: The nuclear moments I have integral values for even nuclear numbers P, and half-integral values for odd nuclear numbers.

The apparent exceptions are K, Cu, and Ag in whose atomic spectra no fine structure has as yet been observed. It is probable that further examination of their spectra will reveal a fine structure. This is a very important rule because if it can be contradicted experimentally the analogy upon which this paper is based fails.

[2] For equivalent s, p, d, f protons with (*kr*) coupling see the paper of Gibbs, Wilber, and White, Phys. Rev. **29**, 790 (1927). For equivalent s, p, d, f, protons with (*ii*) coupling see the paper of S. D. Bryden, Phys. Rev. **38**, 1145 (1931).

B. The observed nuclear moment I is one of the values allowed by Pauli's exclusion principle.

The exceptions are: (a) Mn^{55} indicating $4f$, not $6s$, starts at $P=55$. (b) Cl^{35} $3d^9 \cdot 4p^6$ instead of $3d^{10} \cdot 4p^5$? (c) Cd^{111} indicates following order: $5f$, $6d$, $7s$, $7p$.

C. The observed nuclear moment I is one of the values of the lowest I group with (ii) coupling.

The exceptions are: (a) N^{14} $3s^1 \cdot 3p^3$ instead of $3s^2 \cdot 3p^2$? (b) In^{115} indicates following order $5f$, $6d$, $7s$, $7p$. (c) Pb^{207} smallest I of next to lowest I group.

D. The observed nuclear moment I is the smallest I of the lowest I group.

The exceptions are: (a) Pr^{141} next to smallest I value. (b) Bi^{209} largest I value.

The exceptions to B, C, D, indicate: (1) Departures from the tentative order of filling of the protonic subgroups given in Table IV occur particularly for nuclear numbers greater than 55. Making the suggested changes in the order of the subgroups brings all observed nuclear moments into agreement up to nuclear number 119. (2) There is little definite evidence for deviation from (*ii*) coupling. Absence of data makes deviation from (*ii*) coupling indistinguishable from incorrectly assigned protonic configuration. If, for example, it is assumed that the assigned protonic configurations of Pr and Bi are correct, then their exceptions under D above indicate a tendency toward (*kr*) coupling. This is suggestive. (3) The exceptions may be due to incorrect experimental values of the nuclear moment.

The agreements with A, B, C, D, indicate that: (1) There is an analogy between the construction of the nucleus of equivalent protons and the construction of the extranuclear portion of the atom of equivalent electrons. (2) The rules of Pauli and Hund may be applied to the nuclear protons. (3) (*ii*) coupling predominates for the protons. (4) The nuclear moment is to be identified with the inner protonic quantum number of the normal nuclear state. (5) The nuclear moment I is in general the smallest I value of the lowest I-group. (6) The order of filling of the protonic subgroups is somewhat similar, especially for small nuclear numbers, to the order of filling of the electronic subgroups of an atom.

It is suggested that the nuclear moment be determined for those elements which have an appreciable fraction of their isotopes with an odd nuclear number, for example, P, Cs, Na, Be, Al, K, Sc, V, Co, As, Y, I, Xe, W, Os, Hg, etc. This will give the information necessary for verifying and correcting the assumed order of filling of the protonic subgroups.

This method of building up the nuclei from equivalent protons with the aid of the rules of Pauli and Hund will, if correct, correlate and predict other nuclear phenomena.

A NOTE ON THE EXCITATION OF THE ARC SPECTRUM OF NITROGEN

By K. R. More and O. E. Anderson
Department of Physics, the University of British Columbia

(Received August 28, 1931)

ABSTRACT

The arc spectrum of nitrogen has been excited with low voltage arcs in mixtures of argon and nitrogen. A comparison of the intensities of the lines showed that the strong N I lines were as intense as the moderately strong argon lines. The excitation takes place probably in two steps, the first being the dissociation of the nitrogen molecules into normal and metastable nitrogen atoms by collisions with metastable argon atoms, and the second being the excitation of the metastable nitrogen atoms by collisions with metastable argon atoms.

Introduction

IT IS known from the work of Johnson,[1] Cameron,[2] McLennan and Shrum[3] and others that the presence of a rare gas often modifies the character of the spectra emitted by diatomic gases. By this means Merton and Pilley[4] excited the arc spectrum of nitrogen by passing a discharge through a Geissler tube containing helium and a trace of nitrogen. They also tried mixtures of argon and nitrogen but with moderate currents obtained no evidence of the N I lines. They accounted for the emission by assuming that the helium atoms acted as safety valves limiting the electron velocities to 20.5 volts, which is greater than that required to excite the arc lines but less than the excitation potential of the spark lines. At about the same time Compton[5] suggested that metastable helium atoms were the effective agents. He showed that in mixtures of helium and nitrogen a high current density should be favorable to the dissociation of the nitrogen molecules into neutral atoms by collisions with metastable helium atoms.

Many new N I lines were found by Duffendack and Wolfe[6] who used a high current density in mixtures of helium and nitrogen. They found that the lines were more intense in low voltage arcs than in Geissler discharges. This is in agreement with Compton, since the higher current density of the low voltage arc tends to produce a higher concentration of metastable helium atoms. Compton predicted that the N I spectrum would not be excited in mixtures of argon and nitrogen, since at the time the heat of dissociation of the nitrogen molecule was believed to be about 19 volts, which was much

[1] Johnson, Roy. Soc. Proc. **A108,** 343 (1924); Phil. Mag. **48,** 1069 (1924); Roy. Soc. Proc. **A106,** 195 (1924).
[2] Cameron, Phil. Mag. **1,** 405 (1926).
[3] McLennan and Shrum, Roy. Soc. Proc. **A108,** 501 (1925).
[4] Merton and Pilley, Roy. Soc. Proc. **A107,** 411, (1925).
[5] Compton, Phil. Mag. **50,** 512, (1925).
[6] Duffendack and Wolfe, Phys. Rev. **34,** 409 (1929).

higher than any of the resonance potentials of argon. According to the work of Kaplan,[7] however, the heat of dissociation of molecular nitrogen must be taken as 9.1 volts rather than 19 volts and since there are strong metastable levels of argon at 11.5 and 11.67 volts, which are sufficient to dissociate the nitrogen, it seemed reasonable to expect that under favorable conditions the N I spectrum could be excited in mixtures of argon and nitrogen.

Experimental

In accordance with the above considerations a low voltage arc discharge tube was used in this investigation. It was made of Pyrex glass 25 mm in diameter and 50 cm in length, with the electrodes in bulbs sealed to the side of the tube. This design made it possible to use the tube "end-on" so as to increase the intensity. The hot cathode consisted of an internally heated nickel cylinder coated with a thin layer of barium and calcium oxides. Liquid air traps were used wherever necessary to keep the tube free of mercury vapor.

Before each set of experiments the discharge tube was thoroughly exhausted and baked at a temperature of 350°C. For purposes of degassing the electrodes were brought to a red heat by passing a high current discharge through the tube.

It was found convenient to use commercial argon purified by means of a magnesium arc, while the nitrogen was generated by heating a mixture of sodium azide and alumina.

The argon pressure most suitable to the passage of high currents was found to be 1 to 3 mm while a nitrogen partial pressure of 0.01 to 0.3 mm was found satisfactory for the excitation of the N I lines. The best results were obtained with discharge currents of the order of 2 amperes at 70 volts.

A Hilger E-I quartz spectrograph for the region 3200 to 6000A and a Hilger constant deviation spectrograph with a flint glass prism for the region 6000 to 9000A were used. With the quartz spectrograph one hour exposures were sufficient to record all the N I lines observed. The strong lines could easily be photographed in ten minutes. With the flint glass spectrograph one hour exposures were taken.

The wave-lengths of the lines were measured by using international iron lines for comparison, and the relative intensities determined with a Moll selfregistering microphotometer.

Results

In the region from 3400 to 5000A the plates showed most of the intense lines and many of the weak lines of the N I spectrum found by Merton and Pilley and by Duffendack and Wolfe. Many of the weaker lines were obscured by the positive bands of nitrogen which were usually present when the arc lines were strong. The negative bands of nitrogen were not present on any of the plates. It was found that higher nitrogen pressures were required to bring out the arc lines in the longer wave-length regions than in the violet and ultraviolet. The higher pressures also brought out the first positive

[7] Kaplan, Phys. Rev. **33**, 638, (1929).

bands prominently and this together with the small dispersion prevented the identification of any lines in the region 5000 to 8000A. Some of the more intense lines above 8000A were photographed by using the flint glass spectrograph and infrared sensitive plates.

A comparison of photographic densities made from the microphotometer curves showed that the relative intensities of the lines were, in most cases, the same as those found by Duffendack and Wolfe in mixtures of helium and nitrogen. It was found that the stronger arc lines were as intense as the moderately strong argon lines. The lines observed are given in Table I.

TABLE I. *Observed lines of N I. The first two columns contain the wave-lengths and the intensities of the lines in helium mixtures as given by Duffendack and Wolfe. In the third column are listed the estimated intensities in argon-nitrogen mixtures.*

Wave-lengths (I.A.)	Intensity in He mixture	Intensity in A mixture	Wave-lengths (I.A.)	Intensity in He mixture	Intensity in A mixture
8711.9	2	2	4554.21	1	1
8703.4	2	unresolved	4553.38	1	1
			4503.53	1	0
8686.4	3	5	4502.27	2	2
8683.6	4	unresolved			
8680.3	5	unresolved	4499.08	0	1
			4492.40	7	4
8629.5	4	2			
			4358.27	10	8
8594.3	3	1	4313.11	4	2
			4305.46	6	4
8242.5	4	3			
			4230.35	4	2
8223.3	5	10	4224.74	4	2
8216.45	7	unresolved	4223.04	5	3
8210.9	3	unresolved	4215.92	2	1
			4214.73	5	3
8188.2	5	7			
8185.0	5	unresolved	4187.06	1*d*	1*d*
			4151.46	12	9
4935.03	10	10	4143.42	obscured by He	1
4914.90	5	4	4137.63	7	2
			4114.00	6	4
4881.79	1	1	4109.98	12	12
4753.13	2	2	4099.94	9	10
4669.77	3	6	3834.84	2	1
4660.05	2	3	3834.24	4	3
4657.72	1	0	3830.39	9	4
4656.65	1	0	3822.07	6	2
4651.08	1	3			
			3650.19	5	1
			3532.65	4	0

DISCUSSION

The two important agencies for the dissociation of the nitrogen molecules and for the excitation of the atomic spectrum are collisions with electrons and with metastable argon atoms. Many experimenters have shown that electron impacts seldom produce simple dissociation of nitrogen molecules. In fact,

Duncan[8] has shown that the only atomic spectrum excited by electron bombardment is the spark spectrum, and this results only when the electrons have energy of 70 volts or more. He found that electrons with energy of the same order as the heat of dissociation of the nitrogen molecule or as the resonance potentials of argon did not excite any line spectrum of nitrogen, but were evidently totally consumed in exciting the molecular spectra. It seems reasonable to assume that since the nitrogen molecules are not dissociated by electron impacts, they must be dissociated by collisions with metastable argon atoms. Moreover a metastable argon atom has sufficient energy (11.5 or 11.67 volts) to dissociate a nitrogen molecule into a normal atom and a metastable atom, since this requires the sum of the energy required to dissociate the molecule into two normal atoms (about 9 volts[7,9]), and the energy necessary to raise one of the atoms from the normal state $^4S_{1\frac{1}{2}}(2p^3)$ to the metastable $^2D_{2\frac{1}{2},1\frac{1}{2}}(2p^3)$ states (2.37 volts), a total of about 14 volts. As this is in close resonance with the energy of the metastable argon atoms it is probable that a nitrogen molecule would be dissociated into a normal atom and a metastable atom by a collision with a metastable argon atom.

It is also probable that the metastable argon atoms are the active agents for the excitation of the nitrogen atoms. According to the classification of Ingram[10] and of Compton and Boyce[11] the nitrogen atom has energy levels varying from 10.3 to 14.2 volts, as well as metastable levels at 2.37 and 3.56 volts. Thus a metastable argon atom could excite a normal nitrogen atom to levels as high as 11.67 volts energy, or a metastable nitrogen atom (2.37 volts) to levels as high as 14 volts energy. Also it is known that there is a high concentration of metastable argon atoms in high current low voltage arcs. Thus the nitrogen arc spectrum could be excited with considerable intensity by metastable argon atoms. Electrons with energy of the same order are present in the discharge and could also excite the nitrogen atoms. However the number of collisions between electrons and nitrogen atoms is small compared with the number of collisions between electrons and argon atoms because the nitrogen pressure is much lower than the argon pressure. Thus, since the stronger N I lines are of the same order of intensity as the argon lines, it is probable that metastable argon atoms are the most important agents in the excitation of the nitrogen atoms.

According to the classification of the N I lines, the initial levels of the lines reported arise from the configurations $3p^23p$ and $3p^24p$. The excitation potentials of all these levels lie between 11.7 volts for the $^4D_{\frac{1}{2}}$ state (built upon ^3P, $2p^2$ of the ion) and 13.85 volts for the $2P_{1\frac{1}{2}}$ state (built upon $^1D_2$, $2p^2$ of the ion). Thus a metastable argon atom has sufficient energy to raise a metastable nitrogen atom to any of these levels, but has not sufficient energy to raise a normal nitrogen atom to them. Hence the N I lines observed are probably excited by collisions of metastable argon atoms with metastable

[8] Duncan, Astrophys. J. **62**, 145 (1925).
[9] Birge, Phys. Rev. **34**, 1062 (1929).
[10] Ingram, Phys. Rev. **34**, 421 (1929).
[11] Compton and Boyce, Phys. Rev. **33**, 145 (1929).

nitrogen atoms. Nevertheless the metastable argon atoms have sufficient energy to excite the normal nitrogen atoms to the levels $3p^2 3s^2 P_{1\frac{1}{2},\frac{1}{2}}$ and $3p^2 3s\ ^4P_{2\frac{1}{2},1\frac{1}{2},\frac{1}{2}}$ (energies 10.6 and 10.3 volts respectively). Also it has been found by Compton and Boyce[11] and by Ekefors[12] that these are initial levels for transitions giving rise to ultraviolet lines. Moreover the transitions from the $3p^2 3s\ ^2P_{1\frac{1}{2},\frac{1}{2}}$ states are to the metastable states of 2.37 and 3.56 volts energy and not to the normal state of zero energy. In addition the $3p^2 3s\ ^2P_{1\frac{1}{2},\frac{1}{2}}$ states are the final levels of many of the transitions giving rise to the more intense lines reported. Hence many of the metastable atoms that are further excited return to the metastable state in two steps, radiating visible and ultraviolet light. Thus since metastable atoms result from the dissociation of the nitrogen molecules and from the radiation of light by excited atoms, it is probable that there is a high concentration of metastable nitrogen atoms in the discharge. These are probably excited to the initial levels of the lines reported by collisions with metastable argon atoms.

The experiments with argon indicate therefore that the excitation of the N I lines takes place probably in two steps, the first being the dissociation of the nitrogen molecules into neutral and metastable nitrogen atoms by collisions with metastable argon atoms, and the second being the excitation of the metastable nitrogen atoms by collisions with metastable argon atoms.

The authors wish to express their appreciation to Dr. G. M. Shrum for suggesting the problem and for his assistance in the work.

[12] Ekefors, Zeits. f. Physik **63**, 437 (1930).

THE EMISSION SPECTRUM OF CARBON DIOXIDE

By H. D. Smyth
Palmer Physical Laboratory, Princeton University

(Received August 25, 1931)

Abstract

The emission spectrum of carbon dioxide has been studied by the electron beam excitation method used by Smyth and Arnott. The whole range of the spectrum from 6500 to 1400 has been examined and only the bands reported by Fox, Duffendack and Barker in the region from 2700 to 5000 have been observed. A particular effort was made to get in emission the extreme ultraviolet bands reported by Leifson in absorption but it was unsuccessful. The "second negative bands of carbon" are shown to be probably identical with parts of the Fox, Duffendack and Barker system. This system of some two hundred bands is partially analyzed into fifteen progressions of band heads given by the formula $\nu = 26{,}271 - \nu_x + 1136.85v - 1.85v^2$ where ν_x takes on a particular value for each progression and $v = 0, 1 \cdots 10$. About one hundred bands fit into this arrangement. This empirical analysis is shown to be consistent with a scheme of energy levels involving two normal modes of vibration (ν_1' and ν_2') in the upper electronic state and two (ν_1'' and ν_3'') in the lower electronic state. The $2\nu_2'$ state is split into two separated by 166 cm^{-1}; this and the values of the frequencies are consistent with Dennison's and Barker and Martin's analysis of the infrared spectrum but since the spectrum here analyzed presumably does not involve the normal state the frequencies are numerically different.

DURING the past fifteen years the study of band spectra has made enormous contributions to our knowledge of molecular structure and of radiation processes. Most of this work has been concerned with diatomic molecules and naturally so, since even diatomic band spectra offer complications requiring the greatest ingenuity and care for their interpretation. There remain many details of diatomic spectra still to be examined, but there seems little doubt that the main principles of interpretation have been laid down. Perhaps it is time, therefore, to consider the possibility of applying these principles to the study of molecules containing more than two atoms.

Of course a start has already been made by the study of infrared spectra, Raman effect and absorption spectra. But little or no progress has been made in the study of emission spectra. The difficulties are two. In the first place, the excitation of a gas is very likely to disrupt its molecules and, therefore, the spectrum obtained may well come, not from the molecule it is desired to study, but from one of its component parts. In the second place, once a spectrum is obtained it is likely to be so complicated as to defy analysis. Both these difficulties have been overcome in some measure in older work but it seems worth while to attempt a systematic attack on the general problem aided by recent developments in technique and theory.

The present writer was inspired to undertake such an attack by some experiments which Arnott and he[1] had made on the excitation of the band spec-

[1] Smyth and Arnott, Phys. Rev. **36**, 1023–33 (1930).

tra of nitrogen by electron impact. In these experiments the spectrum was excited by a beam of electrons passing into a water-cooled chamber into which fresh gas flowed continually. Such conditions should be very unfavorable to the excitation of dissociation products. Furthermore, in the nitrogen spectra excited by this method nearly the entire intensity was concentrated in a few bands. It was thought that similar effects might occur in triatomic gases and simplify the spectrum. Such a method of excitation, therefore, might hope to overcome the two main difficulties cited above.

Carbon dioxide was chosen as the first gas to be studied because much is already known about its structure, its ionization potentials and, most important of all, the spectra of its components, carbon monoxide, oxygen and carbon.

Previous Work

According to Kayser[2] the first discontinuous spectrum ever observed was that from a candle flame studied by Wollaston in 1802. It is not surprising therefore that there is a vast body of literature on the spectra of carbon and its compounds. The results of the work up until 1910 have been digested and presented by Kayser. Of the groups of bands that he gives only one seems possibly attributable to CO_2. It is the so-called "second negative group of carbon," a group of some twenty bands as reported by Kayser and later by Hof[3] and Bair.[4] Most of the bands in this group can be identified in the much more extensive system studied by Fox, Duffendack and Barker[5] and discussed in detail later in the present paper. They are observed in the negative glow of discharge tubes through which CO_2 is flowing but give way to CO bands as soon as the flow is stopped. This suggests that they should be assigned to carbon dioxide, probably to CO_2^+.

In their study of the carbon dioxide system Fox, Duffendack and Barker[5,6] excited it by impact of low voltage electrons. Duffendack and Smith[7] also excited it by collisions of the second kind in mixtures of CO_2 with the rare gases and finally Duncan[8] studied the fine structure of the two strongest bands by using a low voltage arc and a 21-foot grating. The conclusion of these authors was that the excitation potential of this spectrum was about nineteen volts and that it probably came from CO_2^+ ions.

Further evidence on the probable origin of the two strongest bands of the system (λ2883 and λ2896) is to be found in their frequent appearance in lists of the first negative bands of CO though authors[9] usually have some difficulty in fitting them in this system. Also, Maxwell[10] studied the effect of electric fields on the emission of these two bands and the comet tail bands of CO. He

[2] Kayser, Handbuch der Spectroskopie **V**, 198, 190–234 (1910).
[3] Hof, Zeits. f. wiss. Photo. **14**, 83 (1914).
[4] Blair, Astrophys. J. **52**, 301 (1920).
[5] Fox, Duffendack and Barker, Proc. Nat. Acad. **13**, 302 (1927).
[6] Duffendack and Fox, Astrophys. J. **65**, 234 (1927).
[7] Duffendack and Smith, Phys. Rev. **34**, 68 (1929).
[8] Duncan, Phys. Rev. **34**, 1148 (1929).
[9] For example see Jevons, Phil. Mag. **47**, 586 (1924).
[10] Maxwell, Jour. Frank. Inst. **210**, 427 (1930).

found the former unaffected by the field and concluded that they came from an excited ion of very short lifetime or from a neutral molecule. The balance of the evidence seems to be in favor of CO_2^+ as the originator of this whole band system.

A second emission spectrum has been found by Kondratjew[11] who studied the spectrum of CO burning in O_2. He photographed a group of diffuse bands in the same general region as the emission bands discussed above and believes them due to CO_2. They are arranged in series with wave number differences of approximately 600 cm^{-1}. These bands probably form an entirely separate system from those considered here. Besides these emission spectra an absorption spectrum in the Schumann region was reported by Leifson;[12] it consisted of a number of bands, only four of which he was able to measure. These have never been observed in emission.

The object of the present work has been three-fold. First, to study the emission spectrum by high speed electron impact in flowing gas in order to confirm its origin and possibly to get a simplified intensity distribution. Second, to obtain the absorption spectrum in emission, and finally to extend some regularities already observed in the wave numbers of the known spectrum. Of these aims only the last has met with much success but the entire work will be reported in full.

Part I. Experimental

Apparatus and procedure

The excitation chamber in which the spectrum was observed was the same as that used by Smyth and Arnott[1] and the arrangement of filament, transverse magnetic field, and so on were very similar. Figure 1 is repeated from their previous paper but will not be discussed here.

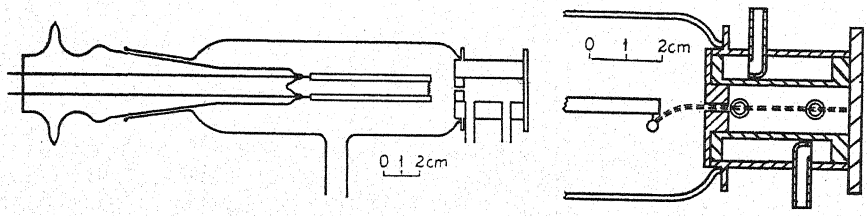


Fig. 1. (a) Schematic diagram of electron beam apparatus. (b) Details of filament, electron beam and water-cooled anode.

Commerical carbon dioxide was resublimed twice in vacuum with liquid air and then stored over phosphorous pentoxide. It was admitted through an artificial leak and during an exposure flowed steadily through the apparatus. Besides CO_2 a small amount of stop-cock grease vapor and a varying amount of mercury vapor were present. Traces of the CH bands were observed in some of the spectrograms. The mercury lines could be varied at will from moderate intensity almost to the vanishing point without any effect on the CO_2 spectrum.

[11] Kondratjew, Zeits. f. Physik **63**, 322 (1930).
[12] Leifson, Astrophys. J. **63**, 73 (1926).

Of three different spectroscopes used, a constant deviation glass Hilger covered the range from 7000A down to 4000, with Ilford panchromatic, Wratten and Wainwright hypersensitive panchromatic, and Ilford Golden Iso-zenith plates; for the region down to 2000A a medium size quartz Hilger, (E 315), with Iso-zenith plates proved very satisfactory; and finally for the Schumann region, a fluorite window was sealed on the excitation chamber and a small fluorite vacuum spectrograph of the type described by Cario and Schmidt-Ott[13] was attached to the apparatus; Schumann plates obtained from the Hilger were used in this instrument. With these spectroscopic arrangements the entire spectrum from about 6500 to about 1400AU was studied though none of it at very high dispersion.

The nature of the luminosity in excitation chamber was of two distinct types. At low pressures, (0.04 mm as measured by a McLeod connected to the excitation chamber) and small currents (5 to 30 m.a. in the main discharge) a sharply defined beam of a deep purple color extended from the orifice of the main discharge tube across the excitation chamber toward the window. The magnetic field was usually adjusted so that this beam was bent downwards striking the wall of the chamber just short of the window. Under these conditions the rest of the excitation chamber was dark. We will refer to this condition as the beam discharge. If the pressure was raised or the current increased the sharp beam became fuzzy and eventually the entire excitation chamber was filled with luminosity as if from a secondary discharge. We will refer to this condition as the high pressure discharge.

Observed spectra

As we had hoped the "beam discharge" showed no trace of the CO spectrum in the visible and near ultraviolet. Long exposures brought out the "first negative" CO^+ bands and traces of the OH band at 3300 and the CH bands at around 4200; a few bands of the 4th positive group appeared faintly on some of the plates taken with the fluorite spectrograph. By far the most prominent feature of the spectrum was the CO_2 band spectrum already mentioned as observed by Fox, Duffendack and Barker.[5] This was so intense that a plate could be obtained with the quartz spectrograph in an hour's exposure even when the current in the discharge tube was only 20 or 30 milliamperes. Apart from this spectrum no bands not definitely attributable to CO were observed between 6500 and 1400 except the CH and OH bands already mentioned.

A particular effort was made to get in emission the bands reported by Leifson in absorption. In spite of variations of the field accelerating the electrons from 700 volts down to 60 and of increases of pressure and current up to the high pressure condition where the 4th positive bands of CO came out prominently no trace of CO_2 emission bands was observed in this region. On some of the first spectrograms there did appear to be bands, though of different wave-length from those given by Leifson, but more careful adjustment of the spectrograph and measurement of the plates showed them to be groups of

[13] Cario and Schmidt-Ott, Zeits. f. Physik **69**, 719 (1931).

TABLE I.

NOTE: The meaning of the designations given in the fourth column and of the values of $\nu_c-\nu_0$ in the fifth column are explained in the text of part II. When they are enclosed in parentheses they refer to the wave numbers in column six.

Wave-lengths and wave numbers in columns one and two marked with asterisks are accurate only to 1.0A or 10 cm^{-1} respectively. All wave numbers in column six are accurate only to 10 cm^{-1}.

Fox, Duffendack and Barker λ	ν_0	Int.	Desig.	$\nu_c-\nu_0$	This Paper ν_0	Int.	
					37,662	1	
					623	1	
					35,433	0	
					410	1	
			a_8?		284	1	
					115	0	
2849.5*	35,084*	4	b_5*	−4*	090		
56.4*	34,999*	5	d_{10}*	0*	008	1	
62.5*	924*	6	n_9*	+29*	34,930	2	
—	—	—			916	00	
—	—	—	j_{10}	+27	831	00	
			e_{10}	+9			
74.3	781	7	r_9	−6	783	5	
77.2	746	5			758	3	
78.2	734	5	k_{10}	−6	—	—	
80.7	704	6			705	10	
82.1	687	10			—	—	
82.6	681	9			—	—	
83.1	675	10			675	11	
					600	4	
90.4	587	7			—	—	
—	—	—			561	4	
—	—	—	(l_{10})?	(+19)?	545	11	
95.4	527	10			—	—	
95.9	522	9			—	—	
96.4	516	10			515	10	
2907.5*	34,384*	0			—	—	
10.2*	352*	0			—	—	
16.3*	280*	0			—	—	
19.1*	247*	0	m_{11}*	+10*	—	—	
24.8*	180*	1			—	—	
25.2*	175*	1			—	—	
2928.3*	34,139*	1	a_7*	−1*	—	—	
29.4*	127*	1			—	—	
33.1*	085*	3			34,082	2	
35.7*	054*	3	c_8*	+4*	063	2	
45.2*	33,944*	2	b_7*	+27*	33,951	1	
49.4*	895*	4	d_9*	+3*	900	2	
56.8*	810*	0			—	—	
58.7*	789*	2	g_{10}*	+6*	785	1	
61.8*	753*	2	j_9*	0*	750	0	
63.8*	731*	5	e_9*	+4*	732	2	
			(r_8)	(+20)	649	0	
			(k_8)	(−23)	490	00	
88.6*	451*	2	l_9*	+6*	—	—	
90.3*	432*	2			420	0	
—	—	—			404	00	
3005.3*	265*	3			263	1	
07.3*	243*	3	f_{11}*	−23*	236		
17.8*	127*	2	m_{10}?	+32*	122	00	
19.6*	107*	0			—	—	
22.6*	075*	1			080	2	
—	—	—			060	1	
—	—	—			039	0	
27.0	026	3	a_6	−1	026	2	2nd Neg. C
—	—	—			32,990	0	λ3030?
34.2	32,948	6	c_7	+1	949	4	
—	—	—			858	1	
43.9	843	5	b_6	+15	837	3	
48.6	792	6	d_8	0	791	5	
58.3*	688*	5	g_8*	+5*	689	4	
63.5*	633*	5	e_8	−4*	640	4	
			j_8	+2*			
67.7*	588*	5	r_7*	−27*	587	2	
72.1	542*	4	k_8*	−21*	537	2	
—	—	—	(k_8)	(+10)	510	1	
—	—	—			498	00	
—	—	—			475	00	
—	—	—			461	00	
—	—	—	(p_9)	(−7)	442	0	OH?
—	—	—			422	0	
—	—	—			403	0	
—	—	—			380	0	
3090.0*	3235*	5	l_8*	+2*	32,355	2	
					323	1	

Fox, Duffendack and Barker λ	ν_0	Int.	Desig.	$\nu_c-\nu_0$	This Paper ν_0	Int.	
—	—	—			301	1	
—	—	—			283		
					257	2	
—	—	—	(h_9?)	(+5)	221	2	
—	—	—			185	2	
—	—	—			148	1	
—	—	—	(f_{10}??)	(−3)	125	0	OH band?
—	—	—			095	0	
—	—	—	(m_9)	(−6)	064	1	
—	—	—			043	00	
—	—	—			014	2	
—	—	—			31,985	3	
—	—	—			921	2	
3132.9	31,910	8	a_5	−2	909	4	
34.6	893	8					
35.7	882	6			886	4	
36.7	871	9					
					869	5	
39.2	846	9	c_6	−6	? 856	4	
					835	5	
42.4	814	5			—	—	
49.5	742	6	b_5	0	743	4	
50.7	730	6			—	—	2nd Neg C
55.2	685	9	d_7	−2	690	5	λ3153
64.9	588	5	g_6	0	588	3	55
70.1	536	5	e_7?		530	3	59
			j_7	+6			
74.3	494	5			488	3	
—	—	—	(r_6)	(+4)	443	1	
—	—	—	(k_7)	(+9?)	402	2	
					382		
—	—	—	(p_8)	+4	325	0	
					291		
—	—	—	(l_7)	(−7)	255	0	
—	—	—	(h_8?)	(?)	150	00	
					100		
—	—	—	(f_9?)	(−15)	035	00	
—	—	—	(f_9?)	(+26)	30,994	1	
—	—	—	(m_8)	(−21)	972	2	
—	—	—			901	0	
—	—	—			854?	00	
—	—	—			831	00	2nd Neg C
3246.9	30,790	10	a_4	−1	790	6	λ3249.4
53.9	723	10	c_5	−3	716	6	51.0
64.6	623	9	b_4	−1	621	5	54.6
69.9	573	10	d_6	−2	568	5	70.5
—	—	—	(n_6)	(+19)	490	0	
80.5	474	3	g_7	+4	468	3	
83.3	448	4			—	—	
84.3	439	8	j_8	−10	439	5	
85.8	425	3		+4	—	—	
87.7	408	3	e_8	−1	—	—	
92.6	363	4	r_5?		371	1	
3301.1	284	4	k_6?	+14	279	1	
—	—	—	(p_9)	0	220	0	
—	—	—	(l_8)	(+22)	111	00	
—	—	—	(h_7)	(−1)	013	00	
—	—	—	(f_8)	(+3)	29,911	1	
—	—	—	(m_7)	(−1)	844	1	
—	—	—			692	0	
3370.0	29,665	10	a_3	0	665	8	2nd Neg C
72.5	643	5			—	—	λ3372.8
75.2	619	3			—	—	75.4
77.5	599	10	c_4	+1	594	8	77.9
82.2	558	5			—	—	
86.2	523	3			—	—	
88.9	500	7	b_3	−2	492	4	
94.5	451	7	d_5	+3	450	4	
96.9	439	3			—	—	
99.4	409	4			—	—	
99.9	404	3			—	—	
3400.9	396	3	n_4	−7	398	5	
02.2	384	1			—	—	
04.3	366	1	g_5	0	—	—	
3413.3	29,289	3	e_5	+2	29,280	1	
—	—		(r_4)	(0)	211	0	
26.6	175	3	k_5	+7	176	2	
43.5	032	2	l_5?	−13	025	2	
—	—	—			28,988	1	
—	—	—	(h_6)	(−4)	902	00	

TABLE I. (*Continued*).

Fox, Duffendack and Barker λ	ν_0	Int.	Desig.	$\nu_c-\nu_0$	This Paper ν_0	Int.	
64.5*	28,856*	0					
71.0*	802*	0	f_7*	+3*	?820	0	
—	—	—	(m_6)	(+9)	721	1	2nd Neg C
3503.2	537	7	a_2	0	537	3	λ3503.6
10.8	475	9	c_3	+1	470	3	06.8
17.1	424	7			—	—	11.5
—	—	—			408	1	
—	—	—	(b_2)	+5	365	0	
28.3	334	4	d_4	0	324	2	
33.8	290	9	n_3?	−25	287	4	
45.9	194	10	j_4	−3	201	7	
51.4	150	7	e_4?	+21 (+12)	163	6	
62.2	065	9	r_3? k_4	−2	061	6	
65.5	039	6			032	5	
81.1	27,916	4			27,915	3	
83.3	899	2	l_4	0	—	—	
86.0	878	2			871	2	
99.1*	777*	6	h_5*	+5*	756?	3	
3615.8	649	3	f_6??		—	—	
16.9	640	3			642		
18.6	635	3			—	7	
21.0	609	7	m_6	+5	600		
34.3	508	2			—	—	
37.7	482	6			—	—	
38.5	476	6			468	4	
47.8	406	3	a_1	0	390	3	2nd Neg C.
61.6	303	7	c_2??		302	5	3663.0
68.1	254	6			—	—	
70.1	240	6	b_1	0	242	2	3671
74.1	210	9	d_3	0	200	5	3674.9
79.6	169	7			—	—	
83.1	143	2	n_2	−6	151	2	
87.9	108	2	g_4?	+19	—	—	
90.9	086	4			—	—	
91.8	072	8	j_3 e_3?		074	6	
3708.0	26,961	3	r_2	−2	26,960	3	
13.9	918	3	k_3?	+17	910	2	
—	—	—	(p_4)	+1	870		
—	—	—	(l_3)	−5	780	1	
40.3	729	5			718	2	
49.1	666	4			—	—	
49.7	661	4	h_4	+1	661	3	
56.4	614	2			—	—	
61.4	578	6	f_5	−2	576	4	
74.6	485	6	m_4	+9	483	4	
89.3	383	5			373	2	
3805.4	271	5	a_0	0	266	3	
09.8	241	5	c_1?	−22	—	—	
—	—	—	b_0??		152	0	
—	—	—	(d_2)	(−3)	085	2	

Fox, Duffendack and Barker λ	ν_0	Int.	Desig.	$\nu_c-\nu_0$	This Paper ν_0	Int.	
38.8	042	6	n_1?		039	4	2nd Neg C.
53.2	25,945	4	j_2	−4	25,950	6	λ3849.5
53.8	941	4		0	—	—	52.9
55.7	928	9	e_2	−9	—	—	
66.8	854	3			—	—	
70.5	829	5	r_1	−1	824	7	
72.7	815	7	k_2	−4	—	—	
74.5	803	6			—	—	
90.4	697	5			690	4	
99.3	638	5	l_2	+9	—	—	
3904.5	604	3	p_3?	+15	593	2	
14.1	541	7	h_3	−3	—	—	
—	—	—			523	3	
20.2	502	4			—	—	
22.2	489	4			—	—	
27.3	456	4	f_4	0	—	—	
—	—	—			434		
—	—	—	(m_3)	(+19)	351	2	
59.4	249	3			—	—	
60.9	240	7			241	7	
64.1	219	5			—	—	
4002.3*	24,979*	2	d_1*	−28*	24,970	3	
25.0*	838*	1	j_1*	−28*	830	2	
—	—	—	(e_1)	(+10)	778	2	
48.9	691	3	r_0	+2	691	5	
50.5	681	5	k_1	−2	—	—	
58.6	632	4			—	—	
68.1	575	5			—	—	
70.7	559	5			568	5	
71.7	553	4			—	—	
—	—	—			452	2	
95.7	409	3	h_2	+1	401	1	
4103.4	363	3			—	—	
07.9	337	7			335	5	
09.2	329	5	f_3	+3	—	—	
20.8	260	6			260	6	2nd Neg C.
22.6	250	8	m_2	−8	—	—	λ4125?
37.6	162	7			158	6	
40.1	147	3			—	—	
44.7	120	2			—	—	
59.5	035	4			045	5	
70.5	23,971	2			—	—	
85.3*	886*	2			23,901	1	
96.6*	822*	0	d_0*	−6*	—	—	
4208.6*	23,754*	1	g_1*	−8*	23,752	0	
64.*	496*	3					
81.6*	349*	4	l_0*	+32*			
4308.4	204	3	f_2	0			
23.8	121	4	m_1	−10			
39.7	038	6					2nd Neg C. λ4340?
41.0	030	5					
59.6	22,932	5					
64.7	905	3					
67.4	891	3					

carbon lines. A further study of this part of the spectrum with different types of excitation is desirable.

The appearance of the 4th positive bands of CO when the discharge was in the "high pressure" condition has been mentioned. A similar condition photographed with the glass spectrograph and panchromatic plates showed the Angstrom bands of CO very strong but the CO_2 bands remained as strong as ever.

In the experimental work up to this point only the electron beam method of excitation had been tried but the anticipated simplification of the spectrum had not been obtained. Furthermore, in spite of the implication of Duffendack and his collaborators that the spectrum which they observed was new, the author came to a different conclusion. After a careful review of the literature, he became convinced that the spectrum under consideration was identical with the second negative bands of carbon although much richer and

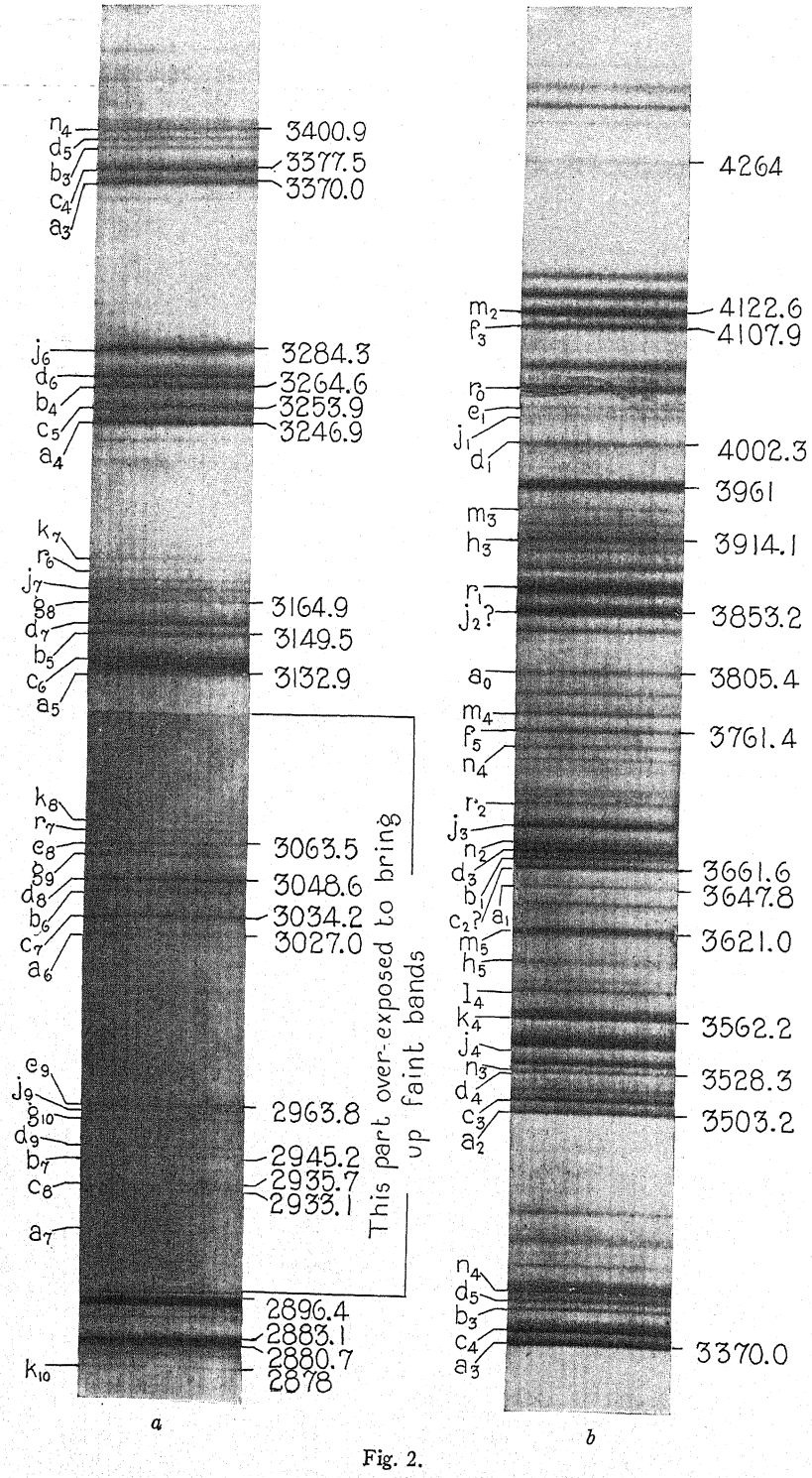

n4
d5
b3
c4
a3
3400.9
3377.5
3370.0
j6
d6
b4
c5
a4
3284.3
3264.6
3253.9
3246.9
k7
r6
j7
g8
d7
b5
c6
a5
3164.9
3149.5
3132.9
k8
r7
e8
g9
d8
b6
c7
a6
3063.5
3048.6
3034.2
3027.0
e9
j9
g10
d9
b7
c8
a7
2963.8
2945.2
2935.7
2933.1
This part over-exposed to bring up faint bands
2896.4
2883.1
2880.7
2878
k10
a
4264
m2
p3
4122.6
4107.9
r0
e1
j1
d1
4002.3
3961
m3
h3
3914.1
r1
j2?
3853.2
a0
3805.4
m4
p5
n4
3761.4
r2
j3
n2
d3
b1
c2?
a1
3661.6
3647.8
m5
h5
3621.0
l4
k4
3562.2
j4
n3
d4
c3
a2
3528.3
3503.2
n4
d5
b3
c4
a3
3370.0
b

Fig. 2.

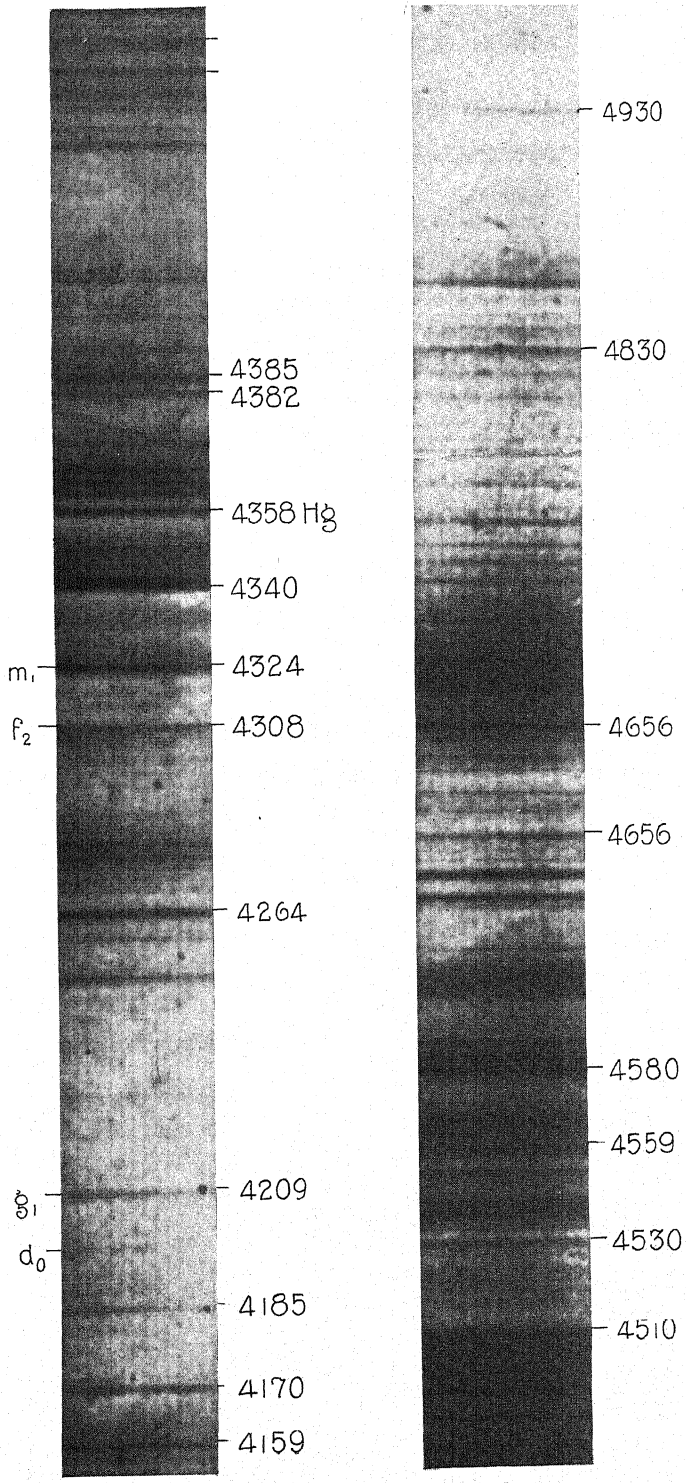

4385
4382
4358 Hg
4340
m1
4324
f2
4308
4264
g1
4209
d0
4185
4170
4159
c
4930
4830
4656
4656
4580
4559
4530
4510
d

Fig. 2.

more extensive than the older work on them indicated. It seemed desirable therefore to try a much simpler method of excitation. The test was easily made. A discharge tube of the simplest type was connected to an old vacuum system. CO_2 from a tank was run through with no particular effort at purification. A high potential outfit was connected to the tube and the flow of gas adjusted until a bright discharge was running smoothly. A spectrogram of the negative glow was taken and showed the complete CO_2 spectrum that had been studied by the electron beam method. It should be added that the Angstrom bands and probably also some other CO bands were quite strong so that this method of excitation is not as clean cut as that previously described. Nor was the intensity as high. Obviously, since this is exactly the method of excitation used in older work to get the second negative bands of carbon and since nearly all wave-lengths given in previous lists of that spectrum are found on our plates the two spectra are identical. It remains a question why the older work reports such a small number of bands.

If the reproductions given in Figs. 2a and 2b be compared with that of Fox, Duffendack and Barker* they will be seen to be almost identical except for the presence of the OH 3300 and CH 4300 bands. The general run of intensity is the same on our plates as on the older ones and therefore the hope that this method of excitation would give a simplified intensity distribution was not justified. Figs. 2c and 2d showing as they do the long wave-length end of the spectrum photographed by the small glass Hilger, indicate that there are a great many more bands than are given in Fox, Duffendack and Barker's list but the measurements on these small dispersion plates did not seem of sufficient accuracy to be included in the list of wave numbers used below for analysis. The measurements from the plate taken with the medium Quartz Hilger which is reproduced in Figs. 2a and 2b should be accurate to about ten wave number units and therefore are a useful check on the more accurate measurements of Fox, Duffendack and Barker on plates taken with the El Quartz Hilger. The probable accuracy which they estimate for their wave-lengths is 0.1A in most cases and 1.0A for bands which they were unable to study with the large instrument. Converted to wave number units these errors are about 1 and 10 cm^{-1} for the region concerned. To allow a detailed comparison of the old results and the new and to serve as a basis for an analysis Table I has been prepared giving both sets of measurements and including also the wave-lengths of the 2nd negative bands.

Part II. Analysis

First inspection of the spectra shows that from λ2900 to λ3500 the bands occur in five well-defined groups of similar but not identical structure; then from 3500 to 4000 is a terrific tangle; then two more groups appear at about λ4100 and λ4270; then another confused array of bands petering out to the end of the spectrum at about λ5000. On the violet side are the two strong bands at λ2893 and λ2883, resolved by Duncan into fine structure, and be-

* The writer is very much obliged to Professor Duffendack who was kind enough to send him one of his CO_2 plates.

yond them some weaker bands that appear again like the groups around λ3000. Fox, Duffendack and Barker arranged six of the strong bands at the violet edges of these groups in a progression. The author has been able to extend their analysis very considerably. His results will be presented first in an entirely empirical way and then possible interpretations will be discussed.

Adding one band on either end of the set arranged by Fox, Duffendack and Barker we get the series given in Table II and find the observed wave

TABLE II. *a-series.*

Desig. of band	λ	νobs.	Int.	νcal.	νcal.−νobs.	Desig. of level
a_0	3805.4	26.271.0	5	26,271.0	0	A_0
a_1	3647.8	27,406.0	3	27,406.0	0	A_1
a_2	3503.2	28,537.2	7	28,537.3	+0.1	A_2
a_3	3370.0	29,665.1	10	29,664.9	−0.2	A_3
a_4	3246.9	30,789.8	10	30,788.8	−1.0	A_4
a_5	3132.9	31,910.8	8	31,909.0	−1.8	A_5
a_6	3027.0	33,026.3	3	33,025.5	−0.8	A_6
a_7	2928.3*	34,139.5*	1	34,138.3	−1.2	A_7
				35,247.4		A_8
				36,352.8		A_9
				37,454.5		A_{10}
				38,552.5		A_{11}

numbers very accurately expressed by the formula $\nu=\nu_a+1136.85v-1.85v^2$ where $\nu_a=26{,}271.0$ and $v=0, 1, \cdots 7$. This implies transitions from a series of vibrational levels of an upper electronic state to a single lower level. This is to be considered merely as a convenient working assumption. The bands in this progression will be designated $a_0, a_1, a_2 \cdots a_0$ and the upper levels $A_0, A_2, A_3 \cdots A_7 \cdots$ where the values of the levels are calculated from the formula. These levels could be adjusted to get a slightly better fit with the a-progression but such an adjustment makes greater errors later on.

Further examination of the spectrum shows that most of the strong bands in the separate groups and many bands in the more confused part of the spectrum can be represented by transitions between the A-levels and different lower levels, i.e., by formulas of the type $\nu=\nu_a-\nu_x+1136.85v-1.85v^2$. Such bands may be symbolically represented by $A_i-\nu_x$, e.g. A_4-2454 would be a band represented by the above formula if ν_x were put equal to 2454 cm^{-1} and $v=4$. As may be seen from the small coefficient of the quadratic v-term the differences between successive A-levels are very nearly the same and therefore it is difficult to be certain of the proper v-values unless the bands observed in a progression are very accurately measured. This means that the value of ν_x may in some cases be too large or too small by approximately 1130 cm^{-1} or even by integral multiples of that number.

In order to save space the results of the analysis have been included in Table I where column four shows the assignment of the bands to various progressions and column five gives the errors of the wave numbers calculated by the use of the various values of ν_x given in Table V below. But to illustrate their nature more clearly two progressions will be presented separately in detail. The first, the d-progression is the most satisfactory one of all except

the intial a-series. As may be seen from Table III below, the value of ν_x is fixed within very narrow limits, probably 2454 to 2456 and the agreement with observed values is excellent except in one or two cases. In this table, as in Table I and elsewhere except Table II, tenths of cm^{-1} have been ignored.

TABLE III. *d-progression.* $A_i - 2454$.

Desig.	ν_c	ν_0	$\nu_c - \nu_0$	Intensity F. D. & B.	Intensity This paper
d_0	23,816	23,822*	−6*	0	—
d_1	24,951	24,979*	−28*	2	3
d_2	26,082	(26,085)	(−3)	—	2
d_3	27,210	27,210	0	9	5
d_4	28,334	28,334	0	4	2
d_5	29,454	29,451	+3	7	4
d_6	30,571	30,573	−2	10	5
d_7	31,683	31,685	−2	9	5
d_8	32,792	32,792	0	6	5
d_9	33,898	33,895*	+3*	4	2
d_{10}	34,999	34,999*	0*	5	1

* Indicates accuracy of only ±10.
( ) Indicates wave number from author's plate. All others are from Fox, Duffendack and Barker.

As typical of the other extreme, a value of ν_x has been chosen that was suggested by other combinations. The agreement with observed ν's is very poor, perhaps not more than chance, and ν_x could certainly be altered by ±20 or even by ±1130 as discussed above without making it much worse.

TABLE IV. *n-progression.* $A_i - 1400$.

Desig.	ν_c	ν_0	$\nu_c - \nu_0$	Intensity F. D. & B.	Intensity This paper
n_0	24,871	—	—		
n_1	26,006	26,042	−36	6	4
n_2	27,137	27,143	−6	2	—
n_3	28,265	28,290	−25	9	4
n_4	29,389	29,396	−7	3	—
n_5	30,509	(30,490)	+19	—	0

The whole gamut of progressions is given in Table V where the values of ν_x are in column one and the intensities of the bands of the corresponding progression follow along the row. If an intensity is given and unmarked it is the intensity of a band in Fox, Duffendack and Barker's list whose wave number agrees to within 10 cm^{-1} with that calculated. If it is marked with an asterisk it is one of Fox, Duffendack and Barker's less accurately measured bands and if in parentheses it is from the author's plate and does not appear on Fox, Duffendack and Barker's list. In either of these last two cases the $\nu_c - \nu_0$ may be as great as 30 cm^{-1}. The values of ν_x are taken empirically to give the best agreement throughout each particular progression and the ± error indicates the limits outside of which there is noticeably poorer agreement. In most cases this error could be considerably exceeded without bringing the disagreement about 10 cm^{-1} or 30 cm^{-1} for the two grades of accuracy of measurement respectively. The actual value of $\nu_c - \nu_0$

TABLE V.

Desig.	ν_x	A_0	A_1	A_2	A_3	A_4	A_5	A_6	A_7	A_8	A_9	A_{10}	A_{11}
a	0	5	3	7	10	10	8	3	1*				
b	167 ± 2	—	6	(0)	7	9	6	—	2*	5	—	—	—
c	1189 ± 2	—	—	—	9	10	10	9	6	3	—	—	—
n	1400 ± 20	—	—	2	—	3	(0)	—	—	—	—	—	—
r	1578 ± 10	3	5	3	—	(0)	—	(1)	5*	(0)	7		
d	2454 ± 2	0	2*	(2)	9	4	7	10	9	6	4	5	
j	2596 ± 4	—	1*	4	8	10	—	3	7	5*	2*		
e	2618 ± 10	—	(2)	9	—	(6)	3	3	7	5*	5*	(00)	
k	2727 ± 10	—	5	7	—	9	3	—	(2)	4*	(0)	5	
l	2890 ± 10	4*	—	5	(1)	2	2	—	(0)	5	2	?	
g	3660 ± 7	—	1*	—	—	—	—	1	3	5	5*	2*	
p	3918 ± 20	—	—	—	—	(1)	—	—	(0)	(0)	(0)	—	
h	4127 ± 4	—	—	3	7	4	6	(00)	(00)	(00)	(2)	—	
m	4295 ± 10	—	4	8	(2)	6	7	(1)	(1)	(2)	(1)	—	0*?
f	5333 ± 4	—	—	3	5	4	6	—	0*	(0)	(1)	(0)	3*

for each particular band is given in column five of Table I. In the fourth column of Table I and in Figs. 2a and 2b the assignments of the bands are given and in many cases even where the $\nu_c - \nu_0$ is obviously too large an assignment is still given indicating the approximate location expected for that particular band of that progression. In making these assignments fifteen different progressions have been used and in the neighborhood of a hundred bands accounted for. Of these fifteen progressions, all but four (*m*, *n*, *r*, *p*) were found independently of the scheme of energy levels now preferred for their representation and are the residue of some thirty odd different trial values of ν_x, both positive and negative, suggested by various observed regularities in the spectrum. They are believed to be established with reasonable certainty. Of the four progressions, *m*, *n*, *r*, *p*, only two, *m* and *r*, seem pretty good; the other two, *n* and *p*, are decidedly wobbly. The reason for including them will emerge from explanation of these progressions which will be advanced presently.

The most striking of the progressions are the *a*, *b*, *c*, *d* and *e*, having ν_x values of 0, 167, 1189, 2454 and 2618. It will be noted that the difference between the first two and between the last two is approximately the same, 166 cm^{-1}. Furthermore this difference occurs quite frequently elsewhere in the spectrum, for example between the *k* and *l* and the *h* and *m* progressions. For a long time the writer[14] believed this separation to indicate a splitting of one of the electronic levels. This point of view made it possible to explain all but one of the values of ν_x in terms of combinations of two fundamental modes of vibration with quadratic anharmonic terms.[15] But this explanation never seemed really satisfactory particularly as two strong progressions, the *c* and *g*, could not be associated with others at separations of 167, that seemed to have any reality. Therefore, in spite of its attractive simplicity and initial success, it has been abandoned.

Before advancing the present explanation it is necessary to review some of the recent work on the infrared spectrum of CO_2. Dennison[16] has recently

[14] Smyth and Chow, Phys. Rev. **37**, 1023 (1931).
[15] Smyth and Chow, Phys. Rev. **37**, 1710 (1931).
[16] Dennison, Revs. of Mod. Phys. **3**, 280 (1931).

discussed the normal modes of vibration to be expected in triatomic molecules of various types. He shows that in a linear molecule there are four normal modes of vibration instead of three. This arises from the fact that the vibration of the central atom perpendicular to the axis of symmetry is not confined to a particular line but merely to a plane. To characterize this motion completely two quantum numbers, v_2 and l, are necessary. To a first approximation the energy of the molecule is independent of l but if the assumption that the motion of the atoms is infinitesimal compared with the equilibrium distances between them is given up the energy becomes dependent on l. Dennison gives the following equation for the total energy:

$$W/h = \text{const.} + v_1\nu_1 + v_2\nu_2 + v_3\nu_3 + x_{11}v_1^2 + x_{22}(v_2^2 - \tfrac{1}{3}l^2) + x_{33}v_3^2 + x_{12}v_1v_2 + x_{13}v_1v_3 + x_{23}v_2$$

where $v_1v_2v_3$ are quantum numbers, the coefficients x_{11}, x_{12} etc. are constants and l has the values $v_2, v_2-2, \cdots 0$. This expression differs from the general formula for the vibrational energy of a triatomic non-collinear molecule only in the presence of the factor $(1/3)l^2$.

At the last Washington meeting of the American Physical Society, Martin and Barker[17] reported the application of these ideas to the explanation of the observed infrared and Raman spectra of CO_2. Professor Barker has been kind enough to send the writer the frequencies and energy level diagram which he showed on the screen at that time. The frequencies are $\nu_1=1361$ cm^{-1}, $\nu_2=668$ cm^{-1} and $\nu_3=2350$ cm^{-1}. The $v_2=2$ level splits into two ($l=2$ and $l=0$) in the manner described above and the amount of splitting, determined from Raman lines, is 102 cm^{-1}. The similar spread of the $v_2=3$ level is 147 cm^{-1}. The Raman lines correspond to changes of two in v_2.

How can this be applied to the present problem? Obviously not directly since this emission spectrum does not involve the normal state of the molecule. Very possibly the initial and final electronic configurations are such that the molecule is no longer linear; particularly as it seems likely that the spectrum comes from CO_2^+. But the frequencies that emerged in the empirical analysis are of the order of magnitude of the ν_1, $2\nu_2$ and ν_3 given above, which suggests that the shape and binding forces of the excited molecule or ion may be similar to those of the molecule in its normal state.

Working from this point of view it is suggested that the various progressions are all v_1' progressions. That is that the ν_1 of the upper state is about 1140 cm^{-1}. The observed separation of 166 cm^{-1} between a number of pairs of progressions is interpreted as a splitting of the $v_2'=2$ level. On this basis the $v_2'=2$, $l'=0$ and $v_2'=2$, $l'=2$ levels have values 1029 and 1195 cm^{-1} respectively above the lowest vibration state of the upper electronic level. The value of ν_3' remains undetermined as there appears no ν_x that requires a v_3' different from zero. In the lower electronic state are four vibration levels besides the zero. Three, at 1400, 2727, and 4127 are probably $v_1''=1$, 2 and 3, respectively. The fourth at 2456 is $v_3''=1$, probably; perhaps it is $v_1''=2$ and

[17] Martin and Barker, Phys. Rev. 37, 1708 (1931).

2727 is $v_3''=1$, 4127 then being a combination, $v_1''=1$ and $v_3''=1$. In this state no values of v_2'' other than zero appear and therefore v_2'' remains undetermined. The complete absence of any transitions from the $v_2'=1$ state is an unexplained difficulty with this whole arrangement. Perhaps it is the result of some selection rule which an extension of Dennison's analysis to electronic transitions might explain.

In the scheme of levels as shown in Fig. 3, the $v_1'>0$ levels have been omitted so that each transition shown represents an entire progression. The levels are labeled by letters to avoid any insistence on their suggested inter-

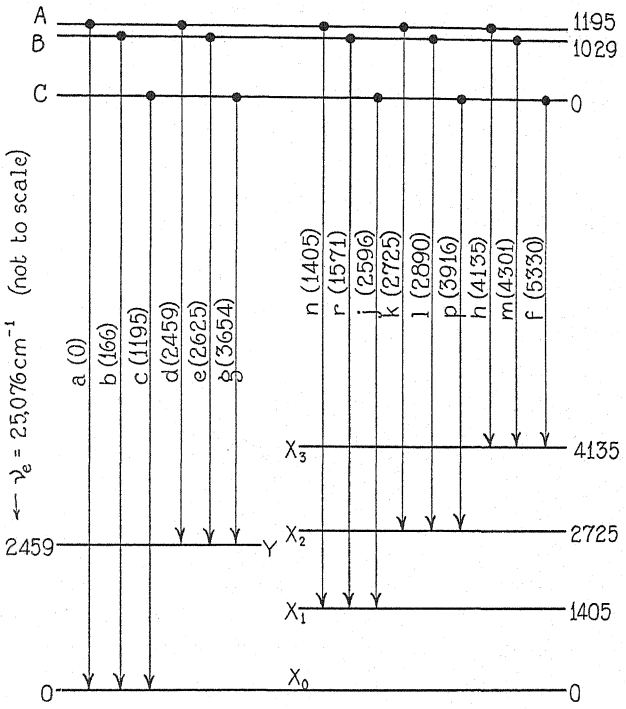


Fig. 3.

pretation. Their numerical values are chosen to give the most general agreement with the observed $\nu_x s$. That this agreement is good in most cases can be seen from Table VI. A slightly different choice of separations of the levels gives a good deal better agreement for all but the *g* and *h* progressions. This may be accidental or as seems more likely the scheme may be over simplified. In any case the values given in Table VI which represent exactly combinations of the levels in Fig. 3 give computed wave numbers that agree within 10 cm^{-1} with sixty-two of the more accurately measured bands in Fox, Duffendack and Barker's table, within 30 cm^{-1} with twenty-eight of the less accurately measured bands and within 30 cm^{-1} with seventeen bands that were observed on the author's plate but not by Fox, Duffendack and Barker.

If the empirical values of ν_x are used only some half dozen more bands are brought within the limits of error but the average value of $\nu_c - \nu_0$ is very considerably reduced. Furthermore, if the doubtful n and p progressions and the A_0 and A_{10} combinations are omitted only twenty-three of the 117 predicted bands are not observed within the limits of error. Considering the overlapping of the bands, their varying intensity and the fact that the measurements are of edges, often ill-defined, rather than of origins, this agreement seems good.

TABLE VI.

Progression	Empirical	Calc.	Diff.	Transition
a	0	0	—	$A-X_0$
b	167	166	−1	$B-X_0$
c	1189	1195	6	$C-X_0$
d	2454	2459	5	$A-Y$
e	2618	2625	7	$B-Y$
f	5333	5330	−3	$C-X_3$
g	3660	3654	−6	$C-Y$
h	4127	4135	8	$A-X_3$
j	2596	2596	0	$C-X_1$
k	2727	2725	−2	$A-X_2$
l	2890	2891	1	$B-X_2$
m	4295	4301	6	$B-X_3$
n	1400	1405	5	$A-X_1$
p	3918	3916	−2	$C-X_2$
r	1578	1572	−6	$B-X_1$

Obviously this scheme of levels is not the only possible way of explaining the observed regularities. The observed A-progressions can not even be assigned with certainty to the upper electronic state. They are cut off at either end about equally sharply, as is the spectrum, so that the A_{10} level may well be actually a $v_1''=0$ level. That this was the case was assumed by the author in papers presented to the Physical Society at the New York[14] and Washington[15] meetings. But this now seems unlikely and attempts to construct a satisfactory energy level scheme on this basis have met with no success.

Granted the A-progressions are ν_1' progressions it might still be expected that all three normal modes of vibration of both upper and lower states should be present in the spectrum. Analytically the spectrum would then be represented by the difference between two equations like that of Dennison's given above, with an electronic term added in. This would give eighteen undetermined constants and could certainly be adjusted to give the observed regularities but it would also predict many regularities that are not observed. Attempts to apply such formulas have not been successful.

There remain a number of bands in Table I, among them the two strongest in the spectrum, which have not been fitted into the scheme. Separations of about 160 cm^{-1} and about 1400 cm^{-1} occur in them with fair regularity showing signs of something like a ν_1'' progression but no definite analysis has been achieved as yet. There also seem to be smaller differences of the order of 10 cm^{-1} that are repeated but these are too near the limits of accuracy of measurement to be dependable.

In connection with some data[18] on the ionization of CO_2 it is of interest to consider the energies of excitation of the upper levels here postulated. The ν_e, that is the energy to go from zero vibration in the lower state to zero vibration in the upper state, is 25,076 $cm^{-1} = 3.1$ volts while the excitation of the A_{10} level requires 4.6 volts. The interpretation of a particular secondary ionization process in CO_2 suggests the existence of an excitation level in the ion (or molecule) at about 4.5 volts.

It should also be pointed out that the long wave-length end of the spectrum from 4000 to 5000 has hardly been touched. The bands included in Table I are only a small part of what is shown on plates taken with the glass spectrograph (see Figs. 2c and 2). In fact the bands in this region are so thick that much greater dispersion is necessary before an analysis can be convincing. For this reason no great weight is given to the fact that some of the progressions given above can be extended in this region and such extensions have not been included in the discussion.

It is probable that the analysis presented above will have to be considerably revised as our knowledge of this spectrum is increased. Yet it seems significant and encouraging that so large a proportion of the observed bands can be fitted into a plausible and not very complicated scheme. If this can be done with an emission spectrum not involving the normal state, it may be possible to do even better in cases where absorption spectrum data can be applied. Such a case is offered by SO_2 whose absorption spectrum has recently been partly analyzed by Watson and Parker.[19] Chow and the author[20] have already pointed out an interesting correlation between this analysis and an emission spectrum previously observed and are beginning a systematic study of the emission spectrum.

In conclusion I wish to thank Miss Janet MacInnes and Mr. T. C. Chow for their help in various phases of this work.

[18] Smyth, Revs. of Mod. Phys. **3**, 382 (1931).
[19] Watson and Parker, Phys. Rev. **37**, 1484 (1931).
[20] Chow and Smyth, Phys. Rev. **38**, 838 (1931).

AUTO-IONIZATION IN THE ALKALINE EARTH METALS AND THE INERT GASES

By H. E. White
University of California, Berkeley

(Received October 19, 1931)

Abstract

The atomic process of auto-ionization put forward by Shenstone[1] is discussed in connection with the alkaline earth metals, calcium, strontium, and barium, and the inert gases, krypton and xenon. The phenomenon is quite similar to the Auger[2] effect in x-rays and analogous with the predissociation of molecules in band spectra put forward by Kronig.[3] Certain characteristics of energy levels in Ca and Sr, known to lie above the first series limit and to give rise, in combination with lower levels, to sharp and nebulous lines, are attributed to the process of auto-ionization. In a similar manner the cutting off at the first or second member of certain series of lines in krypton and xenon and the continuance of other series of the same electron configurations to five, six, seven and eight members is attributed to the process of auto-ionization in those atomic states of the neutral atom which lie above the first series limit.

THE process of *auto-ionization* put forward by Shenstone[1] to account for the ultraionization potentials observed in mercury vapor is of considerable importance in that it clears up a great many of the difficulties previously unaccounted for in atomic spectra. One of the well-known anomalies that may be accounted for, as pointed out by Shenstone and to be given later,[1] is the diffuseness of certain lines in the arc spectrum of copper. The observation of sharp lines and of broad diffuse lines in the same multiplet finds a plausible explanation in this process, auto-ionization.

Above the series limit of any series lies a continuum of possible energy states. This continuum is characterized by the same quantum numbers as the series of discontinuous levels below the limit, i.e. the same L, S, J, and the same odd or even sign of the electron configurations involved. An electron configuration or term is said to be *odd* when Σl_i is *odd*, and *even* when Σl_i is *even*, (i.e. *odd* for an *odd* number of $p, f, h, \cdots$ electrons, otherwise *even*). An atom excited to a discrete energy state above the first ionization potential and into a region accompanied by a continuum characterized by the same L, S, J, and *sign* is in a condition for auto-ionization. The transition from the discrete energy state into the continuum may be interpreted as a "resonance" phenomenon between two states of the same energy, which results in the spontaneous ejection of an electron with kinetic energy and the return of the atom to a lower series limit. Several good examples of this process of auto-ionization are to be found in the alkaline earth elements.

[1] Shenstone, Phys. Rev. **38**, 873 (1931).
[2] Auger, Comptes Rendus **187**, 1141 (1928); **188**, 447, 1287 (1929); **192**, 672 (1931).
[3] Kronig, Zeits. f. Physik **62**, 300 (1930).

In the early development of complex spectrum analysis Russell and Saunders[4] found in calcium a series of triplet p' terms which are now famous. These terms, then designated as $2p'_{1,2,3}$, $3p'_{1,2,3,}$, $4p'_{1,2,3}$ and $5p'_{1,2,3}$ with term values $T=741$, -5000, -8334, and -10086 cm^{-1} respectively, are now designated as $^3P_{2,1,0}$ and are attributed by Russell[5] to the electron configurations $3dmd$. All but the first member of this series, see Fig. 1, lie above the first series limit $4^2s_{1/2}$ of the four chief series of singlets and triplets. The continuum above these four chief series corresponds to *even* S and D terms and to *odd* P and F terms. The $^3P_{2,1,0}$ terms being characteristically *even* enables the electron to have in this state a mean-life sufficiently great to combine normally with lower odd terms and to give the respectably sharp spectrum lines observed.

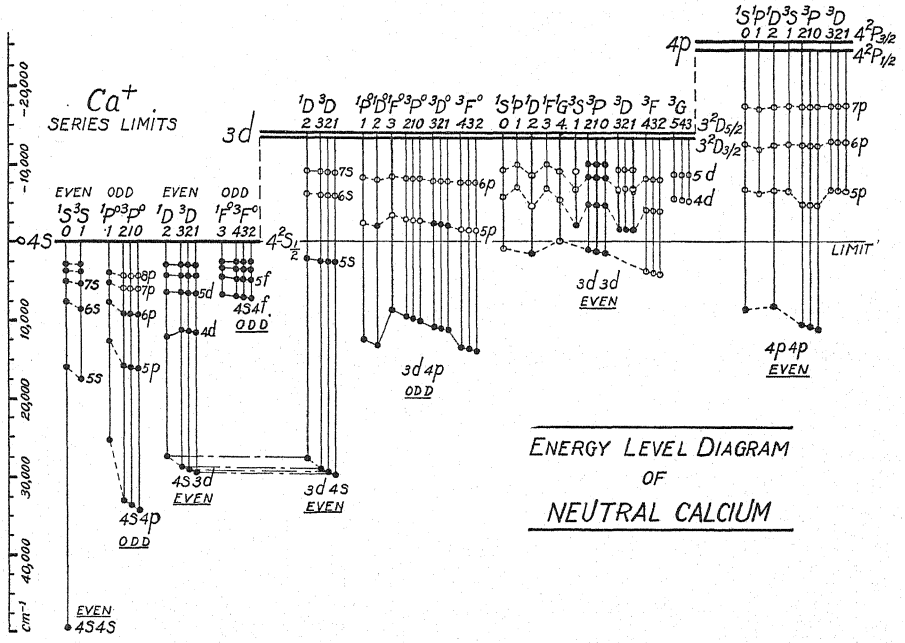


Fig. 1. Energy level diagram of calcium.

The *even* $^3S_1$ term in calcium ($T=-2266.9$ cm^{-1}, and attributed by Russell[3] to $3d4d$) because it is found to combine with other *odd* terms at all, would be expected to have a short mean-life, and to give, as a result, diffuse lines. This level $^3S_1$, $3d4d$, combining with $^3P^0{}_{2,1,0}$, $4s4p$, in a double electron jump gives rise to three hazy lines λ2757.40, λ2749.34, and λ2745.49.

In strontium a $^3F^0$ term, $4d6p$, (the corresponding term in calcium, see Fig. 1, is $^3F^0$, $3d5p$,) lies above the $5^2S_{1/2}$ limit and, as in calcium, is in a continuum of $^3F^0$ terms, $5smf$. These negative $^3F^0{}_{4,3,2}$ terms, $4d6p$, with term

[4] Russell and Saunders, Astrophys. J. **61**, 38 (1925).
[5] Russell, Astrophys. J. **66**, 1 (1927).

values $T=3729.4$, 3621.6 and 3473.3 cm^{-1}, if they are observed to combine with lower terms at all, would also be expected to have a short mean-life and to give rise to extremely diffuse lines. Combining with the $^3D_{3,2,1}$ terms, $5s4d$, with term values $T-27606.0$, 27706.6, and 27766.6 cm^{-1} respectively, these $^3F^0$ terms give rise to five very diffuse lines.[4]

STRONTIUM[4]

Int.*	λ	ν	Designation
4n	3189.23	31346.5	$^3D_3-{}^3F_4^0$
3n	3189.93	31339.6	$^3D_2-{}^3F_3^0$
2n	3198.99	31250.9	$^3D_1-{}^3F_2^0$
2n	3200.22	31238.9	$^3D_3-{}^3F_3^0$
1n	3205.13	31191.0	$^3D_2-{}^3F_2^0$

* The letter *n* indicates that the lines are "nebulous" in appearance.

In barium these same $^3F^0_{4,3,2}$ terms, $5d7p$, with term values $T=4558.6$, 4747.5, and 4966.3 cm^{-1} respectively, lie below the first limit $6^2S_{1/2}$ and in combination with the corresponding terms, $6s5d$, with term values $T=$ 32433.0, 32814.1 and 32995.6 cm^{-1} respectively, give rise to six relatively sharp lines as expected.

BARIUM[4]

Int.	λ	ν	Designation
10	3586.50	27874.4	$^3D_3-{}^3F_4^0$
10	3561.94	28066.6	$^3D_2-{}^3F_3^0$
10	3566.66	28029.2	$^3D_1-{}^3F_2^0$
15	3610.96	27685.6	$^3D_3-{}^3F_3^0$
3	3589.95	27847.6	$^3D_2-{}^3F_2^0$
2	3639.72	27466.9	$^3D_3-{}^3F_2^0$

It is suggested in what follows that an extension of the process of auto-ionization to the spectra of the inert gases where *jj*-coupling, rather the *LS*-coupling, predominates may account for certain apparent anomalies. In the noble elements neon, argon, krypton and xenon all observed series approach, as limits, the inverted $^2P_{1/2,3/2}$ terms of the corresponding ions Ne II, A II, Kr II and Xe II respectively. With almost perfect *jj*-coupling in krypton[6] and xenon[7] each series of energy levels arising from the electron configurations p^5ms, p^5mp, p^5md, and p^5mf, consists of two distinct groups of series. From the energy level diagram for xenon, shown in Fig. 2, it may be seen that in each configuration there is one group of terms approaching the lower limit $^2P_{3/2}$ of the ion, and another group of terms approaching the upper limit $^2P_{1/2}$.

The circles, representing unobserved terms, Fig. 2, and the dots, representing observed terms, indicate that transitions from negative levels to lower levels seldom occur, if at all. It is seen that series built upon the lower

[6] Meggers, de Bruin, and Humphreys, Bur. Stand. Jour. Res. **3**, 129 (1929).
[7] Meggers, de Bruin, and Humphreys, Bur. Stand. Jour. Res. **3**, 731 (1929).

limit $^2P_{3/2}$ are in general observed for some five to eight members, whereas, the series built upon the upper limit $^2P_{1/2}$ are observed for only one or two members. It is reasonable to expect any one of the series arising from the electron configurations $5p^5mp$, for example, to be observed for as many members as any other series belonging to these same configurations. In cases such as this the explanation has been that excitation energies somewhat greater than the first ionization potential ionize the atom rather than excite it to an energy level above the first ionization potential. The process of auto-ionization put forward by Shenstone,[1] however, is a plausible explanation of what happens,

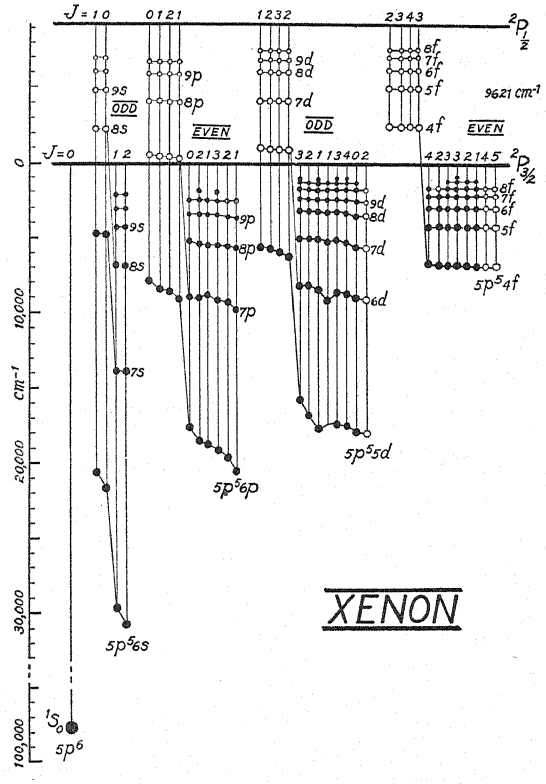


Fig. 2. Energy level diagram of xenon.

and would indicate that excitation into these negative atomic states takes place first and that ionization without radiation is a secondary process.

The energy level diagram for krypton, being so nearly like that of xenon, may be obtained from Fig. 2, by lowering the $^2P_{1/2}$ limit and the series built thereon, about half-way to the $^2P_{3/2}$ limit ($^2P_{3/2}-^2P_{1/2}=5371$ cm^{-1}). This drops one more member of each upper limit series below $^2P_{3/2}$ in a region where its mean-life is sufficiently great to combine normally with lower terms, as observed.

With *jj*-coupling in krypton and xenon the quantum conditions necessary for auto-ionization should be somewhat different than for *LS*-(*Russell-*

Saunders) coupling. For every *odd* state above $^2P_{3/2}$ there is an *odd* continuum characterized by the same J value. It would appear from observation that these conditions might be sufficient for auto-ionization. In some cases, however, the small j's are found to be the same for the two states in "resonance." For example, for the electron configuration $5p^5mp$ there are two *even* terms $J=1$, and $J=2$ above $^2P_{3/2}$, accompanied by *even* continua with $J=1$, and $J=2$, from the same configuration. In addition the discrete states have $j_1=\frac{1}{2}$, $(5p^5)$, and $j_2=3/2$, (mp), and the continua have $j_2=\frac{1}{2}$, (mp), and $j_1=3/2$, $(5p^5)$. Similarly there are two *odd* states $J=1$, and $J=2$, $(5p^5md)$, with $j_1-\frac{1}{2}$, $(5p^5)$, and $j_2=3/2$, (md) in the *odd* continua characterized by $J=1$ and $J=2$ respectively, $(5p^5ms)$, with $j_2=\frac{1}{2}$, (ms), and $j_1=3/2$, $(5p^5)$. This is not the case for all discrete states. In every case, however, *odd* continua do exist where the resultant J's, and the relative directions of the electron spins s_1 and s_2, are the same as in the *odd* discrete states. This is also true for *even* states. The quantum conditions for the so-called "resonance" between two states having approximately the same energy values in jj-coupling should be determined on the quantum mechanics.

THE PRODUCTION OF HEAVY HIGH SPEED IONS WITHOUT THE USE OF HIGH VOLTAGES

By David H. Sloan and Ernest O. Lawrence
University of California

(Received October 19, 1931)

Abstract

A method has been developed for the multiple acceleration of ions to high speeds without the use of high voltages. The ions travel through a series of metal tubes in synchronism with an oscillating electric potential applied alternately to the tubes such that the electric field between tubes is always in a direction to accelerate the ions as they pass from the interior of one tube to the interior of the next. The ions are thereby successively accelerated to speeds corresponding to voltages as many times greater than the high frequency voltage applied to the tubes as there are tubes. In the present experiments a high frequency voltage of 42,000 volts at a wave-length of 30 meters applied to 30 such accelerator tubes in line resulted in the production of a current of 10^{-7} amp. of 1,260,000 volt singly charged Hg ions. The surprising effectiveness of this experimental method for the generation of intense beams of high speed ions is due to the development of simple, convenient and effective methods for focusing and synchronizing the ions as they pass through the accelerating system. The present experiments show that ions having kinetic energies in excess of 1,000,000 volt-electrons can be produced in this way with quite modest laboratory equipment and with a convenience surpassing the direct utilization of high voltages, that the limit to the attainable ion speeds is determined mainly by the length of accelerating system and the size of the high frequency oscillator system, and consequently that the production of 10,000,000 volt ions is an entirely practicable matter.

Introduction

RECENT advances in our knowledge of the structure of matter and its interaction with radiation have in a large measure resulted from experimental studies of collision processes. Apart from experiments in the realm of radioactivity, practically all of these investigations have been concerned with energy interchanges in amounts less than 100,000 volt-electrons. A survey of this situation impresses one that the unexplored domain of higher energy processes awaits the experimenter with promise of much new and important knowledge of the properties of atoms.

There is of course a general recognition of the importance of this field of investigation and several laboratories are developing the technique of the production of high voltages and their direct application to vacuum tubes for the generation of high speed electrons and ions. Highly significant progress in this direction has been made by Coolidge,[1] Lauritsen,[2] Tuve,[3] Brasch and Lange,[4] Cockroft and Walton,[5] Van de Graaff[6] and their collaborators who

[1] W. D. Coolidge, Am. Inst. E. Eng. **47**, 212 (1928).
[2] C. C. Lauritsen and R. D. Bennett, Phys. Rev. **32**, 850 (1928).
[3] M. A. Tuve, G. Breit and L. R. Hafstad, Phys. Rev. **35**, 66 (1930).
[4] A. Brasch and J. Lange, Zeits. f. Physik **70**, 10 (1931).
[5] J. J. Cockroft and E. T. S. Walton, Proc. Roy. Soc. **A129**, 477 (1930).
[6] R. J. Van de Graaff, Schenectady meeting American Physical Society, 1931.

have each developed distinct techniques for voltages of the order of magnitude of one million.

These methods, involving as they do the direct application of high voltage, are subject to certain important limitations. In the first place, it appears that experimental difficulties go up so rapidly with voltage that though the region of one million volts is within the realm of practicability, the region of ten million volts is beyond the present experimental domain. In the second place, these high voltage methods involve apparatus quite beyond the equipment of most physical laboratories and are somewhat cumbersome for detailed experimental investigations of the types that have been carried out in the range of low velocities.

It is for these reasons that we are concerning ourselves with the development of methods for the production of high speed particles which do not require the use of high voltages. Our objective thus is two-fold; first, to make practicable the production of particles having kinetic energies considerably greater than those producible by direct high voltage methods and second, to make the production of particles having kinetic energies in the region of one million volt-electrons a matter than can be carried through with quite modest laboratory equipment and with an experimental convenience which, it is hoped, will lead to a wide-spread attack on this highly important domain of physical phenomena.

Three distinct methods are being developed in our laboratory. One of the methods is for the production of high speed electrons and at the present time is in its early stages of development.[7] Another method designed for the acceleration of relatively light ions has reached a rather advanced stage of development and has already been briefly described;[8,9] a detailed account is expected to be published soon. The third method applicable to heavier ions is the subject of the present paper.

The fundamental principle of this method was experimentally demonstrated several years ago by Wideroe[10] who succeeded in producing 50,000 volt potassium ions in a tube to which the maximum applied voltage was about 25,000 volts. In our initial experiments[11] the method was developed to the production of 210,000 volt mercury ions with an applied voltage of 10,000; i.e., a voltage amplification of 21 was obtained. In the present work new developments have lead to a voltage amplification of 30 and the production of 1,260,000 volt singly charged ions. It is shown also that the method can be readily extended to the production of ions having kinetic energies of the order of magnitude of 10,000,000 volt-electrons.

The Experimental Method

An outline of the experimental arrangement will make clear the important features of the method. A series of metal tubes arranged in line (labeled ac-

[7] This method was discussed briefly at the symposium on high voltages at the Pasadena meeting of the American Physical Society (June 1931).

[8] E. O. Lawrence and N. E. Edlefsen, Science **72**, 376 (1930).

[9] E. O. Lawrence and M. S. Livingston, Phys. Rev. **38**, 834 (1931).

[10] R. Wideroe, Arch. f. Elektrotech. **21**, 387 (1929).

[11] E. O. Lawrence and D. H. Sloan, Proc. Nat. Acad. Sci. **17**, 64 (1931).

celerators in Fig. 1) are attached alternately to the inductance of a high frequency oscillatory circuit. A high frequency voltage applied in this manner produces at any instant electric fields between successive accelerator tubes of opposite direction and equal magnitude. If at one instant an ion finds itself between the first and second tubes with the field in the right direction it will be accelerated into the second tube, and if the time consumed in passing through this tube is equal to the half period of the oscillating field, it will arrive between the second and third tubes with the field reversed in direction in such a manner that it will receive an additional acceleration on passing into the third tube. If the tubes are made successively longer in the proper way

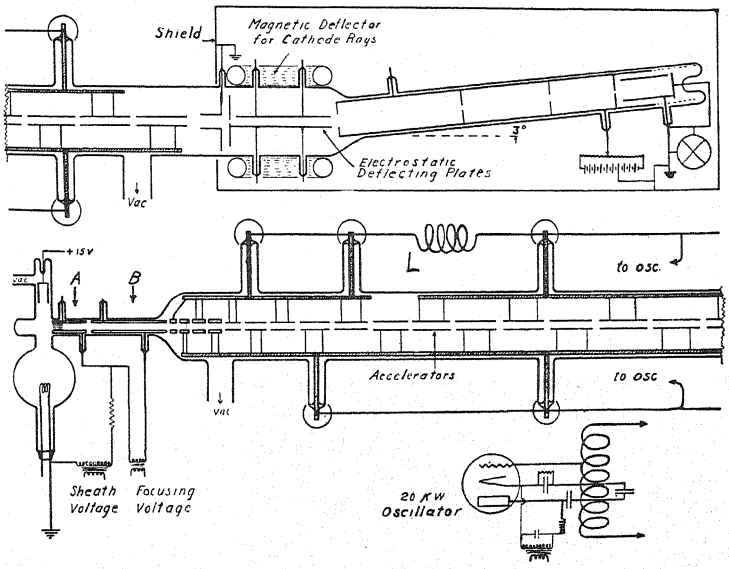


Fig. 1. Diagram of apparatus.

(approximately the square roots of integers times the length of the first tube), for any frequency of the applied oscillations there will be a corresponding voltage such as will cause the ion to move up through the series of accelerators in synchronism with the oscillating field, gaining between each pair of accelerators an increase in kinetic energy corresponding to the applied potential difference. Thus, for example, in the present experimental tube 42,000 volts applied to the 30 accelerators resulted in the production of ions having kinetic energies corresponding approximately to 30 times 42,000 volts, i.e., 1,260,000 volts.

The Experimental Arrangement

The essential components of the experimental arrangement are the line of accelerator tubes in a suitable vacuum, an intense source of ions with focusing devices to draw them properly into the first of the accelerators, electrostatic deflecting plates in conjunction with a collector and galvanometer to select

out and measure the speeds of the ions, a high frequency oscillator, and a satisfactory vacuum system. It is perhaps well to describe these parts of the experimental arrangement in some detail.

The ion source

Because the ion beam must travel a long path of restricted cross section the initial focus of the beam is of an importance comparable with its intensity. The ions must start out approximately in the right direction if they are to succeed in passing all the way through the accelerator tubes.

The hot cathode arc discharge was chosen as the source, not only because it gives a copious supply of ions at low vapor pressures, but also because of the circularly symmetric fields so readily obtained about circular electrodes in the positive ion sheath which are an important help in focusing. Without the arc plasma slight irregularities in the construction and position of all the electrodes in the source would have unpredictable effects upon the focus of the emergent ion beam. The arc has the added advantage that ions so formed have random velocities very small compared to that acquired in falling through the positive ion sheath of the electrode drawing the ions out.

The ions are formed in a hot cathode mercury vapor discharge at 10^{-3} mm of mercury pressure. The accelerating system receives positively charged mercury ions from this arc by means of a negative electrode A (Fig. 1) inserted into the positive column. Between this electrode and the arc is a positive ion sheath or space charge region from which the electrons are repelled by the 10,000 volts negative potential of the electrode. Some of the ions from the arc plasma which acquire 10,000 volts velocity by falling through this space charge enter a hole drilled through the electrode along the principal axis of the accelerator system.

The canal rays thus projected through the hole in the first electrode form a divergent beam, the amount of the divergence depending on the arc current density, the vapor pressure, and the negative potential of the electrode (sheath voltage) as well as the shape of the opening in the face of the electrode at the boundary of the sheath. The second electrode B, 15,000 to 20,000 volts more negative than the first, has its end tapered to provide a suitably curved axially symmetric field between the electrodes which sharply focuses the beam into the region of the high frequency accelerators.

These first two electrodes are each about 8 cm long with a 5 mm hole which, with the small opening 1 mm in diameter and 10 mm long into the arc region, provide a pressure drop between the latter at 10^{-3} mm of mercury pressure and the high frequency accelerator region which is evacuated by two high speed condensing and pumping systems to less than 10^{-5} mm Hg pressure.

The accelerating system

The accelerator cylinders consist of short lengths of copper tubing 5 mm in diameter, all in line with the beam from the ion source, and supported alternately from copper bus bars above and below the group of hollow cylinders. These bars are the opposite terminals of the inductance of the oscillating

circuit. The lengths of the tubes increase as the square roots of integers since the ions gain equal increments of energy between successive accelerators, i.e., the velocities of the ions increase with the square root of the number of times they are accelerated. The lengths of the cylinders are adjusted on the basis of the first one having an effective length of 1 cm, the overall length of the 30 cylinders being about 114 cm. The actual length of the cylinders is decreased by the length of the insulating gap between them.

Since the applied potential is sinusoidal the ions travel part of the distance across the gap in fields perceptibly different from peak values. The shorter the gap between successive cylinders the greater is the effective potential fall for the ions on crossing a gap. On the other hand the gap must be fairly long to permit the use of high voltages, to reduce the inter-electrode capacity, and to give greater equality between the fields at points on and off the axis.

A gap of 20 percent of the distance between centers of cylinders yields effectively 96 percent of the applied potential; this makes the first ten gaps too short to give sufficiently uniform fields, the first three even being too short to prevent sparking between electrodes; the necessary separations of the first three electrodes reduces them to mere rings. To enhance the field uniformity large disks with a hole in the center of each are therefore used for the first few accelerators (the disk arrangement is not shown in Fig. 1). Though disks of this type provide greater homogeneity of the fields, an ion passing from one to the next in a half cycle receives only 63 percent of the maximum of the applied voltage. Rather than increase the voltage applied to these first few enough to compensate for this loss, two extra stages of these disk accelerators are added. The first ten accelerators are of this hybrid design and are attached to a variable loading inductance (L, Fig. 1) which makes possible easy adjustment of the high frequency voltage applied to them relative to the voltage applied to the rest of the accelerators.

Electrostatic resolution and measurement of the ion beam

The beam of high velocity ions emerging from the final accelerator passes through a slit 3 mm wide and between a pair of electrostatic deflecting plates 20 cm long and 1 cm apart, across which are applied suitable potential differences to deflect the beam through an angle of 3 degrees into a line of slits leading to a Faraday collector as shown in Fig. 1.

The purpose of deflecting the ion beams is two-fold; in the first place, electrostatic deflection of the beam in this way serves as a velocity analyzer, and secondly, the collector being off the line of the accelerators, the slit system provides essential shielding of the collector from x-rays generated in the accelerators and in the ion source as well as on the deflecting plates. A magnetic field perpendicular to the axis of the tube deflects to the walls cathode rays generated along the tube, thereby preventing them from striking the deflector plates and generating x-rays which would pass freely through the line of slits to the Faraday collector. Protected thus from all stray radiations and charged particles, the collector is available to locate ion beams of 10^{-12} ampere using a high resistance leak across the electrometer. Without this rela-

tively high current sensitivity the correct initial adjustment of focusing voltages, the discharge current, the synchronizing voltage, and phase correction voltage for each new frequency of the oscillator would be a difficult matter of chance.

The high frequency oscillator

A 20 K. W. Federal Telegraph water-cooled power oscillator tube is used in a self excited Hartley oscillator circuit. Working into a very low resistance load, the tube impedance is readily matched by connecting it across only a small portion of the total inductance, thus giving a greatly increased voltage at the terminals of the entire inductance. Applying a 60 cycle peak voltage of 15,000 volts to the oscillator, the high frequency voltage obtained across some preliminary accelerator tubes was as high as 90,000 volts at 42 meters wavelength. Because of close spacing and dirty electrodes, the present accelerator tube sparks between electrodes at 45,000 volts. The high frequency voltage is adjusted by varying the 60 cycle voltage on the plate of the oscillator tube. The importance of being able to vary this voltage at will is suggested by the fact that changing the applied voltage 1 percent below the optimum value reduces the number of ions getting through the accelerating system to a few percent of the optimum current.

The vacuum system

Little difficulty is experienced in maintaining a satisfactory vacuum in the region of the accelerators. Two condensation pumps with large liquid air traps attached to the tube as indicated in Fig. 1 suffice to maintain a vacuum of about 10^{-5} mm of Hg (ionization gauge measurement) in all parts of the tube excepting the ion source. This pressure is low enough to give the high speed ions requisite free paths and to allow the application of high frequency voltages to the accelerators. It is found that the maximum voltage that can be applied is determined essentially by the condition of the surfaces of the electrodes and not by the degree of vacuum obtained.

Production of an Intense High Speed Ion Beam

Proper synchronization and focus of the ion beam all along its path naturally are essential to the production of an intense beam of high speed ions.

Synchronization

The first requirement for synchronization of the ions with the oscillating field is obviously that voltages are applied to the ion source electrodes AB such as will cause the ions to arrive at the first accelerator tube with proper speeds.

The problem of applying the correct high frequency voltages to the several accelerators is not a simple one. The first ten of hybrid design require a voltage different from that applied to the remaining stages. Moreover, though the remaining accelerators are attached to the same bus bars the potential distribution along them is not uniform, due to the distributed capacity and inductance; this effect depends on the frequency and cannot readily be cal-

culated. Even if for a given frequency and tube design the voltages on the accelerators were calculated, it would be difficult to estimate accurately the percentage of the applied sinusoidal potential effectively contributing to the kinetic energy of an ion crossing various shapes of gaps between accelerator electrodes. Indeed, this percentage is very much dependent on the distance from the axis of the ion path, which must remain somewhat uncertain because of mechanical inaccuracies of alignment. Add to this the change in potential distribution with operating frequencies and it becomes apparent that some sort of flexible adjustment must be available for empirical synchronization of the ions all along their paths.

Many synchronizing devices have been considered. The simplest in principle is to alter the gap separations of the accelerators individually until the ions do experience accelerations which cause them to travel through the tube in synchronism. The same end would be achieved by a system for changing the length of each accelerator itself to correspond to the velocity of the ions passing through it. Such empirical mechanical adjustments would undoubtedly be cumbersome; a much more feasible method is the adjustment of the high frequency voltage applied to the several accelerators by the introduction of variable loading inductances along the busses supporting the line of accelerators.

A single loading coil (L, Fig. 1) for the first ten accelerators has been found to be sufficient; a longer tube which might require several is impractical in a single oscillatory circuit at these high frequencies. In the present experiments, the loading coil determines the voltage on the first ten accelerators relative to that on the remaining stages such as to give the ions velocities upon entering the eleventh tube which enable them to proceed in approximate synchronism with the oscillations. The introduction of the loading coil in the first few stages has proved to be very effective for purposes of synchronization and, therefore, is of cardinal importance in the scheme.

The possible variations in phase between the alternating potential and the velocity of the ions through the column of accelerator electrodes indicate the latitude of adjustment of the applied potentials. Exact synchronism occurs when the ions cross the center of each gap at the same phase angle of the applied sinusoidal potential. While this is the ideal case and not difficult to realize in practice, large deviations from this behavior will still permit acceleration of the ions which as a result emerge with final velocities varying as widely as 5 percent above or below the synchronizing value.

With the loading inductance and the applied high frequency voltage adjusted to the optimum values giving continuous synchronism of the ion beam, the reduction of the high frequency voltage by 2 percent practically eliminates the current of ions which have final velocities corresponding to those of synchronism—though several percent of the ions still get through the system out of synchronism and with reduced final emergent velocities.

If now instead of decreasing the applied voltage it is increased beyond the value for synchronism a complex array of possible phase relations of velocity and frequency occur. An ion crossing the center of an accelerator

gap before or after the instant of maximum applied potential may still receive sufficient energy to pass on in synchronism; indeed, it may receive more than this required amount and thereby its velocity becomes greater than that for synchronism. If this were the situation when it leaves the accelerator system, the ion would emerge with more energy than that acquired when traveling in precise synchronism. If, however, when only partly through the system, it gets so far ahead in phase that it crosses between accelerators before the potential has built up to the synchronizing value, the accelerations will be insufficient for the ion to gain further excessive velocity and the main portion of the beam traveling in synchronism would soon overtake it. Thus, while its average velocity through the system equals that of a synchronized ion, due to its early excess velocity, its final velocity will be below that of the main group. So it is that an excessive oscillator voltage transmits ions over a

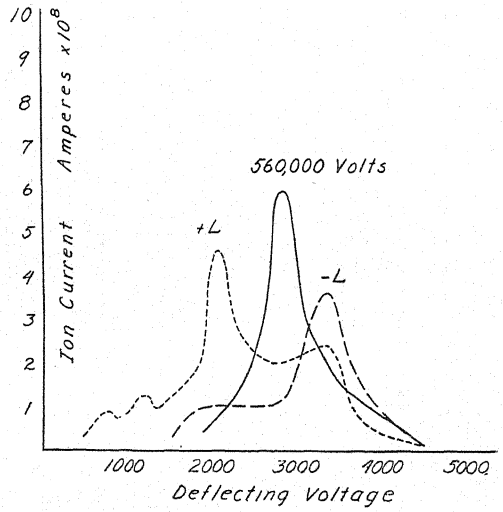


Fig. 2. Variation of current as ions of various velocities are deflected into the collector.

greater phase angle and with a wider emergent velocity distribution, only slightly reducing the number acquiring the normal velocity. This spread in velocities is always observed experimentally.

When the synchronism is not uniform, due to a distortion of the optimum potential distribution along the system, even more striking phase variations occur. Fig. 2 shows the variation of current as ions of various velocities are deflected into the collector; the ordinates are the currents to the collector corresponding to various deflecting voltages on the deflecting plates given by the abscissas. The velocity distributions for three distinct cases are shown. The heavy central curve is obtained with a potential distribution along the accelerators similar to that described in the preceding paragraph; i.e., when the optimum voltage is applied resulting in continuous acceleration of the ions. Less voltage eliminates the peak and reduces the whole curve nearly to

zero. More voltage on the oscillator broadens the peak and reduces it slightly due to the phase displacements mentioned. With the inductance loading the first ten accelerators increased, raising thereby the voltage applied to them, and with the voltage applied to the remaining accelerators lowered to an optimum value giving a sharp peak in the current versus deflecting potential curve, it is seen that the peak (labeled $+L$) represents velocities below those for synchronism. These ions started out too fast and required less acceleration later on to be kept in approximate phase with the oscillations. Similarly, if the inductance is decreased lowering the voltage on the first set of accelerators and the voltage on the remaining accelerators correspondingly increased to bring the ions through with a sharp peak of intensity (curve labeled $-L$), the beam is found now to consist of higher velocity ions than those of synchronism. These ions fall behind in phase in the first accelerations and the higher

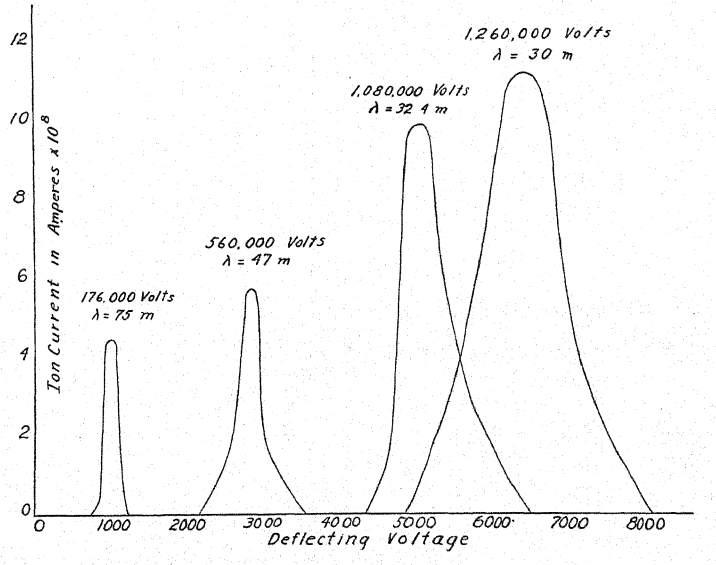


Fig. 3. Ion current plotted against deflector potential; curves for four different oscillator frequencies.

voltages bring their velocities up until they are crossing the gaps at or even before the instant of maximum of this excessive potential, resulting in the excessive final velocities.

These remarks account in a qualitative way for the larger portion of the ion beams. However, it is seen that the velocity distributions of the ions in all cases extend over a wide range and indeed for curves $-L$ and $+L$ there are subsidiary peaks. The presence of two peaks in each of these cases is probably to be ascribed to ions traveling through the accelerators in phases approximately 90 degrees apart. This remark becomes clear when it is realized that there are two portions of each cycle during which the ions are synchronously accelerated. A more detailed discussion of this matter can profitably be reserved for a later time.

In Fig. 3 are plotted ion current versus deflector potential curves for four different oscillator frequencies. In each case the curves represent data obtained with the loading inductance on the first ten accelerators adjusted to give continuous acceleration of the ions with the applied high frequency voltage on the remaining accelerators slightly above the optimum value, thereby resulting in some broadening of the peaks of the curves. Calculations from the deflecting voltages and geometry of the arrangements show that the peaks in each case correspond approximately to ion velocities corresponding to synchronous acceleration. Thus, the curve corresponding to the wavelength of 30 meters represents the production of singly charged mercury ions having energies in excess of 1,260,000 volts. It will be noticed that as the frequency is increased and the voltage and velocities are higher, the maximum ion currents are also greater. This may be attributed to the decreasing relative magnitude of random velocities and the ever present space charge repulsion forces and other stray fields compared to the focusing action of the applied electric fields. This matter of focusing is discussed more fully below.

The above considerations make it evident that if the applied sinusoidal voltage has a peak value somewhat in excess of that corresponding to synchronization of the ions with the frequency used, a quite appreciable portion of the cycle is effective. It is partly for this reason that this method is capable of producing relatively large high speed ion currents.

Focusing the ion beam

In considering the experimental arrangement one is inclined to the belief that it is not capable of yielding relatively intense beams of high speed ions; at first sight it would appear that the number of ions traversing the whole group of accelerators would be a very small portion of the number entering the first accelerator. It would seem that stray fields and space charge effects together with imperfect alignment of the tubes would be the cause of deflection of most of the ions from the very restricted solid angle defined by the final accelerator.

In the early stages of the experiments we were very much concerned with this matter of beam intensities and devoted much thought to ways and means of focusing the ions all along their paths through the system. The methods developed are quite successful, since about 10 percent of the ions starting through the accelerators which have the possibility of traveling through the system actually emerge from the final accelerator.

The first requirement in the production of an intense beam of high speed ions is of course the projection into the first accelerator of a copious supply of ions traveling with proper velocities axially with the cylinders. This initial focusing adjustment is accomplished by trial and error methods, the procedure being to raise the high frequency voltage on the accelerators slightly above the theoretical value for synchronism, and then to adjust the voltages on the ion source electrodes AB until a maximum ion current is obtained at the collector.

The most important focusing occurs along the accelerators and is ac-

complished quite automatically by the curved electric fields between adjacent cylindrical accelerators. An ion crossing the gap between the tubes in synchronism receives an acceleration in towards the axis during the first half of the distance from the inside of one cylinder to the inside of the other, and an approximately equal outward acceleration during the remaining half of the gap length. In first approximation, the net result is a displacement of the ion towards the axis of the cylinders. Because the ion traverses the second half of the gap in a slightly shorter time than it does the first half, the inward velocity component gained in the first half is not quite overcome in the second half, and therefore, the ion retains a slight inward component of velocity as a result of crossing the gap. An ion slightly out of phase with the oscillations may gain a much greater component of velocity at right angles to the line of accelerators. For example, if the ion arrives at the center of the gap after the peak of the oscillations, then during the second half of its course across the gap the average outward component of the electric field is smaller than the corresponding inward component during the first half of the path across the gap, and hence the inward velocity gained in the first half is not neutralized in the second half. This effect is a rather important one and makes it desirable to use applied high frequency voltages with peak values not too greatly in excess of that corresponding to resonance.

This focusing action of the curved fields between accelerators has proved to be highly efficacious; it appears that the decrease of intensity of the beam due to imperfect focus through the accelerators is really insignificant in the case of the 30 accelerators of the present experiments, suggesting that many more accelerators may be incorporated without appreciable loss in beam intensity.

Discussion

This method is most conveniently used in the production of high speed heavy ions because the heavier ions travel slower and, consequently, require shorter accelerating systems. For a given kinetic energy, the speeds of ions vary inversely as the square roots of their masses. For a given oscillating frequency, the required length of the accelerating system is proportional to the ion speeds. It follows that for ions of atomic weight 22 an accelerating system must be three times as long as that required for mercury ions to produce the same kinetic energies. This increase in length is not excessive, and therefore it may be concluded that the method is applicable to the majority of ions.

The present experimental development has achieved one of the objectives outlined in the introduction, namely, the production of ions having energies of the order of magnitude of one million volt-electrons without the use of cumbersome high voltage equipment and with considerable experimental convenience. It is interesting to inquire to what extent the present work has progressed along the road to the other goal, i.e., the production of 10,000,000 volt ions.

To reach higher energies in this way, it is clearly necessary either to in-

crease correspondingly the high frequency voltages at shorter wave-lengths applied to the accelerators or increase the number of accelerators. From experience with the present tube it seems that the voltage on the accelerators cannot conveniently be increased by more than a factor of two and, consequently, the region of 10,000,000 volts can be attained only by increasing the number of accelerators.

With but one oscillatory circuit the limit to the number of accelerators that can be used is established by the capacity of the system. The arrangement of accelerator tubes, bus bars, leads and inductances can be improved considerably over that of the present arrangement; a quite considerable reduction of capacity and increase in general circuit efficiency can be achieved by putting the inductances in the vacuum along with the accelerators. However, these improvements can hardly decrease the capacity per accelerator by much more than a half.

It is evident, therefore, that recourse must be taken to the use of several oscillators in parallel, each exciting a separate group of accelerators. Experiments are now under way to develop this idea. A new tube under construction has a longer accelerating system divided into two sections, the first 36 accelerators being driven by one radio frequency power amplifier, the next set of 20 accelerators being energized by another amplifier, both being excited by a master oscillator which thereby keeps the voltage on all accelerators in phase. The electrode construction is of much lower resistance and capacity and should withstand an applied potential of 80,000 volts at a wave-length of 27 meters. An average current of more than 10^{-7} amperes of singly charged Hg ions should thus be produced with energies of about 4,500,000 volt-electrons. The use of multiply charged ions, as in the earlier work, should greatly increase the ion speeds obtainable. Triply charged Hg ions traversing the accelerating system of the tube now being built would possibly gain 8,000,000 volt-electrons of energy.

If these next experiments are successful, they will be regarded as strong evidence that the experimental limit to the obtainable ion speeds is determined simply by the length of the tube and the number of oscillators. For example, it is estimated that 10,000,000 volts singly charged Hg ions would be produced by an accelerating system 40 feet long with 8 power amplifiers in parallel.

We are much indebted to the Federal Telegraph Company through the courtesy of Dr. Leonard F. Fuller, Vice-President, for the loan of essential equipment. One of us (D. H. S.) also is grateful to the Coffin Foundation for the award of a fellowship.

PHOTOELECTRIC AND THERMIONIC EMISSION FROM COBALT

By Alvin B. Cardwell
Department of Physics
University of Wisconsin

(Received October 27, 1931)

Abstract

The total photoelectric emission from a strip of cobalt foil excited by the undispersed radiation from a quartz mercury arc was studied during an extended outgassing process and after stable conditions had been reached. The sensitivity rose quickly in the initial period, then decreased to a stable value. A change in the long-wave limit consistent with the change in the sensitivity was observed. Curves are plotted showing the variation of the full arc sensitivity with temperature. At a temperature near 850°C abrupt changes in these curves were observed. X-ray analyses seemed to indicate that this resulted from a structural change. The long-wave limit for cobalt which had been cooled suddenly from above 850°C and which was known by x-ray analysis to have a face-centered cubic structure was between 2967A and 3022A (4.25 ± 0.08 volts). A sample which was cooled slowly from above 850°C and which was known from x-ray analysis to have a hexagonal close pack structure had a long-wave limit between 2757A and 2967A (4.12 ± 0.04 volts). A plot of the thermionic current as a function of temperature indicates that there is an abrupt change in the Richardson (A) or (b) and perhaps both at a temperature near 850°C.

IN A previous paper[1] the writer presented a brief account of some studies on the electron emission from carefully outgassed cobalt. An interpretation of the results indicated that the structural change, in the case of a "gas-free" sample, occurred at a somewhat higher temperature than had previously been observed[2,3] for a gas-filled sample. It therefore seemed wise to extend the observations. The present paper is a brief report including investigations of the following: (1) The variation of the photoelectric sensitivity and long-wave limit of cobalt as it undergoes a process of outgassing by extended heat treatment. (2) The effect of temperature and a structural change on the photoelectric sensitivity and long-wave limit. (3) The effect of the structural change on the thermionic emission.

Apparatus

The apparatus was identical with that used in the previous work. A ribbon of cobalt 0.03 mm thick, 3 mm wide, and 18 cm long was rolled from a sample of Kahlbaum cobalt which was known, from a chemical analysis, to be more than 99.9 percent pure. Tungsten leads, through which a current for heating the filament could be passed, served as a means of supporting the sample in a molybdenum collecting cylinder. Through a small window cut in

[1] Cardwell, Proc. Nat. Acad. Sci. 15, 544 (1929).
[2] Masumato, Sci. Rep. Tohoku Univ. 15, 449 (1926).
[3] Schulze, Zeits. f. tech. Physik 9, 365 (1927).

the central part of the cylinder, the undispersed radiation from a vertical Cooper-Hewitt quartz mercury arc could be focused onto the sample. A quartz window was sealed directly to the Pyrex tube by means of a graded quartz-to-Pyrex seal. Condensation of cobalt onto this window, during the intervals when the sample was being heated, was prevented by means of a magnetically controlled door over the opening in the cylinder. A Compton quadrant electrometer, shunted with a high resistance made of fused cupric oxide and soda glass, was used to measure the currents. Pressures in the early stages of the outgassing process were measured with a McLeod gauge and in the later stages with an ionization manometer. An optical pyrometer of the disappearing filament type served as a means of measuring the temperatures. However, since no very reliable emissivity data are available, the temperatures could not be very accurately determined.

Procedure

The entire tube and gauge were baked at 525°C until the pressure became 10^{-6} mm of Hg or better. This usually required about 100 hours. By means of conduction currents the strip was then heated at temperatures which were very slowly increased from 700° to 1100°C. Beginning at this low temperature and gradually increasing to a higher one enormously increased the life of the filaments. Samples which were started at 1000°C lasted only a few hours.

Frequent observations of the photoelectric sensitivity and long-wave limit were taken as the heat treatment progressed. The threshold frequency was determined by the use of absorption cells in the path of the incident light. Absorption limits for solutions which cut off just above and just below the threshold frequency were determined by using a quartz spectrograph. The threshold was placed between these limits. In every case the electrometer sensitivity was increased for these observations, and in many cases the rate-of-charge method was utilized.

At intervals the sample was allowed to stand at room temperature while observations were taken on the change in sensitivity as gas formed on the surface of the cobalt. Curves of this kind are usually called "fatigue curves."

Finally, after a stable condition had been reached, data for the thermionic and photoelectric-temperature curves were taken.

Results

The effect of heat treatment on the photoelectric emission from one particular sample is shown in Fig. 1. This curve may be considered as typical of the several filaments for which readings were taken. In some cases the time required to reach stable conditions was less but in every case the general form of the outgassing curve was the same as that shown in Fig. 1. The points on this curve show the emission from the cold filament immediately after the heating current had been discontinued. At several points on the curve the long-wave limit has been indicated.

In Fig. 2 are shown several fatigue curves which were taken at various intervals during the outgassing process. On each curve is indicated the num-

ber of hours of outgassing to which the sample had been subjected at the time it was taken.

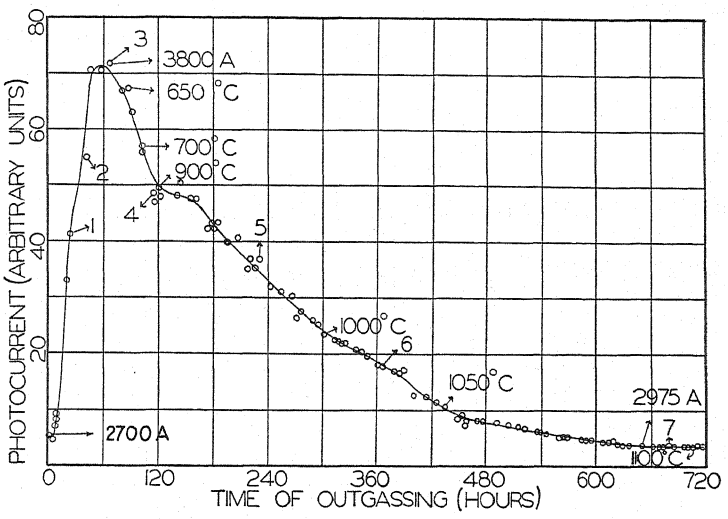


Fig. 1.

The pressures varied a great deal during the outgassing process. In the initial stages of this treatment the ionization gauge showed great increases in

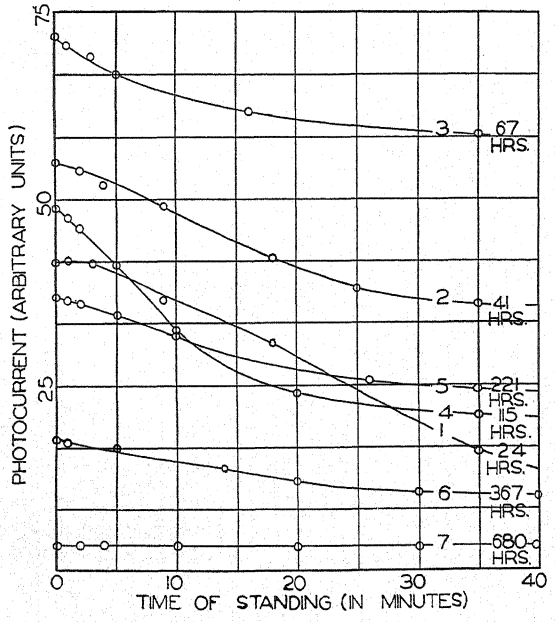


Fig. 2.

pressure while the filament was being heated. These increases became smaller and smaller as the outgassing progressed, and finally the pressure with the

specimen hot was not different from the pressure with the specimen cold. The final pressures obtained were 1 to 3×10^{-8} mm Hg.

Data for Figs. 3, 4, 5, and 6 were taken after the sample had gone through the entire outgassing process, and thus after it had reached a stable condition.

Fig. 3* shows the change in the photoemission with the heating current through the sample at the time observations were made. The temperatures corresponding to two points have been indicated. In connection with Fig. 3 it is important to notice that cobalt having either of two photoelectric sensitivities may exist at room temperature. Cooling suddenly (in a fraction of a second) from temperatures above 850°C produced a surface having a greater

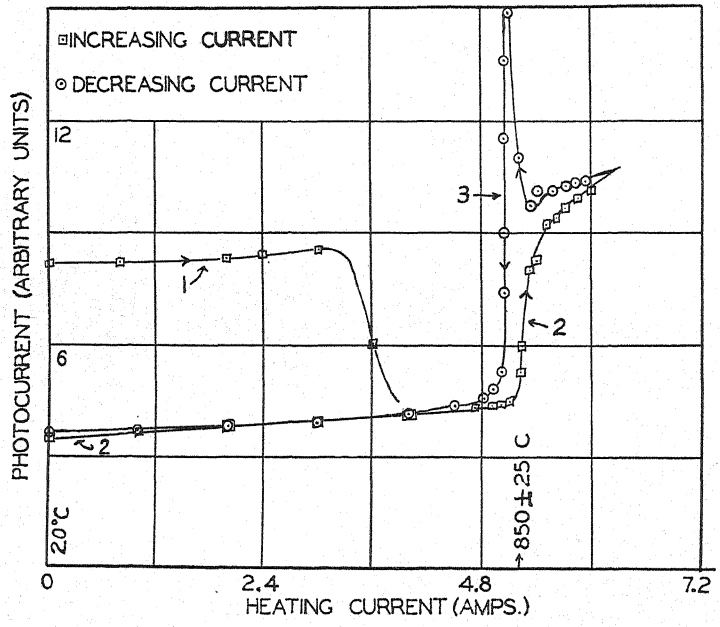


Fig. 3.

sensitivity (curve 1, Fig. 3) than that produced by cooling very slowly. In the former case the switch controlling the heating current was opened, thus allowing the filament to cool very rapidly. In the latter case the current was gradually diminished during an interval of a few minutes to a zero value by means of a variable external resistance.

An x-ray analysis of a slowly cooled and a suddenly cooled sample showed respectively a hexagonal close-packed and a face-centered cubic structure. Hence curve 1 of Fig. 3 shows the variation of the photosensitivity with temperature for a sample which existed at room temperature in the face-centered cubic form, whereas curve 2 shows the analogous change for a sample which

* Fig. 3 is similar to the curve published in the previous article.

existed at room temperature in the hexagonal close-packed form. To avoid confusion, points for curve 1 have not been plotted beyond a temperature corresponding to a heating current of 3.5 amperes. The variation from this point was essentially identical with that shown in curve 2.

The photoelectric sensitivity as a function of decreasing temperatures is plotted in curve 3 of Fig. 3. For a detailed discussion of the time characteris-

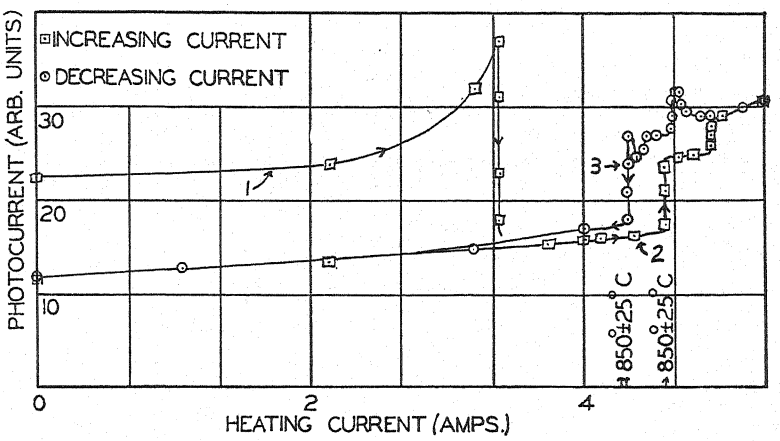


Fig. 4.

tics of such a curve, the reader is referred to the preliminary report.[1] A set of curves similar to those in Fig. 3, but for a sample which was not uniform in thickness, is reproduced in Fig. 4. The filament on which these observations were made was suspended at such an angle with respect to the window that the radiation struck portions of both halves of the loop. When one considers the fact that the two halves of the loop were at different temperatures, curves

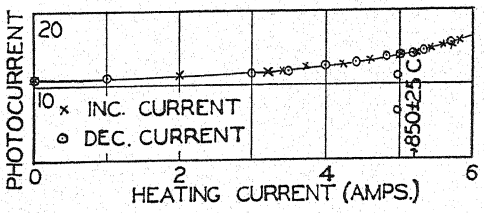


Fig. 5.

2 and 3 of this figure seem quite consistent with the corresponding curves in Fig. 3. Curve 1 is, however, slightly different in the two cases. This point will be discussed later.

It was thought that the marked change in the photocurrent with temperature might be a direct result of a change in the reflecting power of the cobalt strip. In an effort to get some information on this point, the photocurrent produced from the cylinder by radiation reflected from the cobalt was measured as a function of the temperature of the filament. To obtain such a

curve, it was only necessary to make the cylinder negative with respect to the filament. The light had already been carefully focused onto the cobalt. The results of this investigation are shown in Fig. 5. Obviously the large changes observed in the photoelectric current cannot be accounted for by a change in reflecting power.

By means of absorption solutions, the threshold wave-length for hexagonal cobalt—produced by a slow cooling process—was found to lie between 2757A and 2967A. Similarly, the threshold for the face-centered cubic form—produced by rapid cooling—was between 2967A and 3022A. Hence the work functions for hexagonal and face-centered cubic cobalt at room temperature may be placed respectively at 4.12 ± 0.04 volts and 4.25 ± 0.08 volts. In obtaining the data for Fig. 1 the sample was in every case cooled rapidly; hence

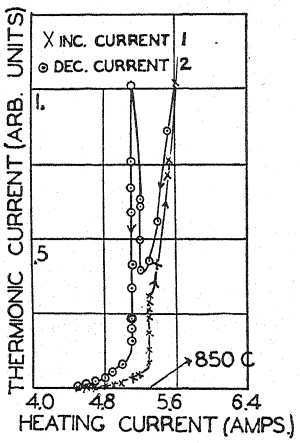


Fig. 6.

the threshold indicated on that curve for the outgassed sample corresponds to that given above for the cubic form.

Curves 1 and 2 of Fig. 6 show the values of the thermionic current for increasing and decreasing temperatures. The current sensitivity of the electrometer was increased approximately thirty-fold for these observations. However, for comparison purposes, the deflections have been reduced so that the scale in absolute magnitude is identical with that used in Fig. 3. It can be seen that the maximum thermionic current is in reality only about 1/15 of the maximum photocurrent. It should be stated at this point that the curves in Figs. 3 and 4 have been corrected for thermionic emission and therefore represent the net photoemission.

Discussion

Two things of particular interest are shown in Figs. 1 and 2. As in the case of platinum, molybdenum, iron, silver, and gold, the change in the photosensitivity is consistent with the shift in the long-wave limit. The fatigue curves are, however, rather peculiar in their behavior. In spite of the fact that

the photosensitivity was decreasing during the second stages of the outgassing process, the fatigue curves always showed a decrease in sensitivity with time of standing. One could account for a behavior as is shown in these fatigue curves by assuming that during the initial stages of the heat treatment one kind of gas was liberated, whereas during the second part another kind of gas was driven from the surface, and that always the former gas settled (perhaps because it had a smaller reflection coefficient) on the surface much more rapidly than the latter.

Evidences for believing that metals which have undergone severe heat treatments in a very high vacuum are "gas-free" and thus yield results which are characteristic of the metals themselves have been discussed in several papers. Characteristics on which like arguments would be made in the case of cobalt are as follows: (a) The photosensitivity and long-wave limit reached a constant value which did not change with more heat treatment. (b) While in this so-called gas-free condition no fatigue could be detected during one hour of standing. (c) The pressures indicated by the sensitive ionization gauge were independent of the temperature of the filament.

The x-ray evidence presented in this paper leads one to associate the abrupt changes in the photoelectric and thermionic curves at a temperature of 850°C with a crystallographic change. Quite analogous changes have been reported in the case of iron[4] and tin.[5]

Cobalt has long been known to exist in two forms. The hexagonal close-packed, which is the normal structure at low temperatures, changes to the face-centered cubic form at temperatures which vary a great deal with the purity of the samples. Schulze[2] and Masumato[3] studied several samples which showed structural changes at various temperatures between 300°C and 600°C. They found that the temperature at which the transition occurs increases with the purity of the sample used. None of the samples for which they published analyses was as pure as the sample used in the present work. One might therefore expect this specimen to have its transition point at a higher temperature than any reported by them. Furthermore, it is quite possible that the gas contained in the cobalt samples used by these workers acted in the same way as metallic impurities, thus further lowering the transition temperature observed by them. At present, this point is being investigated in this laboratory. It should be pointed out that the structural change for a sample of the present cobalt which has received no outgassing occurred at about 570°C.

The peaks (curves 3 of Fig. 3 and 2 of Fig. 6) which occur as the face-centered cubic lattice changes to the hexagonal can be explained by assuming that during the transition from one crystal lattice to another there exists an intermediate structure which is much more sensitive both photoelectrically and thermionically than either of the stable crystal forms. A condition corresponding to the high sensitivity observed for decreasing temperatures does

[4] Cardwell, Proc. Nat. Acad. Sci. **14**, 439 (1928).
[5] Goltz, Phys. Rev. **33**, 373 (1929).

not develop while the temperature is rising, indicating that the intermediate structure may be different in the two cases.

The decrease in the sensitivity with rising temperature as shown in curve 1 of Fig. 3, no doubt occurs as the less stable face-centered cubic cobalt, produced by super-cooling from above 850°C, changes into the more stable hexagonal close-packed form. Since this structural change is identical with that for which the unusually high sensitivity was observed at a higher temperature (curve 3, Fig. 3), one might expect that such a peak would appear in this curve. Such is the case in the corresponding curve of Fig. 4. However, such peaks were not observed in the case of any of the other four samples investigated.

In Fig. 4 two distinct points (near a heating current of 4.3 amperes) at which rather sharp changes in the sensitivity occur, are shown in both the increasing and decreasing temperature curves. It has already been pointed out that for any given heating current one loop of the filament was hotter than the other, and that the radiation struck both halves of the loop. The curves show clearly that the two sides changed at different heating currents, thus producing the two abrupt changes in each curve.

The upward shift in the thermionic curve at 850°C can be accounted for by a change in either the A or b of Richardson's equation. However, Richardson[6] and DuBridge[7] have pointed out that these two change together. One is therefore led to the conclusion that the thermionic work function for face-centered cubic is smaller than the work function for hexagonal cobalt. This conclusion is quite in agreement with the change in the photoelectric threshold which was observed.

Although the above explanation seems quite self-consistent and satisfactory, lack of x-ray analysis of the samples while hot makes it impossible to state positively that the structural change occurs near 850°C. It has been suggested that the abrupt change at this temperature may be due to the formation or breaking down of a surface gas layer or compound. However, as has already been pointed out, the changes which occur in the photoelectric sensitivity of iron and tin, as they go through a structural change, leads one to believe that the change in this case is due to a crystallographic transformation.

In conclusion, the writer desires to express his appreciation to Dr. C. E. Mendenhall under whose guidance this work was done.

[6] Richardson, Proc. Roy. Soc. **A91**, 524 (1927).
[7] DuBridge, Proc. Nat. Acad. Sci. **30**, 705 (1927).

THE PHOTOELECTRIC PROPERTIES OF TANTALUM

By Alvin B. Cardwell
Department of Physics
University of Wisconsin

(Received October 27, 1931)

Abstract

Tantalum was carefully outgassed and it's photoelectric properties studied after stable conditions were reached. Heating 1000 hours at temperatures up to 2200°K produced an apparent stable condition of the surface. Curves, showing the variation of the photoelectric current as a function of the temperature, are plotted for different wave-lengths. For wave-lengths near the threshold, there is a great increase in the photoemission with increasing temperature. With decreasing wave-lengths, this variation becomes very much smaller. Extrapolated values from the $F(\lambda)$ curves show the long-wave limit to be at 20°C, 2750A; and at 700°C, 2825A. Further heat treatment at temperatures up to 2500°K produced a final stable condition. Here again are plotted curves showing the variation of the photoelectric current as a function of the temperature for different wave-lengths. In this case, the great increase in the photoelectric sensitivity with temperature for wave-lengths near the threshold becomes smaller as the wave-lengths used decreases, finally reaching negative values for wave-lengths more than 300A shorter than the threshold value. Extrapolated values from $F(\lambda)$ curves taken at 293°K and 973°K show the long-wave limit at the respective temperatures to be 3050A and 3160A. From curves plotted according to Fowler's theory, the true threshold wave-lengths were found to be as follows: (1). For tantalum in first apparent stable condition (average = 2742A (4.50 volts). (2). For tantalum in final stable condition (average) = 2974A (4.15 volts).

IN A recent paper Professor R. H. Fowler[1] developed a theory for the effect of temperature on the photoelectric sensitivity of a clean metal near the threshold. As a part of the experimental evidence offered in substantiation of the theory the writer was delighted to supply Professor Fowler with some data on tantalum which, although taken more than a year ago, had never been published. The present paper is a report of these results along with a description of the photoelectric and gas characteristics of the metal as it went through a very extensive outgassing process.

Apparatus

The apparatus used in the present work was only slightly different from that used by numerous other investigators. A schematic diagram of the experimental tube and ionization gauge is shown in Fig. 1. The strip to be tested consisted of a ribbon of tantalum 0.03 mm thick, 4 mm wide, and 18 cm long, suspended in the form of a loop by the tungsten leads *W*. *C* is a molybdenum receiving cylinder connected by means of a flexible molybdenum lead to the collecting electrode *L*. The quartz window *Q* is sealed directly to the Pyrex

[1] Fowler, Phys. Rev. **38**, 45 (1931).

tube by means of a graded joint. Just opposite this window is a circular opening in the cylinder. By means of a magnetically controlled iron door this opening could be covered while the sample was being heated to high temperatures. This prevented the distillation of metal onto the quartz window. The insulated ring G supported by the heavy tungsten wire T was always kept at the same potential as C. Thus it was possible to measure only the current from the portion of the loop which had been subjected to a rather uniform heat treatment. The ionization gauge is of the general type described by Dushman and Found.[2]

Photoelectric currents were measured by a Compton quadrant electrometer having a sensitivity of 30,000 mm per volt. A high resistance made of

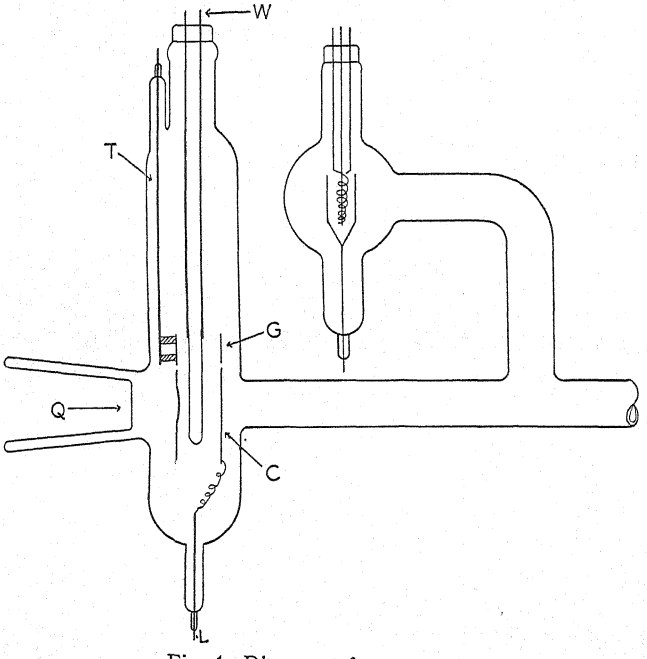


Fig. 1. Diagram of apparatus.

fused soda glass and cupric oxide[3] was shunted across the quadrants so that the steady deflection method could be used.

During a great part of the outgassing period the source of light was the undispersed radiation from a vertical Cooper-Hewitt quartz mercury arc. For a study of the characteristics during the latter part of the period, a Bausch and Lomb quartz single monochromator was placed between the arc and the tantalum sample. Mr. J. H. Dillon[4] had made a study of the particular monochromator used, finding that the impurity of the dispersed radiation (with slit widths 0.02 mm) was not sufficient to produce appreciable errors in

[2] Dushman and Found, Phys. Rev. **23**, 743 (1924).
[3] Andrewes, Davies, and Horton, Proc. Roy. Soc. **A117**, 649 (1928).
[4] Dillon, Phys. Rev. **38**, 408 (1931).

the $F(\lambda)$ curve. The relative intensities of the mercury lines were determined by a thermopile connected to a Leeds and Northrup low resistance galvanometer.

Temperatures were measured by an optical pyrometer of the disappearing filament type, which had been calibrated by observations upon the gold point and the palladium point. Black-body temperatures were corrected for the emissivity of tantalum according to data by Mendenhall and Forsythe.[5]

The tantalum filaments, obtained from the Fansteel Company of North Chicago, were made from a very pure sample of the metal.

Procedure and Results

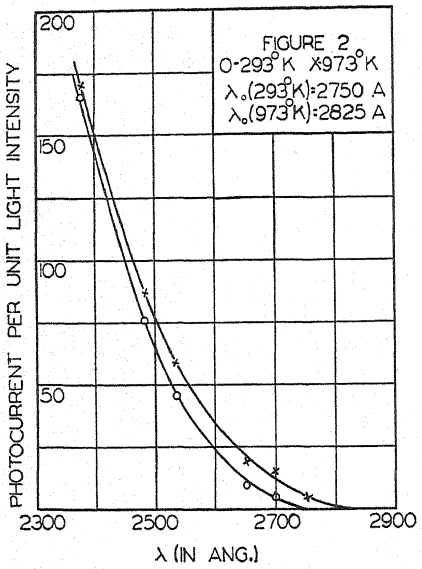
The receiving cylinder was placed in an auxiliary vacuum system where it was heated to 900°C for five days by electronic bombardment. It was then transferred to the experimental tube and sealed in the vacuum system with the sample. The tube and gauge were then encased in an electric furnace and baked for 20 days at 500°C. During the last fourteen days of this interval the filament was heated by a conduction current at temperatures which were slowly increased up to 1400°C.

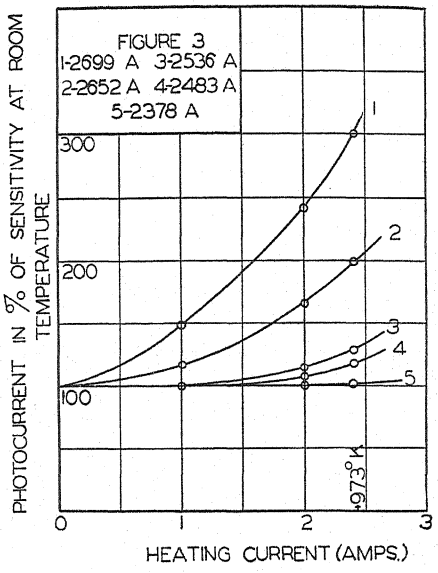
At the end of this twenty-day period the furnaces were removed and the tube was properly shielded for photoelectric observations. The full arc sensitivity varied a great deal, and in a most irregular fashion, during the next few hundred hours of heat treatment. It was only after approximately 1000 hours of heat treatment at temperatures up to 2200°K that the sample showed indications of becoming photoelectrically stable. This is, (1) no further change in its full arc sensitivity resulted with 100 additional hours of heat treatment at the same temperature, and (2) during a one-hour interval no fatigue was observed. At this point attention should be called to the fact that, although the latter condition has been found up to the present to be characteristic only of surfaces which seemed to be gas-free, the surface in this case was not gas-free. This point will be clarified in what follows.

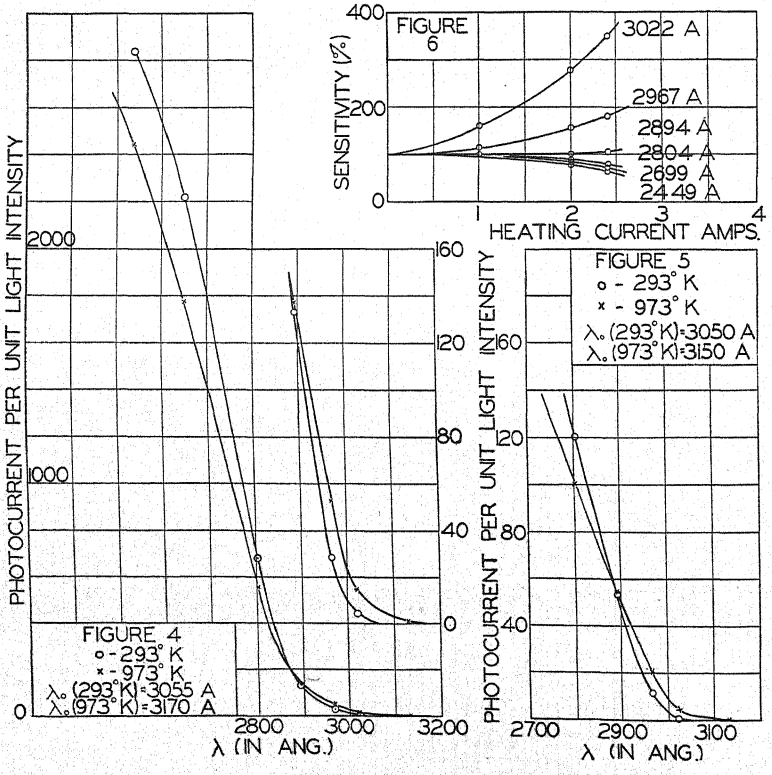
While the sample was in the somewhat stable condition described above, the monochromator was adjusted so that a further study could be made. Fig. 2 shows the $F(\lambda)$ curves for two temperatures. The extrapolated values for the threshold wave-length at the two temperatures have been indicated in the figure. A study of photoelectric sensitivity for individual lines as a function of the temperature is shown in Fig. 3. It is quite obvious that the curves in Figs. 2 and 3 are entirely consistent and that an $F(\lambda)$ curve for any temperature within the range covered can be plotted from the data used in obtaining the curves in Fig. 3.

After several curves, identical with those reproduced in Figs. 2 and 3, were taken, the temperature of the sample was increased to 2300°K. Heating 12 hours at this temperature produced a shift in the threshold toward the red. Fifty hours' additional heat treatment at temperatures up to 2500°K produced no further change in the photoelectric characteristics. It is therefore believed that the metal in this condition was gas-free.

[5] Mendenhall and Forsythe, Astrophys. J. **37**, 380 (1913).


FIGURE 2
0-293°K X-973°K
λ₀(293°K)=2750 A
λ₀(973°K)=2825 A
PHOTOCURRENT PER UNIT LIGHT INTENSITY
200
150
100
50
2300
2500
2700
2900
λ (IN ANG.)


FIGURE 3
1-2699 A 3-2536 A
2-2652 A 4-2483 A
5-2378 A
PHOTOCURRENT IN % OF SENSITIVITY AT ROOM TEMPERATURE
300
200
100
1
2
3
4
5
973°K
0
1
2
3
HEATING CURRENT (AMPS.)


FIGURE 6
SENSITIVITY (%)
400
200
0
3022 A
2967 A
2894 A
2804 A
2699 A
2449 A
1
2
3
4
HEATING CURRENT AMPS.
FIGURE 4
o - 293° K
x - 973° K
λ₀ (293°K)=3055 A
λ₀ (973°K)=3170 A
PHOTOCURRENT PER UNIT LIGHT INTENSITY
2000
1000
0
160
120
80
40
0
2800
3000
3200
λ (IN ANG.)
FIGURE 5
o - 293° K
x - 973° K
λ₀ (293°K)=3050 A
λ₀ (973°K)=3150 A
PHOTOCURRENT PER UNIT LIGHT INTENSITY
160
120
80
40
2700
2900
3100
λ (IN ANG.)

The data for the $F(\lambda)$ curves in Figs. 4 and 5* were taken after the sample had been subjected to this severe heat treatment. In Fig. 4 the points near the threshold are replotted on a much larger scale just above the regular curve. Again the extrapolated values for the threshold frequencies have been indicated in the figures. The crossing of the high and low temperature curves show that the variation of the photoelectric emission with temperature is quite different for various individual wave-lengths. Fig. 6 brings this out much more clearly.

In Fig. 5, the change in slope near the shorter wave-lengths suggests that the $F(\lambda)$ curves may be approaching a maximum value. This would be in agreement with the theoretical deductions of Wentzel,[6] Frohlich,[7] and Tamm

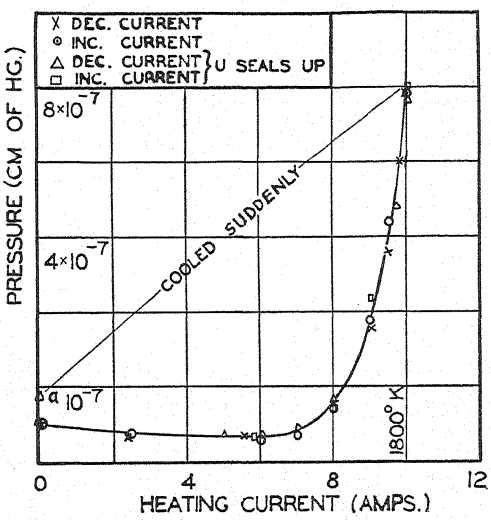


Fig. 7. Equilibrium pressure as a function of the heating current through the filament.

and Schubin[8] that in all cases such curves should have a maximum. Data for much shorter wave-lengths would be desirable to clarify this point.

Throughout the greater part of the outgassing process the pressures underwent rather striking changes as the temperature of the filament was changed. Fig. 7 is a characteristic curve showing the equilibrium pressure as a function of the heating current through the sample. It should be pointed out that one complete set of the data shown graphically was taken while the tube and gauge were "cut off" from the pumping system by means of a mercury U-seal. Clearly, the equilibrium pressure was identical in the two cases. It should also be stated that within wide limits the rapidity with which the heating current was changed made no difference in either the final equilibrium pressure or the time required to reach that pressure. Usually this

* Fig. 5 is identical with that reproduced by Fowler.

[6] Wentzel, Sommerfeld's Festschrift, p. 20 (1928).

[7] Frohlich, Ann. d. Physik **7**, 103 (1930).

[8] Tamm and Schubin, Zeits. f. Physik **68**, 97 (1931).

equilibrium value was reached within an interval of 12 seconds after the heating current was changed. In fact, in only one case was an exception to the above statement observed. The pressure 12 seconds after a heating current of 10 amperes was broken (thus allowing the sample to cool very rapidly to room temperature) was greater (point a, Fig. 7) than when the current was gradually decreased to zero during an interval of 30 seconds. When the sample was suddenly cooled, about 3 minutes elapsed before the pressure decreased to a value corresponding to that reached by the slower cooling process. Here again these values were practically independent of whether the U-seal was or was not closed.

TABLE I.

Temperature °K	λ (A)	Photo-current per unit light intensity	$h\nu/kT$	log I/T^2	log $I/T^{3/2}$	$h\nu_0/kT$	λ_0 (A)	Work function (volts) (Average)
(a) Sample in first apparent stable condition (Fig. 2)								
293	2699	5.0	181.0	−9.75	−6.91	—	Theory 1	
	2652	11.0	184.5	−8.96	−6.12	177.3	2750	
	2537	46.0	192.5	−7.53	−4.69	—		4.53
	2480	76.0	197.0	−6.93	−4.19	—	Theory 2	
	2376	166.0	206.0	−6.25	−3.41	179.3	2725	
973	2754	5.0	53.6	−12.15	−8.71	—	Theory 1	
	2699	14.5	54.6	−11.09	−7.65	53.5	2745	
	2652	20.0	55.6	−10.75	−7.32	—	—	4.49
	2537	59.0	58.1	−9.68	−6.24	—	Theory 2	
	2480	87.0	59.4	−9.27	−5.83	—	—	
	2376	170.0	62.1	−8.62	−5.18	53.4	2750	
(b) Sample in final stable condition (Fig. 4)								
293	3022	4.5	161.5	−9.856	−7.016	—	Theory 1	
	2967	28.7	164.6	−8.003	−5.163	163.0	3000	
	2894	133.0	169.0	−6.470	−3.630	—		4.12
	2804	680.0	174.3	−4.838	−1.998	—		
	2652	2220.0	184.5	−3.655	− .815	—	Theory 2	
	2537	2840.0	192.5	−3.409	− .569	163.5	2990	
973	3132	1.5	47.1	−13.355	−9.915	—	Theory 1	
	3022	14.5	48.7	−11.086	−7.646	50.0	2942	
	2967	53.0	49.7	−9.790	−6.350	—		4.19
	2894	137.0	50.9	−8.841	−5.401	—		
	2804	555.0	52.5	−7.442	−4.002	—	Theory 2	
	2652	1780.0	55.6	−6.276	−2.836	50.0	2942	
	2537	2440.0	58.1	−5.961	−2.521	—		
(c) Sample in final stable condition (Fig. 5)								
293	3022	1.0	161.5	−11.360	−8.520	—	Theory 1	
	2976	11.6	164.6	−8.909	−6.069	162.5	3005	
	2894	53.2	169.0	−7.386	−4.546	—	Theory 2	4.13
	2804	120.0	174.3	−6.573	−3.733	163.0	3000	
973	3132	.3	47.1	−14.965	−11.524	—	Theory 1	
	3022	4.5	48.7	−12.257	−8.816	49.5	2970	4.18
	2967	20.9	49.7	−10.721	−7.281	—		
	2894	53.3	50.9	−9.748	−6.308	—	Theory 2	
	2804	100.0	52.5	−9.155	−5.715	50.0	2942	

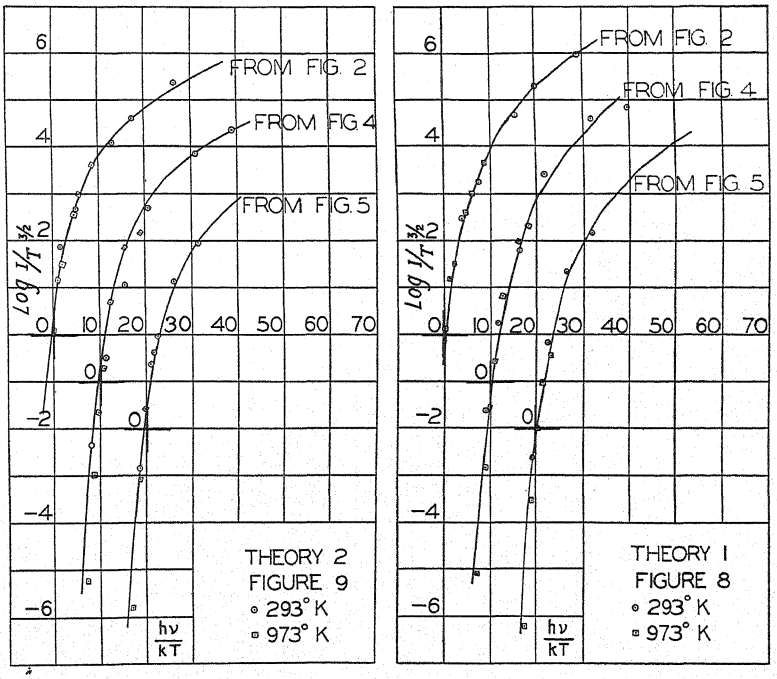
Data for the curves shown in Fig. 7 were taken after the sample had been outgassed 480 hours. With further heat treatment the equilibrium pressures became smaller and the pressure-heating current curves approached nearer and nearer a straight line with a zero slope. The pressure at the end of 1000 hours of heat treatment was 10^{-8} mm of Hg. This corresponds to a galvanometer deflection of only 1 mm. It is therefore impossible to say that the final pressures were *absolutely* independent of the temperature of the filament. A change of 10 to 15 percent could not have been detected.

Tantalum greedily absorbs hydrogen[9] when heated to redness, thus forming the hyride, and nitrogen[10] has been found to react with it at high temperatures (up to 1200°C) forming the nitride. Consequently, there is a possibility that the minimum value of the pressure in the pressure-temperature curve (See Fig. 7) is a direct result of one or both of these chemical actions.

The peculiar affinity of tantalum for hydrogen and nitrogen, and the gas characteristics reported herewith cast somewhat of a doubt as to the "cleanness" of the surface. It is quite possible that at least one, and perhaps both, of the stable conditions reported herewith are characteristic of tantalum with a stable compound on the surface. It is hoped that the thermionic data will give some additional information on this point.

Application of Fowler's Theory

In Fowler's paper, to which reference has already been made, the shift in the long-wave limit with temperature is completely accounted for by the change of the energy distribution of the electrons with temperature. A graphical method is given enabling the whole of the observed points near the threshold for all temperatures to be used in determining the "true threshold" wave-length. By true threshold is meant the threshold which would be observed if the metal were at absolute zero.



In Table I a summary of data from which such an analysis can be made is given. For Fowler's first theory the general method is as follows. First, the

[9] W. von Bolton, Zeits. f. Elektrochem. **11**, 47 (1905).
[10] W. Muthmann, Liebig's Ann. **355**, 62 (1907).

theoretical curve is plotted, then log I/T^2 is plotted against $h\nu/kT$, the scales of the log and $h\nu/kT$ being the same. The origin is then adjusted so as to bring as nearly as possible the observed points into coincidence with the theoretical curve and the points transferred to the theoretical curve. From the $h\nu/kT$ shift the threshold frequency, ν_0, is calculated. Exactly the same procedure is followed for theory 2 except in this case T^2 is replaced by $T^{3/2}$. Fig. 8 shows the curves obtained, on the basis of theory 1 as described above, from data taken on the metal while in both the first state of apparent stability and the final state of stability (Figs. 2, 4, and 5). Similar curves on the basis of theory 2 are reproduced in Fig. 9. The values of the threshold as determined by the shift in the abscissa are shown in Table I. The values for the metal in the final stable state (Figs. 4 and 5) are almost identical with Dushman's[11] value of 4.01 volts for the thermionic work function. In every case the general agreement of the actual points with the theoretical curves is quite good. It is interesting to note that the theory seems to hold to the same degree of accuracy for the metal in both the final state and first state of apparent stability (Figs. 2, 8 and 9).

Fowler[1] discussed the change in slope which leads to the intersection of the curves shown in Figs. 4 and 5, but was unable to arrive at any reasonable explanation. The fact that both gold[9] and silver[10] show a similar crossing, to a much less degree, however, leads one to believe that the effect is a normal one for clean metals. No crossing was observed for the metal while in its first apparent stable condition. There is, however, a possibility that the curves might have crossed had observation been made with much shorter wavelengths.

In conclusion, it is a pleasure to thank Professor Mendenhall under whose invaluable guidance the experiment was performed.

[11] Dushman, Phys. Rev. **25**, 338 (1925).

THE DIELECTRIC CONSTANT OF COMMERCIAL NITROGEN AT HIGH PRESSURES

By James W. Broxon
University of Colorado

(Received October 15, 1931)

Abstract

The dielectric constant of commercial nitrogen, 99 percent pure, was measured at pressures up to 167 atmospheres by the same electrometric method previously employed by the writer in the determination of K for air. $(K-1)$ was again found to vary directly with the pressure, at the rate of 556×10^{-6} per atmosphere at 16.5°C, with the exception of an apparent slight deviation from linearity in the sense of a smaller rate of increase of K with P at pressures above 150 atmospheres. The greatest departure from linearity was only of the order of the probable error, however, and is not considered to be definitely established.

THE values of the dielectric constant of nitrogen herein presented were obtained from data secured during an investigation of the residual ionization in the gas at high pressures. The method of measurement was precisely the same as that described in detail in a paper[1] dealing with the dielectric constant of air at high pressures.

It was mentioned in the report[2] of the residual ionization measurements that the nitrogen was only slightly more than 99 percent pure. An impurity of only 0.2 percent of argon and oxygen had been claimed by the company manufacturing the nitrogen. Local analysis of the gas actually used showed 0.72 ± 0.02 percent oxygen, however, with no carbon dioxide or water vapor, no test for argon being made. Subsequent analysis of some of the unused nitrogen by the commercial concern showed the greater impurity.

Because the temperature varied between 15.35°C and 17.5°C during the measurements, the observed pressures were reduced to corresponding pressures at 16.5°C rather than 18°C as in the case of the air measurements, and these reduced pressures are shown plotted against the resistance ratios in Fig. 1.

In the case of air the resistance ratio and hence the dielectric constant was found to vary linearly with the pressure over the entire range of the observations. In the case of nitrogen the linear relation is again observed at all pressures below 150 atmospheres. At higher pressures, however, there is an apparent slight deviation from the linear relation in the direction to be expected on the basis of the departure from Boyle's law in that region. According to the experimental curve the dielectric constant of the commercial nitrogen is 1.000556+ at 1 atmosphere and 16.5°C, increasing at the rate of 556×10^{-6} per atmosphere up to 150 atmospheres, above which the pressure-rate of increase is slightly less. The experimental curve gives the value of $K=1.0920$ at 167 atmospheres, whereas if the straight line were continued the value 1.0929 would be obtained.

[1] J. W. Broxon, Phys. Rev. **37**, 1338 (1931).
[2] J. W. Broxon, Phys. Rev. **38**, 1704 (1931).

In view of the discussion of the accuracy of the measurements included in the earlier paper it would seem that the deviation observed in the present instance, amounting to about one percent of $(K-1)$ at 167 atmospheres, may extend only to the neighborhood of the limit of the experimental accuracy. Consequently, there is some doubt relative to the reality of the curvature at the high pressure end of the curve. It is regretted that an entirely independent series of observations extending to higher pressures was not immediately feasible.[3] However, the readings are well distributed over the range of the observations and the linear relation between dielectric constant and pressure in the region below 150 atmospheres is clearly designated.

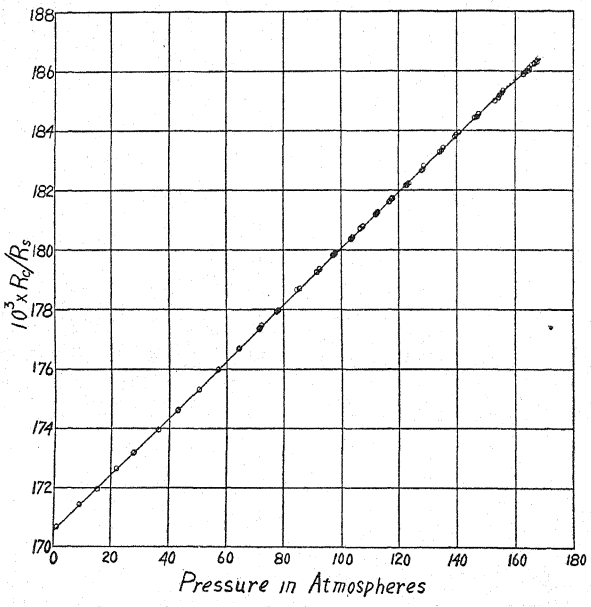


Fig. 1. Resistance ratio for nitrogen.

The relation of these observations to those of other investigators is about the same as in the case of air. Tangl[4] found the Clausius-Mossotti relation to hold for nitrogen at pressures up to 100 atmospheres, while Bodareu[5] arrived at a similar conclusion for the region between 87 and 226 atmospheres. At N.T.P., Tangl found $K=1.000581$ while Bodareu's value, obtained by extrapolation, was 1.000587. If the constancy of $(K-1)/P$ and of P/T is assumed for the region between 0°C and 16.5°C, the corresponding value yielded by the present investigation is 1.000590 for the commercial nitrogen used.

[3] Further work on the dielectric constants of gases at high pressures, including the application of high frequency methods, is in progress.

[4] K. Tangl, Ann. d. Physik **26,** 59 (1908).

[5] E. Bodareu, Accad. Lincei, Atti **22,** 480 (1913). Only an abstract of this paper was available.

MAGNETIC PROPERTIES OF GOLD-IRON ALLOYS

By J. W. Shih
Physics Department, University of Illinois

(Received October 1, 1931)

Abstract

The alloys of gold and iron of different compositions ranging from 0.07 to 10 percent iron by weight have been studied. It was found that the alloys containing 0.1 to 5 percent iron are paramagnetic. Their susceptibilities decrease with rising temperature in a characteristic way, but do not follow either Curie's law or Weiss' law exactly. The square root of susceptibility increases linearly with the percentage of iron atoms added. Thus the gold-iron series does not show the same property as the nickel-copper alloys whose susceptibility increases with temperature in certain ranges. The behavior of the iron atoms in the alloy and some correlations between magnetic susceptibility, density and melting point are discussed.

Introduction

DR. E. H. WILLIAMS[1] of this laboratory has found that alloys of nickel and copper in certain compositions yield paramagnetic substances, in which the paramagnetic susceptibility increases with increasing temperature. This phenomenon also appears in some pure elements such as titanium, chromium, rhodium, boron and one modification of solid oxygen (13°−33°K) but is in conflict with all theories of magnetism. Kamerlingh Onnes[2] has suggested that if paramagnetic atoms unite into a crystal structure, they will only be able to show typical paramagnetic behavior if the carriers are free to change their orientation, but this will be impossible if the magnetic electrons form the binding links which build up the stable crystal structure. Increased temperature, resulting in increased freedom, allows the magnetic carriers to change their orientation under the influence of a field to a greater extent than at low temperature and there may actually be an increase in paramagnetic susceptibility. At the same time the temperature becomes more and more effective in disturbing the magnetic equilibrium. An increasing or decreasing susceptibility will therefore be observed according to the predominating effect. This explanation might be applicable to the nickel-copper alloys, but the question arises as to whether this anomalous paramagnetic phenomenon is a general property of alloys of ferro-magnetic and diamagnetic elements. It would therefore be very interesting to study other alloys of this type to determine whether this anomalous paramagnetic property appears in them likewise. Unfortunately there are only a few pairs of diamagnetic and ferromagnetic metals which lend themselves to such investigations. One of these consists of gold and iron.

[1] E. H. Williams, Phys. Rev. **38**, 828 (1931).

[2] E. C. Stoner, Magnetism and Atomic Structure, E. P. Dutton and Co., New York, 1926, p. 170.

Experimental Details

Pure gold was supplied by Baker and Company and pure iron was kindly furnished by Dr. T. D. Yensen of the Westinghouse Electric and Manufacturing Company. The purity of the former was not guaranteed but the latter was believed to be the purest obtainable in this country. Gold and iron form homogeneous solid solutions[3] in the range 0 to 15 percent iron by weight. The melting point of the alloy depends upon the amount of iron. It has a minimum of about 1040°C for an iron content of about 5 percent. Nine samples of different compositions from 0.07 to 10 percent iron were prepared in an atmosphere of hydrogen (which is insoluble in the alloy). In order to make the alloy very homogeneous the process of melting and cooling was repeated three times for each sample and the ingot was then annealed for two hours. Among all the alloys prepared only the 10 percent specimen changes its color from golden to gray.

The magnetic susceptibility was determined with a Curie balance having an electric control torsion head.[4] The apparatus was calibrated both with distilled water and with cobalt sulphate. The latter was used as practical standard because of its convenience in handling and since its paramagnetic susceptibility[5] is accurately known. The non-uniform field was produced by a large Dubois magnet with two pole pieces specially designed.[6] It was found that these pole pieces gave a region of about two cm in length in which the product $H(\delta H/\delta X)$ is practically constant, where H is the field strength and $\delta H/\delta X$ the field gradient. The value of H at the position of the specimen is about 4500 gausses. The sensitivity of the apparatus depends on the size of the suspension. Phosphor-bronze wire of diameter 0.0202 cm (32 B. & S.) gave about 20 cm deflection at a scale distance of one meter for one gram of water in a field of the above value.

The furnace was such that a temperature of about 1000°C could be obtained. A chromel-alumel thermocouple was used for the temperature measurement. In order to prevent the specimen from oxidizing at high temperatures, hydrogen was passed gently into the furnace during the time of the experiment. The alloy did not lose its lustre after heating, thus indicating that oxidation was completely eliminated.

Results

Nine alloys ranging from 0.07 to 10 percent iron by weight have been measured in the temperature range from 20° to 800°C. Paramagnetism begins for the alloy containing about 0.1 percent iron and continues to a point between 5 and 10 percent iron where it is replaced, at room temperature, by ferromagnetism. The paramagnetic susceptibility decreases first very rapidly and then slowly with rising temperature. The diamagnetic susceptibility of the pure gold is practically constant over the same temperature range. Its

[3] G. Tammann, Zeits. f. anorg. Chem. **53**, 281 (1907).
[4] A. N. Guthrie and L. T. Bourland, Phys. Rev. **37**, 309 (1931).
[5] E. C. Stoner, reference 2, p. 134.
[6] G. Foëx and R. Forrer, Jour. de physique [6], **7**, 180 (1926).

value, as here measured, is -0.148×10^{-6} at room temperature and -0.150×10^{-6} at 800°C. This checks very well with Honda's[7] results. A test on the variation of susceptibility with field has been made on the 5 percent alloy which is important in regarding this effect. It shows that its susceptibility is fairly constant in a wide range of field strength (300-5700 gausses).

TABLE I. *Mass susceptibilities of gold-iron alloys at room temperature.*

Percent of Fe	Suscept., $\chi\times10^6$	Percent of Fe	Suscept., $\chi\times10^6$
0.07	−0.041	2.0	4.33
0.085	−0.023	3.5	12.72
0.1	+0.01	5.0	29.76
0.5	0.559	10.0	Ferromagnetic
1.0	1.52		

Table I gives the susceptibilities of the different alloys at room temperature and their variation with temperature is shown in Fig. 1. In order to show

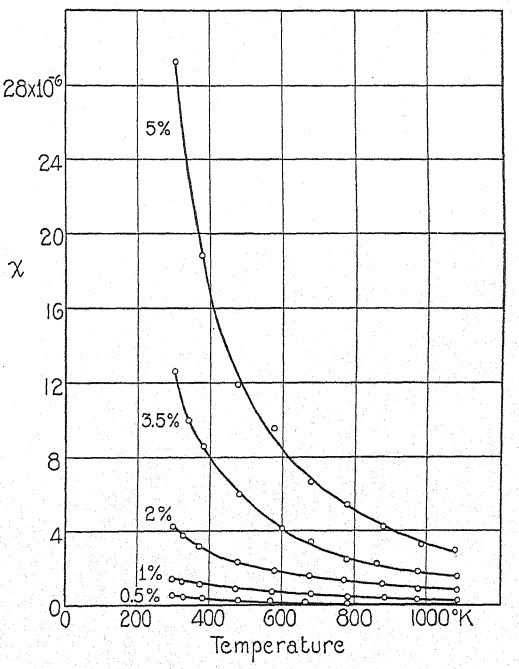


Fig. 1. $\chi-T$ curves for gold-iron alloys.

how the temperature-susceptibility relation deviates from Curie's or Weiss' law, a typical $\chi^{-1}-T$ curve is given in Fig. 2.

Since the volume susceptibility of hydrogen is only about one six-thousandth of that of the 0.5 percent alloy, its maximum possible effect upon the susceptibility is negligibly small. The total error introduced due to the un-

[7] K. Honda, Ann. d. Physik [4], **32**, 1027 (1910).

certainty of the position of the specimen in field, to the fluctuation of field strengths, to the inaccuracy of weighing, etc., is less than 1 percent.

Discussion

The results show that the paramagnetic susceptibility of gold-iron alloys decreases with increasing temperature. It changes in a characteristic way but it follows neither Curie's law nor the Weiss law, exactly. Thus, the gold-iron alloy does not behave in the same way as the nickel-copper alloy. There is no sudden change of susceptibility in the neighborhood of 790° which is the Curie point of pure iron. It seems that the iron atoms lose their ferromagnetic properties in the alloy. Moreover, if the iron atoms remain in their ferromagnetic state only about three ten-thousandths of 1 percent of iron would be necessary to compensate completely all the diamagnetic effect of the gold. But the alloy remains diamagnetic until the iron content amounts to 0.1 percent. This fact is completely in accord with the recent quantum interaction theory[8] of ferromagnetism which deduces the fundamental mechanism of the Weiss molecular field from the resonance between the spinning electrons of neighboring atoms, i.e., if the iron atoms are sufficiently separated they will become nonferromagnetic.

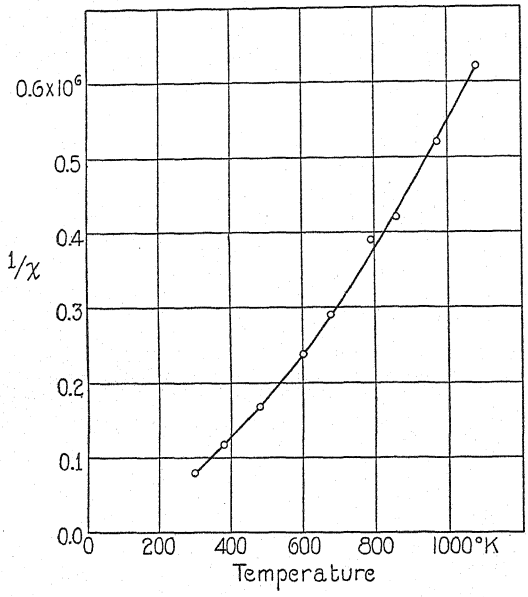


Fig. 2. $\chi^{-1}-T$ curve for the 3.5 percent Fe alloy.

Another interesting result is observed if we plot (Fig. 3) the square root of susceptibility at different temperatures as ordinates and the percentage of iron atoms as abscissas. Except for the point at the lowest iron content the variation of $\chi^{1/2}$ is linear. There is another point [(a), as indicated in Fig. 3]

[8] W. Heisenberg, Zeits. f. Physik 49, 619 (1928).

corresponding to the 5 percent alloy at room temperature, far from the straight line. This, perhaps, is due to the possibility that this alloy begins to become ferromagnetic or it may not be so homogeneous magnetically as the others at the low temperature. Davies and Keeping[9] found in both copper-magnesium and copper-antimony alloys the maximum susceptibilities which correspond to the eutectics. The 5 percent alloy has the lowest melting point and also its density suffers a greater decrease than would be expected from

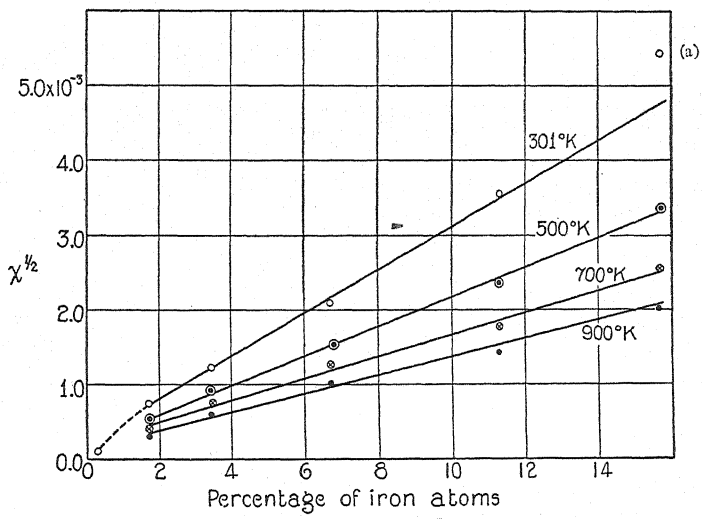


Fig. 3. The square root of susceptibility at different temperatures plotted against the percentage of iron atoms.

the density-percentage curve (not shown). Thus, it may have a peculiarly high susceptibility due to its structure at room temperature, masked by the effect of thermal agitation at high temperature.

In conclusion the writer wishes to express his thanks to Professor J. Kunz for the suggestion of the problem and discussion of the results, and also to Professor E. H. Williams for his valuable help in conducting this investigation.

[9] W. G. Davies and E. S. Keeping, Phil. Mag. [7], **7**, 145 (1929).

certainty of the position of the specimen in field, to the fluctuation of field strengths, to the inaccuracy of weighing, etc., is less than 1 percent.

Discussion

The results show that the paramagnetic susceptibility of gold-iron alloys decreases with increasing temperature. It changes in a characteristic way but it follows neither Curie's law nor the Weiss law, exactly. Thus, the gold-iron alloy does not behave in the same way as the nickel-copper alloy. There is no sudden change of susceptibility in the neighborhood of 790° which is the Curie point of pure iron. It seems that the iron atoms lose their ferromagnetic properties in the alloy. Moreover, if the iron atoms remain in their ferromagnetic state only about three ten-thousandths of 1 percent of iron would be necessary to compensate completely all the diamagnetic effect of the gold. But the alloy remains diamagnetic until the iron content amounts to 0.1 percent. This fact is completely in accord with the recent quantum interaction theory[8] of ferromagnetism which deduces the fundamental mechanism of the Weiss molecular field from the resonance between the spinning electrons of neighboring atoms, i.e., if the iron atoms are sufficiently separated they will become nonferromagnetic.

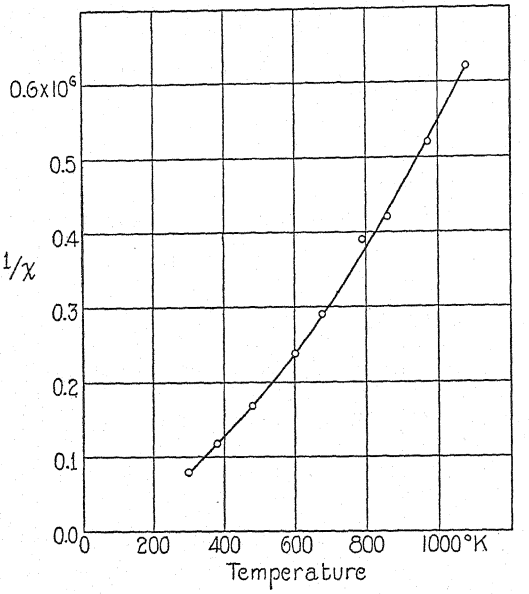


Fig. 2. $\chi^{-1}-T$ curve for the 3.5 percent Fe alloy.

Another interesting result is observed if we plot (Fig. 3) the square root of susceptibility at different temperatures as ordinates and the percentage of iron atoms as abscissas. Except for the point at the lowest iron content the variation of $\chi^{1/2}$ is linear. There is another point [(a), as indicated in Fig. 3]

[8] W. Heisenberg, Zeits. f. Physik 49, 619 (1928).

corresponding to the 5 percent alloy at room temperature, far from the straight line. This, perhaps, is due to the possibility that this alloy begins to become ferromagnetic or it may not be so homogeneous magnetically as the others at the low temperature. Davies and Keeping[9] found in both copper-magnesium and copper-antimony alloys the maximum susceptibilities which correspond to the eutectics. The 5 percent alloy has the lowest melting point and also its density suffers a greater decrease than would be expected from

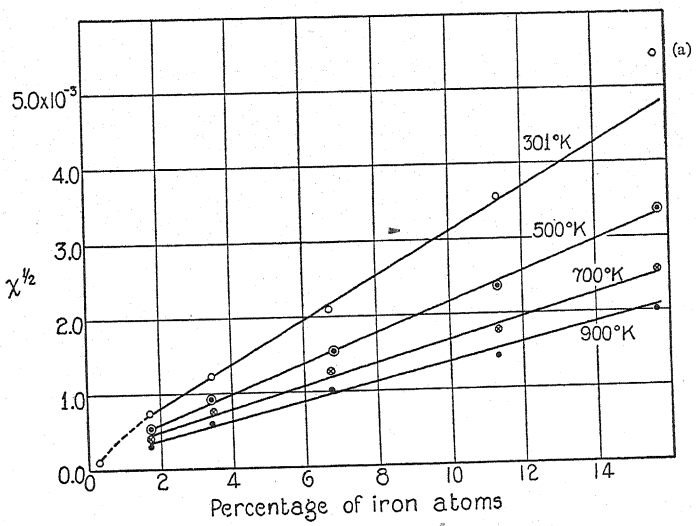


Fig. 3. The square root of susceptibility at different temperatures plotted against the percentage of iron atoms.

the density-percentage curve (not shown). Thus, it may have a peculiarly high susceptibility due to its structure at room temperature, masked by the effect of thermal agitation at high temperature.

In conclusion the writer wishes to express his thanks to Professor J. Kunz for the suggestion of the problem and discussion of the results, and also to Professor E. H. Williams for his valuable help in conducting this investigation.

[9] W. G. Davies and E. S. Keeping, Phil. Mag. [7], 7, 145 (1929).

THE POTENTIAL DUE TO A BURIED SPHEROID

By J. H. Webb
Williams College

(Received August 24, 1931)

Abstract

A series solution of the problem dealing with the electrical potential due to a buried conducting spheroid under the influence of a surface point electrode is given. The problem is complicated by the boundary condition requiring the vanishing of the normal derivative of potential on the surface of the half space. This condition is satisfied by placing an image spheroid in the upper half space. The problem then reduces to that of finding the potential due to two spheroids whose potentials react upon each other. The interaction of the potentials is handled analytically by means of a transformation theorem in spheroidal harmonics due to B. Datta. The method of solution employed leads to an infinite number of equations in an infinity of unknowns. An approximate method for solving these equations is given. It is believed by the author that the inverse distance formula in spheroidal harmonics, which is derived, is new.

THE problem of finding the potential due to a buried conducting sphere under the influence of a surface point electrode has been completely solved.[1] It is the purpose of the present paper to extend the solution of this

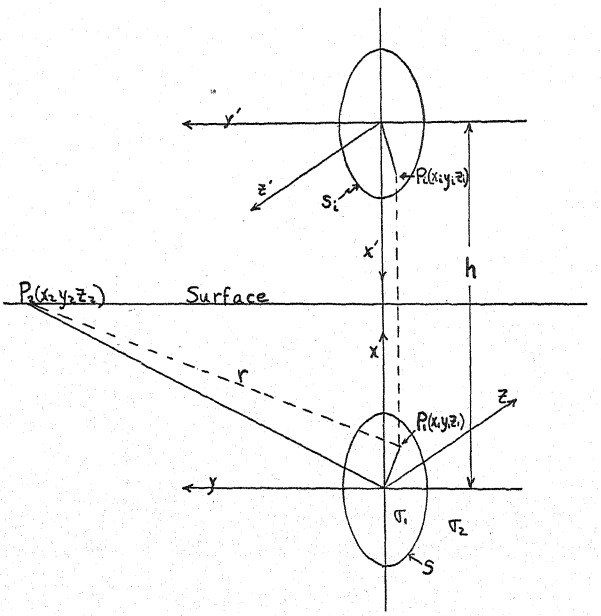


Fig. 1. Buried and imaged spheroids.

problem to the case of a buried spheroid. The solution here given for the oblate and prolate spheroid affords, for the purpose of ore exploration, much greater generality than does the solution for the case of the buried sphere.

[1] J. H. Webb, Phys. Rev. **37**, 292 (1931).

The general procedure in the present case is the same as in the former paper dealing with the sphere. Assume the center of a buried spheroid to be situated at the origin of the set of cartesian coordinates x, y, z as shown in Fig. 1. Assume an electrode, at which a current I is being introduced, to be placed at the point $P_2(x_2, y_2, z_2)$.

As a first step toward a solution of the problem, we shall express the potential due to the electrode alone, in a series of spheroidal harmonics. The purpose of this is to have the potential in a suitable form for substitution in one of the boundary conditions over the surface of the buried spheroid. The desired expression is obtained by finding an expression in spheroidal harmonics for r^{-1}, r being the distance from the electrode to any point $P_1(x_1, y_1, z_1)$ in space. It is possible to express r^{-1} in the following integral form,[2]

$$\frac{1}{r} = \frac{1}{2\pi}\int_{-\pi}^{\pi} \frac{d\theta}{[(x_2 - x_1) + i(y_2 - y_1)\cos\theta + i(z_2 - z)\sin\theta]}, \tag{1}$$

and we can express the integrand in the slightly altered form,

$$\frac{1}{b\left[\dfrac{x_2 + iy_2\cos\theta + iz_2\sin\theta}{b} - \dfrac{x_1 + iy_1\cos\theta + iz_1\sin\theta}{b}\right]} \tag{2}$$

in which b is any quantity. Now it has been shown by Heine[3] that the quantity $(t-z)^{-1}$ can be expressed as follows in a series of Legendre functions P_m and Q_m, of the first and second kind respectively,

$$\frac{1}{t - z} = \sum_{m=0}^{\infty}(2m + 1)P_m(z)Q_m(t), \tag{3}$$

and the expansion can be shown to be convergent when the point z lies inside the ellipse which passes through the point t and has the points ± 1 for its foci. If we identify t and z with the quantities $(x_2+iy_2\cos\theta+iz_2\sin\theta)/b$ and $(x_1+iy_1\cos\theta+iz_1\sin\theta)/b$ respectively, we obtain for the integral (1),

$$\frac{1}{r} = \frac{1}{2\pi b}\int_{-\pi}^{\pi}\sum_{m=0}^{\infty}(2m+1)P_m\left(\frac{X_1}{b}\right)Q_m\left(\frac{X_2}{b}\right)d\theta \tag{4}$$

in which $X_1=(x_1+iy_1\cos\theta+iz_1\sin\theta)$ and $X_2=(x_2+iy_2\cos\theta+iz_2\sin\theta)$. We shall now express (4) in terms of spheroidal coordinates. Supposing the spheroids are oblate, we write

$$\begin{aligned}
&\frac{x_1^2}{\lambda_1^2} + \frac{y_1^2}{\lambda_1 - b^2} + \frac{z_1^2}{\lambda_1^2 - b^2} = 1,\\
&\frac{x_1^2}{\mu_1^2} + \frac{y_1^2}{\mu_1^2 - b^2} + \frac{z_1^2}{\mu_1^2 - b^2} = 1,\\
&z_1 = \nu_1 y_1.
\end{aligned} \tag{5}$$

[2] See Whittaker and Watson, Modern Analysis, 4 Ed., p. 391.
[3] See Whittaker and Watson, Modern Analysis, 4 Ed., p. 321.

For oblate spheroids, $b^2=a^2-c^2$ is a negative quantity, hence we shall write $b^2=-k^2$, or $k=ib$. Making this substitution and also the additional ones,

$$\xi_1^2 = -\frac{\lambda_1^2}{k^2},$$
$$\eta_1^2 = -\frac{\mu_1^2}{k^2}, \tag{6}$$
$$\phi_1 = \tan^{-1}\nu_1,$$

we find

$$\frac{x_1^2}{-k^2\xi_1^2}+\frac{y_1^2}{k^2-k^2\xi_1^2}+\frac{z_1^2}{k^2-k^2\xi_1^2}=1,$$
$$\frac{x_1^2}{-k^2\eta_1^2}+\frac{y_1^2}{k^2-k^2\eta_1^2}+\frac{z_1^2}{k^2-k^2\eta_1^2}=1, \tag{7}$$
$$z_1 = y_1\tan\phi_1.$$

Solving the Eqs. (7), it is readily found that

$$x_1 = ik\xi_1\eta_1,$$
$$y_1 = k(1-\xi_1^2)^{1/2}(1-\eta_1^2)^{1/2}\cos\phi_1,$$
$$z_1 = k(1-\xi_1^2)^{1/2}(1-\eta_1^2)^{1/2}\sin\phi_1,$$

and making the further substitution $i\xi_1=\rho_1$, we have

$$x_1 = k\rho_1\eta_1,$$
$$y_1 = k(1+\rho_1^2)^{1/2}(1-\eta_1^2)^{1/2}\cos\phi_1, \tag{8}$$
$$z_1 = k(1+\rho_1^2)^{1/2}(1-\eta_1^2)^{1/2}\sin\phi_1.$$

If we substitute the above values into the expression for $P_m(X_1/b)$, we find

$$P_m\left(\frac{X_1}{b}\right) = P_m\left[-i\rho_1\eta_1-\left\{1-(i\rho_1)^2\right\}^{1/2}\left\{1-\eta_1^2\right\}^{1/2}\cos(\phi_1-\theta)\right],$$

and this is readily shown to be equal to[4]

$$P_m\left(\frac{X_1}{b}\right) = (-)^m\left[P_m(i\rho_1)P_m(\eta_1) + 2\sum_{q=1}^{m}\frac{(m-q)!}{(m+q)!}P_m^q(i\rho_1)P_m^q(\eta_1)\cos q(\phi_1-\theta)\right]. \tag{9}$$

Similarly, it can be shown that[4]

$$Q_m\left(\frac{X_2}{b}\right) = (-)^{m+1}\left[Q_m(i\rho_2)P_m(\eta_2) + 2\sum_{n=1}^{\infty}\frac{(m-n)!}{(m+n)!}Q_m^n(i\rho_2)P_m^n(\eta_2)\cos n(\phi_2-\theta)\right]. \tag{10}$$

[4] Whittaker and Watson, Modern Analysis, 4 Ed., p. 328–9.

Substituting the expressions (9) and (10) in the Eq. (4), we obtain

$$\frac{1}{r} = \frac{1}{2\pi b}\int_{-\pi}^{\pi}\sum_{m=0}^{\infty}(2m+1)\left[P_m(i\rho_1)P_m(\eta_1) + 2\sum_{q=1}^{m}\frac{(m-q)!}{(m+q)!}P_m{}^q(i\rho_1)P_m{}^q(\eta_1)\cos q(\theta-\phi_1)\right]\times$$
$$\left[Q_m(i\rho_2)P_m(\eta_2) + 2\sum_{n=1}^{\infty}\frac{(m-n)!}{\cdot(m+n)!}Q_m{}^n(i\rho_2)P_m{}^n(\eta_2)\cos n(\theta-\phi_2)\right]d\theta. \quad (11)$$

Eq. (11) simplifies when we carry out the indicated multiplication and integration. Because of the limits of the integration, the only terms which yield anything other than zero are the constant terms (with respect to θ) and the terms containing products of the form

$$\cos q(\theta-\phi_1)\cos n(\theta-\phi_2),$$

in which $q=n$. Carrying out the multiplication and integration indicated in Eq. (11), we find that

$$\frac{1}{r} = \frac{1}{b}\sum_{m=0}^{\infty}(2m+1)\left[P_m(i\rho_1)P_m(\eta_1)Q_m(i\rho_2)P_m(\eta_2) + 4\sum_{q=1}^{m}\left(\frac{(m-q)!}{(m+q)!}\right)^2 P_m{}^q(i\rho_1)P_m{}^q(\eta_1)Q_m{}^q(i\rho_2)P_m{}^q(\eta_2)\cos q(\phi_2-\phi_1)\right]. \quad (12)$$

If the spheroids are of the prolate type, we write

$$\frac{x_1^2}{\lambda_1^2} + \frac{y_1^2}{\lambda_1^2-b^2} + \frac{z_1^2}{\lambda_1^2-b^2} = 1$$
$$\frac{x_1^2}{\mu_1^2} + \frac{y_1^2}{\mu_1^2-b^2} + \frac{z_1^2}{\mu_1^2-b^2} = 1 \quad (13)$$
$$z_1 = \nu_1 y_1$$

in which $b^2=a^2-c^2$, and $\lambda_1^2>b^2>\mu_1^2$. Solving the Eqs. (13), we find

$$x_1 = b\xi_1\eta_1,$$
$$y_1 = b(\xi_1^2-1)^{1/2}(1-\eta_1^2)^{1/2}\cos\phi_1, \quad (14)$$
$$z_1 = b(\xi_1^2-1)^{1/2}(1-\eta_1^2)^{1/2}\sin\phi_1,$$

in which $\lambda_1/b=\xi_1$, $\mu_1/b=\eta_1$ and $\phi_1=\tan^{-1}\nu_1$. By use of these values for x_1, y_1 and z_1 and going through the same procedure as in the case for the oblate spheroids, we find for the expansion of r^{-1}

$$\frac{1}{r} = \frac{1}{b}\sum_{m=0}^{\infty}(2m+1)\left[P_m(\xi_1)P_m(\eta_1)Q_m(\xi_2)P_m(\eta_2) + 4\sum_{q=1}^{m}\left(\frac{(m-q)!}{(m+q)!}\right)^2 P_m{}^q(\xi_1)P_m{}^q(\eta_1)Q_m{}^q(\xi_2)P_m{}^q(\eta_2)\cos q(\phi_2-\phi_1)\right]. \quad (15)$$

The Eqs. (12) and (15) bear a striking similarity to the corresponding equation for the expansion of r^{-1} over the surface of a sphere. The expansion in that case is,

$$\frac{1}{r} = \sum_{m=0}^{\infty} \left(\frac{a}{\rho}\right)^{m+1} \left[P_m(\mu_1) P_m(\mu_2) + 2 \sum_{n=1}^{m} \frac{(m-n)!}{(m+n)!} P_m{}^n(\mu_1) P_m{}^n(\mu_2) \cos n(\phi_2 - \phi_1) \right]$$

in which r is the distance from an external point x_2, y_2, z_2 to a point x_1, y_1,z_1 on the surface of the sphere, a is the radius of the sphere, ρ is the distance from the point x_2, y_2, z_2 to the center of the sphere and the origin of coordinates, and θ_2, ϕ_2 and θ_1, ϕ_1 are the angle coordinates of the points x_2, y_2, z_2 and x_1, y_1, z_1 respectively.

It is believed by the writer that the Eqs. (12) and (15), the expansions for r^{-1}, are new. We shall write these expansions, for brevity, in the following form,

$$\frac{1}{r} = \frac{1}{b} \sum_{m=0}^{\infty} (2m+1) W_m(i\rho_1, \eta_1, \phi_1, i\rho_2, \eta_2, \phi_2), \tag{16}$$

and a similar one for Eq. (15). It is readily seen that Eq. (12) simplifies greatly when the point x_2, y_2, z_2 is taken on the x axis at a distance $x_2 = s$ from the origin. Then $y_2 = 0$, $z_2 = 0$, $i\rho_2 = s/ik$, $\eta_2 = 1$, and since $P_m{}^q(1) = 0$,

$$\frac{1}{r} = \frac{1}{b} \sum_{m=0}^{\infty} (-)^m (2m+1) P_m(i\rho_1) P_m(\eta_1) Q_m\left(\frac{s}{ik}\right). \tag{17}$$

This equation has been given by several authors previously.[5] The corresponding equation for the prolate spheroidal case, for $x_2 = s$, $y_2 = 0$, $z_2 = 0$, is, since under these conditions $\eta_2 = 1$ and $\xi_2 = s/b$,

$$\frac{1}{r} = \frac{1}{b} \sum_{m=0}^{\infty} (2m+1) P_m(\xi_1) P_m(\eta_1) Q_m\left(\frac{s}{b}\right). \tag{18}$$

Having expressed r^{-1} in the desired form, we are now in a position to solve the problem at hand. Let us take the buried spheroid to be the one for which λ_1 has the value λ_{10}. Assume the spheroid to be of the oblate type, of conductivity σ_1, and buried at a depth $h/2$ from the surface in an infinite half space of conductivity σ_2. (See Fig. 1.) The potential due to the electrode alone is $I/4\pi r\sigma_2$ in which r is the distance from the electrode $P_2(x_2, y_2, z_2)$ to any point $P_1(x_1, y_1, z_1)$ and I is the current. It is desired to find the potential at all points in space due to the buried spheroid S. Designate by u and U the inside and outside potentials, respectively, due to the spheroid alone. Then the functions u and U must satisfy Laplace's equation,

$$\Delta^2 \Phi = 0, \tag{19}$$

[5] Phil. Trans. of Roy. Soc. of Lon. **224**, p. 55; Amer. Jour. Math. **43**, 135 (1921).

at all points in space, and are further subject to the conditions:

$$\kappa \frac{\partial u}{\partial \rho_1} - \frac{\partial U}{\partial \rho_1} = -(\kappa - 1)\frac{\partial U_e}{\partial \rho_1}, \quad \rho_1 = \rho_{10}, \tag{20}$$

$$u = U, \quad \rho_1 = \rho_{10}, \tag{21}$$

$$U = 0, \text{ at } \infty \tag{22}$$

and

$$\frac{\partial \Phi}{\partial x} = 0, \quad \text{at} \quad x = \frac{h}{2}, \tag{23}$$

in which U_e denotes the potential due to the electrode and κ represents the ratio of conductivities σ_1/σ_2. The complication which arises in the solution of the problem is due to the boundary condition (23). In order to satisfy this condition, an image spheroid S_i is placed in the upper half space which is also assumed to be filled with material of conductivity σ_2. Then, from symmetry, the normal derivative of the potential on the boundary,

$$x = h/2,$$

will vanish. The inclusion of this image spheroid makes it necessary to take into account the interaction of the potentials of the two spheroids. This can be readily done[6] by changing the boundary condition (20) so as to read

$$\kappa \frac{\partial u}{\partial \rho_1} - \frac{\partial U}{\partial \rho_1} = -(\kappa - 1)\frac{\partial U_a}{\partial \rho_1}, \quad \rho_1 = \rho_{10}, \tag{24}$$

where

$$U_a = U_e + U_i$$

U_i being the potential at $P_1(x_1, y_1, z_1)$ due to the image spheroid. A solution satisfying Eqs. (19) and conditions (21), (22) and (24) will be the solution of our problem. Laplace's equation written in curvilinear coordinates is

$$h_1 h_2 h_3 \left[\frac{\partial}{\partial \rho_1}\left(\frac{h_1}{h_2 h_3}\frac{\partial}{\partial \rho_1}\Phi\right) + \frac{\partial}{\partial \eta_1}\left(\frac{h_2}{h_1 h_2}\frac{\partial}{\partial \eta_1}\Phi\right) + \frac{\partial}{\partial \phi_1}\left(\frac{h_3}{h_1 h_2}\frac{\partial}{\partial \phi_1}\Phi\right)\right] = 0. \tag{25}$$

From the Eqs. (8), it is found that

$$h_1 = \frac{1}{k}\left(\frac{1+\rho_1^2}{\eta_1^2+\rho_1^2}\right)^{1/2}, \; h_2 = \frac{1}{k}\left(\frac{1-\eta_1^2}{\eta_1^2+\rho_1^2}\right)^{1/2}, \left(h_3 = \frac{1}{k((1+\rho_1^2)(1-\eta_1^2))^{1/2}}\right).$$

Substituting the above values in Eq (25), we obtain Laplace's equation in the form,

$$\frac{\partial}{\partial \rho_1}\left\{(1+\rho_1^2)\frac{\partial \Phi}{\partial \rho_1}\right\} + \frac{\partial}{\partial \eta_1}\left\{(1-\eta_1^2)\frac{\partial \Phi}{\partial \eta_1}\right\} + \frac{(\eta_1^2+\rho_1^2)}{(1+\rho_1^2)(1-\eta_1^2)}\frac{\partial^2 \Phi}{\partial \phi_1^2} = 0. \tag{26}$$

Similarly for prolate spheroids, we find from Eqs. (14),

$$h_1 = \frac{1}{b}\left(\frac{\xi_1^2-1}{\xi_1^2-\eta_1^2}\right)^{1/2}, \quad h_2 = \frac{1}{b}\left(\frac{1-\eta_1^2}{\xi_1^2-\eta_1^2}\right)^{1/2}, \quad h_3 = \frac{1}{b((\xi_1^2-1)(1-\eta_1^2))^{1/2}},$$

[6] J. H. Webb, reference 1.

and from Eq. (25),

$$\frac{\partial}{\partial \xi_1}\left\{(\xi_1^2 - 1)\frac{\partial \Phi}{\partial \xi_1}\right\} + \frac{\partial}{\partial \eta_1}\left\{(1 - \eta_1^2)\frac{\partial \Phi}{\partial \eta_1}\right\} + \frac{(\xi_1^2 - \eta_1^2)}{(\xi_1^2 - 1)(1 - \eta_1^2)}\frac{\partial^2 \Phi}{\partial \phi_1^2} = 0. \quad (27)$$

Solutions of the Eqs. (26) are given in a number of places[7] and are

$$u_1 = \sum_{m=0}^{\infty}\left[A_{0m}P_m(i\rho_1)P_m(\eta_1) + \sum_{q=1}^{m}(A_{qm}\cos q\phi_1 + B_{qm}\sin q\phi_1)P_m^q(i\rho_1)P_m^q(\eta_1)\right], \quad (28)$$

$$u_2 = \sum_{m=0}^{\infty}\left[A'_{0m}Q_m(i\rho_1)P_m(\eta_1) + \sum_{q=1}^{m}(A'_{qm}\cos q\phi_1 + B'_{qm}\sin q\phi_1)Q_m^q(i\rho_1)P_m^q(\eta_1)\right]. \quad (29)$$

If we replace in Eq. (28) and (29) $i\rho_1$ by ξ_1, we shall have the solutions of Eq. (27). As the further treatment of the problem is identical for prolate and oblate spheroids, we shall treat only the case of the oblate spheroid. By a consideration of the boundary condition (22) and in order to have the potential due to the spheroid finite at points within the spheroid, u_1 and u_2 are chosen as u and U, the inside and outside potentials respectively of the spheroid. The solution of the problem now consists in finding values for the constants A_{qm} and B_{qm} which will make u and U satisfy the remaining boundary conditions.

Eqs. (28) and (29) satisfy Laplace's equation and condition (22). They will satisfy condition (21) if the constants in Eqs. (28) and (29) are related as follows,

$$A_{0m}' = A_{0m}\frac{P_m(i\rho_{10})}{Q_m(i\rho_{10})}, \quad \left.\begin{matrix} A'_{qm} \\ B'_{qm} \end{matrix}\right\} = \left\{\begin{matrix} A_{qm} \\ B_{qm} \end{matrix}\right\}\frac{P_m^q(i\rho_{10})}{Q_m^q(i\rho_{10})}, \quad (30)$$

in which $i\rho_{10}$ is the value of $i\rho_1$ on the boundary of the spheroid for which $\lambda_1 = \lambda_{10}$. The boundary condition (23) is satisfied by means of the image spheroid, and is handled analytically by using, in place of (20) the revised boundary condition (24), in which

$$U_a = U_e + U_i.$$

Now since the potential U_i at points P, due to the image spheroid, is identical with the potential U at points P_i, due to the buried spheroid, i.e.,

$$U_i(P) \equiv U(P_i), \quad (31)$$

we can write for U_a,

$$U_a = \frac{D}{b}\sum_{m=0}^{\infty}(2m+1)W_m(i\rho_1, \eta_1, \phi_1, i\rho_2, \eta_2, \phi_2) + \sum_{m=0}^{\infty}\left[A_{0m}Q_m(i\rho_i)P_m(\eta_i) + \sum_{q=1}^{m}(A_{qm}\cos q\phi_i + B_{qm}\sin q\phi_i)Q_m^q(i\rho_i)P_m^q(\eta_i)\right] \quad (32)$$

[7] Jeans, Electricity and Magnetism, 1908, p. 251.

in which D represents $I/4\pi\sigma_2$, and the subscript i refers to image points $P_i(x_i, y_i, z_i)$ of $P_1(x_1, y_1, z_1)$. The second member of Eq. (32) can be expressed in terms of the variables $(i\rho_1, \eta_1, \phi_1)$, as desired, by means of the following transformation theorem due to B. Datta,[8]

$$\begin{aligned} Q_m{}^q(i\rho_i)P_m{}^q(\eta_i)\cos q\phi_i &= \sum_{k=q}^{\infty}\frac{(m+q)!}{(m-q)!}(2k+1)\frac{(k-q)!}{(k+q)!}w(k,m)P_k{}^q(i\rho_1)P_k{}^q(\eta_1)\cos q\phi_1 \\ &= \sum_{k=q}^{\infty}\beta_{kqm}, \end{aligned} \tag{33}$$

where

$$w(k,m) = (-)^m\frac{2^m m!}{(2m+1)!}\rho^{m+1}\left[\frac{\partial^m}{\partial t^m}+\frac{\rho^m}{2(2m+3)}\frac{\partial^{m+2}}{\partial t^{m+2}} + \frac{\rho^4}{2\cdot 4(2m+3)(2m+5)}\frac{\partial^{m+4}}{\partial t^{m+4}}+\cdots\right]Q_k(t), \tag{34}$$

in which $\rho = b_i/b = 1$, and $t = h/b$. The expression for $w(k, m)$ can be written more simply[9]

$$w(k,m) = (-)^m\left(\frac{\pi}{2D}\right)^{1/2}J_{m+1/2}(D)\times Q_k(t) = L_k{}^m(t),$$

where $D = \partial/\partial t$.

If we substitute the value of

$$Q_m{}^q(i\rho_i)P_m{}^q(\eta_i)\begin{Bmatrix}\cos q\phi_i\\ \sin q\phi_i\end{Bmatrix}$$

from the Eq. (33) in Eq. (32), we find

$$\begin{aligned} U_a = \frac{D}{b}\sum_{m=0}^{\infty}(2m+1)W_m(i\rho_1,\eta_1,\phi_1,i\rho_2,\eta_2,\phi_2) \\ + \sum_{m=0}^{\infty}A_{0m}\sum_{k=0}^{\infty}\beta_{k0m} + \sum_{q=1}^{m}(A_{qm}\cos q\phi_1 + B_{qm}\sin q\phi_1)\sum_{k=q}^{\infty}\beta_{kqm}. \end{aligned} \tag{35}$$

Since for the determinations of the constants A_{qm} and B_{qm} we shall equate coefficients of like tesseral harmonics,

$$P_m{}^q(\eta_1)\begin{Bmatrix}\cos q\phi_1\\ \sin q\phi_1\end{Bmatrix},$$

after the substitution in the boundary Eq. (24), it is convenient to rearrange the terms in the triple series of the second member of Eq. (35) in such a way that the tesseral harmonics will be summed by the index m. This rearrange-

[8] B. Datta, Tohoku Math. Journ. **15**, 166 (1919.)

[9] J. W. Nicholson, Phil. Trans. Roy. Soc. Lon. **224**, 311.

ment can be effected by simply interchanging the indices m and k, such a process being justifiable since the series is absolutely convergent. Hence, we have,

$$U_a = \frac{D}{b} \sum_{m=0}^{\infty}(2m+1)W_m(i\rho_1, \eta_1, \phi_1, i\rho_2, \eta_2, \phi_2) + \sum_{m=0}^{\infty} \sum_{k=0}^{\infty} A_{0k}\beta_{m0k} + \sum_{q=1}^{m} \sum_{k=q}^{\infty}(A_{qk}\cos q\phi_1 + B_{qk}\sin q\phi_1)\beta_{mqk}. \quad (36)$$

If now the values of u, U and U_a be substituted in Eq. (24) ρ_1 set equal to ρ_{10} and coefficients of like tesseral harmonics, $P_m{}^q(\eta_1)\cos q\phi_1$ and $P_m{}^q(\eta_1)\sin q\phi_1$, be equated, the following sets of linear equations, for the determinations of the constants, result:

$$\begin{aligned} A_{0m}\alpha_{0m} &= K_{0m} - \sum_{k=0}^{\infty} A_{0k}a_{m0k}, \quad (m = 0, 1, 2 \cdots \infty), \\ A_{qm}\alpha_{qm} &= K_{qm} - \sum_{k=q}^{\infty} A_{qk}a_{mqk}, \quad (q = 1, 2 \cdots \infty), \ (m = q, q+1, \cdots \infty), \\ B_{qm}\alpha_{qm} &= M_{qm} - \sum_{k=q}^{\infty} B_{qk}b_{mqk}, \quad (q = 1, 2 \cdots \infty), \ (m = q, q+1, \cdots \infty), \end{aligned} \quad (37)$$

in which

$$\begin{aligned} \alpha_{qm} &= \frac{1}{\kappa - 1}\left\{\kappa - \frac{P_m{}^q(i\rho_{10})Q_m{}^{q\prime}(i\rho_{10})}{P_m{}^{q\prime}(i\rho_{10})Q_m{}^q(i\rho_{10})}\right\}, \\ K_{qm} &= \frac{4D}{b}(2m+1)\left(\frac{(m-q)!}{(m+q)!}\right)^2 Q_m{}^q(i\rho_2)P_m{}^q(\eta_2)\cos q\phi_2 = M_{qm}\frac{\cos q\phi_2}{\sin q\phi_2}, \\ a_{mqk} &= \frac{\beta_{mqk}}{P_m{}^q(\eta_1)\cos q\phi_1 P_m{}^q(i\rho_1)} = b_{mqk}\frac{\sin q\phi_1}{\cos q\phi_1}, \end{aligned} \quad (38)$$

and where the prime indicates differentiation with respect to ρ_1. The theory of the solution of the equations of type (37) has been given by various writers, Hill,[10] von Koch,[11] Schmidt[12] and others. Hence the values of the constants can be found, and the problem is definitely solved. However, the general values thus determined for the constants A_{qm} and B_{qm} are of little practical use, for they do not admit of easy numerical calculation. A method for approximating the values of the constants A_{qm} and B_{qm} is given below. We have

$$w(m, k) = \frac{(-)^k 2^k k!}{(2k+1)!}\left[\frac{\partial^k}{\partial t^k} + \frac{1}{2(2k+3)}\frac{\partial^{k+2}}{\partial t^{k+2}} + \cdots\right]Q_m(t),$$

where $t = h/b$.

[10] G. W. Hill, Acta Math. **8**, 1 (1886).

[11] H. von Koch, Jahres Bericht der Deutschen Mathematiker Vereinigung. **22**, 285–291 (1913).

[12] E. Schmidt, Rendiconti del circolo Matematico di Palermo, **25**, 53 . E. Goldschmidt, Wurzburg Univ. Press Series Reprint, 1912. H. Sturtz, A.G.

Now,

$$Q_m(t) = \frac{2^m m!m!}{(2m+1)!}\left[\left(\frac{b}{h}\right)^{m+1} + \frac{(m+1)(m+2)}{2(2m+3)}\left(\frac{b}{h}\right)^{m+3} + \cdots\right],$$

and if we neglect terms of order greater than
$(b/h)^3$ = (dimensions of spheroid/distance of separation)^3,
we find

$$\begin{aligned} w(m,k) = (-)^k \frac{2^{m+k}m!m!k!}{(2m+1)!(2k+1)!}\Bigg[&(m+1)(m+2)\cdots(m+k)\left(\frac{b}{h}\right)^{m+k+1} \\ &+ \frac{(m+1)(m+2)\cdots(m+k+2)}{2(2m+3)}\left(\frac{b}{h}\right)^{m+k+3} \\ &+ \frac{(m+1)(m+2)\cdots(m+k+2)}{2(2k+3)}\left(\frac{b}{h}\right)^{m+k+3} + \cdots\Bigg] \end{aligned} \tag{39}$$

and on rearranging terms,

$$\begin{aligned} w(m,k) = (-)^k \frac{2^{m+k}m!k!}{(2m+1)!(2k+1)!}\Bigg[&(m+k)!\left(\frac{b}{h}\right)^{m+k+1} \\ &+ (m+k+2)!\left(\frac{b}{h}\right)^{m+k+3}\left\{\frac{1}{2(2m+3)} + \frac{1}{2(2k+3)}\right\}\Bigg]. \end{aligned} \tag{40}$$

Calculating all the values of $w(m, k)$ to this order of approximation (remembering that the indices m and k are now reversed in (34)), we have

$$\begin{aligned} &w(0,0) = \frac{b}{h} + \frac{2}{3}\left(\frac{b}{h}\right)^3, \quad w(0,1) = -\frac{1}{3}\left(\frac{b}{h}\right)^2, \quad w(0,2) = \frac{2}{15}\left(\frac{b}{h}\right)^3, \\ &w(1,0) = \frac{1}{3}\left(\frac{b}{h}\right)^2, \qquad w(1,1) = -\frac{2}{9}\left(\frac{b}{h}\right)^3, \quad w(2,0) = \frac{2}{15}\left(\frac{b}{h}\right)^3. \end{aligned} \tag{41}$$

Therefore, to terms of order higher than $(b/h)^3$, we have for the determination of the constants A_{qm} and B_{qm}, the equations,

$$\begin{aligned} &A_{00}[\alpha_{00} + w(0,0)] + A_{01}w(0,1) + A_{02}w(0,2) = K_{00}, \\ &A_{00}3w(1,0) + A_{01}[\alpha_{01} + w(1,1)] = K_{01}, \\ &A_{00}5w(2,0) + A_{02}\alpha_{02} = K_{02}, \\ &A_{03} = \frac{K_{03}}{\alpha_{03}}, \quad A_{11} = \frac{K_{11}}{\alpha_{11} + 3w(1,1)}, \quad A_{2m} = \frac{K_{2m}}{\alpha_{2m}}, \\ &A_{0m} = \frac{K_{0m}}{\alpha_{0m}}, \quad A_{12} = \frac{K_{12}}{\alpha_{12}}, \quad A_{qm} = \frac{K_{qm}}{\alpha_{qm}}. \\ &\qquad\qquad A_{1m} = \frac{K_{1m}}{\alpha_{1m}} \end{aligned} \tag{42}$$

The equations for the determination of the constants B_{qm} can be written from symmetry. Because of the appearance of the factor $\sin q\phi_1$ in the expression for the potential, the terms containing B_0m do not occur, hence

$$B_{11} = \frac{M_{11}}{\alpha_{11} + 3w(1,1)}, \qquad B_{2m} = \frac{M_{2m}}{\alpha_{2m}},$$
$$\vdots \qquad\qquad \vdots$$
$$B_{12} = \frac{M_{12}}{\alpha_{12}}, \qquad B_{qm} = \frac{M_{qm}}{\alpha_{qm}}. \tag{43}$$
$$\vdots \qquad\qquad \vdots$$
$$B_{1m} = \frac{M_{1m}}{\alpha_{1m}},$$

It may be seen from Eqs. (38) that the values of the constants A_{qm} and B_{qm} will fall off rapidly as q and m increase, and it will usually be unnecessary to go to higher values than four for q and m, although this will depend somewhat on the case at hand. Solving the first three equations of (42) for the first three unknowns, we find,

$$A_{00} = \frac{K_{00}}{\alpha_{00} + w(0,0)} - \frac{K_{01}w(1,0)}{f} - \frac{K_{02}w(0,2)}{f},$$
$$A_{01} = \frac{K_{01}}{\alpha_{01} + w(1,1)} + \frac{K_{00}3w(1,0)\alpha_{02}}{f}, \tag{44}$$
$$A_{02} = \frac{K_{02}}{\alpha_{02}} - \frac{K_{00}5w(2,0)\alpha_{01}}{f},$$

in which $f = \{\alpha_{00}\alpha_{01} + w(0,0)\alpha_{01} + \alpha_{00}w(1,1)\}$.

The value of the potential at all points in the half space, outside the buried spheroid, is given by the Eq. (28) plus a similar term

$$\sum_{m=0}^{\infty} A_{0m}Q_m(i\rho_1')P_m(\eta_1') + \sum_{q=1}^{m}(A_{qm}\cos q\phi_1 + B_{qm}\sin q\phi_1)Q_m{}^q(i\rho_1')P_m{}^q(\eta_1'), \tag{45}$$

which arises from the image spheroid. The value of the potential at all points within the buried spheroid is given by the sum of Eq. (29) and the term (45). The values of the constants A_{qm}' and B_{qm}' are given by the relation (30), and the values of the constants A_{qm} and B_{qm} are found from the Eqs. (42), (43), and (44).

At first sight, the above approximate solution for the potential may seem to be too crude an approximation. However, a similar solution was given for the case of the sphere[13] and the values of the potential thereby calculated were compared with the values as calculated by an exact method. It was

[13] J. H. Webb, Phys. Rev. **37**, 302 (1931).

found that the approximation there made was sufficiently good for practical purposes in all cases where the sphere was at a depth equal to or greater than three times the radius of the sphere. In the present case of the spheroid, the cross effect of the potentials due to the two spheriods is of the same order of magnitude as in the case of the sphere, and hence the approximation will be just as valid for cases where the spheroid is buried at a depth equal to or greater than three times the mean dimension of the spheroid.

It is hoped by the writer that a further paper can be presented in the near future giving a numerical illustration and an investigation of the limiting expressions obtained when very long prolate and very flat oblate spheroids are considered.

In conclusion, I should like to express my sincere appreciation to Professor Warren Weaver for reading the manuscript and for a number of helpful suggestions.

THE STABILITY OF A SINGLE FILE OF STRAIGHT VORTICES

By Arthur Taber Jones
Smith College

(Received October 2, 1931)

Abstract

An infinite number of straight vortices of equal strengths and the same sense of rotation are parallel and uniformly spaced in an infinite plane. If one vortex is slightly displaced, remaining parallel to the others, its velocity does not in general lie in a plane which passes through its original position. There are, however, two planes inclined at 45° to the plane of the file, such that if the displacement is in one of these planes the vortex moves directly away from its original position, and if the displacement is in the other plane the vortex moves directly back toward its original position.

AMONG the problems which arise in the study of vortex motion certain questions of considerable interest have to do with the two files of vortices which frequently form in the wake of a moving body. The stability of such a "street" or "avenue" of straight vortices was examined some twenty years ago by Kármán and Rubach[1], and various other authors have dealt with related matters. But in the literature which I have examined the only treatments I have found of the problem when the file of vortices is single instead of double are brief discussions in the paper by Kármán and Rubach and in Lamb's Hydrodynamics.[2] In these treatments it is assumed that the vortices are straight, parallel, of equal strengths and the same sense of rotation, and at first are uniformly distributed in a plane. Lamb follows Kármán and Rubach in assuming that the vortices are slightly displaced in a sinusoidal manner. It is then shown that the original distribution is unstable. The following

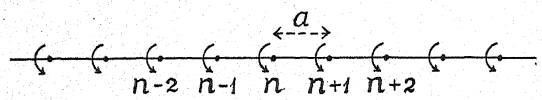


Fig. 1. Single file of straight vortices.

very simple treatment brings out one point which I have not found in the literature, and which may be of sufficient interest to make it worthy of a brief note.

Consider an infinite file of uniformly spaced straight vortices, all having the same strength and the same sense of rotation, all perpendicular to the plane of the paper, and all lying in a single plane as indicated in Fig. 1. If we consider any one of them, say the nth from some chosen origin, we see that the $(n+s)$th and $(n-s)$th give to the chosen vortex equal velocities in opposite senses. The vortices are therefore in equilibrium.

[1] Th. v. Kármán and H. Rubach, Phys. Zeits. **13**, 49 (1912).
[2] Horace Lamb, Hydrodynamics p. 219, Ed. 4 (1916).

Is the equilibrium stable? Let a single one of the vortices, say the nth, receive a small displacement in which it remains parallel to the other vortices. We recall that the velocity which any other vortex imparts to the given vortex is perpendicular to the line joining them, and decreases with their distance apart. Thus if the displacement is to the point A in Fig. 2 it is easy to see that the velocity due to the $(n+s)$th and $(n-s)$th vortices will be in the direction of the arrow A'. Similarly a displacement to B, C, or D leads to a velocity in the direction of one of the arrows B', C', or D'. These facts suggest that if the displacement is to a position in some such plane as J_1J_2 the

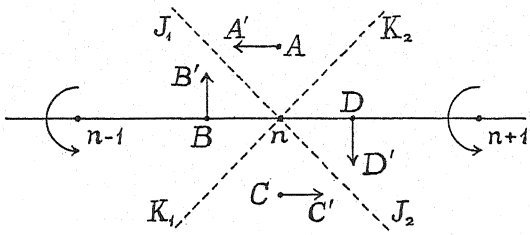


Fig. 2. Direction of velocity of displaced vortex.

vortex will move farther from its original position, whereas if the displacement is in some such plane as K_1K_2 the vortex will return to its original position. That is, it seems likely that the vortex may be unstable for displacements along J_1J_2 and stable for displacements along K_1K_2.

It is not difficult to show that these suggestions are correct, and to obtain the angles at which the planes J_1J_2 and K_1K_2 lie. Let the x and y components of the displacement of the nth vortex be b and c, the x and y components of the velocity which the $(n+s)$th and $(n-s)$th vortices impart to the nth be u and v, the distance from one vortex to the next be a, and the common strength of all the vortices be κ. Then it is easy to show[3] that

$$u = -\frac{\kappa}{2\pi}\left\{\frac{c}{(sa-b)^2+c^2}+\frac{c}{(sa+b)^2+c^2}\right\}$$

and

$$v = -\frac{\kappa}{2\pi}\left\{\frac{sa-b}{(sa-b)^2+c^2}-\frac{sa+b}{(sa+b)^2+c^2}\right\}.$$

If we neglect the squares of small quantities, these equations lead to the extremely simple relation

$$\frac{u}{v}=\frac{c}{b}.$$

It follows that the velocity is not in general directed through the undisplaced position of the vortex. Along the planes J_1J_2 and K_1K_2, where the velocity

[3] These equations are readily obtained from the expressions that follow Eqs. (7) in art. 154 of Lamb's Hydrodynamics, Ed. 3 or 4.

does prove to be thus directed, we must have $u/v = b/c$, and therefore, from the preceding equation, $c = \pm b$. That is, the planes J_1J_2 and K_1K_2 make angles of 45° with the plane in which the vortices lay originally.

Since this result holds for the velocity imparted by the $(n+s)$th and $(n-s)$th vortices it also holds for every similar pair, and therefore for the velocity due to all of them. The given vortex is unstable for displacements toward J_1 or J_2, and it is stable for displacements toward K_1 or K_2.

Cases in which a body is unstable for slight displacements in one direction and stable for slight displacements in some other direction are of course nothing new. But this particular case is an interesting one, and so far as I know is one that has not heretofore been described.

LETTERS TO THE EDITOR

Prompt publication of brief reports of important discoveries in physics may be secured by addressing them to this department. Closing dates for this department are, for the first issue of the month, the twenty-eighth of the preceding month; for the second issue, the thirteenth of the month. The Board of Editors does not hold itself responsible for the opinions expressed by the correspondents.

Nebular Red Shift and Universal Constants

Hubble and Humason (Astrophys. J. 74, 43 (1931)) confirm the linear proportionality to distance of "velocity displacements" in the spectra of extra-galactic nebulae, to a distance of 100 million light years. The "velocity of recession" equals 558 km/sec. per million parsecs, with an uncertainty believed no greater than 20 percent. The authors avoid interpretation and use the term *velocity of recession* only for convenience.

The datum established by their observations is that a red shift exists such that $\Delta\lambda/\lambda_0$ is linearly proportional to distance—where $\Delta\lambda$ is the observed increase in the normal wavelength λ_0 of any line in the observed region of the spectrum. That is:

$$\frac{\Delta\lambda}{\lambda_0} = \frac{x}{H}, \tag{1}$$

where x is the distance of a nebula, and H is a constant observationally determined as about 538,000,000 parsecs or 1.66×10^{27} cm.

The relativistic interpretations have tended to consider that H represents a new constant of nature, independent of previously known universal constants. On the hypothesis, however, that the nebular red shift is not indicative of a true velocity of recession, but rather of what has been called the "fatigue" of light quanta which have come so far, one might look for a connection between H and other universal constants. If light is not transmitted perfectly through empty space, each quantum might be expected to lose energy in proportion to the distance of transmission. A lowering of frequency would result, presumably according to the exponential rule,

$$\nu = \nu_0 e^{-x/H}, \tag{2}$$

where ν_0 is the initial and ν the observed frequency. The observations to date are insufficient to distinguish between the forms (2) and (1).

The purpose of the present note is to point out an empirical relation between the observational H and universal constants. Since H has the dimensions of length, the attempt to relate it to universal constants must begin by setting up a formula applicable to a quantity of such dimensions. The universal constants may be selected from the group e, h, c, G, m_0, M_P (symbols and values employed by R. T. Birge: Phys. Rev. Sup. **1**, 59–62 (1929)). These six determine three presumably independent pure numbers, namely: hc/e^2, or about 863, (e being in electrostatic units); e^2/Gm_0^2, or 4.22×10^{42}; and M_P/m_0, or about 1840. Let A, B, C, respectively, represent those numbers. Quantities having dimensions of length, (or other assigned dimensions) may be defined in various ways, as e^2/m_0c^2, h/m_0c, etc. As the ratios within such a group obviously can be expressed in terms of A, B, C, it is a matter of indifference which quantity is taken as a base.

Trial and error shows that

$$H' = \frac{Bb}{A} = \frac{e^6}{hGm_0^3c^3}, \tag{3}$$

or 1.37×10^{27} cm, approximately, where b is e^2/m_0c^2 (or 2.81×10^{-13} cm) gives the simplest formula for an H' having a magnitude of the order of the observational H of Eq. (1). If this formula is physically valid the more precise observation of H should result in establishing a simple numerical ratio H/H'. The Hubble-Humason H yields the ratio 1.21—but the uncertainty in the observational H is at present too great to make profitable a precise comparison. Considering the large numbers involved, the formula (3) is simpler than would be expected if it is assumed to represent a relationship due merely to chance.

JOHN Q. STEWART
Princeton University Observatory,
Princeton, New Jersey,
November 10, 1931.

Regions of Reversed Magnetization in Strained Wires

In a paper on the propagation of large Barkhausen discontinuities along wires,[1] it has been shown that under certain conditions a phase boundary could be made to move along a wire. The two phases separated by the boundary were distinguished by the direction of magnetization which was axial but of opposite sign. In order to obtain propagation, the main field H, to which the wire was subjected, had to exceed a critical value H_0.

By a small "stopping coil" a local field H_S can be produced opposing H and reducing the field in a short portion of the wire below H_0. Two search coils are placed on opposite sides of the stop coil and the change in induction in these places is measured ballistically. When the propagation is started from one end, the coils show to what extent the wire has changed from phase I to phase II. If the stopping field is below a critical value, complete reversal is indicated in both coils. If, on the other hand, H_S exceeds this critical value, a change is only observed in the first search coil, no change occurring in the second coil on the other side of the stop coil. This shows that the discontinuity has been stopped and by repeating the experiment with search coil I in different places along the wire, the part of the wire which has changed from phase I to phase II can be found.

The "frozen" discontinuity, like the moving one, is cone-shaped, but its length (of the order of 10 cm) is smaller and depends on H. If now a second stopping field is applied in a place along the boundary region, and the first stopping field is removed, the tail of the boundary is held by the second coil. The front edge, however, no longer held by the first stop coil, acts as a nucleus to start propagation over the rest of the wire. The shape of the phase boundary can be determined ballistically as before and is that of a long and narrow kernel, symmetrical with respect to its center. (See Fig. 1.) The same result can be obtained by starting the propagation from both ends of the wire with one stop coil in its center. An analysis of the resulting magnetic field in the boundary region agrees with the hypothesis that the field at the boundary must be H_0.

Whereas in the former experiments the propagation was initiated either by artificial nuclei or, in the case of a spontaneous start, by accidental nuclei, whose shape in either case was unknown, we now have produced a nucleus whose size may be varied and whose shape is known, and whose behavior under various conditions can be studied. The difference and sum of the two values of external field, H_1 and H_2, e.g., at which a certain point of the boundary will start to move in opposite directions, presumably give a direct measure of $2H_0$ and the field due to the internal phase respectively.

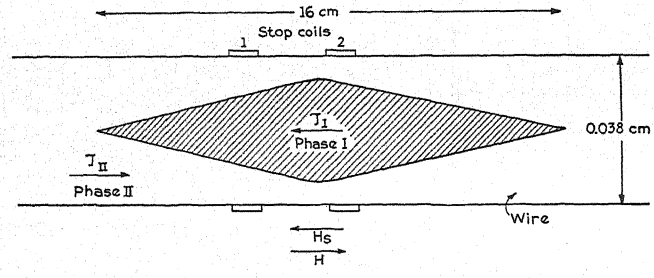


Fig. 1.

A detailed report of these investigations will be published soon.

IRVING LANGMUIR
K. J. SIXTUS

Research Laboratory,
General Electric Company,
Schenectady, New York,
October 29, 1931.

[1] K. J. Sixtus and L. Tonks, Phys. Rev. **37**, 930 (1931).

Do Protons in the Nucleus Possess Orbital Angular Momentum?

The most favored proposal to date as to the origin of nuclear spin appears to be the one in which a spin angular momentum of $\frac{1}{2} \cdot h/2\pi$ is assigned to each proton and zero spin to each electron. Such an assignment agrees with the observed data in that it gives half integral spin values for odd numbers of protons and integral spin values for even numbers of protons. In accounting for the hyperfine structure splitting of energy levels in Tl, Bi and Pb, McLennan, McLay and Crawford (Proc. Roy. Soc. **A133,** Oct. 1931) suggest that in addition to a spin of $\frac{1}{2} \cdot h/2\pi$ each proton may be assigned an orbital angular momentum of $h/2\pi$. Although proton orbital motions have been suggested before this, McLennan, McLay and Crawford point out that such assignments give half integral resultants for an odd number of protons and integral resultants for an even number of protons, as observed. In addition to this they add that orbital protons may be made to give large splitting factors, $g(I)$, to account for the wide normal hyperfine separations observed in thallium, and may be made to give negative splitting factors to account for the inverted hyperfine separations observed in cadmium. Regardless of the quantum conditions or the quantum numbers assigned to each proton, *something corresponding to the Pauli exclusion principle for electrons would be expected to be in operation in the nucleus.* Consequently if, by analogy with extra-nuclear electrons, we assign to each proton in addition to spin, the quantum numbers n and l there is then a possibility that a nucleus containing q protons might have the same configuration as that containing q extranuclear electrons.

In the following table, column two, I have listed the normal proton configuration for the first few elements in the periodic table, on the assumption that it is identical with the normal electron configuration of that atom having the same number of extranuclear electrons. The S, L and J values of the lowest multiple term in each of these proton configurations are given in column three, and the observed nuclear spins in column four. The J value subscripts which give the lowest term in optical spectra are set in heavy type. The agreement between J values and the observed nuclear spins is quite remarkable and it seems unlikely that it is due purely to chance. For Li_7, I equals $\frac{3}{2}$, a resultant composed wholly of proton spin. Here the resultant orbital motion of three protons is zero and the hyperfine splitting factor $g(I)$ should be the same as that expected from the proton spin theory, a result already shown to be in quite good agreement with observation. Like the partially inverted ^3P ($1s\,2p$) spectral term in Li II and the completely inverted ^3P ($1s\,2p$) term in helium, $^3P_1$ in the N_{14} nucleus and $^3P_0$ in the O_{16} nucleus could well lie deepest.

TABLE I.

Element	Proton config.	Lowest nuclear term	Nuclear spin observed
H_1	$1s$	$^2S_{\frac{1}{2}}$	$\frac{1}{2}$
He_4	$1s^2\ 2s^2$	$^1S_0$	0
Li_6	$1s^2\ 2s^2\ 2p^2$	$^3P_{0,1,2}$	0
Li_7	$1s^2\ 2s^2\ 2p^3$	$^4S_{1\frac{1}{2}}$	$\frac{3}{2}$
Be_9	$1s^2\ 2s^2\ 2p^5$	$^2P_{1\frac{1}{2},\frac{1}{2}}$	
B_{10}	$1s^2\ 2s^2\ 2p^6$	$^1S_0$	
B_{11}	$(\ )\ 3s$	$^2S_{\frac{1}{2}}$	
C_{12}	$(\ )\ 3s^2$	$^1S_0$	0
N_{14}	$(\ )\ 3s^2\ 2p^2$	$^3P_{0,1,2}$	1?
O_{16}	$(\ )\ 3s^2\ 2p^4$	$^3P_{2,1,0}$	0
F_{19}	$(\ )\ 3s^2\ 2p^6\ 4s$	$^2S_{\frac{1}{2}}$	$\frac{1}{2}$
Ne_{20}	$(\ )\ 3s^2\ 2p^6\ 4s^2$	$^1S_0$	0

Though it is difficult to say how far the analogy between proton configurations and electron configurations can be carried, it is highly improbable that after the first few elements in the periodic table the order of proton binding would be the same as that for extranuclear electrons. The whole question of binding energy and the stability of the nucleus, brought out by abundance relations, enters the problem at this point.

The tabulation of Table I is not to be considered as an explanation of nuclear structure.

It is given for the purpose of showing that in addition to proton spin another quantum number may be assigned to each proton and the result brought into agreement with observed nuclear spins. Finally (as pointed out by McLennan, McLay and Crawford) the resultant angular momentum of the nucleus can be made to account for the large positive, as well as negative, splitting factors.

H. E. WHITE

Department of Physics,
University of California,
Berkeley, California,
November 13, 1930.

The Entropies of Methane and Ammonia

There has recently appeared in the Physical Review (**38,** 1565 (1931)), an article by D. S. Villars on the entropy of polyatomic molecules. In this paper, Villars applies the symmetry considerations of Hund and Elert to the cases of methane and ammonia, and deduces from them the effect of symmetry and nuclear spin on the *a priori* probabilities of the various rotational states. Knowing these *a priori* weights, it is a simple matter to write out the expression for $Q=\sum_i P_i e^{-\epsilon_i/kT}$ and from this to calculate the rotational entropy. The values obtained by Villars differ from those calculated by Giauque, Blue and Overstreet (Phys. Rev. **38,** 196 (1931)) for methane and ammonia gases with the Sackur-Tetrode equation for translational and rotational entropy, modified to include the effect of symmetry and nuclear spin. There seemed no evident reason why the entropy calculated by these two methods should not agree exactly, provided that the gas under consideration had reached the limiting rotational specific heat, and the same molecular constants were used in both. Therefore we undertook to recalculate Villars' results, by using his *a priori* probabilities in the series for Q, but evaluating Q and $dQ/d\sigma$ by means of summations, instead of by using his approximations. Both for methane and ammonia, the entropy we calculated was identical, within 0.01 unit, with the Tetrode value. It is evident that Villars has made some error in evaluating Q and $dQ/d\sigma$. Moreover, his statement that the values of Giauque, Blue and Overstreet deviated from his own due to an inaccurate approximation on the part of the former, is unfounded, as we shall show.

If we assume methane to be a regular, rigid tetrahedron, the rotational energy levels are given by the formula,

$$E=\frac{h^2}{8\pi^2 I}j(j+1).$$

For I, we have used the value obtained by Dickinson, Dillon and Rasetti (Phys. Rev. **34,** 582 (1929)) from Raman effect, 5.17×10^{-40} gram cm^2. According to Villars, there are three non-combining varieties of methane, nuclear quintet, triplet and singlet, which result from the effect of nuclear spin. They are present in the ratio of 5:9:2 in ordinary methane. Therefore

$$S_r CH_4 = 5/16\,{}^5S_r + 9/16\,{}^3S_r + 2/16\,{}^1S_r + S_{\text{mix}}$$

where ${}^5S_r$ is the rotational entropy of a mole of the pure quintet variety, and ${}^3S_r$ and ${}^1S_r$ have an analogous significance. By using the definitions

$$Q=\sum_i P_i e^{-E_{r,i}/kT} \qquad \sigma=\frac{h^2}{8\pi^2 I k T}$$

we have

$$S_r = R\left[\ln Q - \sigma\frac{d\ln Q}{d\sigma}\right]$$

An evaluation of Q and $dQ/d\sigma$ by the usual method of calculating Boltzmann factors for each level and multiplying by the appropriate *a priori* weights and then summing, yields the following results, at 298.1°K:

$${}^5S_r = 13.28, \quad {}^3S_r = 14.45, \quad {}^1S_r = 11.46.$$

With the above formula,

$$S_r CH_4(298.1°) = 5/16 \times 13.28 + 9/16 \times 14.45 + 2/16 \times 11.46 + 1.88 = 15.59.$$

The Sackur-Tetrode translational entropy is 34.27 units. The entropy of vibration has been calculated by Villars as 0.11 unit. The absolute entropy of methane is therefore

$$S^{298.1°}_{CH_4} = 15.59 + 34.27 + 0.11 = 49.97 \text{ cal. deg.}^{-1} \text{ mole}^{-1}.$$

This is in exact agreement with the value 49.86 calculated by Giauque, Blue and Overstreet, since they neglected the vibrational entropy. It differs, however, from Villars' value of 50.13.

The entropy to be used in connection with entropies in common use for other substances is the absolute entropy minus the limiting nuclear spin entropy, $49.97-R\ln 16=44.46$.

The same procedure was followed in treating ammonia. Assuming a rigid symmetrical pyramid as the structure of the ammonia molecule, the rotational energy levels are given by the formula:

$$E=\frac{h^2}{8\pi^2}\left[\frac{j(j+1)}{A}+\left(\frac{1}{C}-\frac{1}{A}\right)T^2\right] \quad T\leqq j.$$

Defining $\sigma_1=h^2/8\pi^2AkT$

$$\sigma_1=\frac{h^2}{8\pi^2AkT} \qquad \sigma_2=\frac{h^2}{8\pi^2kT}\left[\frac{1}{C}-\frac{1}{A}\right]$$

the rotational entropy, S_r, of the symmetrical top is

$$S_r=R\left[\ln Q-\sigma_1\frac{\partial \ln Q}{\partial\sigma_1}-\sigma_2\frac{\partial \ln Q}{\partial\sigma_2}\right].$$

According to Villars there are two varieties of ammonia, nuclear quartet and doublet, existing in equal amounts in ordinary ammonia.

For A, the moment of inertia perpendicular to the symmetry axis, (the one occurring twice), we use the value of Dickinson, Dillon and Rasetti (loc. cit.), 2.792×10^{-40} gram cm^2. For C, the moment of inertia around the symmetry axis, we use the value 3.49×10^{-40} gram cm^2 given by Badger (Phys. Rev. **35**, 1036 (1930)). With these constants in the two Q series of Villars, we obtain the following results for the rotational entropy at 298.1°:

$$^4S_r=13.98 \qquad ^2S_r=13.98.$$

Therefore $S_r NH_3=13.98+R\ \ln\ 2=15.36$. With the same vibrational frequencies selected by Villars, we obtain 0.11 unit for the vibrational entropy at 298.1°. Villars calculated this to be 0.06, but made an arithmetical error. The Sackur-Tetrode translational entropy is 34.45. Since the nitrogen nucleus has a spin of one unit, we must add to the quantities enumerated above, R ln 3, to obtain the absolute entropy.

$$S^{298.1}_{NH_3}=34.45+15.36+0.11+2.18$$
$$=52.10 \text{ cal. deg.}^{-1} \text{ mole}^{-1}.$$

The difference between this value and that of Giauque, Blue and Overstreet is exactly accounted for by the difference in the amount assigned to vibrational entropy and by the difference in the value used for C in the two calculations. We wish to emphasize the fact that the value calculated from the Tetrode equation is in exact agreement with the above value if the same constants are used.

The absolute entropy of ammonia minus the limiting spin entropy is $52.10-R\ln 24=45.79$. This is in good agreement with the experimental value 46.1, calculated by Giauque, Blue and Overstreet from the entropies of N_2 and H_2 and the free energy data of Lewis and Randall (Thermodynamics, p. 557).

The question as to whether the value 45.79. will be equal to that obtained for the entropy of ammonia by means of the third law of thermodynamics cannot be answered *a priori*. This will depend on the situation existing in the solid, and must be decided by experiment. Nevertheless, regardless of any complications such as rotation in the solid, and so forth, the value 45.79 is the one which should be used in thermodynamic calculations.

D. P. MacDougall
Chemical Laboratory of the
University of California,
Berkeley, California,
November 9, 1931.

Macroscopic and Lattice Expansion of Bi Single Crystals

J. K. Roberts[1] has been the first one to measure the thermal expansion coefficient of Bismuth single crystals normal ($\alpha\perp$) and parallel ($\alpha\parallel$) to the principal axis in the range between room temperature and melting point (272°C), in order to check the relation between specific heats (c) and the thermal expansion in anisotropic metal crystals proposed by Grüneisen and Goens.[2]

Roberts found an almost perfect constancy of $\alpha\parallel$ and $\alpha\perp$ for three Bi crystals between 30°C and 230°C. The values obtained in this region were: $\alpha\perp=12.0\times10^{-6}$ and $\alpha\parallel=16.2\times10^{-6}$. Above 230°C however $\alpha\parallel$ as well as $\alpha\perp$ decreased rapidly to almost one half of their value at 260°, i.e., still 10° below the melting point of the crystal. Since Robert's experiments prove the effect to be reversible one cannot ascribe it to a plastic deformation of the heated crystal caused by the weight of the measuring device.

In order to study this anomaly closer the expansion coefficient of the lattice was stud-

[1] J. K. Roberts, Proc. Roy. Soc. **A106**, 385 (1924).

[2] E. Grüneisen and E. Goens, Phys. Zeits. **24**, 506 (1923); Zeits. f. Physik **29**, 141 (1924).

ied by means of x-rays. A Bragg spectrometer of high accuracy was used, of which the detailed description will be published soon. The reflected intensities of a carefully selected bismuth crystal at the (111) plane were measured as a function of temperature, with an ionization chamber of special design and a Hoffmann electrometer. By these means it was possible to obtain an accuracy of the thermal expansion of the same order as the macroscopic observations, and it thus has been possible to decide whether or not the "decay" of the crystal found macroscopically is due to a gradual disintegration of the lattice as Roberts suggested.

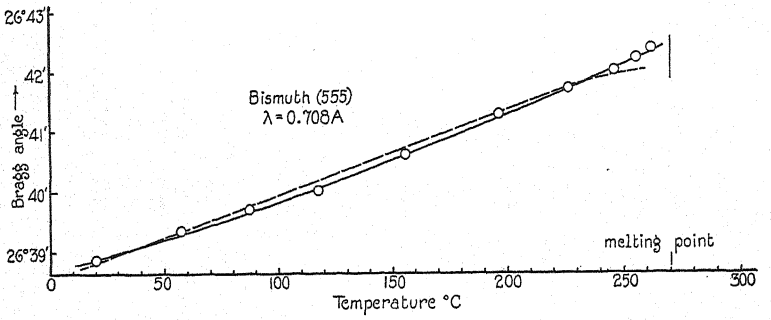
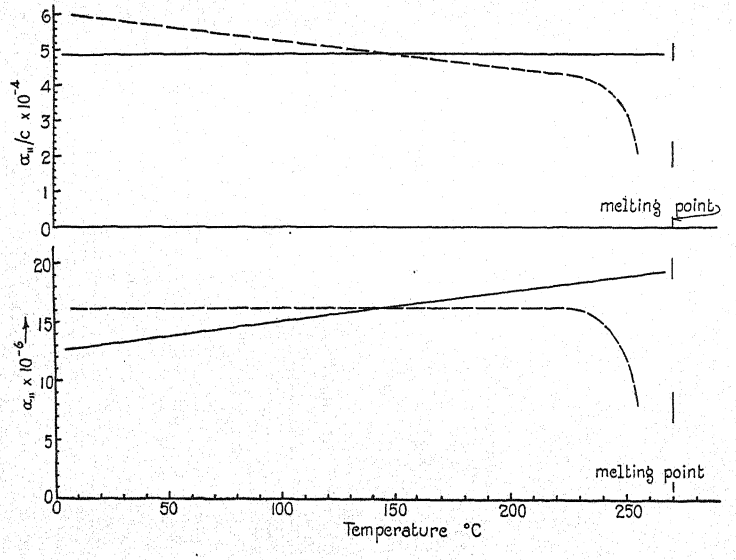


Fig. 1.

Fig. 1 shows the Bragg angle as a function of the temperature in °C. The dashed curve gives the mean of the observations of Roberts when these are translated to Bragg angles for the 5th order reflection of $K\alpha$Mo$=0.708$A with the known lattice spacing of the (111) plane ($D=3.945$A[3] at 23°C). The circles give our data obtained from the position of the intensity maximum of the Bragg-reflexions from the (111) plane of Mo$K\alpha$-radiation in the fifth order at different temperatures. (The diameters of the circles indicate the estimated error.) Although the points are more scattered about this curve than the accuracy of the measurement should permit, the quantitative agreement of the average $\alpha_{\parallel}=16.1\times10^{-6}$



Figs. 2 and 3.

[3] R. C. Hergenrother, Thesis (1931). California Institute of Technology.

with Roberts' value (16.2×10^{-6}) is however surprisingly good.

The solid line indicates the best fitting curve drawn through the experimental points, showing that $\alpha\|$ increases with temperature as far as the lattice expansion is concerned.

Special care was taken in the observations above 220°C where our measurements have shown a distinct deviation from Roberts' measurements, indicating that the macroscopic "decay" of the crystal is not caused by the lattice, since our $\alpha\|$ continues even to increase beyond 230°.

The above relations are shown more clearly in Fig. 2 in which is plotted directly against the temperature. The dashed line is the curve given by Roberts which shows distinctly the decline of $\alpha\|$ above 230°C. The solid line represents the values of $\alpha\|$ obtained from the solid curve of Fig. 1, i.e., the best representation of our measurements in terms of $\alpha\|$.

Since the specific heats of Bi between room-temperature and 700°C have been measured meanwhile by S. Umino[4] the validity of Grüneisen's postulate can be tested much more accurately than Roberts was able to do. Umino found a uniform increase in the true specific heats of Bi between 0° and melting point. Fig. 3 shows the curves obtained if the respective values of $\alpha\|$ shown in Fig. 2 are divided by the corresponding values of c measured by Umino. The dashed curve represents the values of the macroscopic expansion, the solid line the lattice expansion. The fact that the latter does *not* show any temperature variation proves the validity of the postulate of Grüneisen and Goens for the lattice expansion parallel to the axis of Bi. The macroscopic expansion however is shown to deviate to a much larger degree from the relation than can possibly be explained by Roberts' experimental error.

Our observations together with those of Roberts seem to prove that there exists a distinct difference between the macroscopic and the lattice expansion. The spacing of the atoms in the lattice follows the $\alpha\|/c=$ const-relation up to the melting point, whereas the expansion of the crystal as a whole stays constant over a comparatively large region of temperature and begins to decline to nearly half its value during the last 30°–40° before the fusion.

Apparently we have the deal here with a phenomenon hithertofore unknown, which may be ascribed to the existence of a secondary structure in a macroscopic crystal, the thermal variation of which cannot be found by x-ray reflections due to its large parameter (*ca.* 10^{-4} cm.)[5] A method however which integrates overall thermal variations in a large crystal, such as the usual measurement of thermal expansion, is bound to obtain different results, in case such a substructure exists as was already made highly probable in the case of Bi. With this assumption the "decay" of the macroscopic expansion had to be ascribed to a gradual disintegration of the secondary structure, which does not affect the crystal elements and therewith the x-ray reflections.

A detailed description of the methods and observations together with a more extended discussion of this effect will be published soon.

ALEXANDER GOETZ
R. C. HERGENROTHER
California Institute of Technology,
Norman Bridge Laboratory of Physics,
Pasadena, California,
November 3, 1931.

[4] S. Umino, Sc. Rep. Tohoku Univ. **15**, 604 (1926).

[5] A. Goetz, Proc. Nat. Acad. **16**, 99 (1930).

A New Long Wave-Length Absorption Band of CS_2

In a recent paper C. R. Bailey and A. B. D. Cassie (Proc. Roy. Soc. **A132A**, 236 (1931)) have reported the result of an investigation of the infrared spectrum of CS_2 with a prism spectrometer. They observed four bands at 2330, 2179, 1523, and 878 cm^{-1} of which the band at 1523 was found to be much the most intense. All bands (except one which was not resolved) showed a simple doublet structure with a mean spacing of about 13 cm^{-1}. The Raman spectrum of CS_2 has also been measured (Krishnamurti, Ind. J. Phys. **5**, 109 (1930)) and consists of two lines at 655.5 and 795.0 cm^{-1} of which the first was found to be strong and the latter weak. These data may be examined in the light of the selection rules proposed by Dennison (Rev. Mod. Phys. **3**, 297 (1931)) with the view of determining the form of the molecule. While the number of bands so far observed is few, their positions distinctly favor the assumption that the molecule is both linear and symmetrical, since no

band is observed whose frequency is equal to the sum or difference of any two observed bands. On the other hand differences between observed infrared bands do correspond exactly to the Raman frequencies.

Assuming that the molecule is linear and symmetrical we would conclude that the strong band at 1523 cm^{-1} is the active fundamental ν_3 (with the notation employed by Dennison, l.c. p. 292). Of the two Raman lines we would suppose that one should represent the inactive frequency ν_1 and that the other is twice the active fundamental ν_2. From a paper by G. Placzek (Zeits. f. Physik **70**, 84 (1931)) on the intensity of Raman lines of molecules of this type it would appear very probable that the stronger line at 655.5 cm^{-1} is the inactive fundamental.

To test these ideas we have made a search for the active fundamental ν_2 in the region of 25μ. The spectrometer used employed a reflection grating of the echelette type. The thermopile window was of KBr. To prevent overlapping spectra a band of radiation from 21 to 34μ was obtained by reflection from a fluorite crystal. The observations were further freed from effects of short wave-length impurity by use of a fluorite plate as shutter. The absorption cell, which was 3 cm long and fitted with lacquer film windows, contained CS_2 vapor saturated at room temperature (26°C).

A very intense absorption band was found whose envelope structure could be obtained although the individual rotation lines were not resolved. The envelope possessed P, Q, and R branches lying at 389.4, 396.8, and 405.8 cm^{-1} respectively. Thus the existence and position of the band as well as its structure (existence of a Q branch) are completely in accord with our theory. The doublet separation, 16.4 cm^{-1}, leads to a moment of inertia $I=172\times10^{-40}$ and a distance between S atoms of 2.54×10^{-8} cm. These values are considerably lower than the figures obtained by Bailey and Cassie ($I=264\times10^{-40}$ and $S-S=3.20\times10^{-8}$ cm), but it appears possible that our results might be the more accurate by reason of the larger dispersion obtainable in this region.

A very important paper has appeared recently by E. Fermi (Zeits. f. Physik **71**, 250 (1931)) dealing with the Raman spectrum of symmetrical, linear tri-atomic molecules. Fermi has shown that for such molecules important modifications must be made in the existing theory when one of the frequencies ν_1 is approximately equal to twice the frequency ν_2. These modifications show on the one hand that the Raman spectrum should consist principally of two lines. On the other hand they show that the energy levels of the molecule may possess perturbation terms which are of first order in contradistinction to the usual theory in which the perturbations are always of second order. The first order perturbation whose existence Fermi has pointed out may be shown to go over into the usual second order perturbation expression when the difference between ν_1 and $2\nu_2$ is large compared with certain of the anharmonic constants. We have substituted the experimental values for the infrared and Raman frequencies of CS_2 into the theoretical formulae and find that for this case $\nu_1-2\nu_2$ is sufficiently large so that the energy levels may be described in the usual manner using second order terms. The molecule of CO_2 differs from CS_2 in that $\nu_1-2\nu_2$ is very nearly zero and thus the positions of the bands show certain anomalies which are however beautifully explained by the Fermi theory. It might be mentioned that the circumstance of $\nu_1\cong2\nu_2$ does not alter the validity of the selection rules.[3]

Our interpretation of the CS_2 spectrum is given in Table I and agrees completely with the scheme proposed by Placzek. The exactness with which the combination relations are obeyed is a verification of our calculation which showed that the energy levels of CS_2 might be described with the aid of perturbations terms of second order only.

TABLE I.

Identification	Frequency (obs.)	Frequency (calc.)
ν_2	396.8 cm	—
ν_1	655.5	—
$2\nu_2$	795.0	793.6
ν_1	878	867.5
ν_3	1523	—
$\nu_3+\nu_1$	2179	2178.5
$\nu_3+2\nu_2$	2330	2318

DAVID M. DENNISON
NORMAN WRIGHT

Department of Physics,
University of Michigan,
Ann Arbor, Michigan,
November 7, 1931.

Photoelectric Efficiencies in the Extreme Ultraviolet

Measurements of the photoelectric efficiencies of the extreme ultraviolet radiations of Ne and A have been carried out which confirm earlier results[1] that these efficiencies are considerably higher than the known efficiencies in the nearer ultraviolet.

Photoelectric and energy measurements were made in a side arm to a tube carrying a positive column discharge. A quartz filter, movable magnetically, permitted the separation, in the case of each rare gas, of the effects of the extreme ultraviolet radiations from the effects of the rest of the spectrum. The spectral regions so isolated are: $\lambda 744A - \lambda 575A$ for Ne, and $\lambda 1050A - \lambda 790A$ for A, approximately.

For the energy measurements a thermopile was used of the absolute type devised by Coblentz and Emerson.[2] The receiver of this instrument as constructed was a constantan sheet 2.3 cm $\times$ 1.8 cm $\times$ 0.00063 cm mounted 1 mm in front of the 19 hot junctions of an iron-constantan thermopile. A known calibrating current could be passed through the receiver. Photoelectric currents were measured either from the receiver itself, in which case all questions of reflection are eliminated, or from a Ni plate of the same size which could be moved magnetically to a position close in front of the receiver. In the latter case it can be assumed that the extreme ultraviolet energy absorbed by the Ni surface is approximately the same as that absorbed by the receiver since O'Brien[3] has shown that reflection coefficients are very small in the wave-length region here considered. The Ni plate could be withdrawn into a side arm for degassing purposes. An open mesh grid placed about 1 cm in front of the receiver served as an anode to collect the electrons. The receiver of the thermopile was left bright in order to decrease, relatively, the sensitivity to the visible and infrared rays. The thermopile, except for the front face of the receiver was completely surrounded by a Ni housing which prevented any radiation from entering the interior. The sensitivity of the instrument, with the galvanometer used, was of the order of 1 mm for a few microwatts, varying considerably, with the nature and pressure of the gas used.

Experiments, showing that the emission of electrons by metastable atoms under circumstances like the present is small compared with the photoelectric effect, have already been reported.[1] The details of these experiments will be given in a later paper, but it may be stated here that electron currents obtained from a micabacked Mo disk, mounted some centimeters in front of the thermopile of the present apparatus so that it could be rotated magnetically were about six times as great when the disk was perpendicular to the direction of the radiation as when the disk was parallel to the radiation. This showed that at least the main part of the currents involved were caused by an agent having directional properties and which therefore must have been radiation rather than metastable atoms, or ions and electrons diffusing in from the discharge.

Gas pressures of the order of 0.1 mm were used. The gases were purified by the action of a mischmetal arc, and also in the case of Ne by circulation over charcoal in liquid air.

In each case, energy measurements were made with and without the quartz filter, and the difference, making allowance for reflection at the quartz surface, was taken to be the energy in the extreme ultraviolet. This difference amounted to from 20 percent to 50 percent of the total energy absorbed. The arc was left on in each case only long enough (10 seconds) for the thermopile reading to reach an approximate equilibrium value. The effects of heat rays from the glass, warmed by the discharge, were found to be relatively small and were allowed for. Approximate saturation photoelectric currents were measured at the same time as the energy. Photoelectric currents were undetectable when the quartz filter was in place.

The values found for the photoelectric efficiencies for a Ni surface degassed by heating in a vacuum until considerable evaporation had taken place were of the order of 2 percent for Ne (2 electrons per hundred quanta) and 1 percent for A. The wave-lengths of the resonance radiations were used in the calculations.

It was found with the present and other apparatus that the photoelectric currents from Ni, Fe, constantan and graphite were all of the same order of magnitude and that in the cases of Ni, Fe, and constantan a non-degassed surface gave two to three times as

[1] Carl Kenty, Phys. Rev. **38**, 377 (1931).

[2] W. W. Coblentz and W. B. Emerson, Bulletin of the Bureau of Standards **12**, 503 (1915–16).

[3] H. M. O'Bryan, Phys. Rev. **38**, 32 (1931).

much current as a surface which had been well degassed. Thus the efficiencies found for such surfaces were of the order of 5 percent and 2 percent for Ne and A respectively.

Photoelectric currents obtained with Hg discharges were relatively very small and sufficiently in accord with the known values of the efficiency of the normal photoelectric effect in the general region of λ2500A (taken to be of the order of 0.1 percent or 0.2 percent for metals like Ni.) The present results may also be compared with the maximum efficiencies reported for the total currents in the selective effect in the case of sensitive films of the order of 1 percent or 2 percent.

Preliminary experiments with He have yielded values of the efficiency comparable with those in Ne. The experimental conditions were not, however, as favorable in He as in the other cases and the evidence was not as clear that the action of metastable atoms was unimportant.

The experiments are being continued and extended to surfaces of different work functions. Details will be given in a later paper.

CARL KENTY

Research Laboratory,
General Electric Vapor Lamp Company,
Hoboken, New Jersey,
October 29, 1931.

Zeeman Effect in Solids

J. Becquerel,[1] Freed and Spedding,[2] and others have reported that the absorption lines of the rare earth spectra split into doublets of enormous separation when a magnetic field is applied. Both Becquerel and ourselves have stated that some lines under certain conditions resolve into more components; however, both emphasized that the doublets were the most striking facts observed. In a letter to the Physical Review of March 15, 1931, I announced that all lines of the Gd^{+++} ion spectra were complex in a magnetic field and that the doublets really consisted of several components, and that they appeared as doublets only on account of the low resolving power of the instrument used.*

Since that time I have combined the prism from a Hilger E2 spectrograph with a large three-meter Hilger (*L* mounting) and obtained in effect a three-prism instrument which gives a dispersion of 1.3A per mm at the 2700A band of the Gd^{+++} ion.

While unfortunately only three plates were obtained at this dispersion before it became necessary to have the magnet rebuilt, nevertheless the results were so interesting that a report of them now seems advisable. In all three cases the bands between 2700A and 2800A were photographed, the light passing through the crystal parallel to the *b* axis of the monoclinic $GdCl_3 \cdot 6H_2O$ crystal. In plates 1 and 2 the field was parallel to the *a* axis, the fields being 17.5 and 18.5 kilograms, respectively. In plate 3 the field of 18.5 kilograms was parallel to the *c* axis.

All the lines of the bands, which were separated from each other so that they did not overlap when the field was applied, split into nine lines of approximately equal spacing with an overall separation of 16 times the normal Larmor precession.

The intensities of these lines varied greatly; In some cases the outer components were very intense while the inner three or five were barely visible, thus giving rise to an apparent doublet under low dispersion. In other instances the inner components were the more intense giving the appearance of a single, unaffected or slightly widened line under low dispersion. Frequently the intense components in plates 1 and 2 were the faint ones in plate 3. For a few lines the nine components were intense in all three plates.

A Paschen-Back effect was clearly discernible in most of the lines, being small in plate 1 and fairly pronounced in plates 2 and 3. With increased Paschen-Back effect the lines tended to widen and blur and the dissymmetries in intensities became very pronounced. The dissymmetries in position were not so great, especially in overall separation. They did tend to make the intervals between the lines more irregular. These irregularities in the intervals, with two exceptions where the lines in question were close together, were never greater

* Note: J. Becquerel for some time has stated that many of the doublets in the case of other rare earths are actually quartets. It appears, however, from the following work they are really even more complex.

[1] Many papers. Leiden Comm. 1906–1931.

[2] Freed and Spedding. Phys. Rev. **35**, 1408 (1930); ibid. **38**, 670 (1931).

than 20 percent, on any of the plates investigated.

In the exceptions mentioned, lines 2788–9A and 2790–5A, while they gave the nine lines distinctly in plates 1 and 2 did not in plate 3. Also line 2790–5A did not seem to have an overall splitting of 16 ω (ω being the Larmor precession). However, the Paschen-Back effect here was pronounced so that the lines were badly blurred. In addition weak components may have been present.

The lines upon which the splitting could be observed were as shown in Table I.

TABLE I.

Line	Plate 1	Plate 2	Plate 3
A	Field 17.5 K.G. parallel to a	18.5 K.G.	18.5 K.G. parallel to c
2793.07	9 c ?	9 c ?	9 o.f.
2790.49	9	9	9 ? blurred
2788.90	9	9	9 ? blurred
2786.68	9 f	9 o ?	9 c ?
2766.47	9 c.f.	9 c ?	9 c
2764.29	9	9	9 o.f.
2745.57	9 c.f. blurred	9 c ?	9 o.f.
2743.54	9 c.f. blurred	9 c ?	9

c = center compounds; o = outside components
f = faint but definitely present; ? = doubtful

In my last letter[3] I called attention to the fact that many investigators have shown the basic level of Gd^{+++} ion in solids must be a $4f^7$; $^8S_{7/2}$ level, which is not split apart appreciably by the electric field of the crystal and which is free to take all orientations in a magnetic field. This level would then split into eight equally spaced levels of 2ω separation when a magnetic field is applied. Of course as Kramers[3] showed there would be a slight second order splitting due to the crystal field, so that the spacings would be distorted somewhat depending on the magnitude of the effect, but it is certainly small.

I also pointed out that the excited level most probably arises from one of these electrons jumping out through the completed $5s$ and $5p$ shells, giving rise to a configuration such as the $4f^8 5d$.†

I showed there, that one might expect the six $4f$ electrons to couple with Russell-Saunders coupling to give a ^7F term, and that the external electron would be coupled more loosely due to the partial shielding action of the completed $5s$ and $5p$ shells. The external electron would have its orbit coupled strongly with the electric field of the crystal[5] (Case II Bethe)[6] so that it could not orient in a magnetic field. The magnetic moment set up by this orbit however would tend to couple with the moment of the ^7F term inside and the energy of the coupling would presumably be strong enough to prevent the orientation of this core in a magnetic field.

The spin of the external electron, however, would be very loosely coupled as its resonance effect with the other electrons would be small due to the partial shielding action of the completed $5s$ $5p$ shells, and would be of the order of magnitude of the coupling energy of a single electron. It would therefore orient in the

† $4f^7$ electrons give rise to only one octet term, $^8S_{7/2}$ as Pauli's exclusion principle excludes all others. Therefore, for the electron to remain under the influence of the shielding effect of the completed $5s$, $5p$ shells, it would be necessary for a spin to reverse itself when Δn and Δl are 0, giving rise to a sextet term. Reversals such as these rarely occur in atomic spectra. Also the energy involved would probably be large.

[3] F. H. Spedding. Phys. Rev. **37**, 777 (1931).

[4] Kramers. Proc. Amst. Acad. **33**, No. 9 (1930).

[5] E. C. Stoner, in order to account for the magnetic susceptibilities of the iron group has suggested that the orbits are bound and only the spins are free to orient in a magnetic field. Phil. Mag. **8**, 250 (1929).

[6] Bethe. Ann. d. Physik **3**, 133 (1929).

fields obtainable in the laboratory, giving rise to two levels with a separation of 2ω.

Bethe[6] has shown that in crystals the ordinary selection rule of $\Delta m = \pm 1$ does not hold, but that new selection rules apply which permit large jumps in m. These depend on the symmetry of the fields, etc., and in this case are rather uncertain; however, if one assumes all transitions are possible between the levels, exactly nine equally spaced lines are obtained with an overall separation of 16ω. This is true regardless of the term of the upper level.

If the magnetic field splitting becomes of the order of magnitude of the splitting due to the crystal field, then a Paschen-Back effect will be observed and the lines will first blur and then resolve into two components. Also if the coupling of the basic term with the crystal field is large enough so that the magnetic field is not strong in comparison with it, the pattern will be destroyed, and thirdly, if the coupling energy of the spin in the upper term is of the same magnitude as the applied field, again the pattern will not be obtained.

From the above results it seems that the spin of the external electron is very weakly coupled with the orbit, also that the splitting of the basic level due to the crystal field is small.

It seems probable that the excited levels of the rare earths are of the type $(({}^7F_0d)_2)_{5/2}$, $(({}^7F_1g)_4)_{9/2}$,[7] which are split apart due to the various coupling of the external electron orbit with the field of the crystal.

I hope shortly to resume these investigations, studying the polarization of the lines and the effect of various field strength on their splitting. Mr. G. Nutting and myself have investigated the effect of crystal symmetry on the splitting of these terms and expect to publish the results very shortly in the Journal of the American Chemical Society.

F. H. SPEDDING
National Research Fellow in Chemistry,
University of California, Berkeley,
November 5, 1931.

[7] Professor R. T. Birge very kindly suggested this type of nomenclature for the terms in question.

Comparison of Viscosity and Molecular Arrangement in Twenty-two Liquid Octyl Alcohols

In my recent article just published (Phys. Rev. **38**, 1575 (1931)), the values of viscosity for approximately 0°C were used, whereas the x-ray observations were taken between 20° and 30°C. But the rate of change of the viscosity with temperature is of approximately the same order of magnitude in all cases so that the comparison between x-ray diffraction and viscosity is essentially correct if regarded as referring to same temperature conditions. As a matter of fact, the comparison would be slightly improved by using the viscosity at 25°C. The values of viscosity are those obtained by Bingham and Darrell (Rheology **1**, 174 (1930)).

G. W. STEWART

University of Iowa,
Iowa City, Iowa,
November 5, 1931.

Measurement of Nuclear Spin

Hyperfine structures of spectral lines and alternating intensities of band spectra constitute at present the only available means of determining angular momenta of atomic nuclei. We wish to point out another means of finding nuclear spins. It is well known that the Stern Gerlach experiment allows one to determine the angular momentum of an electronic configuration. If the atom has an angular momentum $j(h/2\pi)$ there are $2j+1$ lines in the Stern Gerlach pattern for conditions where the velocity of the atomic beam is sharply defined. It is also obvious that if the inhomogeneous magnetic field used in the experiment is not too strong, the coupling of the electrons to the nucleus will not be destroyed. There will now be $(2j+1)$ $(2i+1)$ distinct states in a magnetic field, where $i(h/2\pi)$ is the angular momentum of the nucleus. It is possible, in some cases, to observe the pattern due to these states and to follow the transition to the strong field condition with $2j+1$ lines.

The number of Stern-Gerlach lines observed in a weak field, their positions, and the magnetic field strength necessary to bring about a partial transition to the strong field pattern will be seen to determine the value of the nuclear spin.

As an example consider an atom in a state

with inner quantum number $j=\frac{1}{2}$ and nuclear spin i. The energy of the atom in a magnetic field is

$$W = -\frac{\Delta W}{2(2i+1)} \pm \frac{\Delta W}{2}\left(1+\frac{2m}{i+\frac{1}{2}}x+x^2\right)^{1/2};$$

$$x = \frac{g\omega}{\Delta W}, \quad \omega = \frac{eh}{4\pi mc} \quad H = \mu_0 H$$

where ΔW is the separation between the two hfs components in the absence of a magnetic field, g is the Landé g factor for the electronic configuration (e.g. 2 for ^2S terms), m is the magnetic quantum number and H is the magnetic field. The force due to an inhomogeneous magnetic field is

$$F = -\frac{dW}{dH}\frac{\partial H}{\partial y}$$

where dH/dy is the gradient of the magnetic field. Thus

$$F = \pm\frac{\frac{2m}{2i+1}+x}{2\left(1+\frac{4m}{2i+1}x+x^2\right)^{1/2}}\cdot g\mu_0\frac{\partial H}{\partial y}.$$

For

$$i=\tfrac{1}{2}, \quad F = \pm\frac{x+m}{2(1+2mx+x^2)^{1/2}}\cdot g\mu_0\frac{\partial H}{\partial y}.$$

For

$$m = 1,\ 0,\ 0,\ -1$$

$$F = \left(1, \frac{x}{(1+x^2)^{1/2}} - \frac{x}{(1+x^2)^{1/2}} - 1\right)(g/2)\mu_0\frac{\partial H}{\partial y}.$$

In a weak field the Stern-Gerlach pattern should consist of three lines the central one having twice the intensity of the two deflected lines. In intermediate fields there are 4 lines and in strong fields (complete Paschen-Back effect for hfs) there are only two lines both of which are displaced. The weak field region may be said to correspond to $x<0.1$, the intermediate to $x=1$, and the strong to $x>3$. If ΔW measured in cm^{-1} is denoted by $\Delta\nu$ then H in gauss is

$$H = 2.14\times 10^4 \times (\Delta\nu)/g.$$

For the normal ^2S state of $Cs\ \Delta\nu=0.30$ cm^{-1} and the low field region $x=0.1$ lies below 320 gauss while $x=3$ for 9.6×10^3 gauss. For $x=1/(8)^{1/2}=0.354$ the four lines will be equidistant. This corresponds to a field of $1.14\times 10^{+3}$ gauss.

The nuclear spins of Cs and Rb are at present being investigated with this method by one of us (I. I. R.).

G. Breit
I. I. Rabi

New York University,
Columbia University,
November 10, 1931.

BOOK REVIEWS

Photochemistry. D. W. G. STYLE. Pp. vii+96, figs. 9, E. P. Dutton and Company, 1931. Price $1.10.

The essential facts of photochemistry are outlined fluently and clearly in this brief review. The first chapter consists of a short introduction to the quantum theory of light absorption, particularly absorption by molecules. The fundamental laws of photochemistry, typical secondary chemical processes, and the dependence of the quantum yield on temperature and pressure are discussed in the following chapters. The final chapter is devoted to a brief survey of experimental methods.

This book should prove very valuable to anyone who wishes to obtain a clear understanding of the fundamental principles of photochemistry without being forced to disentangle them from a mass of rather confusing experimental results. However, if it is used as an introductory text the student should realize that the experimental material has been carefully selected to eliminate individual complexities and to illustrate general laws.

ROBERT LIVINGSTON
University of Minnesota

A Monograph of Viscometry. GUY BARR. xiv+318 pp., figs. 54. Oxford University Press, 1931. Price 30 s.

This book is devoted almost entirely to considerations of the theory and technic of viscosity measurements.

On the theoretical side the various formulae which have been proposed are considered in detail, each quantity is discussed in relation to the available physical knowledge and is accordingly evaluated in so far as its relationship to accuracy of measurement is concerned.

On the technical side the precautions which must be observed if one wishes to make accurate measurements are strongly stressed. Almost every conceivable detail of technic is considered including even such items as the maintenance of sensitivity and the accuracy of thermoregulators for the temperature bath. Anyone who believes that it is relatively easy to make reasonably accurate measurements of absolute viscosity will certainly be disabused of that idea by a careful perusal of this monograph.

Chapter I is devoted to a brief introductory statement and a short history of the development of viscosity measurements. The reviewer was interested to note that Poiseuille was lead to his classical studies by a desire to obtain some understanding of the laws governing the passage of blood through the capillaries. The author notes that Poiseuille's researches have been more fruitful than has any other biophysical investigation.

Chapter II considers "The Viscous Flow of Fluids in Tubes," Chapter III "Tube Viscometers for Absolute Measurements" where we learned that if the length of the capillary tube is 20 cm the *maximum* radius of the capillary must not exceed 0.0268 cm and that if the length is decreased the radius must also be decreased ($l=8.6$ cm, $r=0.0172$ cm). It may be parenthetically added that the reviewer believes that some confusion may arise from the *apparent* change of symbols in certain of the formulae, thus a denotes the radius of a right cylindrical capillary tube (although r is apparently sometimes used to denote tube radius) and r is in general used to denote the radius of a cylindrical surface coaxial with the capillary tube; on p. 20 "Q" denotes the "volume of liquid flowing through the tube in unit time," on p. 21 "V" is used to denote "the volume of liquid discharged in time 't' ", and on page 80 "V" is used as the symbol for the "volume of the measuring bulb." It is thus difficult to follow the derivation of certain of the formulae and to compare one formula with another; all of which emphasizes the desirability of international agreement on a code of symbols used to denote physical quantities.

The later chapters deal with (IV) Commercial Absolute Viscometers; (V) Capillary Viscometers for Relative Measurements; (VI) Flow between Parallel Planes; (VII) The Transpira-

tion of Gases; (VIII) The Falling Sphere Method (the author notes that the tube containing the liquid through which the sphere is allowed to fall must have a diameter at least 20 times that of the falling sphere if the effect of the wall is to be eliminated and an accuracy of 0.5 percent secured. The ratio of these diameters also depends on the viscosity of the liquid, thus for a viscosity of 40 poises a "1/8 inch ball requires a fall tube 3 inches in diameter which for a 1/16 inch ball reduces to 1 1/2 inches;)" (IX) Rotational and Oscillational Viscometers in which the Couette, Hatschek, Searle, Stormer and MacMichael viscometers are analyzed (no mention is made of the Majonnier-Doolittle viscosimeter which has been used to a certain extent in the dairy industry of America); (X) Miscellaneous Methods of Viscometry; (XI) The Study of Anomalous Systems followed by appendices which contain detailed specifications of the Redwood, Saybolt and Engler viscometers; a chart to enable the interconversion of readings obtained by the use of various industrial viscometers, and viscosity-temperature tables of water and various concentrations of sucrose solutions. Water at 20°C is given a viscosity of 1.009 cp. Refined castor oil is recommended as a reference fluid for viscosities ranging from 2.31 (40°C) to 37.60 (5°C) poises.

An author and a subject index close the volume.

The reviewer was especially interested in Chapter XI, for this deals largely with the lyophilic colloid systems and introduces some discussion of "plasticity" in the sense of Bingham. It is to be regretted that the author did not devote more than 20 pages to these anomalous systems, but there is much food for thought in that brief discussion.

The book is recommended to all who are interested, be it ever so little, in either the theory or technic of viscometry. It will be invaluable to those whose special interest lies in this field.

R. A. GORTNER
University of Minnesota

Astronomy. FOREST RAY MOULTON. Pp. 549+xxiii, figs. 213. The Macmillan Company, New York, 1931. Price $3.75.

Dr. Moulton whose several previous text books on astronomical subjects enjoyed the distinction of becoming classics almost as soon as they appeared is to be congratulated upon the completion of this latest addition. As the foreword states, the "book is in no sense a revision of the author's Introduction to Astronomy, but an entirely new publication." Even the most casual glance will reveal that this is no ordinary text book, but a masterful summary of contemporary astronomy stimulating to teacher and student alike, and an invaluable reference book to the research worker.

One can heartily applaud the noble attempt made to relegate to oblivion that misnomer *asteroids*, and to reintroduce the proper term planetoids for these objects. The appended table of physical and astronomical constants is a particularly useful feature of the book though here one might regret the spurious accuracy of the astronomical unit—given to one kilometer exact—and the unfortunate misprint in the length of the sidereal year—16 hrs. instead of 6. A regrettable modesty on the part of the author has resulted in his own name being absent from the index while one has to search diligently before discovering the important part played by the author's in the modern theories of cosmogony. It would seem a little incautious at the present time to class Pluto with the planetoids—after all Pluto is still some 5 magnitudes brighter than would be Ceres at that distance. The importance of the solar system appears overemphasized since after 79 pages of introduction and descriptive remarks on the constellation 325 pages are devoted to the solar system, and only 131 pages to the stellar universe beyond.

Other minor criticisms and corrections are: On map I (p. 32) the precession circle should read pole of *equator*, instead of ecliptic; on p. 149 Lorentz's name is omitted in the mention of the Lorentz contraction; on p. 180 the impression is given that from the moon the earth would be seen to rise and set instead of remaining always stationary in the sky, subject only to a small swaying to and fro; on p. 486 the validity of the argument using the star density near the sun for the estimation of the dimensions of the Milky Way system appear doubtful; on pp. 520–521 the genitive of Dorado is Doradûs instead of Doradi.

W. J. LUYTEN
University of Minnesota

The Electrical Conductivity of the Atmosphere and Its Causes. VICTOR F. HESS. Translated from the German by L. W. Codd. Pp. 204, figs. 15. D. Van Nostrand Company, New York, 1928. Price $4.00.

It is a great boon to students of atmospheric electricity to have this excellent volume on the conductivity of the atmosphere from the authoritative pen of Professor Hess. The author has succeeded in condensing a very large amount of information into a comparatively small volume, and yet has produced a book which is very easy and agreeable to read. The older methods of atmospheric electric measurements pertaining to conductivity are described, but the subject is brought up to date by a continual reference to the more detailed considerations in the light of which the record of such instruments must be interpreted. Even when a detailed account of more recent methods is not given, the author calls attention to such methods and gives the references where details may be found.

In view of the fact that a very large amount of the literature of atmospheric electricity exists in the German language, it is particularly fortunate for English and American readers to have this very excellent translation by L. W. Codd of Professor Hess' book.

W. F. G. SWANN
Bartol Research Foundation

Das Vorkommen der Chemischen Elemente in Kosmos. HARALD VON KLUBER. Pp. 170 +vii, figs. 12. Barth, Leipzig, 1931. Price RM 20.

This excellent book gives a detailed resumé of the results achieved in investigating the occurrence of the chemical elements in the various parts of the universe. The chapter headings are: The Meteorites, The Moon, The Planets, The Comets, The Sun, The fixed Stars and Nebulae. The methods at the disposal of the investigator are well described and critically evaluated. The author lays great stress on the facts of observation and avoids as much as possible uncertain and controversial speculation. This book should be read by chemists and physicists; it should be extremely valuable to astrophysicists.

F. H. MACDOUGALL
University of Minnesota

The Atomic and Molecular Forces of Chemical and Physical Interaction in Liquids and Gases, and Their Effects. R. D. KLEEMAN. Pp. 133+vi, figs. 6. Taylor and Francis, London, 1931. Price 10s. 6d.

The author of this book has also written "A Kinetic Theory of Gases and Liquids," selecting this title, presumably, to indicate that his theory is not *the* kinetic theory of Maxwell and Boltzmann. At any rate, he seems to think that the average velocity of molecules in a liquid varies from one region of the liquid to another. The author starts from a very general law of molecular attraction expressed by means of a very indefinite equation containing a number of pliable constants. He deals with the attraction constants of the atoms, with intrinsic pressure, with the Joule-Thomson effect, with the latent heat of evaporation and with many other related topics. In the opinion of the reviewer, most of the striking agreements obtained by the author between experimental data and results calculated by some equation or other are merely illustrations of the general principle that if an equation by means of its adjustable constants is made to fit a part of a mass of comparable data, it will probably do pretty well for the remainder. It might be added that the author evidently considers that an experiment in which a gas is adiabatically expanded without doing any external work is a Joule-Thomson experiment.

F. H. MACDOUGALL
University of Minnesota

Mathematical and Physical Papers. SIR JOSEPH LARMOR. Vol. I and II, Pp. 1510. Cambridge University Press, London, 1929.

Students of mathematical physics, and particularly thsoe who have occasion to trace the historical development of the subject during the last half centruy, will welcome the appearance of this admirable compilation of papers which represents the work of one of the chief leaders in

applied mathematics during that period. Starting with two short papers on "Planimetry on a Moving Plane" and " 'Apparently Neutral' Equilibrium," of the regular old-time type, suggestive of the things which delighted the hearts of the mathematicians of bygone days, we pass through a series of papers of increasing virility, reaching their maximum of importance in "A Dynamical Theory of the Electric and Luminiferous Medium," published in three parts in the Philosophical Transactions of the Royal Society between the years 1894 and 1898. The maximum is, however, a flat one, and the papers continue with undiminished interest throughout the period of the last thirty years, comprising the extension of the work whose basis was outlined in the papers on the luminiferous medium, the continual development of new points of view, and critical surveys associated with the progress of physics through relativity, thermodynamics and heat radiation, up to the quantum theories of atomic structure of the present day.

Of the 104 papers reprinted, about 25 percent are devoted to electrodynamics in the broadest sense, including electro-optics and applied phenomena. About 18 percent are devoted to ordinary dynamics with special attention to problems of a cosmological nature. Radiation and thermodynamics receive about 10 percent; pure optics, about 11 percent; pure mathematics, 6 percent, and the remainder is devoted to miscellaneous subjects, including a number of addresses before learned societies. However, the actual proportion of material on electrodynamics is much larger than is indicated by the number of papers. Thus, the three papers on "A Dynamic Theory of the Electric and Luminiferous Medium" alone occupy one-fifth of the contents of the two volumes.

At the time when Sir Joseph Larmor commenced to take an active interest in electrodynamics, the work of Maxwell, although twenty years old, was still fresh in the minds of the mathematical physicists, as a theory of very abstract type, unintelligible to many, on account of mathematical difficulties, and a matter of suspicion to not a few. Even as late as 1904, Sir Arthur Schuster, in the preface to his famous "Theory of Optics," writes:

"There is at present no theory of Optics in the sense that the elastic solid theory was accepted fifty years ago. We have abandoned that theory, and learned that the undulations of light are electromagnetic waves differing only in linear dimensions from the disturbances which are generated by oscillating electric currents or moving magnets. But so long as the character of the displacements which constitute the waves remains undefined we cannot pretend to have established a theory of light. This limitation of our knowledge, which in one sense is a retrogression from the philosophic standpoint of the founders of the undulatory theory, is not always sufficiently recognized and sometimes deliberately ignored. Those who believe in the possibility of a mechanical conception of the universe and are not willing to abandon the methods which from the time of Galileo and Newton have uniformly and exclusively led to success, must look with the gravest concern on a growing school of scientific thought which rests content with equations correctly representing numerical relationships between different phenomena, even though no precise meaning can be attached to the symbols used."

The work of Maxwell, founded as it was in the initial instance upon the ideas of continuous currents in closed rigid circuits, sought to perpetuate that idea in the most vivid possible form to a description of the phenomena for the more general case. In this, there arose a certain incompleteness which could only satisfactorily be removed by a more general formulation of the problem in terms of aether on the one hand and electrons on the other. Maxwell's theory did not develop itself to this extent. Speaking of Maxwell's work, Sir Joseph Larmor writes, in his "Aether and Matter:"

"His efforts to fit the range of physical phenomena into an entirely new analytical frame, involving brilliant strokes of explanation diversified by abrupt transitions and unbridged *lacunae*, his essays at utilizing the analytical machinery of the older method of attractions towards the development of a new descriptive scheme that was to wholly supersede it, impart all the interest of nascent discovery to his 'Treatise.' . . . yet the conception of a struggle with confusion—successful but unfinished—not unfitly expresses the feeling that gains strength on each successive survey of the 'Treatise,' and which mainly arises from the necessary initial imperfections of a reconstruction of ideas in a vast domain in which the natural order and logical precision in exposition have not had time to be elaborated."

It fell to the lot of Larmor to take the next step in developing the dynamics of an aetherial

medium loaded with discreet electrons and in conjunction with Lorentz and a few others to bring the science of electrodynamics to the stage in which, while yet unfinished as regards its application to atomic phenomena, it represents the perfection of what we may call the classical electrodynamics of today. In his papers, we find the moulding of classical electric phenomena into a dynamical scheme under the general principle of least action, in such a way as to include the electrons and the aether as joint participants in the phenomena. Then we find the development of the consequences of these general laws to the field of optics of dielectric phenomena, and indeed to all of those originally disconnected aspects of physics which today we regard as forming part of the general electron theory of matter. We also find those theorems of the transformation of the electromagnetic equation which, improved later in the hands of Lorentz, finally developed by the elimination of the electromagnetic theory itself into the relativity equation of Einstein's restricted theory. In the subsequent papers, we see frequent returns to an attack upon the general problem of radiation, and critical discussions on the significance of the development of the restricted and general theory of relativity.

The value of the collection of papers is greatly enhanced by the additions in the form of appendices at the end, in which comments upon the earlier papers are made. The side notes on the margins of each page, indicating the general trend of the discussions in the papers, are also of very great value, as are the author's footnotes, clarifying certain points in the original text, and adding, here and there, corrections whose absence might tend to confuse the reader. The publishers are to be congratulated upon the successful preparation of this most valuable series of papers, which serves to crystallize into one unit a major portion of the developments in electrodynamics and allied fields during the last half century.

W. F. G. SWANN
Bartol Research Foundation

Flussige Kristalle und Lebewesen. VON REINHARD BRAUNS. Pp. 111+xi. E. Schweizerbart'sche Verlagsbuchandlung, Stuttgart, 1931. Price RM 10.

This is a new type of book. It is a collection of 172 abstracts of papers and books which have been published in the field of liquid crystal phenomena, the abstracts originally appearing in either the "Neuen Jahrbach" or in the "Centralblatt" "für Mineralogie Geologie und Paläontologie." The abstracts are arranged chronologically, the first being 1881 and the last 1931. A subject and an author index close the volume.

The author points out that this book is unique in that it does not represent the opinion of a single worker in the interpretation of liquid crystal behavior, but rather the opinions and viewpoints of the 57 authors whose papers are abstracted, accordingly it supplements the monographs which are already a part of the literature. The book contains as a frontispiece a portrait of Otto Lehmann and an appreciation (p. 5–11) of his scientific work.

As the title indicates, many of the abstracts deal with the role of liquid crystals in living processes. Anyone interested in the literature of liquid crystals or in double refraction phenomena will find this collection of abstracts an invaluable aid. The reviewer hopes that this book will be taken as a model for similar treatment of the literature in other special fields.

R. A. GORTNER
University of Minnesota

Second Series *December 15, 1931* *Vol. 38, No. 12*

THE

PHYSICAL REVIEW

THE GRATING CONSTANT OF CALCITE CRYSTALS

By J. A. Bearden

Department of Physics, Johns Hopkins University

(Received November 7, 1931)

Abstract

The precise methods of measuring x-ray wave-lengths, now in use, raise two important questions concerning the crystal grating used. First, what variation in the grating constant is to be expected for crystals grown under different conditions? Second, what is the most accurate value of the grating constant? Since calcite crystals are the most used crystals in x-ray spectroscopy the present work was undertaken to answer as well as possible the above questions for this crystal. The variations in the grating constants of six calcite crystals from four sources (Iceland, Montana, Argentina, and Spain) have been determined by measuring the angle of diffraction for the molybdenum $K\alpha_1$ line in the fourth order. A high precision two crystal spectrometer was used for measuring the diffraction angles. The results are given in the table below. The density of these crystals was then carefully determined. Six to nine independent determinations were made at a temperature of 20.00 ± 0.01°C. The averages of these values are given for a temperature of 20.00°C, in the fourth column of the table. The probable error determined by the method of least squares is given in the fifth column. The mass of the crystals used in determining the density is given in the sixth column. Considering the density measurements of DeFoe and Compton the writer gives the density ρ in g/cm^{-3} at 20°C as $\rho = 2.71030 \pm 0.00003$. The crystals were then chemically analyzed. The results showed that all samples contained about 0.01 percent ferrous oxide, 0.01 percent manganous oxide, and 99.98 percent calcium carbonate. The angle between the cleavage faces of the calcite crystals was determined by three methods. X-rays were used for determining the angle in the first two methods and an optical method for the third. The results for 20°C were $\alpha = 105° 3' 29''$ or $\beta = 101° 54' 4''$, where α is the interior obtuse dihedral angle, and β the angle between the edges of the crystal. The grating constant of the crystal can be calculated from the equation $d = (nM/\rho N\phi)^{1/3} = 3.02816$A at 20°C, $= 3.002810$A at 18°C. The values of the constants used were, $n = 1/2$, $M = 100.078$, $\rho = 2.71030$, $N = 6.0669 \times 10^{23}$, $\phi = 1.09594$.

Origin	Diffraction angle θ	Difference from mean	Density g/cm^{-3}	Probable Error	Mass of crystals g
Iceland	37° 51′ 34.0″	−0.4″	2.7104	±0.000021	12.9764
Iceland	27° 51′ 34.0″	−0.4″	2.71035	±0.000015	15.5780
Montana	27° 51′ 34.6″	+0.2″	2.7102	±0.000081	7.1467
Montana	27° 51′ 34.7″	+0.3″	2.7102	±0.000024	14.8650
Argentina	27° 51′ 34.7″	+0.3″	2.7102	±0.000042	11.0769
Spain	27° 51′ 34.4″	0.0″	2.7102	±0.000036	13.0083
Mean	27° 51′ 34.4″		2.71026		

Introduction

IT IS now possible to measure the diffraction angles of certain x-ray lines to one part in 400,000, or better, by using a double crytal spectrometer[1,2] or a high precision photographic spectrometer.[3] Thus, it is essential to know more about the grating constant of the crystals used. This is especially true if the results obtained by different observers are to be compared. Since calcite crystals are the most used crystals in x-ray spectroscopy, the present work has been undertaken to remove as far as possible any existing uncertainty in the use of this crystal as an x-ray grating. This report may be divided into the following six divisions: (1) X-ray comparison of the grating constant of calcite. (II) Chemical analysis of samples used. (III) Density of calcite. (IV) A determination of the angle between the cleavage faces of calcite. (V) Calculation of the grating constant from chemical data. (VI) Discussion of results.

I. X-ray Comparison of the Grating Constant of Calcite

A comparison of the grating constant of different samples can be precisely made by measuring the diffraction angle of a given x-ray line for each sample.[2] In order to obtain the maximum precision in the comparison, several considerations are necessary. A large angle of diffraction is desired which could be secured by using either a long wave-length or a high order of diffraction. The latter was chosen because in using a high order of a shorter wave-length one has a much greater penetration of the rays into the crystal, and consequently a more reliable estimate of the variation in the grating constant. The method of measuring the diffraction angle must be such that a lack of perfect adjustment of each sample would make a minimum variation in the diffraction angle. A two crystal spectrometer has been used for the measurements because when properly adjusted it fulfills all the necessary conditions for a precise comparison.

The two crystal spectrometer used was a high precision type made by the Societe Genevoise.* The second crystal of this instrument is on the main axis of the spectrometer[1] thus permitting the angle through which this crystal is rotated to be measured very precisely. The graduated circle was calibrated by using a plane mirror on the axis of the spectrometer which reflected the images of two distant filaments into a telescope. As this calibration showed no error greater than 0.6″, which was the limit of resolution of the telescope used, another method was employed to obtain the absolute diffracting angle for one crystal.

A modified Michelson interferometer[4] was attached to the base of the in-

[1] A. H. Compton, Phys. Rev. **37**, 1694 (1931)A; Rev. Sci. Inst. **2**, 365 (1931).

[2] J. A. Bearden, Phys. Rev. **38**, 1389 (1931).

[3] The most precise photographic spectrometers in use are probably those used by Siegbahn and his collaborators.

* The author wishes to express his appreciation to Mr. Alfred L. Loomis of Tuxedo, New York, who so kindly furnished the necessary funds for the purchase of this instrument.

[4] J. A. Bearden, Phys. Rev. **37**, 1217 (1931).

strument and at the height of the crystal tables. This was used to adjust a three point support parallel to and on the axis of the spectrometer. A telescope with a Gauss eyepiece was placed perpendicular to the axis of the spectrometer. A crystal was then placed against the three points and held in place by three light springs. Thence by using the telescope, the cleavage plane of the crystal could be adjusted parallel to the axis of the spectrometer. The interferometer was used to place the part of the crystal which actually diffracted the x-rays on the axis of the spectrometer. The first crystal was then adjusted to diffract the molybdenum $K\alpha_1$ line over the axis of the spectrometer. It was then adjusted parallel to the second crystal by making the width of the rocking curve a minimum.

The slits, one near the x-ray tube and the other in front of the ionization chamber, were placed on a horizontal line perpendicular to the axis of the spectrometer to within 0.1 mm. As is well known, the height of these slits affects the width and angular position of a diffracted line. For a uniformly illuminated source and slits of equal height the correction may be written

$$d\theta''_{\text{eff}} = 0.204 \frac{a^2}{L^2} \tan\theta$$

where a is the height of the slit and L their separation. This equation was tested for four slit heights from 0.5 mm to 3.0 mm, and a separation of 52 cm.

The measured angles have been reduced to 18° C by using the equation[5]

$$d\theta = -1.04(t - 18°\text{C}) \tan\theta \times 10^{-5}$$
$$\text{or } d\theta'' = -2.15(t - 18°\text{C}) \tan\theta$$

where t is the temperature of the crystal at the time of the measurement of the diffracting angle θ.

The diffraction angle for one crystal was then very carefully measured in three different positions on the graduated circle (120° apart). The maximum variation observed was 0.4″ and an average variation slightly less than 0.2″. The average angle was accepted as the absolute diffraction angle for this crystal, and all other results have been obtained relative to this crystal. I do not believe the diffraction angle for this crystal is in error by more than 0.2″ and is probably less.

Some very clear and perfect samples of calcite crystals from Montana, Argentina, Spain, and Iceland have been obtained. (These samples will now be referred to by the first letter of each.) Slabs about 10 mm thick have been carefully cleaved from these samples. Some surfaces were obtained which were almost free from "steps," and the others showed only a few small "steps." Adjacent pairs were selected and the width of the rocking curves measured. The widths varied from 5.5″ to 7″. It was also found that pairs selected even from crystals of different origin gave the same rocking curve widths as adjacent pairs from the same crystal. Only one large I crystal (12×

[5] The value of the expansion coefficient α was misprinted as 1.09×10^{-5} in the Phys. Rev. 38, 1390 (1931). The value actually used was $\alpha=1.04\times10^{-5}$.

8×3 cm) was available, so two samples were cleaved from it in order to see how well the various observations would check. Two M samples were cleaved from different crystals but from the same region.

The grating constants of these crystals were compared by using the molybdenum $K\alpha_1$ line and the fourth order of diffraction. That is, (1, +4), (1, −4) in Allison's notation. Fig. 1 shows typical data forming one set of measure-

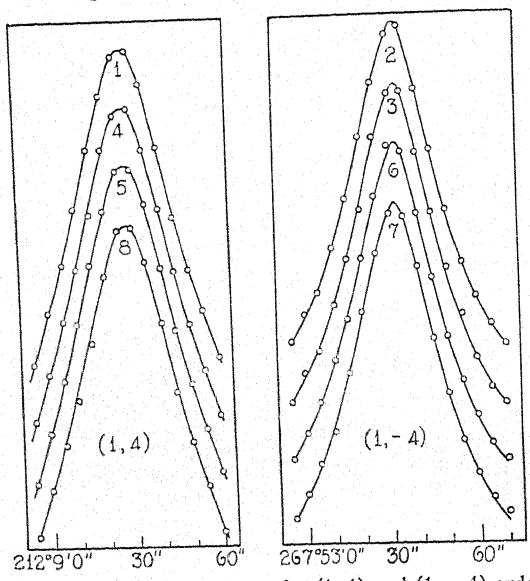


Fig. 1. One set of diffraction curves for (1, 4) and (1, −4) orders. The curves were taken in the order of the numerals.

ments. The curves were taken in the order of the small numerals so that any errors due to a slow change in the adjustment of the apparatus would be eliminated. Two such sets of measurements were made on each crystal in the order I_1, I_2, M_1, M_2, A, and S. Then two more sets in the order S, A, M_2, M_1, I_2, I_1. The results are given in Table I. The angles have been reduced to 18° C

TABLE I.

Origin	Diffraction angle	Difference from mean
Iceland	27° 51′ 34.0″	−0.4″
Iceland	27° 51′ 34.0″	−0.4″
Montana	27° 51′ 34.6″	+0.2″
Montana	27° 51′ 34.7″	+0.3″
Argentina	27° 51′ 34.7″	+0.3″
Spain	27° 51′ 34.4″	0.0″
Mean	27° 51′ 34.4″	0.26″

and corrected for the height of the slit. They have also been slightly corrected for the small error in the graduated circle. Since in each case the measurements have been made on the same part of the graduated circle, I believe the relative values are not in error by more than 0.1″. Thus, there is a real dif-

ference in the grating constant of the various crystals. However, the maximum difference is only one part in 145,000, and the maximum difference from the average is about 1 part in 250,000. If one only considers the M_1, M_2, A, and S crystals the maximum variation from the average is about one part in 500,000. These variations are so small that the differences in x-ray wavelengths reported by some observers must be due to the method used, and not to a variation in the grating constant of the crystals. A redetermination of a series of x-ray lines from 0.5A to 2.25A will be given in this Journal in a few weeks.

II. A Chemical Analysis of Crystals

After the above x-ray data had been secured, two samples were cut from each crystal near the point on the surface that had been used for diffracting the x-rays. Then samples, one from each crystal, were carefully analyzed for the writer by Dr. W. B. D. Penniman and Dr. A. L. Browne. The results are given in Table II. Thus, chemically there appears to be very little difference

Table II.

Origin	Silica	Alumina	Ferrous oxide	Manganous oxide	Magnesium oxide	Calcium carbonate
Iceland	absent	absent	0.007	0.008	absent	99.98%
Iceland	absent	absent	0.006	0.007	absent	99.98
Montana	absent	absent	0.005	0.011	absent	99.97
Montana	absent	absent	0.006	0.011	absent	99.97
Argentina	absent	absent	0.006	0.010	absent	99.98
Spain	0.004	absent	0.007	0.006	absent	99.98

between the various samples. These samples were selected because of their optical clearness and perfection, so that one might expect them to be almost chemically pure. It is well known that colored calcite may contain several percent of some impurity. However in x-ray work it is the general practice to select the best samples available, so that the above results are probably a fair estimate of the chemical purity of the crystals normally used.

III. Density of the Crystals

The other pieces of calcite which were cut from each crystal above, were prepared for determining the density. Five of the crystals were finely ground and all surface flaws due to cleaving the crystal were removed. The edges were rounded off so there would be no possibility of occlusion of air on the surface. Four of these crystals were used in this condition and the fifth was polished with rouge. The sixth crystal was left unground. The masses of the crystals were determined by weighing in air with calibrated weights and correcting for the buoyancy of the air. The crystals were then weighed in kerosene at a temperature of 20° $\pm$0.01° C. The density of the kerosene can be determined very accurately and thus the density of the crystals. Corrections were, of course, made for the weight of the rough gold plated copper supporting wire and surface tension. From 6 to 9 independent measurements have been made

on each crystal. In Table III the results, with the probable errors for each crystal, are given for a temperature of 20° C. The probable error was calculated according to least squares method as was used by Birge.[6] The best previous determinations of the density of calcite crystals were made by De Foe

TABLE III.

Origin	Density-g/cm 20°C	Probable error	Mass of crystal -g
Iceland	2.7104	±0.00002	12.9764
Iceland	2.71035	±0.00002	15.5780
Montana	2.7102	±0.00008	7.1467
Montana	2.7102	±0.00002	14.8650
Argentina	2.7102	±0.00004	11.0769
Spain	2.7102	±0.00004	13.0083
Mean	2.71026		

and Compton.[7] Their results are given in Table IV. They give as a probable error for each sample ± 0.0001 g/cm^{-3}. The variations in Table IV are much greater than those in Table III. This may be due to a fortuitous selection of crystals used in the present experiment. However if this were true, one would hardly expect the mean value for the two sets of crystals to agree so closely.

TABLE IV.

Origin	Density at 20°C g/cm^{-3}
Missouri	2.7106
U.S.A.	2.7102
Iceland	2.7103
Iceland	1/2 (2.7090)
Unknown	2.7101
Unknown	2.7103
Mean	2.7102

The second Iceland crystal in Table IV differs so much from the others that I believe the crystal must have been imperfect and should be given zero weight instead of 1/2. Thus, the mean would have been 2.71034. Taking this result into consideration with the present results of Table III, the writer believes that the most probable value of the density ρ is

$$\rho = 2.71030 \pm 0.00003 \text{ g/cm}^{-3} \text{ at } 20°\text{C}.$$

This probable error given assumes that the variations from this value were experimental errors. The maximum variation would be 0.0003 g/cm^{-3} for De Foe's and Compton's[7] results, and 0.0001 for the present results.

[6] R. T. Birge, Phys. Rev. Supplement **1**, 1 (1929).
[7] O. K. DeFoe and A. H. Compton, Phys. Rev. **25**, 618 (1925).

IV. A Determination of the Angle Between the Cleavage Faces of Calcite

Since the angle between the cleavage faces of a crystal enter into the calculation of the grating constant, it is important to know this angle as precisely as possible. This angle can be measured with high precision by using a two crystal spectrometer as described above. It has also been reported[8] that this angle varies slightly for different crystals.

In the first measurements crystals from 4 to 6 mm square and 10 to 20 mm long were used. The cleavage planes were aligned parallel to the spectrometer axis. The crystals were placed so that the molybdenum $K\alpha_1$ line could be reflected from two faces by simply rotating the crystal through the angle α where α is the angle between the planes of the crystal. Since the results obtained by this method differed from those of previous investigators two other methods were used.

In the second method, crystals about 1 mm $\times$ 1 mm $\times$ 10 mm were mounted parallel to and on the axis of the double crystal spectrometer. The first crystal was adjusted to diffract the silver $K\alpha_1$ line over the axis of the spectrometer. The small crystal was then rotated until it diffracted this line into the ionization chamber. Thus, when the crystal was rotated through an angle α or $180° - \alpha$ the same line was again diffracted into the ionization chamber.

In the last method, the crystals used in the first method were spluttered with gold and adjusted on the spectrometer as above. Optically the angles were determined by using the telescope with a Gauss eyepiece. The results of the three methods are given in Table V in terms of the interior obtuse dihe-

Table V.

Origin	1st method α	2nd method α	3rd method α
Iceland	105° 3′ 28″	105° 3′ 30″	105° 3′ 35″
Montana	105° 3′ 31″	105° 3′ 31″	105° 3′ 20″
Argentina	105° 3′ 29″	105° 3′ 27″	105° 3′ 25″
Spain	105° 3′ 30″	105° 3′ 28″	105° 3′ 25″

dral angle α. The angles were measured at 25° C to 26° C and reduced to 20° C by using the known expansion coefficients parallel to and perpendicular to the axis of the crystal. This correction can be calculated in terms of the angle β between the edges of the crystal β and α are connected by the trigonometric relation

$$\cos\frac{\beta}{2} = \left(2\sin\frac{\alpha}{2}\right)^{-1/2}.$$

The correction is then

$$\frac{d\beta}{dt} = 2\tan\frac{\beta}{2}\left(1 - \frac{3}{4}\sin^2\frac{\beta}{2}\right)(\alpha_1 - \alpha_{11})$$

[8] H. N. Beets, Phys. Rev. **25**, 621 (1925).

by using the values $\alpha_\perp = -0.0000056$ deg.$^{-1}$C and $\alpha_\parallel = 0.000025$ deg.$^{-1}$C. one obtains $d\beta/dt = -3.1''$ per degree C.

The weighted mean of methods one and two gives

$$\alpha = 105^\circ\ 3'\ 29''$$
$$\beta = 101^\circ\ 54'\ 4''.$$

The value of α differs by about 90 seconds from the value obtained by Beets.[8] The present results also show very little, if any, variation in the angle α for different samples. The writer is unable to explain the difference but feels that the above experiments are conclusive.

V. Calculation of the Grating Constant d

From fundamental considerations of crystal structure it can be shown that the grating space of a rhombohedral crystal is given by

$$d = \left(\frac{nM}{N\phi}\right)^{1/3}$$

where n is the number of molecules in each elementary rhombohedron, M the molecular weight of the crystal, N is Avogadro's number, ρ the density of the crystal, and ϕ is the volume of a rhombohedron, the perpendicular distance between whose opposite faces is unity. It can also be shown that

$$\phi = \frac{(1 + \cos\beta)^2}{(1 + 2\cos\beta)\sin\beta}$$

where β is the same as in the last section. ϕ thus becomes

$$\phi = 1.09594 \pm 0.00001.$$

For a calcite crystal $n = \frac{1}{2}$.[9] Birge[6] gives for the molecular weight of calcite $M = 100.078 \pm 0.005$. The density as determined above is, $\rho = 2.71030 \pm 0.00003$. Avogadro's number can be most accurately determined from the relation

$$N = \frac{FC}{e}$$

where F is the Faraday constant, C the velocity of light, and e the charge on the electron. Birge[6] gives $FC = 2.8987 \pm 0.0002 \times 10^{14}$ Abs. e.s.u. and $e = 4.770 \pm 0.005 \times 10^{-10}$ e.s.u. From Millikan's experiments Birge obtained a value of $e = 4.768 \times 10^{-10}$ e.s.u. and in consideration of Wadlun's[10] grating wavelength measurements of x-ray spectra which gave $e = 4.774 \times 10^{-10}$ e.s.u. raised Millikan's value to 4.770×10^{-10} e.s.u. More recent grating measurements by the writer[11] have shown that e, from such experiments, is 4.806×10^{-10} e.s.u. It appears to the writer to be out of the question to average this

[9] W. H. Bragg and W. L. Bragg, X-rays and crystal structure.
[10] A. P. R. Wadlung, Phys. Rev. 32, 841 (1928).
[11] J. A. Bearden, Phys. Rev. 37, 1210 (1931).

result with that of Millikan's. The difference of such an average from the results of either experiment would be many times the experimental error of either. The writer thus believes it is preferable to retain Millikan's value

$$e = 4.768 \pm 0.005 \times 10^{-10} \text{ e.s.u.}$$

until the magnitude of the mosaic structure can be determined and the validity of the grating formula established for x-ray wave-lengths. From this value of e one obtains

$$N = 6.0669 \times 10^{23} \text{ molecules/mole.}$$

The value of d is then calculated to be

$$d = 3.02816\text{A at } 20°\text{C}$$
$$d = 3.02810\text{A at } 18°\text{C.}$$

The probable error is ± 0.001, which is almost entirely due to the probable error in e. This value is about one part in 3000 lower than the value adopted by Siegbahn.[12]

In order to calculate the true wave-length of an x-ray line with the true grating constant as determined above, the complete Bragg law

$$n\lambda = 2d\left(1 - \frac{1-\mu}{\sin^2\theta}\right)\sin\theta$$

must be used where λ is the true wave-length, d the true grating space, μ the index of refraction, and θ the diffraction angle for the n-th order. If we use the value $(1-\mu)/\lambda^2 = 3.69 \times 10^{-6}$ the above equation becomes

$$n\lambda = 2d\left(1 - \frac{135 \times 10^{-6}}{n^2}\right)\sin\theta$$
$$= 2d_n \sin\theta$$

where d_n is the effective grating constant for the n-th order. With the true grating constant $d = 3.02810$, the calculated values of d_n and $\log 2d_n$ are given in Table VI.

TABLE VI.

$d_1 = 3.02769$A	$\log 2d_1 = 0.7821415$
$d_2 = 3.02799$	$\log 2d_2 = 0.7821752$
$d_3 = 3.02805$	$\log 2d_3 = 0.7821937$
$d_4 = 3.02807$	$\log 2d_4 = 0.7821966$
$d_5 = 3.02808$	$\log 2d_5 = 0.7821980$
. . . . .	. . . . .
$d_\infty = 3.02810$	$\log 2d_\infty = 0.7822002$

VI. DISCUSSION

Attention should be called to some of the results in the present experiment. Chemically all the samples seemed to be very similar and almost pure

[12] M. Siegbahn, Spectroskopie der Roentgenstrahlen.

calcium carbonate. In the calculation of the grating constant the effect of the slight impurities was neglected. In the x-ray comparison of the samples the variations in the diffraction angles were small, but the angles I_1 and I_2 were definitely smaller than the others. This would suggest a smaller crystal density. On the contrary the densities of I_1 and I_2 were the largest in the group. This indicates that a difference in density does not reflect itself as a corresponding change in the grating constant of the crystal. Consequently the measured density may not be the real density of the crystal lattice which is responsible for the diffraction of the x-rays.

It has been pointed out[2] that the absolute value of the diffraction angle for the molybdenum $K\alpha_1$ line, obtained by the writer, differs by about 1.4″ from the precision measurement reported by Compton.[1] This difference is about five times the apparent probable error of either experiment. However, the writer has recalculated the correction for the height of the slits in Compton's experiment and finds a value $d\theta_{\text{eff}} = -0.6''$ instead of $-2.2''$ as used by him. Thus his diffraction angle would be increased to 27° 51′ 34.6″ which agrees, within the experimental error, with the present results.

The difference between the writer's ruled grating wave-length measurements[11] and the corresponding crystal results now is 0.25 percent instead of 0.22 percent as previously given. Such a great difference must be due to a failure of the ruled grating diffraction equation to be valid for the x-ray region. The boundary conditions are probably not the same for optical wave-lengths and x-rays and might thus alter the position of the diffraction maxima. A careful analysis of the diffraction theory for x-ray wave-lengths and for the conditions under which x-ray spectra are obtained is badly needed in order to settle the questions raised by such experimental differences.

THE NORMAL STATE OF THE HYDROGEN MOLECULE

By N. Rosen
Massachusetts Institute of Technology

(Received October 30, 1931)

Abstract

The dissociation energy, moment of inertia, and fundamental vibration frequency are calculated for a normal hydrogen molecule by a variational method and are found to be 4.02 v, $4.66 \cdot 10^{-41}$ gm-cm^2, and 4260 cm^{-1} as compared to the experimental values 4.42, $4.67 \cdot 10^{-41}$, and 4380, respectively. The calculation is carried through with the simplest possible improvements in the wave functions. In the appendix a number of integrals are listed and two tables of functions are included that may be useful to calculators.

I. Introduction

THE problem of calculating some of the properties of the normal hydrogen molecule by wave-mechanical methods has been hitherto successful qualitatively but not quantitatively. Thus Sugiura[1] by completing the calculations of Heitler and London[2] based on a first-order perturbation method, obtained 3.2 volts for the dissociation potential as compared to the experimental value, 4.4 volts. Wang,[3] by using a variational method involving the introduction of a shielding constant, obtained 3.7 volts for this energy, which is a distinct improvement but still rather far from the goal. It is true that Condon[4] obtained an almost exact agreement with experiment, but it is questionable as to whether one can call his method of doing this a straight-forward calculation. Eisenschitz and London,[5] by carrying through a second order perturbation method, got 9.5 volts.

Similarly in the case of the two other quantities which are generally calculated at the same time as the energy, namely the equilibrium distance and the fundamental vibration frequency, the calculated results are not in very good agreement with the experimental values. If one surveys the available methods of calculating the quantities mentioned, it is at once evident that the only method for getting quantitative results is that based on the use of a variational principle, because the wave equation for this case cannot be solved exactly, and because solving it by the perturbation method is not to be trusted, as is shown by the fact that the second-order perturbation calculation gave a much worse result than the first-order calculation. In using the variational method one has the comforting assurance that one cannot go astray. If one starts with wave functions of sufficient complexity and having a large

[1] Sugiura, Zeits. f. Physik **45**, 484 (1927).
[2] Heitler and London, Zeits. f. Physik **44**, 455 (1927).
[3] Wang, Phys. Rev. **31**, 579 (1928).
[4] Condon, Proc. Nat. Acad. Sci. **13**, 466 (1927).
[5] Eisenschitz and London, Zeits. f. Physik **60**, 491 (1927).

enough number of parameters, and if one puts in enough labor one can generally approach the right answer, at least as far as the energy is concerned.

However, rather than to do this, it seems preferable to try to get an appreciable improvement in the calculated results with but a small increase in the complexity of the calculation. It is therefore the purpose of the present paper to try to improve the theoretical results for the normal hydrogen molecule, at the same time keeping the wave functions and the calculation as simple as possible.

II. Theory

To carry out this policy of simplicity, we begin with the understanding that we shall deal only with wave functions made up of products of individual electron wave functions. We than inquire as to what happens to the electron charge distribution in a hydrogen atom when it is brought up to another similar atom so as to combine with it. It is apparent that because of the various complicated interactions that occur, the charge distribution will be altered, this distortion becoming greater as the two atoms approach each other. The wave functions (from which the charge distributions are calculated) also become altered. The exact nature of the changes can be investigated only in a six-dimensional space, but for the purposes of the present problem one can try to consider the approximate distortion of an individual wave function in ordinary space. The simplest way to represent this distortion is to consider the radius of the atom to change with the distance to the other atom. This is effectively what Wang[3] did in his calculations, and it led to a definite improvement in the energy value.

However, since the perturbations involved are not spherically symmetrical this cannot be a very good approximation to the true state of affairs, and the next improvement that suggests itself is to introduce a change in the wave function that will depend on the direction with respect to the molecular axis and will be greatest in the direction of the latter. Since the interactions can be thought of roughly as being along this axis, it seems likely that the electron cloud tends to bulge out in the direction of the second atom.

Let us denote the nuclei by a and b, the electrons by 1 and 2, the internuclear distance by R, other distances by r with subscripts and the angle between a radius vector and the axis (the line joining the nuclei) by θ with subscripts. In accordance with the previous considerations we take as the simplest individual wave function

$$\psi = \psi^0 + \sigma\psi' \tag{1}$$

where ψ^0 is the hydrogenic wave function for the lowest state, but with a shielding constant, ψ' is a function symmetrical about the axis but not about a plane through the nucleus perpendicular to it, and σ is a parameter the magnitude of which is to be determined so as to minimize the variational integral.

The conditions imposed on the choice of ψ' are: (1) that it satisfy the boundary conditions for a wave function, (2) that it have reasonable direc-

tional properties, (3) that it be orthogonal to ψ^0, (4) that it satisfy a simple wave equation. Of these, (1) and (2) are necessary, but (3) and (4) are convenient in calculating. If we consider electron 1 on atom a and write the hydrogenic function in the form

$$\psi^0(a1) = N_0 e^{-\alpha r_{a1}} \tag{2}$$

then the simplest perturbation function satisfying these conditions seems to be

$$\psi'(a1) = N_1 e^{-\alpha r_{a1}} r_{a1} \cos\theta_{a1} \tag{3}$$

where N_0 and N_1 are the corresponding normalizing factors which, on integrating the squares of the wave functions over all space, one finds to have the values:

$$N_0 = (\alpha^3/\pi)^{1/2} \tag{4}$$

$$N_1 = (\alpha^5/\pi)^{1/2}. \tag{5}$$

In these expressions, we have used α to represent the quantity Z/a_0, where Z is the effective charge of the nucleus and a_0 the normal hydrogen radius. Accordingly, the wave equation satisfied by $\psi^0(a1)$ is

$$H_{a1}{}^0\psi^0(a1) = Z^2E_0\psi^0(a1) \tag{6}$$

where

$$H_{a1}{}^0 = -\frac{h^2}{8\pi^2 m}\nabla_1{}^2 - Ze^2/r_{a1} \tag{7}$$

and E_0 is the energy of a normal hydrogen atom.

Now ψ' can be seen to be identical with the wave function corresponding to the $2p$ state in a hydrogenic atom of nuclear charge $2Z$. Hence the equation which it satisfies is:

$$H_{a1}'\psi'(a1) = Z^2E_0\psi'(a1), \tag{8}$$

where

$$H_{a1}' = -\frac{h^2}{8\pi^2 m}\nabla_1{}^2 - 2Ze^2/r_{a1}. \tag{9}$$

Of course similar expressions can be written for the wave functions for the other electron or atom. Incidentally, it may be mentioned that for the atom b we take for the wave function

$$\psi'(b1) = -N_1 e^{-\alpha r_{b2}} r_{b1} \cos\theta_{b1} \tag{3a}$$

so as to keep all quantities symmetrical about the plane midway between the nuclei.

For the combined wave function of the normal state of the molecule we take

$$\Psi = \psi(a1)\psi(b2) + \psi(b1)\psi(a2). \tag{10}$$

The wave-mechanical Hamiltonian is given by

$$H = -\frac{h^2}{8\pi^2 m}(\nabla_1{}^2 + \nabla_2{}^2) + e^2[1/R - 1/r_{a1} - 1/r_{a2} - 1/r_{b1} - 1/r_{b2} + 1/r_{12}], \tag{11}$$

and according to the theory of the variational method it is necessary to minimize the quantity

$$W = \int \Psi H \Psi dv_1 dv_2 \Big/ \int \Psi^2 dv_1 dv_2, \tag{12}$$

which then gives the value of the energy.

Now by making use of Eqs. (6) and (8) we can write

$$H\psi^0(a1)\psi^0(b2) = \{2Z^2E_0 + e^2[1/R + s/r_{a1} + s/r_{b2} - 1/r_{a2} - 1/r_{b1} + 1/r_{12}]\}\psi^0(a1)\psi^0/(b2), \tag{13}$$

$$H\psi^0(a1)\psi'(b2) = \{2Z^2E_0 + e^2[1/R + s/r_{a1} + (2s+1)/r_{b2} - 1/r_{a2} - 1/r_{b1} + 1/r_{12}]\}\psi^0(a1)\psi'(b2), \tag{14}$$

$$H\psi'(a1)\psi'(b2) = \{2Z^2E_0 + e^2[1/R + (2s+1)/r_{a1} + (2s+1)/r_{b2} - 1/r_{a2} - 1/r_{b1} + 1/r_{12}]\}\psi'(a_1)\psi'(b_2), \tag{15}$$

where

$$s = Z - 1. \tag{15a}$$

By means of these relations and similar ones derived from them by replacing a by b or 1 by 2, W can be evaluated. If we adopt the following notation,

$$I_{00} = \int \psi^0(a1)\psi^0(b1)dv_1, \tag{16}$$

$$F_0 = \int \frac{[\psi^0(a1)]^2}{r_{a1}} dv_1, \tag{17}$$

$$G_{00} = \int \frac{[\psi^0(a1)]^2}{r_{b1}} dv_1, \tag{18}$$

$$K_{00,01} = \int \frac{[\psi^0(a1)]^2\psi^0(b2)\psi'(b2)}{r_{12}} dv_1 dv_2, \tag{19}$$

$$J_{01} = \int \frac{\psi^0(a1)\psi'(b1)}{r_{a1}} dv_1; \quad J_{10} = \int \frac{\psi'(a1)\psi^0(b1)}{r_{a1}} dv_1, \tag{20}$$

$$L_{01,10} = \int \frac{\psi^0(a1)\psi'(b1)\psi'(a2)\psi^0(b2)}{r_{12}} dv_1 dv_2, \tag{21}$$

with corresponding changes in the numbering when ψ^0 is replaced by ψ' or vice versa, we can then write W in the form:

$$W = \frac{e^2}{R} \sum_{i=0}^{4} \sigma^i(P_i + sQ_i) \Big/ \sum_{i=0}^{4} \sigma^i D_i + 2Z^2E_0, \tag{22}$$

where the quantities D_i, P_i, and Q_i are made up of the various integrals over wave functions and are defined as follows. In each case the "exchange" terms are grouped in brackets.

$$\left.\begin{aligned}
D_0 &= 1 + [I_{00}^2],\\
D_1 &= [4I_{00}I_{01}],\\
D_2 &= 2 + [4I_{01}^2 + 2I_{00}I_{11}],\\
D_3 &= [4I_{01}I_{11}],\\
D_4 &= 1 + [I_{11}^2].
\end{aligned}\right\} \quad (23)$$

$$\left.\begin{aligned}
P_0 &= 1 + R(K_{00,00} - 2G_{00}) + [I_{00}^2 + R(L_{00,00} - 2I_{00}J_{00})],\\
P_1 &= 4R(K_{00,01} - G_{01}) + [4I_{00}I_{01} + R(4L_{00,01} - 4I_{01}J_{00} - 2I_{00}J_{01})],\\
P_2 &= 2 + R(4K_{01,01} + 2F_1 + 2K_{00,11} - 2G_{00} - 2G_{11}),\\
&\quad + [4I_{01}^2 + 2I_{00}I_{11} + R(2L_{01,10} + 2L_{01,01} + 2L_{00,11}\\
&\quad - 2I_{11}J_{00} - 4I_{01}J_{01})],\\
P_3 &= 4R(K_{01,11} - G_{01}) + [4I_{01}I_{11} + R(4L_{01,11} - 2I_{11}J_{01})],\\
P_4 &= 1 + R(2F_1 + K_{11,11} - 2G_{11}) + [I_{11}^2 + RL_{11,11}].
\end{aligned}\right\} \quad (24)$$

$$\left.\begin{aligned}
Q_0 &= 2RF_0 + [2RI_{00}J_{00}],\\
Q_1 &= [R(4I_{00}J_{10} + 2I_{00}J_{01} + 4I_{01}J_{00})],\\
Q_2 &= R(2F_0 + 4F_1) + [R(4I_{00}J_{11} + 2I_{11}J_{00} + 4I_{01}(J_{01} + 2J_{10}))],\\
Q_3 &= [R(8I_{01}J_{11} + 2I_{11}(J_{01} + 2J_{10}))],\\
Q_4 &= 4RF_1 + [4RI_{11}J_{11}].
\end{aligned}\right\} \quad (25)$$

These integrals can be evaluated without great difficulty. The discussion of them is to be found in the appendix. It is easy to see that the various D_i, P_i, and Q_i are functions only of the quantity

$$\rho = \alpha R \quad (26)$$

and can be calculated for various values of ρ and plotted. If we let

$$\rho_0 = R/a_0, \quad (27)$$

then

$$Z = \rho/\rho_0, \quad (28)$$

$$s = (\rho - \rho_0)/\rho_0. \quad (29)$$

For a given value of R or ρ_0 one can then vary ρ and, by reading the values of the functions from the curves, minimize W. By repeating this for a number of values of ρ_0 one thus obtains a series of energy values which can be plotted as a function of ρ_0 and a smooth curve drawn. However, unless the points for which calculations are made are very close together it is not possible in general to determine the minimum of the energy curve very accurately in this way. If the points are fairly close together one can pass a parabola through the points in the vicinity of the minimum. But if, as was the case in the calculation carried out, the points are not sufficiently close together, one must resort to some other method.

What was done was to use instead of a parabola a curve of the type discussed by Morse[6] in connection with interatomic potentials:

$$\Delta E = De^{-2a(\rho_0-\rho_m)} - 2De^{-a(\rho_0-\rho_m)}. \tag{31}$$

A curve of this sort is known to fit molecular energy curves very well especially in the neighborhood of the minimum. By fitting this curve to three points near the minimum one can get the dissociation energy D and the equilibrium distance $\rho_m a_0$. (The details of the curve-fitting are given in the appendix.)

From the latter the moment of inertia follows:

$$J_0 = \tfrac{1}{2}M_H(\rho_m a_0)^2, \tag{31}$$

where M_H is the mass of a hydrogen atom

Since at the minimum

$$\frac{d^2E}{d\rho_0^2} = 2a^2D \tag{32}$$

the fundamental vibration frequency is given by

$$\nu_0 = \frac{a}{\pi a_0 c}(D/M_H)^{1/2}. \tag{33}$$

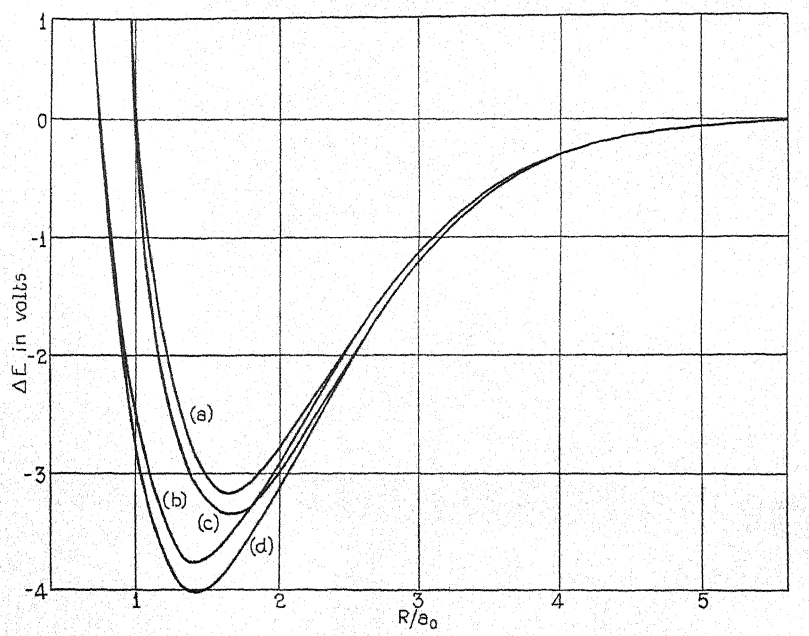


Fig. 1. Calculated energy of normal hydrogen molecule: (a) first order perturbation, (b) varying s, (c) varying σ, (d) varying σ and s.

[6]Morse, Phys. Rev. **34**, 57 (1929).

III. Results

The minimization was carried out first by keeping $\sigma=0$ and varying s. This is essentially what Wang[3] did except that his results were only for the equilibrium distance. The energy curve obtained is shown in Fig. 1 (b) and may be compared with the first-order perturbation energy 1 (a).

The value of s as function of the interatomic distance is shown in Fig. 2. For $R=0$ of course we have a helium atom and for this the effective nuclear charge (as given by a variational method calculation) is 1.6875 e, so that $s=0.6875$. For large distances s falls off rapidly. It is interesting to note that beyond a certain distance, s changes sign. This may be interpreted by saying that for large distances the second electron has more of an effect upon the atom than the second nucleus. Geometrically one may say that as the atoms

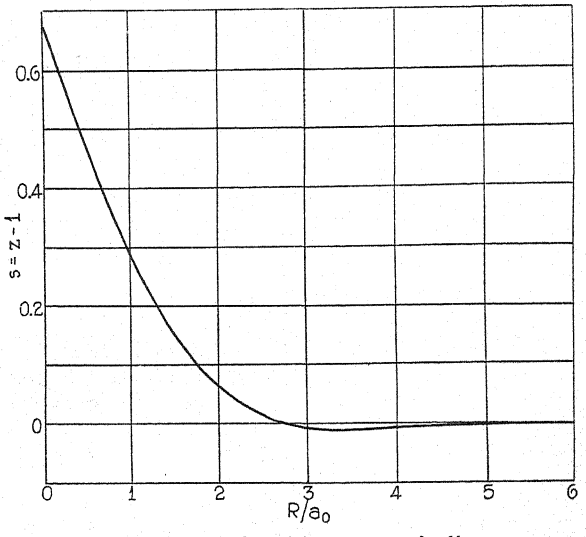


Fig. 2. Variation of s with interatomic distance.

approach each other, there is first an expansion of the charges and then, for smaller distances, a contraction.

The next step in the procedure was to set $s=0$, and minimize W with respect to σ. The energy resulting from this calculation is shown in Fig. 1 (c). Comparison with 1 (a) shows that the improvement in the energy near the equilibrium distance is rather small, but that there is a distinct improvement at somewhat larger distances. The curve of σ thus obtained, denoted by σ_0, is shown in Fig. 3 (a).

The quantity σ can be taken as a rough measure of the longitudinal distortion of the wave function. As the graph shows, for small distances there seems to be a sudden distortion of the wave function which disappears as the atoms merge to give helium. This apparent behavior at small distances is probably without significance, since the wave functions obtainable from a variational calculation need not approximate the true wave functions as closely as the calculated energy does the true value. In the present case, the

behavior of the true wave functions for small internuclear distance is exceedingly complex, and an attempt to fit this behavior into the narrow mold provided by a single parameter cannot be expected to be very successful.

To get a better approximation, the values of s obtained previously were put into W and then σ was varied once more. The energy obtained this time is given in Fig. 1 as curve (d). As is to be expected, it is below the other curves and merges with (b) for small distances and with (c) for large distances. The curve of the values of σ thus calculated, denoted by σ_1, is shown in Fig. 3 (b). It agrees with σ_0 down to about $\sigma_0 = 1.5$. For smaller distances the two differ widely, and this is probably the region in which they lose any physical significance they may have at larger distances.

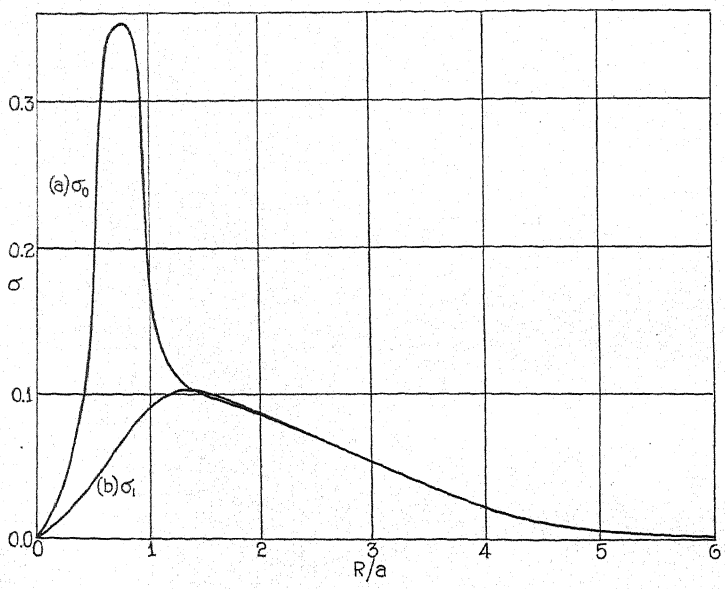


Fig. 3. Parameter σ to minimize energy: (a) without shielding constant, (b) with shielding constant.

The parameter was kept fixed at the set of values σ_1 and s was recalculated. It was found that within the accuracy available in reading graphs, s did not change appreciably—at least in the regions of any importance. Hence the energy curve 1 (d) represents the best result obtainable by the present method.

For this curve the dissociation energy was found to be 4.02 volts, the equilibrium distance between atoms 1.416 a_0 corresponding to a moment of inertia of 4.66×10^{-41} gm-cm^2 and a fundamental vibration frequency of 4260 cm^{-1}. In the following table[7] these results are compared with those obtained in previous calculations and with the experimental values.

[7] This table (except for obvious changes) is taken from the paper of Wang (reference 3). The experimental values given these are those of Witmer, Proc. Nat. Acad. Sci. **12**, 238 (1926), and Phys. Rev. **28**, 1223 (1926). Cf. Birge, Int. Crit. Table V, 409 (1929).

	E (Rh)	$\Delta E(v)$	J_0(gm−cm²)	ν_0(cm^{-1})
Present paper	−2.297	−4.02	4.66×10^{-41}	4260
Wang[3]	−2.278	−3.76	4.59	4900
Condon[4]	−2.325	−4.40	4.26	5300
Sugiura[1]	−2.24	−3.2	5.2	4800
Observed[7]	−2.326	−4.42	4.67	4380

It is seen that the dissociation energy as calculated here is about 10 percent too small. However, if we consider the total energy of the molecule, the error is only about 1 percent. If we compare this to the helium problem—it is only fair that the total molecular energy be considered in this comparison—we note that the Hartree method[8] gives for the total energy of an He atom 5.75 Rh as compared to 5.81 Rh as observed, so that the error is also about 1 per cent. Now the Hartree method gives the greatest possible accuracy obtainable with wave functions made up of the products of individual wave functions, it being equivalent to a variational method with a function of complete flexibility. Since in the present case the wave function is likewise made up of products of individual wave functions, it is questionable whether one could hope to exceed this accuracy by very much, the situation in the hydrogen molecule being rather similar to that in the helium atom.

In concluding the main part of this paper, the writer wishes to acknowledge the advice and encouragement received from Drs. J. C. Slater and R. M. Langer and the assistance from Dr. S. Ikehara in checking parts of the calculation and in compiling the tables.

Note added in proof (December 4, 1931)—Shortly after the present article had been sent to the publisher, the writer learned of the paper of E. A. Hylleraas, Zeits. f. Physik **71**, 739 (1931) "Uber die Elektronenterme des Wasserstoffmolekuls," in which, among other things, he calculates the energy of the lowest state of H_2 in very close agreement with the experimental value. However, it ought to be pointed out that one should not compare the results of the present paper with his results, since he multiplies through his calculated value of the energy by a factor obtained by interpolating between values for $R=0$, and $R=\infty$, to get his final result.

Appendix

1. Integrals

Many of the integrals arising in the present calculations are not new. Thus a number are to be found in the papers of Heitler and London,[2] Sugiura,[1] and Bartlett.[9] However, for the sake of completeness they will all be given here (in perhaps a different form). All but a few of the integrals present no great difficulties in the evaluation. The ones which do give trouble are the exchange integrals and they can be handled in the following way:

On replacing $1/r_{12}$ by its Neumann expansion in terms of Legendre func-

[8] Gaunt, Proc. Camb. Phil. Soc. **24**, 328 (1928).
[9] Bartlett, Phys. Rev. **37**, 507 (1931).

tions of the elliptic coordinates any one of the exchange integrals arising here can be broken up into a sum of terms of the form $H(m, n, \alpha)$ and $S(m, n, \alpha)$ where

$$H(m, n, \alpha) = \int_1^\infty \lambda_1{}^m e^{-\alpha\lambda_1} Q_0(\lambda_1) d\lambda_1 \int_1^{\lambda_1} \lambda_2{}^n e^{-\alpha\lambda_2} d\lambda_2 \tag{A1}$$

$$+ \int_1^\infty \lambda_1{}^n e^{-\alpha\lambda_1} Q_0(\lambda_1) d\lambda_1 \int_1^{\lambda_1} \lambda_2{}^m e^{-\alpha\lambda_2} d\lambda_2, \tag{A2}$$

$$S(m, n, \alpha) = \int_1^\infty \lambda_1{}^m e^{-\alpha\lambda_1} d\lambda_1 \int_1^{\lambda_1} \lambda_2{}^n e^{-\alpha\lambda_2} d\lambda_2,$$

and

$$Q_0(\lambda) = \tfrac{1}{2} \ln \frac{\lambda + 1}{\lambda - 1}. \tag{A3}$$

To treat these quantities, use is made of the simpler functions[10]

$$A_n(\alpha) = \int_1^\infty \lambda^n e^{-\alpha\lambda} d\lambda, \tag{A4}$$

$$F_n(\alpha) = \int_1^\infty \lambda^n e^{-\alpha\lambda} Q_0(\lambda) d\lambda. \tag{A5}$$

These can be shown to satisfy the following recursion formulae[8,9]:

$$A_n(\alpha) = \frac{1}{\alpha}[e^{-\alpha} + nA_{n-1}(\alpha)], \tag{A6}$$

$$F_n(\alpha) = F_{n-2}(\alpha) + \frac{1}{\alpha}[nF_{n-1}(\alpha) - (n-2)F_{n-3}(\alpha) - A_{n-2}(\alpha)]. \tag{A7}$$

These, together with the "starting" formulae:

$$A_0(\alpha) = e^{-\alpha}/\alpha, \tag{A8}$$

$$F_0(\alpha) = \tfrac{1}{2}[(\ln 2 + C)e^{-\alpha}/\alpha - Ei(-2\alpha)e^{\alpha}/\alpha], \tag{A9}$$

$$F_1(\alpha) = \tfrac{1}{2}[(\ln 2 + C)e^{-\alpha}(1/\alpha + 1/\alpha^2) - Ei(-2\alpha)e^{\alpha}(-1/\alpha + 1/\alpha^2)] \tag{A9a}$$

$$C = 0.577216\cdots, \tag{A10}$$

are sufficient to compile tables of these functions. Such tables are included in the present paper[11] (Tables I and II).

By using these functions the integrations in (A1) and (A2) can be carried out. Thus on inverting the order of integration it follows readily that:

$$S(m, n, \alpha) = \int_1^\infty \lambda_1{}^n e^{-\alpha\lambda_1} d\lambda_1 \int_{\lambda_1}^\infty \lambda_2{}^m e^{-\alpha\lambda_2} d\lambda_2 \tag{A11}$$

[10] Zener and Guillemin, Phys. Rev. **34**, 999 (1929). See also Rosen, Phys. Rev. **38**, 255 (1931).

[11] Table I is essentially an enlargement of a table of $A_n(\alpha)$ given in the paper by the present writer mentioned in reference[8], but corrected for several errors mainly in the 5th and 6th figures. Cf. list of errata at the end of the present paper.

TABLE I. $A_n(\alpha)$.

α	n = 0	1	2	3	4	5	6	7	8	9	10
0.5	1.21306	3.63918	1.57698 · 10	9.58318 · 10	7.67868 · 10^2	7.67989 · 10^3	9.21599 · 10^4	1.29024 · 10^6	2.06438 · 10^7	3.71589 · 10^8	7.43178 · 10^9
1.0	3.67879 · 10^{-1}	7.35759 · 10^{-1}	1.83940 · 1	5.88607 · 1	2.39122 · 10	1.19929 · 10^2	7.19940 · 10^2	5.03995 · 10^3	4.03200 · 10^4	3.62880 · 10^5	3.62880 · 10^6
1.5	1.48753	2.47922	4.79317 · 10^{-1}	1.10739	3.10178 · 1	1.04880 · 10	4.21009 · 10	1.96620 · 10^2	1.04879 · 10^3	6.29287 · 10^3	4.19526 · 10^4
2.0	6.76676 · 10^{-2}	1.01501	1.69169	3.21421 · 10^{-1}	7.10510 · 10^{-1}	1.84394 · 1	5.59950 · 1	1.96659 · 10	7.87313 · 10	3.54359 · 10^2	1.77186 · 10^3
2.5	3.28340	4.59676 · 10^{-2}	6.96081 · 10^{-2}	1.16364	2.19016	4.70866 · 10^{-1}	1.16291	3.28899 · 1	1.05576	3.80402 · 10	1.52193 · 10^2
3.0	1.65957	2.21276	3.13474	4.79431 · 10^{-2}	8.05198 · 10^{-2}	1.50795	3.18186 · 10^{-1}	7.59031 · 10^{-1}	2.04068 · 1	6.13863 · 1	2.04787 · 10
3.5	8.62782 · 10^{-3}	1.10929	1.49666	2.14564	3.31494	5.59841 · 10^{-2}	1.04601	2.17829	5.06522 · 10^{-1}	1.31111	3.75467 · 1
4.0	4.57891	5.72364 · 10^{-3}	7.44073 · 10^{-3}	1.01595	1.47384	2.30019	3.90871 · 10^{-2}	7.29719 · 10^{-2}	1.50523	3.43255 · 10^{-1}	8.62716 · 10^{-1}
4.5	2.46867	3.01726	3.80967	5.00845 · 10^{-3}	6.92062 · 10^{-3}	1.01582	1.60130	2.73778	5.11402 · 10^{-2}	1.04749	2.35245
5.0	1.34759	1.61711	1.99443	2.54425	3.38299	4.73058 · 10^{-3}	7.02428 · 10^{-3}	1.11816	1.92381	3.59762 · 10^{-2}	7.33000 · 10^{-2}
6.0	4.13125 · 10^{-4}	4.81980 · 10^{-4}	5.73785 · 10^{-4}	7.00018 · 10^{-4}	8.79804 · 10^{-4}	1.14630	1.55942	2.23245 · 10^{-3}	3.38972 · 10^{-3}	5.49771 · 10^{-3}	9.57598 · 10^{-3}
7.0	1.30269	1.48879	1.72806	2.04328	2.47028	3.06717 · 10^{-4}	3.93169 · 10^{-4}	5.23438 · 10^{-4}	7.28484 · 10^{-4}	1.06689	1.65440
8.0	4.19328 · 10^{-5}	4.71744 · 10^{-5}	5.37264 · 10^{-5}	6.20802 · 10^{-5}	7.29729 · 10^{-5}	8.75409 · 10^{-5}	1.07589	1.36073	1.78006	2.42189 · 10^{-4}	3.44669 · 10^{-4}
9.0	1.37122	1.52358	1.70979	1.94115	2.23395	2.61231	3.11276 · 10^{-5}	3.79225 · 10^{-5}	4.74211 · 10^{-5}	6.11333 · 10^{-5}	8.16381 · 10^{-5}
10	4.53999 · 10^{-6}	4.99399 · 10^{-6}	5.53879 · 10^{-6}	6.20163 · 10^{-6}	7.02065 · 10^{-6}	8.05032 · 10^{-6}	9.37018 · 10^{-6}	1.10991	1.34193	1.66174	2.11573
12	5.12018 · 10^{-7}	5.54686 · 10^{-7}	6.04465 · 10^{-7}	6.63134 · 10^{-7}	7.33062 · 10^{-7}	8.17460 · 10^{-7}	9.20748 · 10^{-7}	1.04912 · 10^{-6}	1.21143 · 10^{-6}	1.42059 · 10^{-6}	1.69584 · 10^{-6}
14	5.93949 · 10^{-8}	6.36374 · 10^{-8}	6.84860 · 10^{-8}	7.40705 · 10^{-8}	8.05579 · 10^{-8}	8.81656 · 10^{-8}	9.71802 · 10^{-8}	1.07985 · 10^{-7}	1.21101 · 10^{-7}	1.37245 · 10^{-7}	1.57427 · 10^{-7}

TABLE I. $A_n(\alpha)$.(*Cont.*)

α	n = 11	12	13	14	15	16	17	18	19	20
1.0	3.99168 · 10^7	4.79002 · 10^8	6.22702 · 10^9	8.71783 · 10^{10}	1.30767 · 10^{12}	2.09228 · 10^{13}	3.55687 · 10^{14}	6.40237 · 10^{15}	1.21645 · 10^{17}	2.43290 · 10^{18}
2.0	9.74530 · 10^3	5.84719 · 10^4	3.80067 · 10^5	2.66047 · 10^6	1.99539 · 10^7	1.59628 · 10^8	1.35684 · 10^9	1.22116 · 10^{10}	1.16010 · 10^{11}	1.16010 · 10^{12}
3.0	7.51051 · 10	3.00437 · 10^2	1.30191 · 10^3	6.07560 · 10^4	3.03780 · 10^4	1.62016 · 10^5	9.18091 · 10^5	5.50855 · 10^6	3.48875 · 10^7	2.32583 · 10^8
4.0	2.37705 · 1	7.13573 · 1	2.31957 · 10	8.11895 · 10	3.04465 · 10^2	1.21787 · 10^3	5.17593 · 10^3	2.32917 · 10^4	1.10636 · 10^5	5.53178 · 10^5
5.0	1.62608 · 10^{-1}	3.91606 · 10^{-1}	1.01952 · 1	2.85601 · 1	8.56938 · 1	2.74234 · 10	9.32408 · 10	3.35668 · 10^2	1.27554 · 10^3	5.10216 · 10^3
6.0	1.79691 · 10^{-2}	3.63513 · 10^{-2}	7.91743 · 10^{-2}	1.85153 · 10^{-1}	4.63296 · 10^{-1}	1.23587 · 1	3.50204 · 1	1.05065 · 10	3.32711 · 10	1.10904 · 10^2
7.0	2.73004 · 10^{-3}	4.81034 · 10^{-3}	9.06375 · 10^{-3}	1.82578 · 10^{-2}	3.92541 · 10^{-2}	8.98538 · 10^{-2}	2.18347 · 10^{-1}	5.61593 · 10^{-1}	1.52445 · 1	4.35572 · 1
8.0	5.15853 · 10^{-4}	8.15712 · 10^{-4}	1.36747	2.43500 · 10^{-3}	4.60755 · 10^{-3}	9.25704 · 10^{-3}	1.97131 · 10^{-2}	4.43965 · 10^{-2}	1.05484 · 10^{-1}	2.63751 · 10^{-1}
9.0	1.13492	1.65035	2.52096 · 10^{-4}	4.05862 · 10^{-4}	6.90148 · 10^{-4}	1.24064	2.35715 · 10^{-3}	4.72801 · 10^{-3}	9.99506 · 10^{-3}	2.22250 · 10^{-2}
10	2.78131 · 10^{-5}	3.79157 · 10^{-5}	5.38304 · 10^{-5}	7.99025 · 10^{-5}	1.24394	2.03570 · 10^{-4}	3.50609 · 10^{-4}	6.35639 · 10^{-4}	1.21225	2.42904 · 10^{-3}
12	2.06654 · 10^{-6}	2.57856 · 10^{-6}	3.30546 · 10^{-6}	4.36838 · 10^{-6}	5.97250 · 10^{-6}	8.47535 · 10^{-6}	1.25188 · 10^{-5}	1.92902 · 10^{-5}	3.10548 · 10^{-5}	5.22700 · 10^{-5}
14	1.83088 · 10^{-7}	2.16327 · 10^{-7}	2.60270 · 10^{-7}	3.19665 · 10^{-7}	4.01893 · 10^{-7}	5.18702 · 10^{-7}	6.89247 · 10^{-7}	9.45569 · 10^{-7}	1.34267 · 10^{-6}	1.97949 · 10^{-6}

TABLE II. $F_n(\alpha)$.

α	n = 0	1	2	3	4	5	6	7	8	9	10
0.5	$7.11802 \cdot 10^{-1}$	1.41200	3.93368	1.63121 · 10	9.72429 · 10	$7.73476 \cdot 10^{2}$	$7.71272 \cdot 10^{3}$	$9.24193 \cdot 10^{4}$	$1.29282 \cdot 10^{6}$	$2.06747 \cdot 10^{7}$	$3.72021 \cdot 10^{8}$
1.0	3.00133	$4.67340 \cdot 10^{-1}$	$8.66934 \cdot 10^{-1}$	2.03225 · 1	6.22186 · 1	2.46547 · 10	$1.22109 \cdot 10^{2}$	$7.28378 \cdot 10^{2}$	$5.08127 \cdot 10^{3}$	$4.05651 \cdot 10^{4}$	$3.64585 \cdot 10^{5}$
1.5	1.44136	2.01240	3.13287	$5.66441 \cdot 10^{-1}$	1.23593	3.32138 · 1	1.09431 · 10	4.32774 · 10	$2.00403 \cdot 10^{2}$	$1.06355 \cdot 10^{3}$	$6.36072 \cdot 10^{3}$
2.0	$7.34145 \cdot 10^{-2}$	$9.61588 \cdot 10^{-2}$	1.35740	2.12310	$3.79616 \cdot 10^{-1}$	$7.97031 \cdot 10^{-1}$	1.99083 · 1	5.89394 · 1	2.03758 · 10	8.07840 · 10	$3.61354 \cdot 10^{2}$
2.5	3.86961	4.85789	$6.44256 \cdot 10^{-2}$	$9.20242 \cdot 10^{-2}$	1.44958	2.58084	$5.29515 \cdot 10^{-1}$	1.26246	3.48483 · 1	1.10096	3.92603 · 10
3.0	2.08628	2.54062	3.22684	4.33445	$6.26745 \cdot 10^{-2}$	$9.95525 \cdot 10^{-2}$	1.77147	$3.58173 \cdot 10^{-1}$	$8.27106 \cdot 10^{-1}$	2.17314 · 1	6.43555 · 1
3.5	1.14309	1.36042	1.67396	2.15170	2.92805	4.28677	$6.87058 \cdot 10^{-2}$	1.22455	2.45229	5.53394 · 10^{-1}	1.40174
4.0	$6.33936 \cdot 10^{-3}$	$7.41008 \cdot 10^{-3}$	$8.89967 \cdot 10^{-3}$	1.10691	1.44035	1.98589	2.94382	$4.76208 \cdot 10^{-2}$	$8.51210 \cdot 10^{-2}$	1.69383	3.75707 · 10^{-1}
4.5	3.54908	4.08877	4.81772	$5.84140 \cdot 10^{-3}$	$7.34625 \cdot 10^{-3}$	$9.67909 \cdot 10^{-3}$	1.35214	2.02926	3.31332	5.94416 · 10^{-2}	1.17786
5.0	2.00209	2.27912	2.64422	3.14181	3.84713	4.89356	$6.52936 \cdot 10^{-3}$	$9.24142 \cdot 10^{-3}$	1.40385	2.31333	$4.16712 \cdot 10^{-2}$
6.0	$6.48493 \cdot 10^{-4}$	$7.24630 \cdot 10^{-4}$	$8.21182 \cdot 10^{-4}$	$9.46806 \cdot 10^{-4}$	1.11521	1.34889	1.68626	2.19580	$3.00521 \cdot 10^{-3}$	$4.36423 \cdot 10^{-3}$	$6.78624 \cdot 10^{-3}$
7.0	2.13850	2.35680	2.62577	2.96395	$3.39922 \cdot 10^{-4}$	$3.97474 \cdot 10^{-4}$	$4.75955 \cdot 10^{-4}$	$5.86811 \cdot 10^{-4}$	$7.49738 \cdot 10^{-4}$	1.00003	1.40364
8.0	$7.14706 \cdot 10^{-5}$	$7.79300 \cdot 10^{-5}$	$8.57115 \cdot 10^{-5}$	$9.52412 \cdot 10^{-5}$	1.07134	1.22298	1.42115	1.68747	2.05690	$2.58789 \cdot 10^{-4}$	$3.38179 \cdot 10^{-4}$
9.0	2.41359	2.60941	2.84110	3.11898	$3.45747 \cdot 10^{-5}$	$3.87708 \cdot 10^{-5}$	$4.40776 \cdot 10^{-5}$	$5.09427 \cdot 10^{-5}$	$6.00541 \cdot 10^{-5}$	$7.25006 \cdot 10^{-5}$	$9.00590 \cdot 10^{-5}$
10	$8.21890 \cdot 10^{-6}$	$8.82415 \cdot 10^{-6}$	$9.52973 \cdot 10^{-6}$	1.03618	1.13557	1.25606	1.40453	1.59094	1.82994	2.14372	2.56673
12	$9.71638 \cdot 10^{-7}$	$1.03210 \cdot 10^{-6}$	1.10099	$1.18015 \cdot 10^{-6}$	$1.27198 \cdot 10^{-6}$	$1.37963 \cdot 10^{-6}$	$1.50733 \cdot 10^{-6}$	$1.66079 \cdot 10^{-6}$	$1.84798 \cdot 10^{-6}$	$2.08007 \cdot 10^{-6}$	$2.37322 \cdot 10^{-6}$
14	$1.17125 \cdot 10^{-7}$	$1.23441 \cdot 10^{-7}$	$1.30517 \cdot 10^{-7}$	$1.38497 \cdot 10^{-7}$	$1.47561 \cdot 10^{-7}$	$1.57939 \cdot 10^{-7}$	$1.69925 \cdot 10^{-7}$	$1.83903 \cdot 10^{-7}$	$2.00383 \cdot 10^{-7}$	$2.20045 \cdot 10^{-7}$	$2.43820 \cdot 10^{-7}$

TABLE II. $F_n(\alpha)$.(*Cont*)

α	n = 11	12	13	14	15	16	17	18	19	20
1.0	$3.64239 \cdot 10^{6}$	$4.00388 \cdot 10^{7}$	$4.80219 \cdot 10^{8}$	$6.24040 \cdot 10^{9}$	$8.73387 \cdot 10^{10}$	$1.30976 \cdot 10^{12}$	$2.09519 \cdot 10^{13}$	$3.56125 \cdot 10^{14}$	$6.40936 \cdot 10^{15}$	$1.21764 \cdot 10^{17}$
2.0	$1.79936 \cdot 10^{3}$	$9.86767 \cdot 10^{3}$	$5.90791 \cdot 10^{4}$	$3.83389 \cdot 10^{5}$	$2.68033 \cdot 10^{6}$	$2.00822 \cdot 10^{7}$	$1.60527 \cdot 10^{8}$	$1.36357 \cdot 10^{9}$	$1.22653 \cdot 10^{10}$	$1.16466 \cdot 10^{11}$
3.0	2.12426 · 10	7.73360 · 10	$3.07733 \cdot 10^{2}$	$1.32831 \cdot 10^{3}$	$6.18018 \cdot 10^{3}$	$3.08280 \cdot 10^{4}$	$1.64105 \cdot 10^{5}$	$9.28490 \cdot 10^{5}$	$5.56382 \cdot 10^{6}$	$3.51998 \cdot 10^{7}$
4.0	$9.25241 \cdot 10^{-1}$	2.51229 · 1	7.46274 · 1	2.40722 · 10	8.37697 · 10	$3.12734 \cdot 10^{2}$	$1.24650 \cdot 10^{3}$	$5.28245 \cdot 10^{3}$	$2.37150 \cdot 10^{4}$	$1.11425 \cdot 10^{5}$
5.0	$8.23454 \cdot 10^{-2}$	$1.78373 \cdot 10^{-1}$	$4.21918 \cdot 10^{-1}$	1.08379 · 1	3.00563 · 1	8.94923 · 1	2.84677 · 10	9.63304 · 10	$3.45448 \cdot 10^{2}$	$1.30850 \cdot 10^{3}$
6.0	$1.13816 \cdot 10^{-2}$	$2.06797 \cdot 10^{-2}$	$4.07512 \cdot 10^{-2}$	$8.69442 \cdot 10^{-2}$	$2.00110 \cdot 10^{-1}$	$4.94626 \cdot 10^{-1}$	1.30697 · 1	3.67594 · 1	1.09623 · 10	3.45451 · 10
7.0	$2.08938 \cdot 10^{-3}$	$3.32048 \cdot 10^{-3}$	$5.66027 \cdot 10^{-3}$	1.03720	$2.04246 \cdot 10^{-2}$	$4.31281 \cdot 10^{-2}$	$9.73308 \cdot 10^{-2}$	3.33886 · 10^{-1}	5.96233 · 10^{-1}	1.60690 · 1
8.0	$4.62110 \cdot 10^{-4}$	$6.64774 \cdot 10^{-4}$	1.01289	$1.64220 \cdot 10^{-3}$	$2.84083 \cdot 10^{-3}$	$5.24692 \cdot 10^{-3}$	1.03355	2.16629 · 10^{-2}	4.81711 · 10^{-2}	1.13286 · 10^{-1}
9.0	1.15726	1.54733	$2.16547 \cdot 10^{-4}$	$3.18946 \cdot 10^{-4}$	$4.96609 \cdot 10^{-4}$	$8.19859 \cdot 10^{-4}$	$1.43697 \cdot 10^{-3}$	2.67310 · 10^{-3}	5.26965 · 10^{-3}	1.09841 · 10^{-2}
10	$3.15400 \cdot 10^{-5}$	$3.99623 \cdot 10^{-5}$	$5.24757 \cdot 10^{-5}$	$7.17886 \cdot 10^{-5}$	1.02825	1.54852	2.45950 · 10^{-4}	4.12686 · 10^{-4}	7.13745 · 10^{-4}	1.36990 · 10^{-3}
12	$2.75117 \cdot 10^{-6}$	$3.24967 \cdot 10^{-6}$	$3.92398 \cdot 10^{-6}$	$4.86160 \cdot 10^{-6}$	$6.20504 \cdot 10^{-6}$	$8.19299 \cdot 10^{-6}$	1.12371 · 10^{-5}	1.60689 · 10^{-5}	2.40296 · 10^{-5}	3.76551 · 10^{-5}
14	$2.72997 \cdot 10^{-7}$	$3.09398 \cdot 10^{-7}$	$3.55645 \cdot 10^{-7}$	$4.15593 \cdot 10^{-7}$	$4.90034 \cdot 10^{-7}$	$6.02868 \cdot 10^{-7}$	$7.53104 \cdot 10^{-7}$	$9.68341 \cdot 10^{-7}$	1.28599 · 10^{-6}	1.76966 · 10^{-6}

$$= \frac{m!}{\alpha^{m+1}} \sum_{\nu=0}^{m} \frac{\alpha^\nu}{\nu!} A_{n+\nu}(2\alpha). \tag{A12}$$

Rather than to calculate $S(m, n, \alpha)$ by this formula it is more convenient when compiling a table of values to use the recursion formula which the expression in A12) satisfies. This is:

$$S(m, n, \alpha) = \frac{1}{\alpha}[mS(m-1, n, \alpha) + A_{m+n}(2\alpha)] \tag{A13}$$

with

$$S(0, n, \alpha) = A_n(2\alpha)/\alpha. \tag{A14}$$

As a check in such calculation, one may use the following relation, easily derivable by the use of expressions of the form (A2) and (A11), namely:

$$S(m, n, \alpha) + S(n, m, \alpha) = A_m(\alpha)A_n(\alpha). \tag{A15}$$

By analogy with (A12) one can define the quantity

$$T(m, n, \alpha) = \frac{m!}{\alpha^{m+1}} \sum_{\nu=0}^{m} \frac{\alpha^\nu}{\nu!} F_{n+\nu}(2\alpha), \tag{A15}$$

which will have an analogous recursion formula,

$$T(m, n, \alpha) = \frac{1}{\alpha}[mT(m-1, n, \alpha) + F_{m+n}(2\alpha)] \tag{A17}$$

with

$$T(0, n, \alpha) = F_n(2\alpha)/\alpha. \tag{A18}$$

By means of this function, it is found that one can write

$$H(m, n, \alpha) = A_m(\alpha)F_n(\alpha) + A_n(\alpha)F_m(\alpha) - T(m, n, \alpha) - T(n, m, \alpha). \tag{A19}$$

Since the functions (A12), (A18), and (A19) are characterized by three parameters they are too bulky to be tabulated here; however, to calculate them from the tables of $A_n(\alpha)$ and $F_n(\alpha)$ is a simple matter.

By the help of these functions the "exchange" integrals can now be evaluated; the remaining integrals require no special comments. The integrals are as follows:

$$RF_0 = R\int \frac{[\psi^0(a1)]^2}{r_{a1}} dv_1 = \rho \tag{A20}$$

$$RF_1 = R\int \frac{[\psi'(a1)]^2}{r_{a1}} dv_1 = \rho/2 \tag{A21}$$

$$RG_{00} = R\int \frac{[\psi^0(a1)]^2}{r_{b1}} dv_1 = 1 - e^{-2\rho}(\rho + 1) \tag{A22}$$

$$RG_{01} = R\int \frac{\psi^0(a1)\psi'(a1)}{r_{b1}} dv_1 = 1/\rho - e^{-2\rho}(\rho^2 + 2\rho + 2 + 1/\rho) \tag{A23}$$

$$RG_{11} = R\int \frac{[\psi'(a1)]^2}{r_{b1}}\,dv_1 = 1 + 3/\rho^2 - e^{-2\rho}(\rho^3 + 3\rho^2 + 11\rho/2 + 7 + 6/\rho + 3/\rho^2) \tag{A24}$$

$$RK_{00,00} = R\int \frac{[\psi^0(a1)]^2[\psi^0(b2)]^2}{r_{12}}\,dv_1dv_1 = 1 - e^{-2\rho}(\rho^3/6 + 3\rho^2/4 + 11\rho/8 + 1) \tag{A25}$$

$$RK_{00,01} = R\int \frac{[\psi^0(a1)]^2\psi^0(b2)\psi'(b2)}{r_{12}}\,dv_1dv_2 = 1/\rho - e^{-2\rho}(\rho^4/12 + 11\rho^3/24 + 59\rho^2/48 + 2\rho + 2 + 1/\rho) \tag{A26}$$

$$RK_{00,11} = R\int \frac{[\psi^0(a1)]^2[\psi'(b2)]^2}{r_{12}}\,dv_1dv_2 = 1 + 3/\rho^2 - e^{-2\rho}(\rho^5/20 + 41\rho^4/120 + 301\rho^3/240 + 25\rho^2/8 + 89\rho/16 + 7 + 6/\rho + 3/\rho^2) \tag{A27}$$

$$RK_{01,01} = R\int \frac{\psi^0(a1)\psi'(a1)\psi^0(b2)\psi'(b2)}{r_{12}}\,dv_1dv_2 = 2/\rho^2 - e^{-2\rho}(\rho^5/30 + \rho^4/5 + 77\rho^3/120 + 71\rho^2/48 + 263\rho/96 + 4 + 4/\rho + 2/\rho^2) \tag{A28}$$

$$RK_{01,11} = R\int \frac{\psi^0(a1)\psi'(a1)[\psi'(b2)]^2}{r_{12}}\,dv_1dv_2 = 1/\rho + 9/\rho^3 - e^{-2\rho}(\rho^6/60 + 7\rho^5/60 + 113\rho^4/240 + 697\rho^3/480 + 3577\rho^2/960 + 8\rho + 14 + 19/\rho + 18/\rho^2 + 9/\rho^3) \tag{A29}$$

$$RK_{11,11} = R\int \frac{[\psi'(a1)]^2[\psi'(b2)]^2}{r_{12}}\,dv_1dv_2 = 1 + 6/\rho^2 + 54/\rho^4 - e^{-2\rho}(\rho^7/140 + 141\rho^6/2520 + 19\rho^5/70 + 893\rho^4/840 + 23809\rho^3/6720 + 6411\rho^2/640 + 30731\rho/1280 + 49 + 84/\rho + 114/\rho^2 + 108/\rho^3 + 54/\rho^4) \tag{A30}$$

$$I_{00} = \int \psi^0(a1)\psi^0(b1)dv_1 = e^{-\rho}(\rho^2/3 + \rho + 1) \tag{A31}$$

$$I_0 = \int \psi^0(a1)\psi'(b1)dv_1 = \rho I_{00}/2 = \tfrac{1}{2}e^{-\rho}(\rho^3/3 + \rho^2 + \rho) \tag{A32}$$

$$I_{11} = \int \psi'(a_1)\psi'(b1)dv_1 = e^{-\rho}(\rho^4/15 + 2\rho^3/15 - \rho^2/5 - \rho - 1) \tag{A33}$$

$$RJ_{00} = R\int \frac{\psi^0(a1(\psi^0(b1)}{r_{a1}}\,dv_1 = \rho e^{-\rho}(\rho + 1) \tag{A34}$$

$$RJ_{10} = R\int \frac{\psi'(a1)\psi^0(b1)}{r_{a1}}\,dv_1 = \tfrac{1}{3}\rho^2 e^{-\rho}(\rho+1) \tag{A35}$$

$$RJ_{01} = R\int \frac{\psi^0(a1)\psi'(b1)}{r_{a1}}\,dv_1 = \tfrac{2}{3}\rho^2 e^{-\rho}(\rho+1) = 2RJ_{10} \tag{A36}$$

$$RJ_{11} = R\int \frac{\psi'(a1)\psi'(b1)}{r_{a1}}\,dv_1 = \tfrac{1}{2}\rho e^{-\rho}(\rho^3/3-\rho-1) \tag{A37}$$

$$RL_{00,00} = R\int \frac{\psi^0(a1)\psi^0(b1)\psi^0(a2)\psi^0(b2)}{r_{12}} = (\rho^6/15)[9H(2,2,\rho) - 6H(2,0,\rho) + H(0,0,\rho) - 3S(1,2,\rho) + S(1,0,\rho)] \tag{A38}$$

$$RL_{00,01} = R\int \frac{\psi^0(a1)\psi^0(b1)\psi^0(a2)\psi'(b2)}{r_{12}} = (\rho/2)RL_{00,00} \tag{A39}$$

$$R(L_{01,01}+L_{01,10}) = R\int \frac{\psi^0(a1)\psi'(b1)[\psi^0(a2)\psi'(b2)+\psi'(a2)\psi^0(b2)]}{r_{12}}\,dv_1dv_2 = (\rho^2/2)RL_{00,00} \tag{A40}$$

$$RL_{00,11} = R\int \frac{\psi^0(a1)\psi^0(b1)\psi'(a2)\psi'(b2)}{r_{12}}\,dv_1dv_2 = R\left(\frac{\rho^2}{4}L_{00,00} - L'\right) \tag{A41}$$

$$RL_{01,11} = R\int \frac{\psi^0(a1)\psi'(b1)\psi'(a2)\psi'(b2)}{r_{12}}\,dv_1dv_2 = (\rho/2)RL_{00,11} \tag{A42}$$

$$RL_{11,11} = R\int \frac{\psi'(a1)\psi'(b1)\psi'(a2)\psi'(b2)}{r_{12}}\,dv_1dv_2 = R\left(\frac{\rho^4}{16}L_{00,00} - \frac{\rho^2}{2}L' + L''\right). \tag{A43}$$

The primed quantities are given by:

$$RL' = (\rho^8/840)[-21H(6,2) + 7H(6,0) + 60H(4,2) - 20H(4,0) - 27H(2,2) + 9H(2,0) + 21S(5,2) - 7S(5,0) - 18S(3,2) + 6S(3,0) + 21S(1,6) - 25S(1,4) + 6S(1,2)], \tag{A44}$$

$$RL'' = (\rho^{10}/15120)[147H(6,6) - 315H(4,6) + 225H(4,4) + 63H(2,6) - 135H(2,4) + 27H(2,2) - 294S(5,6) + 315S(5,4) - 63S(5,2) + 217S(3,6) - 240S(3,4) + 51S(3,2)]. \tag{A45}$$

The argument of these functions is ρ as before.

2. Curve Fitting

To fit a curve of the form

$$\Delta E = De^{-2a(\rho_0-\rho_m)} - 2De^{-a(\rho_0-\rho_m)} \tag{A46}$$

to the energy curve nears its minimum requires a knowledge of the energy at three points in that vicinity. In the calculation discussed the fitting was very easy because the minimum was near $\rho_0=1.5$, and values of ΔE had been calculated for $\rho_0=1$, 1.5, 2. Thus, if we denote these values of ΔE by E_1, E_2, E_3, and let

$$B = e^{-a/2}, \tag{A47}$$

$$C = e^{a\rho_m}, \tag{A48}$$

than the equations to be satisfied are:

$$E_1 = CD(CB^4 - 2B^2), \tag{A49}$$

$$E_2 = CD(CB^6 - 2B^3), \tag{A50}$$

$$E_3 = CD(CB^8 - 2B^4). \tag{A51}$$

The solutions are given by the appropriate root of:

$$E_1B^3 - E_2B^2 - E_2B + E_3 = 0, \tag{A52}$$

and by the relations:

$$C = \frac{2}{B^2}\left(\frac{E_1B - E_2}{E_1B^2 - E_2}\right), \tag{A53}$$

$$D = \frac{1}{2B^3C}\left(\frac{E_1B^2 - E_2}{1 - B}\right), \tag{A54}$$

$$a = 2\ln(1/B), \tag{A55}$$

$$\rho_m = \frac{1}{a}\ln C. \tag{A56}$$

Thus the constants required in (A46) have been evaluated.

Errata: In a recent paper by the author, Phys. Rev. **38**, 255, (1931), several errors appear which may cause inconvenience to anyone using it. The corrected portions should read as follows:

p. 254, Eq. (45): ${}_n{}^m(\alpha) = \sum_{\nu=0}^{m}\alpha^\nu F_{n+\nu}(\alpha)/2^\nu\nu!$

p. 266: $A_8(1, 3.5) = 5.06522$ instead of 5.06553

$A_{10}(1, 3.0) = 2.04787 \cdot 10$ instead of $2.04787 \cdot 1$

$A_{13}(1, 8.0) = 1.36747 \cdot 10^{-3}$ instead of $8.36747 \cdot 10^{-3}$

p. 267: $A_5(-1, 2.0) = 9.23632 \cdot 10^{-1}$ instead of $1.84726 \cdot 10^{-1}$

p. 274, line 5: $\alpha = 1.385\,A^{-1}$

p. 274, line 20: 0.87 instead of 1.11.

A NOTE ON THE GENERAL SOLUTION OF SCHRÖDINGER'S EQUATION AND THE UNCERTAINTY PRINCIPLE

By E. L. Hill
Department of Physics, University of Minnesota

(Received November 13, 1931)

Abstract

It is shown that the general solution of Schrödinger's equation in one dimension for a given energy can be written in a form representing two beams travelling in opposite directions with the classical velocity. This permits an interpretation of the uncertainty principle in which an electron in a conservative field, with a definite energy, has also a definite speed, but its direction of motion is indeterminate. In regions in which the classical velocity is imaginary this interpretation becomes indefinite. A brief consideration is given to the generalization to three dimensions.

Introduction

THE uncertainty principle is often characterized by the statement that "the position and velocity of an electron cannot be determined simultaneously." There are two general theoretical ways of explaining this result; (1) by saying that a localized electron can only be vizualized in terms of a wave packet, and (2) by appealing to the statistical interpretation of the function

$$e^{+i(2\pi/h)pq} \tag{1}$$

as the probability amplitude connecting a coordinate q and its conjugate momentum p. These two arguments are more or less equivalent since one can build up a wave packet by a superposition of functions of the type of Eq. (1); i.e., by a Fourier integral

$$\psi(q) = \int_{-\infty}^{+\infty} g(p) e^{i(2\pi/h)pq} dp. \tag{1'}$$

From this point of view it seems necessary to conclude that if an electron is considered to be at a given point, then its velocity can have any magnitude and any direction.

In a conversation with the writer some months ago, Professor Frenkel suggested that one might interpret the uncertainty principle in terms of an uncertainty in the *direction* of motion of the electron, and of a possible reflection coefficient for the electron at every point in a field of force. Due to the reflection the electron may change, and even reverse, its direction of motion at any point. This development will be made in the English edition of Frenkel's book on wave mechanics.

The purpose of the present note is to present some furthur ideas which have occurred to the present writer on this topic, principally for the purpose of making the above argument more precise and definite. It may be stated

here that the essential point about which our discussion turns is the possibility of expressing the general solution of Schrödinger's equation for a given value of the energy E by means of an integral of type somewhat different from (1′), but in a form in which the integration extends not over all values of the momentum, but over only those values which are consistent with the requirement that the absolute magnitude of the momentum of an electron at a given point with a given total energy shall be just the classical value. For one-dimensional motion the integral reduces to a sum since there are only two possible directions of motion. We discuss first motion in one dimension.

One Dimensional Case

Consider the "collision" of a group of electrons, all having energy E, with a field of force having a potential function $V(x)$, where we assume $E \geqq V(x)$. For simplicity in the later interpretation we assume that

$$\left.\begin{aligned} V(x) &= V_0 \text{ when } x \leqq \xi_0 \\ V(x) &= V_1 \text{ when } x \geqq \xi_1 \end{aligned}\right\} \tag{2}$$

where V_0 and V_1 are constants.

The wave equation to be solved is

$$d^2\psi/dx^2 + 4\pi^2\alpha^2(x, E)\psi = 0 \tag{3}$$

with

$$\alpha(x, E) = + [2m(E - V(x))]^{1/2}/h. \tag{4}$$

Let us try to solve Eq. (3) by replacing $V(x)$ by a "step-function," a portion of which is shown in Fig. (1). For such a step-function the solution can be obtained by elementary means, and one can then approach the actual case by

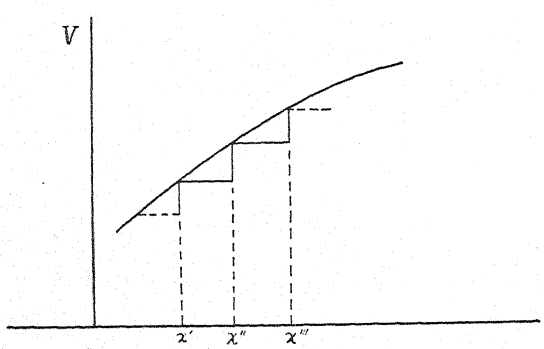


Fig. 1.

making the steps smaller, at the same time increasing their number. Let α' and α'' be the values of $\alpha(x)$ at x' and x'' respectively. For the step-function the solutions can be written as

$$x' \leqq x < x'' \quad \psi = c_1(x')e^{+i2\pi\alpha' x} + c_2(x')e^{-i2\pi\alpha' x} \tag{5}$$

$$x'' \leqq x < x''' \quad \psi = c_1(x'')e^{+i2\pi\alpha'' x} + c_2(x'')e^{-i2\pi\alpha'' x} \tag{6}$$

where $c_1(x')$, $c_2(x')$, $c_1(x'')$, and $c_2(x'')$ are constants.

Applying the usual boundary conditions of continuity for ψ and $d\psi/dx$ at x'', one obtains the expressions

$$\left.\begin{aligned} c_1(x'') &= \tfrac{1}{2}\{c_1(x')(1+\alpha'/\alpha'')e^{+i2\pi(\alpha'-\alpha'')x''} + c_2(x')(1-\alpha'/\alpha'')e^{-i2\pi(\alpha'+\alpha'')x''}\} \\ c_2(x'') &= \tfrac{1}{2}\{c_1(x')(1-\alpha'/\alpha'')e^{+i2\pi(\alpha'+\alpha'')x''} + c_2(x')(1+\alpha'/\alpha'')e^{-i2\pi(\alpha'-\alpha'')x''}\}. \end{aligned}\right\} \quad (7)$$

We now consider the interval $x''-x'=\Delta x$ to become an infinitesimal, and the c's as well as α to be functions of x which can be expanded in Taylor's serious about the point x':

$$\left.\begin{aligned} \alpha'' &= \alpha' + (d\alpha/dx)_{x=x'}\Delta x + \cdots \\ c_1(x'') &= c_1(x') + (dc_1/dx)_{x=x'}\Delta x + \cdots \text{etc.} \end{aligned}\right\} \quad (8)$$

Inserting these relations in Eq. (7) we get, after some elementary manipulations, in the limit $\Delta x \to 0$:

$$\left.\begin{aligned} (dc_1/dx) &= [d(\ln \alpha^{1/2})/dx][-(1+i4\pi\alpha x)c_1 + e^{-i4\pi\alpha x}c_2] \\ (dc_2/dx) &= [d(\ln \alpha^{1/2})/dx][e^{+i4\pi\alpha x}c_1 - (1-i4\pi\alpha x)c_2] \end{aligned}\right\}. \quad (9)$$

With the functions $c_1(x)$ and $c_2(x)$ as determined by these relations we can write for the general solution of Eq. (3):

$$\psi(x) = c_1(x)e^{+i2\pi\alpha(x)x} + c_2(x)e^{-i2\pi\alpha(x)x}. \quad (10)$$

It can easily be verified[1] directly that this function satisfies Eq. (3). In order completely to specify the solution (10) we must subject the functions $c_1(x)$ and $c_2(x)$ to some initial or boundary conditions. It is for this reason that we have introduced Eqs. (2). If we make $c_1(\xi_1)=1$, $c_2(\xi_1)=0$, then Eqs. (9) show that c_1 and c_2 retain these values[2] for all larger values of x, and also that c_1 and c_2 are both constant for $x \leqq \xi_0$, so that we can interpret the problem by saying that a beam of electrons of density $|c_1(\xi_0)|^2$ impinges on the force field from the left, a beam of density $|c_2(\xi_0)|^2$ is reflected, and a beam of unit density is transmitted. The reflection coefficient for the lattice is hence $|c_2(\xi_0)|^2/|c_1(\xi_0)|^2$.

Let us calculate the current at any point in the lattice. For $d\psi/dx$ we get, by using Eq. (9)

$$(d\psi/dx) = i2\pi\alpha(x)[c_1(x)e^{+i2\pi\alpha(x)x} - c_2(x)e^{-i2\pi\alpha(x)x}], \quad (11)$$

and for the current[2a]

$$\left.\begin{aligned} I &= (h/4\pi mi)(\psi^* d\psi/dx - \psi d\psi^*/dx) \\ &= [h\alpha(x)/m][|c_1(x)|^2 - |c_2(x)|^2] = \text{constant}. \end{aligned}\right\} \quad (12)$$

Here $h\alpha(x)/m$ is just the classical velocity which an electron would have at the point x. Since this expression is in the form

$$\text{current} = \text{density} \times \text{velocity}$$

[1] Use of Eq. (11) will simplify the work.

[2] As by Eq. (2), $d\alpha/dx=0$ when $x>\xi_1$ or $x<\xi_0$. If $(d\alpha/dx)_{x=\xi_1}\neq 0$ we can choose a point just to the right of ξ_1 for which $d\alpha/dx$ will be zero. This point ξ_0 can be treated similarly.

[2a] These results were given in a previous note. E. L. Hill, Phys. Rev. 38, 1258 (1931).

it seems very reasonable to conclude that the solution (10) can be interpreted as representing two beams of electrons, one of density $|c_1(x)|^2$ moving to the right, the other of density $|c_2(x)|^2$ moving to the left, each beam, however, having the *classical* velocity appropriate to that point.

This result is foreshadowed by Eq. (11) which shows that the application of the momentum operator

$$p_x = (h/2\pi i)d/dx$$

to ψ, makes $h\alpha(x)$ appear formally like a proper value of p_x, having the proper sign for each of the beams.

This argument makes it very plausible indeed that it is legitimate to think of an electron with a given energy as having a definite velocity at a given point; i.e., the classical velocity, but that the direction of motion is incompletely specified. The average drift of electrons is just sufficient to account for the correct current. The uncertainty in momentum becomes an uncertainty in direction, but not in absolute magnitude. This is all on condition, however, that one confine himself to electrons having one given energy; if one considers electrons in different energy regions, then the resultant solution would contain electrons having different velocities, but for the electrons in each energy state the magnitude of the momentum would have just the classical value.

These two beams, however, cannot be considered as representing *independent* or *alternative* states for the electrons, for in the first place neither of the two terms in Eq. (10) is a solution of Eq. (3) when taken separately, and further, Eqs. (11) and (12) are true only when both terms are included in (10); e.g.,

$$p_x[c_1e^{i2\pi\alpha x}] \neq h\alpha[c_1e^{i2\pi\alpha x}].$$

This simply means that the resolution into beams is not analogous to the resolution of a general ψ-function into a set of mutually orthogonal proper functions. The physical reason for this is obvious: under the influence of the force field the electron can, and in general must, transfer from one beam to the other. However, if one treats the force field as a small perturbation, the electrons being practically free, then in the zeroth order calculation the two directions of motion do represent independent states, between which transitions occur under the influence of the field. This type of treatment has been considered by Brillouin[3] in his theory of metallic conduction. In the general case the two states are so tightly coupled that the idea of a *rate* of transition between them becomes evanescent.

It is to be particularly emphasized here that there is no question of a "measurement" of the velocity or position of an electron involved in this reasoning, just as there is no real question of a physical measurement in any of the purely mathematical treatments of the uncertainty principle; e.g., as in Weyl, "Gruppentheorie und Quantenmechanik," 1st edition, p. 67. To the writer it seems fairly clear that derivations of this nature are logically not

[3] L. Brillouin, Jour. de Physique (7) 1, 377 (1930).

related in any simple way, if indeed they are related at all, to arguments based on γ-ray microscopes and the like. The one is valid for isolated systems while the other depends upon interactions between systems, and although one may choose to say that an isolated system is a meaningless concept, yet there can be little question of the necessity of the concept for the purposes of general theoretical development.

We have explicitly limited ourselves to electron energies for which $E \geqq V(x)$. For regions in which $E < V(x)$ there is no reason to suppose that Eqs. (9) and (10) do not still hold formally. Since $\alpha(x)$ is a pure imaginary number, Eq (11) becomes

$$d\psi/dx = -2\pi|\alpha|\left[c_1(x)e^{-2\pi|\alpha|x} - c_2(x)e^{+2\pi|\alpha|x}\right] \tag{11'}$$

and Eq (12) changes to

$$I = i(h|\alpha|/m)[c_1c_2^* - c_1^*c_2]. \tag{12'}$$

Our interpretation is thus no longer valid unless we consider the imaginary part of $c_1c_2^*$ as a sort of density, but there seems to be no apparent meaning to this. Rojansky[4] has shown that one can formally still make the separation into two beams moving with the velocity $h|\alpha|/m$, but the densities of these beams are not governed by Eq. (9) through the whole range of the variable x.

This constitutes the essence of the physical argument of this note. In the remaining section we shall make some remarks about the generalization to three dimensions, but since the writer has not been able to give the complete solution of the problem for this more complicated case, these remarks must be regarded as being tentative. We shall restrict ourselves to energies for which the total energy is always greater than the potential energy.

Three Dimensional Case

The physical situation is here quite similar to the case of one dimension except that the degree of liberty for the direction of motion of the electron is infinitely greater, since an electron moving originally in a given direction can be reflected not only in the reverse direction, but also in any other direction.

On the basis of our physical idea that the velocity of an electron with definite energy has the classical value, we expect that at any point in coordinate space (x, y, z) designated by the position vector $\boldsymbol{r}$, we can write

$$\psi(\boldsymbol{r}) = \int_0^{2\pi} d\mu \int_0^{\pi} \sin\sigma d\sigma \left\{c(\sigma, \mu; \boldsymbol{r})e^{+i2\pi\alpha(\boldsymbol{r})\boldsymbol{n}\cdot\boldsymbol{r}}\right\} \tag{13}$$

where

$$h\alpha(\boldsymbol{r}) = [2m(E - V(\boldsymbol{r}))]^{1/2}$$

is the magnitude of the classical momentum, and $\boldsymbol{n}$ is an unit vector specifying the direction of the momentum, defined by the angles σ and μ in an ob-

[4] V. Rojansky and W. Wetzel, Phys. Rev. 38, 1979 (1931).

vious manner. The quantity $|c(\sigma, \mu; \boldsymbol{r})|^2$ should then represent the number of electrons, at $\boldsymbol{r}$ moving in the direction of $\boldsymbol{n}$, per unit solid angle.

It is not easy to give a proof that the general solution of Schrödinger's equation (for a given energy E) can be put in the form (13), as we were able to do directly in one dimension. Assuming the correctness of the physical view of the problem it seems very plausible. A still stronger, although qualitative argument, can be made by examining Whittaker's proof[5] of the fact that the general solution of the equation

$$\nabla^2\Phi + \Phi = 0$$

can be represented by a superposition of plane waves of type similar to (13). If we imagine the function $\alpha(x, y, z)$ to be replaced by a three dimensional step-function in which α is constant over certain regions, then for each region Schrödinger's equation can be put in this form, and the general solution can be written in the form (13) with the appropriate value of α. On shrinking the size of the regions, just as we did in the one dimensional case we should expect to get a formula like (13). We are prevented from carrying out the process in detail because of the complexity of the boundary conditions in three dimensions.

We can make a reasonable guess at the equation for $c(\sigma, \mu; \boldsymbol{r})$ by writing down the three dimensional generalization of Eqs. (9); i.e.,[6]

$$\text{grad}\left[c(\sigma, \mu; \boldsymbol{r})e^{+i2\pi\alpha(\boldsymbol{r})\boldsymbol{n}\cdot\boldsymbol{r}}\right] = \boldsymbol{n}i2\pi\alpha(\boldsymbol{r})c(\sigma, \mu; \boldsymbol{r})e^{+i2\pi\alpha(\boldsymbol{r})\boldsymbol{n}\cdot\boldsymbol{r}}$$
$$-(3/4\pi\alpha)\,\text{grad}\,\alpha\left[\boldsymbol{n}\cdot\int_0^{2\pi}d\mu'\int_0^{\pi}\sin\sigma' d\sigma'\left\{\boldsymbol{n}'c(\sigma', \mu'; \boldsymbol{r})e^{+i2\pi\alpha(\boldsymbol{r})\boldsymbol{n}'\cdot\boldsymbol{r}}\right\}\right]. \quad (15)$$

It can readily be verified that

$$\text{grad}\,\psi(\boldsymbol{r}) = i2\pi\alpha(\boldsymbol{r})\int_0^{2\pi}d\mu\int_0^{\pi}\sin\sigma d\sigma\left\{\boldsymbol{n}c(\sigma, \mu; \boldsymbol{r})e^{i2\pi\alpha(\boldsymbol{r})\boldsymbol{n}\cdot\boldsymbol{r}}\right\} \quad (16)$$

which is the expected generalization of Eq. (11), and that ψ, as given by Eq. (13), formally satisfies Schrödinger's equation.

The writer has, however, not succeeded in giving a satisfactory proof that the current is given by the formula

$$I = (h\alpha(\boldsymbol{r})/m)\int_0^{2\pi}d\mu\int_0^{\pi}\sin\sigma d\sigma\,|\,c(\sigma, \mu; \boldsymbol{r})\,|^2\boldsymbol{n}$$

which is the generalization of Eq. (12), and is required by our physical interpretation. The trouble seems to lie in the continuity for the range of direc-

[5] E. T. Whittaker, Mathematische Annalen 57, 333 (1903). Whittaker and Watson, "Modern Analysis,. Cambridge Univ. Press, Chapter 18.

[6] The factor $3/4\pi$ arises from the theorem that for any constant vector Γ

$$\int_0^{2\pi}d\mu\int_0^{\pi}\boldsymbol{n}\sin\sigma d\sigma\{\boldsymbol{n}\cdot\Gamma\} = \frac{4\pi}{3}\Gamma.$$

This is used in the proof that (13) satisfies Schrödinger's equation.

tions of the momentum which causes nearby directions to be related, in the sense of all continuous spectrum problems. One can make some progress towards the desired end by introducing delta functions for the sharp definition of a particular direction of motion, but the passage to the limit of a continuous distribution of directions then appears to be quite artificial. On the other hand, it may be that Eq. (15) is not the proper generalization of Eq. (9).

Added in Proof: Further consideration shows that while Eq. (10) yields a representation of the *momentum*, one must not attempt to apply it too generally to other quantities. One can correctly calculate the average value of p and the standard deviation of p by considering the two beams as independent. The first of these can be calculated from the current and the second by using Eqs. (10) and (11) for the calculation of c_1 and c_2

$$c_1 e^{i2\pi\alpha x} = \tfrac{1}{2}[\psi + (1/i2\pi\alpha)(d\psi/dx)]; \quad c_2 e^{-i2\pi\alpha x} = \tfrac{1}{2}[\psi - (1/i2\pi\alpha)(d\psi/dx)]$$

from which one obtains, for a closed system

$$(\Delta p)^2 = \int h^2\alpha^2[|c_1|^2 + |c_2|^2]dx.$$

This makes it clear that the existence of a mathematical uncertainty principle follows at once from the lack of knowledge of the phases of the motion, and not *primarily* because of any difficulty in the specification of the position or velocity of the electron. One must not, however, overlook the fact that the two "momentum beams" are really not independent: for some questions the interference between the two beams is of importance. The analogy with the classical motion in which the initial conditions are unspecified is thus incomplete; the wave equation contains more than an indeterminacy in the phases of motion.

ELECTRONIC TRANSITIONS BETWEEN AN INNER SHELL AND THE VIRTUAL OUTER SHELLS OF THE IONS OF THE RARE EARTHS IN CRYSTALS

By Simon Freed*

The Physical Laboratory of the University, Leyden, Holland

(Received September 18, 1931)

Abstract

In the rare earths, the inner $4f$ shell is incomplete and its electrons are much less stable than those in the outer complete $5s$ and $5p$ electronic shells. The rare earths possess sharp absorption lines which are ascribed to initial and final quantum states arising from different orientations of the spin and orbital moments of the electrons within the $4f$ shell. Ce^{+++} has only one electron in this shell giving rise to only one term ^2F, a doublet, with an interval of about 1000 cm^{-1}. Absorption in the ultraviolet must correspond, then, to a transition from the $4f$ shell to virtual outer shells such as $5d$ or $6s$, or to the lattice. The ultraviolet absorption spectra were taken of single crystals of hydrated cerium chloride and cerium ethylsulfate at room temperatures, at that of liquid nitrogen, and of liquid hydrogen. The crystals varied in thickness from about 0.2 mm to 3 mm, about the same thickness as has been employed in studying the line spectra of other rare earths. Aside from the very faint diffuse band at about 3020A found in one of the chloride crystals and which doubtless exists in the ethylsulfate also, the crystals were completely transparent from the visible to about 2700A and there, absorption set in and occupied the rest of the ultraviolet (to 2000A). To discover whether this continuum was caused by the overlapping of several regions of selective absorption, the cerium ions were diluted in the isomorphous lanthanum crystals which are transparent and possess practically the same electric fields as the cerium crystals. The ratio of Ce^{+++} to La^{+++} in the solution from which the crystals were grown varied from about 1 to 10 to about 1 to 5000. Three new diffuse bands were discovered which remained structureless even at great dilution and at the temperature of liquid hydrogen. The bands were recognized as transitions from a rather sharp inner quantum state ^2F (the electron in the $4f$ shell) to a diffuse outer quantum state ^2D (the electron in the virtual $5d$ shell). The electron of the activated Ce^{+++} is subject to enormous inhomogeneous electric fields because it is very close to the water molecules (and the negative ions) in the lattice. The ^2D term is decomposed by these fields into sublevels of wide separation which are extremely sensitive to all the variations in electric fields. The substitution of one negative ion for another or a change in the fields accompanying thermal contraction displaces the bands in some instances by a hundred times as much as the lines of Gd^{+++} are displaced under similar conditions. Whence, we return to the conclusion that the *lines* of the rare earths in general are associated with inner quantum states. It was predicated that transitions from the $4f$ electron to the outer shells would occur in other rare earths Pr^{+++}, Nd^{+++} etc., but the bands would begin further in the ultraviolet than they do in Ce^{+++}. A band extending from 2280A to 2100A was found in undiluted neodymium chloride which also remained without structure at the temperature of liquid hydrogen. Pr^{+++} exhibited no absorption band within the range of the spectrograph although the existence of one beginning at about 2100A would not have been determined. It is expected that the first band of Pr^{+++} begins somewhere in this region. The breadth of the bands has been discussed.

* Fellow of the John Simon Guggenheim Memorial Foundation.

IT HAS been proved[1] that the electronic configurations of the rare earths in crystals are the following:

Ionic number*	Ion	Basic term	$1s$, to $4d$	$4f$	$5s$, $5p$
54	La^{+++}	^1S	full	0	full
55	Ce^{+++}	^2F	"	1	"
56	Pr^{+++}	^3H	"	2	"
57	Nd^{+++}	^4J	"	3	"
68	Lu^{+++}	^1S	"	14	"

* Ionic number is the atomic number less three.

The energy required to liberate an electron in the $5s$ shell from these ions is about 45 volts and to liberate an electron in the $5p$ shell about 34 volts.[2] However, an extrapolation is necessary to learn the ionizing energies for the electrons in the $4f$ shell. The $4f$ shell becomes less stable than the $5s$ shell at about atomic number 85 and less stable than the $5p$ shell at atomic number 79 and it remains so for all lower atomic numbers. It appears that the energy of the electron in the $4f$ shell of the rare earths may correspond to radiation in the ultraviolet. It would presumably be the least in Ce^{+++} because the effective nuclear charge is probably the least here.

The extraordinary sharpness of the absorption lines of the rare earths in crystals has been ascribed to stationary states arising from the electrons within the inner ($4f$) shell. The different states owe their origin to the different orientations of the orbital and spin moments of the electrons in this shell. Because of the enormous positive charge acting on these internal electrons, they are doubtless close to the nucleus and rather distant from the fluctuating perturbations of the oscillating molecules and ions. In addition the completely filled $5s$ and $5p$ shells serve as screens against these perturbations. Ce^{+++} has but one electron in the $4f$ shell and it can give rise to but one basic term.[3] Any absorption in the ultraviolet must imply a transition of the $4f$ electron to outer electronic shells such as $5d$,—, $6s$ etc. The possibility is open, of course, that the electron may end in the closely spaced quantum states which are equivalent to ionization in the lattice.

The absorption lines of most of the rare earths are diffuse at room temperature but they sharpen remarkably at lower temperatures. As a rule they are

[1] Hund, Linienspektren, Springer, Berlin (1927).

[2] The actual values differ little from one ion to another. Those given here apply to Nd^{+++} and were read from the Bohr-Coster diagram. See, for example, Ruark and Urey, Atoms, Molecules and Quanta, p. 253, McGraw-Hill, New York (1930).

[3] The basic term is ^2F, a doublet, with an interval of about 1000 cm^{-1} as calculated from Sommerfeld's formula for relativity doublets. These levels are further decomposed by the inhomogeneous electric fields of the surrounding molecules and ions. The magnitude of the electrical separation cannot be as much as several hundred cm^{-1} when the positive ions are surrounded with H_2O dipoles since the magnetic susceptibilities of these ions are almost the same as Hund calculated for the gaseous ions. If the separations reached any such order of magnitude, deviations from Curie's law would have been serious at room temperature. Kramers Proc. Acad. Amsterdam **32**, 1176 (1929).

fine at the temperature of liquid nitrogen. The total intensity of the diffuse lines seems to be concentrated within a very narrow range so that the lines are easy to observe. As a precaution, the temperature was reduced even further to that of liquid hydrogen where the intensification progresses still further.

The apparatus employed was a quartz Dewar tube furnished with four plane quartz windows. The single crystals were always immersed in the refrigerating liquid and were held in a metallic strip fastened to a tube of German silver which could be raised and lowered. In this way any one of several crystals could be placed in the path of the light. The source of continuous radiation in the ultraviolet was a hydrogen discharge tube similar to the type recommended by Bay and Steiner.[4] It was constructed of Pyrex glass and permitted the continuous use of more than 500 milliamperes. An E_2 spectrograph from Hilger was employed through the kindness of Professor Blanksma of the Organic Chemical Laboratory of this university. It contained one quartz prism and had a dispersion of about 5A per mm at 2500A.

Crystals of the following salts were investigated: cerium chloride, cerium ethylsulfate, cerium acetate, praseodymium chloride, neodymium chloride, lanthanum chloride. All contained water molecules of crystallization. The cerium salts were recrystallized many times; the chloride from absolute alcohol. The cerium chloride was obtained as the hydrated chloride "pur" from the Societé des Produits Chimiques des Terres Rares. The ethylsulfate of cerium and the acetate were made from a hydrated nitrate "reinst" of the Auer Gesellschaft. *All* the chemical operations and crystallizations were carried out at practically room temperatures to avoid oxidation. The oxidation of cerium, observed by the yellowing of the solution, sets in rapidly if the solution is boiled in air, but this reaction does not occur in alcohol. (It was later found reported that the oxidized cerium salt reverts easily in the presence of alcohol to the form desired for this work.)[5]

Thereafter, all crystallizations were performed at room temperature from solutions containing considerable concentration alcohol. The crystals were grown by the slow evaporation of a saturated solution in a dessicator containing calcium chloride.

The crystals of the three cerium salts varying in thickness from about 0.2 mm to 3 mm showed similar absorption spectra at all temperatures. They were completely transparent from the visible region of the spectrum to about 2700A and then absorption began rather abruptly and occupied the rest of the ultraviolet region (until about 2000A, the limit of transparency of the quartz spectrograph). The absorption edge moved toward the red with increasing thickness of crystal.

It was inferred at this stage of the work that the continuum corresponded to an ionization of the ion, a transition of the electron immediately to the lattice rather than to an outer shell such as $5d$, . . . , or $6s$ etc. Transition to the latter would presumably have resulted in broad lines or bands since the

[4] Bay and Steiner, Zeits. f. Physik 45, 337 (1927).

[5] Treadwell-Hall, Analytical Chemistry, p. 471, Vol. I, New York (1916).

outer shells are susceptible to the oscillating electric fields of the water molecules. (Additional broadening influences will be discussed later.)

It was of course necessary to establish that the absorption was not due to the negative ions. For this purpose salts of other rare earths containing the same negative ions were examined so as to be entirely assured that the fields emanating from the positive ion, that is, the fields associated with the size and charge of Ce^{+++} could not displace the "natural" obsorption of the negative ions into the observed spectral region. (It is hardly necessary to remark that the ionic radii of the rare earths are almost identical, the well-known difficulty of separating them attests to the minutest differences.)

Lanthanum *chloride* was found to be completely transparent throughout the entire spectral range. This behaviour was expected since the chloride ion is known to be transparent here and lanthanum with no electrons in the $4f$ shell would require for the disruption of the completed shell many times the energy available in the shortest wave-lengths. Apart from a line spectrum, praseodymium *acetate* was also found to be transparent down to the shortest measurable wave-lengths. Dysprosium *ethyl sulfate* behaved similarly.

It was still possible that the unbroken continuum was really the superposition of several absorption bands either because of an interaction of neighboring cerium ions or because of an enormous intrinsic absorption of these ions. The consequences of both these influences could be obviated by separating the Ce^{+++} in the crystal lattice and by keeping the thickness of the resulting crystal about the same as in the previous experiments. The cerium ions were separated from each other by making mixed crystals of the cerium salts with the same lanthanum salts, the cerium comprising but a small fraction of the total. Mixed crytals of cerium and lanthanum chlorides and of cerium and lanthanum ethyl sulfates were investigated. La^{+++} was selected for the dilution because of its complete transparency. Mixed crystals of the La^{+++} and Ce^{+++} salts can be made in all proportions because the radii of these ions are almost identical. In the ethylsulfates and in the chlorides, both the Ce^{+++} ions and La^{+++} ions are immediately surrounded, with the same number of water molcules probably as $La(H_2O)_6^{+++}$, $Ce(H_2O)_6^{+++}$ and the fractional differences in the radii of these increased ions is even less than in the unhydrated ions. In addition the slight difference between the action of one cerium upon another and that of a lanthanum ion upon a cerium ion is lessened by the negative ions between them in the crystal lattice.[6]

Crystals prepared from a *solution containing* about ten times as much lanthanum chloride as cerium chloride exhibited a new faint diffuse absorption band with a maximum at about 3025A at room temperature and the continuum occurred in approximately the same region as before. This ab-

[6] The research of J. Becquerel (Gedenkboek H. Kammerling Onnes (1922)) shows that many absorption lines of the rare earths are sharp even in complicated mixtures such as minerals. The substitution of Br^- for Cl^- in $GdCl_3\,6H_2O$ (Freed and Spedding, Jour. Am. Chem. Soc. **52**, 3747 (1930)) shifted the absorption lines of Gd^{+++} on an average by about $4cm^{-1}$. The substitution of La $(H_2O)_6^{+++}$ for Gd $(H_2O)_6^{+++}$ would doubtless produce so small a displacement that it would be scarcely measurable with the quartz spectograph employed in this work.

sorption was never observed in crystals containing Ce^{+++} in smaller concentration such as are about to be discussed.[7] These crystals varied in thickness from about 0.3 mm to 2 mm. When the concentration of cerium in solution was about two percent of that of lanthanum, the continuum previously noted decomposed into three diffuse bands which remained as diffuse at the temperature of liquid hydrogen as at room temperature. The corresponding ethylsulfates showed similar absorption spectra. When the Ce^{+++} in solution was diluted further, about one hundred fold relative to the La^{+++}, the same absorption bands persisted, became fainter and narrower but showed no structure either to the eye or to a microphotometer. Lowering the temperature to that of liquid hydrogen did not perceptibly alter the diffuseness of the bands. (See Table I.)

TABLE I. *Data of mixed crystal of lanthanum and cerium ethylsulfate and mixed crystal of lanthanum and cerium chloide.*

Temperature	Number of band	$La^{+++}(Ce)^{+++}(C_2H_5SO_4)_3 \cdot 9H_2O$ Center of band	*Width of band A	$La^{+++}(Ce)^{+++}Cl_3 \cdot 6H_2O$ Center of band A	Width of band
	I			3020	
Room	II	2565	110	2575	50
	III	2380	100	2455	50
	IV	2200	50	2300	very wide
	II	2550	80		
Liquid nitrogen	III	2370	60		
	IV	2230	60		
Liquid nitrogen	II	2540	115	2540	80
	III	2365	90	2440	65
	IV	2245	very wide	2300	45

* The width of the band is only of qualitative significance since it varies with the time of exposure, especially in the wider bands.

Different crystals gave roughly the same maxima within 10A for the narrow bands and 15A for the wider ones. This is about the reproducibility with which the maxima of any single bands are known.

The same crystal of the ethylsulfate was employed at the three temperatures. It was grown from a solution containing about fifty times as much lanthanum as cerium.

The same crystal of the chloride was also employed at the two temperatures but it is possible that at room temperatures there was some moisture on the faces of the crystal. The chlorides differ from the ethylsulfates in being very hygroscopic.

The diffuseness of the bands, the magnitude of their separations the great displacement in their positions when one negative ion is substituted for another or when the temperature is reduced, confirm the expectations that the absorption represents a transition from the 4*f* shell to virtual outer shells of the ion. There is no escape from this interpretation if the final quantum

[7] After this research was finished, this band was recognized faintly in the spectrum of a crystal of cerium chloride undiluted with lanthanum.

states are to be identified with the positive ion. The diffuseness of the bands may be attributed to the outer quantum state or states. (I shall refer to an "outer quantum state" when I mean the quantum state of the ion if the electron is in an outer shell.) The latter is exposed to all the perturbations of the neighbors of the positive ion and to all the oscillations that the neighbors experience. In addition, the unordered electric fields resulting from the strains

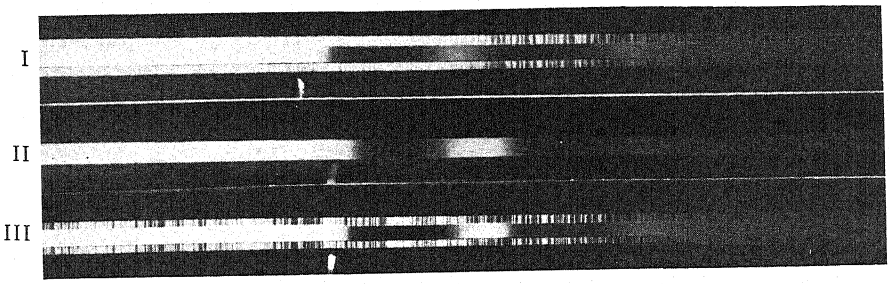


Fig. 1. Mixed crystal of lanthanum and cerium ethylsulfate. I. Room temperature, II. Temperature of liquid nitrogen, III. Temperature of liquid hydrogen.

in the crystal exercise a broadening on these sensitive levels. Even more important in this connection, the electronic levels probably couple with the oscillational levels of the water molecules of the crystal lattice in a way such as has already been anticipated.[8,9] On the other hand, the inner quantum state, the basic state, is relatively free from these oscillating perturbations. The coupling between the electronic motion in the $4f$ shell and the oscilla-

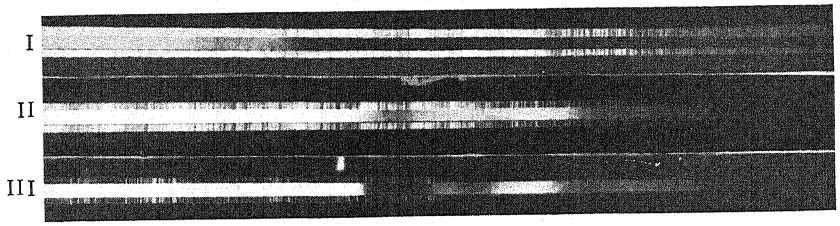


Fig. 2. Mixed crystal of lanthanum and cerium chloride. I. Room temperature: crystal grown from solution containing about ten times as much lanthanum as cerium. II. Room temperature: crystal grown from solution containing about 200 times as much lanthanum as cerium. III. Temperature of liquid hydrogen: crystal containing same concentration as II.

tional motion of the lattice is weak and judging by the sharpness of the absorption lines of the other rare earths such as Nd^{+++}, Gd^{+++}, Dy^{+++} etc., we would estimate the energy of the coupling to be less than the width of a rather sharp absorption line. The energy of this coupling must fall off rapidly with distance.

The H_2O molecules may be fairly well represented as dipoles in their action upon the relatively distant $4f$ electron. However, the proximity of the

[8] Ehrenfest, Gedenboek, H. Kammerling Onnes (1922).
[9] Frenkel, Phys. Rev. **37**, 17 and 1276 (1931).

H_2O groups to the outer electron of the activated Ce^{+++} brings into play their detailed electronic structures with their stupendous inhomogeneous electric fields. The influence of the negative ions also becomes more intense. We find that an alteration in the dipole attending the substitution of one negative ion for another displaces the bands of the Ce^{+++} by as much as 1000 cm^{-1} whereas a similar substitution displaces the lines of Gd^{+++} by less than 10 cm^{-1}. The contraction of the crystal, induced by lowering the temperature, with the resulting change in the electric fields, also effects a disproportionate readjustment of the inner and outer shells. In Gd^{+++} where both the basic and the activated states are in all probability inner states an absorption lines shifts about 6 cm^{-1} when the temperature is reduced from room temperature to that of liquid hydrogen.[10] Under like conditions we find a displacement in Ce^{+++} of from 200 cm^{-1} to 500 cm^{-1}. There is no reason for believing that transitions to outer shells are restricted entirely to Ce^{+++}. We should expect

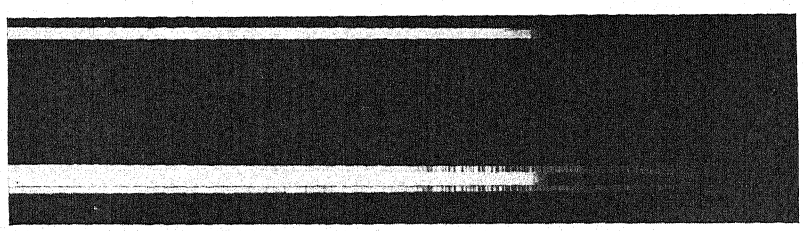


Fig. 3. Absorption spectrum of Nd^{+++} in $NdCl_3 \cdot 6H_2O$ at 20°K. Band begins at about 2280A and ends at about 2100A, (very faint).

Pr^{+++}, Nd^{+++} etc. to have similar bands in their absorption spectra. Pr^{+++} and Nd^{+++} with higher nuclear charges than Ce^{+++} probably hold the $4f$ electrons more strongly and require more energy for analogous transitions. (Such is the ordinary progression in gases also.) Hence we should expect to find their bands further in the ultraviolet region of the spectrum. No bands were found in a hydrated crystal of praseodymium chloride which Professor Urbain had kindly purified for the Cryogenic Laboratory. Nd^{+++} ("Reinst" Auer Gesellschaft) definitely possessed such a band in our extreme ultraviolet. The band of the hydrated neodymium chloride extended from 2280A to 2100A and showed no structure even at the temperature of liquid hydrogen. It is probable that Pr^{+++} can be similarly activated but its first band lies just out of range of the quartz spectrograph. A faint band near 2100A would not have been detected for the general intensity of the radiation was feeble in this region.

It was surprising to observe so little contraction in the bands at the temperature of liquid hydrogen. The breadth of the bands which can be related to thermal oscillations (namely, the variation in the external electric fields and the coupling with the oscillations themselves) are doubtless greatly reduced. However, the low temperature would be accompanied by an in-

[10] Freed and Spedding, Phys. Rev. **34**, 945 (1929).

crease in the number and in the intensity of the strains and their "surface" fields would undo the normal effects of reduced temperatures.[11]

We have mentioned[3] that the separation between the levels of the basic doublet ^2F is expected to be about 1000 cm^{-1}. Corresponding to this difference in energy about 5 percent of the total Ce^{+++} ions would be activated and in the upper level at room temperature. At the temperature of liquid hydrogen, only one Ce^{+++} ion out of 10,000,000 would be activated. Transitions beginning at this activated level would produce faint bands at room temperature and they would disappear at the temperature of liquid hydrogen. Since there is little change in the relative intensities of the bands, we must accept that practically all the Ce^{+++} occupy the basic level or levels so close together that they behave as one relative to the width of the bands.[12] This statement, while almost certainly true, is not necessary for the conclusion that the electron occupies the 5*d* shell. It is sufficient and it makes the discussion more direct. The necessary condition is that the Ce^{+++} ions in these dilute crystals are not present in appreciable amounts at the temperature of liquid hydrogen in more than three levels 2500 cm^{-1} or more apart. There is no question but that this condition is rigorously fulfilled.

If we look at the electronic configurations of the metals of the rare earths, we observe that one 5*d* electron and two 6*s* electrons had been removed in the process of ionization. The 5*f* shell does not become a stable shell for an electron until the atomic number 90 (thorium) is reached and no atom has an electron in the 5*g* shell. We shall try to decide between the 5*d* shell and the 6*s* shell as the final state of the electron. The former would give rise to a ^2D term and the latter to a ^2S term. It is known[13,14] that *S* terms are not decomposed by electric fields (or as Kramers points out, only to a degree of several cm^{-1}) and since they are single, a transition to the 6*s* shell from the basic level could account for only one band. However at least four bands exist and hence we must conclude that the electrons of many cerium ions end in the 5*d* shell. The final state is then $^2D_{3/2,5/2}$ decomposed further by the electric fields of the lattice. On grounds of symmetry Bethe[13] has concluded that a $D_{3/2}$ term is decomposed into three terms in a hexagonal crystal (ethyl sulfate) and in tetragonal crystals and into at least as many in crystals of lower symmetry. (The chloride is probably monoclinic.) The $D_{5/2}$ term will be decomposed into more than three.

[11] These strains are only feebly effective in broadening the lines associated with inner quantum states. Er^{+++} with an ionic number of 66 exhibits very broad and diffuse bands at room temperature which undergo a striking refinement into sharp lines at lower temperatures such as that of liquid nitrogen (Freed and Spedding Nature, **123,** 525 (1929)).

[12] Possibly, the faint band observed at room temperature in some crystals of the chloride, originates at this activated level. The intensities referred to have been shown by the same crystal of the ethylsulfate at the three temperatures. Here we can see little difference in the relative intensities. In the chloride, band II has apparently gained somewhat in intensity at the expense of band III at the temperature of liquid hydrogen. The chlorides, however, are very hygroscopic. At room temperature, there was possibly a little moisture on the faces of the crystal which would influence the absorption and hence make comparison of the intensities, invalid.

[13] Bethe, Ann. d. Physik **3,** 133 (1929).

[14] Kramers, Proc. Acad. Amsterdam **32,** 1176 (1929).

Transitions from the $2F$ term to $D_{3/2}$ and $D_{5/2}$ states would conserve the selection rules of $\Delta j = \pm 1$ and 0 and $\Delta l = \pm 1$ and such transitions would be highly probable. Only very high probabilities of transitions can accord with such enormous intensities in the absorption as have been found. Transitions to the $6s$ shell would introduce $\Delta j = 2$ and $\Delta l = 3$ which would be of much lower probability.[15] The high positive charge on Ce^{+++} would probably make the $5d$ electron more stable than the $6s$, $6p$ etc. electrons. (The concept of many virtual orbits in the crystals becomes more and more vague.) There are numerous examples in gases where a high nuclear charge stabilizes an inner shell. The best known are the iso-electronic gases K and Sc^{++} and their electronic configurations are

	$1s$ to $3p$	$3d$	$4s$
K	full		1
Sc^{++}	"	1	

In a recent letter to this review[16] Spedding advanced the hypothesis that the sharp absorption lines of the rare earths are due quite generally to transitions from the inner $4f$ shell to the outer shells $5d$, $-6s$, etc. He was led to this supposition because the transitions between the states arising within the $4f$ shell in Gd^{+++} must result in intercombination lines, that is in transitions between ^8S and ^6P, for example, intercombination lines occur frequently in the heavier gases free from perturbations and hence there is no reason to dismiss such possibilities in ions imbedded in a lattice where many influences are still unknown. It was observed that the intensity of the absorption bands in Ce^{+++} was much greater than in Nd^{+++} or Pr^{+++} since upon diluting Ce^{+++} with La^{+++} and Nd^{+++} with La^{+++} the bands of Ce^{+++} persisted long after the lines of Nd^{+++} had disappeared. The greater intensity confirms the view that the bands of Ce^{+++} arise from permitted transitions while most of the lines of Nd^{+++} are transitions of less probability, such as intercombination lines. The extreme sensitivity of the bands of Ce^{+++} to external conditions shows clearly that electrons close to the sources of perturbation are responsible for the absorption. In Gd^{+++} the initial and final states are either insensitive to the surrounding molecules or are almost equally sensitive to them. They must then have almost identical electron distributions and hence both the initial and final states of the absorption lines are due to electrons in the $4f$ shell.

I should like to express here my gratitude to Professor W. J. de Haas and to all in his laboratory for their kind hospitability.

[15] As Bethe observes, the presence of the electric fields introduces different quantum numbers and a selection principle applies to them. Nevertheless, the above discussion on transition probabilities is qualitatively valid since in the limit of feeble fields, the above considerations are approximated.

[16] Spedding, Phys. Rev. **37**, 777 (1931).

THE ABSORPTION SPECTRUM OF CHLORINE DIOXIDE*

HAROLD C. UREY AND HELEN JOHNSTON[1]
COLUMBIA UNIVERSITY

(Received October 5, 1931)

ABSTRACT

The wave-lengths of 134 absorption bands of ClO_2 have been measured with the Hilger E–1 and E–185 quartz instruments. The bands have been arranged in progressions and the energy levels deduced. Five vibrational levels of the normal electronic state have been found; the vibrational levels of the excited electronic state can be described with the use of two vibrational quantum numbers. Formulae for these bands and their isotope separations are given. The shapes of the molecule in the normal and excited electronic states have been calculated from Bjerrum's formulae for the vibrations assuming valency forces and all but one solution for each electronic state is excluded by the isotope effect or the intensity distribution of the bands. The central force formulae give no possible solutions. The normal modes of vibration for the molecule have been calculated. The intensity distribution is consistent with the extension of the Franck-Condon principle to polyatomic molecules. The predissociation limit agrees with a very approximate extrapolated value for the energy of dissociation through one mode of vibration of the excited electronic state into a ClO molecule and an O atom. Dissociation through a second mode of vibration of the excited electronic state gives only a very rough value. A discontinuity in the $\Delta E{:}v_2'$ curve noted by Goodeve and Stein appears at about the energy required for an oscillation of the molecule through a straight line position and it is proposed that this is the cause of the discontinuity.

OF THE various triatomic molecules whose electronic bands lie in the more accessible wave-length regions, chlorine dioxide seems to be one of the most promising molecules. It has an intense absorption spectrum lying between λλ 5225 to 2600A and because chlorine has two isotopes of comparable abundance, it is possible to study the isotope effect, giving another way of attacking the assignment of vibrational quantum numbers to its energy levels. This research was undertaken on this molecular spectrum in order to make use of this particular advantage.

The first attempt to classify the bands of ClO_2 was made by Käbitz.[2] Mayer[3] succeeded in arranging them into progressions. In both of these researches only about forty nine bands were considered. Goodeve and Stein[4] investigated the spectrum of ClO_2 and measured 138 bands, and found that many of the observed bands were isotopic bands. These bands were arranged

* Contribution No. 683 from the Department of Chemistry, Columbia University.

[1] The material in this paper is taken from the dissertation submitted by Helen Johnston in partial fulfillment of the requirements of the degree of Doctor of Philosophy, Columbia University, 1931.

[2] B. Käbitz, Diss. Bonn, 1905.

[3] H. Mayer, Zeits. f. physik. Chem. **113**, 220 (1924).

[4] C. F. Goodeven and C. P. Stein, Trans. Faraday; Soc. **25**, 738 (1929).

into 4 principal and 5 sub-"series." They also observed the phenomenon of predissociation, which they located at λ3293A. Very recently Finkelnburg and Schumacher[5] have published a paper on ClO_2. These experimentors have photographed the band heads with a two meter grating, but have not arranged the bands into progressions. They have also determined the limit of predissociation λ3753.28A.

Experimental

The chlorine dioxide was prepared by the reaction of oxalic acid and potassium chlorate as described by Bray.[6] The gas evolved was collected in a trap cooled with dry ice. This trap was connected directly to the absorption cell.

Since chlorine dioxide is decomposed rather rapidly by light, it was necessary to keep a stream of the gas flowing through the absorption cell during the time of exposure. To do this we connected a glass needle valve to an outlet tube of the absorption cell to regulate the rate of flow of the ClO_2 and evacuated the system protecting the pump with a liquid air trap. When this procedure was used, the trap containing the chlorine dioxide was cooled in dry ice or dry ice-alcohol mixtures in order to regulate the pressure of ClO_2. In some cases a stream of nitrogen was passed through the chlorine dioxide trap and then through the absorption cell and thus the cell was kept filled with undecomposed chlorine dioxide. The dry ice-alcohol bath provided a range of temperatures from -76°C to 10°C. The bath was easily regulated to within ± 0.5° by the addition of dry ice about every 15 or 20 minutes.

Three absorption cells were used in these experiments. The first cell was made of Pyrex with plane Pyrex windows. There were three compartments in this cell, the two end ones ten cm long being evacuated and sealed off. The middle compartment was 30 cm long. This construction was used so that the middle compartment containing the ClO_2 gas could be cooled in dry ice in order to sharpen the band heads and simplify the general band structure. This could only be used for the stronger bands. The second cell consisted of a Pyrex tube 60 cm long with quartz windows sealed on which de Khotinsky cement. (ClO_2 is said to explode when brought in contact with organic matter, but we had no such difficulty.) The third cell was an all quartz one of the same general design as the first described above.

As sources of light in the visible and near ultraviolet we used a tungsten filament lamp or a point-o-lite lamp. A Pfund iron arc was used as a reference source. This was mounted directly in front of the slit with the lower electrode remaining in place during the exposure of the absorption spectrum to insure its correct alignment during the exposure of the reference spectrum.

The Hilger E–1 Quartz Spectrograph was used for nearly all our measurements, only a small number being made with the Hilger E–185 three meter instrument.

[5] W. Finkelnburg and H. J. Schumacher, Zeits. f. physik. Chemie, Bodenstein-Festband, 704 (1931).

[6] W. Bray, Zeits. f. physik. Chemie 54, 575 (1906).

Experimental Results

We have measured 134 bands of ClO_2 between λλ5042 and 3226. The reproducibility of our measurements on different plates is about 0.7A or from 3 to 6 cm^{-1} depending on the wave-length range. Table I gives the wave numbers of all bands measured by us and the wave numbers given by Finkelnburg and Schumacher and by Goodeve and Stein. Goodeve and Stein say that their results could be duplicated to within a few wave numbers but that sometimes readings differed by as much as 10 cm^{-1}. In the far ultraviolet, they claimed not to be able to repeat within 15 cm^{-1}. Finkelnburg and Schumacher claim an accuracy of ± 0.05A in the visible and ± 0.5A in the far ultraviolet. We find that the measurements of the latter authors do not follow smooth formulae as well as ours and we do not feel certain that these band heads can be measured so precisely as they claim. The wave-lengths which we secured were reduced to vacuum by reducing the wave-lengths of the standard iron lines to vacuum and making the entire calculation with these standards. The wave-lengths were calculated by using the usual Hartmann formula.

Classification of Bands

Inspection of Goodeve and Stein's results immediately shows that it is impossible to derive a formula that will fit the isotope effect. A formula can be made to fit the isotope effect from the sixth member of their "sequence," but their classification up to this point must be incorrect or the isotope effect surprisingly irregular. Our arrangement of the bands into progressions differs in many details from that of Goodeve and Stein though the main features remain.

In discussing our arrangement, it is convenient to adopt the assignment of vibrational quantum numbers at this point and justify this selection later. We find it necessary to use three quantum numbers for the normal state, v_1'', v_2'' and v_3'', and two for the excited state, v_1' and v_2'. Transitions can be indicated by the symbol $(v_1', v_2') \leftarrow (v_1'', v_2'', v_3'')$, the arrow indicating the direction of the change in absorption.

Anticipating the final assignment of quantum numbers, the progression with the most intense bands is $(0, v_2') \leftarrow (0, 0, 0)$, $v_2' = 0$ to 30, the third most intense band system $(1, v_2') \leftarrow (0, 0, 0)$, $v_2' = 1$ to 17, the second $(0, v_2') \leftarrow (0, 0, 1)$, $v_2' = 4$ to 15, and the fourth $(1, v_2') \leftarrow (0, 0, 1)$, $v_2' = 0$ to 13. If the progression difference between progressions $(0, v_2') \leftarrow (0\ 0, 0)$ and $(0, v_2') \leftarrow (0, 0, 1)$ and between progressions $(1, v_2') \leftarrow (0, 0, 0)$ and $(1, v_2') \leftarrow (0, 0, 1)$ are taken it will be found that this difference is 528.8 cm^{-1}. It would thus appear that the first and third most intense progressions originate from the same unexcited level and go to different excited levels and the second and fourth in intensity come from a level with 528.8 cm^{-1} more energy and terminate on the same two sets of excited levels. If the differences between the bands having the same value of v_2' of the progressions $(0, v_2') \leftarrow (0, 0, 0)$ and $(1, v_2') \leftarrow (0, 0, 0)$ and of progressions $(0, v_2') \leftarrow (0, 0, 1)$ and $(1, v_2') \leftarrow (0. 0, 1)$ and of progressions $(1, v_2') \leftarrow (0, 0, 1)$ and $(2, v_2') \leftarrow (0, 0, 1)$ are taken it is found to be about 300

TABLE I.

U. & J. $\tilde{\nu}$ in cm^{-1} in vacuo	F. & S. $\tilde{\nu}$ in cm^{-1} in vacuo	G. & S. $\tilde{\nu}$ in cm^{-1} in air	U. & J. $\tilde{\nu}$ in cm^{-1} in vacuo	F. & S. $\tilde{\nu}$ in cm^{-1} in vacuo	G. & S. $\tilde{\nu}$ in cm^{-1} in air
	19134.1	19140	*23938.2		23944
	19424.4	19423	23959.1		23967
†	19625.4	19635	*24058.6		24062
19831.9	19841.7	19848	24078.2	24079.3	24084
†		19900	††24169.6		
20070.2		20079	24227.7	24228.3	24232
*20080.2	20081.5		†	24241.0	
20125.8	20130.4	20130	*24463.9		24471
†20185.3			24488.1	24488.4	24495
20332.7		20341	*24610.9		
20359.8		20368	24635.8	24636.8	24641
*20368.4	20369.9		24709.7		
20542.3		20548	*24732.2		24738
20569.4		20574	24757.2	24757.1	24763
*20574.2	20572.7		24899.1	24907.4	24904
20782.1	20778.8	20786			24986
*20785.9			25116.3		
20825.1		20835	*25132.8		25141
21014.2	21016.4	21023	25163.9	25164.2	25170
21064.6	21064.1	21070	25238.7		
21275.8	21276.2	21283	*25274.6		25284
21307.7	21305.4	21310	25307.0	25307.5	25313
21479.8	21480.4	21483	*25397.8		25397
*21716.8			25428.0	25428.0	25436
21724.8	21724.3	21733	*25536.9		25544
21760.6	21761.2	21769	25569.2	25571.4	25575
21842.2		21849			25656
21979.1		21980	25769.9		
22009.7	22010.3	22016	*25799.7		25810
22172.3	22173.7	22178	25834.2	25835.4	25843
†22369.4			25903.4		
22426.4	22425.4	22437	†25916.5		
22449.2	22450.2	22457	*25936.2		25948
22536.2	22537.0	22542	25972.1	25973.6	25979
22590.9	22598.7	22580	26029.9		
		22675	*26059.5		26065
*22703.2		22703	26094.4	26095.4	26107
22706.4	22706.3	22711	††26151.9		
*22860.6	22860.7	22856	26195.5		26208
22873.2	22875.0	22869	26230.7	26232.2	26242
†23029.2			26303.4	26310.6	26306
*23107.6		23116	*26459.4		
23120.5	23119.2	23124	26500.4	26504.9	26503
23140.5			26549.5		
23221.7		23225	*26591.4		
23280.5	23281.7	23277	26633.5	26635.8	26648
*23382.2		23391	26664.0		
23395.7	23395.8	23402	26686.5		
23548.6	23553.0	23556	*26715.5		
*23789.7		23796	26756.0	26757.4	26764
23806.3	23813.8	23812	*26843.5		26860
23902.0		23904	†26875.8		

* Isotopic bands.

† Unclassified bands.

‡ These are the two bands that agree approximately with the calculated values for transitions $(2, 6)\leftarrow(1, 0, 0)$ and $(2, 9)\leftarrow(1, 0, 0)$.

The Editors of the Physical Review suggest that the accuracy of our measurements probably does not justify the use of six significant figures. We fully agree with them but we retain the sixth significant figure because all of our tables and calculation would have to be revised if this figure were dropped. Also the precision of the isotopic separations probably warrants the retension of the fractional values.

TABLE I.—(*Continued*)

U. & J. $\tilde{\nu}$ in cm^{-1} in vacuo	F. & S. $\tilde{\nu}$ in cm^{-1} in vacuo	G. & S. $\tilde{\nu}$ in cm^{-1} in air	U. & J. $\tilde{\nu}$ in cm^{-1} in vacuo	F. & S. $\tilde{\nu}$ in cm^{-1} in vacuo	G. & S. $\tilde{\nu}$ in cm^{-1} in air
26887.0	26888.6	26900	†		29900
26963.8	26967.2	26971	*		29936
*27117.4			29980.9	29982.2	29996
27162.3		27163		30153	
*27240.2			*		30307
27288.6	27293.2	27302	30375.3	30380	30377
*27368.6		27377	*		30400
27412.9	27414.9	27424	30435.6		30477
*		27507	†		30529
†27525.0			†30570.9		
27536.6	27540.4	27550			30613
27625.2	27618.5	27623	*		30976
*27761.5		27772	30989.3	30996	31014
27815.7		27821	†		31142
†27829.7					31218
*27883.1			*		31539
27939.0	27946.7	27956		31601	31619
*		28021	†		31749
†28037.3					31847
28063.0	28065.1	28079		32190	32202
*		28148		32768	32779
28172.8	28186.0	28194		33330	33336
*28415.0		28424	*		33761
28470.7		28475		33848	33877
*28523.5			*		34238
28583.7	28590.2	28603		34346	34341
28704.5	28713.8	28724	*		34746
†28762.8				34841	34855
†28843.9		28840		35288	
29112.4		29114			35370
†29170.1				35805	35840
29223.8	29229.3	29236			36260
*		29304		36321	
29346.0	29351.8	29365			36700
*29685.1		29686			37106
29748.7		29745			37509
29843.0	29850.5	29858			37922

cm^{-1} if v_2' is small and that this difference decreases with increasing v_2'. With this procedure it was found necessary to postulate three upper sets of energy levels and two unexcited energy levels. This is essentially the scheme used by Goodeve and Stein.

The search for further vibration levels of the normal electronic state was then made by first plotting all bands not included in these progressions and then moving a scale having the differences of the $(0, v_2')$, $(1, v_2')$ and $(2, v_2')$ levels along this until agreement with the positions of the unclassified bands was secured. In this way evidence for five vibrational levels of the normal state was secured.

We have not been able to find convincing evidence for the third fundamental vibration frequency of the excited state. Those agreements we have found could be explained as due to chance coincidences.

The final arrangement of bands and combination differences are given in Tables II, III, and IV. The wave number differences are indicated by numbers placed between the columns and rows. The differences indicated by the

Δ's at the top of the columns are the differences between the column of wave numbers following a particular Δ and the first column of the table in each case. In this way the Δ's represent the wave number differences between the lowest lying level and the four higher vibrational levels of the normal state.

TABLE II.

(v_1', v_2')	(v_1'', v_2'', v_3'') (0, 0, 0)	Δ_1	(0, 0, 1)	Δ_2	(0, 1, 0)	Δ_3	(1, 0, 0)
0, 0	20332.7						
	681.5						
0, 1	21014.2						
	710.6						
0, 2	21724.8						
	701.6						
0, 3	22426.4						
	694.1						
0, 4	23120.5	529.6	22590.9				
	685.8		689.6				
0, 5	23806.3	525.8	23280.5				
	681.8		678.6				
0, 6	24488.1	529.0	23959.1				
	675.8		676.7				
0, 7	25163.9	528.1	24635.8				
	670.3		671.2				
0, 8	25834.2	527.2	25307.0	717.9	25116.3	855.2	24979.0*
	666.2		665.1		653.6		669.8
0, 9	26500.4	528.3	25972.1	730.5	25769.9	851.6	25648.8*
	661.9		661.4				654.6
0, 10	27162.3	528.8	26633.5			858.9	26303.4
	653.4		655.1				660.4
0, 11	27815.7	527.1	27288.6			841.9	26963.8
	655.0		650.4				661.4
0, 12	28470.7	531.7	27939.0			845.5	27625.2
	642.0		644.7				
0, 13	29112.7	529.0	28583.7				
	636.0		640.1				
0, 14	29748.7	524.9	29223.8				
	626.6		619.2				
0, 15	30375.3	532.3	29843.0				
	614.0						
0, 16	30989.3						
Ave.		528.5		724.2		850.6	

Some variation in these differences is present but no evidence of trends in values. The wave numbers marked with an asterisk are those of Goodeve and Stein corrected to vacuum.

The energy levels of the normal electronic state are spaced as follows above the lowest level:

(0, 0, 0)	0	cm^{-1}
(0, 0, 1)	528.8	"
(0, 1, 0)	727.0	"
(1, 0, 0)	857.7	"
(0, 2, 0)	1471.3	"

The last level is classified as the first harmonic of the 727.0 cm^{-1} level. It is greater than twice the value of the fundamental but this is quite common among polyatomic molecular levels. These values do not represent average

value of all the differences of Table II, III, and IV but only average values of our own measurements.

All but 21 bands have been assigned to progressions, of this number six were reported by Goodeve and Stein and one by Finkelnburg and Schu-

TABLE III.

(v_1'', v_2'', v_3'') (v_1', v_2')	(0, 0, 0)	Δ_1	(0, 0, 1)	Δ_2	(0, 1, 0)	Δ_3	(1, 0, 0)	Δ_4	(0, 2, 0)
1, 0			20070.2						19134.7*
			711.9						697.2
1, 1	21307.7	525.6	20782.1	738.3	20569.4			1475.8	19831.9
	702.0		697.7		706.4				710.4
1, 2	22009.7	529.9	21479.8	733.9	21275.8			1467.4	20542.9
	696.7		692.5		703.3				
1, 3	22706.4	534.1	22172.3	727.3	21979.1	864.2	21842.2		
	689.3		700.9		689.8		694.0		
1, 4	23395.7	522.5	22873.2	727.0	22688.7*	859.5	22536.2		
	682.5		675.4				685.5		
1, 5	24078.2	529.6	23548.6			856.5	23221.7		
	679.0		679.1				680.3		
1, 6	24757.2	529.5	24227.7			855.2	23902.0		
	670.8		671.4						
1, 7	25428.0	528.9	24899.1	718.3	24709.7				
	666.4		670.1						
1, 8	26094.4	525.2	25569.2			855.7	25238.7		
	661.6		661.5				664.7		
1, 9	26756.0	525.3	26230.7	726.1	26029.9	852.6	25903.4		
	656.9		656.3		656.5		646.1		
1, 10	27412.9	525.9	26887.0	726.4	26686.5	863.4	26549.5		
	650.1		649.6						
1, 11	28063.0	526.4	27536.6						
	641.5		636.2						
1, 12	28704.5	531.7	28172.8						
	638.5								
1, 13	29343.0								
	637.9								
1, 14	29980.9								
	Ave.	527.9		728.2		858.2		1471.6	

macher and have not been confirmed by the authors of this paper and fourteen were first reported by us. Two of the latter fourteen agree very approxi-

TABLE IV.

(v_1'', v_2'', v_3'') (v_1', v_2')	(0, 0, 1)	$\Delta_4 - \Delta_1$	(0, 2, 0)
2, 0	20359.8	942.2	19417.6*
	704.8		708.2
2, 1	21064.6	938.8	20125.8
	696.0		699.3
2, 2	21760.6	935.5	20825.1
	688.6		
2, 3	22449.2		
	691.3		
2, 4	23140.5		
Ave.		938.8	

mately with the calculated values using the formulae below for the transitions (2, 6)←(1, 0, 0) and (2, 9)←(1, 0, 0). These unclassified bands are denoted by a dagger in Table I.

TABLE V.

$(v_1'', v_2'', v_3'') \rightarrow$ v_2'	$(0,0,0)$ $v_1'=0$	$(0,0,1)$ $v_1'=0$	$(0,0,0)$ $v_1'=1$	$(0,0,1)$ $v_1'=1$	$(0,0,1)$ $v_1'=2$	$(0,1,0)$ $v_1'=1$	$(0,1,0)$ $v_1'=0$	$(1,0,0)$ $v_1'=1$	$(1,0,0)$ $v_1'=2$	$(0,2,0)$ $v_1'=1$	$(0,2,0)$ $v_1'=2$
0	+27.8			−3.3	+6.1					+3.7*	−5.8*
1	−2.0		−1.0	+2.4	−2.8	−12.3				−5.9	+0.9
2	+3.0		+0.3	−0.8	−1.7	−6.6				+3.6	+4.3
3	+4.6		+1.9	−3.4	−4.3	+1.6		−4.6			
4	+4.3	+3.4	+1.7	+8.0	+2.5	+1.7*		−0.1			
5	+1.4	+4.4	+0.4	−0.4				+1.6	+8.2		
6	+0.1	−0.1	+1.2	+0.5				+3.7			
7	−1.5	−0.6	−0.6	−0.7		+8.1	−0.6*	+0.9			
8	−3.0	−1.4	−1.1	+2.5		+6.1	+3.1*	+4.3	+4.4		
9	−3.0	−2.5	−0.8	+2.7		−6.5	−2.9	−5.7			
10	−1.7	−1.7	+0.4	+3.3		+0.1	+2.6				
11	−3.2	−1.5	+0.5	+2.9		+1.0	+14.7				
12	+3.3	−0.4	−1.4	−5.3							
13	+0.9	−5.3	−2.6								
14	−1.6	+2.3	+1.7								
15	−7.3	−10.1									
16	−20.1										

TABLE VI.

v_2'	$v_1''=0, v_2''=0, v_3''=0$ $v_1'=0$		$v_1''=0, v_2''=0, v_3''=1$ $v_1'=0$		$v_1''=0, v_2''=0, v_3''=0$ $v_1'=1$		$v_1''=0, v_2''=0, v_3''=1$ $v_1'=1$		$v_1''=0, v_2''=0, v_3''=1$ $v_1'=2$		$v_1''=0, v_{2,}=1, v_{3,}=0.$ $v_1'=1$	
	Obs.	Calc.	Obs.	Calc.	Obs.	Calc.	Obs.	Calc.	Obs.	Calc.	Obs.	Calc.
0		8.1		11.3		8.3	10.0	10.5	8.6	9.7		
1		2.7		6.0		2.9	5.0	5.2		4.4	4.8	6.5
2	−4.5	−2.7		0.6		−2.5		−0.2				0.1
3		−8.0		−4.8		−7.8		−5.6				
4	−12.9	−13.4		−10.2	−13.5	−13.2	−12.6	−11.0				
5	−16.6	−18.8		−15.2	−19.6	−18.6		−16.3				
6	−24.2	−24.2	−20.9	−20.9	−25.0	−24.0		−21.7				
7	−31.1	−29.5	−24.9	−26.3	−30.2	−29.3		−27.1				
8	−34.5	−34.9	−32.4	−31.6	−34.9	−34.7	−32.3	−32.4				
9	−41.0	−40.3	−35.9	−37.0	−40.5	−40.1	−35.2	−37.8				
10	−44.9	−45.6	−42.1	−42.4	−44.3	−45.4	−43.5	−43.2				
11	−54.2	−51.0	−48.4	−47.8		−50.8	−53.7	−48.6				
12	−55.7	−56.4	−55.9	−53.1				−53.9				
13		−61.7	−60.2	−58.4								
14	−63.6	−67.1		−63.8								
15												
16												

The wave numbers of these classified bands can be calculated by an equation of the type,

$$\tilde{\nu} = \tilde{\nu}_e + a(v_2' + \tfrac{1}{2}) - b(v_2' + \tfrac{1}{2})^2 + c(v_1' + \tfrac{1}{2}) - d(v_1' + \tfrac{1}{2})^2 - e(v_1' + \tfrac{1}{2})(v_2' + \tfrac{1}{2}) - \tilde{\nu}''$$

where $\tilde{\nu}_e$ is the wave number for the electronic transition and $\tilde{\nu}''$ is the wave number of the normal vibrational level and a, b, c, d, and e are constants. With the numerical values of the constants which we have secured this becomes,

$$\tilde{\nu} = 19795.38 + 719.34(v_2' + \tfrac{1}{2}) - 2.817(v_2' + \tfrac{1}{2})^2 + 304.82(v_1' + \tfrac{1}{2}) - 2.488(v_1' + \tfrac{1}{2})^2 - 4.892(v_1' + \tfrac{1}{2})(v_2' + \tfrac{1}{2}) - \tilde{\nu}''. \quad (1)$$

This formula applies to bands for which v_2' is equal to or less than 14. The precision with which the measurements in the far ultraviolet can be made is so low that it is impossible to derive a satisfactory formula for this region. In Table V we have given the results of the observed minus the calculated values for the band heads. In most cases there is very close agreement, and the agreement in the case of nearly all the bands is satisfactory and probably within the limits of error of the measurements.

Fig. 1 is the energy level diagram consisting of the levels required by our assignment of quantum numbers. The black circles indicate the observed bands.

The Isotope Effect

The isotope effect is very prominent in these bands. We have indicated the isotopic bands in Table I with an asterisk. This selection was made partly by inspection and partly by means of the formulae derived in this section. The $Cl^{37}O_2$ bands lie on the high frequency side of $Cl^{35}O_2$ bands in the case of bands involving transitions to the lowest excited vibrational levels, but otherwise on the low frequency side.

We have found it possible to fit the experimental differences, $(Cl^{37}O_2) - (Cl^{35}O_2)$, to the formula

$$\Delta\tilde{\nu} = -5.37(v_2' + \tfrac{1}{2}) - 0.80(v_1' + \tfrac{1}{2}) - \Delta\tilde{\nu}'', \quad (2)$$

where $\Delta\tilde{\nu}''$ is -11.16 cm^{-1}, -14.42 cm^{-1} and -15.75 cm^{-1} for the (0, 0, 0), (0, 0, 1) and (0, 1, 0) normal vibrational levels, respectively. The agreement between this formula and the observed values is shown in Table VI, which also shows which isotope bands have been observed. The isotopic bands in many cases could not be observed because of fine structure, superposition of the weaker $Cl^{37}O_2$ band on the strong $Cl^{35}O_2$ band, diffuseness of band heads in the predissociation region, and the general weakness of many of the bands, both $Cl^{35}O_2$ and $Cl^{37}O_2$.

The separations of the vibrational levels in either the excited or normal electronic state should follow a formula of the form,

$$\frac{\Delta E}{hc} = a(v_1 + \tfrac{1}{2}) + b(v_2 + \tfrac{1}{2}) + c(v_3 + \tfrac{1}{2})$$

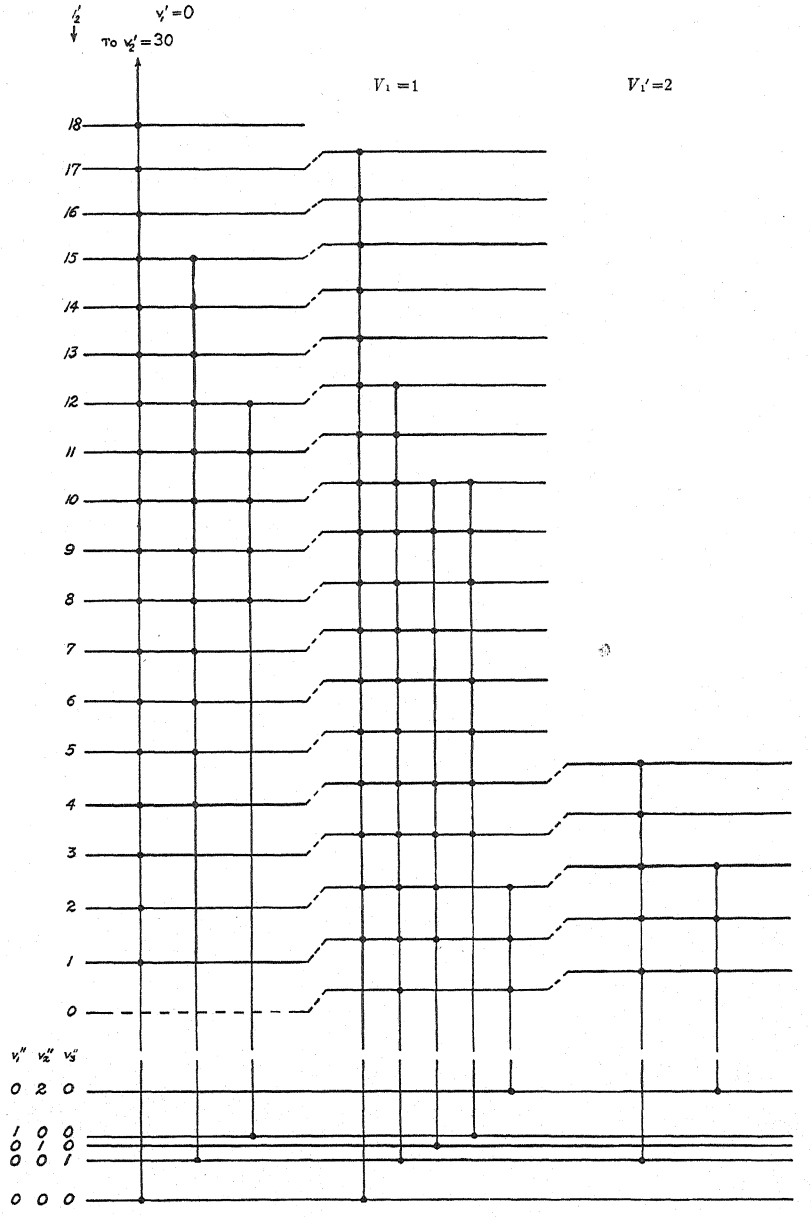


Fig. 1. Energy level diagram of the ClO_2 molecule. Bands that agree approximately with the calculated values for the transitions. (0, 8)←(0, 1, 0); (0, 9)←(0, 1, 0); (2, 6)←(1, 0, 0) and (2, 9) – (1, 0, 0) are omitted. These transitions are discussed in the text.

where the a, b, and c will be negative if ΔE is the energy of the $Cl^{37}O_2$ molecule minus that of the $Cl^{35}O_2$ molecule and higher power terms in the v's are neglected. If we assume that $v_3' = 0$ for all levels which we have observed the isotope separation is then,

$$\tilde{\nu}_{37} - \tilde{\nu}_{35} = \Delta\tilde{\nu} = a'(v_1' + \tfrac{1}{2}) + b'(v_2' + \tfrac{1}{2}) + c'/2 - a''(v_1'' + \tfrac{1}{2}) - b''(v_2'' + \tfrac{1}{2}) - c''(v_3'' + \tfrac{1}{2}). \quad (3)$$

With our assignment of quantum numbers we see from Eqs. (2) and (3) and the values of $\Delta\tilde{\nu}''$, that

$$a' = -0.80 \qquad \frac{c'}{2} - \frac{a''}{2} - \frac{b''}{2} - \frac{c''}{2} = -\Delta\tilde{\nu}''$$

$$b' = -5.37 \quad b'' = -15.76 + 11.16 = -4.60$$

$$c'' = -14.42 + 11.16 = -3.26$$

and thus

$$\frac{c'}{2} - \frac{a''}{2} = 7.23. \quad (4)$$

Our calculated value (see below) for this difference is 3.19 cm^{-1}. This difference would be diminished, if the 11.16, 14.42, and 15.76 cm^{-1} differences in our formula (2) were decreased. This would mean that our calculated differences for the bands having $v_2' = 0$ should be less than those given in Table VI by about 4 cm^{-1}. Examination of that table shows that a change of a few wave numbers in these values may be possible. We shall discuss this further after the theoretical formulae have been presented.

The Normal Modes of Vibration of the ClO_2 Molecule

Bjerrum[7] has considered the problem of the vibrations of molecules of this kind assuming two types of binding; (1) the potential energy is a function of the linear distances between the nuclei, that is the forces are central; (2) the restoring forces consist of harmonic forces along the chemical bond and perpendicular to this direction, that is, the forces are valency forces as he called them. The three frequencies of vibration in each case are functions of three constants, two force constants and the half angle at the apex of the isosceles triangle. All solutions for this angle using the formulae based on assumption (1) gave imaginary angles.

The equation for θ the half angle at the apex by using the formulae based on assumption (2) is a cubic in $\cos^2\theta$ and there are three possible ways of assigning the observed frequencies to the theoretical formulae for the frequencies. This gives nine possible solutions. The possible values of $\cos^2\theta$ must be real and lie between 0 and 1. We find that there are three possible values for θ in the normal electronic state and thus three possibilities for the two force constants k_1, and k_2 as well. In the case of the ClO_2 normal state, our experimental data give us the isotope effect constants as well and it must

[7] N. Bjerrum, Verh. d. D. phys. Ges. **16**, 737 (1914).

TABLE VII.

Assumed assignment of frequencies			Normal electronic state									
$\tilde{\nu}_1$	$\tilde{\nu}_2$	$\tilde{\nu}_3$	$k_1\times10^4$	$k_2\times10^4$	θ	2θ	$\Delta\tilde{\nu}_1$ Calc.	$\Delta\tilde{\nu}_1$ Obs.	$\Delta\tilde{\nu}_2$ Calc.	$\Delta\tilde{\nu}_2$ Obs.	$\Delta\tilde{\nu}_3$ Calc.	$\Delta\tilde{\nu}_3$ Obs.
528.8	857.7	727.0	26.06	34.17	1°19′	2°38′	−0.0073	−3.20		—		−4.60
727.0	857.7	528.8	38.71	11.61	31°55′	63°55′	−4.17	−4.60	−10.90	—	−0.39	−3.26
857.7	727.0	528.8	38.59	8.41	65°10′	130°20′	−10.32	—	−5.88	−4.60	−2.80	−3.26
			Excited electronic state									
661.1*	719.34	304.8	36.65	3.015	55°19′	110°38′			(−5.37)	−5.37	−1.88	−0.80
226.1*	719.34	304.8	6.03	18.33	34°39′	69°18′			(−5.32)	−5.37	−1.90	−0.80
I 719.34	779.6*	304.8	35.86	3.62	38°28′	76°56′	(−5.37)	−5.37	−8.53	—	−0.83	−0.80
II 304.82	719.34	382.1*	7.96	21.81	18°47′	37°34′	(−0.80)	−0.80	−6.06	−5.37	−3.93	—

* These are calculated frequencies.

be possible to calculate these from the formulae by using the same set of values of k_1, k_2 and θ.

In the case of the excited electronic state we have observed two fundamental frequencies and the isotope effects for each of these. With three of these quantities we can solve for the constants k_1, k_2 and θ again and the fourth quantity must also agree with the calculated value. We find four possible values of θ of which two give sets of values for k_1, k_2 and θ from which the second isotope effect can be calculated. The formulae for ν_1, ν_2 and ν_3 and for the isotope effects for each of these are given below. Table VII gives the results of the calculations for the normal and excited states. Columns 1, 2, 3 give the possible assignments of the observed frequencies to the three theoretical formulae, columns 4, 5, 6, 7 the calculated constants, and columns 8, 9, 10 the calculated and observed isotope effects.

$$\nu_1 = \frac{1}{2\pi} k_1^{1/2} \left(\frac{1}{m} + \frac{2 \sin^2 \theta}{M} \right)^{1/2} \tag{5}$$

$$\nu_{2,3} = \frac{1}{2\pi} \left\{ \frac{k_1 + 2k_2}{2m} + \frac{k_1 \cos^2 \theta + 2k_2 \sin^2 \theta}{M} \pm \left[\left(\frac{k_1 + 2k_2}{2m} + \frac{k_1 \cos^2 \theta + 2k_2 \sin^2 \theta}{M} \right)^2 - 2k_1 k_2 \frac{2m + M}{m^2 M} \right]^{1/2} \right\}^{1/2} \tag{6}$$

$$\Delta\nu_1 = \frac{\partial \nu_1}{\partial M} \Delta M = - \frac{\Delta M k_1 \sin^2 \theta}{4\pi^2 \nu M^2} \tag{7}$$

$$\Delta\nu_{2,3} = \frac{\partial \nu_{2,3}}{\partial M} \Delta M = \frac{\Delta M}{8\pi^2 \nu_{2,3} M} \left\{ - \frac{k_1 \cos^2 \theta + 2k_2 \sin^2 \theta}{M} \pm \frac{1}{2\left[\left(\frac{k_1 + 2k_2}{2m} + \frac{k_1 \cos^2 \theta + 2k_2 \sin^2 \theta}{M} \right)^2 - 2k_1 k_2 \frac{2m + M}{m^2 M} \right]^{1/2}} \cdot \left[- \left(\frac{k_1 + 2k_2}{m} \right) \left(\frac{k_1 \cos^2 \theta + 2k_2 \sin^2 \theta}{M} \right) - 2 \left(\frac{k_1 \cos^2 \theta + 2k_2 \sin^2 \theta}{M} \right)^2 + \frac{4k_1 k_2}{mM} \right] \right\} \tag{8}$$

We have calculated the one possible set of normal coordinates for the normal state and the two possible sets of coordinates for the excited state. The results are shown in Fig. 2.[8] Since the calculations for the excited state make

[8] The normal coordinates for these modes of vibration in terms of Cartesian coordinates with origin at the center of mass and x-axis parallel to the line joining the like atoms in the equilibrium position, are

$$q_1 = 2(x_1 + x_2) + y_1 - y_2$$
$$q_2 = B(x_1 - x_2) - 2(y_1 + y_2)$$
$$q_3 = A(x_1 - x_2) + 2(y_1 + y_2)$$

use of the small and inaccurate isotope effects, the shape, normal coordinates and force constants for this state are very approximate. These quantities in the case of the normal state should be much more reliable. Of course, the assumption of valency forces may be only approximate.

Intensities and the Application of the Franck-Condon Principle

Intensities have not been given in the tables for we have been unable to get consistent relative intensities for the bands by comparing spectra with different times of exposure and different pressures of ClO_2 gas in the absorption cell. We can see no evidence of irregularities in intensities of the bands in any progression and therefore we have constructed curves giving the approximate intensity distributions for the four most intense progressions as shown in Fig. 3 in the following way. The strongest bands are found to be suitable for measurement when the partial pressure of ClO_2 in the cell is about 0.2 mm. This was secured by cooling the trap containing the ClO_2 in

---

where x_1, x_2, y_1 and y_2 are the displacements of the like atoms from the equilibrium position and A and B are constants. The conservation of momentum and angular momentum (both taken equal to zero) give the relations

$$y_2 = y_1 + \cot\theta(x_1 + x_2),\quad x_3 = -\frac{m}{M}(x_1 + x_2) \text{ and } y_3 = -\frac{m}{M}(y_1 + y_2),$$

x_3 and y_3 being the displacements of the unlike atom from the equilibrium position. From these equations it is a simple matter to secure the values of the Cartesian coordinates of each atom for each mode of vibration.

The values of A and B were secured by making the transformation of coordinates from the $x, y, \cdots$ etc. to q_1, q_2, q_3 and expressing the potential and kinetic energies in these coordinates. The determinental equation for the frequencies is diagonal then, if,

$$AB = \frac{4M}{M + 2m} \equiv \frac{4}{\mu}$$

and

$$A - B = -\frac{M}{M + 2m}\,\frac{2k_1\tan\theta + 4k_2\cot\theta}{k_1 - 2k_2} + \frac{2k_1\cot\theta + 4k_2\tan\theta}{k_1 - 2k_2}.$$

Setting the quantity on the right equal to X and solving for A and B,

$$A = \frac{X}{2} + \left[\frac{X^2}{4} + \frac{4}{\mu}\right]^{1/2}$$

$$B = -\frac{X}{2} + \left[\frac{X^2}{4} + \frac{4}{\mu}\right]^{1/2}.$$

(Other values for A and B are secured by using the minus sign before the radical, but this gives nothing new for q_2 only becomes q_3 and q_3 becomes q_2.) The frequencies associated with the coordinates q_2 and q_3 are then,

$$\nu_2 = \frac{1}{2\pi}\left[\frac{\frac{1}{2}k_1(\sin\theta - \frac{1}{2}\cos\theta\mu B)^2 + k_2(\cos\theta + \frac{1}{2}\sin\theta\mu B)^2}{\frac{1}{2}m + \frac{1}{8}B^2m/\mu}\right]^{1/2}$$

and

$$\nu_3 = \frac{1}{2\pi}\left[\frac{\frac{1}{2}k_1(\sin\theta + \frac{1}{2}\cos\theta\mu A)^2 + k_2(\cos\theta - \frac{1}{2}\sin\theta\mu A)^2}{\frac{1}{2}m + \frac{1}{8}B^2m/\mu}\right]^{1/2}.$$

These expressions are equivalent to those given above except that either ν_2 or ν_3 may be the greater of the two depending on the values of the constants k_1, k_2 and θ.

dry ice so that the vapor pressure of ClO_2 was about 2 mm[9] and passing 1/10 of a stream of air through the trap and cell and the remainder past the trap and through the cell, the gas stream being divided by using capillary tubes of different lengths. The weakest bands were photographed with the trap containing the ClO_2 at about 5°C at which temperature the vapor pressure of ClO_2 is about 600 mm. Thus the ratio of most intense to least intense bands is considerably more than 3000 probably, for the strongest bands were yet easily measureable and the weakest difficult to observe. From our plates we can determine the most intense bands of each progression and also the bands

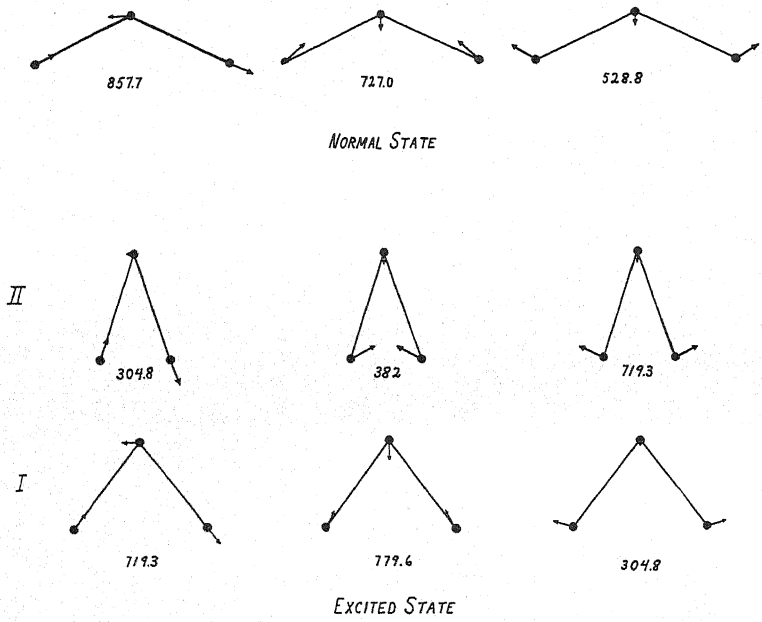


Fig. 2. Normal coordinates of the ClO_2 molecule. The acute angles between the direction of vibration of the oxygen atoms and a horizontal line are:
Normal state: $\tilde{\nu}_1=857.7$, $\alpha=24°50'$; $\nu_2=727.0$, $\alpha=41°39'$; $\nu_3=528.8$, $\alpha=30°25'$;
Excited state: Configuration I; $\tilde{\nu}_1=719.3$, $\alpha=51°32'$; $\tilde{\nu}_2=779.6$, $\alpha=60°23'$; $\tilde{\ }_3=304.8$, $\alpha=16°33'$.
Configuration II; $\tilde{\nu}_1=304.8$, $\alpha=71°13'$; $\tilde{\nu}_2=719.3$, $\alpha=22°30'$; $\tilde{\nu}_3=382$, $\alpha=51°34'$.

at which two progressions have the same intensity. We have determined the bands of greatest intensity from plates taken with a hydrogen discharge tube as source since it gives a more uniform intensity in this region. No correction has been attempted for the changing dispersion of the instrument, which, of course, changes the blackening on the plate at different wave-lengths even if the intensity of the source were uniform.

[9] This was determined by passing a slow stream of N_2 gas through the trap, catching the ClO_2 with liquid air, measuring the volume of gas passed through and determining the amount of ClO_2 vaporized by the method described by Bray (W. Bray, Zeits. f. physik. Chemie **54**, 569 (1906)).

The most intense band of the system is in the progression $(0, v_2')\leftarrow(0, 0, 0)$ and has been assigned the intensity 3000, while the first observed band of each progression has been given the intensity 1. The most intense band of the $(0, v_2')\leftarrow(0, 0, 1)$ progression has been assigned an intensity of 300. This appears to be about right and would be the intensity, if the Boltzmann factor, $e^{-h\nu/kT}$, giving the relative abundance of molecules in the two normal levels were the only factor determining the relative intensities. The maximum intensity of the strongest band of the $(1, v_2')\leftarrow(0, 0, 0)$ comes at $v_2' = 11$ which has the same intensity as the $v_2' = 6$ band of the $(0, v_2')\leftarrow(0, 0, 0)$ progression. The maximum of the $(1, v_2')\leftarrow(0, 0, 1)$ progression is taken as 1/10 that of the $(1, v_2')\leftarrow(0, 0, 0)$ progression agreeing again with the Boltzmann factor

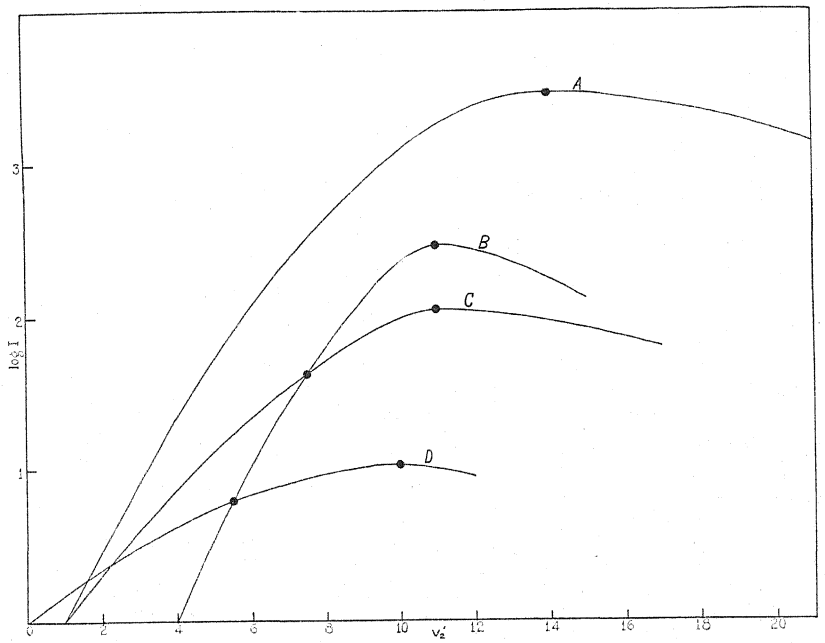


Fig. 3. Log I plotted against v_2'. A. Progression $(0, v_2')\leftarrow(0, 0, 0)$; B. Progression $(0, v_2')\leftarrow(0, 0, 1)$; C. Progression $(1, v_2')\leftarrow(0, 0, 0)$; D. Progression $(1, v_2')\leftarrow(0, 0, 1)$.

as mentioned above. The intersections marked by the dots have been determined by comparing the intensities of the bands of the two progressions. The The curves are terminated at the last observed band. The intensities are probably not small in this region but observation of the bands is difficult because of the diffuseness due to predissociation. The figure is somewhat more than a qualitative representation of the intensities, and does represent the general trend of intensities in the bands.

Large changes in the vibrational quantum number associated with the 719.34 cm^{-1} vibration have been observed and only small changes in that associated with the 304.8 cm^{-1} vibration while the third frequency has not been observed. The most intense bands of the $(0, v_2')\leftarrow(0, 0, 0)$ and $(1, v_2')\leftarrow(0, 0, 0)$ progressions are those to the levels with $v_2' = 14$ and 11. (This is using the

final assignment of quantum numbers which has been done throughout this paper.) The Franck-Condon[10] principle should be applicable to polyatomic molecular spectra and enables us to make a choice between the two possible assignment of frequencies to the normal modes of vibrations of the excited state.

We consider the configuration I of Table VIII and Fig. 2 first. In the electronic transition from the normal state to the excited state, we assume with Condon that the dimensions of the molecule do not change. (The velocities are small in the normal state and thus need not be considered.) Superimposing the normal molecule (Fig. 2) on the excited molecule assuming configuration I, we see that the molecule should vibrate strongly with frequency 304.8 cm^{-1} thus leading us to expect large changes in the associated vibrational quantum number, in contradiction to observation. A large change in the equilibrium distance between Cl and O should cause large changes in the quantum number associated with the calculated 779.6 cm^{-1} frequency. Failure to observe this would be consistent with no change in this distance. The large change in the angle at the apex should not cause a large amplitude of oscillation of the 719.34 cm^{-1} frequency and thus small changes in the quantum number associated with this frequency should be observed again in contradiction to observation. Thus configuration I for the excited state appears to be impossible.

The configuration II for the excited state is consistent with the intensity distribution. Superposition of the normal molecule on this configuration II, shows that the frequency 719.34 should be strongly excited in agreement with observation. The frequency 382.1 (calc.) should be strongly excited if the equilibrium distance Cl-O changed markedly. That it is not observed indicates that this distance is not changed. The asymmetric vibration 304.8^{-1} should not be strongly excited again in agreement with observation. This qualitative agreement enables us to decide between configurations I and II and is, we believe, the first application of the Franck-Condon principle to polyatomic molecular spectra.

The Assignment of Quantum Numbers

Thus far we have anticipated our final assignment of quantum numbers and we shall justify it at this point. The calculated structure of ClO_2 in the normal state requires that $\tilde{\nu}_1 = 857.7$ cm^{-1}, $\tilde{\nu}_2 = 727.0$ cm^{-1} and $\tilde{\nu} = 528.8^{-1}$. From these calculations the assignment of quantum numbers in the normal state is $v_1'' = 1$ for the 857.7 cm^{-1} level, $v_2'' = 1$ for the 727.0 cm^{-1} level and $v_3'' = 1$ for the 528.8 cm^{-1} level. Since the 1471.3 cm^{-1} level is assumed to be a harmonic of the 727.0 cm^{-1} level it is designated by $v_2'' = 2$. Thus the assignment of quantum numbers in the normal state becomes

Level	v_1'', v_2'', v_3''
0. cm^{-1}	0, 0, 0
528.8 cm^{-1}	0, 0, 1

[10] J. Franck, Trans. Faraday Soc. **21,** Part 3 (1925); E. U. Condon, Phys. Rev. **28,** 1182 (1926).

727.0 cm^{-1} 0, 1, 0
857.7 cm^{-1} 1, 0, 0
1471.3 cm^{-1} 0, 2, 0.

For the reasons given above v_1' is the quantum number associated with the 304.8 cm^{-1} frequency, v_2' with the 719.3 cm^{-1} frequency and v_3' with the calculated 382.1 cm^{-1} frequency. No transitions have been observed in which the 382.1 cm^{-1} frequency is involved and therefore we assume that v_3' is zero for all observed bands. We believe that the most intense progression has for its higher levels a set with $v_1'=0$ because we have been unable to find any evidence for levels with a smaller value of v_1', though we have found levels with v_1' one and two units larger.

In Eq. (4) we give the relation between the constants c' and a'' required by our experimental data. Our calculated values of c' and a'' taken from Table VII are -3.93 and -10.32 which make $c/2'-a/2''=+3.19$ instead of 7.23 required by our data, a difference of about 4 cm^{-1}. This may be partially accounted for on the assumption that the $\Delta\tilde{\nu}''$ of Eq. (2) may be too large as pointed out above. The isotope effects of the $\tilde{\nu}_1'$ and $\tilde{\nu}_2'$ frequencies have been estimated from the energy levels having large values of v_2'. Thus, we have calculated the configuration and frequencies of vibration and their isotope effects by using two frequencies for infinitesimal amplitudes of vibration and two isotope effects for large amplitudes of vibration. Thus even if the model were exact, some discrepancy between calculated and observed might be expected.

The difference between the calculated and observed values of $c/2'-a/2''$ could be eliminated by assuming that all bands having $v_2'=0$, as we have assigned the quantum numbers, do not belong to this band system and that the bands having $v_2'=1$ (our numbering) should be numbered as $v_2'=0$. However, we see no experimental reason for doing this and believe that the reason for the discrepancy lies in the approximate character of our calculations.

The Dissociation of the Molecule and Predissociation

From our assignment of frequencies to the normal modes of vibration, it is evident that the unsymmetric vibration of the excited state with $\tilde{\nu}_1'=$ 304.8 cm^{-1}, if the amplitude is large, will lead to dissociation into the ClO molecule and the O atom, either or both with energy of excitation. The formula (1) permits an extrapolation to dissociation though the value for the dissociation energy will probably be very approximate. This extrapolation gives 28968 cm^{-1} above the normal level of the molecule for this energy.

Goodeve and Stein observed predissociation from λ3293A, toward the ultraviolet. Our own plates indicate that the limit is about λ3595A, while Finkelnburg and Schumacher using highest dispersion have observed this limit as λ3753A. We believe their observation to be most reliable because of their higher resolving power.[11] Interpreting this in terms of our energy level

[11] Dr. G. M. Murphy working in our laboratories has attempted to observe the resonance radiation of ClO_2 excited by the λ3660 lines of mercury with negative results as would be expected on the basis of Finkelnburg and Schumacher's value for the predissociation limit but not on the basis of either of the other values.

diagram we place the predissociation at 27162 cm^{-1} above the lowest level, which is as close to our value of 28968 cm^{-1} for dissociation as can be expected considering the likely errors in this extrapolation. The agreement shows that the predissociation limit *does* correspond to dissociation into ClO and O as has been assumed by the previous observers.

Goodeve and Stein[4] showed that there is a distinct break in the curve when the first differences of the progression $(0, v_2')\leftarrow(0, 0, 0)$ are plotted as ordinates against v_2' as abscissa. This is shown in Fig. 4 where we have plotted

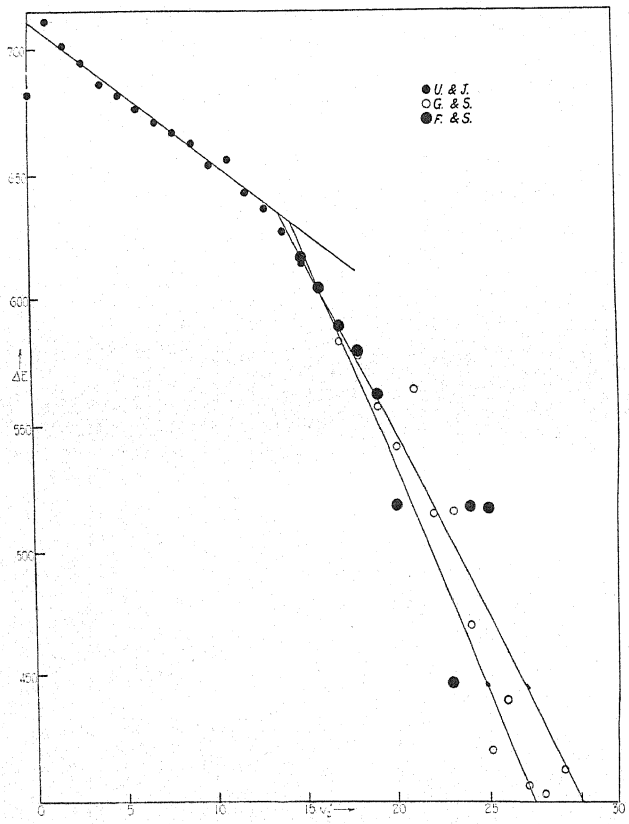


Fig. 4. Values of $E(v_2'+1)-E(v_2')$ plotted against v_2'.

our values up to $(v_2'=15)-(v_2'=14)$ difference and both Goodeve and Stein's and Finkelnburg and Schumacher's from that point on. The discontinuities in these differences is evident and the scattered character of the points from $v_2'=15$ on shows that any formula fitting this part of the energy level diagram would be very doubtful and that any extrapolation to $\Delta E=0$ would be doubtful using either set of data in this region of large values of v_2'. The extrapolated value of v_2' at dissociation might lie anywhere between about $v_2'=59.11$ and $v_2'=67.98$ and the energy of dissociation, assuming a straight line for the $\Delta E:v_2'$ curve from $v_2'=15$ on and these two values of v_2', should lie be-

tween 48268.3 cm^{-1} and 51300.7 cm^{-1}. These wave numbers correspond to 137.1 and 145.7 cal. per mol., respectively. The scattered nature of the points, see Fig. 4, and the very doubtful extrapolation makes us feel that any energy of dissociation derived from such data and calculations is very doubtful except between very wide limits, perhaps even wider than those assumed in the above calculations.

Fig. 5 shows a plot of $\Delta E:v_2'$ in the region of small values of v_2' on a larger scale and including the points of all three sets of data. The straight line drawn

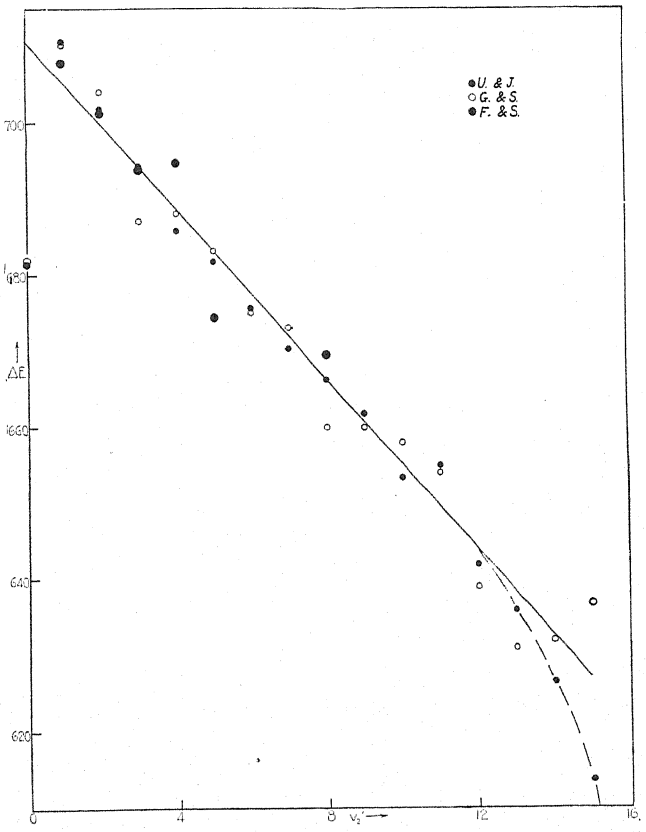


Fig. 5. Values of $E(v_2'+1)-E(v_2')$ plotted against v_2'.

through the data is that required by Eq. (1). It will be seen that our values follow a smoother curve than either of the other sets of data. Finkelnburg and Schumacher claim a higher precision for their work than we do and thus the greater irregularities which their data show may be real. Our values indicate that this curve is not a straight line but the precision of the data does not warrant a definite conclusion.

The broken curve at the lower end of the figure shows the marked way in which the break in the curve occurs. The break in the curve at the left is very similar to the discontinuities in the SO_2, $\Delta E:v'$ curve as observed by Watson

and Parker.[12] The curve with positive slope in the case of SO_2 extended over 3 or 4 differences whereas in ClO_2 it is apparent for only one difference, and therefore the discontinuity in this case may not be real.

The Character of the High Amplitude Vibrations

The half angle at the apex of the isoceles triangle in the excited state is nearly a normal coordinate of the molecule as can be seen from Fig. 2. The application of the Franck-Condon principle for the intensity distribution indicates that the oscillation using the classical model for the most intense band of any progression having the v_2' levels as higher levels, is between $\theta = 65°$, its value for the normal state, and something less than 18.5°. This most intense band appears to be that with $v_2' = 12$ approximately. It should not require much more energy in this mode of vibration to make the molecule oscillate between $\theta = 90°$ and some small angle. Such an oscillation would be an oscillation through the straight line position and would be similar to that of a straight line molecule.

The discontinuity in the plot ΔE against v_2 discovered by Goodeve and Stein and discussed above appears at $v_2' = 15$, just a few levels above the value of v_2' for the most intense band. Therefore it seems that the discontinuity in the $\Delta E : v_2'$ curve at $v_2' = 15$ may occur when the molecule first acquires sufficient energy to vibrate through the straight line position.

We wish to thank the Physics department and particularly Professor H. W. Webb for the privilege of using the Hilger E−1 instrument and the comparator in this work.

[12] W. W. Watson and A. E. Parker, Phys. Rev. **37**, 1484 (1931).

ROTATIONAL STRUCTURE OF THE RED BANDS OF POTASSIUM

By F. W. Loomis[1]
The Alfred Loomis Laboratory, Tuxedo Park, New York

(Received November 6, 1931)

Abstract

A rotational analysis has been made of four bands of the red system of K_2 which had been photographed under high dispersion. The principal molecular constants of the ground state ($^1\Sigma_g^+$) and of the upper state ($^1\Pi_u$) are as follows:

$B_0'' = 0.05611$ $r_e'' = 3.91 \times 10^{-8}$ $\alpha'' = 0.000219$
$B_0' = 0.04812$ $r_e' = 4.22 \times 10^{-8}$ $\alpha' = 0.000235$

The magnitude of the Λ type doublings of the $^1\Pi$ state agrees with Van Vleck's formula for it. The relationships between the molecular constants show that all rotational levels, with both even and odd values of J, are present. Alternating intensities are observed, the lines with odd J'' being stronger. It is concluded that the nuclear spin of K^{39} is definitely not zero, and that the nucleus obeys the Fermi-Dirac statistics.

THE red absorption bands of diatomic potassium were photographed, with the cooperation of Professor R. W. Wood, primarily with the object of determining whether or not the nuclear spin of the principal isotope, K^{39}, was zero, as had been concluded by two independent observers[2,3] of the hyperfine structure of arc and spark lines respectively. We were able to report immediately[4] that an inspection of our plates showed conclusively that this could not be true, for alternating intensities were clearly apparent in the well resolved branches; and moreover the spacing of the lines was such as to preclude the possibility that alternate ones were missing, as they must be if the spin were zero. This latter statement was based on a comparison of the observed spacing with that estimated by extrapolating the known spacings of the corresponding bands of Li_2 and Na_2.

A rotational analysis of four bands of this spectrum has now been completed and thoroughly checked by the combination relations, with the result that our earlier conclusions are verified, independently of the extrapolation from Li_2 and Na_2.

As stated in the joint paper,[4] the spectrum was photographed in absorption in the fourth order of the Tuxedo forty foot spectrograph with a particularly fine seven inch plane grating with 15,000 lines per inch. Sunlight was used as a background and the solar lines as a comparison, their wavelengths being obtained from the revised Rowland's Table.[5]

The red band system of potassium is expected to be, like the green ones of

[1] The University of Illinois.
[2] Schüler and Brück, Zeits. f. Physik **58**, 735 (1929).
[3] Frisch and Kronig, Naturwiss. **19**, 444 (1931).
[4] Loomis and Wood, Phys. Rev. **38**, 854 (1931).
[5] Revision of Rowland's Preliminary Table of Solar Wave-lengths, St. John, Moore, Ware, Adams and Babcock. Published by Carnegie Inst. of Washington (1928).

lithium and sodium, a $^1\Pi - ^1\Sigma$ transition and this is confirmed by the analysis, since each band is found to consist of one P, one Q and one R branch.

The analysis was carried out in much the same way as that[6] of the green bands of Na_2. The lines belonging to the branches were found, where possible, by picking out series of regularly spaced lines by inspection and the assignments were checked and completed by the construction of graphs similar to Figs. 2 of the paper on sodium.[6] In this way three series were found in each band, though there were some regions where two or even three series coalesced. The Q branches could be identified by inspection because of their greater intensity. The P and R branches were identified and triplets of lines with common values of J'' were picked out from them and the Q branches by application of the PQR combination relation

$$R(J'') - Q(J'') \cong Q(J''+1) - P(J''+1). \quad (1)$$

It is true, of course, that this relation is theoretically not exact, since there is Λ type doubling in the upper state and hence the initial levels for the Q lines differ from those of the P and R lines and there is a "combination defect". In the case of potassium, however, this combination defect is so small that it is barely detectable and the PQR combination relation is quite sufficient for the identification of the lines in the three branches which have common J''.

The measured frequencies of the lines of the (1, 0) (1, 1) (0, 1) and (0, 2) bands, with the quantum numbers assigned to them, as described below, are given in Table I.

TABLE I. *Measured frequencies of band lines.*

(1, 0) band				(1, 1) band		
P	Q	R	J''	P	Q	R
	15438.82		21	15345.08		
	38.45		22	44.63		
	38.08		23	44.14		
15435.34	—		24	43.69		
34.88	37.27		25	43.20		
34.35	36.83		26	42.66		
33.80	36.38		27	42.14		
33.25	35.94		28	41.61		
32.68	35.44		29	—		
32.12	34.95		30	40.47		
31.48	34.45	15437.39	31	39.91		
30.89	33.92	37.09	32	39.28		
30.24	33.39	36.63	33	38.67	15341.84	15345.08
29.59	32.82	36.17	34	38.00	—	44.63
28.90	32.25	35.71	35	37.37	40.75	44.14
28.23	31.66	35.22	36	36.70	40.14	43.69
27.50	31.05	34.68	37	36.00	39.57	43.20
26.80	30.43	34.13	38	—	38.96	42.66
26.07	29.78	33.61	39	34.63	38.34	42.14
25.32	29.14	33.05	40	33.86	37.71	41.61
24.58	28.45	32.46	41	33.13	—	—
23.77	—	31.86	42	—	36.36	40.47
22.97	27.04	31.26	43	31.60	35.69	39.91
22.17	26.34	30.70	44	30.82	34.98	39.28
21.32	25.60	30.00	45	30.00	34.26	38.67

[6] Loomis and Wood, Phys. Rev. **32**, 223 (1928).

TABLE I. (*Continued*).

(1, 0) band				(1, 1) band		
P	*Q*	*R*	*J''*	*P*	*Q*	*R*
15420.43	15424.85	15429.36	46	15329.16	15333.54	15338.00
19.60	24.09	28.65	47	28.33	32.80	37.37
18.62	23.30	27.97	48	27.49	32.04	36.70
17.83	22.47	27.23	49	26.60	31.24	36.00
16.90	21.67	26.51	50	25.72	30.45	35.27
15.98	20.80	25.76	51	24.80	29.62	34.55
14.97	19.96	25.04	52	—	28.78	33.86
14.07	19.09	24.23	53	22.94	27.94	33.08
13.09	18.22	23.45	54	22.02	27.10	32.33
12.08	17.29	22.64	55	21.03	26.21	31.49
11.09	16.38	21.82	56	20.08	25.34	30.73
10.06	15.44	20.98	57	19.04	—	29.90
09.01	14.48	20.11	58	18.05	23.48	29.08
07.99	13.52	19.24	59	16.95	22.55	28.23
06.91	12.56	18.35	60	15.94	21.59	27.35
05.80	11.53	17.41	61	14.86	20.60	26.50
04.65	10.53	16.49	62	13.75	—	25.60
03.58	09.51	15.55	63	12.68	18.64	24.67
02.39	08.47	14.59	64	11.57	17.62	23.75
01.21	07.42	13.60	65	10.44	16.57	22.82
00.11	06.32	12.56	66	09.30	15.51	21.81
15398.92	05.22	11.63	67	08.14	14.45	20.88
97.70	04.12	10.62	68	07.01	13.37	—
96.49	02.97	09.51	69	05.80	12.28	18.86
—	01.82	08.47	70	04.57	11.18	17.82
94.00	00.66	07.42	71	03.36	10.03	16.81
92.74	15399.46	06.32	72	—	08.86	15.76
91.44	98.28	05.22	73	00.88	07.71	14.66
—	97.06	04.12	74	15299.60	06.54	13.60
88.82	95.86	02.97	75	98.31	05.34	12.47
—	94.60	01.82	76	96.98	—	11.36
86.14	93.33	00.66	77	95.72	02.92	10.22
84.77	—	15399.46	78	94.37	01.67	09.07
83.40	90.76	98.28	79	93.04	—	07.91
81.99	89.47	97.06	80	91.64	15299.14	06.79
80.58	88.15	95.86	81	90.28	97.86	05.54
79.15	86.82	94.60	82	88.87	96.55	—
77.68	85.45	93.33	83	87.50	95.22	03.07
76.25	84.09	—	84	86.06	—	01.82
74.75	82.71	90.76	85	84.62	92.52	—
73.25	—	89.41	86	83.17	91.15	15299.31
71.74	—	88.10	87	81.68	89.78	—
—	78.42	86.76	88	80.18	88.40	96.71
68.68	—	85.39	89	78.70	86.98	95.37
67.12	75.47	83.98	90	—	85.54	—
—	73.99	82.55	91	75.59	84.09	—
63.95	72.50	—	92	74.07	82.63	91.29
62.31	70.95	79.72	93		81.12	89.90
60.71	69.43	78.20	94		79.64	88.48
59.05	67.86	76.83	95		78.15	87.06
57.40	—	75.34	96		76.64	—
55.70	64.69	73.85	97		75.09	84.17
54.02	—	72.29	98		73.54	82.71
52.32	—	70.74	99			81.24
50.58		69.23	100			
48.86	58.19	67.63	101			
47.12	56.54	66.28	102			
	54.84	64.49	103			
	53.14	62.85	104			
	51.42	61.24	105			
	49.69	—	106			
		57.94	107			

TABLE I. (*Continued*).

(1,0) band				(1,1) band		
P	*Q*	*R*	*J''*	*P*	*Q*	*R*
		15356.22	108			
		54.56	109			
		52.86	110			
			10		15184.77	
			11		84.60	
			12		84.42	
			13		84.17	
			14		83.98	
			15		83.75	
			16		83.51	
			17		83.23	
			18		82.94	
			19		82.71	
			20		82.39	
			21	15180.08	82.07	
			22	79.66	81.75	
	15272.34		23	79.18	81.42	
	71.97		24	78.78	81.02	
	—		25	78.28	80.69	
	71.18		26	77.82	80.33	
15268.17	70.75		27	77.28	79.88	15182.59
67.64	70.32		28	76.76	79.48	—
67.09	69.86		29	76.23	79.01	81.91
—	69.38		30	75.72	78.58	81.53
65.95	68.91		31	75.14	78.10	81.15
65.35	68.43		32	74.57	77.61	80.69
64.76	67.91		33	73.93	77.12	80.33
64.14	67.39		34	73.36	76.61	79.88
63.51	66.86		35	72.74	76.07	79.48
62.84	66.28		36	—	75.52	79.01
62.18	65.71		37	71.45	74.97	78.58
61.50	65.13		38	—	74.39	78.10
60.79	64.52		39	—	73.79	77.61
60.06	63.88		40	—	73.19	77.12
59.34	63.27		41	68.63	72.58	76.61
58.58	62.62		42	67.89	71.98	76.07
57.84	61.94		43	67.16	71.28	75.52
57.07	61.27	15265.49	44	66.35	70.61	74.97
56.27	60.54	64.97	45	65.63	69.95	74.39
55.47	59.84	64.34	46	64.86	69.26	73.79
54.64	59.12	63.71	47	64.05	68.63	73.19
53.80	58.39	63.07	48	63.23	67.89	72.58
52.97	57.63	62.39	49	62.40	67.16	71.98
52.09	—	61.71	50	61.54	66.35	71.28
51.20	56.05	61.01	51	60.73	65.63	70.61
50.29	55.24	60.34	52	59.84	64.86	69.95
49.36	54.43	59.59	53	58.96	64.05	69.26
48.48	53.60	58.81	54	58.05	63.23	68.43
47.52	52.75	58.10	55	57.14	62.40	67.72
46.55	51.86	57.33	56	56.20	61.54	66.88
45.59	50.99	56.53	57	55.27	60.73	66.20
44.62	50.11	55.71	58	54.30	59.84	65.46
43.60	49.19	54.92	59	53.32	58.96	64.67
42.57	48.26	54.06	60	52.32	58.05	63.81
41.53	47.32	53.20	61	51.30	57.14	63.04
40.47	—	52.35	62	50.30	56.20	62.18
39.43	45.38	51.46	63	49.27	55.27	—
38.32	44.37	50.57	64	48.20	54.30	60.42
37.20	43.40	49.65	65	47.13	53.32	59.54
36.10	42.36	48.76	66	46.07	52.32	58.68
35.01	41.33	47.74	67	44.97	51.30	57.76
—	40.26	46.82	68	43.86	50.30	56.82

TABLE I. (*Continued*).

(0, 1) band				(0, 2) band		
P	Q	R	J''	P	Q	R
—	15239.23	15245.84	69	15142.72	15149.27	15155.87
15231.50	38.16	44.86	70	41.59	48.20	54.92
30.33	37.01	43.84	71	40.43	47.13	53.95
29.12	35.92	42.81	72	39.26	46.07	52.98
27.92	34.80	41.80	73	38.08	44.97	51.96
26.72	—	40.74	74	36.88	43.86	50.94
25.47	—	39.67	75	35.66	42.72	49.89
24.16	31.32	38.57	76	34.44	41.59	48.90
22.89	30.14	37.53	77	33.21	40.43	47.82
21.60	28.94	36.37	78	31.94	39.26	46.73
20.32	27.72	35.26	79	30.67	38.08	45.63
18.95	26.47	—	80	29.40	36.88	44.51
17.65	25.27	—	81	28.10	35.66	43.40
16.26	23.97	—	82	26.76	34.44	42.26
14.92	22.69	30.61	83	25.44	33.21	41.11
13.51	21.41	29.43	84	24.11	31.94	39.91
12.15	20.08	28.17	85	22.73	30.67	38.78
10.72	18.76	26.96	86	21.37	29.40	37.58
09.30	17.45	25.68	87	19.97	28.10	36.35
07.83	16.07	24.40	88	18.56	26.76	35.09
06.39	14.70	23.13	89	17.14	25.44	33.88
04.92	13.33	21.84	90	15.71	24.11	32.65
03.43	11.92	20.55	91	14.25	22.73	31.38
01.94	10.51	19.21	92	12.79	21.37	30.07
00.42	09.08	17.87	93	11.32	19.97	28.75
15198.88	07.64	16.52	94	09.82	18.56	27.45
97.34	06.16	15.15	95	08.30	17.14	26.15
95.78	—	13.74	96	06.79	15.71	24.76
—	03.16	12.33	97	05.25	14.25	23.42
92.53	01.70	10.87	98	03.72	12.79	22.06
91.04	00.20	09.50	99	02.12	11.32	20.66
89.40	15198.61	08.02	100	00.55	09.82	19.24
87.77	97.10	06.59	101	15098.96	08.30	17.84
	95.53	05.14	102	97.33	06.79	16.41
	—	03.62	103			
	—	02.08	104			
	90.72	00.56	105			
	89.06	15199.04	106			
	87.44	97.47	107			
		95.88	108			
		94.32	109			
		92.69	110			
		91.04	111			
		89.40	112			
		87.77	113			

After the lines of the branches had been sorted out, the Δ_2F's were obtained and used to determine the absolute values of the quantum numbers and the magnitude of the constants B' and B'' according to the equations:

$$\Delta_2F'(J') = R(J'') - P(J'') = 4B'(J' + \tfrac{1}{2}) + 8D'(J' + \tfrac{1}{2})^3 \quad (2)$$

$$\Delta_2F''(J'') = R(J'' - 1) - P(J'' + 1) = 4B''(J'' + \tfrac{1}{2}) + 8D''(J'' + \tfrac{1}{2})^3 \quad (3)$$

The higher power terms, $12F(J+\frac{1}{2})^5$ etc., have been omitted from these equations because calculation shows them to be negligible in the case of potassium. The calculation of the B's was made by successive approximations and least squares, the D's being determined by the equations

$$D_v = D_e + \beta(v + \tfrac{1}{2}) \quad (4)$$

$$D_e = \frac{-4B_e^3}{\omega_e^2} \tag{5}$$

$$\beta = \frac{\alpha^2}{6\omega_e} + \frac{20\alpha B_e^2 - 32x_e B_e^3}{\omega_e^2}. \tag{6}$$

The values of ω_e and x_e in Eqs. (5) and (6) were taken from a paper by Crane and Christy[7] which gives the vibrational constants of the red system of K_2 as follows:

$$\begin{aligned}\nu &= \nu_0 + \omega_e'(v'+\tfrac{1}{2}) - \omega_e' x_e'(v'+\tfrac{1}{2})^2 - \omega_e''(v''+\tfrac{1}{2}) + \omega_e'' x_e''(v''+\tfrac{1}{2})^2 \\ &= 15377.73 + 74.73(v'+\tfrac{1}{2}) - 0.327(v'+\tfrac{1}{2})^2 - 92.64(v''+\tfrac{1}{2}) \\ &\quad + 0.354(v''+\tfrac{1}{2})^2\end{aligned} \tag{7}$$

The constants α' and α'' of the equation

$$B_v = B_e - \alpha(v+\tfrac{1}{2}) \tag{8}$$

were calculated, after the true J's had been assigned as just described, but before the final adjustment of the B's was made, from the variation of the differences of the Q lines of different bands, according to the equations

$$Q(1,0) - Q(1,1) = Q_0(1,0) - Q_0(1,1) - \alpha''(J+\tfrac{1}{2})^2 + \beta''(J+\tfrac{1}{2})^4 \tag{9}$$

$$Q(1,1) - Q(0,1) = Q_0(1,1) - Q_0(1,0) - \alpha'(J+\tfrac{1}{2})^2 + \beta'(J+\tfrac{1}{2})^4 \tag{10}$$

Finally, the combination defects in the (1, 0), (1, 1) and (0, 1) bands were expressed by the theoretical relations

$$\begin{aligned}R(J'') - Q(J'') - Q(J''+1) + P(J''+1) &\\ = (B_{PR}' - B_Q')((J''+3/2)^2 + (J''+\tfrac{1}{2})^2) &\\ \cong 2(B_{PR}' - B_Q')(J+1)^2 &\end{aligned} \tag{11}$$

and the coefficient $(B'_{PR} - B'_Q)$ determined by least squares to be 2.02×10^{-6}. This is in adequate agreement with the theoretical expression for this quantity.

$$B_{PR}' - B_Q' = 4B^2/\nu(^1\Pi_u\,^1\Sigma_u^+) = 2.52\times10^{-6} \tag{12}$$

which has been found by Mulliken and Christy[8] to hold well for the corresponding $^1\Pi$ states of the similar molecules H_2, Li_2 and Na_2. The combination

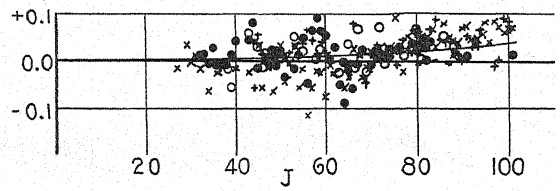


Fig. 1. PQR combination defect. Full circles, hollow circles, ×'s and +'s represent data from bands (1, 0), (1, 1), (0, 1) and (0,2) respectively.

defects of Eq. (11) are plotted in Fig. 1. The curve represents the function $4.04\times10^{-6}(J+1)^2$.

[7] Crane and Christy, Phys. Rev. **36**, 421 (1930).
[8] Mulliken and Christy, Phys. Rev. **38**, 87 (1931).

The rotational constants as above determined are summarized in Table II.

TABLE II. *Rotational constants of K_2^{39} molecule.*

	Ground state ($^1\Sigma_g^+$)				Upper state ($^1\Pi_u$)		
v	equil.	0	1	2	equil.	0	1
B	0.05622	0.05611	0.05589	0.05567	0.04824	0.04812	0.04788
$D\times10^8$	−8.28	−8.32	−8.41	−8.49	−8.06	−8.09	−8.17
α	0.000219				0.000235		
β	-0.083×10^{-8}				-0.074×10^{-8}		
I_e	492.0×10^{-40}				573.4×10^{-40}		
r_e	3.91×10^{-8}				4.22×10^{-8}		
$B_{PR}-B_Q$					2.0×10^{-6}		

The accuracy with which the values of B and D in Table II represent the Δ_2F's, as well as the precision with which the combination relations hold, is

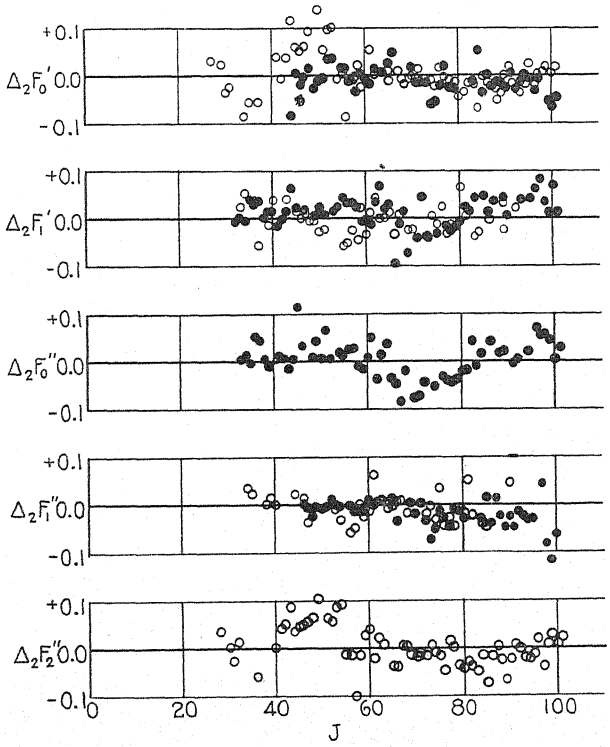


Fig. 2. Residuals of Δ_2F's from those calculated by Eqs. (2) and (3) with constants in Table II. Full circles represent data from bands (0, 1) and (1, 0), hollow circles data from bands (1, 1) and (0, 2).

shown in Fig. 2, wherein the residuals of the observed Δ_2F's from those calculated by Eqs. (2) and (3) are plotted against J. The fact that these representations are within the experimental error of observation (which is far from true of the representations with the quadrupled value of D/B which would have been called for by Eq. (5) had it been assumed that alternate

TABLE III. *Comparison of constants of similar molecules*[9]

	Ground state: $^1\Sigma_g^+$				Upper state: $^1\Pi_u$				Upper state: $^1\Sigma_u^+$			
	H_2	Li_2	Na_2	K_2	H_2	Li_2	Na_2	K_2	H_2	Li_2	Na_2	K_2
F_0	0	0	0	0	99086	20398	20302	15369	90083	14022	15007	11672
B_0	59.19	0.6691	0.1543	0.05611	29.4	0.5532	0.1254	0.04812	19.45	0.495	0.1085	(0.042)
$r_e\times10^8$	0.74	2.67	3.07	3.91	1.05	2.93	3.41	4.22	1.30	3.11	3.67	(4.5)
α	2.79	0.00744	0.00082	0.000219	1.2	0.00804	0.00094	0.000235	(0.4)	0.005	0.0004	(0.00010)
$-D_0\times10^6$	33596	9.952	0.5860	0.0832	18051	9.531	4.076	0.0809	16470	7.7	0.38	(0.063)
ω_e	4371	349.9	159.2	92.64	2446	270.4	125.0	74.73	1354	253.2	115.6	69.09
$\omega_e x_e$	113.5	2.5	0.73	0.354	66.5	3.1	0.84	0.327	16	1.5	0.38	0.153
B_e/ω_e	0.0139	0.00192	0.00097	0.000607	0.0123	.00206	0.00101	0.000646	0.0145	0.00196	0.00094	(0.00061)
$R=2x_eB_e/\alpha$	1.13	1.29	1.73	1.96	1.36	1.59	1.81	1.80	(1.25)	1.2	1.8	(1.9)
D (volts)	4.34	1.14	0.76	0.51	2.25	0.46	0.35	0.22	3.37	1.25	1.01	0.68

[9] The data in Table III have been taken from the following sources: for hydrogen, Hyman, Phys. Rev. **36,** 187 (1930) and Birge, Proc. Nat. Acad. **14,** 12 (1928); for lithium, Harvey and Jenkins, Phys. Rev. **35,** 789 (1930), Wurm, Zeits. f. Physik **58,** 562 (1929) and **59,** 35 (1929), Loomis and Nusbaum, Phys. Rev. **38,** 147 (1931); for sodium, Loomis, Phys. Rev. **31,** 323 (1928), Loomis and Nile Phys. Rev. **32,** 873 (1928), Loomis and Wood, reference 6; for potassium, Crane and Christy, Phys. Rev. **36,** 421 (1930), and as yet unpublished information from Loomis and Nusbaum as to the heats of dissociation for potassium and sodium.

lines of the bands were missing) is additional definite proof that the latter hypothesis is wrong and that the spin of the K^{39} nucleus is not zero. A further and independent proof of this is that the frequencies of the band lines can be represented by the formulae

$$R,\ P(J'') = \nu_0 + B' \pm 2B'(J''+\tfrac{1}{2}) + (B'-B'')(J''+\tfrac{1}{2})^2 \pm 4D'(J''+\tfrac{1}{2})^3 + (D'-D'')(J''+\tfrac{1}{2})^4 \quad (13)$$

$$Q(J'') = \nu_0 + (B'-B'')(J''+\tfrac{1}{2})^2 + (D'-D')(J''+\tfrac{1}{2})^4 \quad (14)$$

in which the constants are those, given in Table II, which were determined from the $\Delta_2 F$'s. Had alternate lines been missing the quadratic coefficients in Eqs. (13) and (14), for instance, would have been twice the difference of the B's determined as above. It has not been thought worthwhile to include graphs showing the agreement between measured and calculated frequencies, but it is within about 0.3 cm^{-1} and systematic deviations could be practically eliminated by adjusting the coefficients, within the limits of error with which they can be determined from the $\Delta_2 F$'s. The result would not, however, be an increase in the precision of our knowledge of these coefficients, but only of certain differences between them which are not particularly significant, so it has not been done.

In Table III a comparison is made between some of the constants of these two states of the K_2 molecule and those of the corresponding states of the similar molecules H_2, Li_2 and Na_2. Data for the upper ($^1\Sigma_u^+$) states have been added for completeness. Since the rotational constants of this state of potassium have not been determined (it would necessitate an analysis of the infrared K_2 system) they have been estimated by extrapolating values for B_e/ω_e and for $R = 2x_e B_e/\alpha$ and by using these to calculate the others. Values based on these extrapolations are given in parentheses. The data in Table III have been compiled from various sources, as indicated in the footnotes. Particularly in the case of hydrogen, difficulties have been encountered owing to contradictions and incompleteness with which the data have been reported, but the data are more than good enough for the purpose of Table III, which is to show the nature of the variations of the various constants along the series of homologous molecules.

The alternation of intensities is most obvious in the 0, 2 band and especially so in the region where for a long interval the lines $Q(M)$ fortuitously coincide closely with $P(M-6)$. It is the lines with odd values of J'' which are stronger, just as has been found to be the case with H_2, Li_2 and Na_2.[10] This signifies that the K^{39} nuclei also obey the Fermi-Dirac statistics. The present observations were made under conditions that do not permit the determination of nuclear spin from the ratio of alternating intensities, but it is hoped to make this determination at a later time.

It is probable that lines due to the molecule $K^{39}K^{41}$ would be sufficiently intense to be found if they were sought for, but as no particular interest attaches to them this has not been done. The lines of the molecule $K^{41}K^{41}$, which would be interesting, are probably too faint to be found.

[10] Urey, Phys. Rev. **38**, 1074 (1931).

HIGH RESOLUTION IN THE INFRARED

By J. D. Hardy*
Physics Laboratory, University of Michigan

(Received November 6, 1931)

Abstract

An instrument is described which is capable of giving an experimental resolving power of ten thousand in the near infrared region. With this instrument several of the infrared lines of helium I have been examined and their components resolved. The exceedingly faint lines of the neon I spectrum lying between 1μ and 2μ have been discovered and their wave-lengths measured.

THE following paper is the result of the work done during the winter of 1930–31 in an attempt to increase the resolution of infrared spectrometers. The work to be done in the near infrared region now consists almost entirely of the examination of fine structures; a work which is constantly demanding higher resolving powers. With the help of the resonance radiometer[1] and a carefully constructed spectrometer it is believed than an instrument has been developed which partially fulfills the requirements of high resolution and of wavelength accuracy. The resonance radiometer has been used only in those cases where the more easily manipulated direct deflection amplifier has proved not sensitive enough.[2]

Resolving power in the infrared has already been carried as high as ten thousand by Ignatief[3] when he resolved the helium line at 1.0830μ. The method he employed to obtain such high resolution was that of using a Fabry and Perot interferometer arrangement. However, the difficulty of interpreting the results and the minuteness of the spectral range of such an instrument render it unsuitable for most purposes. Therefore the work described here was devoted entirely to the grating spectrometer with the hope of increasing its efficiency to that obtained by Ignatief. This would mean that it would be possible to resolve lines as close together as one frequency unit throughout the near infrared range. The two factors tending to increase the sensitivity of the spectrometer which have been most carefully considered in this paper are the optical perfection of the spectrometer and increased bolometric sensitivity. It is recognized that the matter of suitable sources for infrared use is a most important factor, and although some work has been done along that line nothing very definite has been accomplished.

Pfund and later Barnes[4] have described methods for obtaining very sharp

* National Research Fellow.

[1] J. D. Hardy, Rev. Sci. Inst. **1**, 429–448 (1930).

[2] The instrument referred to here is not the "Moll thermo-relay," but is the Pfund grid amplifier which is used to amplify the deflections of galvanometers. See reference 6.

[3] Ignatief, Ann. d. Physik **43**, 1117–1136 (1914).

[4] R. B. Barnes, Phys. Rev. **36**, 296–304 (1930).

lines by using the mirrors of a spectrometer exactly upon their optic axes. Barnes has discussed the futillity of using very narrow slits, in order to increase the resolving power of an instrument, beyond the point where the defects in the optical images formed by the mirrors become noticeable. The test for this lower value of slit width can be easily made by placing the eye behind the exit slit and observing the illumination of the grating as the slits are narrowed. As soon as it becomes evident that further narrowing of the slits results in rather large unilluminated areas in the grating the narrow limit of useful slit widths has been reached. A further narrowing will not only not increase the available detail in the spectrum but will result in a great loss of energy. Several tests were made by the author on spectrometers whose mirrors were used but ten degrees off their optic axes, and when the slits had been narrowed to 0.1 mm only about sixty percent of the grating was illuminated. It was thus evident that where high resolution is desired more carefully constructed optical systems must be employed. Is is obvious that with more perfect optical systems a saving in energy will be had.

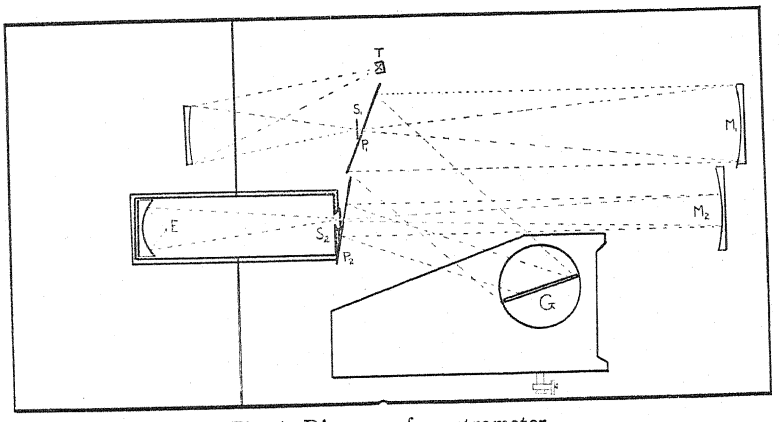


Fig. 1. Diagram of spectrometer.

In accord with this idea a spectrometer was constructed on the plan suggested by Barnes with the difference that the mirrors were of one meter focus and that the last focusing mirror could be replaced by a mirror of four meters focus when high dispersion was desired. A diagram of the spectrometer is shown in Fig. 1. The light from the source T is received by a convex mirror and brought to a focus upon the entrance slit of the spectrometer. (While investigating emission spectra between 1μ and 2μ no fore-prism was used to separate the orders, but an infrared filter was placed in the path when wavelengths longer than 1.2μ were to be examined.) The light on passing through the first slit passes through a hole in the center of the plane mirror P_1. It is then received by the parabolic mirror M_1 and returned directly back to the plane mirror P_1 which reflects the parallel beam onto the grating. The diffracted beam is received by a second plane mirror and sent to the focusing mirror M_2 which focuses the light through a hole in P_2 onto the exit slit. The image thus formed is very sharp and well defined on both sides even when

examined under considerable magnification. The light is finally received by a short focus mirror and brought to a focus upon the thermocouple.

The mirrors M_1 and M_2 are parabolic mirrors with their optic axes through the centers; they are eight inches in diameter and of one meter focus. They were tested and found to be acceptable, although no by and means perfect, as were also the plane mirrors. The last mirror M_2 could be removed and a spherical mirror of four meters focus substituted for it. The reason for substituting such a long focus mirror is simply to spread out the spectrum and allow the use of slightly wider slits, because after the width of the slits has been reduced to a certain point the dust lines, slit imperfections, and diffraction become very important. The introduction of this mirror causes a decrease in energy of six fold, due to the increased size of the image formed; the increase in dispersion is four fold. The grating used in this experiment was a five inch Rowland grating with 15,000 lines to the inch, which gives very sharp lines and a good intensity in the first order. The position of the grating was determined by means of a graduated circle provided with a reading microscope, and any position could be determined with an accuracy of one second of arc, which corresponds to 0.2A.

The thermocouple is of Pfund's design and was constructed by the author. It is exceedingly sensitive and was so constructed that its action in a vacuum is rapid enough to permit its being used with the resonance radiometer without appreciable loss of sensitivity. Direct comparisons, under identical conditions, were made between the thermopiles (three junctions) constructed by Firestone[5] and the single junction element in use in the spectrometer. It was found that in vacuum the single junction thermocouple would give more than three times the deflection produced by the three junction thermopile and its action more than twice as rapid. More recent experiments with thermocouples of this type have lead to the conclusion that an additional increase in sensitivity of five fold can be expected when the elements are used at the temperature of liquid air.

The thermocouple, by a switching arrangement, could be connected to either the resonance radiometer or to a Leeds and Northrup galvanometer. The Pfund thermoelectric amplifier[6] served equally well for both instruments. The amplifier, set upon a small table, could be set up in front of the first resonance galvanometer, and with the second thermocouple connected to the second resonance galvanometer the spectrometer was ready to be used with the resonance radiometer. By moving the table with the amplifier over in front of another shelf, upon which were mounted two Leeds and Northrup high sensitivity galvanometers, with one galvanometer connected to the thermocouple in the spectrometer and the other connected to the thermocouple in the amplifier, a very efficient steady-deflection amplifier could be obtained. (This arrangement, which is more rapid in its response, was used for all survey work and was replaced by the resonance radiometer only in those cases where the highest possible sensitivity was needed.) The amplifi-

[5] F. A. Firestone, Rev. Sci. Inst. **1**, 630–649 (1930).
[6] A. H. Pfund, Science **69**, 71 (1929).

cation could be varied both by changing the intensity of the amplifier lamp and by changing the spacing of the grids. Two sets of grids were used with this amplifier; one set, with a spacing of 1 mm, to give amplifications ranging from 2500 to 15,000 was used entirely with the resonance radiometer; the other set, with 2 mm spacing, to give a range from 50 to 2500, was used with both instruments. The advantage of this type of amplifier is obviously the large range of amplifications and its steadiness even while being pushed to the highest amplification possible. When working with the Leeds and Northrup galvanometers an amplification of six hundred was used, and the steadiness was such that readings could be made in the daytime as well as at night. The principal source of unsteadiness was found to be of an electrical nature and

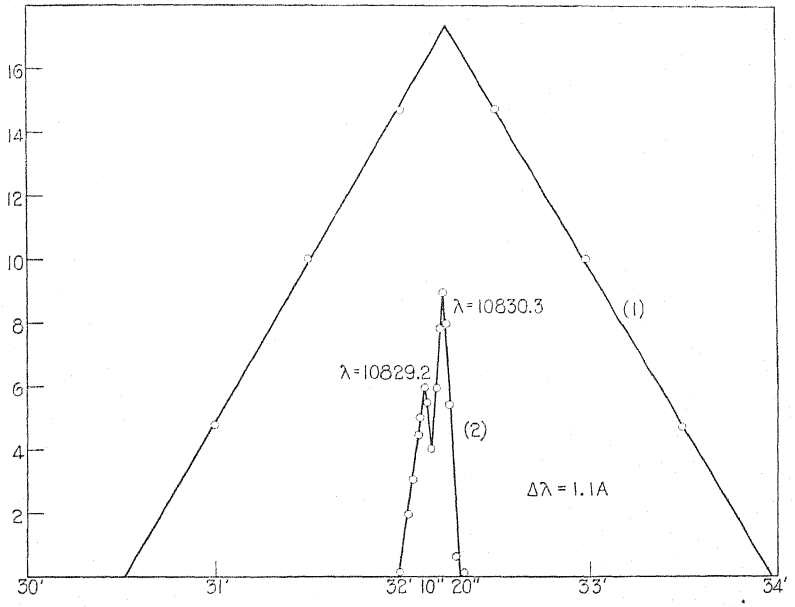


Fig. 2. Helium line at 10,830A. (1) Energy curve with astigmatic spectrometer (unamplified deflections). (2) Energy curve under high dispersion with new type spectrometer (resonance radiometer).

this was reduced, although not eliminated, by carefully shielding every part of the galvanometer circuit. When working with the resonance radiometer an amplification of 6000 was generally used.

After the spectrometer had been set up and focused, tests similar to the ones described above were made to determine the advantage to be gained in line sharpness with narrow slits. It was found that the grating was completely illuminated even with slits so narrow that diffraction prevented further examination. The instrument was calibrated by means of the visual and infrared lines of helium, and the calibration was checked along with the position of the central image at frequent intervals, although they appeared to change very little. The temperature in the basement room in which the spectrometer is located did not vary more than one degree centigrade over long periods of time, and therefore the grating error due to temperature was found to be negligible.

In order to test for the highest resolution that could be realized with the instrument by using ordinarily strong and constant sources, it was decided to examine the 1.0830μ line of helium and see if it were possible to resolve it into its components. The source of radiation was a small glass Geissler tube provided with a capillary 1 mm in diameter. The tube was used 'side on,' and was connected to a neon-sign transformer which was operated from the 110 volt a.c. circuit. The intensity of this source was such that with the spectrometer set on the line and with slits 0.1 mm wide, a deflection of 4 cm was produced by a L and N galvanometer with scale at three meters. The amplifying system was set up and the slits narrowed until no deflection could be detected. However, the helium line could not be resolved. The long focus mirror was then substituted for the parabolic mirror and the slits opened up until the entrance slit was 0.01 mm and the exit slit 0.03 mm. Then with the

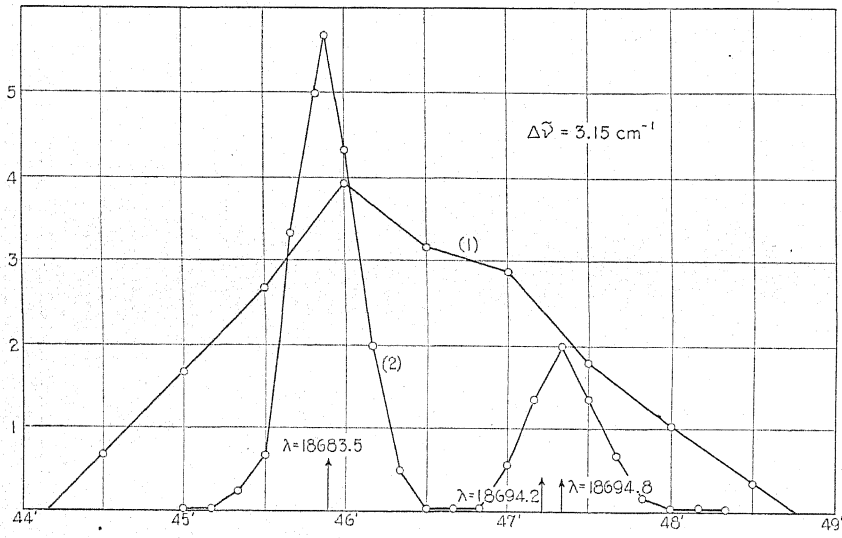


Fig. 3. Helium line at 1.868μ. (1) Curve by Paschen 1908. (λ' position of companion line as deduced by Paschen). (2) Curve with new spectrometer.

help of the resonance radiometer the line could be very nicely resolved. During later experiments a much more powerful source was developed so that it was possible to resolve the line even with the amplified deflections of a L and N galvanometer.

It will be noticed that the "effective slit width" used above is about 0.3A. while the separation between the lines is narly four times that amount. The author has found repeatedly that the "slit-width" must be from a third to a half the amount to be resolved.

Several other lines of the helium spectrum were observed and the line at 1.868μ is shown in Fig. 3, with the line as first observed by Paschen[7] in 1908. This line was observed with wider slits and without the use of the long focus mirror.

The efficiency of the spectrometer was next tested in the matter of energy

[7] F. Paschen, Ann. d. Physik 27, 537–564 (1908).

conservation. The infrared spectrum of neon, which is very faint, was examined between 1μ and 2μ. The slits of the spectrometer had to be opened to a width of 0.8 mm, with the result that the wave-lengths of the lines could not be determined with as great an accuracy as might be desired. The spectrum of neon had been extended photographically by Gremmer[8] out to a wave-length of 9665.0A, and beginning with this line the region out to 2μ was examined. Most of the lines found gave deflections about one hundredth that produced by the visible yellow line at 5852A.

TABLE I.

Wave-length (vacuum)	Intensity	Frequency		Combination
9667.6	8	10343.8	0.5	$(^2P_{1\frac{1}{2}})3p1_1-(^2P_{1\frac{1}{2}})4s1_2$
10564.3	10	9466.1	0.7	$(^2P_{\frac{1}{2}})3p10_0-(^2P_{\frac{3}{2}})3d12_1$
10624.8	1	9411.8	0.3	$(^2P_{1\frac{1}{2}})3p4_1-(^2P_{\frac{1}{2}})4s4_1$
10800.6	3	9258.7	0.3	$(^2P_{1\frac{1}{2}})3p4_1-(^2P_{\frac{1}{2}})4s3_0$
10849.5	7	9217.5	0.5	$(^2P_{1\frac{1}{2}})3p5_2-(^2P_{\frac{1}{2}})4s4_1$
11142.5	13	8974.9	0.1	$(^2P_{1\frac{1}{2}})3p3_2-(^2P_{1\frac{1}{2}})4s2_1$
11178.8	14	8945.6	0.9	$(^2P_{1\frac{1}{2}})3p2_3-(^2P_{1\frac{1}{2}})4s1_2$
11391.6	4	8778.5	0.7	$(^2P_{1\frac{1}{2}})3p3_2-(^2P_{1\frac{1}{2}})4s1_2$
11410.6	3	8764.0	1.3	$(^2P_{\frac{1}{2}})3p7_1-(^2P_{\frac{1}{2}})4s4_1$
11527.7	25	8674.5	0.1	$(^2P_{1\frac{1}{2}})3p4_1-(^2P_{1\frac{1}{2}})4s2_1$
11540.0	5	8665.5	0.4	$(^2P_{\frac{1}{2}})3p10_0-(^2P_{1\frac{1}{2}})3d6_1$
11616.8	3	8608.0	0.1	$(^2P_{\frac{1}{2}})3p7_1-(^2P_{\frac{1}{2}})4s3_0$
11771.1	4	8495.0	0.3	$(^2P_{\frac{1}{2}})3p9_1-(^2P_{\frac{1}{2}})4s4_1$
11789.4	4	8482.4	0.1	$(^2P_{\frac{1}{2}})3p4_1-(^2P_{1\frac{1}{2}})4s2_1$
11989.5	2	8341.0	0.5	$(^2P_{\frac{1}{2}})3p9_1-(^2P_{\frac{1}{2}})4s3_0$
12069.2	10	8285.7	0.4	$(^2P_{1\frac{1}{2}})3p5_2-(^2P_{1\frac{1}{2}})4s1_2$
12461.0	1	8024.8	0.8	$(^2P_{1\frac{1}{2}})3p7_1-(^2P_{1\frac{1}{2}})4s1_2$
12597.4	1	7938.4	0.2	$(^2P_{\frac{1}{2}})3p8_2-(^2P_{1\frac{1}{2}})4s2_1$
12692.7	2	7878.4	0.6	$(^2P_{1\frac{1}{2}})3p6_0-(^2P_{1\frac{1}{2}})4s2_1$
12770.0	0.3	7830.8	1.8	$(^2P_{\frac{1}{2}})3p7_1-(^2P_{1\frac{1}{2}})4s1_2$
12915.0	2	7742.8	0.1	$(^2P_{\frac{1}{2}})3p8_2-(^2P_{1\frac{1}{2}})4s1_2$
13222.0	1	7563.1	0.2	$(^2P_{\frac{1}{2}})3p9_1-(^2P_{1\frac{1}{2}})4s1_2$
15237.0	2	6562.9	0.1	$(^2P_{\frac{1}{2}})3p10_0-(^2P_{\frac{1}{2}})4s4_1$
17168.0	1	5824.8	0.2	$(^2P_{\frac{1}{2}})3p10_0-(^2P_{1\frac{1}{2}})4s2_1$
18081.0	1	5530.7	2.2	$X-(^2P_{1\frac{1}{2}})3d2_1$
18274.0	3	5472.3	5.0?	$Y-(^2P_{1\frac{1}{2}})3d4_3$
18309.0	1	5462.0	0.2	$X-(^2P_{1\frac{1}{2}})3d3_4$
18389.0	2	5438.0	5.0?	$Y-(^2P_{1\frac{1}{2}})3d6_1$?
18433	1	5425		
18552	1	5390		

In Table 1 are given the wave-lengths, the intensities, and the probable classification of these lines. The intensities given are proportional to the deflections produced and are therefore purely arbitrary. The lines in the region around 1.8μ are apparently due to combinations between the $3d$ levels and the X and Y groups, and although the wave-lengths have been checked as well as possible the agreement with the calculated frequencies from the known terms does not check very well with the experimental values.

The usefulness of the spectrometer in the matter of band spectra has been demonstrated in the examination of the 3μ absorption band of ammonia; the results of which will appear shortly. The infrared emission spectra of krypton and xenon are now under investigation.

The author wishes to express his appreciation to Professor H. M. Randall for his advice and many helpful suggestions.

[8] W. Gremmer, Zeits. f. Physik 50, 716 (1928).

RAMAN EFFECT FOR BENZENE SUBSTITUTION PRODUCTS BY IMPROVED TECHNIQUE

By R. W. Wood
Johns Hopkins University

(Received November 2, 1931)

DURING the past summer a book entitled "The Smekal-Raman effect" by K. W. F. Kohlrausch has been published. It contains tables of the Raman lines, expressed in frequency differences for some three or four hundred organic compounds and a vast number of inorganic salts.

So much discussion has occurred in the past as to the reality of certain faint lines recorded in various publications, that it seems worth while to publish results obtained during the past winter on the spectra of some of the substances which have been studied by many observers. The object of the investigation was to improve the technique of mercury arc excitation to the highest possible degree, as this is the most generally available source of light. Few observers are equipped to work with a helium lamp, which as I showed some years ago, was superior in some respects to the mercury lamp.

My feeling was that many of the published tables contain errors. Some observers work with unfiltered radiation, measuring all the lines, and taking frequency differences of the various combinations, and finally selecting the true lines due to a monochromatic excitation. This is a very laborious and risky proceeding.

Filters should always be used. Quinine sulphate dissolved in dilute sulphuric acid is the most efficient for removing 4046, but it turns yellow under the action of the light and must be renewed every half hour or so.

After trying to stabilize it chemically, I finally found that the photochemical change is due chiefly to the 3650 group of lines, and these are absorbed by noviol glass, which however transmits 4046.

If noviol is used of sufficient density to cut off 4046, the 4358 line is also much reduced in intensity. This is the trouble with the Zeiss glass filter recommended for 4358 excitation. It appears to be the same as noviol, showing a red fluorescence when under mercury arc illumination. A thin sheet of pale noviol combined with quinine is the most efficient filter, for complete absorption of 4046 and perfect transmission for 4358. The most suitable thickness is noviol "O", 2.5 mm obtainable ground and polished from the Corning Glass Company, Corning, N.Y. A plate six inches square should be ordered, cut into strips 2×6. I now use a Hanovia 220-volt quartz arc in the metal housing turning on trunnions as supplied by the manufacturers. The burner is operated in a horizontal position just below a narrow aperture in the roof of the iron box. The noviol plate is supported about 1 cm above the aperture as shown in Fig. 1, and a bent sheet of thin aluminum directs the air blast of an electric fan across the aperture under the noviol plate. The fluid filter is

contained in a glass tube 5 cm in diameter and 25 cm in length mounted just above the aperture. This acts as a cylindrical lens as well, forming an image of the arc along the axis of the tube containing the liquid under investigation, constructed as described in my earlier papers. Over this is placed a reflector of thin highly polished sheet aluminum now obtainable in the market. This disposition has proved the most satisfactory of any I have tried. It should be mounted about two meters from the spectrograph, and an image of the end of the tube focussed on the slit with a lens of about 25 cm focus. I made this adjustment by mounting a small disk of white paper against the front window of the tube, and illuminating this strongly with a lamp. Its image can then be seen on the slit. This arrangement gives maximum illumination with a minimum of parasitic light. For excitation by 4046 I employ a tube filled with a solution of iodine in carbon tetrachloride, a saturated solution should first be made, and diluted for use. A 1:10 dilution will reduce 4358 by about the right amount. It can be abolished entirely with a 1:5 dilution, but 4046 will then be considerably reduced as well. With a dilution of 1:35 the excitation is by both 4046 and 4358 but the continuous background is considerably reduced

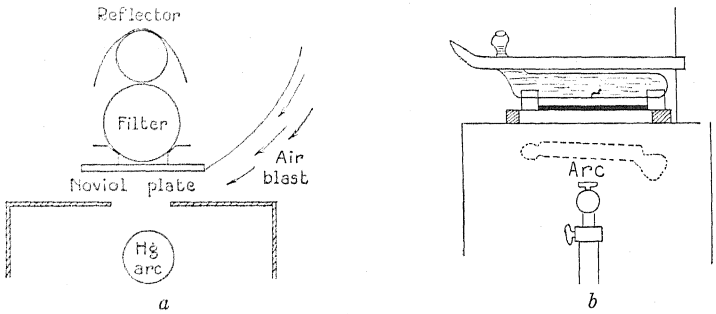


Fig. 1.

between these two lines and faint Raman lines come out which cannot be well seen without the iodine filter. I believe that the best method to follow, and the one most likely to give results free from error is to take two photographs of each substance, one with the noviol quinine filter, and one with noviol iodine, the noviol suppressing 3650, and the iodine 4358.

It is very helpful to make enlargements of each, on such scales that the Raman lines can be brought into coincidence, as shown by Plate I, Figs. *a* and *b*. In other words enlarge the 4358 excitation more than the 4046, which is more dispersed by the prism spectrograph, mark on the 4046 plate or enlargement all lines excited by 4077. This can be done by simply making two marks on a plate or slip of paper separated by the distance between 4066 and 4077 and then fitting the left-hand mark to all of the strongest lines; if the right-hand mark coincides with a much fainter line the chances are that this was excited by 4077. The distance between the two marks must be slightly reduced as we move up the spectrum, of course. Examining spectrum *a*, we see at once that line 177 obtained with 4358 excitation would not be found with 4046 excitation as it is in coincidence with 4077. In general we can be fairly

sure that lines which appear in both spectra are real. For example, in spectrum *a* one might easily come to the conclusion that lines 1161 and 997 were

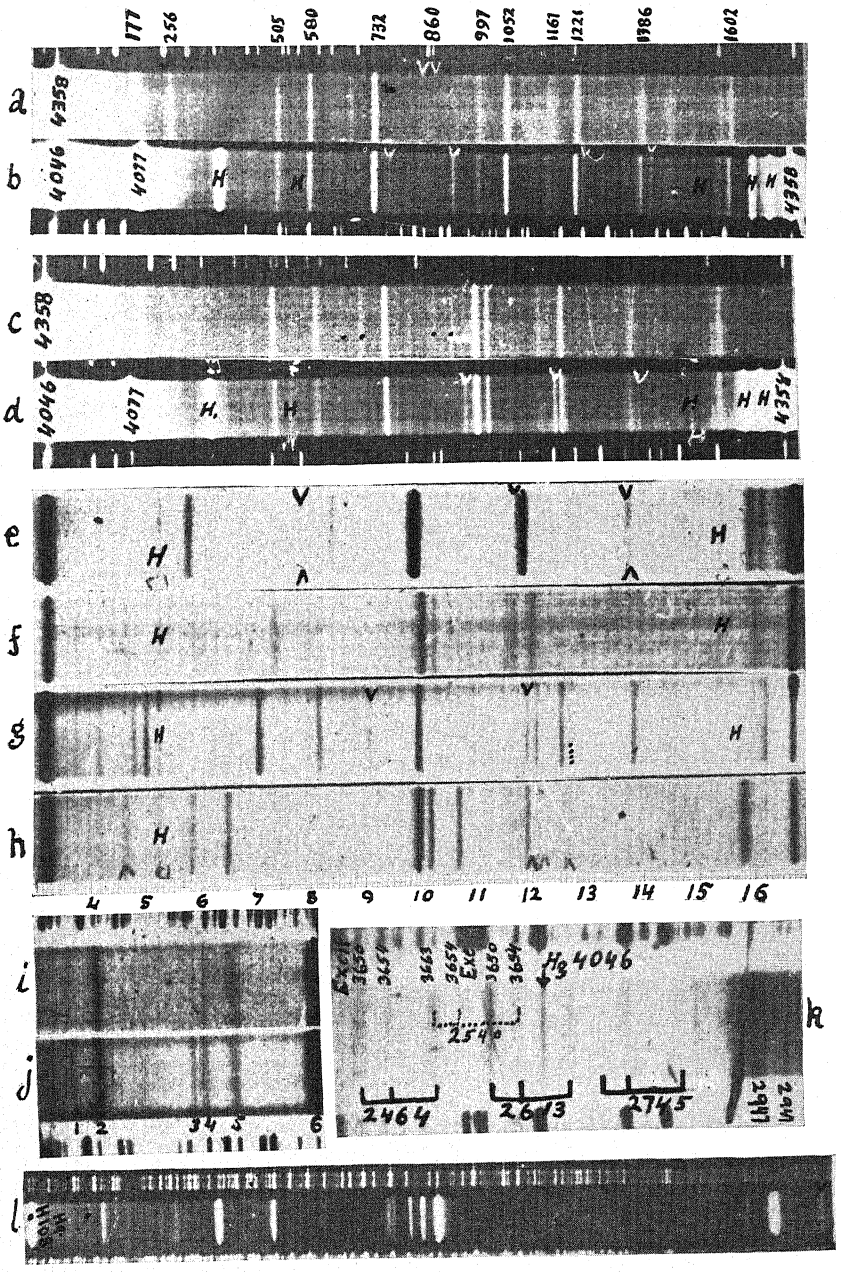


Plate 1.

merely the 4348 excitation of lines 1221 and 1052 (exicted by 4358) but they are found also in the lower spectrum, though much narrower, as in spectrum *a* they are fused with the lines excited by 4348.

In general the spurious lines are more readily picked out by mere inspection in the case of 4358 excitation than with 4046, as they form triplets with the real lines which can usually be recognized at a glance shown by dots in Fig. *c*. The greater separation of 4046 and 4077, makes it difficult or impossible to pick out the lines due to 4077 without measuring their distance from the 4046 lines as described. For study of the fine structure of the complicated Raman band at 3050, excitation by 4046 is all that is necessary, as the band then occurs in a region free from mercury lines and of high photographic sensitivity. With 4358 excitation, however, the band falls at a point of very low sensitivity just above the two mercury lines at 4915.

We will now examine in detail some of the results obtained by this method.

Benzene

The lines given in the table in Kohlrausch's book are the only ones which are real. Bhagavantam reported some new lines not recorded by others. I have investigated these with great care. 4163.8 does not exist. 4494.2 was wrongly assigned to 4358; it is excited by 4046 and gives $\Delta\nu = 2455$, one of the faint lines in the group which I reported in an earlier paper and which will be more fully discussed presently. 4438 assigned by Bhagavantam to 4046 excitation is probably in reality excited by 3906 giving $\Delta\nu = 3068$. Line 4397 was not found. It may have the band of reflected light from the back of the plate, which often resembles a broad line.

4513 unassigned by Bhagavantam (he suggests 4358) is in reality excited by 4046 giving $\Delta\nu = 2543$ which belongs to the group mentioned above.

The spectrum excited by 4046 with a filter of noviol glass and iodine in carbon tetrachloride is reproduced on Plate I Figs. *e* and *l*. In the former lines excited by 4077 are marked with a *v*. In the latter the entire spectrum up $\Delta\nu = 3050$ is reproduced in coincidence with the iron spectrum. Hg 4339–4358 appears at the center greatly reduced in intensity and giving rise to no Raman lines. Line 2947 is very distinct, and 3162–3185 show in the print. The line at the extreme right is due to 4077 excitation.

Toluene

In previous tables a single line only is given $\Delta\nu = 1604$. There are really two lines here as with benzene, the one of shorter wave-length being less intense. The double line was obtained both with 4046 and 4358 excitation as is shown by Figs. *c* and *d* of Plate I. With 4046 excitation they fall just to the left of 4339 Hg. $\Delta\nu = 1604$ and 1583. The other lines of the table in Kohlrausch's book are correct but there seems to be in addition, a faint line to the left of the single bright line at the center of the spectra. In spectrum *c*, the two lines marked with dots are evidently due to 4339–4348 excitation, but in spectrum *d* a faint doublet appears, the left hand member of which may be due to 4077 excitation, and corresponds to the line to the left of the faint mercury line *H*. The right-hand member must be regarded as a real line $\Delta\nu = 720$ and possibly both are. This point can be settled by helium excitation. Lines excited by 4077 are marked with a *v*.

Ortho-xylene

Plate I Figs. *a* and *b* gives a doublet $\Delta\nu = 1602–1580$ instead of the single line 1599 given in Kohlrausch. I cannot understand why other observers have reported only one line here for toluene and the xylenes, as the doublet is almost as conspicuous as in the case of benzene for which all report a doublet. It lies just to the left of the Hg 4358 group in spectrum *b*. The faint line near the center of each spectrum marked *w* is not given in Kohlrausch. Its $\Delta\nu$ is 860. Line 1023 given by Kohlrausch does not appear on either spectrogram. His other lines are correct. The $\Delta\nu$ values are given above the lines of spectrum *a*.

Meta-xylene

Plate I Fig *g*. We find a doublet as with ortho-xylene, $\Delta\nu = 1612–1593$, instead of a single line as given in Kohlrausch. A new line not recorded previously, and marked by a vertical row of dots, $\Delta\nu = 1265$. For the next two lines to the left, I obtain 1250 and 1205. Kohlrausch gives 1245 and 1180, the latter is obviously incorrect as it gives too great a separation of the lines. This can be seen at once if the $\Delta\nu$ values given in Kohlrausch's table are plotted on millimeter cross-section paper and the map thus obtained fitted to Fig. *g*. This scale is the same for both except for a slight variation due to prismatic dispersion. It is thus seen that Kohlrausch's 1180 line is the line marked with a *v* and excited by 4077. It can be seen also that the relative intensities recorded in Kohlrausch's table are far from correct, as he gives 1030 and 1180 at the same intensity one while the spectrogram shows the latter many times brighter. A millimeter scale graduated to $\Delta\nu$ values is given below spectrum *h*. This is only approximately correct, but serves for the identification of the lines.

Para-xylene

The lines 959 and 1012 given in the table in Kohlrausch were not found with 4358 excitation. With 4046 excitation a line was found giving a $\Delta\nu$ of about 1012 but it was due to 4077 excitation of the 826 line, and is therefore to be rejected. $\Delta\nu = 540$ was not found. The short wave-length component of the doublet at 1600 was very faint in this case. 1460 is diffuse and faint and a new line $\Delta\nu = 1325$ narrow and moderately strong was recorded.

Brom-benzene

The lines checked well with Kohlrausch's values, but 1369 failed to appear. It is recorded as very faint however.

Diphenyl oxide

This substance has not been previously investigated. Its spectrum was photographed when in the fluid state, the following lines being found.

$\Delta\nu = 1600$ (2) broad, 1195 (4), 1160 (2), 1020 (3), 1000 (3), 750 (2), 565 (0)? and about a dozen of smaller values not yet measured.

Diphenyl

Previously reported by the author shows the double line 994–1022, as well as lines 1191 and 1146. The strong line 1283 of diphenyl does not appear with the oxide.

Diphenyl-disulphide

In liquid state: 1600 broad (2), 1060 (2), 1020 (2), 1000 (2). These have about the same intensity while, in the case of the oxide 1000 is about three times stronger than 1020.

Anti-Stokes lines of benzene, toluene, and xylene

The existence of anti-Stokes lines in the case of benzene has been so vigorously denied by some investigators, working under conditions which were claimed to be superior to those previously employed, that it seems worthwhile to publish a spectrogram proving conclusively that such lines exist. Traces of them were shown in one of my earlier publications, but I now have plates which really bear reproduction and from which intensity ratios can be determined. Two spectrograms are shown on Plate I Figs. *i* and *j*, the upper made by Hg 4046–4077 excitation, the lower with 4046 and 4358. Line No. 3 appears only in the latter. It is the anti-Stokes line excited by 4358, its wavelength being 4178 and the frequency difference -990. The upper spectrogram was taken with the dense iodine filter combined with noviol glass, which absorbs 3650 and 4358. The lines in the spectrogram are as follows:

1. Mercury
2. $\Delta v =$ 606 excited by 4046
3. $\Delta v = -990$ excited by 4358
4. $\Delta v =$ 606 excited by 4077
5. $\Delta v =$ 845 excited by 4046
6. $\Delta v =$ 990 excited by 4046.

We see from the photograph that the anti-Stokes line has very nearly the same intensity as the 606 line excited by 4077. The superior contrast in this spectrogram was due to the suppression of the continuous background. A filter of noviol glass was employed combined with a very dilute iodine solution, not sufficiently dense to reduce greatly 4358. (saturated solution diluted 1:35.) This combination gives much cleaner spectra than those obtained with no filter. On a plate taken with a quinine filter combined with noviol glass only line No. 3 appeared, together with the other anti-Stokes line $\lambda = 4246.7$, $\Delta v = -606$. Two anti-Stokes lines came out very clearly in the case of toluene excited by 4358, also with para-xylene. In the latter case, the lines were measured giving Δv values -458 and -314, in good agreement with the values 461 and 315.

In a previous communication on the Raman effect, I recorded the presence of a number of faint lines in the spectrum of benzene in the region lying on the short wave-length side of the strong double band with $\Delta v = 3060$. One of these ($\Delta v = 2947$) has been noted by other observers. These lines appear only when

the continuous background has been suppressed to the highest possible degree. Further investigation, with improved technique has confirmed the suspicion that the actual presence of certain of these lines depended on the wave-length of the exciting light, lines obtained with excitation by helium 3888 not being found with mercury 4046.

The $\Delta\nu$ frequencies for these lines are given in the following table:

New lines of benzene

2465	2745
2545	2765
2596 (obtained only with helium excitation.)	2930
2615	2947.

Their presence has been verified with the following excitation wave-lengths; 5461, 4358, 4046, 3888, 3663, 3654, and 3650. Their relative intensities with these different types of excitation is roughly shown in Fig. 2.

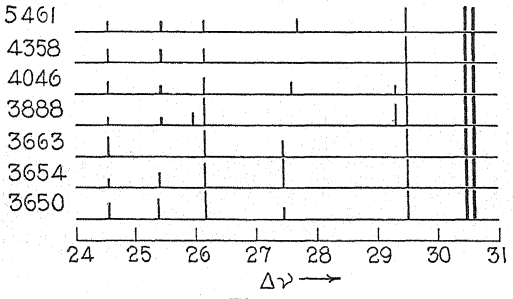


Fig. 2.

It was at first thought that the intensity differences found at different times with different excitations might result from a change in the benzene, due to continued illumination or impurities. But this seems not to be the case, for a marked difference in the intensity ratios was found when the lines were excited simultaneously by the three lines making up the mercury group at wave-length 3650–3663, in which case each Raman line appears in triplicate. A filter of nickel oxide glass was used in this case. A portion of the spectrogram is reproduced much enlarged on Plate I, Fig. *k*. In the interpretation of this spectrum we must remember that the intensities of the exciting lines are very different. 3650 is much brighter than 3663, which in turn is brighter than 3654.

I have bracketed the lines which I believe belong together, the $\Delta\nu$ values being written below the brackets. It appears that two superpositions occur, which complicates the interpretation. There seems, however, to be strong evidence of a change in the intensity ration of the Raman lines for the three different excitations. The most conspicuous effect is obtained with helium 3888 excitation. Here we have a very distinct doublet at $\Delta\nu = 2596$–2615. No trace of the former line being found with any other excitation. Helium excitation also seems to be peculiar in that it gives benzene lines $\Delta\nu = 1178$, 1584,

and 1603 of the same intensity, while with 4046 and 4358 excitation the 1178 line is very much brighter than the other two. This matter will be more fully investigated shortly.

Explanation of plate

a. Raman spectrum of ortho-xylene excited by Hg 4358. Filter of noviol glass and sulphate of quinine. Line $\Delta v = 860$ not previously recorded marked with white *w*.

b. Ortho-xylene spectrum excited by 4046–4077. Filter of noviol glass and iodine in carbon tetrachloride. Lines excited by 4077 marked with a white *v*. Line $\Delta v = 860$ appears here also. The 4358 mercury group is at extreme right. Lines marked *H* are mercury.

c. Spectrum of toluene excited by 4358. Note doublet at right recorded as single line by previous observers. This doublet also appears in *a* and *b*. Quinine and noviol filter.

d. Toluene spectrum excited by 4046–4077. Lines due to 4077 marked *v*, mercury lines marked *H*. Iodine and noviol filter.

4046 *Excitations*

e. Benzene spectrum, reproduced as a negative. Iodine in carbon tetrachloride plus noviol glass as filter. Lines due to 4077 marked *v*. Mercury lines marked *H*. The strong line at the left is mercury 4108, that at the right 4339. The doublet at the left of 4339, ($\Delta v = 1584$–1606) is found with toluene and all three xylenes, contrary to observations by others. It is absent in brom-benzene. Fig. *h*. One 4077 excitation coincides with one by 4046.

f. Diphenyl-oxide. The doublet has fused. No lines excited by 4077 appear.

g. Meta-xylene. Lines excited by 4077 marked *v*.

h. Brom-benzene. The doublet at right shown by other substitution products replaced by a single broad line shifted towards shorter wave-length.

i. j. Anti-Stokes line (No. 3) of benzene. Spectrum *i* taken with iodine filter, which absorbs 4358, and the anti-Stokes line is absent. The lines are as follows: 1. Mercury, 2. $\Delta v606$, excited by 4046. 3. $\Delta v = -990$, excited by 4358. 4. $\Delta v606$, excited by 4077. 5. $\Delta v = 845$. 6. $\Delta v = 990$.

k. New faint lines of benzene in region $\Delta v = 2465$–2947 excited by 3650–54–63. The strong lines at right are $\Delta v = 2947$.

l. Complete spectrum of benzene excited by 4046 with iodine filter the line at right being $\Delta v = 3050$.

THE PASCHEN-BACK EFFECT OF HYPERFINE STRUCTURE I. THALLIUM II AND III

By J. B. Green* and John Wulff*
Mendenhall Laboratory of Physics and Massachusetts Institute of Technology.

(Received September 10, 1931)

Abstract

The Zeeman effect of several characteristic lines of Tl II and Tl III has been studied at field strengths of 14700, 32500 and 43350 gauss. The transition from weak to strong fields shows exceedingly good agreement with the theory of Goudsmit and Bacher. Careful measurements of the magnetic patterns of certain lines indicate that McLennan and Allin's results are inaccurate.

THE magnetic analysis of hyperfine structure permits a more definite determination of nuclear moment than the value interpreted from the interval separations of the hyperfine structure pattern of the fieldless line. The work of Heisenberg and Jordan,[1] Darwin,[2] and Mensing[3] on the Zeeman effect of multiplets for all field strengths has been extended by Goudsmit and Bacher[4] for hyperfine structure. The formulae in both cases are quite similar, yet in the latter the quantum vectors for electron spin and angular momentum, s and l respectively are replaced by the nuclear moment and the total momentum of the remainder of the atom, i and j respectively.

The additional quantum vector i, attributable to the nucleus, causes each line to separate into a tiny multiplet (hyperfine structure) and complicates the Zeeman pattern of the line, analogous to the way in which the electron spin produces an ordinary multiplet and alters the simple Lorentz triplet. The line λ4722 Bi I is no doubt the best example of the objectivity of determination of nuclear moment from the Zeeman effect. Each of the components of this line splits up in a strong magnetic field into ten lines which can be attributed to the presence of a nuclear moment $i=9/2$ having $2i+1=10$ orientations in the magnetic field.

Detailed magnetic analyses have been carried out for the arc spectra of Bi I and Tl I by Goudsmit and Bacher as well as Back and Wulff.[5] McLennan and Durnford[6] have investigated the Zeeman effect of Tl spark lines, yet the lack of resolving power of the spectroscopic instrument as well as the weak

* John Simon Guggenheim Memorial Fellow.
† International Education Board Fellow.
[1] Heisenberg and Jordan, Zeits. f. Physik **37**, 263 (1926).
[2] C. G. Darwin, Proc. Roy. Soc. **A115**, 1 (1927); K. Darwin, Proc. Roy. Soc. **A118**, 264 (1928).
[3] Mensing, Zeits. f. Physik **39**, 24 (1926).
[4] Goudsmit and Bacher, Zeits. f. Physik **66**, 13 (1930).
[5] Back and Wulff, Zeits. f. Physik **66**, 31 (1930).
[6] McLennan and Durnford, Proc. Roy. Soc. **A129**, 48 (1930).

field employed does not permit a complete interpretation. The instruments used in the present work have enabled us to give a more careful analysis of the problem.

Experimental Procedure

The quality of the large concave grating of the Physical Institute in Tübingen permitted the photography of 3rd and 4th order patterns in the visible and 5th order patterns in the ultraviolet. The multicomponent patterns present in the Zeeman effect of hyperfine structure and the small separations involved necessitated the maximum obtainable resolving power. For this purpose the focus of the grating was redetermined with the aid of a series of especially sharp tin lines. The plates rested at an angle, the middle of the plate being on the Rowland circle, the lower half toward the grating and the upper half away from the grating. The spectrograms showed a systematic deviation of the focal curve from a true circle. The final curve determined was found to be slightly elliptical with the minor axes approximately in the position of the normal to the grating. On the empirically determined curve it was possible to adjust the plate holders to insure maximum resolution.

The light source used is described in detail elsewhere. Briefly is consisted of a negative tungsten electrode and a positive electrode of rilled manganin upon which 0.5 mm thickness of Tl was melted. The latter electrode is stationary and isolated from the pole-shoe by a thin strip of mica. The tungsten electrode which is given an intermittent action by a spring eccentric on a constant speed motor makes some 300 contacts per minute. The vacuum chamber was kept at an average argon or hydrogen pressure of 5 mm Hg during the entire exposure. Current was applied at 110 volts and adjusted to 3–5 amperes with suitable rheostats. An inductance of about 100 turns of heavy wire around an iron core in series with the rheostats and a capacity of 5000 cm across the arc served to reduce fluctuations to a minimum. Under these conditions a new positive electrode was inserted about every half hour, and three hours net exposure usually sufficed for proper intensity.

The Weiss magnet had a interferricum of 3.8 mm and the special ferrocobalt pole-tips a diameter of 7 mm. A current of 73 amperes through the water-cooled coils of the magnet gave a field of 43350 gauss. Variations of 1 ampere have no effect on the sharpness of the lines at this field strength and are not detectable with a flip coil. This is to be expected from the calibration curve which shows that saturation is reached in this neighborhood. This was not the case with the two other field strengths employed, namely 32500 and 14700 gauss. Especially with the latter a variation in current of 0.05 amp. affects the sharpness of the lines. Easily controllable rheostats and continual observation were necessary to keep the current constant. During and after the exposure typical cadmium and zinc lines were flashed on the plates to serve as standards for field strength determinations. In many of the patterns studied the separations are at the limit of the resolving power of the grating, an great care had to be exercised in the choice and development of the photographic plate. The special Flieger plates of Perutz in Munich fulfilled all our re-

quirements, of speed, fineness of grain, and sensitivity (2200–5800A). The photometer curves were made with the photoelectric recording photometer at the University of Munich. (Magnification 13 ×) and show fringes which though often attributed to large grain size are here the direct result of the fine photometer slit employed. A wider slit alleviated this disturbance but also failed to bring out some of the fine structure. In any case, it is quite easy to distinguish the real from the apparent maxima.

Theory

The theory of the Paschen-Back effect of hyperfine structure has been admirably discussed by Goudsmit and Bacher[4] and the reader is referred to this paper for a complete discussion of the problem. We shall repeat here only those conclusions necessary for a clearer understanding of the present work.

The hyperfine structure of spectrum lines is caused by the interaction of the total momentum of the rest of the atom with the nuclear momentum, i, (which may have any half or full integral value, including zero). Up to the present, it has not been possible to predict the value of this nuclear moment, and we have had to rely entirely upon experimental data. Further, the different isotopes of the same element may have different nuclear moments. Thus, the progress in this field has not been so rapid as was the case some years ago with complex spectra, when Hund proposed his theory of the coupling of electron spin and angular momentum. Also, the experimental technique involved in the resolution of the very close patterns is very much more difficult than for gross multiplet structure.

In zero field, i and j interact to give a new quantum number f of hyperfine structure, which has either $2i+1$ or $2j+1$ values depending on whether i or j is the smaller of the two interacting vectors. On the basis of the old model theory of the atom, this vector precesses regularly about the field direction H, if H is small, and in the same way as we calculate a g-formula for the vector j, we find for f, a g-formula.

$$g(f) = g(j)\frac{f(f+1) + j(j+1) - i(i+1)}{2j(j+1)}. \tag{1}$$

Thus, in a weak field, each hyperfine energy level is split up into $2f+1$ levels symmetrically situated about the zero field level.

In a strong field the coupling between the i and j vectors is destroyed, and each of the vectors interact independently with the magnetic field. The effect is to introduce a new type of symmetry in which there are associated $2i+1$ equally spaced levels with each of the $2j+1$ orientations of j, m_j, in the magnetic field, the spacings of the $2i+1$ levels being proportional to the value of m_j with which they are associated. Here is seen the origin of the patterns found by Back and Goudsmit[7] in the spectrum of bismuth.

For medium field strengths all symmetry is lost and for the calculation of the positions of the energy levels, we must use the following formula of Goudsmit and Bacher.

[7] Back and Goudsmit, Zeits. f. Physik **47**, 174 (1928).

$$X_{m_i+1,m_j-1}(A/2)(i+m_i+1)(j-m_j+1)+X_{m_i,m_j}$$
$$(E-Am_im_j-m_jg\omega)-X_{m_i-1,m_j+1}(A/2)(i-m_i+1)(j+m_j+1)=0 \qquad (2)$$

where A is the hyperfine structure separation factor, ω the Lorentz separation factor corresponding to the field strength used, E the position of the magnetic level with reference to the center of gravity of the fieldless pattern, and X represents a transition probability.

For a given value of $m_i+m_j=m_f$, the above equation is written for all possible values of m_i and m_j. The determinant of this set of homogeneous equations is set equal to zero and its roots are the values of E for the given m_f. The order of the determinant will be $2j+1$ or $2i+1$ depending on whether j or i has the smaller value.

Thus, in the case of thallium the problem of determining the positions and intensities of the lines from a theoretical standpoint becomes exceedingly simple, since it has been definitely established that the nuclear moment of the Tl atom is 1/2. The equations are, then, all quadratic or linear.

The above theory has been applied very successfully to the spectrum of thallium I and so far has been checked in all details. Spark spectra have much greater hyperfine structure intervals and are therefore easier to resolve. In the spectrum of Tl II and Tl III the visible lines were studied in the magnetic field by McLennan and Durnford[6] but the apparatus used had not a sufficiently high resolving power to give a complete analysis of the lines. Schüler and Keyston[8] have studied the hyperfine structure of Tl II in zero field and we have used their values of the separations in our calculations of the magnetic patterns.

In particular, the lines 3092, 2530 and 2298 of Tl II have been studied at three different field strengths, and 5949 of Tl II and 4110 of Tl III at the maximum field strength, 43350 gauss. The line 3092 has been discussed by us in complete detail elsewhere, and is included here for the sake of completeness, as the simplest example of the Paschen-Back effect of hyperfine structure.

For the line 2298 ($6p^3P_2-7s^3S_1$) as an example, the positions of the levels of $6p^3P_2$ are found from equation (2) as

$$\begin{aligned}
m_f &= 5/2 \quad & E &= A+2\omega g \\
m_f &= 3/2 \quad & E^2+E(A/2-3\omega g)+(2\omega^2g^2-3A^2/2) &= 0 \\
m_f &= 1/2 \quad & E^2+E(A/2-\omega g)-3A^2/2 &= 0 \\
m_f &= -1/2 \quad & E^2+E(A/2+\omega g)-3A^2/2 &= 0 \\
m_f &= -3/2 \quad & E^2+E(A/2+3\omega g)+(2\omega^2g^2-3A^2/2) &= 0 \\
m_f &= -5/2 \quad & E &= A-2\omega g
\end{aligned} \qquad (3)$$

while for the levels of $7s^3S_1$ we get

$$\begin{aligned}
m_f &= 3/2 \quad & E &= A/2+\omega g \\
m_f &= 1/2 \quad & E^2+E(A/2-\omega g)-A^2/2 &= 0 \\
m_f &= -1/2 \quad & E^2+E(A/2+\omega g)-A^2/2 &= 0 \\
m_f &= -3/2 \quad & E &= A/2-\omega g.
\end{aligned} \qquad (4)$$

[8] Schüler and Keyston, Zeits. f. Physik 70, 1 (1931).

The intensities of the components are given by

$m_f \rightarrow m_f$	Parallel polarization
$3/2 \rightarrow 3/2$	$12[X_{1/2,1}X'_{1/2,1}]^2$
$1/2 \rightarrow 1/2$	$8[2X_{1/2,0}X'_{1/2,0} + 3X_{-1/2,1}X'_{-1/2,1}]^2$
$-1/2 \rightarrow -1/2$	$8[3X_{1/2,-1}X'_{1/2,-1} + 2X_{-1/2,0}X'_{-1/2,0}]^2$
$-3/2 \rightarrow -3/2$	$12[X_{-1/2,-1}X'_{-1/2,-1}]^2$
$m_f \rightarrow m_f - 1$	Perpendicular polarization
$3/2 \rightarrow 1/2$	$4[X_{1/2,1}X'_{1/2,0}]^2$
$1/2 \rightarrow -1/2$	$2[3X_{1/2,0}X'_{1/2,-1} + 2X_{-1/2,1}X'_{-1/2,0}]^2$
$-1/2 \rightarrow -3/2$	$6[4X_{1/2,-1}X'_{1/2,-2} + X_{-1/2,0}X'_{-1/2,-1}]^2$
$-3/2 \rightarrow -5/2$	$12[X_{-1/2,-1}X'_{-1/2,-2}]^2$
$m_f \rightarrow m_f + 1$	Perpendicular polarization
$3/2 \rightarrow 5/2$	$12[X_{1/2,1}X'_{1/2,2}]^2$
$1/2 \rightarrow 3/2$	$6[X_{1/2,0}X'_{1/2,1} + 4X_{-1/2,1}X'_{-1/2,2}]^2$
$-1/2 \rightarrow 1/2$	$2[2X_{1/2,-1}X'_{1/2,0} + 3X_{-1/2,0}X'_{-1/2,1}]^2$
$-3/2 \rightarrow -1/2$	$4[X_{-1/2,-1}X'_{-1/2,0}]^2$

The X's are found by substituting the values of E, found by Eqs. (3) and (4), in the original determinantal equations. The umprimed terms refer to the level $^3S_1$, and the primed terms to $^3P_2$.

For the complete details of the calculations the reader is referred to Goudsmit and Backer.

Results

The results are shown in graphical form in Figs. 1–5; below are the theoretical patterns calculated from the theory of Goudsmit and Bacher and above the photometer curves made from the original plates. In comparing the theoretical and experimental curves several facts should be noted: (1) the photometer at best gives integrated results which seldom show the resolution detectable by the human eye; (2) lines just resolvable by the grating may be too close together for the resolving power of the plate which results in a broad diffuse line for a group of adjacent components; (3) lines not resolved by the grating will integrate their intensities in such a fashion that a strong line takes the place of a number of extremely close weak lines.

λ3092. Fig. 1, a, b, c show the parallel and perpendicular polarizations of 3092 Tl II ($6s6p\,^1P_1, -6s7s\,^1S_0$) in the fifth order at field strengths of 14700, 32500 and 43350 gauss. The transition from weak to strong fields is quite evident from the photometer curves. It need only be noted that the separation of the strong doublets in the perpendicular polarization approaches the same value with increasing field, while the two middle parallel components at 14700 gauss merge at 43350 gauss. The magnetic analysis in this case is an excellent check of the theory of the Paschen-Back effect of hyperfine struc-

ture and the value of the fieldless separation deduced therefrom is 0.092 $\pm$0.002A or 0.96$\pm$0.02 cm^{-1} a value slightly different from that found by McLennan and Crawford.

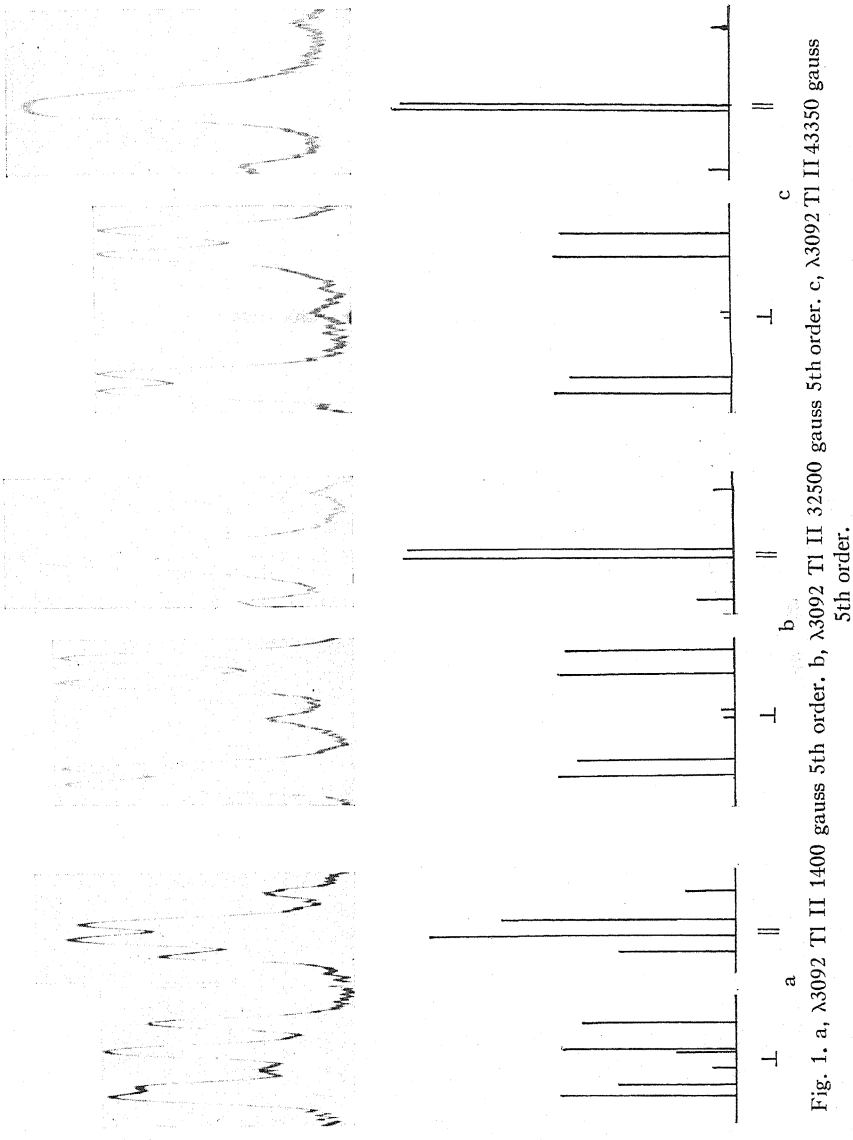


Fig. 1. a, λ3092 Tl II 1400 gauss 5th order. b, λ3092 Tl II 32500 gauss 5th order. c, λ3092 Tl II 43350 gauss 5th order.

λ2298. Figs. 2 a, b, c are taken from the 4th order spectograms of 2298 Tl II ($6s6p^3P_2-6s7s^3S_1$). The magnetic analyses of this line is not so complete as in the previous case (λ3092) yet it may be noted that the unresolved components of the weak fields become more apparent with increasing field strength. The faint side component (so called "forbidden components" of the Paschen-

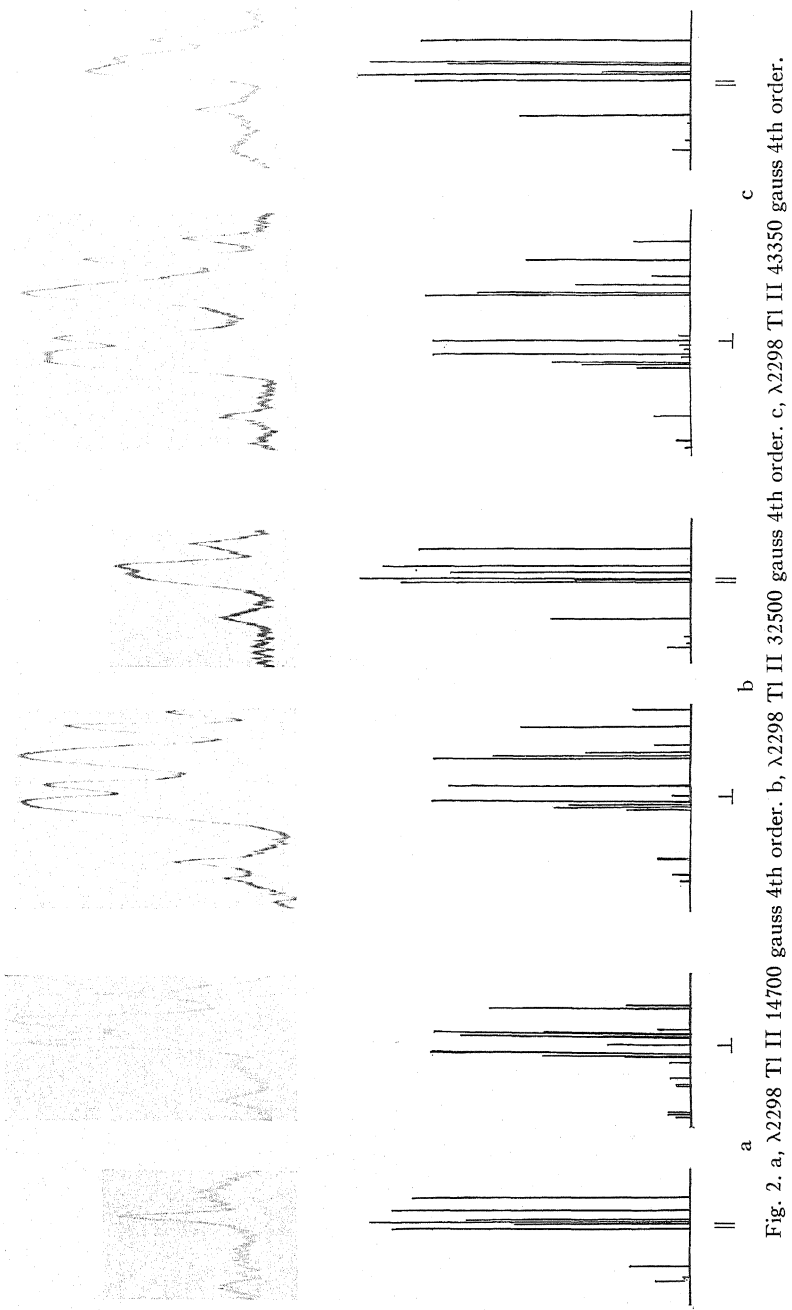


Fig. 2. a, λ2298 Tl II 14700 gauss 4th order. b, λ2298 Tl II 32500 gauss 4th order. c, λ2298 Tl II 43350 gauss 4th order.

Back effect) seem to decrease in intensity with increasing field strength in accordance with the theory.

λ2530. Figs. 3 a, b, c represent 5th order patterns of λ2530, Tl II (6*s*

$6p^1P_1-6s6d^1D_2$) at the above field strengths. Though the perpendicular polarization is in good agreement with the theory, there are discrepancies in the faint side components which have not as yet been accounted for. Here

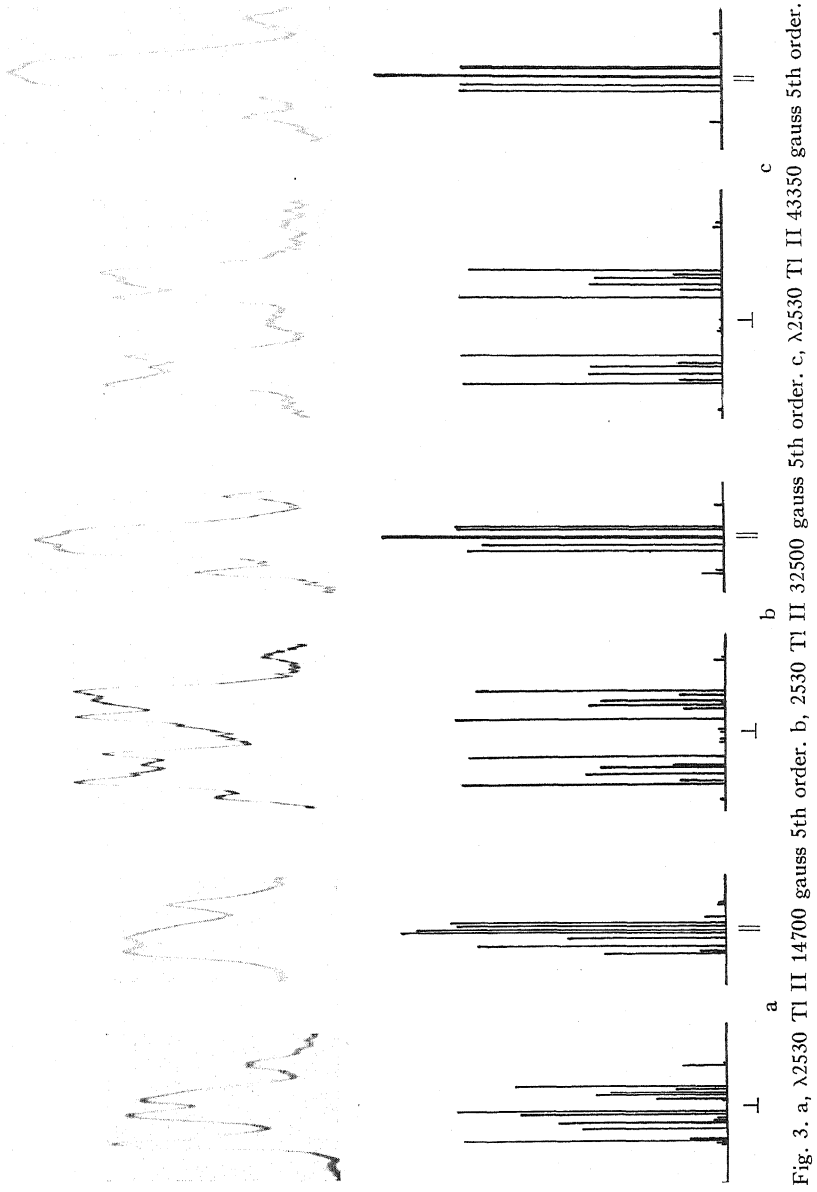


Fig. 3. a, λ2530 Tl II 14700 gauss 5th order. b, 2530 Tl II 32500 gauss 5th order. c, λ2530 Tl II 43350 gauss 5th order.

again it may be noted that the forbidden components decrease in intensity with increasing field.

λ5950. Fig. 4 a and b show both polarizations in the first order of λ5950 Tl II ($6s7s^3S_1-6s7p^2P_2$) at 43350 gauss. From its transition it is evident that

this line is the inverted counterpart of λ2298, which is also evident from the photograph. The increased scale of wave numbers brings out some of the very fine components not apparent in λ2298. The weak component in the center of the perpendicular polarization (on Fig. 4a) belongs to a neighboring line of argon.

λ4110. Fig. 5a, b gives the perpendicular and parallel polarizations of 4110 Tl III ($7s^2S_{1/2}-7p^2P_{3/2}$) in the second order at the high field strength. This line is the counterpart of Tl I 5350 and shows the same general charac-

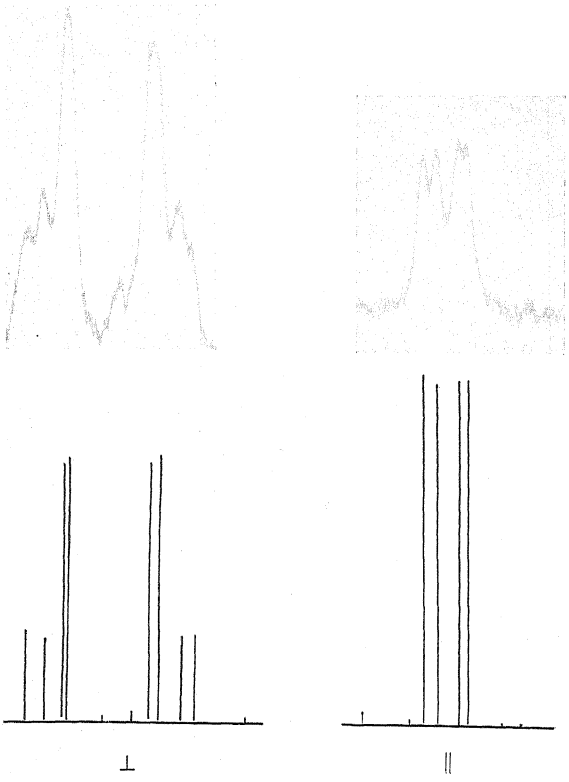


Fig. 4. λ4110 Tl III 43350 gauss second order.

teristics except that the $^2P_{3/2}$ is sufficiently large to influence the separations of the doubling resulting from the nuclear moment $i=1/2$. McLennan and Allin[9] report the separations of $7s^2S_{1/2}$ and $7p^2P_{3/2}$ as 1.37 and 0.44 cm^{-1} respectively. Our measurements on this line are not consistent with these results and indicate that the separation of $7s^2S_{1/2}$ is somewhat smaller, namely 1.24 cm^{-1}. (The faint middle component does not belong to the line; it is the O line 4111).

Conclusion

In the experimental material discussed we have again a very good argument in support of the present status of the theory of the Paschen-Back effect

[9] McLennan and Allin, Proc. Roy. Soc. **A129**, 43 (1930).

of hyperfine structure. The work of Goudsmit and Bacher as well as Back and Wulff has now been definitely applied to spark spectra, such discrepancies which occur are in most cases of a negligible order.

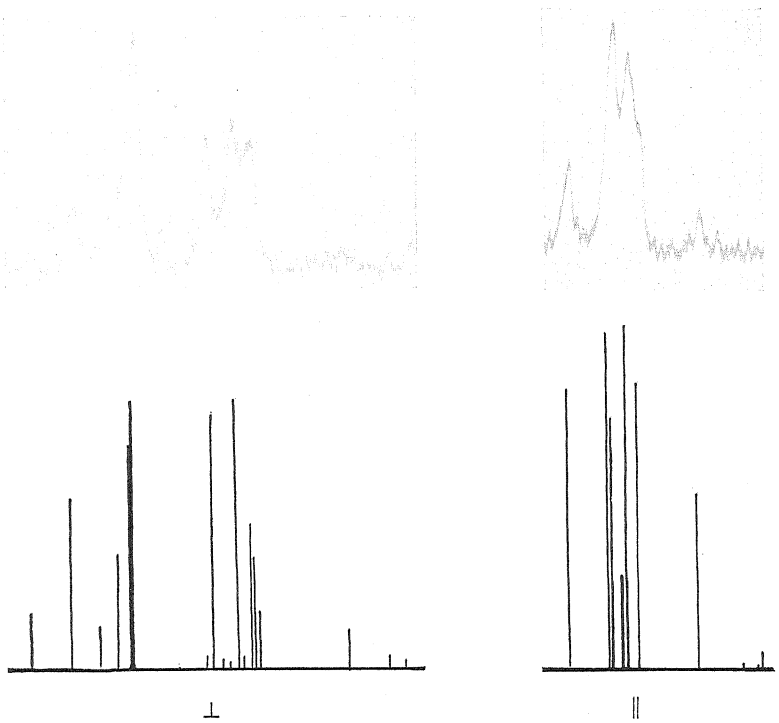


Fig. 5. λ5950 Tl II 43350 gauss first order.

The success of the work can be attributed largely to the excellent apparatus available in Tübingen. To Professors Geiger and Back we extend our thanks for the privilege of working in Tübingen as well as to Professor Gerlach for permitting us the use of the large recording photometer in Munich.

THE PASCHEN-BACK EFFECT OF HYPERFINE STRUCTURE II. Bi II AND Bi III

By J. B. Green* and John Wulff†
Mendenhall Laboratory of Physics and Massachusetts Institute of Technology.
(Received September 10, 1931)

Abstract

Goudsmit and Bacher's theory is successfully applied to the spectra of Bi II and Bi III. The lines λλ5719 of Bi II and 4561 and 3695 of Bi III are used as typical examples of these spectra. λ5719, like 3092 of Ti II, serves as an excellent check on the theory, because of its especially simple transition.

IN A previous paper, the authors showed that Goudsmit and Bacher's[1] theory is quite adequate to explain the complicated Zeeman patterns observed for the hyperfine structure components of the spectra of Tl II and Tl III. The present paper is a continuation of the work and treats the spectra of Bi II and Bi III.

The experimental arrangement was exactly the same as in the previous

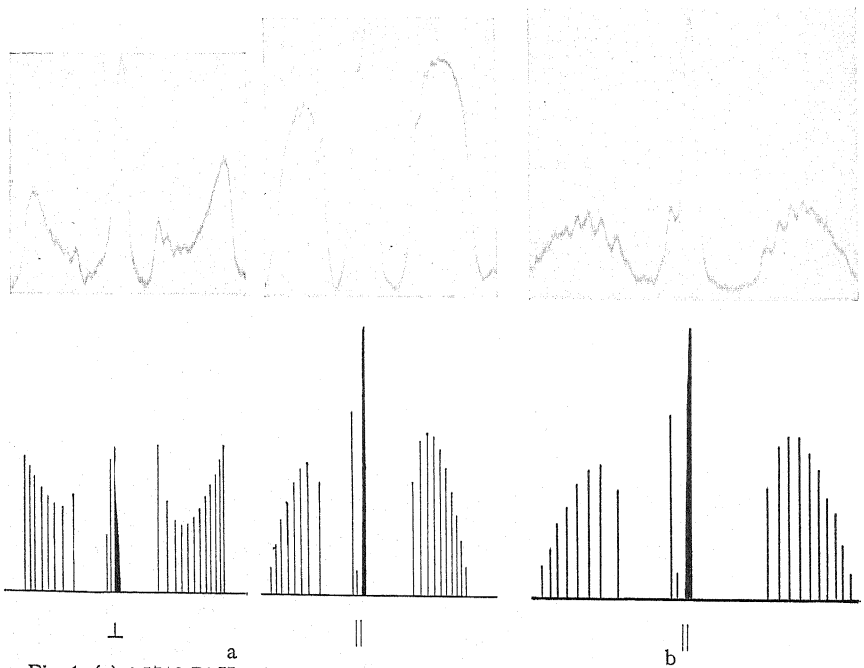
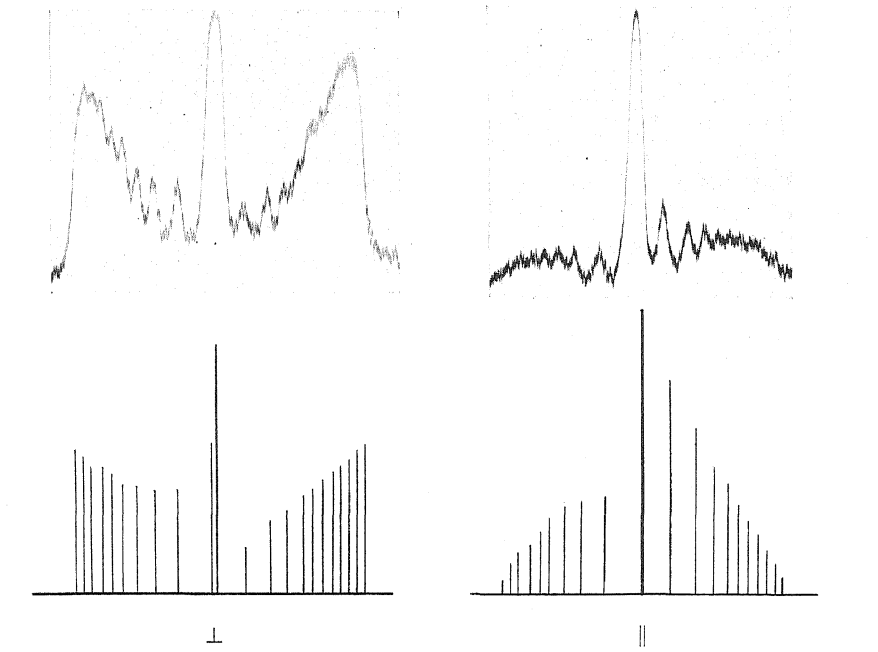
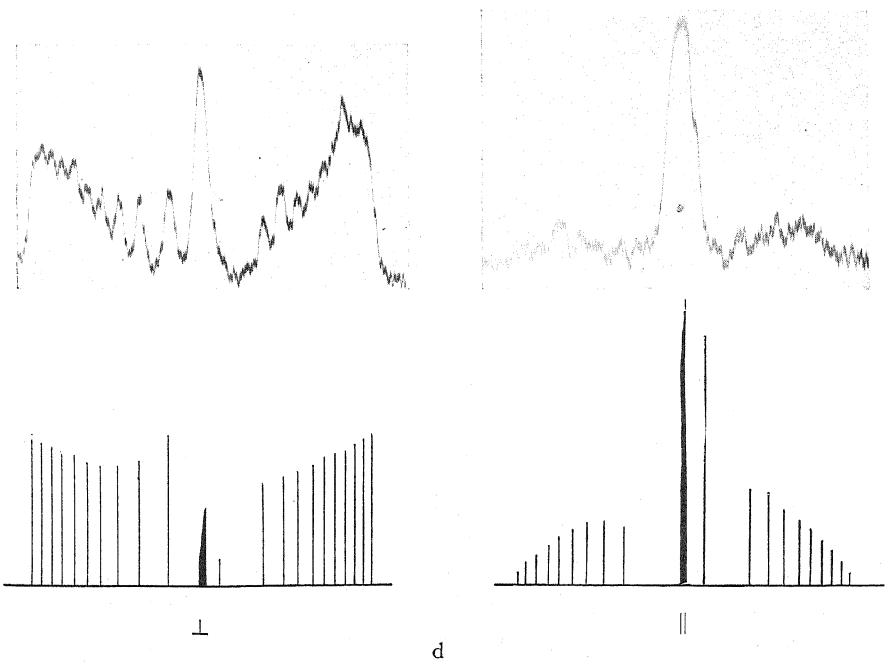


Fig. 1. (a). λ5719 Bi II 14700 gauss second order. (b). λ5719 Bi II 14700 gauss third order

* John Simon Guggenheim Memorial Fellow.
† International Education Board Fellow.
[1] Goudsmit and Bacher, Zeits. f. Physik **66**, 13 (1930).



c



d

Fig. 1. (c). λ5719 Bi II 32500 gauss second order. (d). λ5719 Bi II 43350 gauss second order.

work, except that the thallium metal used on the positive electrode was replaced by pure bismuth metal. For the excitation of spark spectra, alloys of the metal did not prove at all satisfactory. It seems that large quantities of the metallic vapor must be present in order to bring out the spark lines; a condition that must be avoided in the study of arc lines, for it leads almost certainly to self-reversal of some of the components of the lines.

In all other respects too, it was necessary to pay strict attention to all the details. As may be seen from the microphotometer reproductions, the magnetic patterns of the lines are extremely complicated, and in order to prevent the groups of lines from becoming mere smears, the pressure on the vacuum chamber, the current in the arc, and the speed of the motor, had to be kept constant.

Flieger plates of the Perutz Company in Munich were again used, and long tank development with Perutz fine-grain developer served to bring out to the best advantage the really fine work that the grating is capable of doing.

The results of Back and Goudsmit,[2] and Back and Wulff[3] have shown conclusively that the nuclear moment of the bismuth atom is 9/2. Consequently, the Zeeman patterns of the bismuth lines are considerably more complicated than the thallium lines, for in the latter cases, the tendency of each Zeeman component was break up into two in strong magnetic fields, while in the latter, the tendency is to break up into ten!

In the theoretical calculations it would also be possible for the determinantal equation to be of the tenth order and the tedium of the solution of the problem would be enormous, unless one used approximate methods as suggested by Goudsmit and Back. We have therefore chosen a particularly simple type of transition in Bi II to illustrate the theory. The line λ5719 has been classified as $2_1{}^0-7_0$ (possibly $6p\ 7s^3P_1-6p\ 7p^3P_0$). We are thus dealing with a transition $j=1$ to $j=0$, exactly similar to λ3092 of Tl II. A glance at Eq. (2) of the previous paper shows that the determinantal equation will be of the third order. There is one further complication in the calculations for Bi II. This is a two-electron spectrum, and the coupling between the electrons is practically jj in type. Hence we cannot use the Landé g-value in our equations. Applying Houston's[4] theory to the case, we are able to calculate the g-values from the interval separations and for $6p\ 7s\ ^3P_1$ we find the value $g=1.35$ instead of 1.50, the Landé g-value. With this value, the agreement between theory and experient was excellent.

The results of the calculations are shown graphically in Figs. 1a,b,c,d. Fig. 1a is taken at a field strength of 14700 gauss in the second order. Above is the microphotometric reproduction of the original plate (13× enlarged), and below the calculated positions and intensities of the lines. Fig. 1b is a reproduction of the third order, parallel polarization. Figs. 1c and 1d were taken from second order plates with magnetic fields of 32500 and 43350 gauss respectively. The wide black lines indicate a large number of very close com-

[2] Back and Goudsmit, Zeits. f. Physik **47**, 174 (1928).
[3] Back and Wulff, Zeits. f. Physik **66**, 31 (1930).
[4] Houston, Phys. Rev. **33**, 297 (1929).

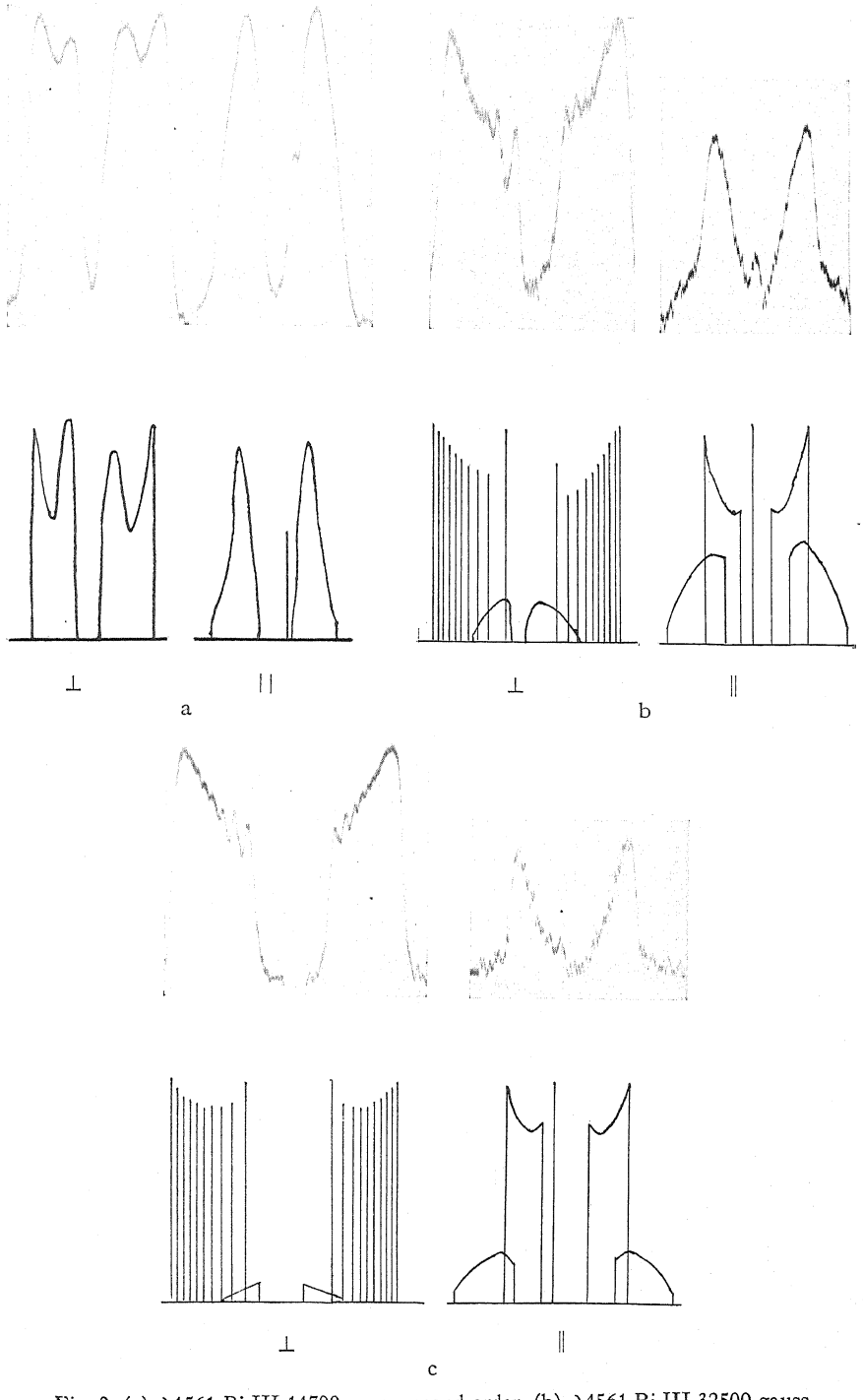


Fig. 2. (a). λ4561 Bi III 14700 gauss second order. (b). λ4561 Bi III 32500 gauss second order. (c). λ4561 Bi III 43350 gauss second order.

ponents and in Fig. 1d, parallel polarization, although these are relatively weak, the grating has integrated their intensities and shows them as one strong line. It is to be noted that the side components in the parallel polarization de-

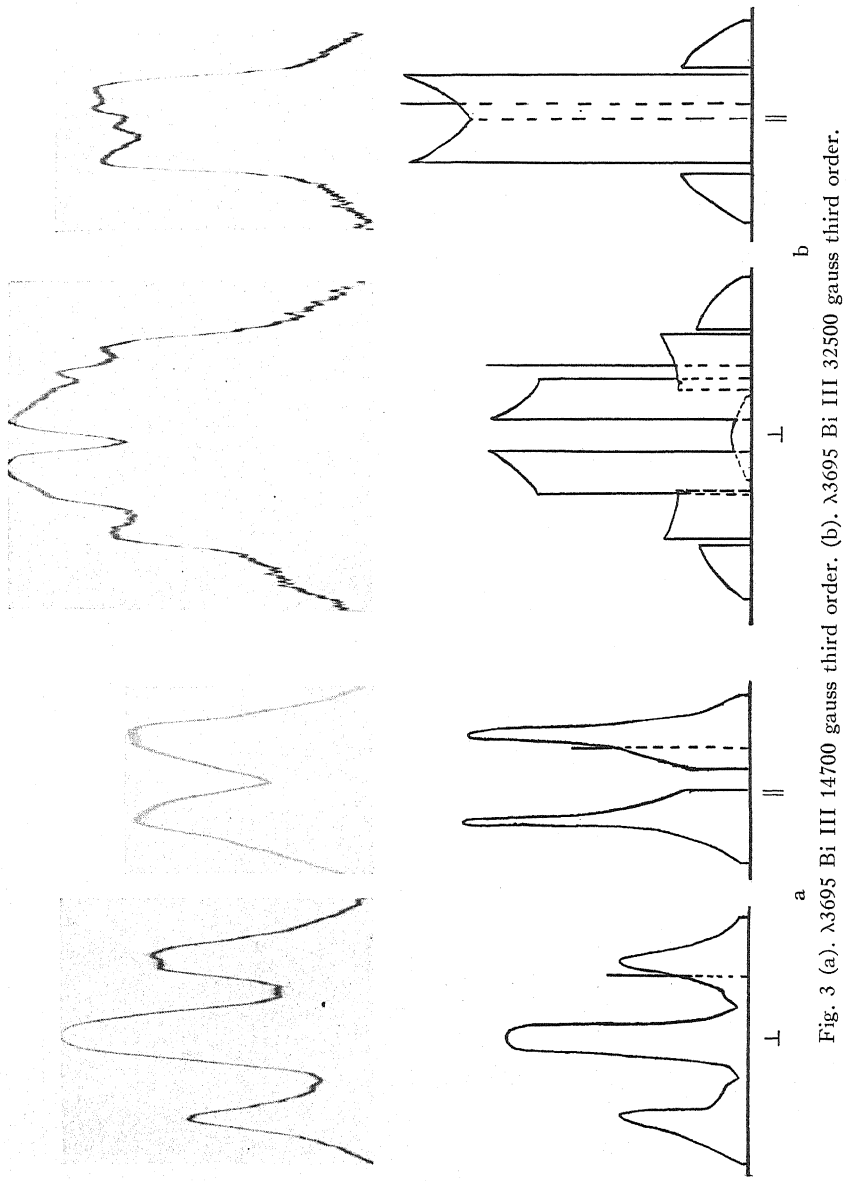
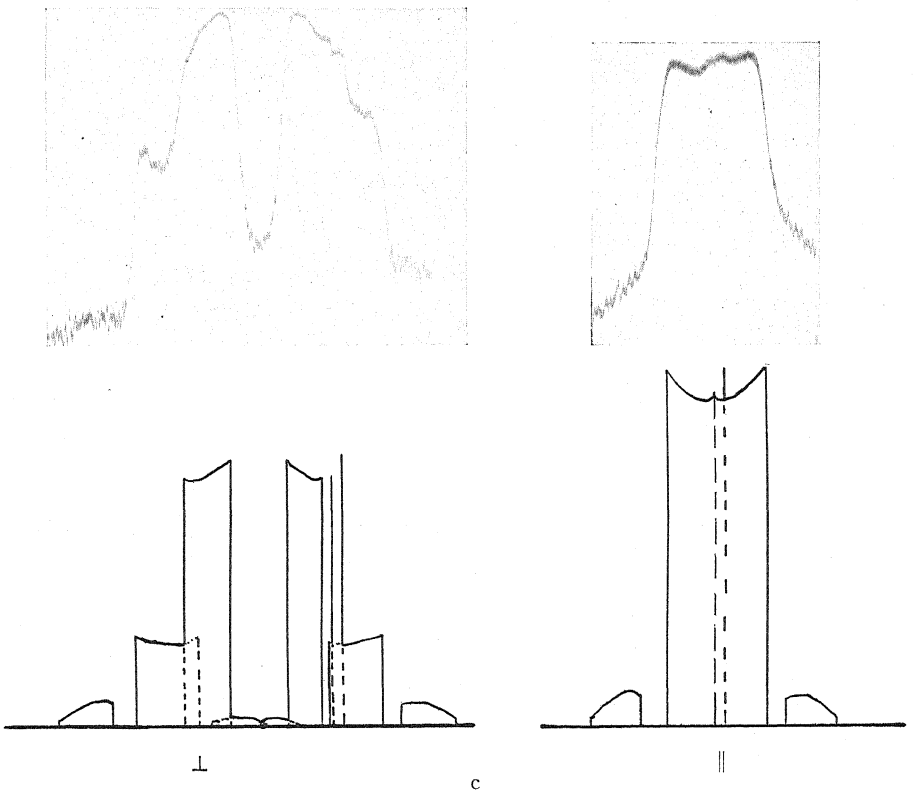


Fig. 3 (a). λ3695 Bi III 14700 gauss third order. (b). λ3695 Bi III 32500 gauss third order.

crease in intensity with increasing field strength, while the outside perpendicular components increase in intensity with increasing field strength. The side parallel components at 43350 gauss are barely perceptible on the photographic plate and their positions are very difficult to determine on the microphotometer record.

As representative lines in the spectrum of Bi III, we chose λλ4561 and 3695. These lines represent the transitions $7s^2S_{1/2}-7p^2P_{1/2}$ and $7s^2S_{1/2}-7p^2P_{3/2}$. These lines were also observed at the three field strengths used in the previous work, namely 14700, 32500 and 43350 gauss, and are represented in Figs. 2a, b,c and 3a b,c respectively.

λ 4561 in strong fields was completely resolved in the perpendicular polarization in the second order, as can be seen on the microphotometer record.



c

Fig. 3 (c). λ3695 Bi III 43350 gauss third order.

In the parallel components, the thing of interest to be noted is that the component marked with an arrow, the only resolvable component in this polarization, moves from the long wave-length group to the short wave-length group as the field strength increases, in complete accordance with the theory. The broad blocks on the computed patterns indicate groups of lines possibly resolvable by the grating but not by the phtographic plate. Fig. 2c shows the result of broadening the photometer slit. The parallel components were recorded with a very fine slit and show plate grain very noticably, while the perpendicular components were recorded with a wider slit, and the plate grain is hardly apparent, but the real breaks in the curve are also reduced so that in some cases they are barely perceptible.

Figs. 3a, b, c represent the results for λ3695 in the third order. The hyperfine separation of the $^2P_{3/2}$ term as given by Fisher and Goudsmit is very small, so that for this term, the approximate formula

$$E = m_j g\omega + A m_i m_j$$

sufficed to determine the energy levels. Here again, in the computed patterns, the blocks represent unresolved groups of lines. When a line sufficiently strong and separated from a group can be seen on the photometer curve, its position is also shown on the theoretical pattern. Unfortunately, the photometer curves are not nearly so rich as the patterns that could be observed with the eye. For example, in the perpendicular polarization for the strong field four sharp lines could easily be distinguished on the long wave-length side of the pattern, while only two show on the photometer curve; and three lines of the corresponding group on the short wave-length side could be separated from the pattern, while none appear on the photometer records. For the low field strength, the blocks on the theoretical pictures overlapped so badly that a sum curve was built and that is the one represented in the figure. This was also done for λ4561. The transition of one line in the parallel polarization from one side of the figure to the other is also noted here.

Here again, then, as in the case of Tl II and Tl III the present status of the theory of the Paschen-Back effect for hyperfine structure is verified in all of its details.

In concluding this work, it gives us great pleasure to acknowledge our thanks to Professors Geiger and Back for the privilege of working at Tübingen, and to the Rockfeller and Guggenheim Foundations for their financial assistance.

PHENOMENA IN OXIDE COATED FILAMENTS II. ORIGIN OF ENHANCED EMISSION

By J. A. Becker and R. W. Sears
Bell Telephone Laboratories, New York, N. Y.
(Received November 6, 1931)

Abstract

Various theories have been advanced regarding the mechanism of emission of electrons from oxide coated filaments. These theories postulate that; (1) the active layer is (a) at the outer oxide surface, (b) at the core-oxide interface; (2) the thermionic electrons come from (a) the adsorbed barium, (b) the oxide just underneath the adsorbed layer; (3) the current is carried through the oxide coating by (a) an entirely electrolytic process, (b) thermionic electrons which come from the core, diffuse through the pores of the coating and form a space charge therein, (c) electrolytic conduction through the oxide crystals and thermionic conduction between crystals, (d) electronic conduction, a small portion being carried by ions. A number of experiments were designed to test these various hypotheses. These experiments show that; (1) When barium is brought to the outer surface of the oxide, either by electrolysis or evaporation from an external source, the emission increases at first, passes through a maximum and then decreases. This change in activity is similar to that for barium on tungsten. (2) When oxygen is brought to the surface of the oxide of an activated filament, the activity decreases rapidly at first and then more slowly. (3) In these two respects, a filament with a core made of an alloy called "Konel" and consisting of nickel, cobalt, iron and titanium acts just like filaments with other cores. (4) When the oxide was stripped from a Konel core filament, the activity decreased by a factor of 6000. (5) The emission-limited current is independent of the area of the core provided that the area of the outer oxide surface remains constant. (6) The conductivity of the oxide varies with the time of sending current through the oxide. (7) The conduction current in the oxide obeys Ohm's law and does not saturate even though its value is hundreds of times larger than the saturated emission. (8) The oxide acquires a positive potential with respect to the core regardless of whether the space current is limited by space charge or by emission. This potential varies linearly with the space current drawn to the plate and is of the order of a few tenths of a volt. (9) The emission for the optimum amount of barium on the oxide surface depends upon the previous treatment of the oxide. From these results we conclude that; (1) The active layer is at the outer oxide surface. The activity depends on the concentration of barium and oxygen on this surface and also upon the amount of metallic barium dispersed through the oxide. The core material does not directly affect the emission but it does greatly affect the ease with which free barium is produced by heat treatment or electrolysis. (2) The thermionic electrons originate in the oxide just underneath the adsorbed barium. (3) Most of the current through the oxide is conducted by electrons, a small portion being carried by barium and oxygen ions.

Introduction

In 1929 one of us proposed a comprehensive theory to account for the complex phenomena observed in oxide coated filaments.[1] The essential points of this theory were: The activity depends upon the concentration of barium[2]

[1] Becker, Phys. Rev. **34**, 1323–1351 (1929).

[2] Throughout this article the word "barium" will be used for barium and / or strontium and / or calcium.

and oxygen on the surface of the oxide and on the composition of the coating. Both barium and oxygen diffuse quite readily from the surface into the oxide and vice versa. When current passes through the oxide most of it is carried by electrons, but a small portion is carried by oxygen and barium ions.

Since that time we have enlarged or extended the theory or made it more explicit. Others too have proposed theories which, in some respects, conflict with ours. Insofar as these extensions or conflicts deal with the production of the barium or the conduction of current through the oxide, they have been dealt with elsewhere.[3] The present article will deal with the question: Where do the thermionic electrons originate?

It has been quite generally held that these electrons come from the region near the outer oxide surface. Recently, however, in two important papers it has been proposed that the electron space current is or may be limited by the emission from the metallic core surface of the filament. Lowry[4] states that, "the source of emission is assumed to be a layer of metallic barium occluded on the surface of the base metal or alloyed with it". He further postulates that "the electrons emitted from this composite surface must diffuse through the pores of the coating". Reimann and Murgoci[5] believe that electrons are thermionically emitted from the core to an adjoining oxide crystal and from one oxide crystal to the next. In each crystal the current is carried exclusively by barium ions. The barium atoms adsorbed on the surface of the outermost oxide crystals emit the electrons which pass to the plate. They conclude that the observed current may be limited by "whichever of the two systems (core or oxide surface) has the lesser emissivity".

Koller,[6] Rothe,[7] Detels,[8] Espe,[9] Becker,[1] Schottky,[10] Gehrts,[11] Huxford[12] and others believe that the emission depends upon the concentration of barium on or very near the surface of the oxide and that the core surface does not determine or limit the emission. There are differences of opinion, however, concerning the origin of the thermions near the oxide surface. Some believe that the thermions come from barium atoms adsorbed on the oxide; that the activity is proportional to the concentration of this adsorbed barium; and that the work function is the same for all appreciable concentrations of barium. Others believe that the thermions originate in the oxide just beneath the surface and that the absorbed barium makes it easier for them to escape from the surface. On this view the work function depends on the concentration of barium and the activity is not directly proportional to this concentration.

In order to decide between these various theories we have designed and

[3] Becker, Trans. Amer. Electrochem. Soc. **59**, 207–220 (1931).
[4] Lowry, Phys. Rev. **35**, 1367–1378 (1930).
[5] Reimann and Murgoci, Phil. Mag. **9**, 440–464 (1930).
[6] Koller, Phys. Rev. **25**, 671–676 (1925).
[7] Rothe, Zeits. f. Physik **36**, 737–758 (1926).
[8] Detels, Jahrb. d. drahtl. Telegr. u. Teleph. **30**, 10–14 and 52–60 (1927).
[9] Espe. Zeits. f. techn. Physik **10**, 489–495 (1929).
[10] Schottky, See Wien-Harms Handbuch der Physik, Vol. XIII, part 2.
[11] Gehrts, Zeits. f. techn. Physik **11**, 246–253 (1930).
[12] Huxford, Phys. Rev. **38**, 379–395 (1931).

performed a number of crucial tests. These were so chosen that the predictions based on one theory were distinctly different from those predicted by some other theory. The first group of tests was designed to decide between the core-surface or the oxide-surface theory; the second group was intended to decide whether the electrons come from the adsorbed atoms or the underlying oxide. We shall describe these tests and discuss the deductions based on them and on tests described by others.

The experiments were conducted in radically different types of tubes. A description of each tube will be given in connection with the particular tests performed with it.

All of the tubes were evacuated on a four-stage mercury diffusion pump. During the pumping, which usually consumed two or three days, a tube was baked, the metal parts were outgassed and the tube was rebaked. The filaments were glowed at suitable temperatures until they were completely outgassed. The tubes were sealed from the pumps with the metal parts quite hot while the pressure was about 1×10^{-6} mm of Hg. All of the tubes contained auxiliary thoriated tungsten filaments which were used as "clean-up filaments" for several days or weeks after seal-off, until the pressure was about 3×10^{-8} mm of Hg or less, even when the oxide coated filaments were glowing.

The oxide coated filaments consisted of a mixture of barium and strontium carbonates, in a suitable suspension, coated on a metallic core. The carbonates were decomposed to the oxides by glowing while the tubes were on the pumps.

The Effect of Barium on the Emission

In a previous article[1] it was shown that the activity of an oxide coated filament changes as barium is put onto the outer oxide surface either by evaporation from an external source or by electrolysis of the oxide itself. From such results the conclusion was drawn that the source of the enhanced emission was at the outer oxide surface or within the oxide very close to the surface. The experiments were conducted with filaments having platinum and nickel cores. It has been reported[4] that oxide coated filaments having cores made of an alloy called "Konel" and consisting of nickel, cobalt, iron and titanium behave differently from filaments with other cores. It was therefore deemed advisable to repeat these experiments with a Konel core filament.

These experiments were conducted in a tube containing an oxide coated Konel filament and an auxiliary filament which could be used either as a source of electrons or as a source from which barium would evaporate under the proper conditions. A cross section of the tube showing the relative arrangement of filaments and plates is shown in Fig. 1. F_1 and F_2 are ribbon filaments mounted parallel to the plates P. F_1 is an oxide coated Konel filament and F_2 a barium-platinum alloy filament. The filaments F_3 were of thoriated tungsten. S is a shield between F_1 and F_2 extending along their entire length. When it was desired to evaporate barium from F_2 onto F_1, the shield could be removed into position S' by tilting the tube.

In these experiments, tests of the activity of the coated filament were made after subjecting the filament to various treatments. These treatments

consisted in: (1) Sending various amounts of current into the coated filament from the auxiliary filament F_2, (2) subsequent glowing of filament F_1 at various temperatures, (3) evaporating various amounts of barium onto F_1 from F_2, (4) subsequently glowing F_1 at various temperatures.

The results are shown in Fig. 2 which is a plot of the emission current in amperes on log scale at a filament temperature of 500°K versus the time of subjecting the filament to the various treatments. The coated Konel filament was conditioned initially by glowing at a temperature of 1100°K until the emission reached an equilibrium value. Then a current of 450 microamperes was sent into the cold coated filament from the auxiliary filament F_2. After various intervals the current was stopped and the activity of the coated filament determined at a temperature of 500°K. The activities at these intervals are shown on the curve by the black dots. The activity increased at first until

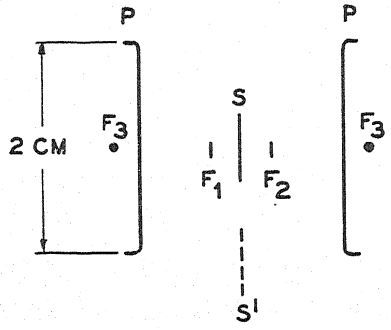


Fig. 1. Arrangement of plates and filaments in tube-152-S.

it reached an optimum value after which it decreased but at a slower and slower rate. A total of 7200 microampere minutes was sent into the coated filament.

The second treatment consisted in glowing the coated filament at 1040°K and later at 1100°K. The activity was again determined periodically at the testing temperature. The values of the activity thus obtained are shown on the curve by the first set of circles. The activity increased back to the optimum value and then decreased. The glowing at 1100°K caused the activity to fall rapidly to its equilibrium value.

The third treatment consisted in evaporating barium onto the surface of the cold coated filament. This was accomplished by removing the shield and glowing the auxiliary filament F_2 at a suitable temperature. During this evaporation no current passed between the two filaments. At intervals the evaporation was stopped and the activity determined as in the previous experiments. The activities at the various times of evaporation are shown on the curve by the crosses. The activity increased initially until it reached an optimum value after which it decreased. An increase in the rate of evaporation from the auxiliary filament increased the rate at which the activity decreased.

The last treatment consisted in glowing the coated filament at 1040 and 1100°K as before. The activities at the various intervals of glowing are shown

by the second set of circles. The activity again increased to an optimum and then decreased to an equilibrium value.

Several auxiliary tests were made on this filament to show that the phenomena observed in Fig. 2 were caused directly by the treatment. The testing temperature of 500°K was sufficiently low that glowing or drawing testing currents at this temperature did not change the emission, regardless of the state of activation.

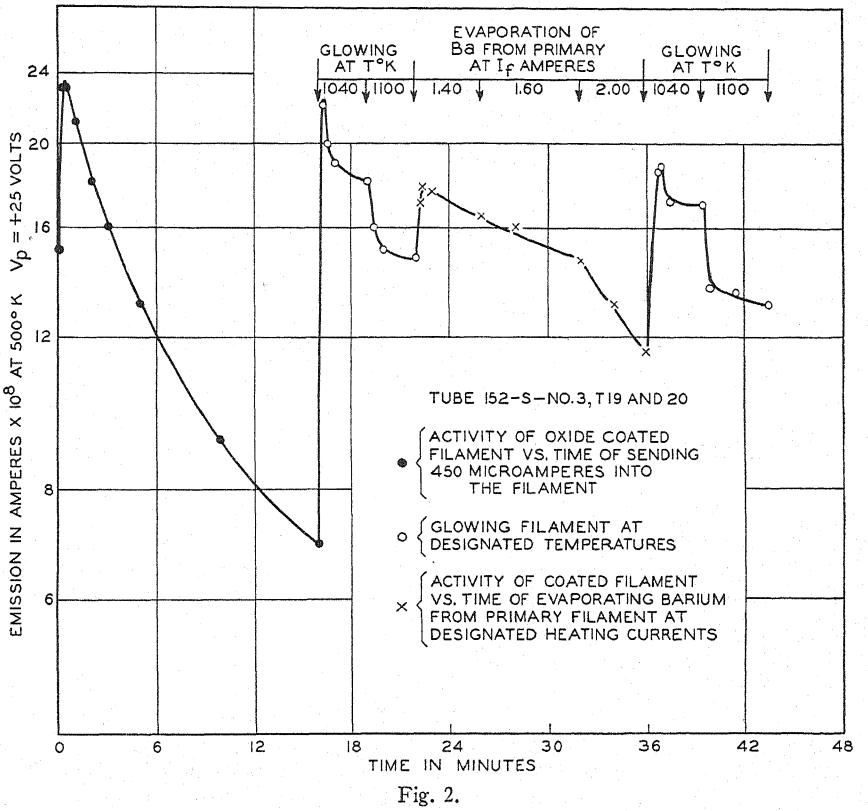


Fig. 2.

That the changes in emission, when electrons were sent into F_1, were due only to the action of the current entering the filament, was demonstrated in two ways. If the potentials of the various electrodes in the tube were arranged so that no electrons reached F_1 even though electrons left F_2, the activity of F_1 was not altered. In the second place, the change in activity of F_1 was the same whether the shield was between F_1 and F_2 or not, provided only that the current into F_1 was the same in the two cases. The insertion of the shield would prevent barium from reaching F_1, even if it did evaporate from F_2.

This last fact was demonstrated by inserting the shield when the temperature of F_2 was such that barium did evaporate from it. In that case the activity of F_1 was not affected until the shield was removed.

It should be noted that in order to obtain reproducible results when barium was evaporated onto the coated filament, it was necessary to have the pressure less than 5×10^{-8} mm of Hg. This is due to the fact that at higher pressures the rate of adsorption of gas atoms and molecules is appreciable. Such adsorbed gas will, of course, alter the activity. It was also necessary to have the platinum-barium alloy filament well conditioned in order that barium and only barium evaporated.

The results of the experiment shown in Fig. 2 can readily be interpreted on the view that the emission is dependent upon the amount of barium on barium oxide. When electrons are sent into an oxide coated filament, the direction of the electrolysis of the oxide is such that the barium ions travel toward the outer surface. Since the changes in emission noted in this experiment were caused by electrons entering the filament, we conclude that the emission changed as various amounts of barium were deposited on the oxide surface. As more and more barium was deposited on the surface the emission increased until it reached an optimum value, after which it decreased. Glowing the filament at 1040°K caused this excess of surface barium to diffuse into the interior of the oxide or to evaporate. The emission, therefore, increased back through the optimum value. Glowing at 1100°K caused the emission to decrease to its equilibrium activity on glowing at that temperature.

This interpretation is confirmed by the second part of this experiment in which barium was evaporated directly onto the oxide surface. The emission changed as the surface concentration of barium changed. As the amount of barium on the surface increased, the emission increased to the optimum value and then decreased just as in the previous case where barium was put on the surface by electrolysis. Subsequent glowing at 1040 and 1100°K again caused this barium to diffuse into the oxide or to evaporate. This in turn caused the emission to increase back to the optimum and then decrease to an equilibrium value.

The first two optima in Fig. 2 have the same value. From this we may conclude that the entire oxide surface was uniformly covered with barium. Presumably the electrons entered the coating from all directions and deposited barium uniformly over the entire surface. The optimum obtained by evaporation of barium onto the surface was less than these optima. The reason is that barium was evaporated onto only one side of the filament. Consequently, the emission from the back side of the ribbon remained constant while that from the front side increased to the optimum. The ratio of the first and third optima in Fig. 2 is of the proper magnitude to agree with this interpretation.

The last optimum emission on glowing at 1040°K was slightly higher than the optimum which just preceded it. After barium had been evaporated onto the ribbon, the front side was covered beyond the optimum while the back side was covered with less than the optimum amount of barium. The fourth optimum in Fig. 2 was slightly higher than the third because during the initial stages of glowing at 1040°K some of the barium from the front side migrated to the back side of the ribbon and increased the barium concentration there.

Thus far we have interpreted the changes in activity when current was

sent into the oxide coated filament in terms of the barium deposited at the outer oxide surface by electrolysis. The oxygen deposited near the core was assumed to have no effect on the activity. This assumption can be verified by comparing the results when the oxide was electrolized with those obtained when barium was evaporated onto the oxide surface. The third optimum in Fig. 2, when corrected for the fact that barium was evaporated onto only one side of the ribbon, is equal to the first optimum. Since oxygen was deposited near the core face in one case and not in the other we conclude that oxygen on the core face does not affect the activity.

Our observed changes in activity when barium was made to appear or to leave the surface of the oxide are qualitatively similar to those observed for barium on tungsten. They are strikingly different, however, in one respect. For barium on tungsten, the optimum activity is thousands of times greater than that for clean tungsten, while for the cases of barium on the oxide discussed above, the optimum activity is less than twice the initial activity. This dissimilarity is due to the fact that when an activated oxide filament is glowed at moderate temperatures, its surface is not freed from adsorbed barium. In fact, the surface in some cases may be nearly completely covered, as was shown in a previous paper.[1]

These results do not seem to be readily interpretable on the view that the emission is determined by the amount of barium on the core face. The testing temperature was so low that the barium could not have diffused into the oxide and increased the barium concentration at or near the core. The observed changes in emission were, therefore, not due to any change in the system at or near the core surface but must have been due to changes in barium concentration on the surface of the oxide.

The Effect of Oxygen on the Emission

Whether the emission is determined by the core surface or oxide surface can also be tested by observing the effects of oxygen on the emission. It has been shown[1] that if oxygen is brought to the surface of an active oxide coated platinum-nickel core filament, the activity decreases. The effect is the same whether the oxygen is deposited by evaporation from an external source or whether it is produced by electrolysis of the oxide. From these experiments it follows that in active filaments with a platinum nickel core, the emission is determined by the outer oxide surface. We have used a Konel core filament in repeating the experiments in which oxygen is brought to the surface by electrolysis.

These experiments were performed in a tube of the same type as that used in studying the effect of barium on the emission and shown in Fig. 1. As emission-limited current was drawn from the coated filament to the plates, the activity decreased rapidly and then more and more slowly. This is illustrated in Fig. 3. Curve 1 shows how the emission current decreased as current was drawn to the plates at a temperature of 660°K and a plate potential of 100 volts. At intervals, during this drawing of current, the activity was tested at a lower temperature, 500°K. Curve 2 shows how the activity under the nor-

mal testing conditions decreased with the time that current was drawn at a temperature of 660°K. The activity at the testing temperature decreased by a factor of ten. The filament was then glowed at 770°K and the emission increased rapidly at first and then more and more slowly as shown by curve 3. The glowing temperature was finally raised to 900°K and the activity increased back to its normal value as shown by curve 4.

These results are very similar to those previously found with a platinum-nickel core filament as can be seen by comparing Fig. 3 of this paper with Fig. 10 of the previous paper.[1] From this it seems clear that the behavior of coated filaments with Konel cores is not essentially different from that in filaments with platinum-nickel or platinum-iridium core. In both cases the decrease in activity is due to oxygen on the surface. This means that the thermionic emission is determined by the condition of the outer oxide surface.

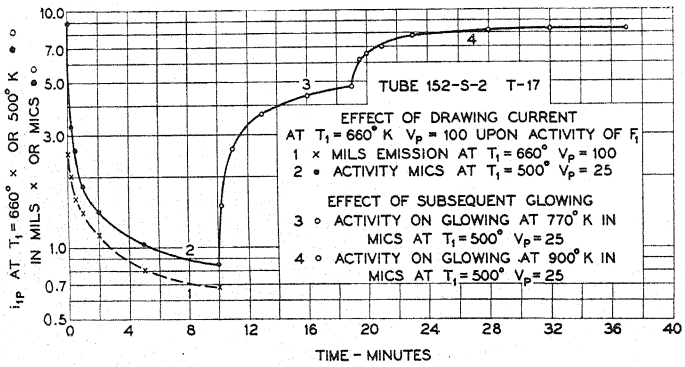


Fig. 3.

These time changes caused by the electrolytic deposition of oxygen are obtained most readily at moderate plate currents and moderate temperatures. However, in vacuum tubes operating normally, heavy currents are usually drawn from the filament to the plate at temperatures around 1050°K. Under these conditions the activity usually remains quite constant with the time of drawing current. There are two reasons for this: (1) The currents are usually limited by space charge and the proportion of current in the oxide carried by ions is very small.[1] (2) At this temperature the rates of diffusion of barium and oxygen in the oxide are high so that the oxygen and barium ions upon becoming neutralized at or near the outer oxide and core surfaces respectively diffuse quite rapidly back into the oxide.

Effect of Removing Oxide Coating

The next type of experiment was designed to make a test of the hypothesis that the enhanced emission is due to barium adsorbed on the core surface. On this view, if the oxide were removed from the core, the emission should be at least as great as before. The tube used for this test consisted of two parallel plates, in the center of which was placed an oxide coated filament with a

Konel core. The filament was in the from of a ribbon approximately 0.125 cm (50 mils) wide. The adherence of the coating to the core of this particular filament was exceptionally poor so that if the filament was subjected to a mechanical vibration or strain, the coating would completely peel off.

The experiment consisted in observing the activity before and after the coating was removed. The filament was activated initially by glowing. The activity of the coated filament on glowing for a number of hours at approximately 1050°K is shown by power-emission line A in Fig. 4. After this activity was observed, the filament was cooled to room temperature and the tube

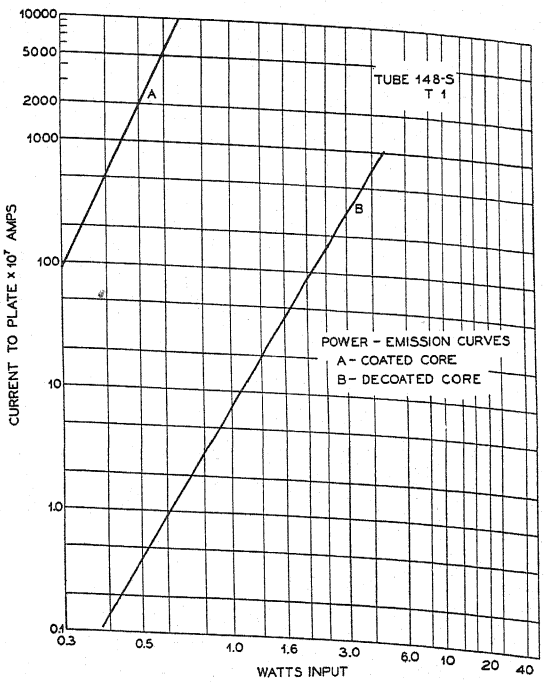


Fig. 4.

jarred. This caused all of the coating to fall off. The activity was again measured at low temperatures and is shown by power-emission line B. The activity decreased by a factor of about 6000. Subsequent glowing of the decoated core failed to change the emission appreciably. The decoated core was of a greyish appearance due to the usual oxidation of the core metal during the treatment of the filament.

Power-emission line B was taken at temperatures sufficiently low that barium could not have evaporated from the decoated core surface had it been there directly after the removal of the oxide. It is known that barium will not evaporate from a tungsten surface even at much higher temperatures than those used in determining line B.[13]

The results of this experiment can readily be interpreted on the view that

[13] Eglin, Phys. Rev. **31**, 1127 (1928).

the emission is dependent upon the amount of barium on barium oxide. The large decrease in emission was due to the loss of the oxide coating which carried the outer oxide surface of low work function with it.

The large decrease in emission is not in accord with the view that the emission is determined by the amount of barium adsorbed on the core face unless the assumption is made that the barium adsorbed on the core adheres more tenaciously to the oxide than to the core and that when the oxide and core are parted, the barium chooses to remain with the oxide. We know of no way of testing such an assumption. We do know that barium sticks tenaciously to both metallic and oxide surfaces. It seems quite probable, therefore, that some of the barium should have remained on the core. If the core had been

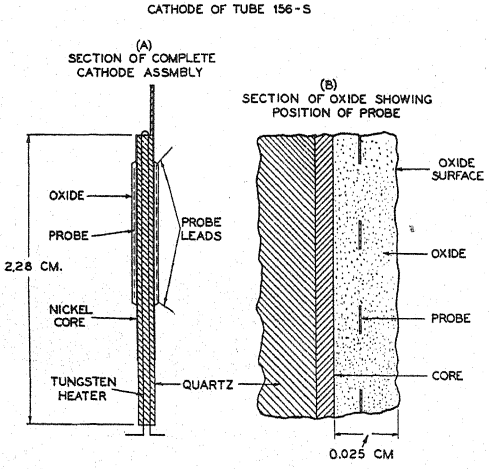


Fig. 5.

"active" when the coating was present it should have been partially "active" when the coating was removed and subsequent glowing at high temperatures should have changed the activity.

Effect of Changing the Area of Supposed Emitter

On the view that the electrons are emitted thermionically between core and coating, the current that reaches the plate may be limited by the number of electrons that are able to leave the core. If the area of the metallic core surface, from which the electrons are supposed to escape, could be reduced, the emission should be reduced proportionately. On the other hand, if the emission is limited by the external oxide surface, it should not change when the area of the core surface is changed.

Such an experiment was conducted in a tube containing an equipotential cathode cylinder coated with a mixture of barium and strontium oxide in which was embedded a metallic ribbon or probe completely insulated from the core. An enlarged cross-section of the cathode is shown in Fig. 5A. An indirectly heated cathode was employed, consisting of a tubular nickel core covering a quartz rod in which was a tungsten heater wire. The nickel core

was coated with a layer of oxide; then a 0.0025×0.0127 cm (1×5 mil) nickel ribbon, which had previously been coated with a layer of oxide, was wound helically about the coated core and the whole coated over with a second coat of oxide. A much enlarged cross-section of the oxide showing the relative positions of core, nickel ribbon or probe and oxide, is shown in Fig. 5B. The area of one side of the probe is equal to about one-third of the area of the core. The cathode assembly shown in Fig. 5A was placed in the axis of three cylindrical anodes, 1.5 cm in diameter. The outside two cylinders are 0.8 cm and the central collector 0.6 cm long. Six thoriated tungsten filaments were placed outside of these collectors for use as clean-up filaments.

The experiments consisted in measuring the emission from the cathode to the plate when the negative terminal of the battery was connected to: (1) the core with the probe floating, (2) the probe with the core floating and, (3) both core and probe. The metallic surface areas are as 1, 2/3 and 5/3.

The results of this test are shown in Table I. The emission currents, when the negative terminal of the battery was connected to the core, probe, and core and probe together are given for several different temperatures. At any temperature, the emission currents in all three cases are practically equal.

TABLE I.

Temp. °K	Emission current in amps. with 40 volts applied between plate and		
	Core (Probe floating)	Probe (Core floating)	Core and probe
545	4.85×10^{-8}	4.78×10^{-8}	4.80×10^{-8}
643	3.06×10^{-6}	2.84×10^{-6}	2.98×10^{-6}
711	2.42×10^{-5}	2.14×10^{-5}	2.31×10^{-5}

These results cannot be interpreted on the view that the electron current is limited by emission from the core. Since the current "emitted" from the core alone was equal to the current "emitted" from the probe alone, one would certainly expect the resultant emission, when the plate battery was connected to both core and probe, to be appreciably larger than the emission from either one alone. This was not verified as can readily be seen from the table.

On the other hand the results are to be expected on the view that the electrons are emitted thermionically from the external oxide surface. The emission was the same in all three cases simply because the area of the outer oxide surface was unchanged.

OXIDE CONDUCTIVITY

Reimann and Murgoci[5] have investigated the variation of the conduction current between two coated filaments, twisted together, with the potential. They found that the current varied linearly with the voltage at low current densities but sometimes showed incipient saturation at potentials of a few volts. They state that, "at current densities comparable with those in the coatings of oxide cathodes from which saturated thermionic space current is being taken, the current conducted through an oxide powder between two electrodes, embedded therein, also saturates". From this they conclude that

the conduction current in any individual oxide crystal obeys Ohm's law and that the current is carried by thermionic electrons between the various crystals and between core and oxide. At low current densities, the currents across the gaps are limited by space charge and most of the potential drop is across the oxide crystals. This accounts for the linear portion of their curves. At high current densities, the current is limited by thermionic emission in one or more gaps. This interpretation is the basis of their conclusion that there is a limitation of thermionic space current, "between the core metal and coating or within the coating itself".

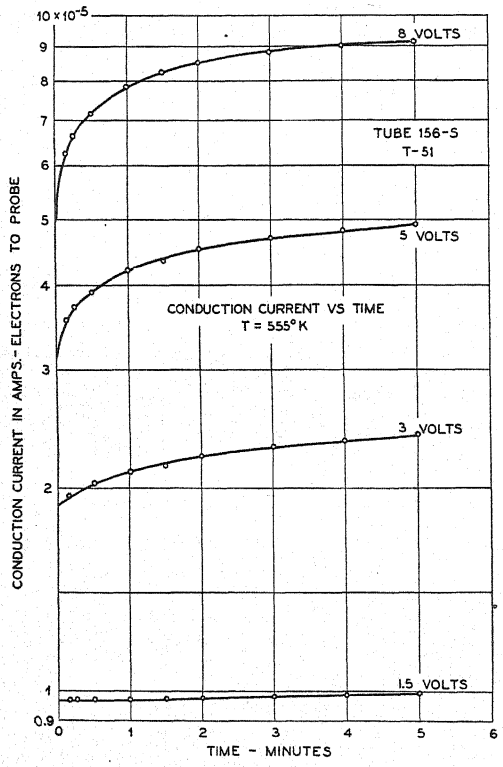


Fig. 6.

Due to the importance of this experiment, we have repeated their measurements with an improved design of tube. The tube contained the special equipotential cathode shown in Fig. 5. and was described in the preceding section.

The measurements consisted in noting the value of the conduction current when various potentials were applied between core and probe. It was found that as long as the currents and voltages were small, Ohm's law was obeyed, but if the applied potential was more than about one volt, the conduction current sometimes varied with the time. When the conduction current varied with the time, it always increased at a fast rate initially and then more and more slowly. In some cases it increased to an optimum value and

then decreased but did not fall below its initial value. The increase of conduction current with time is illustrated in Fig. 6. The conduction current on a logarithmic scale is plotted against the time that electrons were flowing from the core to probe at a temperature of 555°K. Four curves are shown for potentials between the core and probe of 1.5, 3, 5 and 8 volts. After each of these curves, the cathode was glowed for ten minutes at 555°K with no potentials applied. The curves were reproducible, showing that this glowing was sufficient to bring the oxide back to its initial condition. The conduction current always increased with time until at the end of five minutes it had reached an almost constant value. The phenomenon is attributed to an increase in oxide conductivity due to an accumulation of the products of electrolysis in the oxide. A more detailed study of this phenomenon is now in progress.

A current voltage curve can be obtained from the data of Fig. 6. Such a curve is shown in Fig. 7. Curve *A* was obtained by plotting the initial values of

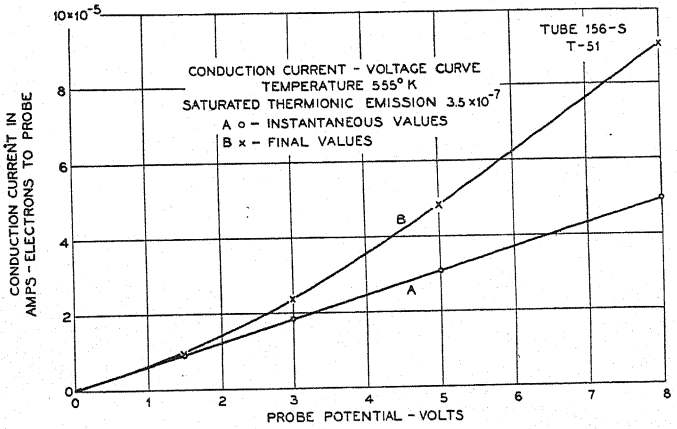


Fig. 7.

the conduction current against the applied potential. The points form a good straight line indicating that the oxide obeys Ohm's law. The final values of conduction current gave curve *B* which is concave toward the current axis. There is no indication of current saturation as reported by Reimann and Murgoci even though the current density at the highest potential is 300 times larger than the total saturated thermionic emission at this temperature. For these cathodes there can be no limitation of thermionic space current at the core face or in the oxide.

This particular test has been made on three cathodes with the same result. Furthermore we have never found a case in a large number of different types of coated filaments in which the behavior indicated such a limitation of thermionic current at the core surface. We therefore believe that the reported deviations from linearity may be attributed to changes in conductivity with time or to polarization since we have found the shape of our current voltage curves to be affected by these factors. It may also be that two filaments twisted together actually do form a gap in the oxide and that the current is limited at this gap.

Potential Distribution in the Oxide

By means of the probe it is possible to test whether the electrons are emitted thermionically from the core and then drift through the pores of the oxide where they form a pseudo space charge. On this view the probe should sometimes be negative with respect to the core and the probe potential should not vary linearly with the current emitted to the plate. On the other hand, if the electrons are emitted thermionically from the outer oxide surface and if they

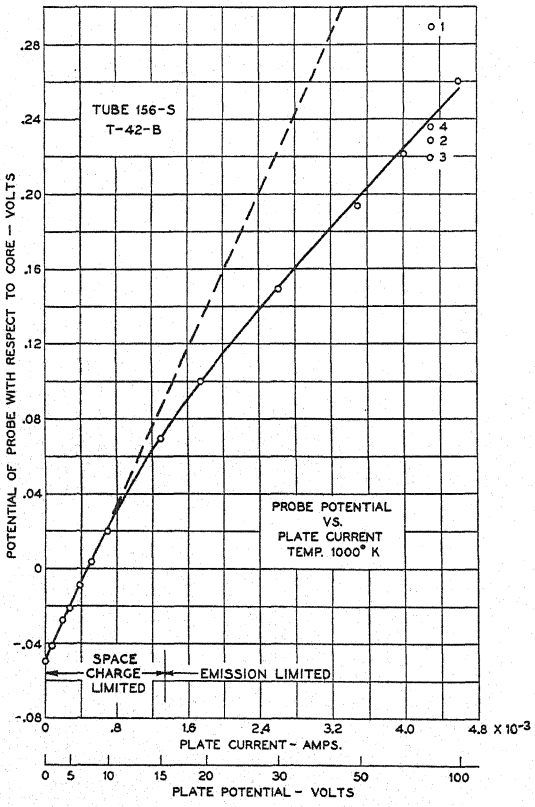


Fig. 8.

pass through the oxide as they would through a metal of high resistivity, the probe should always be positive with respect to the core and the probe potential should be directly proportional to the current through the oxide. Furthermore the ratio of the probe potential to the plate current should give the resistance of the oxide between the core and probe. The value of this resistance should agree with that determined in the conductivity measurements described above.

In the experiments to differentiate between these views, the potential of the probe in the oxide was measured as current was drawn from the core to the plate. A null method was used in measuring the probe potential. The results are illustrated in Fig. 8, which is a plot of the potential of the probe with re-

spect to the core versus the current to the plate in amperes at a temperature of 1000°K. The current to the plate was varied by changing the plate potential. The values of plate potential are indicated in Fig. 8 below the current values. The current was limited by space charge up to approximately 1.2 milliamperes. When the current was limited by emission, the current varied with the plate potential because of the characteristic poor saturation of these oxide cathodes.

These data show that the oxide is positive, regardless of whether the current reaching the plate is limited by space charge or by emission, as was predicted on the basis of our theory. However, the observed curve differs from the predicted in two respects.

In the first place the curve does not pass through the origin. When the plate current is zero, the probe has a negative potential with respect to the core. Since there is a constant flow of energy across the oxide, there must exist a temperature difference between the core and probe. The intercept, therefore, measures the thermal e.m.f. generated by the two nickel-barium oxide junctions at the two temperatures. The temperature difference is estimated to be something like 20 degrees. All of our conduction current voltage curves show this intercept. It does not appear in Fig. 7, however, due to the low temperature and the large voltage range plotted.

That the intercept is due to a thermal e.m.f. was demonstrated in the following manner: The core and probe were connected together through a variable resistance and a galvanometer. The current indicated by the galvanometer was changed by varying the external resistance. A plot was made of the reciprocal of the current versus the external resistance. The plot gave a straight line relation whose slope was equal to the floating probe potential at this temperature. Furthermore, the oxide resistance, as determined from this plot, agrees with the resistance determined from the slope of a current voltage curve at this temperature. This means that the core-oxide-probe system acts just like a source of e.m.f. with a definite internal resistance. The value of the e.m.f. or resistance varies with the temperature. It was found that the intercept of Fig. 8 varied linearly with the power input to the cathode as is to be expected if the temperature difference between any two points in a medium conducting heat is directly proportional to the rate at which energy flows through the medium.

The second deviation from the predictions is the fact that the curve in Fig. 8 is linear only in the region which is well defined by space charge. Over the portion of the curve in which the current is limited by emission, the potential increases more slowly than the current. This is due to the fact that the probe potential varies with the time and the points shown on the curve represent equilibrium values. Thus, when the plate current was suddenly changed from a low value to 4.3 milliamperes, by raising and maintaining the plate potential to approximately 80 volts, the probe potential changed rapidly with time, as illustrated by points 1, 2, 3 and 4, which were taken 5, 25, 80 and 300 seconds respectively after the plate current was increased.

This phenomenon is the same as that observed when conduction current

is drawn between core and probe and which was described above. If instantaneous values of probe potential had been taken, the straight dashed line would have been obtained. The slope of this line represents the resistance of the oxide between the core and a point in the plane of the probe.

If this interpretation is correct, the resistance as thus determined should be somewhat less than the resistance obtained from the initial line of a conduction current-voltage curve at the same temperature. From Fig. 8 the oxide-resistance is 105 ohms. The resistance determined from the slope of a conduction current voltage curve at the same temperature is 268 ohms. The ratio of these resistances is 2.65. At a temperature of 756°K, the resistance obtained from the probe potential plate current curve is 0.54×10^4 ohms and the resistance determined from the slope of the conduction current-voltage curve is 1.15×10^4 ohms. The ratio between these resistances is 2.12. Since the ratios of the cross-sections of the current paths in the two types of curves is somewhat greater than 1 and somewhat less than 3, it is to be expected that the ratio of the resistances would be somewhere between these values. The observed ratios 2.65 and 2.12 are entirely reasonable. Furthermore, the plate current-probe potential curves are similar to the conduction current-voltage curves as regards their deviation from linearity. This deviation from linearity occurs at the same potential difference between core and probe for the two curves. The magnitude of the deviation at any probe potential is approximately the same in the two cases.

These results fully confirm the prediction that the potential of a point in the oxide with respect to the core should be positive and should be directly proportional to the current through the oxide. It is therefore reasonably certain that the electrons pass through the oxide as they would through a metal of a high resistivity and that they do not become occluded on the oxide particles and thus set up a pseudo space charge.

The conclusion that the active layer is on the oxide surface and that the current is not carried thermionically between core and coating is based thus far on tests in special experimental tubes. It can be extended to numerous other tubes by a consideration of the potential distribution between two insulated bodies both of which are thermionic emitters. Let us assume that the electrons are transferred thermionically from the core to the coating and then reemitted thermionically from the coating to the plate. Let us further assume that the electron emissivity of the core is considerably less than that of the coating. Before any potential is applied to the plate, the potential of the oxide will differ from that of the core by a potential equal to the contact potential difference at the core-oxide interface. At the instant when a positive plate potential is applied, the coating will give up more electrons to the plate than it receives from the core. Consequently the coating will become positively charged with respect to the core and the potential difference between coating and plate will decrease. As long as this potential difference between coating and plate is sufficient to keep the current from the coating saturated, the electron emission from the coating will exceed that received by the coating, and the coating will become more and more positively charged. This process

will continue until the current from the coating is limited by space charge and is just equal to the emission limited current from the core to the coating. When this steady state is reached, an appreciable part if not most of the potential difference applied between core and plate will be used up between the core and the coating. Consequently, when the space current is limited by emission; (1) the potential of a probe embedded in the oxide should be an appreciable fraction of the applied potential; (2) an appreciable part if not the major part of the energy dissipated in the tube should be dissipated in the coating, which should consequently get very hot.

These predictions are not confirmed by experiment. The data for Fig. 8 show that the probe potential is only about 0.3 volt even when the plate potential is 100 volts and even this 0.3 volt is to be ascribed to an iR drop rather than to a potential difference across the core-oxide interface. Furthermore, it is a well-known fact that in commercial tubes, a negligible part of the energy represented by the product of the space current and the applied plate potential is dissipated in the filament. It is only in unusual filaments with very thick, shaggy coatings that any appreciable part of the applied potential is used up in the oxide and in this case the resistance of the coating is sufficient to account for the energy dissipated in the filament. These facts make it appear improbable that the emission is ever limited by the core in ordinary oxide coated filaments.

Do the Electrons Come from the Adsorbed Barium Atoms or from the Underlying Oxide?

While it is obviously impossible to observe directly whether the emitted electrons come from the adsorbed barium or from the underlying oxide, nevertheless experiment can indirectly decide between these two views. The predictions made on these two views are quite distinct and can be tested by experiments.

If the thermions come from the adsorbed barium, the activity or emission current at a fixed temperature should be directly proportional to the number of monatomically adsorbed atoms and should increase steadily from a low value characteristic of a bare surface to a value characteristic of solid barium. On the other hand if the electrons come from the underlying oxide and if the barium is ionized and thus helps the electrons escape, one might reasonably expect the activity to increase at a rate which is much more than proportional to the concentration of adsorbed barium and that it might reasonably reach an optimum value for a monatomic layer before it decreases to its value characteristic of sold barium. Of course, eventually as the concentration of barium increases, the electrons must originate in the barium.

The experiments described above and in previous publications in which barium was deposited on the oxide surface either by electrolysis or by evaporation from an outside source, decidedly favor the second hypothesis and definitely contradict the predictions of the first hypothesis.

The behavior of barium on the oxides is strikingly similar to that of barium on tungsten. In both cases as the surface concentration increases log i

increases rapidly at first then more and more slowly, passes through an optimum and then decreases to approach the value for solid barium; when the surface concentration is subsequently decreased, log i again increases to the same optimum and then decreases toward its original value. This striking similarity in behavior points to a similarity in the mechanism of emission in the two cases.

For a layer of barium or other electropositive elements adsorbed on tungsten, it is generally held that at least some of the adsorbed barium is ionized and that the emitted electrons come from the underlying tungsten rather than from the adsorbed barium. On this adion grid theory one can readily explain: (1) Why the work function decreases,[14] passes through a minimum and then increases,[15] (2) why the contact potential changes correspondingly,[14] (3) why the current voltage curves saturate poorly if the surface is not uniformly covered,[16] (4) why the barium sticks to the tungsten at relatively high temperatures,[15] (5) why the adsorbed elements sometimes come off as positive ions,[14] (6) why the rate of positive ion emission decreases as the surface concentration increases.[14]

Because this adion grid theory is capable of interpreting these experimental facts we believe that for one or perhaps even two layers of barium the emitted electrons come from the tungsten or oxide rather than from the barium.

There is one aspect in which barium on the oxides differs from barium on tungsten. In tungsten the number of "free" electrons or those available for emission is fixed; in the oxides this number probably increases by large factors as the amount of barium dispersed through the oxide increases. This view is based on the observation that the conductivity of oxides increases by large factors when the amount of free metal dispersed in the oxide increases. Presumably the electrons that take part in the conduction are also "free" to leave the surface of the oxide if they have sufficient kinetic energy when close enough to the surface. Consequently it is to be expected that the emission will depend not only on the amount of barium on the surface but also on the amount dispersed through the oxide. The barium on the surface makes it easier for each electron to leave the surface: It decreases the work function ϕ in Richardson's equation, $i=AT^2\epsilon^{-\phi e/kT}$. The barium dispersed through the oxide increases the number of electrons that approach the surface: It increases the "A" in Richardson's equation.

We arrive at this view partly as a result of the following experiment. In the tube described in Fig. 1, the cathode was glowed at 1040°K until its activity as tested at 500°K reached a steady and reproducible value. A measured electron current was then sent into the cold oxide coating from an external filament for a measured time. The activity of the oxide filament as tested at 500°K was determined periodically. It was found that the activity increased, passed through an optimum and then decreased. Following this treatment,

[14] Becker, Trans. Amer. Electrochem. Soc. 55, 153–175 (1929).
[15] Becker, Bell Laboratories Record 9, 54–58, Oct. 1930.
[16] Becker, Phys. Rev. 35, 1431 (1930).

the cathode was glowed at 1040°K while its activity at 500°K was again tested periodically. It was found that the activity increased at first, came to an optimum, which differed slightly from the preceding optimum, and then decreased until it approached a steady value. This steady value was greater than the preceding steady value on glowing at 1040°K. Electrons were then again sent into the oxide until the activity passed through an optimum and decreased. This treatment was again followed by a glowing treatment. Both processes were repeated again and again.

Fig. 9 shows some of the results. The various activities are plotted as a function of the total number of milliampere minutes (m.a.m.) of current sent into the oxide cathode. At any value of m.a.m. there are, in general, four characteristic activities shown in the figure. The first set of points do not

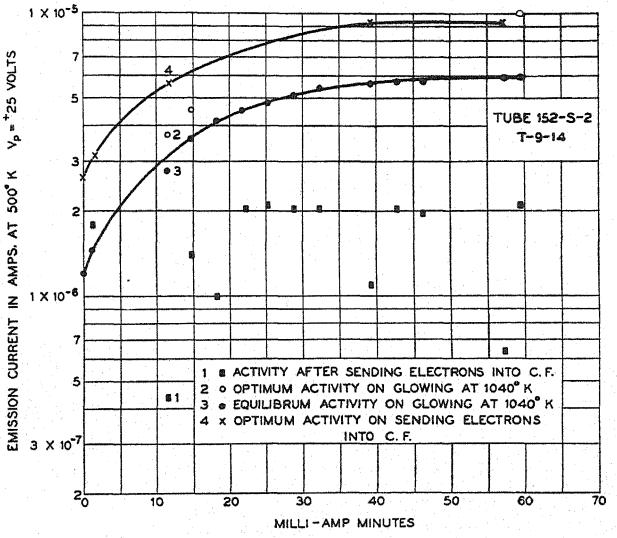


Fig. 9.

and should not form a smooth curve since the m.a.m. between successive glowings at 1040°K was irregular. If the interval between two successive glowings is unusually long, the initial activity is unusually low as it should be. The other sets of points form smooth curves as they should. The most important curve is the uppermost one for the optima on sending electrons into the oxide since each point represents the emission when the surface is covered with a monatomic layer of barium. This confirms the previously known fact, that the concentration of barium on the surface is not the only factor determining the activity.

We interpret this experiment as follows: After the initial glowing at 1040°K the concentrations of barium in the oxide and on the surface had reached a steady state. When electrons were sent into the oxide, oxygen was deposited on the core while barium was brought to the surface by electrolysis. The oxygen combined with the core since it is well known that a Konel core is readily oxidized. When the concentration of barium on the sur-

face reached a monatomic layer, the activity had an optimum value. We estimate that as the electrolysis continued in some cases several layers of barium were deposited on the surface. During the glowing at 1040°K this barium diffused back into the oxide and thus increased the concentration of barium dispersed through the oxide. After each treatment this concentration in the oxide was greater than after the preceding treatment. This is the reason why the optima and the steady value glowing curves increased with the m.a.m.

This experiment seems to us to be a crucial test between the two hypotheses; (1) that the electrons originate in the adsorbed barium itself, (2) they originate in the oxide underneath the adsorbed barium. On the first hypothesis it is difficult or impossible to see why there should be any optimum and why the optima should depend on the treatments to which the oxide was subjected. On the other hand, the second hypothesis is able to explain readily the observed facts.

The Rôle of the Core Metal

In this laboratory it has long been recognized that the nature of the core material has a very great influence on the activities that can be attained and the ease with which they can be attained. King[17] has shown that the average electron emissivity of a number of "combined" coated filaments with platinum-nickel core was higher than the emissivity of similar coatings on platinum-iridium cores. More recently Lowry[4] has shown that uncombined coated filaments with Konel metal cores were better electron emitters than some coated filaments with platinum cores. The emission from oxide coated nickel is also usually much better than from oxide coated platinum. According to Beese,[18] if 0.1 percent of barium is alloyed with the core, the easily attainable activity is appreciably improved.

The influence of the core material on the easily attainable activities is thus a well established fact. It has usually been assumed that this influence is an indirect one. Recently Lowry[4] has expressed the belief that the core material directly affects the activity. As a result he, "assumes that the source of the emission is the composite layer formed by occlusion of alkaline earth metal on the surface of the core". He admits however, "that no crucial tests of this explanation have been offered except that of showing the pronounced influence of the core metal". The experiments described above constitute such a crucial test since they show that the activity is determined by the outer oxide surface. It is well known that thermionic properties are directly affected by only a few atomic layers near the surface. It is also well known that the oxide coating is thousands of layers deep. Consequently the effect of the core material must be an indirect one.

The ways in which the core material may indirectly affect the activity are numerous. Anything which increases the concentration of barium adsorbed on the surface of the oxide or dispersed through the oxide, or anything which changes the composition or physical structure of the oxide will affect the ac-

[17] King, Bell Tech. Jrl. **2**, 31–100 (1923).
[18] Beese, Phys. Rev. **36**, 1309–1313 (1930).

tivity. The oxide very likely reacts chemically with some core constituents to form metallic barium some of which reaches the surface by diffusion. Carbon which is frequently present in cores as an impurity almost certainly reacts with the oxides. In some cases certain core materials, nickel for example, may be dispersed through the oxides. Such dispersed materials change the conductivity of the oxide and the ease with which electrolytic decomposition takes place. It is quite likely that such impurities in the oxide affect the crystal size of the oxide and thus influence diffusion, adsorption, and electrolytic phenomena which in turn affect the activity. If the core is purposely made to contain metallic barium, this barium will diffuse through the oxide and become adsorbed on the surface. The core material may also influence the ease with which the carbonates are decomposed to the oxides when the filament is first heated. Finally, the core material certainly affects the composition of the compounds which are formed when oxide filaments are heated in air to make "combined" filaments. The nature of these compounds and the products of their decompostion when the filament is heated in a vacuum, certainly affects the activity. In these and numerous other cases the core affects the activity in a round-about way rather than directly.

Conclusions

From these experimental results we conclude that: (1) The active layer is at the outer oxide surface.[19] The activity depends upon the concentration of barium and oxygen on this surface and also upon the amount of metallic barium dispersed through the oxide. The core material does not directly affect the emission but it does greatly affect the ease with which free barium is produced by heat treatment or electrolysis. (2) The thermionic electrons originate in the oxide just underneath the adsorbed barium. (3) Most of the current through the oxide is conducted by electrons, a small portion being carried by barium and oxygen ions.

[19] Huxford (Phys. Rev. **38**, 379–395 (1931)) comes to this same conclusion as a result of his work on the photoelectric emission from oxide cathodes.

WAVE-LENGTH STANDARDS IN THE SPECTRA OF ALUMINUM. SILICON AND BISMUTH IN THE SCHUMANN REGION

By R. V. Zumstein
Mendenhall Laboratory, Ohio State University
(Received October 5, 1931)

Abstract

The second order spectra of these elements have been photographed along with first order iron lines with a two meter vacuum grating. Between 1900 and 1500A values are found for the aluminum lines which check very closely the work of Bowen and Ingram. The silicon wave-lengths are 1816.922, 1808.01, 1533.42 and 1526.71. For bismuth the values are 1902.33, 1823.71, 1791.82, 1787.39 and 1777.01. These values are believed to be accurate to within about 0.02A.

IN A previous communication[1] certain wave-lengths in the spectra of carbon and tin were determined to about 0.02A. With a few improvements the same method has been used to obtain standard wave-lengths in the spectra of aluminum, silicon and bismuth. The details of the method may be obtained from the above mentioned article. The results obtained are recorded in Table I. Each measurement is the average of about five plates.

Aluminum

The source of light was a carbon arc in an atmosphere of hydrogen or nitrogen at 1 cm pressure. The lower carbon was 3.5 cm diameter with a shallow hole in the center. About 4 gm aluminum and 0.5 gm of very pure iron wire were placed in the lower electrode. The upper electrode was a solid carbon rod 1 cm diameter with a distance between the electrodes of about 3 mm. The current of 80 amperes was obtained from a 110 volt d.c. generator. The lower electrode was positive and the exposure lasted about 8 minutes. A fluorite window was cemented over the slit in order to allow a good vacuum to be maintained in the spectrometer and any desired gas pressure in the arc chamber. Bowen and Ingram[2] have also made measurements of aluminum lines by direct comparison with iron and their results are included in the table. Although the two sources of light and the methods of producing the spectra were different yet the agreement is very good. The aluminum arc works best in the nitrogen atmosphere. It was, however, necessary to use hydrogen when the lines were near the strong cyanogen band at 3884A. Recent measurements of these lines have also been made by Sawyer and Paschen,[3] Selwyn[4] and Fowler.[5]

[1] R. V. Zumstein and D. S. Marston, Phys. Rev. **38**, 305 (1931).
[2] I. S. Bowen and S. B. Ingram, Phys. Rev. **28**, 444 (1926).
[3] R. A. Sawyer and F. Paschen, Ann. d. Physik **84**, 1 (1927).
[4] E. W. H. Selwyn, Proc. Phys. Soc. **41**, 402 (1929).
[5] A. Fowler, Proc. Roy. Soc. **A123**, 427 (1929).

TABLE I. *Wave-length standards (I.A. vac).*

Aluminum II and III

Bowen and Ingram			Zumstein			Classification	
Int.	λ	error	Int.	λ	error		
10	1862.775	0.02	5	1862.782	0.02	III	$3s^2S_{\frac{1}{2}}-3p^2P_{\frac{1}{2}}^0$
			6	1862.34	0.03	II	$3s3p^3P_2^0-3s4s^3S_1$
			4	1858.05	0.03	II	$3s3p^3P_1^0-3s4s^3S_1$
			2	1855.95	0.03	II	$3s3p^3P_0^0-3s4s^3S_1$
10	1854.715	0.02	6	1854.722	0.02	III	$3s^2S_{\frac{1}{2}}-3p^2P_{1\frac{1}{2}}^0$
4	1767.730	0.01	2	1767.76	0.02	II	$3s3p^3P_2^0-3p^2\,{}^3P_1$
4	1765.814	0.01	1	1765.84	0.02	II	$3s3p^3P_1^0-3p^2\,{}^3P_0$
5	1763.939	0.01	5	1763.95	0.02	II	$3s3p^3P_{21}^0-3p^2\,{}^3P_{21}$
4	1761.973	0.01	1	1762.00	0.02	II	$3s3p^3P_0^0-3p^2\,{}^3P_1$
4	1760.101	0.01	2	1760.13	0.02	II	$3s3p^3P_1^0-3p^2\,{}^3P_2$
5	1724.982	0.01	5	1724.981	0.01	II	$3s3p^3P_2^0-3s3d\,{}^3D_{321}$
5	1721.273	0.01	3	1721.279	0.01	II	$3s3p^3P_1^0-3s3d\,{}^3D_{21}$
4	1719.455	0.01	1	1719.459	0.01	II	$3s3p^3P_0^0-3s3d\,{}^3D_1$
6	1670.802	0.03	4	1670.78	0.03	II	$3s^2\,{}^1S_0-3s3p\,{}^1P_1^0$
	Fowler			*Silicon II* Zumstein			
10	1816.98		4	1816.922	0.01		$3s^23p^2P_{1\frac{1}{2}}^0-x?$
8	1808.09		3	1808.01	0.02		$3s^23p^2P_{\frac{1}{2}}^0-x?$
10	1533.55		7	1533.42	0.02		$3s^23p^2P_{1\frac{1}{2}}-3s^24s^2S_{\frac{1}{2}}$
8	1526.38		5	1526.71	0.02		$3s^23p^2P_{\frac{1}{2}}^0-3s^24s^2S_{\frac{1}{2}}$
	McLennan, etc.			*Bismuth II* Zumstein			
100U	1902.42		25	1902.33	0.02		$6p_{\frac{1}{2}}6p_{1\frac{1}{2}}3_2-6p_{\frac{1}{2}}7s\,2_1^0$
80	1823.80		5	1823.71	0.02		$6p_{1\frac{1}{2}}6p_{1\frac{1}{2}}4_2-6p_{1\frac{1}{2}}7s\,9_2^0$
70	1791.93		9	1791.82	0.02		$6p_{\frac{1}{2}}6p_{1\frac{1}{2}}2_1-6p_{\frac{1}{2}}7s\,1_0^0$
80	1787.47		4	1787.39	0.02		$6p_{1\frac{1}{2}}6p_{1\frac{1}{2}}4_2-6p_{1\frac{1}{2}}7s\,10_1^0$
90u	1777.13		10	1777.01	0.02		$6p_{\frac{1}{2}}6p_{1\frac{1}{2}}2_1-6p_{\frac{1}{2}}7s\,2_1^0$

U Very diffuse, u diffuse

Silicon

There are two strong pairs of lines due to Si II. They should be very useful standards because a small quantity of silicon brings them out in the arc. I frequently find them in the spectra of vacuum tubes from the glass or quartz wall of the tube. Fowler's[5,6] wave-lengths are included in the table. His value 1526.38 seems to be a misprint of 1526.83, the silicon lines were obtained from an arc with a smaller lower carbon, about 1 cm diameter having a hole 0.5 cm diameter which contained the silicon and iron. It was necessary to use the hydrogen atmosphere as bands were always present in the nitrogen atmosphere. The current was 60 amperes d.c.

Bismuth

There are five Bi II lines which are very strong in the arc and spark. They may also be obtained from a fused quartz vacuum tube if a small piece of bis-

[6] A. Fowler, Phil. Trans. **A225**, 46 (1925).

muth is placed in the tube. The most recent measurement of the bismuth lines seems to be by McLennan, McLay and Crawford[7] and their values are given in the table. The classification is also taken from their paper. The second order bismuth and first order iron spectra were obtained from an arc in which the lower electrode was a 2.5 cm iron rod with a hole 0.5 cm diameter and 3 cm deep to contain the bismuth. The upper electrode was carbon as before. The current was 35 amperes d.c. in hydrogen at 1 cm pressure for most of the plates. A few were taken with 60 and 90 ampere alternating current arcs in nitrogen. Because there was no systematic shift of the wavelength with increase of current it is felt that the iron lines are free from pole effect in spite of the large current used (to the order of accuracy that may be obtained from a spectrum having the dispersion of 6A/mm).

At present there is great interest in the fine structure of the bismuth lines. 1902.33 was very intense and broad if there was much bismuth present. It is only of value as a standard where there is a slight concentration of bismuth atoms. 1777.01 was always slightly diffuse even at small concentrations. It would perhaps resolve into components in a higher order or with a finer slit. The other bismuth lines are sharp. It may be mentioned that our spectroscope has a slit 0.05 mm wide and clearly resolves the carbon lines 1658.12 and 1657.90. It is hoped that others will publish similar (or better) wavelength determinations. We should have a much larger number of lines in this region of the spectrum for which at least three independent observers check to within 0.02A. I am indebted to Dr. J. B. Green for helpful discussion of the classification of these lines.

[7] McLennan, McLay and Crawford, Proc. Roy. Soc. **A129**, 587 (1930).

CERTAIN SPECTRA IN THE VANADIUM I ISO-ELECTRONIC SEQUENCE

By Helen T. Gilroy
Physical Laboratory, Cornell University
(Received July 24, 1931)

Abstract

Displacement of multiplets in the iso-electronic sequence which begins with the arc spectrum of vanadium.—Regular displacements were observed for analogous quartets and sextets in the spectra of Mn III, Fe IV, Co V and Ni VI, continuing those already known for V I and Cr II. In addition a new sextet sequence has been found for V I to Co V. The configuration changes investigated were $3d^4\,4p$ to $3d^4\,4s$, $3d^4\,4d$ to $3d^4\,4p$, $3d^4\,4p$ to $3d^5$ and $3d^3\,4sp$ to $3d^3\,4s^2$.

Moseley diagrams and the irregular doublet law.—The irregular doublet law was applied to systems of sextets and quartets due to electronic changes in atoms having five electrons in outer shells. When the change did not involve a change in total quantum number, the law was closely followed.

Centroid diagram.—Shifts of energy levels for sextets and quartets of $(P^\circ\ D^\circ\ F^\circ)$ $3d^4\,4p$ have been calculated for V I to Co V, using the centroid method. Values are not absolute because not all the levels of this configuration are known. But relative values are useful for predicting higher states in the sequence.

Landé interval rule.—Typical tests of the Landé interval rule are given.

Regular doublet law.—The $(\Delta\nu)^{1/4}$ is linear with atomic number in some cases, but not in all.

Tables are given for the new lines and new term values.

THE regular and irregular doublet laws have been shown to hold for several iso-electronic sequences in the first long period of the table of elements.[1,2,3]. This report gives the results of a further application of these laws to the iso-electronic sequence which starts with the arc spectrum of vanadium, and also of an attempt to find radiated lines due to changes in energy level involving L values which are less than the maximum.

The neutral vanadium atom has, in addition to the closed sub-shells of electrons called $1s^2\ 2s^2\ 2p^6$ and $3s^2\ 3p^6$, five valence electrons which, for this iso-electronic sequence, may have the configuration $3d^3\ 4s^2$. Lines in the arc spectrum of vanadium will be due then, to excitation of any one or more of these valence electrons and their subsequent return to a lower energy state. Several sextets and quarters have previously been found in this spectrum, due to changes in electron configuration from $3d^4 4p$ to $3d^4 4s$, $3d^4 4p$ to $3d^5$, $3d^3 4sp$ to $3d^3 4s^2$, $3d^3 4sp$ to $3d^4 4s$ and $3d^4 4p$ to $3d^3 4s^2$.[4,5,6].

[1] Gibbs and White, Phys. Rev. **29**, 426 and 655 (1927); Gibbs and White, Phys .Rev. **33**, 157 (1929).
[2] Gibbs and White, Proc. Nat. Acad. Sci. **13**, 525 (1927); and **12**, 598 and 448 (1926).
[3] White, Phys. Rev. **33**, 538, 672 and 914 (1929).
[4] W. F. Meggers, J. of Wash. Acad. of Sci. **13**, 317 (1923); **14**, 151 (1924).
[5] O. Laporte, Die Naturwissenschaften **11**, 779 (1923).
[6] H. N. Russell, Astrophys. J. **66**, 184 (1927).

Of the second member of this sequence, the first spark spectrum of chromium, only quartets and sextets of the electron changes $3d^44p$ to $3d^44s$ and $3d^44p$ to $3d^5$ have been reported.[6,7,8]. Since the chromium atom which is emitting the first spark spectrum has lost one electron, it will have as many electrons outside the completed sub-shells as the neutral vanadium atom. Hence the spectra have been found to be similar in several respects, though the relative order of energy levels may differ. This will be shown later in one of the graphs. Very few data have been published about the remaining spectra of

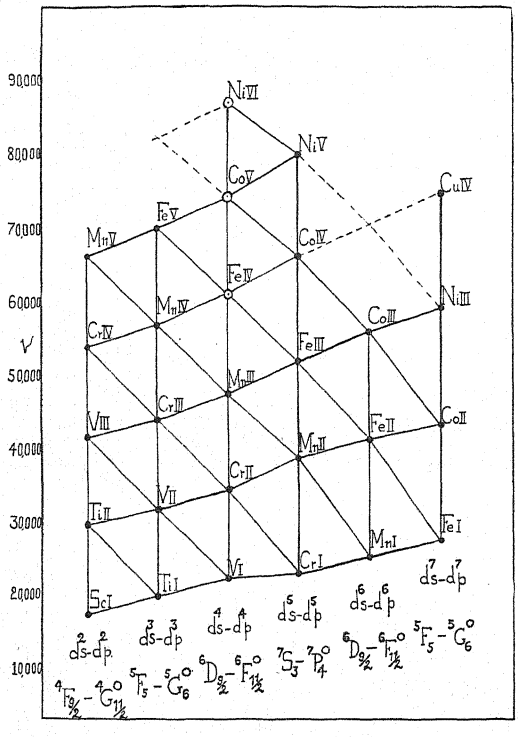


Fig. 1. Regular displacement of multiplets.

this sequence, Mn III, Fe IV, Co V and Ni VI. One sextet group in Mn III, $3d^44s\ ^6D-3d^44p\ ^6F^\circ$, has been identified.[2]

According to the present theory of atomic structure and line spectra, a space quantization of the electrons $3d^44s$ give the following energy levels;—$^2(S, D, G)$, $^{2,4}(P, F)$, $^2(S, D, F, G, I)$, $^{2,4}(P, D, F, G, H)$ and $^{4,6}(D)$. Of these, only the $^{4,6}(D)$ which are involved in the emission of the more intense lines, have been considered in this investigation. Similarly, from the $3d^44p$ configuration only those levels which are derived from the ^5D level of a d^4 configuration, have been studied, that is $^{4,6}(P^\circ, D^\circ, F^\circ)$. In the next higher configuration, $3d^44d$, we have levels $^{4,6}(S, P, D, F, G)$ from the same $d^4\ ^5D$ limit. In the d^5

[7] Meggers, Kiess and Walters Jr., J. Opt. Soc. Amer. 9, 361 (1924).
[8] C. C. Kiess and O. Laporte, Science 63, 234 (1926).

configuration there are levels $^4(D, G)$ and ^6S from the same limit. Since there are two possible methods of ionizing an atom having valence electrons d^4s, one by the removal of an s electron and the other by the removal of a d electron, we might build a five-electron system on the $3d^34s$ configuration, whose lowest energy levels should be $^5(P, F)$. The addition of an s electron to this configuration gives levels $^{4,6}(P, F)$ of the $3d^34s^2$ configuration, while the addition of a p electron gives $3d^34sp$ $^{4,6}(S°, P°, D°, F°, G°)$. This report includes the wave-lengths of a few multiplets due to the electronic change ($3d^34s^2-3d^34sp$).

Displacement of Multiplets

The method employed for predicting the spectral regions in which these multiplets should be found, is that of Gibbs and White.[1,2] Figure 1 is in part a reproduction of their graph showing the regular displacement of multiplets with increasing atomic number but the same number of outer electrons, and with increasing number of d electrons in the incompleted sub-shell but in the same state of ionization. For one electron transition, $3d^44s-3d^44p$, and one multiplet group, $^6D-^6F°$, radiated frequencies have been found for V I[4], Cr II[7] and Mn III[2] with separations of about 13,000 cm^{-1}. From this regularity one may expect that the corresponding line for Fe IV will be at about 61,000 cm^{-1}, for Co V at about 74,000 cm^{-1} and for Ni VI at about 87,000 cm^{-1}. These points are indicated by circles instead of solid dots in Figure 1. In Fe V the line $3d^34s$ $^5F_5-3d^34p$ $^5G°_6$ found by White[3] at 69,905 cm^{-1} fits into this diagram, as do $3d^54s$ $^7S_3-3d^54p$ $^7P°_4$ for Co IV and Ni V at 66,573 cm^{-1} and 80,376 cm^{-1} respectively, both determined by Morell.[9] With these frequencies and those now identified for lines $^6D-^6F°$ in Fe IV, Co V and Ni VI, it is possible to predict with a fair degree of accuracy the most intense lines in parallel sequences. For instance, the line $3d^34s$ $^5F_5-3d^34p$ $^5G°_6$ of Co VI should be at 82,500 cm^{-1} and $3d^64s$ $^6D_{9/2}-3d^64p$ $^6F°_{11/2}$ of Ni IV at 70,700 cm^{-1}.

Photographs taken with a vacuum spectrograph in the regions indicated for the five-electron sequences, show the head line of ($^6D-^6F°$) ($3d^44s-3d^44p$) from Fe IV at 61,312 cm^{-1}, from Co V at 74,312 cm^{-1} and from Ni VI at 87,388 cm^{-1}. These are plotted in Figure 2. In the same manner, from a knowledge of quartets and sextets in the spectra of V I and Cr II, corresponding multiplets have been found for the remainder of the sequence. Some of these are shown in Fig. 2. This completes the multiplet groups produced by the electron change $3d^44s-3d^44p$, which approach the limit $3d^4$ ^5D, a multiplet arising from the configuration $3d^4$ of the corresponding atom, in the next higher state of ionization.

Another possible configuration change involved in this same iso-electronic sequence is from $3d^44p$ to $3d^5$. Since ^6S is the only sextet in the $3d^5$ configuration the only probable sextet group of lines of any intensity is $^6S-^6P°$. This results in three lines, $^6S_{5/2}-^6P°_{3/2,5/2,7/2}$ whose term differences are already known for all the elements in the sequence, having been found in one of the

[9] Morell, Thesis, Cornell, 1928.

sets of multiplets mentioned above; i.e $(3d^44s-3d^44p)$ $(^6D-^6P^\circ)$. This group of lines has been followed through the sequence except in Ni VI, where the lines should appear at about 318A. At this very short wave-length the lines are so faint and the probable error in reciprocal cm so large, that this group has been omitted from the tables of wave-lengths and term values, although two lines were found approximately in this position. Lines due to two more changes in electronic configuration, $3d^44p-3d^44d$ and $3d^34s^2-3d^34sp$, have been found for the sequence to Co V. The group $^6F^\circ-^6G$ from the $3d^44p-3d^44d$ change, involving the largest L values, contains the strongest lines of the first configuration change, though much weaker than the strong lines of the $3d^44s-3d^44p$ groups. For Mn III two additional sextet groups, $^6F^\circ-^6F$ and $^6F^\circ-^6D$, have been found for $3d^44p-3d^44d$.

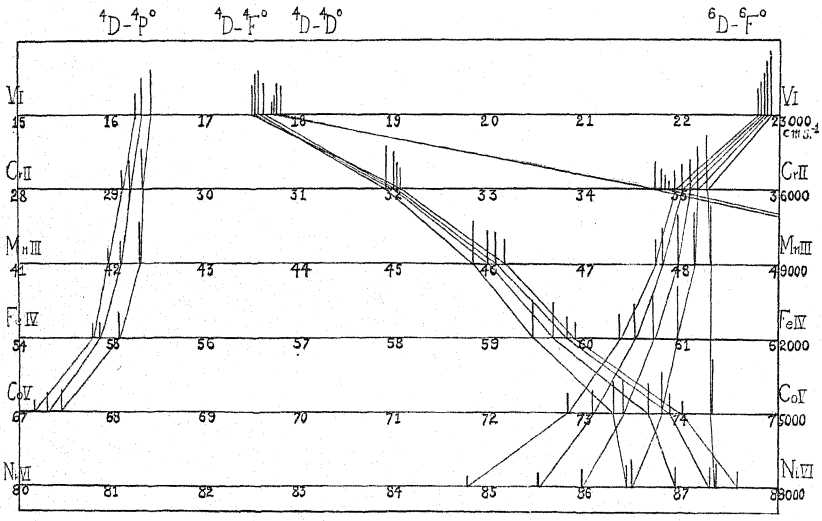


Fig. 2. Displacement of multiplets. Iso-electronic sequence $3d^44s-3d^44p$.

In Figure 2 the nearly linear increase in radiated frequency with increasing atomic number, can be observed from the small change in direction of the connecting lines. This is also true of other multiplets not shown in this chart. A $3d^44p-3d^44d$ change involves approximately 20,000 cm^{-1} shift in frequency from any element to the next higher in the sequence, a $3d^44s-3d^44p$ change involves 13,000 cm^{-1} shift and a $3d^34s^2-3d^34sp$, about 13,500 cm^{-1}. Where the change in electronic configuration involves a change in total quantum number, the lines are displaced somewhat irregularly toward the shorter wave-lengths. In the case of a $3d^5-3d^44p$ change the displacement is about 60,000 cm^{-1} between any two members of the sequence.

One of the tests which has been used throughout to distinguish between lines due to high and low stages of atomic ionization, is apparently not absolutely reliable when adjacent lines belong to different sequences. In general, the presence of an inductive resistance in series with the spark gap very

greatly reduces the intensity of the high ionization lines.[10,11]. In the manganese spectrum the $(3d^44p-3d^44d)$ $(^6F^\circ-{}^6G)$ group of Mn III is closely adjacent to $(3d^34s-3d^34p)$ $(^5F-{}^5G^\circ)$ of Mn IV and $(3d^24s-3d^24p)$ $(^2F-{}^2F^\circ)$ of Mn V. An inductance which is sufficient nearly to efface the strongest line and completely to efface the other lines of the Mn III group, reduces the intensities of the lines of the Mn IV and Mn V groups to a much less extent. Without the inductance the intensities of the latter two groups are nearly the same as that of the strongest Mn III line in the multiplet under discussion.

Irregular Doublet Law

These same data may be combined in another manner to illustrate the irregular doublet law. Bowen and Millikan[12] have shown that the irregular doublet law for x-rays may be transferred to doublets of the second and third periods which are due to one-electron systems. Gibbs and White[1,2,3,13] have extended this application to doublets of the fourth, fifth and sixth periods and to triplets, quartets and quintets in the first and second long periods of the elements. Table I gives the results of a test of this law for systems of lines due to five electrons in outer shells, quartets and sextets having the largest L

TABLE I. *Irregular doublet law.* Values of $\nu^{1/2}$ referred to $3d^4\ {}^5D_0$ of V II, Cr III, Mn IV, etc.

Config.	T.	V I	Δ	Cr II	Δ	Mn III	Δ	Fe IV	Δ	Co V	Δ	Ni VI
$3d^44s$	$^6D_{9/2}$	228	120	348	122	470	122	592	122	714	122	836
$3d^44p$	$^6F^\circ_{11/2}$	171	122	293	122	415	123	538	122	660	122	782
$3d^44d$	$^6G_{13/2}$	90	126	216	121	337	122	459	122	581	122	703
$3d^5$	$^6S_{5/2}$	182	184	366	162	528	150	678	143	821	129	(950)
	Values of $\nu^{1/2}$ referred to $3d^4\ {}^5D_0$ of V II, Cr III, Mn IV, etc.											
$3d^44s$	$^4D_{7/2}$	214	124	338	123	461	124	585	122	707	123	830
$3d^44p$	$^4F^\circ_{9/2}$	167	120	287	121	408	123	531	122	653	123	776
	Values of $\nu^{1/2}$ referred to $3d^34s\ {}^5F_1$ of V II, Cr III; etc.											
$3d^34s^2$	$^4F_{9/2}$	237.5	77.5	315	77.5	392.5	77.5	470	78	548		
$3d^34sp$	$^4G^\circ_{11/2}$	158	78	236	77.5	313.3	77.3	390.6	77.8	468.4		

values being selected to represent each system. Graphically this can be shown in a Moseley diagram, as in Fig. 3. In this figure are plotted the square roots of term values referred to $3d^4\ {}^5D_0$ of the corresponding atom in the next higher state of ionization. In the case of V I, for instance, Russell's[14] value of 52,300 for the limit of $3d^44s\ {}^6D_{1/2}$ was assumed, giving 51,988 for $3d^44s\ {}^6D_{9/2}$. The square root of 51,988, that is 228, was then used as the starting point for the graph. Knowing the radiated frequency of $3d^44s\ {}^6D_{9/2}-3d^44p\ {}^6F^\circ_{11/2}$ we may

[10] Fowler, Phil. Trans. Roy. Soc. **A225**, 1 (1925).

[11] Gibbs, Vieweg and Gartlein, Phys. Rev. **34**, 406 (1929).

[12] Bowen and Millikan, Phys. Rev. **24**, 209 (1924); Phys. Rev. **25**, 295, and **26**, 150 (1925); **27**, 144 (1926).

[13] Gibbs and White, Proc. Nat. Acad. Sci. **12**, 551 and 675 (1926); **14**, 345 and 559 (1928); Phys. Rev. **29**, 359 (1927); **31**, 520 (1928); **33**, 157 (1929).

[14] Russell, Astrophys. J. **66**, 233 (1927).

determine the term value of $3d^4p\ {}^6F^\circ_{11/2}$ referred to the same limit. The square root of this term value gave the first point on the $3d^44p\ {}^6F^\circ_{11/2}$ curve. For the Cr II spectrum Russell's approximate value of 122,000 for $3d^44s\ {}^6D_{1/2}$ referred to $3d^4\ {}^5D_0$ of Cr III, was used and the square roots of term values for $3d^44s\ {}^6D_{9/2}$ and $3d^44p\ {}^6F^\circ_{11/2}$ were determined as in the case of V I. The limits of the sextet series are not known for Mn III, so an extrapolated number for the square root of the term value was read from the graph, assuming that

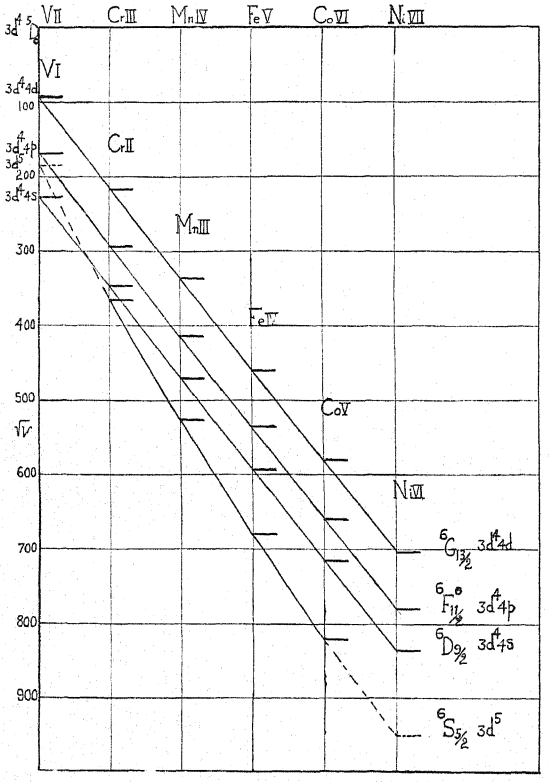


Fig. 3. Moseley Diagram. $\nu^{1/2}$ vs. atomic number.

$3d^44s\ {}^6D_{9/2}$ could be represented by a straight line. This assumption was made on the strength of curves for four sequences reported by White.[3] Since the radiated frequency $3d^44s\ {}^6D_{9/2}-3d^44p\ {}^6F^\circ_{11/2}$ is known, the square root of the term value for $3d^44p\ {}^6F^\circ_{11/2}$ can be readily calculated. A continuation of this method for the remaining elements in the sequence resulted in parallel lines, showing that $\Delta\nu^{1/2}$ is constant, independent of the atomic number, as required by the irregular doublet law. When the same method was applied to the lines $3d^44d\ {}^6G_{13/2}$ and $3d^5\ {}^6S_{5/2}$ corresponding curves were obtained. In the former case the curve is very nearly parallel to those for $3d^44p\ {}^6F^\circ_{11/2}$ and $3d^44s\ {}^6D_{9/2}$, but not in the latter case. Since the irregular or screening doublet law in x-ray spectra holds only for levels between which the transition involves no change in total quantum number of the electrons, the line representing

$\nu^{1/2}$ for $3d^5\ {}^6S_{5/2}$ should not be parallel to those for $3d^44s$, $3d^44p$ and $3d^44d$, in all of which the total quantum numbers of all the electrons involved in the electronic configuration, are the same.

The term values for the quartets, recorded in Table I, are referred to the lowest level, $3d^4\ {}^5D_0$, of the sextet limits, and the same method was used in calculating the $\nu^{1/2}$ for successive elements. A slightly different method was

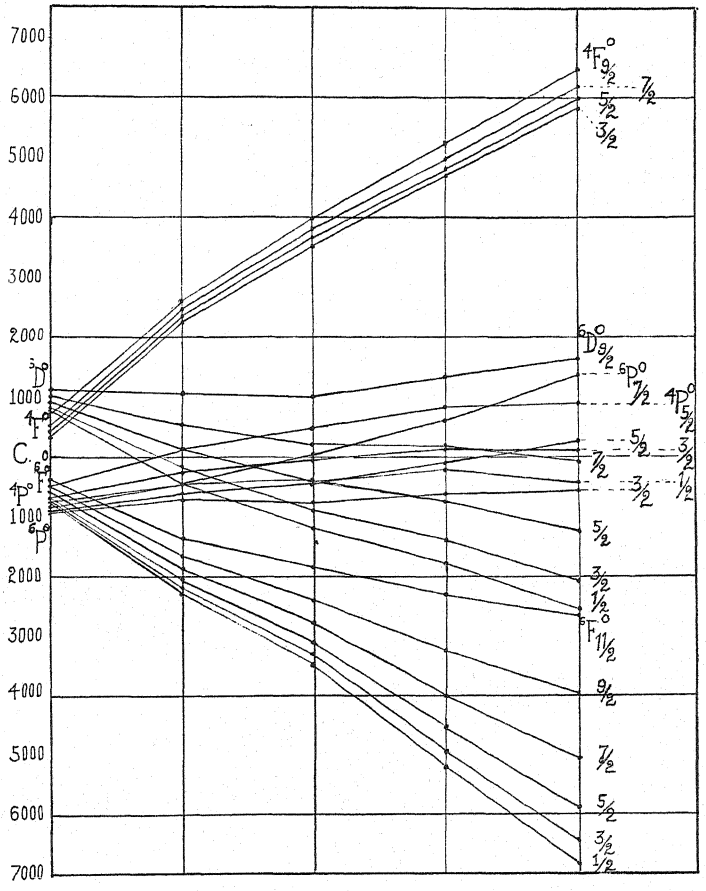


Fig. 4. Shift of Energy Levels. $3d^44p\ {}^4(F^\circ P^\circ)\ {}^6(P^\circ D^\circ F^\circ)$

used for the second set of quartets in Table I, because the limits were known only in the case of $3d^34s^2\ {}^4F_{9/2}$ of V I. For convenience, the reference level taken is $3d^34s\ {}^5F_1$ of V II rather than the actual limit, $3d^34s\ {}^5F_5$. From the radiated frequency $3d^34s^2\ {}^4F_{9/2}-3d^34sp\ {}^4G^\circ_{11/2}$ and the known term value of $3d^34s^2\ {}^4F_{9/2}$, the term value for $3d^34sp\ {}^4G^\circ_{11/2}$ can be found and hence the $\nu^{1/2}$ for each level. Assuming that $\Delta\nu^{1/2}$ is constant and knowing the values of $3d^34s^2\ {}^4F_{9/2}-3d^34sp\ {}^4G^\circ_{11/2}$ for the remainder of the sequence, values for $\nu^{1/2}$ can be calculated. With these values plotted for both $3d^34s^2\ {}^4F_{9/2}$ and $3d^34sp\ {}^4G^\circ_{11/2}$, the lines are observed to be straight, which is in agreement with the

results for the sextets and the first set of quartets having the same total quantum number. The one exception is the $3d^5\ {}^6S_{5/2}$ line, already mentioned, which is related to the others by means of an electronic change involving a change in total quantum number and hence not a violation of the irregular doublet law.

A comparison of Table I with Fig. 3, shows that $3d^34s^2\ {}^4F_{9/2}$ represents the lowest energy level of V I, but does not for the remainder of the sequence. Instead, $3d^5\ {}^6S_{5/2}$ has dropped slightly below $3d^34s^2\ {}^4F_{9/2}$ for Cr II and with rapidly increasing frequency difference, continues to be the lowest level for the rest of the sequence. The level $3d^5\ {}^6S_{5/2}$ for Ni VI has not been definitely determined, but there is small probability that the $\nu^{1/2}$ will not be in the position indicated by the dotted line in Fig. 3.

TABLE II. *Landé interval rule.* Term separations of $3d^14s$ in cm^{-1}.

Spectrum	$^6D_{9/2}$	$^6D_{7/2}$	$^6D_{5/2}$	$^6D_{3/2}$	$^6D_{1/2}$	
V I	113 (4.5)	91 (3.6)	67 (2.7)	41 (1.6)		(4)
Cr II	192.7 (4.5)	156 (3.6)	115 (2.7)	70.8 (1.7)		(7)
Mn III	296 (4.5)	241 (3.7)	180 (2.7)	132 (2.0)		
Fe IV	594.5 (4.5)	476 (3.6)	341 (2.6)	253 (1.9)		
Co V	851 (4.5)	678 (3.6)	524 (2.7)	314 (1.66)		
Ni VI	1272 (4.5)	976 (3.5)	642 (2.3)	341 (1.2)		
Theory	4.5	3.5	2.5	1.5		

	$^4D_{7/2}$	$^4D_{5/2}$	$^4D_{3/2}$	$^4D_{1/2}$	
V I	137 (3.5)	102 (2.6)	63 (1.6)		(4)
Cr II	226 (3.5)	166.7 (2.6)	103 (1.6)		(7)
Mn III	328 (3.5)	241 (2.6)	146 (1.6)		
Fe IV	448 (3.5)	307 (2.4)	184 (1.4)		
Co V	626 (3.5)	428 (2.4)	265 (1.5)		
Ni VI	852 (3.5)	625 (2.6)	373 (1.5)		
Theory	3.5	2.5	1.5		

Centroid Diagram

Greater detail in analysing the shift of energy levels is presented in Fig. 4. The zero line in this figure is the centroid of the configuration under consideration for each element, in so far as the levels have been determined. Vertical distances are the frequency differences between this centroid and each level. The centroid, according to the usual method[15] is calculated as the mean of all the levels weighted in proportion to $2j+1$, where j is the inner quantum number of the level. The final grouping of the levels in Co V indicates a possible coupling which differs from the Russell-Saunders but is not sufficiently different to follow the jj coupling of much heavier elements.[15,16] Addition of other quartet and doublet levels, now unknown, will change the values of the levels given, but should not appreciably change their relative shift. The relative values are useful in predicting higher states in the sequence.

The Landé Interval Rule

The Landé interval rule was found useful in locating most of these multiplets. Though it does not hold for all cases, Table II gives a typical illustration of the extent of variation in the spectra studied. In this table term separations are given in reciprocal centimeters; in brackets under each separation is a number to be compared with the theoretical ratios of term separations given at the bottom of the table. The spread of the multiplets, which appears

Table III. *Regular doublet law.*

			$\Delta\nu$	$\Delta\nu^{1/4}$	s
$3d^4 4s$	$^4D_{7/2}-{}^4D_{5/2}$	V I	137	3.42	14.36
		Cr II	226	3.88	14.20
		Mn III	328	4.28	14.18
		Fe IV	448	4.61	14.34
		Co V	626	5.02	14.31
		Ni VI	852	5.41	14.32
$3d^4 4s$	$^6D_{9/2}-{}^6D_{7/2}$	V I	113	3.26	17.85
		Cr II	193	3.73	18.22
		Mn III	296	4.16	18.50
		Fe IV	594	4.92	18.30
		Co V	851	5.41	18.55
		Ni VI	1272	5.98	18.68
$3d^4 4p$	$^6F^\circ_{11/2}-{}^6F^\circ_{9/2}$	V I	142	3.46	17.65
		Cr II	287	4.12	17.62
		Mn III	490	4.71	17.78
		Fe IV	935	5.54	17.63
		Co V	1374	6.10	17.62
		Ni VI	2183	6.82	17.50
$3d^4 4d$	$^6G_{13/2}-{}^6G_{11/2}$	V I	99	3.15	17.83
		Cr II	159	3.56	18.14
		Mn III	317	4.24	18.05
		Fe IV	575	4.90	17.96
		Co V	929	5.53	17.93

[15] Mack, Laporte and Lang, Phys. Rev. **31**, 748 (1928).
[16] Mack, Phys. Rev. **34**, 17 (1929).

TABLE IV. *Configuration change* $3d^34s^2-3d^34sp$.

Mn III.

s^2 / sp	$^4F_{9/2}$	632	$^4F_{7/2}$	460	$^4F_{5/2}$	340	$^4F_{3/2}$
$^4G^\circ_{11/2}$	55850.6 50 1790.49						
495							
$^4G^\circ_{9/2}$	55355.7 23 1806.50		55987.9 50 1786.10				
338							
$^4G^\circ_{7/2}$	55017.6 18 1817.60		55650.2 25 1798.05		56110.1 40 1782.19		
292							
$^4G^\circ_{5/2}$					55818.2 12 1793.57		56158.3 6 1780.68

Fe IV.

s^2 / sp	$^4F_{9/2}$	824	$^4F_{7/2}$	626	$^4F_{5/2}$	450	$^4F_{3/2}$
$^4G^\circ_{11/2}$	68268.2 40 1464.81						
595							
$^4G^\circ_{9/2}$	67673.2 5 1477.69		68496.9 40 1459.92				
425							
$^4G^\circ_{7/2}$	67246.8 5 1487.35		68071.7 37-x 1469.04		68697.4 25 1455.66		
356							
$^4G^\circ_{5/2}$					68341.0 4 1463.25		68791.4 15 1453.67

Co V.

s^2 / sp	$^4F_{9/2}$	1088	$^4F_{7/2}$	966	$^4F_{5/2}$	544	$^4F_{3/2}$
$^4G^\circ_{11/2}$	80844.0 20 1236.95						
846							
$^4G^\circ_{9/2}$	80198.2 8 1246.91		81186.6 15 1231.73				
532							
$^4G^\circ_{7/2}$			80654.9 2 1239.85		81420.6 8 1228.19		
419							
$^4G^\circ_{5/2}$					81001.2 2 1234.55		81545.4 3 1226.31

in Fig. 2, is here shown in the increasing value of $\Delta\nu$ with increasing atomic number.

Regular Doublet Law

The other doublet law which has already been mentioned, the relativity or regular doublet law in x-ray spectra, serves as another check on the selection of multiplets. This "doublet" must be tested by the $\Delta\nu$ between levels having the same L values but different inner quantum numbers.[17] Landé first noticed that this relation could be applied to optical spectra.[18] Bowen and

Table V. *Mn III. Configuration change* ($3d^4 4s - 3d^4 4p$).

	s	$^4D_{7/2}$	329	$^4D_{5/2}$	242	$^4D_{3/2}$	145	$^4D_{1/2}$
p								
$^4F^\circ_{9/2}$		45818.2 80 2182.54						
167								
$^4F^\circ_{7/2}$		45641.0 30 2190.53		45979.9 70 2174.86				
149								
$^4F^\circ_{5/2}$		45503.9 1 2197.61		45830.4 3 2181.96		46072.5 90 2170.49		
59								
$^4F^\circ_{3/2}$						46013.4 2 2173.28		46158.7 25 2166.44
$^4D^\circ_{7/2}$		51348.9 80 1947.46		51677.4 5 1935.08				
209								
$^4D^\circ_{5/2}$				51468.4 45 1942.94		51707.9 4 1933.94		
168								
$^4D^\circ_{3/2}$						51539.5 30 1940.26		51684.9 1 1934.80
91								
$^4D^\circ_{1/2}$						51450.6 2 1943.61		51593.5 1 1938.23
$^4P^\circ_{5/2}$		42328.76 40 2362.46		42657.93 12 2344.23		42898.39 2 2331.09		
542								
$^4P^\circ_{3/2}$				42113.06 50-x 2374.56		42357.45 50 2360.86		42504.18 8 2357.72
390								
$^4P^\circ_{1/2}$						41967.96 30 2382.77		42113.06 x 2374.56

[17] Sommerfeld, "Atombau" 4th Ed. p. 420.
[18] Landè, Zeits. f. Physik **16**, 394 (1923).

Millikan[13] and Gibbs and White[14] have tested the law for one-electron systems and the latter have applied it to the location of similar multiplets in higher electronic states. One form of this law is

$$\Delta\nu = K(Z - s)^4$$

Table III gives the values of $\nu^{1/4}$ for a few multiplets reported in this investigation. Column 1 gives the configuration, column 2, the levels whose $\Delta\nu$ is used in the calculation and column 6 gives the screening constant. The increase in $\nu^{1/4}$ is nearly linear, but not exactly so in all cases. The introduction of Landé's correction for penetrating orbits does not eliminate the variations from linearity.

TABLE VI. *New term values for V I and Cr II.*

V I. Referred to $3d^34s^2\ {}^4F_{3/2}$ (Russell, Astrophys. J. 66, 233, 1927)			Cr II Referred to $3d^5\ {}^6S_{5/2}$ (C. C. Kiess, Bur. of St. J. of Res. 5, 775 (1930))		
$3d^44d$	${}^6G_{3/2}$	45850.3	$3d^44d$	${}^6G_{3/2}$	86571.0
	${}^6G_{5/2}$	45883.6		${}^6G_{5/2}$	86629.0
	${}^6G_{7/2}$	45938.5		${}^6G_{7/2}$	86715.7
	${}^6G_{9/2}$	46007.1		${}^6G_{9/2}$	86827.8
	${}^6G_{11/2}$	46085.2		${}^6G_{11/2}$	86964.9
	${}^6G_{13/2}$	46183.7		${}^6G_{13/2}$	87124.2

TABLE VII. *Term values of Mn III, referred to the limit of the sextets, estimated from the Moseley diagram.*

Config.	T.	Value	Config.	T.	Value	Config.	T.	Value
$3d^44d$	${}^6F_{11/2}$	111,373	$3d^44p$	${}^4D^\circ_{7/2}$	161,172	$3d^44p$	${}^6F^\circ_{11/2}$	172,583
		314			209			490
	${}^6F_{9/2}$	111,687		${}^4D^\circ_{5/2}$	161,381		${}^6F^\circ_{9/2}$	173,073
		207			168			400
	${}^6F_{7/2}$	111,894		${}^4D^\circ_{3/2}$	161,549		${}^6F^\circ_{7/2}$	173,473
		151			91			313
	${}^6F_{5/2}$	112,045		${}^4D^\circ_{1/2}$	161,640		${}^6F^\circ_{5/2}$	173,786
		90						224
	${}^6F_{3/2}$	112,135		${}^4F^\circ_{9/2}$	166,703		${}^6F^\circ_{3/2}$	174,010
		52			167			158
	${}^6F_{1/2}$	112,187		${}^4F^\circ_{7/2}$	166,870		${}^6F^\circ_{1/2}$	174,168
					149			
	${}^6D_{9/2}$	112,595		${}^4F^\circ_{5/2}$	167,019	$3d^44s$	${}^4D_{7/2}$	212,521
		207			59			328
	${}^6D_{7/2}$	112,802		${}^4F^\circ_{3/2}$	167,078		${}^4D_{5/2}$	212,849
		160						242
	${}^6D_{5/2}$	112,962		${}^6D^\circ_{9/2}$	169,684*		${}^4D_{3/2}$	213,091
		157		${}^4P^\circ_{5/2}$	170,192 *			146
	${}^6D_{3/2}$	113,119		${}^6D^\circ_{7/2}$	170,467*		${}^4D_{1/2}$	213,237
		84		${}^6P^\circ_{7/2}$	170,682 *			
	${}^6D_{1/2}$	113,203		${}^4P^\circ_{3/2}$	170,734 *		${}^6D_{9/2}$	220,900
	${}^6G_{13/2}$	113,701		${}^6D^\circ_{5/2}$	171,103*			298
		317		${}^6P^\circ_{5/2}$	171,118 *		${}^6D_{7/2}$	221,198
	${}^6G_{11/2}$	114,018		${}^4P^\circ_{1/2}$	171,124 *			241
		275		${}^6P^\circ_{3/2}$	171,466 *		${}^6D_{5/2}$	221,439
	${}^6G_{9/2}$	114,293		${}^6D^\circ_{3/2}$	171,567*			178
		211		${}^6D^\circ_{1/2}$	171,855*		${}^6D_{3/2}$	221,617
	${}^6G_{7/2}$	114,504						132
		102					${}^6D_{1/2}$	221,749
	${}^6G_{5/2}$	114,606						
		33				$3d^5$	${}^6S_{5/2}$	278,552
	${}^6G_{3/2}$	114,639						

TABLE VIII. *Term values of Fe IV, referred to the limit of the sextets, estimated from the Moseley diagram.*

Config.	T.	Value	Config.	T.	Value	Config.	T.	Value
$3d^44d$	$^6G_{13/2}$	210,479	$3d^44p$	$^6D^\circ_{9/2}$	283,473*	$3d^44p$	$^6F^\circ_{5/2}$	291,379
		575						388
	$^6G_{11/2}$	211,054		$^4P^\circ_{5/2}$	285,994 *		$^6F^\circ_{3/2}$	291,767
		509						240
	$^6G_{9/2}$	211,563		$^6P^\circ_{7/2}$	286,217 *		$^6F^\circ_{1/2}$	292,007
		417						
	$^6G_{7/2}$	211,980		$^6D^\circ_{7/2}$	286,633*	$3d^44s$	$^4D_{7/2}$	341,056
		247						448
	$^6G_{5/2}$	212,227		$^4P^\circ_{3/2}$	286,639 *		$^4D_{5/2}$	341,504
		88		$^6P^\circ_{5/2}$	286,921 *			308
	$^6G_{3/2}$	212,315		$^4P^\circ_{1/2}$	287,032 *		$^4D_{3/2}$	341,812
								184
$3d^44p$	$^4D^\circ_{7/2}$	273,472		$^6P^\circ_{3/2}$	287,446 *		$^4D_{1/2}$	341,996
		265						
	$^4D^\circ_{5/2}$	273,737		$^6D^\circ_{5/2}$	287,566*		$^6D_{9/2}$	350,464
		143			663			597
	$^4D^\circ_{3/2}$	273,880		$^6D^\circ_{3/2}$	288,231*		$^6D_{7/2}$	351,061
		111			391			476
	$^4D^\circ_{1/2}$	273,991		$^6D^\circ_{1/2}$	288,622*		$^6D_{5/2}$	351,537
				$^6F^\circ_{11/2}$	289,152			342
	$^4F^\circ_{9/2}$	281,584			935		$^6D_{3/2}$	351,879
		246		$^6F^\circ_{9/2}$	290,087			253
	$^4F^\circ_{7/2}$	281,830			736		$^6D_{1/2}$	352,132
		180		$^6F^\circ_{7/2}$	290,823			
	$^4F^\circ_{5/2}$	282,010			556	$3d^5$	$^6S_{5/2}$	460,278
		97						
	$^4F^\circ_{3/2}$	282,107						

TABLE IX. *Term values of Co V referred to the limit of the sextets, estimated from the Moseley diagram.*

Config.	T.	Value	Config.	T.	Value	Config.	T.	Value
$3d^44d$	$^6G_{13/2}$	337,287	$3d^44p$	$^6D^\circ_{9/2}$	431,194*	$3d^44p$	$^6F^\circ_{5/2}$	438,762
		929						573
	$^6G_{11/2}$	338,216		$^6P^\circ_{7/2}$	431,488 *		$^6F^\circ_{3/2}$	439,335
		785						376
	$^6G_{9/2}$	339,001		$^4P^\circ_{5/2}$	431,976 *		$^6F^\circ_{1/2}$	439,711
		631						
	$^6G_{7/2}$	339,632		$^6P^\circ_{5/2}$	432,622 *	$3d^44s$	$^4D_{7/2}$	501,264
		425						626
	$^6G_{5/2}$	340,057		$^4P^\circ_{3/2}$	432,757 *		$^4D_{5/2}$	501,890
		312						428
	$^6G_{3/2}$	340,369		$^6D^\circ_{7/2}$	432,934*		$^4D_{3/2}$	502,318
								265
$3d^44p$	$^4F^\circ_{9/2}$	426,409		$^4P^\circ_{1/2}$	433,306 *		$^4D_{1/2}$	502,583
		274						
	$^4F^\circ_{7/2}$	426,683		$^6P^\circ_{3/2}$	433,437 *		$^6D_{9/2}$	509,796
		197						851
	$^4F^\circ_{5/2}$	426,880		$^6D^\circ_{5/2}$	434,130*		$^6D_{7/2}$	510,647
		145						677
	$^4F^\circ_{3/2}$	427,025		$^6D^\circ_{3/2}$	434,977*		$^6D_{5/2}$	511,324
								524
				$^6D^\circ_{1/2}$	435,463*		$^6D_{3/2}$	511,848
								314
				$^6F^\circ_{11/2}$	435,484		$^6D_{1/2}$	512,162
					1,374			
				$^6F^\circ_{9/2}$	436,858	$3d^5$	$^6S_{5/2}$	673,859
					1,073			
				$^6F^\circ_{7/2}$	437,931			
					831			

Tables of Term Values and Wave-lengths

Two illustrations of multiplet groups of lines are given in Tables IV and V. Each line is represented by its frequency, intensity and wave-length in a vacuum. About fifty lines have been traced for the change in configuration $3d^44s-3d^44p$ through the sequence which starts with V I. Approximately half of these go through to Ni VI, the remainder to Co V. In the other three electronic changes, $3d^44p-3d^44d$, $3d^5-3d^4p$ and $3d^44s^2-3d^34sp$, twenty lines have been traced to Co V, and in addition some fainter multiplet lines found in Mn III. Tables VI, VII, VIII, IX and X give the energy level values referred to the lowest level, $3d^4\ {}^5D_0$ of the corresponding atom which has lost one more electron. These values depend on the limits of the sextets in V I and

TABLE X. *Term values of Ni VI referred to the limit of the sextets, estimated from the Moseley diagram.*

Config.	T.	Value	Config.	T.	Value	Config.	T.	Value
$3d^44d$	$^6G_{13/2}$	494,090	$3d^44p$	$^6F^\circ_{9/2}$	613,691	$3d^44s$	$^4D_{3/2}$	692,038
		1,286			1,485			373
	$^6G_{11/2}$	495,376		$^6F^\circ_{7/2}$	615,176		$^4D_{1/2}$	692,411
					1,146			
$3d\ 4p$	$^4F^\circ_{9/2}$	604,140		$^6F^\circ_{5/2}$	616,322		$^6D_{9/2}$	698,896
		333			1,045			1,273
	$^4F^\circ_{7/2}$	604,473		$^6F^\circ_{3/2}$	617,367		$^6D_{7/2}$	700,169
		270			507			976
	$^4F^\circ_{5/2}$	604,743		$^6F^\circ_{1/2}$	617,874		$^6D_{5/2}$	701,145
		100						642
	$^4F^\circ_{3/2}$	604,843	$3d^44s$	$^4D_{7/2}$	690,561		$^6D_{3/2}$	701,787
					852			341
	$^6P^\circ_{7/2}$	606,982		$^4D_{5/2}$	691,413		$^6D_{1/2}$	702,128
		1,727			625			
	$^6P^\circ_{5/2}$	608,709						
		1,154						
	$^6P^\circ_{3/2}$	609,863						
	$^6F^\circ_{11/2}$	611,508						
		2,183						

TABLE XI. *Wave-lengths of new lines.*

Vanadium I				Chromium II			
λ(I.A. air)	Int.	ν (vac.)	Origin	λ (I.A. air)	Int.	ν (vac.)	Origin
			$3d^44p$ $3d^44d$				$3d^44p$ $3d^43d$
4799.01	8	20831.9	$^6F^\circ_{11/2}-{}^6G_{11/2}$	2558.28	12	39075.3	$^6F^\circ_{11/2}-{}^6G_{9/2}$
4785.46	1	20890.8	$^6F^\circ_{7/2}-{}^6G_{5/2}$	2549.43	40	39211.2	$^6F^\circ_{11/2}-{}^6G_{11/2}$
4784.48	30-x	20895.1	$^6F^\circ_{9/2}-{}^6G_{9/2}$	2539.76	10	39360.8	$^6F^\circ_{9/2}-{}^6G_{9/2}$
4776.44	60	20930.3	$^6F^\circ_{11/2}-{}^6G_{13/2}$	2539.11	60	39370.8	$^6F^\circ_{11/2}-{}^6G_{13/2}$
4773.06	10	20945.1	$^6F^\circ_{7/2}-{}^6G_{7/2}$	2537.60	12	39392.7	$^6F^\circ_{7/2}-{}^6G_{5/2}$
4766.68	50	20973.1	$^6F^\circ_{9/2}-{}^6G_{11/2}$	2531.79	40	39485.0	$^6F^\circ_{7/2}-{}^6G_{7/2}$
4764.13	4	20984.3	$^6F^\circ_{5/2}-{}^6G_{5/2}$	2530.93	60	39498.4	$^6F^\circ_{9/2}-{}^6G_{11/2}$
4757.48	50	21013.7	$^6F^\circ_{7/2}-{}^6G_{9/2}$	2525.47	8	39583.9	$^6F^\circ_{5/2}-{}^6G_{5/2}$
4756.01	1	21020.2	$^6F^\circ_{3/2}-{}^6G_{3/2}$	2524.52	40	39598.8	$^6F^\circ_{7/2}-{}^6G_{9/2}$
4751.58	35	21039.8	$^6F^\circ_{5/2}-{}^6G_{7/2}$	2520.42	20	39663.3	$^6F^\circ_{3/2}-{}^6G_{3/2}$
4748.51	38	21053.4	$^6F^\circ_{3/2}-{}^6G_{5/2}$	2519.79	40	39673.6	$^6F^\circ_{5/2}-{}^6G_{7/2}$
4746.66	35	21061.6	$^6F^\circ_{1/2}-{}^6G_{3/2}$	2516.70	30	39722.1	$^6F^\circ_{3/2}-{}^6G_{5/2}$
				2515.20	8	39745.8	$^6F^\circ_{1/2}-{}^6G_{3/2}$

Cr II as calculated by Russell,[14] and the Moseley diagram of Fig. 3. From the most recent values of the constants involved in the relation between principal ionization potential and term value, the ionization potentials were calculated from the equation,

$$V = 0.00012336 \times \text{term value in cm}^{-1}.$$

In this case "principal ionization potential" is used to designate the potential necessary to remove, completely, one electron, changing the atom from the lowest energy in the state under discussion to the lowest energy in the next

TABLE XII. *Wave-lengths of Mn III, in order of increasing frequency.*

λ(I.A.)	Int.	ν (vac.)	Origin
			$3d^44s$ $3d^44p$
2382.77	30	41967.9	$^4D_{3/2}-{}^4P^\circ_{1/2}$
2374.56	50-x	42113.1	$^4D_{5/2}-{}^4P^\circ_{3/2}$
2362.46	40	42328.8	$^4D_{7/2}-{}^4P^\circ_{5/2}$
2360.86	50	42357.4	$^4D_{3/2}-{}^4P^\circ_{3/2}$
2352.72	8	42504.2	$^4D_{1/2}-{}^4P^\circ_{3/2}$
2344.23	12	42657.9	$^4D_{5/2}-{}^4P^\circ_{5/2}$
2331.09	2	42898.4	$^4D_{3/2}-{}^4P^\circ_{5/2}$
2197.61	1	45503.9	$^4D_{7/2}-{}^4F^\circ_{5/2}$
2190.53	30	45651.0	$^4D_{7/2}-{}^4F^\circ_{7/2}$
2182.54	80	45818.2	$^4D_{7/2}-{}^4F^\circ_{9/2}$
2181.96	3	45830.4	$^4D_{5/2}-{}^4F^\circ_{5/2}$
2174.86	70	45979.9	$^4D_{5/2}-{}^4F^\circ_{7/2}$
2173.28	2	46013.4	$^4D_{3/2}-{}^4F^\circ_{3/2}$
2170.49	90	46072 5	$^4D_{3/2}-{}^4F^\circ_{5/2}$
2166.44	28	46158.7	$^4D_{1/2}-{}^4F^\circ_{3/2}$
2009.80	1	49756 2	$^6D_{3/2}-{}^6D^\circ_{1/2}$
2005.27	3	49868.6	$^6D_{5/2}-{}^6D^\circ_{3/2}$
2004.45	2	49889.0	$^6D_{1/2}-{}^6D^\circ_{1/2}$
2001.32	20	49967.0	$^6D_{5/2}-{}^6P^\circ_{3/2}$
1998.16	30	50046 0	$^6D_{3/2}-{}^6D^\circ_{3/2}$
1997.04	25	50074.1	$^6D_{7/2}-{}^6P^\circ_{5/2}$
1996.30	1	50092.7	$^6D_{7/2}-{}^6D^\circ_{5/2}$
1994.19	25	50145.7	$^6D_{3/2}-{}^6P^\circ_{3/2}$
1992.94	5	50177.1	$^6D_{1/2}-{}^6D^\circ_{3/2}$
1991.32	25	50217.9	$^6D_{9/2}-{}^6P^\circ_{7/2}$
1987.57	4	50312.7	$^6D_{5/2}-{}^6P^\circ_{5/2}$
1986.86	30	50330.7	$^6D_{5/2}-{}^6D^\circ_{5/2}$
1982.83	40	50433.0	$^6D_{9/2}-{}^6D^\circ_{7/2}$
1979.78	1	50510.7	$^6D_{7/2}-{}^6P^\circ_{7/2}$
1971.29	40	50728.2	$^6D_{7/2}-{}^6D^\circ_{7/2}$
1962.07	40	50966.6	$^6D_{5/2}-{}^6D^\circ_{7/2}$
1952.52	50	51215.7	$^6D_{9/2}-{}^6D^\circ_{9/2}$
1947.46	80	51348.9	$^4D_{7/2}-{}^4D^\circ_{7/2}$
1943.61	2	51450.6	$^4D_{3/2}-{}^4D^\circ_{1/2}$
1942.94	45	51468.4	$^4D_{5/2}-{}^4D^\circ_{5/2}$
1941.34	40	51510.8	$^6D_{7/2}-{}^6D^\circ_{9/2}$
1940.26	30	51539.5	$^4D_{3/2}-{}^4D^\circ_{3/2}$
1938.23	1	51593.5	$^4D_{1/2}-{}^4D^\circ_{1/2}$
1935.08	5	51677.4	$^4D_{5/2}-{}^4D^\circ_{7/2}$
1934.80	1	51684.9	$^4D_{1/2}-{}^4D^\circ_{3/2}$
1933.94	4	51707·9	$^4D_{5/2}-{}^4D^\circ_{3/2}$
			$3d^34s^2$ $3d^34sp$
1817.60	15	55017.6	$^4F_{9/2}-{}^4G^\circ_{7/2}$
1806.50	18	55355.7	$^4F_{9/2}-{}^4G^\circ_{9/2}$
1798.05	18	55650.2	$^4F_{7/2}-{}^4G^\circ_{7/2}$
1793.57	10	55818.2	$^4F_{5/2}-{}^4G^\circ_{5/2}$
1790.49	50	55850.6	$^4F_{9/2}-{}^4G^\circ_{11/2}$
1786.10	50	55987.9	$^4F_{7/2}-{}^4G^\circ_{9/2}$
1782.19	40	56110.1	$^4F_{5/2}-{}^4G^\circ_{7/2}$
1780.68	6	56158.3	$^4F_{3/2}-{}^4G^\circ_{5/2}$
			$3d^44p$ $3d^43d$
1707.46	35	58566.5	$^6F^\circ_{11/2}-{}^6G^\circ_{11/2}$
1701.12	2	58784.8	$^6F^\circ_{9/2}-{}^6G_{9/2}$
1698.31	35	58882.1	$^6F^\circ_{11/2}-{}^6G_{13/2}$
1695.55	1	58977.9	$^6F^\circ_{7/2}-{}^6G_{7/2}$
1693.22	40	59059.1	$^6F^\circ_{9/2}-{}^6G_{11/2}$
1689.52	15	59188.1	$^6F^\circ_{7/2}-{}^6G_{9/2}$
1686.62	25	59290.2	$^6F^\circ_{5/2}-{}^6G_{7/2}$
1684.10	1	59378.5	$^6F^\circ_{3/2}-{}^6G_{3/2}$
1683.17	20	59411.7	$^6F^\circ_{3/2}-{}^6G_{5/2}$
1679.69	10	59534.8	$^6F^\circ_{1/2}-{}^6G_{3/2}$
1666.99	60	59988.4	$^6F^\circ_{11/2}-{}^6D_{9/2}$
1659.21	25	60269,6	$^6F^\circ_{9/2}-{}^6D_{7/2}$
1653.50	40	60477.8	$^6F^\circ_{9/2}-{}^6D_{9/2}$
1652.66	10	60508.5	$^6F^\circ_{7/2}-{}^6D_{5/2}$
1648.30	15	60668.6	$^6F^\circ_{7/2}-{}^6D_{7/2}$
1644.39	5	60812.8	$^6F^\circ_{3/2}-{}^6D_{1/2}$
1644.05	tr.	60825.4	$^6F^\circ_{5/2}-{}^6D_{5/2}$
1642.72	18	60874.6	$^6F^\circ_{7/2}-{}^6D_{9/2}$
1642.14	1	60896.2	$^6F^\circ_{3/2}-{}^6D_{3/2}$
1640.13	tr	60970.0	$^6F^\circ_{1/2}-{}^6D_{1/2}$
1639.77	10	60984.2	$^6F^\circ_{5/2}-{}^6D_{7/2}$
1633.71	45	61210.4	$^6F^\circ_{1/2}-{}^6F_{11/2}$
1629.15	30	61383.6	$^6F^\circ_{9/2}-{}^6F_{9/2}$
1623.89	25	61580.5	$^6F^\circ_{7/2}-{}^6F_{7/2}$
1619.59	20	61744.0	$^6F^\circ_{5/2}-{}^6F_{5/2}$
1618.46	2	61787.1	$^6F^\circ_{7/2}-{}^6F_{9/2}$
1615.96	10	61882.7	$^6F^\circ_{3/2}-{}^6F_{3/2}$
1615.62	8	61895.7	$^6F^\circ_{5/2}-{}^6F_{7/2}$
1613.63	5	61972.1	$^6F^\circ_{3/2}-{}^6F_{5/2}$
1613.22	1	61987.8	$^6F^\circ_{1/2}-{}^6F_{1/2}$
1611.86	2	62040.1	$^6F^\circ_{1/2}-{}^6F_{3/2}$
			$3d^5$ $3d^44p$
925.2	10	108081.	$^6S_{5/2}-{}^6P^\circ_{3/2}$
922.2	40	108431	$^6S_{5/2}-{}^6P^\circ_{5/2}$
918.5	100	108870	$^6S_{5/2}-{}^6P^\circ_{7/2}$

higher state of ionization. Since $3d^5\ {}^6S$ is the lowest level for Mn III, Fe IV and Co V, the value of this level referred to $3d^4\ {}^5D_0$ of each atom in its next higher state of ionization, was used in the calculation. The results are; Mn III 34.4 volts, Fe IV 56.8 volts and Co V 83.1 volts.

The final tables, XI to XV, give the new lines for this sequence. For each element studied, the values of wave-length, intensity, frequency and origin are given, the order being that of increasing frequency.

The writer wishes to take this opportunity to express her thanks for the use of the vacuum spectrograph and her appreciation of the very helpful advice of Professor R. C. Gibbs during the progress of this investigation.

TABLE XIII. *Wave-lengths of Fe IV in order of increasing frequency.*

λ (I.A.)	Int.	ν (vac.)	Origin	λ(I.A.)	Int.	ν (vac.)	Origin.
			$3d^44s \quad 3d^44p$				$3d^34s^2 \quad 3d^34sp$
1825.55	8	54778.0	${}^4D_{3/2}-{}^4P^\circ_{1/2}$	1487.35	5	67246.8	${}^4F_{9/2}-{}^4G^\circ_{7/2}$
1822.72	2	54863.1	${}^4D_{5/2}-{}^4P^\circ_{3/2}$				$3d^44s \quad 3d^44p$
1819.29	1	54966.5	${}^4D_{1/2}-{}^4P^\circ_{1/2}$	1485.48	12	67318.3	${}^4D_{7/2}-{}^4D^\circ_{5/2}$
1815.61	25	55061.8	${}^4D_{7/2}-{}^4P^\circ_{5/2}$	1479.65	38	67583.6	${}^4D_{7/2}-{}^4D^\circ_{7/2}$
1812.53	1	55171.5	${}^4D_{3/2}-{}^4P^\circ_{3/2}$				$3d^34s^2 \quad 3d^34sp$
1801.53	5	55508.4	${}^4D_{5/2}-{}^4P^\circ_{5/2}$	1477.69	5	67673.2	${}^4F_{9/2}-{}^4G^\circ_{9/2}$
1688.44	2	59226.3	${}^4D_{7/2}-{}^4F^\circ_{7/2}$				$3d^44s \quad 3d^44p$
1681.45	25	59472.5	${}^4D_{7/2}-{}^4F^\circ_{9/2}$	1475.67	28	67765.8	${}^4D_{5/2}-{}^4D^\circ_{5/2}$
1680.86	1	59493.4	${}^4D_{5/2}-{}^4F^\circ_{5/2}$	1474.52	2	67818.7	${}^4D_{3/2}-{}^4D^\circ_{1/2}$
1675.78	25	59673.7	${}^4D_{5/2}-{}^4F^\circ_{7/2}$	1472.13	35	67928.8	${}^4D_{3/2}-{}^4D^\circ_{3/2}$
1674.89	5	59705.4	${}^4D_{3/2}-{}^4F^\circ_{3/2}$	1470.54	2	68002.2	${}^4D_{1/2}-{}^4D^\circ_{1/2}$
1672.18	5	59802.2	${}^4D_{3/2}-{}^4F^\circ_{5/2}$	1469.92	20	68030.9	${}^4D_{5/2}-{}^4D^\circ_{7/2}$
1669.73	2	59889.9	${}^4D_{1/2}-{}^4F^\circ_{3/2}$	1469.04	37-x	68071.7	${}^4D_{3/2}-{}^4D^\circ_{5/2}$
1663.52	10	60113.4	${}^6D_{3/2}-{}^6F^\circ_{3/2}$				$3d^34s^2 \quad 3d^34sp$
1663.21	10	60124.7	${}^6D_{1/2}-{}^6F^\circ_{1/2}$	1469.04	x	68071.7	${}^4F_{7/2}-{}^4G^\circ_{7/2}$
1662.26	20	60159.1	${}^6D_{5/2}-{}^6F^\circ_{5/2}$				$3d^44s \quad 3d^44p$
1660.07	20	60238.4	${}^6D_{7/2}-{}^6F^\circ_{7/2}$	1468.11	2	68114.8	${}^4D_{1/2}-{}^4D^\circ_{3/2}$
1656.61	15	60364.2	${}^6D_{1/2}-{}^6F^\circ_{3/2}$				$3d^34s^2 \quad 3d^34sp$
1656.25	10	60377.5	${}^6D_{9/2}-{}^6F^\circ_{9/2}$	1464.81	40	68268.2	${}^4F_{9/2}-{}^4G^\circ_{11/2}$
1652.85	20	60501.6	${}^6D_{3/2}-{}^6F^\circ_{5/2}$	1463.25	4	68341.0	${}^4F_{5/2}-{}^4G^\circ_{5/2}$
1647.05	45	60714.6	${}^6D_{5/2}-{}^6F^\circ_{7/2}$	1459.92	40	68496.9	${}^4F_{7/2}-{}^4G^\circ_{9/2}$
1640.03	65	60974.5	${}^6D_{7/2}-{}^6F^\circ_{9/2}$	1455.66	25	68697.4	${}^4F_{5/2}-{}^4G^\circ_{7/2}$
1630.99	75	61312.4	${}^6D_{9/2}-{}^6F^\circ_{11/2}$	1453.67	15	68791.4	${}^4F_{3/2}-{}^4G^\circ_{5/2}$
1579.73	3	63302.0	${}^6D_{5/2}-{}^6D^\circ_{3/2}$				$3d^44p \quad 3d^44d$
1574.68	8	63505.0	${}^6D_{1/2}-{}^6D^\circ_{1/2}$	1280.43	10	78098.8	${}^6F^\circ_{11/2}-{}^6G_{11/2}$
1571.21	10	63645.2	${}^6D_{3/2}-{}^6D^\circ_{3/2}$	1273.49	2	78524.4	${}^6F^\circ_{9/2}-{}^6G_{9/2}$
1566.54	3	63834.9	${}^6D_{9/2}-{}^6D^\circ_{7/2}$	1271.08	15	78673.2	${}^6F^\circ_{11/2}-{}^6G_{13/2}$
1565.05	2	63895.7	${}^6D_{1/2}-{}^6D^\circ_{3/2}$	1268.40	2	78839.5	${}^6F^\circ_{7/2}-{}^6G_{7/2}$
1563.30	10	63967.2	${}^6D_{5/2}-{}^6D^\circ_{5/2}$	1265.28	15	79033.9	${}^6F^\circ_{9/2}-{}^6G_{11/2}$
1560.26	15	64091.8	${}^6D_{5/2}-{}^6P^\circ_{3/2}$	1263.47	15	79147.1	${}^6F^\circ_{5/2}-{}^6G_{5/2}$
1559.08	15	64140.4	${}^6D_{7/2}-{}^6P^\circ_{5/2}$	1261.72	10	79256.9	${}^6F^\circ_{7/2}-{}^6G_{9/2}$
1556.48	15	64247.4	${}^6D_{9/2}-{}^6P^\circ_{7/2}$	1259.54	30	79394.1	${}^6F^\circ_{5/2}-{}^6G_{7/2}$
1555.01	1	64308.2	${}^6D_{3/2}-{}^6D^\circ_{5/2}$	1258.68	2	79448.3	${}^6F^\circ_{3/2}-{}^6G_{3/2}$
1552.11	15	64428.3	${}^6D_{7/2}-{}^6D^\circ_{7/2}$	1257.29	6	79536.1	${}^6F^\circ_{3/2}-{}^6G_{5/2}$
1547.58	15	64616.9	${}^6D_{5/2}-{}^6P^\circ_{5/2}$	1254.80	10	79694.0	${}^6F^\circ_{1/2}-{}^6G_{3/2}$
1546.03	8	64681.6	${}^6D_{1/2}-{}^6P^\circ_{3/2}$				$3d^5 \quad 3d^44p$
1542.15	15	64844.4	${}^6D_{7/2}-{}^6P^\circ_{7/2}$	587.6	2	172829.	${}^6S_{5/2}-{}^6P^\circ_{3/2}$
1540.77	1	64902.5	${}^6D_{5/2}-{}^6D^\circ_{7/2}$	576.8	40	173368.	${}^6S_{5/2}-{}^6P^\circ_{5/2}$
1538.67	25	64991.1	${}^6D_{9/2}-{}^6D^\circ_{9/2}$	574.5	50	174061	${}^6S_{5/2}-{}^6P^\circ_{7/2}$
1524.67	15	65587.9	${}^6D_{7/2}-{}^6D^\circ_{9/2}$				

TABLE XIV. *Wave-lengths of Co V in order of increasing frequency.*

λ(I.A.)	Int.	ν (vac.)	Orign.	λ(I.A.)	Int.	ν (vac.)	Origin.
			$3d^4 4s \quad 3d^4 4p$				$3d^3 4s^2 \quad 3d^3 4sp$
1488.73	20	67171.4	${}^4D_{3/2} - {}^4P^\circ_{1/2}$	1246.91	8	80198.2	${}^4F_{9/2} - {}^4G^\circ_{9/2}$
1486.02	25	67293.8	${}^4D_{5/2} - {}^4P^\circ_{3/2}$	1239.85	2	80654.9	${}^4F_{7/2} - {}^4G^\circ_{7/2}$
1482.91	20	67435.0	${}^4D_{1/2} - {}^4P^\circ_{1/2}$	1236.95	20	80844.0	${}^4F_{9/2} - {}^4G^\circ_{11/2}$
1482.62	25	67448.2	${}^4D_{7/2} - {}^4P^\circ_{5/2}$	1234.55	2	81001.2	${}^4F_{5/2} - {}^4G^\circ_{5/2}$
1476.65	30	67720.8	${}^4D_{3/2} - {}^4P^\circ_{3/2}$	1231.73	15	81186.6	${}^4F_{7/2} - {}^4G^\circ_{9/2}$
1468.98	35	68074.4	${}^4D_{5/2} - {}^4P^\circ_{5/2}$	1228.19	8	81420.6	${}^4F_{5/2} - {}^4G^\circ_{7/2}$
1459.77	15	68503.9	${}^4D_{3/2} - {}^4P^\circ_{5/2}$	1226.31	3	81545.4	${}^4F_{3/2} - {}^4G^\circ_{5/2}$
1389.11	32	71988.5	${}^6D_{5/2} - {}^6F^\circ_{3/2}$				$3d^4 4p \quad 3d^4 4d$
1380.21	10	72452.2	${}^6D_{1/2} - {}^6F^\circ_{1/2}$	1028.08	1	97268.7	${}^6F^\circ_{11/2} - {}^6G_{11/2}$
1379.05	10	72513.7	${}^6D_{3/2} - {}^6F^\circ_{5/2}$	1021.14	10	97853.1	${}^6F^\circ_{9/2} - {}^6G_{9/2}$
1378.12	25	72562.1	${}^6D_{5/2} - {}^6F^\circ_{5/2}$	1018.36	10	98197.1	${}^6F^\circ_{11/2} - {}^6G_{13/2}$
1375.20	30	72716.7	${}^6D_{7/2} - {}^6F^\circ_{7/2}$	1017.43	1	98286.9	${}^6F^\circ_{7/2} - {}^6G_{7/2}$
1373.09	30	72828.4	${}^6D_{1/2} - {}^6F^\circ_{3/2}$	1013.80	10	98638.8	${}^6F^\circ_{9/2} - {}^6G_{11/2}$
1371.01	10	72938.9	${}^6D_{9/2} - {}^6F^\circ_{9/2}$	1010.94	10	98917.8	${}^6F^\circ_{7/2} - {}^6G_{9/2}$
1369.30	4	73030.0	${}^4D_{7/2} - {}^4F^\circ_{7/2}$	1009.02	15	99106.1	${}^6F^\circ_{5/2} - {}^6G_{7/2}$
1368.24	30	73086.6	${}^6D_{3\ 2} - {}^6F^\circ_{5/2}$	1007.51	10	99254.6	${}^6F^\circ_{3/2} - {}^6G_{5/2}$
1364.17	30	73304.6	${}^4D_{7/2} - {}^4F^\circ_{9/2}$	1006.86	4	99318.7	${}^6F^\circ_{1/2} - {}^6G_{3/2}$
1362.46	30	73393.9	${}^6D_{5/2} - {}^6F^\circ_{7/2}$				$3d^5 \quad 3d^4 4p$
1361.32	20	73458.3	${}^4D_{5/2} - {}^4F^\circ_{5/2}$	415.94	1	240419.	${}^6S_{5/2} - {}^6P^\circ_{3/2}$
1357.67	30	73655.6	${}^4D_{5/2} - {}^4F^\circ_{7/2}$	414.52	5	241243	${}^6S_{5/2} - {}^6P^\circ_{5/2}$
1356.09	tr.	73741.9	${}^4D_{3/2} - {}^4F^\circ_{3/2}$	412.59	10	242371	${}^6S_{5/2} - {}^6P^\circ_{7/2}$
1355.20	40	73789.8	${}^6D_{7/2} - {}^6F^\circ_{9/2}$				
1353.42	15	73886.9	${}^4D_{3/2} - {}^4F^\circ_{5/2}$				
1351.22	6	74007.2	${}^4D_{1/2} - {}^4F^\circ_{1/2}$				
1345.67	50	74312.4	${}^6D_{9/2} - {}^6F^\circ_{11/2}$				
1301.12	35	76856.9	${}^6D_{5/2} - {}^6D^\circ_{5/2}$				
1295.87	40	77168.2	${}^6D_{3/2} - {}^6D^\circ_{5/2}$				
1295.55	25	77187.3	${}^6D_{7/2} - {}^6D^\circ_{7/2}$				
1286.95	28	77703.2	${}^6D_{9/2} - {}^6D^\circ_{9/2}$				
1284.00	15	77881.6	${}^6D_{5/2} - {}^6P^\circ_{3/2}$				
1281.63	30	78025.6	${}^6D_{7/2} - {}^6P^\circ_{5/2}$				
1277.01	50	78307.9	${}^6D_{9/2} - {}^6P^\circ_{7/2}$				
1275.52	2	78399.4	${}^6D_{3/2} - {}^6P^\circ_{3/2}$				
1272.23	20	78602.1	${}^6D_{11/2} - {}^6D^\circ_{11/2}$				
1270.70	20	78696.8	${}^6D_{5/2} - {}^6P^\circ_{5/2}$				
1270.44	tr.	78712.9	${}^6D_{1/2} - {}^6P^\circ_{3/2}$				
1263.28	5	79159.0	${}^6D_{7/2} - {}^6P^\circ_{7/2}$				
1258.61	6	79452.7	${}^6D_{9/2} - {}^6D^\circ_{11/2}$				

TABLE XV. *Wave-lengths for Ni VI in order of increasing frequency.*

λI.A.	Int.	ν (vac.)	Origin.	λ(I.A.)	Int.	ν (vac.)	Origin.
			$3d^4 4s \quad 3d^4 4p$				
1191.72	5	83912.3	${}^6D_{3/2} - {}^6F^\circ_{1/2}$	1144.32	18	87388.1	${}^6D_{9/2} - {}^6F^\circ_{11/2}$
1186.90	2	84253.1	${}^6D_{1/2} - {}^6F^\circ_{1/2}$	1141.96	10	87568.7	${}^4D_{1/2} - {}^4F^\circ_{3/2}$
1184.56	4	84419.5	${}^6D_{3/2} - {}^6F^\circ_{3/2}$	1095.49	8	91283.3	${}^6D_{5/2} - {}^6P^\circ_{3/2}$
1179.80	20	84760.2	${}^6D_{1/2} - {}^6F^\circ_{3/2}$	1093.37	40	91460.4	${}^6D_{7/2} - {}^6P^\circ_{5/2}$
1170.08	15	85464.2	${}^6D_{3/2} - {}^6F^\circ_{5/2}$	1087.97	50	91914.3	${}^6D_{9/2} - {}^6P^\circ_{7/2}$
1163.20	10	85969.7	${}^6D_{5/2} - {}^6F^\circ_{7/2}$	1083.98	5	92252.6	${}^6D_{1/2} - {}^6P^\circ_{3/2}$
1161.61	2	86088.2	${}^4D_{7/2} - {}^4F^\circ_{7/2}$	1081.82	1	92436.8	${}^6D_{5/2} - {}^6P^\circ_{5/2}$
1157.13	15	86420.7	${}^4D_{7/2} - {}^4F^\circ_{9/2}$	1074.51	15	93065.7	${}^6D_{3/2} - {}^6P^\circ_{5/2}$
1156.36	12	86478.3	${}^6D_{9/2} - {}^6F^\circ_{9/2}$	1073.11	12	93187.1	${}^6D_{7/2} - {}^6P^\circ_{7/2}$
1153.79	2	86670.9	${}^4D_{5/2} - {}^4F^\circ_{5/2}$				$3d^4 4p \quad 3d^4 4d$
1150.22	10	86940.6	${}^4D_{5/2} - {}^4F^\circ_{7/2}$	861.09	2	116132	${}^6F^\circ_{11/2} - {}^6G_{11/2}$
1146.85	8	87195.4	${}^4D_{3/2} - {}^4F^\circ_{3/2}$	851.66	20	117418	${}^6F^\circ_{11/2} - {}^6G_{13/2}$
1145.53	15	87295.8	${}^4D_{3/2} - {}^4F^\circ_{5/2}$	844.69	20	118386	${}^6F^\circ_{9/2} - {}^6G_{11/2}$

A NEW TYPE OF CRYSTAL FINE-STRUCTURE: LITHIUM FERRITE ($Li_2O \cdot Fe_2O_3$)

By E. Posnjak and Tom. F. W. Barth
Geophysical Laboratory, Carnegie Institution, Washington, D. C.

(Received October 9, 1931)

Abstract

The interpretation of the x-ray diffraction obtained from the isometric modification of lithium ferrite resulted in the conclusion that the smallest "unit" of this structure contains four anions and four cations. The anions, oxygens, occupy the four equivalent points 4*b* while the cations, iron and lithium, occupy together the four equivalent points 4*c*. The large difference in the scattering power of iron and lithium makes it possible to arrive at the definite conclusion that in the structure of lithium ferrite the same set of equivalent positions is occupied by the two chemically different elements (variate atom equipoints). It is shown that the distribution of iron and lithium in this set of equipoints is not regular, that is, there are not always two of each cation present in the "unit"; the distribution is one of chance, which, however, must comply with the requirement that an equal number of each of the cations is always present within a relatively small space. In view of these findings the conception of the unit cell loses its traditional chemical significance and becomes strictly a geometric conception. The "unit cell" of lithium ferrite has a meaning only if its lattice be regarded as geometric points in space. The lattice of lithium ferrite is then identical with the one of the "sodium chloride" structure (4b, 4c); the unit cube contains one molecule of $Li_2O \cdot Fe_2O_3$, and the length of its edge is 4.141 ± 0.005A. The density of lithium ferrite is 4.368 and its refractive index $n_{Li} = 2.40 \pm 0.04$.

Introduction

In the course of studies of ferrites it became of interest to prepare and examine the properties of the alkali ferrites. Although sodium and potassium ferrites have been described in the literature, there is apparently no record of the preparation of lithium ferrite. It will be appropriate therefore to mention that the experiments showed that this compound could be prepared in two modifications, an isotropic and an anisotropic one. The latter resulted from the interaction of a concentrated solution of lithium hydroxide and ferric oxide when heated in a pressure bomb somewhat below 600°C, while above this temperature the cubic modification was formed. The isometric modification was also prepared by heating the appropriate mixture consisting of lithium carbonate and ferric oxide, at red heat. The relation of the two modifications of lithium ferrite has not been determined. In this paper we shall be concerned only with the one formed at the higher temperature which is isotropic, and which was found not to invert when cooled to and kept at room temperature. The optical examinations were kindly made by Dr. George Tunell of this Laboratory, who found that the isotropic modification has a refractive index $n_{Li} = 2.40 \pm 0.04$. The determination of the density of this modification by the pycnometer method[1] resulted in the value of 4.368.

[1] J. Johnston and L. H. Adams, J. Am. Chem. Soc. **34**, 563 (1912).

X-RAY DIFFRACTION MEASUREMENTS

When lithium ferrite was prepared in the bomb by crystallization from solution, minute single octahedral crystals were obtained, the edges and corners of which were modified by rounded faces which were apparently dodecahedra and cubes. They were, however, too small to be utilized singly for x-ray measurements. Diffraction was therefore obtained only by the powder method. The apparatus was one made by the General Electric Company, equipped for using K_α radiation of molybdenum. The spacings were standardized in the usual way by exposure of sodium chloride on the same film alongside of lithium ferrite. Data obtained from such a powder spectrogram are given in Table I. By using the customary equation

TABLE I. *Powder diffraction data from lithium ferrite* ($Li_2O \cdot Fe_2O_3$).

Planar spacing	Intensity (estimated)	Indices	a_0
2.39	4	111(1)	4.143
2.07	10	100(2)	4.142
1.461	9	110(2)	4.128
1.247	3	113(1)	4.144
1.195	4	111(2)	4.144
1.035	2	100(4)	4.141
0.949	1	133(1)	4.140
0.925	5	120(2)	4.139
0.845	4	112(2)	4.143
0.798	1	111(3) 115(1)	4.150
0.732	1—	110(4)	4.144
0.690	2	100(6) 122(2)	4.132
0.654	2	130(2)	4.139
0.624	1	113(2)	4.141
0.575	1—	230(2)	4.145
0.553	1	123(2)	4.138
			$a_0 = 4.141 \pm 0.005$A

$m = a_0^3 \rho / M$, where m is the number of molecules of $Li_2O \cdot Fe_2O_3$ within the unit, M the mass of a molecule of the substance, ρ its density, and a_0 the length of the edge of the unit cube, we find $m = 0.993$. This is, within experimental error, a whole number, as it should be, and one may therefore assume that one molecule of $Li_2O \cdot Fe_2O_3$ is associated with the unit cube.

APPLICATION OF SPACE GROUP CRITERIA

From the reflections given in Table I it is immediately obvious that the lattice underlying the structure of lithium ferrite is a face-centered one. An examination of the tabulation of the results of the theory of space groups shows, however, that there is no space group with an underlying face-centered lattice, or for that matter of any other cubic lattice, which would accommodate two lithium, two iron, and four oxygen ions. This fact would suggest that it may be necessary to multiply the number of molecules of $Li_2O \cdot Fe_2O_3$, and therefore the length of the edge of the unit cell in which they are contained, by a simple integer, as for instance by two; however, we shall show later that this will be found to conflict with the experimental data.

Atomic Arrangement of $Li_2O \cdot Fe_2O_3$

The comparison of the diffraction data from lithium ferrite with those of magnesium and ferrous oxides presents a clue for the solution of the problem. Thus it was found that the diffraction from lithium ferrite bore a very close similarity to that of the two substances just mentioned. The powder diffraction patterns of all three are reproduced in Fig. 1 and it will be readily seen how small the differences in spacings and intensities are. In view of recent experience in the study of spinels[2] in which the present authors had shown that different elements occupy crystallographically equivalent positions, it was thought not to be improbable that lithium ferrite presented another case of variate atom equipoints. Both magnesium oxide[3] and ferrous oxide[4] had been shown to have the sodium chloride structure containing four cations and four anions per unit cell in a face-centered arrangement (4*b*, 4*c*). In the case of lithium ferrite it was thought that by analogy lithium and iron together may occupy four equivalent positions and the oxygens the other four; thus com-

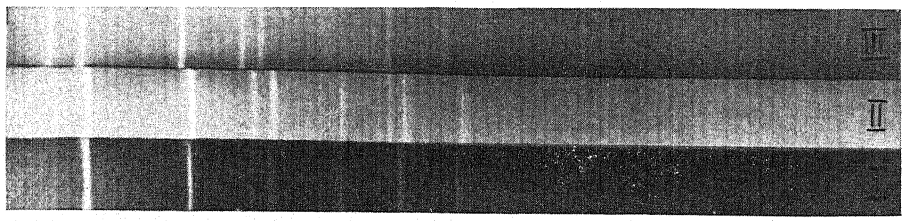


Fig. 1. Spectrograms of I, MgO; II, $Li_2O \cdot Fe_2O_3$; and III, FeO.

plying with the experimental evidence of the presence of two lithium, two iron, and four oxygen ions per unit cell of the lithium ferrite structure.

By making this assumption, the next question that arises concerns the interrelation between the lithium and iron ions within the crystal: are the points in arrangement 4*c* occupied in a regular or an irregular fashion by the two different kinds of ions? The following discussion will prove that it is necessary to conclude that the distribution of lithium and iron among the points of arrangement 4*c* must be one of chance, complying only with the requirement of an equal number of each within a relatively very small space.

The simplest regular arrangement which we may assume would be obtained by placing the lithium and iron ions alternately between the oxygens. Then in the direction of the edge of the cube we would have O–Fe–O–Li–O—. It is quite obvious that in this case the length of the edge of the unit cube would be twice that of the "sodium chloride" arrangement where it extends only from one oxygen over a cation to the next oxygen. The length of the edge of the unit cell given in Table I corresponds to the one in the "sodium chloride" structure, and if we assume the regular distribution of iron and

[2] Tom. F. W. Barth and E. Posnjak, J. Wash. Acad. Sci. **21**, 255 (1931).

[3] W. P. Davey and E. O. Hoffmann, Phys. Rev., [2], **15**, 333 (1920); W. Gerlach and O. Pauli, Zeits. f. Physik **7**, 116 (1921); R. W. G. Wyckoff, Am. J. Sci. [5], **1**, 138 (1921).

[4] R. W. G. Wyckoff and E. D. Crittenden, J. Am. Chem. Soc. **47**, 2876 (1925).

lithium it would therefore be necessary to conclude that the true length of the edge of the cube is $2a_0$. This would of course result in the necessity of reassigning all our indices to higher orders—they would all be multiplied by two, which means that no first order reflections at all would occur in the lithium ferrite structure. However, such a conclusion can be shown to be incompatible with the established theory of the interaction of x-rays and crystals. The proof in this case is identical with that advanced by L. Vegard and H. Schjelderup[5] and more precisely brought out by M. v. Laue[6] in clearing up the theory of diffraction in the case of mixed crystals. The discussion may be confined to the consideration of the structure factor of the face-centered cubic crystal resulting from the regular arrangement of lithium and iron mentioned above, the length of the edge of the unit cell of which is $A_0 = 2a_0$. The structure factor can be expressed as the product of the following three parts:

$$F_1 = \left[1 + e^{2\pi i(h+k)/2} + e^{2\pi i(h+l)/2} + e^{2\pi i(k+l)/2}\right]^2$$

$$F_2 = \left[1 + e^{2\pi i(h+k)/4} + e^{2\pi i(h+l)/4} + e^{2\pi i(k+l)/4}\right]^2$$

$$F_3 = \left[\overline{O}(1 + e^{2\pi i(h+k+l)/2}) + \overline{Li}\cdot e^{-2\pi i(h+k+l)/2} + \overline{Fe}\cdot e^{2\pi i(h+k+l)/2}\right]^2.$$

The part F_1 is due to the fact that the whole lattice is made up of face-centered lattices; the part F_2 because from such a lattice three other identical lattices will be developed by the displacements $A_0/4$, 0, $A_0/4$; 0, $A_0/4$, $A_0/4$ and $A_0/4$, $A_0/4$, 0; and part F_3 shows that in the direction parallel to a body diagonal there are situated equally spaced O–Li–O–Fe. With the help of this structure factor all reflections which can occur may be calculated. When this is done it is found that while all the reflections which have been observed should occur in this structure, there should in addition be present reflections which, however, were not found in the spectrogram. For instance, the reflection from 111(1), the spacing of which would be 4.78A, has the structure factor 16.16 $(\overline{Fe}-\overline{Li})$ and, owing to the difference in the scattering power of iron and lithium, the intensity of this reflection should be stronger than any of those observed. As a matter of fact there is no indication of a diffraction line in this position, and therefore the assumption of the regular distribution of iron and lithium which required doubling the length of the edge of our unit cell must be discarded.

We now have to evaluate our experimental data in regard to the other assumption, namely, the chance distribution of iron and lithium in the four equipoints (4*c*) of the "sodium chloride" arrangement. Taking into consideration not too small a portion of the crystal an equal number of points is occupied by iron and by lithium. Therefore in calculating the intensities the average of the scattering power of the two may be taken, (Fe+Li)/2. The position of the atoms are: O in (4*b*) i.e. 0 0 0 , $\frac{1}{2}\frac{1}{2}0$, $\frac{1}{2}0\frac{1}{2}$, $0\frac{1}{2}\frac{1}{2}$; and 2Fe+2Li in (4*c*) i.e. $\frac{1}{2}\frac{1}{2}\frac{1}{2}$, $\frac{1}{2}00$, $0\frac{1}{2}0$, $00\frac{1}{2}$. The intensities of reflection were calculated on the basis of the equation

[5] L. Vegard and H. Schjelderup, Phys. Zeits. **18**, 93 (1917).
[6] M. v. Laue, Ann. d. Physik [4], **56**, 497 (1918).

$$I = j\frac{1 + \cos^2 2\theta}{\sin 2\theta}F^2,$$

employing the F-values published by W. L. Bragg and J. West[7] for iron and oxygen. For lithium the F-curve given recently by R. W. James and G. W. Brindley[8] was used. The results are given in Table II from which it will be

TABLE II. *Comparison of observed and calculated diffraction intensities from lithium ferrite* ($Li_2O \cdot Fe_2O_3$).

Indices	Estimated	Calculated	Indices	Estimated	Calculated
(111)	4	1.4	(333) } (115) }	1	1.3
(200)	10	10.4			
(220)	9	8.8	(440)	1−	0.8
(113)	3	2.3	(600) } (244) }	2	1.6
(222)	4	3.1			
(400)	2	1.3	(260)	1	1.0
(133)	1	1.5	(226)	1	0.8
(240)	5	4.0	(460)	1−	0.5
(422)	4	2.8	(246)	1	0.8

seen that the calculated intensities are in very good agreement with the estimates made from the spectrogram. Therefore we must conclude that this is the correct structure and that iron and lithium together occupy four equipoints of the "sodium chloride" arrangement filling these points in equal molecular ratio by chance distribution. The holohedral symmetry required by the "sodium chloride" arrangement is in accord with the observed external crystal faces and it may also be mentioned that the lattice dimensions of lithium ferrite agree well with the accepted values of the atomic radii.

CONCLUSIONS

In a recent study of the structure of spinels the authors[9] have shown that the 16 equivalent positions (16*c*) of this structure are not all occupied by chemically equivalent ions, but that eight of them are of one kind, such as the trivalent Fe^{+++}, Al^{+++}, Ga^{+++}, etc., while the other eight are bivalent ions like Mg^{++}, Fe^{++}, etc. The present study of the structure of lithium ferrite, which structurally is the simplest possible case and therefore an even more convincing one, again proves that crystallographically equivalent positions in a crystal may be occupied by chemically different ions (Fe^{+++} and Li^{+}). Such crystals with variate atom equipoints challenge in a certain way our usual conceptions of "crystal" and "chemical compound." Crystallographically, in crystals with variate atom equipoints we find that the usual symmetry requirements (symmetry operations) cannot be extended to its smallest unit, that is, the unit cell. Such an extension can only be accomplished if the atoms are regarded purely as geometrical points in space. Crystals with variate atom equipoints do not exhibit in their lattice the regular

[7] W. L. Bragg and J. West, Zeits. f. Krist. **69**, 118 (1929).
[8] R. W. James and G. W. Brindley, Phil. Mag. [7] **12**, 81 (1931).
[9] Tom. F. W. Barth and E. Posnjak, J. Wash. Acad. Sci. **21**, 255 (1931).

periodicity in regard to the chemical character of the atoms composing it, which is usually associated with our conception of compounds. However, it should be remembered that the conception of the molecule also found no support from the crystal structure of such simple substances as the alkali halides, some oxides, etc.; indeed, the conception of the "unit cell" was introduced and in a sense replaced it, but only as a convenient descriptive term, for it would be very arbitrary to think of the chemical molecule as being identical with the unit cell. In the solid state the only logical limitation of the molecule is the macrocrystal itself.

It may be suggested that the structure with variate atom equipoints be regarded as representing the general case of which the other structures are special cases. We know that the possession of a (geometrical) unit cell of indefinite chemical composition (which is identical with having variate atom equipoints) is apparently the property of all mixed crystals and is therefore a very common phenomenon. There seems to be no obvious reason from the point of view of geometrical and descriptive crystallography why compounds would not require similar treatment.

Several cases are on record in which the same problem arose. For instance, ammonium-oxy-fluoro-molybdate,[10] $(NH_4)_3MoO_3F_3$, whose x-ray diffraction data indicate that the O and F ions occupy crystallographically equivalent positions. In this case it was possible to explain the structure by assuming a larger unit cell, the existence of which, however, could not be brought out by the x-ray spectrograms on account of the similarity of the scattering power of O and F. Other cases were potassium cyanate,[11] KCNO, in which C and N seemed to occupy crystallographically equivalent positions and $Co(NH_3)_5H_2OSO_4I$,[12] in which the NH_3 groups are partly replaced by H_2O. In these cases again the explanation given for ammonium-oxy-fluoro-molybdate appeared reasonable. In the case of lithium ferrite, however, it can be shown in view of the large difference in the scattering power of the cations that an enlargement of the unit cell is inadequate to explain this structure, and thus it becomes much more reasonable to assume that the iron and lithium ions are irregularly distributed within the same set of equipoints.

While very few cases of this type of structure have so far been encountered in compounds, and it is also impossible at present to say what significance attaches to this fact, further studies will show whether or not these cases are fortuitous.

[10] L. Pauling, J. Am. Chem. Soc. **46**, 2738 (1924).
[11] S. B. Hendricks and L. Pauling, J. Am. Chem. Soc. **47**, 2904 (1925).
[12] O. Hassel, Norsk. Geol. Tidsskrift. **10**, 33 (1928). See also *idem*, p. 92.

NATURAL UNITS FOR ATOMIC PROBLEMS

By Arthur E. Ruark
University of Pittsburgh

(Received September 16, 1931)

Abstract

This paper deals principally with two systems of units, designated A and B. In both, the velocity of light and the rest mass of the electron are taken as units. In A, the length unit is $h^2/4\pi^2 m_0 e^2$, which is the radius of the first Bohr hydrogen orbit, in B, it is $h/2\pi m_0 c$, which is $(2\pi)^{-1}$ times the Compton shift in scattering at 90°. In each system, the choice of the above units determines the unit of charge through the equation for the Coulomb force, $f = e^2/r^2$. In system A, the electronic charge is numerically equal to the fine structure constant, α; in system B, the square of the electronic charge is numerically equal to α, and h is equal to 2π. It is shown that many formulas of quantum theory are greatly simplified when written in terms of system B; the coefficients of the Schrödinger and Dirac equations contain only small integers and the electronic charge. The use of these units provides a consistent scheme for simplifying the algebra associated with problems of quantum theory.

§1

WE ARE all familiar with numerous cases in which the mathematical treatment of physical problems is simplified by a suitable choice of units. In the computation of atomic energy levels Hylleraas[1] and others have found it very useful to employ a unit of length of the same order of magnitude as the radius of the first Bohr orbit. Sometimes also, the energy required to ionize the hydrogen atom from its lowest state is taken as the unit of energy. However, when the relativistic wave equations are used, the self-energy of the electron is a more convenient unit. This circumstance led the writer to consider the whole question of natural units for use in problems of atomic and nuclear physics. It soon appeared that rather striking simplifications of the wave-mechanical equations can be achieved by proper choice of units. The determination of the most convenient unit systems was not straightforward, but required considerable searching. The writer's conclusions are presented in this brief paper, which is devoted to methodology, and contains no new physical result.

One of the best-known attempts to simplify the equations of quantum theory and related subjects is that of Planck,[2] who chose new units of length, time, mass and temperature, of such sizes that the velocity of light, the quantum of action, the universal constant of gravitation, and the gas constant are all numerically equal to one. The rounded values of the units of length, time and mass are as follows:

[1] Hylleraas, Zeits. f. Physik **65**, 209 (1930), and earlier papers.
[2] Planck, Heat Radiation, English translation by Masius, p. 175.

Unit of length: 4×10^{-33} centimeter
Unit of time: 1.3×10^{-43} second
Unit of mass: 5.4×10^{-5} gram.

We leave the gas constant out of consideration, since it may always be made unity by properly choosing the unit of temperature.

Obviously, the difficulty with this system is that the new units are not convenient in size for use in atomic problems. The same criticism may be directed against many similar attempts. The writer tried, therefore, to obtain systems of units which fulfill, as far as possible, the following requirements: The fundamental units of length, time and mass must be of such magnitude that atomic lengths, times, and masses are expressible by fairly small numbers, as long as we deal with small quantum numbers; and the coefficients in the principal equations of atomic physics should be simplified when the new units are used. Two of the systems examined will be discussed in detail.

§2

In setting up a system of natural units almost every step consists in abandoning some artificial relation associated with the c.g.s. system. We try to proceed as a Maxwell demon probably would if he were entrusted with the construction of a natural and universal scheme of units. In this section we concern ourselves with two systems, designated A and B. In both, the velocity of light, c, is taken as the unit of velocity. In extranuclear problems, the units of length adopted are as follows:

A: $h^2/4\pi^2m_0e^2$, the radius of the first hydrogen orbit if the motion of the nucleus is neglected.

B: $h/2\pi m_0c$, the Compton wave-length change in scattering at 90°, divided by 2π.

The corresponding units of time are fixed by the choices already made. They are,

A: $h^2/4\pi^2m_0e^2c$.

B: $h/2\pi m_0c^2$.

In both systems we take the rest mass of the electron as the mass unit. At first sight it might seem better to assign the value unity to e, the electronic charge, but this does not simplify the more important equations of quantum theory as much as the choice we have made.[3]

It will often be convenient to prime a quantity measured in c.g.s. units, the unprimed symbol being reserved for the same quantity measured in the new units. Thus $h'=6.547\times10^{-27}$ erg sec., the conventional value of Planck's constant, while it happens that in system B the numerical value of h is 2π.

[3] The essential point is, we cannot make both the elementary charge and the electronic mass *simultaneously* equal to unity, unless we are willing to modify the classical equation for the force between two charges by introducing a constant analogous to the constant of gravitation. The expression $f=\epsilon^2/r^2$, giving the force between two equal charges, ϵ, serves to define the unit of charge. If the numerical values of f and r are unity, then ϵ is the unit of charge. But it is readily verified that the force between two electrons at unit distance is not one in either of the schemes considered here, so the electronic charge cannot be one in these systems.

The unit of action in B is $m_0' \cdot c' \cdot (h'/2\pi m_0' c') = h'/2\pi = (1.042 \pm .0013) \times 10^{-27}$ erg second. This is the quantum of action adopted by Dirac, Weyl and others, in preference to Planck's constant. The use of the symbol h for this quantity has led to so much confusion that a new one seems desirable. Perhaps h_0 would be an acceptable designation. The desire to employ $h'/2\pi$ as the unit of action constituted the writer's reason for choosing $h'/2\pi m_0' c'$ as the new unit of length in system B. Anyone who wishes to employ Planck's constant as the unit of action may do so by taking $h'/m_0' c'$ as the length unit; but then the factor 2π, or some power of it, will appear in many equations.

In Table I we give the c.g.s. numerical values of the new units of certain important physical quantities. These are rounded, since it is not necessary to

TABLE I. *Approximate c.g.s. values of natural units.*

Physical quantity	c.g.s value of unit in system A	c.g.s value of unit in system B
Length	$h'^2/4\pi^2 m_0' e'^2 = 0.5 \times 10^{-8}$	$h'/2\pi m_0' c' = 3.9 \times 10^{-11}$
Time	$h'^2/4\pi^2 m_0' e'^2 c' = 0.17 \times 10^{-18}$	$h'/2\pi m_0' c'^2 = 1.3 \times 10^{-21}$
Velocity	$c' = 3 \times 10^{10}$	$c' = 3 \times 10^{10}$
Mass	$m_0' = 9 \times 10^{-28}$	$m_0' = 9 \times 10^{-28}$
Momentum	$m_0' c' = 2.7 \times 10^{-17}$	$m_0' c' = 2.7 \times 10^{-17}$
Energy	$m_0' c'^2 = 8.1 \times 10^{-7}$	$m_0' c'^2 = 8.1 \times 10^{-7}$
Action	$\alpha h'/2\pi = 1.4 \times 10^{-25}$	$h'/2\pi = 1.0 \times 10^{-27}$
Charge	$e'/\alpha = 6.5 \times 10^{-8}$	$e'/\alpha^{1/2} = 5.6 \times 10^{-9}$

use them in recasting the equations of quantum theory. In the table, α represents the fine structure constant, which is dimensionless. According to Birge,[4] we have

$$\alpha = \frac{2\pi e^2}{hc} = (7.283 \pm 0.006) \times 10^{-3} \tag{1}$$

and

$$\frac{1}{\alpha} = \frac{hc}{2\pi e^2} = 137.29 \pm 0.11. \tag{2}$$

The numerical value of the unit of charge in any system may readily be found with the aid of these relations. In system B, for example, $c = 1$, and $2\pi/h = 1$. Therefore,

$$e^2 = \alpha. \quad (\textit{system } B \textit{ only}) \tag{3}$$

and the new unit of charge measured in c.g.s. electrostatic units must be $e'/\alpha^{1/2} = 4.770 \times 10^{-10}/8.533 \times 10^{-2} = 5.59 \times 10^{-9}$ e.s.u. Similarly,

$$e = \alpha. \quad (\textit{system } A \textit{ only}). \tag{4}$$

It is reasonable to suppose that in nuclear problems it will prove convenient to use units exactly like those of Table I, except that the mass of the proton, or possibly that of the alpha-particle, will replace the electronic mass in the definitions of the units. Attention may be directed to the quantity $e^2/m_0 c^2$, which has the dimensions of length (it is equal to $\alpha h/2\pi m_0 c$) and is of the same order of magnitude as the classical radius of the Lorentz electron.

[4] Birge, Phys. Rev. Supplement **1**, 1 (1929).

Systems involving the so-called gravitational radius of the electron have also been considered by the writer, but will not be discussed here.

§3

It is now possible to state the relative advantages of the proposed systems. Atomic diameters are of the order unity in system A, and frequencies associated with the outer electron shells are of the same order as the corresponding c.g.s. wave numbers. It appears that the units of system A are well adapted in size to the discussion of the outer electrons and of wave-lengths in the optical region, while system B is more useful in dealing numerically with fast electrons and x-ray phenomena. However, the chief benefits to be derived from the use of these units are associated with the facts that algebra is often simplified, and that many atomic constants have small numerical values. For example, in both systems the numerical measures of a mass and of the corresponding energy are identical, since $c=1$. The self energy of the electron is unity. Wave number and frequency are numerically identical and further the electrostatic and electromagnetic units of any quantity are the same. The expression for the Lorentz force per unit charge is $E+[vH]$ and many other electrodynamic formulae are less complex than in c.g.s. units.

It is interesting to note the simple forms assumed by certain equations of atomic theory when the system B is employed. All quantities belonging to the electron have values expressible in terms of integers and of the electronic charge, provided the customary expressions for the electronic angular momentum and magnetic moment are rigorously correct. Thus, the angular momentum is numerically $1/2$, and the magnetic moment $e/2$. Of all electronic properties, then, only the charge requires experimental determination, from the standpoint of both our new unit systems.[5] In both of them, its numeric is connected in a simple way with the fine structure constant, as we see from Eqs. (1) to (4).

Further, in system B the energy, mass and momentum of a photon are all given numerically by $2\pi\nu$, and exponential factors in wave functions are simplified. Thus, numerically $e^{-2\pi iEt/h}$ becomes e^{-iEt}. Such examples could be indefinitely multiplied.

We now illustrate the application of system B to several important equations. Heisenberg's commutation relation is

$$pq - qp = \frac{hI}{2\pi i} \cdot \tag{5}$$

But $h=2\pi$, and (5) may be rewritten as

$$pq - qp = -iI. \quad (\textit{system } B \textit{ only}). \tag{5a}$$

[5] Of course it is not implied that the determination of electronic constants other than the charge can be avoided in connection with *practical* problems. For example, in order to express a length of the order of a few centimeters in terms of the new unit of length, that unit would first have to be found in terms of some familiar unit, such as the centimeter. The new systems are designed to reduce labor for the theoretical and not the experimental physicist.

In this form, the physical units of the right member are submerged, but the algebra of any matrix problem is simplified, and the "lost" constants can easily be reinserted in the final result. It is not necessary to go through laborious transformations in obtaining (5a) or other simplified equations. For example, in the new units as in the old, Schrödinger's equation has the form

$$\Delta\psi + \frac{8\pi^2}{h^2}(E - V)\psi = 0; \tag{6}$$

but in system B, $4\pi^2/h^2 = 1$, numerically, and (6) becomes,

$$\Delta\psi + 2(E - V)\psi = 0. \quad (system\ B\ only). \tag{6a}$$

The relativistic Schrödinger equation and the Dirac equations are also simplified. To summarize, when we use system B, the general equations of quantum mechanics have rational coefficients, except for the occurrence of the electronic charge, which is numerically equal to $\alpha^{1/2}$.

Eddington[6] has brought forward a theory involving space of sixteen dimensions, which indicates that $1/\alpha$ may be exactly 137, that is, $1+1/2$ (17.16). If this were substantiated, all coefficients in the wave equation would be rational. However, Birge's value of $1/\alpha$, cited in Eq. (2), disagrees with Eddington's 137 by more than twice the probable error. Other interpretations of α have been suggested by Lewis and Adams,[7] by Perles,[8] and by Fürth;[9] but such matters, important as they may be, lie outside our present scope.

In conclusion, it may be worth while to note that the use of the natural units discussed focuses attention on certain unsolved problems of quantum theory. The only empirical constants which occur when we apply the Schrödinger Eq. (6a) to the problem of the hydrogen atom are α and m/M. The former enters through the fact that $V = -Ze^2/r = -Z\alpha/r$, in accordance with Eq. (3). No doubt the value of α is connected with the internal mechanism of the electron, as we can see by examining classical electronic models, while it appears probable that m/M will eventually be interpreted as the ratio of two eigenwerte of a still-to-be-discovered wave equation. Pending the elucidation of these matters, the use of our system B reduces the wave equation to very simple terms.

[6] Eddington, Proc. Roy. Soc. **A126**, 696 (1930) and earlier papers.
[7] Lewis and Adams, Phys. Rev. **3**, 92 (1914).
[8] Perles, Naturwiss. **16**, 1094 (1928).
[9] Fürth, Zeits. f. Physik **57**, 429 (1929).

SOME PHYSICAL PROPERTIES OF COMPRESSED GASES. II, CARBON MONOXIDE

By W. Edwards Deming and Lola E. Shupe
Fertilizer and Fixed Nitrogen Investigations
Bureau of Chemistry and Soils
Washington, D. C.

(Received September 5, 1931)

Abstract

The writers have adjusted and extrapolated the compressibility data obtained by Bartlett and his collaborators on carbon monoxide, so that accurate $p-v-T$ relations from $-70°$ to 400° and up to 1200 atm. are available. The relatively low pressure isotherms of Scott at 25° and of Goig-Botella at 0°, 12.44°, and 20.22° are included. Derivatives are obtained by the graphical scheme used for similar calculations on nitrogen. The specific volume, density, expansion coefficients $-(p/v)(dv/dp)_T$ and $(T/v)(dv/dT)_p$ fugacity, C_p, C_p-C_v, C_v, Joule-Thomson coefficient μ are calculated and shown in curves and a table for 14 pressures and 11 temperatures in the range $-70°$ to 400° and 25 to 1200 atm. In particular, C_p vs. p isotherms, C_v vs. t isobars, t vs. p μ = const. graphs are shown; among the last, the $\mu=0$ curve is the inversion curve. There are no direct experimental data for comparison. On account of similarity in the molecular structure and the spectra of the molecules CO and N_2, one might look for some correspondence in the physical properties of the two gases. In general, the trends of the two are qualitatively similar. The C_p-C_v vs. p isotherms all show a maximum. This maximum is very flat at the highest temperatures and comes at about 700 atm. As the temperature decreases, the maximum becomes pronounced and moves to lower pressures; it comes at about 200 atm. along the $-50°$ and $-70°$ curves. Along the $-70°$ isotherm a second maximum appears at about 550 atm., but it is not evident at higher temperatures. C_p-C_v approaches R, of course, along all isotherms as the pressure is decreased to zero. C_p is obtained by adding ΔC_p to $C_p{}^*$. $C_p{}^*$ denotes the heat capacity for a given temperature at zero pressure; ΔC_p is the change in C_p with pressure along a given isotherm. It is evaluated thru $\int_0^p -T(d^2v/dT^2)_p dp$. The derivative occurring under the integral sign is obtained by the authors' graphical scheme at a sufficient number of points for mechanical integration under the isotherm. Along isotherms at 50° and lower, C_p increases rapidly with pressure and reaches a maximum at about 300 atm. Changes in pressure above 500 atm. cause only relatively small changes in C_p at any temperature. Above 200 atm. and below 0°, C_p increases rapidly as the temperature is lowered. The C_v vs. t isobars show that from 300 to 1200 atm. C_v has a minimum at about 100°. On the low temperature side of this minimum the curves are very steep; along the 1200 atm. isobar C_v drops from 4.4 R at $-70°$ to 2.57 R at 100°. Above 100°, C_v is only a few hundredths cal./mole deg. higher than $C_v{}^*$ for pressures up to 400 atm; further increase in pressure to 1200 atm. raises C_v only a few tenths. Below 25°, C_v for $p=25$ is slightly less than $C_v{}^*$. Below 0°, C_v at 100, 150, and 200 atm. drops far below $C_v{}^*$ as the temperature is lowered. A graph showing $\Delta \equiv v(pv/RT-1)$ vs. ρ isotherms and isobars is shown, the data for which are listed in the table. This graph is very convenient for interpolating $p-v-T$ data. Having given two of the three $p-v-T$ coordinates, the third is quickly estimated from the graph, or is readily computed more exactly by reading the ordinate Δ and solving $\Delta=v(pv/RT-1)$ for the unknown desired. Values for the second virial coefficient are found. They are expressible by $B=58.03-19.84\ T^{-1}$ cc/mole between $-70°$ and 400°.

FAIRLY complete compressibility data for several gases over considerable range of pressure and temperature are now available. The work of Bartlett and his collaborators and of others on nitrogen, hydrogen, and their mixtures,[1] carbon monoxide,[2] methane,[3] and helium[4] form valuable extensions of hitherto existing data. A method of determining derivatives such as $(dv/dp)_T$, $(dv/dT)_p$, $(d^2v/dT^2)_p$ from compressibility data enables various physical properties to be computed. The writers have been using a graphical scheme for evaluating derivatives. Curves and a table showing specific volume, density, fugacity, expansion coefficients $-(p/v)(dv/dp)_T$ and $(T/v)(dv/dT)_p$, ΔC_p, C_p, $C_p - C_v$, C_v, and μ for nitrogen over the range $-70°$ to $600°$ and from 20 to 1200 atm. have been published.[5] In the present paper we give the results for carbon monoxide.

This graphical scheme depends on the fact that

$$\Delta \equiv v(pv/RT - 1) \tag{1}$$

and

$$\alpha \equiv RT/p - v \tag{2}$$

and their derivatives with respect to p, v, T express the deviation from Boyle's law; and that any departure of $-(p/v)(dv/dp)_T$ and $(T/v)(dv/dT)_p$ from unity is evidenced by Δ and α and their derivatives being different from zero. In addition to the relations between the derivatives of v, Δ, and α given by Eqs. (3) to (10), we shall need[6]

$$(T/v)(dv/dT)_p = \frac{pv/RT - (d\Delta/dT^{-1})_p/vT}{1 + 2\rho\Delta} \tag{15}$$

$$(T/v)(dv/dT)_p = pv/RT[\rho^2(d\Delta/d\rho)_p + (1 + 2\rho\Delta)] \tag{16}$$

$$(T/v)(dv/dT)_p = (d\alpha/dT^{-1})_p/vT + RT/pv \tag{17}$$

$$-T(d^2v/dT^2)_p = \frac{T}{v}\left\{\left(\frac{dv}{dT}\right)^2 - \frac{1}{p}\frac{d}{dT}\left(pv\frac{dv}{dT}\right)\right\}_p, \tag{18}$$

[1] Bartlett, J. Amer. Chem. Soc. **49**, 687 (1927); **49**, 1955 (1927); Bartlett, Cupples, Tremearne, ibid. **50**, 1275 (1928); Bartlett, Hetherington, Kvalnes, Tremearne, ibid. **52**, 1363 (1930).

[2] Bartlett, Hetherington, Kvalnes, Tremearne, J. Amer. Chem. Soc., **52**, 1374 (1930); G. A. Scott, Proc. Roy. Soc. **125A**, 330 (1929); Severian Goig-Botella, Anales soc. espan. fisquim **27**, 315 (1929); one set of his measurements at 0° is published in duplicate in the Comptes Rendus **189**, 246 (1929).

[3] Kvalnes and Gaddy, J. Amer. Chem. Soc. **53**, 394 (1931). This publication gives data from $-70°$ to 200° and up to 1000 atm. Isotherms at 300° and 400° will soon be undertaken by Dr. Wiebe on the same apparatus.

[4] Wiebe, Gaddy, Heins, J. Amer. Chem. Soc. **53**, 1721 (1931). This publication gives data from $-70°$ to 200° and up to 1000 atm. Isotherms at 300° and 400° will soon be undertaken by Dr. Wiebe on the same apparatus.

[5] W. Edwards Deming and Lola E. Shupe, Phys. Rev. **37**, 638 (1931).

[6] In this paper, the equations, figures, and tables will be numbered as continuations from those in the paper on nitrogen.

because it is more accurate to use Δ and α in isobars against T^{-1} than against T, and because the second derivative is conveniently found from $pv(dv/dT)_p$ vs. T isobars, as will be explained later.

After Bartlett's[2] data on carbon monoxide were published a recalibration of his thermocouple showed that the temperatures recorded as $-25°$, $-50°$, $-70°$ should have been $-24.99°$, $-49.93°$, $-69.90°$. The slight corrections necessary at these temperatures were made, and then Δ vs. p isotherms were plotted from Bartlett's data at $-70°$, $-50°$, $-25°$, $0°$, $25°$, $50°$, $100°$, $150°$, $200°$ to 1000 atm., and from Scott's 25° isotherm, which goes to 170 atm.,

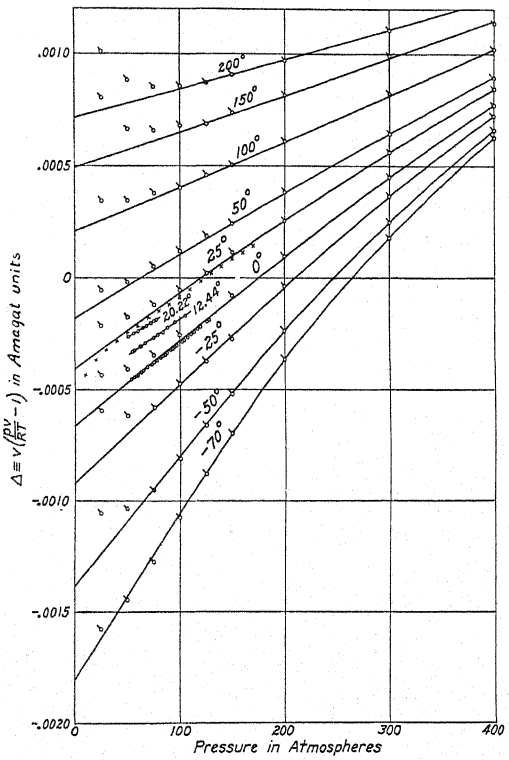


Fig. 7. Δ vs. p isotherms for carbon monoxide to 400 atmospheres. Bartlett's points are flagged circles, Goig-Botella's are circles, Scott's are crosses. Scott's isotherm is at 25°, Goig-Botella's are at 0°, 12.44°, and 20.22°. The data were smoothed according to the curves.

and from Goig-Botella's isotherms at 0°, 12.44°, and 20.22°, which go from 50 to 130 atm. The low pressure portion of these isotherms are shown in Fig. 7. We also plotted Δ vs. T^{-1} isobars obtained from Bartlett's data, at 25, 50, 75, 100, 150, 200, 300, 400, 500, 600, 800, 1000 atm., from $-70°$ to 200°. On these curves were also placed points from Scott's and Goig-Botella's data where they could be used. By trial and error smooth isotherms and isobars were finally placed so that the same value of Δ would be read from a curve on either plot at a given temperature and pressure. This is equivalent to fixing a smooth Δ, p, T^{-1} surface in space.

The $pv/(pv)_s$ value for 800 atm. and 25° was misprinted in Bartlett's paper as 1.9915. It should be 1.0115.

Bartlett's isobars were extrapolated to 1200 atm. and his isotherms to 400°; this is a 20 percent extrapolation with regard to pressure and a 22 percent extrapolation with regard to T^{-1}. Since Bartlett gives nine isotherms and twelve isobars in the range $25 \leqq p \leqq 1000$ atm. and $0.002113 \leqq T^{-1} \leqq 0.004922$, extrapolation to 1200 atm. and to $0.001485°K^{-1}$ should be trustworthy. The value of these extrapolations, if they are any where near as reliable as we think they are, must be considerable; to extend the p-v-T observations to 300° and 400° and to 1200 atm. would require some changes in the apparatus; in fact serious difficulties would have to be overcome in experiments with carbon monoxide at 300° and 400° under high pressure.

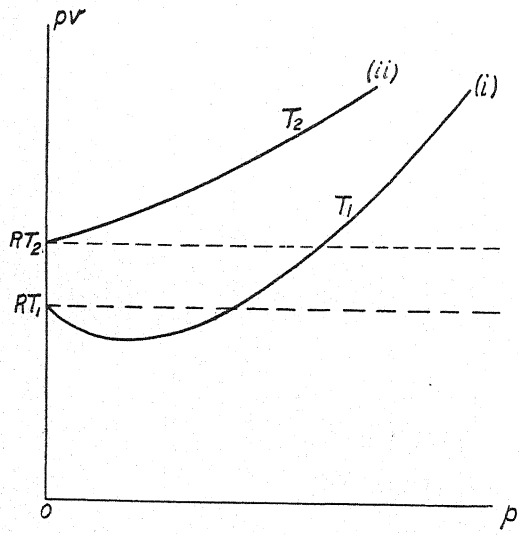


Fig. 8. The isothermal variation of pv with p at low pressure for an actual gas. Carbon monoxide takes the form of (*i*) at 50° or lower, and takes the form of (*ii*) at 100° or higher.

As with nitrogen, the close proximity of the plotted (experimental) values of Δ to the final smooth curves, on which lie the adjusted values of Δ, attests to the high precision of the compressibility data and gives promise that the derived calculations should be reliable. An exception occurs at Bartlett's low pressure observations, as is seen in Fig. 7. The curves shown were drawn from the following considerations.

Holborn and Otto[7] found that the expression

$$pv = RT + ap + bp^2 + cp^4 \tag{19}$$

is capable of following the data of most of the permanent gases along an isotherm from about 20 to 100 atm. Recently William Wild[8] has observed that

[7] Holborn and Otto, Zeits. f. Physik **33**, 1 (1925).
[8] William Wild, Phil. Mag. **12**, 41 (1931).

this power series, when used with constants obtained from data between roughly 20 and 100 atm., extrapolated to 1 atm. gives the "compressibility" (usually denoted by $1+\lambda$, the ratio of the pv product at zero pressure to the product at 1 atm., both at 0°C) in agreement better than 1 in 10,000 with the value obtained from low pressure data where a linear equation $pv=RT+ap$ suffices. These facts mean that the series (19) is capable of expressing the trends of the isotherms from zero pressure up to 50 or 100 atm.

From Eq. (19),

$$\Delta = a + (a^2/RT + b)p + (2ab/RT)p^2 + (b^2/RT + c)p^3 + \cdots \quad (20)$$

A pv vs. p isotherm will take the form (*i*) or (*ii*) in Fig. 8, depending on whether the temperature is below or above the Boyle temperature; at the

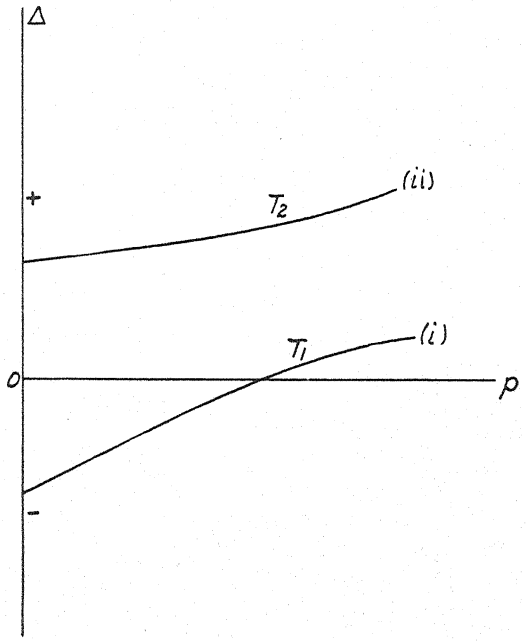


Fig. 9. The graphs of Δ vs. p corresponding to the pv vs. p isotherms in Fig.6.

Boyle temperature $pv=RT$ and the curve is a horizontal line, at least for some distance. Along (*ii*) $a>0$ and $b>0$, hence the corresponding Δ vs. p graph will begin as a straight line with a positive intercept and positive slope and will then curve upward as indicated in Fig. 9, since the coefficients of p and p^2 in (20) are positive. Along (*i*) $a<0$ and $b>0$, so the corresponding Δ curve will begin as a straight line with a negative intercept and positive slope and will then curve downward as shown, since in (20) the coefficients of p and p^2 are positive and negative respectively. The trends thus predicted for the Δ curves are beautifully followed by Goig-Botella's and Scott's points in Fig. 7, but not by Bartlett's. Goig-Botella's and Scott's apparatuses were designed for the low pressure region, but Bartlett's was designed primarily for

work from 100 to 1000 atm., and the upward curl of his points may come from a small systematic error, active only at low pressure. This explanation of the deviation is satisfactory according to a private communication from Dr. Bartlett.

It should be noted that this discrepancy is only slight. The Δ curves are magnified residuals; further, $(dp/d\Delta)_{v,T} = RT\rho^2$ is very small at the low pressure (or low density) end—at 25 atm. and 0° a change in Δ of 0.0001 Amagat units affects the calculated pressure only 0.06 atm.; therefore the points in Fig. 7, instead of showing the data to be unreliable, really show them to be remarkably systematic.

The family of Δ *vs.* T^{-1} isobars (not shown) become nearly straight lines at the higher temperatures and at the lower pressures. The zero pressure isobar is fitted well enough by a straight line, and

$$\Delta = b - (a/R)T^{-1} \tag{21}$$

may be taken for its equation. When Δ is replaced by $v(pv/RT-1)$, this becomes closely

$$(p + a/v^2)(v - b) = RT, \tag{22}$$

which is van der Waals' equation. From this,

$$-T(d^2v/dT^2)_p = 2a/RT^2 \text{ at } p = 0. \tag{23}$$

The slope $-a/R$ of the zero pressure isobar is -0.8856 Amagat units, so

$$\begin{aligned} -T(d^2v/dT^2)_p &= 2 \times 0.8856T^{-2} \text{ Amagat units} \\ &= 960.7T^{-2} \text{ cal./mole atm. deg.} \end{aligned} \tag{24}$$

This quantity will be used later in calculating the heat capacities. It is the value of $(dC_p/dp)_T$ at zero pressure. A more accurate equation of state would give the same result for this purpose, since we need the derivative $-T(d^2v/dT^2)_p$ only at zero pressure.

Eq. (1) can be rewritten as

$$pv/RT = 1 + \Delta\rho. \tag{25}$$

Δ at low pressures is then the second virial coefficient, usually denoted by B; so the Δ vs. T^{-1} zero pressure isobar is really a plot of B. It is expressed by statistical theory in terms of the interaction energy ϵ of two molecules, and the temperature, by

$$B = 2\pi N \int_0^\infty (1 - e^{-\epsilon/kT})r^2 dr. \tag{26}$$

According to London,[9] $-\epsilon$ lies between $3\alpha^2 V_a/4r^6$ and $3\alpha^2 V_i/4r^6$. α here denotes the polarizability of the molecule, and is not the α of Eq. (2). V_a and V_i are the excitation and ionization energies, and r is the molecular separation.

[9] Eisenschitz and London, Zeits. f. Physik **60**, 491 (1930); London, Zeits. f. Physik **63**, 245 (1930).

Margenau[10] evaluated the above integral by assuming that $\epsilon=\infty$ for $r\leqq d$, and $-\epsilon=3\alpha^2V_i/4r^6$ when $r>d$. His result is

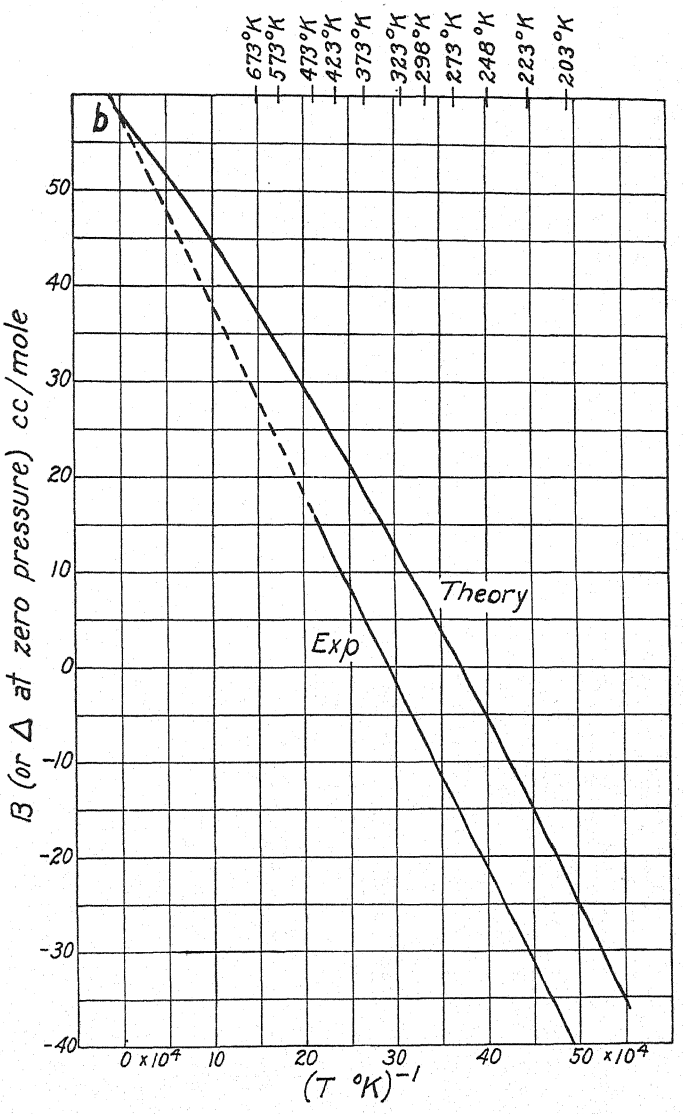


Fig. 10. Carbon monoxide. The curve marked "Exp." shows the experimental values of the second virial coefficient from −70° to 200°C. The extrapolation (dashed) gives $b=58.03$ cc/mole. This value in Eq. (27) gives the curve marked "Theory".

$$B = b(1 - 0.75y - 0.094y^2 - 0.014y^3 - 0.0019y^4 - 0.00022y^5 - 0.000022y^6 - \cdots) \tag{27}$$

[10] H. Margenau, Phys. Rev. **36**, 1782 (1930).

where

$$b = 2\pi Nd^3/3, \quad y = \alpha^2 V_i/d^6 kT = 4\pi^2 N^2 \alpha^2 V_i/9kb^2 T.$$

b is thus four times the volume of N spheres of diameter d. If N is the number of molecules per mole, b is in cc/mole. b can be evaluated by extrapolating the zero pressure Δ vs. T^{-1} isobar back to $T^{-1}=0$. The value so obtained is $b=0.002590$ Amagat units or $22403\times 0.002590 = 58.03$ cc/mole. Zahn and Miles[11] give information from which it is possible to deduce that the polariz-

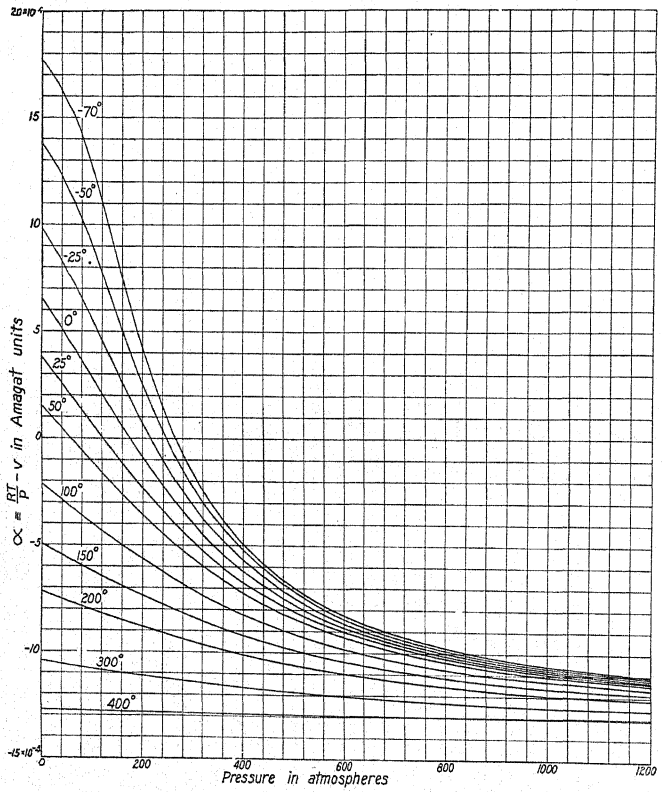


Fig. 11. α vs. p isotherms for carbon monoxide.

ability of CO is 1.97×10^{-24}cc per molecule. John T. Tate and P. T. Smith[12] found 14.20 electron volts for the ionization potential of CO.

With these, $y = 177.7T^{-1}$. The curve given by the series (27) is marked "Theory" in Fig. 10. The curve marked "Exp." is our Δ vs. T^{-1} zero pressure isobar. The agreement is fairly good. The theoretical curve has a perceptible curvature over the range of experiment, $-70° \leqq t \leqq 200°$, while the other does not. According to a recent paper by Kirkwood and Keyes,[13] the second virial

[11] C. T. Zahn and J. B. Miles Jr., Phys. Rev. **32**, 497 (1928).

[12] From a paper read at the Washington meeting of the American Physical Society, May 2, 1931.

[13] J. G. Kirkwood and F. G. Keyes, Phys. Rev. **37**, 832 (1931).

coefficient for He goes through a maximum at about $-100°$, and the same phenomenon should appear at sufficiently high temperatures for other gases. This would imply that the experimental curve should not be extrapolated as a straight line to $T^{-1}=0$ and that $b<58.03$; also that the assumptions underlying the development of Eq. (27) are not fully valid at high temperatures, and that perfect agreement of the curves in Fig. 10 is not to be expected. The experimental curve in Fig. 10, or the list of Δ at zero pressure at the bottom of Table II are probably as good values for the second virial coefficient from $-70°$ to 400° as can be gotten from the data available.

The α vs. p isotherms of Fig. 11 might be of some interest. There has been some conjecture[14] concerning the shape of these curves for a real gas, and Fig. 11 is probably the first publication for an extended range for any gas.[14a] The areas under the curves are used in determining fugacities by Eq. (28).

The tables published by Bartlett and others show compressibility factors $pv/(pv)_s$ at the different pressures and temperatures. The denominator $(pv)_s$ is the value of pv at S. T. P. Baxter[15] gives 1.00048 for $pv/(pv)_s$ at zero pressure. Using Birge's value 22414.1 cc for the volume of a mole of an ideal gas at S. T. P. we have $22414.1/1.00048=22403.3$ for the factor to convert Amagat units of volume into cc/mole. Multiplication of densities in mole/cc by 28.006 converts them into g/cc. We also use $R=82.0489$ cc atm./mole deg. or 1.9864 cal./mole deg., and 273.18° for the ice point, after Birge.

The final values of the physical properties are shown in Table II and in the figures. Care has been taken in each entry to give only as many figures as we consider significant; the last figure is considered doubtful. No points are shown on the curves because they are drawn through the plotted point in every case. Each physical property listed will now be discussed.

Specific volume v, column 2; density ρ, column 3; Δ, column 10 and Fig. 12.

The values of Δ were read from the Δ vs. p isotherms or from the Δ vs. T^{-1} isobars. Those for zero pressure or zero density constitute the second virial coefficient, and are shown at the bottom of the table and in Fig. 10. Eq. (1) solved for v then gives the specific volume for any pressure and temperature at which Δ is known. The densities in column 3 are in g/cc and were obtained by dividing 28.006 by the corresponding v in cc/mole.

The Δ vs. ρ isotherms and isobars of Fig. 12 are convenient for exhibiting and interpolating the p-v-T data, as is described in the title to the figure. Any one of the p-v-T coordinates can be quickly estimated when the other two are given; when greater accuracy is desired, the value of Δ, as read from the graph corresponding to the two given coordinates (ρ and T, v and p, etc.), is substituted in Eq. (1) to obtain the third coordinate. The values of Δ are listed so that anyone desiring to make interpolations in the p-v-T data with more accuracy than can be gotten from the Fig. 12 appearing here can construct a

[14] Lewis and Randall, Thermodynamics, p. 195 (McGraw-Hill Book Company, 1923).

[14a] Added in proof. Since this was written, a table of α for nitrogen from $-148°$ to 300° and to about 100 atm. has appeared in a paper by George Tunell, J. Phys. Chem. **35**, 2885 (1931).

[15] Baxter *et al.*, J. Amer. Chem. Soc. **53**, 1627 (1931).

TABLE II. *Some physical properties of compressed carbon monoxide derived from experimental data on compressibility.*

1 p	2 v	3 ρ	4 f	5 $-\frac{p}{v}\left(\frac{dv}{dp}\right)_T$	6 $\frac{T}{v}\left(\frac{dv}{dT}\right)_p$	7 ΔC_p	8 C_p	9 C_v	10 Δ
atm.	cc/mole	g/cc	atm.			calories/mole degree			cc/mole
			$t=-70°$	$C_p^*=6.953$,	$C_v^*=4.967$	cal./mole deg.			
25	629.0	.04453	23.59	1.057	1.220	.63	7.58	4.94	−35.62
50	298.1	.09395	44.67	1.100	1.465	1.37	8.32	4.86	−31.57
75	189.8	.1475	63.68	1.118	1.710	2.21	9.16	4.71	−27.71
100	138.3	.2025	81.13	1.076	1.899	3.11	10.06	4.54	−23.64
150	92.40	.3031	113.4	.881	1.943	4.57	11.53	4.45	−15.57
200	73.95	.3787	144.9	.667	1.706	5.38	12.34	4.64	−8.33
300	59.32	.4721	214.5	.446	1.188	5.76	12.72	6.01	4.01
400	52.77	.5307	299.5	.366	.888	5.52	12.47	7.05	14.05
500	48.91	.5726	405.9	.320	.780	5.26	12.21	6.67	22.85
600	46.23	.6058	539.7	.293	.708	5.31	12.26	6.62	30.69
800	42.69	.6561	917.8	.257	.552	5.52	12.47	7.63	44.76
1000	40.35	.6941	1509	.238	.467	5.62	12.57	8.17	57.31
1100	39.43	.7103	1917	.231	.426	5.65	12.60	8.54	63.16
1200	38.62	.7252	2422	.223	.396	5.67	12.62	8.75	68.73
			$t=-50°$	$C_p^*=6.953$,	$C_v^*=4.967$	cal./mole deg.			
25	703.6	.03980	24.00	1.038	1.168	.51	7.46	4.95	−27.69
50	339.9	.08239	46.22	1.062	1.352	1.07	8.02	4.85	−24.40
75	220.6	.1269	67.00	1.064	1.500	1.67	8.63	4.83	−21.24
100	162.9	.1719	86.70	1.037	1.619	2.28	9.23	4.77	−17.99
150	109.3	.2561	124.3	.909	1.655	3.28	10.23	4.87	−11.40
200	86.02	.3256	161.7	.751	1.528	3.87	10.82	5.02	−5.20
300	66.20	.4231	242.9	.551	1.172	4.16	11.11	5.74	5.60
400	57.44	.4876	339.4	.433	.942	4.01	10.96	5.86	14.63
500	52.60	.5325	457.9	.374	.810	3.86	10.81	5.80	22.94
600	49.36	.5674	604.6	.337	.710	3.88	10.83	6.02	30.47
800	45.00	.6224	1010	.291	.569	4.02	10.97	6.63	43.46
1000	42.16	.6643	1624	.271	.484	4.08	11.03	7.08	54.91
1100	41.07	.6819	2038	.262	.447	4.10	11.05	7.31	60.27
1200	40.13	.6979	2544	.251	.417	4.11	11.06	7.44	65.42
			$t=-25°$	$C_p^*=6.954$	$C_v^*=4.968$	cal./mole deg.			
25	794.6	.03524	24.36	1.022	1.124	.40	7.36	4.96	−19.33
50	389.7	.07186	47.62	1.032	1.245	.82	7.78	4.93	−16.76
75	256.4	.1092	70.01	1.029	1.348	1.26	8.22	4.90	−14.23
100	191.3	.1464	91.80	1.007	1.421	1.69	8.64	4.90	−11.58
150	128.9	.2173	134.5	.925	1.454	2.36	9.31	5.00	−6.50
200	100.3	.2791	177.5	.808	1.392	2.76	9.71	5.02	−1.46
300	74.75	.3747	270.5	.629	1.152	2.99	9.95	5.31	7.84
400	63.62	.4403	378.8	.509	.969	2.93	9.88	5.30	15.88
500	57.35	.4883	509.2	.437	.833	2.84	9.80	5.36	23.41
600	53.26	.5258	667.6	.393	.724	2.83	9.78	5.61	30.33
800	47.86	.5852	1094	.342	.591	2.86	9.81	5.99	42.14
1000	44.45	.6301	1720	.314	.504	2.87	9.82	6.31	52.58
1100	43.13	.6494	2132	.303	.469	2.88	9.83	6.48	57.35
1200	42.01	.6666	2628	.285	.441	2.88	9.84	6.48	62.01
			$t=0°$	$C_p^*=6.956$,	$C_v^*=4.970$	cal./mole deg.			
25	884.0	.03168	24.62	1.012	1.094	.33	7.28	4.96	−12.55
50	437.6	.06400	48.60	1.015	1.183	.66	7.62	4.94	−10.44
75	290.3	.09649	72.13	1.008	1.255	1.00	7.95	4.94	−8.33
100	217.8	.1286	95.38	.989	1.305	1.32	8.27	4.95	−6.25
150	147.4	.1900	141.7	.926	1.334	1.83	8.79	5.02	−2.02
200	114.2	.2453	189.0	.843	1.299	2.14	9.10	5.05	2.15
300	83.71	.3346	290.8	.674	1.135	2.36	9.32	5.07	10.08
400	69.96	.4003	408.3	.566	.980	2.35	9.31	5.10	17.39
500	62.19	.4504	547.6	.493	.851	2.31	9.27	5.22	24.08
600	57.13	.4902	714.1	.443	.748	2.27	9.23	5.39	30.24
800	50.72	.5521	1152	.380	.616	2.20	9.16	5.57	41.11
1000	46.72	.5995	1778	.352	.531	2.16	9.12	5.81	50.65
1100	45.18	.6199	2183	.340	.496	2.15	9.11	5.93	55.00
1200	43.90	.6380	2663	.319	.467	2.15	9.10	5.92	59.28
			$t=25°$	$C_p^*=6.959$,	$C_v^*=4.973$	cal./mole deg.			
25	971.8	.02882	24.80	1.005	1.073	.27	7.23	4.97	−6.72
50	484.2	.05784	49.31	1.003	1.140	.54	7.50	4.96	−5.04
75	322.8	.08675	73.64	.994	1.193	.81	7.77	4.96	−3.32
100	243.1	.1152	97.94	.977	1.229	1.07	8.02	4.98	−1.52
150	165.1	.1696	147.0	.926	1.248	1.47	8.43	5.04	2.03

TABLE II. (*Continued*).

1	2	3	4	5	6	7	8	9	10
p	v	ρ	f	$-\frac{p}{v}\left(\frac{dv}{dp}\right)_T$	$\frac{T}{v}\left(\frac{dv}{dT}\right)_p$	ΔC_p	C_p	C_v	Δ
atm.	cc/mole	g/cc	atm.			calories/mole degree			cc/mole
200	127.6	.2195	197.5	.851	1.229	1.72	8.68	5.08	5.51
300	92.40	.3031	306.2	.724	1.116	1.93	8.89	5.02	12.30
400	76.25	.3673	430.8	.612	.984	1.95	8.91	4.99	18.82
500	67.04	.4177	576.4	.540	.869	1.93	8.89	5.08	24.82
600	60.94	.4596	748.1	.488	.772	1.89	8.84	5.22	30.13
800	53.55	.5230	1191	.417	.644	1.80	8.76	5.30	40.24
1000	48.97	.5719	1808	.387	.555	1.73	8.69	5.52	49.06
1100	47.22	.5930	2201	.373	.522	1.71	8.66	5.59	53.05
1200	45.77	.6119	2661	.348	.493	1.67	8.63	5.52	56.97
			$t=50°$	$C_p^*=6.965$,	$C_v^*=4.979$	cal./mole deg.			
25	1059	.02645	24.94	1.000	1.058	.23	7.19	4.98	−1.90
50	529.8	.05286	49.82	.995	1.109	.46	7.42	4.97	−.45
75	354.5	.07899	74.74	.985	1.149	.68	7.64	4.97	1.01
100	267.7	.1046	99.81	.969	1.176	.88	7.85	4.99	2.53
150	182.2	.1537	150.8	.925	1.193	1.21	8.17	5.03	5.58
200	140.6	.1992	203.7	.871	1.177	1.42	8.39	5.04	8.54
300	101.0	.2773	317.8	.755	1.097	1.62	8.59	4.97	14.43
400	82.47	.3396	447.5	.650	.984	1.68	8.65	4.97	20.14
500	71.87	.3896	597.7	.580	.883	1.68	8.64	5.02	25.54
600	64.92	.4314	772.9	.527	.796	1.65	8.61	5.11	30.45
800	56.53	.4955	1218	.454	.673	1.58	8.54	5.16	39.88
1000	51.27	.5462	1826	.418	.580	1.50	8.46	5.37	47.88
1100	49.28	.5684	2207	.402	.551	1.46	8.42	5.36	51.46
1200	47.65	.5877	2649	.376	.518	1.42	8.38	5.33	55.11
			$t=100°$	$C_p^*=6.987$,	$C_v^*=5.001$	cal./mole deg.			
25	1231	.02276	25.11	.994	1.037	.17	7.16	5.00	5.94
50	619.3	.04522	50.48	.986	1.069	.34	7.33	5.00	7.03
75	416.2	.06730	76.18	.974	1.092	.50	7.49	5.00	8.07
100	315.1	.08889	102.3	.959	1.108	.64	7.63	5.01	9.16
150	215.0	.1303	155.9	.924	1.119	.87	7.86	5.02	11.43
200	165.7	.1690	211.9	.881	1.112	1.04	8.02	5.01	13.67
300	117.9	.2375	333.1	.792	1.064	1.24	8.22	4.94	18.34
400	95.04	.2947	469.8	.705	.980	1.32	8.31	4.95	22.96
500	81.70	.3428	625.9	.643	.898	1.34	8.33	5.00	27.31
600	73.04	.3835	805.1	.588	.831	1.33	8.32	4.98	31.50
800	62.44	.4485	1249	.514	.715	1.27	8.26	5.04	39.43
1000	55.91	.5009	1835	.470	.635	1.21	8.20	5.08	46.20
1100	53.54	.5231	2194	.453	.600	1.18	8.16	5.13	49.44
1200	51.56	.5431	2604	.428	.569	1.15	8.14	5.10	52.65
			$t=150°$	$C_p^*=7.024$,	$C_v^*=5.038$	cal./mole deg.			
25	1401	.02000	25.21	.991	1.024	.13	7.16	5.04	11.96
50	707.0	.03961	50.86	.980	1.044	.26	7.28	5.04	12.88
75	476.2	.05881	77.00	.968	1.058	.38	7.41	5.04	13.67
100	361.1	.07755	103.7	.954	1.067	.49	7.52	5.05	14.52
150	246.8	.1146	158.8	.923	1.074	.67	7.70	5.05	16.31
200	190.1	.1473	216.6	.888	1.070	.81	7.84	5.03	18.10
300	134.5	.2082	341.9	.814	1.037	1.01	8.03	4.98	21.87
400	107.4	.2607	482.5	.741	.971	1.11	8.13	5.01	25.54
500	91.60	.3057	641.5	.685	.906	1.15	8.17	5.03	29.24
600	81.19	.3449	821.9	.634	.848	1.16	8.19	5.03	32.72
800	68.42	.4093	1260	.562	.743	1.16	8.18	5.10	39.45
1000	60.72	.4612	1825	.514	.668	1.13	8.15	5.13	45.48
1100	57.86	.4840	2164	.495	.638	1.12	8.14	5.14	48.21
1200	55.50	.5046	2548	.473	.606	1.11	8.13	5.17	50.97
			$t=200°$	$C_p^*=7.076$,	$C_v^*=5.090$	cal./mole deg.			
25	1569	.01784	25.26	.989	1.015	.11	7.18	5.09	16.76
50	793.5	.03529	51.08	.977	1.028	.21	7.28	5.09	17.47
75	535.2	.05233	77.48	.964	1.035	.31	7.38	5.10	18.21
100	406.3	.06893	104.5	.951	1.040	.39	7.47	5.10	18.93
150	277.7	.1008	160.5	.923	1.045	.54	7.62	5.09	20.32
200	213.9	.1309	219.4	.892	1.038	.66	7.74	5.09	21.82
300	150.7	.1858	347.1	.830	1.014	.84	7.91	5.04	24.82
400	119.7	.2340	489.8	.769	.962	.94	8.02	5.07	27.91
500	101.4	.2763	649.9	.718	.908	.99	8.07	5.09	30.96
600	89.28	.3137	830.1	.671	.859	1.03	8.10	5.09	33.91
800	73.39	.3765	1261	.600	.767	1.06	8.14	5.15	39.65
1000	65.50	.4276	1805	.550	.692	1.08	8.15	5.24	45.01
1100	62.22	.4501	2128	.531	.664	1.08	8.16	5.25	47.47
1200	59.51	.4706	2488	.510	.632	1.08	8.16	5.30	49.96

TABLE II.—(*Continued*)

1 p	2 v	3 ρ	4 f	5 $\frac{p}{v}\left(\frac{dv}{dp}\right)_T$	6 $\frac{T}{v}\left(\frac{dv}{dT}\right)_p$	7 ΔC_p	8 C_p	9 C_v	10 Δ
atm.	cc/mole	g/cc	atm.			calories/mole degree			cc/mole
			$t=300°$	$C_p^*=7.218$,	$C_v^*=5.232$	cal./mole deg.			
25	1905	.01470	25.31	.988	1.006	.07	7.29	5.23	23.86
50	964.3	.02905	51.27	.975	1.009	.14	7.36	5.23	24.35
75	651.0	.04302	77.88	.962	1.010	.20	7.42	5.24	24.89
100	494.5	.05664	105.2	.950	1.010	.26	7.48	5.24	25.45
150	338.0	.08285	161.9	.924	1.010	.36	7.58	5.21	26.46
200	257.8	.1086	221.6	.900	1.000	.45	7.66	5.22	27.56
300	182.2	.1537	350.8	.850	.976	.58	7.80	5.21	29.60
400	143.6	.1951	494.1	.803	.946	.68	7.90	5.20	31.77
500	120.6	.2322	653.2	.763	.904	.76	7.98	5.25	34.03
600	105.3	.2659	829.7	.722	.864	.82	8.04	5.28	36.20
800	86.42	.3241	1243	.655	.792	.92	8.14	5.34	40.64
1000	75.02	.3733	1749	.606	.721	.99	8.21	5.49	44.67
1100	70.87	.3952	2042	.586	.698	1.01	8.23	5.49	46.62
1200	67.40	.4155	2372	.567	.670	1.03	8.25	5.54	48.53
			$t=400°$	$C_p^*=7.386$,	$C_v^*=5.400$	cal./mole deg.			
25	2238	.01252	25.32	.987	1.000	.05	7.44	5.40	28.90
50	1133	.02472	51.31	.975	.999	.10	7.49	5.40	29.26
75	765.0	.03661	77.96	.962	.997	.15	7.54	5.41	29.68
100	581.0	.04821	105.3	.950	.996	.19	7.58	5.40	30.16
150	396.9	.07057	162.1	.927	.987	.26	7.65	5.40	30.92
200	304.9	.09186	221.8	.905	.978	.33	7.71	5.40	31.70
300	212.9	.1316	350.6	.864	.954	.44	7.82	5.40	33.27
400	166.9	.1678	492.4	.823	.931	.53	7.92	5.39	34.86
500	139.4	.2009	648.6	.790	.897	.62	8.00	5.45	36.52
600	121.0	.2314	820.3	.758	.861	.69	8.08	5.52	38.11
800	98.18	.2852	1215	.696	.793	.83	8.21	5.66	41.45
1000	84.41	.3318	1688	.649	.733	.93	8.32	5.81	44.61
1100	79.42	.3527	1958	.626	.716	.97	8.35	5.78	46.20
1200	75.25	.3722	2252	.605	.696	1.00	8.38	5.78	47.79

$\Delta \equiv v(pv/RT-1)$ in cc/mole extrapolated to zero pressure

t°C	Δ	t°C	Δ
−70	−39.65	100	4.84
−50	−30.89	150	11.09
−25	−21.96	200	16.09
0	−14.63	300	23.37
25	−8.51	400	28.50
50	−3.38		

larger scale chart for that purpose. It is planned to publish large size plots of Δ vs. ρ isotherms and isobars for the gases nitrogen, carbon monoxide, hydrogen, 3:1 hydrogen nitrogen mixture, methane, and helium, as a U. S. Department of Agriculture publication.

Fugacity f, column 4.

Fugacities are computed from the equation

$$f = p \exp(-1/RT) \int_0^p \alpha dp. \tag{28}$$

The integral was evaluated by mechanical integration of the α vs. p isotherms of Fig. 11.

Expansion coefficients $-(p/v)(dv/dp)_T$ and $(T/v)(dv/dT)_p$, columns 5 and 6.

The Δ vs. p, α vs. p, and Δ vs. ρ isotherms and the Δ vs. T^{-1}, α vs. T^{-1}, and Δ vs. ρ isobars are now used to get derivatives. The slopes of these curves can be determined at any point by the graphical method described in the paper

on nitrogen.[5] This method consists of estimating the slope of an α or Δ curve by mechanical means, and then using this slope as a correction term to find the corresponding derivative of v, by Eqs. (3) *et seq.* The three determinations of $-(p/v)\ (dv/dp)_T$ obtained through Eqs. (6), (7), (8) at each point were plotted in isotherms against pressure and in isobars against temperature, and

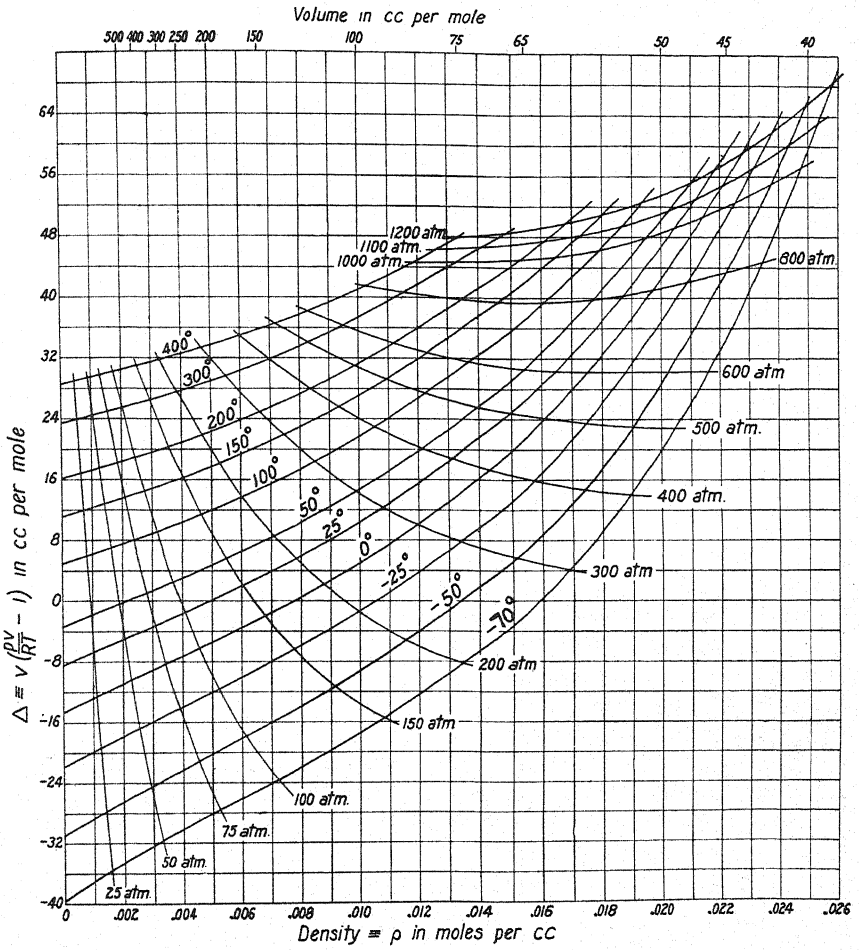


Fig. 12. Δ vs. ρ isotherms and isobars for carbon monoxide. By means of this graph one can readily interpolate the $p-v-T$ data. Thus, for $\rho=0.010$ moles per cc and $t=0°$C, the pressure can be roughly estimated as 240 atm. By reading off $\Delta=5.0$ cc per mole at this point and using $v=1/\rho=100$ cc per mole, $T=273.18°$, $R=82.049$ cc atm./mole deg., the equation $\Delta=v(pv/RT-1)$ gives $p=235.3$ atm.

were adjusted by placing smooth curves that have the same ordinate on both plots at any pressure and temperature, just as the Δ and α curves were smoothed. The ordinates read from either plot are given in column 5.

Likewise there are three determinations of $(T/v)(dv/dT)_p$ at each point, through Eqs. (15), (16), (17). They were adjusted by plotting $pv(dv/dT)_p$ vs.

T isobars at 25, 50, 75, 100 atm.; these isobars turn out to be straight lines. At higher pressures the adjustment was made by drawing smooth curves to $pv(dv/dT)_p$ vs. T and $(dv/dT)_p$ vs. T^{-1} isobars and $(T/v)\ (dv/dT)_p$ vs. p isotherms, and taking the average of $(T/v)\ (dv/dT)_p$ obtained from the three ordinates at a given temperature and pressure.

It should be noted that, at every point, the determinations of an expansion coefficient obtained through the different equations agreed very closely and consequently little smoothing was necessary. Agreement to three figures in all three determinations was not unusual.

ΔC_p, and the heat capacity C_p, columns 7 and 8 and Fig. 14.

ΔC_p is the change in C_p caused by a change in pressure at constant temperature. It is obtained through the thermodynamic equation

$$(dC_p/dp)_T = -T(d^2v/dT^2)_p, \tag{11}$$

which when integrated between 0 and p along an isotherm gives

$$C_p = C_p^* + \Delta C_p = C_p^* + \int_0^p -T(d^2v/dT^2)_p dp. \tag{12}$$

C_p^* is the heat capacity at zero pressure, and it is necessary to assume some value for it at each temperature in order to complete the calculations.

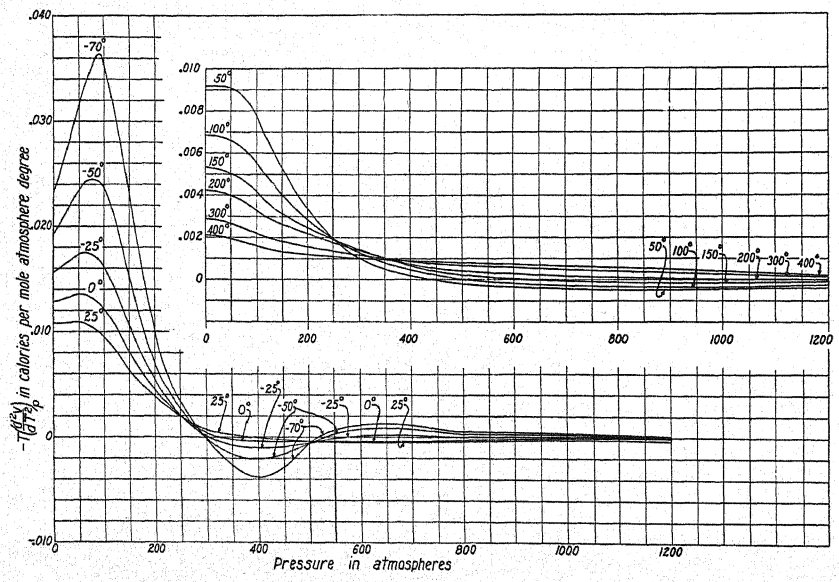


Fig. 13. $-T(d^2v/dT^2)_p = (dC_p/dp)_T$ vs. p isotherms. The area under a curve between any two pressures is the change in heat capacity (at constant pressure) in cal./mole degree between these two pressures, at that temperature.

There are some experimental determinations of C_p at 1 atm., but they are scattered. When corrected to zero pressure by an equation of state they all agree pretty well with the quantum equation

$$C_p^* = 7R/2 + R(3090/T)^2 e^{3090/T}/(e^{3090/T} - 1)^2, \quad (29)$$

which we have accordingly used for C_p^*. $C_v^* = C_p^* - R$. We have assumed that the rotational states remain fully excited down to $-70°$. We wish to thank Dr. W. M. D. Bryant of the Du Pont Ammonia Corporation for advice concerning the choice of a formula for C_p^*.

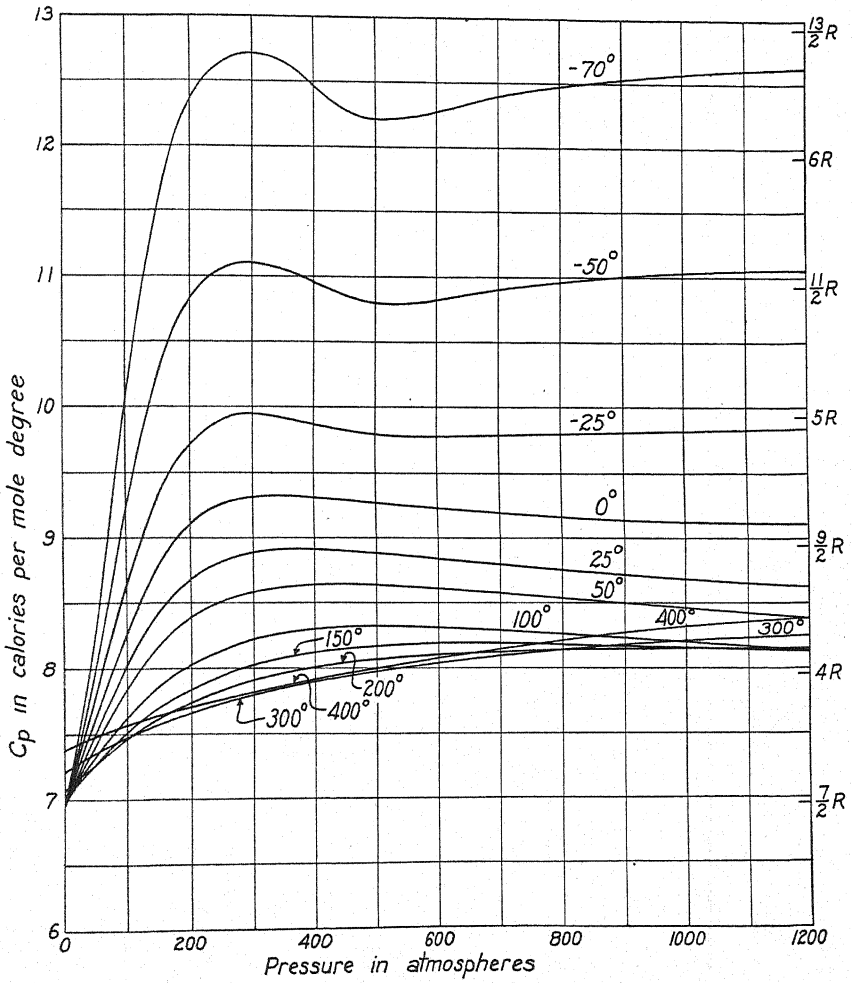


Fig. 14. Carbon monoxide. C_p vs. p isotherms.

The integral in Eq. (12) was evaluated by a mechanical integration under the $-T(d^2v/dT^2)_p$ vs. p isotherms, which are shown in Fig. 13. For these curves at 25, 50, 75, 100 atm., the ordinate was obtained at any point through Eq. (18) from the slope and ordinate of the corresponding $pv(dv/dT)_p$ vs. T isobar, which for the four low pressures was always a straight line, as was previously noted. There is little doubt that the values of $-T(d^2v/dT^2)_p$ therefrom obtained are very accurate, since the slopes and ordinates of straight

lines can be definitely determined. This means that C_p must be quite accurately calculated through these pressures.

Beyond 100 atm. the determination of the second derivative by means of the $pv(dv/dT)_p$ vs. T isobars was supplemented at each point by taking the slopes of the $(dv/dT)_p$ vs. T^{-1} isobars. The two determinations agreed well enough to lead one to expect ΔC_p to be correct to within a few hundredths cal./mole deg. throughout the whole range.

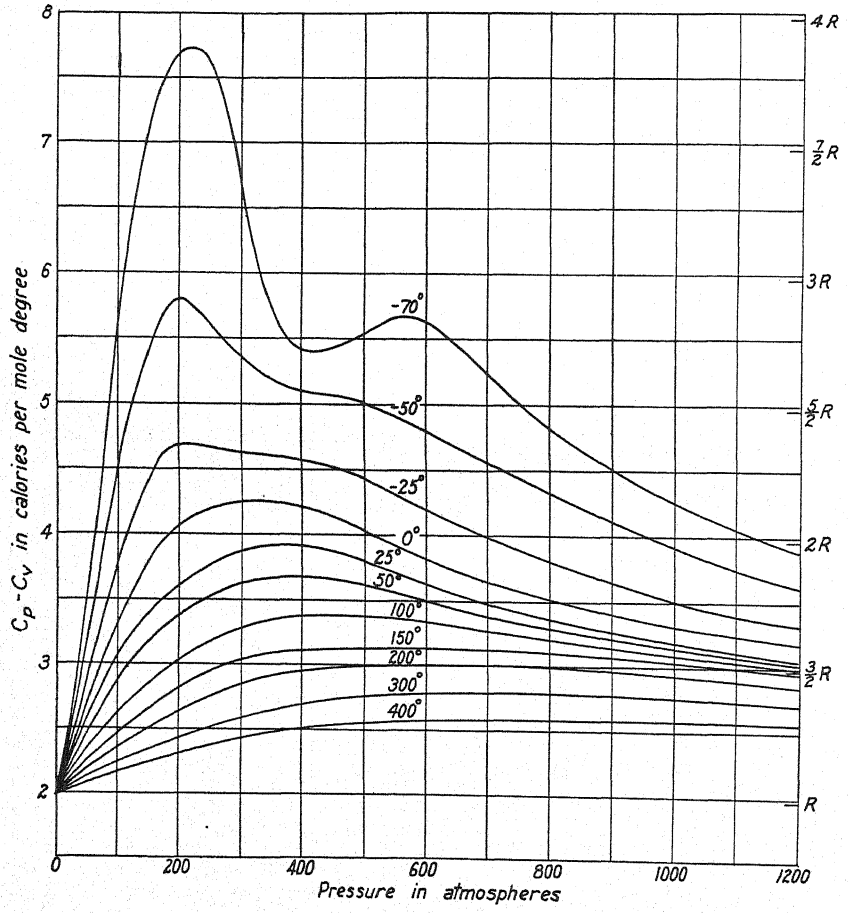


Fig. 15. Carbon monoxide. $C_p - C_v$ vs. p isotherms.

Eq. (24) was used for the zero pressure intercept in Fig. 13. Some time ago the question was raised by the writers[16] whether $-T(d^2v/dT^2)_p$ or $(dC_p/dp)_T \to 0$ as $p \to 0$, as would happen if the behavior of the heat capacity of the actual gas approaches that of a perfect gas. As the gas expands, $pv \to RT$ and $C_p - Cv \to R$, but Eq. (22) shows that $-T(d^2v/dT^2)_p \to 2a/RT^2 \neq 0$, as $p \to 0$.

[16] W. Edwards Deming and Lola E. Shupe, Phys. Rev. 37, 220 (1931).

Since $(dC_v/dp)_T \neq 0$ at very low pressures, the limiting heat capacity C_p^* is not reached except at zero pressure. As the gas expands, there is no

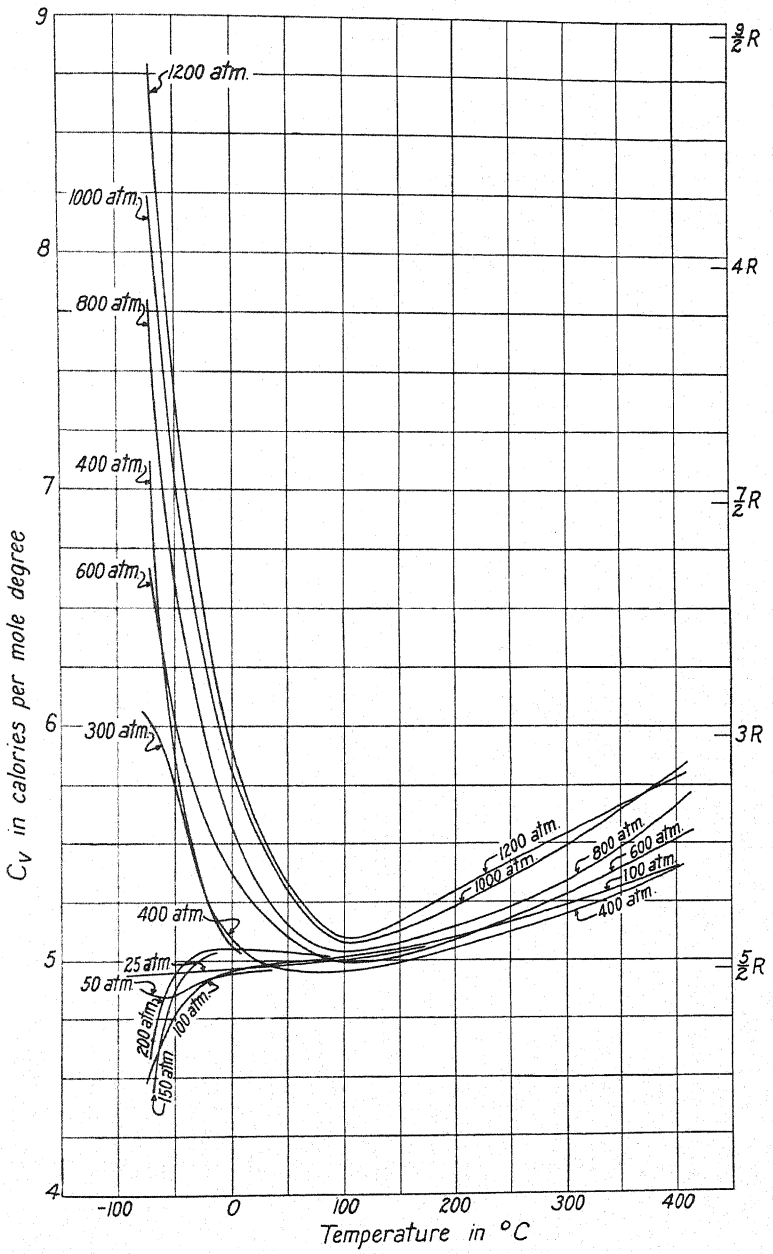


Fig. 16. Carbon monoxide. C_v vs. t isobars.

point reached beyond which further expansion is accompanied by changes in C_p that are infinitesimal compared with the changes in p.

The curves in Fig. 13 show that at low temperatures $(dC_p/dp)_T$ varies considerably with pressure, the lower the temperature the greater the variation. At 25° and above, this derivative is nearly constant through 50 atm.

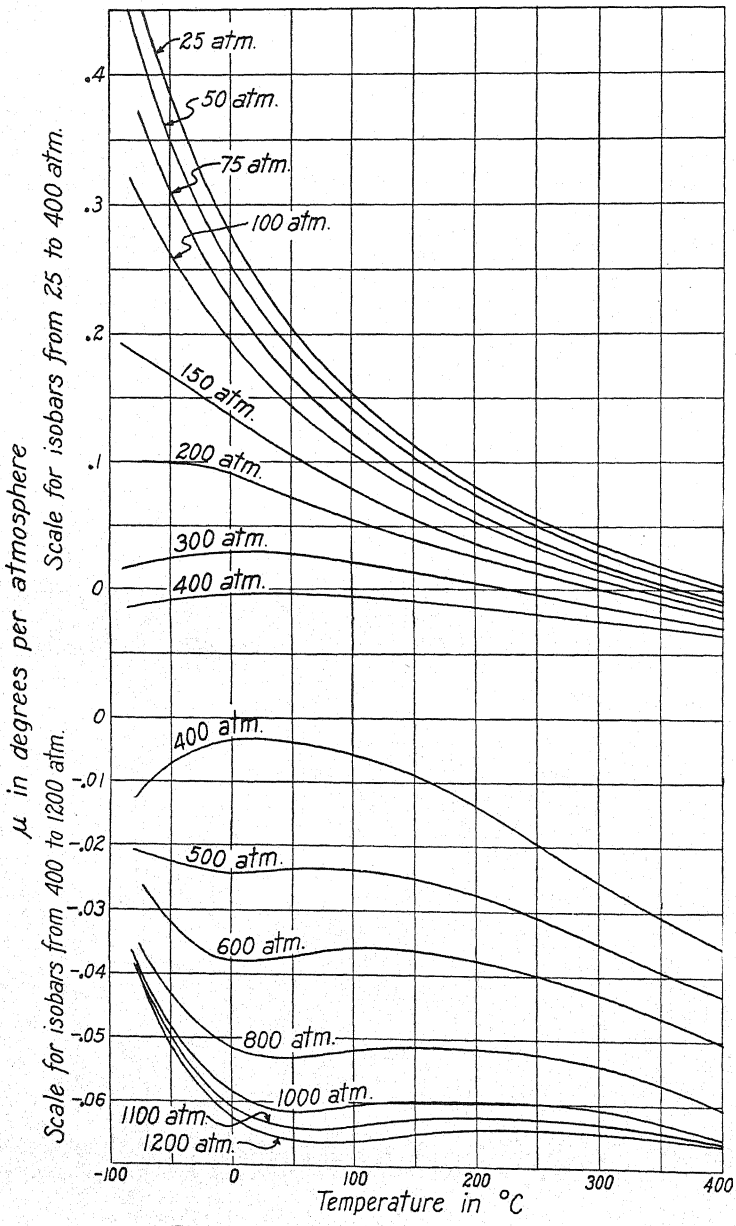


Fig. 17. Carbon monoxide. μ vs. t isobars.

and then decreases with further increase in pressure. Beyond 500 atm. this derivative is small at all temperatures, so very little change in C_p is produced at any of our temperatures by compression beyond 500 atm.

There are no experimental data available on carbon monoxide, but there are the authors'[5] calculations on nitrogen to compare with. Fig. 3 for nitrogen and Fig. 14 for carbon monoxide show that the C_p curves are very similar. At $-50°$ and $-70°$, C_p for carbon monoxide is slightly higher than it is for nitrogen, but at $-25°$ and above, the reverse is true. The difference is nowhere greater than some tenths cal./mole deg.

The quantity $C_p - C_v$, Fig. 15; the heat capacity C_v, column 9 and Fig. 16.

$$C_p - C_v = -T(dv/dT)_p^2/(dv/dp)_T \qquad (13)$$

The derivatives in this equation are simply related to the expansion coefficients in columns 5 and 6, so $C_p - C_v$ can be calculated for each pressure and

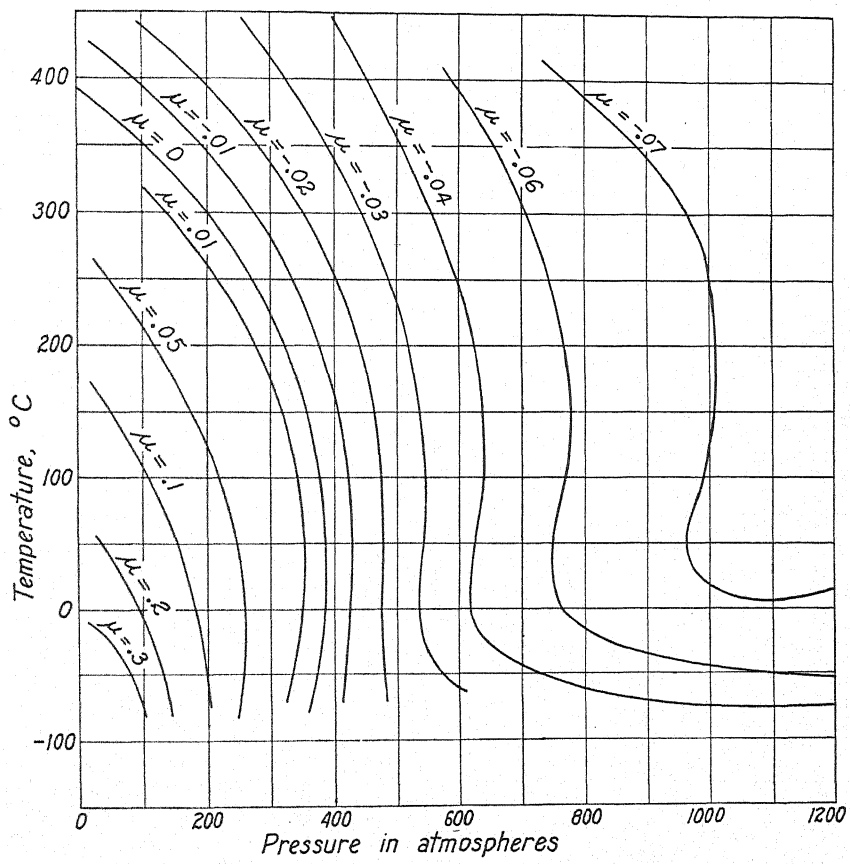


Fig. 18. Carbon monoxide. t vs. p μ = constant curves. μ is given in °C per atm. $\mu > 0$ means that the gas is heated by an adiabatic compression.

temperature. The results are shown in Fig. 15. According to Eq. (22), $C_p - C_v \to R$ as $p \to 0$, at all temperatures.

C_v is calculated by subtracting $C_p - C_v$ from C_p. Some of the C_v vs. t isobars are shown in Fig. 16. More of them could not be drawn without causing

confusion. Above 50°, isobars for $p=0, 25, \ldots, 400$ almost coincide. At higher pressures C_v is higher. Below 50°, C_v at 25 atm. falls a few hundredths cal./mole deg. under C_v*. Below 50°, C_v at 50, 75, 100, 150, 200 atm. deviates considerably from C_v*. The isobars for 100, 150, 200 atm. take peculiar quick descents as the temperature drops below −25°; this is most pronounced for 150 atm. The isobars for 300, 400, . . . , 1200 atm. have a minimum at about 100°. On the low temperature side of this minimum the curves are very steep. The graph for nitrogen in Fig. 5 shows the same characteristics.

Joule-Thomson coefficient μ, Figs. 17 and 18.

The Joule-Thomson coefficient can be calculated from the equation

$$\mu\rho C_p = (T/v)(dv/dT)_p - 1. \tag{14}$$

The values of μ can be read from the curves of Figs. 17 or 18. The latter is a family of μ curves obtained from the μ vs. t isobars (Fig. 17) and μ vs. p isotherms (not shown). The $\mu=0$ curve in Fig. 18 is the inversion curve.

The ultimate accuracy of calculations made by the present method is the accuracy of the p-v-T relations. Data from the various laboratories that have undertaken compressibility work agree very closely, and thus give assurance that calculations made from them should be reliable provided the derivatives can be accurately evaluated. Compressibility data over a wide range of temperature and pressure for a number of gases are now available, and the present method is a quick and accurate means for the determination of a number of physical properties. Calculations for other gases are in progress.

RECIPROCAL RELATIONS IN IRREVERSIBLE PROCESSES. II.

By Lars Onsager
Department of Chemistry, Brown University

(Received November 9, 1931)

Abstract

A general reciprocal relation, applicable to transport processes such as the conduction of heat and electricity, and diffusion, is derived from the assumption of microscopic reversibility. In the derivation, certain average products of fluctuations are considered. As a consequence of the general relation $S=k \log W$ between entropy and probability, different (coupled) irreversible processes must be compared in terms of entropy changes. If the displacement from thermodynamic equilibrium is described by a set of variables $\alpha_1, \cdots, \alpha_n$, and the relations between the rates $\dot{\alpha}_1, \cdots, \dot{\alpha}_n$ and the "forces" $\partial S/d\alpha_1, \cdots, \partial S/d\alpha_n$ are linear, there exists a quadratic dissipation-function,

$$2\Phi(\dot{\alpha}, \dot{\alpha}) \equiv \Sigma \rho_{ij} \dot{\alpha}_i \dot{\alpha}_j = dS/dt = \dot{S}(\alpha, \dot{\alpha}) \equiv \Sigma (\partial S/d\alpha_j)\dot{\alpha}_j$$

(denoting definition by $\equiv$). The symmetry conditions demanded by microscopic reversibility are equivalent to the variation-principle

$$\dot{S}(\alpha, \dot{\alpha}) - \Phi(\dot{\alpha}, \dot{\alpha}) = \text{maximum},$$

which determines $\dot{\alpha}_1, \cdots, \dot{\alpha}_n$ for prescribed $\alpha_1, \cdots, \alpha_n$. The dissipation-function has a statistical significance similar to that of the entropy. External magnetic fields, and also Coriolis forces, destroy the symmetry in past and future; reciprocal relations involving reversal of the field are formulated.

I. Introduction

In A previous communication[1] a reciprocal theorem for heat conduction in an anisotropic medium was derived from the principle of microscopic reversibility, applied to fluctuations. In the following we shall derive reciprocal relations for irreversible processes in general, particularly transport processes: conduction of electricity and heat, and diffusion.

As before we shall assume that the average regression of fluctuations will obey the same laws as the corresponding macroscopic irreversible processes. In (I) we considered fluctuations in "aged" systems, i.e., systems which have been left isolated for a length of time that is normally sufficient to secure thermodynamic equilibrium. For dealing with the conduction of heat we naturally considered the fluctuations of the distribution of heat, and we studied the behavior of the quantities $\alpha_1, \alpha_2, \alpha_3 =$ the total displacements of heat in the directions x_1, x_2 and x_3, respectively.

We brought the laws of irreversible processes into the theory of fluctuations by studying averages

$$\overline{\alpha_1(t)\alpha_2(t+\tau)} = \lim_{t'' \to \infty} \frac{1}{t''-t'} \int_{t=t'}^{t=t''} \alpha_1(t)\alpha_2(t+\tau)dt \qquad (1.1)$$

[1] L. Onsager, Phys. Rev. **37**, 405 (1931). Cited in the following as (I).

of the values of two fluctuating quantities α_1 and α_2 (in this particular case displacements of heat in two perpendicular directions) observed with a prescribed time interval τ. The condition of microscopic reversibility we applied in the form:

$$\overline{\alpha_1(t)\alpha_2(t+\tau)} = \overline{\alpha_2(t)\alpha_1(t+\tau)}\,. \tag{1.2}$$

The calculation of averages of the type (1.1) involves several steps. First of all, something must be known about the distribution of values of the fluctuating quantities α_1, $\alpha_2 \cdots$; we shall employ standard methods for calculating the average products:

$$\overline{\alpha_1^2},\ \overline{\alpha_1\alpha_2},\ \cdots \tag{1.3}$$

with but a slight variation. In addition, we must know the average changes (of quantities α_2, $\alpha_3 \cdots$) which accompany a given deviation α_1' of a quantity α_1 from its normal value $\bar{\alpha}_1(=0)$. On this basis a certain *initial state* of an irreversible process is associated with the displacement $\alpha_1=\alpha_1'$; the average regression towards the normal state will obey the ordinary macroscopic laws governing such processes.

The average regression is described by the functions:

$$\overline{\alpha_i}(\tau,\ \alpha_j')$$

defined as the average of the quantity α_i, taken over all cases, (picked at random for an aged system), in which, τ seconds earlier, the quantity α_j *had* the value α_j'. Whenever these functions are linear in α_j', which will be the common case when reasonable variables α are chosen, the knowledge of the averages (1.3) suffices for evaluating (1.1).

In (I), §4, we derived reciprocal relations for heat conduction in an anisotropic body, showing that the conducting properties of the most general (triclinic) crystal can be represented by a *symmetrical tensor* (ellipsoid). In that particular case it was not necessary to calculate the averages (1.3), nor to determine completely the state associated with a displacement $\alpha_1=\alpha_1'$, because the necessary information could be derived from considerations of symmetry. Even so, these considerations were based on the proposition that, in regard to the probability for a given distribution of energy, the different volume elements of a *homogeneous* crystal would be equivalent, so that the anisotropy of the crystal could be neglected in this particular connection. This proposition involves the fundamental principles of statistical mechanics although it obviates a part of the general mathematical apparatus.

We shall review the derivation briefly. If J_1, J_2, J_3 denote the components of the heat flow along the coordinate axes x_1, x_2, x_3, respectively, and T the absolute temperature, the phenomenological laws of heat conduction in a triclinic crystal take the general form

$$\begin{aligned} J_1 &= L_{11}X_1 + L_{12}X_2 + L_{13}X_3 \\ J_2 &= L_{21}X_1 + L_{22}X_2 + L_{23}X_3 \\ J_3 &= L_{31}X_1 + L_{32}X_2 + L_{33}X_3 \end{aligned} \tag{1.4}$$

where X_1, X_2, X_3 are the components of the "force" on the heat flow

$$X_1 = -(1/T)\partial T/dx_1; \quad X_2 = -(1/T)\partial T/dx_2; \quad X_3 = -(1/T)\partial T/dx_3 \tag{1.5}$$

(Carnot). In order to derive the reciprocal relations

$$L_{12} = L_{21}; \; L_{23} = L_{32}; \; L_{31} = L_{13}$$

we considered the fluctuations of the moments

$$\begin{aligned} \alpha_1 &= \int \epsilon x_1 dV \\ \alpha_2 &= \int \epsilon x_2 dV \end{aligned} \tag{1.6}$$

of the distribution of energy, $\epsilon = \epsilon(x_1, x_2, x_3)$. When we chose the external boundary of the crystal spherical, center at the origin, all questions pertaining to the *instantaneous* distribution of energy have spherical symmetry (cf. above). Thus

$$\overline{\alpha_1} = \overline{\alpha_2} = 0; \; \overline{\alpha_1^2} = \overline{\alpha_2^2}; \; \overline{\alpha_1\alpha_2} = 0, \tag{1.7}$$

and with a displacement of energy there is associated a temperature gradient in the same direction:

$$\begin{aligned} \overline{\partial T/dx_1}^{\alpha_1', \alpha_2'} &= -T\overline{X}_1(\alpha_1', \alpha_2') = C T \alpha_1' \\ &\quad -T\overline{X}_2(\alpha_1', \alpha_2') = C T \alpha_2' \end{aligned} \tag{1.8}$$

where C is for our immediate purposes a mere constant. (Certain rather trivial considerations are needed to justify our assumption of a *linear* relation between displacement (α_1', α_2') and gradient $(T\overline{X}_1, T\overline{X}_2)$. When we take that much for granted, the more special form (1.8) follows from the spherical symmetry.)

The gradient (1.8) determines the heat flow J according to (1.4), and the rate of change $\dot{\alpha}$ of the displacement α is the same as the total flow

$$\begin{aligned} \dot{\alpha}_1(\alpha_1', \alpha_2', \alpha_3') &= d\alpha_1/dt = \int J_1 dV = -CV(L_{11}\alpha_1' + L_{12}\alpha_2' + L_{13}\alpha_3') \\ \dot{\alpha}_2(\alpha_1', \alpha_2', \alpha_3') &= -CV(L_{21}\alpha_1' + L_{22}\alpha_2' + L_{23}\alpha_3'). \end{aligned} \tag{1.9}$$

Then in a short interval of time Δt

$$\overline{\alpha_2}(\Delta t, \alpha_1') = \overline{\alpha_2}(0, \alpha_1') + \dot{\alpha}_2(\alpha_1')\Delta t = 0 - L_{21}CV\alpha_1'\Delta t,$$

where $\bar{\alpha}_2(0, \alpha_1')$ vanishes by symmetry. From this, obviously

$$\overline{\alpha_1(t)\alpha_2(t + \Delta t)} = \overline{\alpha_1'\alpha_2(\Delta t, \alpha_1')} = -L_{21}CV\overline{\alpha_1'^2}\Delta t$$

and, by analogy

$$\overline{\alpha_2(t)\alpha_1(t + \Delta t)} = -L_{12}CV\overline{\alpha_2'^2}\Delta t.$$

Since, by (1.7): $\overline{\alpha_1^2}=\overline{\alpha_2^2}$, the requirement:

$$\overline{\alpha_1(t)\alpha_2(t+\Delta t)} = \overline{\alpha_2(t)\alpha_1(t+\Delta t)}$$

for microscopic reversibility imposes the condition:

$$L_{12} = L_{21}.$$

The more general case of simultaneous transport of heat, electricity and matter (diffusion) in isotropic or anisotropic media leads us to consider the fluctuations of a set of variables $\alpha_1, \alpha_2 \cdots$, measuring displacements of heat, electricity and matter, eventually in different directions. We shall have to actually evaluate the averages (1.3); symmetry considerations can yield the necessary information only in a few cases, as above. The calculation of (1.3) involves directly Boltzmann's fundamental relation between entropy S and probability W:

$$S=k \log W+\text{constant}$$

The exceedingly general character of this relation is the reason that the *rates* of irreversible processes, not solely the ultimate equilibrium, are subject to reciprocal laws, in which *different processes have to be compared in terms of the entropy changes involved.*

Sometimes, of course, it may be more convenient to employ other thermodynamic potentials, particularly the free energy, the main reason being that conditions of *mechanical* equilibrium (pressure, elastic) frequently enter into the laws of irreversible processes, and that the description in terms of energy involves more familiar derived functions (thermodynamic potential, electromotive force, electrical resistance). Above, we purposely considered the "force" on heat, although the concept was not necessary for dealing with the problem in hand, just to demonstrate how the concept of "force" could be extended beyond the familiar.

Fundamentally, however, the *entropy* is the simplest among the thermodynamic potentials, and it is the only one that will serve our purposes in all cases. In our example, where displacements $\alpha_1, \alpha_2, \alpha_3$ of heat are considered, the state of the system being determined by these displacements, so that

$$S = \sigma(\alpha_1, \alpha_2, \alpha_3),$$

the temperature gradients are essentially the same as $\partial S/d\alpha_1$ etc., or rather

$$\partial\sigma/d\alpha_r = \partial(1/T)/dx_r.$$

In order to see this, we recall the fundamental thermodynamic relation

$$\delta S=(1/T)(\delta E-\delta A)-(\mu/T)\delta m,$$

where E = energy; A = work; m = amount of substance; μ = Gibbs' thermodynamic potential. The amount of heat added to a volume element is $\delta Q=\delta E-\delta A$. Now if there is a uniform gradient of temperature (or $1/T$ in the r-direction, then an amount of heat δQ transported a distance Δx_r changes the entropy by the amount

$$\delta S=\delta Q\cdot\Delta(1/T)=\delta Q\cdot\Delta x_r\cdot\partial(1/T)/dx_r=\delta\alpha_r\cdot\partial(1/T)/dx_r,$$

whereby $\delta\alpha_r$ measures a displacement of heat (in units cm $\times$ cal.).

Similarly, where a displacement α of matter (in the x direction) is considered,

$$\partial\sigma/d\alpha = -\partial(\mu/T)/dx,$$

and if α is a displacement of electricity, then

$$\partial\sigma/d\alpha = X/T,$$

where X is the intensity of the electric field.

According to the empirical laws of transport processes the flow J of matter, heat or electricity is proportional to the gradient of the corresponding specific potential, that is

$$J \sim -\operatorname{grad} T$$

for heat conduction and

$$J \sim X;\ J \sim -\operatorname{grad} \mu,$$

respectively, for electrical conduction (Ohm's law) and isothermal diffusion (alternative form of Fick's law). In the following we shall write these empirical relations in the general form

$$d\alpha_r/dt = \dot{\alpha}_r \sim \partial S/d\alpha_r,$$

where the rate of displacement $\dot{\alpha}$ is essentially the same as the flow J, (by definition), except for a volume factor. Whenever different transport processes interfere with each other the simple proportionality is replaced by a system of linear relations

$$\dot{\alpha}_r = G_{r1}\partial\sigma/d\alpha_1 + \cdots + G_{rn}\partial\sigma/d\alpha_n, \quad (r = 1, \cdots, n), \tag{1.11}$$

where again $S=\sigma(\alpha_1, \cdots \alpha_n)$. In taking for granted the linear form (1.11) we are still making use of empirical laws, mostly familiar, which are understood and expected from simple and equally familiar kinetic considerations of very wide scope. Examples have been enumerated in (I), §§ 1–2, and need not be repeated here.

Our object is to show that the condition (1.2) for microscopic reversibility leads to the general reciprocal relation

$$G_{rs} = G_{sr}. \tag{1.12}$$

2. General Theory of Fluctuations

It was shown by L. Boltzmann that a mechanical theory of molecules requires a statistical interpretation of the second law of thermodynamics. Thermodynamic equilibrium is explained as a statistical equilibrium of elementary processes, and Boltzmann gave a direct relation between the entropy S and the "thermodynamic probability" W of a thermodynamic state:

$$S = k \log W + \text{const.}, \tag{2.1}$$

where k is the gas constant per molecule (1.371×10^{-16} erg/degree). The apparent rest associated with thermodynamic equilibrium is explained by the

smallness of the factor k. According to (2.1), under circumstances which normally lead to such equilibrium, the probability

$$e^{\Delta S/k}$$

for a deviation involving an entropy change ΔS (necessarily negative), is appreciable only when ΔS is (at the outmost) of the order of magnitude of k. The *fluctuations* permitted by this restriction can be observed only in very favorable cases, for example the opalescence of liquids near the critical point[2] and Brownian motion of small particles in liquids,[3] or of a mirror in delicate elastic suspension.[4]

The premises and the consequences of Boltzmann's principle (2.1) have been discussed by A. Einstein[5] to an extent which will be practically sufficient for our purposes. It is essential that a thermodynamic equilibrium state, specified in terms of energy and external parameters (volume etc.), is incompletely specified from a molecular point of view; the quantity W measures the number (or extent) of different possibilities for realizing a given thermodynamic state. In order to calculate W one needs a complete (molecular) theory of the system in hand: If one assumes that molecules obey the laws of classical mechanics, then W equals an extension in phase-space, while on the basis of quantum theory W equals the number of stationary states corresponding to the prescribed energy. However, as Einstein has pointed out, the calculation of fluctuations according to (2.1) is *independent of all special assumptions regarding the laws which may govern elementary processes* (we must of course assume that these laws do permit statistical equilibrium of some kind).

We shall have to make certain *general assumptions* about *aged systems*, i.e., systems which have been left isolated for a length of time that is normally sufficient to secure thermodynamic equilibrium. We expect that such a system will in the course of time pass through *all* the (thermodynamic) states $\Gamma^1, \Gamma^2, \cdots \Gamma^l$ that are compatible with the conditions of isolation, whereby the energy, the values of external parameters (volume, etc.) and the numbers of indestructible elementary particles (atoms, molecules) are prescribed.[6] In the course of a long time t the system will spend a total t_r of time intervals in the state Γ^r; we expect that $t_1, t_2 \cdots t_l$ will be proportional to the regions W_1, $W_2 \cdots W_l$. This statement contains an assumption even if $W_1, W_2 \cdots$ are considered as unknown, namely that $t_1/t, t_2/t \cdots$ will be fully determined by the nature of the system, (and the conditions of isolation), independently of the initial state. Granted this assumption, we may define $W_1, W_2 \cdots$ as pro-

[2] M. v. Smoluchowski, Ann. d. Physik [4], **25,** 205 (1909). Theory accompanied by a general discussion of fluctuations is given by A. Einstein, Ann. d. Physik [4], **33,** 1275 (1910).

[3] A. Einstein, Ann. d. Physik [4], **17,** 549 (1905). M. v. Smoluchowski, Ann. d. Physik [4], **21,** 756 (1906).

[4] P. Zeeman and O. Houdyk, Proc. Acad. Amsterdam **28,** 52 (1925). W. Gerlach, Naturwiss. **15,** 15 (1927). G. E. Uhlenbeck and S. Goudsmit, Phys. Rev. **34,** 145 (1929).

[5] Einstein, reference 2.

[6] In a discussion of the fundamental questions involved, W. Schottky introduces the term "resistent groups." Ann. d. Physik [4], **68,** 481 (1922).

portional t_1/t, $t_2/t \cdots$, without reference to any detailed theory of the system. (On the basis of the underlying picture, every W is still a large integer, equal to the number of "microscopic" states contained in a given thermodynamic state. Here, however, we are only interested in the ratios of $W_1, W_2, \cdots$). The various assumptions involved in this application of Boltzmann's principle may be summarized in the formula:

$$S_r = k \log (t_r/t) + \text{const.} \tag{2.2}$$

where S_r is the entropy of the state Γ^r; we shall refer to t_r/t as the *probability* for this state.

A thermodynamic state $\Gamma^r = \Gamma(\alpha_1{}^r, \cdots \alpha_n{}^r)$ may be defined in terms of given values $\alpha_1{}^r, \cdots \alpha_n{}^r$ for such variables $\alpha_1, \cdots \alpha_n$ as can be measured by ordinary means. From a statistical point of view we must allow latitudes $\Delta\alpha_1, \cdots \Delta\alpha_n$ in this specification (the probability for a region of no extension equals zero). We have to introduce a distribution-function

$$f(\alpha_1, \cdots, \alpha_n)$$

and the probability for the state Γ^r becomes equal to the integral of $f(\alpha_1, \cdots \alpha_n)$ over the region

$$\alpha_1{}^{(r)} < \alpha_1 < \alpha_1{}^{(r)} + \Delta\alpha_1$$
$$\cdots\cdots\cdots\cdots$$
$$\alpha_n{}^{(r)} < \alpha_n < \alpha_n{}^{(r)} + \Delta\alpha_n.$$

Then (2.2) takes the form

$$S_r = k \log f(\alpha_1{}^{(r)}, \cdots \alpha_n{}^{(r)}) + k \log (\Delta\alpha_1 \cdots \Delta\alpha_n) + \text{const.} \tag{2.3}$$

Our only direction for the appropriate choice of latitudes $\Delta\alpha$ is that they ought to be taken of the same order of magnitude as the common fluctuations of the quantities α in the state Γ^r. This convention takes care of all important cases; because thermodynamic measurements of entropy are possible only for equilibrium states.[7] A more accurate specification of $\Delta\alpha_1, \cdots \Delta\alpha_n$ is unnecessary because, say, doubling each $\Delta\alpha$ will change the right side of (2.3) only by the amount $nk \log 2$, where $k = 1.371 \times 10^{-16}$ erg/degree, and an entropy difference of this magnitude is far too small to affect any measurement. Actually, where reasonable variables $\alpha_1, \cdots \alpha_n$ are chosen, the order of magnitude of the product $\Delta\alpha_1, \Delta\alpha_2 \cdots \Delta\alpha_n$ varies so little that the contribution $k \log (\Delta\alpha_1' \cdots \Delta\alpha_n'/\Delta\alpha_1'' \cdots \Delta\alpha_n'')$ to the entropy difference between two thermodynamic states is entirely negligible in comparison with $k \log(f(\alpha_1', \cdots \alpha_n')/f(\alpha_1'', \cdots \alpha_n''))$; it is the factor $f(\alpha_1, \cdots \alpha_n)$ that causes the tremendous difference in the probabilities of different thermodynamic states, and is responsible for measurable entropy differences. Thus, as long as we restrict ourselves to cases where S_r is a measured entropy, we may neglect the variability of the term $k \log (\Delta\alpha_1 \cdots \Delta\alpha_n)$ on the right side of (2.3) and write

[7] We allow ourselves, following the custom of thermodynamics, to consider states that may be approximated in some way by equilibrium states. Cf. Schottky, reference 6.

$$S_r = k \log f(\alpha_1^{(r)}, \cdots \alpha_n^{(r)}) + \text{const.} \tag{2.4}$$

So far we have assumed that the variables $\alpha_1, \cdots \alpha_n$ define the state of the system in hand *completely* from the thermodynamic (phenomenological) point of view. As pointed out by Einstein[8] the relation (2.4) remains valid in cases where this definition is incomplete. We merely have to adopt the convention that among all the states which fulfill the given specifications, we select the one with the greatest entropy. This theorem again depends on the probabilities for different states being of different order of magnitude, so that the given set of values of $\alpha_1, \cdots \alpha_n$ will be realized by the chosen state much more frequently than by all other states taken together. We shall summarize these results for subsequent applications. The greatest entropy allowed by a given set $\alpha_1', \cdots \alpha_n'$ of values of the variables $\alpha_1, \cdots \alpha_n$ we denote by

$$\sigma_{1\ldots n}(\alpha_1', \cdots \alpha_n').$$

The corresponding (thermodynamic) state we denote by

$$\Gamma'_{1\ldots n} = \Gamma_{1\ldots n}(\alpha_1', \cdots \alpha_n').$$

Then

$$\sigma_{1\ldots n}(\alpha_1', \cdots \alpha_n') = k \log f(\alpha_1', \cdots \alpha_n') + \text{const.} \tag{2.5}$$

gives the probability for finding the variables $\alpha_1, \cdots \alpha_n$ *with a given set of values* $\alpha_1', \cdots \alpha_n'$. *Practically every time when* $\alpha_1, \cdots \alpha_n$ *assume this set of values, the system will be in the state* $\Gamma_{1\ldots n}(\alpha_1', \cdots \alpha_n')$.

We shall calculate at once certain averages which will be needed for the subsequent derivations. We denote by $f_p(\alpha_p)$ the distribution-function for the variable α_p. We have according to (2.5):

$$k \log f_p(\alpha_p) = \sigma_p(\alpha_p) + \text{const.}, \tag{2.6}$$

where $\sigma_p(\alpha_p')$ is the greatest entropy possible when $\alpha_p = \alpha_p'$, realized by the state $\Gamma_p(\alpha_p')$. The function f_p is determined by (2.6) together with the condition

$$\int_{-\infty}^{\infty} f_p(\alpha_p) d\alpha_p = 1.$$

We obtain from (2.6) by differentiation

$$k df_p/d\alpha_p = f_p(\alpha_p) d\sigma_p/d\alpha_p,$$

assuming that the differential quotient exists. We shall also assume that the entropy $\sigma_p(\alpha_p)$ attains its maximum for a finite value α_p^0 of α_p, corresponding to the equilibrium state Γ^0, and that $(\alpha_p - \alpha_p^0) f_p(\alpha_p)$ approaches zero for large values of $|\alpha_p - \alpha_p^0|$.[9] Then it is easy to calculate the average

$$\overline{(\alpha_p - \alpha_p^0) d\sigma_p/d\alpha_p} = \int_{-\infty}^{\infty} (\alpha_p - \alpha_p^0)(d\sigma_p/d\alpha_p) f_p(\alpha_p) d\alpha_p$$

$$= k \int_{-\infty}^{\infty} (\alpha_p - \alpha_p^0)(df_p/d\alpha_p) d\alpha_p.$$

[8] Einstein, reference 2.

[9] Otherwise this function must have an infinite number of maxima. All the conditions stated are fulfilled whenever α_p is a resonable thermodynamic variable.

Integration by parts yields

$$k[(\alpha_p - \alpha_p{}^0)f_p(\alpha_p)]_{-\infty}^{\infty} - k\int_{-\infty}^{\infty} f_p(\alpha_p)d\alpha_p.$$

The first term vanishes, and the second equals $-k$; thus

$$\overline{(\alpha_p - \alpha_p{}^0)d\sigma_p/d\alpha_p} = -k. \tag{2.7}$$

In the same manner, and under the same assumptions we find

$$\overline{(\alpha_p - \alpha_p{}^0)\partial\sigma_{1\ldots n}/d\alpha_p}$$

$$= \int_{-\infty}^{\infty}\cdots\int(\alpha_p - \alpha_p{}^0)(\partial\sigma/d\alpha_p)f_{1\ldots n}d\alpha_1\cdots d\alpha_n = -k, \tag{2.8a}$$

and

$$\overline{(\alpha_q - \alpha_q{}^0)\partial\sigma_{1\ldots n}/d\alpha_p} = 0, \quad (p \neq q). \tag{2.8b}$$

In the following we shall find it convenient to apply the simple formula (2.7) directly. However, it seems desirable to show the connection with the ordinary formulas for the averages of the products $(\alpha_p-\alpha_p{}^0)(\alpha_q-\alpha_q{}^0)$. We must assume that the entropy $\sigma_{1..n}$ can be expressed by a multiple power series, and that the abridged Taylor development

$$\sigma_{1\ldots n}(\alpha_1,\cdots\alpha_n) = S_0 + \tfrac{1}{2}\sum_{p,q=1}^{n}\eta_{pq}(\alpha_p - \alpha_p{}^0)(\alpha_q - \alpha_q{}^0), \tag{2.9}$$

where

$$\eta_{pq} = \eta_{qp} = [\partial^2\sigma_{1\ldots n}/d\alpha_p d\alpha_q]_{\alpha_1=\alpha_1 0;\ \cdots;\ \alpha_n=\alpha_n 0}, \tag{2.10}$$

will suffice in the entire region of values of $\alpha_1,\cdots\alpha_n$, for which the contribution to any of the averages (2.8 a, b) is at all appreciable. (Since $f\sim\exp(\sigma/k)$, the maximum of $f_{1\ldots n}$ is very sharp). Then we may substitute in (2.8 a, b):

$$\partial\sigma_{1\ldots n}/d\alpha_p = \sum_{p=1}^{n}\eta_{pq}(\alpha_q - \alpha_q{}^0), \tag{2.11}$$

and we obtain a system of linear equations

$$\sum_{r=1}^{n}\eta_{pr}\overline{(\alpha_r - \alpha_r{}^0)(\alpha_q - \alpha_q{}^0)} = -k\delta_{pq} = \begin{cases} -k, & (p=q) \\ 0, & (p\neq q), \end{cases} \tag{2.12}$$

from which the mean squares and products of fluctuations may be computed.

3. The Regression of Fluctuations

We are accustomed to observe that the course of an irreversible process taking place in an isolated system is entirely determined by the initial thermodynamic state according to definite laws, such as the laws for conduction of heat. On the basis of a statistical interpretation of the second law of thermodynamics, no process can be completely predetermined by an initial thermodynamic state; because such a state is itself incompletely defined (from a

molecular point of view; cf. §2). However, we can understand a predetermination with practical certainty, within limits of the order of magnitude of ordinary fluctuations, whereby much greater deviations will be very rare. From this statistical point of view we may still interpret the predictions of irreversible processes from empirical laws as valid for averages taken over a large number of similar cases, which in this connection means cases of irreversible processes starting from the same initial *thermodynamic* state.

Strictly speaking, this rule does not specify uniquely the more refined "microscopic" (molecular) interpretation of laws derived from relatively crude "macroscopic" observations. It makes a considerable difference whether we take an average of the type $\bar{\alpha}=(\alpha'+\alpha'')/2$ or one of the type $\bar{\alpha}=[(\alpha'^5+\alpha''^5)/2]^{1/5}$. However, in all important concrete cases the natural answer to this question will be obvious. For example, if α is a total displacement of heat, itself the sum of many local displacements whose changes depend on local conditions, there may be no doubt that the straight average $\bar{\alpha}=(\alpha'+\alpha'')/2$ is correct.

Now we are able to solve the problem of predicting the *average regression* of fluctuations: Suppose that we start out with a certain isolated system, and watch the fluctuations of the variables $\alpha_1, \cdots \alpha_n$ for a great length of time. Whenever the values of $\alpha_1, \cdots \alpha_n$ happen to be (simultaneously) $\alpha_1', \cdots \alpha_n'$, we make a record of the values which these variables (and perhaps other quantities $\alpha_{n+1}, \cdots \alpha_{n+p}$) assume τ *seconds later*. The averages of such records we denote by

$$\overline{\alpha_1}(\tau, \alpha_1', \cdots \alpha_n'), \cdots \overline{\alpha_{n+p}}(\tau, \alpha_1', \cdots \alpha_n').$$

We know that almost every time when $\alpha_1=\alpha_1'; \cdots ; \alpha_n=\alpha_n'$, the system will be in the (phenomenological) state $\Gamma'_{1\ldots n}=\Gamma(\alpha_1', \cdots \alpha_n')$, and the average course of an irreversible process following that state, described by the functions

$$\overline{\alpha_1}(\tau, \Gamma'_{1\ldots n}), \cdots \overline{\alpha_{n+p}}(\tau, \Gamma'_{1\ldots n}),$$

we know from macroscopic experiments. These functions may be considered as properties (in an extended sense) of the state $\Gamma'_{1\ldots n}$. The "normal" (common) properties of states corresponding to prescribed values $\alpha_1', \cdots \alpha_n'$ of the fluctuating quantities $\alpha_1, \cdots \alpha_n$ are certainly those of the state $\Gamma_1' \cdots {}_n$. The question whether we are allowed to interchange "normal" and average properties must be decided from the consideration of individual cases, as outlined above.

Assuming that the variables $\alpha_1, \cdots \alpha_n$ are suitable in this regard, we have:

$$\overline{\alpha_i}(\tau, \alpha_1', \cdots \alpha_n') = \overline{\alpha_i}(\tau, \Gamma'_{1\ldots n}), \quad (i = 1, \cdots, n+p), \tag{3.1}$$

as a general rule for predicting the average regression of fluctuations from the laws of irreversible processes.

4. Reciprocal Relations

For a discussion of the requirements of microscopic reversibility the averages

$$A_{ji}(\tau) = \overline{\alpha_j(t)\alpha_i(t+\tau)} = \overline{\alpha_j'\bar{\alpha}_i(\tau, \alpha_j')} \tag{4.1}$$

afford a convenient point of attack. The quantities $A_{ij}(\tau)$ may also be defined as time averages (1.1)

$$A_{ji}(\tau) = \lim_{t''\to\infty} \frac{1}{t''-t'} \int_{t=t'}^{t=t''} \alpha_j(t)\alpha_i(t+\tau)dt.$$

In the following it will be convenient to assume that the variables $\alpha_1, \cdots \alpha_n$ measure deviations from the thermodynamic equilibrium, whereby their averages $\bar{\alpha}_1, \cdots \bar{\alpha}_n$ for this state (and also the "normal" values α_j^0) vanish:

$$\overline{\alpha_i} = \alpha_i^0 = 0, \quad (i = 1, \cdots n). \tag{4.2}$$

The assumption of microscopic reversibility requires that, if α and β be two quantities which depend only on the configuration of molecules and atoms, *the event $\alpha=\alpha'$, followed τ seconds later by $\beta=\beta'$, will occur just as often as the event $\beta=\beta'$, followed τ seconds later by $\alpha=\alpha'$.* The same will be true if α and β depend on the velocities of elementary particles in such a manner that they are not changed when the velocities are reversed, for example, when α depends on the distribution of energy in a system.[10] If α_j and α_i are two such "reversible" variables of a reversible system, then obviously

$$A_{ji}(\tau) = \overline{\alpha_j(t)\alpha_i(t+\tau)} = \overline{\alpha_i(t)\alpha_j(t+\tau)} = A_{ij}(\tau). \tag{4.3}$$

We shall consider cases where the course of an irreversible process starting from any state of the type $\Gamma_{1\ldots n}$ can be described by a set of linear differential equations of the form (1.11):

$$\frac{d\overline{\alpha_i}}{dt} = \dot{\alpha}_i = \sum_{r=1}^{n} G_{ir} \frac{\partial\sigma_{1\ldots n}(\alpha_1, \cdots \alpha_n)}{d\alpha_r}, \quad (i = 1, \cdots n). \tag{4.4}$$

According to (3.1) we have

$$\overline{\alpha_i}(\tau, \alpha_j') = \overline{\alpha_i}(\tau, \Gamma_j'),$$

where Γ'_j is the state of maximum entropy for a given value α_j' of the variable α_j. Mathematically this state is characterized by the relations

$$\begin{aligned} \alpha_j &= \alpha_j' \\ \partial\sigma_{1\ldots n}/d\alpha_r &= 0, \quad (r \neq j), \end{aligned} \tag{4.5}$$

and we have for the set of values of $\alpha_1, \cdots \alpha_n$ determined by these conditions:

$$\partial\sigma_{1\ldots n}/d\alpha_j = [d\sigma_j/d\alpha_j]_{\alpha_j=\alpha_j'}. \tag{4.6}$$

[10] Cf. (I) p. 418.

From (4.4) we have in a short interval of time Δt

$$\overline{\alpha_i}(\Delta t, \alpha_j') = \overline{\alpha_i}(0, \alpha_j') + \dot{\alpha}_i \Delta t = \overline{\alpha_i}(0, \alpha_j') + \sum_{r=1}^{n} G_{ir}(\partial \sigma_{1 \cdots n}/d\alpha_r)\Delta t,$$

or substituting (4.5) and (4.6):

$$\overline{\alpha_i}(\Delta t, \alpha_j') = \overline{\alpha_i}(0, \alpha_j') + G_{ij}(d\sigma_j(\alpha_j')/d\alpha_j')\Delta t.$$

Calculating according to (4.1) the average $A_{ji}(\Delta t)$ we obtain

$$A_{ji}(\Delta t) = \overline{\alpha_j(t)\alpha_i(t + \Delta t)} = \overline{\alpha_j' \overline{\alpha_i}(0, \alpha_j')} + G_{ij}\Delta t \overline{\alpha_j d\sigma_j / d\alpha_j},$$

or, observing (2.7) and the convention (4.2):

$$A_{ji}(\Delta t) = A_{ji}(0) - k\Delta t G_{ij}. \tag{4.7}$$

Similarly, of course

$$A_{ij}(\Delta t) = A_{ij}(0) - k\Delta t G_{ji}.$$

Applying the condition (4.3) for microscopic reversibility we find

$$G_{ij} = G_{ji}, \tag{4.8}$$

as announced at the end of §1. The importance of considering fluctuations for the derivation of this result is apparent from the occurrence of Boltzmann's constant k in (4.7).

5. The Principle of the Least Dissipation of Energy

The symmetry relation (4.8) contains the important reciprocal relations in transport processes. An alternative form of (4.8) is convenient for many applications, and commands considerable intrinsic interest. The description (4.4) of a set of simultaneous irreversible processes may be rewritten in the form

$$\frac{\partial \sigma_{1 \cdots n}(\alpha_1, \cdots \alpha_n)}{d\alpha_i} = \sum_{r=1}^{n} \rho_{ir}\dot{\alpha}_r, \quad (i = 1, \cdots n), \tag{5.1}$$

where, according to the equations

$$\sum_{r=1}^{n} \rho_{ir}G_{rj} = \sum_{r=1}^{n} G_{ir}\rho_{rj} = \delta_{ij} = \begin{cases} 1, (i = j) \\ 0, (i \neq j), \end{cases} \tag{5.2}$$

the coefficients (ρ_{ij})form the inverse matrix of (G_{ij}), which enter into (4.4). The symmetry relations (4.8) may be replaced by the equivalent

$$\rho_{ij} = \rho_{ji}, \quad (i = 1, \cdots n). \tag{5.3}$$

We introduce the *dissipation-function*

$$\Phi(\dot{\alpha}, \dot{\alpha}) \equiv \tfrac{1}{2} \sum_{i,j} \rho_{ij}\dot{\alpha}_i\dot{\alpha}_j, \tag{5.4}$$

and incorporate the symmetry relations (5.3) into the description of irreversible processes by writing

$$\partial \sigma_{1 \cdots n}(\alpha_1, \cdots \alpha_n)/d\alpha_i = \partial \Phi(\dot{\alpha}, \dot{\alpha})/d\dot{\alpha}_i, \tag{5.5}$$

in place of (5.1). Further, if we define a function

$$\dot{S}(\alpha, \dot{\alpha}) \equiv \sum_{r=1}^{n} (\partial \sigma_{1 \cdots n}/d\alpha_r)\dot{\alpha}_r, \tag{5.6}$$

representing the rate of increase of the entropy, we can formulate a *variation-principle*, namely

$$\delta[\dot{S}(\alpha, \dot{\alpha}) - \Phi(\dot{\alpha}, \dot{\alpha})] = 0. \tag{5.7}$$

Our convention is that only the velocities $\dot{\alpha}_1, \cdots \dot{\alpha}_n$ should be varied, thus

$$\delta[\dot{S}(\alpha, \dot{\alpha}) - \Phi(\dot{\alpha}, \dot{\alpha})] = \sum_{i=1}^{n} \left(\frac{\partial \sigma_{1 \cdots n}}{d\alpha_i} - \frac{\partial \Phi}{d\dot{\alpha}_i} \right) \delta\dot{\alpha}_i = 0,$$

according to (5.5). The variation principle (5.7), which we shall call the *principle of the least dissipation of energy*, for reasons mentioned in (I), §6, provides convenient means for transforming the reciprocal relations (5.3), or (4.8), to cases where the conventional description of irreversible processes involves an infinite number of variables, for example the temperatures in all parts of a space. The dissipation-function equals half the rate of production of entropy

$$2\Phi(\dot{\alpha}, \dot{\alpha}) = \dot{S}(\alpha, \dot{\alpha}), \tag{5.8}$$

because of (5.5), (5.6) and (5.4), which may be written

$$\Phi(\dot{\alpha}, \dot{\alpha}) = \tfrac{1}{2} \sum_{i,j} \rho_{ij}\dot{\alpha}_i\dot{\alpha}_j = \tfrac{1}{2} \sum_{i} \dot{\alpha}_i \partial\Phi/d\dot{\alpha}_i.$$

It is evident from (5.8) that $\Phi(\dot{\alpha}, \dot{\alpha})$ must be essentially positive (definite or semidefinite), because the second law of thermodynamics demands $\dot{S} \geqq 0$. Therefore the extremum given by (5.7) is always a maximum

$$\dot{S}(\alpha, \dot{\alpha}) - \Phi(\dot{\alpha}, \dot{\alpha}) = \text{maximum}. \tag{5.9}$$

Applications of this principle will be given in a later publication; in (I), §§4–5, a special result was derived by a direct method.

It is worth pointing out that in the dissipation-function has a direct statistical significance. A detailed discussion would be out of place in this article, where a compact presentation of important theorems is intended, but we may state without derivation the result, which is an extension of Boltzmann's principle (2.1). The equilibrium condition of thermodynamics

$$S = \text{maximum}$$

characterizes the most probable state, and the probability W for a state $\Gamma(\alpha_1, \cdots \alpha_n)$ is given by Boltzmann's principle

$$k \log W(\alpha_1, \cdots \alpha_n) = S(\alpha_1, \cdots \alpha_n) + \text{const.};$$

for the precise interpretation of this theorem we must refer to the discussion in §2. In a similar manner, Eq. (5.9) describes the most probable course of an

irreversible process. It is also possible to show, under assumptions approximately equivalent to those that are necessary for deriving, (simultaneously), (5.5) and (2.12), that the probability

$$W(\Gamma', \Delta t, \Gamma'') = W(\alpha_1', \cdots \alpha_n', \Delta t, \alpha_1'', \cdots \alpha_n'')$$

for the states $\Gamma' = \Gamma(\alpha_1', \cdots \alpha_n')$ and $\Gamma'' = \Gamma(\alpha_1'', \cdots \alpha_n'')$ occurring at the times t' and $t'' = t' + \Delta t$, respectively, is given by the formula

$$k \log W(\Gamma', \Delta t, \Gamma'') = S' + S'' - \frac{\Phi(\Delta\alpha, \Delta\alpha)}{\Delta t} + \text{const.}, \tag{5.10}$$

where $S' = S(\alpha_1', \cdots \alpha_n')$, $S'' = S(\alpha_1'', \cdots \alpha_n'')$, and

$$\Phi(\Delta\alpha, \Delta\alpha) = \tfrac{1}{2} \sum_{i,j} \rho_{ij}(\alpha_i'' - \alpha_i')(\alpha_j'' - \alpha_j').$$

(Needless to say, we assume that we are dealing with an aged system.)

6. Nonreversible Systems

As mentioned in (I), §7, we know from our macroscopic experience certain conservative dynamical systems which do not exhibit dynamical reversibility, namely systems where external magnetic fields are acting, and systems whose motion is described relatively to a rotating frame of coordinates, the rotation being equivalent to a field of Coriolis forces. In such cases, where the macroscopic laws of motion are non-reversible, the microscopic motion cannot be reversible.

In dealing with cases of this kind it is advantageous to consider the intensities of magnetic and Coriolis fields as variable external parameters of the system in hand. Then macroscopic dynamical systems subject to external magnetic and Coriolis forces have the following symmetry with regard to reversal of the time: If $[q] = [Q(t-t_0)]$ is a possible motion (succession of configurations $[q]$) of a system left to itself in a magnetic (or Coriolis) field of intensity Θ, then the reverse succession of configurations $[q] = [Q(t_0-t)]$ is a possible motion of the same system when placed in a field of intensity $-\Theta$. Further, let α and β be two functions of the state (and of the parameters) of the system in hand, such that their values are not changed when all the velocities in the system are reversed, (simultaneously with Θ). Then, when we consider the fluctuations in an aged system, as in §4, the succession of events $\alpha = \alpha'$, $\beta = \beta'$, with an intervening lapse of time τ, will occur in a system placed in a field of intensity $+\Theta$, just as often as the succession of events $\beta = \beta'$, $\alpha = \alpha'$, (with a time-interval τ), will occur in a system placed in a field of intensity $-\Theta$.

If we may apply this symmetry condition to the motion of elementary particles, and α_i, α_j are two "reversible" dynamical variables, the averages (4.1) will be functions of the time τ and the field intensity Θ:

$$A_{ji}(\Theta, \tau),$$

and we have the symmetry condition

$$A_{ji}(\Theta, \tau) = A_{ji}(-\Theta, -\tau) = A_{ij}(-\Theta, \tau). \tag{6.1}$$

Supposing that a certain irreversible process can be described in the form (4.4), the coefficients G_{ji} being functions of Θ,

$$\frac{d\alpha_i}{dt} = \dot{\alpha}_i = \sum_{j=1}^{n} G_{ij}(\Theta) \frac{\partial \sigma_{1\cdots n}(\alpha_1, \cdots \alpha_n)}{d\alpha_j}, \quad (i = 1, \cdots n), \tag{6.2}$$

we can derive (4.7) as before

$$A_{ji}(\Theta, \Delta t) = A_{ji}(\Theta, 0) - k\Delta t G_{ij}(\Theta)$$
$$A_{ij}(-\Theta, \Delta t) = A_{ij}(-\Theta, 0) - k\Delta t G_{ji}(-\Theta),$$

and upon applying the symmetry condition (6.1) we find

$$G_{ij}(\Theta) = G_{ji}(-\Theta). \tag{6.3}$$

This theorem contains a reciprocal relation between the Nernst effect and the Ettingshausen effect, which has been derived previously by P. W. Bridgman[11] and by H. A. Lorentz[12] on a quasi-thermodynamic basis.

[11] P. W. Bridgman, Phys. Rev. **24,** 644 (1924); Fourth Solvay Congress ("Conductibilité Electrique des Metaux"), 352 (1924).

[12] H. A. Lorentz, Fourth Solvay Congress, 354 (1924).

THE PROBLEM OF ROTATING MAGNETS

By W. B. Pietenpol and E. C. Westerfield
University of Colorado

(Received September 1, 1931)

Abstract

Ampere's problem of a cylindrical magnet free to rotate about its axis when a current enters at some point on the side of the magnet and leaves along the axis is treated by applying Ampere's original formula directly to the amperian currents which, according to the most commonly accepted theory, account for the magnetic properties of a body. For the torque on a symmetrically magnetised magnet, an expression in agreement with that of Zeleny and Page, and Kimball is obtained. However, this method of attack indicates that this torque is due only to the current in the portions of the circuit not attached to the magnet, contrary to the conclusion of Zeleny and Page. In the case of an asymmetrically magnetised magnet, it is found that the same expression holds provided only that the current is symmetrical in the portion of the circuit not mechanically attached to the magnet. This shows that the expression is more general than indicated by Zeleny and Page, in that they employed a symmetrical distribution of current within as well as without the magnet.

Introduction

THE problem of rotating magnets, which is the converse of unipolar induction, has received considerable attention in recent publications. Ampere first showed that when an electric current is allowed to traverse a cylindrical magnet, entering at some point on the side of the magnet and leaving along the axis of symmetry, the magnet experiences a torque. He explained this effect qualitatively by assuming the magnetism of the magnet to be due to tiny amperian currents and applying his law for the direction of the force between current elements.

In a recent article[1] in which Zeleny and Page have derived the quantitative expression for the torque experienced by the magnet, they conclude that only the current in the portion of the circuit attached to the magnet can contribute to this torque. Kimball[2] obtained the identical expression by deducing the torque exerted on the external circuit by the magnet, and, applying the law of action and reaction, assuming an equal and opposite torque on the magnet. This method of attack seems to imply that only the unattached portions of the current circuit could contribute to the torque on the magnet. These results seem incompatible. However, it is difficult to show experimentally which is correct, since the experimental conditions as well as the resultant expressions are identical.

Zeleny and Page find that when the magnet is asymmetrically magnetised

[1] Zeleny and Page, Phys. Rev. **24**, 544 (1924); Phys. Rev. **27**, 470 (1926); See also, Kennard and Wang, Phys. Rev. **27**, 460 (1926).

[2] A. L. Kimball, Phys. Rev. **28**, 1302 (1926).

the original expression still holds, provided the current both within and without the magnet be symmetrically distributed. Kimball did not treat this case; but, if his original assumption is correct, we readily see that the expression still holds provided only that the current in the portions of the circuit not attached to the magnet be symmetrically distributed. It becomes, therefore, a matter of some importance to determine whether Kimball's assumption is correct.

The present authors have considered this matter theoretically by applying Ampere's original formula[3] directly to the tiny amperian currents which are supposed to account for the properties peculiar to a magnet.

I. Force on a Vector Current Element

In the vector notation, Ampere's formula for the force between two current elements $\mathbf{e}$ and $d\mathbf{r}$[4] separated by the vector distance $\mathbf{r}$ becomes

$$d\mathbf{F} = I_e I_r(2\mathbf{re}\cdot d\mathbf{r} - 3\mathbf{r}\cdot\mathbf{e}dr)(\mathbf{r}:r^4) \tag{1}$$

Taking $\mathbf{e}=r\mathbf{i}$ and $\mathbf{r}=\mathbf{i}u+\mathbf{j}v+\mathbf{k}w$, we have $\mathbf{e}\cdot d\mathbf{r}=e\,du$ and $\mathbf{r}\cdot\mathbf{e}=eu$, and Eq. (1) becomes

$$d\mathbf{F} = eI_e I_r(2r\mathbf{i}du - 3u\mathbf{r}dr)(\mathbf{r}:r^4). \tag{2}$$

From this we obtain as the u, v, and w components of the force

$$dF_u = eI_e I_r d(u^2:r^3) \tag{3}$$

$$dF_v = eI_e I_r(d(uv:r^3) + (vdu - udv):r^3) \tag{4}$$

$$dF_w = eI_e I_r(d(uw:r^3) + (wdu - udw):r^3). \tag{5}$$

II. Axial Torque on an Amperian Current

Formula (3) gives the force along the vector current element $\mathbf{e}$ when $\mathbf{e}$ is directed along the u-axis, and if this expression be integrated between (u_a, r_a) and (u_b, r_b) we obtain

$$F_e = F_u = eI_e I_r(u_b^2:r_b^3 - u_a^2:r_a^3) \tag{6}$$

$$= eI_e I_r(r_b^{-1}\cos^2\phi_b\cos^2\theta_b - r_a^{-1}\cos^2\phi_a\cos^2\theta_a) \tag{7}$$

as the force along $\mathbf{e}$ due to the partial circuit along the path of integration, ϕ being the angle between $\mathbf{r}$ and the (u,v)-plane and θ being the angle between the u-axis and the $(\mathbf{r}, w)$-plane. (Fig. 1). Now suppose $\mathbf{e}$ is translated a small distance $\mathbf{c}$ perpendicular to itself (Fig. 2), then e may be represented by $(c\text{-}d\theta)$; and if c is sufficiently small to permit us to neglect the change in distances between $\mathbf{e}$ and the termini of the partial circuit, we may express the torque on $\mathbf{e}$ about the w-axis as

$$dT = c^2 I_c I_r(r_b^{-1}\cos^2\phi_b\cos^2\theta_b - r_a^{-1}\cos^2\phi_a\cos^2\theta_a)d\theta \tag{8}$$

[3] Carl Cinnamon has applied Ampere's formula to a solenoid, (Abstract, Journal of the Colorado-Wyoming Academy of Science **1**, 41 (1930).

[4] $d\mathbf{r}$=the differential of vector $\mathbf{r}$; ds=the scalar length of $d\mathbf{r}$; dr=the differential of the scalar r.

If we consider e to be an element of an amperian current lying in the (u, v)-plane and having the w-axis as its axis, we may obtain the total torque (about the w-axis) on this amperian current by integrating Eq. (8) as the θ's vary

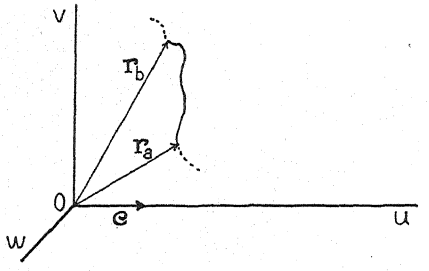


Fig. 1.

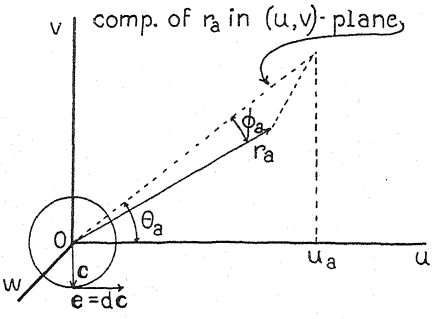


Fig. 2.

through an angle 2π. Since, from symmetry, the initial values of θ_a and θ_b cannot affect the final result, we may replace each by θ. We then have

$$T = c^2 I_e I_r (r_b^{-1} \cos^2 \phi_b - r_a^{-1} \cos^2 \phi_a) \int_0^{2\pi} \cos^2 \theta d\theta$$

$$= 4c^2 I_e I_r (r_b^{-1} \cos^2 \phi_b - r_a^{-1} \cos^2 \phi_a) \int_0^{\pi/2} \cos^2 \theta d\theta \tag{9}$$

$$= \pi c^2 I_e I_r (r_b^{-1} \cos^2 \phi_b - r_a^{-1} \cos^2 \phi_a). \tag{10}$$

If we allow r_b to approach r_a as a limit and ϕ_b to approach ϕ_a as a limit, our partial circuit again approaches the vector element $d\boldsymbol{r}$ as a limit, and our differential expression for the torque on the amperian circuit becomes (from Eq. (10))

$$dT = \pi c^2 I_e I_r d(u^2 : r^3 + v^2 : r^3). \tag{11}$$

III. Force on a Closed Circuit

First assume e to be directed along the u-axis, i.e., $\mathbf{e} = e\boldsymbol{i}$. Since Newton's third law is satisfied by Ampere's formula, we may apply formulae (3), (4), and (5) after reversing the signs. We see that the right member of Eq. (3) and the first term of the right members of Eqs. (4) and (5), being perfect differentials, vanish when integrated around a closed circuit; hence, for the closed circuit o we have

$$F_u = 0.$$

$$F_v = eI_e I_r \int_0 (u dv - v du) : r^3 = eI_e I_r \int_0 \boldsymbol{k} \times \boldsymbol{r} \cdot d\boldsymbol{r} : r^3$$

$$= eI_e I_r \boldsymbol{k} \cdot \int_0 \boldsymbol{r} \times d\boldsymbol{r} : r^3,$$

$$F_w = eI_eI_r \int_0 (udw - wdu):r^3 = - eI_eI_r \int_0 j \times \mathbf{r}\cdot d\mathbf{r}:r^3$$

$$= - eI_eI_r j\cdot \int_0 \mathbf{r} \times d\mathbf{r}:r^3,$$

or replacing $I_eI_r\int_0 \mathbf{r}\times d\mathbf{r}:r^3$ by A, we may write[5]

$$\mathbf{F} = e(A\cdot kj - A\cdot jk) = eA \times j \times k = eA \times i = A \times \mathbf{e}. \qquad (12)$$

(See Fig. 3.) Since $\mathbf{r}$ is a general vector, Eq. (12) is obviously valid even when $\mathbf{e}$ is not directed along the u-axis; and if $\mathbf{e}$ is located at $\mathbf{q}$ and $\mathbf{s}=\mathbf{r}-\mathbf{q}$. Then, $\mathbf{q}$ being constant, we have, replacing $\mathbf{r}$ in A by $\mathbf{s}$,

$$A = I_eI_r \int_0 \mathbf{s} \times d\mathbf{s}:s^3 = I_eI_r \int_0 \mathbf{s} \times d\mathbf{r}:s^3, \qquad d\mathbf{s} = d\mathbf{r},$$

and may write

$$\mathbf{F} = - I_eI_r\mathbf{e} \times \int_0 \mathbf{s} \times d\mathbf{r}:s^3. \qquad (13)$$

IV. Force on an Amperian Current

Suppose now, in Eq. (13), we replace $\mathbf{r}$ by $\mathbf{c}$, where $\mathbf{c}$ is the radius vector which traces out an amperian current lying in the (u, v)-plane with center at origin. (See Fig. 4.) Then $d\mathbf{r}\equiv d\mathbf{c}$ will be a vector current element of this

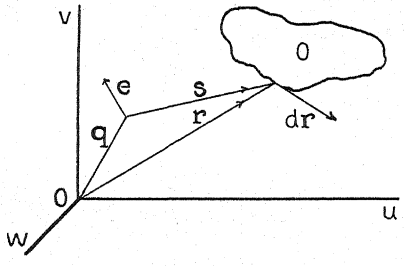


Fig. 3.

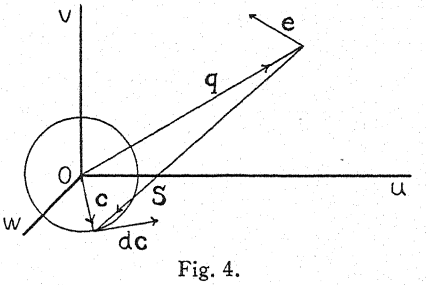


Fig. 4.

amperian current. If we assume the amperian current to be circular, c, being the radius, will be constant. Eq. (13) now becomes

$$\mathbf{F} = I_eI_c\mathbf{e} \times \int_c (\mathbf{q} - \mathbf{c}) \times d\mathbf{c}:s^3 = I_eI_c\mathbf{e} \times \left(\mathbf{q} \times \int_c d\mathbf{c}:s^3 - \int_c \mathbf{c} \times d\mathbf{c}:s^3\right)$$

$$= I_eI_c\mathbf{e} \times \left(\mathbf{q} \times i \int_c du:s^3 + \mathbf{q} \times j \int_c dv:s^3 - c^2k \int_c d\theta:s^3\right), \qquad (14)$$

[5] Triple and higher vector cross-products will be written without parentheses when the operations are to be carried out in inverse order. For example, the expression $\mathbf{a}\times(\mathbf{b}\times(\mathbf{c}\times\mathbf{d}))$ will be indicated by $\mathbf{a}\times\mathbf{b}\times\mathbf{c}\times\mathbf{d}$, while the expression $(\mathbf{a}\times\mathbf{b})\times(\mathbf{c}\times\mathbf{d})$ will be written $(\mathbf{a}\times\mathbf{b})\times\mathbf{c}\times\mathbf{d}$, etc.

where θ is the angle between $\mathbf{c}$ and the u-axis. It remains then to evaluate the three integrals involved in Eq. (14). Since $d\mathbf{c}$ is perpendicular to $\mathbf{c}$ in the (u, v)-plane, it follows that $du = c \sin\theta d\theta$, and $dv = c\cos\theta d\theta$. Moreover, since $\mathbf{s} = \mathbf{c} - \mathbf{q}$, we have, taking $\mathbf{q}$ in the (u, w)-plane, $s^3 = (q^2 + c^2 - 2q_u c\cos\theta)^{3/2}$. Whence, expanding by the binomial theorem and neglecting the third and higher powers of c, (c being small compared to q) we obtain

$$s^{-3} = \frac{2q^4 + 6q^2 q_u c\cos\theta - 3q^2c^2 + 15q_u^2c^2\cos^2\theta}{2q^7}. \tag{15}$$

Or, neglecting the second and higher powers of c, we have the simpler expression

$$s^{-3} = (q^2 + 3q_u c\cos\theta) : q^5. \tag{16}$$

By making use of the above relations, we see that the first integral in Eq. (14) vanishes when integrated around a closed circuit, the integrand being a perfect differential. Applying approximation (16), the second integral becomes

$$\begin{aligned}\int_c dv : s^3 &= (c : q^3)\int_0^{2\pi}\cos\theta d\theta + 3(q_u c^2 : q^5)\int_0^{2\pi}\cos^2\theta d\theta \\ &= 12(q_u c^2 : q^5)\int_0^{\pi/2}\cos^2\theta d\theta = 3\pi(q_u c^2 : q^5).\end{aligned} \tag{17}$$

It is worth while noticing that while we have used only the terms of approximation (16) in obtaining Eq. (17), yet approximation (15) would have added nothing to this result.

Treating the third integral of Eq. (14) in a similar manner, we obtain

$$\begin{aligned}c^2\int_c d\theta : s^3 &= (c^2 : q^3)\int_0^{2\pi} d\theta + 3(q_u c^3 : q^5)\int_0^{2\pi}\cos\theta d\theta \\ &= 2\pi(c^2 : q^3).\end{aligned} \tag{18}$$

And again we observe that approximation (15) would merely give additional terms in the fourth power of c. Thus Eqs. (17) and (18) are accurate to and including the third power of c.

Setting the expressions obtained in (17) and (18) back in Eq. (14) now, we obtain

$$\begin{aligned}\boldsymbol{F} &= 3\pi q_u(c^2 : q^5) I_e I_c \mathbf{e} \times \mathbf{q} \times \boldsymbol{j} - 2\pi(c^2 : q^3) I_e I_c \mathbf{e} \times \boldsymbol{k} \\ &= I_e I_c(\pi c^2 : q^5)(3\mathbf{e} \times \mathbf{q} \times \boldsymbol{k} \times \mathbf{q} - 2q^2 \mathbf{e} \times \boldsymbol{k}).\end{aligned} \tag{19}$$

And since $\pi c^2 \boldsymbol{k} = \mathbf{a}$ is the vector area of the amperian current, we may write Eq. (19) in the somewhat more elegant form

$$\boldsymbol{F} = (I_e I_c : q^5)\mathbf{e} \times (3\mathbf{q} \times \mathbf{a} \times \mathbf{q} - 2q^2 \mathbf{a}). \tag{20}$$

This equation is independent of the coordinate axes; and, since in obtaining this result our only restrictions have been on the position of the coordinate axes, not on the relative position of the amperian current and the vector cur-

rent element, it follows that Eq. (20) is perfectly general,—the only restriction being that q be large compared to c, (i.e., compared to a).

V. Total Axial Torque

If, in Eq. (20), we take our amperian current to lie in the (u, v)-plane with center at $\boldsymbol{r}$; and take the general vector current element $\mathbf{e}$ to lie at $\boldsymbol{b}$: then we

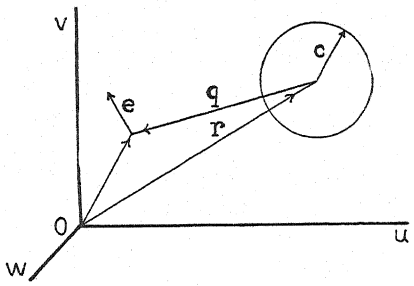


Fig. 5.

have $\boldsymbol{q}=\boldsymbol{b}-\boldsymbol{r}$ (i.e., $\boldsymbol{r}=\boldsymbol{b}-\boldsymbol{q}$), and $\boldsymbol{a}=\pi c^2 k$. (See Fig. 5.) Eq. (20) will then become

$$F = K(2q^2 k \times \mathbf{e} - 3\mathbf{e} \times \boldsymbol{q} \times \boldsymbol{q} \times k), \tag{21}$$

where $K=(\pi c^2 : q^5) I_e I_c$. The torque about the w-axis due to this force will be

$$\begin{aligned} T_1 &= k \cdot \boldsymbol{r} \times F, & \boldsymbol{r} &= \boldsymbol{b} - \boldsymbol{q}, \\ T_1 &= K(2q^2 k \cdot \boldsymbol{r} \times k \times \mathbf{e} - 3k \cdot \boldsymbol{r} \times \mathbf{e} \times \boldsymbol{q} \times \boldsymbol{q} \times k) \\ &= K(2q^2 k \cdot \boldsymbol{b} \times k \times \mathbf{e} - 2q^2 k \cdot \boldsymbol{q} \times k \times \mathbf{e} - 3k \cdot \boldsymbol{b} \times \mathbf{e} \times \boldsymbol{q} \times \boldsymbol{q} \times k \\ &\quad + 3k \cdot \boldsymbol{q} \times \mathbf{e} \times \boldsymbol{q} \times \boldsymbol{q} \times k) \\ &= K(2q^2 k \cdot \boldsymbol{b} \times k \times \mathbf{e} - 2q^2 k \cdot \boldsymbol{q} \times k \times \mathbf{e} - 3k \cdot \boldsymbol{b} \times \mathbf{e} \times \boldsymbol{q} \times \boldsymbol{q} \times k \\ &\quad - 3k \cdot \boldsymbol{q} \times \boldsymbol{q} \times k \; \boldsymbol{q} \cdot \mathbf{e}). \end{aligned} \tag{22}$$

This last result comes from the expansion

$$\begin{aligned} k \cdot \boldsymbol{q} \times \mathbf{e} \times \boldsymbol{q} \times \boldsymbol{q} \times k &= k \cdot (\boldsymbol{q} \cdot \boldsymbol{q} \times \boldsymbol{q} \times k \, \mathbf{e} - \boldsymbol{q} \cdot \mathbf{e} \, \boldsymbol{q} \times \boldsymbol{q} \times k) \\ &= k \cdot (\boldsymbol{q} \times \boldsymbol{q} \cdot \boldsymbol{q} \times k \, \mathbf{e} - \boldsymbol{q} \cdot \mathbf{e} \, \boldsymbol{q} \times \boldsymbol{q} \times k) \\ &= -k \cdot \boldsymbol{q} \times \boldsymbol{q} \times k \, \boldsymbol{q} \cdot \mathbf{e}. \end{aligned}$$

Now, returning to Eq. (11), we find the expression for the torque on the amperian current about its own axis to be

$$\begin{aligned} T_2 &= \pi c^2 I_c I_r d(u^2 : r^3 + v^2 : r^3) \\ &= (\pi c^2 : r^4) I_c I_r (2r(u\,du + v\,dv) - 3(u^2 + v^2)\,dr) \\ &= (\pi c^2 : r^4) I_c I_r (2rk \times \boldsymbol{r} \cdot k \times d\boldsymbol{r} - 3k \times \boldsymbol{r} \cdot k \times \boldsymbol{r} dr) \\ &= (\pi c^2 : r^5) I_c I_r (2r^2 k \cdot \boldsymbol{r} \times k \times d\boldsymbol{r} - 3k \cdot \boldsymbol{r} \times k \times \boldsymbol{r}\, \boldsymbol{r} \cdot d\boldsymbol{r}). \end{aligned}$$

Whence, replacing $\boldsymbol{r}$ by $\boldsymbol{q}$ and $d\boldsymbol{r}$ by $\boldsymbol{e}$ to make the notation agree with that of Eq. (22), we have

$$\begin{aligned} T_2 &= K(2q^2\boldsymbol{k}\cdot\boldsymbol{q}\times\boldsymbol{k}\times\boldsymbol{e} - 3\boldsymbol{k}\cdot\boldsymbol{q}\times\boldsymbol{k}\times\boldsymbol{q}\,\boldsymbol{q}\cdot\boldsymbol{e}) \\ &= K(2q^2\boldsymbol{k}\cdot\boldsymbol{q}\times\boldsymbol{k}\times\boldsymbol{e} + 3\boldsymbol{k}\cdot\boldsymbol{q}\times\boldsymbol{q}\times\boldsymbol{k}\,\boldsymbol{q}\cdot\boldsymbol{e}). \end{aligned} \tag{23}$$

Combining Eqs. (22) and (23), we have for the total torque about the w-axis

$$\begin{aligned} T &= T_1 + T_2 \\ &= K(2q^2\boldsymbol{k}\cdot\boldsymbol{b}\times\boldsymbol{k}\times\boldsymbol{e} - 3\boldsymbol{k}\cdot\boldsymbol{b}\times\boldsymbol{e}\times\boldsymbol{q}\times\boldsymbol{q}\times\boldsymbol{k}) \\ &= K\boldsymbol{k}\cdot\boldsymbol{b}\times\boldsymbol{e}\times(3\boldsymbol{q}\times\boldsymbol{k}\times\boldsymbol{q} - 2q^2\boldsymbol{k}) \\ &= K\boldsymbol{k}\cdot\boldsymbol{b}\times\boldsymbol{e}\times(q^2\boldsymbol{k} - 3\boldsymbol{q}\cdot\boldsymbol{k}\,\boldsymbol{q}) \\ &= K\boldsymbol{k}\cdot\boldsymbol{b}\times\boldsymbol{e}\times(\boldsymbol{q}\times\boldsymbol{k}\times\boldsymbol{q} - 2\boldsymbol{q}\cdot\boldsymbol{k}\,\boldsymbol{q}), \end{aligned} \tag{24}$$

where, as before, $K=(\pi c^2{:}q^5)I_eI_c$.

Suppose now, for comparison, we develop the vector expression for the field of the short magnet to which the amperian current may be supposed to correspond. The field along $\boldsymbol{q}$ at a vector distance $\boldsymbol{q}$ from the center of a short magnet is given by $(2M{:}q^3)\cos\theta$, where M is the magnetic moment of the magnet, and θ is the angle between $\boldsymbol{q}$ and the normal vector. Also, the component of the field perpendicular to $\boldsymbol{q}$ in the plane determined by $\boldsymbol{q}$ and the normal vector, is given by $(M{:}q^3)$ sine θ. If $\boldsymbol{k}$ is the normal vector (as it is in the case under consideration), then from the above expressions we may write as the vector expression of the total field strength at $\boldsymbol{b}$ (where as before $\boldsymbol{q}=\boldsymbol{b}-\boldsymbol{r}$, $\boldsymbol{r}$ being the vector position at the midpoint of the short magnet)

$$\begin{aligned} \boldsymbol{H} &= (2M{:}q^5)\boldsymbol{q}\cdot\boldsymbol{k}\,\boldsymbol{q} + (M{:}q^5)\boldsymbol{q}\times\boldsymbol{q}\times\boldsymbol{k} \\ &= (M{:}q^5)(2\boldsymbol{q}\cdot\boldsymbol{k}\,\boldsymbol{q} + \boldsymbol{q}\times\boldsymbol{q}\times\boldsymbol{k}). \end{aligned} \tag{25}$$

But M is equivalent to $\pi c^2 I_c$ in accordance with the idea of equivalent magnetic shells; hence, combining Eqs. (24) and (25), we may write

$$T = I_e\boldsymbol{k}\cdot\boldsymbol{b}\times\boldsymbol{H}\times\boldsymbol{e}. \tag{26}$$

Or, interchanging dot and cross,

$$T = I_e\boldsymbol{k}\times\boldsymbol{b}\cdot\boldsymbol{H}\times\boldsymbol{e}. \tag{27}$$

This equation really deals with differentials (if we think of the tiny amperian current as an infinitesimal element of the cross-sectional area of a magnet of finite proportions), and should be written

$$d\boldsymbol{T} = I_e\boldsymbol{k}\times\boldsymbol{b}\cdot d\boldsymbol{H}\times\boldsymbol{e} = I_e\boldsymbol{e}\times\boldsymbol{k}\times\boldsymbol{b}\cdot d\boldsymbol{H}, \tag{28}$$

but if we integrate (28) over any finite area in the (u, v)-plane we obtain

$$\boldsymbol{T} = I_e\boldsymbol{e}\times\boldsymbol{k}\times\boldsymbol{b}\cdot\int_A d\boldsymbol{H} = I_e\boldsymbol{e}\times\boldsymbol{k}\times\boldsymbol{b}\cdot\boldsymbol{H}; \tag{29}$$

hence, Eq. (27) is true for any finite area in the (u, v)-plane, being identical in form to Eq. (29).

It follows that if the area under consideration is a right section of a uniformly magnetized, cylindrical magnet whose axis of symmetry coincides with the w-axis, then Eq. (29) may be written

$$T = I_e(N:2\pi), \tag{30}$$

where N is the number of lines of flux which would be cut by $\mathbf{e}$ if it were rigidly attached to a radius vector and swept about the w-axis once. Again, Eq. (30) is really a differential equation (in fact, a second order differential equation), the correct formulation being

$$d^2T = (I_e:2\pi)d^2N. \tag{31}$$

Integrating Eq. (31) along the length of the magnet, we have

$$dT = (I_e:2\pi)\int_L d^2N = (I_e:2\pi)dN. \tag{32}$$

Again, integrating Eq. (32) along the circuit of which $\mathbf{e}$ is an element, we have

$$T = (I_e:2\pi)\int_{b_1}^{b_2} dN = (I_e:2\pi)(N_2 - N_1),$$

or, for simplicity of statement,

$$T = (I_e:2\pi)N, \tag{33}$$

where N is understood to mean the algebraic sum of the lines of flux cutting the annular surface which would be swept out by rotating the segment of circuit in question about the w-axis, (i.e., about the axis of symmetry of the magnet).

The above expression applies to a uniformly magnetised, cylindrical magnet. To treat the case of an asymmetrically magnetised magnet, we may return to Eq. (29). If $\mathbf{e}$ is now considered to be a differential length of a filament of current symmetrically distributed about the axis of the magnet, then (29) becomes

$$dT = I_e r H e_r = r H e_r dI \tag{34}$$

where r is the perpendicular distance from the axis to $\mathbf{e}$, H is the scalar magnitude of the field at $\mathbf{e}$, and e_r is the component of $\mathbf{e}$ along r. But $dI = (I:2\pi)d\theta$, and $dN = He_r d\theta$; hence (34) may be written

$$dT = (I:2\pi)rHe_r d\theta = (I:2\pi)dN. \tag{35}$$

Integrating this expression around a ring having as its axis the axis of the magnet, we obtain

$$T = IN:2\pi \tag{36}$$

corresponding to (30). In this expression, I is the current and N the flux through the ring.

Tracing through steps corresponding to Eqs. (31), (32), and (33), we see that (36) is the right form also for the equation corresponding to (33), where, now, N signifies the flux of a magnet of finite length through a ring region of finite dimensions,—formula (36) holding provided only that the current in this ring region be symmetrically distributed. Since throughout this work we have been dealing with expressions which satisfy Newton's third law, it follows that the torque must be due to the reaction between the amperian currents of the magnet and the current in the portions of the circuit not attached to the magnet. Thus for each infinitesimal force derived for an amperian current, there was an equal and opposite force on the current element e. If both the current element and the amperian current are seated in the same solid body (as they would be in the case of the current traversing the magnet), their mutual reaction could only produce mechanical stresses in the body and could not produce a motion of the body as a whole. It follows that (36) gives the torque on an asymmetrically magnetised magnet provided only that the current in the unattached portions of the circuit be symmetrically distributed, and N represent the total flux which cuts them.

Conclusion

Formula (33) has the same form as the expression obtained by Zeleny and Page, the distinction being that Zeleny and Page were led to attribute the torque to the reaction of the flux of the magnet with the current traversing the magnet and attached arm. In the light of the results contained in the present paper, this seems subject to logical objections; since, as has been pointed out, the reaction between a current element and an amperian circuit situated in the same solid body could only produce mechanical stresses in that body and not rotation of the body as a whole.

Zeleny and Page obtained an expression identical to that of (36) when the entire current sheet was symmetrical, whereas it is shown in the present paper that the current in the portions of the circuit attached to the magnet need not be symmetrical. Zeleny and Page have not treated the case of an asymmetrically magnetised magnet and asymmetrically distributed current within the magnet; however, since in this more general case the torque exerted by the current circuit on the poles would, in general, not be zero, it seems possible that they would find it somewhat difficult to apply their method; and, of course, the logical objections mentioned above would still apply.

It should be pointed out that while there is some doubt as to the validity of Ampere's original formula as applied to partial circuits, it is admittedly valid when one of the circuits is complete as in the present case.

In the experiment performed by Zeleny and Page in which the magnet is replaced by the brass cylinder in a fixed solenoid, the torque on the brass cylinder may be calculated by again applying Ampere's formula for the force between current elements. Here, however, the current-bearing conductors of

the solenoid are not mechanically attached to the cylinder, hence, the torque on it is due to the reaction between the current traversing the brass cylinder and the current in the solenoid. In this case the authors are in agreement with Zeleny and Page. If the solenoid is mechanically attached to the brass cylinder, then the reaction of the current within the brass cylinder with the current in the solenoid can no longer contribute to the torque, and the torque is due to the reaction between the current in the solenoid and the current in the portions of the circuit not attached to the brass cylinder.

In the present paper, only the major torque of the ordinary set-up has been calculated. Actually, the reaction of the current in the portions of the circuit attached to the magnet with that in the portions of the circuit not attached thereto may contribute to the torque, though, as pointed out by Zeleny and Page, this contribution is negligible in the experiments considered. It is obvious, however, that an experiment could be arranged in which this contribution would not be negligible. In asymmetrical cases, external magnetic fields would also affect the torque. To include these factors and extend the treatment to any rigid system, the following general law may be stated: *The torque on any rigid system may be obtained from the integrated reactions of all the current elements mechanically attached, with all the current elements not mechanically attached to the system.* It is understood that magnets are to be treated in terms of the corresponding amperian currents.

LETTERS TO THE EDITOR

Prompt publication of brief reports of important discoveries in physics may be secured by addressing them to this department. Closing dates for this department are, for the first issue of the month, the twenty-eighth of the preceding month; for the second issue, the thirteenth of the month. The Board of Editors does not hold itself responsible for the opinions expressed by the correspondents.

On the Interpretation of the Selective Photoelectric Effect from Two-Component Cathodes

A paper by Mr. A. R. Olpin with the above title appeared in the November 1st issue of the Physical Review. [**38**, 1745, 1931] Mr. Olpin calculates the wave-length of maximal response for a series of alkali hydrides, alkali oxides and alkali sulphides with a striking precision. His interpretation is based upon the Campbell-Fowler theory with the modification that the distance d between successive atomic layers occurring in the expression derived by Fowler has been correlated to the interplanar spacings in crystals of the compounds dealt with.

The object of this letter is to point out that the amazing agreement which Mr. Olpin finds is purely accidental.

Recently Zintl and Harder (Zeits. f. physik. Chemie B. **14**, 265, 1931) have determined the crystal structures of the alkali hydrides. The lattice constants which they give are rather different from those used in Mr. Olpin's calculations as the following table shows:

	Zintl and Harder	Olpin
LiH	4.084A	4.10A
NaH	4.880	4.50
KH	5.700	5.20
RbH	6.037	5.52
CsH	6.376	5.84

The next table shows the wave-lengths of maximal response as calculated on the basis of the correct spacings as compared to the observed wave-lengths.

	Calc.	Obs.
LiH	2750A	2800A
NaH	3930	3400, 3300
KH	5360	4350
RbH	6010	4800
CsH	6710	5400

It will be seen that there is no quantitative agreement except for LiH.

The spacings which Mr. Olpin uses in his calculations for the oxides and sulphides are not correct either, so that the agreement which he finds also for these substances is fictive.

W. H. ZACHARIASEN

Ryerson Physical Laboratory.
University of Chicago,
December 3, 1931.

"Regular Reflection of X-rays from Quartz Crystals Oscillating Piezoelectrically." Some Interpretations

Fox and Cork (Phys. Rev. **38**, 1420 (1931)), with a Y-cut quartz plate as the reflecting crystal in a Bragg spectrometer failed to detect any effect of piezoelectric oscillations on either the intensity or width of the reflected line. In view of the magnitude of the intensity effect usually observed this null result requires explanation.

An important fact to be considered in connection with this result is that it was obtained by surface reflection from the quartz plate, while all other positive results (Fox and Carr; Barrett; Nishikawa, Sakisaka and Sumoto; Barrett and Howe) were obtained by transmission through the quartz plate. It has been shown (Sakisaka, Proc. Phys.-Math. Soc.

Japan **12,** 190 (1930)) that with Mo$K\alpha$ rays reflecting from the surface of quartz, there is no appreciable contribution to the reflected beam from depths in the crystal greater than about 0.12 mm, either when the crystal had a "clean natural face" or when it has a ground surface. Fox and Cork, then, observed in their experiment the reflecting characteristics of the outer tenth millimeter or so of their half-millimeter thick crystal.

In grinding crystals to shape the surfaces become imperfect and intensely reflecting. These imperfect surface layers extend to a depth of about 0.1 mm (Sakisaka, Jap. Jour. Phys. **4,** 171 (1927)) and are not entirely removed by etching for a few minutes, nor by polishing. It is likely that such a layer on the reflecting surface was the seat of practically all of the reflected energy in Fox and Cork's experiment. Their result could be explained by saying that the reflecting layer was already so imperfect that oscillations could not add appreciably to this imperfection and therefore could not appreciably alter the line width and intensity. Sakisaka and Sumoto (Proc. Phys.-Math. Soc. Japan **13,** 211 (1931)) explain in this manner the unchanged surface reflection from quartz when the quartz is subjected to a temperature gradient.

Another interpretation of the negative result is possible that might be valid even with a thoroughly etched surface. Barrett and Howe found the reflecting power of oscillating quartz to be such as to indicate not a condition of random imperfection in the lattice, but, instead, a condition resulting from directed strain gradients. Regions of a crystal may be found where the reflecting power of a plane is practically unchanged by oscillations. The condition of strain in Fox and Cork's oscillating crystal may have been such as to have no effect on their reflected beam. There is too little known at present about the distribution of reflecting power as a function of mode of oscillation, type of cut, accuracy of cut, crystal dimensions and circuit interactions to be able definitely to accept or reject this interpretation.

CHARLES S. BARRETT
CARL E. HOWE

Naval Research Laboratory,
Bellevue, Anacostia, D.C.,
December 1, 1931.

Note on "The Range of Fast Electrons and Neutrons"

In the Physical Review, November 1st, 1931, Messrs. J. F. Carlson and J. R. Oppenheimer,[1] writing on the range of electrons and hypothetical neutrons, make a number of statements which more extensive knowledge of the published experimental facts would have prevented.

(1) To speak of the thinness of the tracks of fast β-rays is misleading; one can really only refer to the line density of droplets which are individually observed in photographs taken under properly controlled conditions.

(2) In 1929, Skobelzyn[2] pointed out from the evidence of track photographs that the number of ions produced per centimeter of a cosmic straight track differs, if at all, but slightly from the number observed under the same conditions in the case of the fastest β particles of radioactive origin.

(3) In the case of radioactive β-rays the exact variation of ionization per centimeter with $\epsilon=(1-v^2/c^2)^{-1/2}$ is known experimentally,[3] and instead of ionization per centimetre increasing with log ϵ, as theory requires according to Messrs. Carlson and Oppenheimer, it decreases. Nevertheless, they say that their "result makes it hard to believe that the particles observed with cosmic rays are electrons or protons since they are observed to ionize less than slower β particles". This reasoning is based on obvious contradiction of the experimental facts.

(4) With regard to the radioactive emission of neutrons from nuclei they write, "it would be of extreme interest to see whether in such a disintegration (radioactive β-ray) thin tracks of the kind observed by Mott-Smith could be found". For the benefit of the writers of this sentence it seems necessary to point out that this experiment has been performed on every occasion in which a β-ray source has been used in an expansion chamber, and that no evidence whatsoever for the emission of neutrons has been obtained.

[1] Carlson and Oppenheimer, Phys. Rev. **38,** 1787 (1931).

[2] Skobelzyn, Zeits. f. Phys. **54,** 686 (1929).

[3] Williams and Terroux, Proc. Roy. Soc., A, **126,** 289 (1930).

Surely it is hardly necessary to insist that the object of physical theories is to describe accurately the experimental facts to which they refer, and to point out that such a purpose is defeated at the outset by neglect of the facts.

W. H. WATSON
F. R. TERROUX
Macdonald Physics Laboratory,
McGill University,
Montreal, Canada,
November 23, 1931.

Neutrons and Cosmic Rays

It has been suggested that cosmic rays are neutrons of high energy.[1] The neutron proposed by Pauli has a magnetic moment and hence should be deflected in a nonhomogeneous magnetic field. This suggests the possibility of an observational verification of the neutron hypothesis, either by a Stern-Gerlach experiment or by displacements in the earth's magnetic field. An exact treatment would require the solution of a wave equation but an approximate result can be obtained classically.

In a Stern-Gerlach experiment the displacement s normal to the original velocity is given by

$$s = \tfrac{1}{4}\,\frac{\mu}{E}\,l^2\frac{\partial H}{\partial s}$$

where μ is the magnetic moment of the particle and E is its energy. The ratio of the displacements of a neutron and an atom is

$$s_N/s_A = (\mu_N/\mu_A)(E_A/E_N).$$

If μ_N and μ_A are of the same order of magnitude S_N will not be measurable since E_N (for cosmic rays) is large compared to E_A, and s_A is almost at the limit of measurability.

Neutrons approaching the earth might be deflected by the earth's magnetic field so that they would not be distributed uniformily over the earth's surface. This would be analogous to the effect found by Epstein[2] for electrons.

For a neutron with a magnetic moment μ and energy E moving radially toward a dipole whose moment is M the component of force perpendicular to the direction of motion is

$$F = \frac{-6\mu M}{r^4}\,\frac{\sin\theta\cos\theta}{(1+3\cos^2\theta)^{1/2}}$$

where r is the distance from the dipole and θ the angle between the axis of the dipole and the direction of motion. An approximate integration gives

$$s = -\mu M/3ER^2$$

for the deflection normal to r for the value of θ giving maximum deflection. If μ is one Bohr magneton, M the magnetic moment and R the radius of the earth and E one million volt-electrons we find s to be approximately 10^{-6} centimeters.

We conclude that it is impossible to distinguish between neutrons and photons by magnetic effects if the energies are of cosmic-ray magnitudes. It is doubtful if neutrons with energy small enough to be appreciably deflected in a magnetic field would produce enough ionization to be observed at all.

L. D. HUFF
Clemson College,
South Carolina,
November 25, 1931.

[1] L. M. Mott-Smith and G. L. Locher, Phys. Rev. **38,** 1399 (1931); J. F. Carlson and J. R. Oppenheimer, Phys. Rev. **38,** 1787 (1931).

[2] P. S. Epstein, Proc. Nat. Acad. **16,** 658 (1930).

Conservation of Energy and the Disintegration of RaE.

The disintegration of RaE is accompanied by the emission of a more or less continuous spectrum of β-rays and by little high-frequency γ-radiation. Since the energy difference between RaE and RaF would be expected to have *some* unique value this peculiar β-ray emission has been cited by Bohr, at the recent meeting of the British Association for the Advancement of Science, as rendering doubtful the conservation of energy in the process of disintegration. There is, however, another mode of escape from the apparent dilemma.

The change from RaD to RaE raises the atomic number by unity and may be regarded as increasing the linear dimensions of the nucleus while decreasing the linear dimensions of the extra-nuclear electron structure. The probability of capture by the nucleus of an extra-nuclear electron is thus increased and we may

regard this event as initiating the next transformation. The captured electron, considered as a projectile entering the nucleus with a definite energy, can transfer this energy, together with the energy difference between that of RaE^+ and RaF^+, to *two* electrons within the nucleus, both of which might thus be emitted with different energies subject only to the condition that the sum of these energies is constant. These are obviously conditions for a continuous β-ray spectrum with a maximum intensity corresponding to the most probable velocity of emergence. The subsequent return of an electron to the shell from which it had been captured would give rise to some x-ray characteristic of RaF. The question whether or not the captured electron is one of the two emitted is probably meaningless.

The idea that a β-ray disintegration may be initiated by the instability of an extra-nuclear electron is not new, since it was proposed by H. T. Wolff as early as 1915.[1] This seems to be the first case in which such an extra-nuclear electron is needed for other reasons. It will be noticed that we must assume so much independence of the intra-nuclear and extra-nuclear systems as may be necessary to provide a certain degree of randomness in the impacts of captured electrons. On these views the number of β-rays emitted in the process should be twice the number of RaE atoms disintegrating.

This note is based upon a discussion with Professor A. H. Compton, who suggested, in particular, that the initial event in the proposed two-electron emission should be the capture of a third electron by the nucleus of RaE.

L. W. McKeehan
Sloane Physics Laboratory,
Yale University,
November 16, 1931.

[1] H. T. Wolff, Phys. Zeits. **16**, 416–419 (1915).

Distribution of Mobilities of Ions in Air

In the last issue of the Physical Review [**38**, 1716 (1931)] Loeb and Bradbury in discussing a paper of mine [Phys. Rev. **34**, 310 (1929)], in which I showed that aged ions in moist air have mobilities spread over a considerable range of values, make the following statement: "In this investigation most sources of error have been critically analyzed with the possible exception of the action of the moving air stream in aspirating more ions (and perhaps a larger spatial extent of ionization) into his chamber than is evident from the measurements". I should like to show that this hypothesized source of error was not present in my experiments. It should be recalled that in these experiments a *slow*, non-turbulent system of air was made to flow axially in the space between two concentric cylinders and that a relatively small amount of air, partially ionized in an auxiliary chamber, was gently forced into the main air stream through 102 small holes along a circumference of the outer of the two cylinders. The rate at which this ionized air entered the apparatus was controlled by water flowing under a constant pressure head into a gasometer and after a steady state of flow was reached this rate could not be affected by an aspiratory action of the main air stream. Moreover, this rate, which entered the calculations as a small quantity, was actually measured during the progress of each set of observations while the main air stream was flowing continuously. Incidentally the rate was found to be the same whether the main air stream was flowing or not. It should be noted, too, that the behavior of the jets of air as they entered the apparatus was carefully studied in a duplicate apparatus made partly of glass. The jets were made visible by an admixture of smoke and showed no widening such as is mentioned in the above quotation as having possibly been present.

John Zeleny
Sloane Physics Laboratory,
Yale University,
November 20, 1931.

The Deepest Term in the Au II Spectrum

The first spark spectrum of gold was analyzed by McLennan and McLay (Trans. Roy. Soc. Can. **22**, 103 (1928)) who did not locate the lowest term, $d^{10}\,{}^1S_0$, because of lack of range of the fluorite spectrograph used in their investigation. In the course of an investigation in this laboratory of the excitation of the gold spectrum in an atmosphere of helium, the spectrum of a gold hollow cathode discharge in helium has been photographed

with a 1 meter vacuum spectrograph. Only three combinations between $d^{10}\ {}^1S_0$ and known terms are possible, *viz.*, combinations with ${}^3P_1{}^0$, ${}^3D_1{}^0$, and ${}^1P_1{}^0$ of the d^9p configuration. Only three lines with the expected frequency differences appear in the region and thus locate ${}^1S_0$ with certainty. The lines are:

Int.	λ	ν	Classification
4	1362.44	73398	${}^1S_0-d^9p\ {}^3P_1{}^0$
7	1224.65	81655	${}^1S_0-d^9p\ {}^1P_1{}^0$
5	1166.81	85704	${}^1S_0-d^9p\ {}^3D_1{}^0$

The wave-lengths are believed good to somewhat better than one-tenth of an Angstrom and the separations somewhat better. The frequency differences agree with McLennan's analysis to within 2 frequency units. The value of ${}^1S_0$ based on McLennan's term values is -15036.

This value of the low level is further confirmed from a study of the spectrum of the low voltage arc in helium and gold vapor. In this excitation lines from the two levels $d^97S\ {}^3D_1$ and ${}^1D_2$, which are respectively 24.11 and 24.15 volts above the normal state of the gold atom and thus nearly in resonance with the He ion (24.47 volts), are very strongly excited.

R. A. Sawyer
Kenneth Thomson
University of Michigan,
November 25, 1931.

A Band Spectrum due to the Molecule N_2O_3

During a study of the absorption of light by N_2O (Abstract No. 19 Chicago Meeting of the American Physical Society, Nov. 27–28, 1931), the authors were lead to an investigation of mixtures of NO and NO_2, and have observed, in the near ultraviolet, an absorption spectrum consisting of apparently diffuse bands, due in all probability to the molecule N_2O_3. The bands are observed in relatively large amounts of NO when small amounts of NO_2 are added, the new bands predominating over the absorption of NO_2 under these conditions. Their centers are located approximately at wave-lengths 3843, 3682, 3539, 3509, 3417, 3386, 3305, 3279. The bands do not appear to possess sharp edges nor to show any pronounced tendency to degrade one way or the other. The first member is exceptionally diffuse. The third member ap pears most intense. The bands grow weaker as they proceed to shorter wave-lengths suggesting that there may be further weaker members among the NO_2 absorption. The new bands show qualitatively the dependence to be expected upon the pressures of NO and NO_2, and upon the temperature, decreasing noticeably with increasing temperature. A more detailed description of this spectrum will be published later.

Eugene H. Melvin
Oliver R. Wulf
U. S. Bureau of Chemistry and Soils,
November 23, 1931.

A. Effect of Crystal Symmetry on the Energy Levels of Solids. B. Experimental Evidence of Definite Orientation of Coordinated Water Molecules About Rare Earth Ions in Solution

Because of its interest to physicists, who perhaps would not see the complete paper in a chemical journal, we think that it is desirable to publish a brief summary of an article which we shall submit soon to the Journal of the American Chemical Society.

A. Photographs were taken of the absorption spectra of the Gd^{+++} ion in monoclinic crystals of $GdCl_3\cdot 6H_2O$, $GdBr_3\cdot 6H_2O$, $Gd_2(SO_4)_3\cdot 8H_2O$; in hexagonal crystals of $Gd(BrO_3)_3\cdot 9H_2O$, $Gd(C_2H_5SO_4)_3\cdot 9H_2O$, and in a triclinic crystal, $Gd(NO_3)_3\cdot 6H_2O$. Gadolinium IV was chosen because it is by far the most desirable ion for this type of work. It gives sharp lines at room temperature, it has the simplest spectrum of any of the rare earths, its lines and multiplets being well separated from one another, and its basic level, ${}^8S_{7/2}$, is known to be single. Its chief disadvantage is that its absorption lines occur in the ultraviolet.[1]

In all cases the same multiplets were observed at approximately the same frequencies, although a slight shift of the multiplets toward shorter wave-lengths was noticeable in the case of crystals of higher symmetry. The lines within the multiplets were, however, greatly affected by changes in the crystal system.

[1] Freed and Spedding, Nature **123,** 525 (1929); Phys. Rev. **34,** 945 (1929); ibid. **38,** 670 (1931); Spedding, Phys. Rev. **37,** 777 (1931).

From the monoclinic crystals the number and spacing of the lines was almost identical, the differences between the spectra of $Gd_2(SO_4)_3 \cdot 8H_2O$ and $GdCl_3 \cdot 6H_2O$ being of the same order as those between $GdCl_3 \cdot 6H_2O$ and $GdBr_3 \cdot 6H_2O$.[2] Only in two cases were distinct differences observed and both occurred in multiplets in which the lines were very closely spaced. The differences were caused by a single line of the chloride spectrum becoming two lines in the case of the sulphate. On the other hand, between the hexogonal and monoclinic crystals, there were notable differences both in the number and spacing of the lines. The over-all spread of the multiplets was less than half that shown by the monoclinic crystals, and in many cases fewer lines were observed. The spectrum of the triclinic crystal was similar to that of the monoclinic type, but its multiplets were farther spread out. Unfortunately, only two groups of lines were obtained from $Gd(BrO_3)_3 \cdot 9H_2O$ and $Gd(NO_3)_3 \cdot 6H_2O$ owing to continuous absorption by the negative ions in the region below 3000A.

In a previous letter[3] to this journal experimental evidence was presented which showed that all the lines arise from a single basic level, $^8S_{7/2}$, which is not appreciably affected by the crystal field. For this reason the position of the lines and multiplets is effectively an energy level diagram of the excited levels. The absence of sensitivity to variations in the crystal field of the mean positions of the multiplets and the great sensitivity of their component lines to this field proves that the multiplets arise from an excited electronic level which has become non-degenerate because of the electric fields of the crystal. To a first approximation, the type and magnitude of the splitting depends only on the symmetry of the crystal, and the chemical differences of the surrounding ions have only a second order effect, except for that which aids in determining the crystal form.

These facts are in good agreement with those predicted by Bethe,[4] who, from considerations of wave mechanics and group theory has shown that degeneracy of the levels of rare earth ions, caused by the force fields of the neighboring ions in the crystal, should depend on the symmetry of the fields about the ions, and that the degeneracy should become less in fields of lower symmetry. In his calculations Bethe has made many simplifying assumptions which are not applicable here, so that better than qualitative agreement should not be expected. While the unique structures are still unknown, careful crystallographic measurements of all our crystals have been made by Professor Adolph Pabst of this university. In general the crystals are from the class of highest symmetry of the system to which they belong. In the case of the hexagonal crystals which we have used, the symmetry about the Gd^{+++} ion appears certainly to be greater than that about the Gd^{+++} ion in the monoclinic crystals.

B. Photographs were taken of the absorption spectra of Gd^{+++} ion in solutions of $GdCl_3 \cdot 6H_2O$ and $Gd(C_2H_5SO_4)_3 \cdot 9H_2O$ of various concentrations. The positions and general spacings of the lines in all cases were very similar to those of the $GdCl_3 \cdot 6H_2O$ crystals except that the lines were very much wider and the multiplets were shifted slightly toward higher frequencies. The fact that the lines of the multiplets can be clearly resolved shows that the water molecules must take definite positions about the Gd^{+++} ion in order to give a field of definite symmetry. If random distribution is assumed, there would be all types of symmetry and the multiplets would become broad, blurred bands on account of the overlapping of the various spectra. The great width of the lines does, however, show that there is considerable thermal agitation and that the water molecules vibrate about their mean positions.

A study of the number of lines in the multiplets, together with their shifts, widths, and so on, should give a great deal of information concerning the effect which temperature, concentration, additional ions, various solvents and the like have on the force fields which surround the ions in solution.

We are continuing this work and hope soon to have more detailed information concerning it.

F. H. SPEDDING
(*National Research Fellow in Chemistry*)
G. C. NUTTING

Chemical Laboratory of the University of California,
Berkeley, California,
November 18, 1931.

[2] Freed and Spedding, J. Am. Chem. Soc. **52**, 3747 (1930).

[3] F. H. Spedding, Phys. Rev. **38**, 2080 (1931).

[4] Bethe, Ann. d. Physik **3**, 133 (1929).

The Heat Capacity of Methane

D. S. Villars and G. Schultze (Phys. Rev. **38,** 998 (1931)) have recently published a paper on the rotational heat capacity of methane gas. By applying the results of Hund and Elert, they obtained the *a priori* probabilities of the rotational states and the series expression for $Q=\sum_i P_i e^{-\epsilon_{ri}/kT}$. According to Villars and Schultze, symmetry and nuclear spin result in the existence of three non-combining types of methane, quintet, triplet and singlet. They have calculated rotational heat capacities for each of the three varieties; for the metastable mixture of 5/16 quintet, 9/16 triplet and 2/16 singlet, and for the equilibrium mixture. The heat capacity of the metastable mixture is that of what we might call "ordinary" methane, while the equilibrium heat capacity is that which would obtain in the presence of some hypothetical catalyst. The results of Villars and Schultze indicate that the rotational heat capacity of methane reaches a maximum around 50°K and then falls off to about 0.6 R at 175°, where it is apparently still decreasing. This result was very surprising, since it seemed to us that the equipartition value of 3/2 R should have been reached by this temperature. If their results were correct, the experimental value of the entropy of methane at 298.1° would be considerably in error, since it has been obtained from the third law value at the boiling point by assuming the rotational heat capacity of the gas to be 3/2 R from the latter temperature to 298.1°K.

The fact that the experimental entropy agrees with that calculated from the Tetrode equation equally well at the boiling point and at room temperature led us to recalculate the results of Villars and Schultze.

Assuming methane to be a regular rigid tetrahedron, the rotational energy levels are given by the equation:

$$E_r = \frac{h^2}{8\pi^2 I} j(j+1).$$

From the definition, $\sigma = h^2/8\pi^2 IkT$, we have the following expression for the rotational heat capacity:

$$C_r = \sigma^2 \frac{d^2 \ln Q}{d\sigma^2} = \sigma^2 \left[Q \frac{\frac{d^2Q}{d\sigma^2} = \left(\frac{dQ}{d\sigma}\right)^2}{Q^2} \right].$$

For I, the moment of inertia, we have used the Raman value, 5.17×10^{-40} gm cm² (Dickinson, Dillon and Rasetti, Phys. Rev. **34,** 582 (1929)), which was also used by Villars and Schultze. We have used the same *a priori* probabilities as those given by Villars and Schultze.

An evaluation of Q, $(dQ/d\sigma)$, $(d^2Q/d\sigma^2)$ by summing, and substitution in the above equation for C_r, gives the results in Table I, and those plotted in Figs. 1 and 2. In Fig. 1, the three curves represent the heat capacity of the three kinds of methane, while in Fig. 2, the two curves are for the equilibrium mixture and the metastable frozen mixture. Above the temperature range of the plots, the heat capacity curves are virtually straight lines, coincident with $C_r/R=1.5$.

Our results differ considerably from those of Villars and Schultze. Below 40°, the two

TABLE I. *Rotational heat capacity of methane.*

T°K	Quintet C_r/R	Triplet C_r/R	Singlet C_r/R	Equilibrium C_r/R	5/16 Quintet 9/16 Triplet 2/16 Singlet C_r/R
3.84	0	0.035	0	0.499	0.020
7.68	0.006	0.481	0.003	0.941	0.290
12.80	0.276	0.981	0.030	1.347	0.642
19.20	1.354	1.328	0.219	1.733	1.198
25.60	2.255	1.457	0.537	1.838	1.592
30.72	2.432	1.487	0.794	1.798	1.696
38.40	2.198	1.498	1.101	1.688	1.667
43.89	1.971	1.499	1.250	1.621	1.615
51.20	1.747	1.500	1.374	1.563	1.561
61.44	1.589	1.500	1.456	1.527	1.527
76.80	1.516	1.500	1.492	1.504	1.504
153.60	1.500	1.500	1.500	1.500	1.500

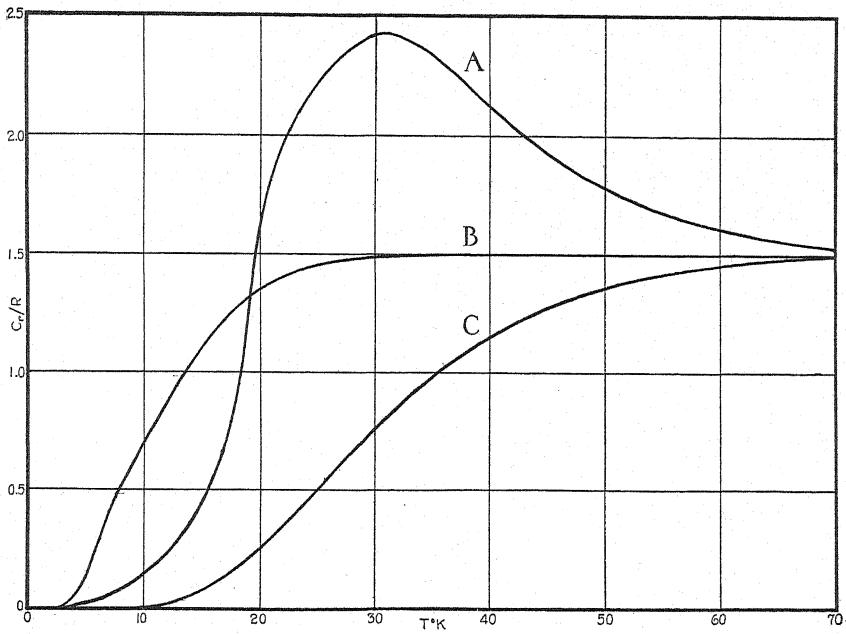


Fig. 1. Rotational heat capacities of methane. *A*, quintet. *B*, triplet. *C*, singlet.

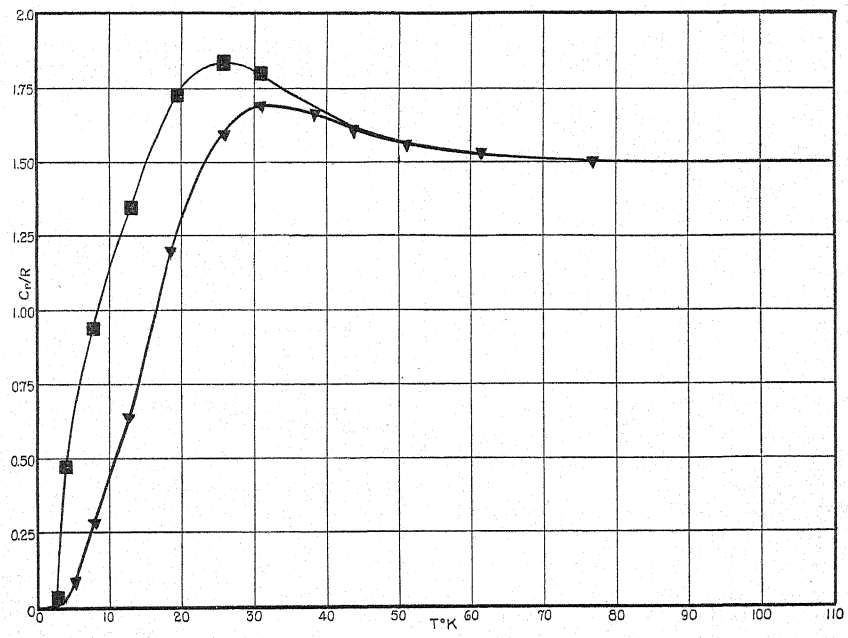


Fig. 2. Rotational heat capacities of methane. Squares, equilibrium. Triangles. frozen.

sets of results agree fairly well, except for the case of the equilibrium mixture, but at higher temperatures the difference is very marked. As may be seen from Fig. 2, according to our calculations, the heat capacity after reaching a maximum, descends asymptotically toward the equipartition value, which it reaches, within a few thousandths of a calorie, at a temperature of 100°K. We have been unable to discover the source of the large deviation, but suspect it lies in the evaluation of the sums involved.

For the sake of completeness, we have calculated the vibrational heat capacity at room temperature. Use is made of the same equation as in rotation, namely $C/R=(\sigma^2 d^2 \ln Q/d\sigma^2)$, but in this case we substitute vibrational energies in the expression for Q. With the frequency assignments of Dennison (D. M. Dennison, Astrophy. J. **62,** 84 (1925)) and assuming simple harmonic motion, we obtain $C_v^{(298.1)}/R=0.296$. For the heat capacity of methane at room temperature, therefore, we have $3/2\ R$ for translation, $3/2\ R$ for rotation, R for C_p-C_v and $0.296\ R$ for vibration. Thus

$$C_p^{298.1} = 8.54 \text{ cal. mole}^{-1}.$$

The International Critical Tables gives $C_p=8.47$ at 15°C, and at this temperature our calculated value would be 8.45.

D. P. MacDougall

Chemical Laboratory of the University of California,
Berkeley, California,
November 18, 1931.

An Estimation of the Spectrum of the Element of Atomic Number 87

During the past two years I have been examining the optical spectra of mineral concentrates in an effort to identify the *raies ultimes* of the missing alkali element, eka-caesium. A comparison of alkali spectra shows that the principal series spectrum of this element will be characterized by a widely separated doublet in the red region, and a closer doublet in the violet. K. T. Bainbridge,[1] basing his computations on the similarity of the spectrum of Ra II with that of unionized eka-caesium, has estimated the wavelength of the $1^2S-2^2P_2$ line to be 7600 ± 200A, and that the component of lesser intensity, $1^2S-2^2P_1$, is further in the red at 8720 ± 200A. F. H. Loring[2] has made another estimate, based on Hick's equation for series spectra, which lead to values of 8061A for the $1^2S-2^2P_2$ line, and 4831A as the wave-length of the $1^2S-3^2P_2$ line. Both estimates of the $1^2S-2^2P_2$ line place it in a region of poor photographic sensitivity, indicating that for purposes of identification, the $1^2S-3^2P_2$ transition, though theoretically not the most persistent line in the spectrum of the element, will be more important than the true *raie ultime* in the red. As the approximated wavelengths of the red line differ considerably from each other, corresponding doubt is placed on the estimate made by Loring of the wavelength of the line in the violet region. In general, a more exact knowledge of the position of the individual lines, together with independent estimates of the doublet separations, are desirable.

Unfortunately, the methods which led to the exact elucidation of the spectra of stripped atoms of the initial series of the periodic table are not applicable to the present case owing to the paucity of analyzed spectra in the 7th period. Spectral regularities in a group of elements, as observed by Ramage[3] among the atomic weights of the alkalis, or by Hicks' for their atomic volumes,[4] cannot be used for extrapolating the spectrum of eka-caesium because of a lack of generality in the correlations.

In an effort to estimate the spectrum of the missing alkali, I observed that for any spectral term T, in a periodic group of elements, the quantum defect Q, is roughly a linear function of the total quantum number n, of the valence electron. If Q is known, T can be calculated from the relationship: (1) $T=r^2R/(n-Q)^2$, where R is the Rydberg constant and $r-1$ is the degree of ionization of the atom. Though this relationship is not precise, it is singularly free from manifest exceptions (see Fig. 1). This generality has been tested and found to be true for the S, P, D, F, G and H levels of the neutral alkali atoms, the singlet and triplet S and P levels in the spectra of the

[1] K. T. Bainbridge, Phys. Rev. **34,** 752 (1929).

[2] F. H. Loring, Chem. News **140,** 178, 202, 242 (1930).

[3] Ramage, Proc. Roy. Soc. **A70,** 1 (1902).

[4] W. N. Hicks, Proc. Roy. Soc. **A83,** 226 (1910).

neutral alkaline earths, the doublet spectra of the neutral atoms of the elements of group III, for the S, P and D levels of the neutral copper, silver and gold atoms, and for the corresponding singlet and triplet levels of zinc, cadmium and mercury. The most marked curvature in the loci is observed in the case of the spectra of the singly ionized alkaline earth atoms, when the levels of radium are included. L. A. Turner[5] observed that if the total quantum numbers assigned by Bohr to the first two groups of elements be given different integral values in the case of the elements of high atomic weight, then the corresponding quantum defects for the S and P levels are, approximately, a linear function of the atomic number. At the end of his paper he states that H. N. Russell observed: "Straight lines will also be obtained if the quantum defects obtained from Bohr's quantum numbers are plotted against integers". The rule postulated above is more general and exact than Turner's formulation, and is better adapted for purposes of extrapolation in so far that the Bohr quantum numbers differ consistently by unity from element to element.

The utility of the rule, for estimating the spectrum of a heavy element, can be tested by calculating the principal series spectrum of radium, from the energy levels of the known alkaline earths, other than radium, and comparing the result with the known spectrum of the element. If the relationship were exactly linear the first difference Δ, (see Table I) should be a constant and ϵ have the value zero. Since in this case the locus has a marked curvature, the value of Δ is not constant, and it may be assumed that the Δ of radium will probably differ from that of barium by as large an amount as the maximum deviation from constancy observed in that group. On this assumption, the quantum defects of the levels of radium were evaluated from the formula: (2) $Q_{Ra}=Q_{Ba}+\Delta_{Ba}+|\epsilon|_{max.}$ The

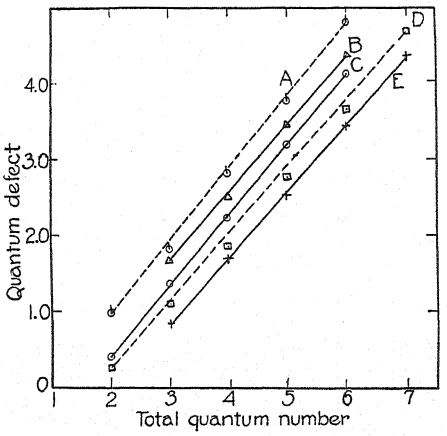


Fig. 1. S Levels for the elements of the first three groups. (Data from the Inter. Critical Tables 5, 392 (1929) 1st ed.) A, 2^2S_1 term for B I, Al I, Ga I, In I and Tl I ($n-1$, instead of n plotted, to avoid intersection with other curves); B, singlet system Mg I, Ca I, Sr I and Ba I (Be I and Ra I spectra not analyzed); C, 1^2S_1 term for Li I, Na I, K I, Rb I and Cs I; D, 1^2S term for Be II, Mg II, Ca II, Sr II, Ba II and Ra II; E, triplet system Be I, Mg I, Ca I, Sr I and Ba I. Dotted lines show marked curvature.

first transition of the principal series so estimated is 3950A for the major line, and 4500A for the component of lesser intensity; the wave-lengths of the observed lines being 3816A and 4683A, respectively.

From the law of spectroscopic displacement, the spectrum of eka-caesium may be expected to be similar to that of Ra II; hence, an equation of form (2) may be assumed valid for the extrapolation of its spectrum. The wave-lengths of the *raies ultimes* computed from the energy levels (see Table II) are:

[5] L. A. Turner, Phil. Mag. **48**, 384, 1010 (1924).

$1^2S-2^2P_2=7460$A, $1^2S-2^2P_1=8130$A, $1^2S-3^2P_2=4260$A, and $1^2S-3^2P_1=4310$A. These estimates are in closer agreement with the values of Bainbridge, than with those published by Loring. If Eq. (1) be investigated for the effect on the value of T produced by a small error in the estimation of Q, vis., (3) $\Delta T=-2r^2R\Delta n^*/(n^{*3}+2n^{*2}\Delta n^*)$, it will be observed that the levels of neutral atoms are much less sensitive than those of singly, or doubly ionized atoms. In (3), n^* is the effective quantum number, equal to $n-Q$.

TABLE I. *Estimation of Ra spectrum (example 1^2S term).*

Element	n	Q	Δ	ϵ
Be	2	0.271		
			0.826	
Mg	3	1.097		−0.064
			0.762	
Ca	4	1.859		+0.157
			0.919	
Sr	5	2.778		−0.030
			0.889	
Ba	6	3.667		
Ra	7	(4.713)	Calc.	
		4.699	Observed	

The doublet separations in the principal series of the alkalis increases progressively with increase in nuclear charge. H. Bell[6] has shown that the separations can be accurately represented by empirical equations of the type: $(\Delta\tilde{\nu})^{1/2}=m(N-N_0)$, and $\log\Delta\tilde{\nu}=p\log N+q$, where N is the atomic number, and m, p, q and N_0 are constants. For element 87, the distance between the doublets, computed with the aid of these equations, are $1450\tilde{\nu}$ and $467\tilde{\nu}$ for the multiplets in the red and violet regions, respectively. The separations obtained from the estimated 2^2P_j and 3^2P_j levels, $1100\tilde{\nu}$ and $330\tilde{\nu}$, are in fair agreement with the values calculated from Bell's equations.

TABLE II. *Estimated energy levels of RaII and Ek−Cs I.*

Level	Radium Obs. $\tilde{\nu}$	Radium Calc. $\tilde{\nu}$	Calc. for element 87
1^2S	82,862	83,880	32,930
2^2P_2	56,653	58,600	19,540
2^2P_1	61,510	61,680	20,560
3^2P_2	—	—	9,416
3^2P_1	—	—	9,750

HERMAN YAGODA

New York University,
Washington Square East,
New York, N. Y.
October 27, 1931.

[6] H. Bell, Phil. Mag. **36**, 337 (1918).

Excitation of High Optical Energy Levels. An Erratum

(Phys. Rev. **38**, 193, 1931)

In a letter to the Editor of the above title, line 12, page 194, read $58\cdot10^{-6}$ henrys instead of $6\cdot10^{-5}$ henrys.

J. E. MACK

Department of Physics,
University of Wisconsin,
Madison, Wisconsin,
November 9, 1931.

BOOK REVIEWS

Thermodynamics. ALFRED W. PORTER. Pp. 96+vii, figs. 21. E. P. Dutton and Company New York, 1931. Price, $1.10.

The fundamental principles and equations of classical thermodynamics, and some of their important applications, are developed briefly but clearly in this monograph. The introductory chapter is rendered especially interesting by a presentation of the historical background of the subject. The reviewer is of the opinion that the various empirical equations of state are treated at greater length than their relative importance warrants. The chapter on Irreversible Operations, which includes a comparatively detailed account of the Joule-Thompson effect, is particularly valuable since this phase of thermodynamics frequently receives scant attention. The application of thermodynamics to solutions is treated rather sketchily. No mention is made of the Third Law or of the Nernst Heat Theorem.

ROBERT LIVINGSTON
University of Minnesota

Fortschritte der Chemie, Physik and physikalischen Chemie, Band 20, Heft 3. Bandenspektra und Ihre Bedeutung für die Chemie. R. M. MECKE. Pp. 87, figs. 20. Gebrüder Borntrager, Berlin, 1929, Price 7.60 RM.

This small book includes a discussion of the theory of molecular spectra, helpful but not always accurate. Useful diagrams are given. Rather complete tables of band spectrum data, including heats of dissociation, are presented, including some data for polyatomic molecules. The effects of isotopy in band spectra are discussed in some detail. The author also discusses the use of band spectrum data for the calculation of chemical constants and specific heats.

R. S. MULLIKEN
University of Chicago

The Universe. FRANK ALLEN. Pp. 145+xiv, figs. 31. Harcourt Brace and Company, New York, 1931.

This "little book" gives a very readable, often amusing, and generally instructive account of the successive conceptions of the material universe held since the days of the Greeks. It presents, in bookform, the substance of a popular lecture delivered at the University of Manitoba in 1928, and, suffers somewhat of the general defects of such publications in that it appears to be a little too rambling in places, and goes off on too many by-paths and side-issues. Such may serve their purpose in elevating a lecture above the level of dullness, but often render a published account of it analogous to the "omnibus" article. It is well illustrated with portraits and photographs of the principal philosophers and savants, and adorned with a number of explanatory diagrams and sketches and may well take its place among the already vast number of books which give the uninitiated the impression that they grasp the idea of relativity whereas they have not really touched the meaning of it yet. A more factual criticism one can make is that the author subscribes to the myth that it was Galileo who invented the telescope.

W. J. LUYTEN
University of Minnesota

Dielectric Constant and Molecular Structure. C. P. SMYTH. Pp. 214. Figs. 31. Chemical Catalog Company, New York, 1931. Price $4.00.

This volume is one that will be welcomed by many readers. In the first place, being written by a physical chemist, it naturally stresses the chemical aspects more carefully than does most existing literature, irrespective of language. Also there is a particular dearth of monographs in English on the general subject of dipole-moment. Debye's "Polar Molecules" is perhaps the best known example, and there is almost no duplication of material between this and Professor

Smyth's new book. In the first place, the latter terminates with a very fine and useful 14 page table of the dipole moments of the molecules so far measured. (The English edition of Debye appeared too early to include the table of moments found in the German one, which has since been supplemented by a "Nachtrag" to the table, and then a "Nachtrag" to the "Nachtrag," each sold independently.)

The content of the book is primarily descriptive rather than mathematical. Even the first chapter called "mathematical theory" is more a presentation of the results than details of the mathematical analysis. A valuable feature is a chapter on experimental technique and apparatus, too often overlooked.

The chapters dealing with the relation of dielectric measurements to the structure of organic molecules are particularly complete. It is unfortunate that Professor Smyth's own measurements on ethylene dichloride were available too late to incorporate in the volume, as they have shed much light on the question of free rotation, i.e., as to whether certain carbon bonds are essentially sockets in which the radical can turn freely. The interesting vector addition of constituent dipoles in benzene substituents is discussed in considerable detail.

The two final chapters are on electronic and atomic polarization and on molecular association. In the discussion of electric refraction, some discussion of the calculations of Pauling could very properly have been included, perhaps at the expense of some of the older work. On page 144 the mistake of certain other writers has been followed in stating that the polarizability should vary as the inverse cube rather than inverse fourth power of the effective charge.

The style of the volume is a clear one. The documentation of literature is quite complete, although in Chap. I some minor results are erroneously attributed to Debye rather than Pauli, Manneback, and others.

J. H. VAN VLECK
University of Wisconsin

Applications of the Absolute Differential Calculus. A. J. MCCONNELL. Pp. xii+318. Blackie and Son, London 1931. Price 20s.

The avowed purpose of this admirable text is to develop the principles of tensor analysis and the absolute differential calculus, and to apply them to a wealth of relatively elementary subjects. It is to be considered as a text which will enable the student of mathematics or physics to "appreciate the power of tensorial methods . . . by seeing them applied to subjects with which he is already familiar," thus adequately preparing him for the study of more advanced disciplines, such as the general theory of relativity and the geometry of hyperspace.

The first two of the four parts into which the book is divided present the algebraic and geometric treatments of tensor algebra, respectively, and refer in the main to linear transformations. The theory of determinants, including the theory of elementary divisors, is concisely presented in terms of tensor notation. The geometrical applications are concerned with (oblique) rectilinear coordinates, the plane, the straight line and quadric surfaces. The absolute differential calculus proper is developed in the third part, which consists in an introduction to the differential geometry of curves and surfaces in three-dimensional Euclidean space. Finally the fourth part, consisting of the last hundred pages, applies the methods developed to the dynamics of a particle, rigid bodies and continuous media and to the special theory of relativity. An appendix correlates the new with the classical notation in dealing with general orthogonal coordinates in mathematical physics.

This excellent text can be recommended unreservedly to any one who wishes to become acquainted with the methods of tensor analysis; it should also prove a valuable auxiliary or reference text for students learning any of the disciplines with which it deals.

H. P. ROBERTSON
Princeton University

Handbuch der Anorganischen Chemie. Eisenatom und Eisenmetall. Vierter Band, dritte Abteilung, zweiter Teil A, Lieferung I. A. ABEGG, F. AUERBACH AND I. KOPPEL. Pp. 336, figs. 136. Verlag von S. Hirzel, Leipzig, 1931. Price, 40 RM.

With this second volume on the properties of iron (the first volume was published a year

ago), the excellent handbook of Abegg, started under his direction more than twenty-five years ago, edited after his death by Auerbach and after the latter's passing away by Professor Koppel, is approaching its completion. The publication of the monograph on the properties of iron and its compounds will be welcomed by all the friends of Abegg's Handbook, who have felt a great need for it during a long time.

The present volume dealing with the physical properties of iron will be of special interest to physicists and covers the following subjects:

Atomic weight (by J. Meyer); iron atom (nucleus, electron shells, x-ray spectrum; size of the atom and the ions, etc., by E. Rabinowitsch); preparation of pure iron; pyrophoric and colloidal iron (D. Deutsch); modifications of iron and their stability limits; space lattice and crystal habit; specific gravity; expansion; compressibility; mechanical and thermal properties (by K. Fischbeck); optical properties (by W. Schütz); magnetic and electrical properties (by K. Fischbeck); electromotive and electrochemical behavior (by H. Danneel).

This modern volume is a worthy addition to the well-known "Handbuch."

I. M. KOLTHOFF
University of Minnesota

Gmelins Handbuch der anorganischen Chemie. Eighth edition. Published by the Deutsche Chemische Gesellschaft, Berlin, 1931.

System-Nummer 8, Jod, Vol. 1, pp. 244, price RM 37.

System-Nummer 45, Germanium, pp. 62, price RM 13.

System-Nummer 58, Kobalt, Vol. A, Part I, pp. 220, price RM 34.

System-Nummer 59, Eisen, Vol. B, part 4, pp. 657–872.

It is with gratitude and admiration that new additions to the eighth edition of "Gmelins Handbuch" will be received by physicists, chemists and biologists. The most successful, complete outline of the physical and chemical properties of elements and their compounds, their occurrence in nature, their technical, biological and pharmacological significance is an achievement by which this compilatory work gains a place in any physical or chemical library. The systematic and exhaustive treatment of the literature, in which not only references are made to the original periodicals, but also to the patents published, will be of invaluable aid to scholars in whatever field they may specialize. The four volumes announced above uphold the high scientific standing of the work.

I. M. KOLTHOFF
University of Minnesota

Annales de l'Institut Henri Poincare, Vol. I, sections iv. Pp. 122. Les Presses Universitaires de France, Paris.

In this section of the first volume, there are three articles. An introduction to the subject of band spectra is given by L. Bloch. Dirac discusses several quantum mechanical problems of interest, and Carleman treats the theory of singular integral equations.

The first article is evidently intended merely to give a sketch of the field. After the usual preliminaries, one is introduced to Hund's theory of vector combinations, with the inclusion of case (a) and case (b) only. A few remarks about some typical electronic transitions conclude the treatment. It is clear, but brief.

Dirac points out the similarity between quantum and classical statistics, and obtains the quantum mechanical analogue of Lionville's theorem. Next, the permutation theory is developed, in practically the same form as in his original article. This theory is rather special, since for most actual problems one must consider the rotation group as well as the permutation group. Perhaps a translation of the group theoretical work on rotations into a language similar to that of Dirac (i.e. where space rotations are constants of the motion) would be helpful. Dirac next shows how a hole in a closed shell may be described by means of a wave equation. Heisenberg, a year and a half later, has arrived at this result independently. It is to be regretted that the delay in the publication of these Annales is so great. A discussion of the relativistic electron forms the remainder of this article.

Carleman at first gives examples of singular integral equations. Then it is shown how every analytic function regular in a certain region is a fundamental function for a certain Hermitian kernel. This leads to a study of singular integral equations with Hermitian kernel and complex eigenvalue. They admit of at least one quadratically integrable solution. The concept of spectral function is defined, and the orthogonality properties of such functions discussed.

If the aim of these Annales is to present up to date subjects, then more speedy publication is necessary.

JAMES H. BARTLETT, JR.
University of Illinois

AUTHOR INDEX TO VOLUME 38

References with (A) are to abstracts of papers presented at meetings of the Physical Society and references with (L) are to Letters to the Editor.

Ahearn, A. J. Emission of secondary electrons from tungsten—1858, 1918(A)

Allison, Samuel K. Resolving power attainable in x-ray spectroscopy by photographic methods—203

——— **and Victor J. Andrew.** Experimental test of the ionization chamber method of measuring the relative intensities of x-ray spectrum lines—441

Almy, G. M. and G. D. Rahrer. Faint branches in the OH bands—1816

Almy, John E. Book review—1396

Anderson, O. E. (see More, K. R.)—1995

Andrew, Victor J. (see Allison, Samuel K.)—441

Aughey, Henry (see Kenny, A. W.)—1388(L)

Austin, J. B. Calculation of the characteristic frequency from the coefficient of compressibility—1788(L)

Bacher, R. F. (see Campbell, J. S.)—1906(L)

——— (see Meggers, W. F.)—1258(L)

Badger, Richard M. and John L. Binder. Absorption band in ethylene gas in the near infrared—1442

Badgley, Ralph E. (see Henderson, Joseph E.)—590(A)

Banta, H. E. (see Heaps, C. W.)—195(L)

Barker, E. F. (see Plyler, E. K.)—1827

Barnes, R. Bowling and M. Czerny. Concerning the reflection power of metals in thin layers for the infrared—338

Barrett, Charles S. Laue spots from perfect, imperfect, and oscillating crystals—832(L)

——— **and Carl E. Howe.** Regular reflection of x-rays from quartz crystals oscillating piezoelectrically. Some interpretations—2290(L)

Barth, Tom. F. W. (see Posnjak, E.)—2234

Bartlett, James H., Jr. Many-electron wave functions—1623

——— **and W. H. Furry.** Valence forces in lithium and beryllium—1615

——— Book reviews—1261, 1394, 1395, 2303

Bartlett, Russell S. Thermionic emission from a plane electrode—1566(L)

Bateman, H. On dissipative systems and related variational principles—815

Beams, J. W. (see Stevenson, E. C.)—133

Beams, J. W. (see Street, J. C.)—416

Bearden, J. A. Determination of e/m by the refraction of x-rays—1919(A)

——— Grating constant of calcite crystals—1389(L), 2089

——— Refraction of the copper K-series by quartz—835(L)

Becker, J. A. and R. W. Sears. Phenomena in oxide coated filaments II. Origin of enhanced emission—2193

Beeck, Otto and J. Carlisle Mouzon. Ionization of Kr and Xe by positive alkali ions and the ionization potentials of Ne, A, Kr, and Xe—967

Bender, Wm. Asymmetric Zeeman patterns at intermediate strengths of field in Ca I—588(A)

Bennett, R. D., J. C. Stearns, A. H. Compton. Constancy of cosmic rays—1566(L)

——— (see Compton, A. H.)—1565(L)

Berkey, W. E. and R. C. Mason. Measurements on the vapor stream from the cathode of a vacuum arc—943

——— (see Mason, R. C.)—1783(L)

——— (see Tanberg, R.)—296

Berry, N. E. and G. K. Rollefson. Transition probabilities and quenching in the $3P$ state of sodium—1599

Betsill, J. L. (see Doan, R. L.)—1922(A)

Binder, John L. (see Badger, Richard M.)—1442

Biswas, Susil Chandra. Diamagnetic susceptibility of the rare gas atoms according to Slater's method—1784(L)

Bitter, Francis. Magnetization and the magnetocaloric effect—528, 588(A)

——— Inhomogeneities in the magnetization of ferromagnetic materials—1903(L)

Blue, R. W. (see Giauque, W. F.)—196(L)

Bowen, I. S. Spectrum of doubly ionized carbon, C III—128

Bowers, Harold E. (see Harkins, William D.)—1845

Bozorth, R. M. and J. F. Dillinger. Transverse Barkhausen effect in iron—192(L)

Brackett, Fredrick S. and Urner Liddel. Infrared absorption bands of hydrogen cyanide in gas and liquid—582(A)

Bradbury, Norris. Absolute values of the mobilities of gaseous ions—1905(L)
——— (see Loeb, Leonard B.)—1716
Bradley, Charles A., Jr. (see Urey, Harold C.)—589(A), 718; 1969
Bramley, Arthur. Radioactive disintegration—1567(L)
Breit, G. Hyperfine structure of heavy elements—463
——— **and I. I. Rabi.** Measurement of nuclear spin—2082(L)
Brewer, A. Keith. Effect of adsorbed K^+ ions on the photoelectric threshold of iron—401
Brice, Brooks A. Absorption band spectra of silver bromide and silver iodide vapors—658
Bridgman, P. W. The P-V-T relations of NH_4Cl and NH_4Br, and in particular the effect of pressure on the volume anomalies—182
——— Book review—1082
Briggs, H. B. (see Ives, Herbert E.)—1477, 1917(A)
Brown, Joseph G. Relation of atmospheric space-charge to turbulence and convection—587(A)
Brown, Weldon G. Infrared absorption band system of iodine—1187
——— Note on the heat of dissociation of iodine—709
——— Vibrational quantum analysis of the visible absorption bands of bromine—1179
Brown, W. L. and H. McN. Cowan. Oscillations in discharge tubes—376(L)
Broxon, James W. Residual ionization in nitrogen at high pressures—1704
——— Dielectric constant of commercial nitrogen at high pressures—2049
Brune, O. Equivalent electrical networks—1783(L)
Bryden, Samuel D., Jr. Allowed levels for equivalent (s, p, d, f) electrons with (jj) coupling—1145
——— The structure of the nucleus and its total moment of momentum—1989
Bush, V. and S. H. Caldwell. Thomas-Fermi equation solution by the differential analyzer—1898

Calbick, C. J. (see Davisson, C. J.)—585(A)
Caldwell, S. H. (see Bush, V.)—1898
Callihan, Dixon (see Hatley, C. C.)—909
Campbell, J. S. and R. F. Bacher. Nuclear moments of indium and gallium—1906(L)
——— **and W. V. Houston.** Revision of values of e/m from the Zeeman effect—581(A)
Campbell, J. W. Book review—1910
Cardwell, Alvin B. Photoelectric and thermionic emission from cobalt—2033
——— Photoelectric properties of tantalum—2041
Carlson, J. F. and J. R. Oppenheimer. Range of fast electrons and neutrons—1787(L)
Child, C. D. Absorption of light by flames containing sodium—699
Chow, T. C. and H. D. Smyth. Emission and absorption spectra in sulphur dioxide—838(L)
Christy, Andrew (see Mulliken, Robert S.)—87
Claus, W. D. Effect of temperature on the intensity of x-rays diffusely scattered from rocksalt—604
Compton, A. H., R. D. Bennett, J. C. Stearns. Ionization as a function of pressure and temperature—1565(L)
——— (see Bennett, R. D.)—1566(L)
Condon, E. U. Book reviews—1081, 1909
Constant, F. W. (see Lowance, F. E.)—1547
Cook, S. R. Electromagnetic theory of sight and color vision—587(A)
Cooke, F. W. Ionization of caesium vapor by light—1351
Copley. M. J. (see Guthrie, A. N.)—360
Cork, James M. (see Fox, Gerald W.)—1420
Cotton, J. C. (see Knauss, H. P.)—1190
Coven, Allen W. Scattering of x-rays from paraffin, aluminum, copper and lead—1424
Cowan, H. McN. (see Brown, W. L.)—376(L)
Crigler, Elizabeth A. Intensity of Raman lines in estimating the concentration of the components present in benzene-toluene mixtures—1387(L)
Czerny, M. (see Barnes, R. Bowling)—338

Dahm, Thos. M. Effect of inductance on the electromagnetically damped galvanometer—590(A)
Danforth, W. E., Jr. Dielectric constant of liquids under high pressure—1224
Davey, Wheeler P. (see Phelps, Robert T.)—1919(A)
Davisson, C. J. and C. J. Calbick. Electron lenses—585(A)
——— Book review—1262
Deming, W. Edwards and Lola E. Shupe. Some physical properties of compressed carbon monoxide—1920(A), 2245
Dennison, David M. and Norman Wright. New long wave-length absorption band of CS_2—2077(L)
Dieke, G. H. Perturbations in the helium band spectrum—646
Dillinger, J. F. (see Bozorth, R. M.)—192(L)
Dillon, J. H. Photoelectric properties of zinc single crystals—408
Doan, R. L. and J. L. Betsill. Force relations in drawing copper wire—1922(A)
Doermann, F. W. and Otto Halpern. Elastic scattering of electrons by spherically symmetrical atoms—193(L)
DuMond, Jesse W. M. and Archer Hoyt. A new K-series x-ray line due to Fermi-Sommerfeld electrons—839(L)

DuMond, Jesse W. M. and Harry A. Kirkpatrick. Dependence of Compton line breadth on primary wave-length with the multi-crystal spectrograph —1094

Dunnington, Frank G. Electro-optical shutter—its theory and technique—1506

——— Optical study of the formation stages of spark breakdown—1535

Edwards, Hiram W. Interference in thin metallic films—166

Edwards, R. L. (see Stewart, G. W.)—1575

Eldridge, John A. Book reviews—1793, 1794

Ellett, A. (see Zahl, H. A.)—977

Ellis, Joseph W. Polymers and new infrared absorption bands of water—582(A), 693

Epstein, Paul S. Modern statistics from the Gibbsian point of view—590(A)

Erikson, Henry A. Book review—1396

Estermann, I., R. Frisch and O. Stern. Diffraction experiments with monochromatic molecular beams —584(A)

Fisher, Thomas F. (see Serduke, James T.)—1922 (A)

Focke, A. B. (see Goetz, A.)—1569(L)

Forsythe, W. E. Intercomparison of the high temperature scale—1247

Fowler, R. H. Analysis of photoelectric sensitivity curves for clean metals at various temperatures— 45

Fox, Gerald W. and James M. Cork. Regular reflection of x-rays from quartz crystals oscillating piezoelectrically—1420

Frank, N. H. Theory of thermionic emission—1918 (A)

——— **and L. A. Young.** Transmission of electrons through potential barriers—80

——— (see Young, L. A.)—838(L)

Freed, Simon. Electronic transitions between an inner shell and the virtual outer shells of the ions of the rare earths in crystals—2122

——— **and Frank H. Spedding.** Diagram of some of the energy levels of gadolinium IV in the crystal lattice as obtained from the ultraviolet absorption spectra of $GdCl_3 \cdot 6H_2O$ and $GdBr_3 \cdot 6H_2O$ —670

Frenkel, J. Some remarks on the theory of the photoelectric effect—309

Frisch, R. (see Estermann, I.)—584(A)

Furry, W. H. (see Bartlett, James H., Jr.)—1615

Gartlein, C. W. and R. C. Gibbs. Production of second and third spark spectra in a hollow cathode lamp—1907(L)

Giauque, W. F., R. W. Blue, Roy Overstreet. Entropies of methane and ammonia—196(L)

Gibbs, R. C. and P. G. Kruger. Some evidence indicating the existence of Ba isotopes 136 and 137 —1921(A)

——— (see Gartlein, C. W.)—1907(L)

——— (see Shapiro, C. V.)—1170

Gideon, Edith (see Henderson, Joseph E.)—586(A)

Gilroy, Helen T. Certain spectra in the vanadium I iso-electronic sequence—2217

Glasoe, G. Norris. Contact potential difference between iron and nickel and their photoelectric work functions—1490

Goetz, A. and A. B. Focke. Metamagnetism in bismuth crystals—1569(L)

——— **and R. C. Hergenrother.** Macroscopic and lattice expansion of Bi single crystals—2075(L)

Gortner, R. A. Book reviews—2084, 2088

Goudsmit, S. and L. Gropper. Many-electron selection rules—225

Gray, Newton M. and Lawrence A. Wills. Note on the calculation of zero order eigenfunctions—248

Green, J. B. and R. A. Loring. Multiplet structure and Zeeman effect—1289

——— **and John Wulff.** Paschen-Back effect of hyperfine structure I. Tl II and Tl III—2176

——— **and John Wulff.** Paschen-Back effect of hyperfine structure II. Bi II and Bi III—2186

Gropper, L. (see Goudsmit, S.)—225

Gunn, Ross. Stability of the atmosphere of a rotating star—1052

Guthrie, A. N. and M. J. Copley. Magnetic moment of the palladium atom—360

Hall, Harvey. Relativistic theory of the photoelectric effect. Part I. Theory of the *K*-absorption of x-rays—57

——— **and J. R. Oppenheimer.** Part II. Photoelectric absorption of ultragamma radiation—57, 589(A)

Halpern, Otto (see Doermann, F. W.)—193(L)

Harder, Oscar E. Book reviews—1573

Hardy, J. D. High resolution in the infrared—2162

Harkins, William D. Periodic system of atomic nuclei and the principle of regularity and continuity of series—1270; a correction—1792(L)

——— **and Harold E. Bowers.** Raman effect and the carbon-halogen bond—1845

Harrington, Marshall C. Secondary emission from nickel by impact of metastable atoms and positive ions in helium—1312

Harrison, George R. Quantitative intensity determinations in the spectra of normal and of singly ionized vanadium, V I and V II—1921(A)

George R. Harrison and M. H. Johnson, Jr. Intensity summation rules and perturbation effects in complex spectra—757
——— **and Philip A. Leighton.** Spectral fluorescence efficiencies of certain substances with applications to heterochromatic photographic photometry—899
Hartig, Henry E. Book review—1081
Harvey, G. G. Diffuse scattering of x-rays from sylvine—593
——— (see Jauncey, G. E. M.)—1071(L); 1925
Hatley, C. C. and Dixon Callihan. Effect of varying concentrations of certain electrolytes on the violet band of the Raman spectra of water—909
Haupt, Curtis R. Probability law governing ionization by electron impact in mercury vapor—282
Heaps, C. W. Thermocouples of longitudinally and transversely magnetized wires—1391(L)
——— **and H. E. Banta.** Effect of internal stress on magnetic susceptibility—195(L)
Heitler, W. Quantum theory and electron pair bond—243
Henderson, Joseph E. and Ralph E. Badgley. Work required to remove a field electron—590(A)
——— **and Edith Gideon.** Effects due to the bombardment of platinum by mercury ions—586(A)
Hergenrother, R. C. (see Goetz, Alexander)—2075(L)
Heyworth, Dorothy. Crystal structure of arsenic triiodide, AsI_3—351
——— Note on the crystal structure of arsenic triodide—1792(L)
Hicks, Victor. Corrected relative intensities of the x-ray lines in the tantalum *L*-series—572(L)
Hiedemann, Egon. Electronic velocities in the positive column of high frequency discharges—198(L)
High, M. E. Raman effect in certain organic compounds—1837
——— **and M. L. Pool.** Removal of continuous background from Raman spectrum of carbon tetrachloride—374(L)
Hill, E. L. Note on the general solution of Schrödinger's equation and the uncertainty principle—2115
——— One-dimensional problems in quantum mechanics—1258(L)
——— Reflection of electrons by a special potential field—1072(L)
——— Book reviews—842, 1260, 1794
Hirsh, F. R., Jr. Satellites of *M*-series x-ray lines—914
Hollaender, Alexander and John Warren Williams. Molecular scattering of light from amorphous and crystalline solids—1739
Holzer, Robert E. Absorption of hydrogen positive rays in helium and argon—585(A)
Houghton, H. G. Transmission of visible light through fog—152
——— (see Stratton, J. A.)—159
Houston, William V. Structure of soft x-ray lines—1797
——— (see Campbell, J. S.)—581(A)
Howe, Carl E. (see Barrett, Charles S.)—2290(L)
Hoyem, A. G. Some electrical properties of spectroscopically pure zinc crystals—1357
——— (see Tyndall, E. P. T.)—820
Hoyt, Archer (see DuMond, Jesse W. M.)—839(L)
Huang, Tzu Ching. Further application of Huang's general equations of energy and entropy of gases: the general adiabatic equation of gases—1385
Hubbard, J. C. Acoustic resonator interferometer: I. the acoustic system and its equivalent electric network—1011
Huff, L. D. Motion of a Dirac electron in a magnetic field—501, 589(A)
——— Neutrons and cosmic rays—2292(L)
Hughes, A. L. Book review—1262
Hughes, D. S. Isotope separation in the spectra of Li I—857
Hulburt, E. O. Temperature of the lower atmosphere of the earth—1876
Hutchisson, Elmer. Band spectrum intensities by graphical methods—1921(A)
Huxford, W. S. Effect of electric fields on the emission of photoelectrons from oxide cathodes—379

Inglis, David R. Energy relations in complex spectra—862
——— **and M. H. Johnson, Jr.** Zeeman effect in intermediate coupling—1642
Ives, Herbert E. Exhibition of parallax panoramagrams made with a large diameter concave mirror—1922(A)
——— Vectorial photoelectric effect in thin films of alkali metals—1209, 1917(A)
——— **and H. B. Briggs.** Photoelectric effect from thin films of alkali metal on silver—1477, 1917(A)

Jackson, Dunham. Book review—1913
Jauncey, G. E. M. Scattering of x-rays by gases and crystals—1
——— Scattering of x-rays from polyatomic gases—194(L)
——— **and G. G. Harvey.** Diffuse scattering of x-rays from sylvine at low temperature—1925
——— **and G. G. Harvey.** Relation between the scattering of x-rays by gases and crystals—1071(L)

Jenkins, F. A., Yale K. Roots and Robert S. Mulliken. Red CN band system—1075(L)
Johnson, J. R. (see Shapiro, C. V.)—1170
Johnson, M. H., Jr. Spectra of two-electron systems—1628
——— (see Harrison, George R.)—757
——— (see Inglis, D. R.)—1642
Johnson, Thomas H. de Broglie wave spectrum from the secondary structure of LiF—586(A)
Johnston, Helen (see Urey, Harold C.)—581(A), 2131
Jones, Arthur Taber. Stability of a single file of straight vortices—2068
Jordan, W. H. (see Roller, Duane)—396

Kaplan, C. Strain-energy function for isotropic bodies—1020
Kaplan, Joseph. Auroral spectrum—582(A)
——— Forced predissociation in nitrogen—373(L)
——— Light of the night sky—1048
——— New criterion for predissociation—1079(L); correction—1792(L)
——— Predissociation in nitrogen and excitation of the green auroral line—1079(L)
——— Book review—1574
Kennard, E. H. (see Roess, Louis C.)—1263
Kennard, R. B. Optical study of heat transfer by convection from solid surfaces to air—1921(A)
Kennedy, Roy J. and Edward M. Thorndike. Search for an electrostatic analogy to the gravitational red shift—591(A)
Kenney, A. W. and Henry Aughey. X-ray diffraction patterns of mixtures—1388(L)
Kenty, Carl. Photoelectric and metastable atom emission of electrons from surfaces—377(L)
——— Photoelectric efficiencies in the extreme ultraviolet—2079(L)
Keyes, F. G. (see Kirkwood, J. G.)—576(L)
King, Arthur S. Features of the spectra of thulium, ytterbium, and lutecium under different excitations—583(A)
——— Spectra of high current vacuum arcs—590(A)
——— (see Meggers, W. F.)—1258(L)
Kingsbury, B. A. Shot effect in photoelectric currents—1458, 1922(A)
Kingsbury, E. F. Thermionic emission in caesium-oxide photocells at room temperatures—1918(A)
Kirkpatrick, Harry A. (see DuMond, Jesse W. M.)—1094
Kirkpatrick, Paul. Lateral space distribution of x-ray photoelectrons—1938
Kirkwood, J. G. and F. G. Keyes. Second virial coefficient—576(L)
Knauss, H. P. and J. C. Cotton. Ultraviolet bands of CO in the electrodeless ring discharge—1190
Knipp, Charles T. and Julian K. Knipp. Electrodeless discharge: Method of measuring induced current, variation of current with pressure for various gases—948
Knipp, Julian K. (see Knipp, Charles T.)—948
Kolthoff, I. M. Book reviews—1793, 2302, 2303
Korff, S. A. Absorption line width in sodium vapor—477
——— Book review—1081
Krishnan, K. S. Magnetic anisotropy of ions of the type XO_3—833(L)
Kruger, P. G. (see Gibbs, R. C.)—1921(A)

Langer, R. M. Absence of spin in nuclear electrons—837(L)
——— Schrödinger potential function—779
——— X-ray reflections from oscillating crystals—573(L)
Langmuir, Irving. Diffusion of electrons back to an emitting electrode in a gas—1656
——— **and K. J. Sixtus.** Regions of reversed magnetization in strained wires—2072(L)
Laporte, Otto, George R. Miller and Ralph A. Sawyer. First spark spectrum of rubidium (Rb II)—843
Lapp, C. J. Book review—1394
Lawrence, Ernest O. and M. Stanley Livingston. Production of high speed protons without the use of high voltages—834(L)
——— **and David H. Sloan.** High velocity mercury ions—586(A)
——— (see Sloan, David H.)—2021
Leighton, Philip A. (see Harrison, George R.)—899
Leland, O. M. Book review—1393
Lewis, Gilbert N. More fundamental thermodynamics—376(L)
Liddel, Urner (see Brackett, Fredrick S.)—582(A)
Linder, Ernest G. Dissociation of water in the glow discharge—679
Lindsay, R. B. Canonical transformation and the vibrations of a loaded string—491
Livingston, M. Stanley (see Lawrence, Ernest O.)—834(L)
Livingston, Robert. Book reviews—1795, 2084, 2301
Llewellyn, F. B. Book review—1397
Locher, G. L. (see Mott-Smith, L. M.)—1399
Loeb, Leonard B. Mobility of Na^+ ions in N_2 and H_2 as a function of time—549, 586(A)
——— Sparking potential and electrode material—1891
——— **and Norris E. Bradbury.** Velocity spectrum of normal gaseous ions in air and the problem of ionic structure—1716

Longden, A. C. Absolute determination of gravity —1920(A)
Loomis, F. W. Rotational structure of the red bands of potassium—2153
——— **and R. E. Nusbaum.** Magnetic rotation spectrum and heat of dissociation of the lithium molecule—1447
——— **and R. W. Wood.** Nuclear spin of potassium —854
Loring, R. A. (see Green, J. B.)—1289
Lowance, F. E. and F. W. Constant. Structure sensitiveness of magnetism in metals—1547
Luhr, Overton. Mass of positive ions in a glow discharge—1730
Luyten, W. J. Book reviews—1911, 1912, 2085, 2301

MacDougall, D. P. Entropies of methane and ammonia—2074(L)
——— Heat capacity of methane—2296(L)
MacDougall, F. H. Book reviews—201, 2086
McKeehan, L. W. Conservation of energy and the disintegration of RaE—2292(L)
McMillan, Edwin. Electrical field giving uniform deflecting force on a molecular beam—1568(L)
Mack, J. E. Excitation of high optical energy levels —193(L), erratum—2300(L)
Mackeown, S. S. Transition from a glow discharge to an arc—584(A)
Margenau, Henry. Equation of state of real gases —1785(L)
——— Role of quadrupole forces in van der Waals attractions—747
——— Surface energy of liquids—365
Marston, D. S. (see Zumstein, R. V.)—305
Mason, R. C. Cathode fall of an arc—427
——— **and W. E. Berkey.** Reaction due to gas molecules leaving the cathode of an arc—1783(L)
——— (see Berkey, W. E.)—943
Matuyama, E. (see Okubo, J.)—1651
Maxwell, Louis R. Average life of the ionized helium atom—1664
Meggers, W. F., A. S. King, R. F. Bacher. Hyperfine structure and nuclear moment of rhenium—1258(L)
Melvin, Eugene H. (see Wulf, Oliver R.)—330
——— **and Oliver R. Wulf.** Band spectra due to the molecule N_2O_3—2294(L)
Meyer, Alfred Wesley. Diffraction of x-rays in organic mixtures—1083
Michels, Walter C. Low voltage excitation of sodium—712
Miller, George R. (see Laporte, Otto)—843
Millis, John S. Zeeman effect in the ortho-helium band spectrum—1148
Milne, W. E. Book review—1913
Mitchell, Allan C. G. Effect of hyperfine structure on the polarization of cadmium resonance radiation—473
Mohler, F. L. Emission spectrum of metallic silver under electron bombardment and its relation to the absorption spectrum—1923(A)
Montgomery, Carol G. Magnetization of colloidal suspensions—1782(L)
More, K. R. and O. E. Anderson. Note on the excitation of the arc spectrum of nitrogen—1995
Morris, Charles S. Raman spectra of certain organic liquids—141
Morton, G. A. Atomic scattering power of copper and oxygen in cuprous oxide—41
Mott-Smith, L. M. and G. L. Locher. New experiment bearing on cosmic-ray phenomena—1399
Mouzon, J. Carlisle (see Beeck, Otto)—967
Mueller, Donald W. and H. D. Smyth. Negative hydrogen ions from H_2O by electrons of a critical velocity—1920(A)
Müller, Hans. Kerr-effect in Rochelle salt—1922(A)
Mulliken, Robert S. Note on the interpretation of the BeF bands—836(L)
——— **and Andrew Christy.** A-type doubling and electron configurations in diatomic molecules—87
——— (see Jenkins, F. A.)—1075(L)
——— Book Review—2301
Murphy, George M. (see Urey, Harold C.)—575(L)
Muskat, Morris. Anomalous scattering of alpha-rays—23

Naudé, S. Meiring. Rotational analysis of the first positive nitrogen (N_2) bands—372(L)
Neher, H. V. Scattering of high velocity electrons by thin foils—585(A), 1321
Nettleton, L. L. Book review—1397
Nickerson, John L. Current-intensity relation of the $\lambda 600$ band of helium—1907(L)
Nielsen, Harald H. Infrared bands of slightly asymmetric molecules—1432
Nielsen, Walter M. Effect of temperature on the continuous band spectrum of mercury vapor—888
Nile, S. W. Calculation of effective nuclear magnetic moments from hyperfine structure—375(L)
Nishikawa, S., Y. Sakisaka and I. Sumoto. Note on "Effect of piezoelectric oscillation on the intensity of x-ray reflections from quartz"—1078(L)
Nottingham, W. B. Transmission of electrons through potential barrier of thoriated filament—1918(A)
Nusbaum, R. E. (see Loomis, F. W.)—1447
Nutting, G. C. (see Spedding, F. H.)—2294

O'Bryan, H. M. Reflecting power and grating efficiency in the extreme ultraviolet—32

Okubo, J. and E. Matuyama. Appearance of the forbidden lines and the intensity modifications of the spectra of mercury, cadmium and zinc under high frequency excitation—1651
Olpin, A. R. Correlating the selective photoelectric effect with the selective transmission of electrons through crystalline surface structures—1917(A)
——— An interpretation of the selective photoelectric effect from two-component cathodes—1745
Onsager, Lars. Reciprocal relations in irreversible processes: II—2265
Oppenheimer, J. R. Note on light quanta and the electromagnetic field—725
——— (see Carlson, J. F.)—1787(L)
——— (see Hall, Harvey)—57, 589(A)
Overstreet, Roy (see Giauque, W. F.)—196(L)

Page, Leigh. Book review—199
Pardue, Louis A. Dispersion of x-rays in calcite—1808
Pauling, Linus. Book review—199
Phelps, Robert T. and Wheeler P. Davey. X-ray study of the nature of solid solutions—1919(A)
Phipps, T. E. (see Shaw, E. J.)—174
Pielemeier, W. H. Supersonic satellites and velocity—1236
Pierce, W. C. Effect of general radiation in the diffraction of x-rays by liquids—1409
——— Higher order effects in the diffraction of x-rays by liquids—1413
Pietenpol, W. B. and E. C. Westerfield. Problem of rotating magnets—2280
Plyler, E. K. Structure of the water vapor molecule—1784(L)
——— **and E. F. Barker.** Infrared spectrum and the molecular configuration of N_2O—1827
Pokrowski, G. I. New effect produced by action of x-rays on matter—925
Pool, M. L. Life of metastable mercury and evidence for a long-lived metastable vibrating nitrogen molecule—955
——— (see High, M. E.)—374(L)
Posnjak, E. and Tom. F. W. Barth. New type of crystal fine-structure lithium ferrite ($Li_2O \cdot Fe_2O_3$)—2234
Potapenko, G. V. Production of ultra-short undamped electromagnetic waves—584(A)
Pyle, W. R. Dielectric constants of certain organic liquids at medium frequency—1057

Rabi, I. I. (see Breit, G.)—2082(L)
Rahrer, G. D. (see Almy, G. M.)—1816
Randall, H. M. and Norman Wright. Infrared spectrum of Sn I—457
Reyerson, L. H. Book review—1910
Rice, Oscar Knefler. Collision problems involving large interactions—1943
Richtmyer, R. D. Upper atomic-number limits for satellites of the x-ray line $L\beta_2$—1802
Rinde, C. A. Note on the relation of wave-length to color sensation—588(A)
Robertson, H. P. Book review—2302
Roess, Louis C. and E. H. Kennard. X-ray absorption by a Thomas-Fermi atom—1263
Rojansky, V. and W. Wetzel. Quantum-mechanical reflection coefficients and their numerical determination—1979
Rollefson, G. K. (see Berry, N. E.)—1599
Roller, Duane, W. H. Jordan and C. S. Woodward. Some photoelectric properties of mercury films—396
Romig, W. Doppler effect in the canal rays in neon—1709
Roots, Yale K. (see Jenkins, F. A.)—1075(L)
Rosen, N. Calculation of interaction between atoms with *s*-electrons—255
——— Normal state of the hydrogen molecule—2099
Ross, William H. Thermocouples whose elements are longitudinally and transversely magnetized wires of nickel and of iron—179
Ruark, Arthur E. Natural units for atomic problems—2240
Rudnick, Philip. Capture and loss of electrons by helium ions in helium—1342

Sakisaka, Y. (see Nishikawa, S.)—1078(L)
Saunders, F. A. Book review—842
Sawyer, Ralph A. (see Laporte, Otto)—843
——— **and Kenneth Thomson.** Deepest term in the Au II spectrum—2294(L)
Schultze, G. (see Villars, D. S.)—998
Schwede, Harold F. (see Struve, Otto)—1195
Sears, R. W. (see Becker, J. A.)—2193
Seass, Stewart. Thermocouples whose elements are longitudinally and transversely magnetized ferromagnetic substances—1254
Serduke, James T. and Thomas F. Fisher. Hall effect in solid mercury—1922(A)
Shapiro, C. V., R. C. Gibbs, and J. R. Johnson. Band spectrum of benzene: existence of a small vibrational frequency in the normal state—1170
Shaw, E. J. and T. E. Phipps. Magnetic moment of the diatomic sulfur molecule—174
Shenstone, A. G. Ultra-ionization potentials in mercury vapor—873
Shih, J. W. Magnetic properties of gold-iron alloys—2051

Shortley, George H. Inverse-cube central force field in quantum mechanics—120
Shrader, J. E. Three-dimensional vibrograph—1923 (A)
Shupe, Lola E. (see Deming, W. Edwards)—1920 (A), 2245
Sixtus, K. J. (see Langmuir, Irving)—2072(L)
Slater, J. C. Molecular energy levels and valence bonds—1109
——— Note on the structure of the groups XO_3—325
——— Quantum theory of the equation of state—237
Sleator, W. W. New absorption bands of ammonia, methyl bromide, methyl iodide and carbon dioxide in the infrared spectrum—147
Sloan, David H. and Ernest O. Lawrence. Production of heavy high speed ions without the use of high voltages—2021
——— (see Lawrence, E. O.)—586(A)
Smith, Lloyd P. Evaluation of the matrix components for helium—1961
Smith, T. Townsend. Book review—578
Smyth, H. D. Emission spectrum of carbon dioxide—2000
——— (see Chow, T. C.)—838(L)
——— (see Mueller, Donald W.)—1920(A)
Soller, Walter. Graphical determination of all crystal lattices from x-ray powder method data—583 (A)
Sommerfeld, A. Angular distribution of photoelectrons—1078(L)
Spedding, Frank H. Zeeman effect in solids—2080(L)
——— **and G. C. Nutting.** A. Effect of crystal symmetry on the energy levels of solids. B. Experimental evidence of definite orientations of coordinated water molecules about rare earth ions in solution—2294
——— (see Freed, Simon)—670
Spencer, Roy G. Absorption of soft x-rays in gases—1932
——— Additional theory of the double x-ray spectrometer—618
——— Study of the shape of the Ag *L*, Mo *K* and Cu *K* lines—630
Stearns, J. C. (see Bennett, R. D.)—1566(L)
——— (see Compton, A. H.)—1565(L)
Stenstrom, K. W. Book reviews—1392, 1398
Stern, O. (see Estermann, I.)—584(A)
Stevens, Daniel S. Rotational analysis of the first negative group of oxygen (O_2^+) bands—1292
Stevenson, E. C. and J. W. Beams. Electro-optical Kerr effect in gases—133
Stewart, G. W. X-ray study of the magnetic character of liquid crystalline para-azoxyanisol and a comparison with the isotropic liquid—931
——— **and R. L. Edwards.** Comparison of viscosity and molecular arrangement in twenty-two liquid octyl alcohols—1575, 2082(L)
Stewart, John Q. Nebular red shift and universal constants—2071(L)
Stewart, O. M. Book review—1794
Stratton, J. A. and H. G. Houghton. Theoretical investigation of the transmission of light through fog—159
Street, J. C. and J. W. Beams. Fall of potential in the initial stages of electrical discharges—416
Strong, John. Investigations in the far infrared—583(A), 1818
Struve, Otto and Harold F. Schwede. Intensities of Balmer emission lines in stellar spectra—1195
Stuart, H. A. Internal molecular potential between the substituent groups in a benzene ring as derived from the heats of combustion—1372
Sumoto, I. (see Nishikawa, S.)—1078(L)
Swann, W. F. G. Book reviews—199, 2086

Tanberg, R. and W. E. Berkey. Temperature of cathode in vacuum arc—296
Terroux, F. R. (see Watson, W. H.)—2291(L)
Thompson, James S. New method producing negative ions—1389(L)
Thomson, Kenneth. (see Sawyer, R. A.)—2293(L)
Thorndike, Edward M. (see Kennedy, Roy J.)—591(A)
Tolman, Richard C. Nonstatic model of universe with reversible annihilation of matter—797
——— On the theoretical requirements for a periodic behaviour of the universe—1758
——— Book review—578
Tonks, Lewi. Increase in surface area due to crystal faces developed by etching—1030
——— Plasma-electron resonance, plasma resonance and plasma shape—1219
Turner, Louis A. Enhancement of predissociation by collisions—574(L)
Tyndall, E. P. T. and A. G. Hoyem. Resistivity of single crystal zinc—820

Uber, Fred M. X-ray absorption coefficients of mercury vapor in the region of its *L*-absorption discontinuities—217
Uhlenbeck, G. E. (see Van Lear, G. A., Jr.)—1583
——— Book review—1392
Urey, Harold C. The alternating intensities of Na_2 bands—1074(L)
——— **and Charles A. Bradley, Jr.** Relative abundances of isotopes—589(A), 718
——— **and Charles A. Bradley, Jr.** Vibrations of pentatonic tetrahedral molecules—1969

Urey, Harold C. and Helen Johnston. Absorption spectrum of chlorine dioxide—581(A), 2131
——— **and George M. Murphy.** Relative abundance of N^{14} and N^{15}—575(L)
Valasek, Joseph. Book review—1573
Van Atta, L. C. Excitation probabilities for electrons in helium, neon, and argon—876
Van de Graaff, Robert J. 1,500,000 volt electrostatic generator—1919(A)
Van Lear, G. A., Jr. and G. E. Uhlenbeck. Brownian motion of strings and elastic rods—1583
Van Vleck, J. H. Book reviews—1260, 2301
Vaughan, Alfred L. Mass spectrograph analyses, and critical potentials for the production of ions by electron impact, in nitrogen and carbon monoxide —1687
Villars, Donald Statler. Entropy of polyatomic molecules—1552, 1920(A)
——— **and G. Schultze.** Low temperature rotational heat capacities and the relative amounts of the nuclear singlet, triplet and quintet symmetry modifications of methane—998
Vollrath, R. E. 500 kilovolt cathode rays—212

Wahlin, H. B. Emission of positive ions from Cu and Ag—1074(L)
Warner, A. H. Determination of the photoelectric threshold for tungsten by Fowler's method—1871
Warren, B. E. Interpretation of the effect of piezoelectric oscillations on the intensity of x-ray reflections from quartz—572(L)
Washburn, E. W. Crystalline rubber hydrocarbon—1790(L)
Washburn, Harold W. Electro-optical shutter—584(A)
Waterman, A. T. Equilibrium distribution of potential and of electrons outside the surface of a conductor—1497
Watson, David L. Quantization of large scale events —1072(L)
Watson, W. H. and F. R. Terroux. Note on range of fast electrons and neutrons—2291(L)
Webb, J. H. Potential due to a buried spheroid—2056
Weizel, Walter. Broadening of the resonance atomic line of helium—642
Wellman, B. Reaction due to gas molecules leaving the cathode of an arc—1077(L)
Westerfield, E. C. (see Pietenpol, W. B.)—2280
Wetzel, W. Transmission of electrons through an electrical condenser—1205
——— (see Rojansky, V.)—1979
White, H. E. Auto-ionization in the alkaline earth metals and the inert gases—1786(L) 2016
White, H. E. Comparison of the classical electron orbital models with the probability density $\psi\psi^*$ of the Schrödinger and the Dirac solutions of hydrogen-like atoms—589(A)
——— Do protons in the nucleus possess orbital angular momentum?—2078(L)
——— Pictorial representations of the Dirac electron cloud for hydrogen-like atoms—513
Whitmer, Charles A. *M*-series absorption spectrum of tantalum—1164
Williams, E. H. Magnetic properties of copper-nickel alloys—828
Williams, John Warren. (see Hollaender, Alexander) 1739
Williamson, R. C. Book reviews—1909
Wills, Lawrence A. (see Gray, Newton M.)—248
Winans, J. Gibson. New emission bands in mercury vapor—583(A)
Winch, Ralph P. Photoelectric properties of thin unbacked gold films—321
Wollan, E. O. Experimental electron distribution in atoms of monatomic gases—15
Womer, R. L. Ionization of helium, neon and argon —454
Woo, Y. H. Temperature and diffuse scattering of x-rays from crystals—6
Wood, R. W. Absorption spectra of salts in liquid ammonia—1648
——— Raman effect for benzene substitution products by improved technique—2168
——— Selective thermal radiation of colored and pure fused quartz—487
——— Stereophotographic models of electron motion in Stark effect—346
——— (see Loomis, F. W.)—854
Woodcock, K. S. Emission of negative ions under the bombardment of positive ions—1696
Woodward, C. S. (see Roller, Duane)—396
Workman, E. J. Temperature variation of the specific heat (C_p) of CO_2 at 65.3 kg/cm² pressure; the specific heat (C_v) of helium as a function of pressure—587(A)
Wright, Norman (see Dennison, David M.)—2077 (L)
——— (see Randall, H. M.)—457
Wulf, Oliver R. and Eugene H. Melvin. Effect of temperature upon the ultraviolet band spectrum of ozone and the structure of this spectrum—330
——— (see Melvin, Eugene H.)—2294(L)
Wulff, John (see Green, J. B.)—2176, 2186

Yagoda, Herman. Estimation of the spectrum of the element of atomic number 87—2298(L)
Young, Lloyd A. Note on local momentum in wave mechanics—1612

Young, Lloyd A. and N. H. Frank. Temperature dependence of photoelectric effect in metals—838(L)
——— (see Frank, N. H.)—80
Zachariasen, W. H. Interpretation of the selective photoelectric effect from two-component cathodes —2290(L)
Zahl, H. A. and A. Ellett. Reflection of mercury from alkali halide crystals—977
Zahn, C. T. Temperature variation of the electric moment of ethylene chloride—521
Zeleny, John. Aging of ions in air and nitrogen—969
——— Distribution of mobilities of ions in air—2293(L)
Zener, Clarence. Probabilities of low-velocity inelastic collisions—277, 588(A)
Ziegler, G. E. Crystal structure of sodium nitrite, $NaNO_2$—1040
Zumstein, R. V. Wave-length standards in the spectra of aluminum, silicon and bismuth in the Schumann region—2214
——— **and D. S. Marston.** Wave-length standards in the spectra of carbon and tin in the Schumann region—305
Zwicky, F. Permanent electric and magnetic moments of crystals—1772

ANALYTIC SUBJECT INDEX TO VOLUME 38

References marked (A) are to abstracts of papers presented at meetings of the Physical Society, those marked with (L) are to Letters to the Editor.

Absorption of light (see also **Spectra, absorption**)
By flames containing sodium, C. D. Child—699
Transmission of visible light through fog, H. G. Houghton—152; theoretical investigation, J. A. Stratton, H. G. Houghton—159
Acoustics
Resonator interferometer, equivalent electric network, J. C. Hubbard—1011
Supersonic waves, velocity, W. H. Pielemeier—1236
Alpha-particles (see also **Radioactivity**)
Anomalous scattering, Morris Muskat—23
Arcs (see also **Discharge of electricity in gases**)
Cathode fall for thermionic and high field arcs, R. C. Mason—427
Temperature of cathode, vapor stream, R. Tanberg, W. E. Berkey—296
Transition from glow to arc, S. S. Mackeown—584(A)
Velocity of, vapor stream from cathode, R. Tanberg, W. E. Berkey—296, W. E. Berkey, R. C. Mason—943, 1783(L) B. Wellman 1077(L)
Astrophysics
Intensities of Balmer emission lines in stellar spectra, O. Struve, H. F. Schwede—1195
Nebular red shift and universal constants, J. Q. Stewart—2071(L)
Stability of atmosphere of a rotating star, electromagnetic fields, R. Gunn—1052
Atomic and molecular beams
Absorption of H^+, H_2^+, H_3^+ in A and He, R. E. Holzer—585(A)
Diffraction of He by LiF crystals, I. Estermann, R. Frisch, O. Stern—584(A)
Electrical field giving uniform deflecting force on a molecular beam, E. McMillan—1568(L)
Of Pd, A. N. Guthrie, M. J. Copley—360
Reflection of H atom from LiF, T. H. Johnson—586(A)
Reflection of Hg from alkali halide crystals, H. A. Zahl, A. Ellett—977
Atomic structure (see also **Energy states of atoms, Spectra**)
Dirac electron cloud for hydrogen-like atoms, pictorial representation, H. E. White—513,589(A)
Evaluation of the matrix components for He, L. P. Smith—1961
Natural units for atomic problems, A. E. Ruark—2240
Atomic structure factors
Of Cu and O in Cu_2O, G. A. Morton—41
In polyatomic gases, G. E. M. Jauncey—194(L)
Scattering of x-rays by gases and crystals, G. E. M. Jauncey—1; G. E. M. Jauncey, G. G. Harvey—1071(L)
For sylvine, G. G. Harvey—593; at low temperature, G. E. M. Jauncey, G. G. Harvey—1925
Atmosphere (see **Meteorology, atmospheric electricity**)
Atmospheric electricity (see also **Aurora, Meteorology**)
Relation of atmospheric space-charge to turbulence and convection, J. G. Brown—587(A)
Aurora
Auroral spectrum, nitrogen afterglow, J. Kaplan—582(A)
Green line and predissociation in N_2 J. Kaplan—1079(L); a correction 1792(L)
Light of night sky and aurora lines, J. Kaplan—1048
Book reviews
Allen, Frank. The Universe—2301
Annales de l'Institute Henri Poincare, Vol. I, sections i, ii, and iii—1395, section iv—2303
Barr, Guy. A. Monograph of Viscometry—2084
Bauer, O. and M. Hansen. Der aufbau der Kupfer-Zinklegierungen—1573
Becker, Fr. Uber interstellare Massan und die Absorption des Sternlicktes in Weltraum—1081
Berek, M. Gründlagen der Praktischen Optik—1573
Brauns, von Reinhard. Flussige Kristalle und Lebewesen—2088
Courant, R. Voresungern uber Differential-und Integralrechnung. Erster Band: Funktionen einer Veranderlichen—1913
Culver, Charles A. Electricity and Magnetism, an Advanced Textbook for Colleges—1794.
Dadourian, H. M. Analytical Mechanics—1910
Daniels, Mathews, and Williams. Experimental Physical Chemistry—1793
Debye, P. Elektronen Interferenzen Leipziger Vorträge 1930, 1262
Eve, A. S. and D. A. Keyes. Applied Geophysics in Search for Minerals—1397
Ewald, P. P., Th. Poschl, and L. Prandtl. The Physics of Solids and Fluids—578

Book reviews (continued)
Faraday Society Discussion. Photochemical Processes—1795
Ferry, E. S. in collaboration with O. W. Silvey, G. W. Sherman, Jr, D. C. Duncan. A Handbook of Physics Measurements, Vol. II—1394
Fowler, R. H. Statistical Mechanics—1392
Gmelins Handbuch der anorganischen Chemie. 8 Auflage. System-Nummer 8: Jod, Lieferung 1—2303
Gmelins Handbuch der anorganischen Chemie. 8 Auflage. System-Nummer 45: Germanium—2303
Gmelins Handbuch der anorganischen Chemie. 8 Auflage. System-Nummer 58: Kobalt, Teil A, Lieferung 1—2303
Gmelins Handbuch der anorganischen Chemie. 8 Auflage. System-Nummer 59: Eisen, Teil B, Lieferung 4—2303
Handbuch der anorganischen Chemie IV. Band 3, Abt. 2, Teil a 1, Eisenatom und Eisenmetall—A. Abegg, F. Auerbach, I. Koppel. 2302
Handbuch der Astrophysik, Band III, Erste Halfte Grundlagen der Astrophysik—578
Handbuch der Astrophysik, Band III, Zweite Halfte: Grundlagen der Astrophysik, Dritter Teil—1260
Handbuch der Experimentalphysik, Band XXIII. 2 Teil, Phosphoreszenz und Fluoreszenz von P. Lenard, F. Schmidt, und R. Tomaschek; Lichtelektrische Wirkung von P. Lenard and A. Becker—1262
von Helmholtz, H. Counting and Measuring—1909
Hess, Victor F. The Electrical Conductivity of the Atmosphere and its Causes—2086
Houston, R. A. Intermediate Physics—199
Houtermans, F. G. Neuere Arbeiten uber Quantentheorie des Atomkerns—1081
Jeffreys, Harold. Scientific Inference—1911
Kleeman, R. D. The Atomic and Molecular Forces of Chemical and Physical Interaction in Liquids and Gases, and Their Effects—2086
von Kluber, Harald. Das Vorkommen der Chemischen Elemente in Kosmos—2086
Kneser, H. O. Der Aktiv Stickstoff—1574
Kohl, K. Uber ungedanpfte elektrische Ultrakurzwellen—1397
Larmor, Sir Joseph. Mathematical and Physical Papers. Vol. I and II—2086
Laurence, A. C. S. Soap Films—1910
Lichtenstein, L. Vorlesungen uber einige Klassen nichtlinearer Integralgleichungen und Integrodifferentialgleichungen—1394
Luckiesh, N. Artificial Sunlight—1398
Mackaye, James. The Dynamic Universe—199
McConnell, A. J. Applications of the Absolute Differential Calculus—2302
March, Dr. A. Die Grundlagen der Quantenmechanik, zweite Auflage—1261
Mecke, Dr. R. Fortschritte der Chemie, Physik und physikalischen Chemie—2301
Meyer, Kurt H. and H. Mark. Der Aufbau der hochpolymeren organischen Naturstoffe auf Grund Molekular-Morphologischer, Betrachtungen—199
Milne-Thomson. Die elliptischen Funktionen von Jacobi—1913
Milne-Thomson, L. M. and L. J. Comrie. Standard Four-Figure Mathematical Tables—1911
Moulton, Forest Ray. Astronomy—2085
Ollivier, F. La Topographie sans Topographes—1393
Osborn, F. A. Physics of the Home—1909
Planck, Max. Einführung in die Theoretische Optik—842
Poor, V. C. Electricity and Magnetism—842
Porter, A. W. Thermodynamics—2301
Rabinowitsch, Eugen and Erich Thilo. Periodisches System—1793
Rosseland, Svein. Astrophysik (No. XI of Structur der Materie)—1912
Rosenthal, Josef. Das Jahrhundert der Strahlen—1392
Rutherford, Sir Ernest, Dr. James Chadwick and Dr. C. D. Ellis. Radiations from Radioactive Substances—1396
Sauerwald, F. Lehrbuch der Metallkunde—1573
Saunders, Frederick A. A Survey of Physics for College Students—1396
Searborough, J. B. Numerical Mathematical Analysis—1081
Simon, F. Fünfundzwanzig Jahre Nernstscher Wärmesatz—1082
Smith, C. J. Physics for Students of Pharmacy—1909
Smyth, C. P. Dielectric Constant and Molecular Structure—2301
Style, D. W. G. Photochemistry—2084
Ulich, Hermann—Chemische Thermodynamik—201
Warburg, Emil. Lehrbuch der Experimentalphysik fur Studierende—1794
Wigner, Eugen. Gruppentheorie und ihre Anwendung auf die Quantenmechanik der Atomspektren—1794
Wilson, W. Theoretical Physics, Vol. I—1260

Brownian movement
Of strings and elastic rods, G. A. Van Lear, Jr., G. E. Uhlenbeck—1583

Compressibility
Characteristic frequency from compressibility, J. B. Austin—1788(L)
Compton effect (see **X-rays, diffraction, scattering, reflection and refraction**)
Conductivity, thermal (see **Thermal conductivity**)
Contact potentials
Of Fe—Ni compared with photoelectric work function, G. N. Glasoe—1390
Cosmic radiation
Constancy of rays, R. D. Bennett, J. C. Stearns, A. H. Compton—1566(L)
Detection by Wilson cloud apparatus and Geiger-Müller counter, L. M. Mott-Smith, G. L. Locher—1399
Ionization as a function of pressure and temperature, A. H. Compton, R. D. Bennett, J. C. Stearns—1565(L)
Ionization in N_2 at high pressures, J. W. Broxon—1704, and neutronx, L. D. Huff—2292(L)
Range of fast electrons and neutrons, J. F. Carlson, J. R. Oppenheimer—1787(L), criticism, W. H. Watson. F. R. Terroux—2291(L)
Crystals and crystal structure
Of AsI_3, D. Heyworth—351, errata 1792(L)
Crystalline rubber hydrocarbon, E. W. Washburn—1790(L)
Electrical properties of S. P. single crystal zinc, E. P. T. Tyndall, A. G. Hoyem—820 A. G. Hoyem—1357
Fine-structure of lithium ferrite, E. Posnjak, T. F. W. Barth—2234
Graphical determination of crystal lattices from x-ray powder method data, W. Soller—583(A)
Grating constant for calcite crystals, J. A. Bearden—1389(L), 2089
Increase in surface area due to etching, L. Tonks—1030
Magnetic anisotropy of XO_3 ions, K. S. Krishnan—833(L)
Magneto-caloric effect in single crystals, F. Bitter 528, 588(A)
Of $NaNO_2$, G. E. Ziegler—1040
Permanent electric and magnetic moments, F. Zwicky—1772
Photoelectric properties of zinc single crystals, J. H. Dillon—408
Secondary structure of LiF, T. H. Johnson—586(A)
X-ray diffraction patterns of mixtures, A. W. Kenney, H. Aughey—1388(L)
X-ray reflection from crystals oscillating piezoelectrically, G. W. Fox, J. M. Cork—1420; B. E. Warren—572(L) R. M. Langer—573(L); C. S. Barrett—832(L); S. Nishikawa, Y. Sakisaka, I. Sumoto—1078(L) C. S. Barrett, C. E. Howe—2290(L)
Cybotactic state
In isotropic liquids and liquid crystals, G. W. Stewart—931
In octyl alcohols, G. W. Stewart, R. L. Edwards—1575, G. W. Stewart—2082(L)
Various organic mixtures, A. W. Meyer—1083
Diamagnetism (see **Magnetic properties**)
Dielectric constants
Electric moment of crystals, F. Zwicky—1772
Of liquids under high pressure, W. E. Danforth, Jr.—1224
Of N_2 at high pressure, J. W. Broxon—2049
Of organic liquids, W. R. Pyle—1057
Temperature variation of the electric moment of ethylene chloride, C. T. Zahn—521
Diffraction of atoms (see **Atomic and molecular beams**)
Diffusion
Reciprocal relations in irreversible processes: II, L. Onsager—2265
Discharge of electricity in gases (see also **Arcs, Electrons in gases**)
Capture and loss of He ions in He, P. Rudnick—1342
Cathode fall for thermionic and high field arcs, R. C. Mason—427
Diffusion of electrons back to an emitting electrode, I. Langmuir—1656
Dissociation of water in the glow discharge, E. G. Linder—679
Electronic velocities in high frequency discharges, E. Hiedemann—198(L)
Fall of potential in the initial stages, J. C. Street, J. W. Beams—416
Oscillations in discharge tubes, W. L. Brown, H. McN. Cowan—376(L)
Plasma-electron resonance and plasma resonance, L. Tonks—1219
Secondary electrons from Ni in He glow discharge, M. C. Harrington—1312
Discharge of electricity in high vacua (see also **Electrons, thermionic; High voltage tubes, machines**)
Work required to remove a field electron, J. E. Henderson, R. E. Badgley—590(A)
Dissociation
Of H_2O in glow discharge, E. G. Linder—679
Dissociation, heat of (see also **Molecular structure and constants**)
Of AgBr and AgI, B. A. Brice—658
Of H_2O, E. G. Linder—679
Of I_2 from band spectra, W. G. Brown—709
Of Li_2 and Be_2, J. H. Bartlett, Jr. W. H. Furry—1615

Doppler effect
In Ne canal rays, W. Romig—1709
In x-rays, by electrons in scattering body, J. W. M. DuMond, H. A. Kirkpatrick—1094
Dynamics
Canonical transformation for vibrations of loaded strings, R. B. Lindsay—491
Dissipative systems and related variational principles, H. Bateman—815
Elasticity
Characteristic frequency from compressibility, J. B. Austin—1788(L)
Force relations in drawing Cu wire, R. L. Doan, J. L. Betsill—1922(A)
Strain-energy function for isotropic bodies, C. Kaplan—1020
Electrical conductivity and resistance
Reciprocal relations in irreversible processes: II, L. Onsager—2265
Of single crystal zinc, E. P. T. Tyndall, A. G. Hoyem—820, A. G. Hoyem—1357
Electrical circuits
Acoustic resonator interferometer, equivalent electric network, J. C. Hubbard—1011
Equivalent networks, O. Brune—1783(L)
Electrical oscillations and waves
Ultra-short undamped waves, G. V. Potapenko—584(A)
Electric moment (see **Dielectric constant**)
Electrodeless discharge
Method of measuring induced current, C. T. Knipp, J. K. Knipp—948
Electromagnetic theory
Light quanta and the electromagnetic field, J. R. Oppenheimer—725
Problem of rotating magnets, W. B. Pietenpol, E. C. Westerfield—2280
Electrons
Transmission through potential barriers, N. H. Frank, L. A. Young—80, W. Wetzel 1205, W. B. Nottingham—1918(A)
Value of charge from shot effect, B. A. Kingsbury—1458, 1922(A)
Electron distribution in atoms
Of monatomic gases, E. O. Wollan—15
In rare earths in crystals, S. Freed—2122
By scattering of x-rays, G. E. M. Jauncey—1; G. E. M. Jauncey, G. G. Harvey—1071(L)
Stark effect, stereophotographic models, R. W. Wood—346
Electrons in gases
Capture and loss of He ions in He, P. Rudnick—1342
Electrons in metals
Equilibrium distribution outside conductor, A. T. Waterman—1497
Electrons, scattering of (see also **Electrons in gases**)
Probabilities in He, Ne and A, L. C. Van Atta—876
By spherically symmetrical atoms, F. W. Doermann, O. Halpern—193(L)
In thin metal foils, comparison with theory, H. V. Neher—585(A), 1321
Electrons, secondary
Negative ions by bombardment of Pt, J. S. Thompson—1389(L), K.S. Woodcock—1696(L)
From Ni, bombarded by He ions and metastable atoms, M. C. Harrington—1312
From Pt by bombardment with Hg ions, J. E. Henderson, E. Gideon—586(A)
From thin metal foils, H. V. Neher—585(A), 1321
From W, A. J. Ahearn—1858, 1918(A)
Electrons, thermionic
From Co, change with temperature, A. B. Cardwell—2033
Effect of space charge, R. S. Bartlett—1566(L)
Electron and potential distribution outside conductor, A. T. Waterman—1497
Enhanced emission in oxide coated filaments, J. A. Becker, R. W. Sears—2193
Photoelectric and thermionic work function, W. S. Huxford—379
Theory of emission, N. H. Frank—1918(A)
Transmission through potential barrier of thoriated filament, W. B. Nottingham—1918(A)
Electro-optical effects (see also **Photoelectric effect and properties**)
Electro-optical shutter, electric circuit of, H. W. Washburn—584(A)
Electro-optical shutter, theory and technique, F. G. Dunnington—1506
Kerr effect in gases, E. C. Stevenson, J. W. Beams—133
Kerr effect in Rochelle salt, H. Müller—1922(A)
Electrostatics
Potential due to a buried spheroid, J. H. Webb—2056
1,500,000 volt electrostatic generator, R. J. Van de Graaff—1919(A)
e/m
From quantum mechanical calculation, L. D. Huff—501, 589(A)
By refraction of x-rays, J. A. Bearden—835(L), 1919(A)
From Zeeman effect, J. S. Campbell, W. V. Houston—581(A)
Energy states of atoms (see also **Atomic structure, Spectra, atomic**)
Of Gd IV in crystal lattice, S. Freed, F. H. Spedding—670
Levels for equivalent (s, p, d, f) electrons with (jj) coupling, S. D. Bryden, Jr.—1145
Of rare earth ions in crystals, S. Freed—2122

Energy states of molecules (see **Molecular structure and constants, Spectra, molecular**)
Entropy
Of ammonia and methane, D. S. Villars—1552, 1920(A) W. F. Giauque, R. W. Blue, Roy Overstreet—196(L) D. P. MacDougall 2074(L)
Of the universe, R. C. Tolman—797, 1758
Equations of state
General adiabatic equation for gases, T. C. Huang —1385
P-V-T relations of NH_4Cl and NH_4Br, P. W. Bridgman—182
Properties of CO, W. E. Deming, L. E. Shupe—1920(A), 2245
Quantum theory of, J. C. Slater—237
For real gases, H. Margenau—1785(L)
Second virial coefficient, J. G. Kirkwood, F. G. Keyes—576(L), H. Margenau—1785(L)
van der Waals attractions, H. Margenau,—747
Errata
Excitation of high optical energy levels J. E. Mack—2300(L)
A new criterion for predissociation J. Kaplan —1792(L)
Note on the crystal structure of AsI_3 D. Heyworth—1792(L)
Excitation of atoms and molecules
Average life of H^+, L. R. Maxwell—1664
Of high optical energy levels, J. E. Mack—193(L), errata—2300(L)
Low voltage excitation of Na, probability measurements, W. C. Michels—712
Transition probabilities and quenching in Na, N. E. Berry, G. K. Rollefson—1599
Fluorescence
In iodine, effect of argon, L. A. Turner—574(L)
Transition probabilities and quenching, N. E. Berry, G. K. Rollefson—1599
Gamma-rays
Photoelectric absorption, H. Hall, J. R. Oppenheimer, 57, 589(A)
Gases
Properties of CO, W. E. Denning, L. E. Shupe 1920(A), 2245
Gravitation
Absolute determination of gravity, A. C. Longden —1920(A)
Hall effect
In solid mercury, J. T. Serduke, T. F. Fisher—1922(A)
Heat of combustion
Internal molecular potentials, H. A. Stuart—1372
Heat transfer
From solid surfaces to air, R. B. Kennard—1921(A)
High voltage tubes and machines (see also **Ions, high speed**)
Production of high speed ions without the use of high voltages, D. H. Sloan, E. O. Lawrence—2021; E. O. Lawrence, M. S. Livingston—834(L)
500 kilovolt cathode rays, R. E. Vollrath—212
1,500,000 volt electrostatic generator, R. J. Van de Graaff—1919(A)
Hydrodynamics
Stability of a single file of straight vortices, A. T. Jones—2068
Hyperfine structure
Effect on polarization of Cd resonance radiation, A. C. G. Mitchell—473
Of Bi II and Bi III, J. B. Green, J. Wulff—2193
Of heavy elements, theory, G. Breit—463
Of In and Ga, J. S. Campbell, R. F. Bacher—1906(L)
Of Tl II and Tl III, J. B. Green, J. Wulff—2176
Nuclear magnetic moments from hyperfine structure, S. W. Nile—375(L)
Nuclear moment of Re I, W. F. Meggers, A. S. King, R. F. Bacher—1258(L)
Nuclear moment of K, F. W. Loomis, R. W. Wood —854; F. W. Loomis—2153
Intensities in spectra (see also **Spectra, etc.**)
Of Balmer emission lines (stellar) O. Struve, H. F. Schwede—1195
Band spectrum intensities by graphical methods, E. Hutchisson—1921(A)
Of He band, λ600 J. L. Nickerson—1907(L)
Summation rules and perturbation effects in complex spectra, G. R. Harrison, M. H. Johnson, Jr.—757
Of V I and V II, G. R. Harrison—1921(A)
Interference phenomena
In thin metallic films, H. W. Edwards—166
Ionization by impact (see also **Potentials, critical**)
As function of pressure and temperature, A. H. Compton, R. D. Bennett, J. C. Stearns—1565(L)
Of Kr and Xe by positive alkali ions, O. Beeck, J. C. Mouzon—967
Negative ions by bombardment of Pt. J. S. Thompson—1389(L), K. S. Woodcock—1696(L)
Ionization potentials (see **Potentials critical**)
Ionization by radiation (see **Photoionization**)
Ions, high speed (see also **High voltage tubes and machines**)
Hg ions, E. O. Lawrence, D. H. Sloan—586(A)
500 kilovolt cathode rays, R. E. Vollrath—212
Ions in gases
Average life of H^+, L. R. Maxwell—1664
Bombardment of platinum by Hg, J. E. Henderson, E. Gideon—586(A)

Ions in gases (continued)
Mass of gas ions in air, N_2, O_2, and SO_2 from glow discharge, O. Luhr—1730
Mass spectrograph analyses of ions in N_2 and CO, A. L. Vaughan—1687
Negative hydrogen ions from H_2O, D. W. Mueller, H. D. Smyth—1920(A)
Ions, mobility (see also **Ions in gases**)
Absolute values, N. E. Bradbury—1905(L)
Aging of ions in air and N_2, J. Zeleny—969, 2293(L)
Of Na^+ ions in N_2 and H_2 as a function of time, nature of ion, L. B. Loeb—549, 586(A)
Velocity spectrum of ions in air and problem of ionic structure, L. B. Loeb, N. E. Bradbury—1716, J. Zeleny—2293(L)
Isotopes
Atomic species, regularities and continuity of series, W. D. Harkins—1270, 1792(L)
Of Ba, 136 and 137, R. C. Gibbs, P. G. Kruger—1921(A)
Relative abundance of N^{14} and N^{15}, H. C. Urey, G. M. Murphy—575(L)
Relative abundances, H. C. Urey, C. A. Bradley, Jr.—589(A), 718
Search for $O^{18}H$, G. M. Almy, G. D. Rahrer—1816
Liquids (see also **Hydrodynamics**)
General x-radiation and diffraction by liquids, W. C. Pierce—1409
Higher order effects in x-ray diffraction, W. C. Pierce—1413
Magnetic character of liquid crystalline para-azoxyanisol, G. W. Stewart—931
Surface energy of liquids, H. Margenau—365
Magnetic properties
Of An-Fe alloys, J. W. Shih—2051
Anisotropy of XO_3 ions, K. S. Krishnan—833(L)
Of colloidal suspensions, C. G. Montgomery—1782(L)
Of Cu-Ni alloys, E. H. Williams—628
Diamagnetic susceptibility of the rare gas atoms, S. C. Biswas—1784(L)
Effect of internal stress, C. W. Heaps, H. E. Banta—195(L)
Inhomogeneities in the magnetization, F. Bitter—1903(L)
Of liquid crystalline para-azoxyanisol, G. W. Stewart—931
Magneto-caloric effect and mechanism of magnetization, F. Bitter—528, 588(A)
Metamagnetism in Bi crystals, A. Goetz, A. B. Focke—1569(L)
Moment of the Pd atom, A. N. Guthrie, M. J. Copley—360
Moment of S_2, E. J. Shaw, T. E. Phipps—174
Permanent moments of crystals, F. Zwicky—1772
Reversed magnetization in strained wires, I. Langmuir, K. J. Sixtus—2072(L)
Structure sensitiveness of Cu, Ag, Pt, and Bi, F. E. Lowance, F. W. Constant—1547
Transverse Barkhausen effect in Fe, R. M. Bozorth, J. F. Dillinger—192(L)
Thermocouples of longitudinally and transversely magnetized wires of Ni and of Fe, W. H. Ross—179; S. Sears—1254; C. W. Heaps—1391(L)
Mechanics (see **Dynamics**)
Mechanics, quantum—atomic structure and spectra
Dirac electron cloud for H like atom, pictorial representation, H. E. White—513, 589(A)
Evaluation of the matrix components for He, L. P. Smith—1961
Many-electron wave functions, J. H. Bartlett, Jr.—1623
Of two-electron systems, M. H. Johnson, Jr.—1628
Mechanics, quantum—general
Collision problems involving large interactions, O. K. Rice—1943
General solution of Schrödinger's equation and the uncertainty principle, E. L. Hill—2115
Inelastic collisions, C. Zener—277, 588(A)
Inverse-cube central force field, G. Shortley—120
Light quanta and the electromagnetic field, J. R. Oppenheimer—725
Local momentum in wave mechanics, L. A. Young—1612
Motion of a Dirac electron in a magnetic field, value of e/m, L. D. Huff—501, 589(A)
Natural units for atomic problems, A. E. Ruark—2240
One-dimensional problems in quantum mechanics, E. L. Hill—1258(L)
Quadrupole forces in van der Waals attractions, H. Margenau—747
Quantization of large scale events, D. L. Watson—1072(L)
Reflection coefficients and their numerical determination, V. Rojansky, W. Wetzel—1979
Reflection of electrons by a special potential field, E. L. Hill—1072(L)
Schrödinger potential function, R. M. Langer—779
Tables of integrals and functions, N. Rosen—2099
Theory of equation of state, J. C. Slater—237
Transmission of electrons through potential barriers, N. H. Frank, L. A. Young—80, W. Wetzel—1205
Wave mechanics quantization of loaded string, R. B. Lindsay—491
Zero order eigenfunctions, N. M. Gray, L. A. Wills—248

Mechanics, quantum—molecular structure and spectra
Electron pair bond, W. Heitler—243
Energy levels and valence bonds, J. C. Slater—1109
Interaction between atoms with *s*-electrons, N. Rosen—255
Normal state of H_2, N. Rosen—2099
Mechanics, statistical
Types of statistics, models, P. S. Epstein—590(A)
Metals
Colors of thin films, H. W. Edwards—166
Metastable atoms and molecules
Life of Hg and N_2, M. L. Pool—955
Metastable atom emission of electrons from surfaces, C. Kenty—377(L)
Meteorology
Of the earth, temperature effect of O_3 and CO_2, E. O. Hulburt—1876
Heat transfer from solid surfaces to air, R. B. Kennard—1921(A)
Ultraviolet band of ozone, effect of temperature, O. R. Wulf, Eugene H. Melvin—330
Methods and instruments
Absolute determination of gravity, A. C. Longden—1920(A)
Band spectrum intensities by graphical methods, E. Hutchisson—1921(A)
Concentrations from Raman spectra, E. A. Crigler—1387(L)
Double x-ray spectrometer, R. C. Spencer—618
Effect of inductance on damped galvanometer, T. M. Dahm—590(A)
Electrical field giving uniform deflecting force on a molecular beam, E. McMillan—1568(L)
Electron lenses, apertures in charged conductors, C. J. Davisson, C. J. Calbick—585(A)
Electro-optical shutter, theory and technique, F. G. Dunnington—1506
Excitation of high optical energy levels, J. E. Mack—193(L), errata—2300(L)
Heterochromatic photographic photometry, G. R. Harrison, P. A. Leighton—899
High resolution in the infrared, J. D. Hardy—2162
Improved technique for Raman effect, R. W. Wood—2168
Induced currents in glow discharge, C. T. Knipp, J. K. Knipp—948
Infrared spectroscopy, J. Strong—1818
Ionization chamber method of measuring intensities of x-ray lines, S. K. Allison, V. J. Andrew—441
Intercomparison of the high temperature scale, W. E. Forsythe—1247
500 kilovolt cathode rays, R. E. Vollrath—212
1500 kilovolt electrostatic generator, R. J. Van de Graaff—1919(A)
Method of producing negative ions, J. S. Thompson—1389(L)
Na arc, N. E. Berry, G. K. Rollefson—1599
Reflecting power and grating efficiency in the extreme ultraviolet, H. M. O'Bryan—32
Reflection power of metals in thin layers for the infrared, R. B. Barnes, M. Czerny—338
Removal of continuous background from Raman spectra, M. E. High, M. L. Pool—374(L)
Resolving power of double crystal x-ray spectrometer, S. K. Allison—203
Second and third spark spectra in a hollow cathode lamp, C. W. Gartlein, R. C. Gibbs—1907(L)
Supersonic satellites and velocity, W. H. Pielemeier—1236
Three-dimensional vibrograph, J. E. Shrader—1923(A)
Thomas-Fermi equation solution by the differential analyzer, V. Bush, S. H. Caldwell—1898
Mobility of ions (see **Ions, mobility**)
Molecular structure and constants (see also **Spectra, molecular, Raman spectra**)
Energy levels and valence bonds, J. C. Slater—1109
From heats of combustion, for substituent groups in benzene ring, H. A. Stuart—1372
Of the groups XO_3, J. C. Slater—325
Heat capacities and relative amounts of nuclear modifications of methane, D. S. Villars, G. Schultze—998, D. P. MacDougall—2296(L)
Heat of dissociation of Li_2, F. W. Loomis, R. E. Nusbaum—1447
Magnetic moment of S_2, E. J. Shaw, T. E. Phipps—174
Moments of inertia of ethylene, R. M. Badger, J. L. Binder—1442
Of N_2O, E. K. Plyler, E. F. Barker—1827
Raman effect and the carbon-halogen bond, W. D. Harkins, H. E. Bowers—1845
Normal state of H_2, N. Rosen—2099
Valence forces in Li and Be, J. H. Bartlett, Jr., W. H. Furry—1615
Vibrational frequency in the normal state of benzene, C. V. Shapiro, R. C. Gibbs, J. R. Johnson—1170
Vibrations of pentatonic tetrahedral molecules, H. C. Urey, C. A. Bradley, Jr.—1969
Of the water vapor molecules, E. K. Plyler—1784(L)
Multiplets (see also **Spectra, atomic**)
Displacement in isoelectronic sequence, H. T. Gilroy—2217
Zeeman effect in Sn III and Sb I, J. B. Green, R. A. Loring—1289

Neutrons
Cosmic rays, L. M. Mott-Smith, G. L. Locher—1399, L. D. Huff—2292(L)
Range of fast electrons and neutrons, J. F. Carlson, J. R. Oppenheimer—1787(L), W. H. Watson, F. R. Terroux—2291(L)
Nuclear spin (see also **Hyperfine structure**)
Absence of, R. M. Langer—837(L)
Alternating intensities of Na_2 bands, H. C. Urey—1074(L)
Classification of elements, S. D. Bryden, Jr.—1989
Of In and Ga, J. S. Campbell, R. F. Bacher—1906(L)
Of K, F. W. Loomis, R. W. Wood—854; F. W Loomis—2153
Measurement by Stern-Gerlach experiment, G. Breit, I. I. Rabi—2082(L)
Of Re I, W. F. Meggars, A.S. King, R. F. Bacher——1258(L)
Spin of protons in nucleus, H. E. White—2078(L)
Nucleus
Atomic species, regularities and continuity of series, W. D. Harkins—1270, 1792(L)
Structure and moment of momentum, S. D. Bryden, Jr.—1989
Optical constants and properties
Reflection power of metals in thin layers for the infrared, R. B. Barnes, M. Czerny—338
Optical instruments (see **Methods and instruments**)
Paschen-Back effect (see **Zeeman effect**)
Periodic system of atoms
Atomic species, regularities and continuity of series, W. D. Harkins—1270, 1792(L)
Photoelectric effect and properties
In caesium-oxide photocells at room temperatures, E. F. Kingsbury—1918(A)
Of Co, change with temperature, A. B. Cardwell—2033
Effect of adsorbed K^+ ions on threshold of iron, A. K. Brewer—401
Effect of electric fields on the emission from oxide cathodes, W. S. Huxford—379
Efficiencies in the extreme ultraviolet, C. Kenty—2079(L)
Of Hg, thin films, D. Roller—396
Lateral distribution of x-ray photoelectrons, P. Kirkpatrick—1938
Photoelectric and metastable atom emission of electrons from surfaces, C. Kenty—377(L)
Relativistic theory, H. Hall, J. R. Oppenheimer—57, 589(A)
Selective effect from two-component cathodes, A. R. Olpin—1745, 1917(L), W. H. Zachariasen, 2290(L)
Shot effect in photoelectric currents, B. A. Kingsbury—1458, 1922(A)
Of Ta, effect of temperature, A. B. Cardwell—2041
Temperature variation of photoelectric sensitivity, R. H. Fowler—320, L. A. Young and N. H. Frank—838(L)
Theory of photoelectric effect in hydrogen-like atom, angular distribution, J. Frenkel—309; E. L. Hill—1072(L), A. Sommerfeld—1078(L)
Thin films of alkali metal on silver, H. E. Ives, H. B. Briggs—1477, 1917(A)
Of thin unbacked gold films, R. P. Winch—321
Threshold for W by Fowler's method, A. H. Warner—1871
Vectorial effect in thin films of alkali metals, H. E. Ives—1209, 1917(A)
Work function of Fe and Ni compared with contact potentials, G. N. Glasoe—1490
Of zinc single crystals, J. H. Dillon—408
Photography
Parallax panoramagrams made with a large diameter concave mirror, H. E. Ives—1922(A)
Photoionization
Of Cs vapor, F. W. Cooke—1351
In high pressure chamber, A. H. Compton, R. D. Bennett, J. C. Stearns—1565(L)
In N_2 at high pressure by cosmic rays, J. W. Broxon—1704
Photometry
Fluorescence and heterochromatic photographic photometry, G. R. Harrison, P. A. Leighton—899
Piezoelectric effect
Oscillation of crystals and x-ray diffraction, B. E. Warren—572(L), R. M. Langer—573(L), C. S. Barrett—832(L), S. Nishikawa, Y. Sakisaka, I. Sumoto—1078(L), G. W. Fox, J. M. Cork—1420, C. S. Barrett, C. E. Howe—2290(L)
Plasmoidal discharges (see **Discharge of electricity in gases**)
Polymerization
In water, J. W. Ellis—693
Potentials, critical
For ions by electron impact in N_2 and CO, A. L. Vaughan—1687
Ionization of C III, I. S. Bowen—128
Of Kr and Xe by positive alkali ions, O. Beeck, J. C. Mouzon—967
Potentials, critical (see also **Ionization potentials**)
Probabilities of energy losses in He, Ne and A, L. C. Van Atta—876
Ultra-ionization potentials of Hg, probability law, C. R. Haupt—282

Potentials, critical (see also **Ionization potentials** (continued)
Ultra-ionization potentials of He, Ne and A, R. L. Womer—454
Ultra-ionization potentials in Hg vapor, A. G. Shenstone—873
Ultra-ionization potentials and spectral data, H. E. White—1786(L), 2016
Predissociation
Enhancement of, by collisions, L. A. Turner—574(L)
In N_2, J. Kaplan—373(L), 1079(L); a correction—1792(L)
A new criterion, J. Kaplan—1079(L); errata—1792(L)
Proceedings of the American Physical Society
Pasadena Meeting, June 15 to 20, 1931—579
Schenectady Meeting, September 10 to 12, 1931—1915
Radiation (see **Thermal radiation**)
Radioactivity
Anomalous scattering of alpha-rays, M. Muskat—23
Conservation of energy and the disintegration of RaE, L. W. McKeehan—2292(L)
Induced by action of x-rays, G. I. Pokrowski—925
Radioactive disintegration, A. Bramley—1567(L)
Raman spectra
From amorphous and crystalline solids and their solutions, A. Hollaender, J. W. Williams—1739
Benzene substitution products by improved technique, R. W. Wood—2168
Carbon-halogen bond, W. D. Harkins, H. E. Bowers—1845
In certain organic compounds, C. S. Morris—141, M. E. High—1837
Concentrations in benzene-toluene mixtures, E. A. Crigler—1387(L)
Effect of solutes on spectra of water, C. C. Hatley, D. Callihan—909
Removal of continuous background from spectrum of CCl_4, M. E. High, M. L. Pool—374(L)
Relativity
Electrostatic analogy to the gravitational red shift, R. J. Kennedy, E. M. Thorndike—591(A)
Model of universe with reversible annihilation of matter, R. C. Tolman—797
Periodic behavior of the universe, R. C. Tolman—1758
Theory of photoelectric effect, H. Hall, J. R. Oppenheimer—57, 589(A)
Reststrahlen
Investigations, 20 to 40μ, J. Strong—583(A)
Scattering of electrons (see **Electrons in gases, Electrons, scattering of**)
Selection rules
Many-electron selection rules, S. Goudsmit, L. Gropper—225
Shot effect
In photoelectric currents, B. A. Kingsbury—1458, 1922(A)
Solutions
Orientation of H_2O rare earth ions, F. H. Spedding, G. C. Nutting—2294(L)
X-ray study of the nature of solid solutions, R. T. Phelps, W. P. Davey—1919(A)
Sound (see **Acoustics**)
Spark discharge
Breakdown potential and electrode material, L. B. Loeb—1891
Fall of potential in the initial states, J. C. Street, J. W. Beams—416
Optical study of the formation stages, F. G. Dunnington—1535
Specific heat
Of methane, D. S. Villars, G. Schultze—998; D. P. MacDougall—2296(L)
Temperature and pressure variation of C_p, CO_2 and He, E. J. Workman—587(A)
Spectra, absorption (see also **Absorption of light**)
Of AgBr and AgI, B. A. Brice—658
Of Br_2, infrared, vibrational analysis. W. G. Brown—1187
Of Br_2, visible, vibrational analysis, W. G. Brown—1179
Of ClO_2, H. C. Urey, H. Johnston—58(A), 2131
Of ethane and ethylene in infrared, R. M. Badger, J. L. Binder—1142
Of Gd^{+++} ion in crystals, F. H. Spedding, G. C. Nutting—2294(L)
Of Gd, S. Freed, F. H. Spedding—670
Of HCN in gas and liquid, F. S. Brackett, U. Liddel—582(A)
Of I_2, W. G. Brown—709
Infrared bands of ammonia, NH_3, methyl bromide, methyl iodide and CO_2, W. W. Sleator—147
Of K_2, nuclear spin, F. W. Loomis, R. W. Wood—854, F. W. Loomis—2153
Line width in Na vapor, S. A. Korff—477
Long wave-length absorption band of CS_2, D. M. Dennison, N. Wright—2077(L)
Magnetic rotation spectrum and heat of dissociation, F. W. Loomis, R. E. Nusbaum—1447
Of N_2O_3, E. H. Melvin, O. R. Wulf—2294(L)
New infrared bands in H_2O, J. W. Ellis—582(A), 693
Of rare earths, S. Freed—2122
Of salts in liquid ammonia, R. W. Wood—1648

Spectra, absorption (see also **Absorption of light** (continued)
Ultraviolet band of ozone, effect of temperature, O. R. Wulf, E. H. Melvin—330
Spectra, atomic
Of alkaline earth metals and inert gases, auto-ionization, H. E. White—1786(L), 2016.
Of Bi II and Bi III, Paschen-Back effect of hyperfine structure, J. B. Green, J. Wulff—2186
Broadening of the resonance line of He, W. Weizel—642
Of C III and C II, I. S. Bowen—128
Deepest term in Au II, R. A. Sawyer, K. Thomson—2293(L)
Doppler effect in Ne canal rays, W. Romig—1709
Of Element No. 87, H. Yagoda—2298(L)
Energy relations in complex spectra, D. R. Inglis—862
Excitation of high optical energy levels, J. E. Mack—193(L); erratum—2300(L)
Of Hg, Cd and Zn under high frequency excitation, J. Okubo, E. Matuyama—1651
Infrared lines of Ne I and He I, J. D. Hardy—2162
Intensities of Balmer emission lines in stellar, O. Struve, H. F. Schwede—1195
Levels for equivalent (s, p, d, f) electrons with (jj) coupling, S. D. Bryden, Jr.—1145
Of Li I, isotope separation, D. S. Hughes—857
Low voltage excitation of Na, W. C. Michels—712
Of N I, K. R. More, O. E. Anderson—1995
Of Rb II, O. Laporte, G. R. Miller, R. A. Sawyer—843
Of Sn I, infrared, H. M. Randall, N. Wright—457
Of Tl II and Tl III, Paschen-Back effect of hyperfine structure, J. B. Green, J. Wulff—2176
Of Tu, Yb and Lu under different excitations, A. S. King—583(A)
Of V I isoelectronic sequence, H. T. Gilroy—2217
Spectra, continuous
Emission spectrum of metallic Ag under electron bombardment, F. L. Mohler—1923(A)
Spectra, general
Effect of temperature on band spectrum of Hg, W. M. Nielsen—888
Electrostatic analogy to the gravitational red shift, R. J. Kennedy, E. M. Thorndike—591(A)
High current vacuum arcs, A. S. King—590(A)
Investigations in the far infrared, J. Strong—1818
Light of the night sky and aurora lines, J. Kaplan—1048
Many-electron selection rules, S. Goudsmit, L. Gropper—225
Summation rules and perturbation effects in complex spectra, G. R. Harrison, M. H. Johnson, Jr.—757
Ultra-ionization potentials in Hg vapor, A. G. Shenstone—873
Wave-length standards, C I and Sn in Schumann region, R. V. Zumstein, D. S. Marston—305, of Al, Si and Bi, R. V. Zumstein—2214
Spectra, molecular (see also **Molecular structure and constants**)
Alternating intensities of Na_2 bands, H. C. Urey—1074(L)
Of benzene, vibrational frequency in the normal state, C. V. Shapiro, R. C. Gibbs, J. R. Johnson—1170
Emission spectrum of CO_2, H. D. Smyth—2000
Faint branches in OH bands, G. M. Almy, G. D. Rahrer—1816
Infrared bands of slightly asymmetric molecules, H. H. Nielsen—1432
Intensities by graphical methods, E. Hutchisson—1921(A)
Intensity of $\lambda 600$ band of He, J. L. Nickerson—1907(L)
Interpretation of the BeF bands, R. S. Mulliken—836(L)
New bands in Hg vapor, J. G. Winans—583(A)
Of N_2O, infrared, E. K. Plyler, E. F. Barker—1827
O_2^+ bands, rotational analysis, D. S. Stevens—1292
Ortho-helium, band spectrum, Zeeman effect, J. S. Millis—1148
Perturbations in He band spectrum, G. H. Dieke—646
Red CN band system, F. A. Jenkins, Y. K. Roots, R. S. Mulliken—1075(L)
Rotational analysis of the first positive (N_2) bands. S. M. Naudé—372(L)
In SO_2, T. C. Chow, H. D. Smyth—838(L)
Λ-type doubling, electron configuration in diatomic molecules, R. S. Mulliken, A. Christy—87
Ultraviolet of CO, electrodeless ring discharge, H. P. Knauss, J. C. Cotton—1190
Vibrations of pentatonic tetrahedral molecules, H. C. Urey, C. A. Bradley, Jr.—1969
Spectra, Raman (see **Raman Spectra**)
Spectroscopy, technique
Band spectrum intensities by graphical method, E. Hutchisson—1921(A)
High current vacuum arcs, A. S. King—590(A)
In the far infrared, J. Strong—1818
Second and third spark spectra in a hollow cathode lamp, C. W. Gartlein, R. C. Gibbs—1907(L)

Stark effect
Stereophotographic models of electron motion, R. W. Wood—346
Sun (see **Astrophysics**)
Surface tension
Surface energy of liquids, H. Margenau—365
Thermal conductivity (see also **Heat transfer**)
Reciprocal relations in irreversible processes: II, L. Onsager—2265
Thermal radiation
Of colored and pure fused quartz, R. W. Wood—487
Intercomparisons of the high temperature scale, W. E. Forsythe—1247
Thermal expansion
Macroscopic and lattice expansion of Bi single crystals, A. Goetz, R. C. Hergenrother—2075(L)
Thermionic emission (see **Electrons, thermionic**)
Thermionic emission of positive ions
From Cu and Ag, H. B. Wahlin—1074(L)
Thermodynamics
Fundamental thermodynamics, G. N. Lewis—376(L)
General adiabatic equation for gases, T. C. Huang—1385
Model of universe with reversible annihilation of matter, R. C. Tolman—797
Reciprocal relations in irreversible processes: II, L. Onsager—2265
Relativistic thermodynamics and behavior of the universe, R. C. Tolman—1758
Ultra-ionization potentials (see **Potentials, critical**)
Valence
Directed valence in molecules, J. C. Slater—1109
Forces in Li and Be, J. H. Bartlett, Jr., W. H. Furry—1516
Quantum theory and electron pair bond, W. Heitler—243
Structure of the groups XO_3, J. C. Slater—325
van der Waal forces
Quadrupole forces, H. Margenau—747; 1785(L)
Virial coefficient
Second virial coefficient, application to He, J. G. Kirkwood, F. G. Keyes—576(L); H. Margenau—1785(L)
Viscosity
And molecular arrangement in octyl alcohols, G. W. Stewart, R. L. Edwards—1575, G. W. Stewart—2082(L)
Vision
An electromagnetic theory, S. R. Cook—587(A)
Relation of wave-length to color sensation, C. A. Rinde—588(A)
Wave mechanics (see **Mechanics, quantum, etc.**)
X-ray absorption
By Hg vapor in *L* region, F. M. Uber—217
In ionization chamber, S. K. Allison, V. J. Andrew—441
K absorption calculated for Sn, L. C. Roess, E. H. Kennard—1263
M-series of Ta, C. A. Whitmer—1164
Photoelectric absorption of ultragamma radiation, H. Hall, J. R. Oppenheimer—57, 589(A)
Soft x-rays in gases, R. G. Spencer—1932
X-rays, diffraction, scattering, reflection and refraction
Atomic scattering power of Cu and O in Cu_2O, G. A. Morton—41
Dependence of Compton line breadth on primary wave-length, J. W. M. DuMond—1094
Diffraction patterns of mixtures, A. W. Kenney, H. Aughey—1388(L)
Dispersion in calcite, L. A. Pardue—1808
Effect of temperature on scattering from rocksalt, W. D. Claus—604
By gases and crystals, G. E. M. Jauncey—1, G. E. M. Jauncey, G. G. Harvey—1071(L)
General radiation and diffraction by liquids, W. C. Pierce—1409
Grating constant of calcite crystals, J. A. Bearden—1389(L), 2089
Higher order effects in liquids, W. C. Pierce—1413
In organic mixtures, A. W. Meyer—1083
Piezoelectric oscillation and the intensity of x-ray reflections, B. E. Warren—572(L), R. M. Langer—573(L); C. S. Barrett—832(L); S. Nishikawa, Y. Sakisaka, I. Sumoto—1078(L); G. W. Fox, J. M. Cork—1420; C. S. Barrett, C. E. Howe—2290(L)
From polyatomic gases, G. E. M. Jauncey—194(L); by quartz, of Cu *K*-series, J. A. Bearden—835(L)
Scattering from Al, Cu, and Pb and paraffin, A. W. Coven—1424
From sylvine, G. G. Harvey—593, at low temperature, G. E. M. Jauncey, G. G. Harvey—1925
Temperature and diffuse scattering from crystals, Y. H. Woo—6
X-ray study of the magnetic character of liquid, G. W. Stewart—931
X-rays, emission
Corrected relative intensities of the x-ray lines in the tantalum *L*, V. Hicks—572(L)
New *K*-series line, delta, J. W. M. DuMond, A. Hoyt—839(L)
Relative intensities of lines, S. K. Allison, V. J. Andrew—441

X-rays, emission (continued)
Satellites of $L\beta_2$ for atomic numbers 50 to 60, R. D. Richtmyer—1802
Satellites of M-series, F. R. Hirsh, Jr.—914
Shape of Ag L, Mo K and Cu K lines, R. O. Spencer—630
Structure of soft x-ray lines, W. V. Houston—1797
X-rays, spectroscopy
Double spectrometer, theory of, R. C. Spencer—618
Resolving power of double crystal spectrometer, S. K. Allison—203

Zeeman effect
Hyperfine structure, Paschen-Back effect in Bi II and Bi III, J. B. Green, J. Wulff—2186
Hyperfine structure, Paschen-Back effect in Tl II and Tl III, J. B. Green, J. Wulff—2176
In intermediate coupling, D. R. Inglis, M. H. Johnson, Jr.—1642
Multiplet structure, Sn III and Sb I, J. B. Green R. A. Loring—1289
In ortho-helium band spectrum, J. S. Millis—1148
Patterns at intermediate strengths of field in Ca I W. Bender—588(A)
In solids, F. H. Spedding—2080(L)

X-rays, emission (continued)
Satellites of $L\beta_2$ for atomic numbers 50 to 60, R. D. Richtmyer—1802
Satellites of M-series, F. R. Hirsh, Jr.—914
Shape of Ag L, Mo K and Cu K lines, R. O. Spencer—630
Structure of soft x-ray lines, W. V. Houston—1797
X-rays, spectroscopy
Double spectrometer, theory of, R. C. Spencer—618
Resolving power of double crystal spectrometer, S. K. Allison—203

Zeeman effect
Hyperfine structure, Paschen-Back effect in Bi II and Bi III, J. B. Green, J. Wulff—2186
Hyperfine structure, Paschen-Back effect in Tl II and Tl III, J. B. Green, J. Wulff—2176
In intermediate coupling, D. R. Inglis, M. H. Johnson, Jr.—1642
Multiplet structure, Sn III and Sb I, J. B. Green R. A. Loring—1289
In ortho-helium band spectrum, J. S. Millis—1148
Patterns at intermediate strengths of field in Ca I W. Bender—588(A)
In solids, F. H. Spedding—2080(L)